ORNL/Sub/81-21099/1&03

26 FEBRUARY 1982

REPORT EBT-P010

FUSION ELMO BUMPY TORUS ENERGY

Copy No. 97

Elmo Bumpy Torus Proof Of Principle

PHASE II — TITLE 1 REPORT

Volume III MAGNET SYSTEM

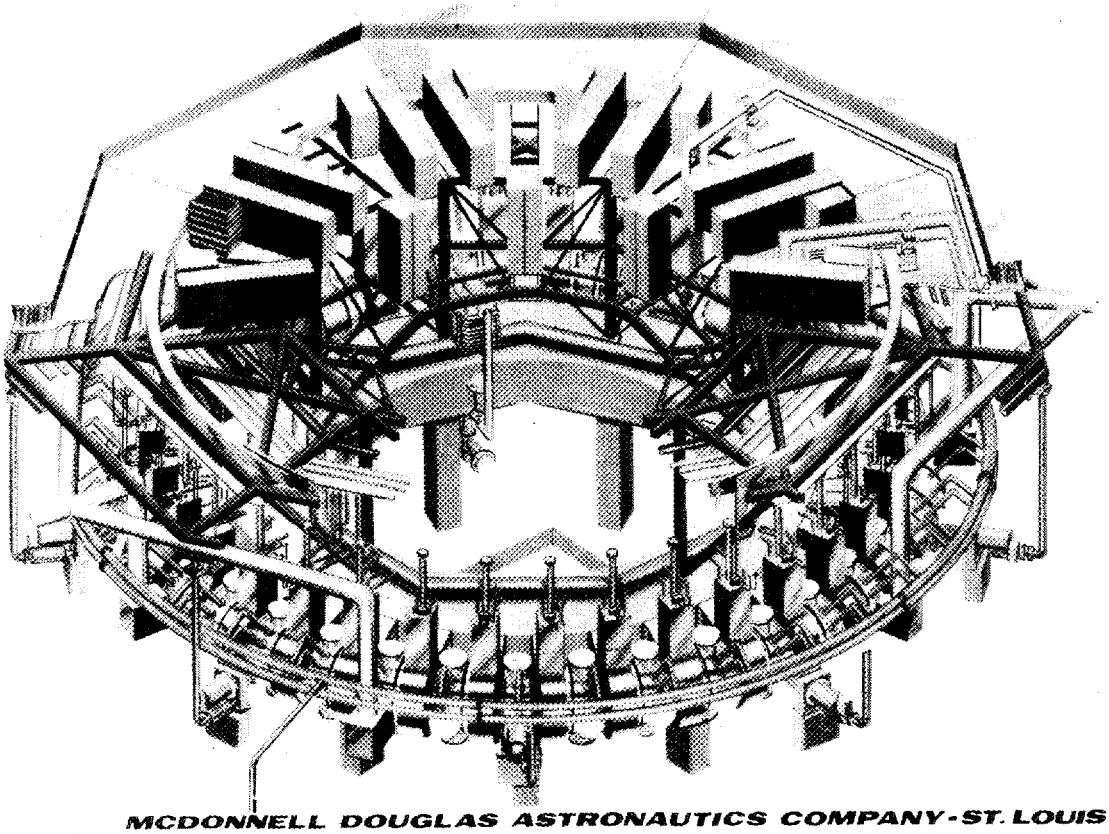

MCDONNELL DOUGLAS ASTRONAUTICS COMPANY-ST. LOUIS DIVISION
Saint Louis, Missouri 63166 (314) 232-0232

MCDONN

MARTIN MARIETTA ENERGY SYSTEMS LIBRARIES
3 4456 0156095 1

EBT–P010
Volume III
26 February 1982

Printed in the United States of America. Available from
National Technical Information Service
U.S. Department of Commerce
5285 Port Royal Road, Springfield, Virginia 22161
NTIS price codes—Printed Copy: A 05; Microfiche A01

PRELIMINARY DESIGN REPORT

MAGNET SYSTEM

VOLUME III

PREPARED BY: S. L. Ackerman
S. Ackerman, Project Manager
EBT-P Magnet System - General Dynamics

APPROVED BY: R. J. Dannenmuller
R. J. Dannenmuller, Manager
EBT-P Magnet System

APPROVED BY: Harry F. Imster
H. F. Imster, Manager
EBT-P Engineering - MDAC

APPROVED BY: Roy J. DeBellis
R. J. DeBellis, Manager
EBT-P Project - MDAC

APPROVED BY: H C McCurdy
H. C. McCurdy, Manager
EBT-P Technology Development - ORNL

APPROVED BY: A. L. Boch
A. L. Boch, Manager
EBT-P Project - ORNL

Reference Index

Volume I — Device Summary

Volume II — Toroidal Vessel

Volume III — Magnet System

Volume IV — Microwave System

Volume V — Vacuum Pumping System

Volume VI — Instrumentation and Control

Volume VII — Cryogenic Systems

Volume VIII — Device Utilities

Volume IX — Support Structure

TABLE OF CONTENTS

Section		Page
1	INTRODUCTION AND SUMMARY	
1.1	ORNL DEVELOPMENT PROGRAM	1-3
1.2	MAGNET DEVELOPMENT PROGRAM BENEFITS	1-6
1.3	TITLE I MAGNET DESIGN ACTIVITIES - CONTRIBUTIONS FROM MDAC/ORNL	1-7
1.4	TITLE I SYSTEM DESIGN ACTIVITIES	1-7
1.4.1	Power Supply and Distribution System	1-7
1.4.2	Quench Protection System	1-7
1.4.3	Instrumentation and Control	1-8
1.5	DESIGN DESCRIPTION	1-8
1.6	MASTER SCHEDULE	1-15
2	PURPOSE AND SCOPE	2-1
3	DESIGN CRITERIA	3-1
3.1	MAGNETICS REQUIREMENTS	3-1
3.2	SUPERCONDUCTOR	3-1
3.2.1	Specification Requirements	3-1
3.2.2	Test Requirements	3-1
3.2.3	Current Density	3-2
3.2.4	Stability	3-2
3.2.5	Protection	3-2
3.3	WINDING ASSEMBLY	3-2
3.3.1	General - Pack Configuration	3-2
3.3.2	Winding Concept and Tension	3-4
3.3.3	Insulation/Cooling Concept	3-4
3.3.4	Bobbin	3-4
3.3.5	Insulation Strength	3-4
3.4	MAGNET DEWAR	3-5
3.4.1	General	3-5
3.4.2	Interfaces	3-6
3.4.3	Dewar Vacuum	3-6
3.4.4	Thermal Performance	3-7
3.5	STRUCTURAL REQUIREMENTS	3-7
3.5.1	Structural Performance Requirements	3-8
3.5.2	Design Environments	3-10
3.6	POWER SUPPLY AND DISTRIBUTION SYSTEM	3-16
3.6.1	Power Supply Design Criteria	3-16
3.6.2	Distribution System Design Criteria	3-21
3.7	MAGNET PROTECTION SYSTEM DESIGN CRITERIA	3-22
3.7.1	Protection Philosophy	3-22
3.7.2	Protection Equipment	3-24
3.8	INSTRUMENTATION AND CONTROL	3-27
3.9	SAFETY & HAZARD DESIGN CRITERIA	3-28
3.10	X-RAY SHIELD	3-31
3.11	DEVELOPMENT PROGRAM	3-32

TABLE OF CONTENTS, Cont'd

Section			Page
4	DESIGN DESCRIPTION		4-1
	4.1	COLD MASS ASSEMBLY DETAILS	4-1
	4.2	DEWAR DETAILS	4-8
	4.3	X-RAY SHIELD	4-13
	4.4	MAGNET INSTRUMENTATION	4-14
	4.4.1	Measurement Program	4-14
	4.4.2	Temperature Measurements	4-14
	4.4.3	Strain Measurements	4-19
	4.4.4	Voltage Measurements — All Magnets	4-19
	4.4.5	Liquid Helium Level Measurement — All Magnets	4-19
	4.4.6	Helium Vessel Pressure — All Magnets	4-19
	4.4.7	Acoustic Emission Measurement — Development Magnet	4-19
	4.4.8	Sensor Descriptions	4-22
	4.4.9	Electrical Wiring	4-22
	4.4.10	Electrical Connectors	4-30
	4.5	ELECTRICAL DISTRIBUTION SYSTEM DESIGN DESCRIPTION	4-42
	4.5.1	Sizing Conductors and Joint Overlaps	4-42
	4.5.2	Field Error	4-43
	4.6	PROTECTION SYSTEM DESIGN DESCRIPTION	4-43
	4.6.1	Circuit Breaker	4-43
	4.6.2	Circuit Breaker Drivers	4-44
	4.6.3	Dump Resistors	4-44
	4.6.4	Bypass Diode Assembly	4-48
	4.6.5	Vapor-Cooled Lead Voltage Monitor	4-48
	4.6.6	Quench Detectors	4-49
	4.6.7	Helium Level Monitor	4-49
	4.6.8	Vacuum Switch/Pressure Switch	4-49
	4.6.9	Ground Referencing Resistors and Steering Diodes	4-49
	4.7	MATERIAL SELECTION	4-49
	4.7.1	Metallic Materials	4-50
	4.7.2	Non-Metallic Materials	4-51
5	SUPPORTING ANALYSIS		5-1
	5.1	MAGNETICS ANALYSIS	5-1
	5.2	STRESS ANALYSIS	5-13
	5.2.1	Helium Vessel Stress Analysis	5-13
	5.2.2	Winding Stress Analysis	5-20
	5.2.3	Cold Mass Supports Stress Analysis	5-22
	5.2.4	Vacuum Vessel Stress Analysis	5-27
	5.2.5	Miscellaneous Stress Analysis	5-31
	5.3	THERMODYNAMIC ANALYSIS	5-34
	5.3.1	Stability	5-34
	5.3.2	Heat Loads to Cryogens	5-43

TABLE OF CONTENTS, Cont'd

Section		Page
5.3.3	Quench Pressure Rise	5-49
5.3.4	Cooldown and Warmup Analysis	5-52
5.4	X-RAY ANALYSIS	5-65
6	PROGRAM PLANS AND SCHEDULES	6-1
6.1	MANUFACTURING PLAN	6-1
6.1.1	Tooling	6-1
6.1.2	Schedule	6-1
6.1.3	Manufacturing	6-1
6.2	QUALITY ASSURANCE	6-3
6.3	PRELIMINARY HAZARD ANALYSIS SUMMARY	6-5
6.4	ACCEPTANCE TEST PLAN	6-6
6.5	INSTALLATION AND ALIGNMENT PLAN	6-11
6.6	TITLE II SCHEDULE	6-12
6.7	MASTER PROGRAM SCHEDULE	6-14
7	REFERENCES	7-1

Appendix

A	DRAWING PACKAGES	A-1
B	SUPPORTING ANALYSES	B-1
B-1	Magnetic Analysis	B-1
B-2	Superconductor	B-14
B-3	Stress Analysis	B-25
B-4	Thermodynamic Analysis	B-136
B-5	Mirror Coil X-Ray Shield Optimization	B-177
C	MAGNETIC SYSTEM ALIGNMENT PLAN	C-1
D	MANUFACTURING PLAN	D-1
E	ACCEPTANCE TEST PLAN	E-1
F	LONG LEAD PROCUREMENT	F-1
G	PRELIMINARY HAZARD ANALYSIS REPORT	G-1
H	MAGNET DEVELOPMENT PROGRAM	H-1

LIST OF FIGURES

Figure		Page
1.5-1	Mirror Coil Design Summary	1-9
1.5-2	EBT-P Magnet Assembly	1-10
1.5-3	EBT-P Magnet Cross-Sectional Arrangement	1-11
1.5-4	Cold Mass Support Structure	1-12
1.5-5	Cold Mass Support	1-13
1.5-6	Mirror Coil/X-Ray Shield/Vacuum Liner	1-14
1.6-1	Elmo Bumpy Torus Master Schedule	1-16
3.3-1	Mirror Coil Parameters	3-3
3.5-1	Factors of Safety Used for Mirror Coil Assembly	3-9
3.5-2	Total X-Ray Doses (5 Years 60 GHz, 5 Years 90 GHz)	3-12
3.5-3	Minimum Magnet Design Loads (Par. 3.2.10)	3-13
3.5-4	Differential Pressure Loads	3-14
3.5-5	Loading Combinations Used in the Analysis of EBT-P	3-15
3.6-1	Magnet Power Supply Alarm/Relay Requirements	3-20
3.11-1	Short Sample Critical Current	3-38
4.1-1	Coil Pack Cross Section	4-2
4.1-2	NbTi Superconductor	4-3
4.1-3	Helium Supply Tube	4-4
4.1-4	Cold Mass Assembly Showing Bosses for Mounting Supports	4-5
4.1-5	LN_2 Cold Wall With LN_2 Tracer Tube	4-7
4.2-1	Dewar With Mounting Lugs Installed	4-9
4.2-2	Dewar With Closeout Plate Welded in Place	4-10
4.2-3	Magnet Mounting Tension Bolts	4-11
4.4-1	EBT-P Development Magnet Measurement Summary	4-15

LIST OF FIGURES, Cont'd.

Figure		Page
4.4-2	EBT-P Production Magnet Measurement Summary	4-16
4.4-3	CLTS Temperature Sensor Installation	4-17
4.4-4	Type E Thermocouple Installation	4-18
4.4-5	Bi-Axial Strain Gage	4-20
4.4-6	Single Axis Support Assy Strain Gages	4-21
4.4-7	Development Magnet Sensor Descriptions - Strain Gages and Temperature Sensors	4-23
4.4-8	Development Magnet Sensor Descriptions - Acoustic Emission Sensor	4-25
4.4-9	Development and Production Helium Pressure and Liquid Helium Level Sensor Descriptions	4-26
4.4-10	Production Magnet Temperature Sensor Descriptions	4-27
4.4-11	Production Magnet Strain Gage Description	4-29
4.4-12	Electrical Wire Summary	4-31
4.4-13	Electrical Connector Summary Part Description	4-33
4.6-1	Circuit Breaker Driver	4-45
4.6-2	Mirror Coil Dump Resistor	4-47
5.1-1	EBT-P Overhead Buswork Schematic (40^{0} Sector)	5-2
5.1-2	Field Point Locations	5-3
5.1-3	EBT-P Field Point Location	5-4
5.1-4	Field Due to Overhead Buswork	5-5
5.1-5	Entry/Exit Lead Path	5-7
5.1-6	Coil Pack Winding Model	5-8
5.1-7	Magnetic Field at Coil Axes Intersections	5-10
5.1-8	Magnetic Field Along Coil Axis	5-11
5.1-9	Quench Analysis Input Data	5-13
5.1-10	Temperature Vs. Time for EBT-P	5-14
5.1-11	Voltage Vs. Temperature for EBT-P	5-15
5.2-1	Finite Element Model Used for Analysis of Helium Vessel	5-17
5.2-2	Helium Vessel Model Loads	5-18

LIST OF FIGURES, Cont'd.

Figure		Page
5.2-3	Conductor Stresses Due to Winding, Cooldown, and Magnet Loads	5-19
5.2-4	Finite Element Model of Cold Mass Supports	5-23
5.2-5	Finite Element Model of Mirror Magnet Including Cold Mass Supports	5-24
5.2-6	Bolt Installation - Cold Mass Support to Cold Mass	5-28
5.2-7	Finite Element Model Used in Analysis of Vacuum Vessel Stack Discontinuities	5-30
5.3-1	EBT-P Unit Cell and Stability Parameters	5-35
5.3-2	Maximum Heated Channel Vertical Length	5-36
5.3-3	Energy Required to Create Minimum Propagating Zone as Function of Maximum Cooling Flux	5-38
5.3-4	Qualitative Illustration of Forces Acting to Produce Slip Against Bobbin During Charge-Up	5-40
5.3-5	Steady-State Liquid Helium Heat Loads per Coil	5-44
5.3-6	Conduction Path Lengths and Areas for Support Heat Leak Calculations	5-45
5.3-7	Schematic of Service Stack Showing Heat Paths from Room Temperature to Cryogens	5-46
5.3-8	Steady-State Liquid Nitrogen Heat Loads per Coil	5-48
5.3-9	Heating Rate to Helium in the Cryostat After a Quench	5-50
5.3-10	Current, Resistance and Time Constant Vs. Time During Worst Observed Quench of Development Coil #1	5-51
5.3-11	Schematic of Emergency Vent Line Showing Contributions to Pressure Drop During Quench Pressure Rise	5-53
5.3-12	Cryostat Pressure, Helium Mass and Exiting Mass Flow Rate After a Quench	5-54
5.3-13	Schematic of Model Used to Determine Cooldown/Warmup Times	5-56
5.3-14	Schematic of Detailed Warmup/Cooldown Model B Used to Compute 3-D Gradients	5-57
5.3-15	Proposal Flowrate and Supply Temperature Schedule During Cooldown and Warmup	5-58
5.3-16	Preliminary EBT-P Cooldown Response	5-59

LIST OF FIGURES, Cont'd.

Figure		Page
5.3-17	Preliminary EBT-P Warmup Response	5-60
5.3-18	Angular Temperature Gradient During Cooldown	5-62
5.3-19	Angular Temperature Gradients During Warmup	5-63
5.3-20	Design Flowrate and Supply Temperature Schedule During Cooldown and Warmup	5-64
6.4-1	Elmo Bumpy Torus Production Acceptance Test Facility	6-8
6.4-2	Production Acceptance Time Requirements	6-9
6.6-1	Elmo Bumpy Torus Title II Schedule Overview	6-13

LIST OF DRAWINGS

Dwg. No.	Title	Page
SK82881	Magnet Busbar Layout	A-3
SK90381-1	EBT Helium Level Monitor and CAMAC Cabinets	A-9
SK90381-2	EBT Power and Digital I/O Cabinet and Strain/Temp. Signal Conditioning Cabinet	A-11
SK90381-3	EBT System Status Display Cabinet and Protection Cabinet	A-13
SK90381-4	EBT Magnet Status Display Cabinet and Helium Pressure Monitor Cabinet	A-15
11-38001	Magnet Assy - EBT-P, Prototype	A-17
11-38002	Cold Mass Assembly - EBT-P Prototype	A-21
11-38003	Helium Supply Tube - EBT-P Prototype	A-23
11-38005	Cold Mass Outer Ring - EBT-P Prototype	A-25
11-38006	Winding Assembly - EBT-P Prototype	A-29
11-38009	Insulation - Slotted - EBT-P Prototype	A-35
11-38010	Insulation - Sidewall - EBT-P Prototype	A-37
11-38011	Housing - Conductor Lead - EBT-P Prototype	A-39
11-38012	Insulation - Layer End - EBT-P Prototype	A-41
11-38013	Bobbin Assembly - EBT-P Prototype	A-43
11-38016	Insulation - Ground - EBT-P Prototype	A-45
11-38020	Vapor Cooled Current Leads - EBT-P Prototype	A-47
11-38030	Stack Assembly - EBT-P Prototype	A-51
11-38031	Liquid Helium Tube - EBT-P Prototype	A-59
11-38032	LHe Level Sensor - EBT-P Prototype	A-61
11-38040	LN_2 Cold Wall Assembly - EBT-P Prototype	A-63
11-38060	Vacuum Vessel Assembly - EBT-P Prototype	A-69
11-38062	Outer Ring/Vacuum Vessel - EBT-P Prototype	A-71

LIST OF DRAWINGS (Cont'd.)

Dwg. No.	Title	Page
11-38063	Side Plate/Vacuum Vessel - EBT-P Prototype	A-73
11-38064	Stack Plate/Vacuum Vessel - EBT-P Prototype	A-75
11-38065	Strut Fitting/Vacuum Vessel - EBT-P Prototype	A-77
11-38066	Support Assembly/Vacuum Vessel - EBT-P Prototype	A-79
11-38067	Side Plate Assembly - EBT-P Prototype	A-83
11-38068	Stack Plate Assembly - EBT-P Prototype	A-85
11-38070	Outlet Assembly - EBT-P Prototype	A-87
11-38080	Cold Mass Support Strut - EBT-P Prototype	A-91
11-38084	Support Installation Cold Mass - EBT-P Prototype	A-93
11-38090	Out of Plane Struts - EBT-P Prototype	A-95
11-38091	Out of Plane Strut Pin - EBT-P Prototype	A-97
D11-38087	Instrumentation Vac and LHe Ves - EBT-P Development	A-99
D11-38088	Instrumentation Wiring Diagram - EBT-P Development	A-111
11-38570	Electrical Architecture - EBT	A-119
70B376000	EBT-P, Magnet Protection System Instl./Envelope	A-155
70B376001	EBT-P, Magnet Envelope/Interface	A-157
70B376002	EBT-P, Magnet Field Lines	A-163
70B376004	EBT-P, Magnet Bus Arrangement - Circuit Breaker/Stack	A-167
70B376005	EBT-P, Magnet Power Line Routing Envelope	A-171
70B376008	EBT-P, X-Ray Shield - Magnet	A-173
70B373008	EBT-P, Magnet Supply/Return Manifolds, Cryo	A-175
70B373009	EBT-P, Magnet Interface, Cryogenics	A-181
70B373010	EBT-P, Magnet Supply/Return Envelopes, Cryo	A-183
70B372009	EBT-P, Magnet Support Alignment Mount	A-189

LIST OF ABBREVIATIONS AND ACRONYMS

A	Ampere
ac	Alternating Current
ASME	American Society of Mechanical Engineers
BCD	Binary Coded Decimal
C	Celcius
CLTS	Cryogenic Linear Temperature Sensor
CMOS	Complimentary Metal Oxide Semiconductor
CRKT	Circuit
Cu	Copper
D-1	First Development Coil
D-2	Second Development Coil
dc	Direct Current
deg	Degree
DOE	Department of Energy
DPDT	Double Pole Double Throw
EBT-P	Elmo Bumpy Torus Proof of Principle
F.S.	Factor of Safety
GDC	General Dynamics Convair Division
GHz	Gigahertz
hr	Hour
Hz	Hertz
I	Electrical Current
I&C	Instrumentation and Control
in	Inch
K	Kelvin

LIST OF ABBREVIATIONS AND ACRONYMS (Cont'd.)

l	Liter
lb	Pound
LED	Light Emitting Diode
LHe	Liquid Helium
LN_2	Liquid Nitrogen
M	Meter
MC	Mirror Coil
MDAC	McDonnell Douglas Astronautics Company
MEV	Megaelectron Volt
MLI	Multilayer Insulation
M.S.	Margin of Safety
NbTi	Niobium Titanium
Nb_3Sn	Niobium-three Tin
NC	Numerical Control
O.D.	Outside Diameter
ORNL	Oak Ridge National Laboratory
PDC	Proposed Design Change
PHA	Preliminary Hazard Analysis
psi	Pounds Per Square Inch
QA	Quality Assurance
QPS	Quench Protection System
R	Major Radius
RAD	Unit of Radiation Dose
R.T.	Room Temperature
SCCS	Standard Cubic Centimeters Per Second
SCR	Silicon Controlled Rectifier
SMF	Stationary Magnetic Field
SPST	Single Pole Single Throw

LIST OF ABBREVIATIONS AND ACRONYMS (Cont'd.)

T	Tesla
TBD	To Be Determined
TTL	Transistor - Transistor Logic
V	Volt
W	Watts

PREFIXES:

c	centi (10^{-2})
G	giga (10^{9})
μ	micro (10^{-6})
m	milli (10^{-3})

SECTION 1

INTRODUCTION AND SUMMARY

During Title I, General Dynamics' principal role as a subcontractor to the McDonnell Douglas Astronautics Company (MDAC) is to assist in the further development of a low-cost superconducting magnet mirror coil system for the EBT-P program consistent with long life and dependable operation. The activity can best be defined as an extension of ORNL's previous development program with further joint ORNL/MDAC/GDC refining of the mirror coil components. MDAC/GDC participation for the entire program can be subdivided into four distinct elements as follows:

- Design, development, and fabrication of two dewar subassemblies to enclose the ORNL developed and fabricated cold mass assemblies.

- Design, development, and fabrication of a production prototype magnet system including conductor (procurement), cold mass components, dewar and x-ray shield. This prototype would form the basis for the production of 36 magnets for the torus and three spares.

- Design, development, and fabrication of an electrical/electronics system including quench protection, instrumentation and control, and power supply to power and protect the mirror coil system during its operation in the torus.

- Fabrication of the 39 production magnets.

Over this past year, Title I design was principally concerned with the detail design and generation of supporting analyses data and documentation for the mirror coil dewars for development and prototype programs. Drawings generated have been fully coordinated with ORNL to ensure interface compatibility and agreement during each step in the design and the fabrication process. Where required, stress, thermal, and electrical analysis and trade studies have been supplied and made part of this PDR report. Specific accomplishments include:

a. Full release of development dewars to house and support the ORNL cold mass assemblies.

   - The development dewars base differs from the prototype dewar base to accommodate the ORNL three (3) coil test facility design. The prototype dewar drawings included with this report reflect the dewar base as designed for the torus facility installation. Further, the development dewars contain instrumentation not included in the prototype or production dewars.

b. Design and development of cold mass supports which meet thermal and stress criteria and x-ray environment.

- The design of the cold mass support system is crucial to maintaining magnetic alignment even after a fault condition has occurred and the system has returned to normal mode operation. Several unique designs have evolved which offer options of lower heat loss (a polyimide insert), lower production costs (single piece support), and lower hysteresis effects, resulting from high tolerance components and assembly tooling. A single piece titanium support (see Figure 1.5-5) has been established for the prototype and production magnet system.

c. Helium stack design which meets refrigeration system, thermal, and quench pressure criteria.

- This design, the last to be released, required a considerable effort. Two designs were evolved since the developmental and prototype dewars required taller stacks for additional helium reserves than the production design. However, the torus facility was modified to accommodate a single (taller) stack design. A unique passive flow-limiting design reduced the complexity of the refrigeration system by simplifying the gas return lines.

d. Dewar design which meets passing particle fraction criteria.

- The dewar design was iterated to meet the revised passing particle fraction criteria established after the development dewars were designed and the side panels were fabricated. By careful redesign and modification of the assembly procedure, additional corner clearance was made available for the passing particles. Therefore, the development dewars differ from the prototype and the production dewars in this design respect.

Task 1 also included conceptual design of the instrumentation and control system. This task is a coordinated effort, principally between MDAC and GDC. The results of this work have previously been reviewed at the I&C Preliminary Design Review which occurred within the past few weeks. However, the quench protection, power supply, and distribution system conceptual designs are all presented as part of this Title I report. Considerable joint effort was expended in coordinating the helium and LN_2 refrigeration systems design as well as the magnet and electrical/instrumentation physical interface criteria.

Task 6 includes the detail fabrication of the two developmental dewars to support and house the ORNL cold mass assembly. Work on this task has been greatly expanded this past year to include additional cold mass and dewar component details of this assembly, and to provide for the modification and installation of the ORNL cold mass into the dewar assembly at GDC. The prototype magnet, where possible and when economically efficient, has been fabricated at the same time components were being produced for the two developmental dewars. In addition, where tooling was common and could be used for the production magnets, such items were fabricated to promote learning experience and lower cost for the production program. Conductor for the prototype is now being procured from two separate sources. The decision in the selection of conductor for the prototype will be made approximately 1 December 1981. To assist in the selection of the conductor for the production magnets, it is recommended that a second cold mass bobbin assembly be fabricated for the alternate conductor in addition to the prototype cold mass, and that this conductor be "open dewar" tested at ORNL. It should also be noted that a GDC representative, Tom Mann, has been "stationed" at ORNL to assist in the transfer of ORNL technology to GDC and the liaison required to coordinate design and document activities. An important technology transfer included witnessing the ORNL open dewar test program and the coil winding operations.

With respect to outstanding potential problems, we must note that the quench protection system demands a unique design to cope with the electron ring collapse-induced voltage phenomena. Alternate quench detection sensors are being explored as a solution to this problem.

1.1 ORNL DEVELOPMENT PROGRAM

The Magnet Development Program was started in mid 1979 with the following stated purposes:

- An experiment iteration of the magnet design is required in order to proceed with final design and manufacture with acceptable risk.
- The development program consists primarily of the design, fabrication, and testing of two instrumented EBT-P type magnets.
- The program is intended to support final design and manufacture by the industrial participant.
- Since the designer and manufacturer will not be selected for about a year, EBT-P would be delayed if development waited for them.

The major activity in the program during 1979 was the superconductor procurement activity.

The original conductor specification required a critical current of 2,800 A at 4.2K for three different grades of conductor. The three grades were for the specified critical current at fields of 8.0 T, 6.0 T, and 2.0 T. The copper was specified to be not less than 75% of the conductor volume in any of the three grades. The 2.0 T conductor grade was subsequently dropped due to a redesign of the EBT-P mirror coil.

It was not felt that the conductor requirements specified were overly restrictive or beyond the state of art. However, three of the four companies bidding on the development conductor took exception to either the amount of copper fraction or the definition of critical current.

Airco won the development conductor order with a bid based on a new processing technique (i.e., compacted monolith). This technique offered the attraction of higher current density while maintaining the desired Cu to superconductor ratio.

A compacted cable is made by putting a number of multifilament strands into either a seamless tube or within a copper strip on a continuous tube mill. The tubes are compacted and drawn down to final round size through conventional wire drawing dies. The twisting of the filaments is done at almost the final round size stage. Rectangular shaping is accomplished with a turkshead roll and a final sizing die. Airco successfully made a number of lengths of low field conductor (6T grade) using the tube mill. The high field conductor (8T) remained a persistent problem which was never fully solved. The high field lengths experienced center bursting. The problem arose from the heat treatment of the NbTi to maximize the intrinsic critical current density. This heat treatment tends to make the superconductor brittle which then results in conductor breakage during the drawing operation. Airco corrected the breakage problem by altering the heat treating and compensating for the decreased current density by adding more superconductor in place of copper.

The result was sufficient current carrying property, but insufficient copper. If the specification for copper fraction had been met on the conductor delivered, then the current carrying property would have been low. For the high field conductor, Airco tried both the seamless tube and the tube mill with 37 and 19 multifilamentary strands.

With this production problem and others, the first acceptable piece of 6T wire was completed and shipped in August 1980. The first 8T conductor was not received until November 8, 1980.

Critical current measurements were performed as soon after the receipt of the conductors as possible, but they were delayed by repairs to the ORNL magnet laboratory. As testing progressed, both grades of conductor exhibited sufficient current carrying capability. However, there were two aspects of the measurement that created concern. First the conductor was highly unstable to small motions. Conductor samples trained during short sample testing. The second concern developed when a resistive voltage was observed with very rapid sweeping of the transport current.

To explain the unexpected behavior of the conductor samples in the short sample tests, a series of tests were performed by ORNL to characterize the conductor's magnetic properties.

The basic question to be addressed was how an internal field will penetrate the conductor when applied perpendicular to its longitudinal axis. In the extreme cases, the external field may be excluded from the entire conductor or may penetrate the conductor without being excluded from large regions. In the first case, shielding currents and stored energy are high. If flux is redistributed in the conductor, the stored energy will be deposited as heat and the conductor may quench. In the second or ideal case, each filament behaves independently and stored energy is low. The size and separation of individual filaments is also a concern as shielding currents are set up in each filament and between filaments.

In summary, NbTi filament diameter should be less than about 200 μm at 4.2K. The ORNL magnetization tests indicated that the Airco compacted monolith (high and low field) exhibited strong coupling with an effective filament diameter of 400 μm. Its magnetization was very sensitive to the rate of field change. Additional testing on a classical monolith reconfirmed that uniform distribution of filaments, vs the strand design, results in a small effective filament diameter.

As a result of these experiments, the Airco compacted monolith conductor was determined not to be appropriate for the EBT-P application. The decision was made to revise the conductor requirements to force the production of a classical monolith with filaments distributed over the entire conductor cross section except for solid copper sections in the core and around the perimeter.

During mid 1980, two 304L stainless steel bobbins were fabricated by ORNL in preparation for winding the two development coils planned under the program.

After the award of the EBT-P contract to McDonnell Douglas in September 1980, there was a reassessment of the Magnet Development Program. This reassessment reviewed the tasks and work divisions in the MDP with the objective of utilizing all the resources at ORNL, MDAC, and GDC. After MDAC submitted the recommendations, ORNL determined that ORNL would proceed with the winding and open dewar testing of the two development cold masses. MDAC/GDC was to proceed at an accelerated pace to design and fabricate the dewars, cold mass supports, cold walls, etc., for the two ORNL development coils.

The installation of the coils into the dewars was to be performed by ORNL at that point. This was later changed to have GDC install the coils in the dewars at the San Diego facilities.

Winding of the first ORNL development coil (D-1) started in November 1980. The high field of the D-1 coil was wound with a 660-meter length of 37-strand high field compacted conductor successfully produced by Airco. The low field region was wound with 9-strand conductor. Winding of the coil was completed in mid March 1981. A significant amount of effort over this span was spent in data collection on the conductor winding pack, recording winding stresses and splice development. The splice development program selected a high lead solder (97.5 Pb 2.5 Ag) as the best material for the side-by-side conductor splice.

Testing of the D-1 coil started in mid April 1981. It successfully achieved a self-field of 7.4T.

In subsequent radiation simulation testing, the D-1 coil quenched at 68 watts at 5.0T and 13 watts at 7.4T. An important result of the D-1 coil testing was the establishment of a more severe quench pressure rise criteria for the development coils. It is based on the I^2R heating rate observed during the open dewar test.

1.2 MAGNET DEVELOPMENT PROGRAM BENEFITS

Significant benefits from the MDP thus far must focus on the successful performance of the D-1 coil at field. This test answered an outstanding issue raised by EBT-P external reviews and validated the basic technical approach to the mirror coils. Beyond this primary result, other benefits include:

- Correlation of practice and development winding data with STANSOL analytical calculations.

- Demonstration of the thermal margin in the coil based on the radiation simulation testing.

- Valuable manufacturing experience has been gained and transferred to MDAC and GDC through observation of the ORNL winding process.

- Development of quench pressure rise criteria for the development coils.

- Accelerated design and fabrication experience gained at MDAC/GDC on the development dewars, cold mass supports, LN_2 cold wall, and stack.

- Development experience and testing performed on various splice concepts and solder materials.

1.3 TITLE I MAGNET DESIGN ACTIVITIES

ORNL design activities predated the award of the MDAC/GDC contract by approximately two years. During this period, the mirror coil design concept was evolved and the superconductor coil winding and insulation configuration was established. These activities and the GDC proposal formed the basis of the current contract. Joint tradeoff studies accomplished by the three organizations (MDAC/ORNL/GDC) were particularly important in the design of the helium and LN_2 refrigeration systems, instrumentation and control, x-ray shielding,magnetic alignment, and quench protection-power supply systems. All three organizations have cooperated in establishing design criteria, reviewing test data, and in-depth review of the detail design. This process has been an iterative process, and we can take satisfaction in the conscientious reviews which accompanied each element of the design.

1.4 TITLE I SYSTEM DESIGN ACTIVITIES

1.4.1 POWER SUPPLY AND DISTRIBUTION SYSTEM. Title I design has entailed expansion and verification of concepts laid down in the EBT proposal. Performance, reliability, and cost were the driving criterion in all analyses.

The series bus architecture has been analyzed, via computer analysis, for steady-state operation as well as transient effects during startup and shutdown. The bus structure layout has been coordinated with MDAC for both mechanical compatibility as well as electrical considerations. The magnet power supply which drives the bus has been sufficiently specified for initial RFPs to be sent.

1.4.2 QUENCH PROTECTION SYSTEM. A baseline design has been established which detects a superconductor normal zone producing a voltage drop of 50mv or more and automatically initiates action within one second to protect the magnet. Potential problems identified during Title I which could affect the baseline design

were (1) the creation of a large induced voltage created by a plasma E ring collapse, and (2) non-balanced voltage inputs from eddy currents in the magnet vessel shells. These potential problems will be investigated in detail during Title II design, and circuit designs will be created to resolve any problems.

1.4.3 INSTRUMENTATION AND CONTROL. This system has been coordinated with MDAC for compatibility and is relatively well defined. The details of the system were given at the Instrumentation and Control PDR presented at MDAC.

1.5 DESIGN DESCRIPTION

The magnetic system consists of 36 superconducting mirror coils, the power and distribution system, the x-ray shielding, and the protection system. Figure 1.5-1 is a design summary of the superconducting mirror coils.

The overall assembled EBT-P magnet is shown in Figure 1.5-2 and its general cross-sectional arrangement is shown in Figure 1.5-3. The magnet assembly, as shown in Figure 1.5-3 consists of:

a. The superconducting winding pack

b. 316L stainless steel coil case

c. Titanium alloy cold mass support structure

d. Liquid nitrogen cooled copper shield

e. Super insulation

f. 304L stainless steel vacuum vessel

The design of the titanium alloy cold mass support structure is shown in Figure 1.5-4. It consists of three tangential trusses which support the helium vessel. A detail of the helium vessel support truss is shown in Figure 1.5-5.

Figure 1.5-6 shows how the magnet is installed in the EBT-P device. The two piece x-ray shield is bolted securely to the magnet external case. The torroidal vessel vaccuum liner is not attached to the magnet and thus allows independent alignment of the magnet and vessel. A more detailed discussion of the installation of the device is presented in volume I of the Title I report.

The structural design criteria is consistent with the ASME Pressure Vessel code (as applicable).

SYSTEM ELEMENT	DESIGN CHARACTERISTICS
o COIL MASS ASSEMBLY	o MONOLITHIC NbTi SUPERCONDUCTOR o HELIUM VENTILATED COIL PACK o LAYER WOUND WITH PANCAKE ENTRY o ALL WELDED AND MACHINED 316L HELIUM VESSEL
o LN_2 SHIELD	o COPPER SHEET WITH TRACE COOLING TUBES o MLI ON BOTH SIDES o LOW LOSS SUPPORTS
o VACUUM DEWAR	o 304L ALL WELDED ASSEMBLY o TITANIUM TRUSS SUPPORTS o DEWAR ALIGNMENT IS EXTERNAL
o SUPPORT STRUCTURE	o MIRROR COIL DEWAR/SUPPORT STRUCTURE IS ADJUSTABLE AFTER INSTALLATION TO PERMIT MAGNET FIELD ALIGNMENT

FIGURE 1.5-1 MIRROR COIL DESIGN SUMMARY

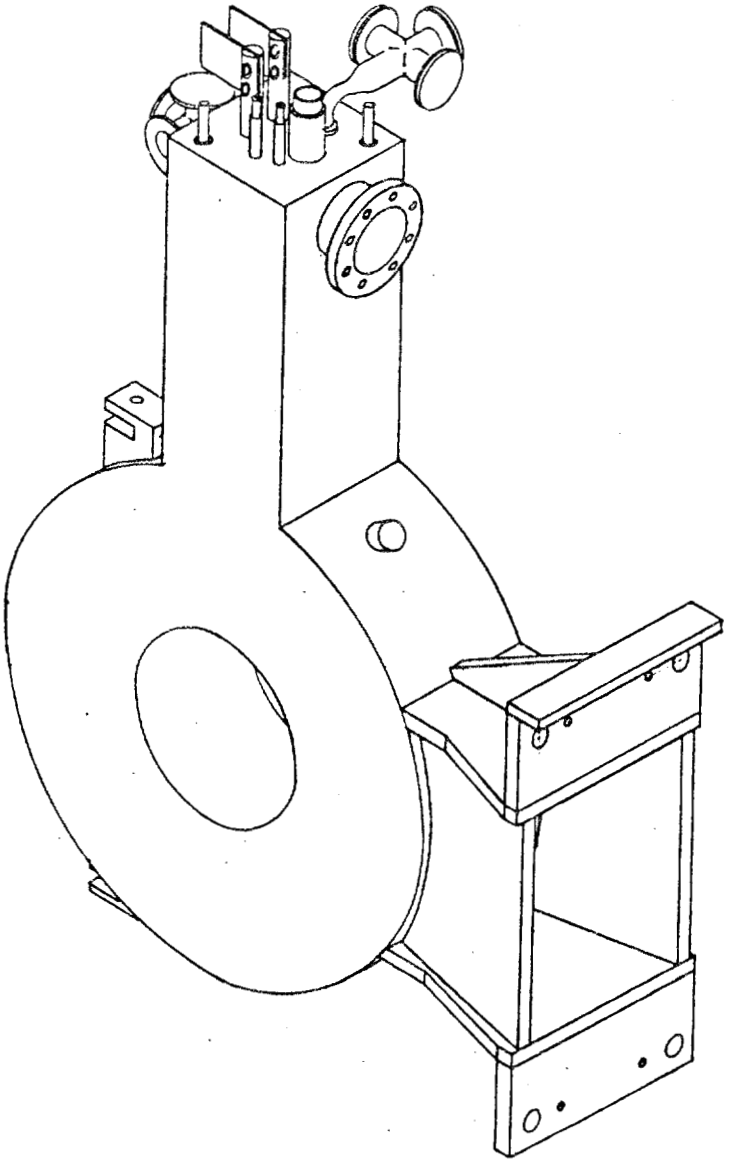

FIGURE 1.5-2 EBT-P MAGNET ASSEMBLY

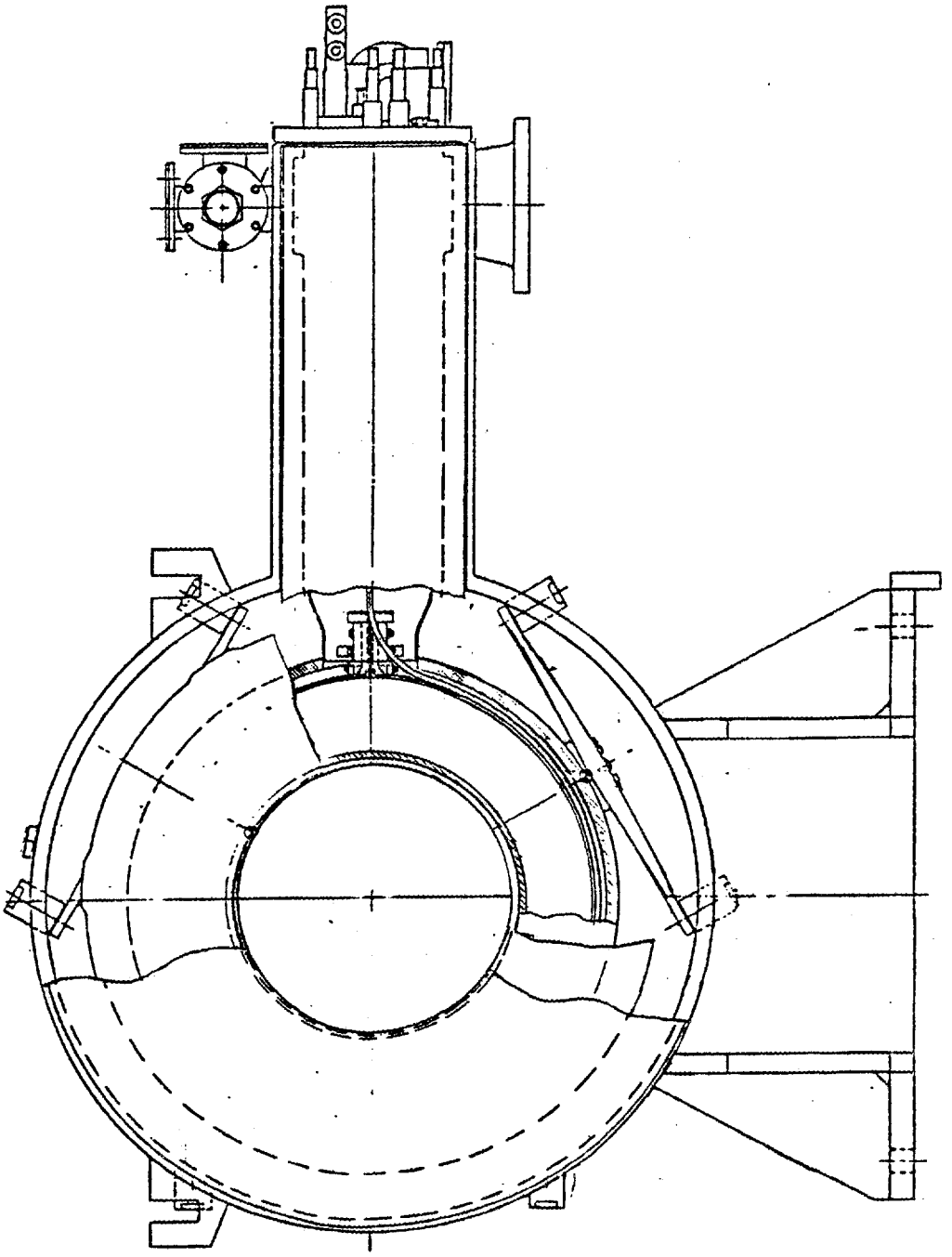

FIGURE 1.5-3 EBT-P MAGNET CROSS-SECTIONAL ARRANGEMENT

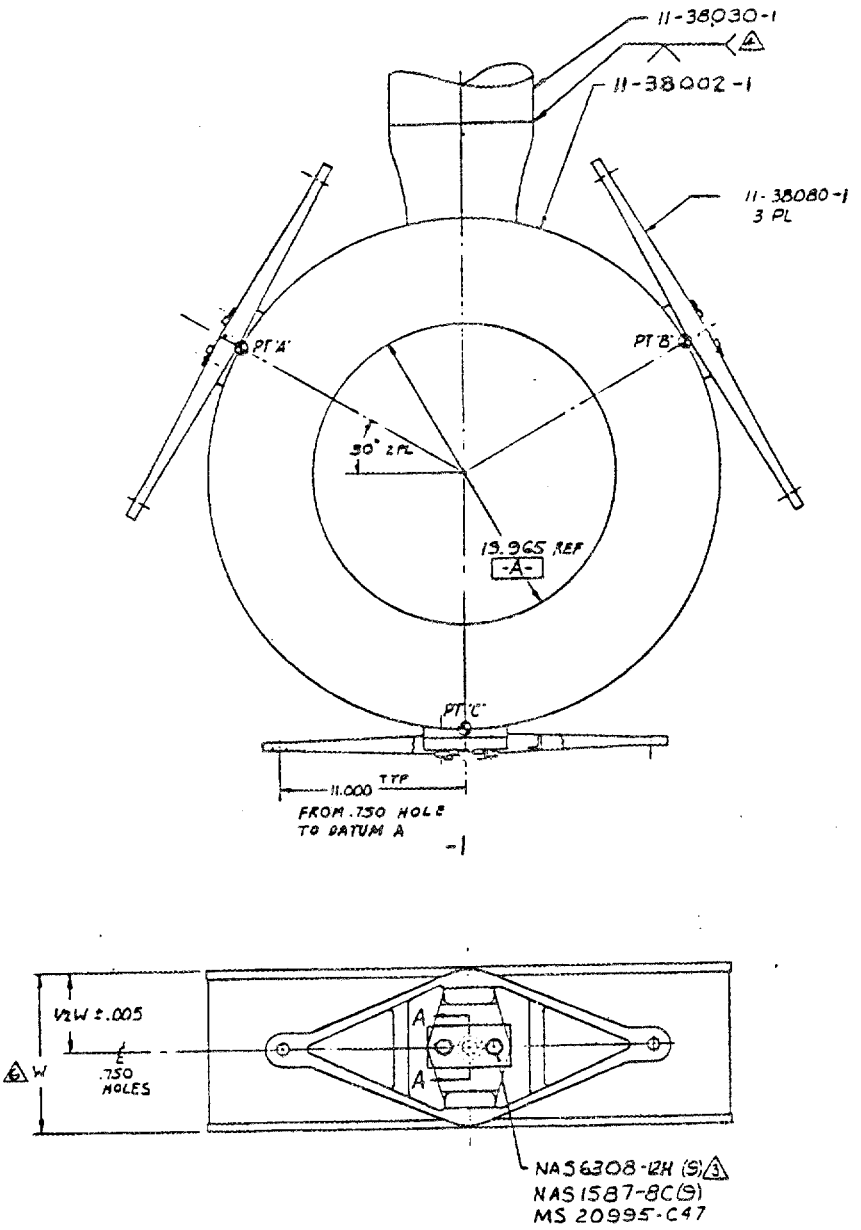

FIGURE 1.5-4 COLD MASS SUPPORT STRUCTURE

COLD MASS SUPPORTS MEET STRESS, THERMAL
AND RADIATION REQUIREMENTS

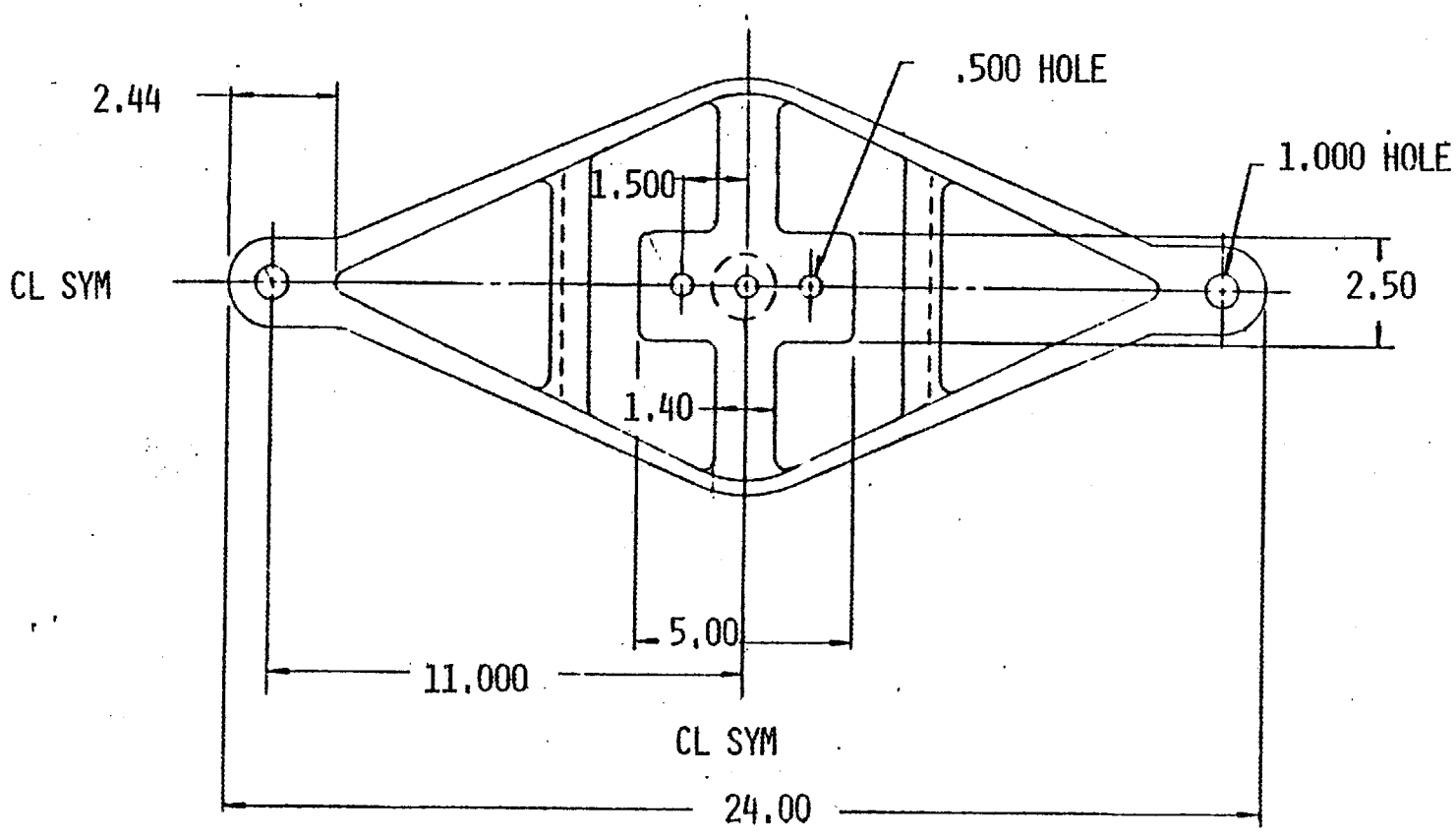

FIGURE 1.5-5

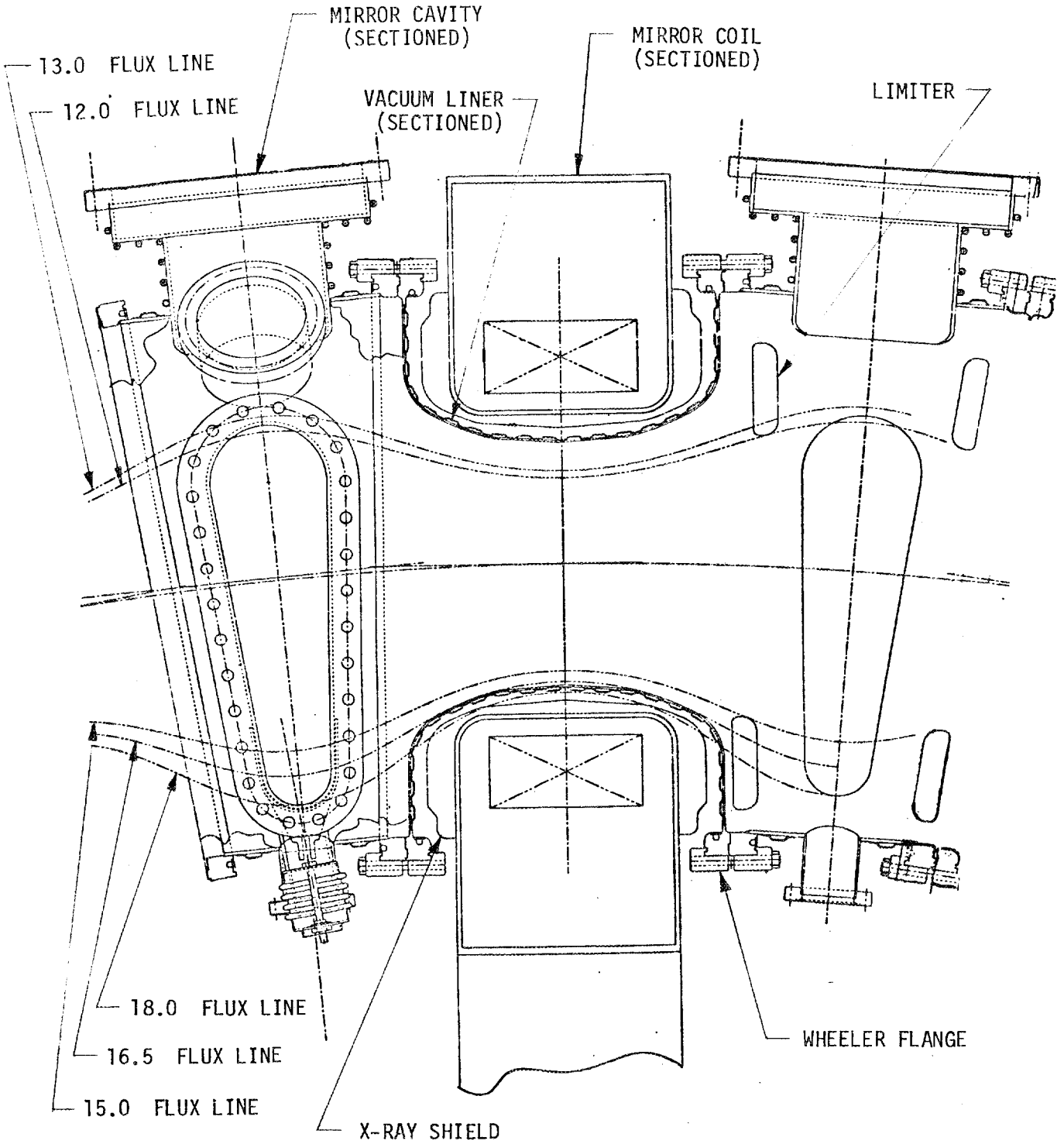

MIRROR COIL/X-RAY SHIELD/VACUUM LINER
INSTALLATION IN EBT-P

FIGURE 1.5-6

1.6 MASTER SCHEDULE

The master schedule for the development program has been altered substantially over that schedule which was generated at the start of the contract on October 1980. These schedule changes have resulted from a desire to increase GDC's role in the fabrication of dewar assemblies for the two ORNL cold mass assemblies; from the unfortunate slip in conductor availability for the development and prototype cold mass assemblies; from the resolution of difficult design problems, especially in the helium stack assembly area and cold mass supports; and finally, from the strike which occurred at the ORNL facility. However, it still appears possible to meet the production program, provided that no new difficulties are encountered with respect to conductor design and additional outstanding technical problems are resolved. To maintain the current production schedule will also require advance procurement of the superconductor and other critical materials well in advance of the start of detailed fabrication for the production magnets. The current Master Schedule is shown in Figure 1.6-1.

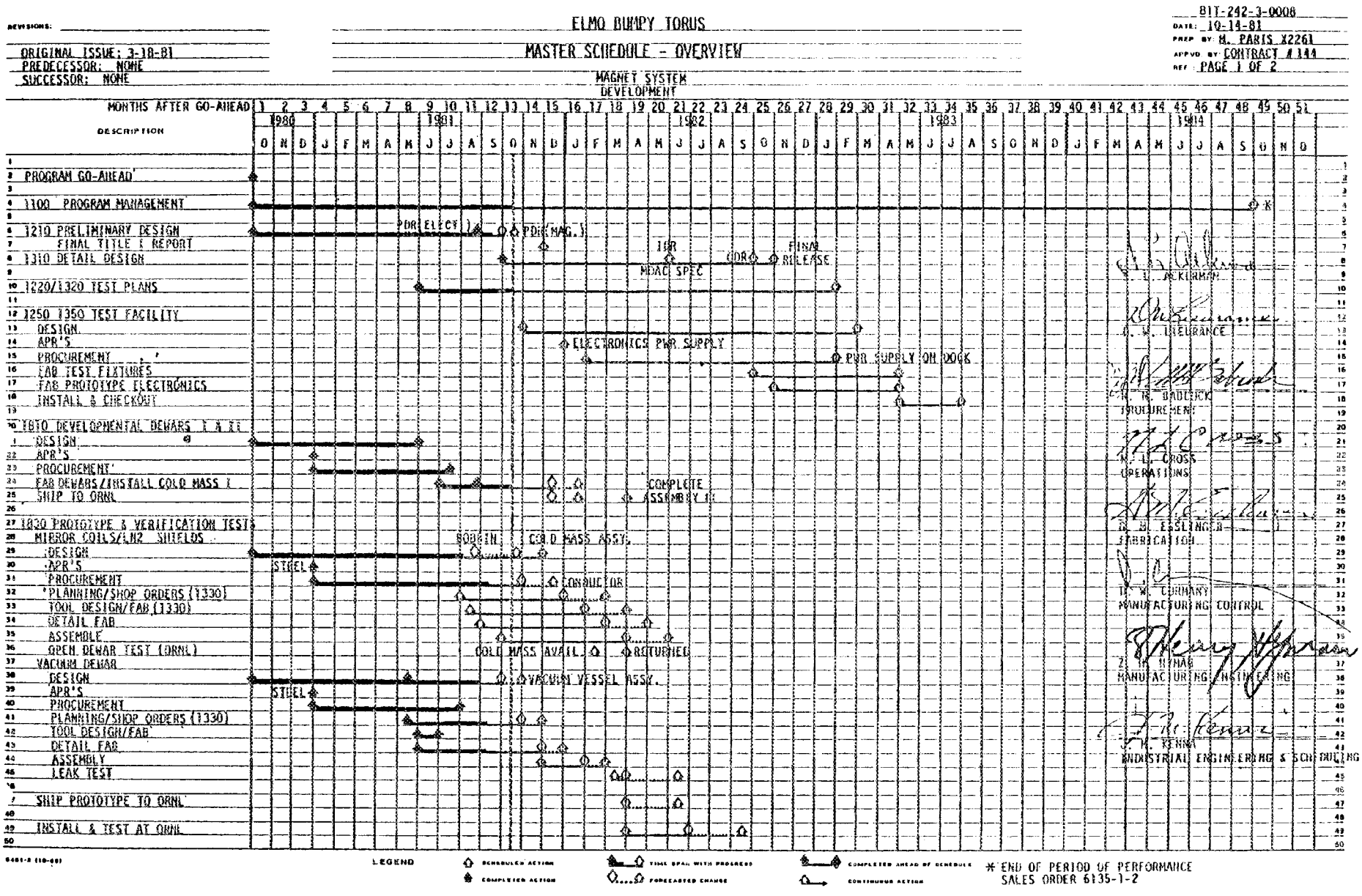

Figure 1.6-1. Elmo Bumpy Torus Master Schedule

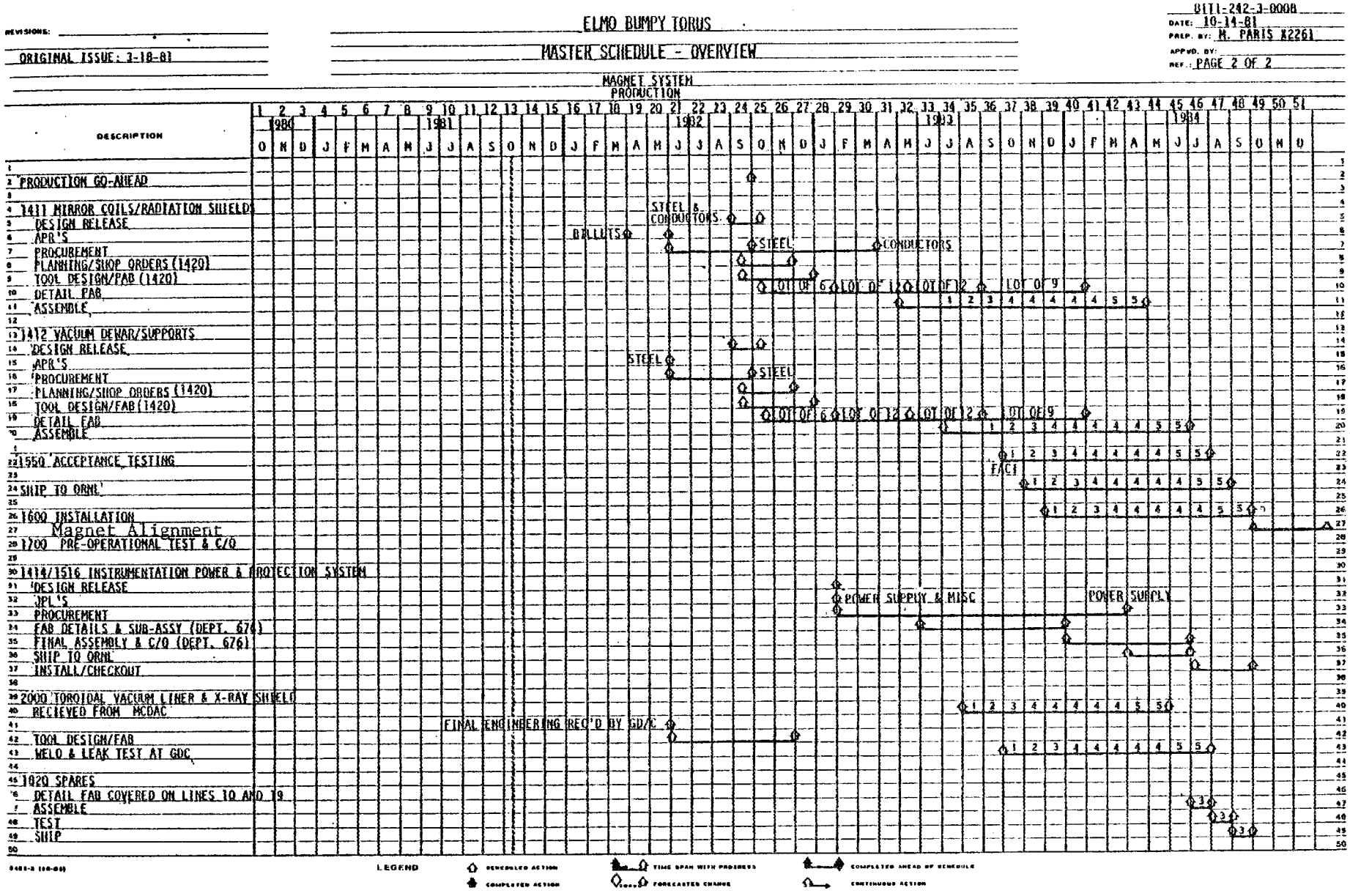

Figure 1.6-1. Elmo Bumpy Torus Master Schedule (continued)

SECTION 2

PURPOSE AND SCOPE

The purpose of the Title I engineering effort has been to extend the early and on-going ORNL development for the magnet coils into the design of components for the mirror coil system. This was verified by the submission of each drawing and accompanying analyses, when required, to both MDAC and ORNL. Changes resulting from these reviews have been incorporated into the final designs which have been approved by both MDAC and ORNL. Test results on the ORNL development coils resulted in the rejection of the first proposed superconductor configuration and a more conventional superconductor design has now evolved. This new superconductor is currently under procurement both by ORNL (AIRCO) and GDC (AIRCO and IGC). Early identification and definition of interfaces has established commonality between development and prototype hardware. This is principally required for both refrigeration systems (helium and LN_2), mechanical marriage of the mirror coil assembly to the torus, instrumentation and control, x-ray shields, and the power supply and quench protection system. Trade studies were numerous and especially important in the design of the helium stack and support systems. The main purpose of this indepth analysis was to minimize both the heat leak and the complexities of the helium refrigeration system. The final design of the cold mass to vacuum dewar supports was a long iterative process and was required to meet the stress criteria during all thermal and fault conditions while reducing the heat loss to the maximum extent possible. A redesign of the dewar assembly resulted in improving the passing particle fraction.

Several elements of the design are still not resolved. Quench protection is complicated by unique induced voltage noises by physics shutdown problems and will be described in detail under Section 3.7. The magnetic axis alignment approach is still undergoing changes in order to provide the simplest and lowest cost system consistent with adjustment and accuracy criteria.

Throughout the GDC design program, industrial and manufacturing engineering personnel have been involved with the intent of reducing development and manufacturing costs by proper tolerance control, welding, fabrication, and tooling techniques. This process has resulted in a good producibility plan which will be discussed under Paragraph 6.2. Proven techniques, welding, and machining, as well as other component fabrication, will all be demonstrated in the prototype design. It is further intended that components supplied by the subcontractors will also be tested in the prototype under simulated operation conditions.

SECTION 3

DESIGN CRITERIA

3.1 MAGNETICS REQUIREMENTS

The magnetic field required for the EBT-P experiment will be provided by 36 superconducting coils. The coils will be located in a toroidal array with a major radius of 4.5 meters. Each coil will have a mean radius of 29cm. The winding will be nominally rectangular, 21.1cm wide and 10cm thick. Each of the coils will be cooled to 4.2K by a liquid helium pool boiling bath.

60 GHz Operation

The coils will initially provide a maximum field, on axis, at the coil throat of 3.3 Tesla and a mirror ratio of 2.2 at a design bulk heating frequency of 60 GHz.

90 GHz Operation

The coils will also be capable of continuous operation at the field levels compatible with 90 GHz bulk heating frequency, with a maximum field of at least 7.4 Tesla at the surface of the conductor and 4.8 Tesla on axis at the coil throat (when operating in the 36-magnet toroidal array).

Field Error

ΔB is defined as the deviation of the field from that produced by ideal solenoidal windings. The cumulative error field, with all coils energized, will not exceed 1×10^{-4} averaged around the torus along the minor axis in the radial direction. The sources of error field include non-solenoidal (i.e., helical and spiral) windings, bus work, current leads, ferromagnetic materials, and alignment error. The analyses dealing with the error field are presented in Section 5.1.

3.2 SUPERCONDUCTOR

3.2.1 SPECIFICATION REQUIREMENTS. The superconducting cable to be used for the coil windings will be an 0.29cm X 0.5cm NbTi/Cu rectangular monolith with twisted superconducting filaments. These filaments will be less than or equal to 66 microns in diameter. The conductor will have a twist pitch of 2-3 inches and a copper-to-superconductor ratio of 2.8 minimum.

3.2.2 TEST REQUIREMENTS. The short sample critical current at 7.5T and 4.2K shall be greater than 2800 amps. The final

conductor zero field composite resistivity ratio shall be a minimum of 120.

3.2.3 CURRENT DENSITY. The operating current in the conductor will be no greater than 1800 amps direct current under maximum field conditions. The windings are designed to operate at a field of 7.4 Tesla and a nominal current density of 10,000 amps/cm^2.

3.2.4 STABILITY. Due to the coil design, overall motion of the insulated conductor when energized will not be sufficient to result in a coil quench. The conductor will be capable of achieving 7.4 Tesla on the first exposure to the design current. Stresses experienced during winding and fabrication will not degrade conductor performance below the specification requirements.

3.2.5 SUPERCONDUCTOR MINIMUM LENGTH CRITERIA. The minimum conductor length for the high field region of an EBT-P coil shall be long enough to wind the first five layers and the 34 layers of the pancake. This requires approximately 1200 feet of conductor. The minimum length of conductor to be used in the low field region shall be long enough to wind four layers of the coil. This allows the splices to be placed on the outside of the coil for maximum cooling and keeps them from being in adjacent layers. This requires approximately 1000 feet, which is the minimum deliverable length.

3.3 WINDING ASSEMBLY

3.3.1 GENERAL — PACK CONFIGURATION. As developed during Phase I and Phase II, the design variables for EBT-P mirror coil winding assembly or pack are closely related to the required physics parameters for the device. The input parameters of plasma radius, number of sectors, coil width, annulus field, coil winding to flux line distances, passing particle fraction, and coil length-to-width ratio determine the mirror requirements. These output variables are mean coil radius, mirror ratio, torus major radius, midplane field on axis, throat field on axis, peak field on coil, and coil current density. The specific physics requirements require the corresponding mirror coil parameters tabulated in Figure 3.3-1.

The conductor pack will have only one grade of conductor designed for the high field requirements. This criteria was changed during Title I design from a two-grade concept. It was determined that the cost savings of two conductor grades were offset by the additional complications associated with a multigrade procurement. This was especially true after the decision was made to have more than one source of supply for superconductor. An added benefit of this criteria change is that the gross stability of the conductor pack is increased with a high field conductor in the lower field regions. On a qualitative basis, a more reliable coil results.

PARAMETER	QUANTITY (60 GHz)	QUANTITY (90 GHz)
INSIDE COIL RADIUS	24.0	24.0
OUTSIDE COIL RADIUS	34.0	34.0
MEAN COIL RADIUS	29.0 cm	29.0 cm
MIRROR RATIO	2.2:1	2.2:1
TORUS MAJOR RADIUS	4.5 m	4.5 m
MIDPLANE FIELD ON AXIS	1.5 T	2.2 T
THROAT FIELD ON AXIS	3.3 T	4.8 T
PEAK FIELD ON COIL	5.1 T	7.4 T
COIL CURRENT DENSITY	6667 A/cm^2	10,000 A/cm^2
CONDUCTOR PACK LENGTH	21.1 cm	21.1 cm
OPERATING CURRENT	1133 A	1700 A
AMPERE TURNS	1.4×10^6	2.1×10^6

FIGURE 3.3-1. MIRROR COIL PARAMETERS

3.3.2 WINDING CONCEPT AND TENSION. The winding concept is to be layer wound with a half-pancake (pie) on one side. This pie approach is specified to minimize the lead effects on the magnet's stray fields. The coil electrical leads are brought out close together over the center of the conductor pack. This concept also maximizes the amount of active conductor in the available winding pack area.

The winding pack/bobbin design is to be based on a winding tension that minimizes conductor pack movements (i.e., lift-off and axial shifting) during operation.

After a conductor pack has been designed as physically stable as possible for operating conditions, credible events will be developed based on the charging scenario and fault conditions. These events/displacements, with their associated forces, will then be utilized as design criteria for the conductor stability and magnetic field accuracy analysis.

3.3.3 INSULATION/COOLING CONCEPT. The conductor pack is an unimpregnated, liquid helium-cooled, pool-boiling configuration. Turn-to-turn and layer-to-layer insulation will consist of a 50% coverage of spiral-wrapped nomex tape. This tape is 6.5 mils thick and .12 inch wide. The ground insulation concept is to be based on a combination of polyimide and G-10CR. The polyimide is to provide coverage at the corners in the bobbin and at joints in the G-10CR. The G-10CR is to be designed so that there is a helium plennum along the sidewalls of the conductor pack. This same G-10CR configuration is to provide a separate helium plennum against the coil bobbin.

Both the ventilated conductor pack and the helium plennum against the bobbin were selected as criteria for the pack, after an evaluation of the non-uniformly distributed 10-watt thermal load which results from the x-ray environment imposed on the mirror coils.

3.3.4 BOBBIN. The coil bobbin is to be designed of stainless steel exhibiting the lowest magnetic permeability in weld areas at liquid helium temperatures. Experience on other programs has led GDC to establish magnetic permeability as an acceptance criteria on the stainless steel plate material. The maximum allowable permeability of the bobbin welds shall not exceed TBD. Base material shall not exceed TBD. Beyond material selection to minimize magnetic permeability, the bobbin shall be designed to give the largest clear bore with an acceptable winding tension.

The bobbin must provide a stable, accurate support structure for the conductor pack under normal operating centering and fault out-of-plane loading conditions specified in Paragraph 3.5.

3.3.5 INSULATION STRENGTH. The factor of safety for insulation gaps within the coil pack shall be determined as follows:

$$F.S. = \frac{\text{Gap Breakdown Voltage in Ambient Helium}}{\text{Maximum Predicted Voltage}}$$

For dielectric materials other than helium, the factor of safety shall be determined similarly as follows:

$$F.S. = \frac{\text{Material Breakdown Voltage}}{\text{Maximum Predicted Voltage}}$$

In call cases, the factor of safety shall be 2.0 minimum.

The minimum gap for conductors seeing the full 400-volt discharge shall be 6mm. (Breakdown voltage for 6mm is greater than 800 volts.)

The insulation test voltage in air from conductor to ground shall be determined as follows:

400 (Design Voltage) X 1.5 (Factor of Safety)
X 4.67 (Ratio of Breakdown in Air to Helium)
= 2800 volts

3.3.6 PROTECTION. Specialized circuitry will be provided to electrically isolate each coil in the event of a quench and allow it to discharge into a resistive element in order to protect the conductor.

Maximum discharge voltage at any point in the magnet system will be compatible with the magnet insulation scheme. Maximum temperature increase at any point within the coil during a quench will be less than 100K. The supporting quench analysis is presented in Section 5.1.

3.4 MAGNET DEWAR

3.4.1 GENERAL. The mirror coil dewar and support structure shall be designed to minimize heat leak into the liquid helium environment, minimize thermal radiation from the dewar wall to helium cooled mirror coil, and withstand gravity and magnetic loads during normal operation and fault conditions. It will be designed for seismic loads during normal operation but not fault conditions. Coil supports shall be designed to prevent the need for coil realignment after a coil quench.

Sufficient coil position adjustments shall be provided to align the coil axis and the axis of the device. If required, readjustment capability will be provided when the coil is at 4.2^{o}K. This adjustment can be provided by moving the coil in the dewar or moving the dewar and coil combination. Future installation of ARE coils shall not require internal modification of the vacuum dewar.

3.4.2 INTERFACES

Structural/Vacuum. The mirror coil dewars shall comply with the interface dimensions shown on MDAC drawing 70B376001.

Cryogenic. The mirror coil dewars shall comply with the physical interfaces imposed by MDAC drawing 70B373009.

3.4.3 DEWAR VACUUM

Base Pressure. The vacuum dewar shall be designed for a base pressure of 10^{-5} torr.

Dewar Pumpdown. The time required to pump down the dewar shall be minimized by selecting materials and surface finishes that minimize outgassing.

Helium Vessel Leakage. The total helium vessel leakage into the dewar at operating temperature shall not exceed 1×10^{-9} SCCS of helium gas.

Outgassing and Bake-out. The dewar shall be designed to facilitate bake-out at 100°C in the event that loss of system vacuum is experienced or required for maintenance.

3.4.4 THERMAL PERFORMANCE

LHe Demand. The following represents the nominal calculated helium allocations to various subassemblies in the vacuum dewar. Acceptance rejection criteria will be established following development testing and incorporated during the Title II design.

Subassembly	Refrigeration	Liquefication
Cold Mass Supports	4.25 watts	
MLI Insulation	.23 watts	
Stack Losses	4.53 watts	
X-ray Heating	10 watts	
Controls & Instrumentation	(Included in Stack)	
Conductor Losses	.03 watts	
Vapor-Cooled Leads		4.9 l/hr
	19.0 watts	4.9 l/hr

LN_2 Demand. The following represents the maximum nitrogen allocation to various subassemblies in the vacuum dewars.

Subassembly	Heat Load
Cold Mass Supports	39.0 watts
Cold Wall Radiation (Thermal)	14.0 watts
Stack Losses	13.4 watts
	66.4 watts

3.5 STRUCTURAL REQUIREMENTS

The structural requirements for the mirror coil are extracted from the preliminary procurement specification, Reference 3.5-1. Reference 3.5-2 was searched to ensure completeness of the requirements. Reference 3.5-1 calls out References 3.5-4 thru 3.5-6 which contain further structural requirements. The most significant of these additional references is 3.5-4 which is the ASME Boiler and Pressure Vessel code.

The structural analysis of the EBT-P is based on the requirements of the ASME Pressure Vessel code. Section VIII, Divisions 1 and 2 are used on the pressure vessel components and Section III, Division 1, Appendix XVII on the component supports. The code provides values for room temperature properties, factors of safety, methods of analysis, and acceptable design configurations. In areas of the pressure vessel which the code does not address, such as the inner bore, the code has been used as a guide for

configuration development, and detailed analysis has been used to confirm adequate margins.

The overall structural requirements are subdivided into Performance Requirements and Design Environments which are tabulated in the following two sections.

3.5.1 STRUCTURAL PERFORMANCE REQUIREMENTS. The governing structural performance requirement is (paraphrased):

> No inelastic deformation which could destroy the alignment or cause coil quench shall occur during any of the anticipated normal or fault environments.

This requirement is satisfied through detailed analysis and use of factors of safety for computing margins of safety. The material properties used are specification guaranteed minimums, and minimum margins are all associated with a 1.5 factor of safety on yield except for the titanium cold mass supports which are critical at ultimate with a factor of safety of 2.0.

Factors of Safety

Factors of safety referred to in this criteria are regarded as design factors of safety. A design factor of safety is intended to raise the design load to a value which is compatible with the design strength property (i.e., yield or ultimate) of the material.

Figure 3.5-1 shows the factors of safety we used for the mirror coil assembly analysis.

The following extracts from Reference 3.5-1 provide a more detailed list of the structural performance requirements imposed on the EBT-P mirror magnets.

a. Overall motion of the insulated conductor when energized shall not be sufficient to result in a coil quench (para. 3.2.2).

b. Stresses experienced during winding and fabrication shall not degrade conductor performance below specification requirements (para. 3.2.4).

c. The conductor-to-conductor joining techniques shall be selected to minimize electrical resistance while maintaining 95% of the mechanical yield strength of the parent conductors (para. 3.2.4.2).

d. The bobbin shall be capable of resisting the stresses incurred during both normal operation and fault conditions (para. 3.2.9).

FIGURE 3.5-1 FACTORS OF SAFETY USED FOR MIRROR COIL ASSEMBLY

CONDITION	BEHAVIOR	FACTOR OF SAFETY	PARAGRAPH NOS. REF. 3.5-1
OPERATIONAL LOADS	ULTIMATE STRENGTH	3.0*	
	YIELD STRENGTH	1.5	3.9.1
	BUCKLING STRENGTH	4.0	3.9.1
	FATIGUE STRENGTH	10 BASED ON CYCLES	3.9.1
HANDLING AND TRANSPORTATION	ULTIMATE STRENGTH	3.0	
	YIELD STRENGTH	2.0	3.9.1
	BUCKLING STRENGTH	4.0	3.9.1
	FATIGUE STRENGTH	10 BASED ON CYCLES	3.9.1

*SEE 5.2.3 FOR EXCEPTION

e. The mirror coil dewar and support structure shall be designed to...withstand gravity and magnet loads during normal operation and under fault conditions. Coil supports shall be designed to prevent the need for coil alignment after a coil quench (para. 3.3).

f. Deleted.

g. All materials, parts, and processes shall be defined and controlled by engineering drawings, specifications, and/or standards (para. 3.9.4).

h. Particular attention shall be paid to operational temperatures, fracture toughness, impact, creep, stress rupture, thermal stability, thermal fatigue, stress corrosion, embrittlement, and magnetic properties (para. 3.9.4.1).

3.5.2 DESIGN ENVIRONMENTS. This section presents the loads, accelerations, temperatures, and other environments which the EBT-P structure must withstand. These environments are extracted from Reference 3.5-1 with cross checks to References 3.5-2 and 3.5-3.

The forces due to magnet loads are reported in Section 5.1 and are not repeated in this section.

Ambient Environment. The mirror magnet shall meet all requirements when operating in air at 38°C and 80% relative humidity.

Temperature. The coil shall be capable of being cooled from 300°K to 4.2°K (para. 3.2.6.1).

Operating Life. The coil shall be capable of operating for a minimum of 10 years including the cycle life specified below, when operating for 4000 hrs/year under EBT-P nominal operating conditions (para. 3.2.7).

Thermal Cycles. The coil shall be capable of meeting all the requirements of this specification after being subjected to 200 thermal cycles. A thermal cycle is defined to be cooldown from 300°K to 4°K and warmup from 4°K to 300°K (para. 3.2.7.1).

Electrical Cycles. The coil shall be capable of meeting the requirements of this specification after being subjected to 2,000 charging cycles. A charging cycle is defined as energizing the coil from zero current to the nominal operating current within 30 minutes and discharging (para. 3.2.7.2).

Fault Loading Cycles. The coil support system shall be capable of withstanding the out-of-plane fault loads for a total of 20 cycles during the life of the machine (para. 3.2.7.3).

Radiation. The mirror coil and support equipment must meet all requirements of the specification after a total x-ray exposure over 10 years as given in Figure 3.5-2 (para. 3.2.8.2). The coil must operate with a maximum steady-state heat load from x-ray radiation of 10 watts per coil.

Loads and accelerations which are applied to the EBT-P mirror magnets are given in Figure 3.5-3. Pressures applied to the helium vessel and dewar are given in Figure 3.5-4.

Figure 3.5-5 presents the load condition combinations which we used for analysis. Most of these combinations were run in the overall finite element model of the mirror coil assembly.

FIGURE 3.5-2 TOTAL X-RAY DOSES (5 YEARS 60 GHz, 5 YEARS 90 GHz)

REGION	R (IN)	H (IN)	θ (DEG)	D RADS X 10^8
	0	70		0.53
CIRCUIT BREAKERS	80	70		0.50
CIRCUIT BREAKERS	102	70		0.53
	0	109		0.43
DUMP RESISTORS	96	109		0.47
DUMP RESISTORS	165	109		0.50
CRYO PUMP	170	22		0.72
TOP OF STACK	177	49		0.72
COIL R = 9.488			0	0.81
COIL Z = 4.134			30	0.62
↓			60	0.51
			90	0.44
			120	0.38
			150	0.37
			180	0.35

FIGURE 3.5-3 MINIMUM MAGNET DESIGN LOADS (PAR. 3.2.10)

LOADING CONDITION		MINIMUM DESIGN LOAD OR ACCELERATION
• NORMAL OPERATION:	IN-PLANE (WITH ARE COIL)	17,900 LB
	OUT-OF-PLANE	0
• FAULT CONDITION:	IN-PLANE	8,000 LB
	OUT-OF-PLANE	73,000
• COIL MISALIGNMENT:	IN-PLANE	TBD
	OUT-OF-PLANE	TBD
• SEISMIC: ZONE 2	VERTICAL	±1.2G
	HORIZONTAL	±0.2G
• HANDLING: (PACKAGED):		
	LATERAL	±1.0G
	VERTICAL	+2.5G, -0.5G
	LONGITUDINAL	±1.5G
		10^3 CYCLES
(UNPACKAGED):		
	LATERAL	±3G
	VERTICAL	±3G
	LONGITUDINAL	±3G

FIGURE 3.5-4 DIFFERENTIAL PRESSURE LOADS
(PAR. 3.3.3)

ITEM	NORMAL PRESSURE (PSI)	YIELD FACTOR SAFETY	PROOF PRESSURE (PSI)	YIELD FACTOR OF SAFETY	BURST PRESSURE (PSI)	ULTIMATE FACTOR OF SAFETY
HELIUM VESSEL (INTERNAL)	50	1.5	62.5	1.0	100	1.0
VACUUM VESSEL (EXTERNAL)	14.7	1.5	--	--	--	--

FIGURE 3.5-5 LOADING COMBINATIONS USED IN THE ANALYSIS OF EBT-P

LOAD SOURCE	OVERALL LOAD CONDITION: NORMAL 4°K OPERATION	FAULT-NORMAL	FAULT-SEISMIC	NORMAL 4°K + SEISMIC	PROOF	SHIPPING
GRAVITY	X	X	X	X	X	
THERMAL (4°K)	X	X	X	X		
NORMAL ELECTROMAGNETIC	X			X		
FAULT ELECTROMAGNETIC		X	X			
INTERNAL PRESSURE - H_E	X	X			X	
SEISMIC			X	X		
SHIPPING & HANDLING						X
VACUUM	X	X	X	X		

3.6 POWER SUPPLY AND DISTRIBUTION SYSTEM

3.6.1 POWER SUPPLY DESIGN CRITERIA. The magnet power supply shall be a continuously variable, current-regulated, dc power supply capable of ON, OFF, RESET, interlock status and digital current ramp, and voltage control from an external sources. The magnet power supply shall feature automatic cross-over, over-current cutoff and reverse voltage protection.

3.6.1.1 Performance. The magnet power supply shall have a basic minimum output rating of ± 50 vdc at 1800 adc. The power supply shall have a long-term stability of ± 0.5% output. From a cold start, the power supply shall attain ± 0.5% stability within two hours.

3.6.1.2 Input Power: 480 vac, 3 phase, 60 Hz.

Line voltage variations:	± 6%
Line voltage imbalance:	5% maximum
Frequency variation:	± 1.0 Hz

3.6.1.3 Output Characteristics: 50 vdc, 0-1800 adc.

Output current variation:	± 0.05% maximum peak-to-peak ripple
Ripple voltage frequency:	720 Hz (fundamental)

3.6.1.4 Current Control. The magnet power supply shall be capable of current control from the process controller. The magnet power supply shall reference its output to an external precision current transducer (such as a shunt) interfaced to the output bus. The power supply shall respond smoothly to the current level specified by the control input, the output voltage required to change the output current shall be limited by the voltage control, but in no case greater than 50 vdc. The power supply controller shall limit the output voltage slew rate to 1 V/sec. The magnet power supply shall operate with a phase margin of at least 30° with the superconducting magnet load as shown. The requirements for the digital input are listed below:

A.	Isolation:	500 V between control input and power supply control circuit
B.	Format:	4 digits BCD
C.	Resolution:	2000 amps should correspond to the BCD code

D.	Input Current:	15 ma max. TTL, CMOS compatible
E.	Noise Immunity:	input shall have common mode transient immunity of at least 1000 V/us
F.	Current Transducer Current Range:	0 to 1800 adc
G.	Current Transducer Voltage Drop:	500 mvdc maximum
H.	Current Transducer Isolation:	1000 vdc to ground
I.	Current Transducer Accuracy and Linearity:	± 0.02% minimum

3.6.1.5 Voltage Control. The magnet power supply shall be capable of current ramp (amps/sec) control from the process controller. The magnet power supply shall reference its output to an external precision current transducer (such as a shunt) interfaced to the output bus. The power supply shall respond smoothly to the level specified by the ramp control input, the output voltage required to change the output current shall be limited to 50 vdc. The power supply controller shall limit the output voltage slew rate to 1.0 volt per second. The magnet power supply shall operate with a phase margin of at least 30° with the superconducting magnet load as shown. The requirements for the digital input are listed below:

A.	Isolation:	500 V between control input and power supply control circuit
B.	Format:	2 digits BCD
C.	Resolution:	50 V should correspond to the BCD code 0101 0000
D.	Input Current:	15 ma max. TTL, CMOS compatible
E.	Noise Immunity:	input shall have common mode transient immunity of at least 1000 V/us

3.6.1.6 Isolated Output Signal. Two isolated digital outputs shall be proved which shall indicate current flowing through the current transducer and output voltage. These outputs shall be accurate to within ± 1 LSB and shall be used to operate a remote digital readout. The outputs shall be latched and the sample rate shall be at least 1 Hz. The requirements for the digital output are listed below:

A.	Isolation:	500 V between transducer and output
B.	Format:	4 digits BCD

C.	Output Current Drive:	15 ma minimum for each output bit
D.	Output Voltage:	TTL, CMOS compatible
E.	Noise Immunity:	Output shall have a common mode transient immunity of at least 1000 V/us.

3.6.1.7 Loads. The main magnet power supply load shall be 36, 1.07 Henry superconducting magnets, series connected, with a total series resistance of 10×10^{-3} ohms. In addition, there shall be a 244×10^{-3} ohm resistive load in parallel with each magnet coil's terminals.

3.6.1.8 Input Circuit Breaker. The input circuit breaker shall have an interrupt capacity asymmetrical with a minimum continuous current rating of 120% full load input current at 480 vac. The circuit breaker shall be capable of instantaneous magnetic trip, ambient compensated thermal trip and manual trip (with safety lockout provisions for a padlock).

3.6.1.9 Main Input Contactor. The main input contactor shall be a three-pole contactor with 1500 V insulation and a minimum continuous current rating of 120% of full-load at 480 vac. Operating coils shall be continuous duty type and shall operate the contactor in the range of 85 to 110% of the rated coil voltage.

3.6.1.10 Rectification. The magnet power supply shall contain two main transformers and shall produce 12-phase rectification. One transformer shall contain a delta primary, the other shall have a wye primary. The two secondaries of these transformers shall be connected in a double wye with interphase transformer configuration.

3.6.1.11 Control, Protection and Function. Indicating devices and switches of this section shall be mounted on the power supply front panel. Circuitry of this section shall be powered from the secondary side of a 480/120 V control transformer. Indicating lights shall be LEDS unless otherwise specified.

3.6.1.12 Metering and Non-Annunciator Indicating Devices.

Ammeters:

Output Current:	2% digital dc ammeter
3-Phase Line Current:	expanded scale ac ammeter with switch

Voltmeters:

Output Voltage:	2% dc voltmeter
3-Phase Line Voltage:	expanded scale ac voltmeter with switch

AC "ON" indicating light

DC "ON-OFF-RESET" control pushbutton switches with indicating lights

3.6.1.13 Alarm Detectors, Annunciators and Contacts. Figure 3.6-1 shows the alarm conditions which shall require annunciators and/or a pair of relay contacts for remote indication of power supply alarms. An annunciator shall be a neon indicating light. The relay contacts required for remote indication shall be normally closed, i.e., the relay contacts shall open for an alarm condition. The contacts shall be rated at 1A and shall be electrically isolated from the power supply and shall be capable of withstanding a 500 vdc high potential test from the contacts to the power supply primary or secondary circuits.

3.6.1.14 Power Supply Protection System. In the event of any of the failures listed in Figure 3.6-1 (1 thru 6 only), the main input contactor shall be latched open. The Magnet Power Supply shall be designed so that in the event of a power failure or other fault that requires interruption of the 480 input power, the Magnet Power Supply shall be capable of passing the current stored in the magnet until the magnet is fully discharged. This requires that the Magnet Power Supply shall absorb the stored energy in free air convection over a period of time.

3.6.1.15 Output Protection. Redundant free-wheeling SCR's across the output shall be used to absorb the magnet energy during power-line disturbances and load overvoltages. The SCR's shall be triggered by redundant means other than the input ac power.

3.6.1.16 Power Failure. The seller shall provide an isolated relay contact for remote indication of "loss of ac power" for loss of 480 vac power. The contact shall open on loss of 480 vac power.

3.6.1.17 Power Supply Malfunction. The seller shall provide an isolated relay contact for remote indication of "power supply malfunction." The contact shall be open as a result of the power supply being shut down by any internal interlock.

3.6.1.18 Output Fault Current. The seller shall limit the output fault current (dead short on dc output) to no more than 20,000 amperes peak.

3.6.1.19. Ground Fault. The Magnet Power Supply shall incorporate a shutdown circuit such that excessive ground current shall shut down the power supply. Vendor shall supply an isolated relay contact which opens when ground current is detected.

#ALARM	ANNUNCIATORS	RELAY CONTACTS **SPST(NC)	DETECTORS
1. 480 VAC POWER FAIL*	1	1	3 DETECTORS, 1 FOR EACH PHASE
2. AC INPUT OVERCURRENT	1	1	3 DETECTORS, 1 FOR EACH PHASE
3. DC OUTPUT OVERCURRENT	1	1	SCREWDRIVER ADJUSTABLE FROM 1500 TO 2200
4. DC OUTPUT OVERVOLTAGE	1	1	SCREWDRIVER FROM 30 VDC TO 50 VDC
5. THYRISTOR OVERTEMPERATURE	1	1	1 FOR EACH THYRISTOR
6. CABINET OVERTEMPERATURE	1	1	
7. THYRISTOR PHASE-BACK ANGLE OVERCURRENT			IN THE EVENT OF AN OVERCURRENT CONDITION, THE THYRISTOR GATE EXCITATION SHALL BE REMOVED

* DEFINED AS WHEN THE INPUT POWER FALLS BELOW THAT REQUIRED TO OPERATE THE SUPPLY AT MAXIMUM RATING.

** SPST(NC) = SINGLE POLE, SINGLE THROW, NORMALLY CLOSED (CONTACT OPENS ON FAULT CONDITION).

FIGURE 3.6-1. MAGNET POWER SUPPLY ALARM/RELAY REQUIREMENTS

3.6.1.20 Transient Protection. Semiconductor transient voltage protection shall be provided for transients 50% and greater than the manufacturer's inverse and forward voltage ratings.

3.6.1.21 Terminals. The ac input terminals shall be located at the rear of the Magnet Power Supply. The dc output terminals shall be located at the top of the Magnet Power Supply.

3.6.1.22 Cooling. Air is preferred, but if water cooling is used, each parallel water path shall be 304 stainless steel and shall be monitored by a flow switch interlocked with the magnet power supply such that loss of return flow on any one of the branches shall inhibit/shut down the magnet power supply.

3.6.1.23 Grounding Practice. The Magnet Power Supply shall be capable of operation either ungrounded or with either side of the dc output grounded, or grounded through a center tap on the resistive load across the output terminals. A ground pad shall be provided for external connection to the frame of the Magnet Power Supply at the rear of the supply. The Magnet Power Supply current transducer shall be capable of operating ± 1000 vdc above frame potential.

3.6.2 DISTRIBUTION SYSTEM DESIGN CRITERIA. The power will be supplied to the magnets by means of a solid copper circular ring bus which is located above the magnets on the torus mezzanine. Connections to the magnet will be made with flexible jumpers to facilitate magnet alignment.

3.6.2.1 Field Error. The bus must be designed to minimize the magnetic field produced in the plasma region. This will be accomplished in two ways. First, a circular return bus will be folded back and run parallel to the series magnet supply bus. Secondly, all to/from lines must be run as close together as possible. This last requirement does not apply to conductors carrying current only during an emergency discharge.

3.6.2.2 Sizing Criteria. The high current conductors will be initially sized at 1 amp/MCM. This value is sufficiently conservative to assure a less than 30°C steady-state temperature rise. Solid buswork will be oriented with the long dimension vertical to maximize convective cooling.

Joints in the solid buswork will be overlapped sufficiently to maintain a resistance less than or equal to an equivalent length of bus. All other joints must have a resistance sufficiently low to assure no more than a 30°C rise locally.

Joint design must recognize that the magnet charging cycles imply a thermal cycling requirement.

3.6.2.3 Insolation/Insulation. Solid copper buswork will be insulated by maintaining a minimum isolation distance of 0.75 inch between it and any other adjacent bus or conductive materials. Buswork will be rigidly held to assure that deflections due to temperature graidents or magnetic forces will not degrade the insulating capability.

Insulating materials must withstand an X-ray dose of approximately 2×10^8 rads over a 10-year life.

All buswork will be dielectric tested to 1500 vdc.

3.7 MAGNET PROTECTION SYSTEM DESIGN CRITERIA

The magnet protection system must monitor the operational status of each of the 36 superconducting magnets and take appropriate action in the event an anomaly is detected. The system is somewhat distributed throughout the electronics. It consists of the monitoring equipment which detects anomalous conditions, decision making equipment which initiates a protective action, and the equipment which implements the chosen protective action.

3.7.1 PROTECTION PHILOSOPHY. There are three protective actions which can be performed by the magnet protection system. The first is the inhibiting of charging. The magnet cannot be charged unless all equipment interlocks indicated a "go". The second protective action is to slowly ramp down the magnet through a free-wheeling SCR which will be located in the power supply. The following tables indicates the equipment interlocks which would either inhibit charging or cause a slow rampdown by maintaining the power supply input contactor in the open position.

MAGNET POWER SUPPLY
INPUT POWER MONITOR (LOW)

MAGNET POWER SUPPLY
INPUT OVERCURRENT

MAGNET POWER SUPPLY
OUTPUT OVERCURRENT

MAGNET POWER SUPPLY
OUTPUT OVERVOLTAGE

MAGNET POWER SUPPLY
THYRISTOR OVERTEMP

MAGNET POWER SUPPLY
CABINET OVERTEMP

BREAKER OPEN/CLOSED (OPEN)

EMERGENCY DISCHARGE
RESISTOR OVERTEMP

PROTECTION SYSTEM ENABLE

Each of these signals will be provided to the I and C system process controller which will control the power supply.

The third potential protective action which can be taken by the protection logic is to initiate an emergency dump. An emergency dump will be initiated for one of three reasons: (1) the magnet is directly in danger due to a quench condition, (2) the magnet can no longer be protected because of an equipment failure, or (3) the operator initiates an emergency dump. When the decision to dump is made, all magnets will be discharged simultaneously to minimize structural imbalances. The quench detection logic will be hardwired directly to the circuit breakers which initiate discharge. No computers or microprocessors shall be used in the emergency discharge logic which directly protects the magnet.

The following direct monitoring devices associated with each magnet will initiate an emergency discharge for all magnets.

QUENCH DETECTOR (PRIMARY)

QUENCH DETECTOR (BACKUP)

VAPOR-COOLED LEAD A OVERVOLTAGE

VAPOR-COOLED LEAD B OVERVOLTAGE

HELIUM LEVEL MONITOR LOW SETPOINT

LOSS OF VACUUM (SWITCH)

HELIUM OVERPRESSURE (SWITCH)

Signals initiating in the above monitoring devices will be normally high such that loss of power to any of the devices will have the same effect as detection of a fault.

The system will be protected from power failures as follows. Loss of power to the magnet power supply will result in a free-wheeling discharge through the free-wheeling SCR. The remaining direct protection equipment will be supplied with uninterruptible power. The breaker drivers will automatically open the breakers using a capacitive discharge circuit should the uninterruptible power fail.

3.7.2 PROTECTION EQUIPMENT. The protection equipment will include or interface to the following devices:

DESCRIPTION	DEVICES/MAGNET	TOTAL
LEAD VOLTAGE MONITOR	2	72
QUENCH DETECTOR	2	72
HELIUM LEVEL MONITOR	1	36
VACUUM SWITCH	1	36
PRESSURE SWITCH	1	36
BREAKER DRIVER	1/4	9
CIRCUIT BREAKER	1/4	9
DUMP RESISTOR	1	36
BYPASS DIODE ASSY	1/2	18

Each of these components must be compatible with the temperature, operating life, and radiation dosage requirements associated with their specific location. The following represents a brief synopsis of the individual operating requirements for each of the above units.

3.7.2.1 Lead Voltage Monitor. The voltage drop across each vapor-cooled lead will be monitored to protect against overtemperature due to loss of helium coolant flow. The monitors must accept an analog differential input which will trigger a discrete output when a preset level is exceeded.

Input Voltage:	
Input Isolation:	500 vdc to ground at either input
Setpoint Adjustment:	5mv - 500mv
Output:	Isolated Contact Set: Normally closed when power is applied and input is less than setpoint.

	Normally open when input exceeds setpoint or loss of power. 200ma at 28 vdc.
Response Time:	20 milliseconds max.

3.7.2.2 Quench Detector. Each magnet must have two means of quench detection, either of which will be capable of triggering the breaker drive. The detailed concept has not yet been determined.

3.7.2.3 Helium Level Monitor. The helium level monitor for each magnet will interface to the helium level probe in the magnet stack. It will provide a 0-100mv analog output proportional to helium level which will serve as an input to the process controller in order to control helium delivery to the magnet. The monitor will also provide an adjustable setpoint for a "helium level low" signal which will interface to the breaker driver. This setpoint signal will be an isolated contact set which is normally closed when power is applied and the helium level is above the adjustable setpoint, and normally open when helium level is either below the setpoint or power fails.

3.7.2.4 Vacuum Switch/Pressure Switch. The vacuum switch will be an adjustable pressure switch with a contact set which is closed when a vacuum exists in the dewar and open upon loss of vacuum. If the device contains active components requiring power, then loss of power must produce the same indication as loss of vacuum.

The magnet also contains a pressure switch which will indicate overtemperature of the helium or an unnoticed quench. The function of the pressure switch is identical to that of the vacuum switch.

3.7.2.5 Breaker Driver. The breaker driver is the controller of the protection system. Each breaker driver will accept inputs from the protection monitoring equipment associated with two magnets and command the breaker open upon receipt of a command. Inputs will be in the form of contact open/closures. Inputs are safe when contact sets are closed. When any input contact set opens, a discharge will be initiated. The breaker driver will be fail-safe in design so that no single component failure can disable its ability to discharge the magnets. The breaker driver will have redundant outputs to each circuit breaker open coil. A loss of both primary and uninterruptible power will initiate an output command to open the breaker. This will be implemented by using capacitive storage as the energy source to the breaker open coil.

INPUTS FOR DUMP	NO.
Lead Voltage Monitor	4
Quench Detector	4
Helium Level Monitor	2
Vacuum Switch	2
Pressure Switch	2
Emergency Shutdown (Process Controller)	2
Manual Emergency Shutdown	1
Dump Bus	2 (Redundant)
OUTPUTS TO BREAKER	
Open Coil	2 (Redundant)
AUXILIARY OUTPUT	
Dump Bus	2 (Redundant)
Status (Shutdown Cause)	6
Quench in Progress	1

The dump bus is monitored by each breaker drive as an input. When any breaker driver initiates a dump, all other breaker drivers are simultaneously triggered.

3.7.2.6 Circuit Breaker. The circuit breaker must be capable of interrupting a DC inductive circuit upon command. Each breaker will be rated at 2000 amps continuous operation. The predicted circuit values are 1800 amps at approximately 800 volts. Due to the potential for transient voltages exceeding 800 volts, the preliminary interrupt voltage requirement has been established at 1500 volts. The breakers will open upon receipt of a 115 vdc, 2 amp signal. Once the breaker is open, a contact in the breaker will open this circuit. A 115 vdc, 50 amp signal will be used to reset the breaker.

The breaker will be installed in a DPST configuration with both poles side by side. Each pole will have individual open and close coils.

The overall size (for the DPST configuration) will be limited to 18 inches wide, 26 inches deep, and 48 inches high.

3.7.2.7 Dump Resistor. Dump resistors will be placed electrically across each of the 36 magnets. Each dump resistor must be able to absorb 1.5 megajoules adiabatically with a temperature rise of less than 150°C. The resistance must be $0.238\Omega \pm 2\%$. The resistors will see a peak voltage of approximately 400 volts but must maintain a ground isolation potential of 2500 vdc.

The dump resistor will be fabricated from 304 stainless steel in an insulated frame. Overall size for a pair mounted together will not exceed 12 inches wide by 26 inches high by 66 inches long.

3.7.2.8 Bypass Diode Assembly. Each bypass diode assembly will contain four silicon high-current diodes. The steady state design current will be 2500 amps. The current through the diodes with a voltage drop of 2.8 volts shall not exceed 25 amps. At full current, the voltage drop should not exceed 20 volts. Steady state power dissipation will be by means of free air convection. The reverse breakdown voltage will be 600 volts minimum. The turn on time for the diode assembly should not exceed 1.0 microsecond. The diode assembly mounting must be insulated to a minimum of 2500 vdc.

3.8 INSTRUMENTATION AND CONTROL

Instrumentation for each magnet will include nine channels (minimum) of strain conditioning circuitry, six channels of temperature conditioning (four channels compatible with carbon glass resistor sensors, and two channels compatible with type E thermocouples). A helium pressure signal conditioner and an LHe level signal conditioner are also required.

The data acquisition system will record analog outputs from the quench detectors and vapor-cooled lead monitors, as well as the temperature and strain monitors. In addition, the status of the breaker driver and manual emergency shutdown will be recorded.

A secondary control console will be located in the control room. In the event of a master control console failure, it will be capable of taking over control of the magnet power supply.

3.9 SAFETY & HAZARD DESIGN CRITERIA

System Safety recognizes certain basic safety design criteria that must be adhered to in the EBT-P system to ensure personnel safety. Under normal operating conditions, the magnetic fringing field, the magnet structure, and the cryogen system are all potentially hazardous.

In spite of a large amount of experimental work done in the field of biomagnetism, understanding of the effects which magnetic fields have on the human body remains rudimentary. However, enough deleterious effects have been recorded to label exposure to magnetic fields a potential hazard. Hence, personnel exposure to stationary magnetic fields should be minimized. Another potential hazard steming from the magnetic field is in incorrect instrument readings. Thus, instruments should be either shielded or removed from high magnetic fields.

In the event that the liquid helium or nitrogen of the cyrogen system go through a phase change to gas, most likely occurring during a transient situation, pressure relief valves and venting system must be included to ensure that personnel will not be exposed to a possibly hazardous gaseous environment. Dump resistors should be located away from personnel, since they produce large amounts of heat (maximum resistor temperature is 350°F) upon coil discharge.

The magnet structure poses potential hazards under both normal operating conditions and during testing and fault isolation. Failure of the magnet structure could cause serious injury to personnel, hence, structural safety factors are incorporated into the design. These are 1.5 for yield strength, 3.0 for ultimate tensile strength, and 4.0 for buckling. Also, the vacuum vessel has a factor of safety of 10 for fatigue strength, based on life cycles. Pressure relief valves are incorporated to ensure that pressure in the structure does not exceed maximum tolerance levels.

During maintenance operations, personnel access to cryopanels should be limited until they return to ambient temperature. In addition, safety devices, such as handrails, scaffolds, and protective equipment must be provided for maintenance personnel.

NORMAL OPERATION

o MAGNETIC FIELD

Personnel exposure to high magnetic fields will be minimized.

- STRUCTURE

All structures in the EBT-P magnet system are designed with safety factors of:

1.5 for yield strength
3.0 for ultimate strength*
4.0 for buckling

Additionally, the vacuum vessel is designed to withstand 10 times the life cycle of fatigue associated with teh EBT-P operations.

Pressure relief devices will be incorporated to assure that pressure of the structure does not exceed maximum tolerance levels.

- CRYOGEN SYSTEM

Pressure relief valves and a venting system assure that personnel will not be subjected to a possibly hazardous gaseous environment.

* See 5.2.3 for exception.

TESTING AND FAULT ISOLATION

- MAGNETIC

  Same exposure standards as in normal operation.

- CRYOGENIC

  Limit personnel exposure to cryopanels during maintenance until they return to ambient temperature.

- MAINTENANCE PERSONNEL

  Provide safety devices for maintenance personnel such as handrails, scaffolds, and protective equipment.

3.10 X-RAY SHIELD

The mirror coil x-ray shield design criteria established in the RFP were revised by the ORNL/MDAC/ANL Internal Shielding Review Meeting of 9 July 1981. The meeting resulted in an agreement to use an extended high energy tail, a higher ring temperature, and a distribution of the x-ray source between the electron rings and limiters. A list of the criteria used for design and analysis of the x-ray shield is as follows:

- The x-ray shield shall be designed to limit mirror coil heating to 10 watts maximum during 90 GHz operation.
- The x-ray spectra is based upon an electron maxwellian distribution out to 14 MEV, ring temperature of 2 MEV, and a plasma impurity level of 2% aluminum.
- The source distribution is 77% from the electron rings and 23% from the limiters.
- Mirror coil/x-ray shield/torridal vessel integrated design shall clear the 16.0 cm flux line.

3.11 DEVELOPMENT PROGRAM

3.11.1 INTRODUCTION. Just after the EBT-P project started, there was a period of about a year before the principle industrial participant and the industrial magnet manufacturer were chosen. The magnet development program was started in May, 1979, at ORNL to take advantage of this year to start the magnet development. The magnet design underwent a number of changes in the fall and early winter of 1979 during the Phase I meetings among the four competing industrial teams and ORNL. The parameters for the current magnet design were established during these meetings. The design is contained in the proposed reference design reviewed in January, 1980.

In addition to demonstrating that the coil design will produce the proper field magnitudes and be able to tolerate the x-ray load, the other program objectives are:

1. To demonstrate design features and fabrication techniques that will produce the required field accuracy and eliminate systematic (cumulative) field errors.

2. To solve the problems of structural containment and of maintaining proper alignment in the dewar after cooldown and energizing.

3. To evaluate thermal design features and determine heat removal capability.

4. To develop techniques, facilities, and criteria for acceptance testing of the coils manufactured for EBT-P.

In short, the magnet development plan is for ORNL to wind two development coils and test them in a general purpose dewar (Open Dewar Tests), while designing and building a facility to test the development coils and the GDC wound prototype coil in their individual dewars. The two-coil tests and the prototype tests will address most of the program objectives listed above. The plan is to test the dewar restraint system for the centering load and fault load cases in the two-coil test, then to test the prototype magnet as the center magnet of a three-magnet array. This will test the prototype in a magnetic environment similar to the environment expected in EBT-P, as well as test it in the worst fault loading case. Since the program began, the two development coils have been wound and have had their open dewar tests; the test facility has been designed and is under construction; GDC is manufacturing the development dewars; and GDC is preparing to wind the prototype coil.

Technology transfer from the development program to the magnet manufacturer is an important part of the magnet development program, but it is only part of the overall plan to reduce risks in getting the magnet system for EBT-P. There are three main

steps in the transition from the magnet development program to magnet manufacturing:

1. Information transfer from the development program to the magnet manufacturer. The information transfer is being done by having a GDC on-site observer for winding and coil testing, by on-site GDC visits during critical winding steps, and by a 40 minute movie that has been made of the winding of the first development coil which will be given to MDAC and GDC in mid-September. Also, MDAC/GDC has participated in the design changes from D-1 to D-2.

2. ORNL is setting design criteria with active participation by MDAC/GDC. ORNL is responsible for evaluating design analysis, reviewing, commenting, and approving the MDAC/GDC magnet system design. This step includes the GDC dewar design and construction for the two development coils and the prototype coil, and the prototype magnet design and construction at GDC.

3. Magnet manufacture according to the manufacturing, QA, and acceptance test plans. These plans will be based on the results of the development program and prototype program.

3.11.2 COIL DESIGN. The following list contains part of the magnet parameters developed during Phase I:

Inside Radius	24 cm
Outside Radius	34 cm
Length	21.1 cm
Peak Field	7.4 T
Peak Current Density	10,000 A/cm^2

Fortunately, these magnets will not be operated in the pulse mode, and will not be subjected to strong externally generated pulsed magnetic fields; however, the magnets will be subjected to x-ray radiation generated in the plasma region. Estimates generated during Phase I set the volume energized x-ray load at 10 watts into the winding. Subsequent source estimates and shielding calculations have lowered this estimate, but the coils were designed and tested with the 10 watt load as the criteria.

The conductor used in the coil is a compacted monolith[2]. Two grades of conductor were used. The high field grade has 71% copper by volume and a critical current of 3500 A at 7.5 T. The low field conductor has a 76% copper volume and a critical current of 4300 A at 6 T; and 3000 A at 7.5 T.

Our preference in magnet designs subjected to external heat, in this case x-ray radiation, is a ventilated design rather than windings potted in epoxy. Liquid helium heat capacity is enormous compared to the NbTi and copper that comprise the superconductor. It is preferable to have heat transfer directly from the surface of the conductor to liquid helium rather than via conduction through a poor thermal conductor, as is the case for all potting compounds.

The insulation in the windings must be thin to achieve the objective current density and allow for helium circulation through the coil windings. The turn-to-turn and layer-to-layer insulation in the coil winding pack is provided by a spiral wrap of 7 mil (nominal dimensions) unimpregnated Nomex lacing tape. The tape is wrapped to cover 50% of the conductor. About 8% of the winding pack volume is free for liquid helium circulation.

The winding scheme for the mirror coils must be chosen carefully to keep the field errors low. These errors are introduced by crossovers, by layer-to-layer transitions in the magnet, and by leads. The largest potential error is the result of the large separation of the leads as they leave the winding. The choice of the winding scheme strongly influences the lead placement. Two common winding types are layer winding and pancake winding. An inappropriate layer winding scheme would feed the conductor onto the bobbin through a hole in a side plate and then wind each layer and bring the other lead off the outside diameter. The bad feature of this scheme is that there is an uncompensated current lead the length of the coil build. One can also design a pancake winding with uncompensated leads on each end of the coil. Pancake-wound coils for this application have the disadvantage that if the conductor is graded, there must be two joints in each pancake to make the grade change. Two more joints are required to connect the pancakes electrically. Joints take considerable time to make, thus increasing the overall winding cost. But as in the layer-wound case, proper designs of pancake-wound coils are also possible (e.g., the mirror magnets for EBT-S).

A hybrid winding scheme has been chosen for the EBT-P coils. Basically, this design consists of a layer-wound coil with a pie (one-half of a pancake) wound on one end to bring the conductor next to the bobbin to the outside diameter as a lead. There will be an even number of layers and the same number of turns in the pie so that the two leads end up on the outside diameter. The leads can either be put on the same end of the coil or the coil can be wound so that the leads are brought out on the coil midplane. The latter method was chosen for the development coils. The leads are then brought out close together for good field error compensation. The lead spacing is set by helium breakdown voltages during a possible dump.

The two development coils (D-1, D-2) are not identical. D-1 is wound with both grades of conductor while D-2 is wound with only the low field grade. The basic reason is that the high field conductor in D-1 is unique; Airco could not produce another length of this material when D-2 was ready to be wound. Fortunately, the low field grade is reproducible and it has sufficient critical current at 7.4 T to warrant using as the only grade in D-2.

The practice winding, winding tests, and coil winding are described in the following papers included in the appendix of this section and presented at the 9th Symposium on Engineering Problems in Fusion Research:

"Design and Construction of the EBT-P Development Coils"

"A comparison Between Experimental and Analytical Winding Prestrain for a Circular Solenoid"

Also included in this section's appendix are three additional papers describing advances in analytical methods developed to aid in the stress analysis of the EBT-P coil.

3.11.3 WELD TEST. The coil design requires that a closure ring be welded on the bobbin after the coils are wound and tested in an open dewar, but before the coils are installed in the GDC designed and built dewars. There was considerable concern about this weld because it might overheat and damage the bobbin insulation, and there may be some weld spatter on the coil. A weld test was done at ORNL on a mock up of the bobbin when it was thought that the welding would be done at ORNL. Because of the strike, this step was moved to GDC and the weld test repeated. There was no damage to the mocked up insulation and there was no weld splatter on the coil side of the weld with either the ORNL test or the GDC test.

3.11.4 CRITICAL CURRENT TESTS. Although both grades of conductor had sufficient current carrying capability to meet or exceed the critical current specifications there were two disturbing aspects to the measurements. The conductor was highly unstable to very small motions as manifested by the training during the short sample measurements even when samples were potted in epoxy. Training is a phenomena usually only observed in highly unstable magnets. It consists in a series of quenches, each one at a higher current (hence higher force) than the previous measurement, until finally some value is asymptotically approached which is considered the critical current.

The second effect which caused doubt about the conductor was the resistive voltage observed at very rapid sweep of the transport current with the sample in a background field. The origin of this voltage became apparent when the magnetization measurements showed a very large magnetization loop. The

area in the loop was sensitive to ramp rate even at very slow rates. This indicated that circulation currents in magnetization currents are very worrisome because their stored energy per unit volume of conductor is larger than the estimated (MPZ Model) allowable sudden heat disposition rate per unit volume. When this was discovered, magnetiziation tests were done on similar monolithic NbTi conductors from ORNL's conductor samples from other projects and on samples supplied by Airco. These tests showed that the problem lay in the distribution of the filaments. The best filament distribution found was a uniform distribution of filaments over an annular region. The filaments should be separated as far apart as possible, but there must be enough filaments to insure that the critical current will meet specs.

The short sample critical current measurements are shown in Figure 3.11-1. The sample numbers are the Airco spool designations. The short sample critical current measurements have a sensitivity of 10^{-12} 56-cm referred to the superconducting friction. The critical current is given for each case where current sharing could be obtained after a number of training steps. The current sharing state was not reached in the high field grade. The critical current in this case is the quench current.

3.11.5 JOINT TESTS. Mechanical and electrical tests of the potential splices used in the development coils were done at room temperature and at helium temperature. One sample splice was made using each of the following solders: 50% Pb, 50% Sn, 97.5% Pb, 2.5% Ag; and 97.5% Pb, 1.5% Ag, 1.0% Sn. An apparatus was made using existing equipment to pull test each joint at helium temperature. The 97.5% Pb, 2.5% Ag solder performed best and was used in the coil.

Another sample using the 97.5% Pb, 2.5% Ag solder was made and put on the short sample apparatus used to test the conductor so the joint resistance can be measured in the proper magnetic field. The joint resistance was 5×10^{-9} ohms and the conductor showed the same short sample critical current as measured without the joint. A theoretical estimate indicated that a joint resistance of 10^{-7} ohms would spontaneously quench the coil at full current and that a joint resistance of 10^{-8} ohms would cause a negligible decrease in coil stability.

3.11.6 OPEN DEWAR TESTS. Each development coil was tested. The tests, referred to as open dewar tests (ODT), were done in a large laboratory dewar rather than in smaller dewars to be used in EBT-P. These coils will be tested again after they are put into the smaller dewars. The purpose of the ODT is to determine if the coils can make field without training, to determine the amount of heat they can tolerate at the 60 GHz and 90 GHz operating points, and to determine if the conductor lifts off the bobbin in the center of the winding pack. The open dewar tests and test results are described in the paper

"Tests of the First Development Coils for EBT-P". This paper is included in Appendix H for this section and was also presented at the 9th Sympsoium on Engineering Problems in Fusion Research.

3.11.7 SUMMARY. The magnet development program has demonstrated that the design of the EBT-P mirror coils is basically sound, that these coils can be manufactured, and that in a large laboratory dewar the coils will operate up to specifications. Questions concerning operation in individual dewars and magnet alignment will be addressed in the two coil tests and prototype test early next year.

Figure 3.11-1. Measured Short Sample Critical Current Values

Sample #	$\mu_o H\perp$[a] (T)	I_c (A)	Sensitivity (Ωcm)	Cu:SC	A_{SC}[b] (mm^2)	λJ_c[c] (Amm^{-2})	Remarks
Low Field Grades							
D-3-80-A	7.5	2840	10^{-12}	3.20:1	3.46	821	
	6.0	4340	10^{-12}			1255	
D-3-80-B	7.5	2830	10^{-12}	3.20:1		818	
	6.0	4320	10^{-12}			1249	
D-4-80	7.5	3020	10^{-12}	2.99:1	3.64	830	An average of two training steps required to reach the critical current at each specified field level.
	6.0	4290	2.5×10^{-13}			1179	
D-7-80	7.5	1820	10^{-12}	3.06:1	3.58	508	
	7.0	2110	10^{-12}			589	
	6.0	2770	10^{-12}			774	
D-10-80	7.5	2750	10^{-12}	3.24:1	3.43	802	
High Field Grades							
P-11-80-A[d]	7.5	3515	quench	2.40:1	4.27	823	Current sharing not observed after 4 training steps.
P-11-80-B	7.5	3565	quench	2.40:1	4.27	835	Current sharing not observed after 6 training steps.
P-11-80-E	7.5	3720	$\sim 6 \times 10^{-13}$	2.40:1	4.27	871	Current sharing observed after 10 training steps.
B-460[e]	7.5	3230	10^{-12}	2.86:1	3.76	859	
	7.0	3870	10^{-12}			1029	Training eliminated by soldering to stainless steel mandrel.
	6.5	4410	10^{-12}			1173	

[a]Field applied perpendicular to the current direction and to the narrow face of the conductor.

[b]Cross sectional area of the superconductor fraction of the conductor.

[c]Current density in the superconducting fraction of the conductor at the critical current.

[d]Samples designated with P refer to the first length of the high field grade received (Type 1).

[e]This number refers to the second length of high field conductor received (Type 2).

SECTION 4

DESIGN DESCRIPTION

4.1 COLD MASS ASSEMBLY DETAILS

The bobbin assembly consists of two side plates and an inner ring welded together to form a spool, see Drawing 11-38013. All materials are 316L stainless steel. The side plates are .650 thick and the inner ring has a thickness of .366 inches. The width of the completed bobbin is 9.80 inches and has an outside diameter of 30.64 inches. The inner bore diameter is 17.966 inches. All parts are completely machined after welding to maintain the required dimensions.

The coil pack, Figure 4.1-1, consists of a monolithic NbTi superconductor, 2.9 mm X 5.0 mm in size, barber pole wrapped with .178 mm thick Nomex to provide 50% coverage of the superconductor, see Figure 4.1-2.

Slotted and solid G-10 CR epoxy-fiberglass is used for the bobbin inner ring and sidewall insulation.

Five sheets of insulation are installed next to the bobbin sidewalls and inner ring (2 slotted, 1 solid and 2 slotted sheets).

The entry wind against one side is a 34 layer pancake lead winding. This is followed by 5 more sheets of insulation and a 32 layer X 37 turn layer winding.

A perforated sheet of .005 thick Kapton is used to cover the slotted insulation at the inner ring to prevent chafing of the Nomex on the superconductor during operation.

The outside of the winding is covered by eight sheets of slotted insulation, another layer of winding to exit the leads, and eight more sheets of slotted insulation. The outer insulation is held in place by two stainless steel ring clamps.

The helium ventilation for the coil pack is provided from a 3/8-inch O.D. 304L stainless steel helium fill tube on the outer diameter of the coil pack, see Figure 4.1-3 and Drawing 11-38002.

The outer ring for the cold mass assy is in two halves. The upper half contains a concentric reducer neck assy welded in place to attach the helium stack. The outer ring half is .50-inch thick 316L stainless steel rolled to a 14.82-inch inside radius as shown in Drawing 11-38005. The weld preparation for the ends and edges are machined to conform to the ASME Pressure Vessel Code. These rings are welded to the bobbin per MIL-STD-278, using ER 316 electrodes. The root and final layer of all welds are penetrant inspected, allowing no defects. Three mounting bosses are welded to the outer ring to mount the cold mass supports, see Figure 4.1-4.

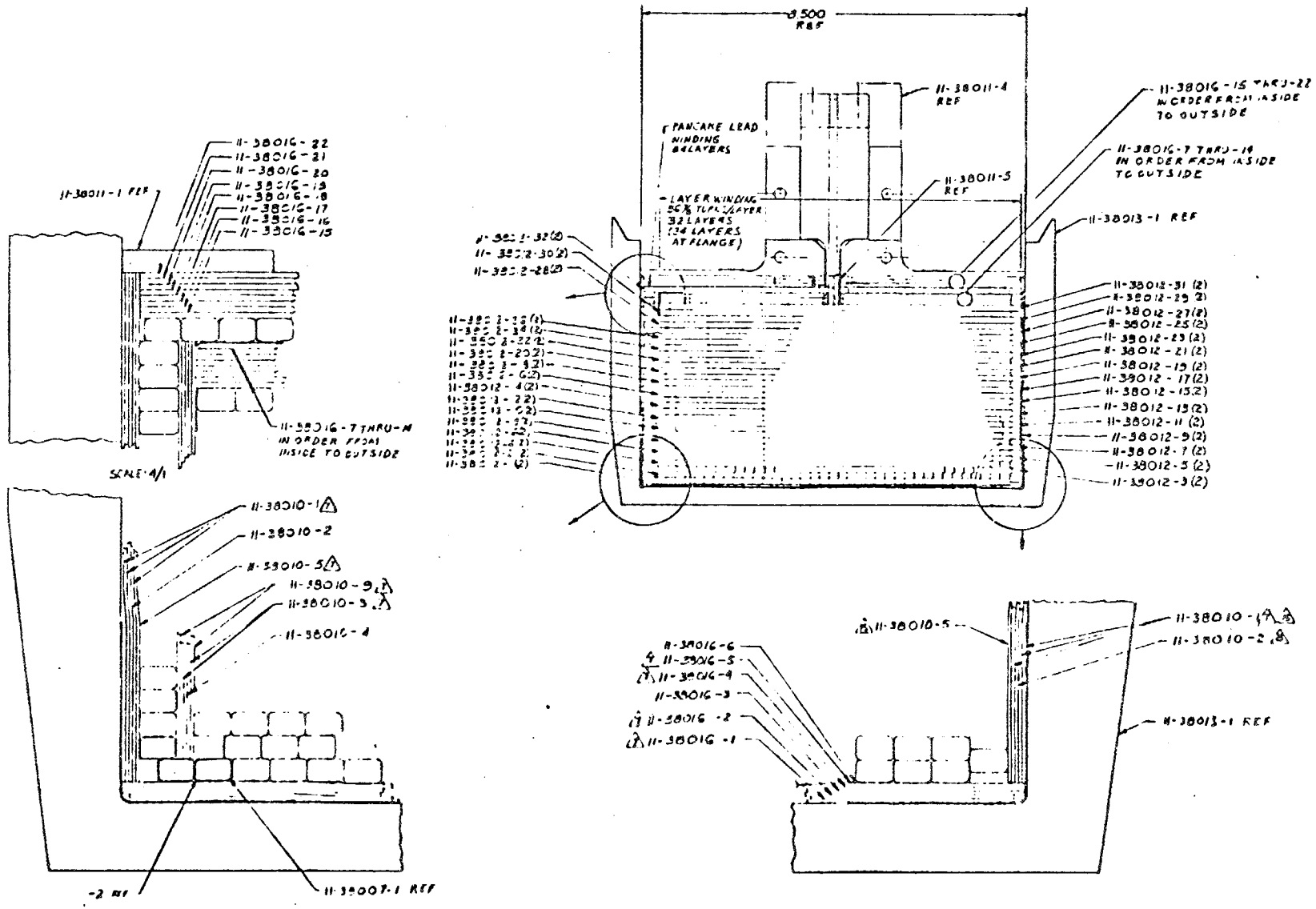

FIGURE 4.1-1 COIL PACK CROSS SECTION

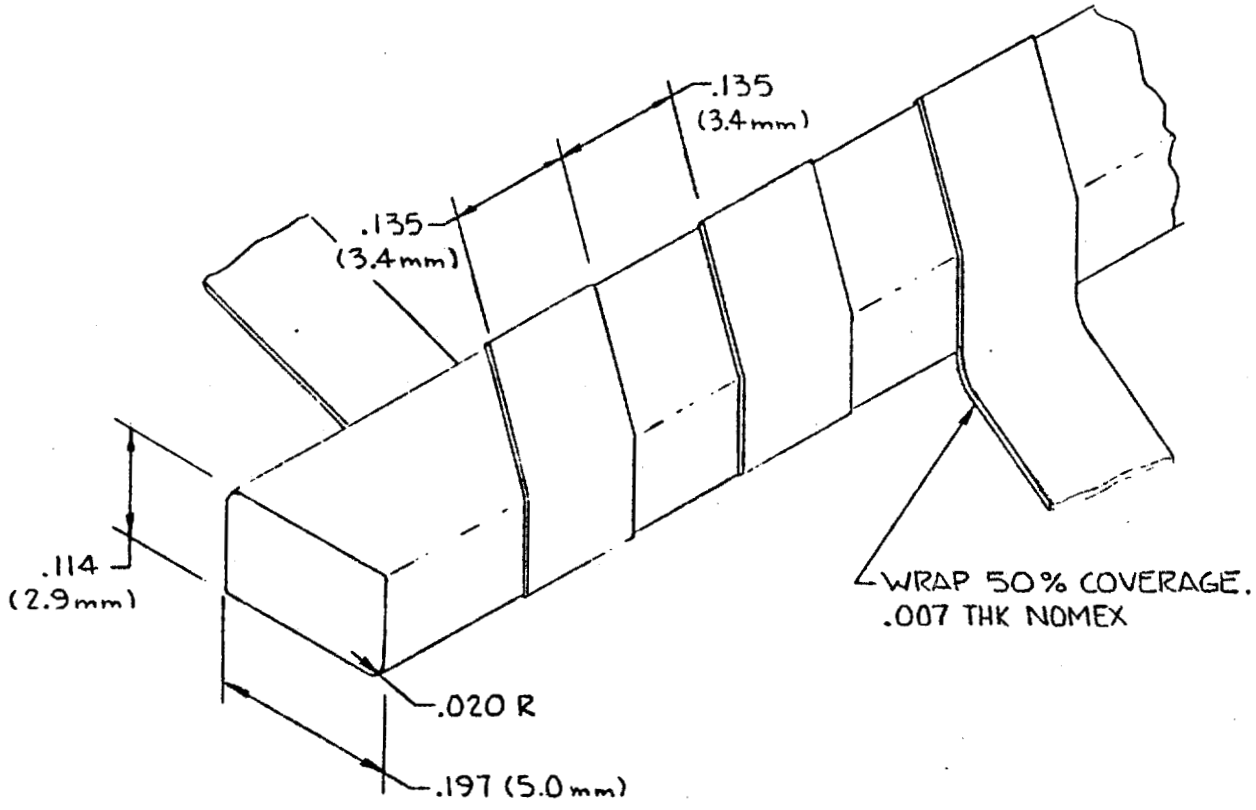

FIGURE 4.1-2 NbTi SUPERCONDUCTOR

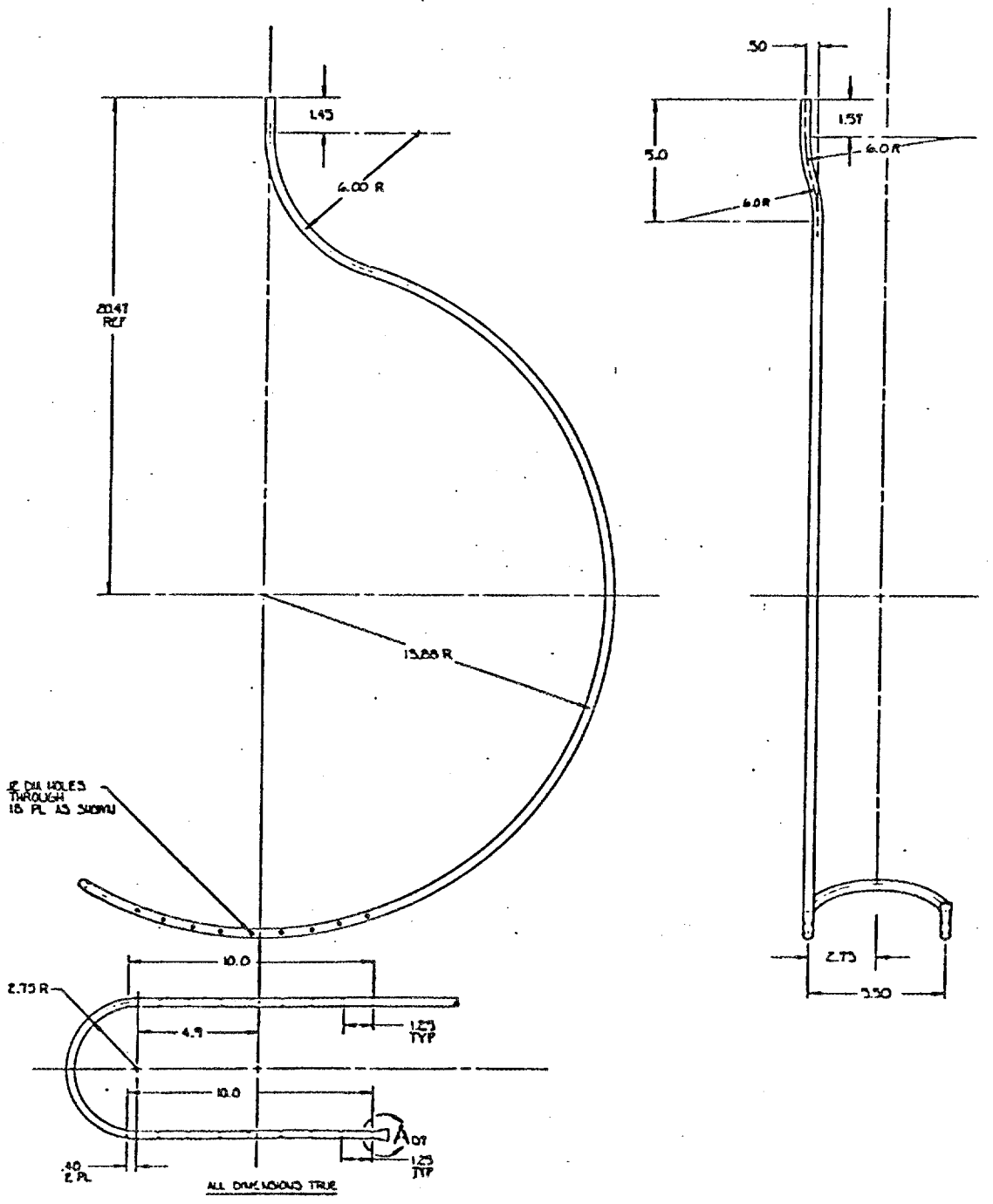

FIGURE 4.1-3 HELIUM SUPPLY TUBE

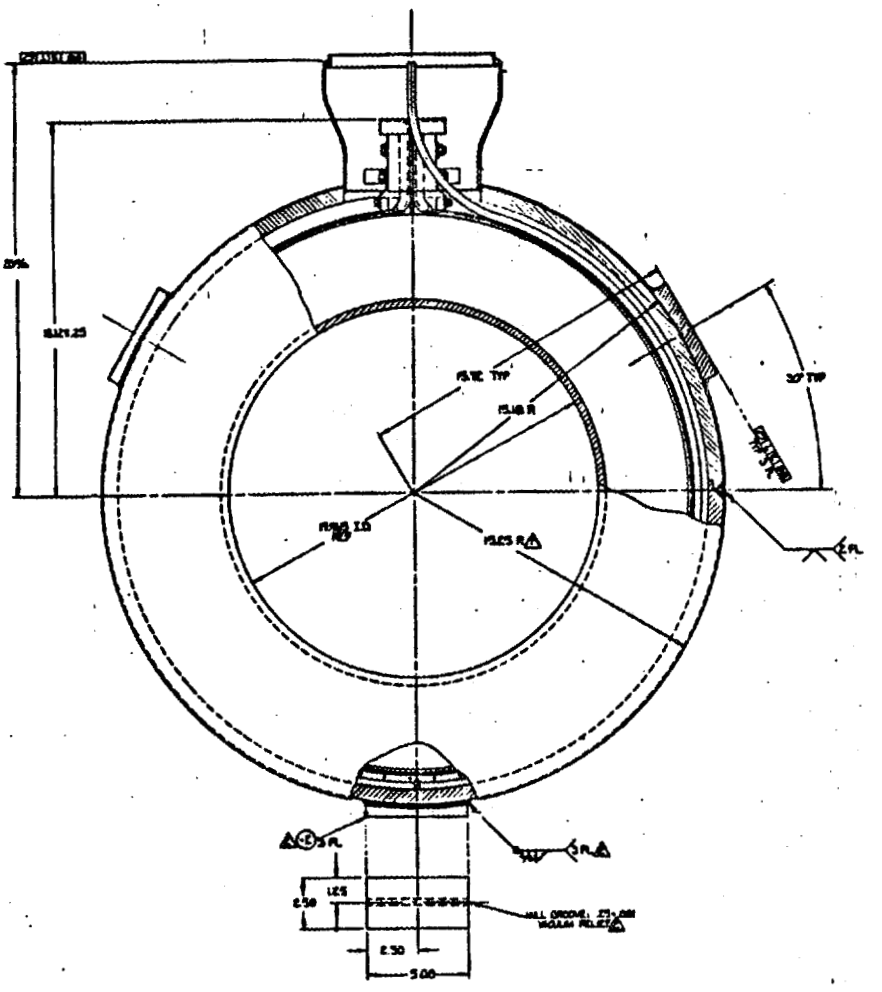

FIGURE 4.1-4 COLD MASS ASSEMBLY SHOWING BOSSES FOR MOUNTING SUPPORTS.

The helium stack, Drawing 11-38030, is an 8.0-inch diameter stainless steel pipe with an 8.0-inch diameter bellows welded to the upper end of the pipe. The lower end of the pipe is welded to the reducer neck assy on the cold mass. The upper end of the bellows is welded to a 1 1/8-inch thick plate to close out the helium vessel. The bellows will accommodate the expansion and contraction of the stack.

The stack contains two 2000 amp vapor-cooled leads, a .50-inch O.D. liquid helium supply operation tube, a .50-inch O.D. liquid helium supply cooldown tube, a 2.375-inch O.D. cold helium return vent tube, a liquid level sensor, and G-10 CR baffles to reduce the heat leak during operation and cooldown.

To further reduce the heat leak in the stack, finger contact strips of beryllium copper are installed around the helium supply tubes and the vent tube to provide LN_2 intercepts. Seven copper straps are also equally spaced around the outside of the helium stack and connected to the inside of the LN_2 shield.

A 10-layer Kapton insulation blanket is installed between the stack and the LN_2 shield.

The cold mass assy is covered with a 20-layer Kapton insulation blanket (MLI) and installed into an .032-inch thick copper alloy LN_2 shield, see Drawing 11-38040. The cold mass supports project beyond the diameter of the LN_2 shield, therefore, it is necessary to fabricate the shield in two halves with cutouts to accept the supports. These halves are installed from each side of the cold mass assy and riveted together at the circumferential centerline. The halves consist of a rolled inner and outer ring brazed to a side plate. The outer ring is 35.14 inches in diameter, and the inner ring is 17.14 inches in diameter. The completed LN_2 shield assy is 10.50 inches wide.

Two 1/2-inch O.D. copper tubes are brazed to the outer ring to provide an LN_2 supply line and an N_2 return line, Figure 4.1-5, to cool the shield.

MLI blankets are installed around the outside of the shield. Twenty (20) layers around the cold mass area, thirty (30) layers in the stack area, and due to space limitations, ten (10) layers in the inner bore.

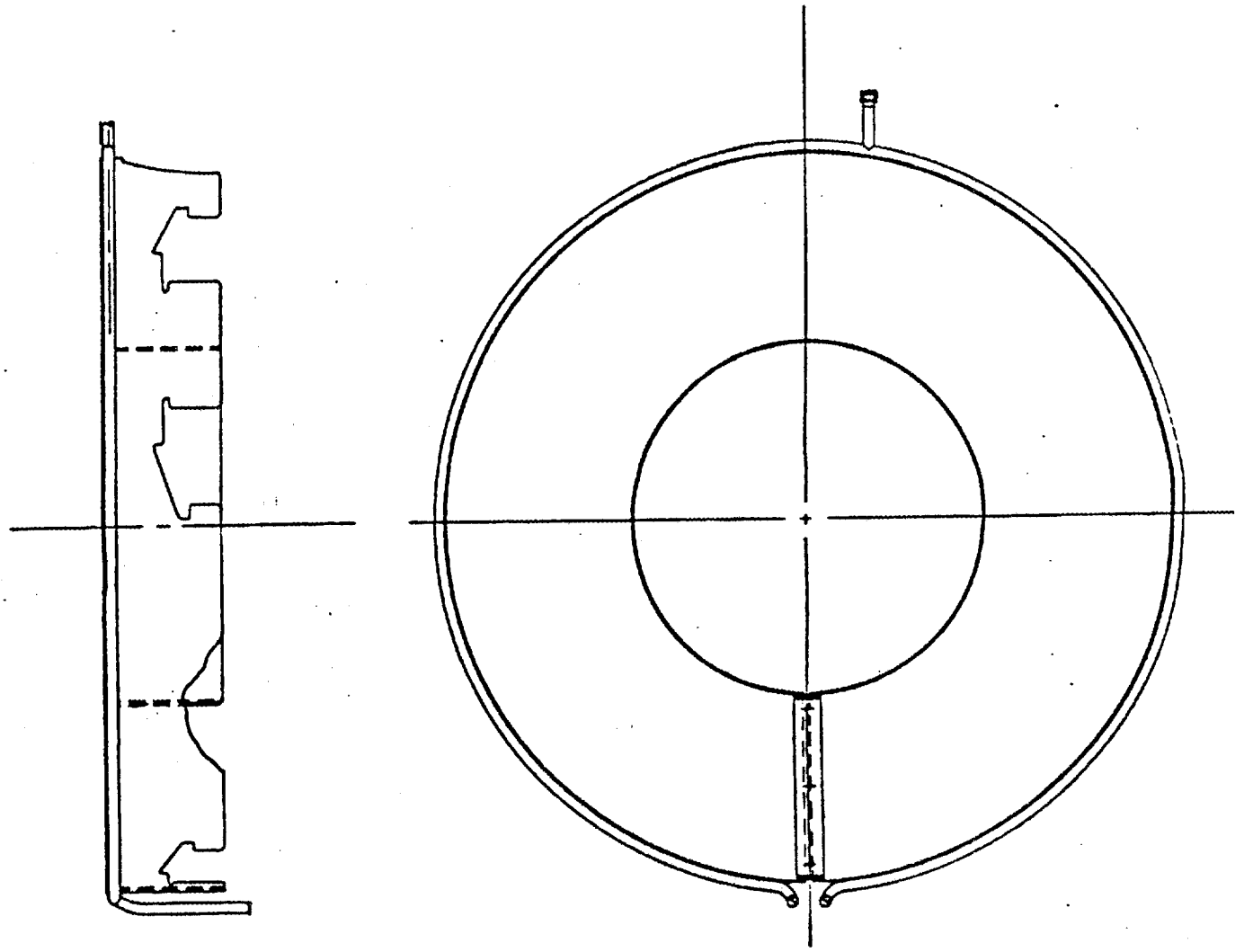

FIGURE 4.1-5 LN_2 COLD WALL WITH LN_2 TRACER TUBE

4.2 DEWAR DETAILS

The vacuum dewar, as shown in Drawing 11-38060, consists of an outer ring, an inner ring, side plates, stack plates, and a support assy. All materials are 304L stainless steel and are welded together using ER316L electrode.

The dewar is 12.0 inches wide and has a 1.00-inch thick outer ring with an outside diameter of 42.75 inches. The side plates are .25 inches thick, with a spun inner bore diameter of 16.50 inches.

The stack plates are .25 inches thick on the sides and .50 inches thick front and back. The stack sits on top of the outer ring and extends 48.0 inches above the horizontal centerline of the dewar.

The support assy. has a 1.5-inch thick plate to bolt to the bucking ring. The support plate is 33.84 inches aft of the vertical centerline of the dewar and is welded to the outer ring with gussets and side plates.

The external structure of the dewar shall have locations for alignment construction balls, fittings for out-of-plane struts, and six undersized holes thru the outer ring to pick up the location of the cold mass support bolt holes.

To complete the overall magnet assy, the cold mass assy is installed in the dewar and temporarily aligned to the proper adjustments. A dial indicator is inserted thru the six undersized holes in the dewar outer ring from the outside, to pick up the exact location of the bolt holes in the cold mass supports. After locating the exact center of the support bolt holes, the holes in the dewar are opened to insert a close-fit mounting lug. These lugs are then bolted to the supports and welded in place to the outside of the dewar, see Figure 4.2-1. This ensures an exact fit with no pre-load on the mounting bolts.

The close-out side plate of the dewar is then welded in place, Figure 4.2-2.

The completed magnet assy will be temporarily installed on the bucking ring and will then be optically aligned, using the construction balls located on the external structure to identify the location of the conductor midplane axes, see MDAC Interface Drawing 70B376001. The assembly will then be adjusted through four sets of spherical washers and spherical nuts bolted through the support structure and bucking ring, Figure 4.2-3, until it is in the required secured position as optically verified by the pre-determined construction ball location.

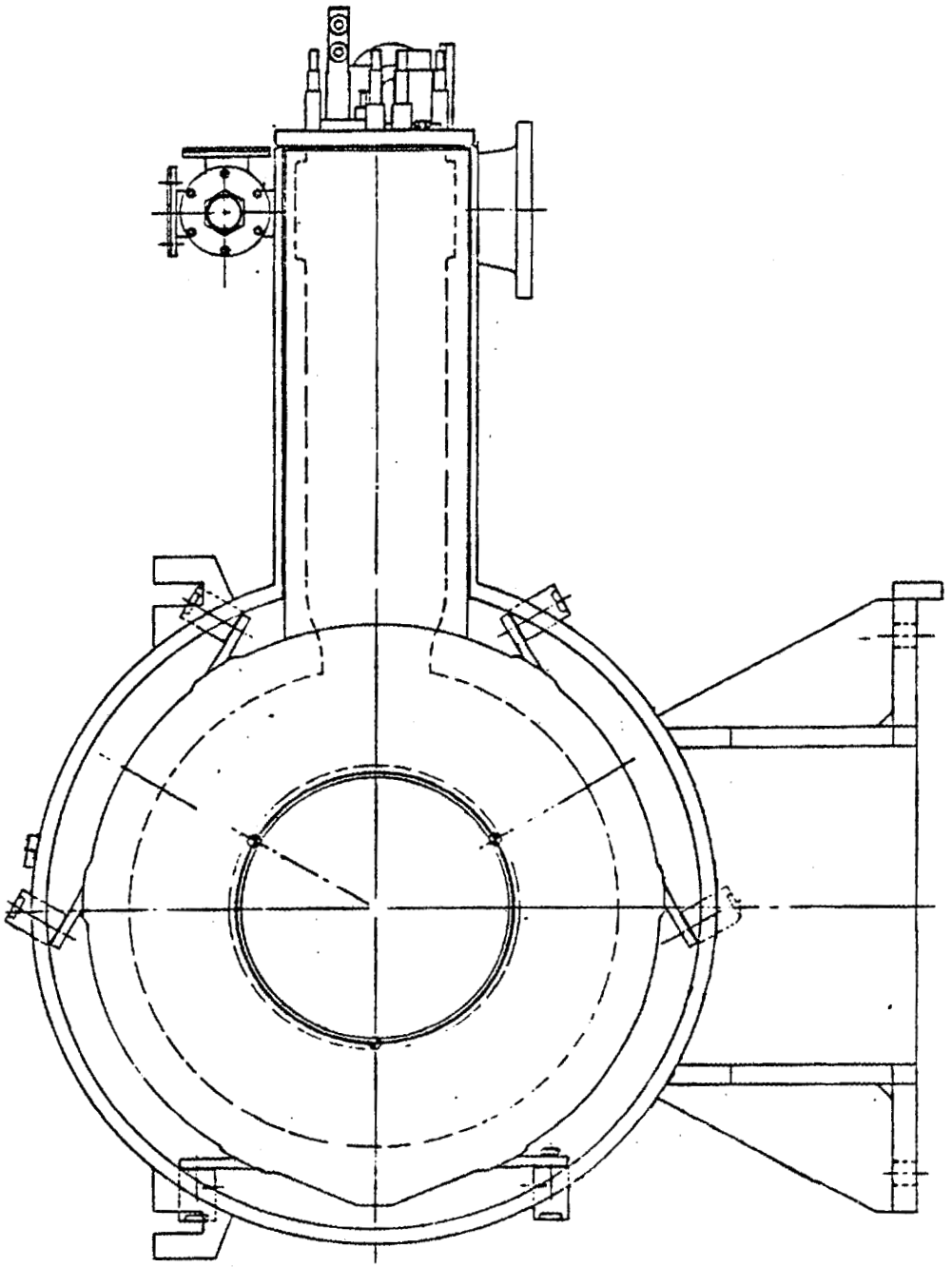

FIGURE 4.2-1 DEWAR WITH MOUNTING LUGS INSTALLED

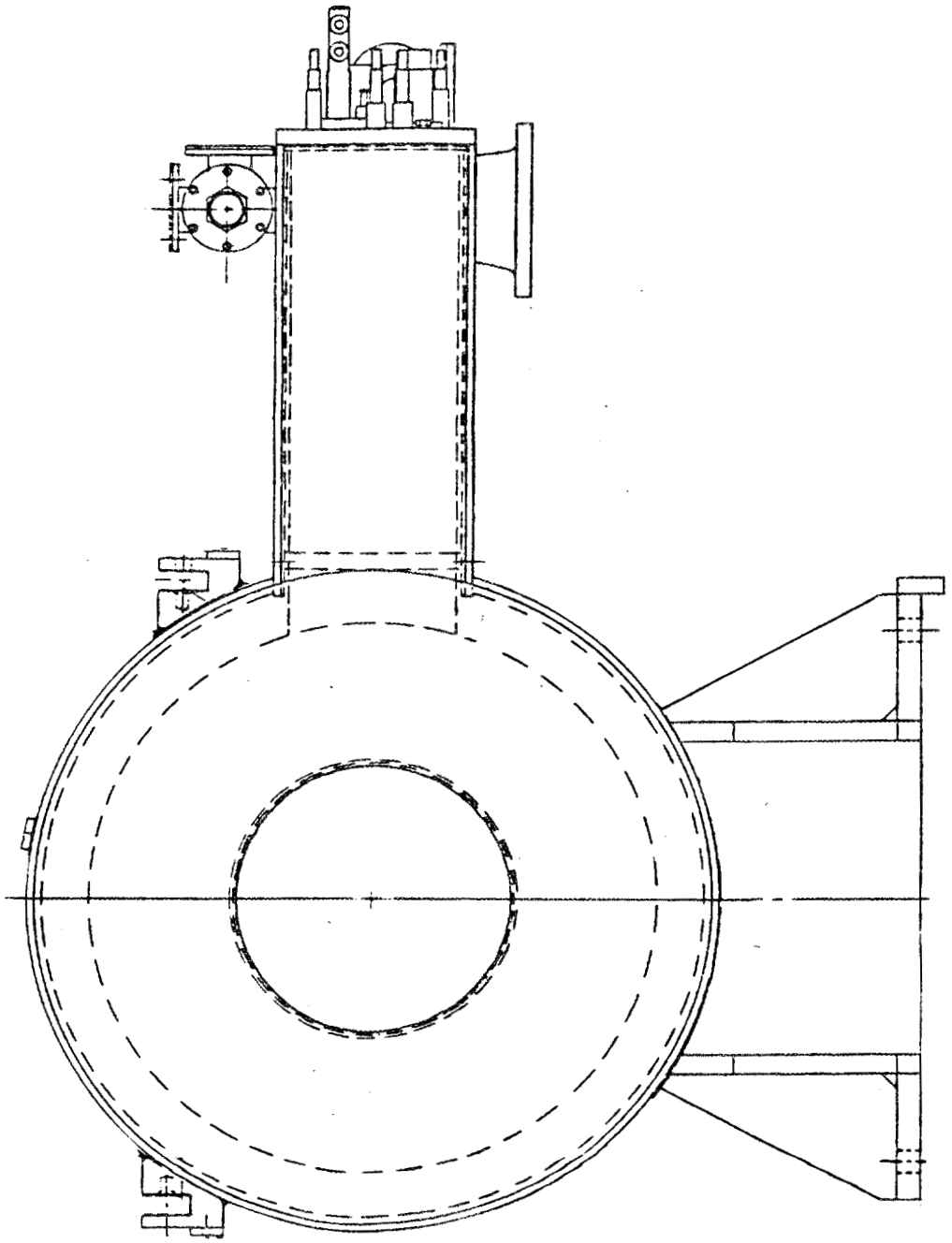

FIGURE 4.2-2 DEWAR WITH CLOSEOUT PLATE WELDED IN PLACE

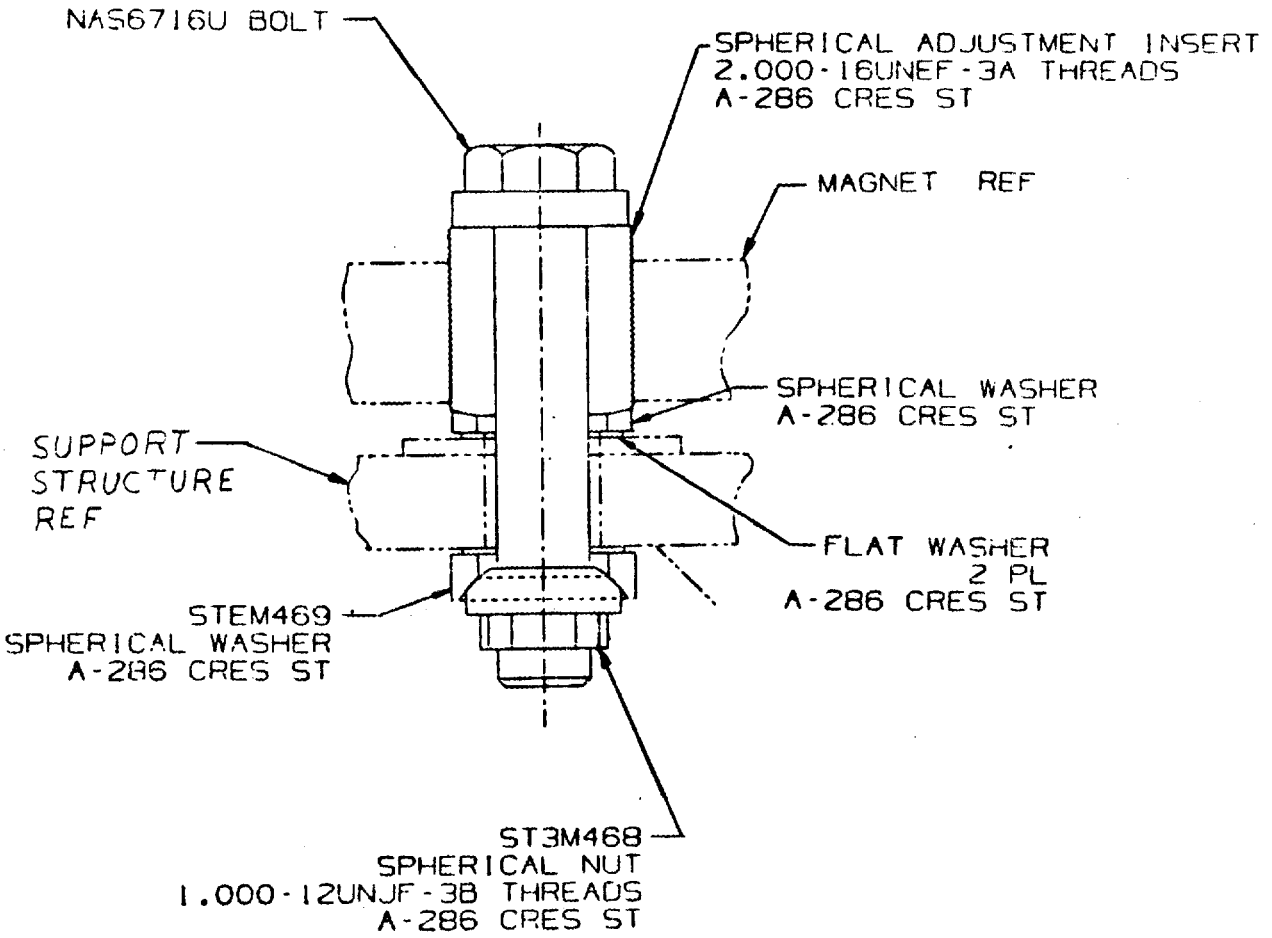

VIEW SHOWING MAGNET MOUNTING
BOLT ASSY
TYPICAL 4 PLCS PER MAGNET

FIGURE 4.2-3. MAGNET MOUNTING TENSION BOLTS

Following alignment verification, four dowel pins will be drilled and reamed through the magnet support structure and the bucking ring support. Locator pins will be inserted, the magnet support structure and bucking ring will be shimmed, and all support fasteners will be torqued.

4.3 X-RAY SHIELD

The baseline shield configuration incorporated a 3/4 inch tungsten throat and 1½ inch lead sides. Detailed analysis indicated that the tungsten throat was not necessary and that a thinner, contoured lead throat was more than sufficient. On the basis of the analysis, MDAC has submitted a Proposed Design Change (PDC) to replace the tungsten/lead baseline by an all lead shield. Additionally, the provision for water cooling of the shield was removed, since the steady-state temperature rise was found to be less than 10°F at upgrade operation. The envelope of the proposed shield is shown in drawing number 70B376008. This design, in conjunction with a stainless steel toroidal vessel, contoured along the 16.5 cm flux line, should provide a passing particle fraction of more than 35%. The shield is to be cast in equal halves, thus requiring only one tooling setup for manufacture. Since the throat is approximately a mean free path thick, streaming is insignificant and a stepped joint in the bore is not required. Any installation gaps can be filled with a lead paste or mortar. The shield is to be bolted to the outside of the magnet dewar prior to installation of the toroidal vessel vacuum liner. This simplified design greatly reduces cost with a very small impact to x-ray heating of the cold mass.

4.4 MAGNET INSTRUMENTATION

4.4.1 MEASUREMENT PROGRAM. The instrumentation measurement quantities and locations for the EBT-P development and production magnet systems have been established. A summary of the development magnet instrumentation quantities and general locations is presented in Figure 4.4-1. These include 27 temperature, 28 strain, and 1 each of liquid helium level, helium pressure, and an acoustic emission measurement to be tried experimentally on the first development magnet. Additionally, four vapor-cooled lead voltage measurements are included.

A development magnet measurement list including measurement number, type, location, range, sensor, installation drawing reference, and measurement period is included at the end of this section.

Figure 4.4-2 summarizes the production magnet measurements. These include six temperature, nine strain, one liquid helium level, one helium pressure, and four vapor-cooled lead voltage measurements and four coil winding voltage taps.

A production magnet measurement list is included at the end of this section.

4.4.2 TEMPERATURE MEASUREMENTS.

4.4.2.1 Development Magnets. Cooldown and warmup temperature sensors located on the helium vessel sidewalls and outer ring are cryogenic linear temperature sensors (CLTS) bonded to the measurement locations with cryogenic strain gage adhesives with the installation technique shown in Figure 4.4-3. The sensor wiring schematic is also depicted.

Similarly, the CLTS sensor is installed at nine additional locations on the support assemblies, three per assembly, and six locations within the stack assembly.

Cooldown, warmup and operational temperature measurements which utilize type E, chromel constantan thermocouples are installed as shown in Figure 4.4-4. The wiring schematic is also shown. The thermocouples are installed on each support assembly at the center attach point to the helium vessel and at three points on the liquid nitrogen shields.

4.4.2.2 Production Magnets. Two thermocouples are installed on the liquid nitrogen shields in the same manner as described for the development magnets, Figure 4.4-4.

Two CLTS sensors are installed on the warm end of the vapor-cooled leads per methods shown in Figure 4.4-3.

Two carbon glass resistors are installed in the liquid helium

FIGURE 4.4-1
EBT-P DEVELOPMENT MAGNET MEASUREMENT SUMMARY

TYPE	GENERAL LOCATION	QTY
TEMP	HELIUM VESSEL SIDEWALLS	5
	HELIUM VESSEL OUTER RING	1
	SUPPORT ASSEMBLY (4 PER ASSEMBLY)	12
	LN_2 SHIELD	3
	STACK ASSEMBLY INTERNAL	6
		27
STRAIN	HELIUM VESSEL INNER BORE	6
	HELIUM VESSEL OUTER RING	6
	HELIUM VESSEL SIDEWALLS	4
	SUPPORT ASSEMBLY (4 PER ASSEMBLY)	12
		28
LEVEL	STACK ASSEMBLY INTERNAL	1
PRESSURE	STACK ASSEMBLY INTERNAL	1
ACOUSTIC	STACK ASSEMBLY INTERNAL	1
VOLTAGE	VAPOR-COOLED LEADS (WARM AND COLD ENDS)	4

FIGURE 4.4-2
EBT-P PRODUCTION MAGNET MEASUREMENT SUMMARY

TYPE	GENERAL LOCATION	QTY
TEMP	HELIUM VESSEL, LHe BATH	2
	LN_2 SHIELD	2
	VAPOR-COOLED LEADS, WARM END	2
STRAIN	HELIUM VESSEL, INNER BORE	3
	SUPPORT ASSEMBLY (2 PER ASSEMBLY)	6
LEVEL	STACK ASSEMBLY INTERNAL	1
VOLTAGE	VAPOR-COOLED LEADS (WARM AND COLD ENDS)	4
	COIL WINDING	4
HELIUM PRESSURE	HELIUM OUTLET ASSY - PRESS. XDUCER	1
	- PRESS. SWITCH	1
VACUUM PRESSURE	VACUUM OUTLET ASSY - VACUUM MONITOR	1
	- VACUUM SWITCH	1

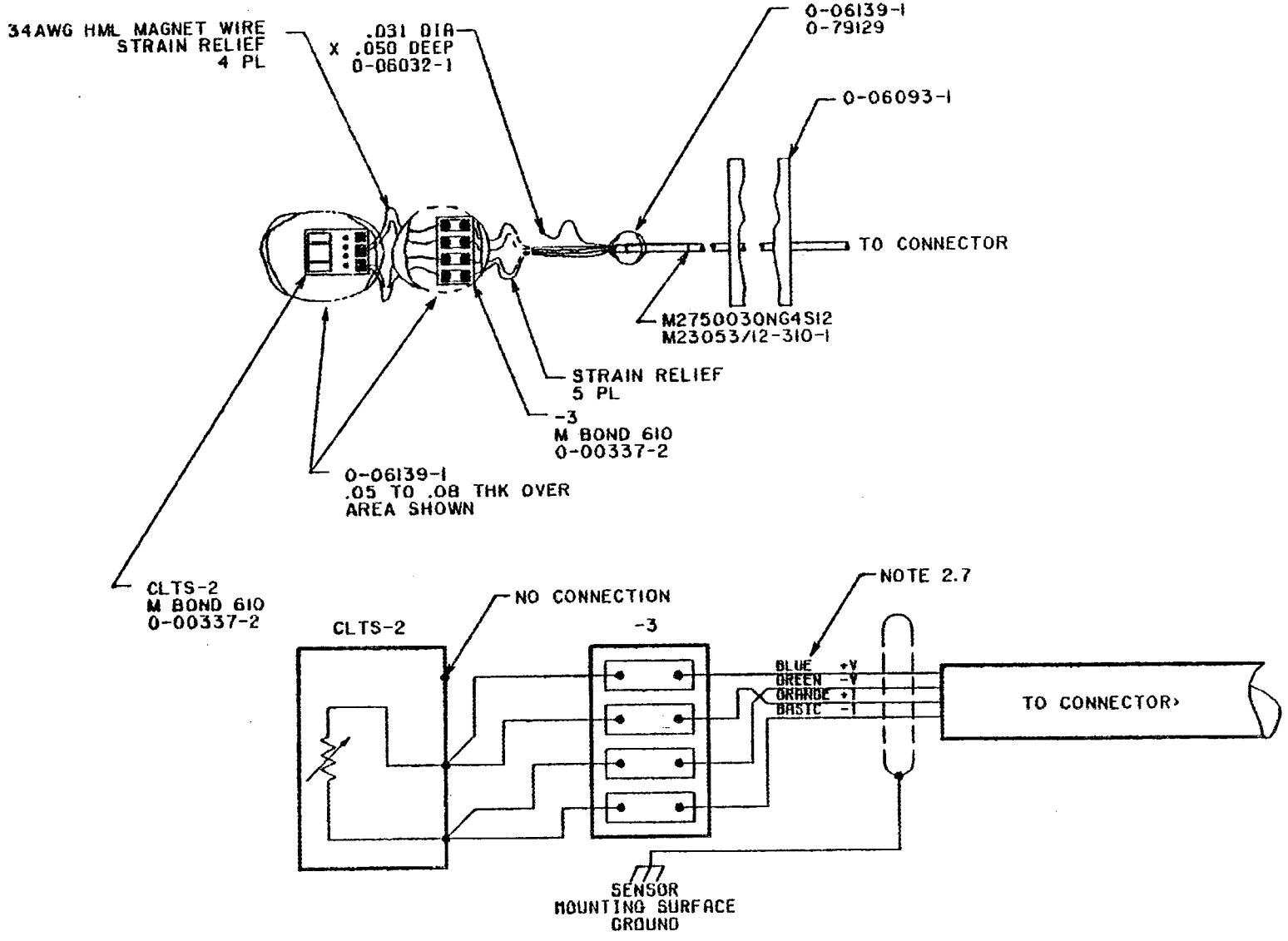

FIGURE 4.4-3 CLTS TEMPERATURE SENSOR INSTALLATION

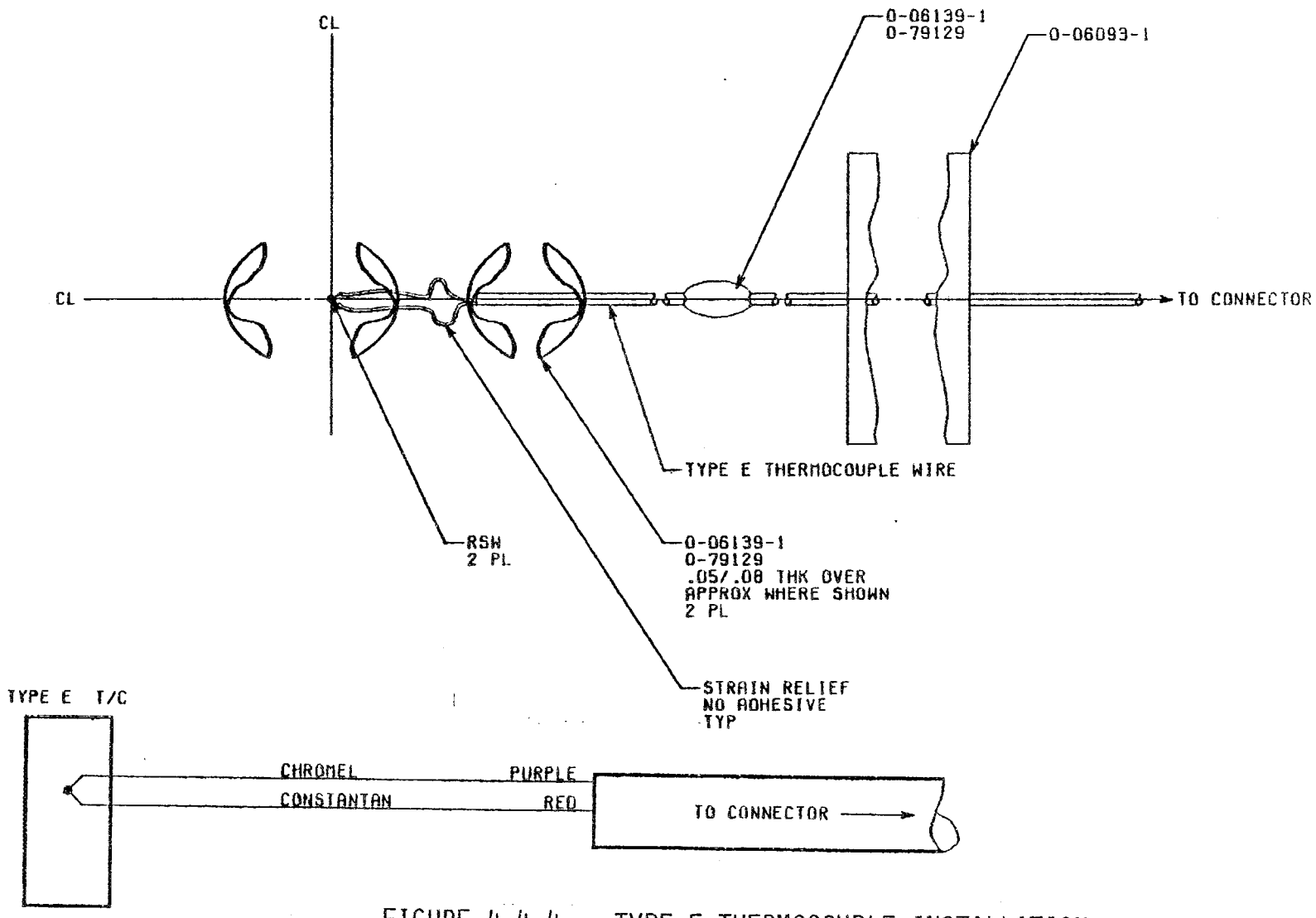

FIGURE 4.4-4. TYPE E THERMOCOUPLE INSTALLATION

to obtain cooldown, warmup and operational bath temperatures. The precise location and installation details have not been finalized at this time.

4.4.3 STRAIN MEASUREMENTS

4.4.3.1 Development Magnets. Karma alloy foil, bi-axial strain gages which are wired to form half-bridge completion networks, are used for the 16 helium vessel structural measurements. The gages are installed with cryogenic strain gage adhesives with the methods shown in Figure 4.4-5.

Karma alloy foil, single axis strain gages which are wired to form one-quarter active arm bridge completion networks, are used for the 12 support assembly measurements. Installation and wiring schematics for these gages are shown in Figure 4.4-6.

4.4.3.2 Production Magnets. Weldable, nickel-chrome alloy, single axis strain gages are used to form half-bridge completion networks for the six support assembly and three helium vessel inner bore measurement points. One of the half-bridge gages is active and the other half is a dummy, strain-free gage, that serves as a temperature compensation device. Each gage is temperature compensated from room temperature to liquid nitrogen temperature. The installation and wiring schematic for this gage has not been detailed at this time.

4.4.4 VOLTAGE MEASUREMENTS — ALL MAGNETS. Two voltage taps are installed on each vapor-cooled lead, one at the attach point to the coil conductor and one at the warm end above the stack area. Single conductor, shielded and jacketed, 30 AWG cables are used. The 30-gage conductor is stripped back and inserted into a .030 to .050 deep hole drilled at the attach point. The hole around the tap wire is filled with silver-filled conductive epoxy.

Voltage tap installations are planned, for production magnets only, at an additional four places within the coil winding. These taps will be soft soldered to the conductor surface.

4.4.5 LIQUID HELIUM LEVEL MEASUREMENT — ALL MAGNETS. An NbTi superconducting helium level sensor is installed in the stack of each magnet. The active level sensing length will extend from the minimum helium level point within the stack to the highest liquid point.

4.4.6 HELIUM VESSEL PRESSURE — ALL MAGNETS. A cryogenic strain gage pressure transducer is installed on each stack assembly. The sensor is close coupled to a pressure tube that penetrates the helium outlet flange.

4.4.7 ACOUSTIC EMISSION MEASUREMENT — DEVELOPMENT MAGNET. One acoustic emission sensor is installed in the first development

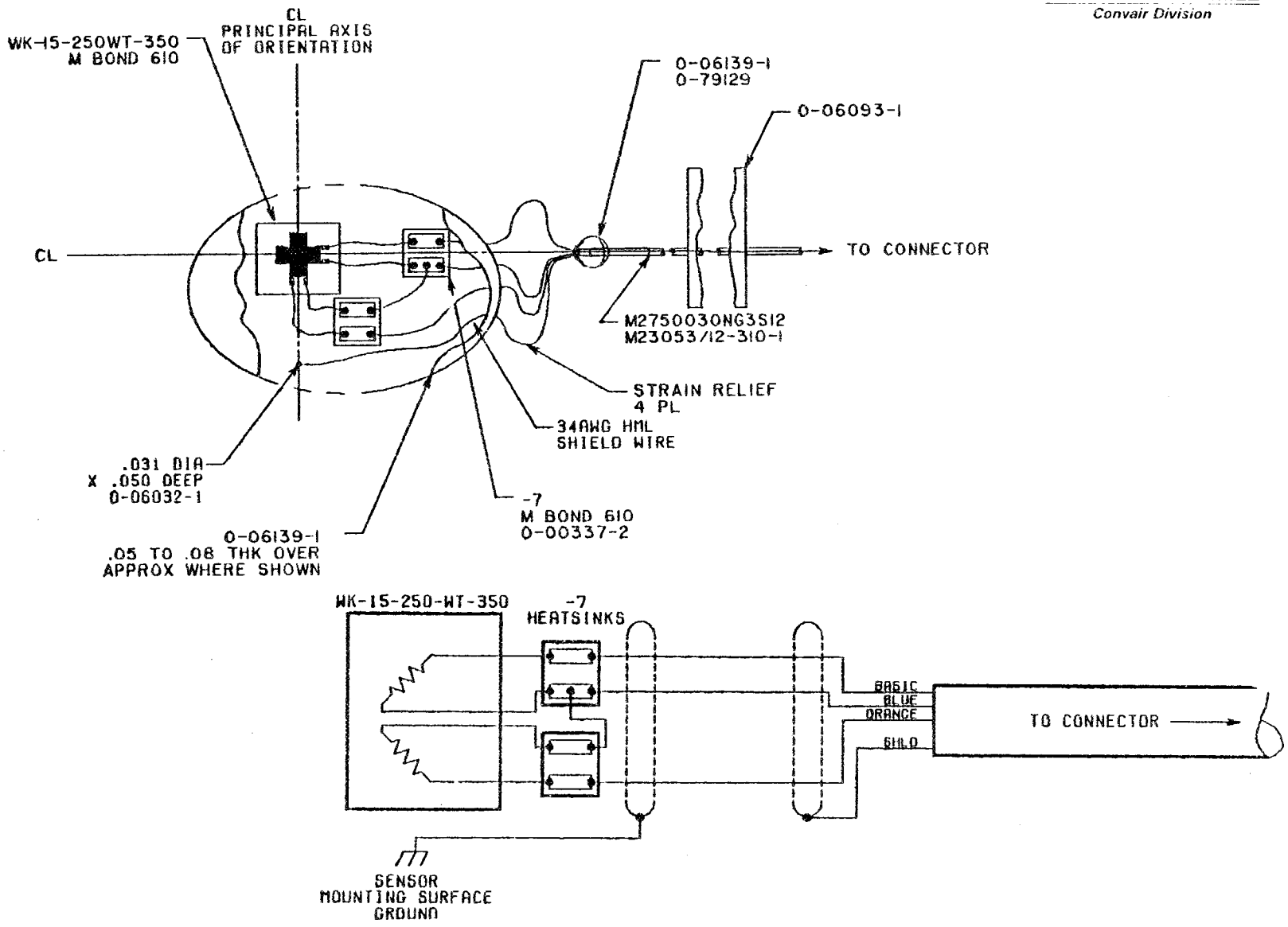

FIGURE 4.4-5 BI-AXIAL STRAIN GAGE

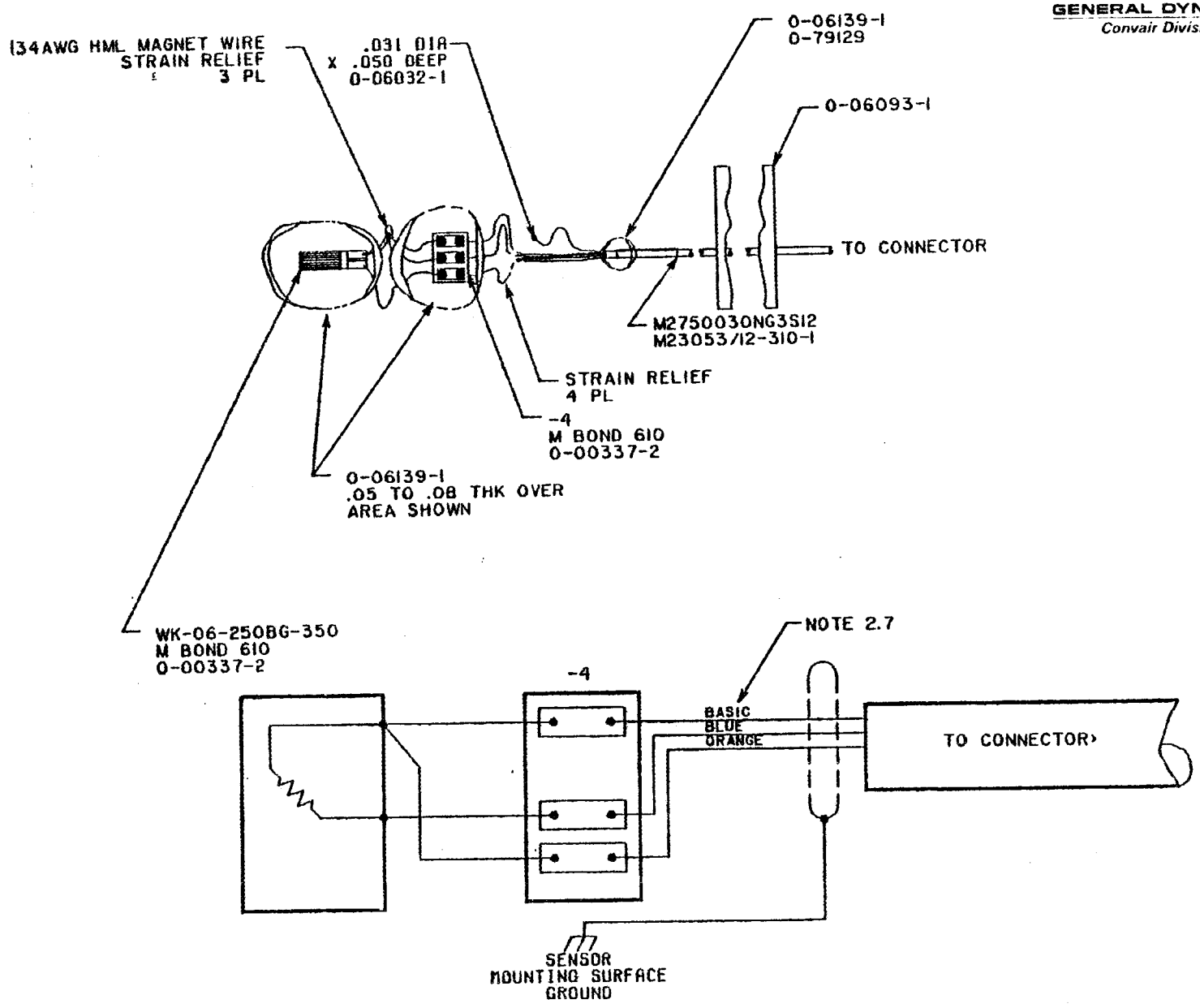

FIGURE 4.4-6 SINGLE AXIS SUPPORT ASS'Y. STRAIN GAGES

magnet for experimental purposes. The sensor is located in the stack assembly at the minimum liquid helium level point. The sensor is a quartz crystal, high frequency, pressure transducer.

4.4.8 SENSOR DESCRIPTIONS

4.4.8.1 Temperature Sensors. The temperature sensor part numbers and descriptions are shown in Figure 4.4-7 for the development magnets and Figure 4.4-10 for the production magnets.

4.4.8.2 Strain Gages. Strain gage part number and descriptions are shown in Figure 4.4-7 for the development magnets and Figure 4.4-11 for production magnets. It is considered necessary to use weldable strain gages instead of adhesive bonded gages for production magnets for the following reasons: 10-year life requirement, limited number of gages, radiation environment, and due to the inaccessibility for replacement. These gages also provide better temperature compensation and less apparent strain due to magnetic field affect.

4.4.8.3 Acoustic Emission. The acoustic emission sensor planned for installation in the first development magnet is described in Figure 4.4-8. The usage of this sensor is considered strictly developmental at this time.

4.4.8.4 Liquid Helium Level Sensor. The superconducting wire helium level sensor is insensitive to magnetic fields up to 10 Tesla. The 70 milliampere current carried by the NbTi assures resistive operation in helium gas and superconducting operation in liquid helium. A description of this sensor is shown in Figure 4.4-9.

4.4.8.5 Helium Vessel Pressure Transducer. The part number and description of the helium vessel pressure transducer is shown in Figure 4.4-9. This transducer is a highly accurate and stable device used where cryogenic temperature and long-term stability is of concern. The sensor has a time response of approximately 50 milliseconds.

4.4.9 ELECTRICAL WIRING. The instrumentation and control wiring is expected to be of three configurations: single conductor, three conductor, and four conductor. Single conductor 30 AWG wire is used for voltage taps, and multiconductor 30 AWG wire is used for the remaining sensor types. All wires are silver plated copper. All cables are insulated with Kapton-FEP insulation for wires and jackets. All insulation materials average approximately .004 inch thick.

All cables are shielded. The single and multiconductor cable has a silver plated copper braided wire shield for added mechanical protection and noise minimization. The shield coverage is specified as 85% minimum.

FIGURE 4.4-7
DEVELOPMENT MAGNET SENSOR DESCRIPTIONS

STRAIN GAGES

PART NO.	WK-06-250BG-350	WK-15-250WT-350
CONSTRUCTION:	THIN FOIL SENSING GRID OF 'K' ALLOY ENCAPSULATED IN GLASS-FIBRE REINFORCED EPOXY RESIN	THIN FOIL SENSING GRIDS (TWO 90° AXIAL GAGES) OF 'K' ALLOY ENCAPSULATED IN GLASS-FIBRE REINFORCED EPOXY RESIN
SIZE:	0.052" LONG X 0.22" WIDE (OVERALL)	0.51" LONG X 0.60" WIDE (OVERALL MATRIX)
RESISTANCE:	350 ± 0.3%	350 ± 0.3%
RANGE:	± 1.5% STRAIN	± 1.5% STRAIN

FIGURE 4.4-7
DEVELOPMENT MAGNET SENSOR DESCRIPTIONS

TEMPERATURE SENSORS

PART NO.:	HF/D-30-E	CLTS-2
CONSTRUCTION:	TYPE E, THERMOCOUPLE WIRE, CROMEL CONSTANTAN 30 AWG CONDUCTORS KAPTON TAPE INSULATION	THIN FOIL SENSING GRIDS OF NICKEL AND MANGANIN LAMINATED INTO GLASS-FIBRE REINFORCED EPOXY RESIN MATRIX WITH INTEGRAL Cu PRINTED CRKT TERMINALS
SIZE:	0.04 INCH OUTER DIA.	0.430" LONG X 0.310" WIDE X 0.0004" THK
RESISTANCE:	N/A	296.9°K = 290 OHMS ± 0.5% 4.1°K = 220 OHMS (NOMINAL)
RANGE:	300 TO 4.2°K	300 TO 4.2°K

-CONTINUED-

FIGURE 4.4-8
DEVELOPMENT MAGNET SENSOR DESCRIPTIONS

ACOUSTIC EMISSION SENSOR

PART NO.:	701H
CONSTRUCTION:	QUARTZ CRYSTAL ELEMENT MOUNTED ON STAINLESS STEEL DIAPHRAGM. THE FLUSH-MOUNTED DIAPHRAGM IS HERMETICALLY WELDED TO A STAINLESS STEEL TRANSDUCER HOUSING.
CALIB. PRESS. RANGES:	0 TO 85 PSI AND 0 TO 850 PSI
RESONANT FREQ.:	65 KHz
RESOLUTION:	0.006 PSI
SENSITIVITY:	≃ 200 MV/PSI

FIGURE 4.4-9
DEVELOPMENT & PRODUCTION HELIUM PRESSURE
AND LIQUID HELIUM LEVEL SENSOR DESCRIPTIONS

HELIUM PRESSURE TRANSDUCER

PART NO.:	CEC 1000-05
CONSTRUCTION:	FOUR ACTIVE, SPUTTERED THIN FILM STRAIN GAGES DEPOSITED ON A DIAPHRAGM HOUSED IN A 17-4PH STAINLESS STEEL HOUSING
RANGE:	0-50 PSIA
PROOF PRESS:	100 PSIA WITHOUT CALIB SHIFT
EXCITATION:	10 VDC
OUTPUT:	0 TO 30 MV
ACCURACY:	± 0.25%
BRIDGE RES.:	300 TO 500 OHMS

LIQUID HELIUM LEVEL GAGE

PART NO.:	11-38032-1
CONSTRUCTION:	NIOBIUM TITANIUM SUPERCONDUCTING WIRE INSTALLED IN .25 DIA. FIBERGLASS TUBE
OPERATING CURRENT:	70 MA
SIZE:	14-INCH ACTIVE SENSOR LENGTH WITH 18.9-INCH TUBE EXTENSION
RESISTANCE:	4.5 OHM/CM IN NORMAL STATE

FIGURE 4.4-10

PRODUCTION MAGNET TEMPERATURE SENSOR DESCRIPTIONS

PART NO.:	HF/D-30-E
CONSTRUCTION:	TYPE E, THERMOCOUPLE WIRE,
	CROMEL CONSTANTAN
	30 AWG CONDUCTORS
	KAPTON TAPE INSULATION
SIZE:	0.04-INCH OUTER DIA.
RANGE:	300 TO 4.2°K

FIGURE 4.4-10

PRODUCTION MAGNET TEMPERATURE SENSOR DESCRIPTIONS

TEMPERATURE SENSORS

PART NO.:	CGR-1-1000	CLTS-2
CONSTRUCTION:	CARBON GLASS ELEMENT HOUSED IN GOLD PLATED Cu CYLINDER FILLED WITH He 4 GAS	THIN FOIL SENSING GRIDS OF NICKEL AND MANGANIN LAMINATED INTO GLASS-FIBRE REINFORCED EPOXY RESIN MATRIX WITH INTEGRAL Cu PRINTED CRKT TERMINALS
SIZE:	0.120" DIA. X 0.335" LONG	0.430" LONG X 0.310" WIDE X 0.0004" THK
RESISTANCE:	$300^{o}K$ = 10 OHMS (NOMINAL) $4.2^{o}K$ = 1000 OHMS (NOMINAL)	$296.9^{o}K$ = 290 OHMS $\pm$ 0.5% $4.1^{o}K$ = 220 OHMS (NOMINAL)
RANGE:	300 TO $4.2^{o}K$	300 TO $4.2^{o}K$

-CONTINUED-

FIGURE 4.4-11

PRODUCTION MAGNET STRAIN GAGE DESCRIPTION

STRAIN GAGES

PART NOS.:	SG-355/12-09-1/4-TITANIUM & SG-355/12-09-1/4-316
CONSTRUCTION:	HALF-BRIDGE (1 ACTIVE, 1 DUMMY) 350 OHM NICROME WIRE GAGES INSTALLED IN 321 STAINLESS STEEL TUBE FILLED WITH MAGNESIUM OXIDE POWDER. THE STRAIN TUBE IS ON A FLANGE USED FOR SPOTWELDING TO THE TEST MAT'L.
SIZE:	1.093 INCH GAGE TUBE LENGTH X 0.187 INCH WIDE WELDING FLANGE
RESISTANCE:	350 ± 5 OHMS
RATED STRAIN:	± 20,000 $\mu\epsilon$

All cables have a voltage rating of 600 volts rms and will be sample tested by the supplier at 1500 volts from conductor to conductor and conductor to shield. (See Figure 4.4-12 for the electrical wire summary.)

4.4.10 ELECTRICAL CONNECTORS

4.4.10.1 Vacuum Vessel Interface Connectors. The development magnets utilize two 128-pin, hermetic, jam-nut mounted receptacles and one 37-pin, hermetic, jam-nut mounted receptacle for wiring all internally mounted temperature sensors and strain gages.

One of the 128-pin receptacles is utilized for all of the 28 strain gage measurements. The second 128-pin receptacle is utilized for all 15 CLTS-2 internally-mounted temperature sensors.

The 37-pin receptacle, which consists of 8 pairs of chromel/constantan contacts plus 21 gold plated, copper alloy contacts, is utilized with the 6 internally located thermocouple measurements.

The 128-pin, hermetic receptacles, manufactured by ITT Cannon, are an environmental resistant class rated for -65 to 150°C temperature operation.

The shell material is aluminum alloy, with cadmium over electroless nickel plating. The shell size is 24-35 which contains 128 number 22 gage, gold plated, copper alloy, crimp contacts.

The part number is KJ7Y24E35PN. The mating plug part number is KJ6F24N35SN which is an environmental resistant, straight plug with strain relief.

The 37-pin, hermetic receptable, also manufactured by ITT Cannon is an environmental resistant class rated for -162 to 232°C temperature operation.

The shell material is stainless steel with clear chromate over cadmium plating. The shell size is 28-21 which contains 8 chromel, 8 constantan, and 21 gold plated, copper alloy, number 16 gage, solder pot contacts.

The part number is BFH20412-117. The mating plug part number is CA24275-4388 which is an environmental resistant, straight plug with strain relief.

The production magnets will utilize one of the above described 37-pin connectors and one 42-pin connector, as described later, on each vacuum vessel interface.

4.4.10.2 Helium Vessel Interface Connector. Each production and development magnet will utilize one 42-pin, hermetic,

FIGURE 4.4-12
ELECTRICAL WIRE SUMMARY

FUNCTION	PART DESCRIPTION	PART NO.
CABLE FOR VOLTAGE TAPS	ONE CONDUCTOR, SHIELDED & JACKETED CONDUCTOR: 30 AWG, Ag PLATED Cu INSULATION: .004 WALL KAPTON-FEP SHIELD: Ag PLATED Cu BRAIDED WIRE VOLTAGE RATING: 600 VRMS	M2750030NG1S12
CABLE FOR STRAIN GAGES	THREE CONDUCTOR, SHIELDED & JACKETED CONDUCTOR: 30 AWG, Ag PLATED Cu INSULATION: .004 WALL KAPTON-FEP SHIELD: Ag PLATED Cu BRAIDED WIRE VOLTAGE RATING: 600 VRMS	M2750030NG3S12
CABLE FOR CARBON GLASS RESISTORS, CLTS TEMP. SENSORS	FOUR CONDUCTOR SHIELDED & JACKETED ALL OTHER PROPERTIES SAME AS ABOVE	M2750030NG4S12

weld-mounted receptacle for wiring connections to all internally mounted voltage taps and temperature sensors.

The 42-pin, hermetic, weld-mount receptacle, manufactured by Hermetic Seal Corp., is an environmental resistant class rated for -55° to 175°C temperature operation.

The shell material is passivated 303 or 304L stainless steel. The shell size is 44-1, which contains 36 number 16 gage and 6 number 12 gage, gold plated copper, solder contacts. The voltage rating for this contact arrangement is 2800 volts rms at sea level.

The part number is SSR-2053-44-1P (gold). The mating plug part number is MS3106B44-1S, which is an environmental resistant straight plug with strain relief.

The connector types are summarized in Figure 4.4-13.

FIGURE 4.4-13
ELECTRICAL CONNECTOR SUMMARY

FUNCTION	PART DESCRIPTION	PART NO.
*VACUUM VESSEL, RECEPTACLE	CIRCULAR, 128, 22 AWG PINS, CRIMP HERMETIC, JAM-NUT MOUNTED ALUMINUM ALLOY, CAD OVER NI SHELL	KJ7Y24E35PN
*PLUG, MATES WITH ABOVE	CIRCULAR, STRAIGHT PLUG WITH STRAIN RELIEF, ENVIRONMENTAL BAYONET COUPLED	KJ6F24N35SN
VACUUM VESSEL, RECEPTACLE	CIRCULAR, 37, 16 AWG PINS, SOLDER 8 CHROMEL, 8 CONSTANTAN, 21 COPPER HERMETIC, JAM-NUT MOUNTED STAINLESS STEEL, CHROMATE OVER CAD SHELL	BFH20412-117
PLUG, MATES WITH ABOVE	CIRCULAR, STRAIGHT PLUG WITH STRAIN RELIEF, ENVIRONMENTAL, THREADED COUPLING	CA24275-4388
HELIUM VESSEL, RECEPTACLE	CIRCULAR, 42, SOLDER CONTACTS 36, 16 AWG AND 6, 12 AWG HERMETIC, WELD MOUNT PASSIVATED STAINLESS STEEL SHELL	SSR-2053-44-1P
PLUG, MATES WITH ABOVE	CIRCULAR, STRAIGHT PLUG WITH STRAIN RELIEF, ENVIRONMENTAL, THREADED COUPLING	MS3106B44-1S

*DEVELOPMENT MAGNETS ONLY

EBT-P DEVELOPMENT PROGRAM

MEASUREMENT LIST

MEAS. NO.	DESCRIPTION/ LOCATION	MEASUREMENT RANGE		UNITS	TRANSDUCER DESCRIPTION	TRANSDUCER PART NO.	INSTALLATION DWG.NO.	MEASUREMENT PERIOD	
		LOW	HIGH					COOL-DOWN WARMUP	OPERATION
T1	TEMP., RT. SIDEWALL	4.2	300	°K	Nickel Manganin Resistance	CLTS-2	D11-38087*	X	
T2								X	
T3								X	
T4	TEMP., RT. SIDEWALL	4.2	300					X	
T5	TEMP., LT. SIDEWALL	4.2	300		Nickel Manganin Resistance	CLTS-2		X	
T6	TEMP., CTR. MTG. SUPPORT STRAP				T/C, Type E	HF/D-30-E		X	X
T7	TEMP., CTR. MTG. SUPPORT STRAP				T/C, Type E			X	X
T8	TEMP., CTR. MTG. SUPPORT STRAP	4.2	300		T/C, Type E			X	X
T9	TEMP., OUTER RING	4.2	300		Nickel Manganin Resistance	CLTS-2		X	
T10	TEMP., SUPPORT STRAP	77	300		Nickel Manganin Resistance	CLTS-2		X	
T11								X	
T12								X	
T13								X	
T14								X	
T15								X	
T16								X	
T17	TEMP., SUPPORT STRAP	77	300		Nickel Manganin Resistance	CLTS-2	D11-38087	X	
T18	TEMP., LN2 SHIELD	77	300		T/C,Type E,CrCn	HF/D-30-E	D11-38089	X	X

*Ref. ORNL SK-TJM-881-001

EBT-P DEVELOPMENT PROGRAM

MEASUREMENT LIST

MEAS. NO.	DESCRIPTION/ LOCATION	MEASUREMENT RANGE		UNITS	TRANSDUCER DESCRIPTION	TRANSDUCER PART NO.	INSTALLA-TION DWG.NO.	MEASUREMENT PERIOD	
		LOW	HIGH					COOL-DOWN WARMUP	OPERA-TION
T19	TEMP., LN2 SHIELD	77	300	°K	T/C,Type E,CrCn	HF/D-30-E	D11-38089	X	X
T20	TEMP., LN2 SHIELD	77	300	↓	T/C,Type E,CrCn	↓	D11-38089	X	X
T21	BETWEEN HT. STA. TEMP., STACK,	77	300	°K	Nickel/Manganin Resistance	CLTS-2	D11-38086	X	X
T22	TEMP., SUPPORT STRAP	77	300	↓	Nickel Manganin Resistance	CLTS-2	D11-38087	X	
T23	CONNECTION TEMP.,STACK,VCL,	4.2	300	°K	↓	↓	D11-38086	X	X
T24	PLATE TEMP,STACK,LOWER G10	4.2	300	↓	↓	↓	↓	X	X
T25	TEMP,STACK,Cu PLATE	77	300	↓	↓	↓	↓	X	X
T26	TUBE TEMP,STACK,He VENT	77	300	↓	↓	↓	↓	X	X
T27	INNER WALL TEMP,STACK, TUBE,	77	300	°K	Nickel Manganin Resistance	CLTS-2	D11-38086	X	X

EBT-P DEVELOPMENT PROGRAM

MEASUREMENT LIST

MEAS. NO.	DESCRIPTION/ LOCATION	MEASUREMENT RANGE		UNITS	TRANSDUCER DESCRIPTION	TRANSDUCER PART NO.	INSTALLATION DWG. NO.	MEASUREMENT PERIOD	
		LOW	HIGH					COOL-DOWN WARMUP	OPERATION
S1	STRAIN, HOOP, INNER BORE			$\mu\xi$	Karma Alloy Foil Gage	WK-15-250WT-350	D11-38087*	X	X
S2								X	X
S3								X	X
S4	STRAIN, HOOP, INNER BORE							X	X
S5	STRAIN, AXIAL, INNER BORE							X	X
S6	STRAIN, AXIAL, INNER BORE							X	X
S7	STRAIN, AXIAL, OUTER RING							X	X
S8								X	X
S9								X	X
S10								X	X
S11								X	X
S12	STRAIN, AXIAL, OUTER RING							X	X
S13	STRAIN, RADIAL, RT. SIDEWALL							X	X
S14	STRAIN, RADIAL, RT. SIDEWALL							X	X
S15	STRAIN, RADIAL, LT. SIDEWALL							X	X
S16	STRAIN, RADIAL LT. SIDEWALL			$\mu\xi$	Karma Alloy Foil Gage	WK-15-250WT-350	D11-38087*	X	X

*Ref ORNL SK-TJM-881-001

EBT-P DEVELOPMENT PROGRAM

MEASUREMENT LIST

MEAS. NO.	DESCRIPTION/ LOCATION	MEASUREMENT RANGE		UNITS	TRANSDUCER DESCRIPTION	TRANSDUCER PART NO.	INSTALL-ATION DWG. NO.	MEASUREMENT PERIOD	
		LOW	HIGH					COOL-DOWN WARM-UP	OPER-ATION
S17	STRAIN, SUPPORT STRAP			$\mu\varepsilon$	KARMA ALLOY FOIL GAGE	WK-06-250BG-350	D11-38087	X	X
S18								X	X
S19								X	X
S20								X	X
S21								X	X
S22								X	X
S23								X	X
S24								X	X
S25								X	X
S26								X	X
S27								X	X
S28	STRAIN, SUPPORT STRAP			$\mu\varepsilon$	KARMA ALLOY ~~FOIL GAGE~~	WK-06-250BG-350	D11-38087	X	X

EBT-P DEVELOPMENT PROGRAM

MEASUREMENT LIST

MEAS. NO.	DESCRIPTION/ LOCATION	MEASUREMENT RANGE		UNITS	TRANSDUCER DESCRIPTION	TRANSDUCER PART NO.	INSTALLA-TION DWG.NO.	MEASUREMENT PERIOD	
		LOW	HIGH					COOL-DOWN WARMUP	OPERA-TION
V1	VOLTAGE, VCL. COLD END	N/A	N/A	MV	VOLTAGE TAP	GDC FABRICATED	D11-38086	X	X
V2	↓	↓	↓	↓	↓	↓	D11-38086	X	X
V3	VOLTAGE, VCL, WARM END	↓	↓	↓	↓	GDC FABRICATED	D11-38086	X	X
V4	↓	↓	↓	MV	VOLTAGE TAP	GDC FABRICATED	D11-38086	X	X
P1	PRESSURE, HELIUM VESSEL	0	50	PSI	STRAIN GAGE, THIN FILM	CEC-1000-05	D11-38086	X	X
L1	HELIUM LEVEL, STACK	0	14	IN	SUPERCONDUCTING WIRE	D11-38032-3	D11-38030	X	X
AE1	ACOUSTIC EMISSION, STACK	0	85	PSI	QUARTZ CRYSTAL	701H	D11-38086	X	X

EBT-P PROTOTYPE AND PRODUCTION

MEASUREMENT LIST

MEAS. NO.	DESCRIPTION/ LOCATION	MEASUREMENT RANGE		UNITS	TRANSDUCER DESCRIPTION	TRANSDUCER PART NO.	INSTALLATION DWG. NO.	MEASUREMENT PERIOD	
		LOW	HIGH					COOL-DOWN WARMUP	OPERATION
T1	TEMP, VCL, WARM END	200	300	°K	Nickel Manganin Resistor	CLTS-2	11-38086 (1) 71E-2086 (2)	X	X
T2	TEMP, VCL, WARM END	200	300	°K	Nickel Manganin Resistor	CLTS-2	11-38086 71E-2086	X	X
T3	TEMP, LN_2 SHIELD	77	300	°K	TYPE E, T/C CR-CN	HF/D-30-E	11-38089 71E-2089	X	X
T4	TEMP, LN_2 SHIELD	77	300	°K	TYPE E, T/C CR-CN	HF/D-30-E	11-38089 71E-2089	X	X
T5	TEMP, LHe BATH	4.2	300	°K	CARBON GLASS RESISTOR	CGR-1-1000	11-38087 71E-2087	X	X
T6	TEMP, LHe BATH	4.2	300	°K	CARBON GLASS RESISTOR	CGR-1-1000	11-38087 71E-2087	X	X

(1) PROTOTYPE
(2) PRODUCTION

EBT-P PROTOTYPE AND PRODUCTION

MEASUREMENT LIST

MEAS. NO.	DESCRIPTION/ LOCATION	MEASUREMENT RANGE		UNITS	TRANSDUCER DESCRIPTION	TRANSDUCER PART NO.	INSTALLATION DWG. NO.	MEASUREMENT PERIOD	
		LOW	HIGH					COOL-DOWN WARMUP	OPERATION
S1	STRAIN, SUPPORT			$\mu\epsilon$	NI CR, WELDABLE, 1/2 BRIDGE	SG-355/12-09-1/4-TI	11-38087 71E-2087	(1) (2) X	X
S2	↓			↓	↓	↓	↓	X	X
S3	↓			↓	↓	↓	↓	X	X
S4	↓			↓	↓	↓	↓	X	X
S5	↓			↓	↓	↓	↓	X	X
S6	STRAIN, SUPPORT			$\mu\epsilon$	NI CR, WELDABLE, 1/2 BRIDGE	SG-355/12-09-1/4-TI	11-38087 71E-2087	X	X
S7	STRAIN, INNER BORE HELIUM VESSEL			$\mu\epsilon$	NI CR, WELDABLE 1/2 BRIDGE	SG-155/12-09-1/4-316	11-38087 71E-2087	X	X
S8	↓			↓	↓	↓	↓	X	X
S9	STRAIN, INNER BORE HELIUM VESSEL			$\mu\epsilon$	NI CR, WELDABLE, 1/2 BRIDGE	SG-355/12-09-1/4-316	11-38087 71E-2087	X	X

(1) PROTOTYPE
(2) PRODUCTION

EBT-P PROTOTYPE AND PRODUCTION

MEASUREMENT LIST

MEAS. NO.	DESCRIPTION/ LOCATION	MEASUREMENT RANGE		UNITS	TRANSDUCER DESCRIPTION	TRANSDUCER PART NO.	INSTALLATION DWG. NO.	MEASUREMENT PERIOD	
		LOW	HIGH					COOL-DOWN WARMUP	OPERATION
V1	VOLTAGE, VCL COLD END	N/A	N/A	MV	VOLTAGE TAP	GDC FABRICATED	11-38086 71E-2086	(1) (2) X	X
V2	↓	↓	↓	↓	↓	↓	↓	X	X
V3	VOLTAGE, VCL WARM END	↓	↓	↓	↓	↓	↓	X	X
V4	↓	↓	↓	MV	VOLTAGE TAP	GDC FABRICATED	11-38086 71E-2086	X	X
V5	VOLTAGE, COIL LAYER 5	↓	↓	↓	↓	↓	11-38006 71E-2006	X	X
V6	LAYER 13	↓	↓	↓	↓	↓	↓	X	X
V7	LAYER 21	↓	↓	↓	↓	↓	↓	X	X
V8	VOLTAGE, COIL LAYER 29	N/A	N/A	MV	VOLTAGE TAP	GDC FABRICATED	11-38006 71E-2006	X	X
P1	PRESSURE, HELIUM VESSEL	0	50	PSIA	STRAIN GAGE, THIN FILM	CEC-1000-05	11-38086 71E-2086	X	X
P2	PRESSURE, SWITCH HELIUM	15	18	PSIA	PRESSURE SWITCH, DIAPHRAGM	21-4C40-1-86	11-38086 71E-2086	X	X
P3	PRESSURE, VACUUM VESSEL	10^{-8}	10^{-4}	TORR	ANALOG MONITORS	MDAC FURNISH		X	X
P4	PRESSURE, SWITCH VACUUM	0.4	1500	TORR	PRESSURE SWITCH, DIAPHRAGM	16073		X	X
L1	HELIUM LEVEL, STACK	0	14	IN	SUPERCONDUCTOR WIRE	11-38032-3 71E-2032-3	11-38030 71E-2030	X	X

(1) PROTOTYPE
(2) PRODUCTION

4.5 ELECTRICAL DISTRIBUTION SYSTEM DESIGN DESCRIPTION

Standard materials, practices and processes have been used when available to keep costs low and reliability high for the electrical distribution system design. The design details the manner in which power is routed from the magnet power supply to the 36 series connected magnets. The power bus and return are standard flat bar conductors made from electrical grade copper and form concentric rings above the magnets on the torus mezzanine as shown in Drawing SK82881 (Appendix A). Breaks in the outer power bus occurring over the magnets allow for series electrical connections. The series connection between the power bus and magnet vapor-cooled leads is made with two sets of four flexible jumper cables.

4.5.1 SIZING CONDUCTORS AND JOINT OVERLAPS. The copper bus bar and flexible jumper cable sizing has been verified using the following standard formulas (Reference 4.5-1) for a 30°C rise above a 40°C ambient temperature:

Flat Bars on Edge:

$$I = 504\ A^{.5}\ P^{.39} \text{ amperes} \qquad \text{(Equation 4.5-1)}$$

Solid or Hollow Round Bars:

$$I = 510\ A^{.5}\ P^{.36} \text{ amperes} \qquad \text{(Equation 4.5-2)}$$

where I = current in amperes

A = cross sectional area of the conductors in square inches.

P = perimeter of the conductor in inches.

A 5" X 1/2" copper flat bar has been selected for the power bus and return. These dimensions give a current capacity of 2030 amps when used to solve Equation 4.5-1.

The flexible jumper cables have been selected to be 535 MCM each. With four in parallel, the current capacity is 1784 amps when Equation 4.5-2 is solved.

Both of the above conductors are more than adequate for carrying the normal power supply current of 1683 amps.

Joint overlaps on the bus bars will be silver-plated or coated with special joint compounds to prevent oxidation and the resulting contact resistance. The overlap region will be bolted to provide a contact pressure of at least 750 psi and will be at least five inches in length (10 times the conductor width). The five-inch overlap and 750 psi contact pressure assure that the resistance of the overlap area is less than or equal to an equivalent length of conductor.

4.5.2 FIELD ERROR. The bus is designed so that the power and return conductors are separated by one inch. Since the conductors are in close proximity and their currents flow in opposite directions, the magnetic fields tend to cancel out. The flexible jumper cables are also designed to be in close proximity for the same reason. A preliminary calculation for the field generated in the plasma region is reported in Section 5.1.

4.6 PROTECTION SYSTEM DESIGN DESCRIPTION

Every effort has been made to assure reliability in the design of the protection system. Redundancy and fail-to-safe operation have been the key design criteria. In addition, cost is an important consideration and off-the-shelf equipment has been used when available.

Drawings of protection system cabinets and electrical schematics are found in Appendix A .

A detailed description of the protection system's subassemblies follow.

4.6.1 CIRCUIT BREAKER. The circuit breaker provides the means for interrupting magnet current during an emergency discharge. It receives its command to open circuit from the circuit breaker driver which is discussed in Section 4.6.2.

Physically, there are nine circuit breakers distributed around the torus as shown in Drawing SK82881 (Appendix A). Electrically, the nine circuit breakers are configured as 9 DPST switches for a total of 18 circuit breakers.

The circuit breakers are of the Westinghouse DMD type and are extensively used in heavy industry. The two poles are rated at 2000 amps each at 1500 vdc.

The control circuitry consists of a closing coil for closing the contacts and an opening coil for opening the contacts. The closing coil requirements are 110 vdc at 50 amps, while the opening coil is rated at 110 vdc and 2 amps.

The physical dimensions are 47.5 inches high by 25 inches deep by 18 inches wide.

The maximum time required to break a circuit from the time the opening coil is energized is 250 msec.

The breakers are interfaced to the power bus by four pairs of 1000 MCM cables and high current lugs. The interfaces between the closing/opening coils and circuit breaker drivers on the north balcony are by hard wire cabling and an overhead wire tray.

4.6.2 CIRCUIT BREAKER DRIVERS. The circuit breaker drivers perform the function of energizing the 18 circuit breaker opening coils when an emergency dump command is received at their respective inputs. A dump will also be initiated in case of low capacitor voltage/charge or loss of both 110 vac primary and back-up power.

Since an emergency dump is a critical protection function, the circuit breaker drivers are designed for maximum reliability. This is accomplished by using redundancy in critical circuits and fail-to-safe operation (emergency dump).

Refering to Figure 4.6-1, the outputs of the protection system monitoring devices are relay contacts. The contacts are normally open when power is off or when a dump command is initiated. With this configuration, a broken wire or loss of power will initiate a dump, i.e., fail-to-safe. The wiring between the monitoring devices and circuit breaker drivers is totally redundant and diode-isolated at both terminations. This allows the wiring to be one fault tolerant to a shorted condition.

The breaker driver circuitry consists essentially of a low power dc voltage supply for charging a capacitor bank which stores the charge for firing the circuit breaker, redundant input diode "or" logic and redundant solid state switches for completing the opening coil circuit. Special detectors will initiate a dump on loss of input ac power or low voltage on any capacitor in the capacitor bank.

The capacitor bank will be over-rated by 50% so that the failure of any one capacitor will not degrade its ability to open the circuit breakers. In addition, every capacitor in the bank will be diode isolated so that a shorted capacitor will have no adverse effect on the rest of the capacitor bank. Discrete outputs such as the status and quench in progress will be buffered before transmission to the data acquisition system. The dump bus will be common to all breaker driver inputs to assure all magnets discharge simultaneously.

The wiring to and from the circuit breaker driver and the circuit breaker opening coil will be fully redundant for reliability.

The 18 circuit breaker drivers are located on the north balcony in nine cabinets. There are two breaker drivers located in each cabinet.

4.6.3 DUMP RESISTORS. The protection system will incorporate emergency dump resistors to discharge the magnets. Each coil will have its own individual resistor. Two resistor elements will be combined into a single structure. The resistors are air-cooled and incorporate over-temperature protection via a thermal switch located on the resistors to inhibit operation of the coil immediately after a discharge. The resistor element will be a

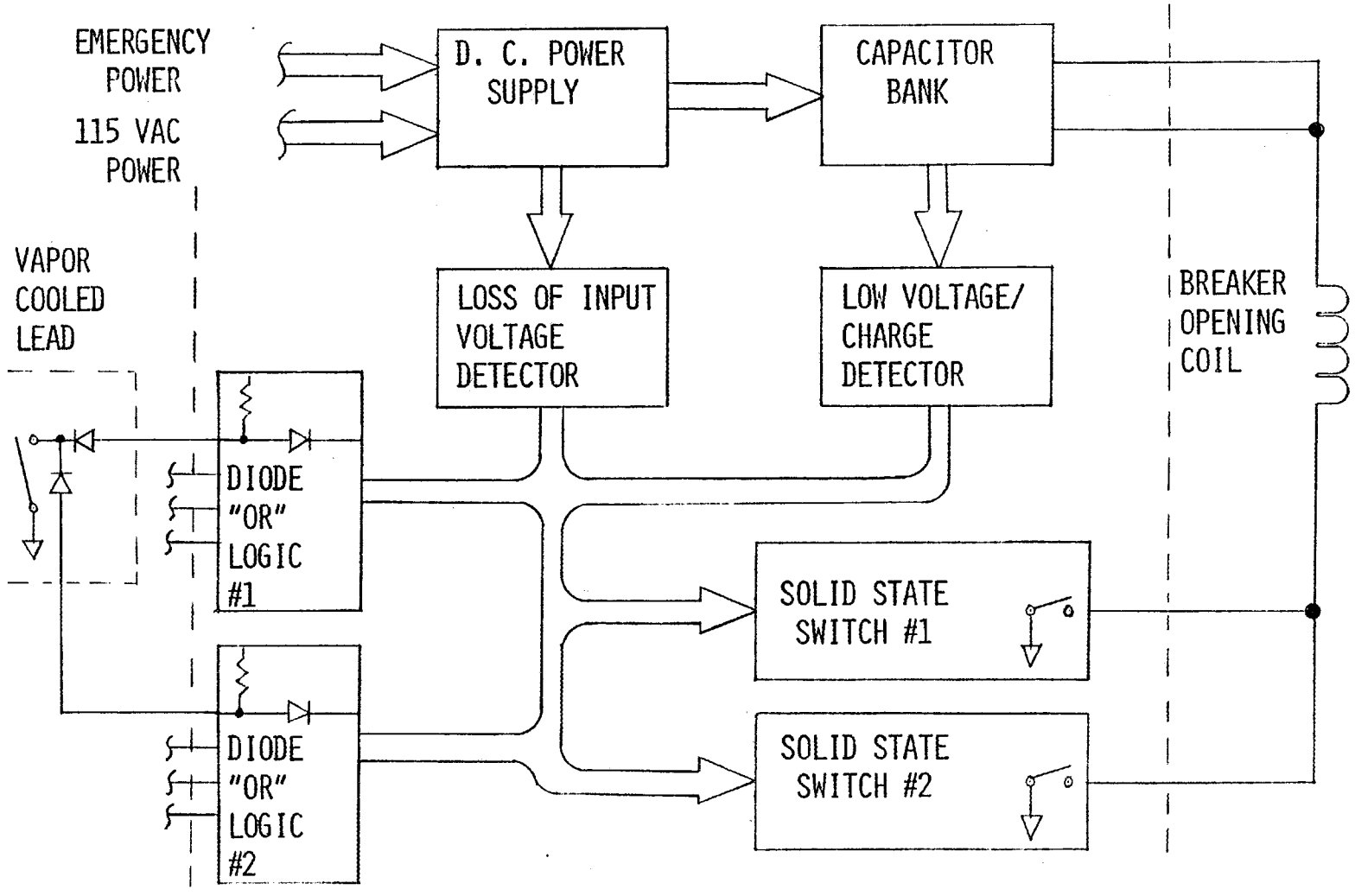

FIGURE 4.6-1 CIRCUIT BREAKER DRIVER

milled (zig zag pattern) sheet of stainless steel and is shown in Figure 4.6-2. The support structure is made from fiberglass epoxy composite.

A worst case thermal analysis assuming a constant energy input and no thermal losses uses the equation:

$$\Delta T = \frac{E}{C \cdot W} \qquad \text{(Equation 4.6-1)}$$

where ΔT is the final temperature rise in ^{o}C, E is the energy input in joules, W is the weight of the resistor in pounds, and C is the thermal capacity in joules per pound per deg. cent. of the steel.

Substituting the following values into Equation 4.6-1:

E = 1.5 megajoules (stored coil energy)

C = 228 Joules/lbs/^{o}C

W = 49 pounds (weight of steel)

ΔT will be equal to a maximum temperature rise of 134°C. Assuming a maximum ambient temperature of 38°C, the peak operating temperature will be 172°C. The dump resistor fiberglass insulation and support structure (G-10) can withstand a flex test with a 50% degradation for 35,000 hours at 185°C which is more than adequate mechanical strength. The G-10 will also provide an electrical ground isolation of at least 2500 vdc.

The peak potential any resistor should see with respect to ground is 400 vdc.

The two dump resistors and frame for each magnet are physically located on the torus superstructure as shown in Drawing SK82881 (Appendix A). They are electrically connected to the power busses by four pairs of 1000 MCM cable and terminated with high current lugs.

The discharge time constant is a function of the resistor value and magnet coil inductance. The time constant follows the equation:

$$t = L/R$$

with L = 1.07 H and R = .238 ohms, the time constant is 4.5 sec.

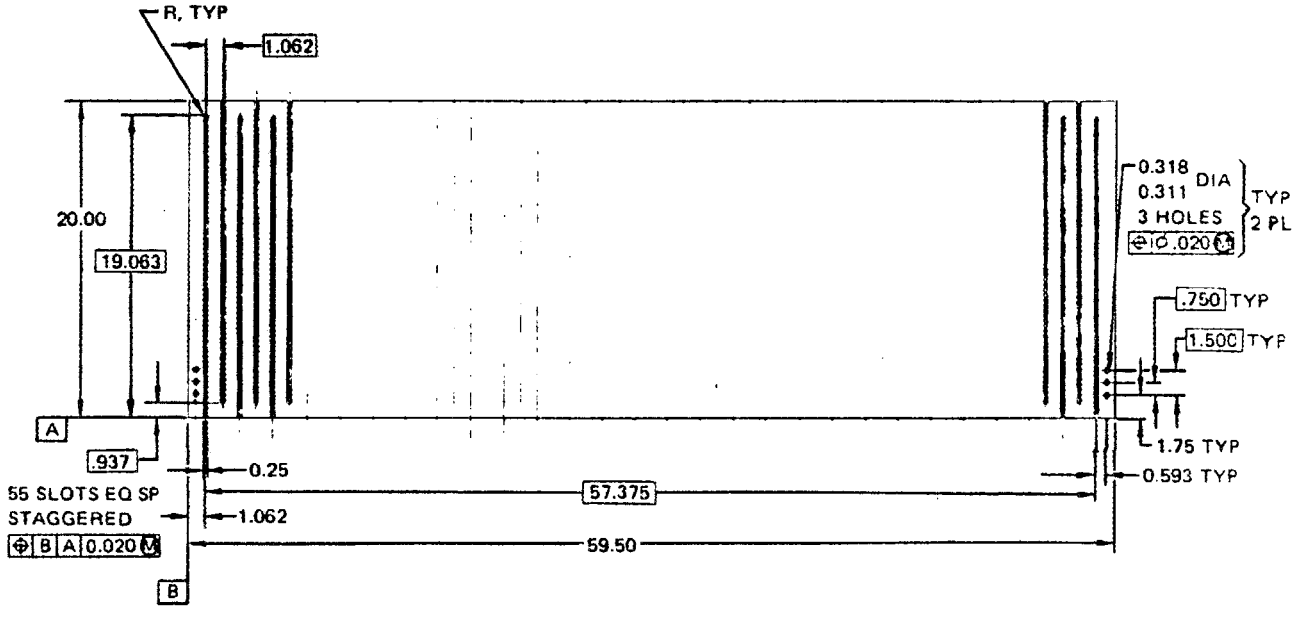

FIGURE 4.6-2 MIRROR COIL DUMP RESISTOR

4.6.4 BYPASS DIODE ASSEMBLY. The bypass diode assembly provides for a current transfer made to limit the magnet's coil voltage to chassis ground during an emergency discharge.

The bypass diode assembly will consist of four Westinghouse type RA201025XXOO disc diodes and two Westinghouse dual diode heat sinks PDAARA201248 with their associated mounting brackets.

The heat sinks allow the diodes to conduct 2,580 amps steady-state at a 40°C ambient temperature and with natural convection cooling. The maximum voltage rating of the assembly is 1200 vdc. It may be isolated from chassis ground to 2500 vdc by using G-10 insulation. Each diode is rated for an average current of 4800 amps at 1.56 vdc or 6.24 vdc across the entire assembly. The repetitive peak reverse voltage is rated at 1200 V.

The diode assemblies are interfaced to the power bus and adjacent diode assemblies with 3 pairs of 1000 MCM cables. The physical layout and location on the torus superstructure is shown in Drawing SK82881 (Appendix A).

4.6.5 VAPOR-COOLED LEAD VOLTAGE MONITOR. The vapor-cooled lead voltage monitor indirectly measures the temperature of the vapor-cooled leads by detecting a voltage increase as a function of a temperature dependent resistance increase at a constant magnet power supply current. There is a separate monitor for each vapor-cooled lead, or two per magnet.

The monitors have an adjustable set point or voltage trip level with a BCD output going to the data acquisition unit and a normally closed contact set going to the circuit breaker drivers.

The monitors will be implemented by using standard Bell and Howell bar graph voltmeters with the following specifications:

a. Operating voltage - 117 vac, 60 Hz, single phase
b. Input common mode voltage - 500 volts minimum
c. Any input to ac supply line isolation - 500 volts minimum
d. Any input to chassis ground - 500 volts minimum
e. Analog differential input range - 0 to and 3 vdc minimum
f. Input impedance 10 megohms
g. Accuracy (at any common mode voltage) - ± 1% minimum
h. Read speed - update every 20 msec's
i. Output - 3 digit BCD minimum, covering the range +.000 to +3.00 volts, TTL compatible
j. The unit has an adjustable set point, externally adjustable from 0.00 to 3.00 volts with a tolerance of 3% of true voltage. The output of the set point trip circuit is an isolated contact set, normally closed when power is applied and when the input is below the set point. The contacts are rated for 200 ma at 28 vdc.
k. The envelope size of this unit is 1.5" wide X 6.97" high X 6.38" deep.

The monitors will be allocated to nine cabinets located on the north balcony.

4.6.6 QUENCH DETECTORS. The design requirements for the quench detector require that each magnet must have two means of quench detection, either of which will be capable of triggering the breaker drive. The detailed concept has not yet been determined.

4.6.7 HELIUM LEVEL MONITOR. There will be one helium level monitor for each magnet. The outputs will provide an analog signal for use by the process controller and an isolated contact set which will trigger the breaker driver when the helium is below a low level set point.

The helium level monitor will be implemented using an off-the-shelf American Magnetics, Inc. liquid helium level monitor and sensor probe. The specifications are as follows:

a.	Sample frequency:	once in three minutes to continuous
b.	Meter:	3 1/2" taut band
c.	Analog output:	0-100 mv
d.	Relay rating:	250 ma or 100 volts maximum
e.	Power:	110 volts, 50-60 Hz, 20 watts
f.	Size:	11" wide X 9 5/8" deep X 3 7/8" high
g.	Weight:	8 lbs.

The probe is described in the magnet sensor Section 4.4. The monitors are located on the north balcony in two cabinets, 18 monitors per cabinet.

4.6.8 VACUUM SWITCH/PRESSURE SWITCH. The vacuum and pressure switch functions are described in Section 3.7.2.4. The physical characteristics are delineated in the magnet sensor section 4.4.

4.6.9 GROUND REFERENCING RESISTORS AND STEERING DIODES. It is necessary to reference the junctions of each discharge magnet pair to chassis ground in order to limit the maximum magnet-to-ground and discharge potential to 400 vdc. This requirement is apparently satisfied by using a ground-referencing resistor in series with a steering diode. The diode prevents ground loop or sneak path currents from flowing.

At present, a Systems Computer Analysis Program (SYSCAP) nodal analysis is being used to evaluate and optimize the circuit design.

4.7 MATERIAL SELECTION

The following specific criteria were used in selecting the materials for the EBT-P magnet.

a. Excellent mechanical and physical properties at room and cryogenic temperatures.

b. High degree of fabricability and producibility.
c. Large data base and specification coverage.
d. Reliability established by service history.
e. Proven fabrication methods and processes.
f. Availability in the required sizes and shapes at reasonable cost.
g. Previous design and fabrication experience.

4.7.1 METALLIC MATERIALS. Based on the above criteria, the following metallic materials were selected for the EBT-P magnet:

- Type 304L stainless steel for the vacuum vessel.
- Type 316L stainless steel for the coil case.
- One hundred ten (110) copper for the LN_2 cold wall assembly.
- Ti-4V-6Al alloy for the cold mass support structure.
- Nb_3Sn superconductor.
- NbTi superconductor.

TYPE 304L STAINLESS STEEL FOR THE VACUUM VESSEL. Type 304L stainless steel is a low carbon/chromium-nickel corrosion-resistant steel which, in the annealed condition, possesses an austentic, face-centered cubic crystalline structure, having low magnetic permeability and freedom from grain boundary carbide precipitation during welding. Of the available 300 series corrosion-resistant steels, type 304L possesses the most economic combination of mechanical and physical properties, fabricability and availability in various forms and sizes, and has a large data base and service reliability in cryogenic applications.

TYPE 316L STAINLESS STEEL FOR THE COIL CASE. Type 316L stainless steel was selected for the coil case. This alloy has essentially the same properties as 304L with the exception that it is more corrosion-resistant and remains non-magnetic at cryogenic temperatures. A non-magnetic material is desirable to prevent interaction with the magnetic field.

ONE HUNDRED TEN (110) COPPER FOR LN_2 COLD WALL ASSEMBLY. One hundred ten (110) copper is 99.9% pure copper with a good combination of thermal, mechanical and joining properties and is non-magnetic at cryogenic temperatures.

Ti-4V-6Al ALLOY FOR COLD MASS SUPPORT STRUCTURE. Ti-4V-6Al alloy was selected because it was radiation-resistant and had the highest strength to thermal conductivity ratio at cryogenic temperatures.

Nb_3Sn SUPERCONDUCTOR STRIP FOR CONNECTING VAPOR-COOLED LEADS TO NbTi SUPERCONDUCTOR. Nb_3Sn superconductor was selected as an intermediary connector between the vapor-cooled leads and the NbTi superconductor because of its high superconducting transition temperature. Introduction of Nb_3Sn will result in a reduced risk

of quench and lower heat loads in the vapor-cooled lead region of the magnet.

In a radiation environment chiefly consisting of x-rays with a total maximum dose of 7.3 X 10^8 rads over a period of ten years, no significant radiation damage is anticipated in the structural materials 304L and 316L stainless steels, copper or Ti-4V-6Al alloy. The mechanical and thermophysical properties of these materials will remain essentially unchanged.

The superconductor Nb_3Sn and NbTi will also retain their superconducting properties, and there will not be any significant change in the critical current, the critical temperature or the critical field.

4.7.2 NON-METALLIC MATERIALS. The principal non-metallic materials used in the EBT-P magnet are as follows:

- NEMA grade G-10 CR fiberglass/epoxy laminate and Kapton film (MIL-P-46112 Type I) for ground insulation.
- Nomex tape (MIL-T-43435 Rev. B, Type V, Size 2, Finish A) for turn-to-turn insulation.
- Ethylene propylene rubber for O-ring seals.
- Eccobond 57C silver-filled conductive epoxy adhesive (GD/C EMS 0-06023-1).
- M-Bond 610 two-part epoxy adhesive (GD/C EMS 0-06072-1) for bonding strain gages.
- Stycase 2850 ft. two-part epoxy adhesive for bonding and anchoring of wires and leads.
- Polyolifin heat shrinkable sleeving (MIL-I-23053/6B) for instrumentation wire insulation.
- Aluminized Kapton for multilayer superinsulation to restrict the thermal radiation load on the cold mass.

These materials are selected on the basis that they remain functional in the operational environment of the EBT-P magnet with a cumulative x-ray radiation dosage of 4.0 X 10^8 rads at the end of ten years of operation (stack region with stainless steel shielding - Figure 3.5-2). The rationale for each selection is based on data available and/or successful usage of the material under a similar operational environment.

Slotted G-10 CR fiberglass/epoxy laminate is placed between the stainless steel bobbin and the conductor pack. Part of the G-10 CR is slotted to allow liquid helium coolant to circulate on all sides of the conductor pack. Layers of 0.005-inch thick by 2-inch wide Kapton film (DuPont Type 500H) are placed around the corners to offer redundant ground insulation, as well as thermal protection, for the G-10 CR laminate during the close-out welding of the outer case. The Kapton film layers are held in place during assemblying by the silicone pressure-sensitive adhesive applied on one side of the film (this is procurable as Permacel Tape No. 222).

The turn-to-turn insulation is provided by a Nomex tape (MIL-T-43435, Rev. B, Type V, Size 2, Finish A, procurable from Western Filament, Inc. under the trade name of Nomex Tape 70H0F25X). The tape is approximately .12 inch wide and 6.5 mils thick spirally wound around the conductor under 1-5 lbs. tension. During the winding of the tape onto the conductor, tape ends are butt-joined and bonded onto the conductor using a cyanoacrylate adhesive (GD/C EMS 0-00089-1). The tape covers approximately 50% of the conductor surface area. The successful use of Nomex tape for turn-to-turn insulation has been demonstrated by the development magnets built by the Oak Ridge National Laboratory.

The radiation resistance of G-10 CR fiberglass/epoxy laminates are shown in Reference 4.7-1 and of polyimide films, such as Vespel and Kapton, in Reference 4.7-1 and 4.7-2. G-10 CR showed a loss in compressive strength, flexure strain, modulus, and strength after 2.4 X 10^9 rads and 10^{10} rads radiation dosage; while the polyimide films are virtually unaffected. Data obtained by Oak Ridge National Laboratory under DOE Contract No. W-7405-eng-26 (Reference 4.7-3) showed that under 2 X 10^8 rad radiation dosage, fiberglass/epoxy laminate showed no change in flexure strength. This is also in agreement with data presented in Science Research Council Report RHEL/R200 (Reference 4.7-4).

Radiation resistance of Nomex has also been studied. The material was found to be able to tolerate 2 X 10^8 rad with no loss in electrical breakdown voltage (Reference 4.7-3) and only a slight discoloration and a less than 0.60% in weight loss after 2.4 X 10^9 rad radiation exposure (Reference 4.7-5).

The silicone pressure-sensitive and the cyanoacrylate adhesives are not expected to endure 10^8 rad radiation dosage. However, these adhesives are strictly used in a very small quantity as an assembly aid, the by-product and the energy liberated as a result of radiation degradation of the adhesives should not affect the performance of the magnet.

Data on the radiation resistance of ethylene propylene rubber, Eccobond 57C silver-filled conductive epoxy adhesive, and M-Bond 610 two-part epoxy adhesive are not available. These materials have been used in other superconducting magnets under cryogenic temperatures. It is not expected that the epoxy adhesives would pose a problem under radiation dosages less than 10^9 rads but further research will be done during Title II. The same can be said for Stycase 2850 ft. (used with 7% 24LV hardever), a two-part epoxy cured at room temperature manufactured by Emerson and Cuming, Inc. Data available to substantiate these claims are given in Reference 4.7-6.

The radiation resistance of heat shrinkable sleeving for wire bundles is not as good as the epoxies. However, the polyalefin type (MIL-I-23053/6B) such as polyethylene was selected since it is more radiation-resistant and cryogenically-reliable than the other thermoplastics used for heat shrinkable sleeving.

Aluminized Kapton will be used for multi-layer superinsulation. Kapton has excellent radiation resistance as discussed earlier. In addition, aluminized Kapton was evaluated by ORNL (Reference 4.7-7) which showed that the material could serve as superinsulation for cryogenic environment at least up to a dose of 10^{10} rads with minimal change in material appearance and outgassing upon warm-up.

5

SUPPORTING ANALYSIS

5.1 MAGNETICS ANALYSIS

FORCE AND FIELD ANALYSIS

Magnetic field strengths and forces were calculated using the program EBTFLD3. This program sums the individual field contributions from an array of filamental circular loops distributed through each coil pack. Each coil was modeled with 200 loops. The field from each loop was calculated using elliptic integrals.

Values of the magnetic field strengths and forces and their locations are tabulated in Appendix B-1 . The peak field was found to be approximately 7.4 Tesla and is located at the center of the coil along the inner radius.

ERROR FIELD ANALYSIS

The error field in the EBT-P will be generated by different sources such as the overhead buswork, the current leads, and also the actual helical and spiral turns with which the coils will be wound. This error analysis was generated in two parts, the first dealing with the buswork and the second dealing with the current leads and the non-solenoidal windings.

The buswork above the torus is a system of current-carrying segments which repeat every 40 degrees (refer to SK82881, sheets 1 and 2 in Appendix A). Only those leads which carry current during normal operation were considered; that is, all power supply leads and dump circuitry were ignored.

This buswork was then divided into a network of straight-line segments which are illustrated in Figure 5.1-1. Coil 4 in this figure was determined to be the coil whose field would be most perturbed by the current network above the torus. Therefore, field points in the bore of coil 4 and at the midplane between coils 3 and 4 were calculated for a worst case determination. Refer to Figures 5.1-2 and 5.1-3 for field point locations.

The magnetic field due to five 40-degree sectors, two on either side of the sector containing the field points (refer to Figure 5.1-3), was calculated using the computer program LINES. This program calculates the magnetic field due to any number of consecutive, current-carrying line segments. This data is summarized in the table in Figure 5.1-4. According to this data, the worst case radial field deviation will be approximately one gauss located in the coil throat at the top of the toroidal array.

The second part of the error analysis deals with the field deviation caused by the vapor-cooled entry leads and the non-

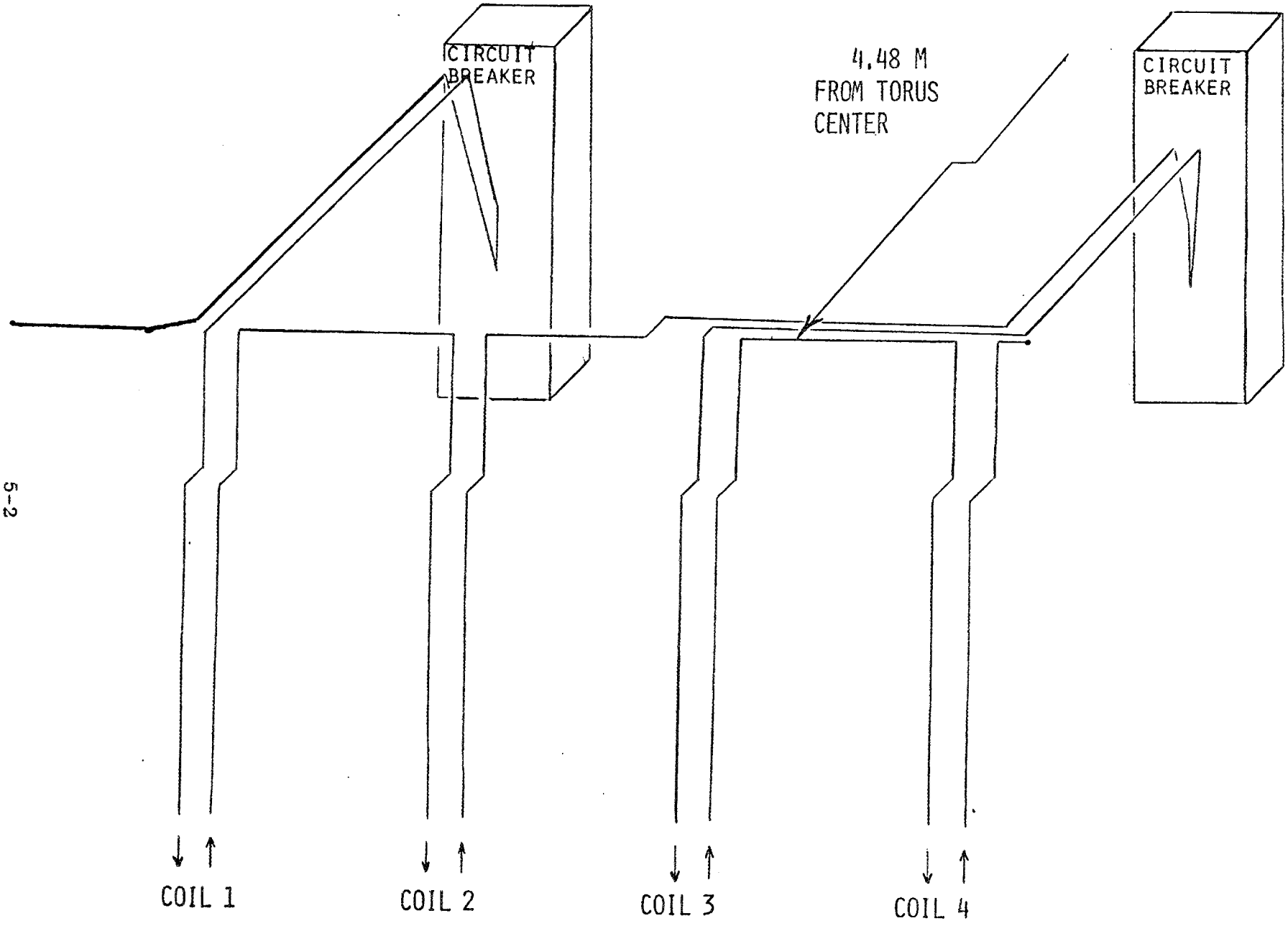

FIGURE 5.1-1 EBT-P OVERHEAD BUSWORK SCHEMATIC (40° SECTOR)

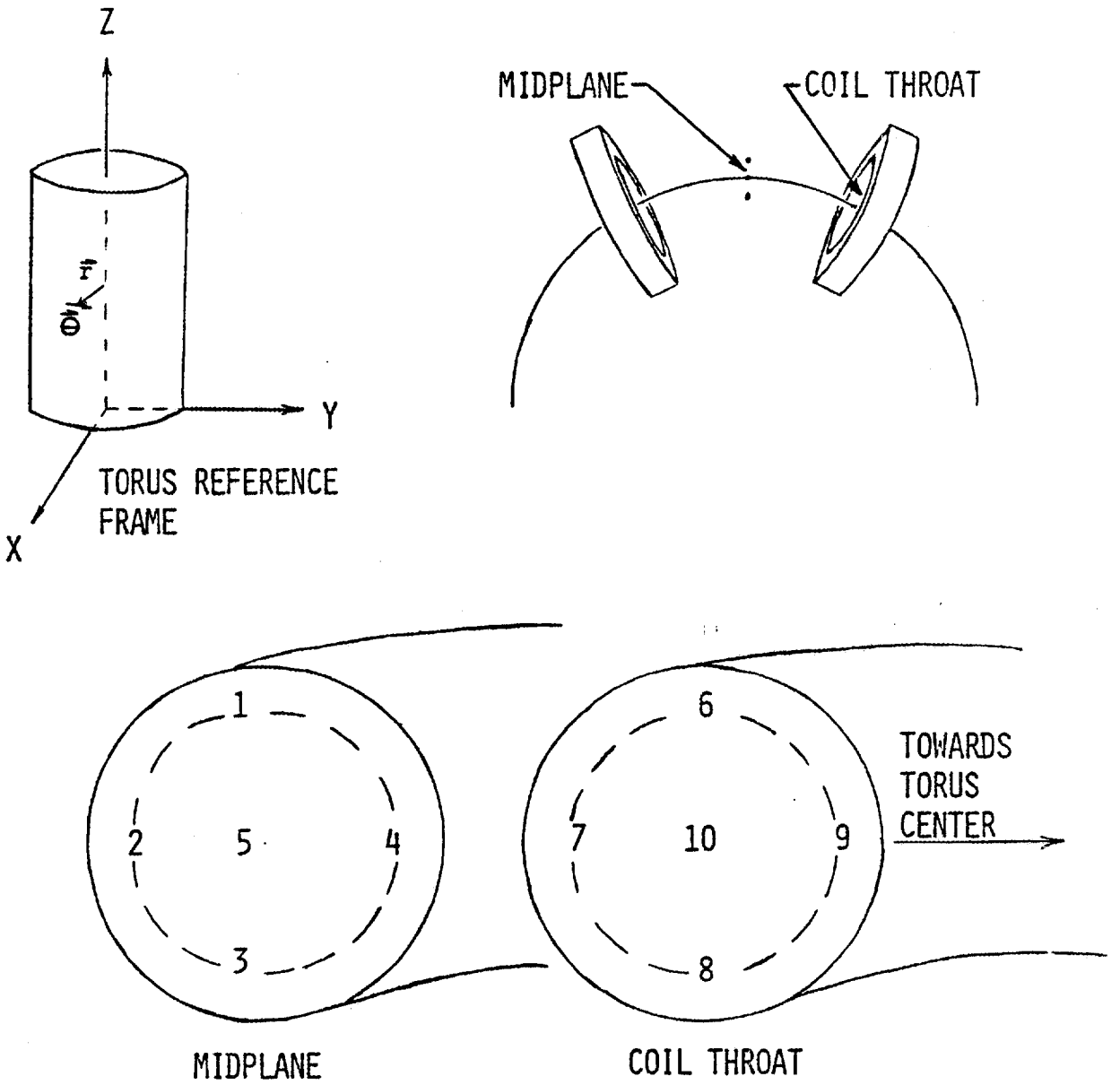

FIGURE 5.1-2 FIELD POINT LOCATIONS

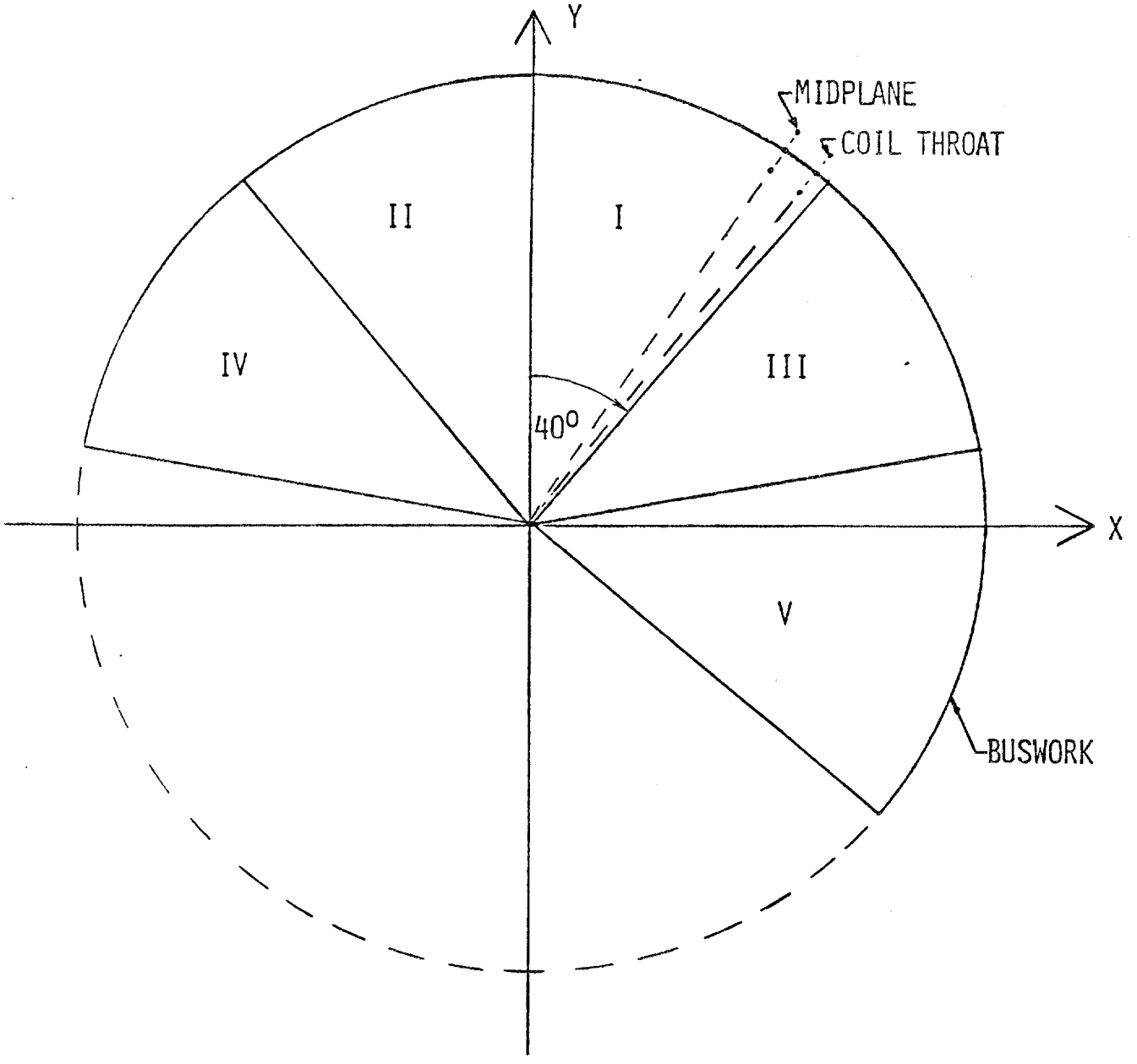

FIGURE 5.1-3 EBT-P FIELD POINT LOCATIONS

	FIELD (WORST CASE) IN GAUSS				
	POINT	BR	Bθ	BZ	MAGNITUDE
MIDPLANE	1	0.46006	0.78168	0.19323	0.92737
	2	0.41544	0.67692	0.18010	0.81440
	3	0.38988	0.63380	0.19897	0.77026
	4	0.42518	0.72097	0.21769	0.86485
	5	0.42232	0.70264	0.19731	0.84320
COIL THROAT	6	0.59487	0.79746	0.19768	1.01434
	7	0.53067	0.68899	0.18123	0.88835
	8	0.49579	0.64328	0.20033	0.83651
	9	0.54671	0.73304	0.22191	0.94010
	10	0.54130	0.71480	0.20004	0.91868

NOTE: MIDPLANE IS BETWEEN COILS 3 AND 4.
COIL THROAT IS IN REFERENCE TO COIL 4.
FIELD IS DUE TO 5 - 40° SECTORS OF BUSWORK.

FIGURE 5.1-4 FIELD DUE TO OVERHEAD BUS WORK

solenoidal windings of the coils themselves.

The as-built coil configuration was performed using the code COILS2, which was prepared specifically for the EBT-P program. The computer code models the coil using a current-carrying filament which traces out the path followed by the superconductor throughout the winding.

The magnetic model can be described most simply by dividing it into six sections:

a. lead entry down through stack,
b. half of 32nd layer from center to left flange (helix),
c. pancake spiral from 32nd layer to 1st layer,
d. 31 helically-wound layers,
e. half of 32nd layer from right-hand flange to center (helix) and,
f. lead exit up through stack.

The dimensional data can be found from Drawing 11-38006 (Appendix A). A more detailed explanation of the model follows.

The computer code models the magnet by sending a single, current-carrying filament down the entry lead path shown in Figure 5.1-5 to the coil pack.

After lead entry, the coil pack itself was modeled by first winding 1/2 of the 32nd layer from the center of the coil to the left-hand flange (as viewed in Drawing 11-38006-1 of Appendix A). The filament was wound in a helical manner, consisting of 360-straight line segments per turn, for 19 turns. The conductor then follows a descending spiral path for 34 turns (layers) to the bobbin. Two extra turns (layers) were incorporated in this pancake to compensate for the double-conductor-width insulation between the 31st and 32nd layers (refer to drawing). The model then moves the current element helically in the first layer until it passes the turn of insulation separating the pancaked layers from the rest of the windings. At this point, the main coil pack winding begins. The current element helically progresses from the insulation on the left-hand side to the flange on the right-hand side (as seen in Figure 5.1-6).

Each time a left- or right-hand boundary dimension is met, a layer transition automatically occurs. During a layer transition, the current element travels a path tangent to the point where it contacted the boundary. This tangent takes the element to the next layer, along the boundary, and then begins its helical traverse back to the other side of the coil. The model of the coil pack is then completed by winding the last (32nd) layer from the right-hand flange back to the center of the coil where the lead exits as seen in Figure 5.1-5.

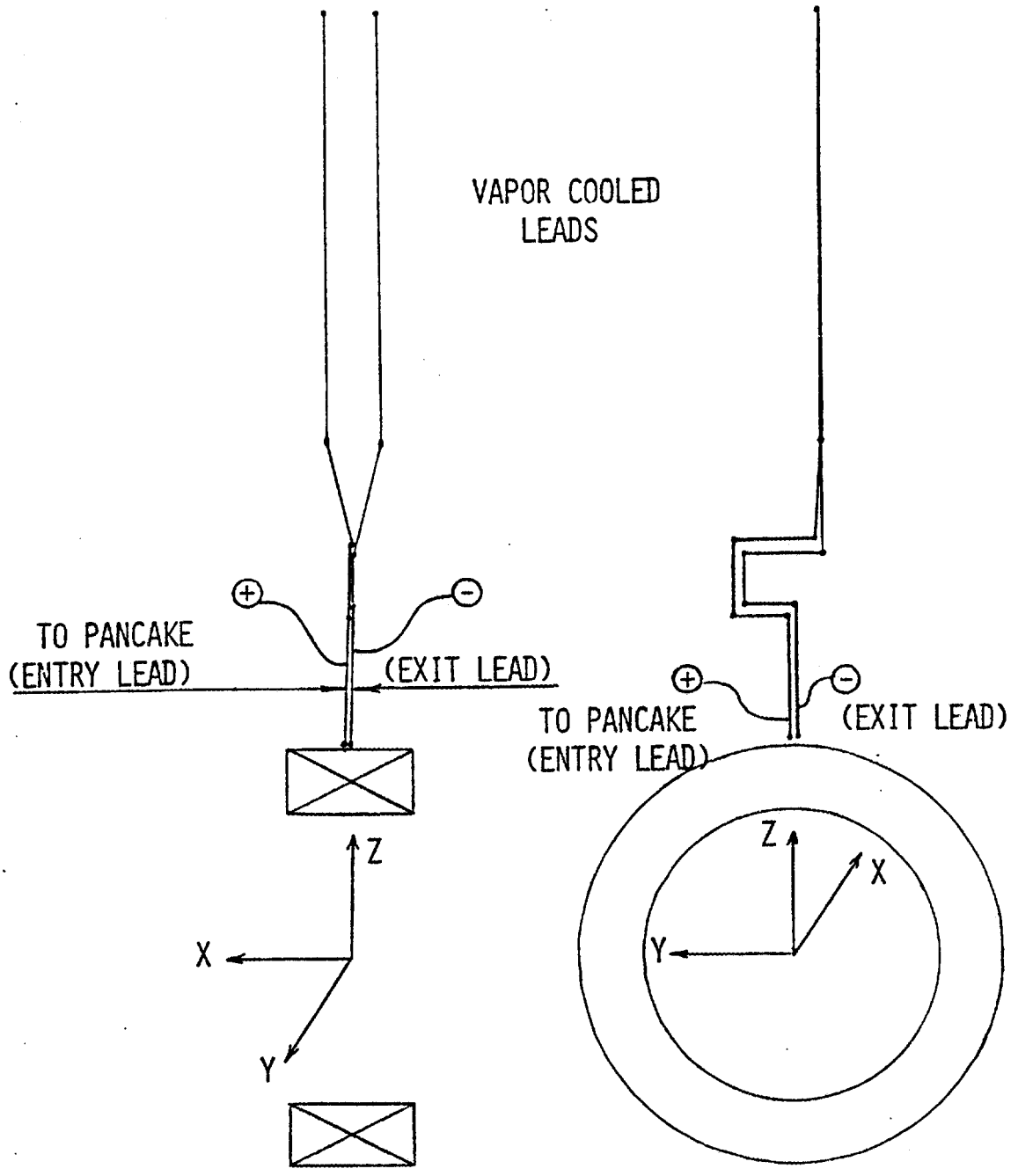

FIGURE 5.1-5 ENTRY/EXIT LEAD PATH

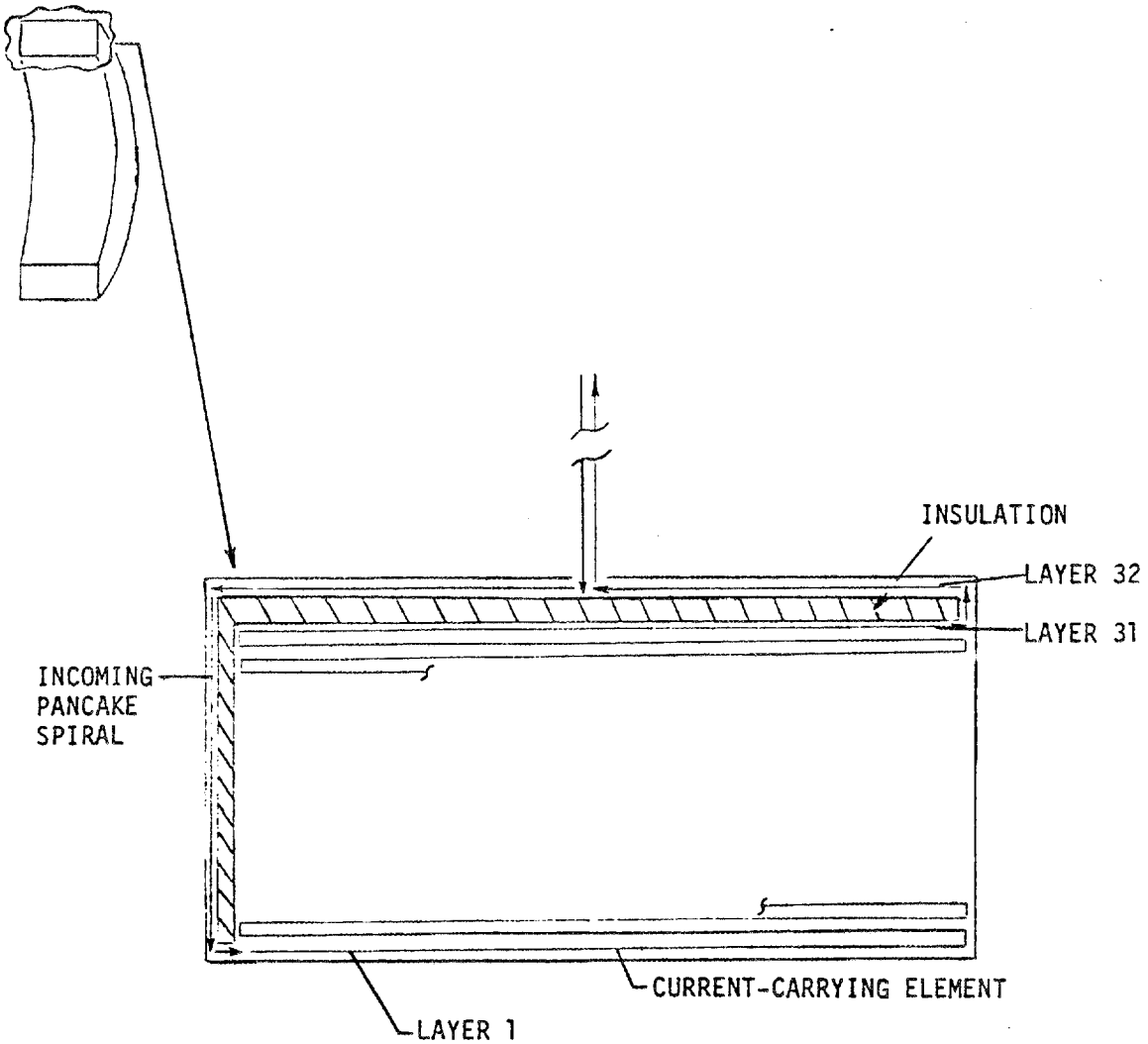

FIGURE 5.1-6. COIL PACK WINDING MODEL

Each helical and/or spiral turn of the conductor was modeled as 360 straight line segments, one segment per degree. The fields, due to each line segment, were calculated and then summed to reach the final field value. A study was performed to determine the deviation caused by using line segments. In this study, the field due to a circular turn of current was compared to those produced by turns of 36,360 and 3600 straight line segments. The field deviations were found to be 0.2%, 2×10^{-3}% and 8×10^{-5}%, respectively. Due to the number of calculations needed when over 1200 turns are segmented into 3600 lines, 360 line segments were determined to be sufficient. Further study of this effect is necessary during Title II.

The field data are presented in Figures 5.1-7 and 5.1-8 for points along the coil axis. Figure 5.1-7 tabulates the non-axial fields at points on either side of the coil. These points are located at the intersections of the axes from two adjacent coils. The data present the effects of individual conductor sections as they influence the field behaviors at these points. The values assigned to these individual sections of conductor may be somewhat misleading. This is due to the fact that the windings of a particular section do not start and stop at the same angular (or circumferencial) positions; therefore, the field error given is partially due to incomplete loops which are completed in another section.

Figure 5.1-8 tabulates the fields at points along the axis from left to right. The average axial field is also shown. In this reference frame, Bx is approximately equal to the axial field and the root mean square of By and Bz is approximately equal to the radial field. With this in mind, the average axial field is 2.49 Tesla and the radial, or error field, is approximately 0.15 gauss. This average should represent a first order attempt at quantifying the toroidal field error due to coil shape. The 0.15 gauss represents a globally-averaged $\Delta B/B$ of approximately 5×10^{-6}.

During the Title II study period, additional field calculations will be necessary. For example, the worst case tolerance buildup effects will be analyzed. The coil model will also be modified so that the layer-layer transitions take place at specified locations. This will include the effects due to next-to-last turn spacers required to equalize the number of turns in each layer.

CONDUCTOR DESCRIPTION

The superconducting cable to be used for the coil windings is described in General Dynamics/Convair Specification No. 11-38007, Rev. A, which is attached as Appendix B-2 .

Briefly, the superconductive material is a niobium-titanium alloy (46.5 $\pm$ 1.5% Wt. Nb) in a high conductivity copper matrix. The conductor as a whole is a rectangular monolith with the follow-

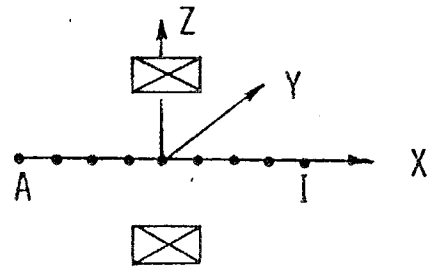

SECTION	LEFT SIDE (PT. A) BY (GAUSS)	LEFT SIDE (PT. A) BZ (GAUSS)	RIGHT SIDE (PT. I) BY (GAUSS)	RIGHT SIDE (PT. I) BZ (GAUSS)
LEAD ENTRY	-1.237	-0.028	+1.349	+0.038
32ND LAYER (LEFT HALF)	-2.623	+1.543	+2.318	-1.102
PANCAKE (LEFT SIDE)	+0.267	+0.513	-0.313	-0.026
LAYERS 1-31	+1.845	-2.809	-1.961	+2.172
32ND LAYER (RIGHT HALF)	+0.518	+0.745	-0.069	-1.078
LEAD EXIT	+1.363	+0.061	-1.224	-0.049
TOTAL:	+0.133	+0.025	+0.100	-0.045

FIGURE 5.1-7. MAGNETIC FIELD AT COIL AXES INTERSECTIONS

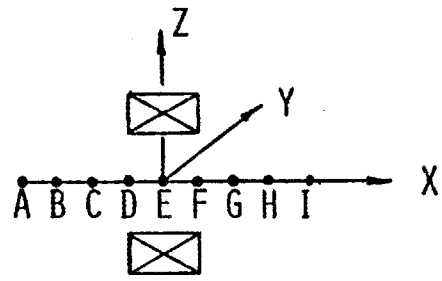

PT	BX (TESLA)	BY (TESLA)	BZ (TESLA)	BR (TESLA)
A	+1.00345	+1.33879E-05	+2.35127E-06	1.3593E-05
B	+1.60879	+1.61234E-05	+4.15350E-07	1.6129E-05
C	+2.61737	+1.88133E-05	+3.07985E-06	1.9064E-05
D	+3.79341	+1.83618E-05	+4.49921E-06	1.8905E-05
E	+4.36235	+1.82903E-05	+8.96304E-06	2.0368E-05
F	+3.79446	+1.59865E-05	-1.13331E-06	1.6027E-05
G	+2.61808	+1.09632E-05	-6.86026E-06	1.2933E-05
H	+1.60906	+9.99710E-06	-5.96136E-06	1.1640E-05
I	+1.00357	+9.97861E-06	-4.35466E-06	1.0887E-05
AXIAL AVERAGE:	+2.49006	+1.4653E-05	+1.1101E-07	1.5505E-05

FIGURE 5.1-8 MAGNETIC FIELD ALONG COIL AXIS

ing dimensions:

Width:	0.1969 ± 0.001 inch (nom: 5.0 mm)
Height:	0.1142 ± 0.001 inch (nom: 2.9 mm)
Corner Radius:	0.02 ± 0.004 inch
Cu:Sc Ratio:	3.0:1 (by volume)

The conductor critical current at 7.5 Tesla and 4.2K is 2800 amps and the zero field composite resistivity ratio is 120.

The coupling time constant is defined as:

$$\tau_o = \frac{\mu_o \ell p^2}{4\pi\rho} ,$$

where:

$\mu_o = 4\pi \times 10^{-7}$ H/m,

ℓp = twist pitch length (m) and

ρ = matrix resistivity at 4.2K and 5.5T ($\Omega \cdot$ m)

and is less than one second for this conductor.

QUENCH ANALYSIS

The data in the table in Figure 5.1-9 were input into the computer program SUPERQ, which relates voltage, temperature, current, and time in the event of a quench situation. SUPERQ is an iterative time step program which includes the enthalpy of both copper and superconductor but does not include helium cooling effects. This represents a realistic case for the situation where a quench is initiated by a low helium level. Referring to Figure 5.1-10, we can see that with an operating current of 1683 amps, the maximum temperature will reach 96K approximately 10 seconds after the start of the quench. Figure 5.1-11 illustrates the dump voltage behavior in this instance.

OPERATING CURRENT	=	1683.	(AMPS)
MAXIMUM DISCHARGE VOLTAGE	=	400.	(VOLTS)
OVERALL CURRENT DENSITY	=	10156.	(AMPS/SQ. CM)
MAGNETIC ENERGY	=	1.44400	(MEGAJOULES)
CRITICAL TEMPERATURE	=	5.0	(DEG K)
NORMAL ZONE LENGTH	=	40.	(CM)
NORMAL ZONE TRIGGER VOLTAGE	=	.04600	(VOLTS)
DELAY	=	.20000	(SEC)
SELF FIELD	=	7.40000	(TESLA)
BACKGROUND FIELD	=	0.00000	(TESLA)
FIELD ANGLE	=	0.00000	(DEGREES)
Cu/Sc RATIO	=	3.0	
PACKING FRACTION	=	.87500	
RRR	=	120.	
AREA OF UNIT CELL	=	.16571	(SQ. CM)
AREA OF CONDUCTOR	=	.14500	(SQ. CM)
AREA OF COPPER	=	.10875	(SQ. CM)
DUMP RESISTANCE	=	.23767	(OHMS)
INDUCTANCE	=	1.01960	(HENRIES)

Figure 5.1-9 Quench Analysis Input Data

5.2 STRESS ANALYSIS

This section presents a summary of the stress analysis done to date on the EBT-P mirror magnets. Detailed stress calculations are contained in Appendix B-3 . These analyses show that the mirror magnet assembly satisfies the requirements of Section 3.5.1 when the assembly is exposed to the environments described in Section 3.5.2.

5.2.1 HELIUM VESSEL STRESS ANALYSIS. The helium vessel was analyzed using both the ASME Boiler and Pressure Vessel Code and an MSC/NASTRAN finite element model. The ASME Code was used to evaluate structural requirements due to uniformally distributed loading, and the NASTRAN model was used to investigate the effects of non-uniform loads. For areas of the structure which do not conform to standard ASME Code configurations, standard engineering analysis practices were followed.

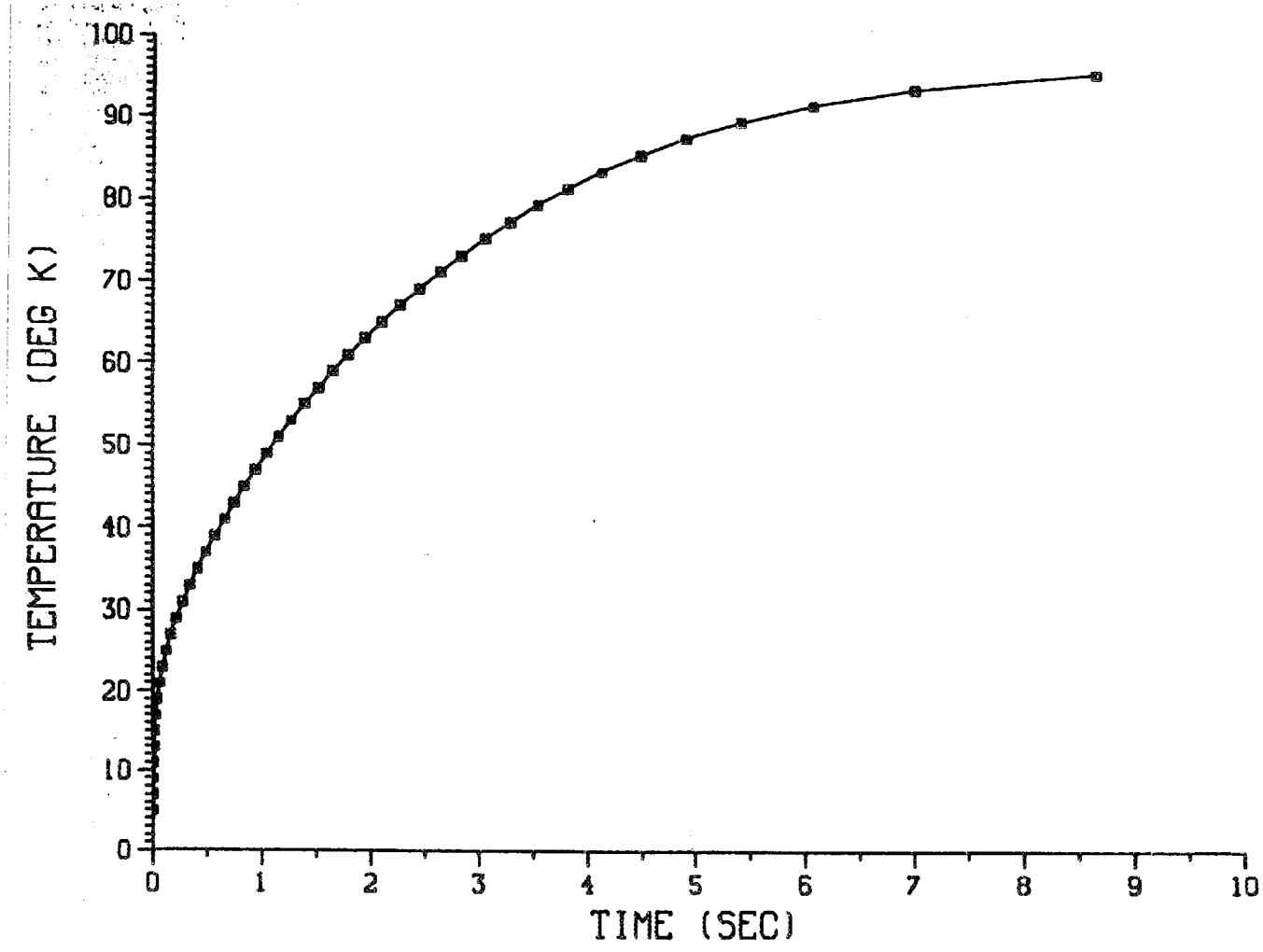

FIGURE 5.1-10 TEMPERATURE VS. TIME FOR EBT-P

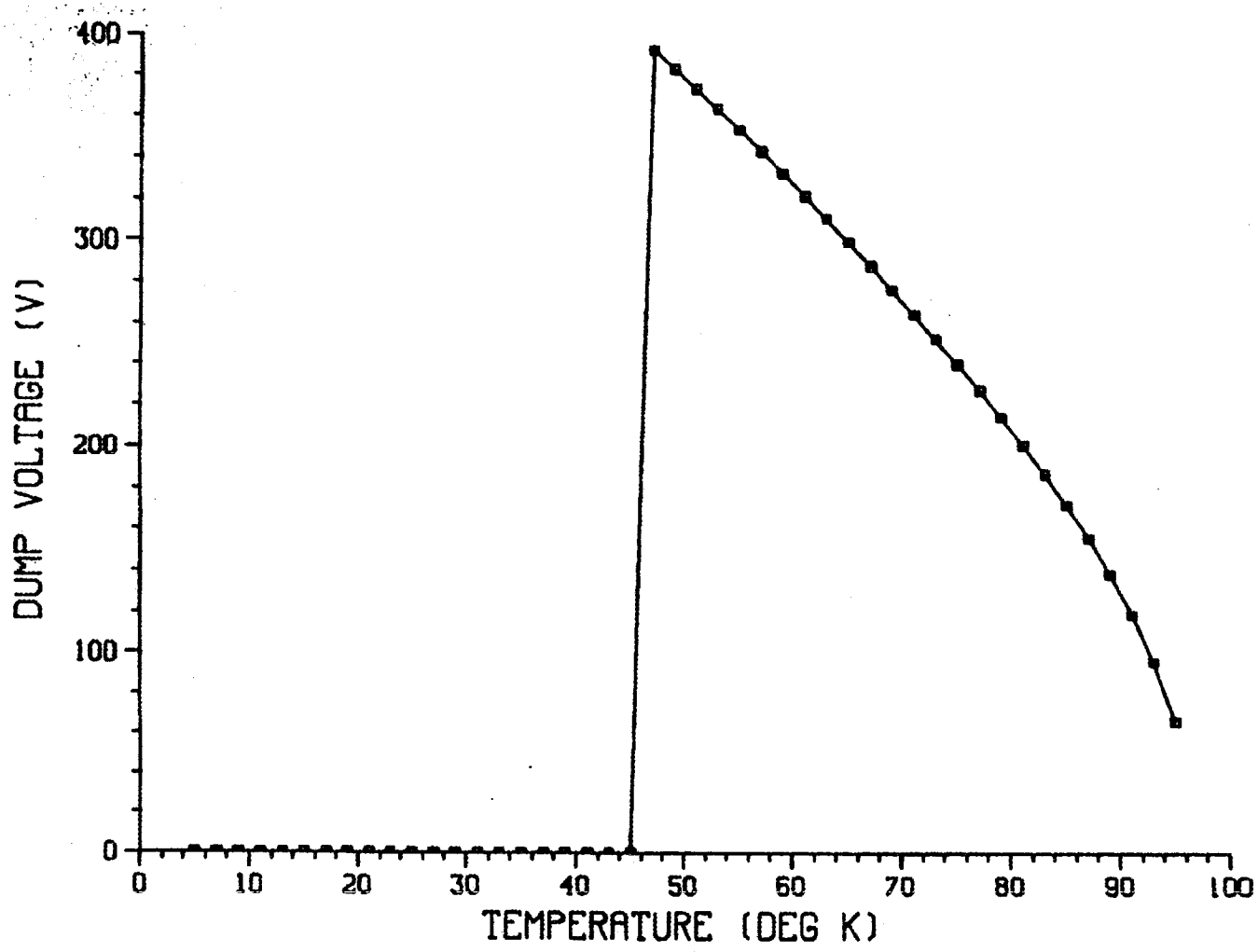

FIGURE 5.1-11 VOLTAGE VS. TEMPERATURE FOR EBT-P

The NASTRAN model is shown in Figure 5.2-1 and contains 144 quad 8 plate elements, 33 bar elements, and has 4575 degrees of freedom. The model is a half symmetric structure, symmetric about the X-Y plane. The outer ring thickness is .75, the inner ring is .375, and the side walls taper from .375 to .625. The model was analyzed under loading conditions shown in Figure 5.2-2.

The inner bore is loaded during coil winding. This produces maximum load condition at room temperature according to the STANSOL analysis (see Figure 5.2-3). This loading can produce both stability and structural yielding. The winding tension used of 180 pounds produces a maximum hoop stress in the inner bore of -14,865 psi and a maximum radial stress of -571 psi. A stability analysis, when using a factor of safety of 4 gives the following margin of safety.

$$MS = \frac{7532}{571\ (4)} - 1 = 2.30 \text{ buckling}$$

The margin of safety on yield is:

$$MS = \frac{25,000}{14,865\ (1.5)} - 1 = +.12 \text{ yield}$$

The inner bore is also loaded by the centering force acting on the coil pack. This produces an unequal load distribution around the bore which was modeled in the finite element model. The results of this analysis indicated the maximum stress condition existed on the side opposite the centering direction. The maximum principal stresses are:

Longitudinal stress = 7,286 psi

Hoop stress = 1,608 psi

Combining these stresses using VonMises criteria gives an effective stress of:

Effective stress = 6,630 psi

$$MS = \frac{25,000}{6,630\ (1.5)} - 1 = +1.51 \text{ yield using R.T. properties}$$

A discontinuity analysis of the inner bore side plate joint indicates a maximum stress of 2,908 psi at proof pressure and 3,877 psi at burst pressure exists. This provides the following margins of safety:

$$MS = \frac{25,000}{1.5\ (2908)} - 1 = +4.73 \text{ proof pressure}$$

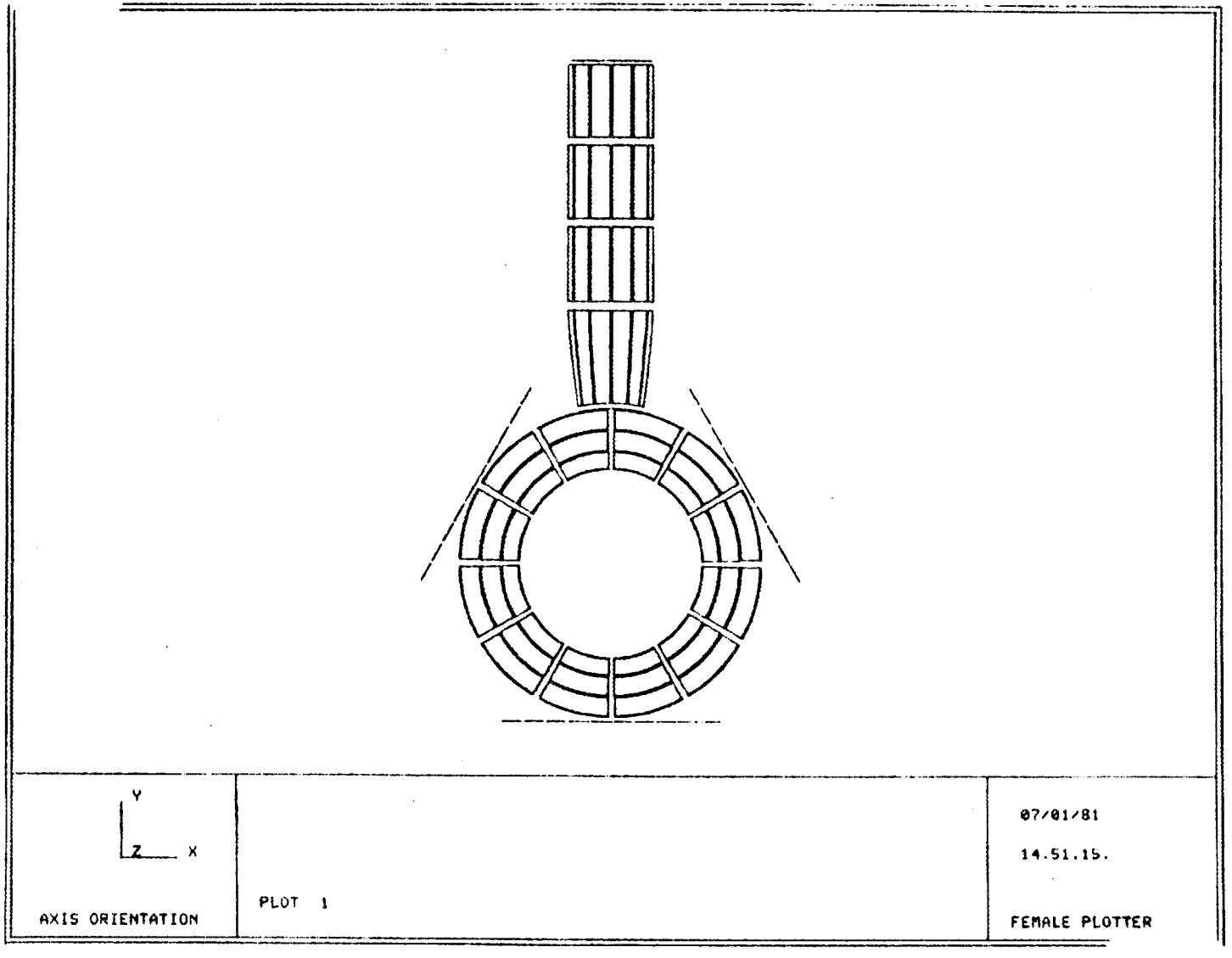

FIGURE 5.2-1 FINITE ELEMENT MODEL USED FOR ANALYSIS OF HELIUM VESSEL

LOAD CONDITION	LOAD
NORMAL PRESSURE	14.7 PSI
FAULT PRESSURE	50.0 PSI
PROOF PRESSURE	75.0 PSI
BURST PRESSURE	100 PSI
NORMAL OPERATION	14.7 PSI + 17,900 CENTERING
FAULT OPERATING	50 PSI + 8,000 CENTERING + 73,000 O.F.P.

FIGURE 5.2-2. HELIUM VESSEL MODEL LOADS

STRESS (PSI)

DESIGN	HOOP		RADIAL	
	MAX	MIN	MAX	MIN
NOMEX	+16,600	+1880	+ 0	- 735
KAPTON	+10,800	+7300	+ 0	-1590

FIGURE 5.2-3. CONDUCTOR STRESSES DUE TO WINDING, COOLDOWN, AND MAGNET LOADS

$$MS = \frac{70,000}{3\ (3877)} - 1 = +5.02 \text{ burst pressure}$$

An analysis of the side flange corner stress when loaded by the fault condition of 50 psi plus 73,000 pounds side load indicates the maximum stress occurs at the inner radius and is 27,718 psi. Since this loading can only occur at operating temperature, the low temperature properties of the material are used. The margin of safety is:

$$MS = \frac{70,000}{27,710\ (1.5)} - 1 = +.68 \text{ fault condition}$$

The NASTRAN model indicates the maximum loading in the outer ring occurs at the attachment point of the bottom cold mass support strut. The indicated stress at this point is 42,922 psi. The model does not account for the localized reinforcement due to the mounting pad for the support, so this stress is conservative. At this condition, the margin of safety is:

$$MS = \frac{70,000}{42,922\ (1.5)} - 1 = +.09 \text{ on yield}$$

The helium vessel stack is a cylinder of varying wall thickness. The bottom section is .11 in. thick, the upper section is .035 in. thick. Analyzing this using the ASME Code indicates the minimum wall thickness is .0169 inches. This is a margin of safety of:

$$MS = \frac{.035}{.0169} - 1 = 1.07 \text{ proof pressure}$$

5.2.2 WINDING STRESS ANALYSIS. The mirror magnet winding was analyzed with computer program STANSOL. Two series of analyses were performed investigating the effects of using Kapton vs. Nomex as the conductor wrapping material. One further difference between the two analyses was the use of 115 lbs. winding tension for the Kapton and 180 lbs. winding tension for the Nomex. Earlier runs with Kapton and 180 lbs. winding tension over-stressed the bobbin in compression. For each configuration, there were three analyses run: the first included all materials and was loaded by the winding preload and a temperature reduction to $4^{o}K$; the second analysis was the same as the first except for the addition of magnetic loads; the third analysis removed the bobbin to simulate lift off and was loaded with magnetic loads only. The actual operating stresses are obtained by combining all three conditions. A summary of the resulting stresses is given in Figure 5.2-3. The Nomex design was selected even though the Kapton design gave a more benign stress state.

The conductor is purchased to Convair specification number 11-38007. This specifies a room temperature yield strength of at least 30 ksi. Available data (Reference M-216 dated 11/29/77) indicates that Type 101 OFHC copper is stronger at $20^{o}K$ than at room temperature.

The material reported which has properties nearest the conductor R.T. yield is 1/4 hard (10% cold work). Its R.T. yield is 29.6 ksi and 20°K yield is 38.5 ksi. Therefore, ratio our specification value to get a 4°K allowable of:

$$F_{TY_{4^oK}} = 30 \times \frac{38.5}{29.6} = 39.0 \text{ ksi}$$

Conductor margins of safety were calculated at each of the four winding pack elevations where magnetic fields were defined. These fields were used for calculation of stresses along the axis of the torus. The critical location was in layer number 5 from the bobbin which had the peak axial tension. The radial stresses from STANSOL and the torus axis stresses are multiplied by four to account for peaking where the Nomex overwraps contact each other. The resulting stresses at the critical layer five are:

$$\text{Hoop} = +16593 \text{ psi}$$

$$\text{Radial} = 4 \times (-391) = -1564 \text{ psi}$$

$$\text{Axial} = 4 \times (-2767) = -11068 \text{ psi}$$

$$\text{D.E. (Actual)} = (16593 + 1564)^2 + (11068 - 1564)^2 + (16593 + 11068)^2$$

$$= 11.85 \times 10^8$$

$$\text{D.E. (Allow)} = \overline{2 \times 39000}^2 = 30.42 \times 10^8$$

$$\text{M.S.} = \frac{\sqrt{30.42 \times 10^8}}{1.5 \times \sqrt{11.8 \times 10^8}} - 1 = +0.07$$

The strain, due to winding and mechanical load, influences the critical current in the superconductor. The winding strain is:

$$\epsilon_\omega = \frac{C}{R} = \frac{0.1142/2}{9.5} = 0.0061$$

$$\epsilon_\sigma = \frac{\sigma}{E} = \frac{24,000}{14.6 \times 10^6} = 0.0016$$

$$\text{Total} = 0.0061 + 0.0016 = 0.0077$$

Based on data from J. W. Ekin, "Mechanical Effects on Superconductor Performance," a strain of 0.77% will degrade the critical current about 3% in a 7 Tesla field. Note that this degradation is only significant at the extreme fibers at the peak field.

5.2.3 COLD MASS SUPPORTS STRESS ANALYSIS. The 11-38060-6 cold mass supports provide a radially flexible, near simple support for the cold mass and react loads to the outside of the dewar. The material used is Ti-6Al-4V which has the desirable properties of high strength and low heat conduction. The analysis criteria used was that of the ASME Boiler and Pressure Vessel Code, Section III, Division 1, Appendix XVII which is for nuclear power plant component supports. The most significant items from this appendix are the step-by-step directions for analyzing bolted joints and the factors of safety of:

F.S. Yield = 5/3

F.S. Ult = 2.0

The internal loads in the cold mass supports were determined using NASTRAN. Three bar models of the supports were created as shown in Figure 5.2-4. Each model contained 22 bars so that varying cross sections were accurately represented. The bar material modulii were input with values appropriate for the operating temperatures. These three support models were incorporated into an overall model of the helium vessel, vacuum vessel, and support structure as shown in Figure 5.2-5. The model was loaded with combinations of gravity, temperature, normal magnetic loads, fault magnetic loads, and pressure. Each bar of each support was searched for critical load conditions and margins of safety calculated. The allowables used were taken from MIL-HDBK-5C and corrected for temperature with data from the same source. Due to the closeness of yield and ultimate in Ti-6Al-4V, the ultimate strength requirement governed the design. The most critical margin of safety is at node 18 in the lower support.

ANALYSIS AT NODE 18

$$T = -27.5^{\circ}F$$

$$F_{tu} = 1.09 \times 130{,}000 = 141{,}700 \text{ psi}$$

$$= P/A \pm \frac{M_1 C_1}{I_1} \pm \frac{M_2 C_2}{I_2}$$

$$= 47{,}723 \text{ psi}$$

$$MS = \frac{141{,}700}{2.0 \times 47723} - 1 = +0.48$$

In addition to stress checks, the legs of the supports were checked for column stability according to ASME Code methods (Reference Equation 19, Appendix XVII).

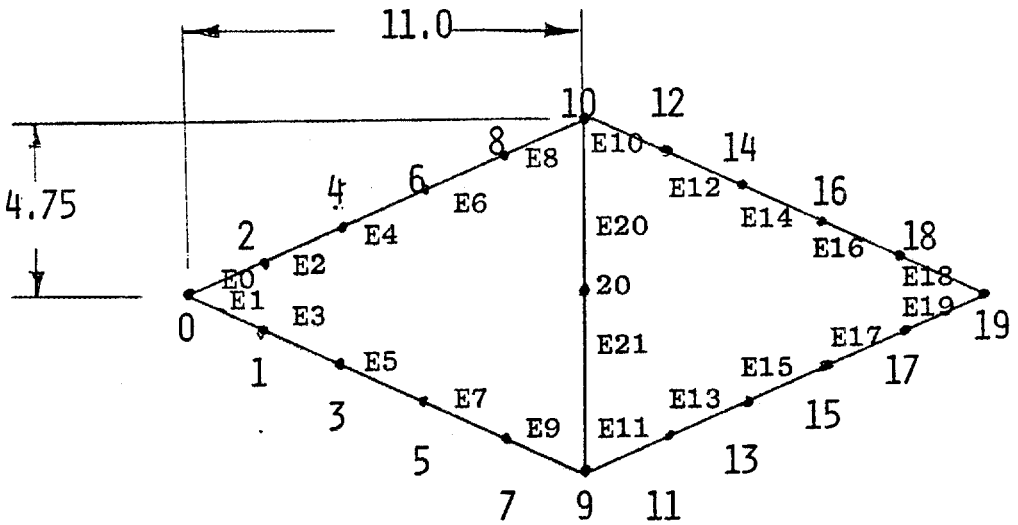

FIGURE 5.2-4 FINITE ELEMENT MODEL OF COLD MASS SUPPORTS

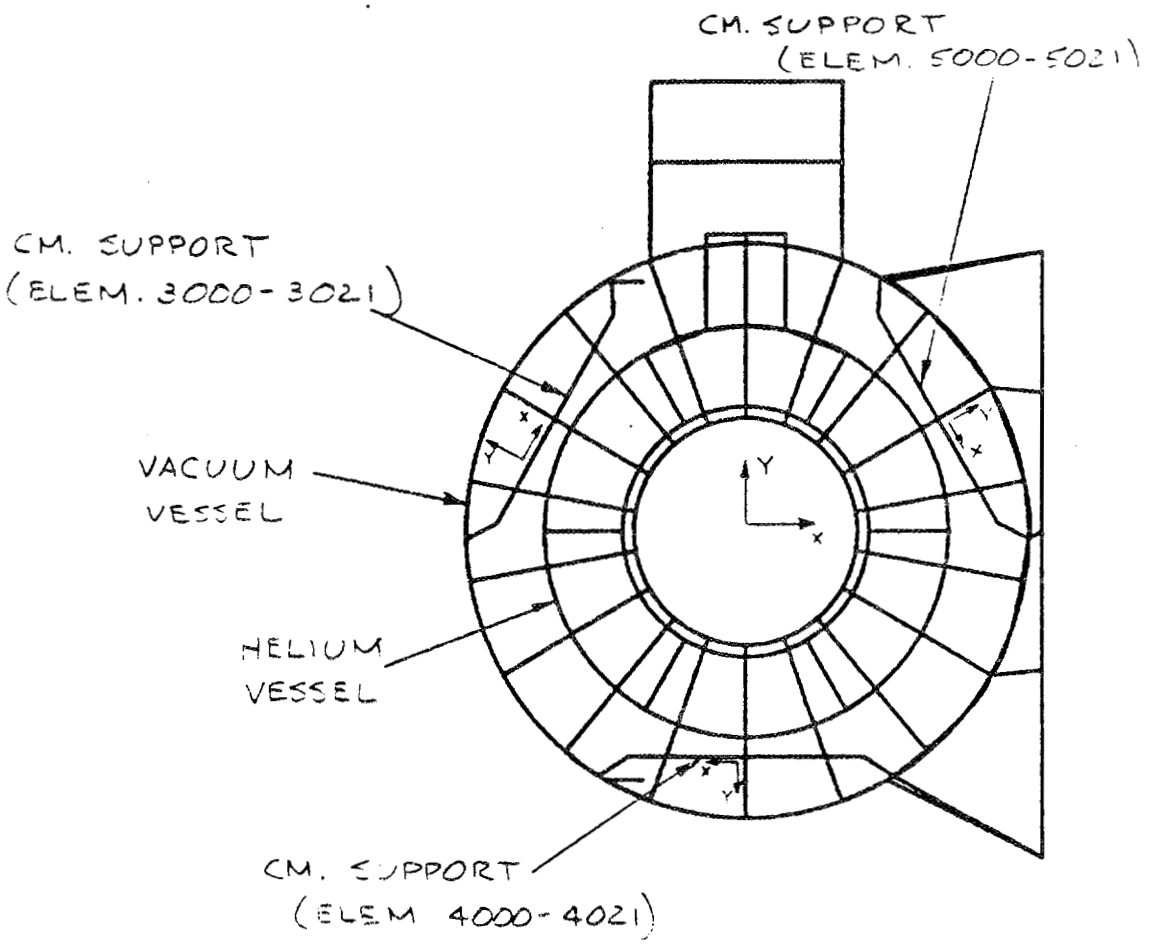

FIGURE 5.2-5 FINITE ELEMENT MODEL OF MIRROR MAGNET INCLUDING COLD MASS SUPPORTS

$$\frac{fa}{Fa} + \frac{Cmxfbx}{(1-fa/F'ex)Fbx} + \frac{Cmyfby}{(1-fa/F'ey)Fby} \leq 1.0$$

where $Fe = \frac{12\pi^2 E}{23\ (K\ l/r)^2}$

with restrained ends, Cm = 0.85

K = 0.80 (pinned - fixed)

Tension in the legs due to cooldown is conservatively ignored. The most critical element is element 14 at cold temperature.

Mx = 65.31 in lbs., My = 735.6 in lbs.,
P = 17650 lbs.

$E = 18.5 \times 10^6$ psi Fa = 98,875 psi

ℓ_x = 4.375 in. ℓ_y = 11.0 in.

r_x = 0.132 in. r_y = 0.317 in.

F'_{ex} = 135,500 psi F'_{ey} = 123,617 psi

fa = 35,300 psi

f_{bx} = 1719 psi f_{by} = 8084 psi

$R_1 + R_2 + R_3 = 0.357 + 0.020 + 0.0973 = 0.474$

$$MS = \frac{1.0}{0.474} - 1 = +1.11$$

<u>END BOLTS</u>. The bolts in the cold mass supports to the vacuum vessel are sized according to the ASME Code, Section III, Division 1, Appendix XVII, Paragraph 2460. The governing equations are:

$L/d \geq 0.5 + 1.43\ (fp/SU)$

$L/d \geq 1.2$

$fp/SU \leq 1.5$

$$\left(\frac{f_t}{F_t}\right)^2 + \left(\frac{f_v}{F_v}\right)^2 \leq 1$$

$$F_v = \frac{0.62\ Su}{3}$$

$$F_t = \frac{Su}{2}$$

Bolt material is Inconel 718 heat treated to Su = 185,000 psi. The bolts attach to the outer vacuum vessel wall and room temperature properties are used.

The critical load condition is fault operation where the lower, inner support bolt is loaded with a shear of 16,814 lbs. The critical margin of safety for the lug is:

$$f_p = \frac{16814}{.56\ X\ .75} = 40{,}033 \text{ psi}$$

$$L/d = \frac{1.0}{.75} = 1.333$$

$$L/d \quad 0.5 + 1.43 \left(\frac{40{,}033}{130{,}000}\right) = 0.9404$$

$$MS_{lug} = \frac{1.333}{.9404} - 1 = +0.42$$

The bolt simultaneously experiences a tensile load of 292 lbs.

$$A_B = \frac{\pi D^2}{4} = \pi\ X\ \frac{.75^2}{4} = 0.4418 \text{ in.}^2$$

$$f_v = \frac{16814}{.4418} = 38059 \text{ psi}$$

$$f_t = \frac{292}{.4418} = 661 \text{ psi}$$

$$F_v = \frac{0.62\ X\ 185000}{3} = 38233 \text{ psi}$$

$$F_t = \frac{185000}{2} = 92{,}500 \text{ psi}$$

$$\Sigma R = \left(\frac{661}{92500}\right)^2 + \left(\frac{38059}{38233}\right)^2 = 0.9910$$

$$MS_{bolt} = \frac{1.0}{0.991} - 1 = +0.009$$

CENTER BOLTS. The bolts at the center of the cold mass supports which attach it to the cold mass are a pattern of three bolts, a single one of which is shown in Figure 5.2-6. These bolts are 0.50 inches in diameter, and made of A-286 heat-treated to a minimum of 160,000 psi tensile strength. The cold mass is near 4^oK. The handbook on materials for superconducting machinerv gives a 1.48 increase in F_{tu} at 17^oK. The ASME allowable shear stress is:

$$F_v = \frac{0.62 \text{ X } 1.48 \text{ X } 160000}{3} = 48,940 \text{ psi}$$

The critical load condition is the fault condition at the lower support where the loads are:

Axial + Lateral = Total

(15027 + 9127) + 9237 = 25860 lbs.

or $\frac{25860}{3}$ = 8620 lbs/bolt shear

$$f_v = \frac{8620}{\pi \text{ X } .25^2} = 43,901 \text{ psi}$$

$$MS_{shear} = \frac{48940}{43901} - 1 = +0.11$$

The critical bearing stress is in the 316 L pads. The procurement specification of a factor of safety of 1.5 on yield is more restrictive than the ASME code. To get a bearing yield value at 4^oK, the 4^oK F_{ty} value is ratioed by the room temperature ratio of F_{bry}/F_{ty} for 301 taken from MIL-HDBK-5C.

$$F_{bry} = 60,000 \text{ X } \frac{50}{30} = 100,000 \text{ psi @ } 4^oK$$

$$f_b = \frac{8620}{0.5 \text{ X } 0.26} = 66308 \text{ psi}$$

$$MS = \frac{100,000}{1.5 \text{ X } 66308} - 1 = +0.005$$

5.2.4 VACUUM VESSEL STRESS ANALYSIS. The vacuum vessel was analyzed using MSC/NASTRAN finite element analysis code and ASME Boiler and Pressure Vessel Code. Nastran models were used to determine thermal and magnetic load distributions, as well as to provide detailed analysis of the stack discontinuity effects.

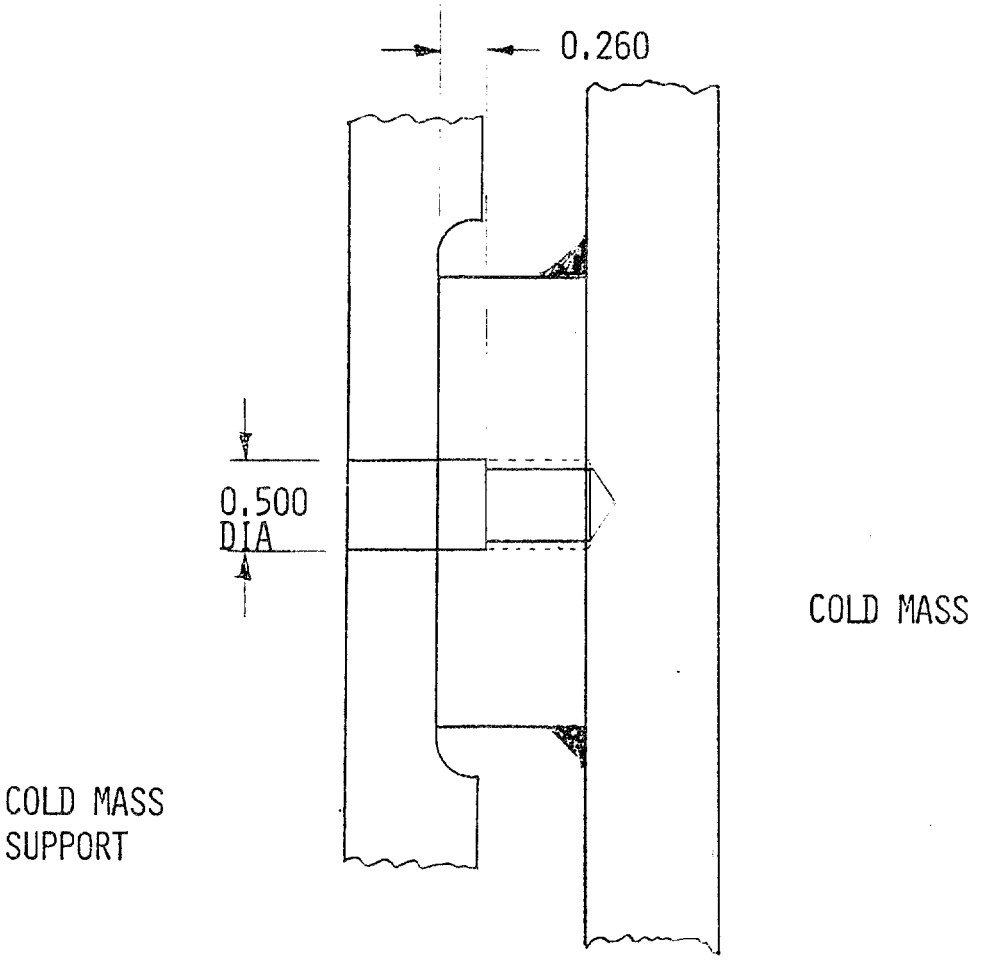

FIGURE 5.2-6 BOLT INSTALLATION - COLD MASS SUPPORT TO COLD MASS

Section VIII, Divisions 1 and 2, were used in the ASME Code analysis.

The Nastran model used to determine the load distributions is shown in Figure 5.2-1. It consists of 150 quad 8 plate elements, 10 triangular plate elements, 74 bar elements, and has 2572 degrees of freedom. Magnetic loads were imposed on the model by applying gravity loads to the cold mass in directions and magnitudes which would simulate the magnetic forces acting on the cold mass. These forces are defined in Figure 3.5-3. The results of this model were used for the cold mass supports and out-of-plane supports analysis. The Nastran model used to investigate the stack discontinuity is shown in Figure 5.2-7. The model consists of 168 quad 8 plate elements and has 2050 degrees of freedom. The model is a half-semetric model of a 70 degree segment which subtends the stack section of the vacuum vessel. The model also includes the inner bore corner radius to provide stress distribution in that region. The ASME Code does not provide for the analysis of side plates, such as are used on the vacuum vessel and so this model also provides data for this portion of the structure, as well.

The results of this model showed the need for reinforcement across the vessel-stack interface. Due to space constraints, the support had to be placed inside and trimmed to only 0.25" thick for a span of 7.5". The pressure load supported is about 12" wide. The bar used is 1.0" thick and welded to 0.25" thick outer plate. Using 10t effective width, I = 0.157, C = 0.304.

$$M = \frac{wl^2}{12} = \frac{14.7 \text{ X } 12 \text{ X } 7.5^2}{12} = 827 \text{ in/lb}$$

$$f = MC/I = 827 \text{ X } 0.304/0.0157 = 16013 \text{ psi}$$

$$MS = \frac{25000}{1.5 \text{ X } 16013} - 1 = +0.04$$

The side plates indicate that stress peaking occurs at approximately the mid radius of the side plates. The principal stress in the radial direction is 9110 psi and the 2099 psi in the tangential direction. This is an effective stress of 8263 psi for a margin of safety of:

$$MS = \frac{25000}{1.5\ (8263)} - 1 = +1.02 \text{ on yield}$$

The peak stress in the inner bore corner radius occurs at approximately 45° of the 90° corner radius. The principal stresses are -5,680 psi and -12,990 psi, respectively. This is an effective stress of 11,279 psi for a margin of safety of:

$$MS = \frac{25000}{1.5\ (11,279)} - 1 = +.48 \text{ on yield}$$

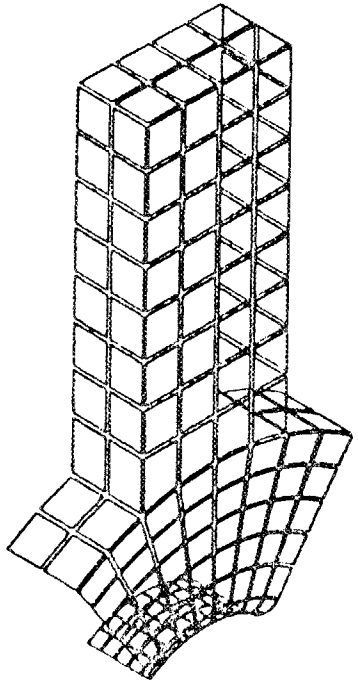

FIGURE 5.2-7 FINITE ELEMENT MODEL USED IN ANALYSIS OF VACUUM VESSEL STACK DISCONTINUITIES

The peak stress in the stack side plates occurs approximately half way up the stack. The principal stresses are 13,117 psi in the vertical direction and 4,957 psi in the horizontal direction. This is an effective stress of 11,472 psi for a margin of safety of:

$$MS = \frac{25000}{1.5\ (11,472)} - 1 = +.45 \text{ on yield}$$

The center bore, corner radius, and side plates were all initially sized using the ASME code. The center bore was sized to permit pressure reversal without collapse. The margin of safety on collapse is +2.94.

The center bore butt weld is sized to permit non-radiographic inspection according to the requirements of Division 1. The margin of safety on this weld is +.20.

The out-of-plane support lugs incur a peak loading of 22,660 lb. during fault condition loading. The bolts which hold the supports to the vacuum vessel are 1.0" Inconel 718, heat treated to 180 ksi. The margin of safety in shear is:

$$MS = \frac{.62\ (180,000)\ \pi\ (.5)^2}{3\ (22,660)} - 1 = +.29 \text{ shear}$$

Bearing margin of safety on the holes in the out-of-plane support lugs is:

$$MS = \frac{.75\ (70,000)\ (1.89)}{2\ (22,660)} - 1 = +1.19 \text{ bearing}$$

5.2.5 MISCELLANEOUS STRESS ANALYSIS.

OUT-OF-PLANE STRUTS. The out-of-plane struts are conservatively sized to carry all out-of-plane loads on a single pair. The maximum load based on finite element analysis is

$$P = 22660 \text{ lb}$$

The struts are made from 304L 2.0" hex stock.

$$S_y = 25,000 \text{ psi}$$

$$A = 3.0 \text{ in.}^2$$

$$r = 0.5270 \text{ in.}$$

$$Kl/r = \frac{1.0 \times 25.6}{0.5270} = 48.573$$

$$C_c = \left(\frac{2\pi^2 E}{S_y}\right)^{\frac{1}{2}} = 148.69$$

The column is checked to the ASME Code, Section III, Appendix XVII, Para. 2213.

$$Fa - f\ (S_y,\ Kl/r,\ C_c) = 13{,}260 \text{ psi}$$

NOTE: This is less than $S_y/1.5$

$$f = P/A = \frac{22660}{3.0} = 7553 \text{ psi}$$

$$MS = \frac{13260}{7553} - 1 = +0.76$$

The high strength rod end threads into the end of the soft 304L hex. The balanced strength shear section thru the threads is at about 80% of the 304L thread section. The thread engagement is at least 1.0 inch.

$$A_s = L \times P.D. \times \pi \times 0.8 = 3.0 \text{ in.}^2$$

$$f_s = 22660/3.0 = 7550 \text{ psi}$$

$$F_{sy} \approx 0.6\ F_{ty} = 15000 \text{ psi}$$

$$MS = \frac{15000}{1.5 \times 7550} - 1 = +0.32$$

The manufacturer's ultimate rating of the BRE-16-2450 rod end is 73,300 lbs. Test data indicates a factor of 1.5 between the proportional limit and ultimate.

$$MS = \frac{73300/1.5}{1.5 \times 22660} - 1 = +0.44$$

AXIAL STIFFNESS ANALYSIS. Information provided by ORNL indicated that the required axial stiffness for stability of a toroidal array is:

$$k_s > 4k_m$$

For EBT-P

$$k_s > 26{,}700 \text{ lb/in}$$

From Nastran model, axial displacement due to an out-of-plane force of 73,000 pounds is .091482 (mean value of 12 pts.).

Then

$$k_s = \frac{73{,}000}{.091482} = 797{,}970 \text{ lb/in}$$

$$MS = \frac{797{,}970}{26{,}700} - 1 = +28.9$$

5.3 THERMODYNAMIC ANALYSIS

5.3.1 STABILITY. The very high overall current density of 10,000 A/cm^2 required for the EBT-P mirror coils necessitates a metastable conductor design. At the 90 GHz operating point, the 1683 amp current and 7.4T peak field produce a joule heat flux of 1.57 W/cm^2 on the wetted perimeter of the conductor. Although transient peak nucleate boiling fluxes in helium are approximately that high (References 5.3-1, 5.3-2), transient recovery fluxes are typically about the same as steady-state recovery fluxes, roughly 10% of the transient nucleate peak levels (Reference 5.3-1). Thus, recovery from the normal state is not expected with the EBT-P conductor, and stability depends on the prevention of the formation of a normal zone. The conductor must withstand transient fault events associated with conductor motion as well as a steady-state heating from x-rays produced in the plasma.

At 90 GHz, the coil is operated at only 60% of the conductor critical current to provide a margin of .7K above the bath temperature of 4.2K before current sharing begins. The critical temperature of the conductor at 1683 amps and 7.4T is 5.8K. The basic unit cell is shown in Figure 5.3-1, together with the pertinent parameters used in the stability analysis.

The magnet system specification (Reference 5.3-3) requires the conductor pack to withstand a steady-state heat load due to x-rays of 10W per coil at 90 GHz. This is equivalent to an average energy deposition of 0.30 mW/cm^3 of conductor or a heat flux of .059 mW/cm^2 of conductor wetted surface. At the inside corner of the coil pack, where the x-ray heating is most severe, the peak deposition rate for a 10W total load is approximately 0.75 mW/cm^3, which corresponds to a wetted surface heat flux of .174 mW/cm^2.

The critical heat flux in the vertical channel shown in Figure 5.3-2 may be estimated from the correlation given in Reference 5.3-4, i.e.,

$$\dot{q}_c = \sigma \frac{W}{\sqrt{Z}} \qquad 5.3\text{-}1$$

Where

$\dot{q}_c$ = maximum heat flux injected into a channel (W/cm^2)

$\sigma \approx 7.0$ (empirical constant)

W = width of channel (cm)

Z = height of channel (cm)

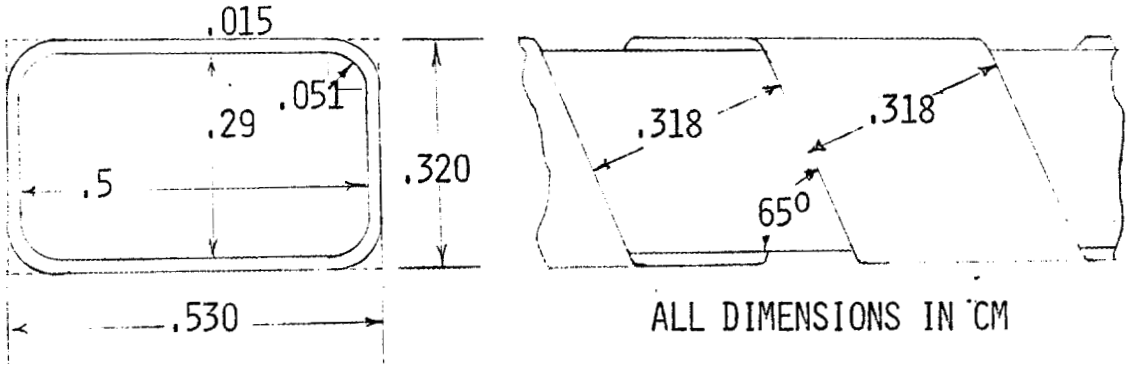

UNIT CELL AREA	= .170 CM^2
CONDUCTOR AREA	= .143 CM^2
COPPER: SUPERCONDUCTOR	= 3:1
SUPERCONDUCTOR AREA	= .0357 CM^2
COPPER AREA	= .107 CM^2
WETTED PERIMETER	= .746 CM
HELIUM VOLUME	= 9% OF UNIT CELL VOLUME
INSULATION COVERAGE	= 50% OF CONDUCTOR SURFACE
Io	= 1683 AMPS
B_{MAX}	= 7.4 T
STABILIZER RRR	= 120
CRITICAL CURRENT	= 2800 AMPS AT 7.4 T, 4.2K
BATH TEMPERATURE	= 4.2K
$\dot{q}_J$	= 1.57 W/CM^2

FIGURE 5.3-1 EBT-P UNIT CELL AND STABILITY PARAMETERS

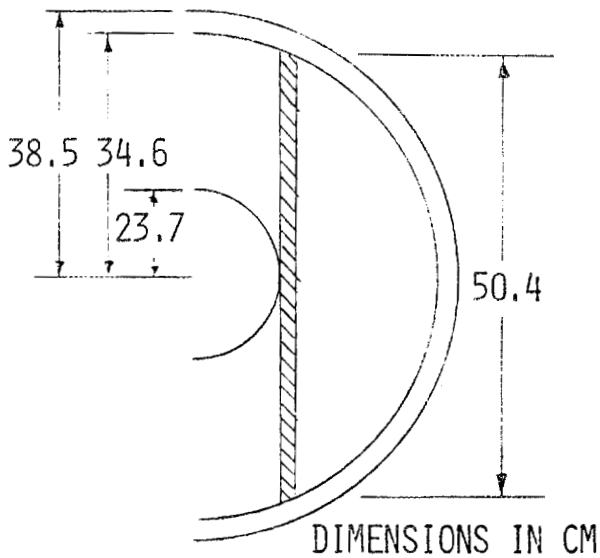

FIGURE 5.3-2 MAXIMUM HEATED CHANNEL VERTICAL LENGTH

Taking the insulating wrap thickness as the channel width (.015 cm), and the chord length indicated in Figure 5.3-2 as the maximum channel height (50cm) gives a critical flux of 15 mW/cm^2. Thus, heat removal should be accomplished in the nucleate boiling regime, even though the effects of vapor accumulation and/or horizontal surfaces blocking upward flow within the conductor pack could degrade the critical flux significantly. However, at the worst heating location, the presence of ground/grid insulation should provide enough helium volume locally to avoid this degradation.

The temperature difference between conductor and bath required to transfer .18 mW/cm^2 must be less than the conductor current sharing margin. At this very low flux level, heat transfer approaches a limiting case of conduction across a liquid film into the interconductor channel. A minimum heat transfer coefficient can be calculated by assuming a channel Nusselt number of unity and using a channel hydraulic diameter of .029 cm. If the channel is assumed vapor locked so that no liquid is present, the heat transfer coefficient is 3.65 mW/cm^2-K, and the maximum temperature difference required to remove .18 mW/cm^2 is .050K.

The analysis indicates that the boiling heat transfer should be sufficient to remove the steady-state x-ray heating with a large margin of safety. This conclusion is at odds with the results of the x-ray heating simulation done in the open dewar test of the first development coil at ORNL, which indicated that 13W is the maximum load for the conductor pack to be stable. One possible explanation for the difference is the possibility of localized vapor locking of the helium within the pack. A test to measure the steady-state helium heat transfer within a simulated conductor pack is recommended to better understand the reasons for this discrepancy.

The open dewar test at ORNL also demonstrated an unexpected level of stability against transient fault events in the first development coil, particularly in light of the fact that the conductor was demonstrated to have lifted off the bobbin. Figure 5.3-3 is a plot of the energy deposition required to create the minimum propagating zone (MPZ) as a function of maximum, or peak, nucleate boiling heat flux. The analysis is documented in Appendix B-4 . The result of the analysis is that if the coil is stable, then the energy deposition from a fault event such as a slip must be very small, even as the peak nucleate boiling flux approaches the high levels associated with transient boiling heat transfer in helium.

Two analyses were done to determine whether the heat fluxes and energy depositions of Figure 5.3-3 are credible in terms of the EBT-P conductor pack. The first analysis was done to estimate the magnitude of energy deposition from two different fault events, one a radial slip, the other an axial slip of a conductor

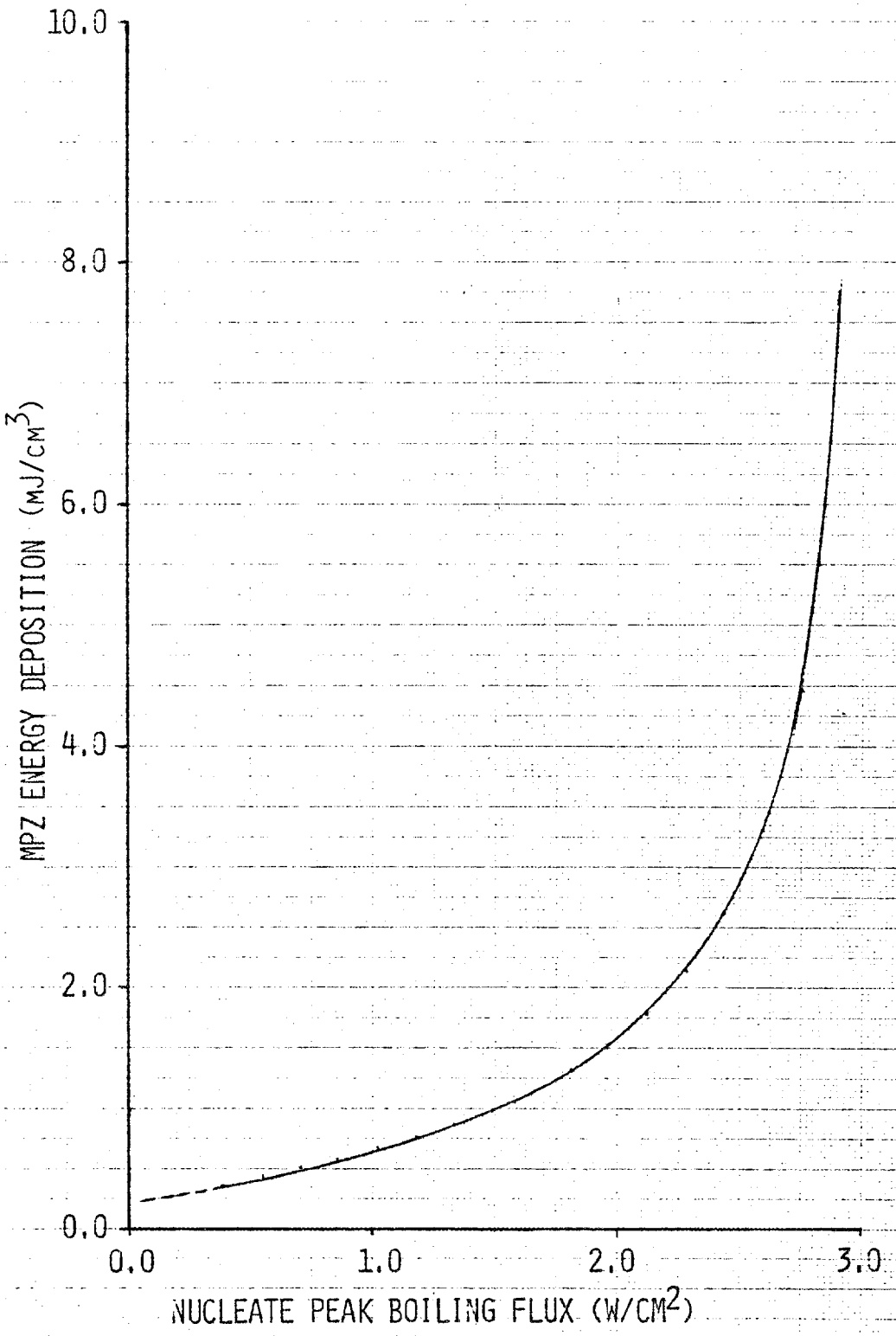

FIGURE 5.3-3. ENERGY REQUIRED TO CREATE MINIMUM PROPAGATING ZONE AS FUNCTION OF MAXIMUM COOLING FLUX

in the first layer of the winding. The second was done to estimate the level of heat transfer within the conductor pack, considering a channel limited boiling mechanism and also an induced flow mechanism utilizing the capillary action of the porous Nomex braid insulation. Both analyses are documented in Appendix B-4 .

The first fault event analyzed assumed that, due to friction between two adjacent turns, the conductors are constrained to move together as the conductor pack lifts off the bobbin. However, since there is an axial gradient in the radial magnetic force, a slip between the conductors can occur. The expression for the energy released during such a slip, derived in Appendix B-3 , is:

$$\Delta U = \frac{(\mu F_a r)^2}{A_c E}\left[\frac{\Delta F_r}{\mu F_a} - 1\right] \qquad 5.3\text{-}2$$

Where

ΔU = energy released/unit length of conductor (J/m)

μ = coefficient of friction at slip plane

F_a = accumulated axial force on conductor at slip plane (N)

ΔF_r = difference in net radial force between adjacent conductors (N)

r = radius of slipping conductor (m)

A_c = cross-sectional area of conductor (m^2)

E = Young's modulus of the conductor (Pa)

If the term $\Delta F_r/\mu F_a$ is greater than one, a slip can occur. Examination of the forces acting on the first layer conductors shows that the quantity $\Delta F_r/F_a$ is small everywhere except at the sidewall (neglecting any axial precompression of the winding), and even at that point, a coefficient of friction smaller than 0.09 is necessary for a radial slip to occur. The maximum slip energy corresponds to μ = 0.05, for which ΔU = 2mJ/m or .150mJ/cm^3.

The second fault event analyzed was an axial slip along the bobbin. In this scenario, as the magnet is charged, at some point the accumulated axial force becomes greater than the frictional forces present because of the winding pretension and can cause a slip if a gap between adjacent conductors exists. This case is more difficult to analyze due to the complex way the axial forces accumulate assuming the conductors haven't lifted off the bobbin. Qualitatively, the forces that would produce an axial slip during a chargeup are shown in Figure 5.3-4. As the magnet is charged, the frictional restraining force

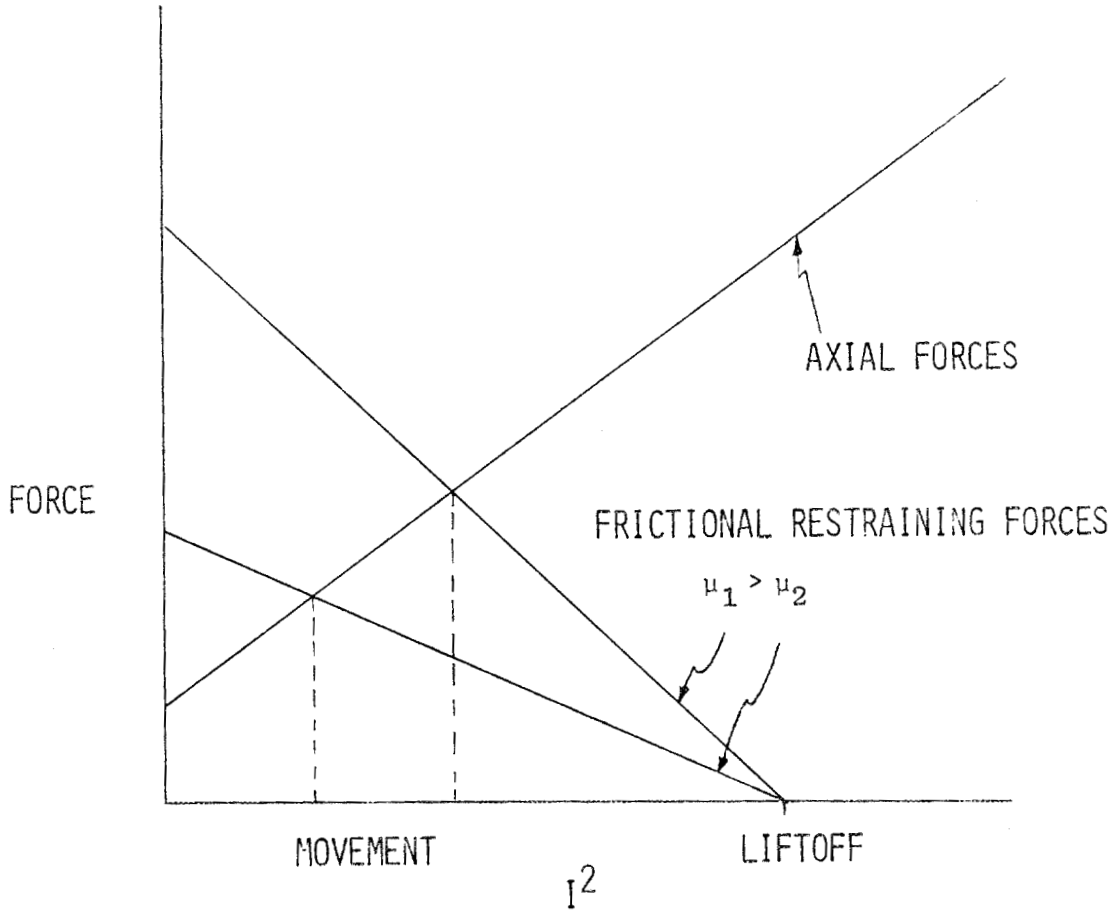

FIGURE 5.3-4. QUALITATIVE ILLUSTRATION OF FORCES ACTING TO PRODUCE SLIP AGAINST BOBBIN DURING CHARGE-UP

decreases because the net inward radial force is decreasing. At the same time, the axial forces that produce the slip are increasing. The net result is that motion can occur at current levels below the current at which liftoff occurs. Motion at lower current levels releases less energy because the forces are small, and there is a larger margin on the current sharing temperature difference because the conductor is operating at a smaller fraction of its critical current. Both effects can account for the observed stability in the first development coil.

All of the energy released as a result of conductor motion does not go directly into the conductor. In Appendix B-4 , it is shown that when two materials slide against each other or collide into each other, the energy is dissipated in each material according to:

$$\frac{\Delta U_1}{\Delta U} \alpha \frac{E_2}{E_1 + E_2} \qquad 5.3\text{-}3$$

Where

ΔU_1 = energy dissipated in material 1

ΔU = total energy released during slip or collision

E_1 = Young's modulus of material 1

E_2 = Young's modulus of material 2

Using values of 1 X 10^5 MPa for the modulus of copper, and 70 MPa for the effective modulus of the Nomex braid, Equation 5.3-3 says that essentially all of the released energy goes into the braid immediately after a slip.

The porosity of the braid allows helium to permeate into it, which in turn means that the energy deposited in the braid is absorbed by the helium directly. The Nomex filaments comprising the braid form channels for helium flow that, qualitatively at least, should exhibit similar transient heat transfer behavior as that observed in internally cooled cabled superconductors. There is also a pumping capability of the braid, due to capillary action, that tends to minimize any local channel dryouts, and keeps the braid, and also the conductor surface underneath the braid, at least partially wetted. It is possible that the braid acts like the wick of a heat pipe, and provides a significant enhancement of the normal boiling heat transfer within the conductor pack. A simple analysis, documented in Appendix B-4 , suggests that the wicking action of the braid could produce heat fluxes within the braid of at least the same order of magnitude as the channel boiling flux that occurs at the bare conductor surface.

The maximum channel boiling flux can be estimated using Eq. 5.3-1. The difficulty is determining what a "channel" is within the conductor pack. A reasonable assumption to determine a maximum flux is to assume a channel one-wrap-thickness wide with a height equal to the short conductor dimension, i.e., the channel formed between two horizontal conductors. With a wrap thickness of .015cm and conductor height of .29cm, Eq. 5.3-1 predicts a maximum boiling flux of 0.20 W/cm^2. This estimate is probably optimistic when compared to the data of Reference 5.3-1, and is considered an upper bound for the steady-state heat flux obtainable within the conductor pack. Maximum transient peak nucleate boiling fluxes might be up to six times this value for very high power, short duration heating pulses deposited directly to the conductor.

The open dewar test x-ray heating simulation suggests that the steady-state heat transfer is considerably less than predicted above. However, it is unknown whether the results of the open dewar test apply only globally or whether they are valid for a single heated conductor. The results do imply that the background heating does degrade the heat removal capacity of the helium during a fault event, however.

The preceding analyses have shown that, due to the low modulus of the Nomex braided insulation and the way the magnetic forces operate within a coil, the fault energies deposited in the conductor are probably the same order of magnitude as the minimum propagating zone energy of the conductor, a few tenths of a millijoule per cm^3. Normal channel boiling fluxes were estimated to be of the order of 10^{-1} W/cm^2, which is too large to explain the x-ray heating results of the first development coil test, and too small to explain the stability of the coil against conductor motion. This implies that another heat transfer mechanism is acting with the coil pack. One possibility is heat transfer due to induced flow caused by capillary action within the braided conductor. To investigate this possibility, and to determine the steady-state heat transfer and operating temperature within the conductor pack, a heat transfer test on a simulated conductor pack is recommended. The pack should model the EBT-P winding configuration, channel sizes, and surface orientations seen within the magnet. The possible effect of the porous braid should be checked by comparing the heat transfer from an identical conductor/wrap configuration utilizing a non-porous insulation such as Kapton tape.

Once the heat transfer characteristics of the conductor pack are accurately determined, it is possible to better understand why the first development coil behaved as it did during the open dewar test. This in turn assures a higher degree of manufacturing quality control as the EBT-P program transitions from development to production phase.

5.3.2. HEAT LOADS TO CRYOGENS. The EBT-P mirror coils are designed to operate in saturated liquid helium at a bath temperature of 4.2K. A liquid nitrogen system is employed to provide a 77K thermal shield between the cold mass and room temperature dewar to minimize the heat leak to the liquid helium.

The major components of the LHe refrigeration and liquefaction loads are shown in Figure 5.3-5. The major sources are the x-ray heating from the plasma, conduction from the LN_2 intercepts in the cold mass supports, and conduction along the various elements comprising the service stack.

The value listed in Figure 5.3-5 for the x-ray heating is a specification maximum limit and not the actual load. A shielding analysis done by MDAC indicates that the actual maximum heat load is 2.5W due to x-rays.

The conduction loads were computed assuming one-dimensional heat transfer and using thermal conductivity integrals to account for the temperature dependence of conductivity at low temperatures. Figure 5.3-6 shows a sketch of one-quarter of a support, identifying the parameters of the analysis performed to determine the support heat leak. The single piece titanium support is shown.

A schematic diagram of the conduction paths in the stack is shown in Figure 5.3-7. The stack wall and gaseous helium/baffle paths are LN_2 intercepted. The vacuum jackets of the vent/cold gas return line and the helium fill tubes are partially intercepted with beryllium/copper finger springs providing some thermal contact. The heat leak calculation allowed for a high thermal contact resistance at that point, and therefore those paths are assumed intercepted at 100K.

The purpose of the G-10 baffles in the stack is to eliminate any natural convection loops above the liquid level. The baffle spacing was determined by requiring the Grashof-Prandtl product of the gas to be less than 2000, which limits the Nusselt number for heat transfer between two adjacent horizontal plates to unity, i.e., heat transfer is by conduction only. (Reference 5.3-5)

The vapor cooled leads are standard Efferson-type leads rated at 2000 amps. The boiloff rate is based on an optimum boiloff of 1.4 ml/A-hr-lead at rated current and is derated according to

$$\frac{\dot{q}_{op}}{\dot{q}_{rated}} = .60 + .40\left(\frac{I_{op}}{I_{rated}}\right)^2 \qquad (5.3\text{-}4)$$

SOURCE	REFRIGERATION LOAD	LIQUEFACTION LOAD
X-RAY HEATING	10.0W	
CONDUCTION THROUGH SUPPORTS	4.25W*	
STACK LOSSES	4.23W	4.9 L/HR**
INSTRUMENTATION WIRING	.30W	
RADIATION THROUGH MLI FROM COLD WALL	.23W	
SPLICES	.03W	
	19.0W	4.9 L/HR

* ONE-PIECE TITANIUM SUPPORT DESIGN

** LOAD PRODUCED BY VAPOR-COOLED LEADS

FIGURE 5.3-5. STEADY-STATE LIQUID HELIUM HEAT LOADS PER COIL

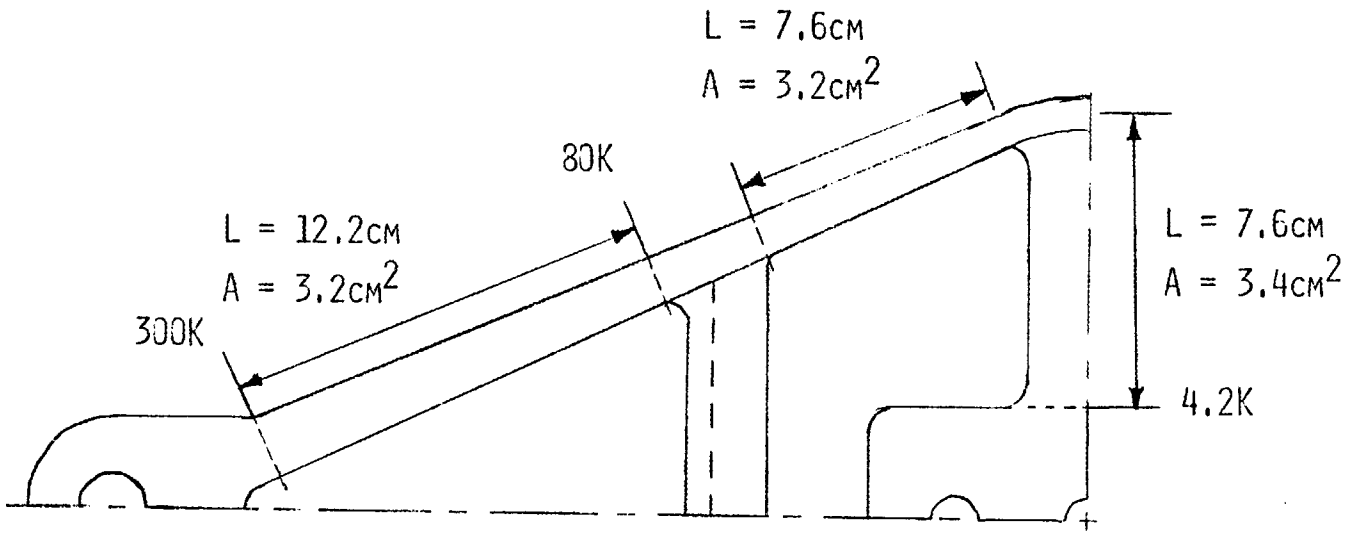

FIGURE 5.3-6. CONDUCTION PATH LENGTHS AND AREAS FOR SUPPORT HEAT LEAK CALCULATIONS

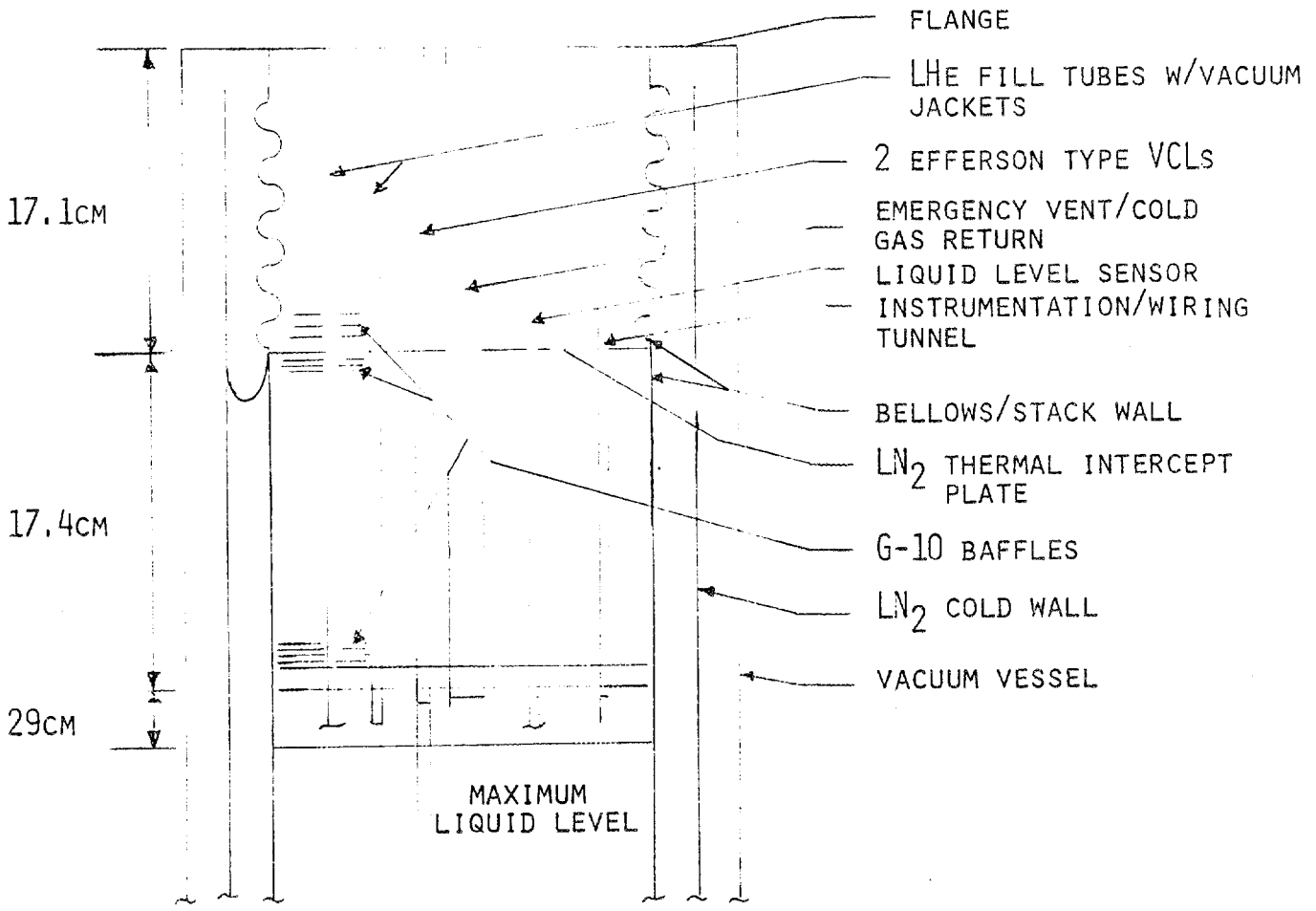

FIGURE 5.3-7. SCHEMATIC OF SERVICE STACK SHOWING HEAT PATHS FROM ROOM TEMPERATURE TO CRYOGENS

Where

$\dot{q}_{op}$ = the operating boiloff

$\dot{q}_{rated}$ = the optimum boiloff at rated current

I_{op} = operating current

I_{rated} = rated current

The loads to the liquid nitrogen system are shown in Figure 5.3-8 and consist of conduction loads to the intercepts in the supports and stack, and thermal radiation from the dewar wall at room temperature through 20 layers of MLI to the cold wall. Intercept locations are indicated in Figure 5.3-6 for the supports and in Figure 5.3-7 for the stack.

The heat load through the MLI, which is double aluminized mylar with dacron spacers, was computed (on both sides of the cold wall) using an effective thermal conductivity for an MLI blanket given by (Reference 5.3-6):

$$K_{eff} = (3.007 \times 10^{-25})(\bar{N}^{8.6})\left(\frac{T_h + T_c}{2}\right) + \frac{(8.33 \times 10^{-2})(\sigma)(T_h^{\,2} + T_c^{\,2})(T_h + T_c)(N)}{(2/\varepsilon - 1)(\bar{N})(N - 1)} \qquad (5.3\text{-}5)$$

Where

$\bar{N}$ = layer density (77 layers/inch)

N = number of layers

T_h = hot side temperature (R)

T_c = cold side temperature (R)

ε = shield emittance (.07 for DAM)

σ = Stefan-Boltzman constant (1.714×10^{-9} BTU/hr-ft^2 - R^4)

K_{eff} = effective conductivity (BTU/hr-ft-R)

To account for pins, seams, and penetrations in a blanket, standard practice at GDC is to multiply the above K_{eff} by a factor of 4.0 before computing radiation loads. However, since the layers in the EBT blankets are perforated, a 25% degradation (increase) in the above value was assumed, as indicated by data from Reference 5.3-7. Therefore, a factor of 5 instead of 4 was used to compute the radiation loads through the MLI.

SOURCE	LOAD
CONDUCTION TO SUPPORT INTERCEPTS	39.0W
RADIATION TO COLD WALL	14.0W
CONDUCTION TO STACK INTERCEPTS	13.4W
TOTAL	66.4W

FIGURE 5.3-8. STEADY-STATE LIQUID NITROGEN HEAT LOADS PER COIL

Details of the analyses to compute the various heat loads are given in Appendix B-4 .

5.3.3 QUENCH PRESSURE RISE.

In the event of a global quench of a coil and subsequent high heat generation rates within the conductor, large amounts of energy will be absorbed by the liquid helium in the cryostat in a short period of time. The internal pressure will rise rapidly and must be relieved before structural failure occurs by allowing helium to vent from the cryostat. An analysis was performed to determine the vent line size required to keep the helium pressure below the cryostat design pressure of 50 psia, given the worst case heating rates expected during a quench. With the present vent system configuration, a vent diameter of 2.3 inches I.D. limits the cryostat pressure rise to approximately 45 psia.*

Figure 5.3-9 shows the heat rate to the helium for a quench. This curve is based on data shown in Figure 5.3-10 measured during the open dewar test of the first development coil and shows current, coil resistance, and dump time constant as a function of time from start of dump. Results from the open dewar test suggested that the best conservative estimate of the heating rate to the helium is to assume that all I^2R heat goes into the liquid. Thus, the curve of Figure 5.3-10 is a plot of

$$\dot{Q} = I_o^2 R_c e^{-2(t - t_o)/\tau} \qquad (5.3\text{-}6)$$

Where

$\dot{Q}$ = heat rate to helium (watts)

I_o = current at time t_o (amps)

R_c = coil resistance at time t_o (ohms)

t_o = time at which measurement is made (seconds from start of dump)

τ = dump time constant at t_o (seconds)

The heating curve does not include the effects of a vacuum loss. An estimate of the heat rate and time constant produced by suddenly raising the outer wall temperature of the cold mass to 90K (the temperature of liquifying air) showed that the heat conducted through the wall is negligible until a point in time after all the liquid has been vented from the magnet due to a simultaneous quench. Loss of vacuum alone is a less severe fault than a coil quench, since the heating

* The quench pressure rise will be re-estimated in Title II when definitive data is available from the development coil tests.

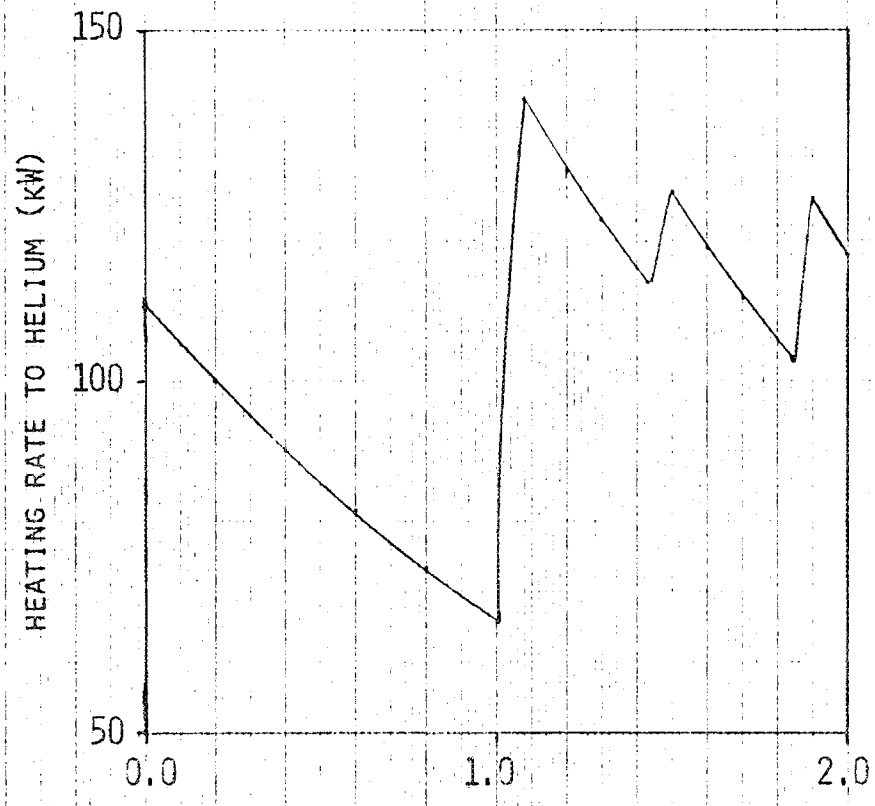

FIGURE 5.3-9. HEATING RATE TO HELIUM IN THE CRYOSTAT AFTER A QUENCH

T_0(SEC)	R_C(OHM)	I_0(AMP)	τ(SEC)
0.0			
	0.0334	1827	3.809
1.08			
	0.0665	1452	3.327
1.426			
	0.0776	1309	3.191
1.84			
	0.0995	1149	2.954
2.99			
	0.1150	780	2.806
∞			

FIGURE 5.3-10. CURRENT, RESISTANCE, AND TIME CONSTANT VS. TIME DURING WORST OBSERVED QUENCH OF DEVELOPMENT COIL #1

occurs at lower levels and over longer periods of time. Details of this analysis are presented in Appendix B-4 .

A schematic of the vent line configuration is shown in Figure 5.3-11. An equivalent loss coefficient for the entire line is required for input to the computer program used to computer the helium pressure during quench. This equivalent loss coefficient was obtained by summing the individual coefficients shown in Figure 5.3-11, plus adding in an $(f \frac{L}{D})$ factor for each straight-section of the vent. The effective coefficient used in the analysis was 8.0. This input value was varied from about 5 to 15 with little effect seen on the maximum pressure. The pressure showed greatest sensitivity to vent line diameter. A 2.0-inch-diameter vent produces a maximum pressure of approximately 61 psia. A 2.3-inch inside diameter line is needed to bring the pressure rise down to 45 psia maximum.

The other factor that affected the pressure rise was the amount of gas or ullage available to absorb the expanding liquid at the start of quench. Various runs made with varying initial ullage volumes showed that the rate at which the pressure rises is sensitive to this parameter, but the peak pressure is relatively unaffected. For the design case, only the gas above the maximum liquid level and below the bottom baffle, and that in the vent line itself below the vacuum vessel flange at the top of the stack, was considered as ullage volume, approximately 3.6 liters. The maximum initial liquid volume is 29.0 liters.

Figure 5.3-12 shows the calculated response of the helium to the heat input. GDC program QCHPRS (Reference 5.3-8) was used to simulate the venting process, since the flow in the vent is essentially Fanno flow (adiabatic, constant area flow). Helium pressure, mass, and exiting mass flow rate are shown as functions of time. Note in particular that after about 1.67 seconds only 10% of the initial mass of helium remains in the dewar. At this point, the heat being generated in the conductor will stay in the conductor, i.e., the heat transfer to the helium becomes limited and the pressure transient is essentially over. The analysis is not valid after this point in time.

5.3.4 COOLDOWN AND WARMUP ANALYSIS.

Two multi-mode thermal models of the EBT-P mirror coils were built to investigate the thermal response during warmup and cooldown. The GDC thermal analyzer program P4560D (Reference 5.3-9) was used to solve the models to obtain temperature vs. time curves and to get temperature gradients through the magnet assemblies during the transients.

A simple model, denoted model A and shown schematically in

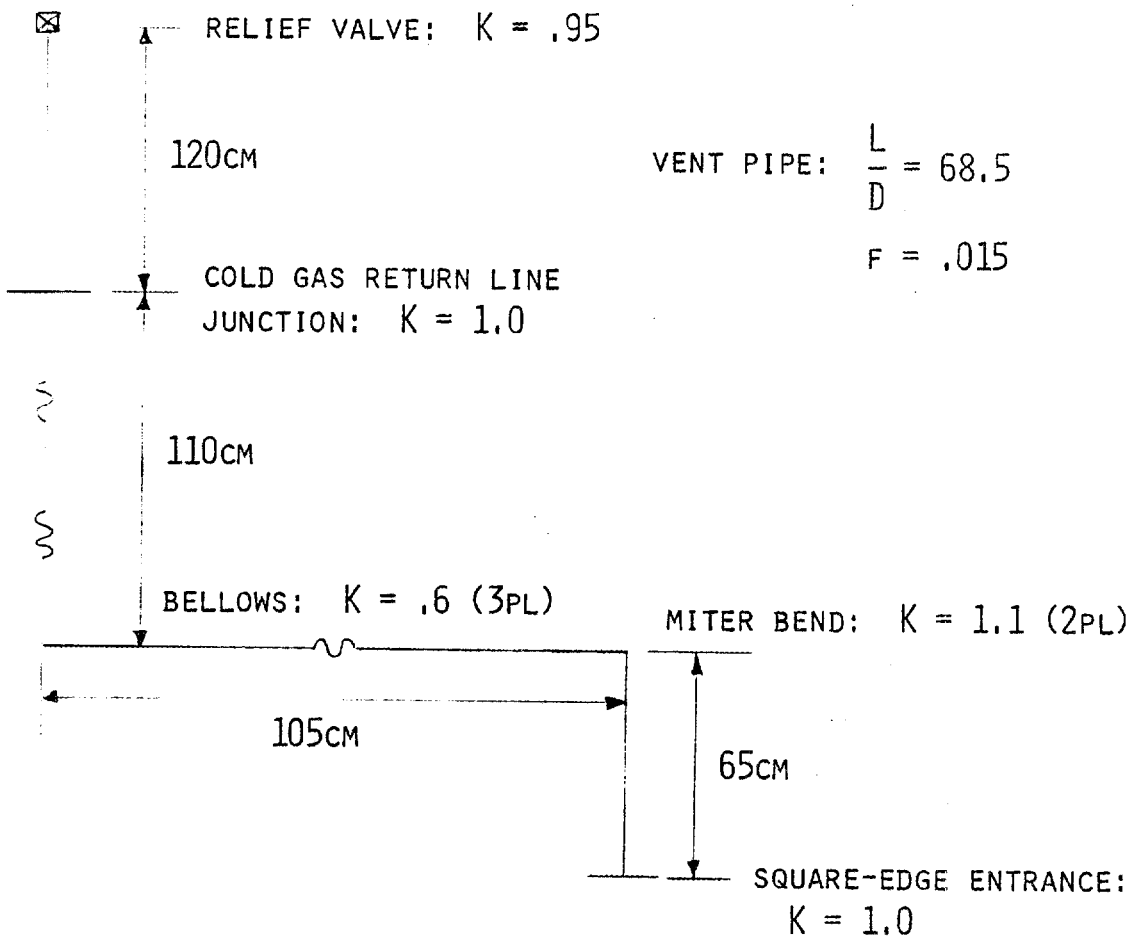

FIGURE 5.3-11. SCHEMATIC OF EMERGENCY VENT LINE SHOWING CONTRIBUTIONS TO PRESSURE DROP DURING QUENCH PRESSURE RISE

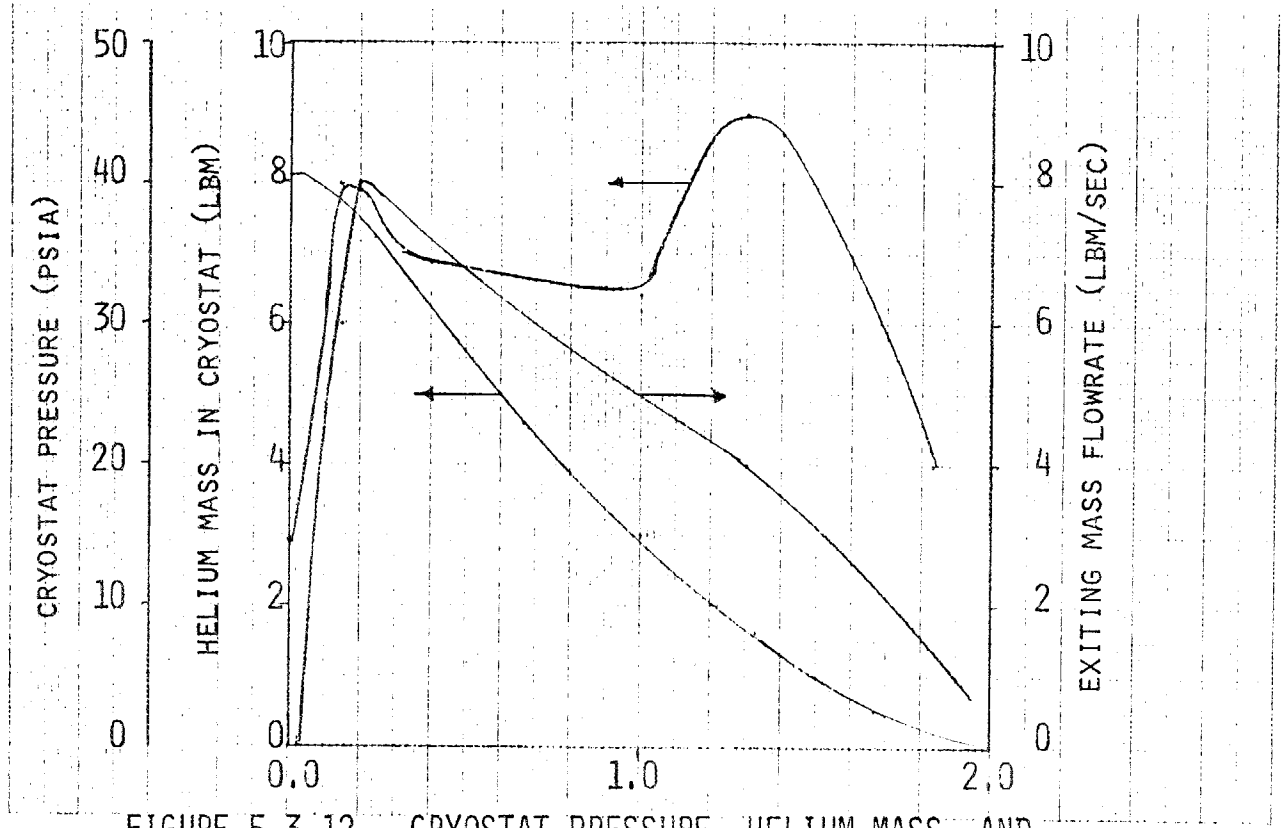

FIGURE 5.3-12. CRYOSTAT PRESSURE, HELIUM MASS, AND EXITING MASS FLOW RATE AFTER A QUENCH

Figure 5.3-13, was used primarily to establish flow rate and helium inlet temperature schedules. A more complex model, model B, shown in Figure 5.3-14, was used to determine temperature gradients, particularly from the bottom to the top of the magnet.

The main difference between the models is that model B has node divisions in the Θ direction (w.r.t. coil reference frame) while the simpler model lumps the thermal mass in that direction into one node.

The heat transfer coefficient between the flowing helium gas and the magnet structure is a major driver in the total time required for cooldown or warmup. If the helium is assumed to flow into the conductor pack, the heat transfer to/from the helium will be very good and the magnet mean temperature will be equal to the exiting helium temperature. This was the case presented in the design proposal (Reference 5.3-10) and resulted in a cooldown time of 11 hours and a warmup time of nine hours with the flow rate and inlet temperature schedule shown in Figure 5.3-15 (Reference 5.3-10). An analysis to determine expected flow rate distributions within the cryostat shows that possibly only 10% of the flow would be distributed within the winding, and 90% would flow in the annular region between the conductor pack and closure ring. To be conservative, it was assumed that none of the flow would penetrate the winding, requiring the conductor pack and bobbin to be conductively cooled from the annular passage. Since the annular passage has such a large cross-sectional area, the flow is laminar, which will further degrade heat transfer. However, the passage is short enough that there is a developing thermal and hydrodynamic boundary layer. The Nusselt number in the passage, then, ranges from about 15.5 at the entrance to about 7.6 at the exit (Reference 5.3-11) with an integrated average Nusselt number of 8.9. The value of 8.9 was used in Model A, while the Nusselt number as a function of length around the circumference of the annulus was incorporated into Model B, in order to see the effect on bottom-to-top gradients. The computation of the local Nusselt number is detailed in Appendix B-4 .

With the flow rate and supply temperature schedule of Figure 5.3-15 and the heat transfer limited to flow in the annular passage only, the cooldown time stretches out to about 25 hours, and the warmup time to 15 hours. The temperature responses vs. time are shown in Figures 5.3-16 and 5.3-17, curves which were generated from a solution of Model A. A check of Model A was made by running Model B with the same input and the results were in agreement to within 10%.

The 6.75 gm/sec warmup and initial cooldown flow rate proposed in Reference 5.3-10 and listed in Figure 5.3-15 is unrealistically high. The cooldown supply line is only .375 inch OD, requiring

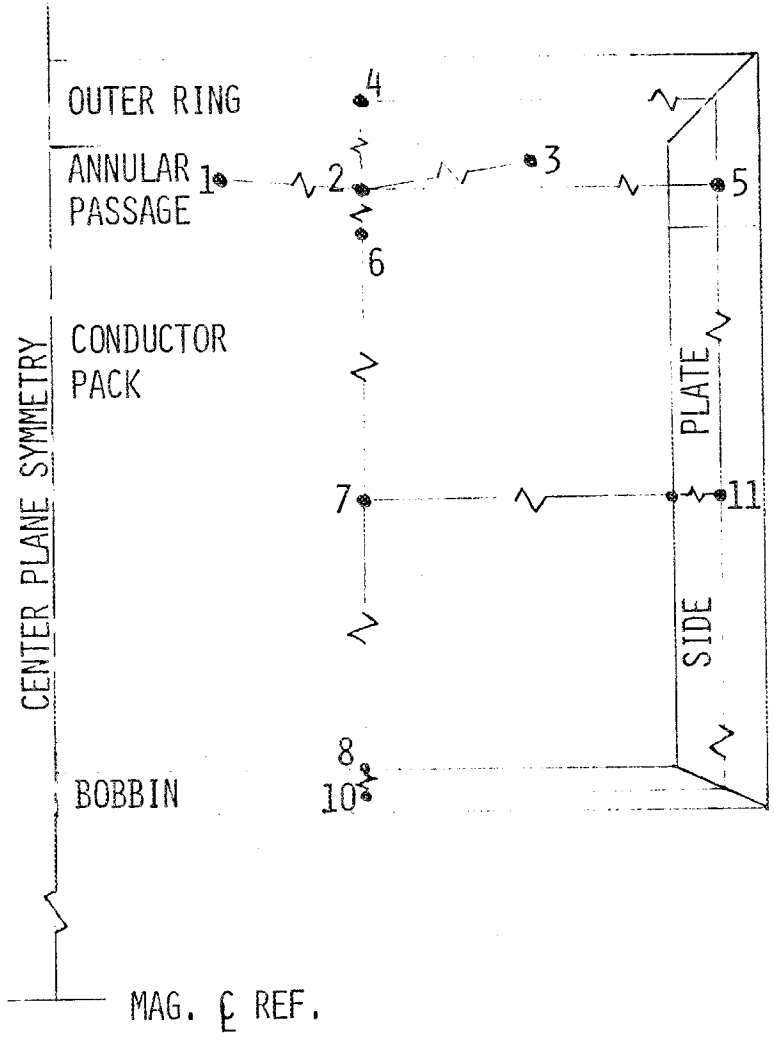

NODES 1, 2, 3 REPRESENT HELIUM GAS FLOW THROUGH THE ANNULAR PASSAGE SURROUNDING THE CONDUCTOR PACK.

NODES 4, 5, 10, 11 MODEL THE STEEL COLD MASS STRUCTURE.

NODE 7 HAS THE LUMPED PROPERTIES OF THE CONDUCTOR PACK CONSTITUENTS.

NODES 6, 8, 9 ARE ENERGY BALANCE NODES AT MATERIAL INTERFACES.

FIGURE 5.3-13 SCHEMATIC OF MODEL A USED TO DETERMINE COOLDOWN/WARMUP TIMES

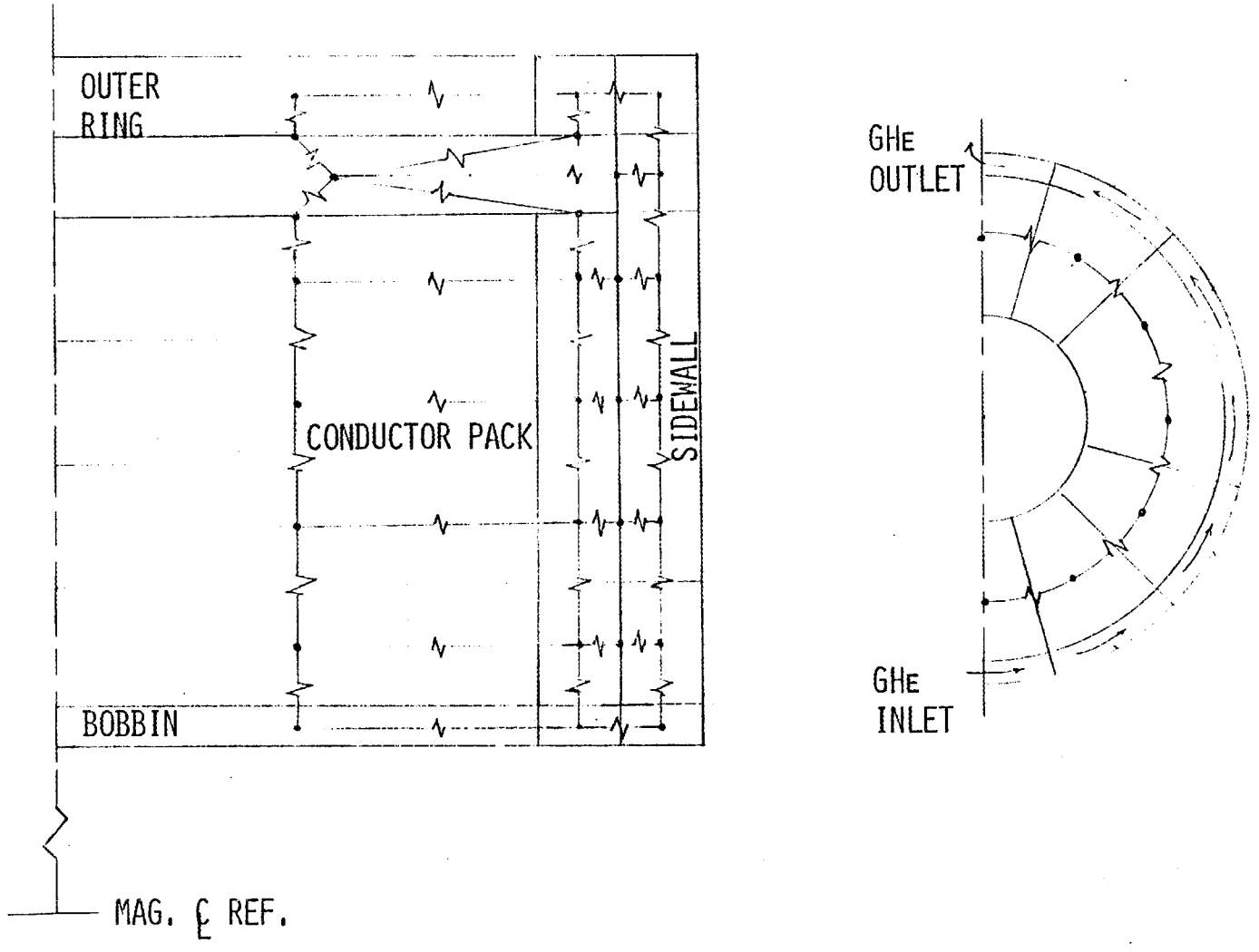

FIGURE 5.3-14 SCHEMATIC OF DETAILED WARMUP/COOLDOWN MODEL B USED TO COMPUTE 3-D GRADIENTS

	RETURN TEMPERATURE (K)	SUPPLY TEMPERATURE (K)	MASS FLOW RATE/COIL (GM/SEC)
COOLDOWN			
	300-85	80	6.75
	85-55	50	4.25
	55-30	25	3.375
	30-15	10	2.5
	15-4.5	4.5	2.0
WARMUP			
	4.5-65	100	6.75
	65-110	150	6.75
	110-150	200	6.75
	150-300	300	6.75

FIGURE 5.3-15. PROPOSAL (REFERENCE 5.3-10) FLOWRATE AND SUPPLY TEMPERATURE SCHEDULE DURING COOLDOWN AND WARMUP

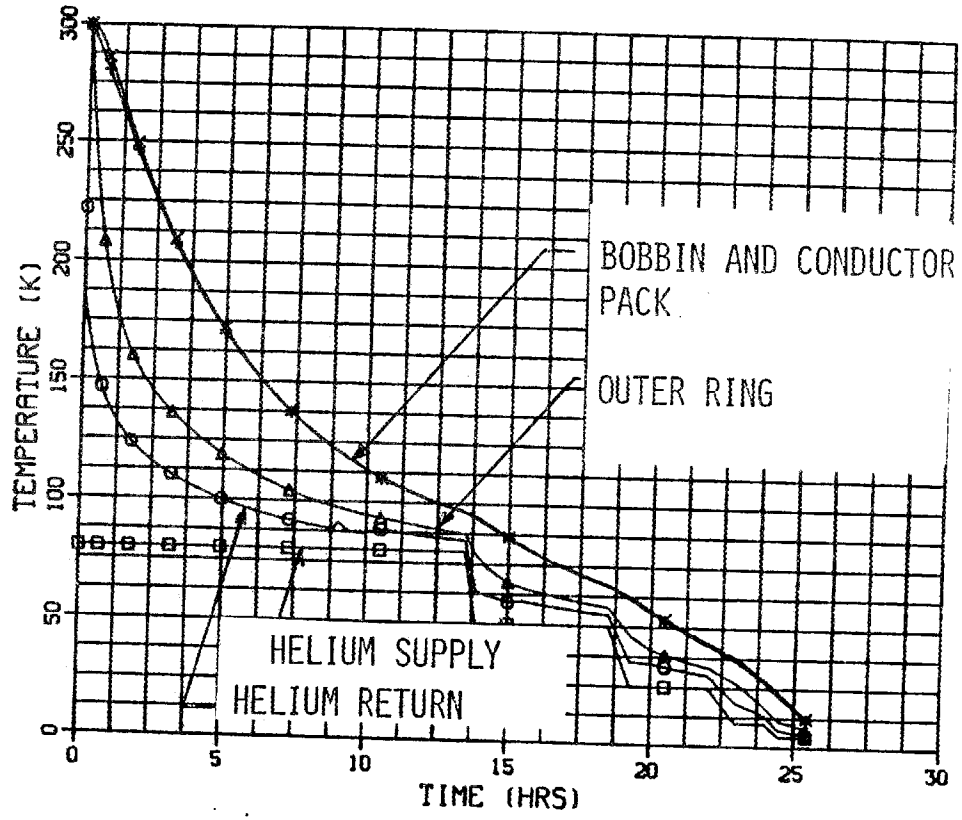

FIGURE 5.3-16 PRELIMINARY EBT-P COOLDOWN RESPONSE

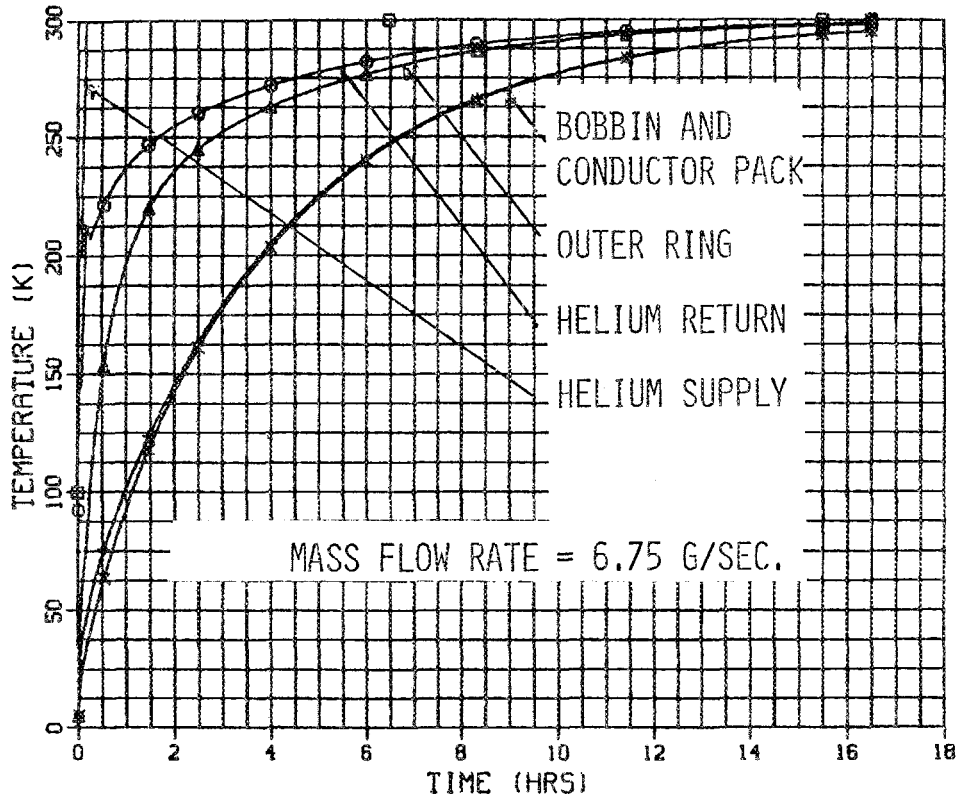

FIGURE 5.3-17 PRELIMINARY EBT-P WARMUP RESPONSE

very high velocities out of the tube. These jets impacting the structure will create localized cold/warm spots which can cause thermal stress problems. However, Figures 5.3-18 and 5.3-19 show angular temperature gradients (assuming no local cold/warm spots) during cooldown and warmup, respectively, for the Figure 5.3-15 schedule. The radial gradients can be seen in Figures 5.3-16 and 5.3-17. Stress analysis has shown these gradients produce acceptable thermal stress levels.

An alternate supply temperature and flow rate schedule is proposed in Figure 5.3-20. Although at this writing no model had been run with this schedule, it is estimated that the 3.375 gm/sec flow will simply double the warmup time to 30 hours and stretch the cooldown time to approximately 42 hours based on simply scaling the times at a given mass flow rate by the ratio of new flow rate/old flow rate. These times will be substantiated during detailed analysis. The slower cooldown times will produce smaller thermal gradients during the transients than those shown in Figures 5.3-16, -17, -18, and -19. However, the specified 72-hour cooldown warmup periods are satisfied with a large margin.

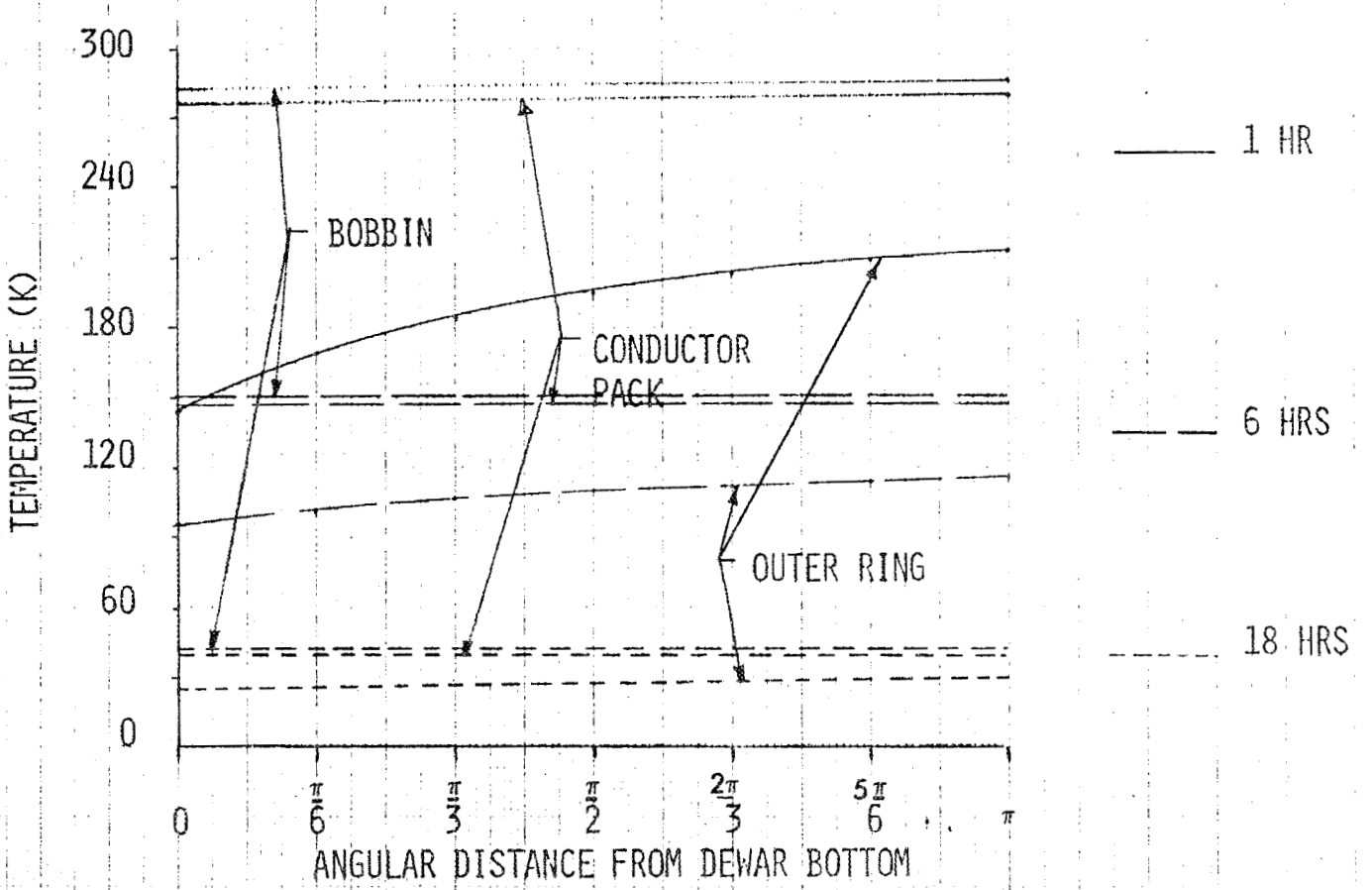

FIGURE 5.3-18 ANGULAR TEMPERATURE GRADIENTS DURING COOLDOWN

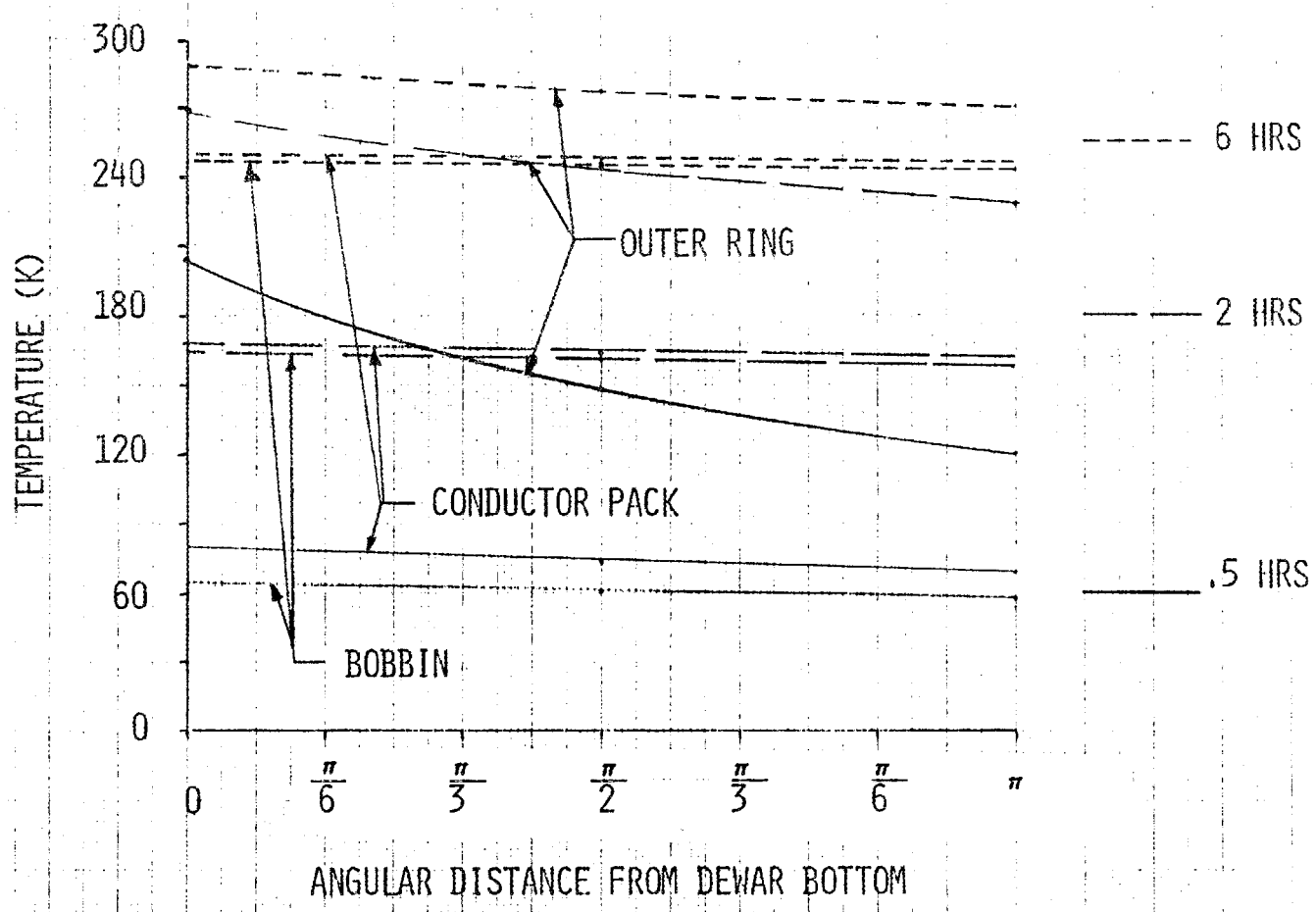

FIGURE 5.3-19 ANGULAR TEMPERATURE GRADIENTS DURING WARMUP

	RETURN TEMPERATURE (K)	SUPPLY TEMPERATURE (K)	MASS FLOW RATE/COIL (GM/SEC)
COOLDOWN			
	300-100	80	3.375
	100-65	50	3.375
	65-40	25	3.375
	40-15	10	2.5
	15-4.5	4.5	2.0
WARMUP			
	4.5-80	100	3.375
	80-150	175	3.375
	150-300	300	3.375

FIGURE 5.3-20. DESIGN FLOWRATE AND SUPPLY TEMPERATURE SCHEDULE DURING COOLDOWN AND WARMUP

5.4 X-RAY ANALYSIS

Several design options for the mirror coil X-ray shield were analyzed to provide data for shield design (see Appendix A.2-5). Since the baseline design could not provide adequate passing particle fraction, the shield envelope was modified in two ways. First, the corners of the shield were trimmed by 0.10 inch. Then, to add conservatism, the sides were increased to 1.5 inches. Options, based on the modified envelope, included a design with a tungsten throat and lead sides, an all-lead design, and a design with tungsten rings placed in the sides. Results indicated that all these designs were overconservative with respect to both total heating and peak heating. This led to examination of an all-lead design with a reduced throat thickness which would allow a greater passing particle fraction. This last design was found to exceed all design criteria by a substantial margin.

SECTION 6

PROGRAM PLANS AND SCHEDULE

6.1 MANUFACTURING PLAN

The Preliminary Manufacturing Plan, Appendix D , has been developed by manufacturing engineers based on current design and in accordance with current schedules. Working closely with the design groups, all drawings have been carefully reviewed from a producibility and manufacturability standpoint. The manufacturing producibility engineers provide manufacturing engineering direction and guidance to EBT design engineers in process selection, material requirements and allowances for forming, machining, welding, and winding. They conduct trade studies on weld joint geometries, welder accessibility, and machining.

The major contribution of this activity is to update the manufacturing sequence and flow chart and manufacturing plan to reflect the latest design changes. This manufacturing sequence and flow plan serves as a road map that defines all major operations required to produce the EBT magnets. The major manufacturing producibility requirement for the EBT program is to ensure the drawings can be used by fabricating shops and the magnet can be manufactured with existing technology and equipment. The producibility engineer's major responsibility is to ensure low cost manufacturing methods are designed into the magnet in the engineering design phase of this program while ensuring the delivery of high quality magnets.

6.1.1 TOOLING. The selection of manufacturing methods and the related tools are based upon the lowest combined cost for tools, manufacturing materials, and quality control, including both non-recurring and recurring costs. General Dynamics tooling plan for EBT-P is designed to meet the objective of minimum tooling expenditures while maintaining program quality requirements. The tooling plan is based on 1 prototype 36 production articles and 3 spares which will be fabricated, tested, and delivered. The preliminary tool list is included in Appendix D .

6.1.2 SCHEDULE. The tooling and manufacturing plan is based on a standard one-shift, 40-hour week. The peak rate requirement of five magnets a month requires the use of two winding and two final assembly stations.

6.1.3 MANUFACTURING. The fabrication and assembly of each major element of the magnet is described in detail in Appendix D . The assemblies addressed are:

- The cold mass, which includes the wound conductor pack and the helium vessel
- The LN_2 cold wall and multilayer insulation, which cover the helium vessel
- The vacuum vessel, which forms the outer container for the entire magnet
- The stack assembly, which contains the high current leads and plumbing components.

6.2 QUALITY ASSURANCE

The EBT-P quality assurance administrator is a functional member of the EBT-P program manager's staff with the responsibility and authority to act for the quality assurance director on the EBT-P Program. He draws upon the entire functional quality assurance organization as needed to satisfy program quality requirements. He also serves as the focal point for all quality assurance requirements and quality assurance coordination. He will provide assurance of design controls, appropriate quality assurance planning, instructions, procedures, and standards necessary to establish and maintain EBT-P quality requirements throughout procurement, fabrication, testing and delivery. His responsibilities also include supporting program and design reviews, participating in verification tests, resolving quality assurance problems, inputting quality assurance requirements to program documents, developing required plans and procedures, identifying required special equipment or personnel training and certification and conducting QA audits.

This organizational structure has an excellent performance implementation record with experience on other magnet programs and larger scale military contracts. The system provides a proven close-coupled cost-effective quality assurance program tailored to provide the specialty requirements of this program.

Special emphasis is being placed on the overall quality program and controls of the superconductor suppliers. In July, a visit was made to each of them at which time a specially-selected GDC resident procurement quality assurance representative was introduced and assigned. Since the two suppliers are in a competitive position for the production contract, a separate representative was assigned to each company. These representatives are chartered to become personally involved and totally familiar with all in-process manufacturing steps and inspection check points. Mandatory inspection hold points have been assigned on critical processes. These representatives will be monitoring the contents of the contractually required lot control history jacket. This jacket will include:

A. Copies of certifications for all conductor constituent materials.

B. A color photograph of the conductor billet, prior to close, showing the location of constituent materials. The photograph shall be identified to the lot and signed and dated by a representative of the Sellers quality assurance organization.

C. Data sheets indicating compliance with the in-process inspections.

D. Data sheets indicating compliance with the dimensional acceptance requirements.

E. Data sheets indicating compliance with the performance acceptance requirements including copies of critical current plots, resistivity plots, and stress-strain curves.

F. Data sheets indicating compliance with the general acceptance requirements.

G. Data sheets indicating conductor length.

H. Non-conformance reports (WARF).

Each folder shall be identified with the spool lot number. The folder shall be presented to the GDC representative at the time of acceptance. The folder shall be maintained up-to-date and available for review at any time during the manufacturing/test cycle.

A weekly written reporting system has been established wherein current supplier engineering and quality activity is presented to our program management. This information, while a useful real time management tool, will also be beneficial when the production phase control is considered.

Thus, this resident representative provides a fully-functional quality assurance and control system that confidently monitors the supplier manufacturer with "in-house" continuity.

6.3 PRELIMINARY HAZARD ANALYSIS SUMMARY

The system safety principal contribution to the preliminary design review is the Preliminary Hazard Analysis (PHA). The PHA is performed to obtain an initial safety evaluation of the EBT-P magnet subsystem with its interfacing subsystems. The information from the PHA will be incorporated into the final GDC design of the ELMO-BUMPY Torus magnet subsystem. The PHA accomplishes this by providing the basis for design criteria and for subsequent subsystem hazard analyses, which will identify safety critical areas, the hazards involved and will delineate the preventative action required.

Each of the six areas of safety concern carry hazards particular to itself. The magnetic field raises concerns about effects of exposure to personnel, disturbance of instrumentation, and attraction of ferromagnetic objects. The electrical subsystem includes the Power and Distribution, Protection, and Instrumentation and Control subsystems. Concerns in this area center on high voltage problems (usually due to transient situations such as charge or dump) and instrumentation failure. Degradation of magnet components is the main safety concern caused by radiation. Potential high pressure, extreme cold, and inert gases are the primary safety interests in the cryogenic system. Safety in the vacuum pumping system focuses on the pressure differential due to the vacuum, and leaks changing heat transfer characteristics possibly leading to undesired helium boil-off. The chief mechanical and structural concerns are fatigue failure and earthquake damage.

Corrective action will be taken to reduce to an acceptable level the hazards identified by the PHA. These actions will consist of design changes, safety devices, warning devices or procedures and training. The system safety group will continue to work closely with the design group throughout the EBT-P development and production to minimize possible safety problems identified by subsequent hazard analyses. The magnetic field produced by the EBT-P stands out as an inherent safety concern, since the field extends outside of the reactor vessel and personnel will undoubtedly be subjected to it. We suggest, on the basis of researched biomagnetism data that personnel adhere to DOE standards for occupational use with stationary magnetic fields (SMF). In addition to the above limitations, it is recommended that people with a history of mental problems, those with implanted electronic medical devices, pregnant women, and persons with chronic health problems, such as sickle cell anemia or heart problems, be excluded from exposure to SMF.

6.4 ACCEPTANCE TEST PLAN

Production magnets will be subjected to the tests listed below to assure each magnet has been properly manufactured and the requirements of MDAC procurement spec. 70P370000 have been satisfied. The tests listed are final acceptance tests and do not include the manufacturing in-process tests.

1. Winding Insulation Resistance Test*
2. Proof Pressure Test*
3. Final GHe Leak Test*
4. Vacuum Liner GHe Leak Test
5. Magnet Operational Test
6. Magnetic Axes Alignment
7. Heat Leak Test

*Performed prior to installation of shield and vacuum liner.

Additional detail information relative to these tests can be found in Appendix E of this report.

A test facility will be provided to accomplish these tests plus certain in-process tests. The facility will become an integral element of the overall manufacturing plan and will be conceived in such a manner as to assure all contractual commitments are satisfied. A preliminary requirements document for the facility is in Appendix E. Because of its importance to the EBT Program, a conceptual discussion relative to its requirements and utilization are provided in the following paragraphs.

Current planning requires the final acceptance testing of 39 magnets over an 11-month span at the following rates:

MONTH	1	2	3	4	5	6	7	8	9	10	11
NO. OF MAGNETS	1	2	3	4	4	4	4	4	5	5	3

In addition, it must be capable of supporting certain manufacturing in-process tests. The most significant of these will be the testing of the winding assembly at liquid helium temperature (referred to as open dewar test). This test will be accomplished prior to welding the outer ring onto the winding assembly.

4. Testing would be accomplished on a one-shift per day basis and no testing on Sunday.

5. The helium refrigeration system will not be used for warmup of the magnet, which would allow the system to be available for the next magnet.

The result is a 27-day time span required to test 5 magnets and 5 winding assemblies. The time can be reduced to 20 days by going to two shifts per day for testing. For planning purposes, one shift per day is recommended. The two-shift per day operation and overtime would be utilized as required to resolve unexpected problems.

The significant features of the facility are:

1. Conveniently located adjacent to EBT manufacturing facility.

2. Power, protection and control systems will allow magnet testing to simulate actual EBT system operating conditions. Automatic data logging will be provided during test runs.

3. Helium refrigeration system will be sized to allow simultaneous chilldown of a completed magnet plus a winding assembly.

4. Four test positions will be provided to allow concurrent test operations.

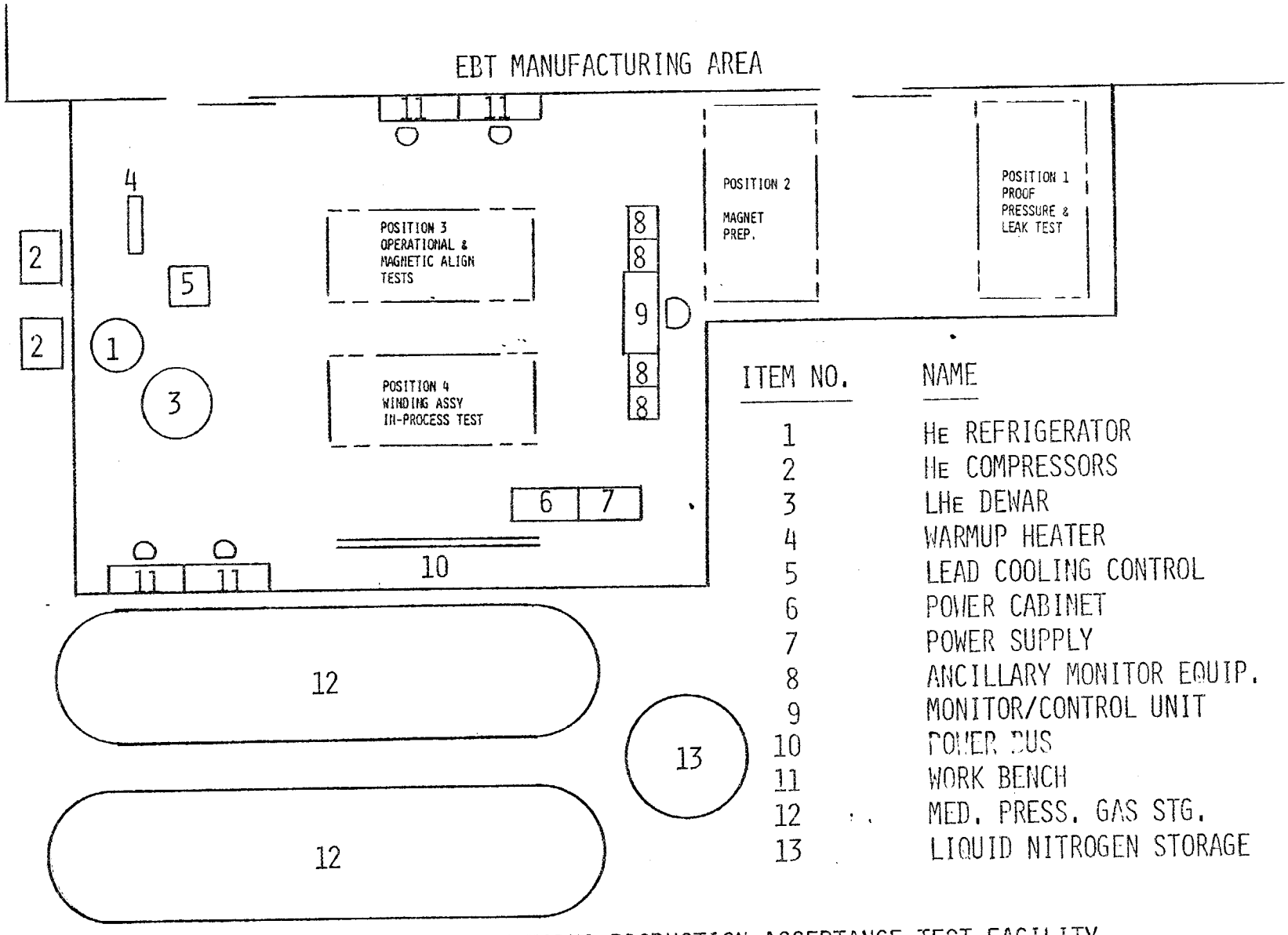

FIGURE 6.4-1 ELMO BUMPY TORUS PRODUCTION ACCEPTANCE TEST FACILITY

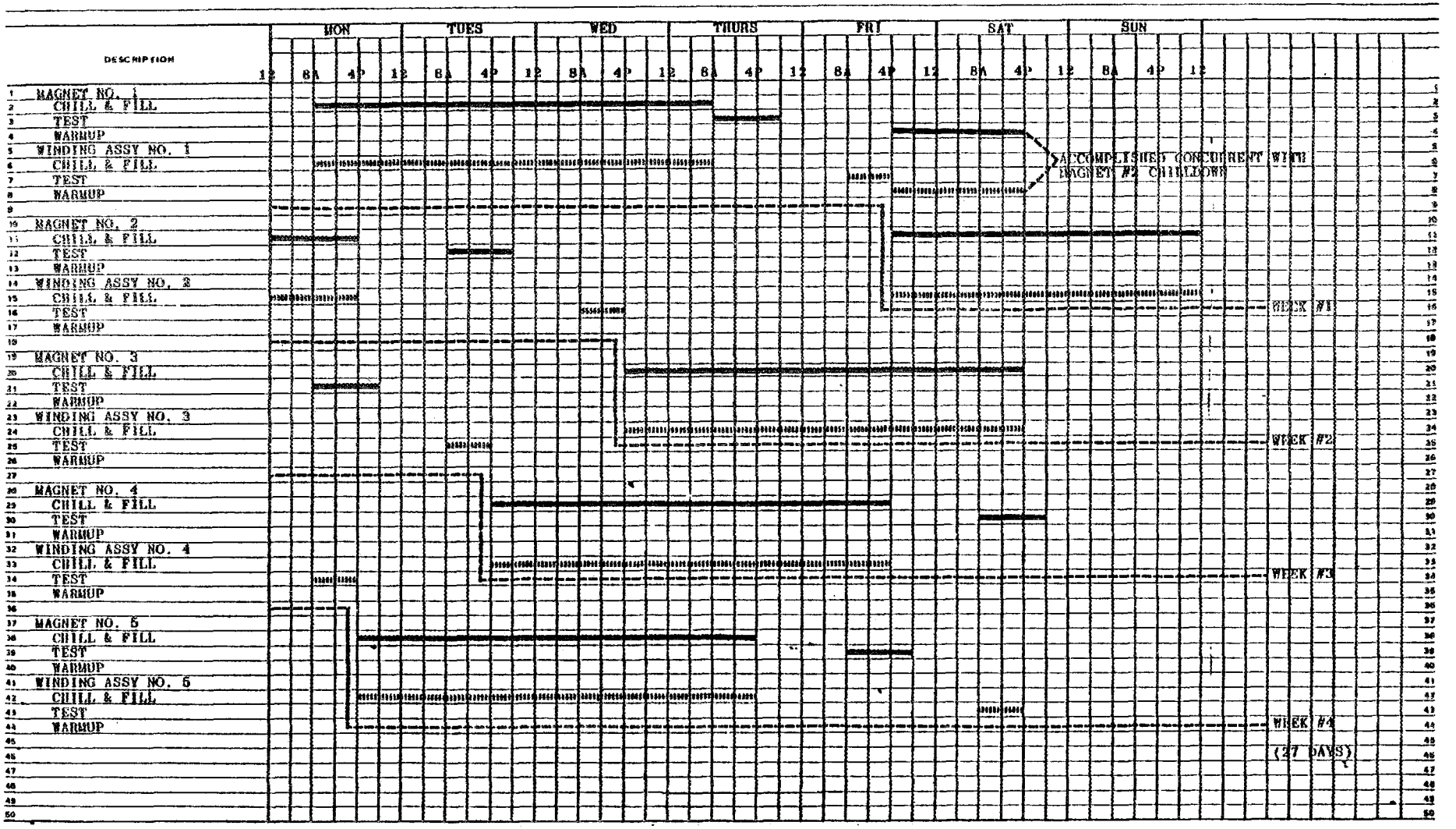

FIGURE 6.4-2 PRODUCTION ACCEPTANCE TIME REQUIREMENTS

To satisfy these requirements, the test facility will be conveniently located adjacent to the manufacturing facility (see Figure 6.4-1). This will allow subassemblies and completed magnets to be easily and quickly moved between the two facilities. Concurrent test operations are necessary to satisfy the production rate requirements and will be accomplished by providing the following four test positions within the facility:

- Position (1) will be used for proof pressure testing and leak checking.

- Position (2) will be used to prepare a magnet for chilldown and operational testing. Tasks performed will be: (1) final electrical tests at room temperature, (2) evacuation of the vacuum vessel, and (3) evacuation and GHe purging of the winding assembly.

- Position (3) is where operational testing, magnetic alignment, and heat leak tests will take place.

- Position (4) will be used for the in-process winding assembly operational test at liquid helium temperature.

The critical path in the facility utilization schedule is the time required to chilldown and complete the operational testing for both the winding assembly and a completed magnet. All other tasks can easily be accomplished concurrent with these activities. The liquid helium refrigeration system will be designed to provide simultaneous chilldown of both a completed magnet at position (3) and a winding assembly at position (4). The power, protection, control and instrumentation systems will be designed to test a single magnet at any given time.

Figure 6.4-2 illustrates the plan for testing 5 magnets per month, and was based upon the following criteria:

1. The helium refrigeration system would be operated and available 24 hours a day, seven days a week.

2. Chilldown, LHe fill and thermal stabilization would take 72 hours.

3. Operational testing would take 12 hours for a completed magnet and 8 hours for a winding assembly.

6.5 INSTALLATION AND ALIGNMENT PLAN

This plan describes the proposed approach for the alignment of the mirror coils and supporting structure to limit the cumulative field error as expressed by the quantity of $\Delta B/B$ to 1×10^{-4} when averaged around the torus along the minor axis.

The alignment plan described herein can be briefly summarized as follows:

1. Magnetic field measurements will be made on each coil to define axes location with respect to construction balls located on the dewar. (Magnetic axes to within $\pm$ 0.005 inches and $\pm$ 1.5 minutes angularity).
2. Aluminum bucking ring structures reference surfaces on the outer perimeter to be optically aligned to within 0.010 inches and vertical to within 0 degrees, 2 minutes.
3. All magnets are to be installed on the torus before starting alignment. A clearance of 0.30 inch is provided between the magnet base and aluminum ring. This allows for cummulative tolerance buildups and magnet adjustments of 0.17 inches or 0.5 degrees.
4. The magnets are aligned optically to within 0.005 inches.
5. 32 magnets are locked into position using tapered pins.
6. 4 magnets (one in each sector) are temporarily locked into position with jack screws.
7. The magnets are cooled and powered to TBD amperes. Alignment is verified and/or vernier adjustments are made on the 4 magnets with the use of an electron beam to determine field line closure.
8. The final 4 magnets are then permanently pinned in the aligned position.

The tooling bars and scopes required for alignment will be disassembled and removed following alignment verification. It is MDAC's understanding that ORNL is currently exploring the possibility for using a toroidal winding for detecting flux linkages between the toroidal coil and the mirror coils which are a measure of alignment error. If this technique has the required sensitivity, it would be highly desireable to incorporate it into the EBT-P design and alignment procedure as it could provide coil alignment status during device operation.

6.6 TITLE II SCHEDULE

The Title II design and fabrication schedule as originally proposed appears to be realistic and achievable. The groundwork accomplished during the Title I design phase is directly applicable and transferable to detail designs for the magnet and I&C systems. Depending on the degree of success of the PDRs for these systems (assuming no major redesigns), we should enjoy an easy transition into the next and final design phase. All of the analysis basic to the design will be further refined and documented and updated as additional physics parameters are defined or substantiated. Where necessary validation tests may be proposed, especially for verifying the stability criteria, these tests would also be accomplished early during this period. Producibility and volume fabrication design will be one of the principle tasks accomplished during this phase. A major portion of effort will be expended in the area of manufacturing technology. Of prime importance is the assurance that each magnet can be wound in a repeatable manner. We will determine the key characteristics, to be verified during the winding process, which will provide this necessary assurance.

New designs, procurement, and fabrication encompassing the test facility, production engineering, and tooling can also proceed in a timely fashion.

A large portion of the Title II task will include detail design of the quench protection and power systems. GDC plans to procure off-the-shelf components and subsystems to minimize the task and maintain the schedule.

REVISIONS:

DATE: 9-11-81
PREP BY: M. PARIS, X2261
APPVD. BY:
REF:

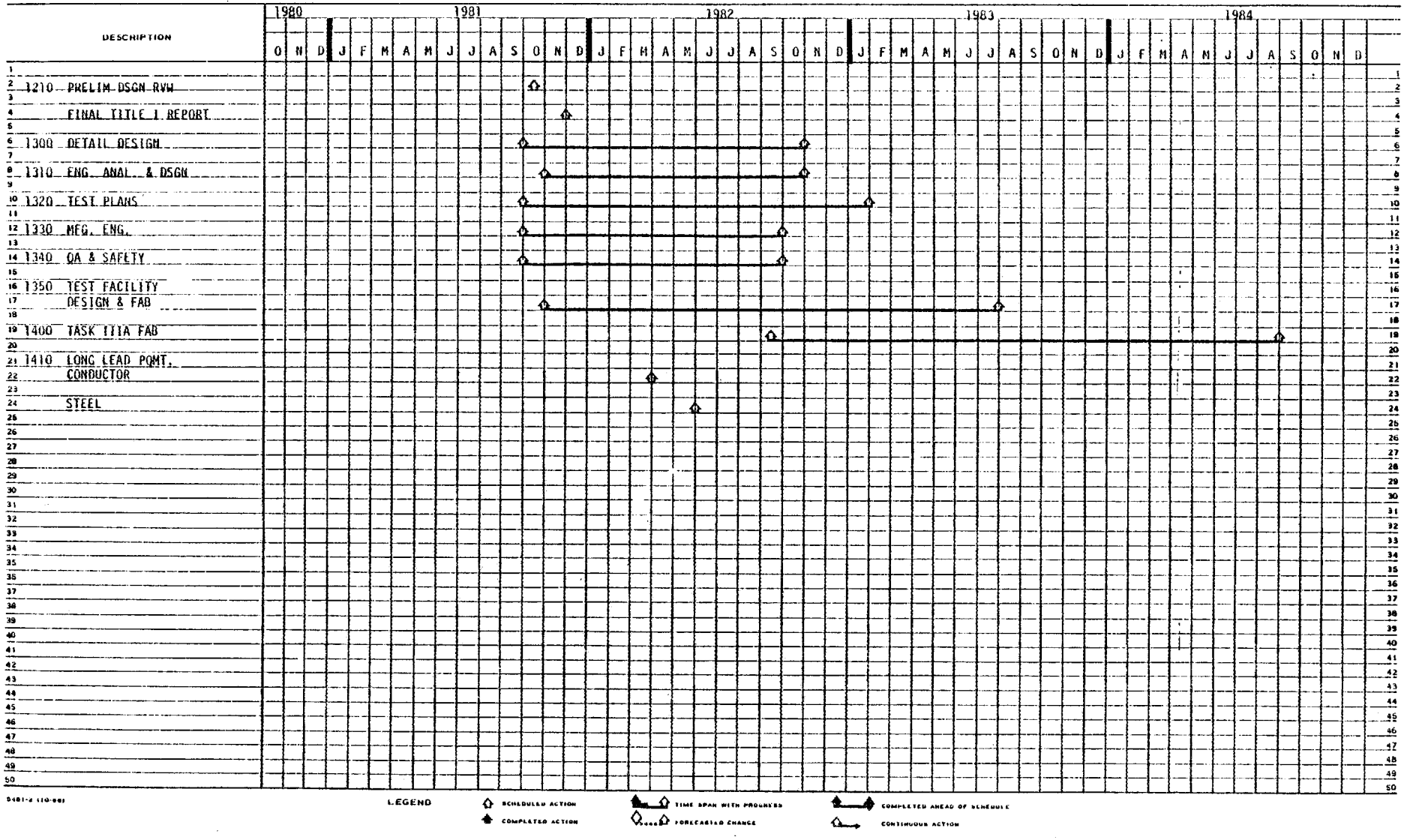

FIGURE 6.6-1. ELMO BUMPY TORUS TITLE II SCHEDULE OVERVIEW

6.7 MASTER PROGRAM SCHEDULE

The General Dynamics master program schedule, which includes the Task 1 and Task 6 phases, has been altered considerably since the start of this project. Initially, changes encountered in the two development dewar elements of the program resulted from an increase in task to accommodate ORNL objectives and later to cope with the ORNL strike problems at Oak Ridge, Tennessee. However, additional delays resulting from superconductor manufacturing difficulties and technical problems, with respect to the design of the helium stack system, have stretched the development dewar delivery program six months (June to December). However, the real program slip is considerably less since GD is now supplying a completely assembled mirror coil magnet. The prototype is now estimated for completion by 1 April 1982 and is paced by superconductor delivery now scheduled for December 1981. If any serious difficulty is encountered in the ORNL development or prototype magnet test program, we can surely predict that this would impact Title III production. It will take a conscientious and disciplined effort of all participants to minimize the impact of these design and procurement delays. Title II schedule remains as originally proposed as indicated by paragraph 6.6 above.

Title III schedule also remains essentially as that originally proposed. Mirror coil production fabrication is based on installing two coil winding stations and two vessel welding table positions. The critical fabrication element and pacing operation is coil winding. It is planned to wind coils on a two-shift basis, which utilizes the third shift for maintenance and to cope with anticipated schedule difficulties. Learning experience will allow us to increase production from one or two coils per month to a maximum of five per month toward the end of the program. We are not anticipating any difficulty in any of the detailed parts fabrication or test areas at this time. A single "all up" refrigeration/power test station is planned in order to test each mirror coil to the maximum extent possible prior to shipment. The magnet coil axis will be determined when the magnet is operated at full field. All electronic components included in the power supply and quench protection will be purchased or fabricated to support the test program. Long lead procurement of materials to support this production is discussed in detail under paragraph 8.0 Appendices. See Figure 1.6-1 for Master Schedule.

SECTION 7

REFERENCES

3.5-1 Procurement Specification for EBT-P Mirror Coil Magnet System, Specification 70P370000, 23 April 1980 (unsigned)

3.5-2 EBT-P, ORNL/MDAC/GDC, Plan for the Evaluation of Alternate Mirror Coil Cold Mass Support Systems, Draft copy, circa November 1980 (unsigned)

3.5-3 Deleted

3.5-4 ASME Boiler and Pressure Vessel Code, Section VIII, Division 1, "Pressure Vessels."

3.5-5 Uniform Building Code

3.5-6 U.S. Department of Energy, ERDA Manual Appendix 6301, General Design Criteria

4.5-1 "Copper for Busbars", Copper Development Association, London, England, 1958

4.7-1 R. R. Coltman, Jr., C. E. Klabunde, and C. J. Long, "The Effect of a 100 MGy (10^{10} Rads) Gamma - Ray Dose at 5K on the Strength of Polymide Insulators", ORNL SSD No. 81-10, January 1981

4.7-2 R. E. Schramm, A. F. Clark, and R. P. Reed, "A Compilation and Evaluation of Mechanical, Thermal, and Electrical properties of Selected Polymers", NBS Monograph 132, pp .653, 657, 658, 659, and 663

4.7-3 C. J. Long, R. H. Kernohan, and R. R. Coltman Jr., "Radiation Effects on Insulators for Superconducting Magnets", DOE Contract No. W-7405-eng-26 with the Union Carbide Corporation.

4.7-4 D. Evans, J. T. Morgan, R. Sheldon, G. B. Stapleton, "Post Irradiation Mechanical Properties of Epoxy Resin/ Glass Composites", Science Research Concil Report No. RHEL/R200, June 1970

4.7-5 R. R. Coltman Jr., C. E. Klabunde, R. H. Kernohan, C. J. Long, "Radiation Effects on Organic Insulators for Superconducting Magnets", Oak Ridge National Laboratory Report ORNL/TM-7077, P. 29 and Table VII, P. 39

4.7-6 Same as Reference 4.7-5, Figures 2, 3, 4, and 5

4.7-7 Same as Reference 4.7-5, P.44

5.3-1 E. H. Christensen, and S. D. Peck, "Large Coil Program Concuctor LHe Heat Transfer and Heater Verification Test Data Analysis", GDC Report 91Z0122, 10 July 1980

5.3-2 P. J. Giarratano and N. V. Fredrick, "Transient Pool Boiling of Liquid Helium Using a Temperature Controlled Heater Surface", Advances in Cryogenic Engineering, Vol. 25, 1980, pp 455-466

5.3-3 Reference 3.5-1

5.3-4 M. N. Wilson, "Heat Transfer to Boiling Liquid Helium in Narrow Vertical Channels", Paper II-2, IIR Commission 1 Meeting, June 1966

5.3-5 Frank Kreith, Principles of Heat Transfer, Intext Educational Publishers, London and New York, 1973, P402

5.3-6 G. D. Fredrickson, "Investigation of High-Performance Insulation Application Problems", MDAC Reprot G4722, August 1973

5.3-7 C. W. Keller, G. R. Cunnington, and A. P. Glassford, "Thermal Performance of Multilayer Insulations", LMSC Report D349866, 5 April 1974

5.3-8 E. H. Christensen and R. P. Krause, "Configuration Dependent Heat Transfer Data and Quench Pressure Program for Superconducting Magnets", GDC Report GDC-ERR-79-059, December 1979

5.3-9 R. F. O'Neill, and E. R. Nauharth, "Convair Thermal Analyzer Computer Program P4560", Version D. Report GDC-005A, 29 May 1969

5.3-10 EBT-P Magnet System Proposal, 11 March 1980

APPENDIX A DRAWING PACKAGES

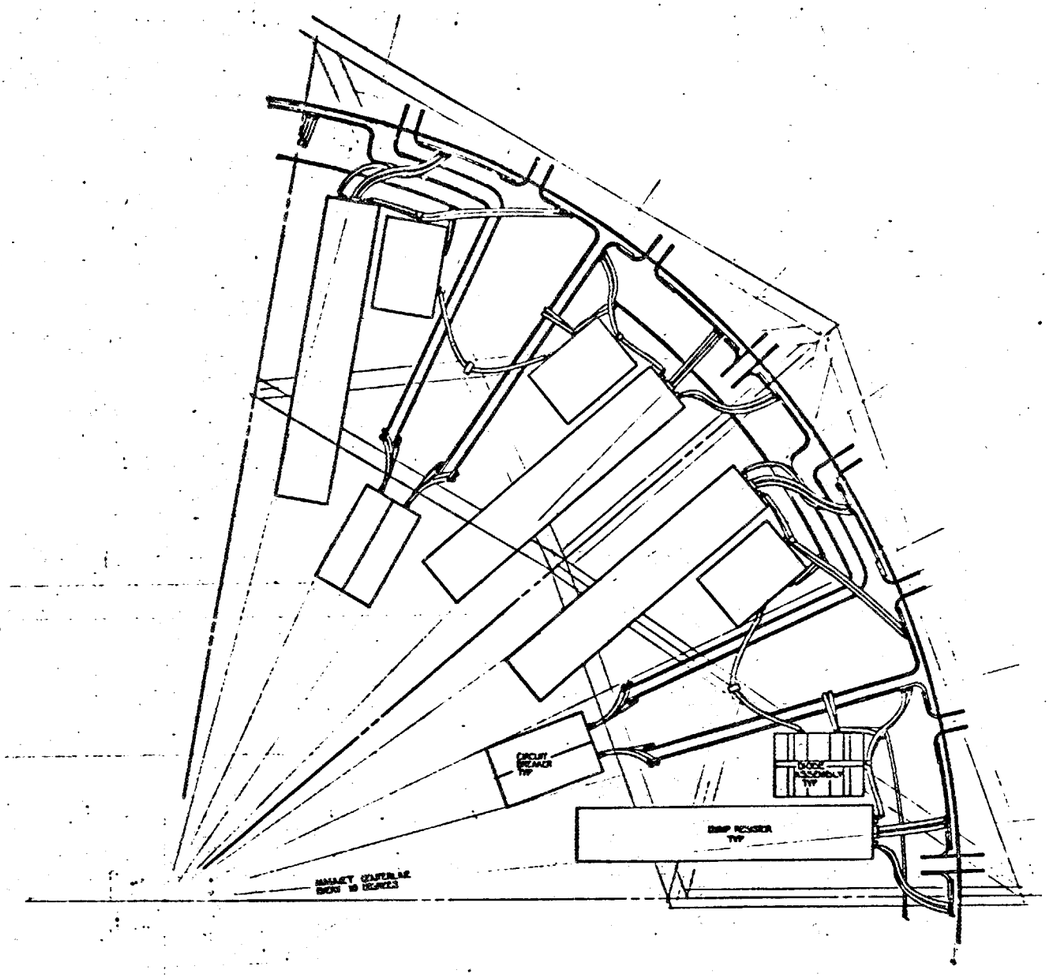

APPROVED TITLE I

REF AL-BOCH LETTER DATED
MARCH 19, 1982

PRELIMINARY

SEE SEPARATE PARTS LIST

SEE G-70914 FOR ABBREVIATION, CODE AND SYMBOL REQUIREMENTS

SEE G-70900 FOR STANDARD MANUFACTURING AND INSTALLATION REQUIREMENTS

UNLESS OTHERWISE SPECIFIED ALL MACHINED SURFACES ✓

UNLESS OTHERWISE SPECIFIED DIMENSIONS ARE IN INCHES
TOLERANCES
X ±1 · .X ±.06 · .XX ±.010
ANGULAR PER G-70900

CHECK
STRESS
DR ENGR
DR SUPT
DRAFT
CONTRACT NO

GENERAL DYNAMICS
CONVAIR DIVISION
SAN DIEGO, CALIFORNIA

MAGNET SUPPORT LAYOUT
EBT-P

SIZE E | CODE IDENT NO 14170 | DWG NO SK 82881

SHEET NO
REV LTR

A-3/A-4

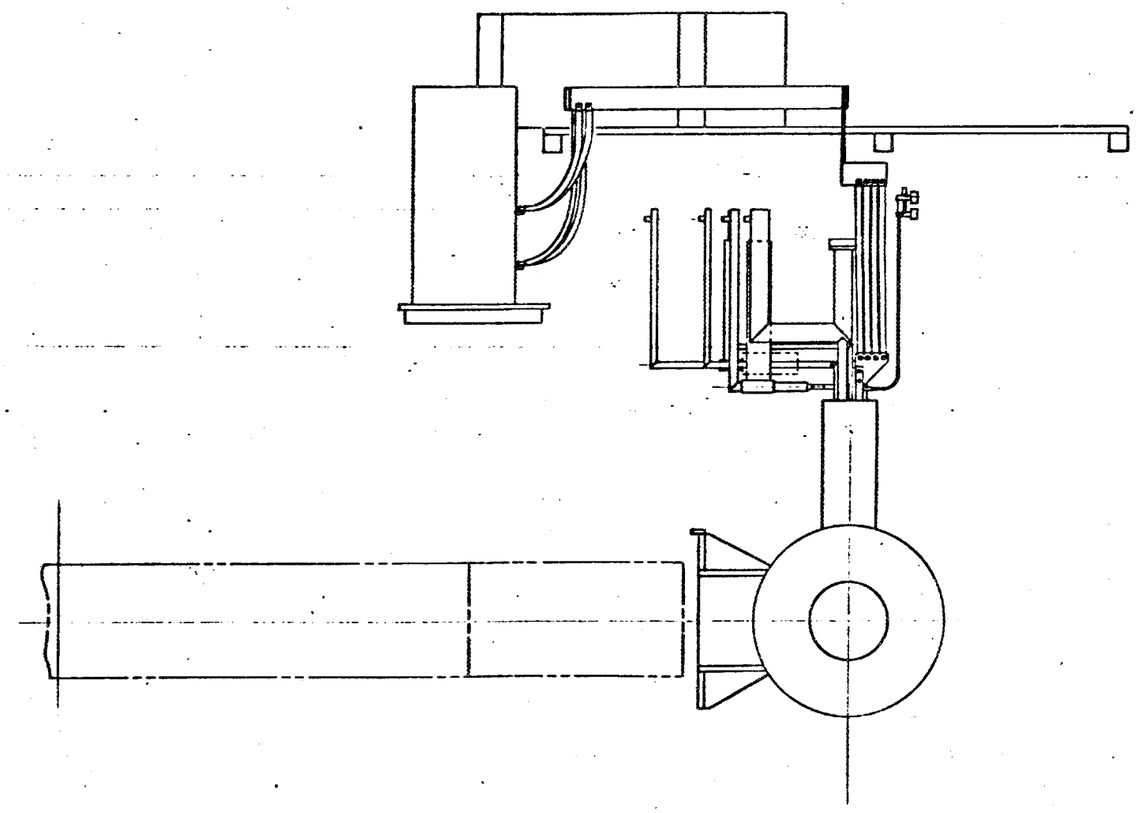

APPROVED TITLE I

REF AL BOCH LETTER DATED
MARCH 19, 1982

PRELIMINARY

GENERAL DYNAMICS
CONVAIR DIVISION
SAN DIEGO, CALIFORNIA

MAGNET BUSBAR LAYOUT
EBT-P

E 14170

5X82831

A–5/A–6

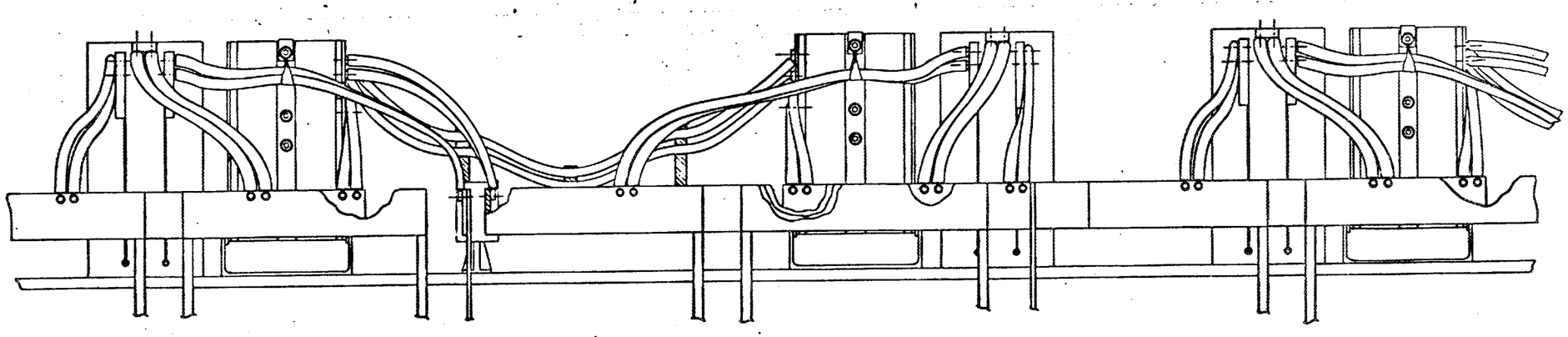

SCALE NONE

PRELIMINARY

APPROVED TITLE I

REF AL BOCH LETTER DATED
MARCH 19, 1982

SEE SEPARATE PARTS LIST

SEE D-70014 FOR ABBREVIATION, CODE AND SYMBOL REQUIREMENTS	UNLESS OTHERWISE SPECIFIED DIMENSIONS ARE IN INCHES	CHECK	GENERAL DYNAMICS CONVAIR DIVISION SAN DIEGO CALIFORNIA
SEE D-70002 FOR STANDARD MANUFACTURING AND INSTALLATION REQUIREMENTS	TOLERANCES X ±1 / XX ±.02 / XXX ±.010 ANGULAR PER D-70002	STRESS	MAGUE T BLOBAK LAYOUT EBT-P
UNLESS OTHERWISE SPECIFIED ALL MACHINED SURFACES ✓	DATE	DESIGN	SIZE E
	PROJ ENGR	CONTRACT NO	SCALE

A–7/A–8

DWG NO. SK90381-1 SH 1 REV

REVISIONS

ZONE	REV	DESCRIPTION	DATE	APPROVED

HELIUM LEVEL MONITOR CABINETS

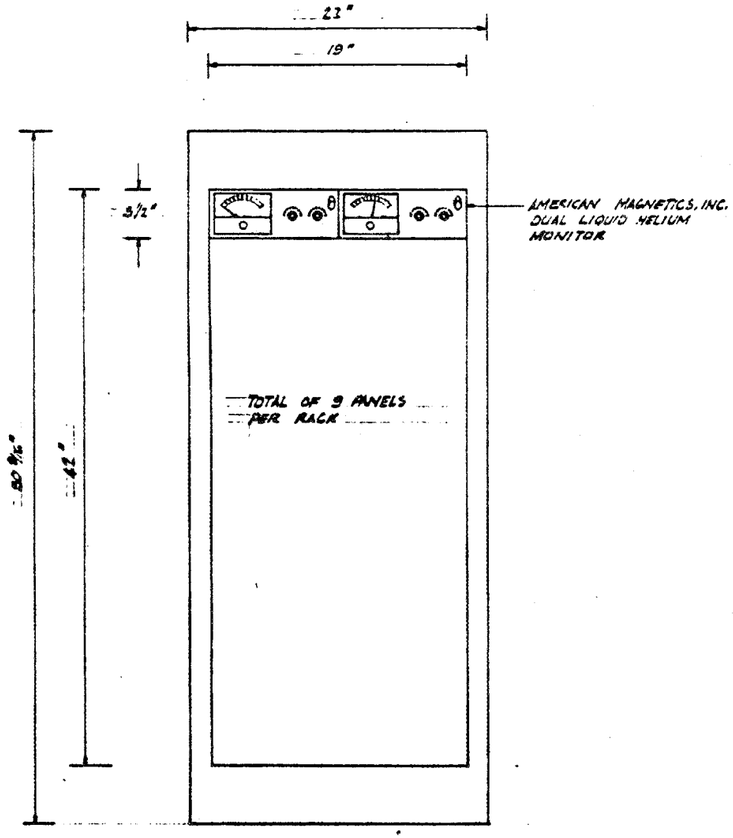

2 RACKS OF 9 PANELS EACH ARE REQUIRED TO MONITOR THE LIQUID HELIUM LEVEL OF THE 36 MAGNETS.

CAMAC CABINET

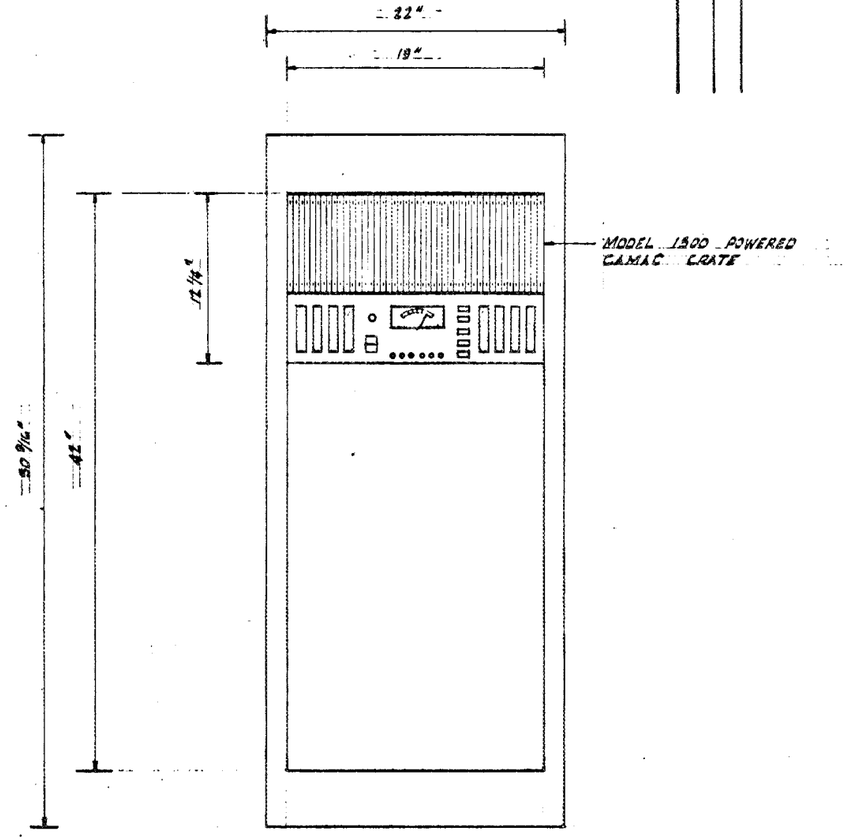

THE CAMAC FUNCTIONS AS THE MAIN LOCAL DATA AQUISITION SUBASSEMBLY.

APPROVED TITLE I

PRELIMINARY.

REF AL BOCH LETTER DATED MARCH 19, 1982

☐ SEE SEPARATE PARTS LIST

SEE 0-70914 FOR ABBREVIATION, CODE AND SYMBOL REQUIREMENTS

SEE 0-70902 FOR STANDARD MANUFACTURING AND INSTALLATION REQUIREMENTS

UNLESS OTHERWISE SPECIFIED ALL MACHINED SURFACES ✓

UNLESS OTHERWISE SPECIFIED DIMENSIONS ARE IN INCHES

TOLERANCES .X ±.1 .XX ±.03 .XXX ±.010 ANGULAR PER 070902

MATL

PROD. ENGR

CHECK

STRESS

GR ENGR

DESIGN

DRAWN A. W. LOAD 7-22-82

CONTRACT NO.

SHEET NO.

REV LTR

GENERAL DYNAMICS
CONVAIR DIVISION
SAN DIEGO, CALIFORNIA

EBT HELIUM LEVEL MONITOR CABINETS & CAMAC CABINET

SIZE D | FSCM NO. 14170 | DWG NO. SK90381-1

SCALE 3/16"=1'-0" | SHEET 1 OF 1

SEC. CLASS | TYPE | LEVEL | CONT | GROUP | DISTR | REPRO | PACKAGE NO. | NO.

A-9/A-10

DWG NO. SK90381-2 SH 1 REV —

REVISIONS				
ZONE	REV	DESCRIPTION	DATE	APPROVED

SIGNAL CONDITIONING POWER AND DIGITAL I/O CABINET

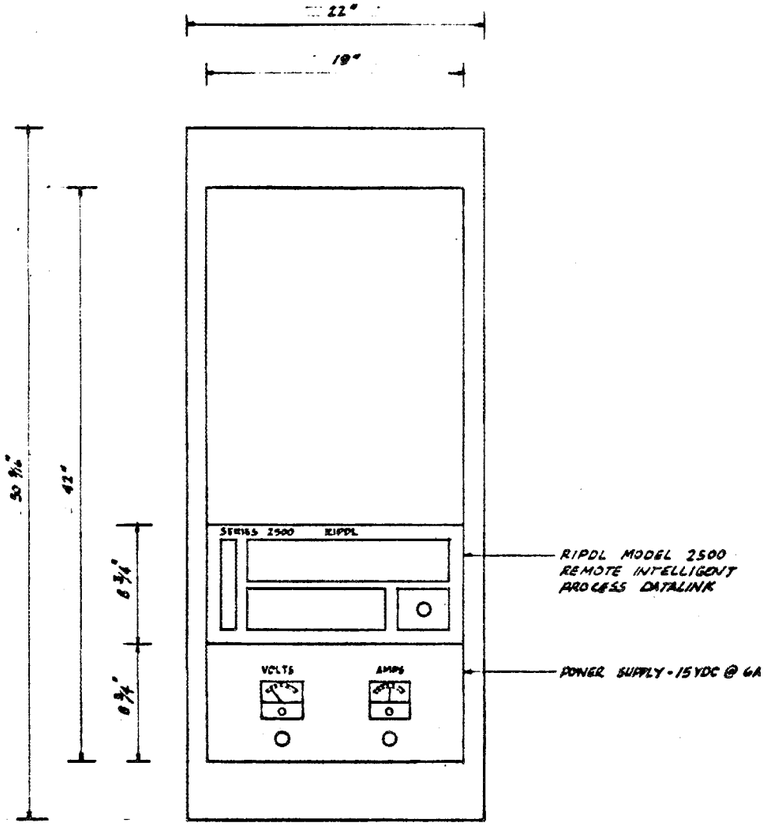

THE POWER SUPPLY PROVIDES POWER TO THE 3 SIGNAL CONDITIONING RACKS - THE RIPDL PROVIDES A DATALINK BETWEEN THE VARIOUS SIGNAL CONDITIONER CHANNELS AND THE CAMAC.

STRAIN / TEMPERATURE SIGNAL CONDITIONING CABINETS

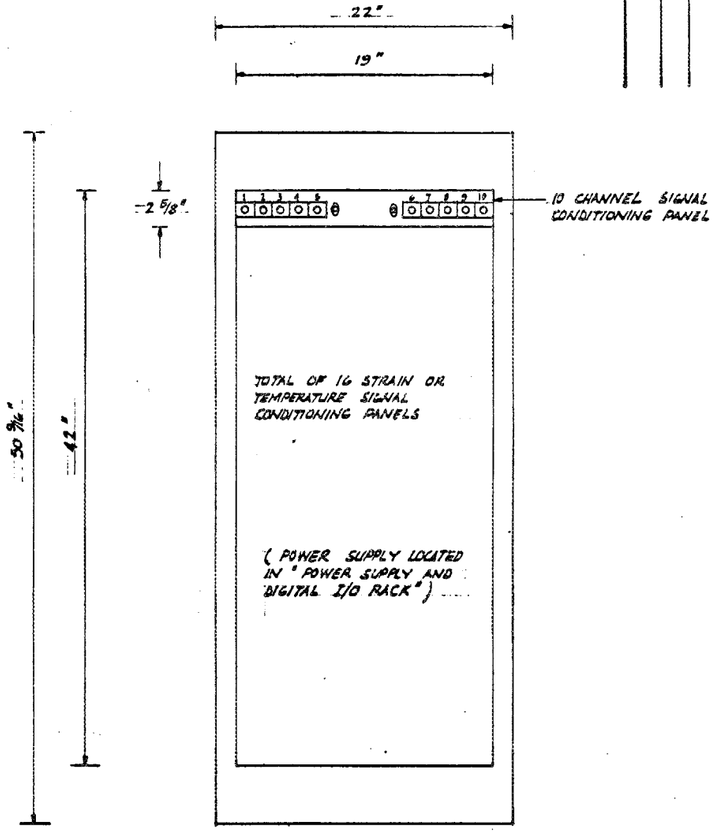

APPROX. 3 1/2 RACKS ARE REQUIRED TO MONITOR THE 324 STRAIN GAGES AND 216 TEMPERATURE SENSORS.

PRELIMINARY

APPROVED TITLE I

REF AL BOCH LETTER DATED MARCH 19, 1982

☐ SEE SEPARATE PARTS LIST

SEE 0-70914 FOR ABBREVIATION, CODE AND SYMBOL REQUIREMENTS

SEE 0-70902 FOR STANDARD MANUFACTURING AND INSTALLATION REQUIREMENTS

UNLESS OTHERWISE SPECIFIED ALL MACHINED SURFACES ✓

UNLESS OTHERWISE SPECIFIED DIMENSIONS ARE IN INCHES

TOLERANCES: .X ±.1, .XX ±.03, .XXX ±.010; ANGULAR PER 070902

MATL

PROD. ENGR

CHECK

STRESS

GR ENGR

DESIGN

DRAWN H. K. URAD 7-22-81

CONTRACT NO.

SHEET NO. | REV LTR

GENERAL DYNAMICS
CONVAIR DIVISION
SAN DIEGO, CALIFORNIA

EET POWER & DIGITAL I/O CABINET & STRAIN/TEMP. SIGNAL CONDITIONING CABINETS

SIZE D | FSCM NO 14170 | DWG NO. SK90381-2

SCALE 3/8 = 1 in | SHEET 1 OF 1

SEC. CLASS | TYPE | LEVEL | CONT | GROUP | DISTR | REPRO | PACKAGE NO. | REL

FORM 7516

DWG NO. SK90381-3 SH 1 REV -

REVISIONS

ZONE	REV	DESCRIPTION	DATE	APPROVED

SYSTEM STATUS DISPLAY CABINET

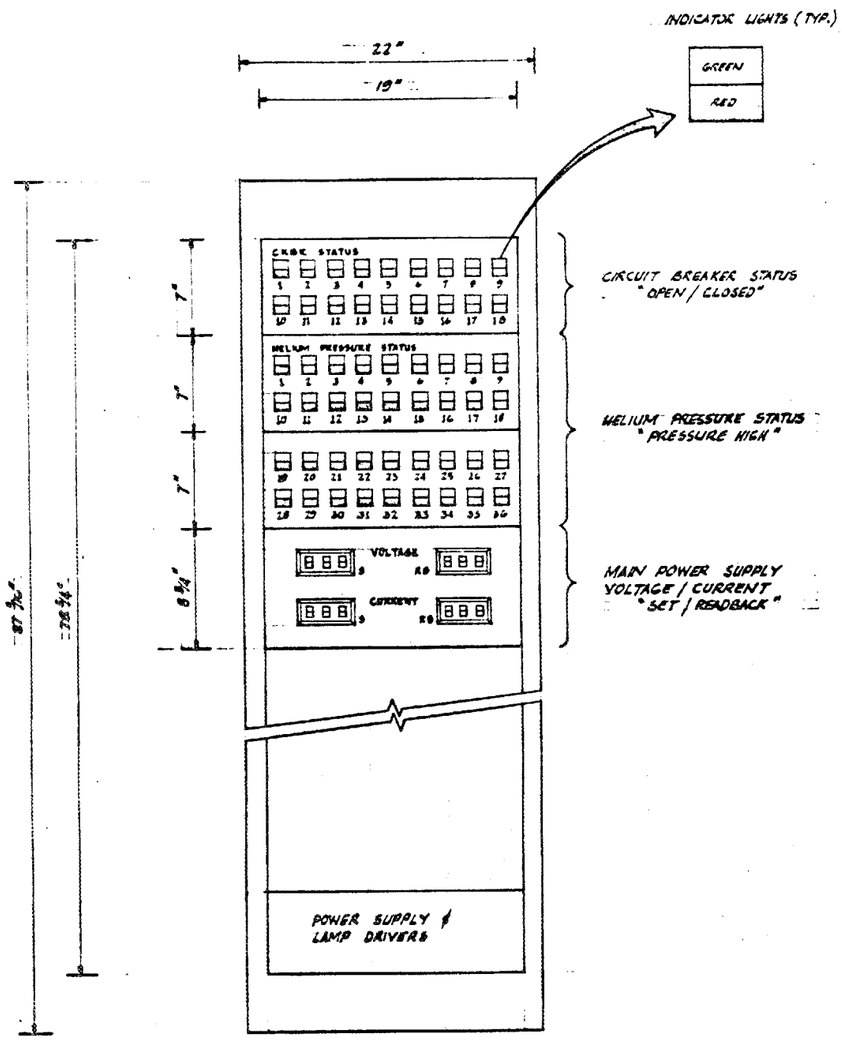

THE LIGHTS INDICATE THE STATUS OF THE 18 CIRCUIT BREAKERS AND 36 HELIUM PRESSURE SWITCHES. THE DIGITAL DISPLAYS REFLECT THE COMMANDED AND ACTUAL VOLTAGE / CURRENT.

PROTECTION CABINET

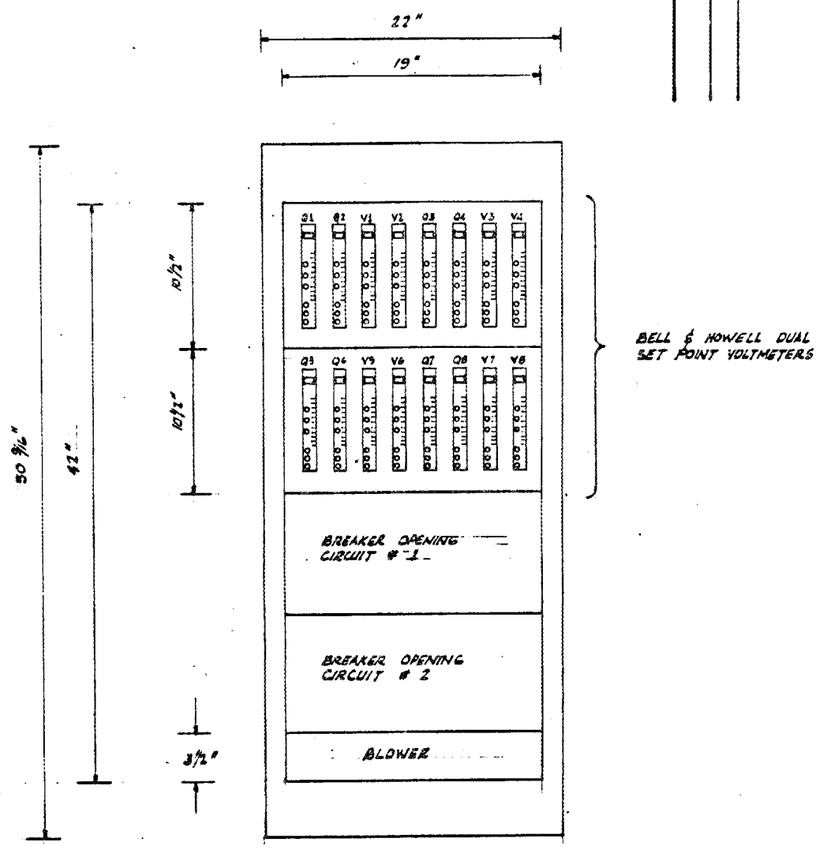

8 RACKS CONTAINING 2 PANELS OF 8 VOLTMETERS EACH PLUS 2 BREAKER OPENING CIRCUITS ARE REQUIRED FOR THE 36 MAGNETS.
EACH PANEL OF VOLTMETERS REPRESENTS 2 QUENCH DETECTORS AND 2 VAPOR COOLED LEAD MONITORS.

PRELIMINARY

APPROVED TITLE I

REF AL BOCH LETTER DATED MARCH 19, 1982

☐ SEE SEPARATE PARTS LIST

SEE 0-70914 FOR ABBREVIATION, CODE AND SYMBOL REQUIREMENTS

SEE 0-70902 FOR STANDARD MANUFACTURING AND INSTALLATION REQUIREMENTS

UNLESS OTHERWISE SPECIFIED ALL MACHINED SURFACES ✓

UNLESS OTHERWISE SPECIFIED DIMENSIONS ARE IN INCHES

TOLERANCES .X ±.1 .XX ± .03 .XXX ± .010 ANGULAR PER 070902

MATL

PROD. ENGR

CHECK

STRESS

GR ENGR

DESIGN

DRAWN H. H. URAO 7-23-81

CONTRACT NO.

SHEET NO.

REV LTR

GENERAL DYNAMICS
CONVAIR DIVISION
SAN DIEGO, CALIFORNIA

EBT SYSTEM STATUS DISPLAY CABINET & PROTECTION CABINET

SIZE D FSCM NO. 14170 DWG NO. SK90381-3

SCALE 3/8 = 1/2 SHEET 1 OF 1

SEC. CLASS | TYPE | LEVEL | CONT | GROUP | DISTR | REPRO | PACKAGE NO. | REL

FORM 75-16

A–13/A–14

DWG NO. SK90381-4 SH 1 REV

REVISIONS

ZONE	REV	DESCRIPTION	DATE	APPROVED

MAGNET STATUS DISPLAY CABINET

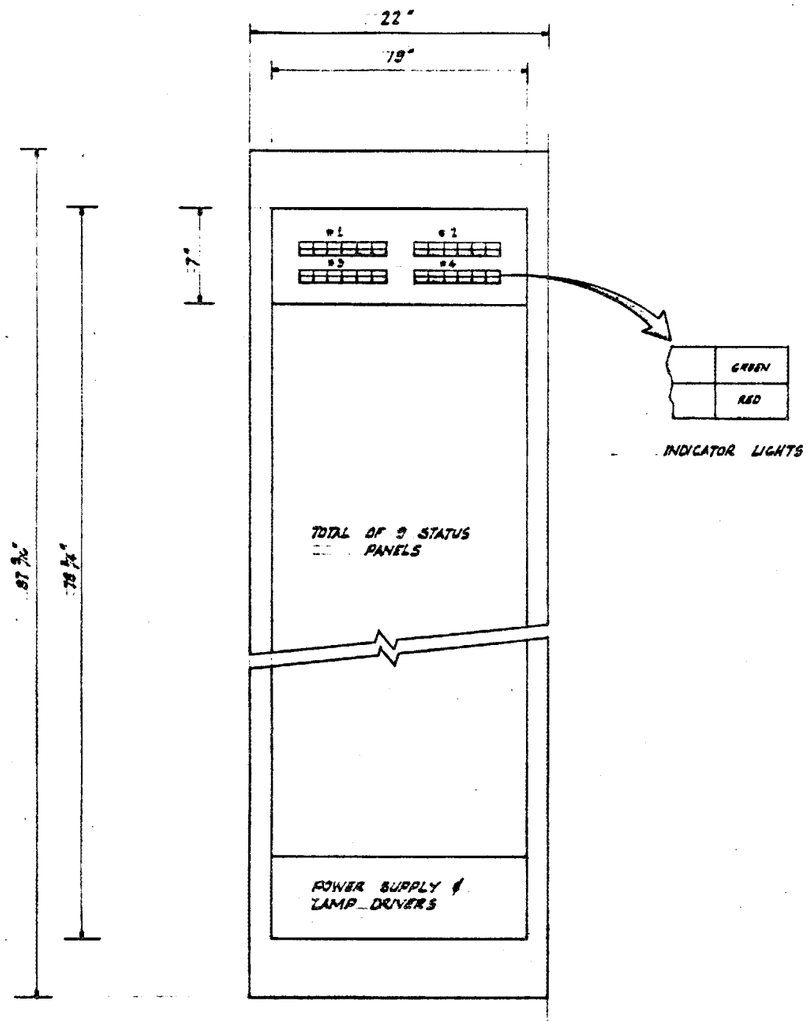

HELIUM PRESSURE MONITOR CABINET

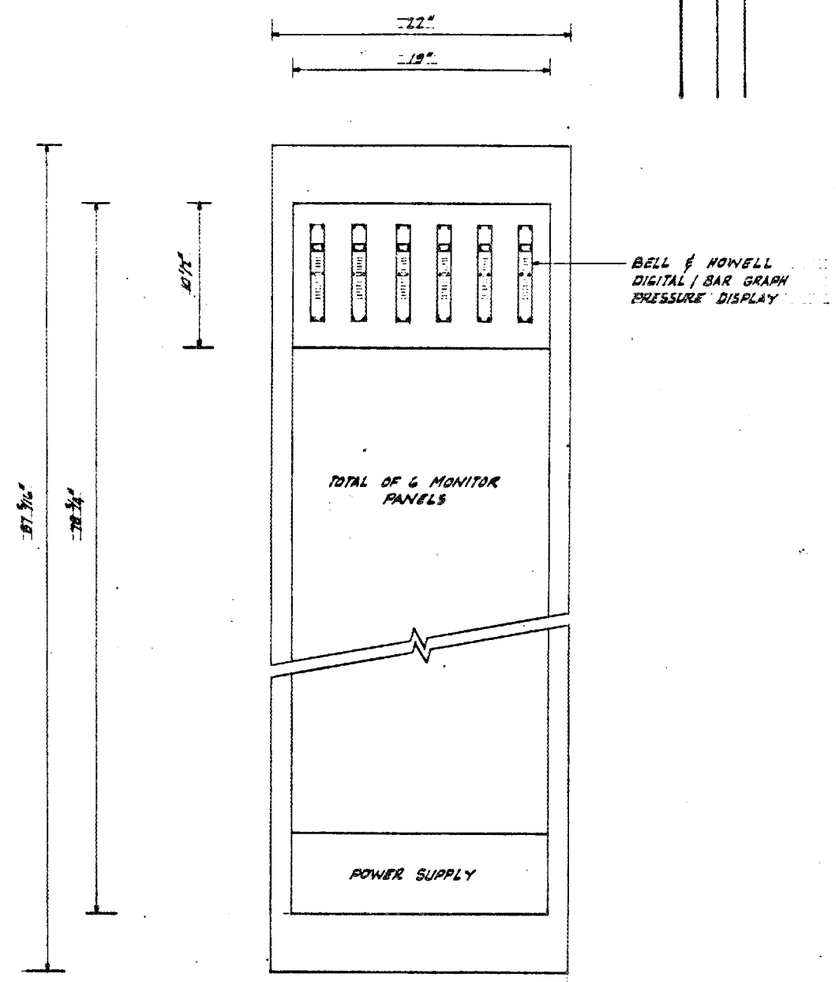

EACH BLOCK OF INDICATOR LIGHTS PROVIDES STATUS FOR: 2 QUENCH DETECTORS
2 VAPOR COOLED LEADS
1 VACUUM SWITCH
1 HELIUM LEVEL SWITCH

EACH PANEL DISPLAYS THE HELIUM PRESSURE OF 6 MAGNETS.

PRELIMINARY

APPROVED TITLE I

REF AL BOCH LETTER DATED MARCH 19, 1982

☐ SEE SEPARATE PARTS LIST

SHEET NO.
REV LTR

SEE 0-70914 FOR ABBREVIATION, CODE AND SYMBOL REQUIREMENTS

SEE 0-70902 FOR STANDARD MANUFACTURING AND INSTALLATION REQUIREMENTS

UNLESS OTHERWISE SPECIFIED ALL MACHINED SURFACES ✓

UNLESS OTHERWISE SPECIFIED DIMENSIONS ARE IN INCHES
TOLERANCES .X ±.1 .XX ± .03 .XXX ± .010
ANGULAR PER 070902

MATL
PROD. ENGR

CHECK
STRESS
GR ENGR
DESIGN
DRAWN H. H. URAO 7-14-81
CONTRACT NO.

GENERAL DYNAMICS
CONVAIR DIVISION
SAN DIEGO, CALIFORNIA

EBT MAGNET STATUS DISPLAY CABINET & HELIUM PRESSURE MONITOR CABINET

SIZE D FSCM NO. 14170 DWG NO. SK90381-4

SCALE 3/16"=1'-0 SHEET / OF /

SEC. CLASS | TYPE | LEVEL | CONT | GROUP | DISTR | REPRO | PACKAGE NO. | REL

FORM 7516

A–15/A–16

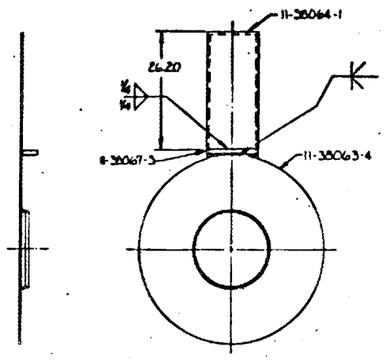

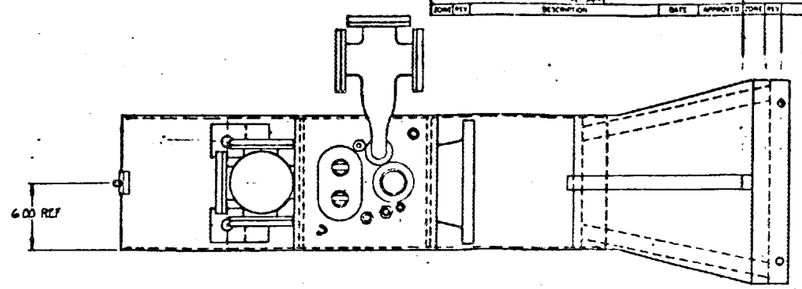

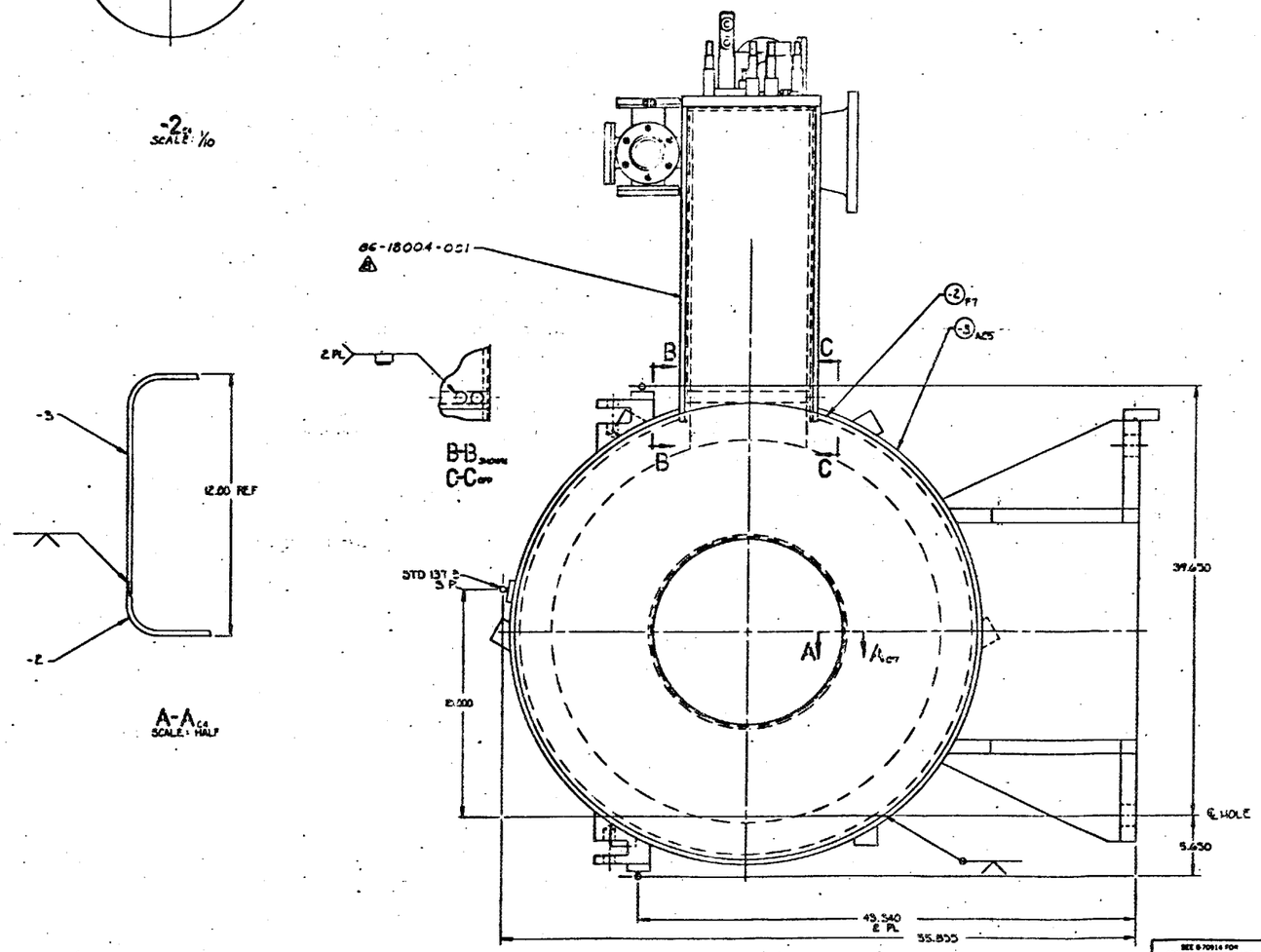

NOTES

1. COLD MASS I.D. SHALL BE CONCENTRIC WITH DATUM A WITHIN .010 AT PTS 'A', 'B' AND 'C'
2. ALL WELDING TO BE PER MIL-STD-278, CLASS A-4 AND BY WELDERS QUALIFIED PER MIL-STD-248.
3. PENETRANT INSPECT ROOT AND FINAL LAYER OF ALL WELDS PER MIL-I-6866, TYPE II, METHOD A. NO DEFECTS PERMITTED.
4. IDENTIFY PER 0-70042-20. LOCATION OPTIONAL.
5. WHERE A FULL .50 FILLET WELD CANNOT BE MADE A SEAL WELD SHALL SUFFICE. FILLET WELD TO ENCOMPASS AT LEAST 90% OF WELDED JOINT.
6. WELDING ELECTRODES SHALL BE ER316L PER MIL-E-19933D AND/OR E316L PER MIL-E-22200/2.
7. LOCKWIRE PER MS 33540.
8. LOCATE IDENT PLATE APPROX AS SHOWN. MARK PER 0-70042-30 OR-60. LINES 1&2: MAGNET ASSY-EBT-P -DEVELOPMENT. PART NO: 11-38001-1 SERIAL NO: AS APPLICABLE. CONTRACT NO: P.O. Y0E206R. AFTER MARKING, COAT FACE OF IDENT PLATE WITH 0-75052-2 CLEAR EPOXY ENAMEL.
9. TESTING TO BE DONE IN ACCORDANCE WITH INTEGRATED TEST PLAN GDC-EBT-81-011, SECTION 4.1

APPROVED TITLE I

REF AL BOCH LETTER DATED MARCH 19, 1982

PRELIMINARY

SEE SEPARATE PARTS LIST

SEE 0-70016 FOR ABBREVIATION, CODE AND SYMBOL REQUIREMENTS

SEE 0-70902 FOR STANDARD MANUFACTURING AND INSTALLATION REQUIREMENTS

UNLESS OTHERWISE SPECIFIED DIMENSIONS ARE IN INCHES

TOLERANCES .X ±.1 .XX ±.03 .XXX ±.010 ANGULAR PER 0-70902

UNLESS OTHERWISE SPECIFIED ALL MACHINED SURFACES ✓

GENERAL DYNAMICS
CONVAIR DIVISION
SAN DIEGO, CALIFORNIA

MAGNET ASSY-EBT-P

SIZE E | CODE IDENT NO 14170 | DWG NO 11-38001

SCALE 1/10 | SHEET 1 OF 2

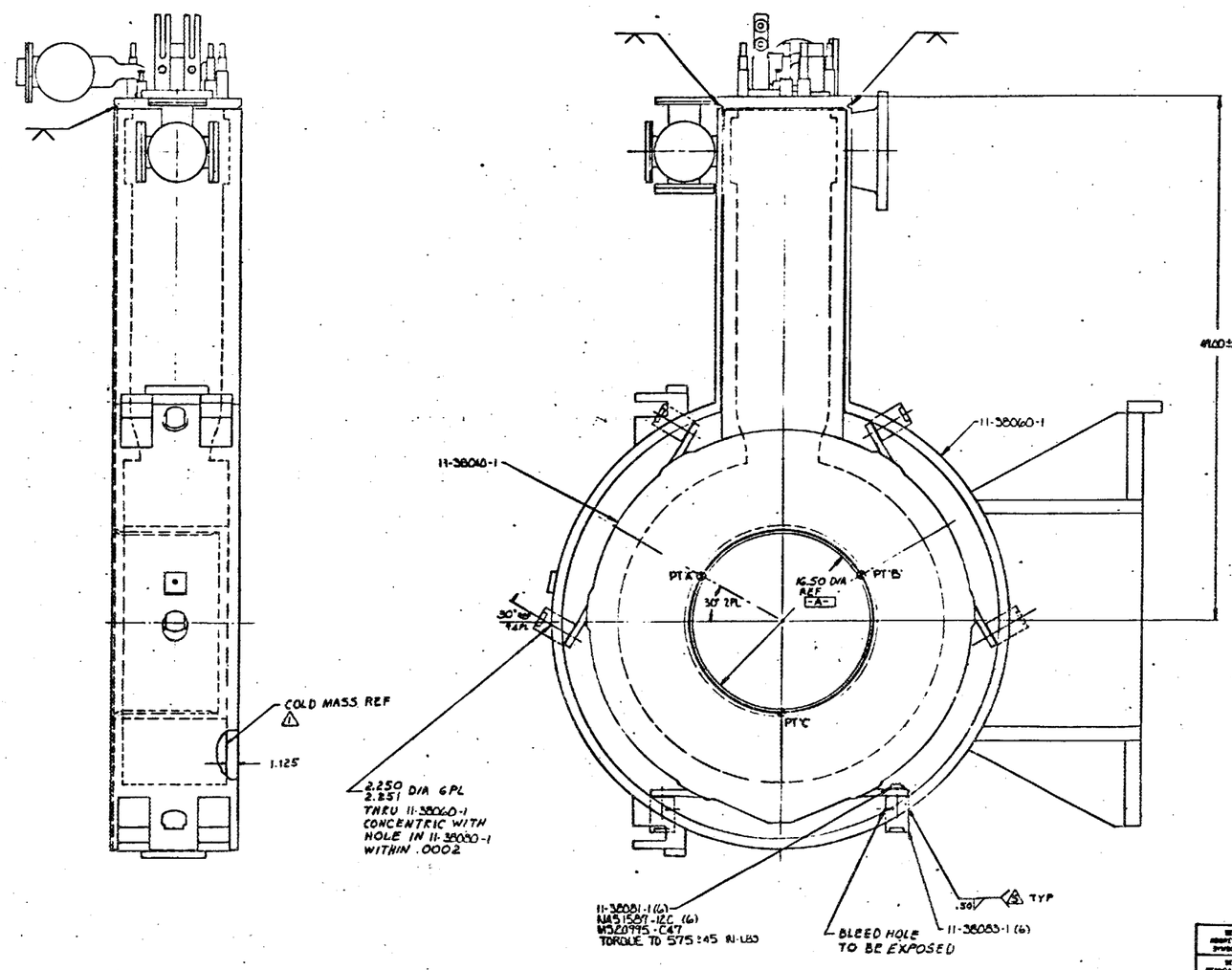

PRELIMINARY

APPROVED TITLE I

REF AL BOCK LETTER DATED
MARCH 19, 1982

SEE SEPARATE PARTS LIST

SEE G 70914 FOR ABBREVIATION CODE AND SYMBOL REQUIREMENTS

SEE G 70902 FOR STANDARD MANUFACTURING AND INSTALLATION REQUIREMENTS

UNLESS OTHERWISE SPECIFIED DIMENSIONS ARE IN INCHES
TOLERANCES
.X ± .1 .XX ± .03 .XXX ± .010
ANGULAR PER G 70902

UNLESS OTHERWISE SPECIFIED
ALL MACHINED SURFACES ✓

MATL
PROD SHOP

CHECK
STRESS
GRINDER
DESIGN
DRAWN
CONTRACT NO

GENERAL DYNAMICS
CONVAIR DIVISION
SAN DIEGO, CALIFORNIA

MAGNET ASSY-EBT-P
PROTOTYPE

SIZE E FSCM NO 14170 DWG NO 11-38001
SCALE 1.5=1.0 SHEET 2 OF

SEC CLASS | TYPE | LEVEL | CONT | GROUP | DISTR | PLFMD | PACKAGE NO | ALL

A–19/A–20

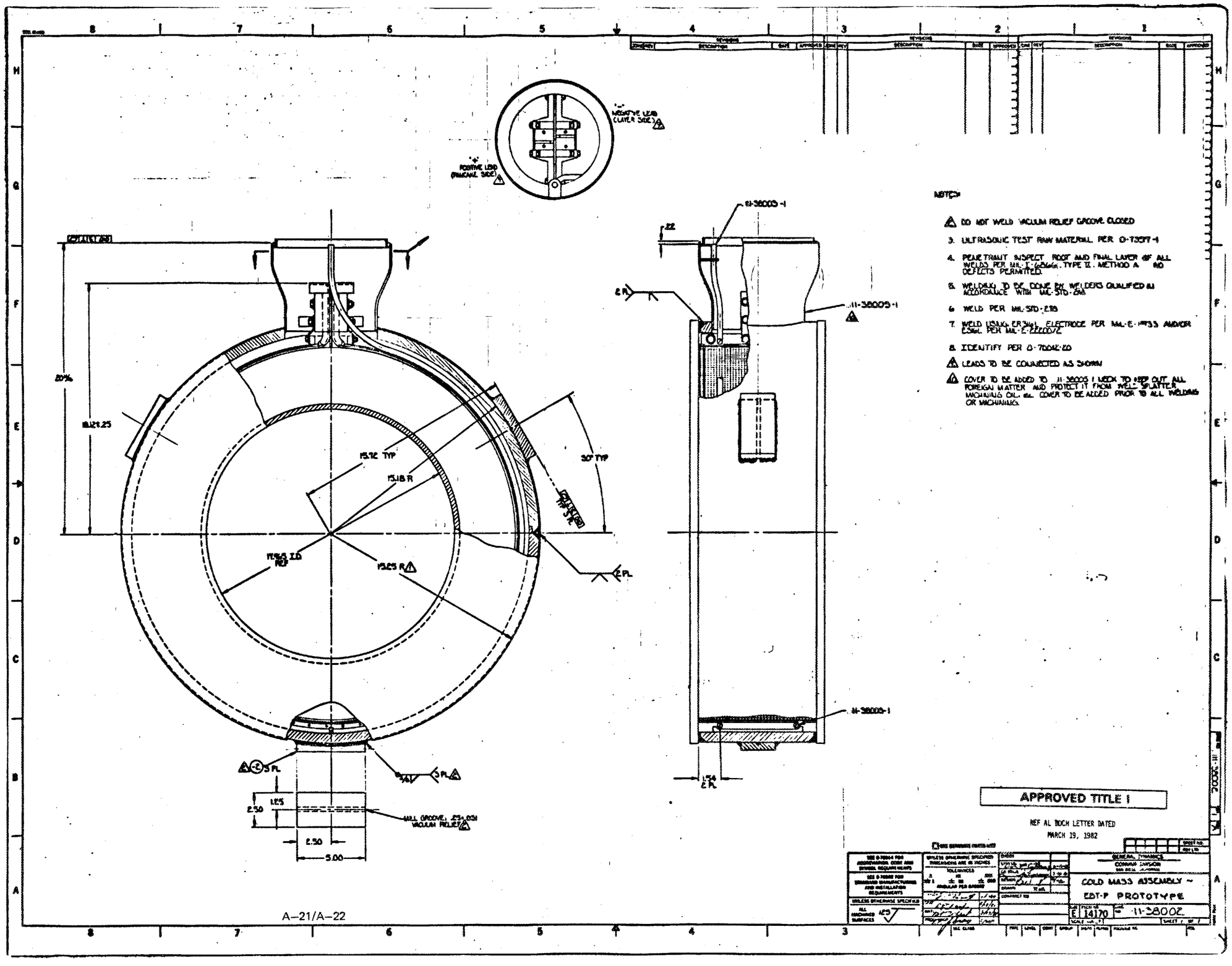
NEGATIVE LEAD (LAYER SIDE)
POSITIVE LEAD (PANCAKE SIDE)
11-38005-1
.22
.11-38005-1
11-38005-1
1.74 ER
20%
R21.25
15.72 TYP
15.18 R
30° TYP
15.25 R
EPL
3 PL
1.25
2.50
2.50
5.00
MILL GROOVE, .25 x .031 VACUUM RELIEF
NOTES:
DO NOT WELD VACUUM RELIEF GROOVE CLOSED
3. ULTRASONIC TEST RAW MATERIAL PER D-73077-1
4. PENETRANT INSPECT ROOT AND FINAL LAYER OF ALL WELDS PER MIL-I-6870A, TYPE II, METHOD A NO DEFECTS PERMITTED.
5. WELDING TO BE DONE BY WELDERS QUALIFIED IN ACCORDANCE WITH MIL-STD-248
6. WELD PER MIL-STD-278
7. WELD USING ER347L ELECTRODE PER MIL-E-19933 AND/OR ER347L PER MIL-E-22200/2
8. IDENTIFY PER D-70042-20
LEADS TO BE CONNECTED AS SHOWN
COVER TO BE ADDED TO 11-38005-1 WEDK TO KEEP OUT ALL FOREIGN MATTER AND PROTECT IT FROM WELD SPLATTER, MACHINING OIL, etc. COVER TO BE ADDED PRIOR TO ALL WELDING OR MACHINING.
APPROVED TITLE I
REF AL BOCH LETTER DATED MARCH 19, 1982
GENERAL DYNAMICS
CONVAIR DIVISION
COLD MASS ASSEMBLY - EBT-P PROTOTYPE
E 14170
11-38002

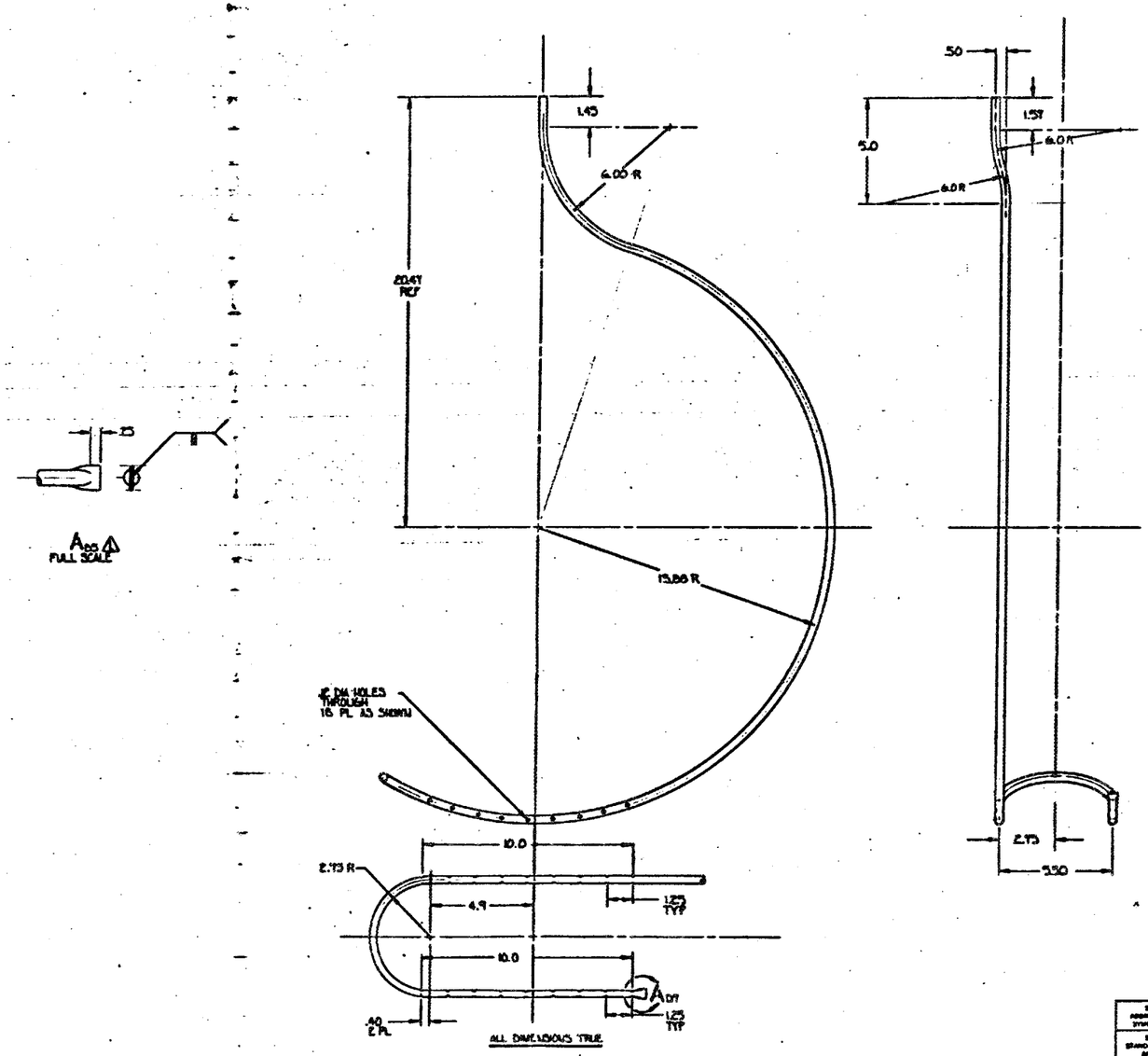

NOTES:

1. ⚠ CRIMP END OF TUBE CLOSED AND WELD AS SHOWN
2. WELDING TO BE DONE BY WELDERS QUALIFIED IN ACCORDANCE WITH MIL-STD-248
3. MAT'L: .375 OD × .020 WALL × 72 LONG 304L SST TUBING; DWG ROD
4. IDENTIFY PER 0-70042-20.
5. WELD PER MIL-STD-248.
6. WELD USING ER316L ELECTRODE PER MIL-E-19933 AND/OR E316L PER MIL-E-22200/2

APPROVED TITLE I

REF AL BOCH LETTER DATED MARCH 19, 1982

PRELIMINARY

GENERAL DYNAMICS
CONVAIR DIVISION
SAN DIEGO, CALIFORNIA

HELIUM SUPPLY TUBE ~
EBT-P PROTOTYPE

E 14170 11-38003

SCALE HALF

SEE D 70914 FOR ABBREVIATION, CODE AND SYMBOL REQUIREMENTS

SEE D 70962 FOR STANDARD MANUFACTURING AND INSPECTION REQUIREMENTS

UNLESS OTHERWISE SPECIFIED ALL MACHINED SURFACES

UNLESS OTHERWISE SPECIFIED DIMENSIONS ARE IN INCHES

TOLERANCES

ANGULAR PER D70962

DATE

PROD. DATE

DWG CLASS

CHECK

STRESS

GP ENGR

DESIGN

DRAWN

CONTRACT NO

SHEET NO

REV LTR

SHEET 1 OF 1

11-38003

A-23/A-24

-1

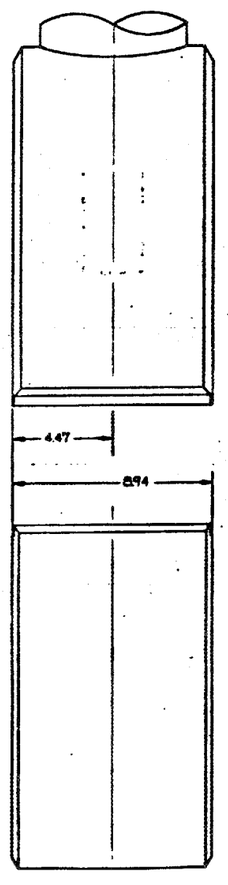

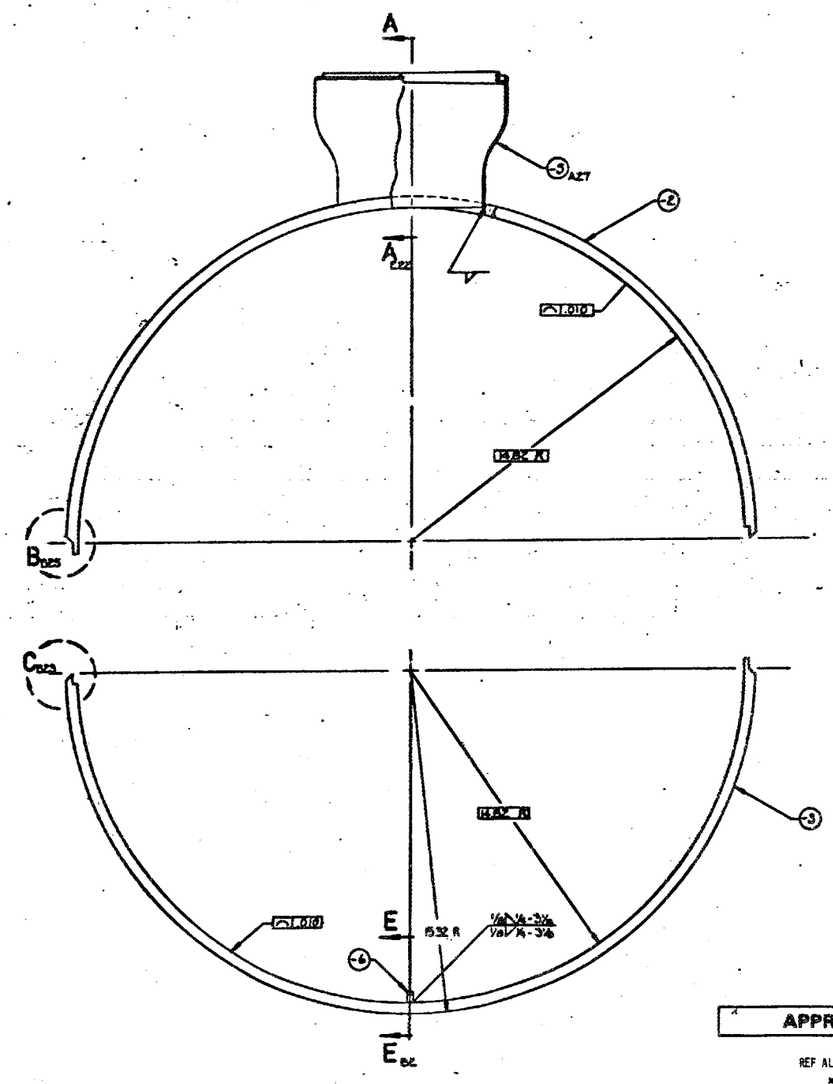

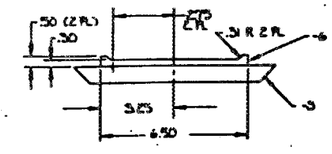

E-E

NOTES:

1. ALL DIMENSIONS SHALL BE FINAL MACHINING DIMENSIONS AND SHALL BE DONE AFTER WELDING -5 AND -4 IN PLACE AND STRESS RELIEVING DONE
2. BRIGHT BUFF OUTSIDE SURFACE OF -2 AND -3
3. IDENTIFY PER 0-70042-20 LOCATION OPTIONAL
4. ULTRASONIC TEST RAW MATERIAL PER 0-73517-1
5. PENETRANT INSPECT ROOT AND FINAL LAYER OF ALL WELDS PER MIL-I-16866 TYPE II METHOD A. NO DEFECTS PERMITTED.
6. WELDING TO BE DONE BY WELDERS QUALIFIED IN ACCORDANCE WITH MIL-STD-248
7. WELD PER MIL-STD-278
8. WELD USING ER316L FILLER WIRE PER MIL-E-17033 AND/OR E316L PER MIL-E-22200/12

APPROVED TITLE I

PRELIMINARY

REF AL BOCH LETTER DATED MARCH 19, 1982

-1

GENERAL DYNAMICS
CONVAIR DIVISION
SAN DIEGO, CALIFORNIA

COLD MASS OUTER RING - EBT-P PROTOTYPE

E 14170 11-38005

A–25/A–26

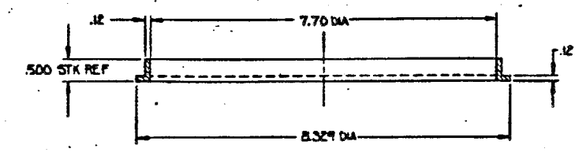

-4 DET
FULL SCALE

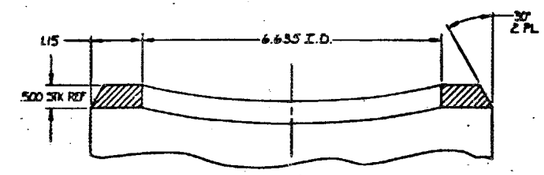

A-A$_{F4}$
FULL SCALE
-5 OMITTED FOR CLARITY

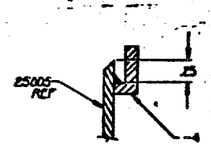

D$_{DET}$
SCALE NONE

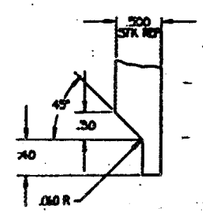

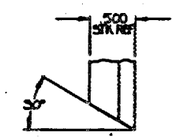

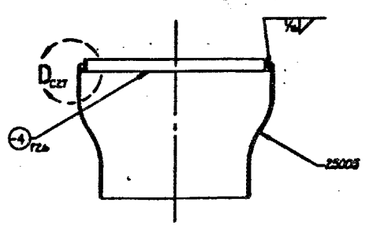

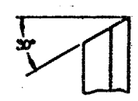

B$_{D4}$
SCALE 2/1

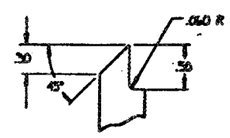

C$_{D4}$
SCALE 2/1

APPROVED TITLE I

REF AL BOCH LETTER DATED
MARCH 19, 1982

PRELIMINARY

-5$_{F4}$

A-27/A-28

SEE D 70914 FOR ABBREVIATION, CODE AND SYMBOL REQUIREMENTS	UNLESS OTHERWISE SPECIFIED DIMENSIONS ARE IN INCHES TOLERANCES .X ±.1 .XX ±.03 .XXX ±.010 ANGULAR PER D70902	CHECK / STRESS / GP ENGR / DESIGN / DRAWN / CONTRACT NO
SEE D 70902 FOR STANDARD MANUFACTURING AND INSTALLATION REQUIREMENTS		
UNLESS OTHERWISE SPECIFIED ALL MACHINED SURFACES 125	MATL / PROD ENGR	

GENERAL DYNAMICS
CONVAIR DIVISION
SAN DIEGO CALIFORNIA

COLD MASS OUTER RING - EBT-P PROTOTYPE

SIZE E | TYPE NO 14170 | CODE NO 11-38005 | SCALE | SHEET 2 OF

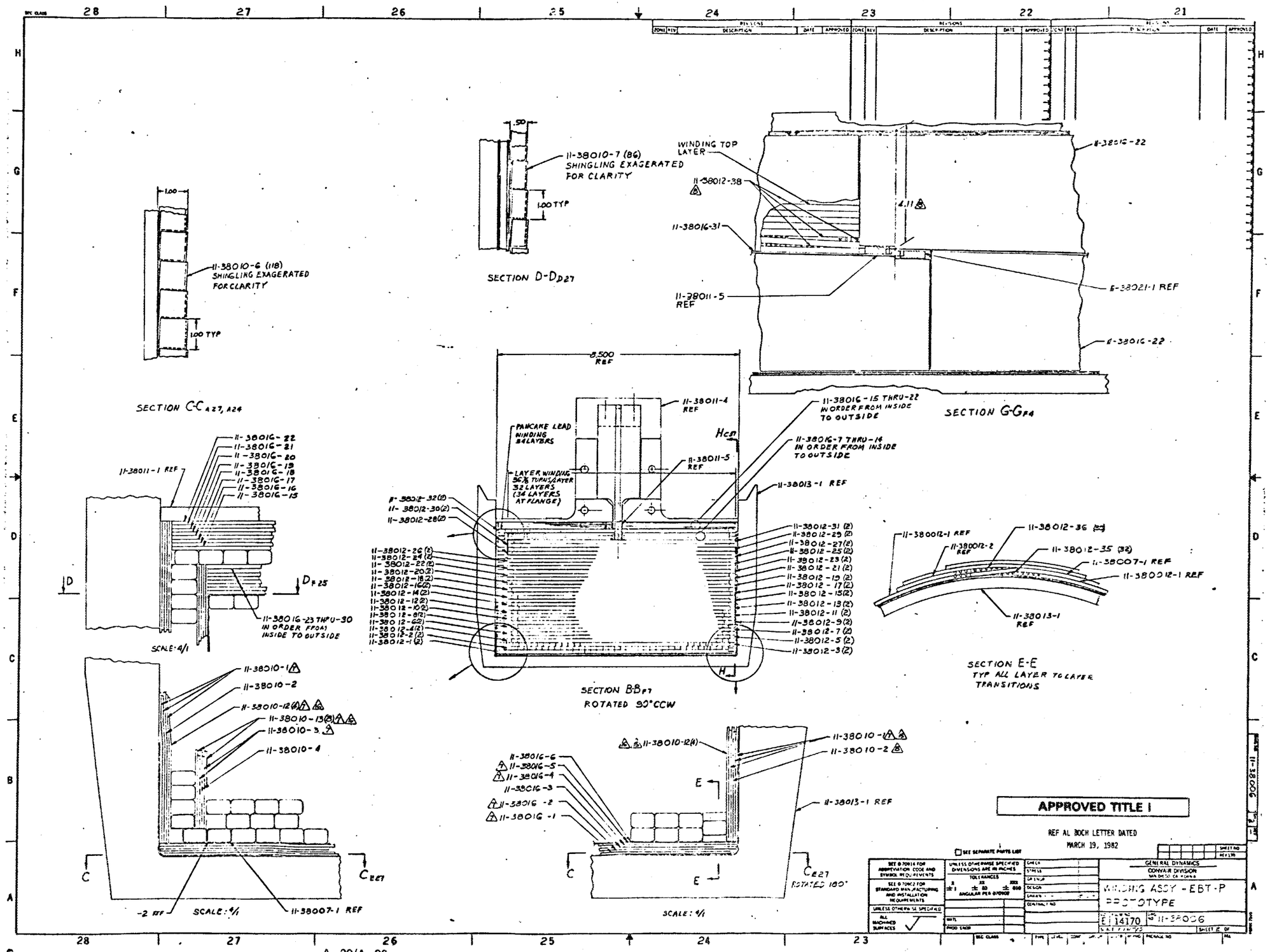
SECTION C-C A27, A24
11-38010-6 (118) SHINGLING EXAGERATED FOR CLARITY
1.00 TYP
SECTION D-D D27
11-38010-7 (86) SHINGLING EXAGERATED FOR CLARITY
1.00 TYP
SECTION G-G F4
WINDING TOP LAYER
11-38012-38
11-38016-31
11-38011-5 REF
4.11
11-38016-22
11-38021-1 REF
11-38016-22
SECTION B-B F7
ROTATED 90°CCW
5.500 REF
11-38011-4 REF
PANCAKE LEAD WINDING 8 LAYERS
LAYER WINDING 56 TURNS/LAYER 32 LAYERS (34 LAYERS AT FLANGE)
11-38011-5 REF
11-38016-15 THRU-22 IN ORDER FROM INSIDE TO OUTSIDE
11-38016-7 THRU-14 IN ORDER FROM INSIDE TO OUTSIDE
11-38013-1 REF
11-38012-32(2)
11-38012-30(2)
11-38012-28(2)
11-38012-26(2)
11-38012-24(2)
11-38012-22(2)
11-38012-20(2)
11-38012-18(2)
11-38012-16(2)
11-38012-14(2)
11-38012-12(2)
11-38012-10(2)
11-38012-8(2)
11-38012-6(2)
11-38012-4(2)
11-38012-2(2)
11-38012-1(2)
11-38012-31(2)
11-38012-29(2)
11-38012-27(2)
11-38012-25(2)
11-38012-23(2)
11-38012-21(2)
11-38012-19(2)
11-38012-17(2)
11-38012-15(2)
11-38012-13(2)
11-38012-11(2)
11-38012-9(2)
11-38012-7(2)
11-38012-5(2)
11-38012-3(2)
SECTION E-E
TYP ALL LAYER TO LAYER TRANSITIONS
11-38012-36
11-38012-35 (32)
11-38007-1 REF
11-38012-1 REF
11-38012-2 REF
11-38013-1 REF
11-38011-1 REF
11-38016-22
11-38016-21
11-38016-20
11-38016-19
11-38016-18
11-38016-17
11-38016-16
11-38016-15
11-38016-23 THRU-30 IN ORDER FROM INSIDE TO OUTSIDE
SCALE: 4/1
11-38010-1
11-38010-2
11-38010-12(4)
11-38010-13(3)
11-38010-3
11-38010-4
-2 REF
SCALE: 4/1
11-38007-1 REF
11-38016-6
11-38016-5
11-38016-4
11-38016-3
11-38016-2
11-38016-1
11-38010-12(4)
11-38010-1
11-38010-2
11-38013-1 REF
SCALE: 4/1
ROTATED 180°
APPROVED TITLE I
REF AL BOCH LETTER DATED MARCH 19, 1982
GENERAL DYNAMICS
CONVAIR DIVISION
SAN DIEGO CALIFORNIA
WINDING ASSY - EBT-P
PROTOTYPE
E 14170
11-38006

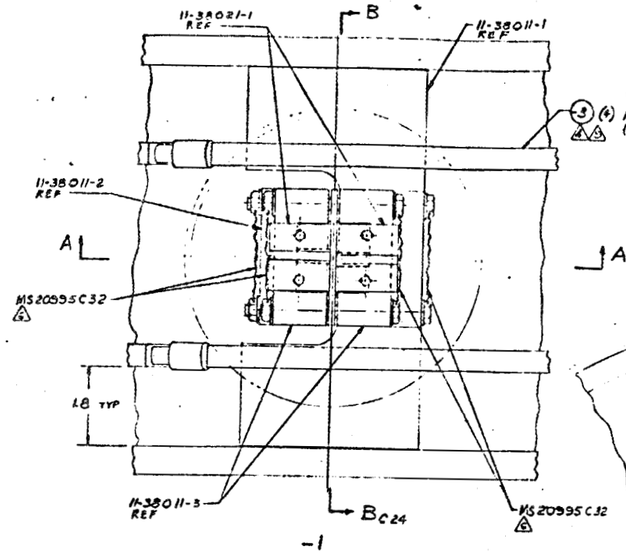

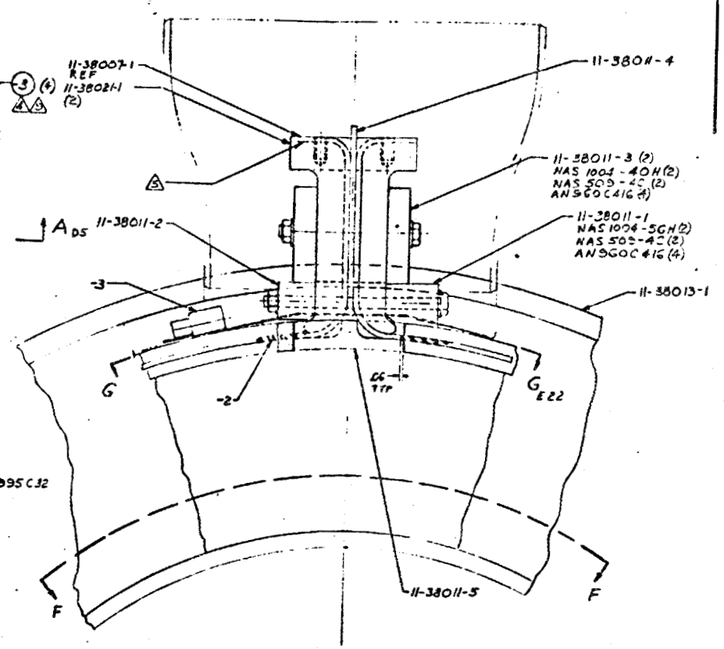

SECTION A-A 6-6

WINDING SCHEDULE 8

START OF FIRST LAYER IS 0

END OF LAYER NO.	NO OF TURNS FROM START	END OF LAYER NO	NO OF TURNS FROM START
1	38 + 180°	17	628 + 180°
2	75 + 135°	18	665 + 135°
3	112 + 90°	19	702 + 90°
4	149 + 45°	20	739 + 45°
5	186	21	776
6	222 + 315°	22	812 + 315°
7	259 + 270°	23	845 + 270°
8	296 + 225°	24	886 + 225°
9	333 + 180°	25	923 + 180°
10	370 + 135°	26	960 + 135°
11	407 + 90°	27	997 + 90°
12	444 + 45°	28	1034 + 45°
13	481	29	1071
14	517 + 315°	30	1107 + 315°
15	554 + 270	31	1144 + 270
16	591 + 225°	32 *	1165 + 315°

* HALF LAYER

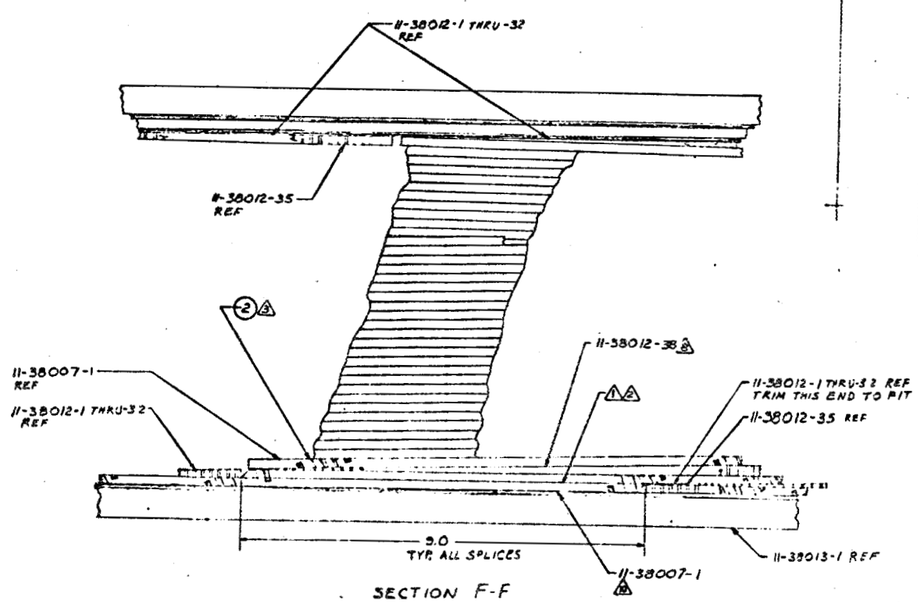

SECTION F-F

NOTES:

1. SOLDER SPLICE USING 97.5% LEAD, 2.5% SILVER SOLDER AND FLUX COMPOSED OF $ZnCl_2$-383G, NH_4Cl-38G, HCl-40 ML AND H_2O-100 ML.
2. ALL SPLICES TO BE LOCATED ADJACENT TO FLANGE. SPLICE PROCEDURE PER MIS(TBD).
3. -2 TO BE HELICALLY WRAPPED ABOUT 11-38007-1 SO THAT 40% TO 60% OF THE STRAND IS COVERED. ATTACH ENDS TO STRAND WITH 0-00089-1 CEMENT OR EQUIVALENT.
4. INSTALL -3 CLAMPS IN TANDEM. TRIM TAILS TO 1.00±.25.
5. SOLDER PER 0-73514-2 USING TIN-LEAD ALLOY, ASTM GRADE 63B PER FED SPEC QQ-S-571.
6. SAFETY IN ACCORDANCE WITH MS33540.
7. INSTALL ADJACENT LAYERS SO THAT THE ANGLE BETWEEN SLOTS IS 45° OR MORE.
8. USE 11-38012-38 AS A SHIM. USE LENGTH REQUIRED TO BRING LAST TURN OF CONDUCTOR TO CORRECT POSITION IN WINDING SCHEDULE
9. TORQUE TO 12-15 IN LB.
10. MAINTAIN 150-180 LB. TENSION WHILE WINDING.
11. IMMEDIATELY PRIOR TO ASSEMBLY CLEAN COMPONENTS WITH CHEESECLOTH, DDD-C-301, SOAKED WITH SOLVENT, 0-78054-1.
12. IDENTIFY PER 0-70042-20. LOCATION OPTIONAL.
13. CLEAN & PRE-TIN 11-38007-1 IN AREA TO BE SOLDERED. SOLDER SHIELD AND CONDUCTOR OF -5 TO 11-38007-1 USING 0-00337-2 EUTECTIC SOLDER.
14. PREPARE SURFACE AND APPLY ADHESIVE PER 0-79129.
15. ALIGN SLOTS AS SHOWN IN SECTION H-H.
16. USE 0-00089-1 CEMENT TO HOLD IN PLACE.

APPROVED TITLE I

REF AL BOCH LETTER DATED MARCH 19, 1982

SEE SEPARATE PARTS LIST

SEE G70814 FOR ABBREVIATION CODE AND SYMBOL REQUIREMENTS

SEE G70902 FOR STANDARD MANUFACTURING AND INSTALLATION REQUIREMENTS

UNLESS OTHERWISE SPECIFIED ALL MACHINED SURFACES ✓

UNLESS OTHERWISE SPECIFIED DIMENSIONS ARE IN INCHES

TOLERANCES: .X ±.1, .XX ±.03, .XXX ±.010, ANGULAR PER G70902

MATL

PROD ENGR

CHECK

STRESS

SP ENGR

DESIGN ENGR

DRAWN

CONTRACT NO

GENERAL DYNAMICS
CONVAIR DIVISION
SAN DIEGO, CALIFORNIA

WINDING ASSY-EBT-P
PROTOTYPE

SIZE E FSCM NO 14170 DWG NO 11-38006

SCALE

SHEET 1 OF 1

SEC CLASS

A-31/A-32

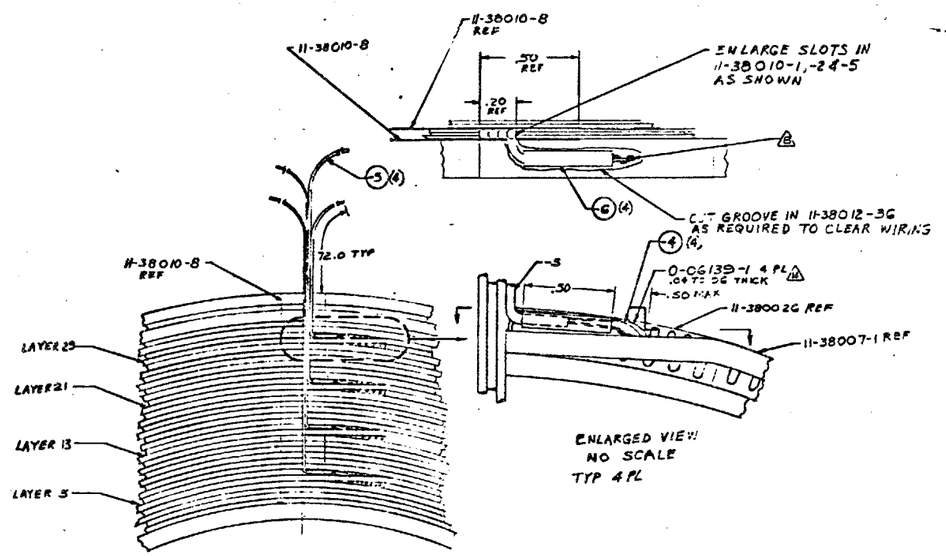

APPROVED TITLE I

REF AL BOCH LETTER DATED MARCH 19, 1982

SEE SEPARATE PARTS LIST

SEE D70014 FOR ABBREVIATION, CODE AND SYMBOL REQUIREMENTS

SEE D70902 FOR STANDARD MANUFACTURING AND INSTALLATION REQUIREMENTS

UNLESS OTHERWISE SPECIFIED ALL MACHINED SURFACES ✓

UNLESS OTHERWISE SPECIFIED DIMENSIONS ARE IN INCHES

TOLERANCES: X ±.1, XX ±.03, XXX ±.010; ANGULAR PER D70922

MATL

PROD ENGR

CHECK

STRESS

OR ENGR

DESIGN

DRAWN

CONTRACT NO

GENERAL DYNAMICS
CONVAIR DIVISION
SAN DIEGO, CALIFORNIA

WINDING ASSY-EBT-P -PROTOTYPE

SIZE E | CODE IDENT NO 14170 | DWG NO 11-38006

SCALE | SHEET 3 OF

SEC CLASS | TYPE | LEVEL | CONT | GROUP | SYSTEM | FIELD | PACKAGE NO | SELL

DWG NO.	SH	REV

REVISIONS

ZONE	REV	DESCRIPTION	DATE	APPROVED

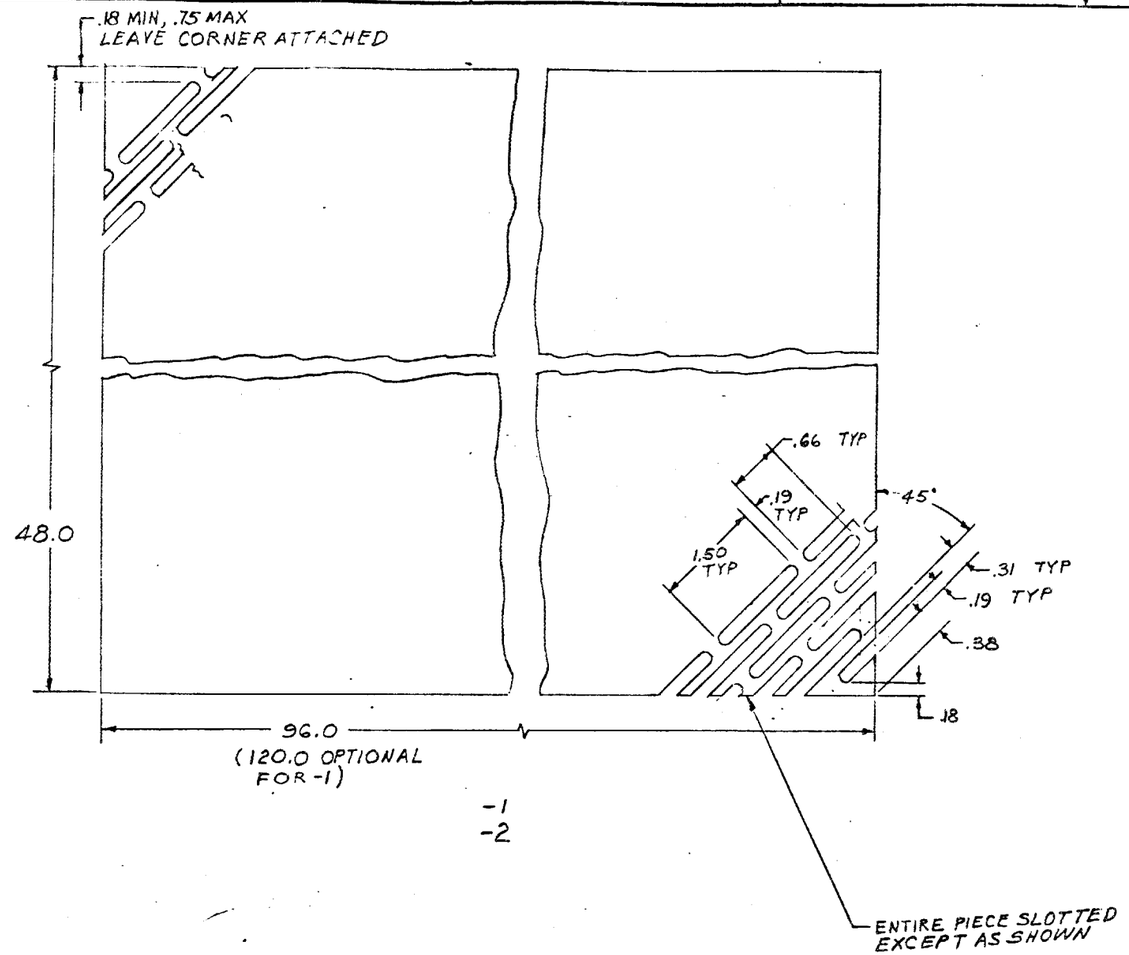

1. MATERIAL: NEMA GRADE G-10 CR FIBERGLASS EPOXY SHEET. -1 .020±.003 THICK. -2 .031±.003 THK.
2. PUNCHED SHEET TO BE FREE OF GLASS FIBERS AND DUST.
3. APPLY PART NO PER 0-70042-20. LOCATION OPTIONAL.
4. APPROVED SOURCES:
   SPAULDING FIBRE CO., INC.
   1 AMERICAN DRIVE
   BUFFALO, N.Y. 14225 PH 716-631-8000

   WESTINGHOUSE ELECTRIC CORP.
   MICARTA DIV.
   HAMPTON, S.C. 29924 PH 803-943-2311

APPROVED TITLE I

REF AL BOCH LETTER DATED MARCH 19, 1982

☐ SEE SEPARATE PARTS LIST

Z-2 ✓ MAG
Z-1 ✓

SHEET NO.
REV LTR

SEE 0-70914 FOR ABBREVIATION, CODE AND SYMBOL REQUIREMENTS

SEE 0-70902 FOR STANDARD MANUFACTURING AND INSTALLATION REQUIREMENTS

UNLESS OTHERWISE SPECIFIED
ALL MACHINED SURFACES ✓

UNLESS OTHERWISE SPECIFIED DIMENSIONS ARE IN INCHES
TOLERANCES
X ±.1 XX ±.03 XXX ±.010
ANGULAR PER 070902

		2/3/82
MAT		6/3/82
PROD ENGR		2/9/82

CHECK		
STRESS		2-2-82
GR ENGR		
DESIGN		
DRAWN	N. HILL	7-6-81
CONTRACT NO.		

GENERAL DYNAMICS
CONVAIR DIVISION
SAN DIEGO, CALIFORNIA

INSULATION-SLOTTED
EBT-P PROTOTYPE

SIZE D | FSCM NO 14170 | DWG NO. 11-38009
SCALE 1/1 | SHEET 1 OF 1

SEC. CLASS | TYPE | LEVEL | CONT | GROUP | DISTR | REPRO | PACKAGE NO. | REL

FORM 7316

A-35/A-36

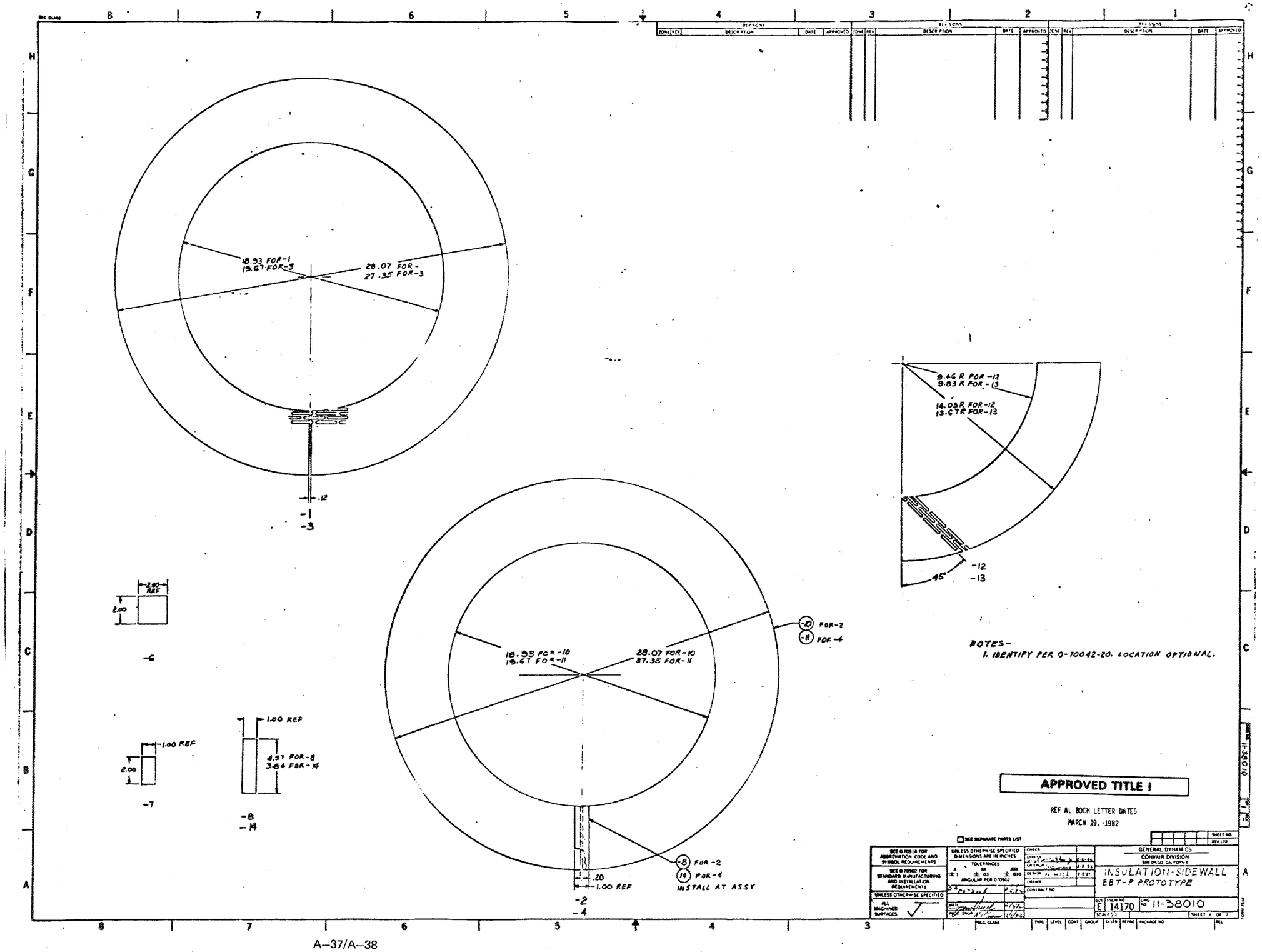
18.93 FOR-1
19.67 FOR-3
28.07 FOR-
27.35 FOR-3
.12
-1
-3
2.00 REF
2.00
-6
1.00 REF
2.00
-7
1.00 REF
4.37 FOR-8
3.84 FOR-14
-8
-14
18.93 FOR-10
19.67 FOR-11
28.07 FOR-10
27.35 FOR-11
-10 FOR-2
-8 FOR-4
.20
1.00 REF
-2
-4
-8 FOR-2
14 FOR-4
INSTALL AT ASSY
9.46 R FOR-12
9.83 R FOR-13
14.03 R FOR-12
13.67 R FOR-13
45°
-12
-13
NOTES-
1. IDENTIFY PER 0-70042-20. LOCATION OPTIONAL.
APPROVED TITLE I
REF AL BOCH LETTER DATED
MARCH 19, 1982
GENERAL DYNAMICS
CONVAIR DIVISION
SAN DIEGO CALIFORNIA
INSULATION-SIDEWALL
EBT-P PROTOTYPE
E 14170
11-38010

DWG NO.	SH	REV
11-38011	1	

REVISIONS

ZONE	REV	DESCRIPTION	DATE	APPROVED

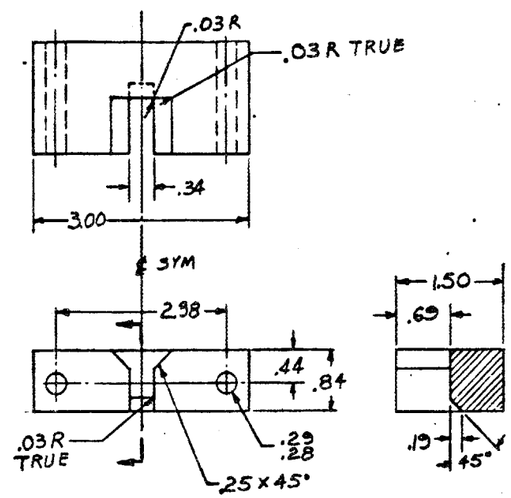

-2

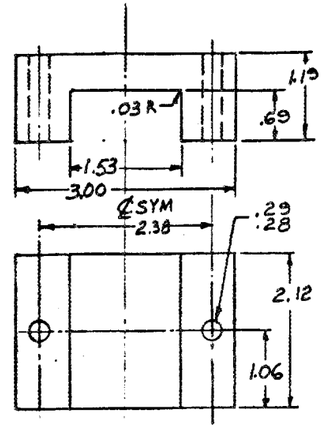

-3

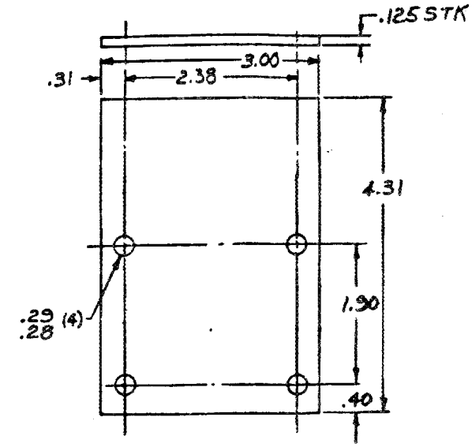

-4

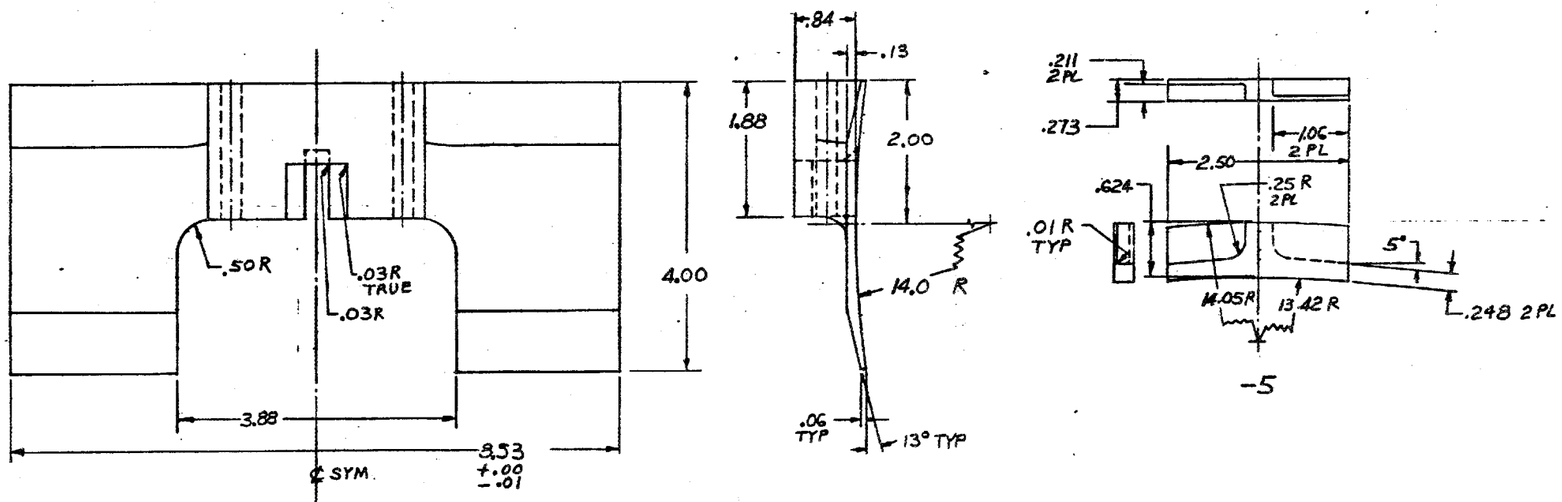

-5

NOTES
1. IDENTIFY PER 0-70042-20. LOCATION OPTIONAL.

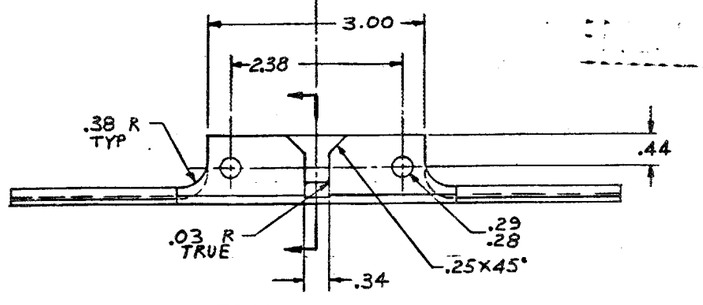

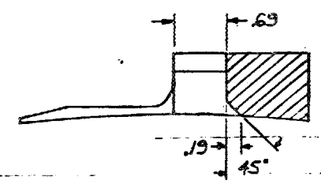

-1

A–39/A–40

PRELIMINARY

APPROVED TITLE I

REF AL BOCH LETTER DATED MARCH 19, 1982

☒ SEE SEPARATE PARTS LIST

SEE 0-70914 FOR ABBREVIATION, CODE AND SYMBOL REQUIREMENTS	UNLESS OTHERWISE SPECIFIED DIMENSIONS ARE IN INCHES	CHECK	GENERAL DYNAMICS CONVAIR DIVISION SAN DIEGO, CALIFORNIA
SEE 0-70902 FOR STANDARD MANUFACTURING AND INSTALLATION REQUIREMENTS	TOLERANCES .X ±.1 .XX ± .03 .XXX ± .010 ANGULAR PER 070902	STRESS	
		GR ENGR	
		DESIGN N. HILL 8-24-81	HOUSING-CONDUCTOR LEAD
		DRAWN	-EBT-P-PROTOTYPE
		CONTRACT NO.	
UNLESS OTHERWISE SPECIFIED ALL MACHINED SURFACES ✓	MATL.		SIZE D / FSCM NO. 14170 / DWG NO. 11-38011
	PROD. ENGR		SCALE / SHEET 1 OF 1

SHEET NO. / REV LTR

SEC. CLASS | TYPE | LEVEL | CONT | GROUP | DISTR | REPRO | PACKAGE NO. | REL.

FORM 2916

DWG NO. 11-38012 SH 1 REV

REVISIONS

ZONE	REV	DESCRIPTION	DATE	APPROVED

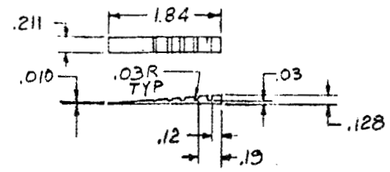

-36

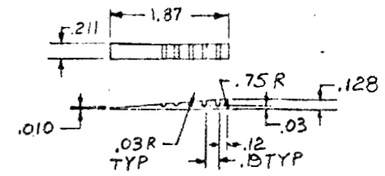

-35

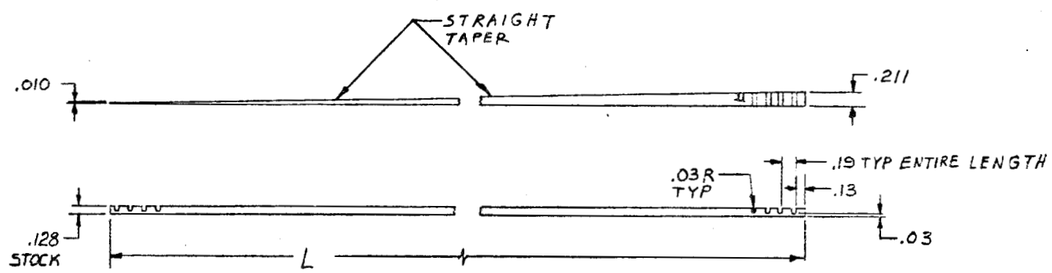

-1 THRU-32 & -38

DASH NO	DIM L
1	54.60
2	55.00
3	55.41
4	55.81
5	56.21
6	56.61
7	57.02
8	57.42
9	57.82
10	58.23
11	58.63
12	59.03
13	59.43
14	59.84
15	60.24
16	60.64

DASH NO	DIM L
17	61.04
18	61.45
19	61.85
20	62.25
21	62.66
22	63.06
23	63.46
24	63.86
25	64.27
26	64.67
27	65.07
28	65.48
29	65.88
30	66.28
31	66.68
32	67.87
38	85.71

NOTES

1. IDENTIFY PER 0-70042-20. LOCATION OPTIONAL.

APPROVED TITLE I

REF AL BOCH LETTER DATED MARCH 19, 1982

☒ SEE SEPARATE PARTS LIST

SEE 0-70914 FOR ABBREVIATION, CODE AND SYMBOL REQUIREMENTS

SEE 0-70902 FOR STANDARD MANUFACTURING AND INSTALLATION REQUIREMENTS

UNLESS OTHERWISE SPECIFIED ALL MACHINED SURFACES ✓

UNLESS OTHERWISE SPECIFIED DIMENSIONS ARE IN INCHES

TOLERANCES X ±.1 .XX ±.03 .XXX ±.010 ANGULAR PER 070902

MAT'L 2/3/82

PROJ. ENGR 2/3/82

SEC. CLASS

CHECK

STRESS 1-29-82

GR ENGR 2-8-82

DESIGN H. HILL 8-21-81

DRAWN

CONTRACT NO.

2/3/82

SHEET NO.

REV LTR

GENERAL DYNAMICS
CONVAIR DIVISION
SAN DIEGO, CALIFORNIA

INSULATION-LAYER END
-EBT-P-PROTOTYPE

SIZE D FSCM NO 14170 DWG NO. 11-380 12

SCALE 1/1 SHEET 1 OF 1

TYPE | LEVEL | CONT | GROUP | DISTR | REPRO | PACKAGE NO. | REL

FORM 7516

A-41/A-42

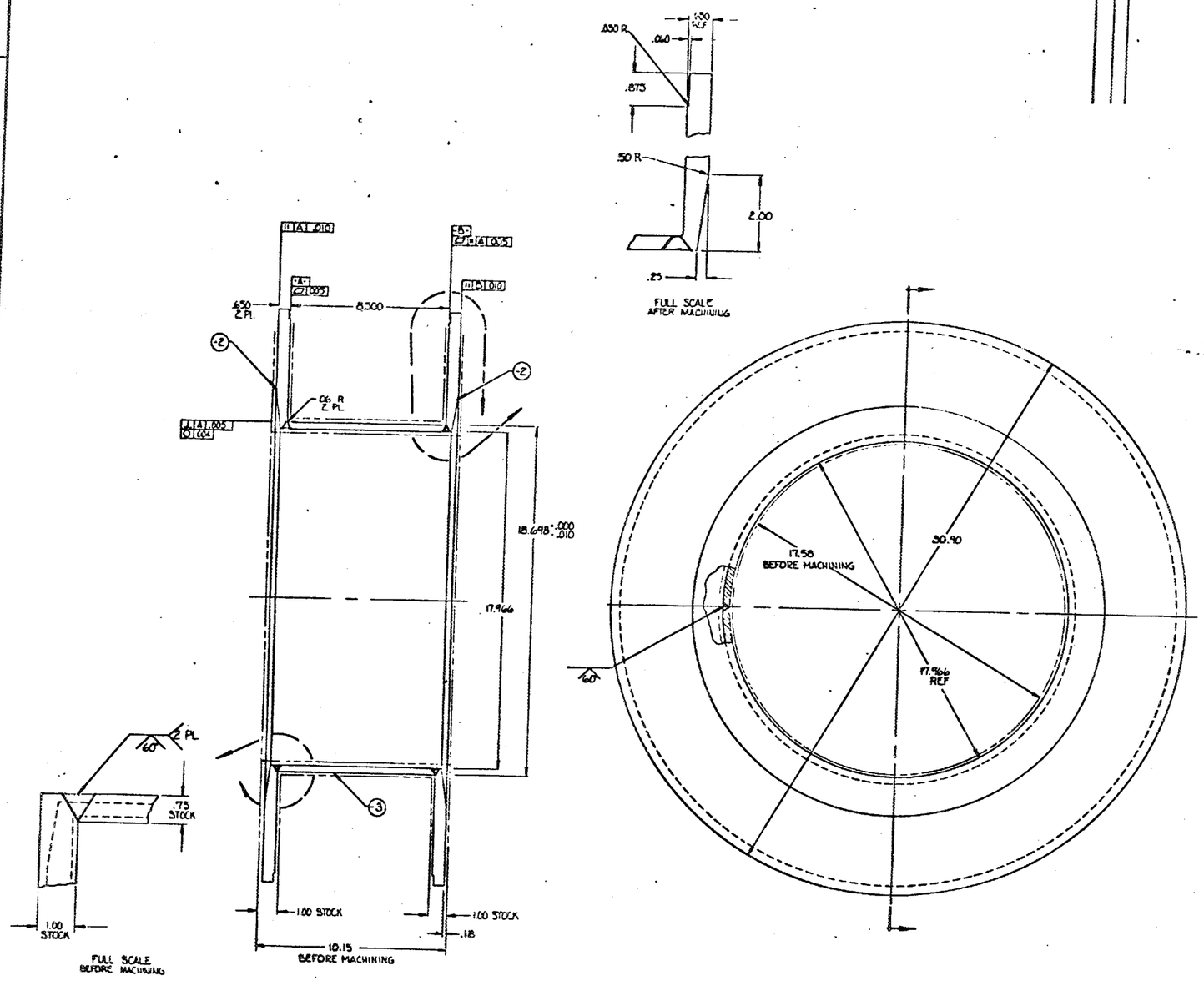

NOTES:

1. PENETRANT INSPECT RAW AND FINAL LAYER OF ALL WELDS PER MIL-I-6866, TYPE II METHOD A OR ASME CODE, SEC VIII, DIV 1, APPENDIX VIII NO DEFECTS PERMITTED
2. WELD AND RADIOGRAPHIC INSPECT PER MIL-STD-278E OR ASME CODE, SECTION VIII, DIV 1.
3. WELDING PROCEDURE AND WELDERS TO BE QUALIFIED IN ACCORDANCE WITH MIL-STD-248C OR ASME CODE, SECTION IX
4. WELD USING EA316L ELECTRODE PER MIL-E-17933 AND/OR E316L PER MIL-E-22200/2
5. IDENTIFY PER 0-70042-20 LOCATION OPTIONAL
6. ALL DIMENSIONS SHOWN ARE FINAL MACHINING DIMENSIONS AND SHALL BE DONE AFTER WELDING EXCEPT AS SHOWN
7. STRESS RELIEF SHALL BE DONE AT 1400°F TO 1450°F AFTER WELDING HOLD AT TEMPERATURE FOR 2 HOURS THEN OIL QUENCH
8. ULTRASONIC TEST RAW MATERIAL PER 0-73517-1 OR ASME CODE SECTION V, ARTICLE 23, SA-435
9. IMPACT TEST RAW MATERIAL, WELD PROCEDURE QUALIFICATION SPECIMENS AND PRODUCTION WELDS FOR 4K SERVICE PER ASME CODE, SECTION VIII, DIV 1, PARA UHA-51, UG-84. ACCEPTANCE CRITERIA SHALL BE 0.015 INCH LATERAL EXPANSION MINIMUM
10. PENETRANT INSPECT ALL MACHINED SURFACES PER MIL-I-6866 TYPE II, METHOD A OR ASME CODE SEC III DIV I APPENDIX VIII NO DEFECTS PERMITTED.
11. THE FOLLOWING LIMITATION APPLYS TO NOTES 1,2,3,8 AND 9: BOTH PROCEDURES MAY NOT BE USED CONCURRENTLY IN ANY ONE FABRICATION PROCESS

APPROVED TITLE I

REF AL BOCH LETTER DATED
MARCH 19, 1982

52 SEE SEPARATE PARTS LIST

SEE 0-70914 FOR ABBREVIATION, CODE AND SYMBOL REQUIREMENTS

SEE 0-70002 FOR STANDARD MANUFACTURING

UNLESS OTHERWISE SPECIFIED DIMENSIONS ARE IN INCHES

TOLERANCES

GENERAL DYNAMICS
CONVAIR DIVISION
SAN DIEGO, CALIFORNIA

SHEET NO

-1

DWG NO.	SH	REV
11-38016	1	

REVISIONS

ZONE	REV	DESCRIPTION	DATE	APPROVED

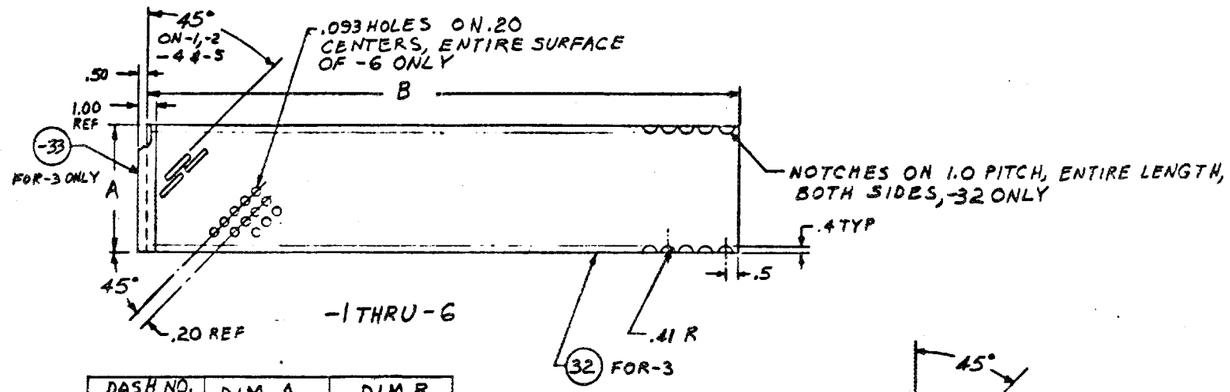

-1 THRU -6

DASH NO.	DIM A	DIM B
-1	8.34	58.72
-2	8.34	58.84
-32	8.43	58.96
-4	8.44	59.08
-5	8.44	59.23
-6	8.44	59.34

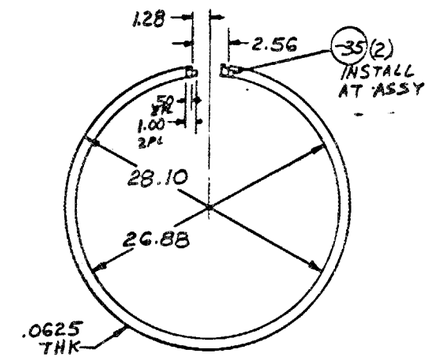

-31

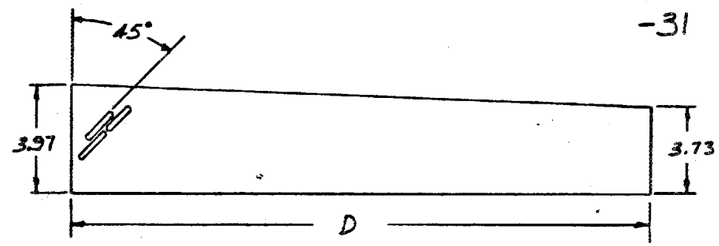

-7 THRU - 14

DASH NO	DIM D
-7	84.34
-8	84.53
-9	84.73
-10	84.92
-11	85.12
-12	85.31
-13	85.51
-14	85.70

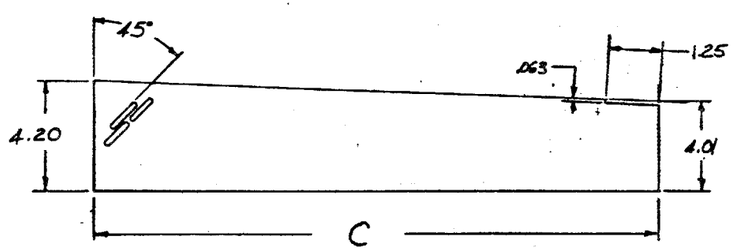

-15 THRU-22

DASH NO	DIM C
-15	86.70
-16	86.90
-17	87.09
-18	87.29
-19	87.48
-20	87.67
-21	87.87
-22	88.06

NOTES:

1. IDENTIFY PER 0-70042-20. LOCATION OPTIONAL.

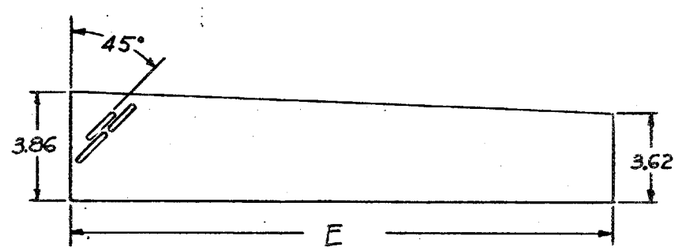

-23 THRU-30

DASH NO	DIM E
-23	84.34
-24	84.53
-25	84.73
-26	84.92
-27	85.12
-28	85.31
-29	85.51
-30	85.70

PRELIMINARY

APPROVED TITLE I

REF AL BOCH LETTER DATED MARCH 19, 1982

☒ SEE SEPARATE PARTS LIST

SEE 0-70914 FOR ABBREVIATION, CODE AND SYMBOL REQUIREMENTS

SEE 0-70902 FOR STANDARD MANUFACTURING AND INSTALLATION REQUIREMENTS

UNLESS OTHERWISE SPECIFIED ALL MACHINED SURFACES ✓

UNLESS OTHERWISE SPECIFIED DIMENSIONS ARE IN INCHES

TOLERANCES: .X ±.1, .XX ±.03, .XXX ±.010; ANGULAR PER 070902

MATL

PROD. ENGR

CHECK

STRESS

GR ENGR

DESIGN N. HILL 8-15-8

DRAWN

CONTRACT NO.

SHEET NO.

REV LTR

GENERAL DYNAMICS
CONVAIR DIVISION
SAN DIEGO, CALIFORNIA

INSULATION-GROUND
EBT -P- PRTOTYPE

SIZE D | FSCM NO. 14170 | DWG NO. 11-38016

SCALE NONE | SHEET 1 OF 1

SEC. CLASS | TYPE | LEVEL | CONT | GROUP | DISTR | REPRO | PACKAGE NO. | REL

FORM 7535

A-45/A-46

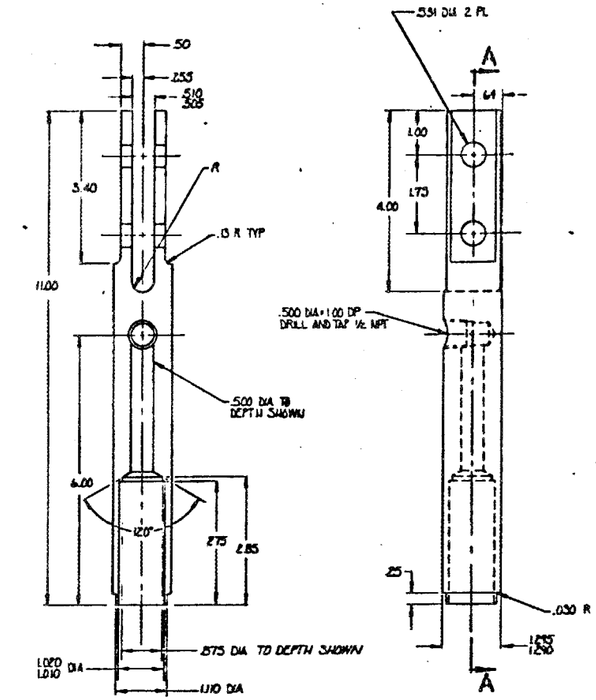

A-A

-3 ⚠

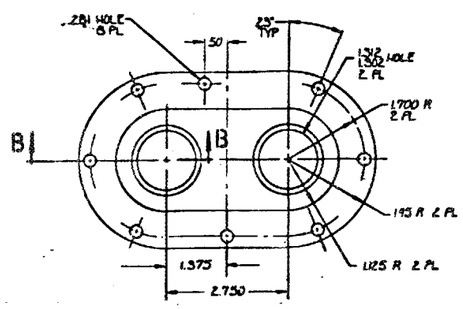

-6

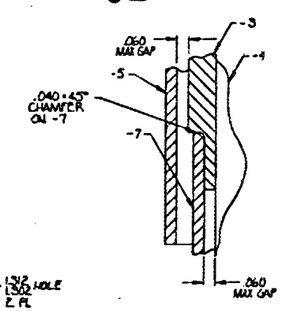

C
SCALE NONE

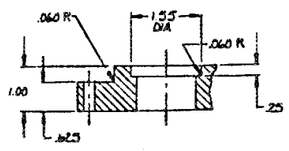

B-B

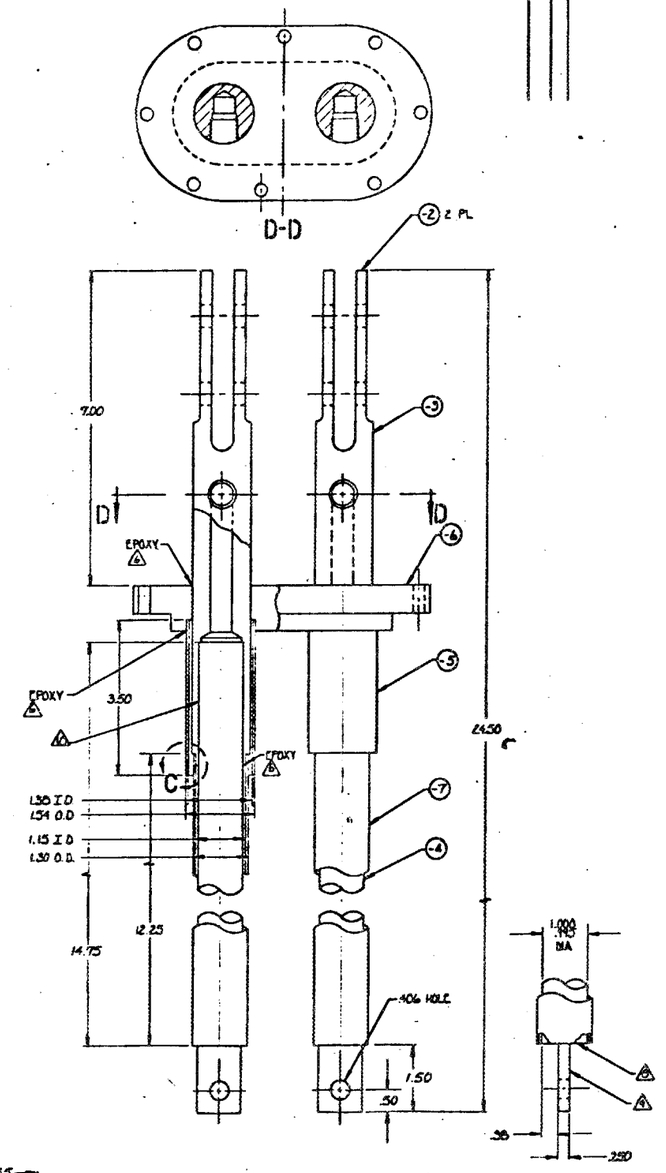

-1 ⚠

NOTES:

1. LEADS TO BE RATED AT 2000 AMPS EACH
2. LEADS TO BE SAME AS ANY L-SERIES LEAD EXCEPT FOR -3 COLLECTORS AND GIO-ER TUBES AND -6 FLANGE
3. LEAD NOT TO SUSTAIN ANY DEGRADATION WHEN SOLDERED TO COPPER TERMINALS USING EUTECTIC TIN/LEAD SOLDER AT TEMPERATURES LESS THAN 400° F
4. BAG AND TAG WITH "14170 SPEC 11-38020-1"
5. SUGGESTED SOURCE OF SUPPLY:
   AMERICAN MAGNETICS INC
   P.O. BOX 8
   OAK RIDGE, TN 37830
   TEL: 615-482-1056
6. ⚠ EPOXY PER MANUFACTURER'S STANDARD PRACTICE
7. ACCEPTANCE TEST TO BE PERFORMED BY GD/C. EACH LEAD LOSS TO BE LESS THAN 2.0 LITERS/HR He AT 2000 AMPS WITH COLD END AT 4.2 K AND WARM END AT 300 K
8. ⚠ COLD END OF LEAD TO INCLUDE Nb_3Sn SUPERCONDUCTOR TO MINIMIZE LOSSES
9. ⚠ COPPER ALLOY PER ASTM B-152-77 UNS NO C10100 TEMPER O60 (SOFT ANNEAL). CERTIFICATION REQUIRED
10. ⚠ SOLDER PER MANUFACTURER'S STANDARD PRACTICE
11. ⚠ TIN WITH "STABRITE" PER MANUFACTURER'S STANDARD PRACTICE.
12. LEADS TO WITHSTAND 100 LB PULL AT TOP OR BOTTOM CONNECTIONS WHEN -6 IS MOUNTED ONTO STACK
13. ⚠ THIS DRAWING IDENTICAL TO DW-38020

APPROVED TITLE I

REF AL BOCH LETTER DATED
MARCH 19, 1982

SPECIFICATION CONTROL DRAWING

SEE 070916 FOR ABBREVIATION, CODE AND SYMBOL REQUIREMENTS	UNLESS OTHERWISE SPECIFIED DIMENSIONS ARE IN INCHES	GENERAL DYNAMICS CONVAIR DIVISION SAN DIEGO, CALIFORNIA
SEE 070902 FOR STANDARD MANUFACTURING AND INSTALLATION REQUIREMENTS	TOLERANCES .X ±.03 .XX ±.010 .XXX ±.1 ANGULAR PER 070902	LIQUID COOLED CURRENT LEADS
UNLESS OTHERWISE SPECIFIED ALL MACHINED SURFACES 125		EBT-P PROTOTYPE
		SIZE E FSCM NO 14170 DWG NO 11-38020
		SCALE FULL SHEET 1 OF 1

A-47/A-48

DWG NO.	SH	REV
11-38021	1	

REVISIONS

ZONE	REV	DESCRIPTION	DATE	APPROVED

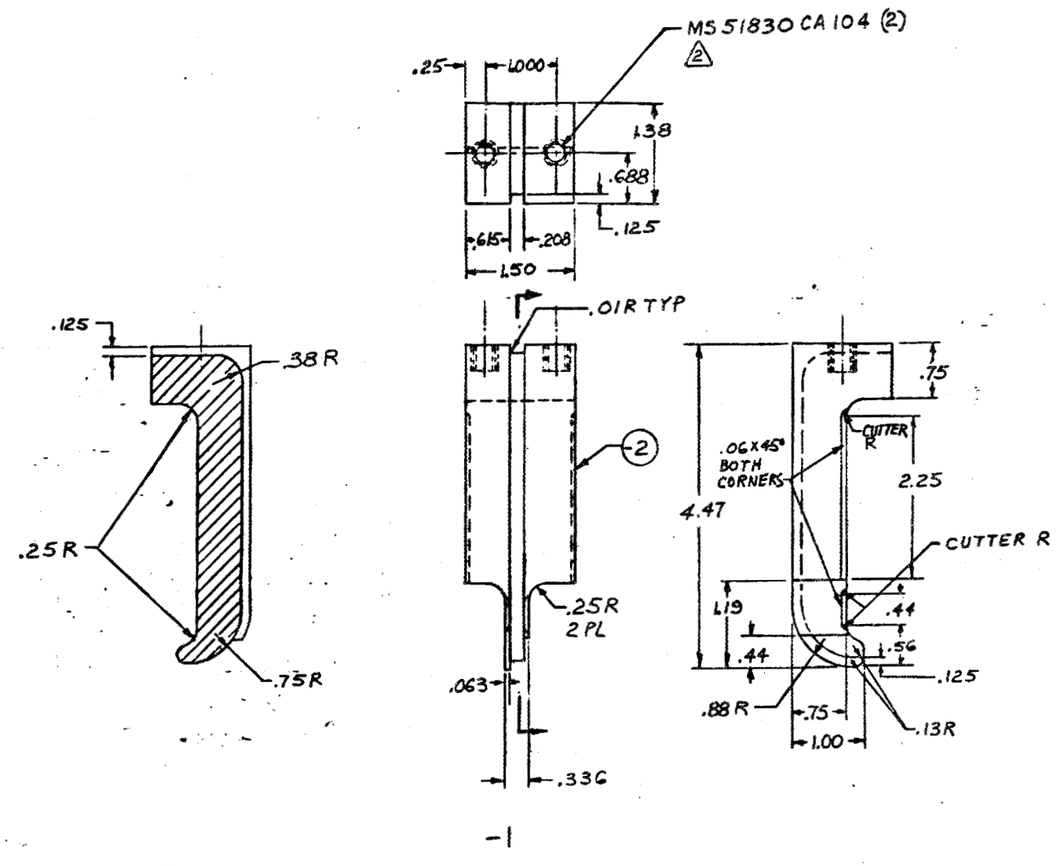

NOTES

1. IDENTIFY PER 0-70042-20. LOCATION OPTIONAL.
2. INSTALL PER MS 51835.

PRELIMINARY

APPROVED TITLE I

REF AL BOCH LETTER DATED MARCH 19, 1982

☒ SEE SEPARATE PARTS LIST

SEE 0-70914 FOR ABBREVIATION, CODE AND SYMBOL REQUIREMENTS	UNLESS OTHERWISE SPECIFIED DIMENSIONS ARE IN INCHES	CHECK	GENERAL DYNAMICS CONVAIR DIVISION SAN DIEGO, CALIFORNIA
SEE 0-70902 FOR STANDARD MANUFACTURING AND INSTALLATION REQUIREMENTS	TOLERANCES .X ±.1 .XX ± .03 .XXX ± .010 ANGULAR PER 070902	STRESS	LEAD LUG - EBT-P - PROTOTYE
UNLESS OTHERWISE SPECIFIED ALL MACHINED SURFACES ✓	MATL	GR ENGR	
	PROD. ENGR	DESIGN	
		DRAWN N. HILL 8-25-81	
		CONTRACT NO.	

SHEET NO. / REV LTR

SIZE D | FSCM NO. 14170 | DWG NO. 11-38021

SCALE | SHEET 1 OF 1

FORM 7958

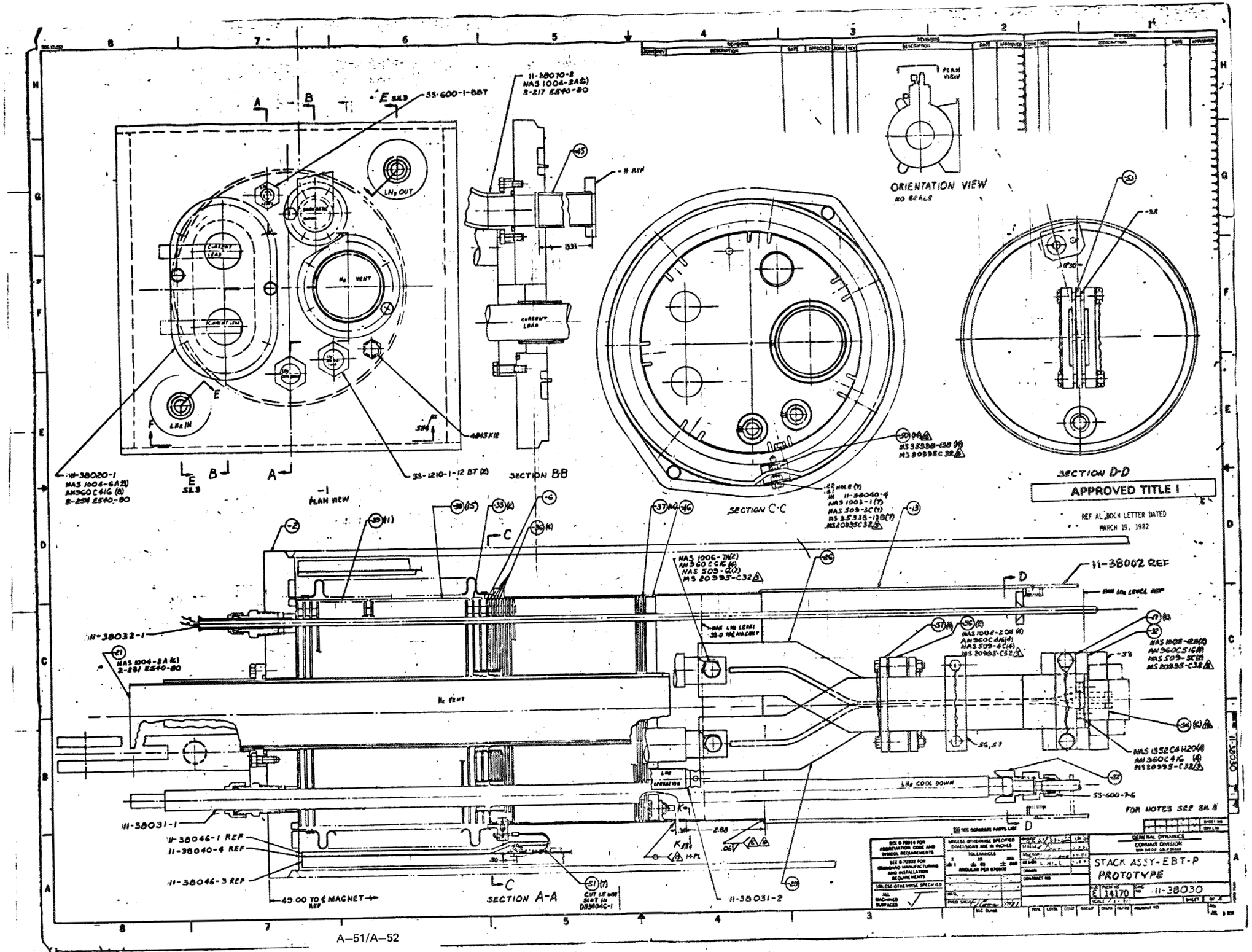
ORIENTATION VIEW
NO SCALE
SECTION B-B
SECTION C-C
SECTION D-D
SECTION A-A
PLAN VIEW
APPROVED TITLE I
REF AL BOCK LETTER DATED MARCH 19, 1982
11-38002 REF
11-38032-1
11-38031-1
11-38046-1 REF
11-38040-4 REF
11-38046-3 REF
11-38031-2
11-38020-1
11-38070-2
NAS 1004-2A(2)
2-281 E540-80
NAS 1006-7H(2)
AN360C6K(4)
NAS 509-6(2)
MS 20995-C32
NAS 1004-2B(4)
AN360C4K(4)
NAS 509-8C(4)
MS 20995-C32
NAS 1008-4B(2)
AN360C5K(8)
NAS 509-5C(2)
MS 20995-C32
NAS 1352C4H204(4)
AN360C4K(4)
MS 20995-C32
MS 35338-138(4)
MS 20995C32
NAS 1003-1(7)
NAS 509-3C(7)
MS 35338-138(7)
MS 20995C32
SS-600-1-8BT
SS-1210-1-12 BT (2)
SS-600-7-6
LN2 OUT
LN2 IN
LN2 VENT
CURRENT LEAD
LN2 OPERATION
LN2 COOL DOWN
FOR NOTES SEE SH. 8
49.00 TO ℄ MAGNET REF
CUT 1/8 WIDE SLOT IN 11-38040-1
GENERAL DYNAMICS
CONVAIR DIVISION
STACK ASSY-EBT-P
PROTOTYPE
E 14170
11-38030
SHEET 1 OF 4

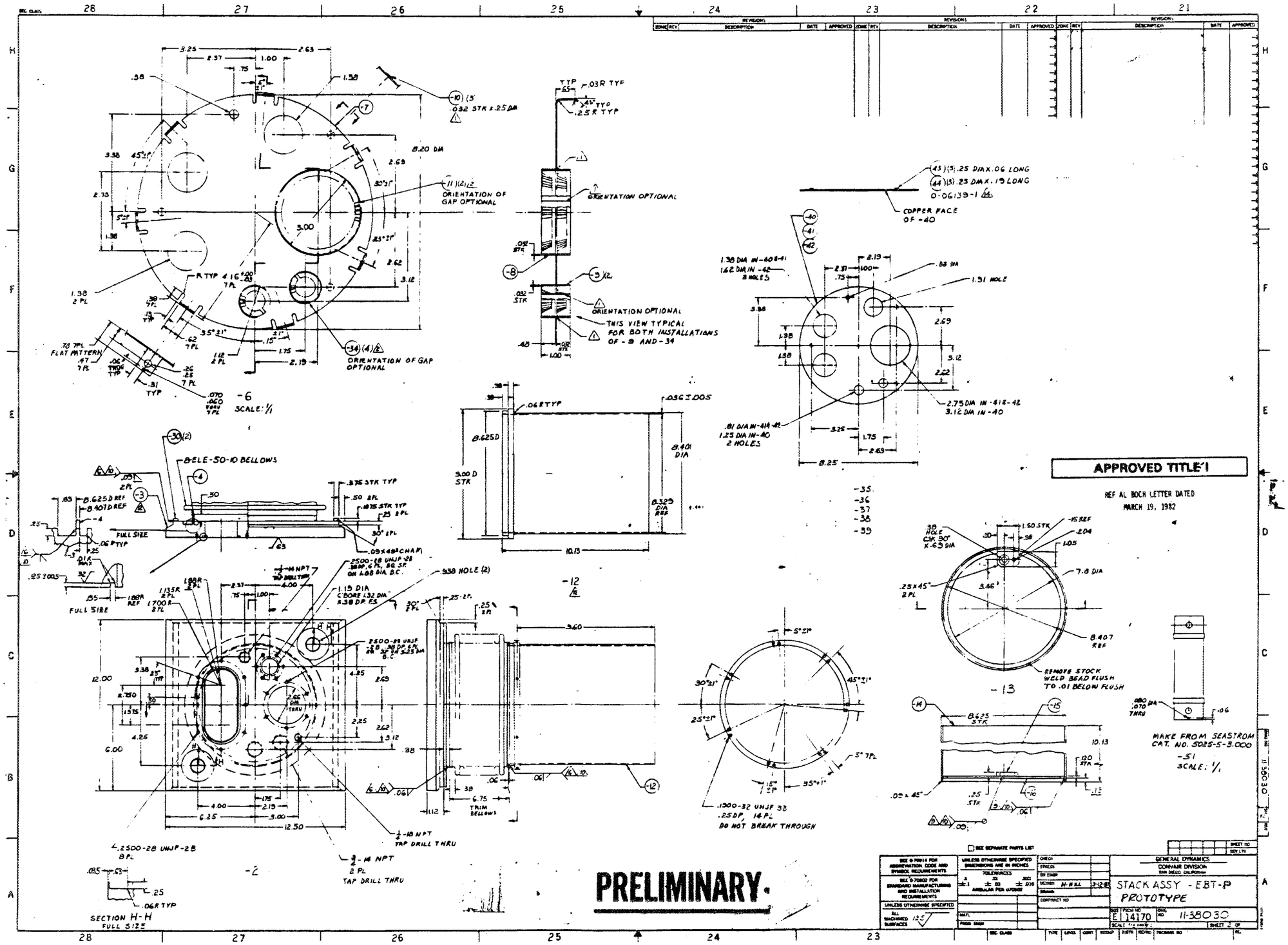
APPROVED TITLE'I
REF AL BOCH LETTER DATED MARCH 19, 1982
PRELIMINARY
STACK ASSY - EBT-P
PROTOTYPE
GENERAL DYNAMICS
CONVAIR DIVISION
SAN DIEGO, CALIFORNIA
E 14170
11-38030
-6
SCALE: 1/1
-2
SECTION H-H
FULL SIZE
-12
-13
-51
SCALE: 1/1
MAKE FROM SEASTROM CAT. NO. 5025-5-3.000
ORIENTATION OF GAP OPTIONAL
ORIENTATION OPTIONAL
THIS VIEW TYPICAL FOR BOTH INSTALLATIONS OF -9 AND -34
8-ELE-50-10 BELLOWS
COPPER FACE OF -40
REMOVE STOCK WELD BEAD FLUSH TO .01 BELOW FLUSH
DO NOT BREAK THROUGH
TAP DRILL THRU
TRIM BELLOWS

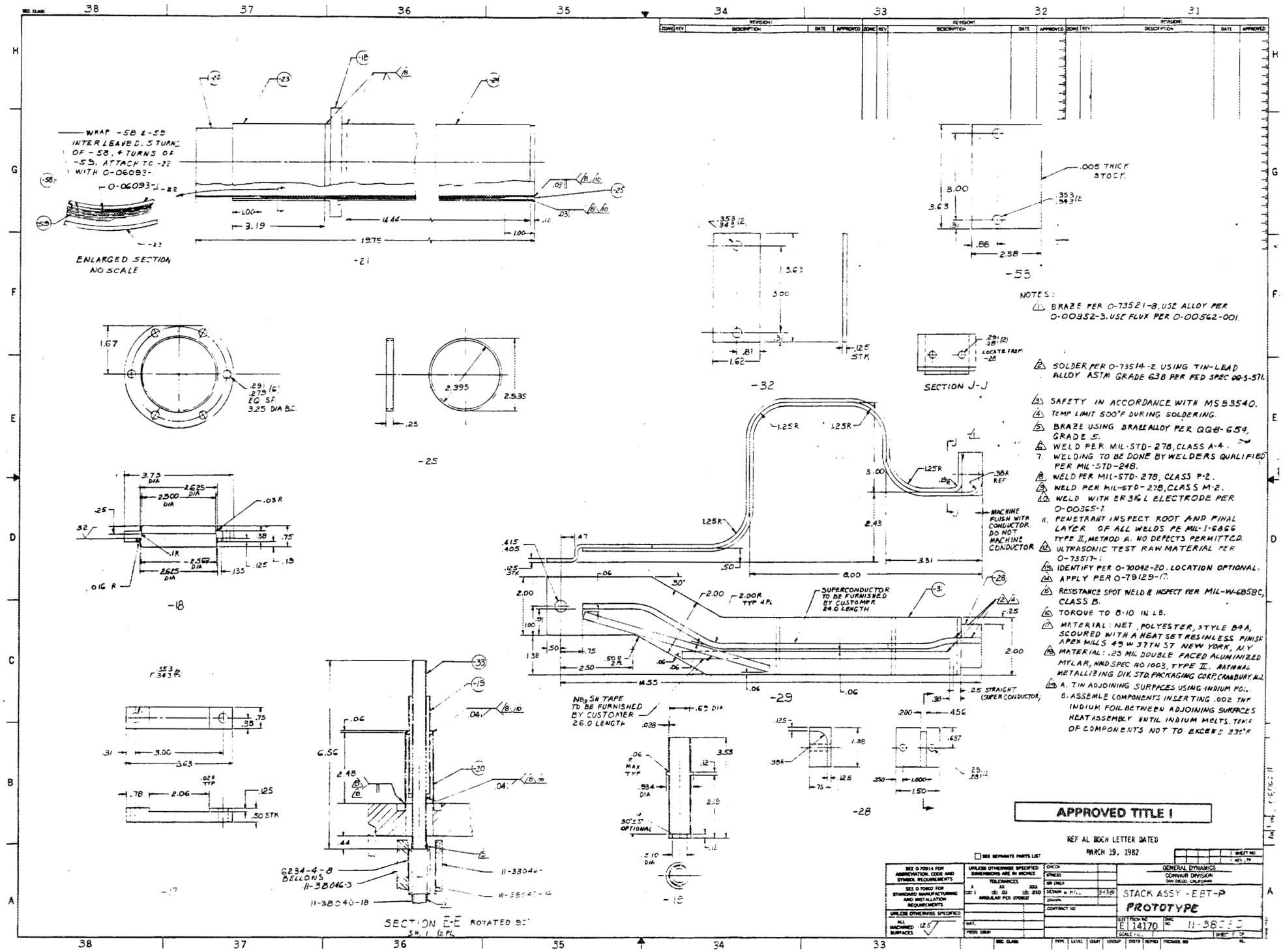
WRAP -58 & -59 INTERLEAVE 5 TURNS OF -58, 4 TURNS OF -59. ATTACH TO -22 WITH O-06093-1
ENLARGED SECTION NO SCALE
-21
-55
-32
SECTION J-J
-25
-18
-29
-28
-17
SECTION E-E ROTATED 90°
NB3 SN TAPE TO BE FURNISHED BY CUSTOMER 26.0 LENGTH
SUPERCONDUCTOR TO BE FURNISHED BY CUSTOMER 24.0 LENGTH
MACHINE FLUSH WITH CONDUCTOR. DO NOT MACHINE CONDUCTOR
.005 THICK STOCK
NOTES:
1. BRAZE PER O-73521-8. USE ALLOY PER O-00952-3. USE FLUX PER O-00562-001.
2. SOLDER PER O-73514-2 USING TIN-LEAD ALLOY ASTM GRADE 63B PER FED SPEC QQ-S-571.
3. SAFETY IN ACCORDANCE WITH MS33540.
4. TEMP LIMIT 500°F DURING SOLDERING.
5. BRAZE USING BRAZEALLOY PER QQB-654, GRADE 5.
6. WELD PER MIL-STD-278, CLASS A-4.
7. WELDING TO BE DONE BY WELDERS QUALIFIED PER MIL-STD-248.
8. WELD PER MIL-STD-278, CLASS P-2.
9. WELD PER MIL-STD-278, CLASS M-2.
10. WELD WITH ER316L ELECTRODE PER O-00365-7.
11. PENETRANT INSPECT ROOT AND FINAL LAYER OF ALL WELDS PE MIL-I-6866 TYPE II, METHOD A. NO DEFECTS PERMITTED.
12. ULTRASONIC TEST RAW MATERIAL PER O-73517-1.
13. IDENTIFY PER O-70042-20. LOCATION OPTIONAL.
14. APPLY PER O-79129-17.
15. RESISTANCE SPOT WELD & INSPECT PER MIL-W-6858C, CLASS B.
16. TORQUE TO 8-10 IN LB.
17. MATERIAL: NET, POLYESTER, STYLE B4A, SCOURED WITH A HEAT SET RESINLESS FINISH APEX MILLS 49 W 37TH ST NEW YORK, N.Y.
18. MATERIAL: .25 MIL DOUBLE FACED ALUMINIZED MYLAR, NND SPEC NO 1003, TYPE II. NATIONAL METALLIZING DIV. STD. PACKAGING CORP. CRANBURY, N.J.
19. A. TIN ADJOINING SURFACES USING INDIUM FOIL. B. ASSEMLE COMPONENTS INSERTING .002 THK INDIUM FOIL BETWEEN ADJOINING SURFACES HEAT ASSEMBLY UNTIL INDIUM MELTS. TEMP OF COMPONENTS NOT TO EXCEED 230°F
APPROVED TITLE 1
REF AL 100CN LETTER DATED MARCH 19, 1982
GENERAL DYNAMICS
CONVAIR DIVISION
SAN DIEGO, CALIFORNIA
STACK ASSY - EBT-P
PROTOTYPE
E 14170

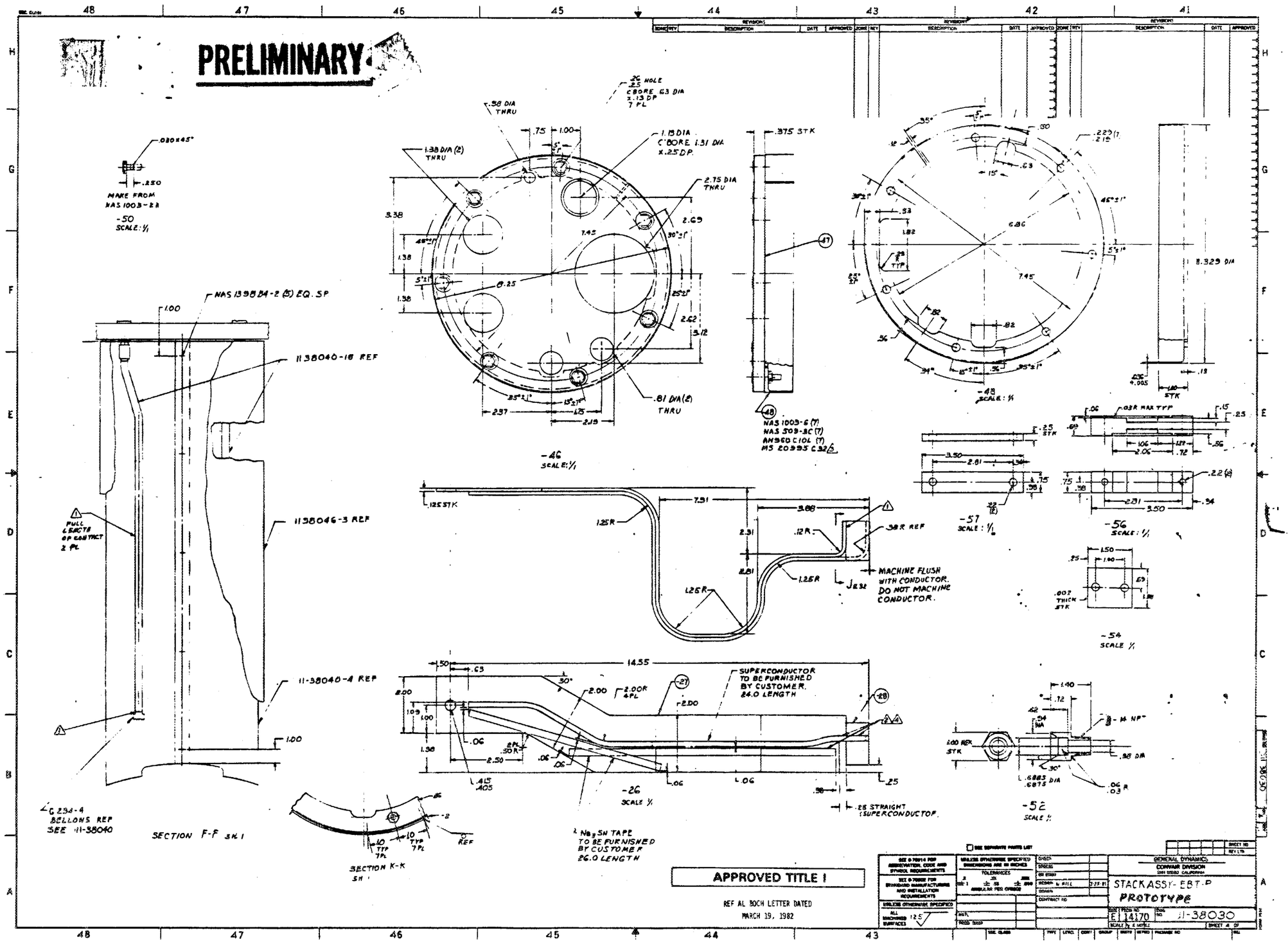
PRELIMINARY
.030x45°
.250
MAKE FROM NAS 1003-2A
-50
SCALE: 1/1
NAS 1398 B4-2 (5) EQ. SP
1.00
11-38040-18 REF
11-38046-3 REF
11-38040-4 REF
FULL LENGTH OF CONTACT 2 PL
1.00
G 238-4 BELLOWS REF SEE 11-38040
SECTION F-F SH 1
SECTION K-K SH 1
.26 HOLE .25 C'BORE .63 DIA x .13 DP 7 PL
.38 DIA THRU
1.38 DIA (2) THRU
1.13 DIA C'BORE 1.31 DIA x .25 DP
2.75 DIA THRU
.81 DIA (2) THRU
-46
SCALE: 1/1
.375 STK
NAS 1003-6 (7)
NAS 509-3C (7)
AN960C10L (7)
MS 20995 C32
-48
SCALE: 1/1
8.329 DIA
.125 STK
1.25R
MACHINE FLUSH WITH CONDUCTOR. DO NOT MACHINE CONDUCTOR.
-57
SCALE: 1/1
-56
SCALE: 1/1
-54
SCALE 1/1
14.55
SUPERCONDUCTOR TO BE FURNISHED BY CUSTOMER. 24.0 LENGTH
2.00R 4PL
.25 STRAIGHT (SUPERCONDUCTOR)
-26
SCALE 1/1
Nb3Sn TAPE TO BE FURNISHED BY CUSTOMER 26.0 LENGTH
-52
SCALE 1/1
APPROVED TITLE I
REF AL BOCH LETTER DATED MARCH 19, 1982
GENERAL DYNAMICS
CONVAIR DIVISION
STACKASSY- EBT-P
PROTOTYPE
E 14170
11-38030

DWG NO. 11-38031 SH 1 REV

REVISIONS

ZONE	REV	DESCRIPTION	DATE	APPROVED

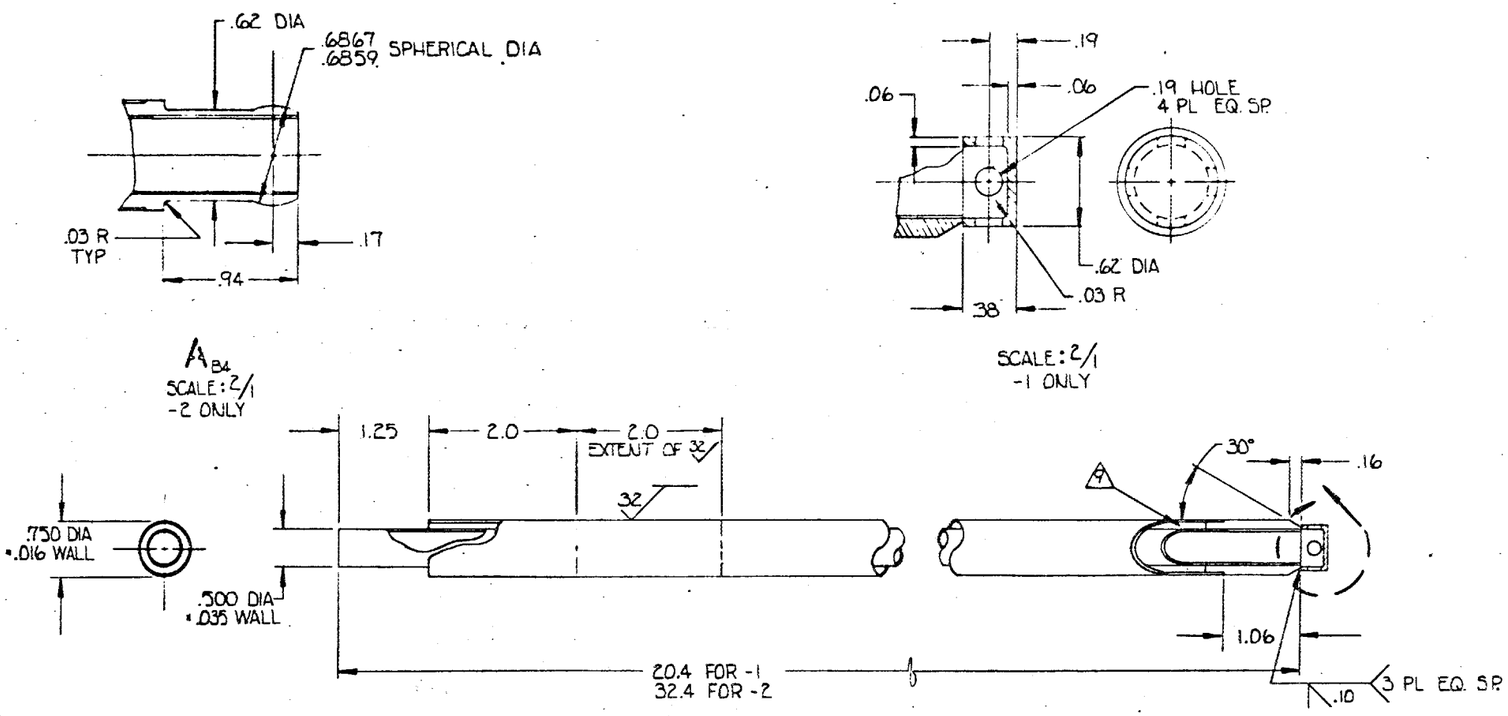

-1 10

-2 SAME AS -1 EXCEPT AS SHOWN 11

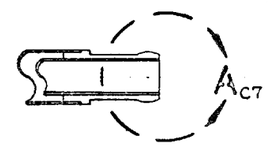

-2 END CONFIGURATION

NOTES:

1. DETAIL DESIGN MAY BE ALTERED TO SUIT VENDOR MANUFACTURING PROCEDURES SUBJECT TO CONVAIR/ GENERAL DYNAMICS APPROVAL
2. COMPLETED ASSEMBLY TO WITHSTAND A 45 PSIA TEST PRESSURE (INTERNAL AND EXTERNAL) WITH VACUUM JACKET OPERATING
3. MARK PART PER CONVAIR STD 0-70041. DO NOT USE IDENT PLATE. IDENTIFY PER 0-70042-20. MARKING SHALL INCLUDE VENDOR'S CODE IDENT Nº AND PART Nº; AND CONVAIR'S CODE IDENT Nº AND PART Nº.
4. SUGGESTED VENDORS:
   CRYOLAB 805 528 1593
   BOX 6008, LOS OSOS, CA. 93402
   CRYOGENIC ASSOCIATES 317 298 7333
   6565 KUFFMAN, INDIANAPOLIS, IND. 46268
5. LEAK TEST PER ASTM-E-498, METHOD A. NO DETECTABLE LEAKAGE ALLOWED
6. MATERIAL TO BE 304L STAINLESS STEEL
7. ENDS TO BE COVERED DURING TRANSPORTATION AND HANDLING
8. ALL WELDING TO BE DONE PER MIL-STD-278 BY WELDERS QUALIFIED PER MIL-STD-248 USING ER316L ELECTRODES.

9 INSTALL MLI ACCORDING TO MANUFACTURERS STANDARD APPLICATION FOR MINIMIZING HEAT LEAK

10 -1 IDENTICAL TO D11-38031-3

11 -2 IDENTICAL TO D11-38031-1

APPROVED TITLE I

REF AL BOCH LETTER DATED MARCH 19, 1982

PRELIMINARY

SPECIFICATION CONTROL DRAWING

☐ SEE SEPARATE PARTS LIST

SHEET NO.
REV LTR

SEE 0-70914 FOR ABBREVIATION, CODE AND SYMBOL REQUIREMENTS

SEE 0-70902 FOR STANDARD MANUFACTURING AND INSTALLATION REQUIREMENTS

UNLESS OTHERWISE SPECIFIED ALL MACHINED SURFACES 125

UNLESS OTHERWISE SPECIFIED DIMENSIONS ARE IN INCHES

TOLERANCES .X ±.1 .XX ± .03 .XXX ± .010 ANGULAR PER 070902

MATL

PROD. ENGR

CHECK
STRESS
GR ENGR
DESIGN
DRAWN SY.VK 9-9-81
CONTRACT NO.

GENERAL DYNAMICS
CONVAIR DIVISION
SAN DIEGO, CALIFORNIA

LIQUID HELIUM TUBE ~
EBT-P PROTOTYPE

SIZE D FSCM NO. 14170 DWG NO. 11-38031

SCALE FULL SHEET 1 OF 1

SEC. CLASS TYPE LEVEL CONT GROUP DISTR REPRO PACKAGE NO. REL

FORM 7316

A-59/A-60

DWG NO.	SH	REV
11-38032	1	-

REVISIONS

ZONE	REV	DESCRIPTION	DATE	APPROVED

NOTES:

1. ELECTRICAL LEADS ARE COLOR CODED AS FOLLOWS: RED: I+; BLACK: I-; BLUE: V+; YELLOW: V-
2. DO NOT BEND LEADS WHEN COLD
3. DO NOT OPERATE IN VACUUM. OK AT 1 K WITH LIQUID HELIUM PRESENT
4. ICE FORMATIONS WILL CAUSE ERRATIC OPERATION (FROZEN WATER OR GAS).
5. APPLY PER 0-79129-17.
6. DURING ROOM TEMPERATURE TESTING LIMIT CURRENT TO 1 MILLIAMPERE.
7. LEVEL SENSOR HAS A NOMINAL RESISTANCE OF 4.5 OHMS/CM (ACTIVE LENGTH) WHEN IN NORMAL STATE AND MAINTAINED JUST ABOVE THE TRANSITION TEMP OF ~ 10 K
8. IDENTIFY PER 0-70042-20. LOCATION OPTIONAL
9. -1 IDENTICAL TO D11-38032-1

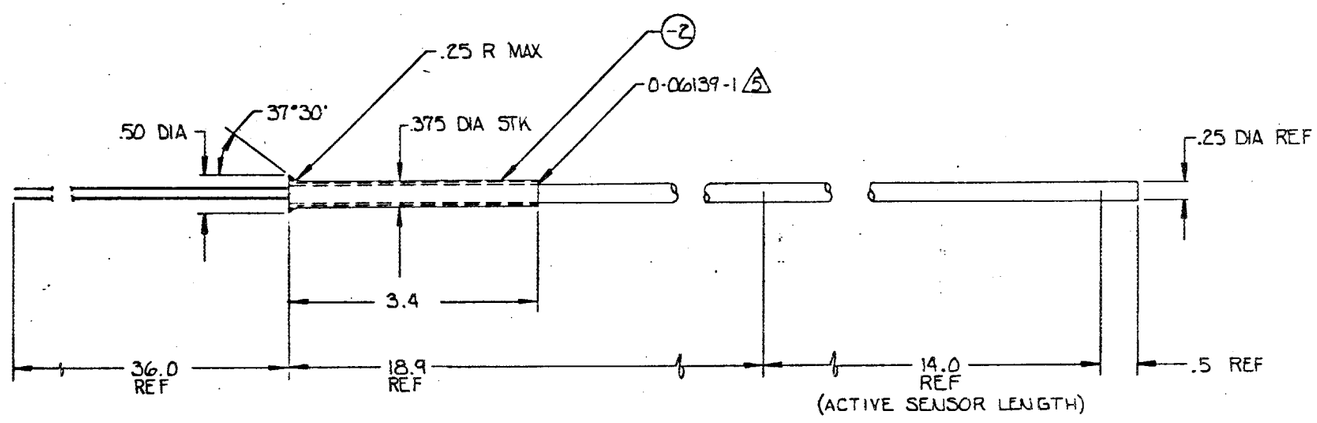

-1

PRELIMINARY

APPROVED TITLE I

REF AL BOCH LETTER DATED MARCH 19, 1982

☐ SEE SEPARATE PARTS LIST

SHEET NO.
REV LTR

SEE 0-70914 FOR ABBREVIATION, CODE AND SYMBOL REQUIREMENTS

SEE 0-70902 FOR STANDARD MANUFACTURING AND INSTALLATION REQUIREMENTS

UNLESS OTHERWISE SPECIFIED ALL MACHINED SURFACES 125

UNLESS OTHERWISE SPECIFIED DIMENSIONS ARE IN INCHES
TOLERANCES
.X ±.1 .XX ±.03 .XXX ±.010
ANGULAR PER 070902

MATL
PROD. ENGR

CHECK		
STRESS		
GR ENGR		
DESIGN		
DRAWN	PGVK	9-9-81
CONTRACT NO.		

GENERAL DYNAMICS
CONVAIR DIVISION
SAN DIEGO, CALIFORNIA

LHe LEVEL SENSOR ~
EBT-P PROTOTYPE

SIZE D | FSCM NO. 14170 | DWG NO. 11-38032

SCALE FULL | SHEET 1 OF 1

SEC. CLASS | TYPE | LEVEL | CONT | GROUP | DISTR | REPRO | PACKAGE NO. | REL

FORM 7516

A-61/A-62

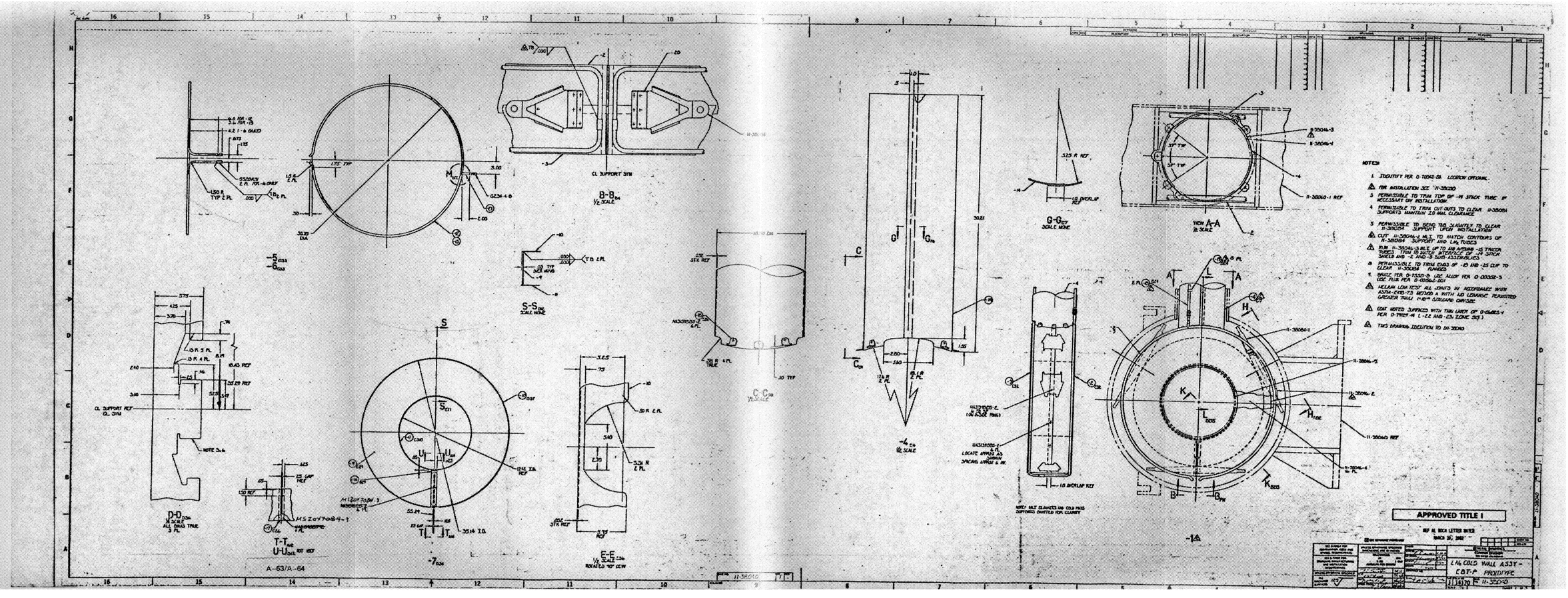
B-B
1/2 SCALE
CL SUPPORT STM
S-S
SCALE NONE
C-C
1/2 SCALE
G-G
SCALE NONE
VIEW A-A
1/2 SCALE
D-D
1/2 SCALE
ALL DIMS TRUE
T-T
U-U
E-E
1/2 SCALE
ROTATED 90° CCW
-4
1/2 SCALE
-7
-1
NOTES
1. IDENTIFY PER 0-70242-DA. LOCATION OPTIONAL.
FOR INSTALLATION SEE 11-38020
3. PERMISSIBLE TO TRIM TOP OF -14 STACK TUBE IF NECESSARY ON INSTALLATION.
4. PERMISSIBLE TO TRIM CUT-OUTS TO CLEAR 11-38084 SUPPORTS TO MAINTAIN 1.0 MIN CLEARANCE.
5. PERMISSIBLE TO BEND TAB SLIGHTLY TO CLEAR 11-38054 SUPPORT UPON INSTALLATION.
CUT 11-38044-3 MLT TO MATCH CONTOURS OF 11-38054 SUPPORT AND LAN FITTINGS.
RUN 11-38046-2 MLT UP TO AIR AROUND -15 TRACER TUBES. TRIM TO MATCH CONTOURS OF -14 STACK SHIELD AND -2 AND -3 SUB ASSEMBLIES.
PERMISSIBLE TO TRIM ENDS OF -15 AND -25 CLIP TO CLEAR 11-38084 FLANGES.
FORGE PER 0-7550-9. LRC ALLOY PER 0-00332-3 USE TILE PER 0-60342-101.
VACUUM LEAK TEST ALL JOINTS IN ACCORDANCE WITH ASTM-E498-73 METHOD A WITH NO LEAKAGE PERMITTED GREATER THAN 1 X 10⁻⁸ STD CC/SEC HE/SEC.
COAT NOTED SURFACES WITH THIN LAYER OF 0-GLASS-1 PER 0-TRSP 14 (-22 AND -24 ZONE 20)
THIS DRAWING IDENTICAL TO 11-38040
APPROVED TITLE I
REF AL BOCK LETTER DATED MARCH 20, 1962
LH2 COLD WALL ASSY - CBT-P PROTOTYPE
11-3500
A-63/A-64

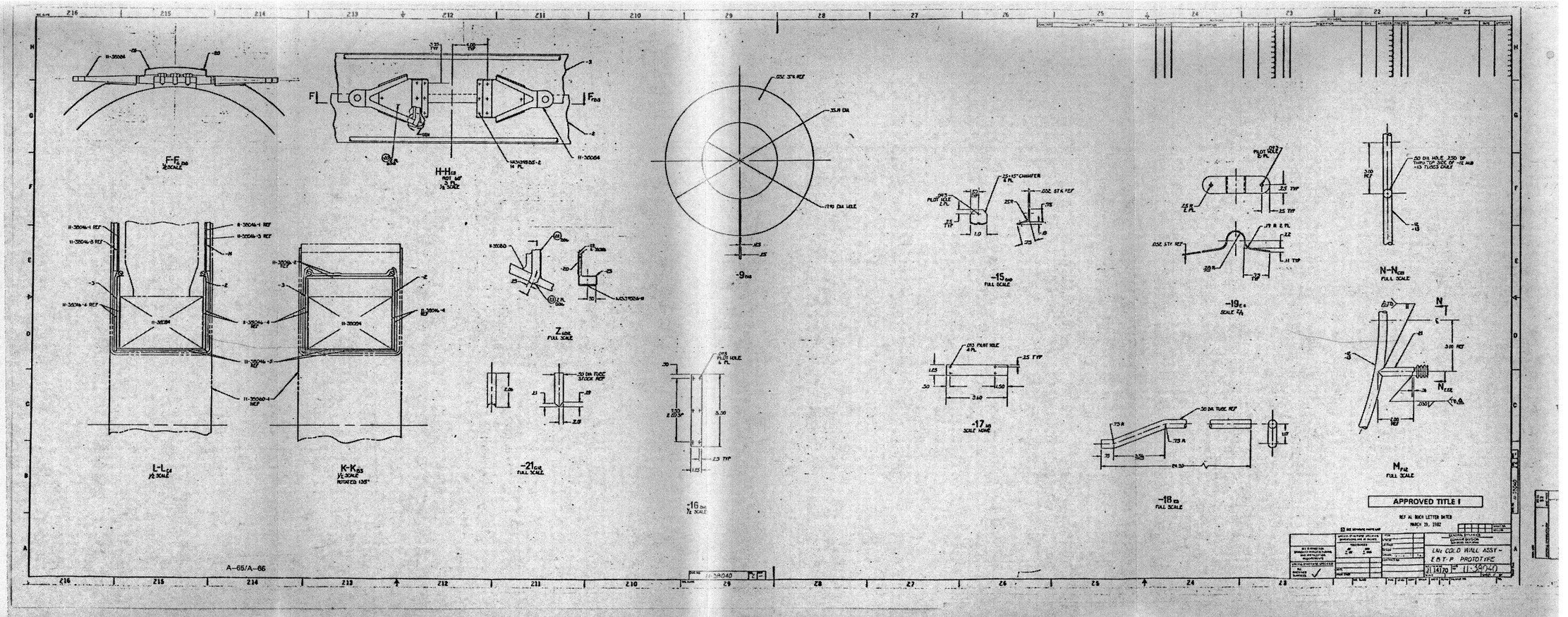
F-F
H-H
L-L
K-K
Z
-9
-15
-19
N-N
-21
-16
-17
-18
M
APPROVED TITLE I
LM: COLD WALL ASSY - E.O.T.P. PROTOTYPE
A-65/A-66

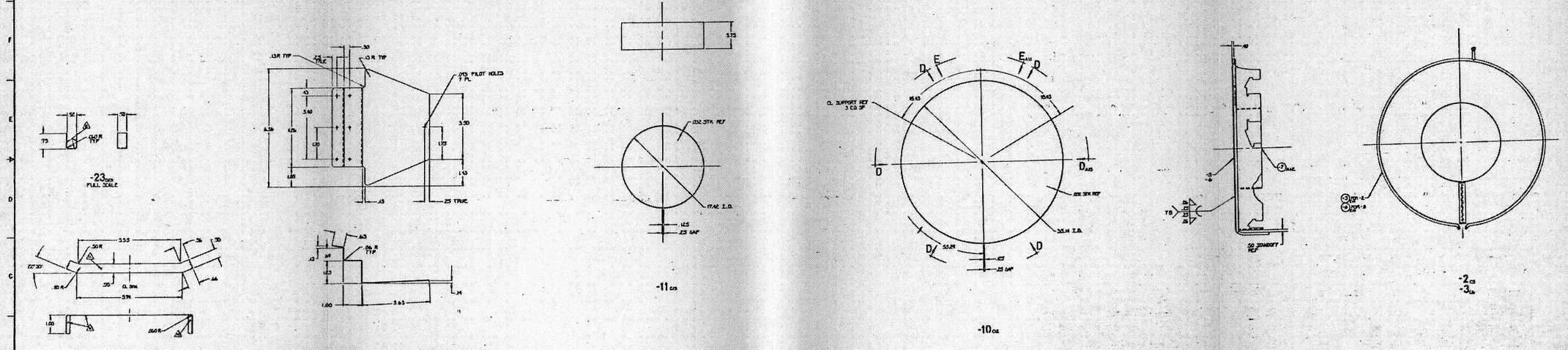
-23 DWG
FULL SCALE
-22 CCD
FULL SCALE
-20 DCSE
FULL SCALE
-11 CCD
-10 CCE
-2 CD
-3 CE
APPROVED TITLE I
REF AL BUCK LETTER DATED
MARCH 15, 1962
LUX COLD WALL ASSY
EOT-P PROTOTYPE
11-35040

A-67/A-68

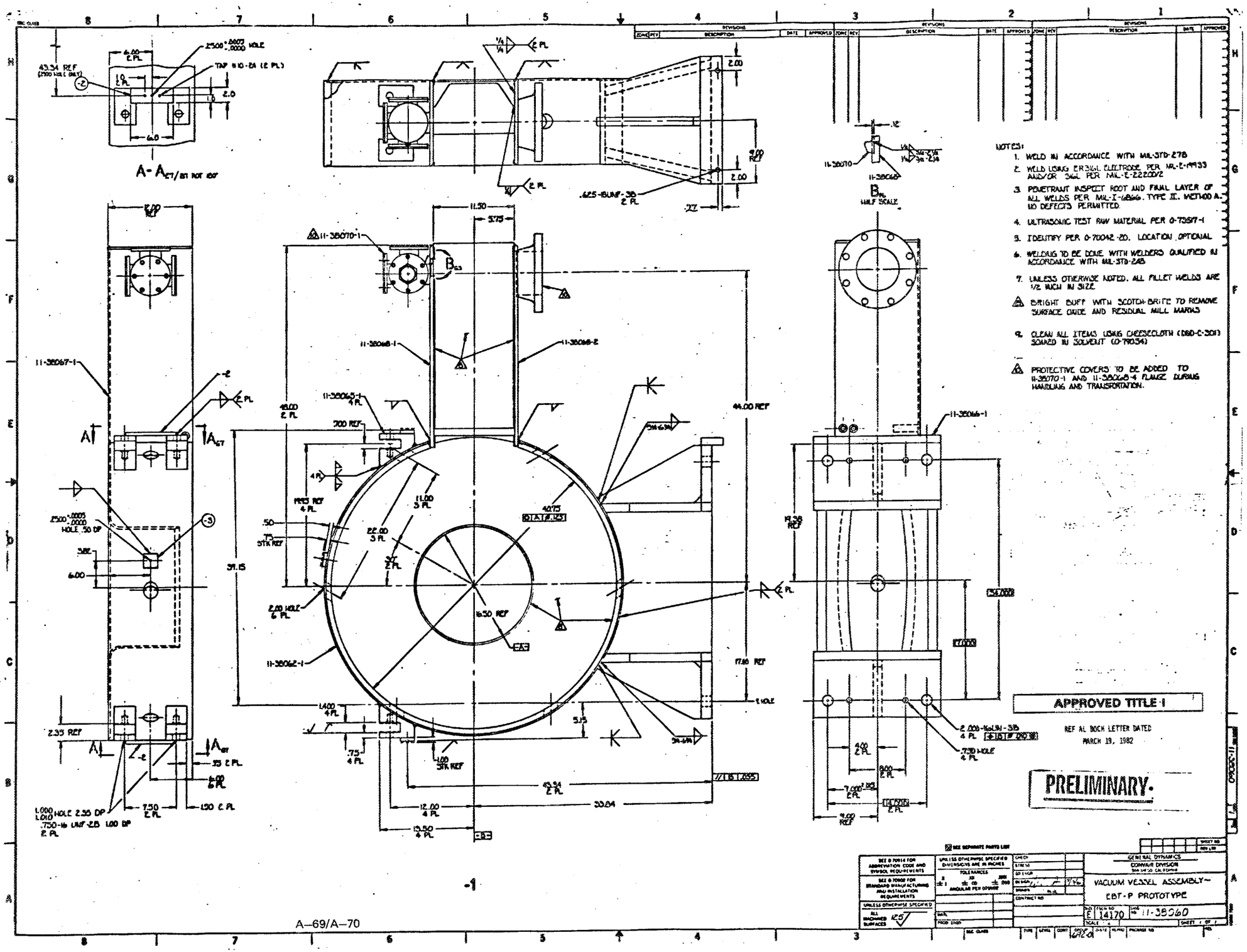
A-A
B
NOTES:
1. WELD IN ACCORDANCE WITH MIL-STD-278
2. WELD USING ER316L ELECTRODE PER MIL-E-19933 AND/OR 316L PER MIL-E-22200/2
3. PENETRANT INSPECT ROOT AND FINAL LAYER OF ALL WELDS PER MIL-I-6866, TYPE II, METHOD A. NO DEFECTS PERMITTED.
4. ULTRASONIC TEST RAW MATERIAL PER 0-73597-1
5. IDENTIFY PER 0-70042-20. LOCATION OPTIONAL
6. WELDING TO BE DONE WITH WELDERS QUALIFIED IN ACCORDANCE WITH MIL-STD-248
7. UNLESS OTHERWISE NOTED, ALL FILLET WELDS ARE 1/2 INCH IN SIZE
BRIGHT BUFF WITH SCOTCH-BRITE TO REMOVE SURFACE OXIDE AND RESIDUAL MILL MARKS
CLEAN ALL ITEMS USING CHEESECLOTH (DDD-C-301) SOAKED IN SOLVENT (O-790341)
PROTECTIVE COVERS TO BE ADDED TO 11-38070-1 AND 11-38068-4 FLANGE DURING HANDLING AND TRANSPORTATION.
APPROVED TITLE I
REF AL DOCK LETTER DATED MARCH 19, 1982
PRELIMINARY
GENERAL DYNAMICS
CONVAIR DIVISION
VACUUM VESSEL ASSEMBLY-
EBT-P PROTOTYPE
E 14170
11-38060
-1

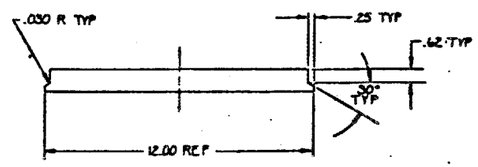

A-A
HALF SCALE

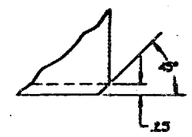

B-B
FULL SCALE
4 PL

NOTES:
1. ULTRASONIC TEST RAW MATERIAL PER 0-75517-1
2. IDENTIFY PER 0-70042-20 LOCATION OPTIONAL
3. MAT'L: 1.00-12.0-1500 304L SST; ASTM-A-240

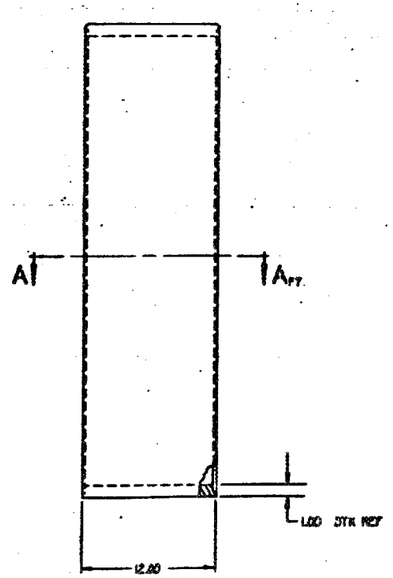

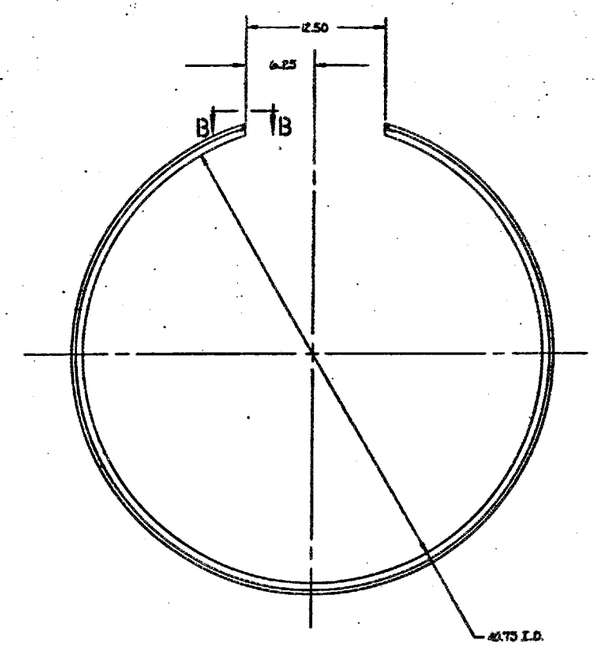

APPROVED TITLE I

REF AL BOCH LETTER DATED
MARCH 19, 1982

PRELIMINARY

-1

SEE SEPARATE PARTS LIST

SEE D 70914 FOR ABBREVIATION CODE AND SYMBOL REQUIREMENTS
SEE D 70107 FOR STANDARD MANUFACTURING AND INSTALLATION REQUIREMENTS
UNLESS OTHERWISE SPECIFIED
ALL MACHINED SURFACES 125

UNLESS OTHERWISE SPECIFIED DIMENSIONS ARE IN INCHES
TOLERANCES
.X ± .1 .XX ± .03 .XXX ± .010
ANGULAR PER D70502

CHECK
STRESS
QA SHOP
DESIGN
DRAWN
CONTRACT NO

GENERAL DYNAMICS
CONVAIR DIVISION
SAN DIEGO, CALIFORNIA

OUTER RING / VACUUM VESSEL ~ EBT-P PROTOTYPE

SIZE E | STOCK NO 14170 | CODE IDENT NO 11-38062
SCALE 1/4 | SHEET 1 OF 1

A–71/A–72

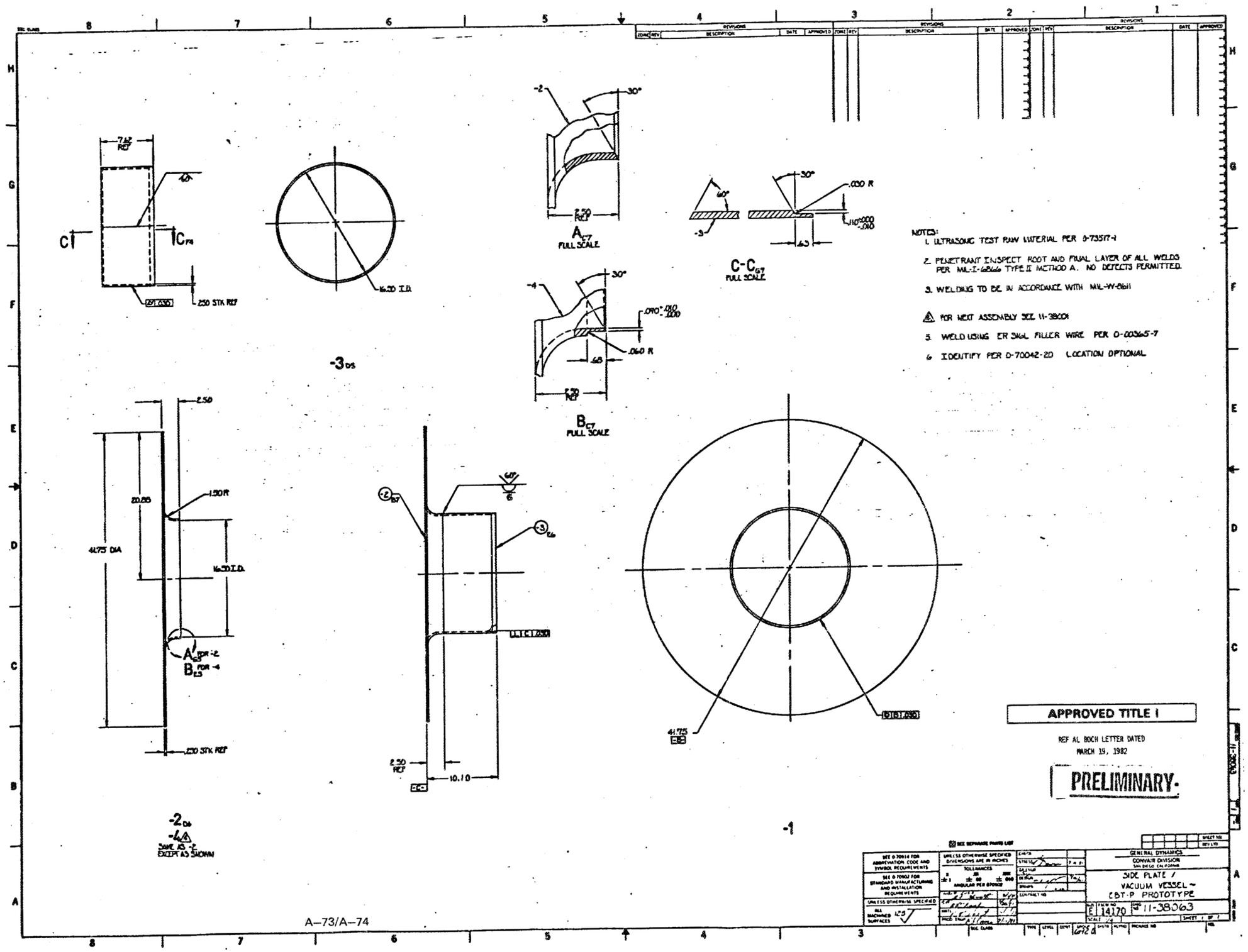
REVISIONS
ZONE REV DESCRIPTION DATE APPROVED
7.62 REF
C
C
.250 STK REF
16.20 I.D.
-3 DS
A C7
FULL SCALE
B C7
FULL SCALE
C-C C7
FULL SCALE
.030 R
.060 R
2.50
1.50 R
20.85
41.75 DIA
16.50 I.D.
A C3 FOR -2
B C3 FOR -4
.250 STK REF
10.10
41.75
-2 DS
-4
SAME AS -2
EXCEPT AS SHOWN
-1
NOTES:
1. ULTRASONIC TEST RAW MATERIAL PER 0-73517-1
2. PENETRANT INSPECT ROOT AND FINAL LAYER OF ALL WELDS PER MIL-I-6866 TYPE II METHOD A. NO DEFECTS PERMITTED.
3. WELDING TO BE IN ACCORDANCE WITH MIL-W-8611
4. FOR NEXT ASSEMBLY SEE 11-38001
5. WELD USING ER 5356 FILLER WIRE PER 0-00365-7
6. IDENTIFY PER 0-70042-20 LOCATION OPTIONAL
APPROVED TITLE I
REF AL BOCH LETTER DATED
MARCH 19, 1982
PRELIMINARY
GENERAL DYNAMICS
CONVAIR DIVISION
SAN DIEGO, CALIFORNIA
SIDE PLATE /
VACUUM VESSEL -
CBT-P PROTOTYPE
E 14170
11-38063
SCALE 1/4
SHEET 1 OF 1

A–73/A–74

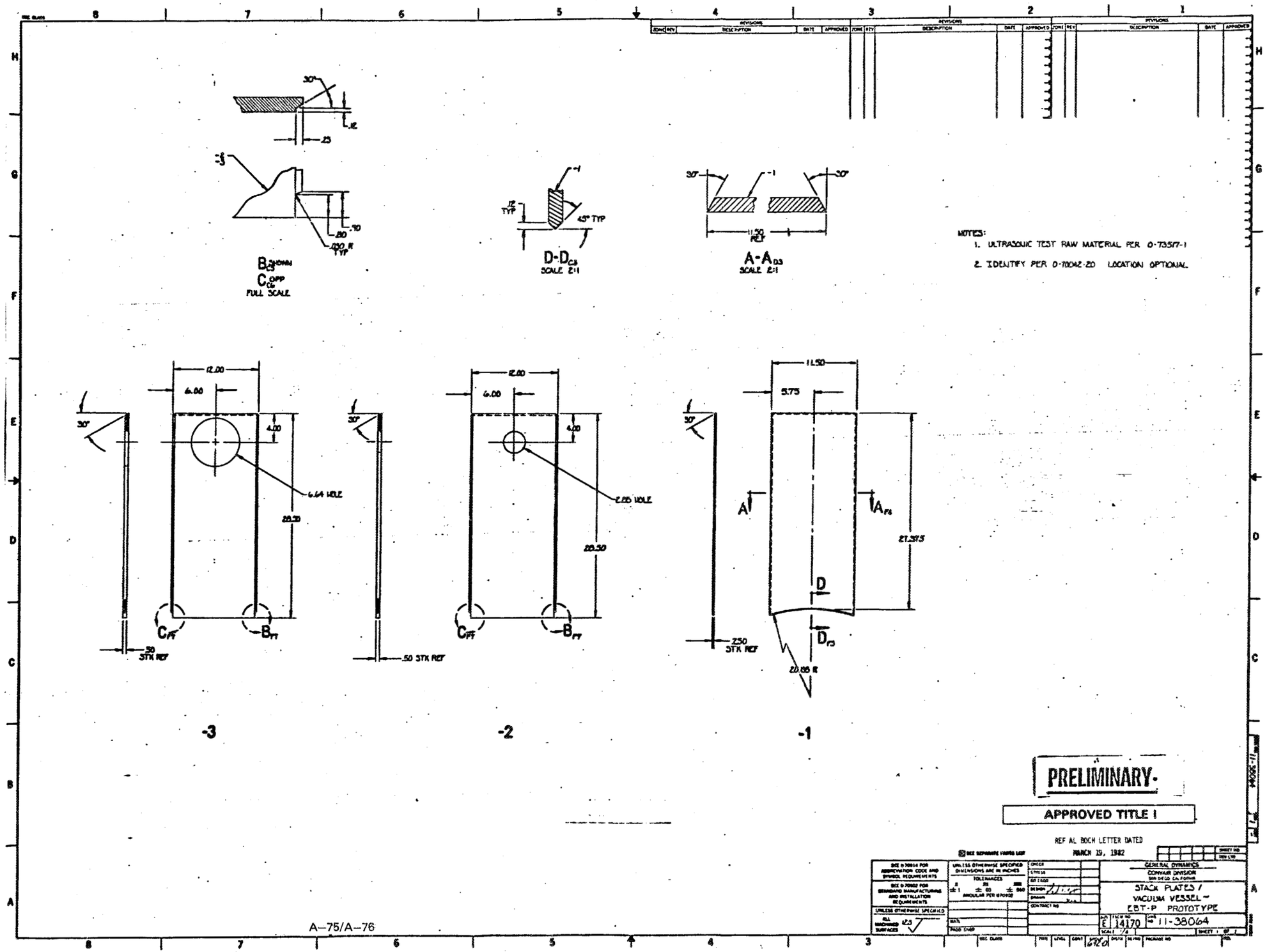
30°
.12
.25
-3
.70
.80
.030 R TYP
B-3 NOMM
C-3 OPP
FULL SCALE
-1
.12 TYP
45° TYP
D-D-3
SCALE 2:1
30°
-1
30°
11.50 REF
A-A-3
SCALE 2:1
NOTES:
1. ULTRASONIC TEST RAW MATERIAL PER D-73577-1
2. IDENTIFY PER D-70042-20 LOCATION OPTIONAL
12.00
6.00
4.00
30°
6.64 HOLE
28.30
C-FF
B-FT
.50 STK REF
12.00
6.00
4.00
2.05 HOLE
28.30
C-FF
B-FT
.50 STK REF
11.50
5.75
30°
A
A-FS
27.375
D
D-FS
2.50 STK REF
20.05 R
-3
-2
-1
PRELIMINARY
APPROVED TITLE I
REF AL BOCH LETTER DATED
MARCH 19, 1982
GENERAL DYNAMICS
CONVAIR DIVISION
SAN DIEGO, CALIFORNIA
STACK PLATES /
VACUUM VESSEL
EBT-P PROTOTYPE
E 14170
11-38064
A-75/A-76

11-38065

REVISIONS				
ZONE	REV	DESCRIPTION	DATE	APPROVED

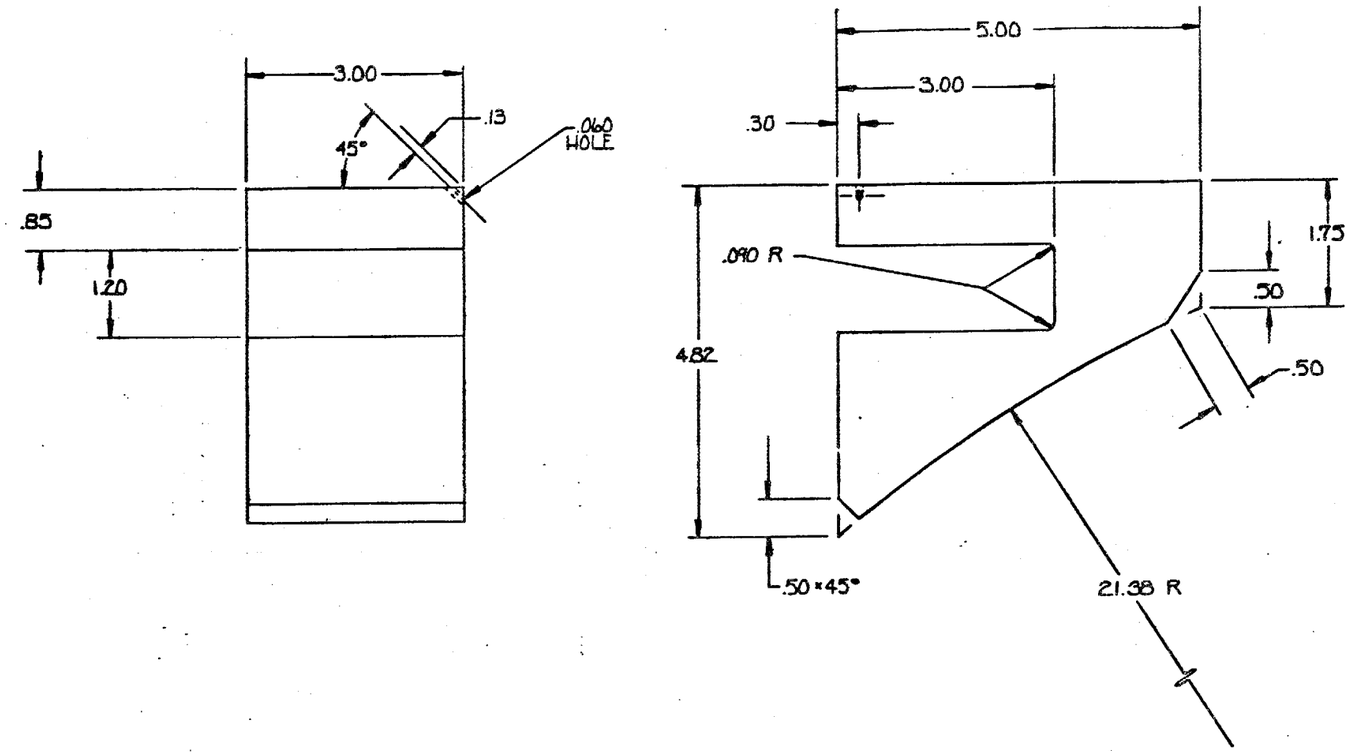

NOTES:

1. ULTRASONIC TEST PER 0-73517-1
2. IDENTIFY PER 0-70042-20 LOCATION OPTIONAL
3. MAT'L: 3.0 × 5.0 × 5.0 304L SST; ASTM-A-240

PRELIMINARY.

-1

APPROVED TITLE I

REF AL BOCH LETTER DATED MARCH 19, 1982

☐ SEE SEPARATE PARTS LIST

SHEET NO.
REV LTR

SEE 0-70914 FOR ABBREVIATION, CODE AND SYMBOL REQUIREMENTS

SEE 0-70902 FOR STANDARD MANUFACTURING AND INSTALLATION REQUIREMENTS

UNLESS OTHERWISE SPECIFIED ALL MACHINED SURFACES 125

UNLESS OTHERWISE SPECIFIED DIMENSIONS ARE IN INCHES

TOLERANCES

X	XX	XXX
±.1	± .03	± .010

ANGULAR PER 070902

MATL.

PROD. ENGR

CHECK
STRESS
GR ENGR
DESIGN 5/1/82
DRAWN
CONTRACT NO.

GENERAL DYNAMICS
CONVAIR DIVISION
SAN DIEGO, CALIFORNIA

STRUT FITTING / VACUUM VESSEL ~ EBT-P PROTOTYPE

SIZE D | FSCM NO. 14170 | DWG NO. 11-38065

SCALE FULL | SHEET 1 OF 1

SEC. CLASS | TYPE | LEVEL | CONT | GROUP 092-0 | DISTR | REPRO | PACKAGE NO. | REL

FORM 7516

A–77/A–78

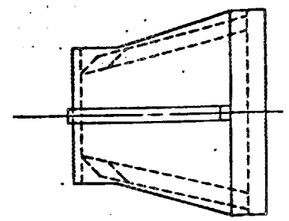

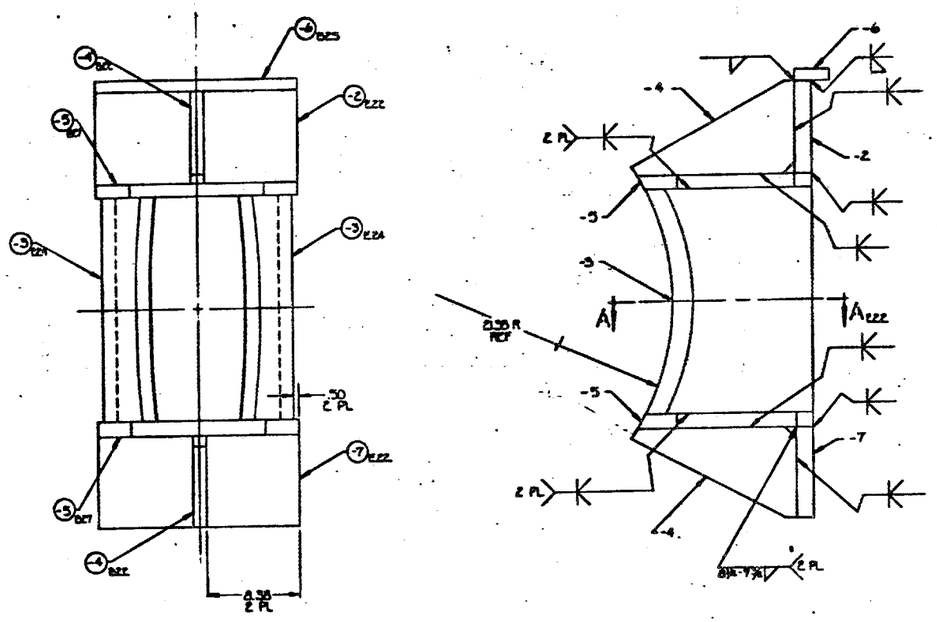

-1

NOTES:

1. ULTRASONIC TEST RAW MATERIAL PER 0-73517-1
2. PENETRANT INSPECT ROOT AND FINAL LAYER OF ALL WELDS PER MIL-I-6866, TYPE II, METHOD A NO DEFECTS PERMITTED.
3. WELDING TO BE DONE BY WELDERS QUALIFIED IN ACCORDANCE WITH MIL-STD-248
4. WELD PER MIL-STD-278
5. WELD USING ER316L ELECTRODE PER MIL-E-19933 AND/OR 316L PER MIL-E-22200/2.
6. IDENTIFY PER 0-70042-20 LOCATION OPTIONAL
7. ⚠ DIMENSIONS BEFORE MACHINING OF 45° WELD PREPS

APPROVED TITLE I

REF AL BOCH LETTER DATED
MARCH 19, 1982

PRELIMINARY

SEE SEPARATE PARTS LIST

SEE D 70914 FOR ABBREVIATION, CODE AND SYMBOL REQUIREMENTS	UNLESS OTHERWISE SPECIFIED DIMENSIONS ARE IN INCHES TOLE RANCES .X ±.1 .XX ±.03 .XXX ±.010 ANGULAR PER D70902	CHECK	GENERAL DYNAMICS CONVAIR DIVISION SAN DIEGO, CALIFORNIA
SEE D 70902 FOR STANDARD MANUFACTURING AND INSTALLATION REQUIREMENTS		STRESS	
		GR ENGR	
UNLESS OTHERWISE SPECIFIED ALL MACHINED SURFACES 25		DESIGN	SUPPORT ASSEMBLY / VACUUM VESSEL ~ EBT-P PROTOTYPE
		DRAWN	
		CONTRACT NO	
	MATL		SIZE E / FSCM NO 14170 / DWG NO 11-230066
	FINISH ENGR		SCALE / SHEET / OF

A–79/A–80

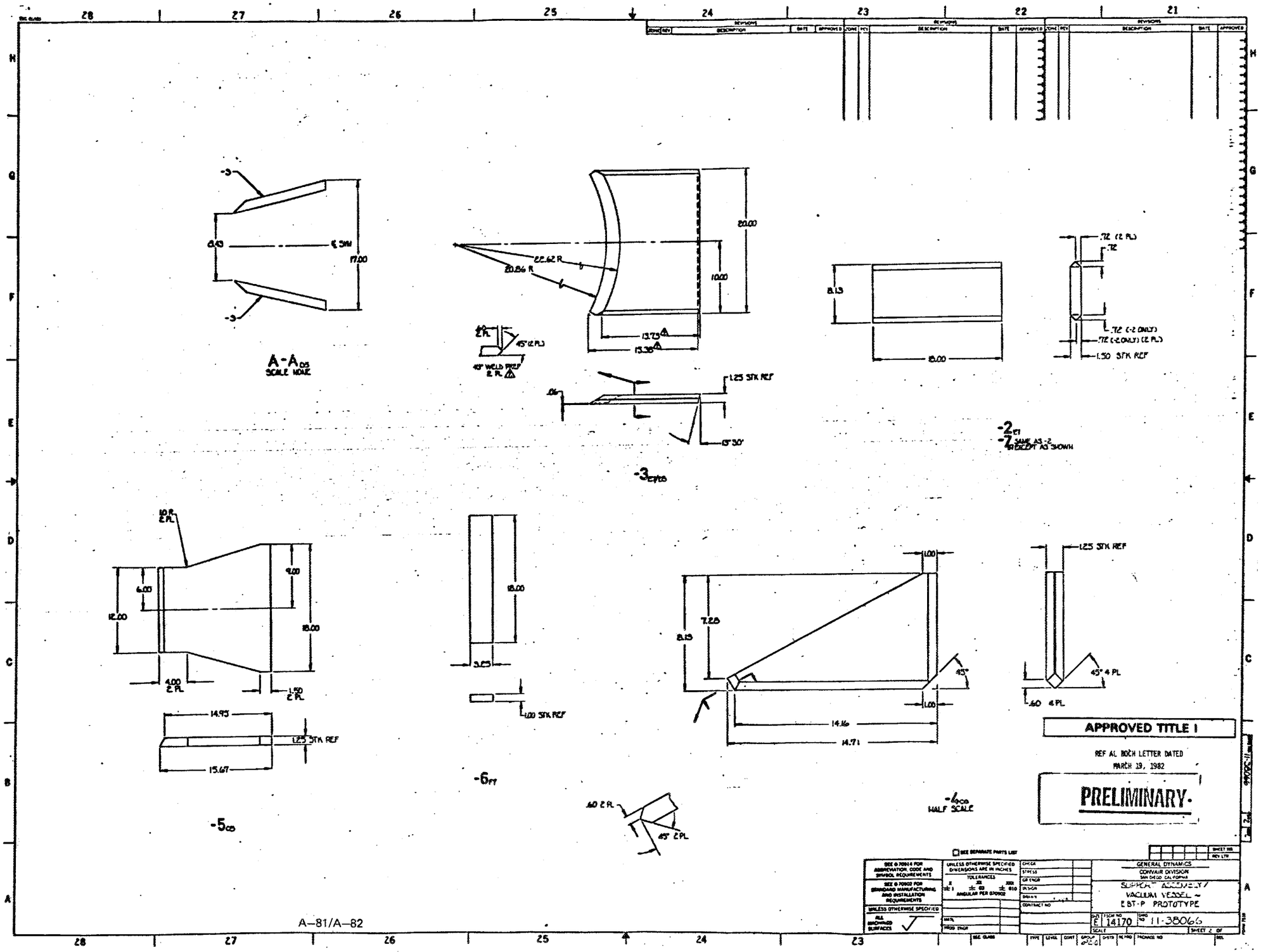
A-A
SCALE NONE
-3
17.00
20.00
10.00
22.62 R
20.86 R
13.73
15.36
45° (2 PL)
1.25 STK REF
15° 30'
-3
8.13
15.00
.72 (2 PL)
.72
.72 (-2 ONLY)
.72 (-2 ONLY) (2 PL)
1.50 STK REF
-2
-7 SAME AS -2 EXCEPT AS SHOWN
10 R 2 PL
6.00
12.00
9.00
15.00
4.00 2 PL
1.50 2 PL
14.95
1.25 STK REF
15.67
-5
15.00
3.25
1.00 STK REF
-6
1.00
7.25
8.15
45°
14.36
14.71
1.25 STK REF
45° 4 PL
.60 4 PL
-4
HALF SCALE
.60 2 PL
45° 2 PL
APPROVED TITLE I
REF AL BOCH LETTER DATED
MARCH 19, 1982
PRELIMINARY
GENERAL DYNAMICS
CONVAIR DIVISION
SAN DIEGO, CALIFORNIA
SUPPORT ASSEMBLY
VACUUM VESSEL -
EBT-P PROTOTYPE
E 14170
11-38066
SHEET 2 OF
A-81/A-82

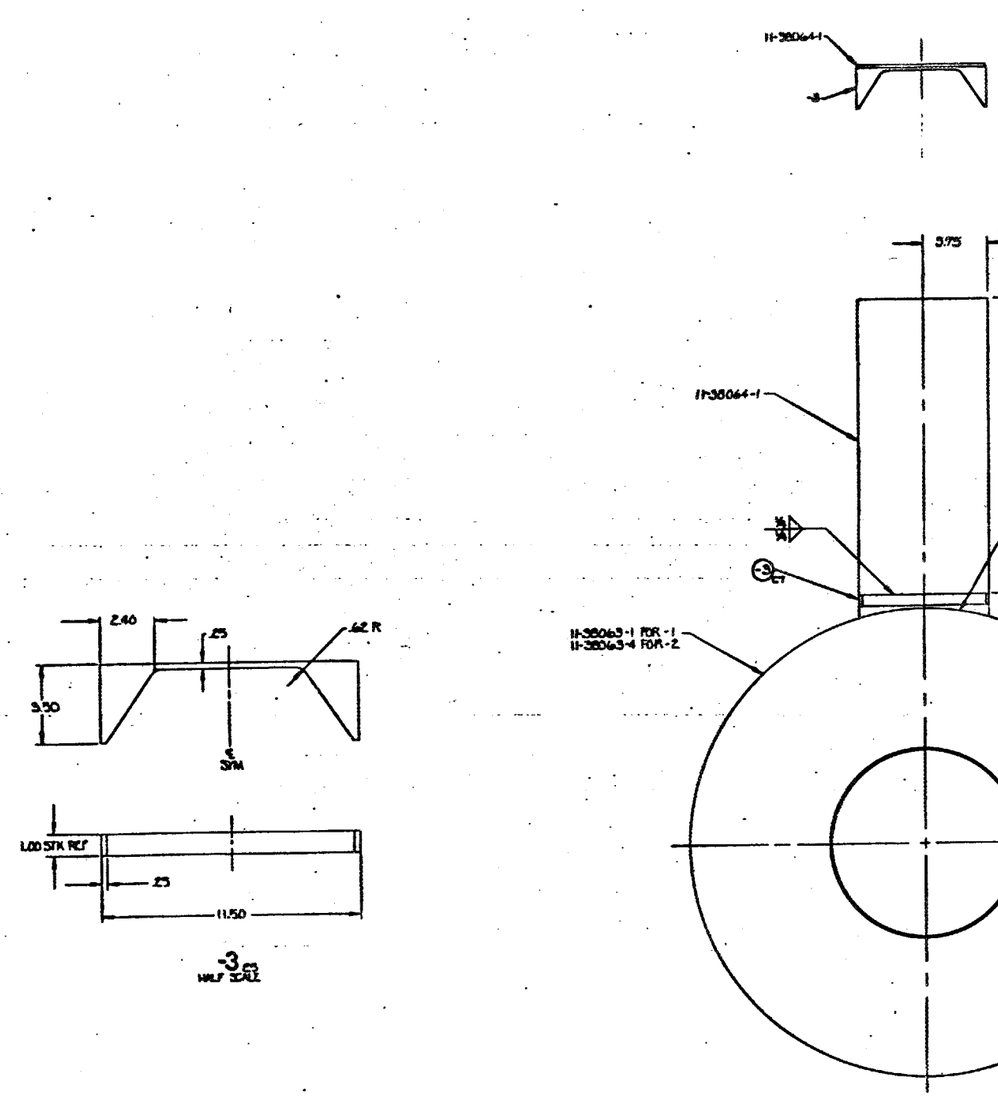

NOTES:

1. PENETRANT INSPECT ROOT AND FINAL LAYER OF ALL WELDS PER MIL-I-6866, TYPE II, METHOD A. NO DEFECTS PERMITTED
2. WELDING TO BE DONE BY WELDERS QUALIFIED IN ACCORDANCE WITH MIL-STD-248
3. WELD PER MIL-STD-278
4. WELD USING ER 316L ELECTRODE PER MIL-E-19933 AND/OR 316L PER MIL-E-22200/2
5. IDENTIFY PER 0-70042-20. LOCATION OPTIONAL
6. ULTRASONIC TEST RAW MATERIAL PER 0-73517-1

PRELIMINARY

APPROVED TITLE I

REF AL BOCH LETTER DATED MARCH 19, 1982

SEE SEPARATE PARTS LIST

SEE 0-70014 FOR ABBREVIATION CODE AND SYMBOL REQUIREMENTS

SEE 0-70002 FOR STANDARD MANUFACTURING AND INSTALLATION REQUIREMENTS

UNLESS OTHERWISE SPECIFIED

ALL MACHINED SURFACES ✓

UNLESS OTHERWISE SPECIFIED DIMENSIONS ARE IN INCHES

TOLERANCES

ANGULAR PER 0-70002

GENERAL DYNAMICS
CONVAIR DIVISION
SAN DIEGO CALIFORNIA

SIDE PLATE ASSY ~
EBT-P PROTOTYPE

SIZE E | FSCM NO 14170 | DWG NO 11-38067

SCALE 1/2 | SHEET 1 OF 1

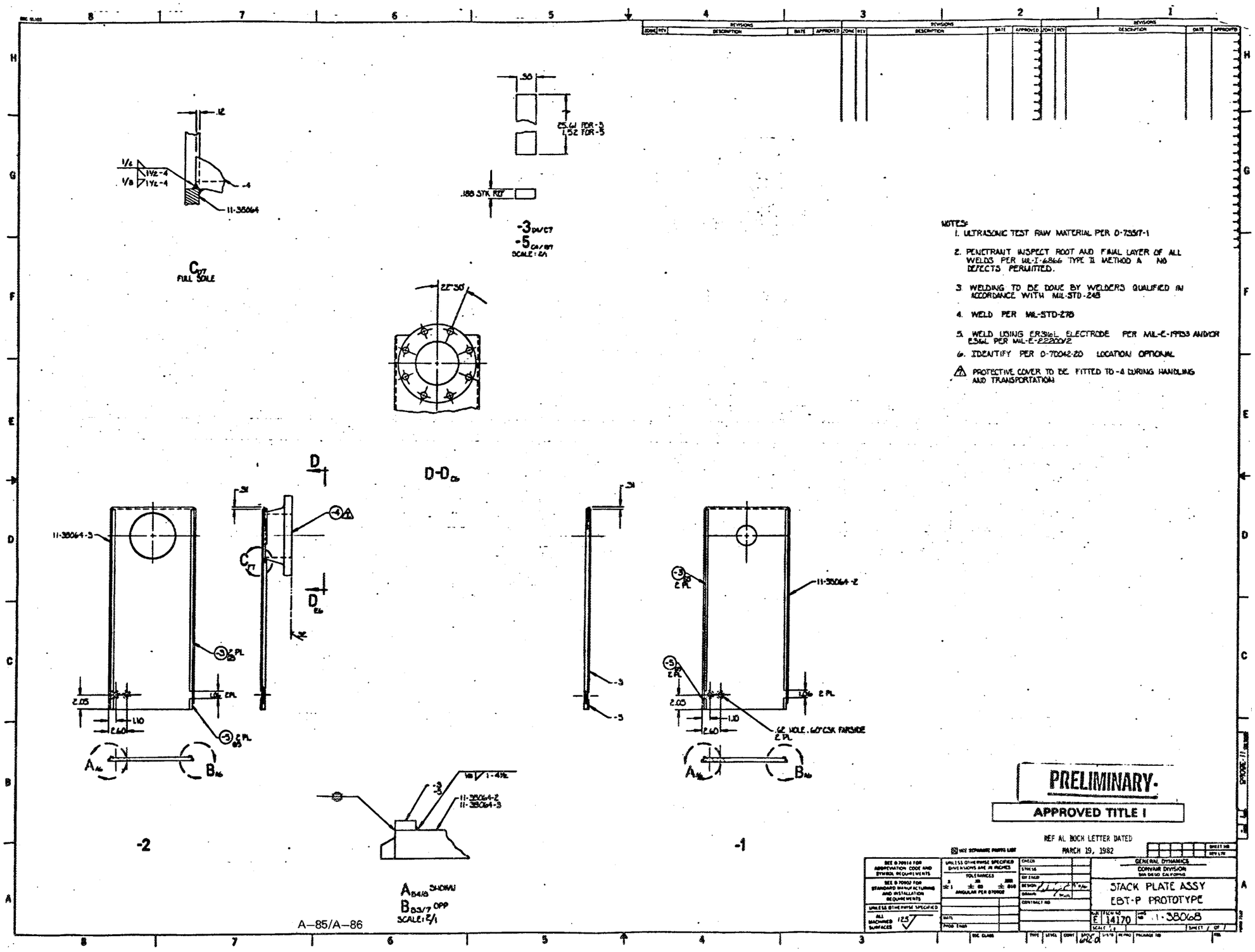
.12
1/4
1 1/2-4
1/8
1 1/2-4
-4
11-38064
C77
FULL SCALE
.50
25.GW FOR-3
1.52 FOR-5
.188 STK RDT
-3 DW/C7
-5 CA/B7
SCALE: 2/1
22°30'
D-D26
D
D26
11-38064-3
-4
C77
-3 2 PL
1.06 2 PL
2.05
1.10
2.60
A46
B46
-3
-5
11-38064-2
2 PL
62 HOLE, 60° CSK FARSIDE
2 PL
-2
-1
11-38064-2
11-38064-3
A54/8 SHOWN
B53/7 OPP
SCALE: 2/1
NOTES:
1. ULTRASONIC TEST RAW MATERIAL PER D-73517-1
2. PENETRANT INSPECT ROOT AND FINAL LAYER OF ALL WELDS PER MIL-I-6866 TYPE II METHOD A NO DEFECTS PERMITTED.
3. WELDING TO BE DONE BY WELDERS QUALIFIED IN ACCORDANCE WITH MIL-STD-248
4. WELD PER MIL-STD-278
5. WELD USING ER316L ELECTRODE PER MIL-E-19153 AND/OR E316L PER MIL-E-22200/2
6. IDENTIFY PER D-70042-20 LOCATION OPTIONAL
7. PROTECTIVE COVER TO BE FITTED TO -4 DURING HANDLING AND TRANSPORTATION
PRELIMINARY
APPROVED TITLE I
REF AL BOCH LETTER DATED
MARCH 19, 1982
GENERAL DYNAMICS
CONVAIR DIVISION
SAN DIEGO CALIFORNIA
STACK PLATE ASSY
EBT-P PROTOTYPE
E 14170
11-38068
A-85/A-86

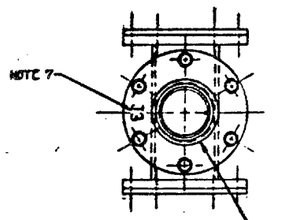

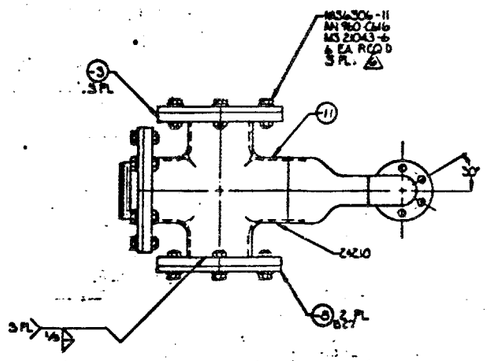

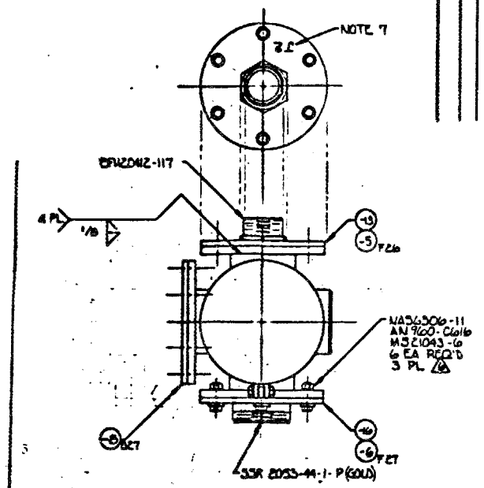

NOTES:

1. IDENTIFY PER 0-70042-20
2. CLEAN USING CHEESECLOTH SOAKED IN FREON TF
3. ULTRASONIC INSPECT RAW MATERIAL PER MIL-I-8950 B CLASS AAA
4. WELD USING ER 316L ELECTRODE PER MIL-E-19933 AND/OR E316L PER MIL-E-22200/2.
5. PENETRANT INSPECT ALL WELDS PER MIL-I-6866. TYPE II. METHOD A NO DEFECTS ALLOWED
6. INSTALL FASTENERS PER 0-70054 USING TORQUE LIMITS PER 0-70058
7. STENCIL PER 0-70042-20 USING 0-79055-6 BLACK EPOXY INK WITH 1/2 INCH HIGH LETTERS AND LOCATION APPROX AS SHOWN STENCIL ON ASSEMBLY
8. LIGHTLY COAT O-RING WITH VACUUM GREASE 0-00021-1
9. WELDING TO BE DONE WITH WELDERS QUALIFIED IN ACCORDANCE WITH MIL-STD-248 OR ASME SECTION IX AND FABRICATE IN ACCORDANCE WITH ASME CODE SECTION VIII DIV I PART UW
10. HELIUM LEAK TEST ALL WELDS IN ACCORDANCE WITH ASTM E 498-73 METHOD A NO DETECTABLE LEAKAGE PERMITTED
11. HELIUM LEAK TEST PER ASTM E498-73 METHOD A. MAX LEAK PERMITTED: 1×10^{-6} SCC He/SEC

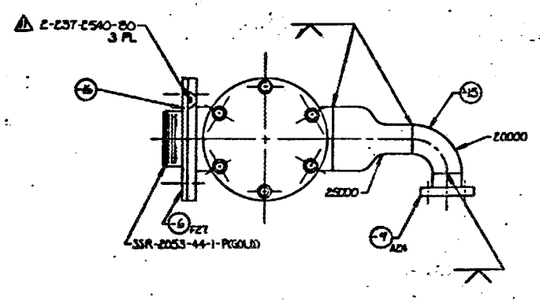

-2

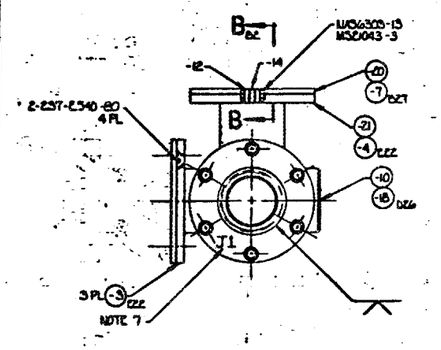

-1

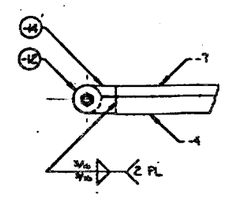

B-B
FULL SCALE

APPROVED TITLE I

PRELIMINARY

REF AL BOCH LETTER DATED
MARCH 19, 1982

SEE SEPARATE PARTS LIST

SEE 0-70014 FOR ABBREVIATION CODE AND SYMBOL REQUIREMENTS

SEE 0-70002 FOR STANDARD MANUFACTURING AND INSTALLATION REQUIREMENTS

UNLESS OTHERWISE SPECIFIED ALL MACHINED SURFACES ✓

UNLESS OTHERWISE SPECIFIED DIMENSIONS ARE IN INCHES
TOLERANCES
.XX ±.03 .XXX ±.010
ANGULAR PER 0-70002

CHECK
STRESS
GR ENGR
DESIGN
DRAWN
CONTRACT NO
SCALE
MATL
PROD ENGR

GENERAL DYNAMICS
CONVAIR DIVISION
SAN DIEGO, CALIFORNIA

OUTLET ASSEMBLY ~
EBT-P PROTOTYPE

SIZE E | FSCM NO 14170 | DWG NO 11-38070
SCALE | SHEET 1 OF 2

A-87/A-88

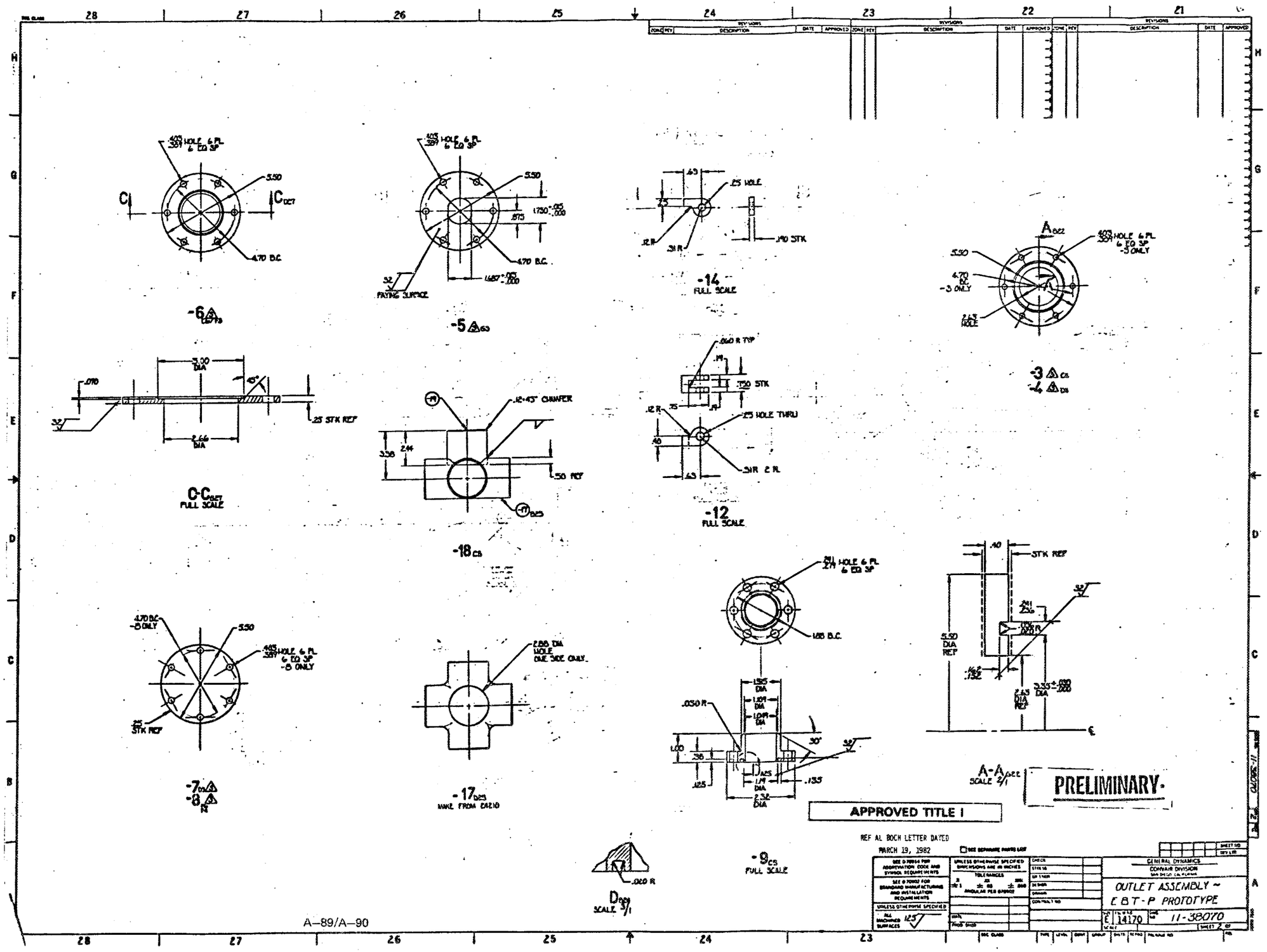
-6
-5
-14
FULL SCALE
-3
-4
C-C
FULL SCALE
-18
-12
FULL SCALE
-7
-8
-17
MAKE FROM 6Al4V
-9
FULL SCALE
A-A
SCALE 2/1
PRELIMINARY
APPROVED TITLE I
REF AL BOCH LETTER DATED
MARCH 19, 1982
GENERAL DYNAMICS
CONVAIR DIVISION
OUTLET ASSEMBLY ~
EBT-P PROTOTYPE
E 14170
11-38070
A-89/A-90

DWG NO. 11-38080 SH 1 REV A

REVISIONS

ZONE	REV	DESCRIPTION	DATE	APPROVED
B5	A	REVISED -1 CONFIGURATION	2/10/82	
C7		ADDED VIEW 'A'	2/10/82	
G11		ADDED NOTES 5 AND 6	2/10/82	
		PANDER KRAATS 2-11-82	2-11-82	

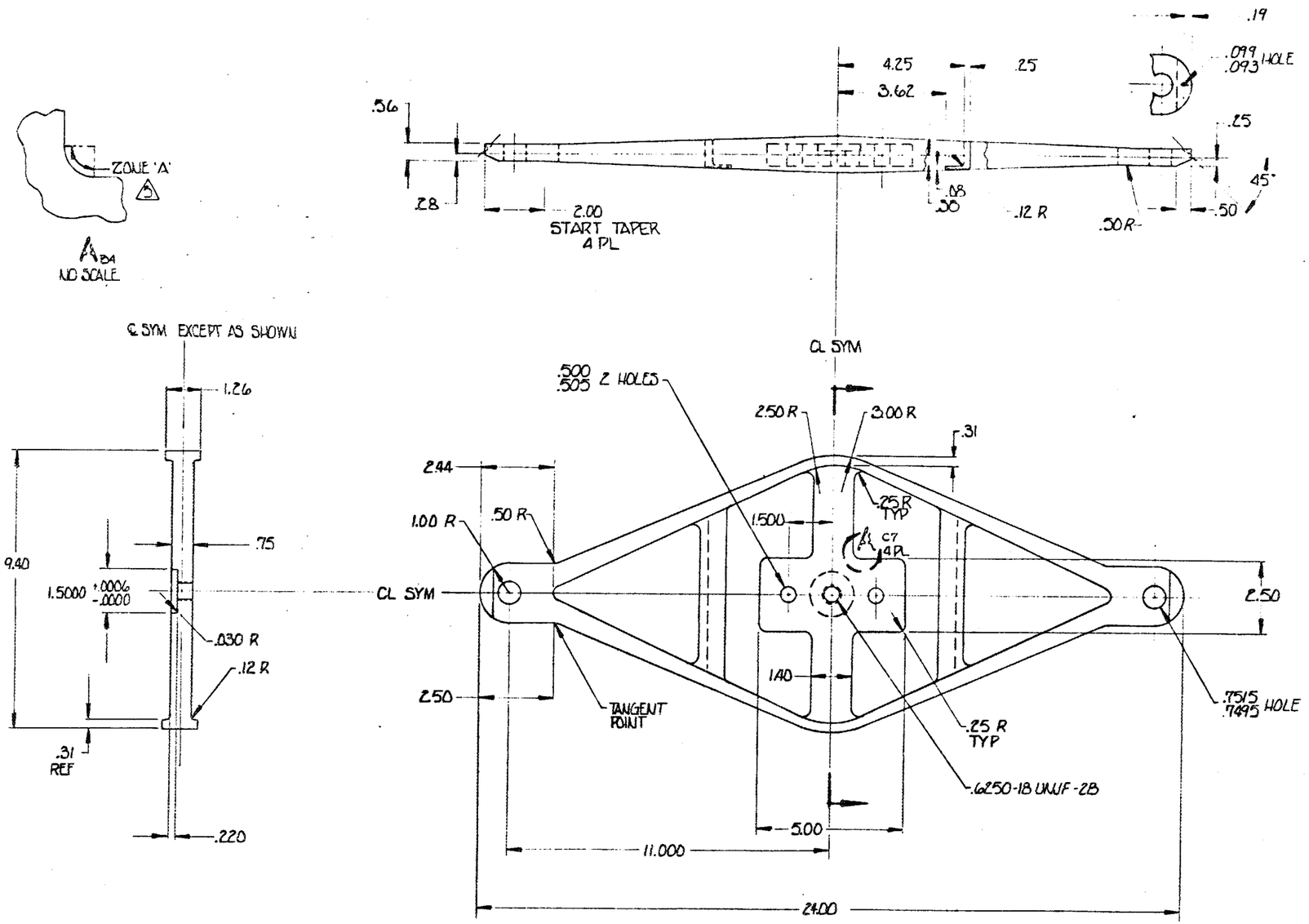

NOTES:

1. ULTRASONIC TEST RAW MATERIAL PER D-73517-1
2. IDENTIFY PER D-70042-20. LOCATION OPTIONAL
3. MAT'L:
   1.375 × 9.5 × 24.0 6AL-4V ELI TITANIUM ANNEALED. MIL-T-9046, TYPE III, COMP 'D'
4. PENETRANT INSPECT PER MIL-I-6866. TYPE I, METHOD A. MAX DEFECT PERMITTED 0.080
5. PENETRANT INSPECT PER MIL-I-6866 TYPE I, METHOD A. MAX DEFECT PERMITTED 0.025
6. -1 IDENTICAL TO D11-38080-6.

APPROVED TITLE I

REF AL BOCH LETTER DATED MARCH 19, 1982

-1

☐ SEE SEPARATE PARTS LIST

SEE D-70914 FOR ABBREVIATION, CODE AND SYMBOL REQUIREMENTS

SEE D-70902 FOR STANDARD MANUFACTURING AND INSTALLATION REQUIREMENTS

UNLESS OTHERWISE SPECIFIED ALL MACHINED SURFACES 125

UNLESS OTHERWISE SPECIFIED DIMENSIONS ARE IN INCHES

TOLERANCES: X ±.1, XX ± .03, XXX ± .010; ANGULAR PER D70902

CHECK
STRESS 2-11-82
GR ENGR
DESIGN 1-29-82
DRAWN (PGVK) 1-29-82
CONTRACT NO.
MATL 2/15/82
PROD ENGR 2/15/82

GENERAL DYNAMICS
CONVAIR DIVISION
SAN DIEGO, CALIFORNIA

COLD MASS SUPPORT STRUT
EBT-P PROTOTYPE

SIZE D | FSCM NO 14170 | DWG NO. 11-38080

SCALE HALF | SHEET 1 OF 1

SEC. CLASS | TYPE | LEVEL | CONT | GROUP | DISTR | REPRO | PACKAGE NO. | REL

FORM 7516

A-91/A-92

DWG NO 11-38084 SH 1 REV

REVISIONS

ZONE	REV	DESCRIPTION	DATE	APPROVED

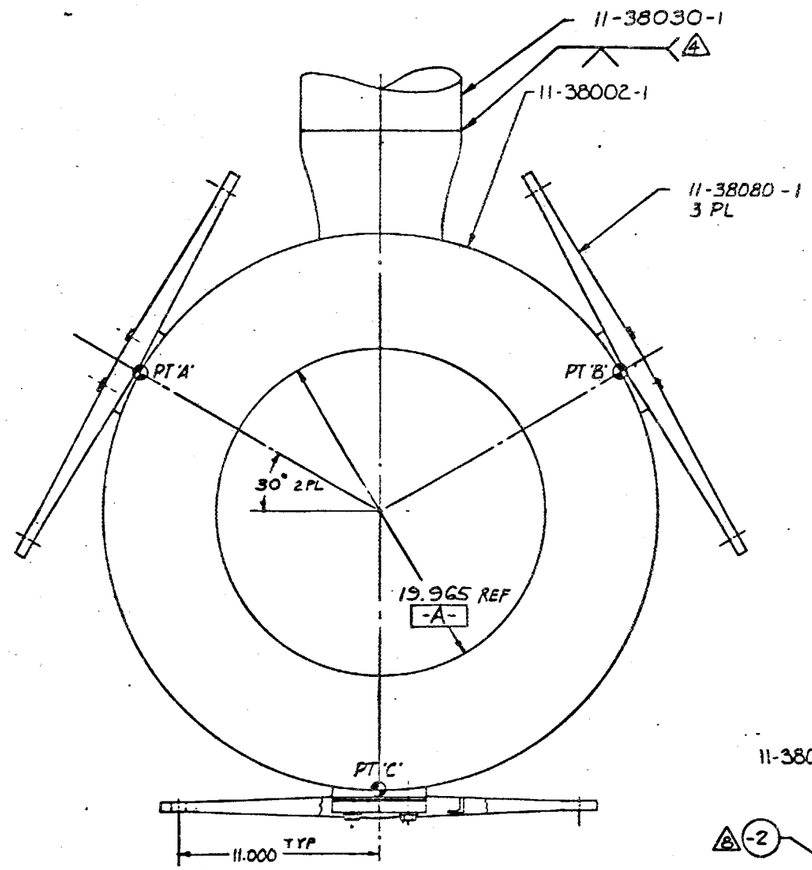

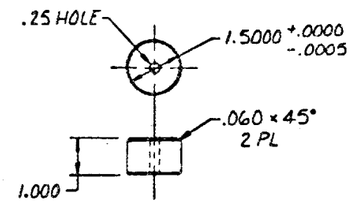

-3
SCALE: 1/2

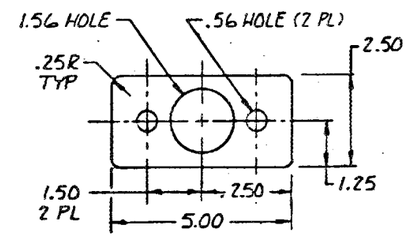

-2
SCALE: 1/2

PRELIMINARY

NOTES:

1. LOCKWIRE PER MS 33540.
2. IDENTIFY PER 0-70042-20.
3. INSTALL FASTENERS PER 0-70054. TORQUE TO 450-520 IN-LBS.
4. WELD PER MIL-STD-278 BY WELDERS QUALIFIED IN ACCORDANCE WITH MIL-STD-248, USING ER316L ELECTRODE PER MIL-E-19933 AND/OR E316L PER MIL-E-22200/2
5. PENETRANT INSPECT ROOT AND FINAL LAYER OF ALL WELDS PER MIL-I-6866, TYPE II, METHOD A. NO DEFECTS PERMITTED.
6. DIM W TO BE MEASURED AT PTS 'A', 'B' & 'C'
7. PRE-INSTALL -3 TO ESTABLISH GAP DIMENSION. TORQUE TO 225 IN-LBS.
8. INSTALL -2 TO MAINTAIN AN INTERFERENCE FIT OF .003 TO .002

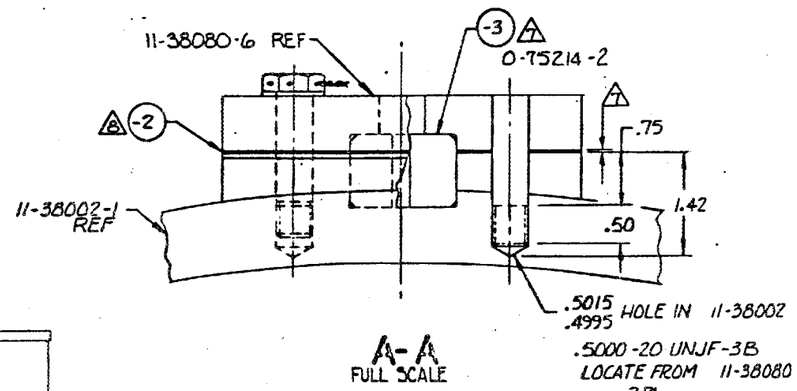

A-A
FULL SCALE

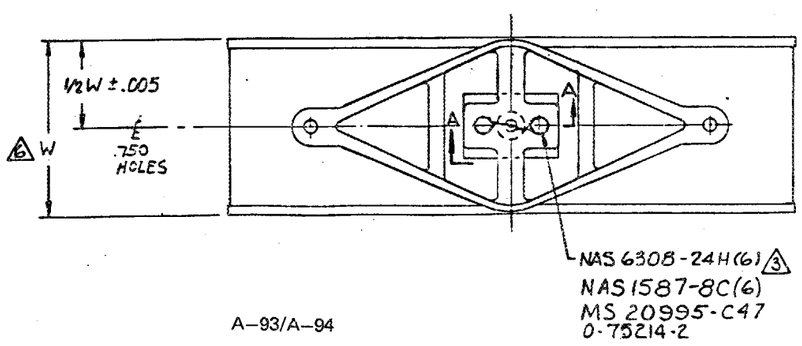

APPROVED TITLE 1

SEE SEPARATE PARTS LIST

REF AL BOCH LETTER DATED MARCH 19, 1982

SHEET NO.	REV LTR

SEE 0-70914 FOR ABBREVIATION, CODE AND SYMBOL REQUIREMENTS	UNLESS OTHERWISE SPECIFIED DIMENSIONS ARE IN INCHES	CHECK	
	TOLERANCES X ±.1 XX ±.03 XXX ±.010 ANGULAR PER 070902	STRESS	5/20/81
SEE 0-70902 FOR STANDARD MANUFACTURING AND INSTALLATION REQUIREMENTS		GR ENGR	7/9/81
		DESIGN N. HILL	5-20-81
		DRAWN N.H.	5-20-81
UNLESS OTHERWISE SPECIFIED		CONTRACT NO.	
ALL MACHINED SURFACES 125			
	MATL		7-7-81
	PROD. ENGR		7-8-81

GENERAL DYNAMICS
CONVAIR DIVISION
SAN DIEGO, CALIFORNIA

SUPPORT INSTL-COLD MASS-EBT-P PROTOTYPE

SIZE	FSCM NO.	DWG NO.
D	14170	11-38084

SCALE 1/2 IN TTD SHEET 1 OF 1

SEC. CLASS | TYPE | LEVEL | CONT | GROUP | DISTR | REPRO | PACKAGE NO. | REL

A-93/A-94

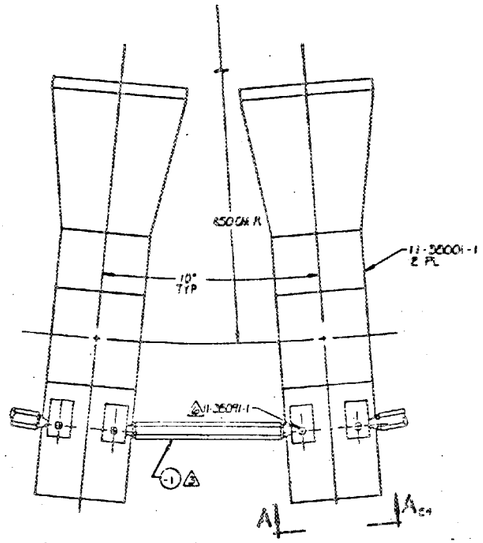

TYPICAL INSTALLATION
1/8 SCALE

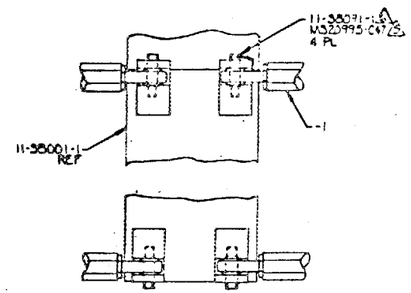

A-A
1/4 SCALE

NOTES:

1. ULTRASONIC TEST RAW MATERIAL PER D-73517-1
2. IDENTIFY PER D-70042-20 LOCATION OPTIONAL
3. TORQUE TO 20 FT-LBS ON ASSEMBLY (TENSION)
4. INSTALL FASTENERS PER D-70054 USING TORQUE LIMITS PER D-70058
5. SAFETY PER MS33540
6. TORQUE TO 50-400 IN LBS
7. -1 ASSEMBLY IDENTICAL TO D11-35090-1

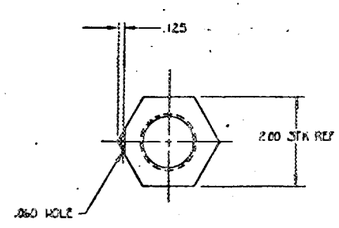

B-B
FULL SCALE

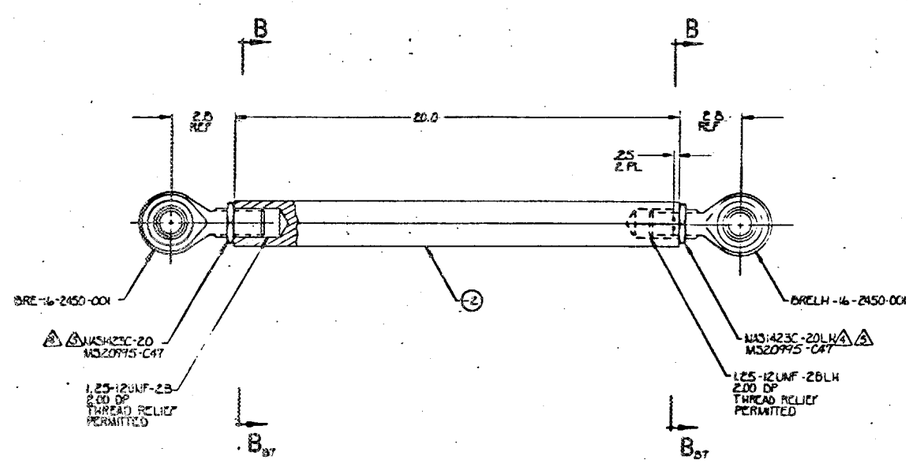

APPROVED TITLE I

PRELIMINARY

REF AL BOCH LETTER DATED
MARCH 19, 1982

SEE SEPARATE PARTS LIST

SEE D-70916 FOR ABBREVIATION, CODE AND SYMBOL REQUIREMENTS

SEE D-70902 FOR STANDARD MANUFACTURING AND INSTALLATION REQUIREMENTS

UNLESS OTHERWISE SPECIFIED DIMENSIONS ARE IN INCHES
TOLERANCES
± 1 ± .03 ± .010
ANGULAR PER D-70902

UNLESS OTHERWISE SPECIFIED
ALL MACHINED SURFACES 125

CHECK
STRESS
DESIGN
DRAWN
CONTRACT NO

GENERAL DYNAMICS
CONVAIR DIVISION
SAN DIEGO CALIFORNIA

OUT OF PLANE STRUTS ~
EBF-P PROTOTYPE

SIZE E FSCM NO 14170 DWG NO 11-35090
SCALE 1/4 = 1 SHEET 1 OF 1

SHEET NO
REV LTR

A-95/A-96

DWG NO. 11-38091

REVISIONS				
ZONE	REV	DESCRIPTION	DATE	APPROVED

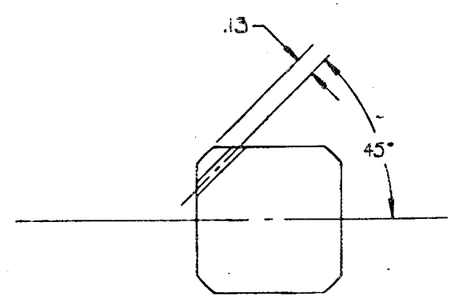

A - A_{A4}

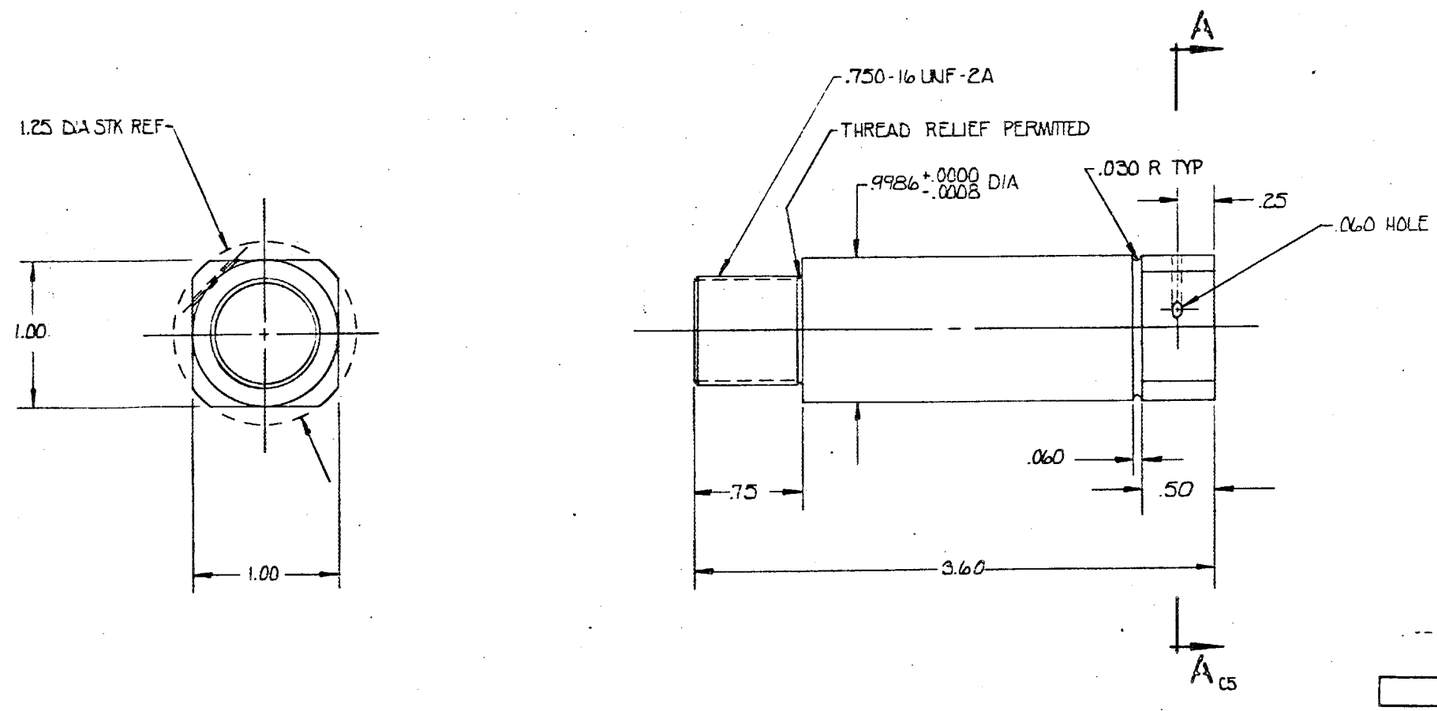

NOTES:

1. ULTRASONIC TEST RAW MATERIAL PER 0-73517-1
2. IDENTIFY PER 0-70042-20 LOCATION OPTIONAL
3. MAT'L: 1.25 DIA × 4.0 ROD INCONEL 718: ASM 5662
4. HEAT TREAT AND AGE TO 180 KSI PER 0-75134

PRELIMINARY

APPROVED TITLE I

REF AL BOCH LETTER DATED MARCH 19, 1982

☐ SEE SEPARATE PARTS LIST

-4

SEE 0-70914 FOR ABBREVIATION, CODE AND SYMBOL REQUIREMENTS	UNLESS OTHERWISE SPECIFIED DIMENSIONS ARE IN INCHES	CHECK	GENERAL DYNAMICS CONVAIR DIVISION SAN DIEGO, CALIFORNIA
SEE 0-70902 FOR STANDARD MANUFACTURING AND INSTALLATION REQUIREMENTS	TOLERANCES .X ±.1 .XX ± .03 .XXX ± .010 ANGULAR PER 070902	STRESS	
		GR ENGR	
		DESIGN	OUT OF PLANE STRUT PIN – EBT-P PROTOTYPE
		DRAWN	
UNLESS OTHERWISE SPECIFIED ALL MACHINED SURFACES 125		CONTRACT NO.	
	MATL		SIZE D FSCM NO. 14170 DWG NO. 11-38091
	PROD. ENGR		SCALE 2/1 SHEET 1 OF 1

SHEET NO. / REV LTR

SEC. CLASS | TYPE | LEVEL | CONT | GROUP 692-01 | DISTR | REPRO | PACKAGE NO. | REL

FORM 7516

A–97/A–98

SEC. CLASS

REVISIONS											
ZONE	REV	DESCRIPTION	DATE	APPROVED	ZONE	REV	DESCRIPTION	DATE	APPROVED	ZONE	REV	DESCRIPTION	DATE	APPROVED

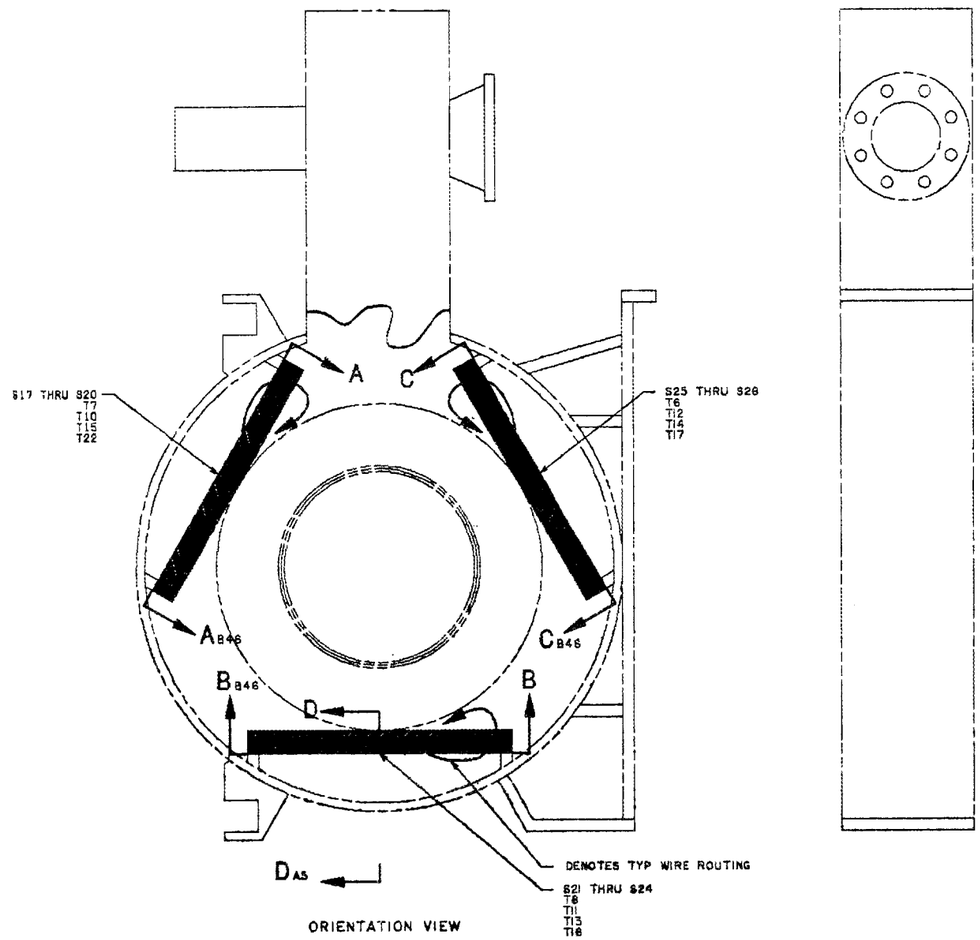

ORIENTATION VIEW

NO SCALE

NOTES:

1.1 WIRING SHALL BE ACCORDANCE WITH WIRING DIAGRAM DRAWING NUMBER D11-38088.

1.2 ROUTE WIRING TO CONNECTOR ALONG TROUGH IN INSULATION USING 0-06093-1 TAPE TO RETAIN AS SHOWN IN SECT D-D IN ACCORDANCE WITH SECT A-A, B-B, C-C.

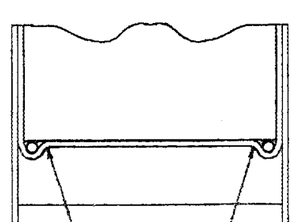

SECT D-D C7

NO SCALE

COMPUTERIZED REPRODUCIBLE

607-0.495.76L2995.01.D.A 8/26//80 3

APPROVED TITLE I

REF AL BOCH LETTER DATED MARCH 19, 1982

SEE SEPARATE PARTS LIST

SEE D-70814 FOR ABBREVIATION, CODE AND SYMBOL REQUIREMENTS

SEE T-70300 FOR STANDARD MANUFACTURING AND INSTALLATION REQUIREMENTS

UNLESS OTHERWISE SPECIFIED ALL MACHINED SURFACES

UNLESS OTHERWISE SPECIFIED DIMENSIONS ARE IN INCHES

TOLERANCES

X	XX	XXX
±.1	±.03	±.010

ANGULAR PER D-70802

MATL

PROD ENGR

CHECK

STRESS

QA CHK

DESIGN

DRAWN R.BISON

CONTRACT NO.

GENERAL DYNAMICS
CONVAIR DIVISION
SAN DIEGO, CALIFORNIA

INSTRUMENTATION
VAC AND L HE VES.
EBT-P DEVELOPMENT

SIZE E | FSCM NO. 14170 | DWG NO. D11-38087

SCALE NOTED | SHEET 1 OF 6

SEC. CLASS | TYPE | LEVEL | CONT | DISTR | PACKAGE NO. | REL

DWG NO. D11-38087 | SHT. 1 | REV

A-99/A-100

SEC. CLASS

REVISIONS											
ZONE	REV	DESCRIPTION	DATE	APPROVED	ZONE	REV	DESCRIPTION	DATE	APPROVED	ZONE	REV	DESCRIPTION	DATE	APPROVED

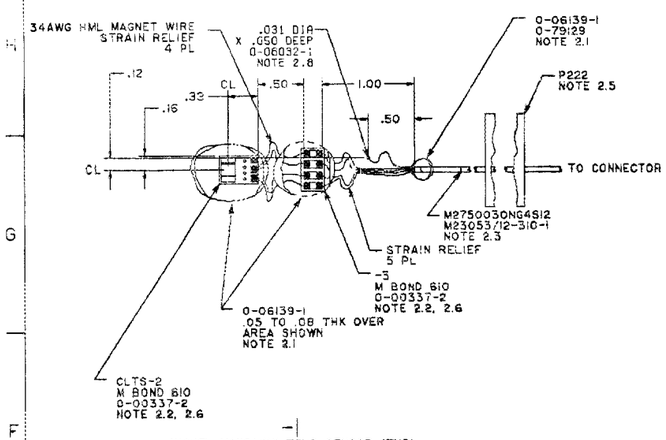

NICKEL MANGANIN TEMP SENSOR (TYP)
SCALE: 2/1

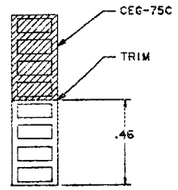

-3
SCALE: 4/1

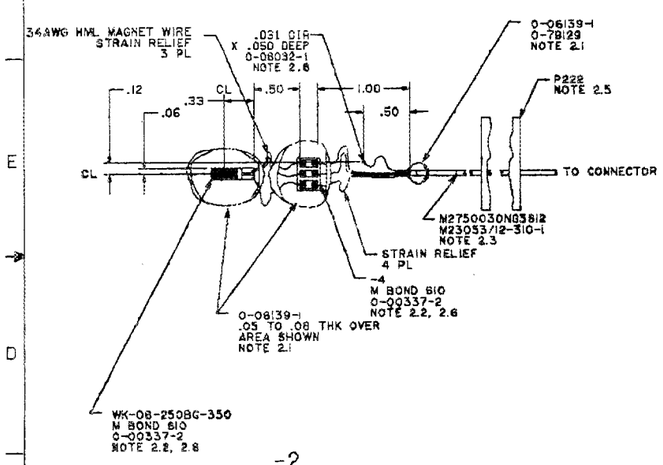

-2
SINGLE AXIS STRAIN GAGE (TYP)
SCALE: 2/1

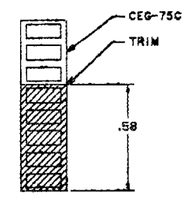

-4
SCALE: 4/1

NOTES:

2.1 PREPARE SURFACES AND APPLY ADHESIVE PER 0-79129.

2.2 SOLDER ELECTRICAL TERMINATIONS PER 0-73522.

2.3 TERMINATE CABLE SHIELD PER 55-01410, PARA 5.4.2. DO NOT INSTALL LUG ON WIRE.

2.4 TEST ALL SENSORS AND COMPLETED SUB-ASSEMBLIES PER APPLICABLE PARAGRAPH OF GDC-EBT-81-011. IDENTIFY END OF CABLE WITH:
SENSOR PART NO
SENSOR SERIAL OR BATCH NO
ASSEMBLY NO
REF DES

2.5 INSTALL CABLE ON SUPPORTS AND ML; USING P222 TAPE AT INTERMEDIATE INTERVALS (MAX 12.0) AS REQUIRED.

2.6 PREPARE SURFACES PER 0-79129 AND MIX AND APPLY ADHESIVE PER APPLICABLE VENDOR INSTRUCTIONS.

2.7 IDENTIFY WIRE COLOR CODES AT END OF CABLE AS REQUIRED.

2.8 TERMINATE CABLE SHIELD IN HOLE USING 0-06032-1 ADHESIVE.
ON MATERIAL LESS THAN .125 THK: SPOT WELD SHIELD ON SURFACE AND COVER TERMINATION WITH 0-06032-1 ADHESIVE. DO NOT DRILL .031 DIA X .050 DEEP HOLE.

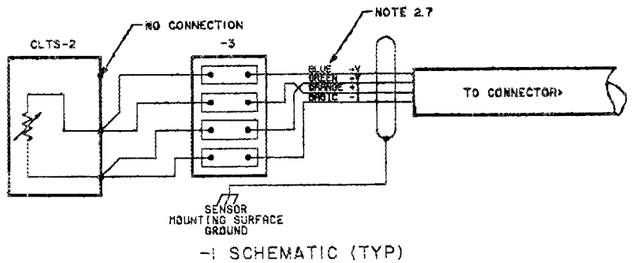

-1 SCHEMATIC (TYP)
NICKEL-MANGANIN TEMP SENSOR WIRING

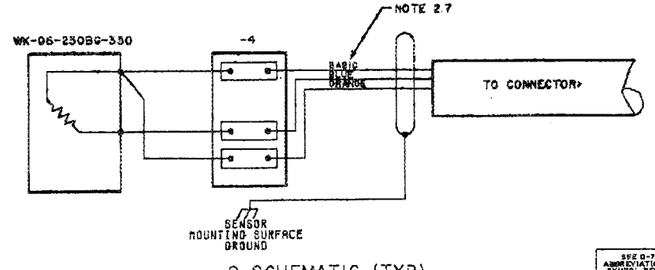

-2 SCHEMATIC (TYP)
STRAIN GAGE WIRING

COMPUTERIZED REPRODUCIBLE
607-0.499.76L2995.01.D.A 8/26/80 3

APPROVED TITLE I

REF AL BOCH LETTER DATED
MARCH 19, 1982

☒ SEE SEPARATE PARTS LIST

SEE D-70914 FOR ABBREVIATION, CODE AND SYMBOL REQUIREMENTS
SEE D-70999 FOR STANDARD MANUFACTURING AND INSTALLATION REQUIREMENTS
UNLESS OTHERWISE SPECIFIED
ALL MACHINED SURFACES ✓

UNLESS OTHERWISE SPECIFIED DIMENSIONS ARE IN INCHES
TOLERANCES
.X ±.1 .XX ±.03 .XXX ±.010
ANGULAR PER D-70902
MATL
FINISH

CHECK
STRESS
QA ENGR
DESIGN
DRAWN R.BIGNI
CONTRACT NO.

GENERAL DYNAMICS
CONVAIR DIVISION
SAN DIEGO, CALIFORNIA

INSTRUMENTATION
VAC AND L HE VES.
EBT-P DEVELOPMENT

SIZE E | FSCM NO. 14170 | CODE IDENT NO. | DII-38087 | REV
SCALE NOTED | SHEET 2 OF

SEC. CLASS | TYPE | LEVEL | CONT | GROUP | DISTR | REPRO | PACKAGE NO. | REL

SHEET NO.
REV LTR

DII-38087 REV

A-101/A-102

SEC.CLASS

REVISIONS				REVISIONS				REVISIONS			
ZONE REV	DESCRIPTION	DATE	APPROVED	ZONE REV	DESCRIPTION	DATE	APPROVED	ZONE REV	DESCRIPTION	DATE	APPROVED

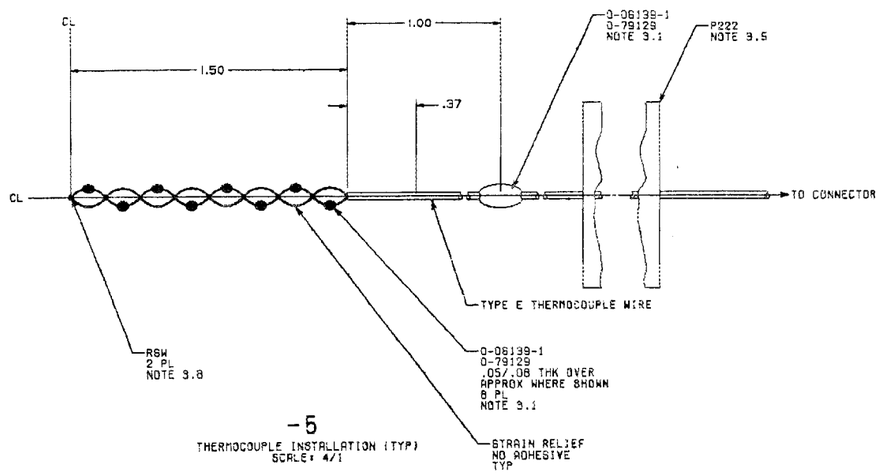

-5
THERMOCOUPLE INSTALLATION (TYP)
SCALE: 4/1

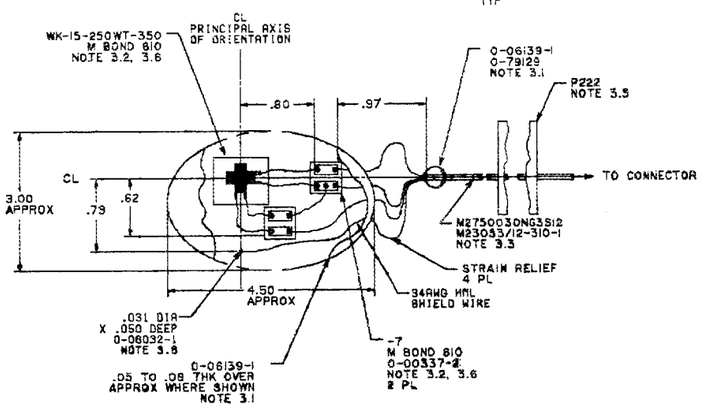

-6
ROSETTE STRAIN GAGE INSTALLATION (TYP)
SCALE: 2/1

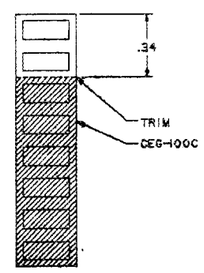

-7
SCALE: 4/1

NOTES:

3.1 PREPARE SURFACES AND APPLY ADHESIVE PER 0-79129.

3.2 SOLDER ELECTRICAL TERMINATIONS PER 0-73522.

3.3 TERMINATE CABLE SHIELD PER 53-01410, PARA 5.4.2. DO NOT INSTALL LUG ON WIRE.

3.4 TEST ALL SENSORS AND COMPLETED SUB-ASSEMBLIES PER APPLICABLE PARAGRAPH OF GDC-EBT-81-011. IDENTIFY END OF CABLE WITH:
SENSOR PART NO
SENSOR SERIAL OR BATCH NO
ASSEMBLY NO
REF DES

3.5 INSTALL CABLE ON SUPPORTS AND MLI USING P222 TAPE AT INTERMEDIATE INTERVALS (MAX 12.0) AS REQUIRED.

3.6 PREPARE SURFACES PER 0-79129 AND MIX AND APPLY ADHESIVE PER APPLICABLE VENDOR INSTRUCTIONS.

3.7 IDENTIFY WIRE COLOR CODES AT END OF CABLE AS REQUIRED.

3.8 TWIST THERMOCOUPLE WIRES TOGETHER AND SPOT-WEL SPOT-WELD THERMOCOUPLE TO MOUNTING SURFACE WHEN ATTACHING TO TITANIUM SUPPORT MATERIAL.

WHEN ATTACHING TO LN2 COPPER SHIELD MATERIAL:
PRE-TIN THERMOCOUPLE AND SURFACE ATTACHMENT AREA
SOLDER THERMOCOUPLE USING 0-00337-2 EUTECTIC SOLDER.

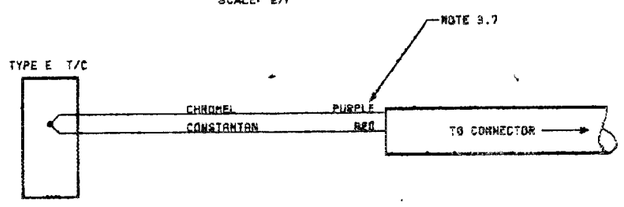

-5 SCHEMATIC (TYP)
THERMOCOUPLE

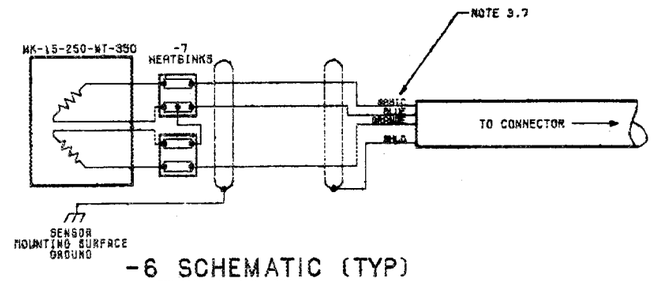

-6 SCHEMATIC (TYP)
ROSETTE STRAIN GAGE

COMPUTERIZED REPRODUCIBLE
607-0.499.76L2995.01.D.A 8/26//80 3

APPROVED TITLE I

REF AL BOCH LETTER DATED
MARCH 19, 1982

☐ SEE SEPARATE PARTS LIST

SEE 0-70914 FOR ABBREVIATION, CODE AND SYMBOL REQUIREMENTS
SEE 0-70962 FOR STANDARD MANUFACTURING AND INSTALLATION REQUIREMENTS
UNLESS OTHERWISE SPECIFIED ALL MACHINED SURFACES ✓

UNLESS OTHERWISE SPECIFIED DIMENSIONS ARE IN INCHES
TOLERANCES
.X ±.1 .XX ±.03 .XXX ±.010
ANGULAR PER 0-70962
MATL
PROD BASIS
SEC. CLASS

CHECK
STRESS
DESIGN
DRAWN H.GIBSON
CONTRACT NO.

GENERAL DYNAMICS
CONVAIR DIVISION
SAN DIEGO, CALIFORNIA

INSTRUMENTATION
VAC AND L HE VES.
EBT-P DEVELOPMENT

SIZE/FSCM NO. E14170
DWG NO. D11-38087
SCALE NOTED
SHEET 3 OF

SHEET NO.
REV LTR

TYPE | LEVEL | CONT | GROUP | DISTR | REPRO | PACKAGE NO. | REL

DWG NO. D11-38087 SHT 3 REV

A-103/A-104

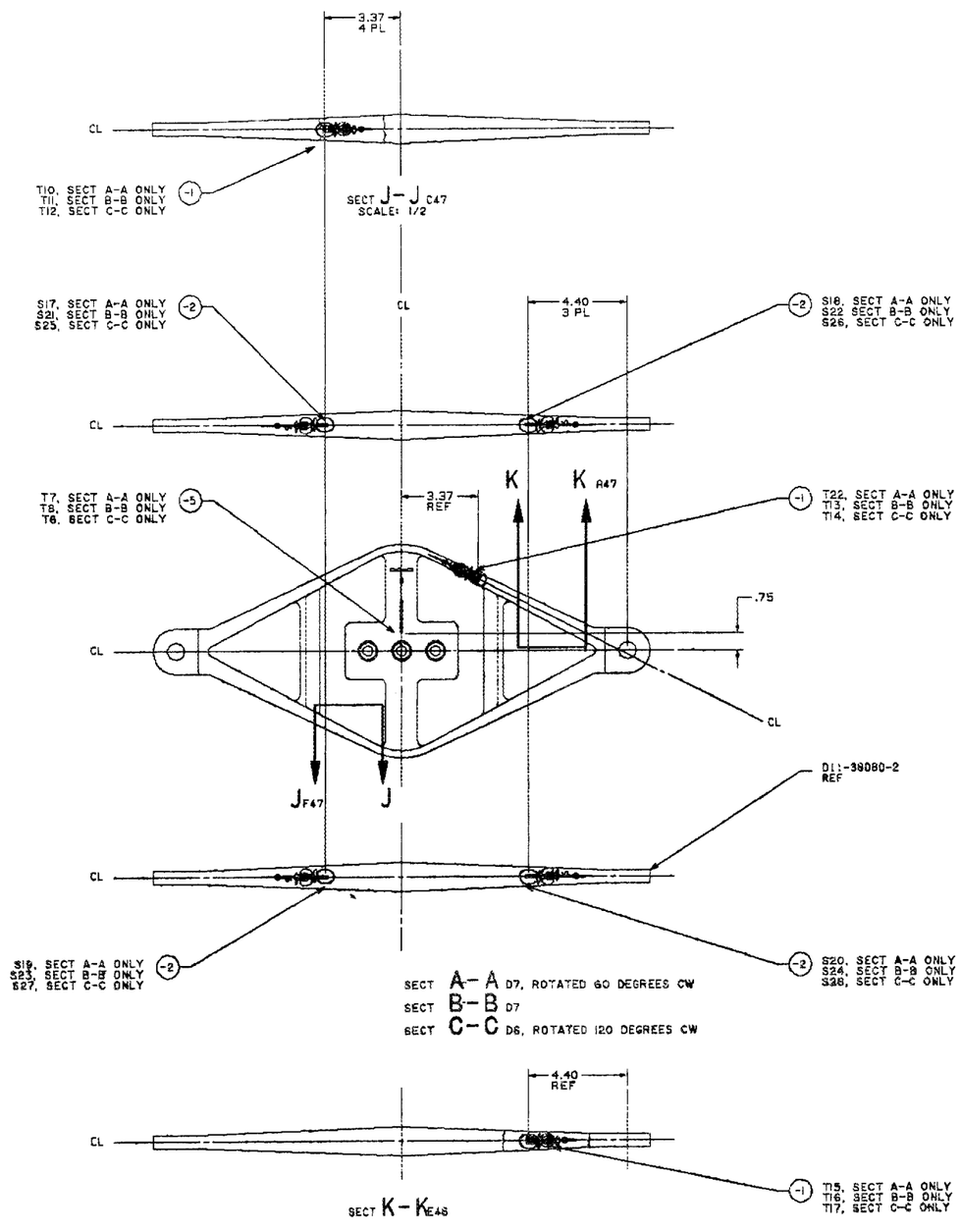

A-105/A-106

NOTES:

4.1 SENSOR LOCATIONS FOR S17 THRU S28; T6, T7, T8, T10 THRU T17, AND T22, ARE SHOWN.

COMPUTERIZED REPRODUCIBLE

607-0.489.76L2995.01.D.A 8/26/80 3

APPROVED TITLE I

REF AL BOCH LETTER DATED MARCH 19, 1982

☐ SEE SEPARATE PARTS LIST

SEE D-70914 FOR ABBREVIATION, CODE AND SYMBOL REQUIREMENTS

SEE D-70902 FOR STANDARD MANUFACTURING AND INSTALLATION REQUIREMENTS

UNLESS OTHERWISE SPECIFIED

ALL MACHINED SURFACES ✓

UNLESS OTHERWISE SPECIFIED DIMENSIONS ARE IN INCHES

TOLERANCES

.X ±.1 .XX ±.03 .XXX ±.010

ANGULAR PER D-70902

MATL

PROJ ENGR

SEC. CLASS

CHECK

STRESS

GR ENGR

DESIGN

DRAWN R.BIBEN

CONTRACT NO.

GENERAL DYNAMICS
CONVAIR DIVISION
SAN DIEGO, CALIFORNIA

INSTRUMENTATION
VAC AND L HE VES.
EBT-P DEVELOPMENT

SIZE E FSCM NO. 14170 DWG NO. D11-38087

SCALE NOTED

SHEET 4 OF

TYPE | LEVEL | CONT | GROUP | DISTR | REPRO | PACKAGE NO. | REL

SHEET NO.

REV LTR

D11-38087

REVISIONS											
ZONE	REV	DESCRIPTION	DATE	APPROVED	ZONE	REV	DESCRIPTION	DATE	APPROVED	ZONE	REV	DESCRIPTION	DATE	APPROVED

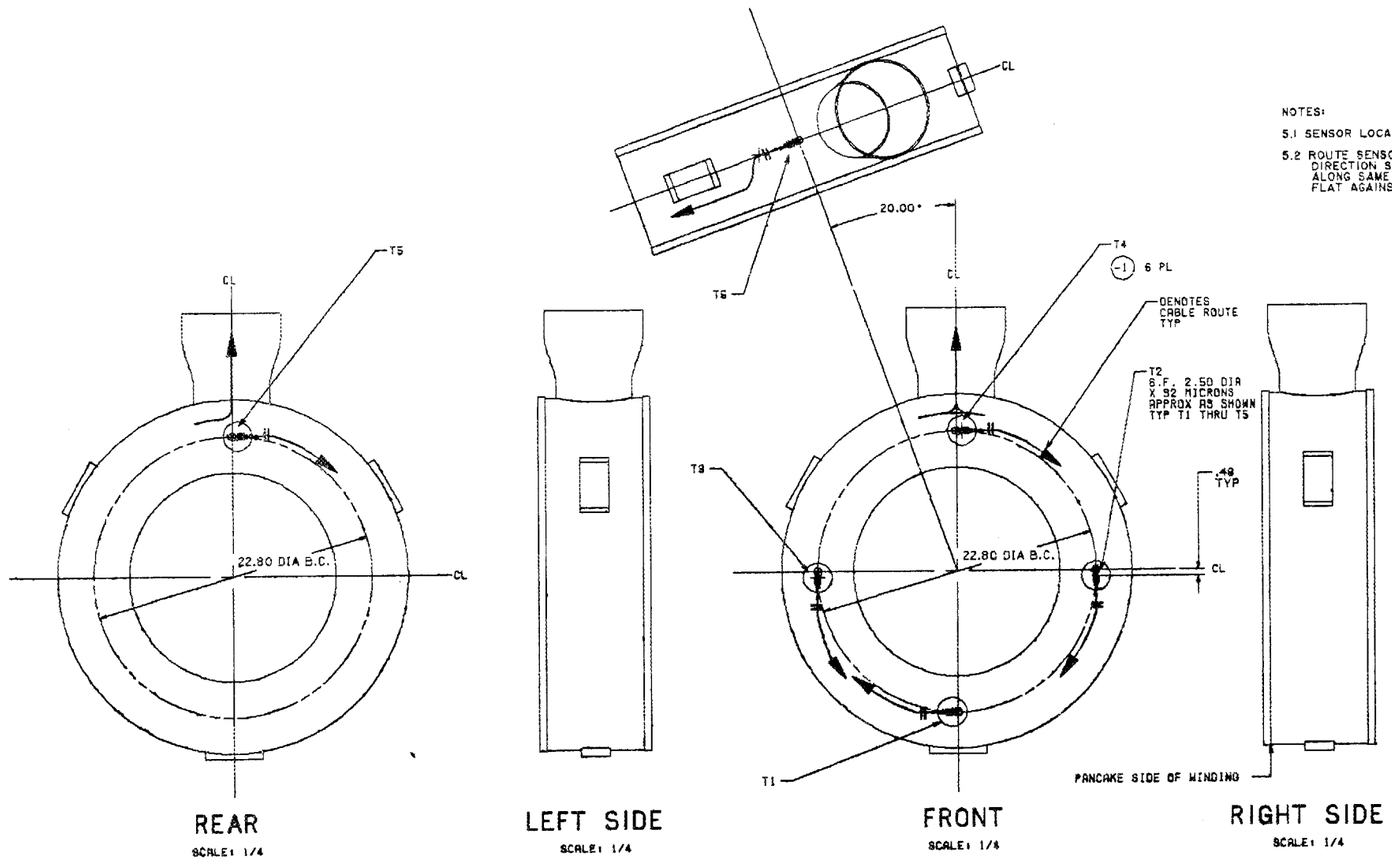

NOTES:

5.1 SENSOR LOCATIONS FOR T1 THRU T5 AND T9 ARE SHOWN.

5.2 ROUTE SENSOR CABLES TO STACK ABOUT CIRCUMFERENCE IN DIRECTION SHOWN. WHEN MORE THAN ONE CABLE IS ROUTED ALONG SAME PATH THEY MAY BE ADJACENT BUT MUST REMAIN FLAT AGAINST THE HELIUM VESSEL SURFACES.

COMPUTERIZED REPRODUCIBLE

607-0.499.76L2995.01.D.A 8/26//80 3

APPROVED TITLE I

REF AL BOCH LETTER DATED MARCH 19, 1982

☐ SEE SEPARATE PARTS LIST

SEE D-70914 FOR ABBREVIATION, CODE AND SYMBOL REQUIREMENTS

SEE D-70902 FOR STANDARD MANUFACTURING AND INSTALLATION REQUIREMENTS

UNLESS OTHERWISE SPECIFIED ALL MACHINED SURFACES ✓

UNLESS OTHERWISE SPECIFIED DIMENSIONS ARE IN INCHES

TOLERANCES

X	XX	XXX
±.1	±.03	±.016

ANGULAR PER D-70902

MATL

PROD ENGR

CHECK

STRESS

ME DYN

DESIGN

DRAWN R.BIBOW

CONTRACT NO.

GENERAL DYNAMICS
CONVAIR DIVISION
SAN DIEGO, CALIFORNIA

INSTRUMENTATION
VAC AND L HE VES.
EBT-P DEVELOPMENT

SIZE E | FSCM NO 11470 | DWG NO D11-38087 | SHEET 5 OF | REL

SCALE NOTED

SEC. CLASS | TYPE | LEVEL | CONT | GROUP | DISTR | REPRO | PACKAGE NO.

SHEET NO. | REV LTR

A-107/A-108

NOTES:

6.1 SENSOR LOCATIONS FOR S1 THRU S16 ARE SHOWN.

6.2 ROUTE SENSOR CABLES TO STACK ABOUT CIRCUMFERENCE IN DIRECTION SHOWN. WHEN MORE THAN ONE CABLE IS ROUTED ALONG SAME PATH THEY MAY BE ADJACENT BUT MUST REMAIN FLAT AGAINST THE HELIUM VESSEL SURFACES.

6.3 ALL GAGES ARE 90 DEG ROSETTES.

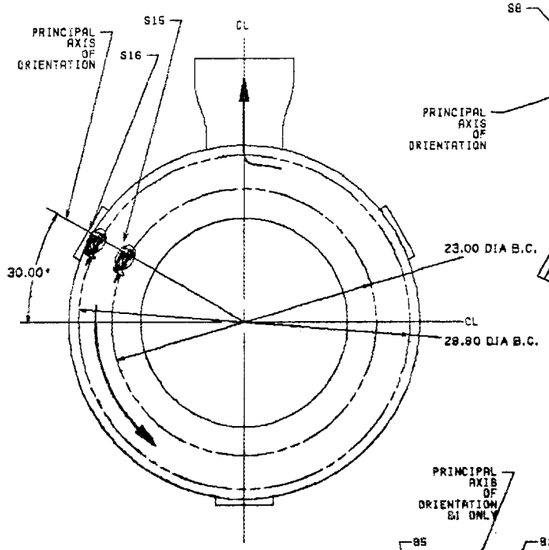

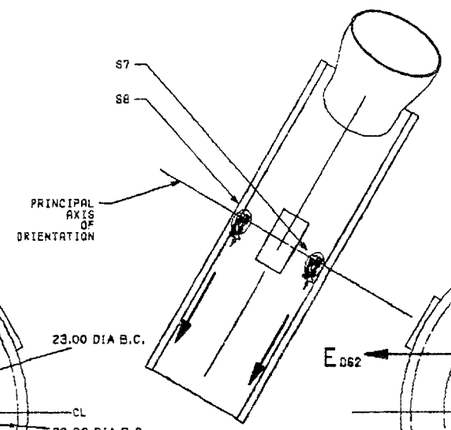

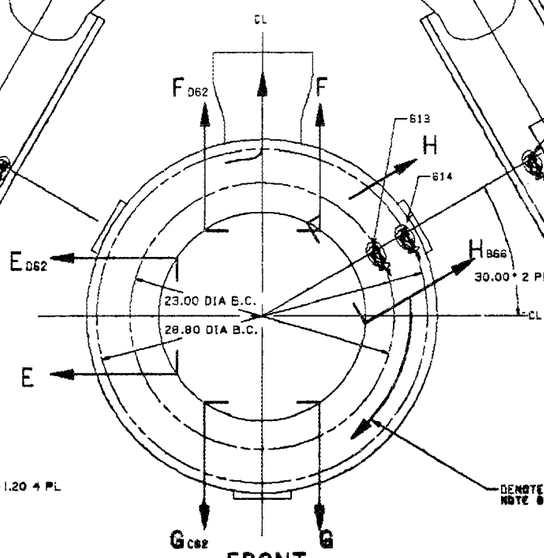

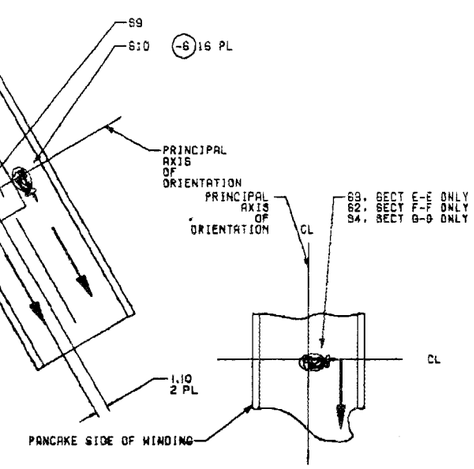

VIEW E-E E66

VIEW F-F F66 ROTATED 90 DEG CCW

VIEW G-G G65 ROTATED 90 DEG CW

SCALE: 1/4

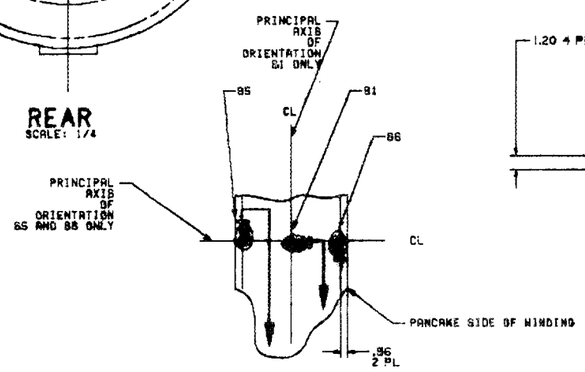

VIEW H-H E64, ROTATED 90 DEG CW
SCALE: 1/4

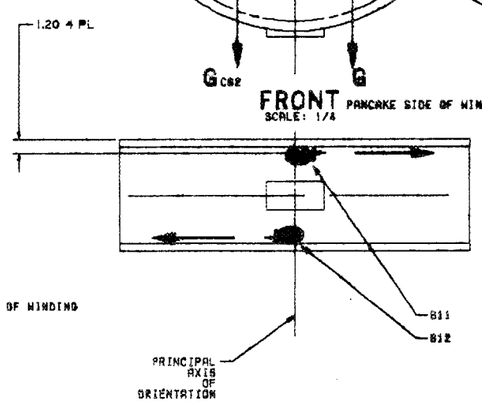

COMPUTERIZED REPRODUCIBLE

607-0.489.76L2995.01.D.A 9/26/80 3

APPROVED TITLE I

REF AL BOCK LETTER DATED MARCH 19, 1982

SEE SEPARATE PARTS LIST

GENERAL DYNAMICS
CONVAIR DIVISION

INSTRUMENTATION VAC AND LHE VES
EBT-P DEVELOPMENT

E1476 LDI-3808

A-109/A-110

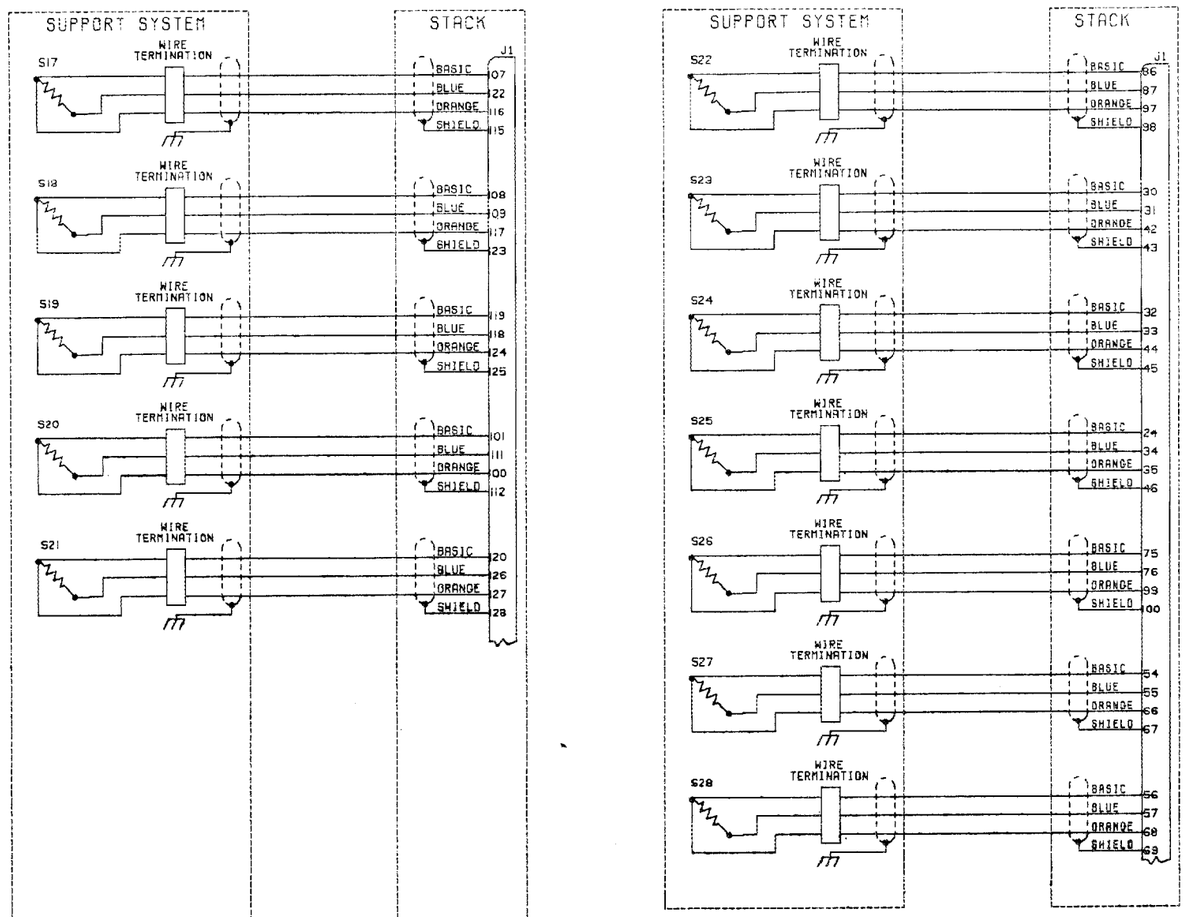

REVISIONS											
ZONE	REV	DESCRIPTION	DATE	APPROVED	ZONE	REV	DESCRIPTION	DATE	APPROVED	ZONE	REV	DESCRIPTION	DATE	APPROVED
											A	DELETED T15, 16, 17 ON SH 1. ADDED T15, 16, 17 TO SH 2.		

NOTES:

1.1 CONNECTIONS FOR S17 THRU S28 ARE SHOWN ON THIS SHEET.

1.2 INSTALLATION OF S17 THRU S28 AND T1 THRU T22 SHALL BE IN ACCORDANCE WITH DRAWING NUMBER D11-38087.

1.3 MATING PLUGS ARE FURNISHED TO ORNL FOR ALL CONNECTORS SHOWN.

COMPUTERIZED REPRODUCIBLE

607-0.499.76L2995.01.D.A 8/26//80 3

APPROVED TITLE I

REF AL BOCH LETTER DATED MARCH 19, 1982

☐ SEE SEPARATE PARTS LIST

SEE D-70914 FOR ABBREVIATION, CODE AND SYMBOL REQUIREMENTS

SEE D-70907 FOR STANDARD MANUFACTURING AND INSTALLATION REQUIREMENTS

UNLESS OTHERWISE SPECIFIED ALL MACHINED SURFACES ✓

UNLESS OTHERWISE SPECIFIED DIMENSIONS ARE IN INCHES

TOLERANCES: .X ±.1, .XX ±.03, .XXX ±.010; ANGULAR PER D-70902

MATL

PROJ ENGR

CHECK

STRESS

DR ENGR

DESIGN

DRAWN R.RISDN

CONTRACT NO.

GENERAL DYNAMICS
CONVAIR DIVISION
SAN DIEGO, CALIFORNIA

INSTRUMENTATION WIRING DIAGRAM
EBT-P DEVELOPMENT

SIZE E | FSCM NO. 14170 | DWG NO. D11-38088 | REV

SCALE NOTED | SHEET 1 OF 4

SEC. CLASS | TYPE | LEVEL | CONT | GROUP | DISTR | REPRO | PACKAGE NO. | REL

SHEET NO. | REV LTR

D11-38088-110 CAD GRAD

A-111/A-112

SEC.CLASS

REVISIONS											
ZONE	REV	DESCRIPTION	DATE	APPROVED	ZONE	REV	DESCRIPTION	DATE	APPROVED	ZONE	REV	DESCRIPTION	DATE	APPROVED
											A	CHANGED T6, T7 AND T8 FROM J2 TO J3. ADDED T15, T16 T17 TO J2. DELETED T21 FROM J3. DELETED V1 DELETED SHIELDS FROM T/C CABLES.		

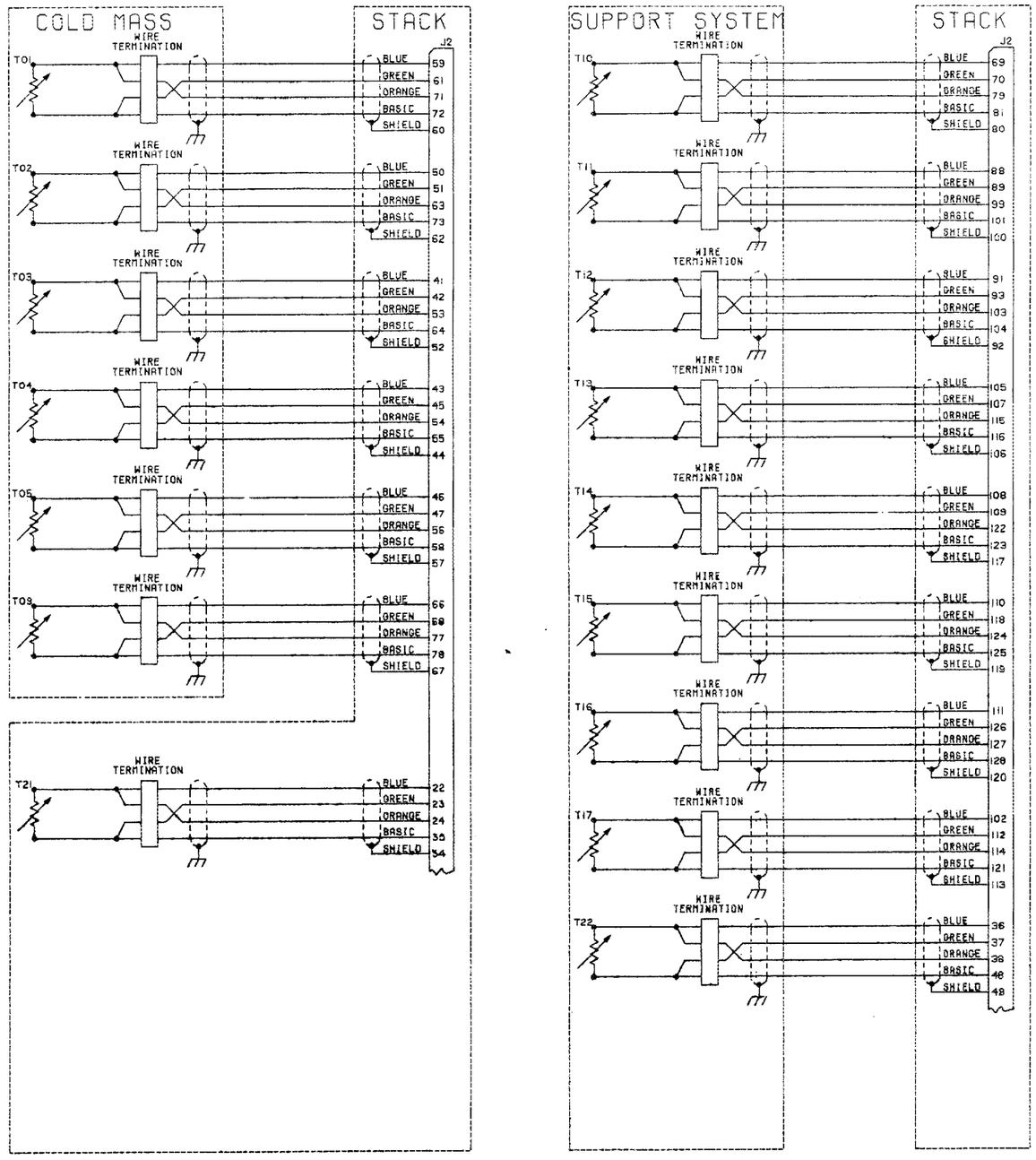

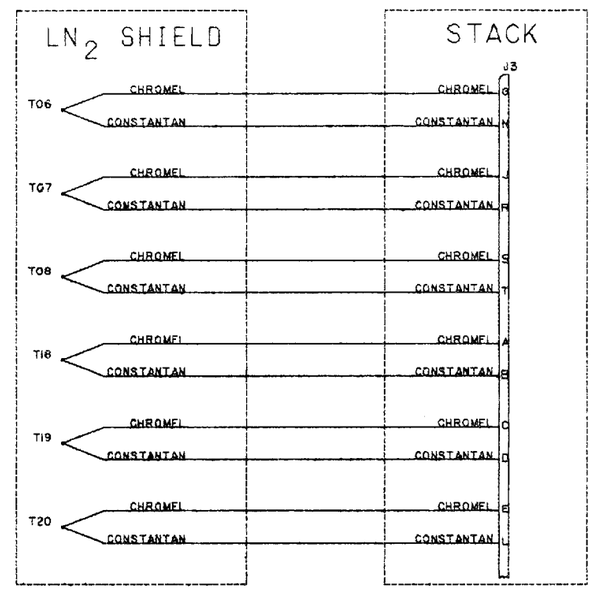

NOTES:

2.1 CONNECTIONS FOR T1 THRU T22 ARE SHOWN ON THIS SHEET.

2.2 MATING PLUGS ARE FURNISHED TO ORNL FOR ALL CONNECTORS SHOWN.

COMPUTERIZED REPRODUCIBLE

676.EBTP.11-38088.2.D.DD 4/16/81 1

APPROVED TITLE I

REF AL BOCH LETTER DATED MARCH 19, 1982

☐ SEE SEPARATE PARTS LIST

SEE D-70914 FOR ABBREVIATION, CODE AND SYMBOL REQUIREMENTS

SEE D-72962 FOR STANDARD MANUFACTURING AND INSTALLATION REQUIREMENTS

UNLESS OTHERWISE SPECIFIED ALL MACHINING SURFACES ✓

UNLESS OTHERWISE SPECIFIED DIMENSIONS ARE IN INCHES

TOLERANCES .X ±.1 .XX ±.03 .XXX ±.010

ANGULAR PER D-70902

MATL

PROD ENGR

CHECK

STRESS

DR ENGR

DESIGN

DRAWN R.RIBBK

CONTRACT NO.

GENERAL DYNAMICS
CONVAIR DIVISION
SAN DIEGO, CALIFORNIA

INSTRUMENTATION WIRING DIAGRAM
EBT-P DEVELOPMENT

SIZE E | FSCM NO. 14170 | DWG NO. D11-38088

SCALE NOTED | SHEET 2 OF

SEC. CLASS | TYPE | LEVEL | CONT | GROUP | DISTR | REPRO | PACKAGE NO. | REL

DWG NO. D11-38088 SHT 2 REV A

SHEET NO. | REV LTR

A-113/A-114

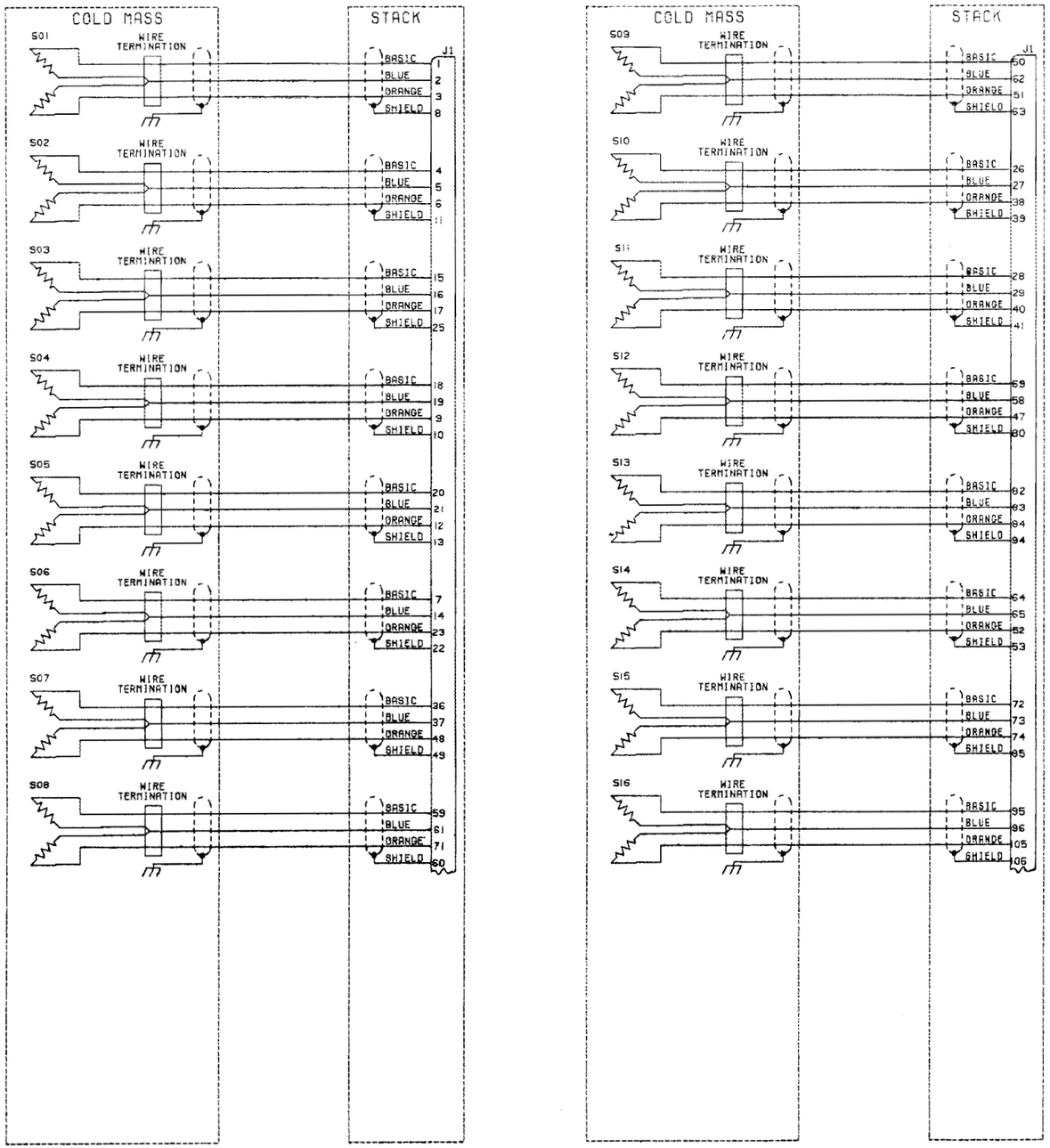

NOTES:

3.1 CONNECTIONS FOR S1 THRU S16 ARE SHOWN ON THIS SHEET.

3.2 MATING PLUGS ARE FURNISHED TO ORNL FOR ALL CONNECTORS SHOWN.

COMPUTERIZED REPRODUCIBLE

607-0.499.76L2995.01.D.A 8/26//80 3

APPROVED TITLE I

REF AL BOCH LETTER DATED MARCH 19, 1982

SEE SEPARATE PARTS LIST

GENERAL DYNAMICS
CONVAIR DIVISION
SAN DIEGO, CALIFORNIA

INSTRUMENTATION WIRING DIAGRAM
EBT-P DEVELOPMENT

SIZE E | FSCH NO. 11470 | DWG NO. D11-38088 | SHEET 3 OF

SCALE DTSD

A-115/A-116

REVISIONS											
ZONE	REV	DESCRIPTION	DATE	APPROVED	ZONE	REV	DESCRIPTION	DATE	APPROVED	ZONE	REV	DESCRIPTION	DATE	APPROVED

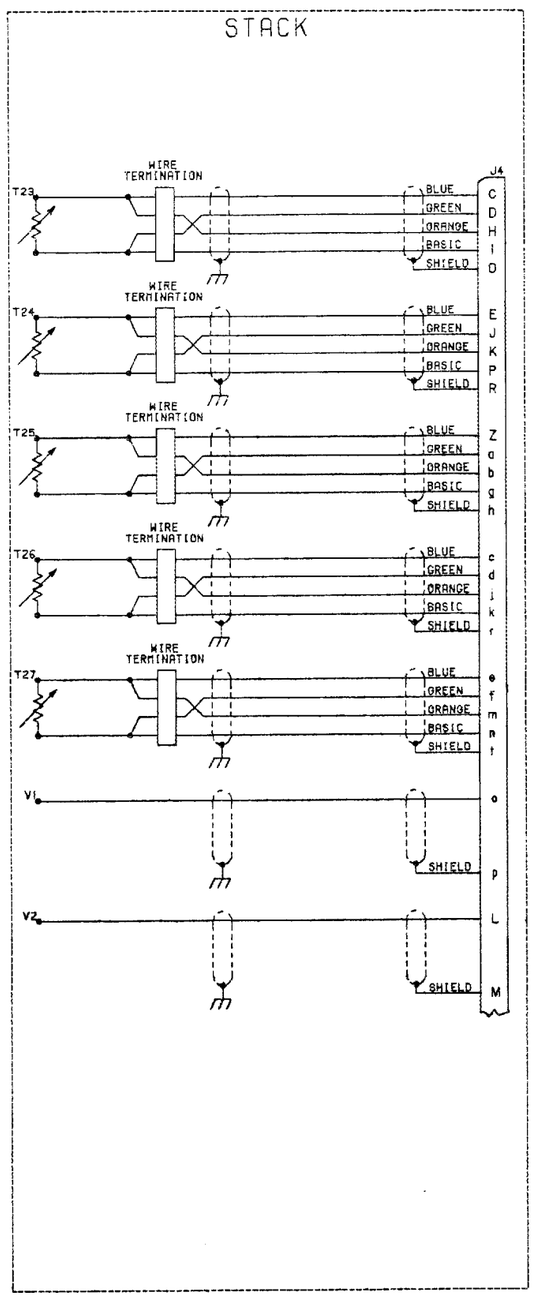

NOTES:

4.1 CONNECTIONS FOR T23 THRU T27 AND V1 AND V2 ARE SHOWN ON THIS SHEET.
4.2 MATING PLUGS ARE FURNISHED TO ORNL FOR ALL CONNECTORS SHOWN.

COMPUTERIZED REPRODUCIBLE
676.EBTP.11-38088.2.D.OD 4/16//81 1

APPROVED TITLE I

REF AL BOCH LETTER DATED
MARCH 19, 1982

☐ SEE SEPARATE PARTS LIST

SEE D-70314 FOR ABBREVIATION, CODE AND SYMBOL REQUIREMENTS
SEE D-70902 FOR STANDARD MANUFACTURING AND INSTALLATION REQUIREMENTS
UNLESS OTHERWISE SPECIFIED
ALL MACHINED SURFACES ✓

UNLESS OTHERWISE SPECIFIED DIMENSIONS ARE IN INCHES
TOLERANCES
.X ±.1 .XX ±.03 .XXX ±.010
ANGULAR PER D-70902

MATL
PROD ENGR
SEC. CLASS

CHECK
STRESS
GR ENGR
DESIGN
DRAWN R.RISON
CONTRACT NO.

GENERAL DYNAMICS
CONVAIR DIVISION
SAN DIEGO, CALIFORNIA

INSTRUMENTATION
WIRING DIAGRAM
EBT-P DEVELOPMENT

SIZE E FSCM NO. 114176 DWG NO. D11-38088
SCALE NOT ED SHEET 4 OF 4

TYPE | LEVEL | CONT | GROUP | SUBTYP | SPND | PACKAGE NO. | REL

SHEET NO.
REV LTR

D11-38088 SHT 4 REV

A–117/A–118

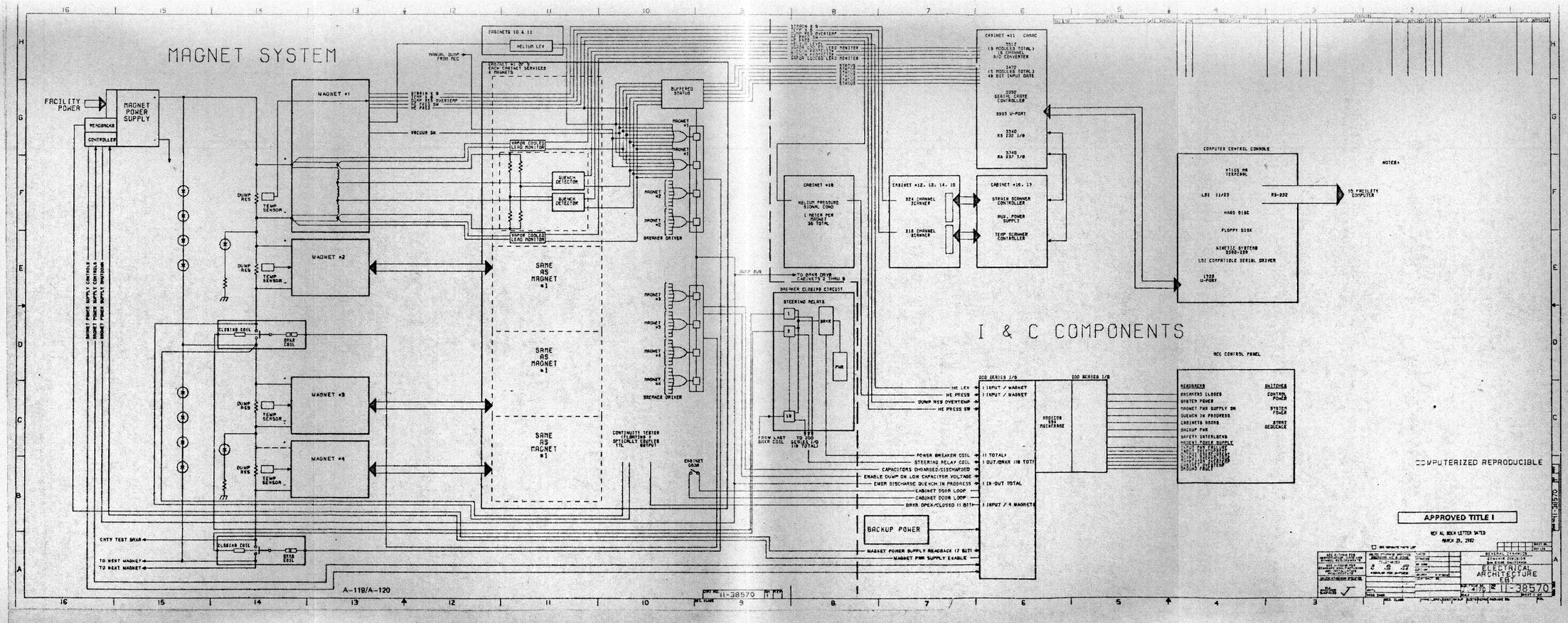
MAGNET SYSTEM
FACILITY POWER
MAGNET POWER SUPPLY
MEASURING
CONTROLLER
MAGNET #1
MAGNET #2
MAGNET #3
MAGNET #4
DUMP RES
TEMP SENSOR
CLOSING COIL
DUMP RES
TEMP SENSOR
CLOSING COIL
MAGNET POWER SUPPLY CONTROLS
MAGNET POWER SUPPLY CONTROLS
MAGNET POWER SUPPLY MONITORS
CNTY TEST DRVR
TO NEXT MAGNET
TO NEXT MAGNET
A-119/A-120
CABINETS 10,8,11
HELIUM LEV
MANUAL DUMP FROM REC
CABINET 9 & 12
HIGH CABINET SERVICES
4 MAGNETS
VAPOR COOLED LEAD MONITOR
QUENCH DETECTOR
QUENCH DETECTOR
VAPOR COOLED LEAD MONITOR
SAME AS MAGNET #1
SAME AS MAGNET #1
SAME AS MAGNET #1
CONTINUITY TESTER (FLOWTRON / OPTICALLY ISOLATED TTL)
CABINET DOOR
BUFFERED STATUS
MAGNET #1
MAGNET #2
MAGNET #3
MAGNET #4
BREAKER DRIVER
BREAKER DRIVER
DUMP BUS
CABINET #10
HELIUM PRESSURE SIGNAL COND
1 METER PER MAGNET 36 TOTAL
TO BRKR DRVR CABINETS 3 THRU 8
BREAKER CLOSING CIRCUIT
STEERING RELAYS
DRVR
PWR
FROM LAST BRKR COIL
TO 2ND BRKR IN TOTAL
CABINET #11 CAMAC
1012
18 MODULES TOTAL)
18 DIGITAL CONVERTER
1477
15 MODULES TOTAL)
48 BIT INPUT CARD
3200
SERIAL/PARALLEL CONTROLLER
3933 U-PORT
3240
RS 232 I/O
3240
RS 232 I/O
CABINET #12, 13, 14, 15
924 CHANNEL SCANNER
918 CHANNEL SCANNER
CABINET #16, 17
STRIPS SCANNER CONTROLLER
MUX. POWER SUPPLY
TEMP SCANNER CONTROLLER
COMPUTER CONTROL CONSOLE
VT100 PWR TERMINAL
LSI 11/23
HARD DISK
FLOPPY DISK
WINCHESTER SCSI-SCM
LSI COMPATIBLE SERIAL DRIVER
1200 U-PORT
RS-232
TO FACILITY COMPUTER
NOTES:
I & C COMPONENTS
HC LEV
HC PRESS
DUMP RES OVERTEMP
HC PRESS SP
POWER BREAKER COIL
STEERING RELAY COIL
CAPACITORS DISCHARGED/DISCHARGED
ENABLE DUMP ON LOW CAPACITOR VOLTAGE
EMER DISCHARGE QUENCH IN PROGRESS
CABINET DOOR LOOP
CABINET DOOR LOOP
BRKR OPEN/CLOSED (1 BIT)
BACKUP POWER
MAGNET POWER SUPPLY READBACK (7 BIT)
MAGNET PWR SUPPLY ENABLE
200 SERIES I/O
1 INPUT / MAGNET
1 INPUT / MAGNET
11 TOTAL)
1 OUT/BRKR (18 TOT)
1 IN-OUT TOTAL
1 INPUT / 4 MAGNETS
200 SERIES I/O
ADDECON 583 MAINFRAME
MCC CONTROL PANEL
MEASURING
BREAKERS CLOSED
SYSTEM POWER
MAGNET PWR SUPPLY ON
QUENCH IN PROGRESS
CABINETS DOORS
BACKUP PWR
SAFETY INTERLOCKS
SWITCHES
CONTROL POWER
SYSTEM POWER
STROBE BEACONS
COMPUTERIZED REPRODUCIBLE
APPROVED TITLE I
REF AL BOOK LETTER DATED
MARCH 25, 1982
ELECTRICAL ARCHITECTURE
EB1
11-38570
11-38210

PARTS LIST

0-70916 REQUIRED FOR ABBREVIATION, CODE AND SYMBOL INTERPRETATION

CONVAIR DIVISION OF GENERAL DYNAMICS
SAN DIEGO, CALIFORNIA

PDA: PL 11-38001 | REV LTR: -

TITLE: MAGNET ASSEMBLY ~ EBT-P PROTOTYPE

PADR | RELEASE/DATE | CODE IDENT NO.: 14170 | SH 1 OF 1 SHS

DOC TYPE | DOC OPT | DOC CONT | GROUP 692-0 | REPRO CODE | CONTRACT NO. | UNDIM DWG

DRAFTSMAN 7/10/81 PGYK | DESIGNER / / | GR ENGR / / | STRESS / / | PROD. ENGR / / | MATERIAL / / | CHECKER / / | / / | / / | / / | / /

PAGE | DISTRIBUTION CODE | PACKAGE NO. | NOTE SYMBOL: * D - DOCUMENT NO. E - END ITEM G - GENERAL NOTE L - LIMIT M - MATERIAL N - NOMENCLATURE R - REF DESIG T - TYPE DESIG/VALUE U - USAGE DATA V - VENDOR ITEM

REQUIREMENTS PER ASSY/INSTL -3	-2	-1	UNIT OF MEAS	FIND NO.	CODE IDENT NO.	PART OR IDENTIFYING NUMBER	NOMENCLATURE OR DESCRIPTION	ZONE LTR	ZONE NO.	NOTE SYM *	NOTES
		X				-1	MAGNET ASSY	A	5		
	X	1				-2	SIDE PLATE ASSY	F	7		
X		1				-3	SUB ASSY	A	25		
6						11-38083-1	BOSS	A	24		
1						11-38060-1	VACUUM VESSEL	D	24		
1						11-38040-1	LN_2 COLD WALL ASSY	D	26		
	1					11-38064-1	STACK PLATE	H	7		
	1					11-38063-4	SIDE PLATE	G	7		
	1					11-38067-3	SUPPORT BAR	G	8		
6						11-38081-1	BOLT	A	25		
6						NAS1587-12C	WASHER				
		3				STD 197 B	CONST. BALL	C	6	V	MDAC FURNISHED PART
		1				86-18004-001	IDENT PLATE	E	6		
AR	AR	AR				ER316L	ELECTRODE				NOTE 6
AR	AR	AR				E316L	ELECTRODE				NOTE 6
AR						MS20995-C47	LOCKWIRE				
		AR				0-75052	EPOXY ENAMEL				
		DOC				M933540	SPEC				PRELIMINARY
		↑				MIL-STD-278	SPEC				
						MIL-STD-248	SPEC				
						MIL-I-6866	SPEC				
						0-70042	SPEC				
						GDC-EBT-81-011	TEST PLAN				
						0-79054	SPEC				
		↓				MIL-E-19933	SPEC				
		DOC				MIL-E-22200/2	SPEC				

6501 (2-76)

PARTS LIST

0-70916 REQUIRED FOR ABBREVIATION, CODE AND SYMBOL INTERPRETATION

CONVAIR DIVISION OF GENERAL DYNAMICS
SAN DIEGO, CALIFORNIA

PDA: PL 11-38002 | REV LTR: –

TITLE: COLD MASS ASSEMBLY ~ EBT-P PROTOTYPE

PADR | RELEASE/DATE | CODE IDENT NO. 14170 | SH 1 OF 1 SHS

DOC TYPE | DOC OPT | DOC CONT | GROUP 692-D | REPRO CODE | CONTRACT NO. | UNDIM DWG

DRAFTSMAN / / | DESIGNER / / | GR ENGR / / | STRESS / / | PROD. ENGR / / | MATERIAL / / | CHECKER / / | / / | / / | / / | / /

PAGE | DISTRIBUTION CODE | PACKAGE NO. | NOTE SYMBOL: * D - DOCUMENT NO. E - END ITEM G - GENERAL NOTE L - LIMIT M - MATERIAL N - NOMENCLATURE R - REF DESIG T - TYPE DESIG/VALUE U - USAGE DATA V - VENDOR ITEM

REQUIREMENTS PER ASSY/INSTL	UNIT OF MEAS	FIND NO.	CODE IDENT NO.	PART OR IDENTIFYING NUMBER	NOMENCLATURE OR DESCRIPTION	ZONE LTR	ZONE NO.	NOTE SYM *	NOTES
-1				-1	COLD MASS ASSY	A	6		
3				-2	SUPPORT BLOCKS	B	7	M	.750 x 3.6 x 5.1 304L SST, ASTM-A-240
1				11-38006-1	WINDING ASSY	C	4		
1				11-38005-1	OUTER RING	F	5		
1				11-38003-1	HELIUM SUPPLY TUBE	G	4		
DOC				0-73517	TEST SPEC				
↑				MIL-I-68866	INSPECT. SPEC				
				MIL-STD-248	WELD SPEC				
				MIL-STD-278	WELD SPEC				
				MIL-E-19933	WELD SPEC				
↓				MIL-E-22200/12	WELD SPEC				
DOC				0-70042	IDENT SPEC				
									PRELIMINARY
AR				ER316L	ELECTRODE				
AR				E316L	ELECTRODE				

6501 (2-76)

PARTS LIST

0-70916 REQUIRED FOR ABBREVIATION, CODE AND SYMBOL INTERPRETATION

CONVAIR DIVISION OF GENERAL DYNAMICS
SAN DIEGO, CALIFORNIA

PDA: PL11-38005 | REV LTR: –

TITLE: COLD MASS OUTER RING ~ EBT-P PROTOTYPE

PADR | RELEASE/DATE | CODE IDENT NO. 14170 | SH 1 OF 1 SHS

DOC TYPE	DOC OPT	DOC CONT	GROUP 692.0	REPRO CODE	CONTRACT NO.	UNDIM DWG

DRAFTSMAN / /	DESIGNER 9/20/81	GR ENGR / /	STRESS / /	PROD. ENGR / /	MATERIAL / /	CHECKER / /	/ /	/ /	/ /	/ /

PAGE | DISTRIBUTION CODE | PACKAGE NO. | NOTE SYMBOL: * D - DOCUMENT NO. E - END ITEM G - GENERAL NOTE L - LIMIT M - MATERIAL N - NOMENCLATURE R - REF DESIG T - TYPE DESIG/VALUE U - USAGE DATA V - VENDOR ITEM

REQUIREMENTS PER ASSY/INSTL				UNIT OF MEAS	FIND NO.	CODE IDENT NO.	PART OR IDENTIFYING NUMBER	NOMENCLATURE OR DESCRIPTION	ZONE LTR	ZONE NO.	NOTE SYM *	NOTES
		-5	-1									
			X				-1	RING ASSEMBLY				
		X	1				-5	NECK ASSEMBLY				
			1				-2	RING HALF			M	.500×9.0×40.0 316L SST; ASTM-A-240
			1				-3	RING HALF			M	.500×9.0×40.0 316L SST; ASTM-A-240
		1					-4	PLATE			M	.500×8.5×8.5 316L SST; ASTM-A-240
		1				10633	25005	REDUCER			V	8×6
		AR	AR				ER 316 L	FILLER WIRE				
		DOC	DOC				0-70042	IDENT SPEC				
		⇧	⇧				0-73517	TEST SPEC				
							MIL-I-6866	INSP SPEC				
							MIL-STD-248	WELD SPEC				
		⇩	⇩				MIL-STD-278	WELD SPEC				
		DOC	DOC				MIL-E-19933	WELD SPEC				
		DOC	DOC				MIL-E-22200/2	WELD SPEC				

PRELIMINARY

6501 (2-76)

PARTS LIST

0-70916 REQUIRED FOR ABBREVIATION, CODE AND SYMBOL INTERPRETATION

CONVAIR DIVISION OF GENERAL DYNAMICS
SAN DIEGO, CALIFORNIA

PDA: PL 11-38006 | REV LTR: -

TITLE: WINDING ASSY-EBT-P PROTOTYPE

PADR | RELEASE/DATE | CODE IDENT NO. 14170 | SH 1 OF 4 SHS

DOC TYPE | DOC OPT | DOC CONT | GROUP | REPRO CODE | CONTRACT NO. | UNDIM DWG

DRAFTSMAN / / | DESIGNER 8/17/81 N. HILL | GR ENGR / / | STRESS / / | PROD. ENGR / / | MATERIAL / / | CHECKER / / | / / | / / | / / | / /

PAGE | DISTRIBUTION CODE | PACKAGE NO. | NOTE SYMBOL: * D - DOCUMENT NO. E - END ITEM G - GENERAL NOTE L - LIMIT M - MATERIAL N - NOMENCLATURE R - REF DESIG T - TYPE DESIG/VALUE U - USAGE DATA V - VENDOR ITEM

REQUIREMENTS PER ASSY/INSTL			-1	UNIT OF MEAS	FIND NO.	CODE IDENT NO.	PART OR IDENTIFYING NUMBER	NOMENCLATURE OR DESCRIPTION	ZONE LTR	ZONE NO.	NOTE SYM *	NOTES
			X				-1	WINDING ASSY	E	7		
			A/R				-2	WINDING INSULATION				NOMEX TAPE .125 WIDE X .007 THICK
												NO. 70 HOF 25X WESTERN
												FILAMENT INC. 4680 SAN FERNANDO
												RD., GLENDALE, CA. 91204. APPROX
												6585 YDS/ASSY.
			4				-3	HOSE CLAMP				MS 35842-9 MUST BE NON MAGNETIC
			A/R				11-38007-1	SUPER CONDUCTOR				APPROX 2550 YARDS/ASSY
			6				11-38010-1	SIDEWALL INSUL. SLOTTED				
			2				11-38010-2	SIDEWALL INSUL. SOLID				
			2				11-38010-3	SIDEWALL INSUL. SLOTTED				
			1				11-38010-4	SIDEWALL INSUL. SOLID				
			2				11-38010-5	SIDEWALL INSUL. SLOTTED				
			118				11-38010-6	SIEWALL INSUL. CORNER				BOTTOM
			86				11-38010-7	SIDEWALL INSUL. CORNER				TOP
			2				11-38010-10	SIDEWALL INSUL SLOTTED				
			1				11-38011-1	CLAMP HALF				
			1				11-38011-2	CLAMP HALF				
			2				11-38011-3	CLAMP HALF				PRELIMINARY
			1				11-38011-4	INSULATOR				
			2				11-38012-1	INSUL - LAYER END				
			2				11-38012-2	" " "				
			2				11-38012-3	" " "				
			2				11-38012-4	" " "				
			2				11-38012-5	" " "				
			2				11-38012-6	" " "				
			2				11-38012-7	" " "				
			2				11-38012-8	INSUL - LAYER END				

6501 (2-76)

PARTS LIST

0-70916 REQUIRED FOR ABBREVIATION, CODE AND SYMBOL INTERPRETATION

CONVAIR DIVISION OF GENERAL DYNAMICS
SAN DIEGO, CALIFORNIA

PDA: PL 11-38006 | REV LTR

TITLE: WINDING ASSY-EBT-P-PROTOTYPE

PADR | RELEASE/DATE | CODE IDENT NO. 14170 | SH 2 OF ___ SHS

DOC TYPE	DOC OPT	DOC CONT	GROUP		REPRO CODE	CONTRACT NO.	UNDIM DWG

DRAFTSMAN / /	DESIGNER 8/17/81 N. HILL	GR ENGR / /	STRESS / /	PROD. ENGR / /	MATERIAL / /	CHECKER / /	/ /	/ /	/ /	/ /

PAGE | DISTRIBUTION CODE | PACKAGE NO. | NOTE SYMBOL: * D - DOCUMENT NO. E - END ITEM G - GENERAL NOTE L - LIMIT M - MATERIAL N - NOMENCLATURE R - REF DESIG T - TYPE DESIG/VALUE U - USAGE DATA V - VENDOR ITEM

REQUIREMENTS PER ASSY/INSTL				UNIT OF MEAS	FIND NO.	CODE IDENT NO.	PART OR IDENTIFYING NUMBER	NOMENCLATURE OR DESCRIPTION	ZONE LTR	ZONE NO.	NOTE SYM *	NOTES
			-1									
			2				11-38012-9	INSUL - LAYER END				
			2				11-38012-10					
			2				11-38012-11					
			2				11-38012-12					
			2				11-38012-13					
			2				11-38012-14					
			2				11-38012-15					
			2				11-38012-16					
			2				11-38012-17					
			2				11-38012-18					
			2				11-38012-19					
			2				11-38012-20					
			2				11-38012-21					
			2				11-38012-22					
			2				11-38012-23					
			2				11-38012-24					
			2				11-38012-25					
			2				11-38012-26					PRELIMINARY
			2				11-38012-27					
			2				11-38012-28					
			2				11-38012-30					
			2				11-38012-31					
			2				11-38012-32	INSUL - LAYER END				
			32				11-38012-35	INSUL-RAMP				
			30				11-38012-36	INSUL - WEDGE				
			A/R				11-38012-37	INSUL - SPLICE				
			132				11-38012-38	INSUL-SPACER				
			1				11-38013-1	BOBBIN ASSY				

6501 (2-76)

PARTS LIST

0-70916 REQUIRED FOR ABBREVIATION, CODE AND SYMBOL INTERPRETATION

CONVAIR DIVISION OF GENERAL DYNAMICS
SAN DIEGO, CALIFORNIA

PDA: PL 11-38006 | REV LTR:

TITLE: WINDING ASSY -EBT-P PROTOTYPE

DOC TYPE	DOC OPT	DOC CONT	GROUP	REPRO CODE	CONTRACT NO.	UNDIM DWG	PADR	RELEASE/DATE	CODE IDENT NO.	SH 3 OF ___ SHS
									14170	

DRAFTSMAN	DESIGNER	GR ENGR	STRESS	PROD. ENGR	MATERIAL	CHECKER				
/ /	/ /	/ /	/ /	/ /	/ /	/ /	/ /	/ /	/ /	/ /

PAGE | DISTRIBUTION CODE | PACKAGE NO.

NOTE SYMBOL: * D - DOCUMENT NO. E - END ITEM G - GENERAL NOTE L - LIMIT M - MATERIAL N - NOMENCLATURE R - REF DESIG T - TYPE DESIG/VALUE U - USAGE DATA V - VENDOR ITEM

REQUIREMENTS PER ASSY/INSTL	UNIT OF MEAS	FIND NO.	CODE IDENT NO.	PART OR IDENTIFYING NUMBER	NOMENCLATURE OR DESCRIPTION	ZONE LTR	ZONE NO.	NOTE SYM *	NOTES
1				11-38016-1	GROUND INSUL-SLOTTED				
1				11-38016-2	GROUND INSUL-SLOTTED				
1				11-38016-3	GROUND INSUL-SOLID				
1				11-38016-4	GROUND INSUL-SLOTTED				
1				11-38016-5	GROUND INSUL-SLOTTED				
1				11-38016-6	GROUND INSUL PERF				
1				11-38016-7	GROUND INSUL-SLOTTED				
1				11-38016-8					
1				11-38016-9					
1				11-38016-10					
1				11-38016-11					
1				11-38016-12					
1				11-38016-13					
1				11-38016-14					PRELIMINARY
2				11-38016-15					
2				11-38016-16					
2				11-38016-17					
2				11-38016-18					
2				11-38016-19					
2				11-38016-20					
2				11-38016-21					
2				11-38016-22					
1				11-38016-23					
1				11-38016-24					
1				11-38016-25					
1				11-38016-26					
1				11-38016-27					
1				11-38016-28					
1				11-38016-29					
1				11-38016-30	GROUND INSUL-SLOTTED				

6501 (2-76)

PARTS LIST

0-70916 REQUIRED FOR ABBREVIATION, CODE AND SYMBOL INTERPRETATION

CONVAIR DIVISION OF GENERAL DYNAMICS
SAN DIEGO, CALIFORNIA

PDA: PL 11-38006 | REV LTR:

TITLE: WINDING ASSY-EBT-P - PROTOTYPE

PADR | RELEASE/DATE | CODE IDENT NO. 14170 | SH 4 OF ___ SHS

DOC TYPE | DOC OPT | DOC CONT | GROUP | REPRO CODE | CONTRACT NO. | UNDIM DWG

DRAFTSMAN / / | DESIGNER 9/23/81 N.HILL | GR ENGR / / | STRESS / / | PROD. ENGR / / | MATERIAL / / | CHECKER / / | / / | / / | / / | / /

PAGE | DISTRIBUTION CODE | PACKAGE NO.

NOTE SYMBOL: * D - DOCUMENT NO. E - END ITEM G - GENERAL NOTE L - LIMIT M - MATERIAL N - NOMENCLATURE R - REF DESIG T - TYPE DESIG/VALUE U - USAGE DATA V - VENDOR ITEM

REQUIREMENTS PER ASSY/INSTL			-1	UNIT OF MEAS	FIND NO.	CODE IDENT NO.	PART OR IDENTIFYING NUMBER	NOMENCLATURE OR DESCRIPTION	ZONE LTR	ZONE NO.	NOTE SYM *	NOTES
			2				11-38021-1	LEAD LUG ASSY				
			A/R					SOLDER				97.5% LEAD, 2.5% SILVER
			A/R					SOLDER				TIN-LEAD ALLOY ASTM GRADE 63B PER
												QQ-S-571
			A/R					FLUX				COMPOSITION IN PROPORTIONS AS FOLLOWS:
												ZINC CHLORIDE - 383 GM, AMMONIUM
												CHLORIDE - 38 GM, HYDROCHLORIC ACID
												- 40 ML, WATER - 100 ML.
			2				NAS 1004-40H	BOLT				
			2				NAS 1004-56H	BOLT				
			4				NAS 509-4C	NUT				
			8				AN960C416	WASHER				
			A/R				MS20995C32	LOCKWIRE				
			A/R				DDD-C-301	CHEESECLOTH				
			A/R				0-79054-1	SOLVENT				
			A/R				0-00089-1	CEMENT				
			A/R				0-06139-1	ADHESIVE				
			A/R				0-00337-2	SOLDER				
			A/R				-4	TAPE 4 MIL X 1.0X2.0				PERMACEL NO 222, JOHNSON & JOHNSON
			4				-5	CABLE				M 81381/19-30-9, 84.0 LONG (.050 DIA)
			4				-6	SHRINK SLEEVE				M 23053/12-309-1, .6 LONG
			DOC				MS 33540	SPEC				
			DOC				QQS-571	SPEC				
			DOC				0-70042	SPEC				
			DOC				0-79129	SPEC				

PRELIMINARY

6501 (2-76)

PARTS LIST

0-70916 REQUIRED FOR ABBREVIATION, CODE AND SYMBOL INTERPRETATION

CONVAIR DIVISION OF GENERAL DYNAMICS
SAN DIEGO, CALIFORNIA

PDA: PL 11-38010 | REV LTR

TITLE: INSULATION-SIDE WALL

PADR | RELEASE/DATE | CODE IDENT NO. 14170 | SH 1 OF 1 SHS

DOC TYPE | DOC OPT | DOC CONT | GROUP | REPRO CODE | CONTRACT NO. | UNDIM DWG

DRAFTSMAN / / | DESIGNER 8/13/71 N. HILL | GR ENGR / / | STRESS / / | PROD. ENGR / / | MATERIAL / / | CHECKER / / | / / | / / | / / | / /

PAGE | DISTRIBUTION CODE | PACKAGE NO.

NOTE SYMBOL: * D - DOCUMENT NO. E - END ITEM G - GENERAL NOTE L - LIMIT M - MATERIAL N - NOMENCLATURE R - REF DESIG T - TYPE DESIG/VALUE U - USAGE DATA V - VENDOR ITEM

REQUIREMENTS PER ASSY/INSTL -9	-5	-4	-2	UNIT OF MEAS	FIND NO.	CODE IDENT NO.	PART OR IDENTIFYING NUMBER	NOMENCLATURE OR DESCRIPTION	ZONE LTR	ZONE NO.	NOTE SYM *	NOTES
							-1	INSULATION, SLOTTED			*	MAKE FROM 11-38009-1
			X				-2	INSULATION ASSY			*	
							-3	INSULATION, SLOTTED			*	MAKE FROM 11-38009-1
		X					-4	INSULATION ASSY			*	
	X						-5	INSULATION ASSY			*	
							-6	2.0X2.0 TAPE				PERMACEL NO 222 (2 MIL KAPTON,
							-7	1.0X1.0 TAPE				SILICONE ADHESIVE) JOHNSON & JOHNSON
	4		1				-8	1.0X4.6 TAPE				6350 ALTURA BLVD. PO BOX 5420
4		1					-14	1.0X3.9 TAPE				BUENA PARK, CA. 90620, 714-523-7531
X							-9	INSULATION ASSY			*	
			1				-10	INSULATION, SOLID				.020±.003 x 29.0 x 29.0 NEMA G-10 CR
		1					-11	INSULATION, SOLID				.020±.003 x 28.0 x 28.0 NEMA G-10 CR
	4						-12	INSULATION, SLOTTED				MAKE FROM 11-38009-1
4							-13	INSULATION, SLOTTED				MAKE FROM 11-38009-1
											*	FOR REQUIREMENTS SEE 11-38006-1

PRELIMINARY

6501 (2-76)

PARTS LIST

0-70916 REQUIRED FOR ABBREVIATION, CODE AND SYMBOL INTERPRETATION

CONVAIR DIVISION OF GENERAL DYNAMICS
SAN DIEGO, CALIFORNIA

PDA: PL 11-38011 | REV LTR

TITLE: HOUSING - CONDUCTOR LEAD - EBT-P - PROTOTYPE

PADR | RELEASE/DATE | CODE IDENT NO. 14170 | SH 1 OF 1 SHS

DOC TYPE	DOC OPT	DOC CONT	GROUP		REPRO CODE	CONTRACT NO.	UNDIM DWG

DRAFTSMAN / /	DESIGNER 8/25/81 N. HILL	GR ENGR / /	STRESS / /	PROD. ENGR / /	MATERIAL / /	CHECKER / /	/ /	/ /	/ /	/ /

PAGE | DISTRIBUTION CODE | PACKAGE NO.

NOTE SYMBOL: * D - DOCUMENT NO. E - END ITEM G - GENERAL NOTE L - LIMIT M - MATERIAL N - NOMENCLATURE R - REF DESIG T - TYPE DESIG/VALUE U - USAGE DATA V - VENDOR ITEM

REQUIREMENTS PER ASSY/INSTL				UNIT OF MEAS	FIND NO.	CODE IDENT NO.	PART OR IDENTIFYING NUMBER	NOMENCLATURE OR DESCRIPTION	ZONE LTR	ZONE NO.	NOTE SYM *	NOTES
							-1	CLAMP				1.000x4.1x8.6 NEMA G-10 CR
							-2	CLAMP				.875 x 1.6 x 3.1 NEMA G-10 CR
							-3	CLAMP				1.250 x 2.2 x 3.1 NEMA G-10 CR
							-4	INSULATOR				.125x 3.1 x 4.4 NEMA G-10 CR
							-5	INSULATOR				.3125x .8 x 2.6 NEMA G-10 CR

PRELIMINARY

6501 (2-76)

PARTS LIST

D-70916 REQUIRED FOR ABBREVIATION, CODE AND SYMBOL INTERPRETATION

CONVAIR DIVISION OF GENERAL DYNAMICS
SAN DIEGO, CALIFORNIA

PDA: PL 11-38012 | REV LTR:

TITLE: INSULATION-LAYER END-EBT-P-PROTOTYPE

DOC TYPE	DOC OPT	DOC CONT	GROUP	REPRO CODE	CONTRACT NO.	UNDIM DWG	PADR	RELEASE/DATE	CODE IDENT NO.	SH 1 OF 2 SHS
									14170	

DRAFTSMAN	DESIGNER	GR ENGR	STRESS	PROD. ENGR	MATERIAL	CHECKER			
/ /	8/24/81 N. HILL	/ /	/ /	/ /	/ /	/ /	/ /	/ /	/ /

PAGE | DISTRIBUTION CODE | PACKAGE NO.

NOTE SYMBOL: * D - DOCUMENT NO. E - END ITEM G - GENERAL NOTE L - LIMIT M - MATERIAL N - NOMENCLATURE R - REF DESIG T - TYPE DESIG/VALUE U - USAGE DATA V - VENDOR ITEM

REQUIREMENTS PER ASSY/INSTL	UNIT OF MEAS	FIND NO.	CODE IDENT NO.	PART OR IDENTIFYING NUMBER	NOMENCLATURE OR DESCRIPTION	ZONE LTR	ZONE NO.	NOTE SYM *	NOTES
2				-1	WEDGE				.128 ± .003 X .22 X 55.0 NEMA G-10 CR
2				-2					56.0
2				-3					56.0
2				-4					56.0
2				-5					57.0
2				-6					57.0
2				-7					58.0
2				-8					58.0
2				-9					58.0
2				-10					59.0
2				-11					59.0
2				-12					60.0
2				-13					60.0
2				-14					60.0
2				-15					61.0
2				-16					61.0
2				-17					62.0
2				-18					62.0
2				-19					62.0
2				-20					63.0
2				-21					63.0
2				-22					64.0
2				-23					64.0
2				-24					64.0
2				-25					65.0
2				-26					65.0
2				-27					66.0
2				-28					66.0
2				-29					66.0
2				-30	WEDGE				.128 ± .003 X .22 67.0 NEMA G-10 CR

PRELIMINARY

6501 (2-76)

11-38012-1

A-130

APPENDIX A

PARTS LIST

G-70916 REQUIRED FOR ABBREVIATION, CODE AND SYMBOL INTERPRETATION

CONVAIR DIVISION OF GENERAL DYNAMICS
SAN DIEGO, CALIFORNIA

PDA: PL 11-38012 | REV LTR

TITLE: INSULATION-EBT-P-PROTOTYPE

PADR | RELEASE/DATE | CODE IDENT NO. 14170 | SH 2 OF ___ SHS

DOC TYPE	DOC OPT	DOC CONT	GROUP		REPRO CODE	CONTRACT NO.	UNDIM DWG

DRAFTSMAN / /	DESIGNER 8/24/81 N. HILL	GR ENGR / /	STRESS / /	PROD. ENGR / /	MATERIAL / /	CHECKER / /	/ /	/ /	/ /	/ /

PAGE | DISTRIBUTION CODE | PACKAGE NO.

NOTE SYMBOL: * D - DOCUMENT NO. E - END ITEM G - GENERAL NOTE L - LIMIT M - MATERIAL N - NOMENCLATURE R - REF DESIG T - TYPE DESIG/VALUE U - USAGE DATA V - VENDOR ITEM

REQUIREMENTS PER ASSY/INSTL	UNIT OF MEAS	FIND NO.	CODE IDENT NO.	PART OR IDENTIFYING NUMBER	NOMENCLATURE OR DESCRIPTION	ZONE LTR	ZONE NO.	NOTE SYM *	NOTES
				-31	WEDGE				.128±.003 X .22 X 67.0 NEMA G-10 CR
				-32	WEDGE				68.0
									43.0
									42.0
				-35	RAMP				2.0
				-36	FILLER				2.0
				-37	FILLER SPLICE				76.0
				-38	FILLER-TOP LAYER				.128±.003 X .22 X 86.0 NEMA G-10CR

PRELIMINARY

6501 (2-76)

PARTS LIST

0-70916 REQUIRED FOR ABBREVIATION, CODE AND SYMBOL INTERPRETATION

CONVAIR DIVISION OF GENERAL DYNAMICS
SAN DIEGO, CALIFORNIA

PDA: PL 11-38013 | REV LTR: —

TITLE: BOBBIN ASSEMBLY ~ EBT-P PROTOTYPE

PADR | RELEASE/DATE | CODE IDENT NO.: 14170 | SH 1 OF 1 SHS

DOC TYPE	DOC OPT	DOC CONT	GROUP	REPRO CODE	CONTRACT NO.	UNDIM DWG
			692-0			

DRAFTSMAN	DESIGNER	GR ENGR	STRESS	PROD. ENGR	MATERIAL	CHECKER	QA
/ / RSVK	/ /	/ / SOK	7/16/81	7/17/81	7/17/81	/ /	7/24/81

DISTRIBUTION CODE | PACKAGE NO. | NOTE SYMBOL: * D - DOCUMENT NO. E - END ITEM G - GENERAL NOTE L - LIMIT M - MATERIAL N - NOMENCLATURE R - REF DESIG T - TYPE DESIG/VALUE U - USAGE DATA V - VENDOR ITEM

REQUIREMENTS PER ASSY/INSTL	UNIT OF MEAS	FIND NO.	CODE IDENT NO.	PART OR IDENTIFYING NUMBER	NOMENCLATURE OR DESCRIPTION	ZONE LTR	ZONE NO.	NOTE SYM *	NOTES
-1				-1	BOBBIN ASSY	B	4		
1				-3	INNER RING	C	6	M	.750 × 9.0 × 60.0 316L SST, ASTM-A-240
2				-2	SIDE PLATE	F	6/7	M	1.00 × 35.0 × 35.0 316L SST, ASTM-A-240
DOC				MIL-I-68166	INSP SPEC				
				MIL-STD-248	WELD SPEC				
				MIL-STD-278	WELD SPEC				
				MIL-E-19933	WELD SPEC				
				0-70042	IDENT SPEC				
				MIL-E-22200/2	WELD SPEC				
DOC				0-73517	TEST SPEC				
AR				ER 316L	FILLER WIRE				

PRELIMINARY

6501 (2-76)

PARTS LIST

0-70916 REQUIRED FOR ABBREVIATION, CODE AND SYMBOL INTERPRETATION

CONVAIR DIVISION OF GENERAL DYNAMICS
SAN DIEGO, CALIFORNIA

PDA | PL 11-38016 | REV LTR

TITLE INSULATION - GROUND - EBT-P - PROTOTYPE

PADR | RELEASE/DATE | CODE IDENT NO. 14170 | SH 1 OF 2 SHS

DOC TYPE | DOC OPT | DOC CONT | GROUP | REPRO CODE | CONTRACT NO. | UNDIM DWG

DRAFTSMAN / / | DESIGNER 8/21/81 N. HILL | GR ENGR / / | STRESS / / | PROD. ENGR / / | MATERIAL / / | CHECKER / / | / / | / / | / / | / /

PAGE | DISTRIBUTION CODE | PACKAGE NO.

NOTE SYMBOL: * D - DOCUMENT NO. E - END ITEM G - GENERAL NOTE L - LIMIT M - MATERIAL N - NOMENCLATURE R - REF DESIG T - TYPE DESIG/VALUE U - USAGE DATA V - VENDOR ITEM

REQUIREMENTS PER ASSY/INSTL				UNIT OF MEAS	FIND NO.	CODE IDENT NO.	PART OR IDENTIFYING NUMBER	NOMENCLATURE OR DESCRIPTION	ZONE LTR	ZONE NO.	NOTE SYM *	NOTES
			-3									
							-1	SLOTTED SHEET				MAKE FROM 11-38009-1
							-2	SLOTTED SHEET				MAKE FROM 11-38009-1
			X				-3	SOLID SHEET ASSY				
							-4	SLOTTED SHEET				MAKE FROM 11-38009-1
							-5	SLOTTED SHEET				MAKE FROM 11-38009-1
							-6	PERFORATED SHEET				.005 x 8.5 X 60 TYPE 500 H KAPTON DUPONT
							-7	SLOTTED SHEET				MAKE FROM 11-38009-2
							-8					
							-9					
							-10					
							-11					
							-12					
							-13					
							-14					
							-15					
							-16					
							-17					
							-18					
							-19					
							-20					
							-21					
							-22					
							-23					
							-24					
							-25					
							-26					
							-27					
							-28					
							-29					
							-30	SLOTTED SHEET				MAKE FROM 11-38009-2

PRELIMINARY

6501 (2-76)

PARTS LIST

D-70916 REQUIRED FOR ABBREVIATION, CODE AND SYMBOL INTERPRETATION

CONVAIR DIVISION OF GENERAL DYNAMICS
SAN DIEGO, CALIFORNIA

PDA: PL 11-38016 | REV LTR

TITLE: INSULATION-GROUND-EBT-P-PROTOTYPE

DOC TYPE	DOC OPT	DOC CONT	GROUP	REPRO CODE	CONTRACT NO.	UNDIM DWG	PADR	RELEASE/DATE	CODE IDENT NO.	SH 2 OF ___ SHS
									14170	

DRAFTSMAN	DESIGNER	GR ENGR	STRESS	PROD. ENGR	MATERIAL	CHECKER				
/ /	8/21/81 N. HILL	/ /	/ /	/ /	/ /	/ /	/ /	/ /	/ /	/ /

PAGE | DISTRIBUTION CODE | PACKAGE NO.

NOTE SYMBOL: * D - DOCUMENT NO. E - END ITEM G - GENERAL NOTE L - LIMIT M - MATERIAL N - NOMENCLATURE R - REF DESIG T - TYPE DESIG/VALUE U - USAGE DATA V - VENDOR ITEM

REQUIREMENTS PER ASSY/INSTL			UNIT OF MEAS	FIND NO.	CODE IDENT NO.	PART OR IDENTIFYING NUMBER	NOMENCLATURE OR DESCRIPTION	ZONE		NOTE SYM *	NOTES
	-31	-3						TYP	NO.		
	X					-31	INSULATION ASSY				
		1				-32	INSULATION-SOLID				
	1	1				-33	TAPE, 1.0X 8.5				.020±.003 x 8.5 x 60.0 NEMA G-10 CR
	2					-34	TAPE, 1.0 x 1.0				PERMACEL # 222, JOHNSON & JOHNSON.
	1					-35	INSULATION, SOLID				.0625 x 29.0 x 29.0 NEMA G-10 CR

PRELIMINARY

6501 (2-76)

PARTS LIST

0-70916 REQUIRED FOR ABBREVIATION, CODE AND SYMBOL INTERPRETATION

CONVAIR DIVISION OF GENERAL DYNAMICS
SAN DIEGO, CALIFORNIA

PDA: PL11-38020 | REV LTR: –

TITLE: VAPOR COOLED CURRENT LEADS ~ EBT-P PROTOTYPE

PADR | RELEASE/DATE | CODE IDENT NO.: 14170 | SH 1 OF 1 SHS

DOC TYPE | DOC OPT | DOC CONT | GROUP: 692-0 | REPRO CODE | CONTRACT NO. | UNDIM DWG

DRAFTSMAN: PGVK 7/13/81 | DESIGNER: 7/13/81 | GR ENGR: / / | STRESS: 7/20/81 | PROD. ENGR: 7/23/81 | MATERIAL: 7/22/81 | CHECKER: / / | 7/20/81 | QA: 7/24/81 | / / | / /

PAGE | DISTRIBUTION CODE | PACKAGE NO.

NOTE SYMBOL: * D - DOCUMENT NO. E - END ITEM G - GENERAL NOTE L - LIMIT M - MATERIAL N - NOMENCLATURE R - REF DESIG T - TYPE DESIG/VALUE U - USAGE DATA V - VENDOR ITEM

REQUIREMENTS PER ASSY/INSTL			UNIT OF MEAS	FIND NO.	CODE IDENT NO.	PART OR IDENTIFYING NUMBER	NOMENCLATURE OR DESCRIPTION	ZONE LTR	ZONE NO.	NOTE SYM *	NOTES
	-2	-1									
		X				-1	LEAD ASSEMBLY	A	4		
	X	2				-2	COLLECTOR ASSEMBLY	G	4		
	1					-3	COLLECTOR	F	4	M	1.50 DIA × 12.0 ROD 110 COPPER; ASTM-B-133
	1					-4	LEAD	D	3	V	AMI STAINLESS STEEL NOTE 5
		1				-5	TUBE	E	3	M	1.54 DIA × 3.6 × .06 WALL G10-CR; NEMA GRADE
		1				-6	FLANGE	E	3	M	4.0 × 1.0 × 7.0 G10-CR; NEMA GRADE
	1					-7	TUBE	D	3	M	1.30 DIA × 12.3 × .06 WALL G10-CR; NEMA GRADE
										G	SUGGESTED SOURCES OF SUPPLY FOR G10-CR MATERIAL:
											- SPAULDING FIBRE CO. INC. SMYRNA TN 37167
											- WESTINGHOUSE ELECTRIC CORP. MICARTA DIVISION HAMPTON SC 29924.
	AR	AR					EPOXY				NOTE 6
	AR	AR					SOLDER				NOTE 10

PRELIMINARY

6501 (2-76)

P-6

PARTS LIST

0-70916 REQUIRED FOR ABBREVIATION, CODE AND SYMBOL INTERPRETATION

CONVAIR DIVISION OF GENERAL DYNAMICS
SAN DIEGO, CALIFORNIA

PDA: PL 11-38021 | REV LTR:

TITLE: LEAD LUG-EBT-P- PROTOTYPE

DOC TYPE	DOC OPT	DOC CONT	GROUP	REPRO CODE	CONTRACT NO.	UNDIM DWG	PADR	RELEASE/DATE	CODE IDENT NO.	SH 1 OF 1 SHS
									14170	

DRAFTSMAN	DESIGNER	GR ENGR	STRESS	PROD. ENGR	MATERIAL	CHECKER				
/ /	8/26/87 N. HILL	/ /	/ /	/ /	/ /	/ /	/ /	/ /	/ /	/ /

PAGE | DISTRIBUTION CODE | PACKAGE NO.

NOTE SYMBOL: * D - DOCUMENT NO. E - END ITEM G - GENERAL NOTE L - LIMIT M - MATERIAL N - NOMENCLATURE R - REF DESIG T - TYPE DESIG/VALUE U - USAGE DATA V - VENDOR ITEM

REQUIREMENTS PER ASSY/INSTL				UNIT OF MEAS	FIND NO.	CODE IDENT NO.	PART OR IDENTIFYING NUMBER	NOMENCLATURE OR DESCRIPTION	ZONE LTR	ZONE NO.	NOTE SYM *	NOTES
			-1				-1	LEAD LUG ASSY				
			1				-2	LUG				1.50X1.6X4.5 UNS NO 10100 COPPER, TEMPER 060 (ANNEALED) ASME B152-77, CERTS REQ'D.
			2				MS51830CA104	THREAD INSERT				(1/4-28, A286, .375 DEEP)
			DOC				0-70042	SPEC				
			DOC				MS 51835	SPEC				

PRELIMINARY

6501 (2-76)

PARTS LIST

0-70916 REQUIRED FOR ABBREVIATION, CODE AND SYMBOL INTERPRETATION

CONVAIR DIVISION OF GENERAL DYNAMICS
SAN DIEGO, CALIFORNIA

PDA: PL 11-38030 | REV LTR

TITLE: STACK ASSY- EBT-P PROTOTYPE

PADR | RELEASE/DATE | CODE IDENT NO. 14170 | SH 1 OF 5 SHS

DOC TYPE | DOC OPT | DOC CONT | GROUP | REPRO CODE | CONTRACT NO. | UNDIM DWG

DRAFTSMAN / / | DESIGNER 9/10/81 N. HILL | GR ENGR / / | STRESS / / | PROD. ENGR / / | MATERIAL / / | CHECKER / / | / / | / / | / / | / /

PAGE | DISTRIBUTION CODE | PACKAGE NO. | NOTE SYMBOL: * D - DOCUMENT NO. E - END ITEM G - GENERAL NOTE L - LIMIT M - MATERIAL N - NOMENCLATURE R - REF DESIG T - TYPE, DESIG/VALUE U - USAGE DATA V - VENDOR ITEM

REQUIREMENTS PER ASSY/INSTL -21	-13	-6	-2	-1	UNIT OF MEAS	FIND NO.	CODE IDENT NO.	PART OR IDENTIFYING NUMBER	NOMENCLATURE OR DESCRIPTION	ZONE LTR	ZONE NO.	NOTE SYM *	NOTES
				X				-1	STACK ASSY	D	6		
			X	1				-2	PLATE ASSY	A	27		
			1					-3	PLATE	D	28		1.25X12.1X12.6 TYPE 304L STLS. STL.
			1					-4	PIPE	D	27		8 IN SCHED 5S X .6 LONG TYPE 304L STLS. STL.
		X		1				-6	HEAT INTERCEPT ASSY	E	27		
		1						-7	PLATE	H	26		.032 X 10.2 X 10.2 COPPER SHEET, QQ-C-576 AY110
		1						-8	TUBE	F	25		.032 X 1.1 X 9.5 COPPER SHEET, QQ-C-576, ALLOY 110
		2						-9	TUBE	F	25		.032 X 1.1 X 4.0 COPPER SHEET, QQ-C-576, ALLOY 110
		3						-10	DISC	H	26		.032 X .3 X .3 COPPER SHEET, QQ-C-576, ALLOY 110
		2						-11	FINGER SPRING	G	26		CAT. NO 97-310A X 9.19 LONG, INSTRUMENT SPECIALTIES
													CO. DELAWARE WATER GAP, PA (717) 424-8510
			1					-12	SLEEVE	D	25		9.00 O.D. X .375 WALL TUBE, TYPE 304L STLS STL.
	X			1				-13	NECK ASSY	C	22		
	1							-14	PIPE	C	23		8 IN. SCHED 5S PIPE X 10.2 LONG TYPE 304L STLS. STL
	1							-15	BAR	C	22		.25 X 1.5 X 1.1 TYPE 304L STLS. STL.
	1							-16	SHEET	B	22		.120 X 8.5 X 8.5 TYPE 304L STLS. STL.
				2				-17	CLAMP HALF	A	37		.50 X .8 X 3.7 PLATE NEMA G-10 CR
1								-18	FLANGE	C	37		3.75 O.D. X .8 LONG BAR OR .75 X 4.0 X 4.0
													PLATE, TYPE 304L STAINLESS STEEL
				2				-19	TUBE	A	34		1.00 O.D. X .250 WALL X 3.6 LONG, 304L STLS. STL.
				2				-20	TUBE	B	36		1.00 O.D. X .028 WALL X 2.5 LONG, 304L STLS. STL.
X				1				-21	VENT ASSY	F	36		
1								-22	TUBE	H	37		2.375 O.D. X .035 WALL X 19.8 L. 304L STLS. STL.
1								-23	TUBE	H	37		2.625 O.D. X .065 WALL X 3.2 L. 304L STLS. STL.
1								-24	TUBE	H	35		2.625 O.D. X .065 WALL X 14.5 L. 304L STLS. STL.
1								-25	RING	G	35		2.625 O.D. X .3 LONG BAR OR .25 X 3.0 X 3.0
													PLATE, TYPE 304L STAINLESS STEEL
			1					8ELE-50-10	BELLOWS, 304 S. STL.	E	27		WITH 304 S. STL END BANDS, PATHWAY
													BELLOWS INC., EL CAJON, CA.
			2					-30	BACK-UP BAR	E	27		.1875 X .375 X 11.6 BAR TYPE 304L STLS. STL.

6501 (2-76)

PRELIMINARY

PARTS LIST

0-70916 REQUIRED FOR ABBREVIATION, CODE AND SYMBOL INTERPRETATION

CONVAIR DIVISION OF GENERAL DYNAMICS
SAN DIEGO, CALIFORNIA

PDA: PL 11-38030 | REV LTR

TITLE: STACK ASSY - EBT-P PROTOTYPE

PADR | RELEASE/DATE | CODE IDENT NO. 14170 | SH 2 OF ___ SHS

DOC TYPE | DOC OPT | DOC CONT | GROUP | REPRO CODE | CONTRACT NO. | UNDIM DWG

DRAFTSMAN / / | DESIGNER / / | GR ENGR / / | STRESS / / | PROD. ENGR / / | MATERIAL / / | CHECKER / / | / / | / / | / / | / /

PAGE | DISTRIBUTION CODE | PACKAGE NO.

NOTE SYMBOL: * D - DOCUMENT NO. E - END ITEM G - GENERAL NOTE L - LIMIT M - MATERIAL N - NOMENCLATURE R - REF DESIG T - TYPE DESIG/VALUE U - USAGE DATA V - VENDOR ITEM

REQUIREMENTS PER ASSY/INSTL -38	-37	-36	-35	-29	-26	-6	-1	UNIT OF MEAS	FIND NO.	CODE IDENT NO.	PART OR IDENTIFYING NUMBER	NOMENCLATURE OR DESCRIPTION	ZONE LTR	ZONE NO.	NOTE SYM *	NOTES
					X		1				-26	TRAY ASSY	B	44		
					1						-27	BAR	C	44		.125X3.4X26.0 UNS NO 10100 COPPER
				1	1						-28	BAR	B	33		.75X1.5X1.4 TEMPER 060 (ANNEALED)
				X			1				-29	TRAY ASSY	C	34		ASME B 152-77
				1							-31	BAR	D	33		.125X3.4X26.0 CERTS REQ'D.
							1				-32	PLATE	E	34		.125X.8X3.7 NEMA G-10 CR
							2				-33	TUBE	C	36		.50 O.D.X.035 WALL X 6.6 LONG, 304L STLSSTL
						4					-34	FINGER SPRING	F	26		CAT NO 97-310A X 3.19 LONG, INSTRUMENT SPECIALTIES CO. DELAWARE WATER GAP, PA.
			X				2				-35	DISC ASSY	D	23		
		X					4				-36	DISC ASSY	D	23		
	X						46				-37	DISC ASSY	D	23		
X							15				-38	DISC ASSY	D	23		
							11				-39	DISC ASSY	D	23		
		1	1								-40	DISC	G	23		.062X8.3X8.3 COPPER CLAD GLASS EPOXY PER MIL-P-13949, FL-GE, 062, CL, CLASS I.
1	1										-41	DISC	F	23		.063X8.3X8.3 NEMA G-10 CR

PRELIMINARY

6501 (2-76)

PARTS LIST

0-70916 REQUIRED FOR ABBREVIATION, CODE AND SYMBOL INTERPRETATION

CONVAIR DIVISION OF GENERAL DYNAMICS
SAN DIEGO, CALIFORNIA

PDA: PL 11-38030 | REV LTR:

TITLE: STACK ASSY - EBT-P PROTOTYPE

PADR | RELEASE/DATE | CODE IDENT NO.: 14170 | SH 3 OF ___ SHS

DOC TYPE | DOC OPT | DOC CONT | GROUP | REPRO CODE | CONTRACT NO. | UNDIM DWG

DRAFTSMAN / / | DESIGNER 9/10/81 N. HILL | GR ENGR / / | STRESS / / | PROD. ENGR / / | MATERIAL / / | CHECKER / / | / / | / / | / / | / /

PAGE | DISTRIBUTION CODE | PACKAGE NO.

NOTE SYMBOL: * D - DOCUMENT NO. E - END ITEM G - GENERAL NOTE L - LIMIT M - MATERIAL N - NOMENCLATURE R - REF DESIG T - TYPE DESIG/VALUE U - USAGE DATA V - VENDOR ITEM

REQUIREMENTS PER ASSY/INSTL -21	-46	-39	-38	-37	-36	-35	-1	UNIT OF MEAS	FIND NO.	CODE IDENT NO.	PART OR IDENTIFYING NUMBER	NOMENCLATURE OR DESCRIPTION	ZONE LTR	ZONE NO.	NOTE SYM *	NOTES
		1									-42	DISC	F	23		.063 X 8.1 X 8.1 NEMA G-10 CR
				3	3						-43	ROD	G	23		.25 DIA X .2 LONG NEMA G-10 CR
		3	3			3					-44	ROD	G	23		.25 DIA X .3 LONG NEMA G-10 CR
							1				-45	TUBE	G	5		1.25 O.D. X .063 WALL X 13.4 NEMA G-10 CR
	X						1				-46	PLATE ASSY	E	45		
	1										-47	PLATE	G	43		.375 X 8.3 X 8.3 NEMA G-10 CR
	1										-48	RING	E	42		1.000 X 8.5 X 8.5 PLATE, 304L STLS. STL.
							14				-50	BOLT	G	48		MAKE FROM NAS 1003-2H
							7				-51	STRAP	A	21		MAKE FROM CAT NO 5025-5-3.000, SEASTROM
																MFG. CO. (714)-560-8955
							1				-52	ADAPTER	B	42		1.00 HEX X 1.5 LONG TYPE 304 STLS. STL.
							1				-53	INSULATION	F	32		.005 X 2.4 X 3.7 KAPTON FILM, TYPE H, DUPONT
							2				-54	SHIM	B	1		.002 X 2.0 X 2.0 INDIUM FOIL, 99.99% INDIUM
																CORP OF AMERICA.
							2				-56	CLAMP	D	41		.750 X .8 X 3.6 PLATE NEMA G-10 CR
							4				-57	INSULATOR	D	42		.250 X .8 X 3.66 PLATE NEMA G-10 CR
1											-58	ALUMINIZED FILM	G	38		NOTE 18, 17 IN X 40 IN
1											-59	SEPARATOR NET	G	38		NOTE 17, 17 IN X 30 IN.
							1				11-38031-1	LIQUID He INLET	B	8		
							1				11-38031-2	LIQUID He INLET	A	4		
							1				11-38032-1	LIQUID LEVEL SENSOR	C	8		
							1				11-38040-4	SHIELD ASSY	C	46		
							2				11-38040-18	TUBE	C	47		PRELIMINARY
							1				11-38046-1	INSULATION ASSY	A	7		
							1				11-38046-3	INSULATION ASSY	D	47		
A/R											0-06093-1	TAPE				
		A/R	A/R	A/R	A/R	A/R					0-06139-1	ADHESIVE	G	23		
							1				11-38020-1	VAPOR COOLED LEADS	E	8		
							1				11-38070-2	OUTLET ASSY	H	5		

6501 (2-76)

PARTS LIST

0-70916 REQUIRED FOR ABBREVIATION, CODE AND SYMBOL INTERPRETATION

CONVAIR DIVISION OF GENERAL DYNAMICS
SAN DIEGO, CALIFORNIA

PDA: PL 11-38030 | REV LTR

TITLE: STACK ASSY-EBT-P - PROTOTYPE

PADR | RELEASE/DATE | CODE IDENT NO. 14170 | SH 4 OF ___ SHS

DOC TYPE	DOC OPT	DOC CONT	GROUP	REPRO CODE	CONTRACT NO.	UNDIM DWG

DRAFTSMAN / /	DESIGNER 9/18/81 N. HILL	GR ENGR / /	STRESS / /	PROD. ENGR / /	MATERIAL / /	CHECKER / /	/ /	/ /	/ /	/ /

PAGE | DISTRIBUTION CODE | PACKAGE NO.

NOTE SYMBOL: * D - DOCUMENT NO. E - END ITEM G - GENERAL NOTE L - LIMIT M - MATERIAL N - NOMENCLATURE R - REF DESIG Y - TYPE DESIG/VALUE U - USAGE DATA V - VENDOR ITEM

REQUIREMENTS PER ASSY/INSTL -46	-28	-26	-1	UNIT OF MEAS	FIND NO.	CODE IDENT NO.	PART OR IDENTIFYING NUMBER	NOMENCLATURE OR DESCRIPTION	ZONE LTR	ZONE NO.	NOTE SYM *	NOTES
			1				SS-600-7-6	ADAPTER	A	1		SWAGE LOK - CRAWFORD FITTING CO.
			1				SS-600-1-8BT	FITTING	H	6		SOLON OHIO
			2				SS-1210-1-12 BT	FITTING	D	6		
			2				G 234-4-8	BELLOWS	B	48		8 CONVOLUTIONS, STUB ENDS, FLEXONICS
												BARTLETT, ILL.
			1				2-217 E540-80	O-RING	H	5		PARKER SEAL CO
			1				2-231 E540-80	O-RING	C	8		COMPOUND E515-80 MAY BE SUBSTITUTED
			1				2-242 E540-80	O-RING	D	8		
			1				4845 K12	PIPE PLUG, 1/4 IN	E	6		McMASTER-CARR SUPPLY, 304 STNLS, STL.
	7	7					AN960C10L	WASHER				
			4				AN960C416	WASHER				
			4				AN960C516	WASHER				
			4				AN960C616	WASHER				
A/R			A/R				MS20995C32	LOCK WIRE				
	21						MS35338-138	LOCK WASHER				
	7	7					NAS509-3C	NUT				
			4				NAS509-4C	NUT				
			2				NAS509-5C	NUT				
			2				NAS509-6C	NUT				PRELIMINARY
	7						NAS1003-1	BOLT				
		7					NAS1003-6	BOLT				
			12				NAS1004-2A	BOLT				
			8				NAS1004-6A	BOLT				
			4				NAS1004-20H	BOLT				
			2				NAS1005-12H	BOLT				
			2				NAS1006-7H	BOLT				
			4				NAS1352C4H16	BOLT				
			5				NAS1398B4-2	RIVET				
			A/R				QQ-S-571, GR 63 B	SOLDER				
			A/R				QQ-B-654, GR 5	BRAZE ALLOY				

6501 (2-76)

PARTS LIST

0-70916 REQUIRED FOR ABBREVIATION, CODE AND SYMBOL INTERPRETATION

CONVAIR DIVISION OF GENERAL DYNAMICS
SAN DIEGO, CALIFORNIA

PDA: PL 11-38030 | REV LTR

TITLE: STACK ASSY-EBT-P PROTOTYPE

PADR | RELEASE/DATE | CODE IDENT NO. 14170 | SH 5 OF ___ SHS

DOC TYPE	DOC OPT	DOC CONT	GROUP		REPRO CODE	CONTRACT NO.	UNDIM DWG

DRAFTSMAN / /	DESIGNER 9/11/81 N. HILL	GR ENGR / /	STRESS / /	PROD. ENGR / /	MATERIAL / /	CHECKER / /	/ /	/ /	/ /	/ /

PAGE | DISTRIBUTION CODE | PACKAGE NO. | NOTE SYMBOL: * D - DOCUMENT NO. E - END ITEM G - GENERAL NOTE L - LIMIT M - MATERIAL N - NOMENCLATURE R - REF DESIG T - TYPE DESIG/VALUE U - USAGE DATA V - VENDOR ITEM

REQUIREMENTS PER ASSY/INSTL				UNIT OF MEAS	FIND NO.	CODE IDENT NO.	PART OR IDENTIFYING NUMBER	NOMENCLATURE OR DESCRIPTION	ZONE LTR	ZONE NO.	NOTE SYM *	NOTES
							0-00352	SPEC				
							0-00365	SPEC				
							0-00562	SPEC				
							0-70042	SPEC				
							0-73514	SPEC				
							0-73517	SPEC				
							0-73521	SPEC				
							0-79129					
							MS 33540	SPEC				
							MIL-I-6866	SPEC				
							MIL-P-13949	SPEC				
							MIL-W-6858	SPEC				
							MIL-STD-248	SPEC				
							MIL-STD-278	SPEC				

PRELIMINARY

6501 (2-76)

PARTS LIST

0-70916 REQUIRED FOR ABBREVIATION, CODE AND SYMBOL INTERPRETATION

CONVAIR DIVISION OF GENERAL DYNAMICS
SAN DIEGO, CALIFORNIA

PDA: PL 11-38032 | REV LTR: –

TITLE: LIQUID HELIUM LEVEL SENSOR – EBT-P PROTOTYPE

PADR | RELEASE/DATE | CODE IDENT NO.: 14170 | SH 1 OF 1 SHS

DOC TYPE	DOC OPT	DOC CONT	GROUP	REPRO CODE	CONTRACT NO.	UNDIM DWG
			692-0			

DRAFTSMAN	DESIGNER	GR ENGR	STRESS	PROD. ENGR	MATERIAL	CHECKER				
9/15/81 RGVK	/ /	/ /	/ /	/ /	/ /	/ /	/ /	/ /	/ /	/ /

PAGE | DISTRIBUTION CODE | PACKAGE NO. | NOTE SYMBOL: * D - DOCUMENT NO. E - END ITEM G - GENERAL NOTE L - LIMIT M - MATERIAL N - NOMENCLATURE R - REF DESIG T - TYPE DESIG/VALUE U - USAGE DATA V - VENDOR ITEM

REQUIREMENTS PER ASSY/INSTL				UNIT OF MEAS	FIND NO.	CODE IDENT NO.	PART OR IDENTIFYING NUMBER	NOMENCLATURE OR DESCRIPTION	ZONE LTR	ZONE NO.	NOTE SYM *	NOTES
			-1									
			X				-1	SENSOR ASSY				
			1				-2	TUBE			M	.375 DIA × .035 WALL × 3.6 LONG
												TYPE 304L SST ; ASTM-A-240
			1				-3	LHe LEVEL SENSOR			V	MAKE FROM LIQUID HELIUM LEVEL SENSOR,
												ACTIVE LENGTH 14.0; FIBREGLAS EXTENSION
												LENGTH 18.9; OVERALL LENGTH 33.4,
												EXTRA LEAD LENGTH 36.0
												AMERICAN MAGNETICS INC.
												OAK RIDGE, TN 37830
			DOC				0-79129	SPEC				
			DOC				0-70042	SPEC				
			AR				0-06139-1	ADHESIVE				
												PRELIMINARY

6501 (2-76)

PARTS LIST

0-70916 REQUIRED FOR ABBREVIATION, CODE AND SYMBOL INTERPRETATION

CONVAIR DIVISION OF GENERAL DYNAMICS
SAN DIEGO, CALIFORNIA

PDA: PL11-38040 | REV LTR: A

TITLE: LN_2 COLD WALL ASSEMBLY ~ EBT-P PROTOTYPE

DOC TYPE	DOC OPT	DOC CONT	GROUP	REPRO CODE	CONTRACT NO.	UNDIM DWG	PADR	RELEASE/DATE	CODE IDENT NO.	SH / OF
			692-0						14170	1 / 2 SHS

DRAFTSMAN	DESIGNER	GR ENGR	STRESS	PROD. ENGR	MATERIAL	CHECKER		Q A		
P.G.V.K. 7/13/81	7/13/81	8/7/81	7/20/81	7/23/81	7/22/81	1 1	7/20/81	7/24/81	7/27/81	1 1

PAGE | DISTRIBUTION CODE | PACKAGE NO. | NOTE SYMBOL: * D - DOCUMENT NO. E - END ITEM G - GENERAL NOTE L - LIMIT M - MATERIAL N - NOMENCLATURE R - REF DESIG T - TYPE DESIG/VALUE U - USAGE DATA V - VENDOR ITEM

REQUIREMENTS PER ASSY/INSTL -4	-3	-2	-1	UNIT OF MEAS	FIND NO.	CODE IDENT NO.	PART OR IDENTIFYING NUMBER	NOMENCLATURE OR DESCRIPTION	ZONE LTR	ZONE NO.	NOTE SYM *	NOTES
2		X	X				-1	SHIELD ASSEMBLY	A	4		
	X	X	1				-2	ASSEMBLY HALF	C	5		
X			1				-3	ASSEMBLY HALF	C	6		
X			1				-4	STACK SHIELD	E	4		
2		1					-5	LN_2 ASSEMBLY	D	33		
2	1						-6	LN_2 ASSEMBLY	D	33		
2	1	1					-7	SHIELD HALF ASSY	D	34		
1							-14	STACK TUBE	D	7	M	.032×36.0×36.0 110 COPPER; QQ-C-576
6							-15	STACK HOLD CLIP	D	10	M	.032×2.0×1.0 316LSST; ASTM-A-240
			2				-18	STACK LN_2 TUBE	E	5	M	.500 DIA×30.0 110 COPPER; ASTM-B-188
			6				-20	SUPPORT INSERT	D	3	M	.032×7.0×8.0 110 COPPER; QQ-C-576
			1				11-38046-1	INSULATION BLANKET				
			12				11-38046-2	↑ ↑				
			1				11-38046-3					
			16				11-38046-4	↓ ↓				
			8				11-38046-5	INSULATION BLANKET				
			1				11-38084-1	C/M SUPPORT INST'L				PRELIMINARY
			DOC				0-70042	IDENT SPEC				
			DOC				0-73521	BRAZE SPEC				
			DOC				0-00352	ALLOY SPEC				
			DOC				0-00562	FLUX SPEC				
			DOC				ASTM-E498-73	HELIUM LEAK SPEC				
			28				MS20470B4-2	RIVET				
			48				NAS1398B5-2	RIVET				
			12				NAS1398B6-11	RIVET				

6501 (2-76)

PARTS LIST

0-70916 REQUIRED FOR ABBREVIATION, CODE AND SYMBOL INTERPRETATION

CONVAIR DIVISION OF GENERAL DYNAMICS
SAN DIEGO, CALIFORNIA

PDA: PL11-38040 | REV LTR: —

TITLE: LN_2 COLD WALL ASSEMBLY ~ EBT-P PROTOTYPE

PADR | RELEASE/DATE | CODE IDENT NO. 14170 | SH 2 OF ___ SHS

DOC TYPE	DOC OPT	DOC CONT	GROUP 692-0		REPRO CODE	CONTRACT NO.	UNDIM DWG

DRAFTSMAN 7/12/67 PEVK	DESIGNER / /	GR ENGR / /	STRESS / /	PROD. ENGR / /	MATERIAL / /	CHECKER / /	/ /	/ /	/ /	/ /

PAGE | DISTRIBUTION CODE | PACKAGE NO. | NOTE SYMBOL: * D - DOCUMENT NO. E - END ITEM G - GENERAL NOTE L - LIMIT M - MATERIAL N - NOMENCLATURE R - REF DESIG T - TYPE DESIG/VALUE U - USAGE DATA V - VENDOR ITEM

PAGE	REQUIREMENTS PER ASSY/INSTL -1	-7	-6	-5	UNIT OF MEAS	FIND NO.	CODE IDENT NO.	PART OR IDENTIFYING NUMBER	NOMENCLATURE OR DESCRIPTION	ZONE LTR	ZONE NO.	NOTE SYM *	NOTES
1				X				-5	LN_2 ASSEMBLY	D	33		
1			X					-6	LN_2 ASSEMBLY	D	33		
1		X						-7	SHIELD HALF ASSY	D	34		
		1						-9	SIDE PLATE	B	13	M	.032×36.0×36.0 110 COPPER; QQ-C-576
		1						-10	OUTSIDE RING	C	12	M	.032×6.0×115.0 110 COPPER; QQ-C-576
		1						-11	INSIDE RING	C	13	M	.032×6.0×60.0 110 COPPER; QQ-C-576
				1				-12	LN_2 TUBE	E	12	M	.500 DIA×130.0 110 COPPER; ASTM-B-188
			1					-13	LN_2 TUBE	E	12	M	.500 DIA×125.0 110 COPPER; ASTM-B-188
		1						-16	INSULATOR STRIP	B	29	M	.031×1.25×9.0 G10-CR; NEMA GRADE
		2						-17	INSULATOR STRIP	C	26	M	.031×1.25×6.0 G10-CR; NEMA GRADE
			1	1				-21	LN_2 MANIFOLD TUBE	B	211	M	.500 DIA×2.5 110 COPPER; ASTM-B-188
			1	1			96142	G234-4-8	BELLOWS	F	12	V	
			2				39428	5520K31	COUPLING	G	10	V	
1	6							-22	INTERCEPT CLIP	B	316	M	.032×9.5×1.5 110 COPPER; QQ-C-576
1	12							-23	END CLIP	D	316	M	.032×.5×2.5 110 COPPER; QQ-C-576
1	DOC							0-06023	EPOXY				
1	DOC							0-79129	EPOXY SPEC				

PRELIMINARY

6501 (2-76)

PARTS LIST

0-70916 REQUIRED FOR ABBREVIATION, CODE AND SYMBOL INTERPRETATION

CONVAIR DIVISION OF GENERAL DYNAMICS
SAN DIEGO, CALIFORNIA

PDA: PL 11-38060 | REV LTR: –

TITLE: VACUUM VESSEL ASSEMBLY ~ EBT-P PROTOTYPE

PADR | RELEASE/DATE | CODE IDENT NO. 14170 | SH 1 OF ___ SHS

DOC TYPE | DOC OPT | DOC CONT | GROUP 692-0 | REPRO CODE | CONTRACT NO. | UNDIM DWG

DRAFTSMAN / / PGVK | DESIGNER 7/17/81 | GR ENGR / / | STRESS / / | PROD. ENGR / / | MATERIAL / / | CHECKER / /

DISTRIBUTION CODE | PACKAGE NO.

NOTE SYMBOL: * D - DOCUMENT NO. E - END ITEM G - GENERAL NOTE L - LIMIT M - MATERIAL N - NOMENCLATURE R - REF DESIG T - TYPE DESIG/VALUE U - USAGE DATA V - VENDOR ITEM

PAGE	REQUIREMENTS PER ASSY/INSTL			-1	UNIT OF MEAS	FIND NO.	CODE IDENT NO.	PART OR IDENTIFYING NUMBER	NOMENCLATURE OR DESCRIPTION	ZONE LTR	ZONE NO.	NOTE SYM *	NOTES
								-1	VACUUM VESSEL	A	5		
				1				11-38062-1	OUTER RING	C	7		
				4				11-38065-1	STRUT FITTING	E	6		
				1				11-38066-1	SUPPORT ASS'Y	E	2		
				1				11-38067-1	SIDE PLATE ASS'Y	E	8		
				1				11-38068-1	STACK PLATE ASSY	F	6		
				1				11-38068-2	STACK PLATE ASSY	F	5		
				1				11-38070-1	OUTLET ASSY	G	6		
				DOC				MIL-STD-248	WELD SPEC				
								MIL-STD-278	WELD SPEC				
								MIL-I-68166	INSP. SPEC				
								0-70042	IDENT SPEC				
				DOC				0-79517	TEST SPEC				
				AR				ER 316L	FILLER WIRE				
				AR				DDD-C-301	CHEESECLOTH				
				AR				0-79054	SOLVENT				
				DOC				MIL-E-19933	WELD SPEC				PRELIMINARY
				DOC				MIL-E-22200/2	WELD SPEC				
				2				-2	MOUNTING PLATE	H	8	M	1.00 x 2.0 x 6.0 304L SST; ASTM-A-240
				1				-3	MOUNTING PLATE	D	7	M	.750 x 2.0 x 2.0 304L SST; ASTM-A-240

6501 (2-76)

PARTS LIST

0-70916 REQUIRED FOR ABBREVIATION, CODE AND SYMBOL INTERPRETATION

CONVAIR DIVISION OF GENERAL DYNAMICS
SAN DIEGO, CALIFORNIA

PDA: PL11-38063 | REV LTR: –

TITLE: SIDE PLATE / VACUUM VESSEL ~ EBT-P PROTOTYPE

PADR | RELEASE/DATE | CODE IDENT NO.: 14170 | SH 1 OF 1 SHS

DOC TYPE | DOC OPT | DOC CONT | GROUP: 692-0 | REPRO CODE | CONTRACT NO. | UNDIM DWG

DRAFTSMAN / / | DESIGNER 5/14/81 | GR ENGR / / | STRESS 7/16/81 | PROD. ENGR 7/17/81 | MATERIAL 7/16/81 | CHECKER / / | Q A 7/20/81

PAGE | DISTRIBUTION CODE | PACKAGE NO. | NOTE SYMBOL: * D - DOCUMENT NO. E - END ITEM G - GENERAL NOTE L - LIMIT M - MATERIAL N - NOMENCLATURE R - REF DESIG T - TYPE DESIG/VALUE U - USAGE DATA V - VENDOR ITEM

REQUIREMENTS PER ASSY/INSTL			-1	UNIT OF MEAS	FIND NO.	CODE IDENT NO.	PART OR IDENTIFYING NUMBER	NOMENCLATURE OR DESCRIPTION	ZONE LTR	ZONE NO.	NOTE SYM *	NOTES
			X				-1	SIDE PLATE ASSY	B	3		
			1				-2	SIDE PLATE	D	6	M	.250×45×45 304L SST; ASTM-A-240
			1				-3	INNER RING	D	5	M	.250×8×65 304L SST; ASTM-A-240
							-4	SIDE PLATE	B	7	M	.250×45×45 304L SST; ASTM-A-240 △4
			DOC				0-73517	TEST SPEC				
			↑				MIL-I-68866	INSP SPEC				
			↓				MIL-W-8611	WELD SPEC				
							0-70042	IDENT SPEC				
			DOC				0-00365	WELD SPEC				
			AR				ER 316L	FILLER WIRE				

PRELIMINARY

6501 (2-76)

PARTS LIST

0-70916 REQUIRED FOR ABBREVIATION, CODE AND SYMBOL INTERPRETATION

CONVAIR DIVISION OF GENERAL DYNAMICS
SAN DIEGO, CALIFORNIA

PDA: PL 11-38064 | REV LTR: –

TITLE: STACK PLATES / VACUUM VESSEL ~ EBT-P PROTOTYPE

PADR | RELEASE/DATE | CODE IDENT NO. 14170 | SH 1 OF 1 SHS

DOC TYPE	DOC OPT	DOC CONT	GROUP 692-0	REPRO CODE	CONTRACT NO.	UNDIM DWG

DRAFTSMAN	DESIGNER	GR ENGR	STRESS	PROD. ENGR	MATERIAL	CHECKER			
/ / PGVE	/ / S/Cabl	/ /	/ /	/ /	/ /	/ /	/ /	/ /	/ /

PAGE | DISTRIBUTION CODE | PACKAGE NO.

NOTE SYMBOL: * D - DOCUMENT NO. E - END ITEM G - GENERAL NOTE L - LIMIT M - MATERIAL N - NOMENCLATURE R - REF DESIG T - TYPE DESIG/VALUE U - USAGE DATA V - VENDOR ITEM

REQUIREMENTS PER ASSY/INSTL				UNIT OF MEAS	FIND NO.	CODE IDENT NO.	PART OR IDENTIFYING NUMBER	NOMENCLATURE OR DESCRIPTION	ZONE LTR	ZONE NO.	NOTE SYM *	NOTES
	-3	-2	-1									
			X				-1	STACK PLATE	B	3	M	.250×12.0×30.0 304L SST; ASTM-A-240
		X					-2	STACK PLATE	B	5	M	.500×12.5×29.0 304L SST; ASTM-A-240
	X						-3	STACK PLATE	B	7	M	.500×12.5×29.0 304L SST; ASTM-A-240
	DOC	DOC	DOC				0-73517	TEST SPEC				
	DOC	DOC	DOC				0-70042	IDENT SPEC				

PRELIMINARY

6501 (2-76)

PARTS LIST

D-70916 REQUIRED FOR ABBREVIATION, CODE AND SYMBOL INTERPRETATION

CONVAIR DIVISION OF GENERAL DYNAMICS
SAN DIEGO, CALIFORNIA

PDA: PL11-38066 | REV LTR: —

TITLE: SUPPORT ASSEMBLY / VACUUM VESSEL ~ EBT-P PROTOTYPE

PADR | RELEASE/DATE | CODE IDENT NO.: 14170 | SH 1 OF 1 SHS

DOC TYPE | DOC OPT | DOC CONT | GROUP: 692-D | REPRO CODE | CONTRACT NO. | UNDIM DWG

DRAFTSMAN: FGVK | DESIGNER: 7/1/81 | GR ENGR | STRESS | PROD. ENGR | MATERIAL | CHECKER

PAGE | DISTRIBUTION CODE | PACKAGE NO.

NOTE SYMBOL: * D - DOCUMENT NO. E - END ITEM G - GENERAL NOTE L - LIMIT M - MATERIAL N - NOMENCLATURE R - REF DESIG T - TYPE DESIG/VALUE U - USAGE DATA V - VENDOR ITEM

REQUIREMENTS PER ASSY/INSTL				UNIT OF MEAS	FIND NO.	CODE IDENT NO.	PART OR IDENTIFYING NUMBER	NOMENCLATURE OR DESCRIPTION	ZONE LTR	ZONE NO.	NOTE SYM *	NOTES
			-1									
			X				-1	SUPPORT ASSEMBLY	B	5		
			1				-2	BACK PLATE - TOP	F	3	M	1.50×8.2×18.1 304L SST; ASTM-A-240
			2				-3	SIDE PLATE	E	6	M	1.25×15.4×20.1 304L SST; ASTM-A-240
			2				-4	WEB PLATE	D	6	M	1.25×8.2×14.8 304L SST; ASTM-A-240
			2				-5	END PLATE	D	3	M	1.25×15.7×18.1 304L SST; ASTM-A-240
			1				-6	ADJUSTER BAR	F	4	M	1.00×3.3×18.1 304L SST; ASTM-A-240
			1				-7	BACK PLATE - BOTTOM	C	3	M	1.50×8.2×18.1 304L SST; ASTM-A-240
			DOC				D-73517	TEST SPEC				
			↑				MIL-I-68466	INSP SPEC				
							MIL-STD-248	WELD SPEC				
							MIL-STD-278	WELD SPEC				
							MIL-E-19933	WELD SPEC				
			↓				D-70042	IDENT SPEC				
			DOC				MIL-E-22200/2	WELD SPEC				
			AR				ER 316L	ELECTRODE				
			AR				E 316L	ELECTRODE				

PRELIMINARY

6501 (2-76)

PARTS LIST

0-70916 REQUIRED FOR ABBREVIATION, CODE AND SYMBOL INTERPRETATION

CONVAIR DIVISION OF GENERAL DYNAMICS
SAN DIEGO, CALIFORNIA

PDA: PL11-38067 | REV LTR: —

TITLE: SIDE PLATE ASSEMBLY ~ EBT-P PROTOTYPE

PADR | RELEASE/DATE | CODE IDENT NO.: 14170 | SH 1 OF 1 SHS

DOC TYPE	DOC OPT	DOC CONT	GROUP	REPRO CODE	CONTRACT NO.	UNDIM DWG
			692-0			

DRAFTSMAN	DESIGNER	GR ENGR	STRESS	PROD. ENGR	MATERIAL	CHECKER				
/ /	5/21/81	/ /	/ /	/ /	/ /	/ /	/ /	/ /	/ /	/ /

PAGE | DISTRIBUTION CODE | PACKAGE NO.

NOTE SYMBOL: * D - DOCUMENT NO. E - END ITEM G - GENERAL NOTE L - LIMIT M - MATERIAL N - NOMENCLATURE R - REF DESIG T - TYPE DESIG/VALUE U - USAGE DATA V - VENDOR ITEM

REQUIREMENTS PER ASSY/INSTL				UNIT OF MEAS	FIND NO.	CODE IDENT NO.	PART OR IDENTIFYING NUMBER	NOMENCLATURE OR DESCRIPTION	ZONE LTR	ZONE NO.	NOTE SYM *	NOTES
		-2	-1									
		X					-1	SIDE PLATE ASSY	B	4		
			X				-2	SIDE PLATE ASSY	B	4		
		1	1				11-38064-1	STACK PLATE	F	5		
			1				11-38063-1	SIDE PLATE	D	5		
		1					11-38063-4	SIDE PLATE	D	5		
		1	1				-3	SUPPORT BAR	E	5	M	1.00 x 3.5 x 11.5 304L SST, ASTM-A-240
		DOC	DOC				MIL-I-6866	TEST SPEC				
		↑	↑				MIL-STD-248	WELD SPEC				
							MIL-STD-278	WELD SPEC				
		↓	↓				0-70042	IDENT SPEC				
		DOC	DOC				MIL-E-19933	WELD SPEC				
		DOC	DOC				MIL-E-22200/2	WELD SPEC				
		AR	AR				ER 316L	ELECTRODE				
		AR	AR				E 316L	ELECTRODE				
		DOC	DOC				0-73517	TEST SPEC				

PRELIMINARY

6501 (2-76)

PARTS LIST

0-70916 REQUIRED FOR ABBREVIATION, CODE AND SYMBOL INTERPRETATION

CONVAIR DIVISION OF GENERAL DYNAMICS
SAN DIEGO, CALIFORNIA

PDA: PL11-38068 | REV LTR: —

TITLE: STACK PLATE ASSEMBLY ~ EBT-P PROTOTYPE

DOC TYPE	DOC OPT	DOC CONT	GROUP	REPRO CODE	CONTRACT NO.	UNDIM DWG	PADR	RELEASE/DATE	CODE IDENT NO.	SH 1 OF 1 SHS
			682-0						14170	

DRAFTSMAN	DESIGNER	GR ENGR	STRESS	PROD. ENGR	MATERIAL	CHECKER				
PGVK	[illegible]	/ /	/ /	/ /	/ /	/ /	/ /	/ /	/ /	/ /

PAGE | DISTRIBUTION CODE | PACKAGE NO.

NOTE SYMBOL: * D - DOCUMENT NO. E - END ITEM G - GENERAL NOTE L - LIMIT M - MATERIAL N - NOMENCLATURE R - REF DESIG T - TYPE DESIG/VALUE U - USAGE DATA V - VENDOR ITEM

REQUIREMENTS PER ASSY/INSTL				UNIT OF MEAS	FIND NO.	CODE IDENT NO.	PART OR IDENTIFYING NUMBER	NOMENCLATURE OR DESCRIPTION	ZONE LTR	ZONE NO.	NOTE SYM *	NOTES
		-2	-1									
		X	X				-1	STACK PLATE ASSY	A	4		
		X					-2	STACK PLATE ASSY	A	7		
		2	2				-3	BACKING STRIP	C D	7 4	M	.188×.375×25.7 304L SST; ASTM-A-240
		1					-4	WELDING NECK FLANGE	C	7	V	MF 11015 × 6.0 LADISH CO. OR EQUIV.
			1				11-38064-2	STACK PLATE	D	3		
		1					11-38064-3	STACK PLATE	D	8		
		2	2				-5	BACKING STRIP	D D	4 7	M	.188×.375×1.6 304L SST; ASTM-A-240
		DOC	DOC				0-73517	TEST SPEC				
		⇧	⇧				MIL-I-68866	INSP SPEC				
							MIL-STD-248	WELD SPEC				
		⇩	⇩				MIL-STD-278	WELD SPEC				
							MIL-E-19933	WELD SPEC				
		DOC	DOC				0-70042	IDENT SPEC				
		DOC	DOC				MIL-E-22200/12	WELD SPEC				
		AR	AR				ER 316 L	ELECTRODE				
		AR	AR				E 316 L	ELECTRODE				

PRELIMINARY

6501 (2-76)

PARTS LIST

0-70916 REQUIRED FOR ABBREVIATION, CODE AND SYMBOL INTERPRETATION

CONVAIR DIVISION OF GENERAL DYNAMICS
SAN DIEGO, CALIFORNIA

PDA: PL11-38070 | REV LTR: —

TITLE: OUTLET ASSEMBLY ~ EBT-P PROTOTYPE

DOC TYPE	DOC OPT	DOC CONT	GROUP	REPRO CODE	CONTRACT NO.	UNDIM DWG	PADR	RELEASE/DATE	CODE IDENT NO.	SH / OF
			692-0						14170	1 / 2 SHS

DRAFTSMAN	DESIGNER	GR ENGR	STRESS	PROD. ENGR	MATERIAL	CHECKER				
/ /	8/4/81	/ /	/ /	/ /	/ /	/ /	/ /	/ /	/ /	/ /

PAGE | DISTRIBUTION CODE | PACKAGE NO.

NOTE SYMBOL: * D - DOCUMENT NO. E - END ITEM G - GENERAL NOTE L - LIMIT M - MATERIAL N - NOMENCLATURE R - REF DESIG T - TYPE DESIG/VALUE U - USAGE DATA V - VENDOR ITEM

REQUIREMENTS PER ASSY/INSTL -15	-13	-11	-10	-2	-1	UNIT OF MEAS	FIND NO.	CODE IDENT NO.	PART OR IDENTIFYING NUMBER	NOMENCLATURE OR DESCRIPTION	ZONE LTR	ZONE NO.	NOTE SYM *	NOTES
					X				-1	OUTLET ASSEMBLY	B	4		
				X					-2	OUTLET ASSEMBLY	B	6		
			X		1				-10	CROSS ASSEMBLY	D	3		
		X		1					-11	CROSS ASSEMBLY	G	6		
	X				1				-13	PLATE ASSEMBLY	G	3		
X				1					-15	NECK ASSEMBLY	C	5		
	1								-5	INSTR PLATE	F	26	M	.250×6.0×6.0 304L SST; ASTM-A-240
				2	1				-8	BLANK PLATE	F	6/4	M	.250×6.0×6.0 304L SST; ASTM-A-240
1									-9	MOUNTING FLANGE	C	6	M	1.50×3.0×3.0 304L SST; ASTM-A-240
		3	3						-3	INSTR. FLANGE	C	4		.500×6.0×6.0 304L SST; ASTM-A-240
2			1						-18	CROSS SUB-ASSY	D	3		
2			1						-21	DISK ASSY				
1								10633	20000	ELBOW	C	5	V	1" SHDL 10S SST
		1						10633	24210	CROSS			V	2½" SHDL 10S SST
1								10633	25000	REDUCER	C	6	V	2½" × 1" SHDL 10S SST
	1								BFH 20412-117	INSTR. RECEPTACLE	G	4	V	ITT CANNON
				18	18				NAS6306-11	BOLT				
				18	18				AN960-C616	WASHER				
				18	18				MS21043-6	NUT				
					1				NAS6303-13	BOLT				
					1				MS21043-3	NUT				
				AR	AR					CHEESE CLOTH				
				AR	AR					FREON TF				
				3	4				2-237-E540-80	O-RING	D	4	V	PARKER SEAL CORP.

PRELIMINARY

6501 (2-76)

PARTS LIST

0-70916 REQUIRED FOR ABBREVIATION, CODE AND SYMBOL INTERPRETATION

CONVAIR DIVISION OF GENERAL DYNAMICS
SAN DIEGO, CALIFORNIA

PDA: PL11-38070 | REV LTR: —

TITLE: OUTLET ASSEMBLY ~ EBT-P PROTOTYPE

DOC TYPE	DOC OPT	DOC CONT	GROUP	REPRO CODE	CONTRACT NO.	UNDIM DWG	PADR	RELEASE/DATE	CODE IDENT NO.	SH 2 OF ___ SHS
			692-0						14170	

DRAFTSMAN	DESIGNER	GR ENGR	STRESS	PROD. ENGR	MATERIAL	CHECKER				
/ /	/ /	/ /	/ /	/ /	/ /	/ /	/ /	/ /	/ /	/ /

PAGE | DISTRIBUTION CODE | PACKAGE NO.

NOTE SYMBOL: * D - DOCUMENT NO. E - END ITEM G - GENERAL NOTE L - LIMIT M - MATERIAL N - NOMENCLATURE R - REF DESIG T - TYPE DESIG/VALUE U - USAGE DATA V - VENDOR ITEM

REQUIREMENTS PER ASSY/INSTL -21	-20	-18	-16	-2	-1	UNIT OF MEAS	FIND NO.	CODE IDENT NO.	PART OR IDENTIFYING NUMBER	NOMENCLATURE OR DESCRIPTION	ZONE LTR	ZONE NO.	NOTE SYM *	NOTES
			X	1	1				-16	PLATE ASSEMBLY	F/G	1/3		
1		X							-18	CROSS SUB-ASSY	D	25		
	X				1				-20	DISK ASSY	D	3		
1	X								-21	DISK				
1									-4	INSTR. FLANGE	D	4	M	.500×6.0×6.0 304L SST; ASTM-A-240
			1						-6	INSTR. FLANGE	F	27	M	.250×6.0×6.0 304L SST; ASTM-A-240
	1								-7	VACUUM PLATE	D	3	M	.250×6.0×6.0 304L SST; ASTM-A-240
1									-12	HINGE HALF	D	24	M	.750×.7 ×1.0 304L SST; ASTM-A-240
	1								-14	HINGE HALF	F	24	M	.190×.7 ×1.0 304L SST; ASTM-A-240
		1							-17	CROSS	B	25	V	MAKE FROM LADISH 24210 2½"
		1							-19	PIPE	E	25	V	2½" × 3.5 LONG SHDL 10S SST PIPE
			1											
									SSR 2053-44-1-P(GOLD)	INSTR RECEPTACLE	E/6	4/6	V	ITT CANNON
				DOC	DOC				0-70042	IDENT SPEC				
				⇧	⇧				MIL-I-8950 B	INSPECT SPEC				
									MIL-E-19933	WELD SPEC				
									MIL-E-22200/2	WELD SPEC				
									MIL-I-68666	WELD SPEC				
				⇩	⇩				0-70059	FASTENER SPEC				
				DOC	DOC				0-70058	TORQUE SPEC				
				AR	AR				0-79055-6	EPOXY INK				
				AR	AR				0-00021-1	GREASE				
				DOC	DOC				MIL-STD-248	WELD SPEC				
				DOC	DOC				ASTM-E 498-73	LEAK SPEC				
				AR	AR				ER316L	ELECTRODE				
				AR	AR				E316L	ELECTRODE				

PRELIMINARY

6501 (2-76)

PARTS LIST

0-70916 REQUIRED FOR ABBREVIATION, CODE AND SYMBOL INTERPRETATION

CONVAIR DIVISION OF GENERAL DYNAMICS
SAN DIEGO, CALIFORNIA

PDA: PL 11-38084 | REV LTR

TITLE: SUPPORT INSTL - COLD MASS -EBT-P PROTOTYPE

PADR | RELEASE/DATE | CODE IDENT NO. 14170 | SH 1 OF 1 SHS

DOC TYPE	DOC OPT	DOC CONT	GROUP	REPRO CODE	CONTRACT NO.	UNDIM DWG

DRAFTSMAN / /	DESIGNER / /	GR ENGR / /	STRESS / /	PROD. ENGR / /	MATERIAL / /	CHECKER / /	/ /	/ /	/ /	/ /

PAGE | DISTRIBUTION CODE | PACKAGE NO.

NOTE SYMBOL: * D - DOCUMENT NO. E - END ITEM G - GENERAL NOTE L - LIMIT M - MATERIAL N - NOMENCLATURE R - REF DESIG T - TYPE DESIG/VALUE U - USAGE DATA V - VENDOR ITEM

REQUIREMENTS PER ASSY/INSTL -1				UNIT OF MEAS	FIND NO.	CODE IDENT NO.	PART OR IDENTIFYING NUMBER	NOMENCLATURE OR DESCRIPTION	ZONE LTR	ZONE NO.	NOTE SYM *	NOTES
			X				-1	SUPPORT INSTL				
			1				-2	SHIM			M	.032 x 2.5 x 5.0 MF 0-00745-2
			1				-3	PIN			M	1.75 DIA x 1.3 6AL-4V, ELI TITANIUM
												ANNEALED. MIL-T-9046, TYPE III, COMP D
			1				11-38002-1	COLD MASS ASSY				
			3				11-38080-1	SUPPORT				
			1				11-38030-1	STACK ASSY				
			6				NAS 6308-24 H	BOLT				
			6				NAS 1587-8C	WASHER				
			A/R				MS 20995-C47	LOCKWIRE				PRELIMINARY
			DOC				MS 33540	SPEC				
			DOC				MIL-STD-248	SPEC				
							MIL-STD-278					
							MIL-I-6866					
							MIL-E-19933					
							MIL-E-22200/2					
							0-70054					
							0-70058					
							0-75214-2	SPEC				
							ER 316L	ELECTRODE				
							E 316L	ELECTRODE				
			DOC				0-70042	SPEC				

6501 (2-76)

PARTS LIST

0-70916 REQUIRED FOR ABBREVIATION, CODE AND SYMBOL INTERPRETATION

CONVAIR DIVISION OF GENERAL DYNAMICS
SAN DIEGO, CALIFORNIA

PDA: PL 11-38090 | REV LTR: —

TITLE: OUT OF PLANE STRUTS ~ EBT-P PROTOTYPE

PADR | RELEASE/DATE | CODE IDENT NO. 14170 | SH 1 OF 1 SHS

DOC TYPE | DOC OPT | DOC CONT | GROUP 692-0 | REPRO CODE | CONTRACT NO. | UNDIM DWG

DRAFTSMAN / / RGVK | DESIGNER / / | GR ENGR / / | STRESS / / | PROD. ENGR / / | MATERIAL / / | CHECKER / / | / / | / / | / / | / /

PAGE | DISTRIBUTION CODE | PACKAGE NO. | NOTE SYMBOL: * D - DOCUMENT NO. E - END ITEM G - GENERAL NOTE L - LIMIT M - MATERIAL N - NOMENCLATURE R - REF DESIG T - TYPE DESIG/VALUE U - USAGE DATA V - VENDOR ITEM

REQUIREMENTS PER ASSY/INSTL				UNIT OF MEAS	FIND NO.	CODE IDENT NO.	PART OR IDENTIFYING NUMBER	NOMENCLATURE OR DESCRIPTION	ZONE LTR	ZONE NO.	NOTE SYM *	NOTES
			-1				-1	STRUT ASSEMBLY	B	4		
			1				-2	ROD	C	4	M	2.0 HEX × 20.5 ROD 304 SST; ASTM-A-276
			1				BRE-16-2450-001	ROD END	C	6	V	SOUTHWEST PRODUCTS CO.
			1				BRELH-16-2450-001	ROD END	C	3	V	SOUTHWEST PRODUCTS CO.
			1				NAS1423C-20	JAM NUT	C	6		
			1				NAS1423C-20LH	JAM NUT	C	3		
			2				11-38091-1	PIN	G	3		
			DOC				0-73517	TEST SPEC				
			↑				0-70042	IDENT SPEC				
							0-70054	TORQUE SPEC				
			↓				0-70058	TORQUE SPEC				
			DOC				MS33540	SAFETY WIRE SPEC				
			AR				MS20995-C47	LOCKWIRE				PRELIMINARY

6501 (2-76)

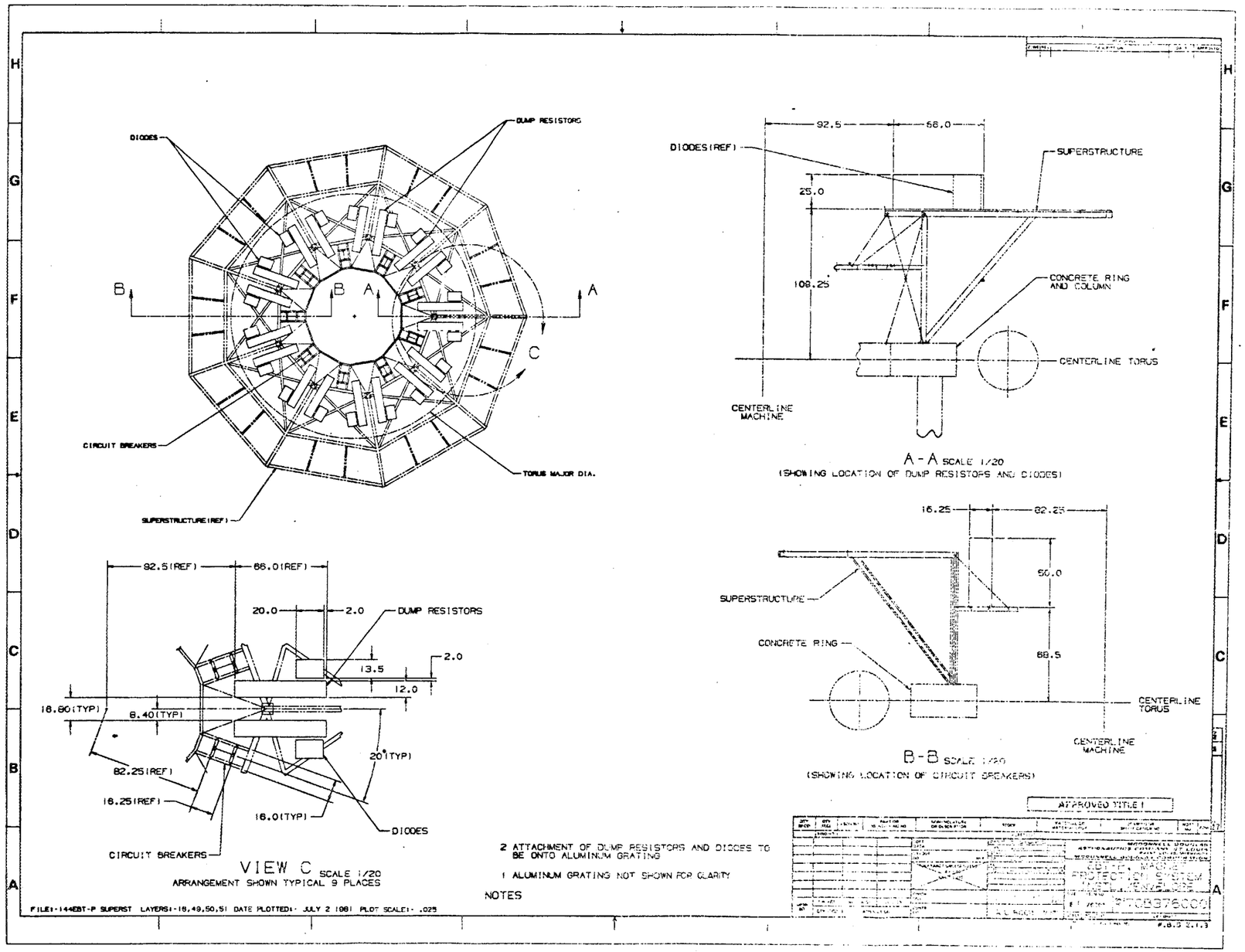
DIODES
DUMP RESISTORS
B
B
A
A
C
CIRCUIT BREAKERS
TORUS MAJOR DIA.
SUPERSTRUCTURE (REF)
92.5
66.0
DIODES (REF)
SUPERSTRUCTURE
25.0
108.25
CONCRETE RING AND COLUMN
CENTERLINE TORUS
CENTERLINE MACHINE
A - A SCALE 1/20
(SHOWING LOCATION OF DUMP RESISTORS AND DIODES)
16.25
82.25
50.0
SUPERSTRUCTURE
CONCRETE RING
68.5
CENTERLINE TORUS
CENTERLINE MACHINE
B - B SCALE 1/20
(SHOWING LOCATION OF CIRCUIT BREAKERS)
92.5 (REF)
66.0 (REF)
20.0
2.0
DUMP RESISTORS
2.0
13.5
12.0
18.80 (TYP)
8.40 (TYP)
20° (TYP)
82.25 (REF)
16.25 (REF)
16.0 (TYP)
DIODES
CIRCUIT BREAKERS
VIEW C SCALE 1/20
ARRANGEMENT SHOWN TYPICAL 9 PLACES
2 ATTACHMENT OF DUMP RESISTORS AND DIODES TO BE ONTO ALUMINUM GRATING
1 ALUMINUM GRATING NOT SHOWN FOR CLARITY
NOTES
APPROVED TITLE 1
FILE: 144EBT-P SUPERST LAYERS: 18,49,50,51 DATE PLOTTED: JULY 2 1981 PLOT SCALE: .025

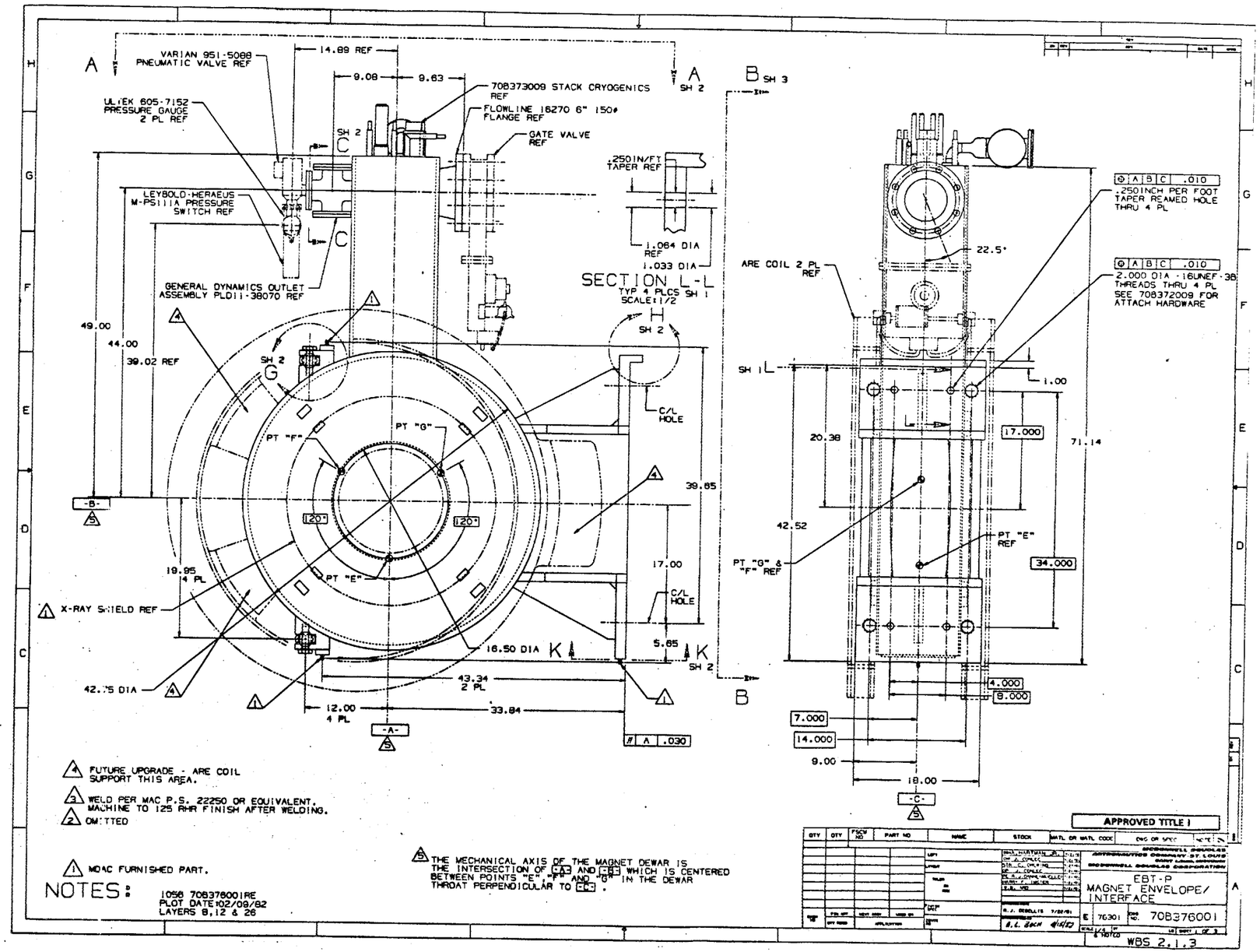
VARIAN 951-5008 PNEUMATIC VALVE REF
ULTEK 605-7152 PRESSURE GAUGE 2 PL REF
LEYBOLD-HERAEUS M-PS111A PRESSURE SWITCH REF
GENERAL DYNAMICS OUTLET ASSEMBLY PL011-38070 REF
708373009 STACK CRYOGENICS REF
FLOWLINE 16270 6" 150# FLANGE REF
GATE VALVE REF
.2501N/FT TAPER REF
1.064 DIA REF
1.033 DIA
SECTION L-L
TYP 4 PLCS SH 1
SCALE 1/2
C/L HOLE
PT "F"
PT "G"
PT "E"
120°
X-RAY SHIELD REF
16.50 DIA
42.75 DIA
43.34 2 PL
12.00 4 PL
33.84
19.95 4 PL
39.65
17.00
5.85
14.89 REF
9.08
9.63
49.00
44.00
39.02 REF
.030
ARE COIL 2 PL REF
22.5°
.2501INCH PER FOOT TAPER REAMED HOLE THRU 4 PL
2.000 DIA -16UNEF-3B THREADS THRU 4 PL SEE 708372009 FOR ATTACH HARDWARE
.010
1.00
20.38
17.000
71.14
42.52
PT "G" & "F" REF
PT "E" REF
34.000
4.000
8.000
7.000
14.000
9.00
18.00
FUTURE UPGRADE - ARE COIL SUPPORT THIS AREA.
WELD PER MAC P.S. 22250 OR EQUIVALENT. MACHINE TO 125 RHR FINISH AFTER WELDING.
OMITTED
MDAC FURNISHED PART.
THE MECHANICAL AXIS OF THE MAGNET DEWAR IS THE INTERSECTION OF "A" AND "B" WHICH IS CENTERED BETWEEN POINTS "E", "F" AND "G" IN THE DEWAR THROAT PERPENDICULAR TO "C".
NOTES:
1056 708376001RE
PLOT DATE 02/09/82
LAYERS 8,12 & 26
APPROVED TITLE 1
EBT-P
MAGNET ENVELOPE/ INTERFACE
76301
708376001
WBS 2.1.3

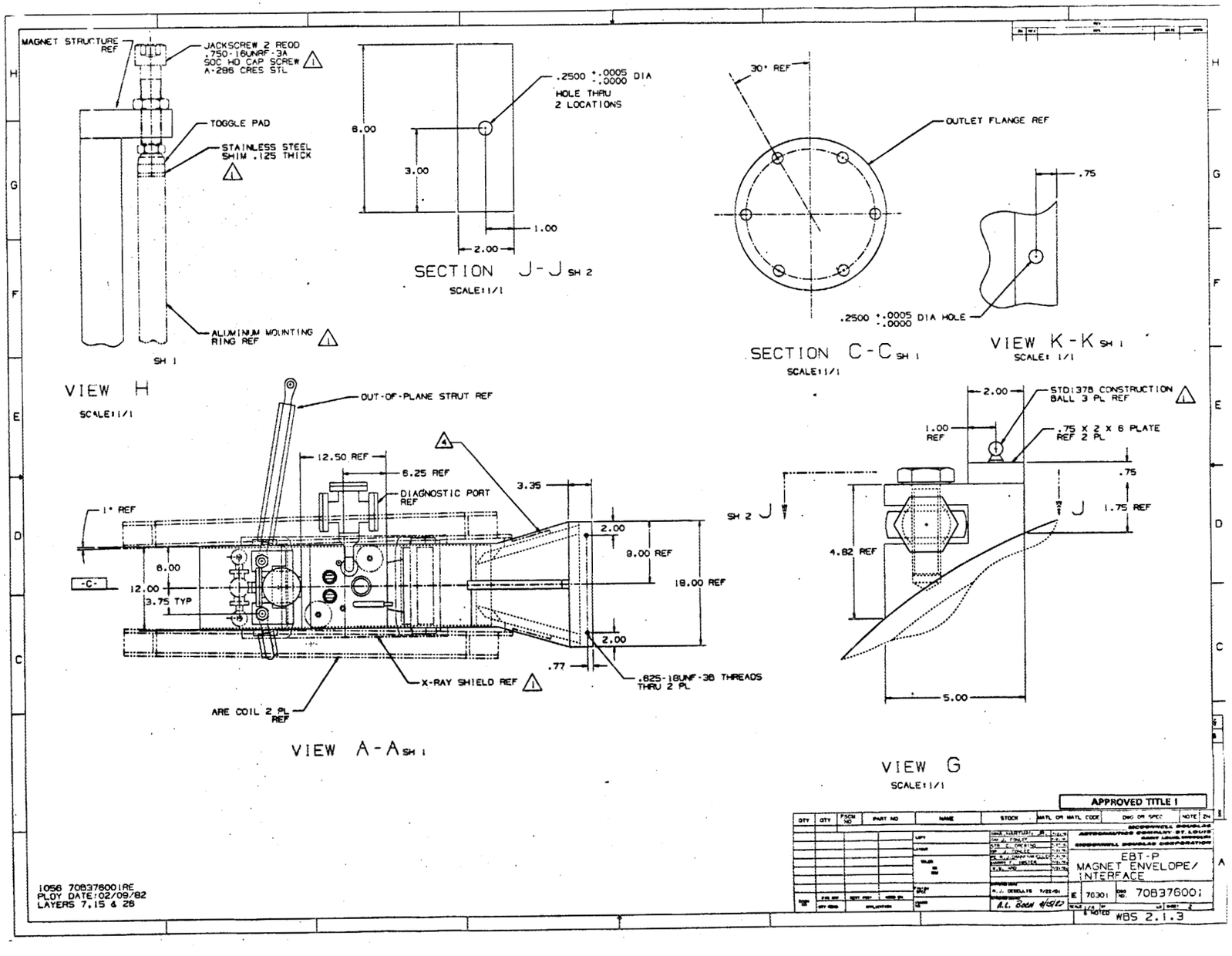
MAGNET STRUCTURE REF
JACKSCREW 2 REQD .750-16UNRF-3A SOC HD CAP SCREW A-286 CRES STL
TOGGLE PAD
STAINLESS STEEL SHIM .125 THICK
ALUMINUM MOUNTING RING REF
SH 1
VIEW H
SCALE:1/1
.2500 +.0005 -.0000 DIA HOLE THRU 2 LOCATIONS
8.00
3.00
1.00
2.00
SECTION J-J SH 2
SCALE:1/1
30° REF
OUTLET FLANGE REF
.75
.2500 +.0005 -.0000 DIA HOLE
SECTION C-C SH 1
SCALE:1/1
VIEW K-K SH 1
SCALE: 1/1
OUT-OF-PLANE STRUT REF
12.50 REF
6.25 REF
DIAGNOSTIC PORT REF
3.35
1° REF
2.00
9.00 REF
18.00 REF
8.00
12.00
3.75 TYP
-C-
2.00
.77
.625-18UNF-3B THREADS THRU 2 PL
X-RAY SHIELD REF
ARC COIL 2 PL REF
VIEW A-A SH 1
2.00
STD1378 CONSTRUCTION BALL 3 PL REF
1.00 REF
.75 X 2 X 6 PLATE REF 2 PL
.75
1.75 REF
SH 2 J
J
4.82 REF
5.00
VIEW G
SCALE:1/1
APPROVED TITLE I
EBT-P
MAGNET ENVELOPE/
INTERFACE
70301
70837600:
WBS 2.1.3
1056 70837600:RE
PLOT DATE:02/09/82
LAYERS 7,15 & 26

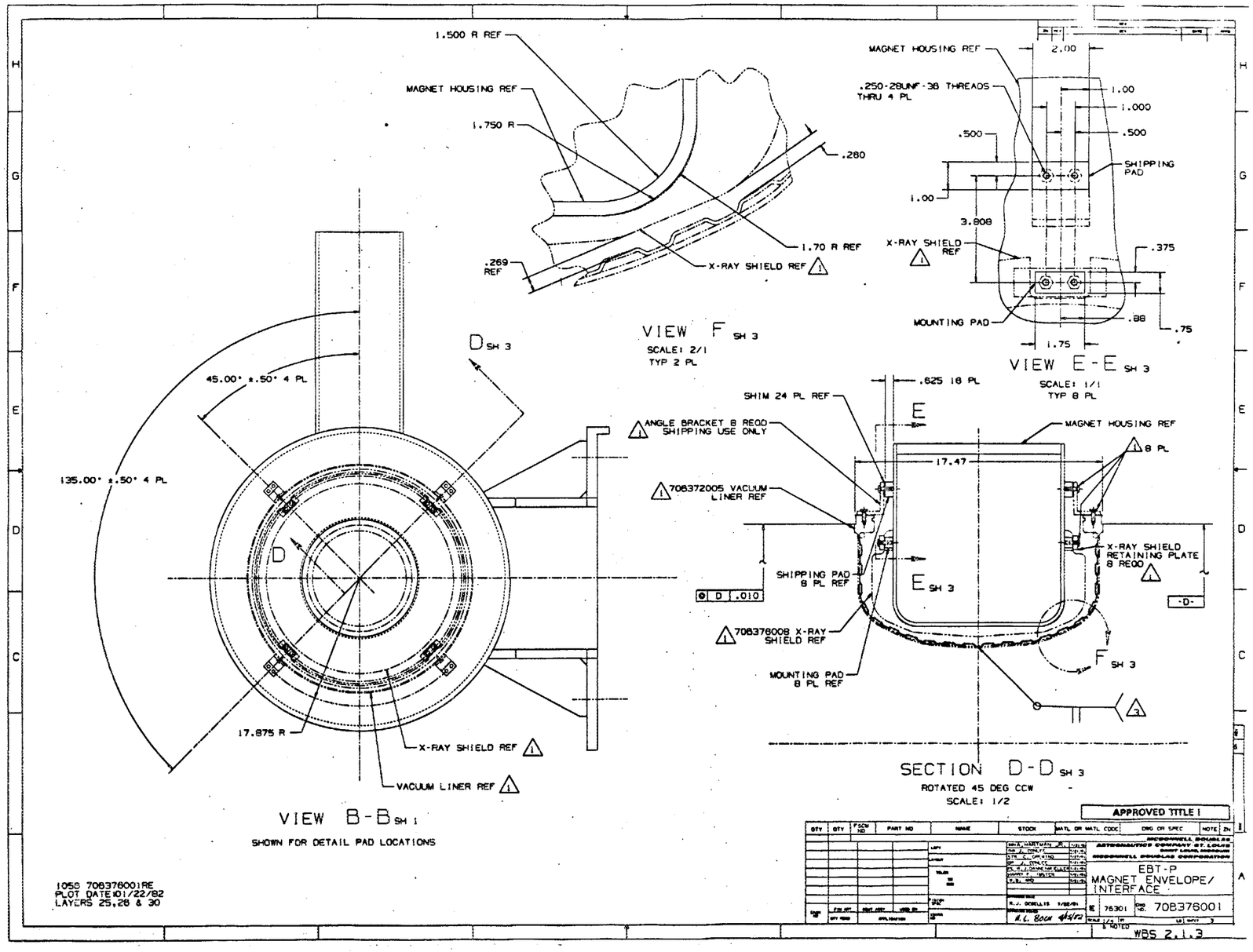
1.500 R REF
MAGNET HOUSING REF
1.750 R
.280
1.70 R REF
.269 REF
X-RAY SHIELD REF
VIEW F SH 3
SCALE: 2/1
TYP 2 PL
MAGNET HOUSING REF
.250-28UNF-3B THREADS THRU 4 PL
2.00
1.00
1.000
.500
.500
SHIPPING PAD
1.00
3.808
X-RAY SHIELD REF
.375
MOUNTING PAD
.88
.75
1.75
VIEW E-E SH 3
SCALE: 1/1
TYP 8 PL
D SH 3
45.00° ±.50° 4 PL
135.00° ±.50° 4 PL
D
17.875 R
X-RAY SHIELD REF
VACUUM LINER REF
VIEW B-B SH 1
SHOWN FOR DETAIL PAD LOCATIONS
.625 18 PL
SHIM 24 PL REF
E
ANGLE BRACKET 8 REQD SHIPPING USE ONLY
MAGNET HOUSING REF
8 PL
17.47
708372005 VACUUM LINER REF
X-RAY SHIELD RETAINING PLATE 8 REQD
SHIPPING PAD 8 PL REF
E SH 3
D .010
-D-
708376008 X-RAY SHIELD REF
F SH 3
MOUNTING PAD 8 PL REF
SECTION D-D SH 3
ROTATED 45 DEG CCW
SCALE: 1/2
APPROVED TITLE I
EBT-P
MAGNET ENVELOPE/
INTERFACE
76301
708376001
WBS 2.1.3
1058 708376001RE
PLOT DATE:01/22/82
LAYERS 25,28 & 30

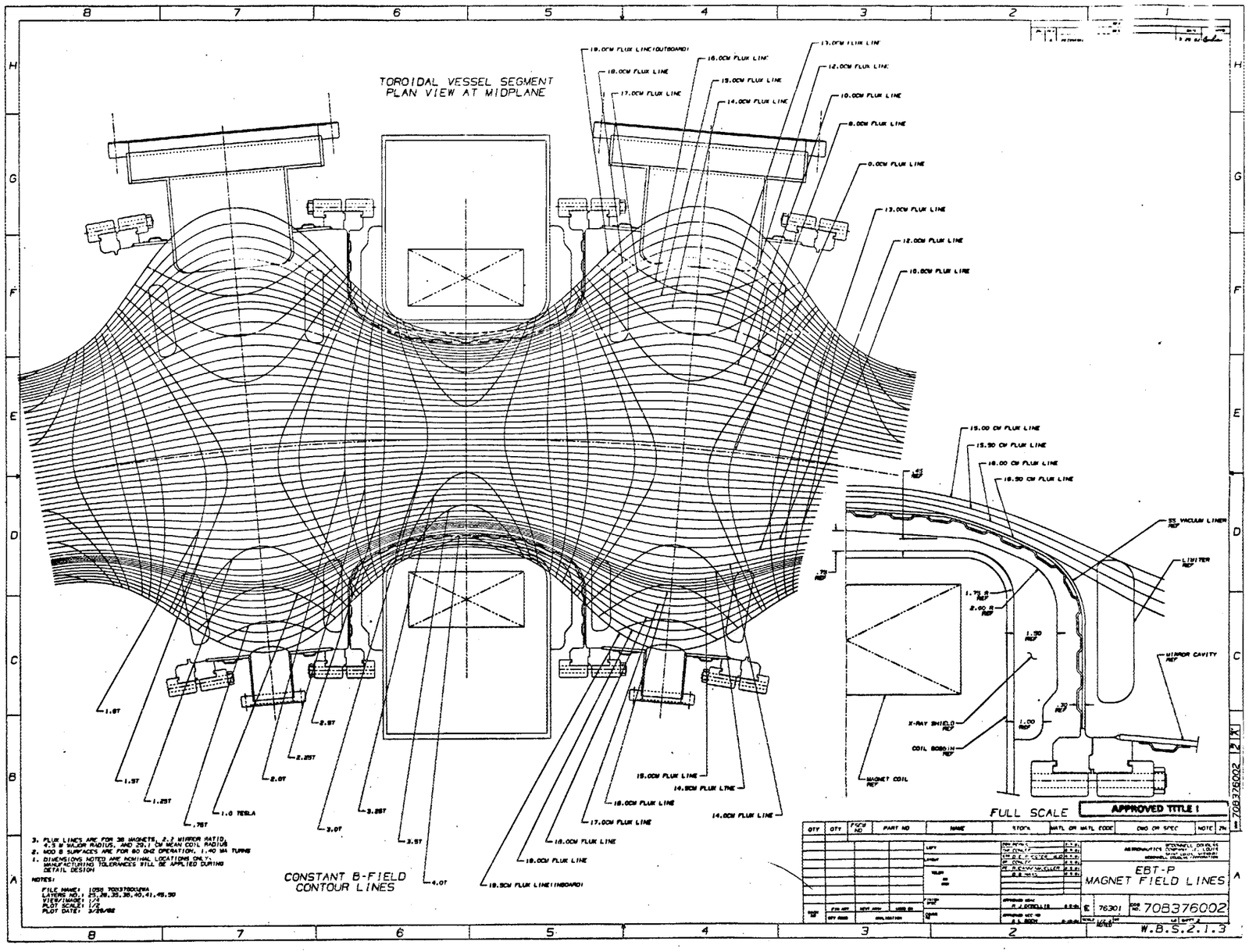
TOROIDAL VESSEL SEGMENT
PLAN VIEW AT MIDPLANE
CONSTANT B-FIELD
CONTOUR LINES
FULL SCALE
APPROVED TITLE !
EBT-P
MAGNET FIELD LINES
708376002
W.B.S.2.1.3

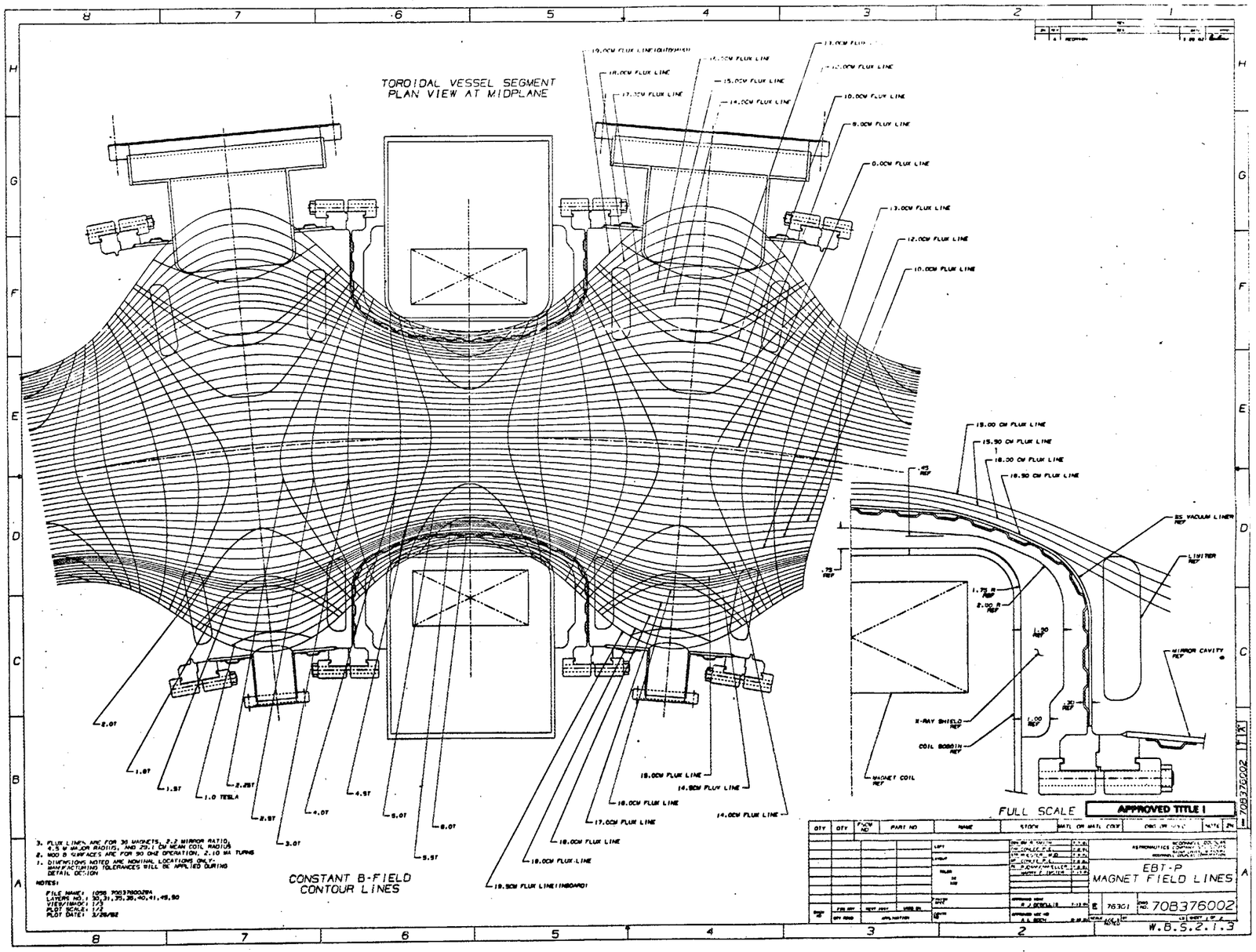
TOROIDAL VESSEL SEGMENT
PLAN VIEW AT MIDPLANE
CONSTANT B-FIELD
CONTOUR LINES
1.0 TESLA
EBT-P
MAGNET FIELD LINES
FULL SCALE
APPROVED TITLE I
708376002
W.B.S.2.1.3

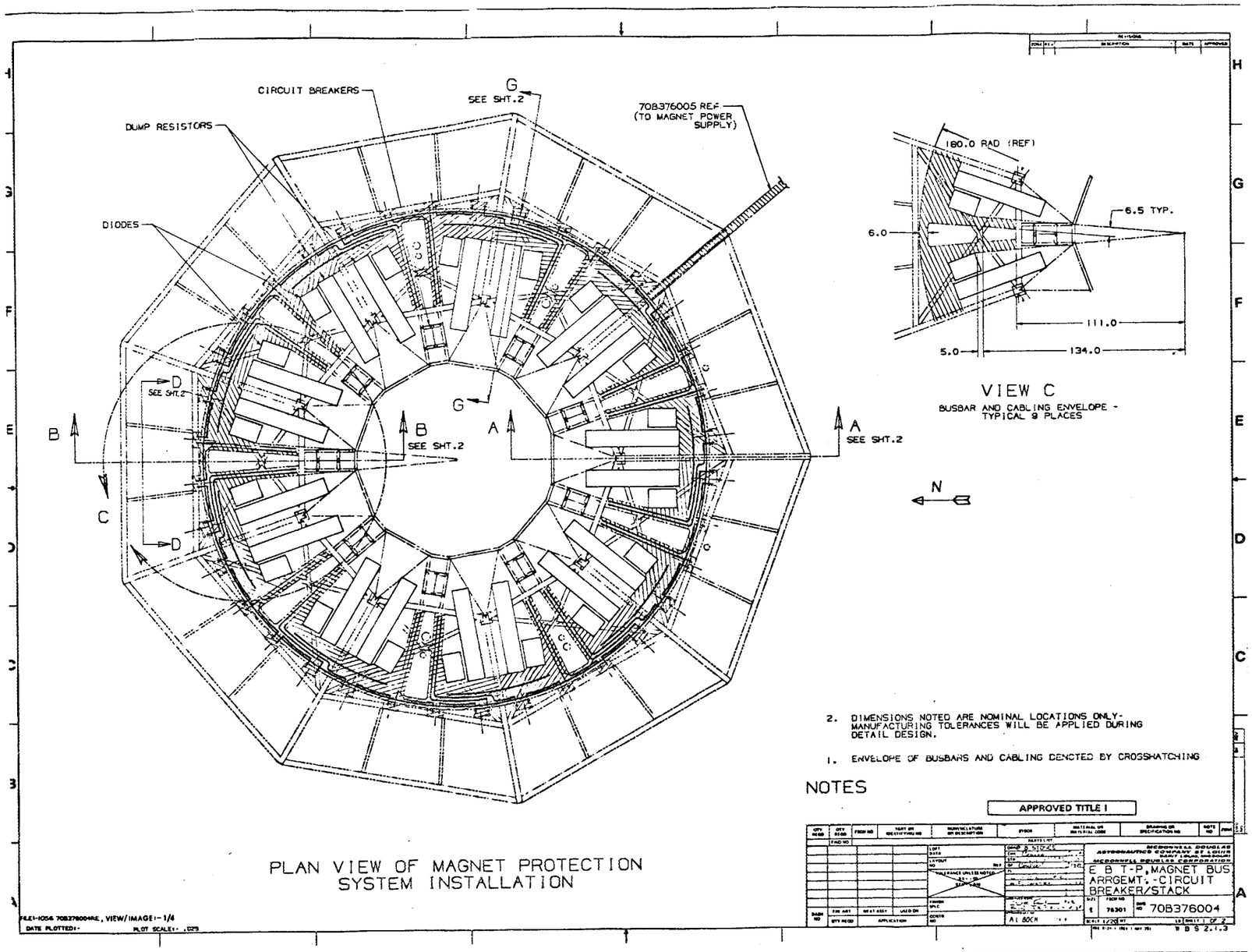
CIRCUIT BREAKERS
DUMP RESISTORS
DIODES
G
SEE SHT.2
708376005 REF
(TO MAGNET POWER SUPPLY)
D
SEE SHT.2
B
B
SEE SHT.2
A
A
SEE SHT.2
C
D
N
180.0 RAD (REF)
6.5 TYP.
6.0
111.0
5.0
134.0
VIEW C
BUSBAR AND CABLING ENVELOPE - TYPICAL 9 PLACES
2. DIMENSIONS NOTED ARE NOMINAL LOCATIONS ONLY- MANUFACTURING TOLERANCES WILL BE APPLIED DURING DETAIL DESIGN.
1. ENVELOPE OF BUSBARS AND CABLING DENOTED BY CROSSHATCHING
NOTES
APPROVED TITLE I
PLAN VIEW OF MAGNET PROTECTION SYSTEM INSTALLATION
MCDONNELL DOUGLAS ASTRONAUTICS COMPANY ST. LOUIS
MCDONNELL DOUGLAS CORPORATION
E B T-P, MAGNET BUS ARRGEMT, -CIRCUIT BREAKER/STACK
76301
708376004
A1 BOCK
SCALE 1/20
SHEET 1 OF 2
FILE1-1054 708376004RE, VIEW/IMAGE1-1/4
DATE PLOTTED1-
PLOT SCALE1- .025

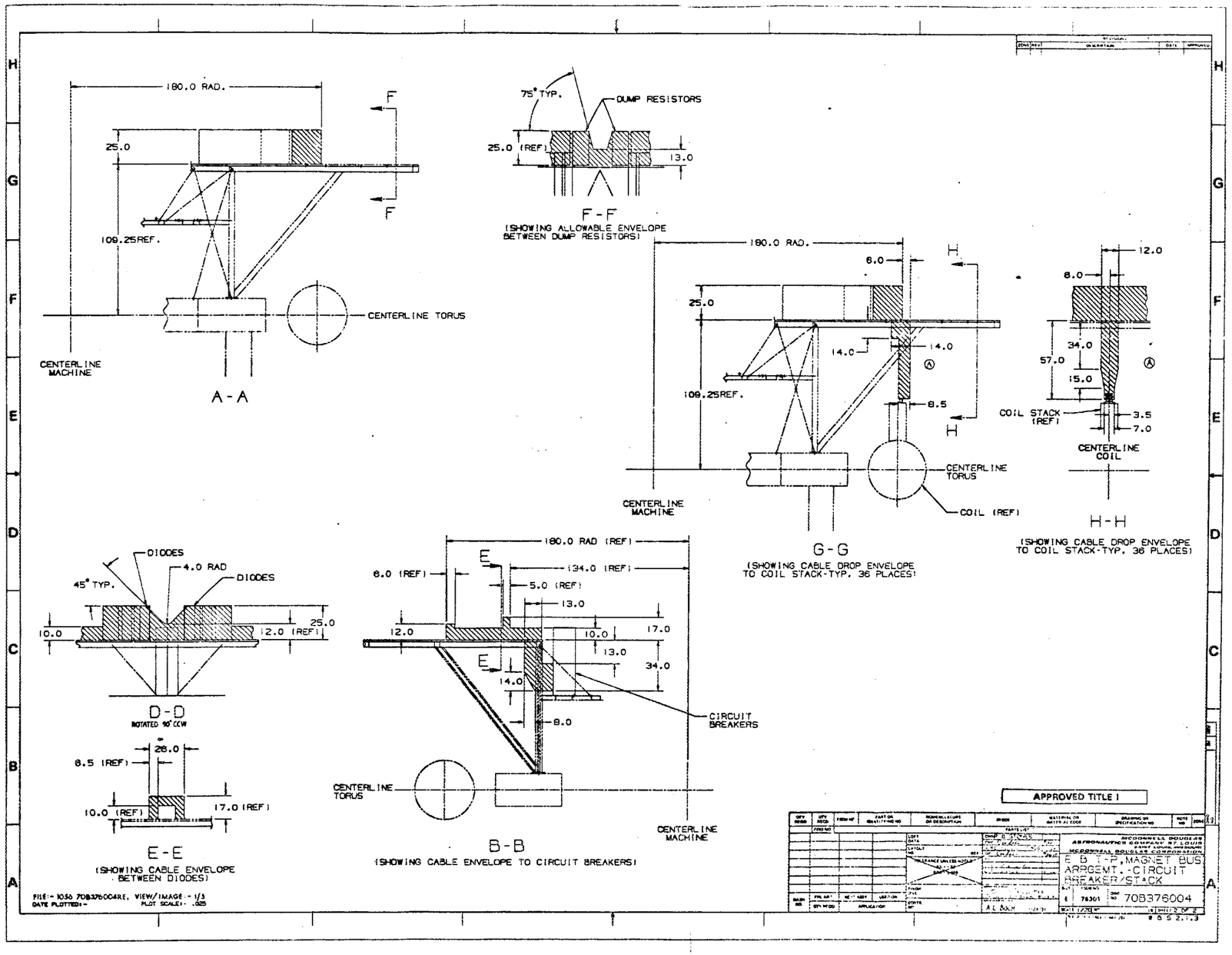
180.0 RAD.
25.0
109.25REF.
CENTERLINE TORUS
CENTERLINE MACHINE
A-A
75° TYP.
DUMP RESISTORS
25.0 (REF)
13.0
F-F
(SHOWING ALLOWABLE ENVELOPE BETWEEN DUMP RESISTORS)
180.0 RAD.
6.0
25.0
14.0
109.25REF.
8.5
CENTERLINE TORUS
CENTERLINE MACHINE
COIL (REF)
G-G
(SHOWING CABLE DROP ENVELOPE TO COIL STACK-TYP. 36 PLACES)
12.0
8.0
34.0
57.0
15.0
COIL STACK (REF)
3.5
7.0
CENTERLINE COIL
H-H
(SHOWING CABLE DROP ENVELOPE TO COIL STACK-TYP. 36 PLACES)
DIODES
4.0 RAD
DIODES
45° TYP.
10.0
12.0 (REF)
25.0
D-D
ROTATED 90° CCW
26.0
8.5 (REF)
10.0 (REF)
17.0 (REF)
E-E
(SHOWING CABLE ENVELOPE BETWEEN DIODES)
180.0 RAD (REF)
134.0 (REF)
6.0 (REF)
5.0 (REF)
13.0
12.0
10.0
17.0
13.0
34.0
14.0
8.0
CIRCUIT BREAKERS
CENTERLINE TORUS
CENTERLINE MACHINE
B-B
(SHOWING CABLE ENVELOPE TO CIRCUIT BREAKERS)
APPROVED TITLE I
MCDONNELL DOUGLAS ASTRONAUTICS COMPANY ST. LOUIS
MCDONNELL DOUGLAS CORPORATION
EBT-P, MAGNET BUS ARRGEMT.-CIRCUIT BREAKER/STACK
708376004

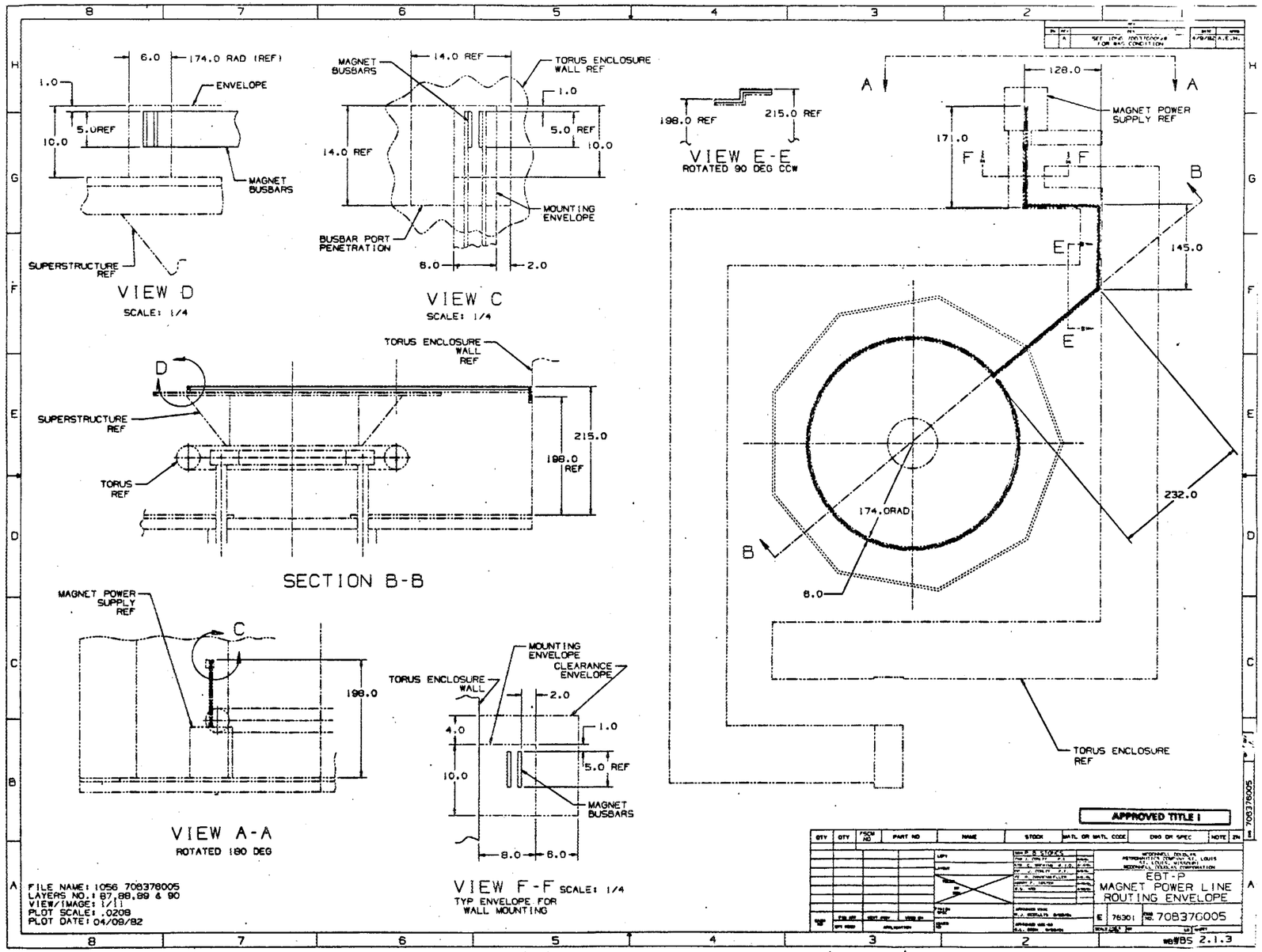
VIEW D
SCALE: 1/4
VIEW C
SCALE: 1/4
VIEW E-E
ROTATED 90 DEG CCW
SECTION B-B
VIEW A-A
ROTATED 180 DEG
VIEW F-F SCALE: 1/4
TYP ENVELOPE FOR WALL MOUNTING
MAGNET POWER SUPPLY REF
TORUS ENCLOSURE REF
MAGNET BUSBARS
MOUNTING ENVELOPE
CLEARANCE ENVELOPE
TORUS ENCLOSURE WALL
SUPERSTRUCTURE REF
TORUS REF
ENVELOPE
BUSBAR PORT PENETRATION
174.0 RAD (REF)
174.0 RAD
232.0
145.0
171.0
128.0
198.0 REF
215.0 REF
FILE NAME: 1056 708376005
LAYERS NO.: 87,88,89 & 90
VIEW/IMAGE: 1/11
PLOT SCALE: .0208
PLOT DATE: 04/09/82
APPROVED TITLE I
EBT-P
MAGNET POWER LINE
ROUTING ENVELOPE
708376005
76301

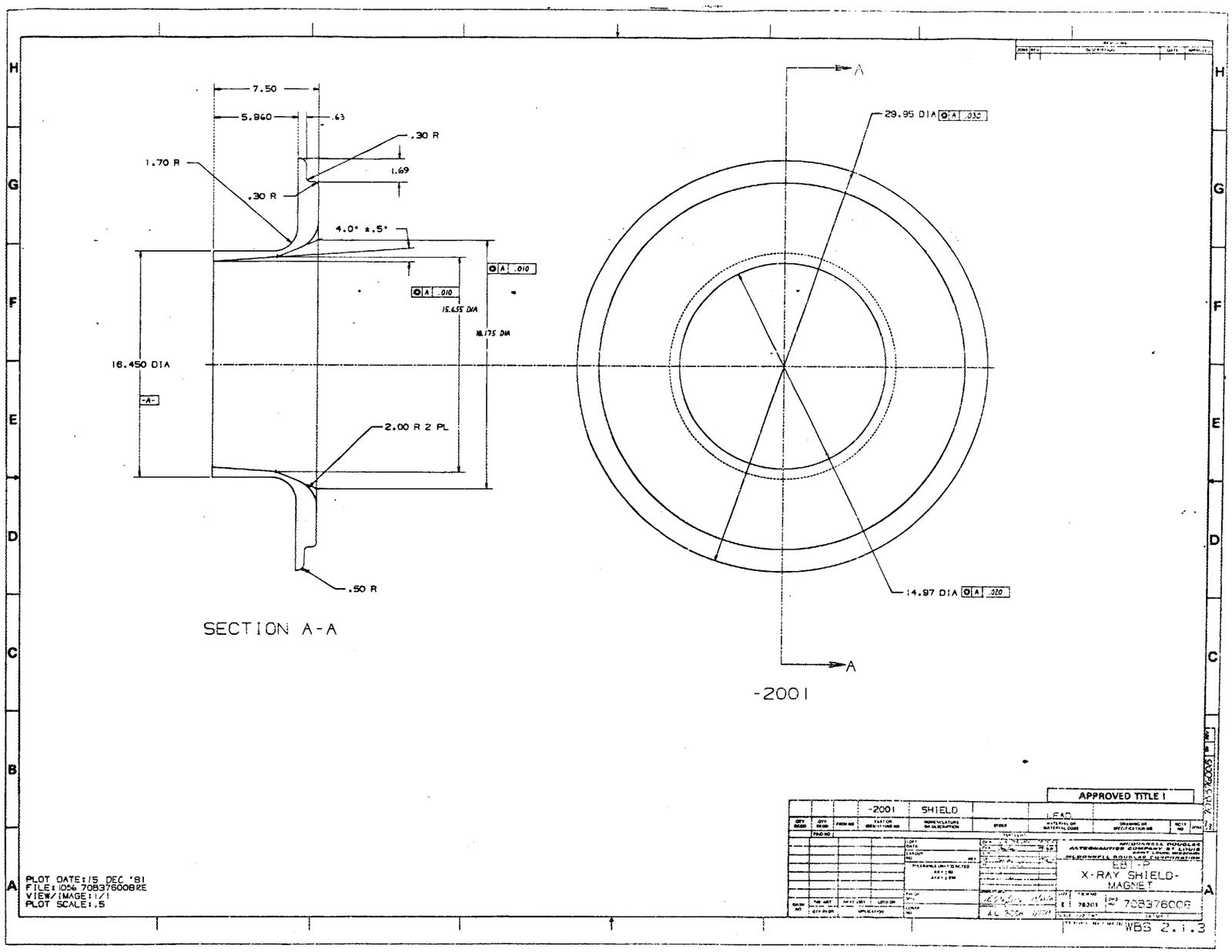
7.50
5.960
.63
.30 R
1.70 R
1.69
.30 R
4.0° ±.5°
.010
.010
15.655 DIA
16.175 DIA
16.450 DIA
-A-
2.00 R 2 PL
.50 R
SECTION A-A
29.95 DIA .030
14.97 DIA .020
A
A
-2001
APPROVED TITLE 1
-2001
SHIELD
LEAD
X-RAY SHIELD-
MAGNET
76301
708376008
WBS 2.1.3
PLOT DATE: 15 DEC '81
FILE: 1056 708376008RE
VIEW/IMAGE: 1/1
PLOT SCALE: .5

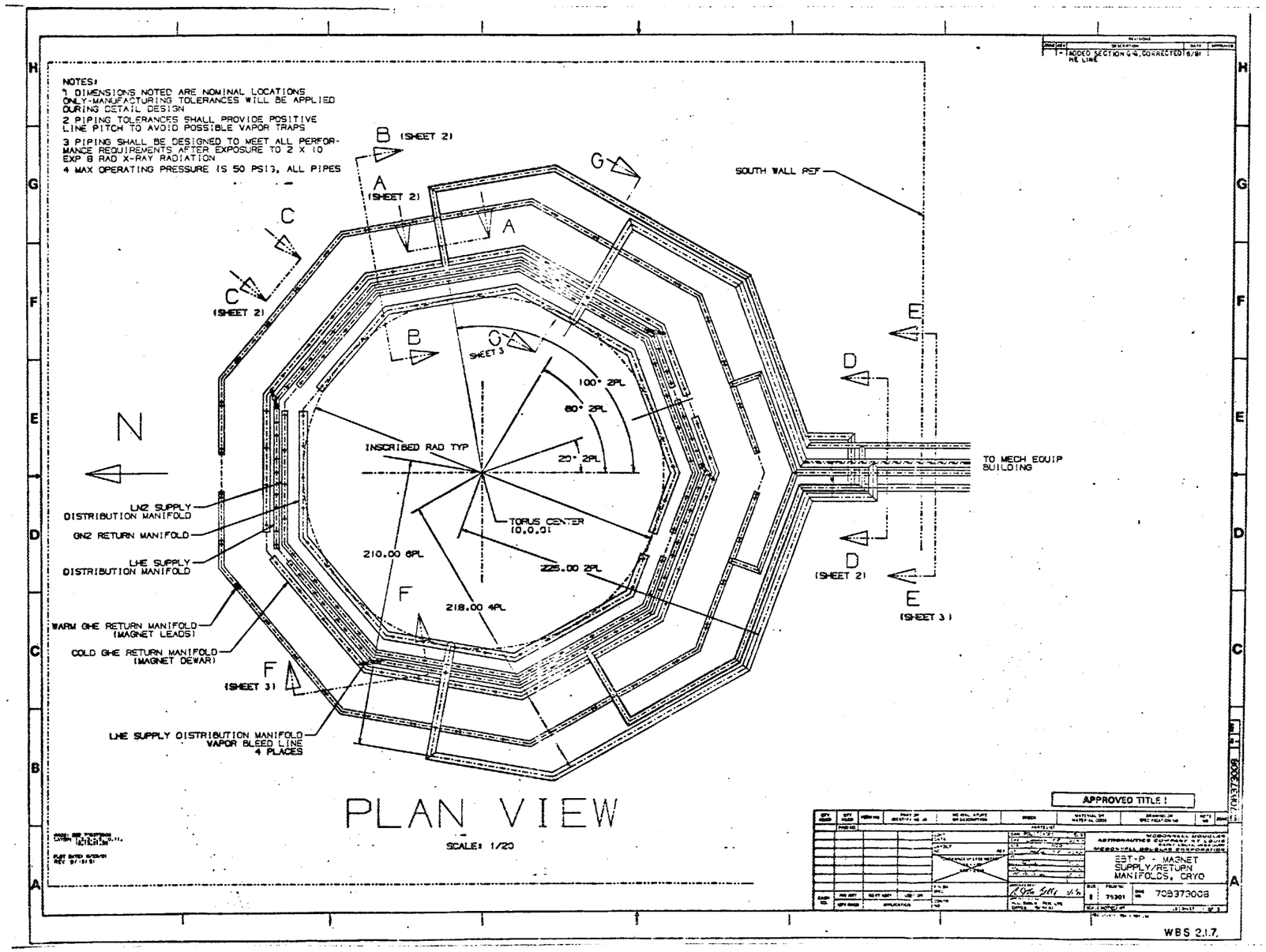
NOTES:
1 DIMENSIONS NOTED ARE NOMINAL LOCATIONS ONLY-MANUFACTURING TOLERANCES WILL BE APPLIED DURING DETAIL DESIGN
2 PIPING TOLERANCES SHALL PROVIDE POSITIVE LINE PITCH TO AVOID POSSIBLE VAPOR TRAPS
3 PIPING SHALL BE DESIGNED TO MEET ALL PERFORMANCE REQUIREMENTS AFTER EXPOSURE TO 2 X 10 EXP 8 RAD X-RAY RADIATION
4 MAX OPERATING PRESSURE IS 50 PSIG, ALL PIPES
B (SHEET 2)
A (SHEET 2)
C
C (SHEET 2)
G
SOUTH WALL REF
A
B
C
SHEET 3
100° 2PL
80° 2PL
20° 2PL
INSCRIBED RAD TYP
TORUS CENTER (0,0,3)
210.00 6PL
225.00 2PL
218.00 4PL
F
F (SHEET 3)
D
D (SHEET 2)
E
E (SHEET 3)
TO MECH EQUIP BUILDING
N
LN2 SUPPLY DISTRIBUTION MANIFOLD
GN2 RETURN MANIFOLD
LHE SUPPLY DISTRIBUTION MANIFOLD
WARM GHE RETURN MANIFOLD (MAGNET LEADS)
COLD GHE RETURN MANIFOLD (MAGNET DEWAR)
LHE SUPPLY DISTRIBUTION MANIFOLD VAPOR BLEED LINE 4 PLACES
PLAN VIEW
SCALE: 1/20
APPROVED TITLE:
EBT-P - MAGNET SUPPLY/RETURN MANIFOLDS, CRYO
709373008
WBS 2.1.7.

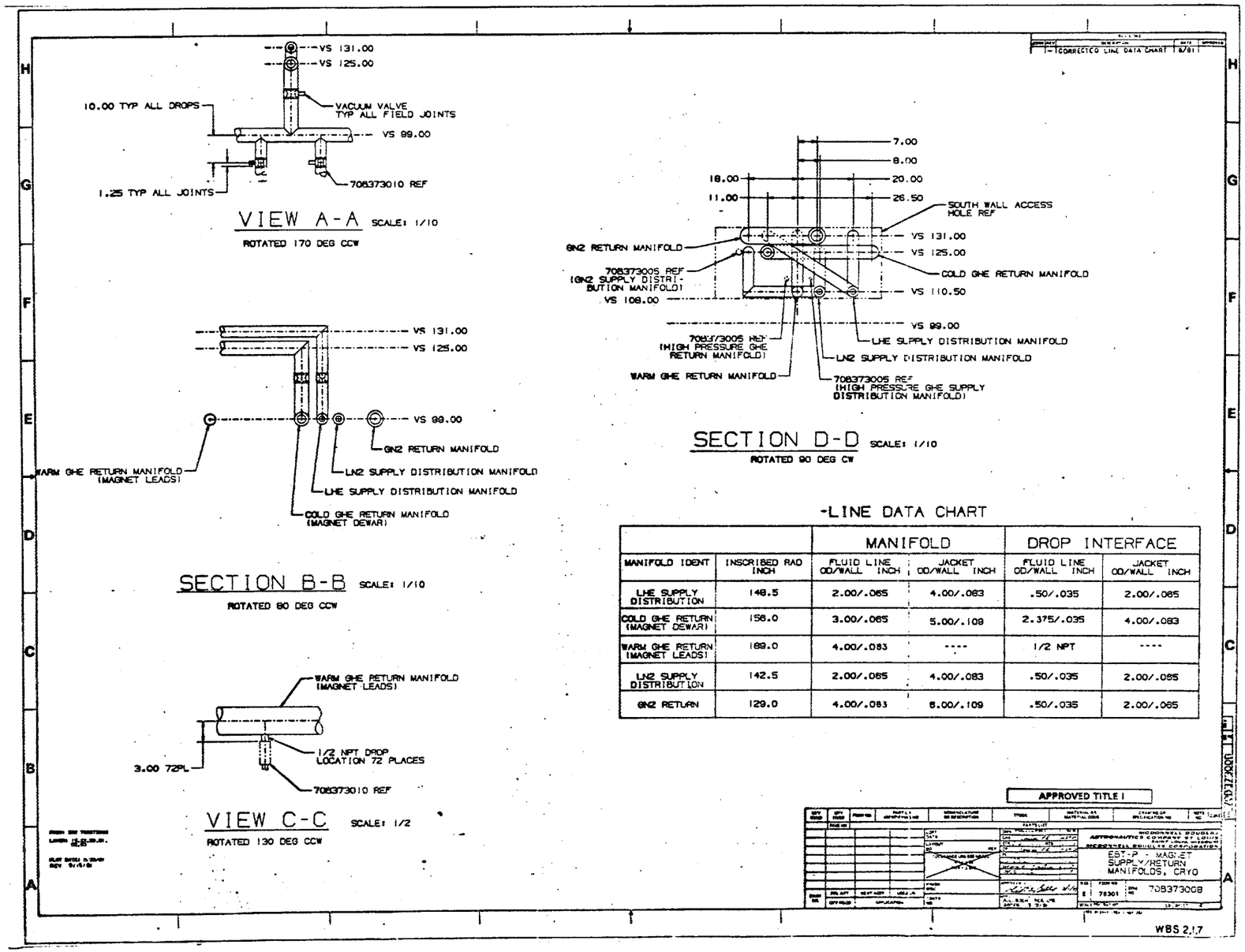

-LINE DATA CHART

		MANIFOLD		DROP INTERFACE	
MANIFOLD IDENT	INSCRIBED RAD INCH	FLUID LINE OD/WALL INCH	JACKET OD/WALL INCH	FLUID LINE OD/WALL INCH	JACKET OD/WALL INCH
LHE SUPPLY DISTRIBUTION	148.5	2.00/.065	4.00/.083	.50/.035	2.00/.065
COLD GHE RETURN (MAGNET DEWAR)	156.0	3.00/.065	5.00/.109	2.375/.035	4.00/.083
WARM GHE RETURN (MAGNET LEADS)	189.0	4.00/.083	----	1/2 NPT	----
LN2 SUPPLY DISTRIBUTION	142.5	2.00/.065	4.00/.083	.50/.035	2.00/.065
GN2 RETURN	129.0	4.00/.083	6.00/.109	.50/.035	2.00/.065

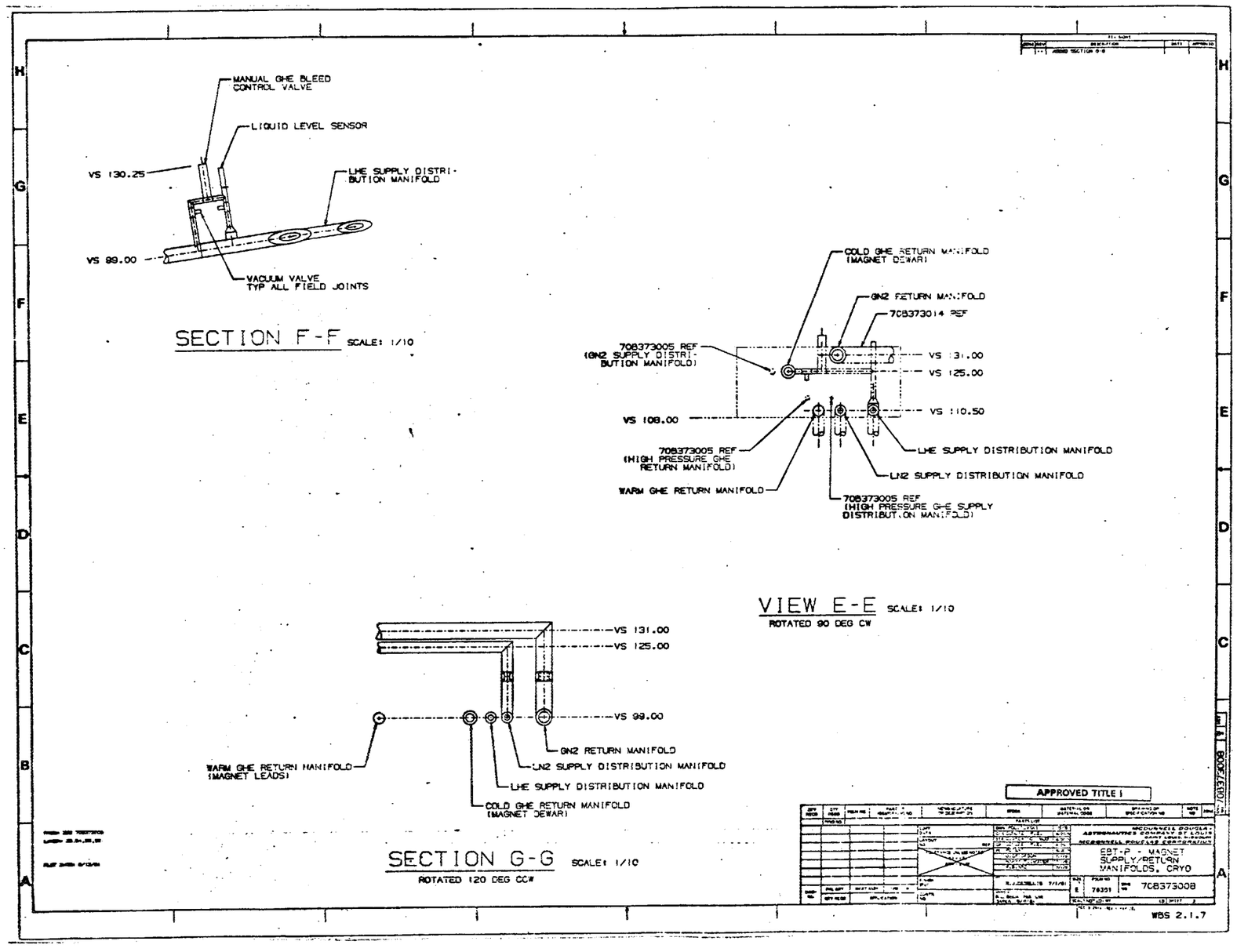
MANUAL GHE BLEED CONTROL VALVE
LIQUID LEVEL SENSOR
VS 130.25
LHE SUPPLY DISTRIBUTION MANIFOLD
VS 99.00
VACUUM VALVE TYP ALL FIELD JOINTS
SECTION F-F SCALE: 1/10
COLD GHE RETURN MANIFOLD (MAGNET DEWAR)
GN2 RETURN MANIFOLD
708373014 REF
708373005 REF (GN2 SUPPLY DISTRIBUTION MANIFOLD)
VS 131.00
VS 125.00
VS 110.50
VS 108.00
708373005 REF (HIGH PRESSURE GHE RETURN MANIFOLD)
LHE SUPPLY DISTRIBUTION MANIFOLD
LN2 SUPPLY DISTRIBUTION MANIFOLD
WARM GHE RETURN MANIFOLD
708373005 REF (HIGH PRESSURE GHE SUPPLY DISTRIBUTION MANIFOLD)
VIEW E-E SCALE: 1/10
ROTATED 90 DEG CW
VS 131.00
VS 125.00
VS 99.00
GN2 RETURN MANIFOLD
LN2 SUPPLY DISTRIBUTION MANIFOLD
WARM GHE RETURN MANIFOLD (MAGNET LEADS)
LHE SUPPLY DISTRIBUTION MANIFOLD
COLD GHE RETURN MANIFOLD (MAGNET DEWAR)
SECTION G-G SCALE: 1/10
ROTATED 120 DEG CCW
APPROVED TITLE:
EBT-P - MAGNET SUPPLY/RETURN MANIFOLDS, CRYO
708373008
WBS 2.1.7

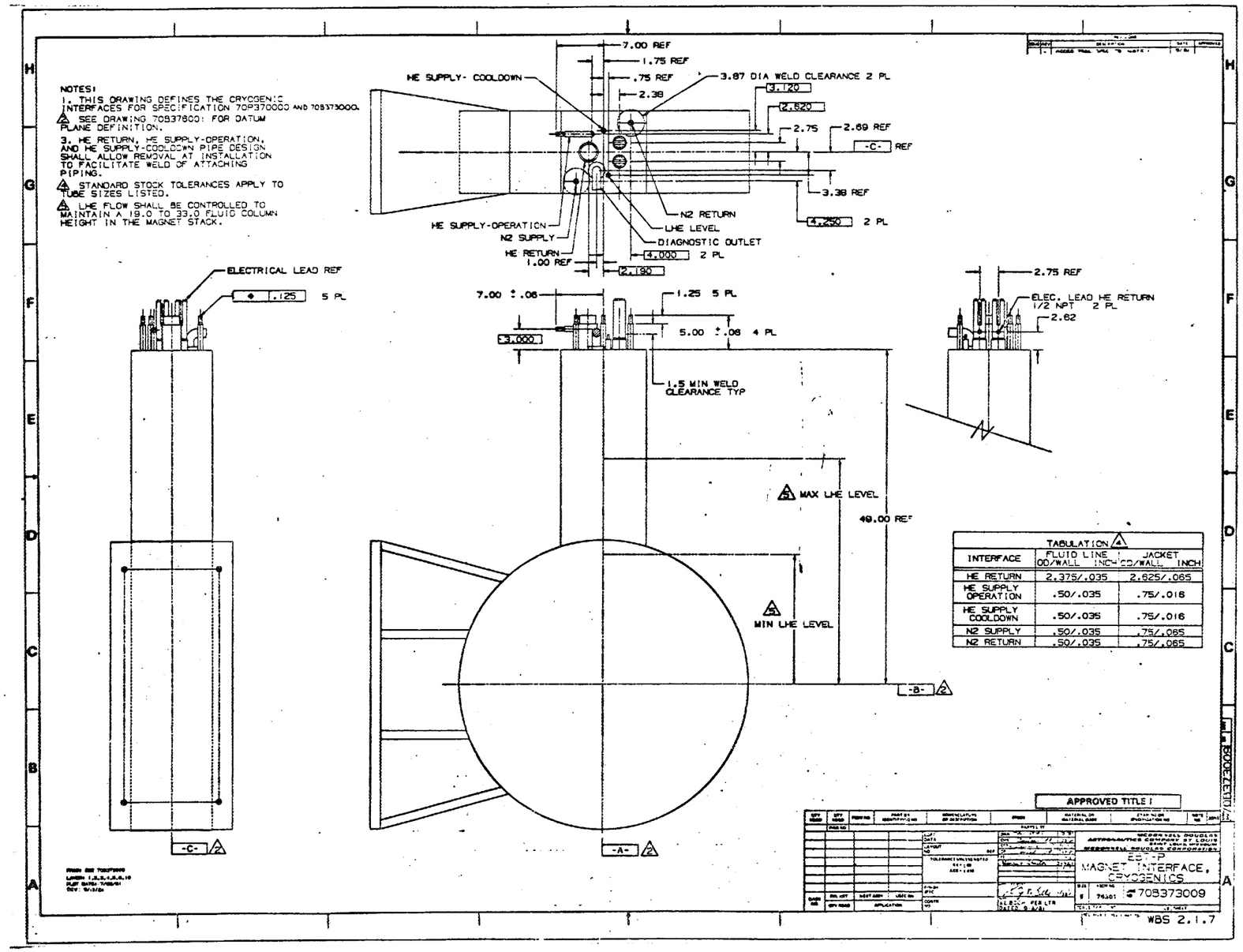
NOTES:
1. THIS DRAWING DEFINES THE CRYOGENIC INTERFACES FOR SPECIFICATION 70P370000 AND 708373000.
2. SEE DRAWING 70B37800: FOR DATUM PLANE DEFINITION.
3. HE RETURN, HE SUPPLY-OPERATION, AND HE SUPPLY-COOLDOWN PIPE DESIGN SHALL ALLOW REMOVAL AT INSTALLATION TO FACILITATE WELD OF ATTACHING PIPING.
4. STANDARD STOCK TOLERANCES APPLY TO TUBE SIZES LISTED.
5. LHE FLOW SHALL BE CONTROLLED TO MAINTAIN A 19.0 TO 33.0 FLUID COLUMN HEIGHT IN THE MAGNET STACK.
HE SUPPLY- COOLDOWN
7.00 REF
1.75 REF
.75 REF
2.38
3.87 DIA WELD CLEARANCE 2 PL
3.120
2.620
2.75
2.69 REF
-C- REF
3.38 REF
4.250 2 PL
N2 RETURN
LHE LEVEL
DIAGNOSTIC OUTLET
HE SUPPLY-OPERATION
N2 SUPPLY
HE RETURN
1.00 REF
4.000 2 PL
2.190
ELECTRICAL LEAD REF
1.125 5 PL
7.00 ±.06
1.25 5 PL
3.000
5.00 ±.06 4 PL
1.5 MIN WELD CLEARANCE TYP
2.75 REF
ELEC. LEAD HE RETURN 1/2 NPT 2 PL
2.62
MAX LHE LEVEL
49.00 REF
MIN LHE LEVEL
-B-
-C-
-A-
TABULATION
INTERFACE
FLUID LINE OD/WALL INCH
JACKET OD/WALL INCH
HE RETURN 2.375/.035 2.625/.065
HE SUPPLY OPERATION .50/.035 .75/.016
HE SUPPLY COOLDOWN .50/.035 .75/.016
N2 SUPPLY .50/.035 .75/.065
N2 RETURN .50/.035 .75/.065
APPROVED TITLE I
MCDONNELL DOUGLAS ASTRONAUTICS COMPANY ST. LOUIS
MCDONNELL DOUGLAS CORPORATION
EBT-P
MAGNET INTERFACE, CRYOGENICS
708373009
WBS 2.1.7

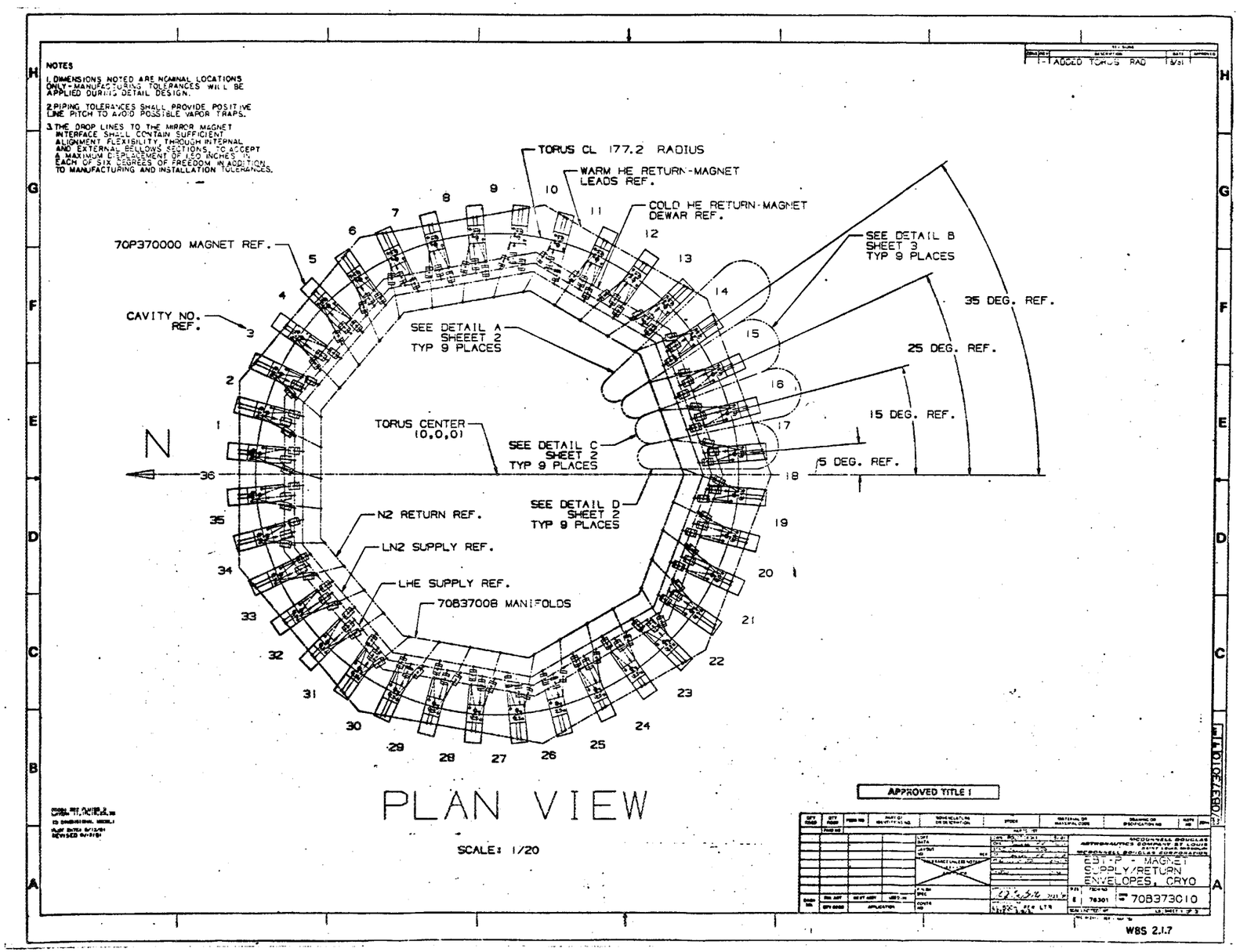
NOTES
1. DIMENSIONS NOTED ARE NOMINAL LOCATIONS ONLY - MANUFACTURING TOLERANCES WILL BE APPLIED DURING DETAIL DESIGN.
2. PIPING TOLERANCES SHALL PROVIDE POSITIVE LINE PITCH TO AVOID POSSIBLE VAPOR TRAPS.
3. THE DROP LINES TO THE MIRROR MAGNET INTERFACE SHALL CONTAIN SUFFICIENT ALIGNMENT FLEXIBILITY THROUGH INTERNAL AND EXTERNAL BELLOWS SECTIONS, TO ACCEPT A MAXIMUM DISPLACEMENT OF 1.50 INCHES IN EACH OF SIX DEGREES OF FREEDOM IN ADDITION TO MANUFACTURING AND INSTALLATION TOLERANCES.
TORUS CL 177.2 RADIUS
WARM HE RETURN-MAGNET LEADS REF.
COLD HE RETURN-MAGNET DEWAR REF.
70P370000 MAGNET REF.
CAVITY NO. REF.
SEE DETAIL A SHEEET 2 TYP 9 PLACES
SEE DETAIL B SHEET 3 TYP 9 PLACES
35 DEG. REF.
25 DEG. REF.
15 DEG. REF.
5 DEG. REF.
TORUS CENTER (0,0,0)
SEE DETAIL C SHEET 2 TYP 9 PLACES
SEE DETAIL D SHEET 2 TYP 9 PLACES
N2 RETURN REF.
LN2 SUPPLY REF.
LHE SUPPLY REF.
70B37008 MANIFOLDS
N
PLAN VIEW
SCALE: 1/20
APPROVED TITLE I
CRYO - MAGNET SUPPLY/RETURN ENVELOPES, CRYO
70B373010
WBS 2.1.7

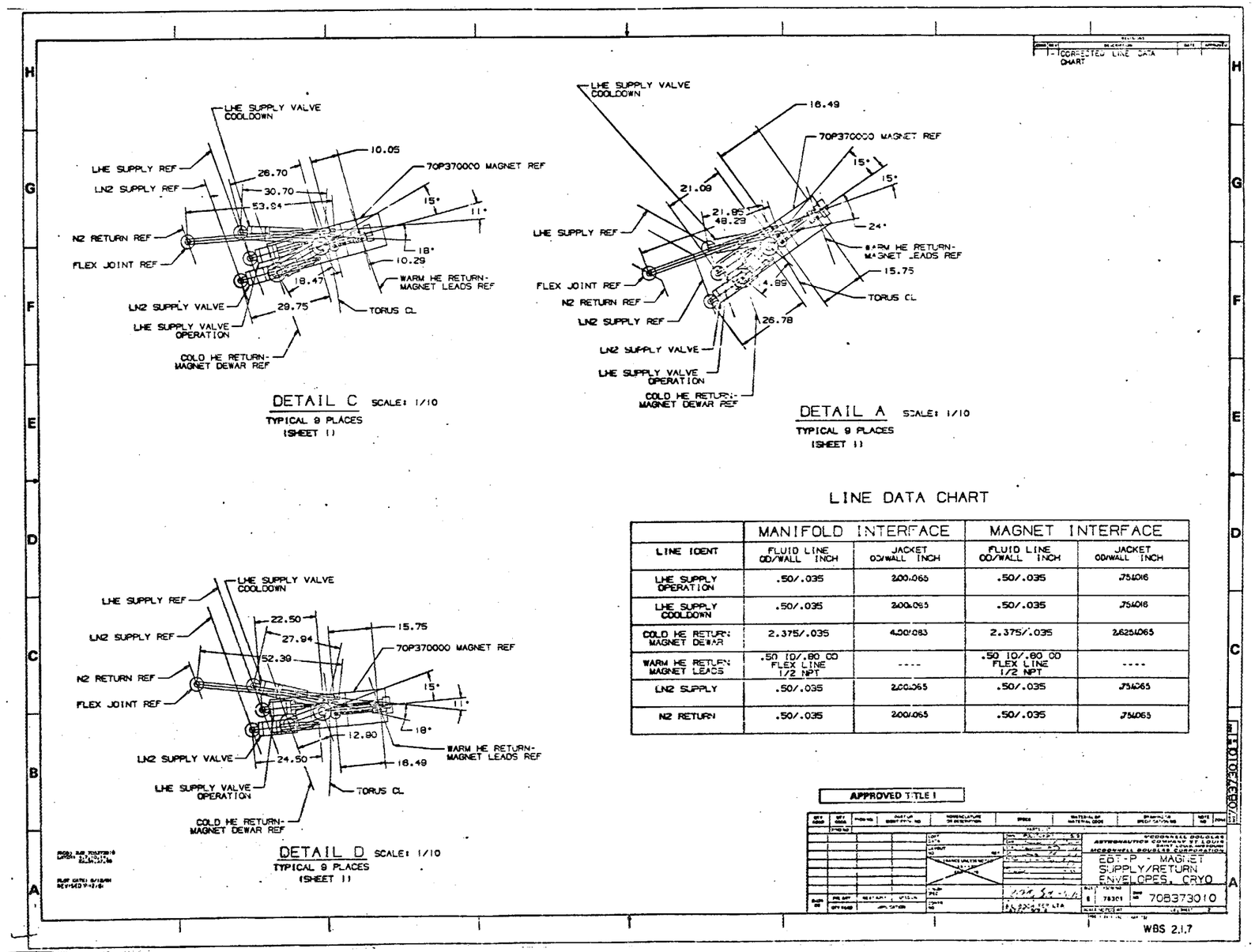

LINE DATA CHART

	MANIFOLD INTERFACE		MAGNET INTERFACE	
LINE IDENT	FLUID LINE OD/WALL INCH	JACKET OD/WALL INCH	FLUID LINE OD/WALL INCH	JACKET OD/WALL INCH
LHE SUPPLY OPERATION	.50/.035	2.00/.065	.50/.035	.75/.016
LHE SUPPLY COOLDOWN	.50/.035	2.00/.065	.50/.035	.75/.016
COLD HE RETURN MAGNET DEWAR	2.375/.035	4.00/.083	2.375/.035	2.625/.065
WARM HE RETURN MAGNET LEADS	.50 ID/.80 OD FLEX LINE 1/2 NPT	----	.50 ID/.80 OD FLEX LINE 1/2 NPT	----
LN2 SUPPLY	.50/.035	2.00/.065	.50/.035	.75/.065
N2 RETURN	.50/.035	2.00/.065	.50/.035	.75/.065

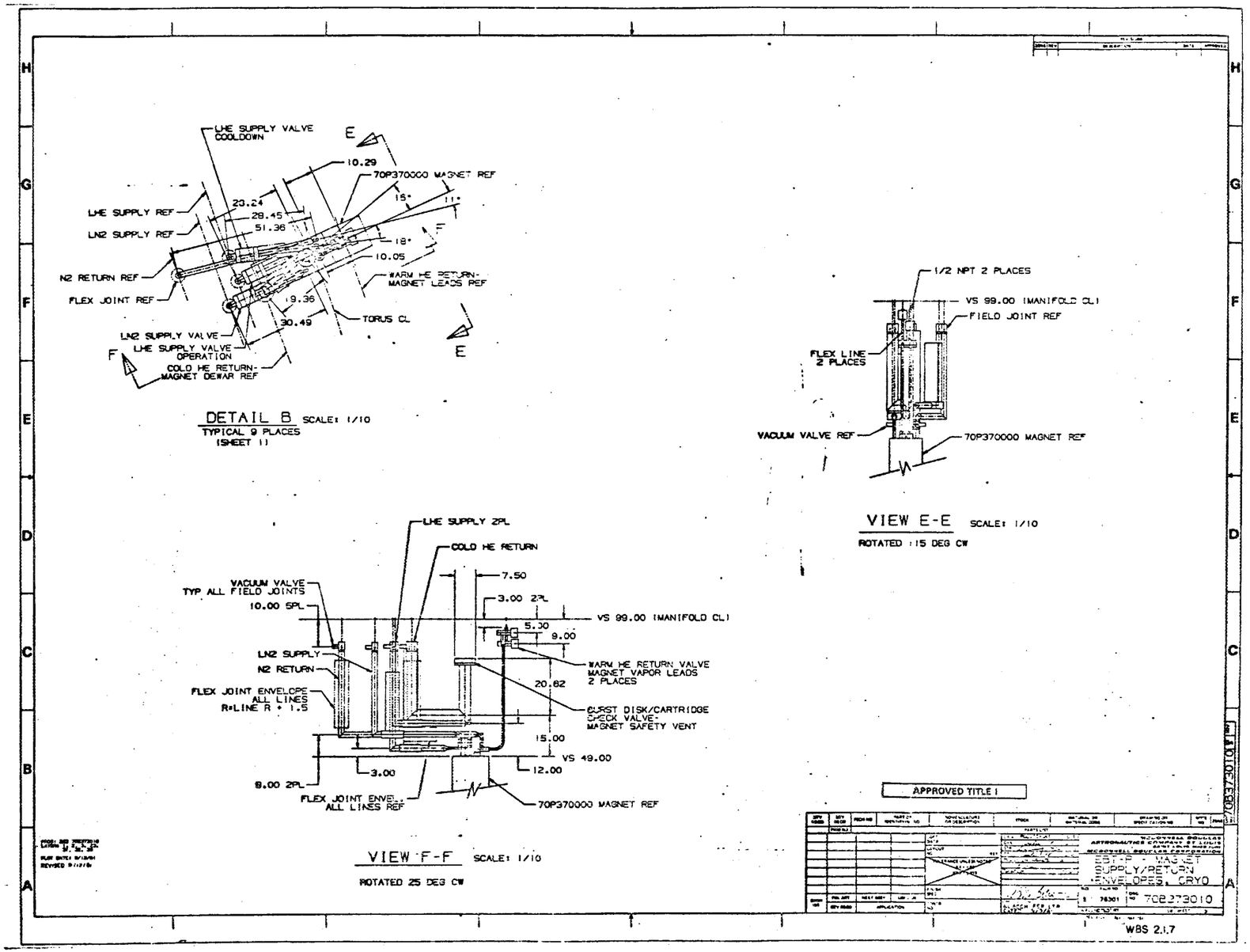
LHE SUPPLY VALVE COOLDOWN
10.29
70P370000 MAGNET REF
23.24
28.45
51.36
LHE SUPPLY REF
LN2 SUPPLY REF
N2 RETURN REF
FLEX JOINT REF
15°
11°
18°
10.05
WARM HE RETURN-MAGNET LEADS REF
19.36
30.49
TORUS CL
LN2 SUPPLY VALVE
LHE SUPPLY VALVE OPERATION
COLD HE RETURN-MAGNET DEWAR REF
DETAIL B SCALE: 1/10
TYPICAL 9 PLACES
(SHEET 1)
1/2 NPT 2 PLACES
VS 99.00 (MANIFOLD CL)
FIELD JOINT REF
FLEX LINE 2 PLACES
VACUUM VALVE REF
70P370000 MAGNET REF
VIEW E-E SCALE: 1/10
ROTATED 15 DEG CW
LHE SUPPLY 2PL
COLD HE RETURN
7.50
3.00 2PL
VACUUM VALVE TYP ALL FIELD JOINTS
10.00 5PL
VS 99.00 (MANIFOLD CL)
5.30
9.00
LN2 SUPPLY
N2 RETURN
WARM HE RETURN VALVE MAGNET VAPOR LEADS 2 PLACES
20.62
FLEX JOINT ENVELOPE ALL LINES R=LINE R + 1.5
BURST DISK/CARTRIDGE CHECK VALVE-MAGNET SAFETY VENT
15.00
VS 49.00
3.00
12.00
8.00 2PL
FLEX JOINT ENVEL. ALL LINES REF
70P370000 MAGNET REF
VIEW F-F SCALE: 1/10
ROTATED 25 DEG CW
APPROVED TITLE I
ASTRONAUTICS COMPANY ST. LOUIS
MCDONNELL DOUGLAS CORPORATION
EBT-P MAGNET SUPPLY/RETURN ENVELOPES, CRYO
76301
702273010
WBS 2.1.7

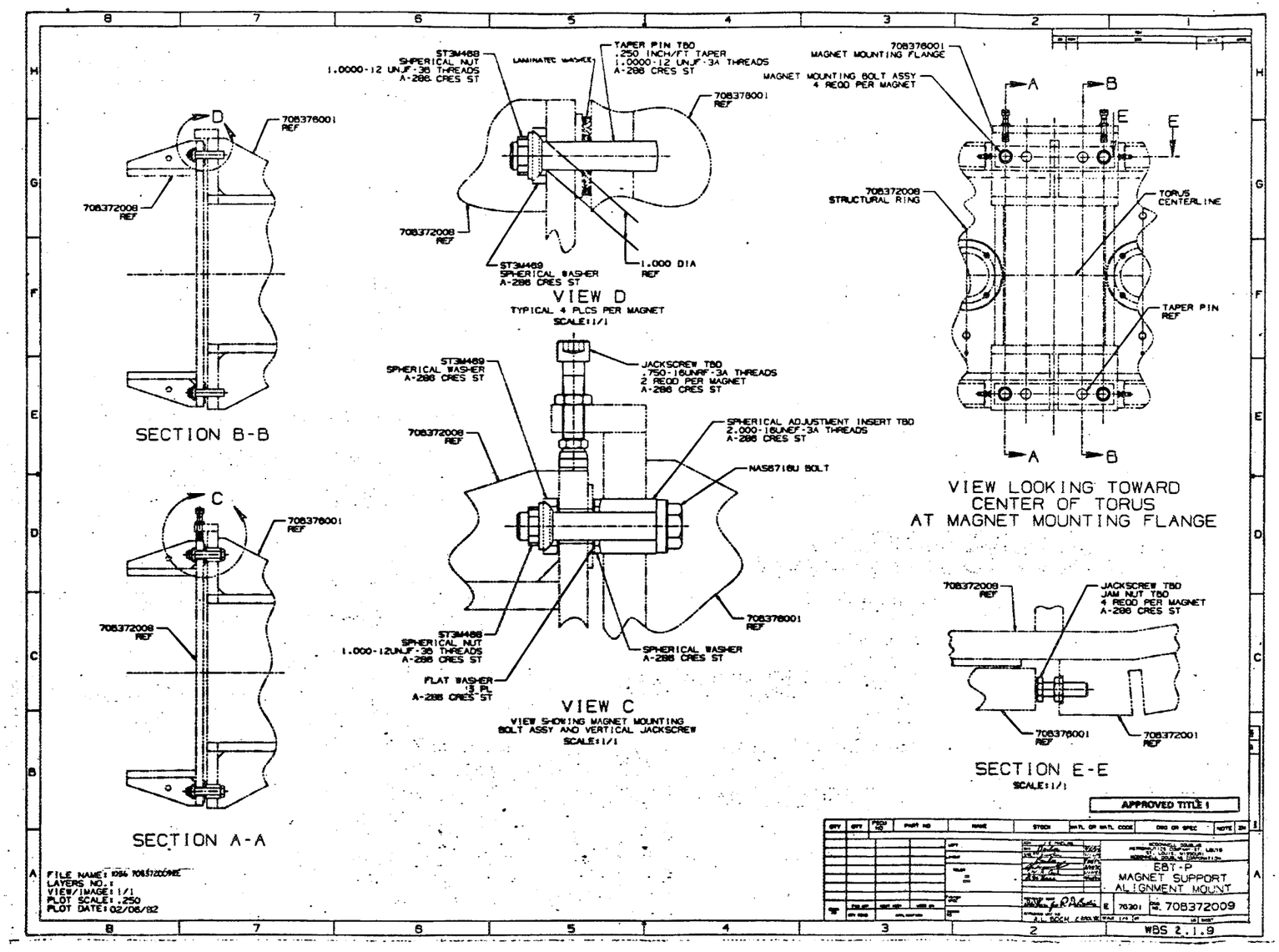
SECTION B-B
SECTION A-A
VIEW D
TYPICAL 4 PLCS PER MAGNET
SCALE:1/1
VIEW C
VIEW SHOWING MAGNET MOUNTING BOLT ASSY AND VERTICAL JACKSCREW
SCALE:1/1
VIEW LOOKING TOWARD CENTER OF TORUS AT MAGNET MOUNTING FLANGE
SECTION E-E
SCALE:1/1
ST3M469 SPHERICAL NUT 1.0000-12 UNJF-3B THREADS A-286 CRES ST
TAPER PIN TBD .250 INCH/FT TAPER 1.0000-12 UNJF-3A THREADS A-286 CRES ST
708376001 REF
708372008 REF
ST3M469 SPHERICAL WASHER A-286 CRES ST
1.000 DIA REF
708376001 MAGNET MOUNTING FLANGE
MAGNET MOUNTING BOLT ASSY 4 REQD PER MAGNET
708372008 STRUCTURAL RING
TORUS CENTERLINE
TAPER PIN REF
JACKSCREW TBD .750-16UNRF-3A THREADS 2 REQD PER MAGNET A-286 CRES ST
SPHERICAL ADJUSTMENT INSERT TBD 2.000-18UNEF-3A THREADS A-286 CRES ST
NAS6716U BOLT
ST3M468 SPHERICAL NUT 1.000-12UNJF-3B THREADS A-286 CRES ST
FLAT WASHER 13 PL A-286 CRES ST
SPHERICAL WASHER A-286 CRES ST
JACKSCREW TBD JAM NUT TBD 4 REQD PER MAGNET A-286 CRES ST
708372001 REF
APPROVED TITLE:
EBT-P MAGNET SUPPORT ALIGNMENT MOUNT
708372009
WBS 2.1.9
FILE NAME: 1984 708372009E
LAYERS NO.: 1
VIEW/IMAGE: 1/1
PLOT SCALE: .250
PLOT DATE: 02/06/82

APPENDIX B-1 SUPPORTING ANALYSES

MAGNETIC ANALYSIS

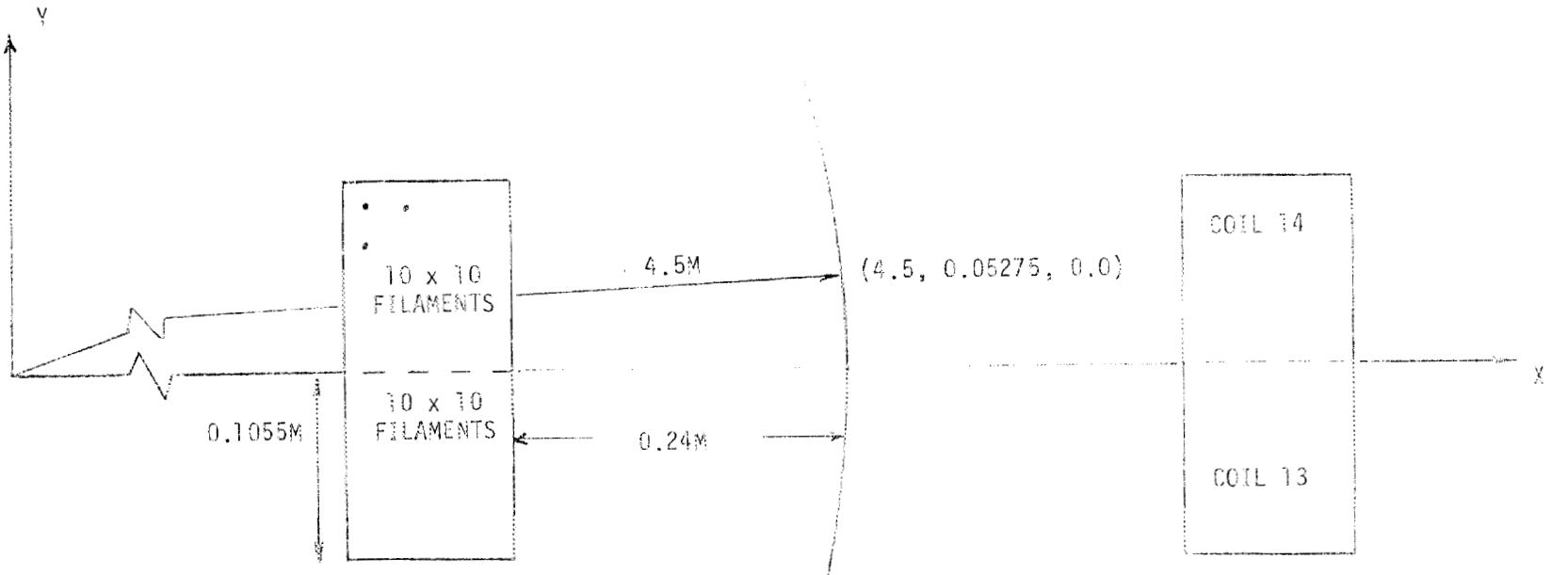

TURN TO TURN SPACING = .01055M (AXIAL)

LAYER SPACING = 0.01M (RADIAL)

200 FILAMENTS TOTAL

COIL FILAMENT LOCATIONS, COIL MID-PLANE

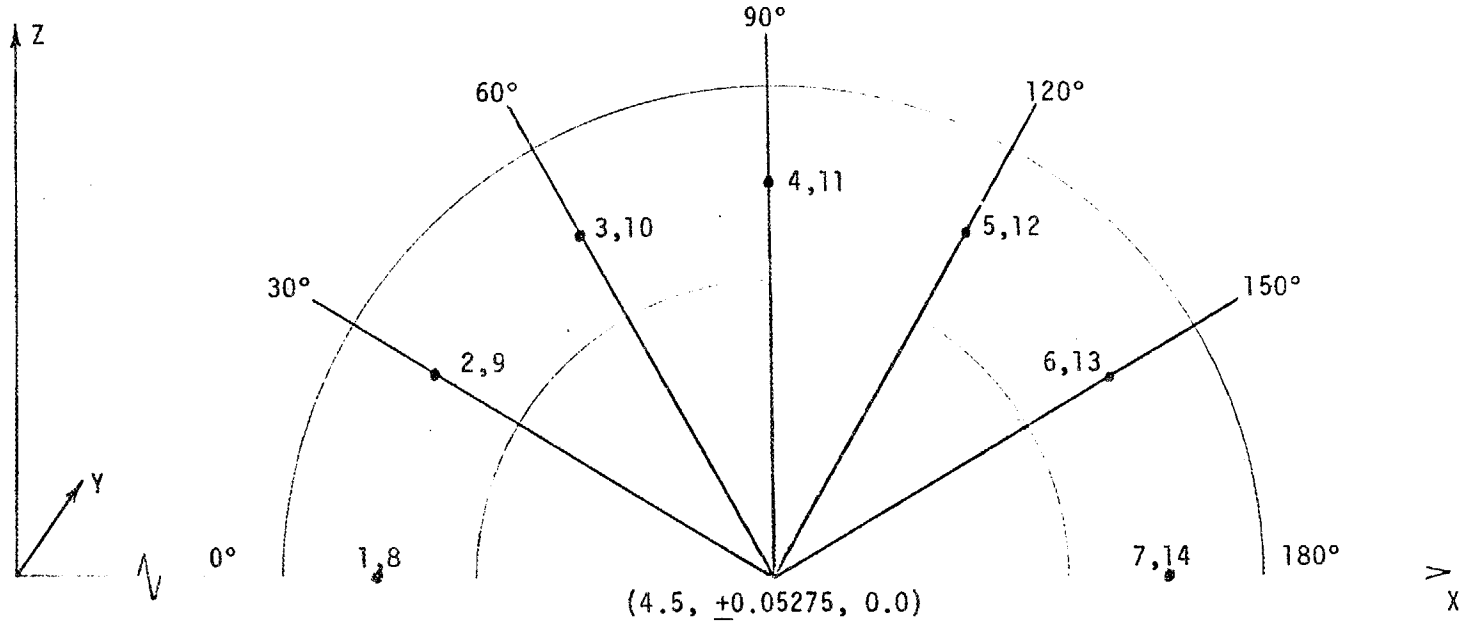

● Perimeter Points

Y = +0.05275M for Points 1-7

Y = -0.05275M for Points 8-14

FIELD POINT LOCATIONS, AXIAL VIEW

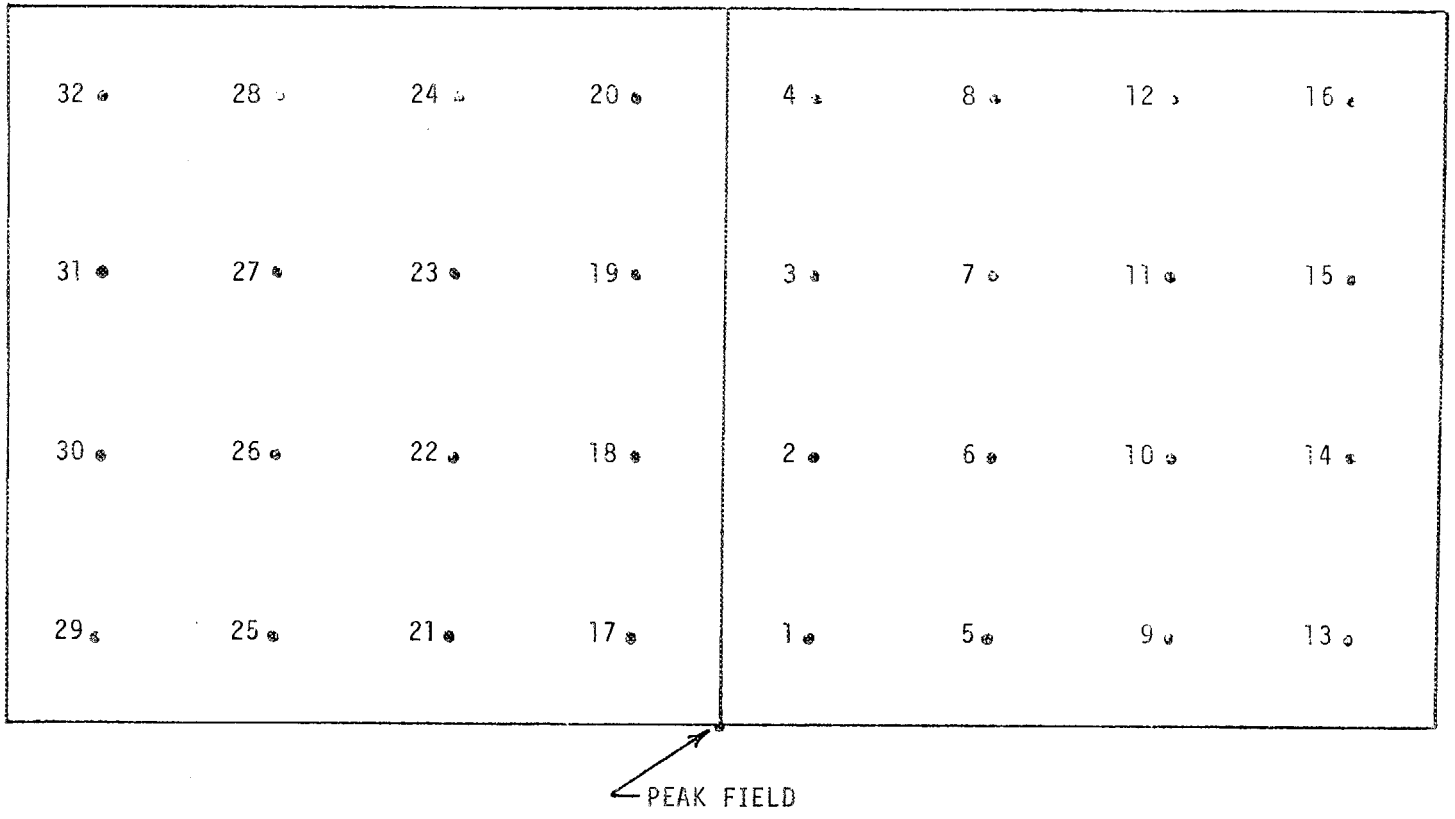

COIL PACK FIELD POINT LOCATIONS

FIELDS COIL 13

NORMAL OPERATION

	X	Y	Z	B_X	B_Y	B_Z
PEAK FIELD	4.26000	0	0	0	7.30705	0
PERIMETER FIELDS						
8 (0°)	4.21000	-.05275	0	+1.73230	2.49840	0
9 (30°)	4.24885	-.05275	.14500	+1.50179	2.49301	.86302
10 (60°)	4.35500	-.05275	.25115	+ .87074	2.47891	1.49676
11 (90°)	4.50000	-.05275	.29000	+ .00609	2.46097	1.73112
12 (120°)	4.64500	-.05275	.25115	+ .86117	2.44441	1.50137
13 (150°)	4.75115	-.05275	.14500	-1.49748	2.43307	.86766
14 (180°)	4.79000	-.05275	0	-1.73066	2.42908	0
MIDPLANE FIELDS						
17	4.25500	-.00528	0	+ .14805	6.85567	0
18	4.22500	-.00528	0	+ .16134	3.99095	0
19	4.19500	-.00528	0	+ .15561	1.15208	0
20	4.16500	-.00528	0	+ .13277	-1.77501	0
21	4.25500	-.03693	0	+1.05779	6.68319	0
22	4.22500	-.03693	0	+1.16740	3.89520	0
23	4.19500	-.03693	0	+1.12667	1.15452	0
24	4.16500	-.03693	0	+ .94962	-1.69823	0
25	4.25500	-.06858	0	+2.06807	6.17625	0
26	4.22500	-.06858	0	+2.36749	3.61882	0
27	4.19500	-.06858	0	+2.29051	1.17781	0
28	4.16500	-.06858	0	+1.86457	-1.44402	0
29	4.25500	-.10023	0	+3.33517	4.99271	0
30	4.22500	-.10023	0	+4.03605	3.06951	0
31	4.19500	-.10023	0	+3.93245	1.24060	0
32	4.16500	-.10023	0	+3.05208	- .70960	0

FIELDS COIL 14

NORMAL OPERATION

	X	Y	Z	B_X	B_Y	B_Z
PEAK FIELD	4.26000	0	0	0	7.30705	0
PERIMETER FIELDS						
1 (0°)	4.21000	.05275	0	-1.73230	2.49840	0
2 (30°)	4.24885	.05275	.14500	-1.50179	2.49301	.86302
3 (60°)	4.35500	.05275	.25115	- .87074	2.47891	1.49676
4 (90°)	4.50000	.05275	.29000	- .00609	2.46097	1.73112
5 (120°)	4.64500	.05275	.25115	.86117	2.44441	1.50137
6 (150°)	4.75115	.05275	.14500	1.49748	2.43307	.86766
7 (180°)	4.79000	.05275	0	1.73066	2.42908	0
MIDPLANE FIELDS						
1	4.25500	.00528	0	-.14805	6.35567	0
2	4.22500	.00528	0	-.16134	3.99095	0
3	4.19500	.00528	0	-.15561	1.15208	0
4	4.16500	.00528	0	-.13277	-1.77501	0
5	4.25500	.03693	0	-1.05779	6.68319	0
6	4.22500	.03693	0	-1.16740	3.89520	0
7	4.19500	.03693	0	-1.12667	1.15452	0
8	4.16500	.03693	0	- .94962	-1.69823	0
9	4.25500	.06858	0	-2.06807	6.17625	0
10	4.22500	.06858	0	-2.36749	3.61882	0
11	4.19500	.06858	0	-2.29051	1.17781	0
12	4.16500	.06858	0	-1.86457	-1.44402	0
13	4.25500	.10023	0	-3.33517	4.99271	0
14	4.22500	.10023	0	-4.03605	3.06951	0
15	4.19500	.10023	0	-3.93245	1.24060	0
16	4.16500	.10023	0	-3.05208	- .70960	0

FIELDS COIL 13

APPENDIX B-1

ONE COIL DOWN

	X	Y	Z	B_X	B_Y	B_Z
PEAK FIELD	4.26000	0	0	+.06392	7.13759	0
PERIMETER FIELDS						
8 (0°)	4.21000	-.05275	0	+1.82540	2.31452	0
9 (30°)	4.24885	-.05275	.14500	+1.57976	2.31193	.91422
10 (60°)	4.35500	-.05275	.25115	+ .90963	2.30509	1.58190
11 (90°)	4.50000	-.05275	.29000	- .00363	2.29633	1.82428
12 (120°)	4.64500	-.05275	.25115	- .91461	2.28816	1.57796
13 (150°)	4.75115	-.05275	.14500	-1.58017	2.28253	.91027
14 (180°)	4.79000	-.05275	0	-1.82352	2.28054	0
MIDPLANE FIELDS						
17	4.25500	-.00528	0	+ .21459	6.68459	0
18	4.22500	-.00528	0	+ .23486	3.82833	0
19	4.19500	-.00528	0	+ .23515	.99866	0
20	4.16500	-.00528	0	+ .21729	-1.91866	0
21	4.25500	-.03693	0	+1.13351	6.49326	0
22	4.22500	-.03693	0	+1.25104	3.71519	0
23	4.19500	-.03693	0	+1.21707	.98528	0
24	4.16500	-.03693	0	+1.04555	-1.85603	0
25	4.25500	-.06858	0	+2.15458	5.96468	0
26	4.22500	-.06858	0	+2.46303	3.41893	0
27	4.19500	-.06858	0	+2.39366	.99062	0
28	4.16500	-.06858	0	+1.97385	-1.61779	0
29	4.25500	-.10023	0	+3.43442	4.75619	0
30	4.22500	-.10023	0	+4.14564	2.84681	0
31	4.19500	-.10023	0	+4.05065	1.03292	0
32	4.16500	-.10023	0	+3.17709	- .90142	0

FIELDS COIL 14

ONE COIL DOWN

	X	Y	Z	B_X	B_Y	B_Z
PEAK FIELD	4.26000	0	0	.06392	7.13759	0
PERIMETER FIELDS						
1 (0°)	4.21000	.05275	0	-1.67116	2.36581	0
2 (30°)	4.24885	.05275	.14500	-1.45014	2.36184	.83015
3 (60°)	4.35500	.05275	.25115	- .84401	2.35147	1.44153
4 (90°)	4.50000	.05275	.29000	- .01108	2.33835	1.66986
5 (120°)	4.64500	.05275	.25115	.82689	2.32632	1.45037
6 (150°)	4.75115	.05275	.14500	1.44317	2.31813	.83903
7 (180°)	4.79000	.05275	0	1.66929	2.31525	0
MIDPLANE FIELDS						
1	4.25500	.00528	0	- .08426	6.69033	0
2	4.22500	.00528	0	- .09085	3.83364	0
3	4.19500	.00528	0	- .07934	1.00351	0
4	4.16500	.00528	0	- .05167	-1.91430	0
5	4.25500	.03693	0	-1.00145	6.53365	0
6	4.22500	.03693	0	-1.10513	3.75254	0
7	4.19500	.03693	0	-1.05924	1.01935	0
8	4.16500	.03693	0	- .87782	-1.82541	0
9	4.25500	.06858	0	-2.01813	6.04059	0
10	4.22500	.06858	0	-2.31229	3.48909	0
11	4.19500	.06858	0	-2.23068	1.05454	0
12	4.16500	.06858	0	-1.80079	-1.56041	0
13	4.25500	.10023	0	-3.29075	4.86931	0
14	4.22500	.10023	0	-3.98694	2.95123	0
15	4.19500	.10023	0	-3.87919	1.12791	0
16	4.16500	.10023	0	-2.99524	- .81633	0

FIELDS COIL 13

APPENDIX B-1

TWO COILS DOWN

	X	Y	Z	B_X	B_Y	B_Z
PEAK FIELD	4.26000	0	0	+ .06769	7.10968	0
PERIMETER FIELDS						
8 (0°)	4.21000	-.05275	0	+1.83104	2.28404	0
9 (30°)	4.24885	-.05275	.14500	+1.58417	2.28190	.91849
10 (60°)	4.35500	-.05275	.25115	+ .91087	2.27624	1.58901
11 (90°)	4.50000	-.05275	.29000	- .00635	2.26897	1.83207
12 (120°)	4.64500	-.05275	.25115	- .92089	2.26216	1.58438
13 (150°)	4.75115	-.05275	.14500	-1.58884	2.25746	.91384
14 (180°)	4.79000	-.05275	0	-1.83302	2.25579	0
MIDPLANE FIELDS						
17	4.25500	-.00528	0	+.21853	6.65643	0
18	4.22500	-.00528	0	+.23961	3.80039	0
19	4.19500	-.00528	0	+.24070	.97101	0
20	4.16500	-.00528	0	+.22362	-1.94596	0
21	4.25500	-.03693	0	+1.13766	6.46332	0
22	4.22500	-.03693	0	+1.25608	3.68549	0
23	4.19500	-.03693	0	+1.22297	.95590	0
24	4.16500	-.03693	0	+1.05230	-1.88504	0
25	4.25500	-.06858	0	+2.15896	5.93281	0
26	4.22500	-.06858	0	+2.46838	3.38732	0
27	4.19500	-.06858	0	+2.39995	.95935	0
28	4.16500	-.06858	0	+1.98105	-1.64865	0
29	4.25500	-.10023	0	+3.43905	4.72222	0
30	4.22500	-.10023	0	+4.15131	2.81313	0
31	4.19500	-.10023	0	+4.05735	.99960	0
32	4.16500	-.10023	0	+3.18478	- .93429	0

FIELDS COIL 14

TWO COILS DOWN

	X	Y	Z	B_X	B_Y	B_Z
PEAK FIELD	4.26000	0	0	.06769	7.10968	0
PERIMETER FIELDS						
1 (0°)	4.21000	.05275	0	-1.66653	2.34088	0
2 (30°)	4.24885	.05275	.14500	-1.44644	2.33721	.82687
3 (60°)	4.35500	.05275	.25115	- .84276	2.32763	1.43603
4 (90°)	4.50000	.05275	.29000	- .01293	2.31554	1.66379
5 (120°)	4.64500	.05275	.25115	.82220	2.30445	1.44533
6 (150°)	4.75115	.05275	.14500	1.43655	2.29692	.83620
7 (180°)	4.79000	.05275	0	1.66200	2.29427	0
MIDPLANE FIELDS						
1	4.25500	.00528	0	- .08039	6.66274	0
2	4.22500	.00528	0	- .08619	3.80626	0
3	4.19500	.00528	0	- .07390	.97641	0
4	4.16500	.00528	0	- .04547	-1.94106	0
5	4.25500	.03693	0	- .99777	6.50765	0
6	4.22500	.03693	0	-1.10072	3.72675	0
7	4.19500	.03693	0	-1.05411	.99382	0
8	4.16500	.03693	0	- .87200	-1.85063	0
9	4.25500	.06858	0	-2.01463	6.01607	0
10	4.22500	.06858	0	-2.30812	3.46475	0
11	4.19500	.06858	0	-2.22584	1.03045	0
12	4.16500	.06858	0	-1.79530	-1.58421	0
13	4.25500	.10023	0	-3.28742	4.84616	0
14	4.22500	.10023	0	-3.98299	2.92825	0
15	4.19500	.10023	0	-3.87462	1.10516	0
16	4.16500	.10023	0	-2.99008	- .83881	0

RUNNING FORCES COIL 13

APPENDIX B-1

(TOP HALF COIL)

	X	Y	Z	F_X	F_Y	F_Z
NORMAL OPERATION PERIMETER FORCES						
8 (0°)	4.21000	-.05275	0	-14,982	10,388	0
9 (30°)	4.24885	-.05275	.14500	-12,947	10,387	7,475
10 (60°)	4.35500	-.05275	.25115	- 7,433	10,384	12,873
11 (90°)	4.50000	-.05275	.29000	0	10,381	14,757
12 (120°)	4.64500	-.05275	.25115	7,329	10,379	12,694
13 (150°)	4.75115	-.05275	.14500	12,635	10,378	7,295
14 (180°)	4.79000	-.05275	0	14,566	10,378	0
ONE COIL DOWN PERIMETER FORCES						
8 (0°)	4.21000	.05275	0	-13,879	10,946	0
9 (30°)	4.24885	.05275	.14500	-12,006	10,945	6,932
10 (60°)	4.35500	.05275	.25115	- 6,911	10,942	11,971
11 (90°)	4.50000	.05275	.29000	0	10,939	13,770
12 (120°)	4.64500	.05275	.25115	6,860	10,937	11,883
13 (150°)	4.75115	.05275	.14500	11,854	10,935	6,844
14 9180°)	4.79000	.05275	0	13,675	10,935	0
TWO COILS DOWN PERIMETER FORCES						
8 (0°)	4.21000	.05275	0	-13,696	10,980	0
9 (30°)	4.24885	.05275	.14500	-11,850	10,980	6,842
10 (60°)	4.35500	.05275	.25115	- 6,825	10,983	11,821
11 (90°)	4.50000	.05275	.29000	0	10,986	13,606
12 (120°)	4.64500	.05275	.25115	6,782	10,989	11,748
13 (150°)	4.75115	.05275	.14500	11,723	10,991	6,768
14 (180°)	4.79000	.05275	0	13,527	10,992	0

RUNNING FORCES COIL 14

(TOP HALF COIL)

	X	Y	Z	F_x	F_y	F_z
				LBS/IN	LBS/IN	LBS/IN
NORMAL OPERATION						
PERIMETER FORCES						
1 (0°)	4.21000	.05275	0	-14,982	-10,388	0
2 (30°)	4.24885	.05275	.14500	-12,947	-10,387	7,475
3 (60°)	4.35500	.05275	.25115	- 7,433	-10,384	12,873
4 (90°)	4.50000	.05275	.29000	0	-10,381	14,757
5 (120°)	4.64500	.05275	.25115	7,329	-10,379	12,694
6 (150°)	4.75115	.05275	.14500	12,635	-10,378	7,295
7 (180°)	4.79000	.05275	0	14,566	-10,378	0
ONE COIL DOWN						
PERIMETER FORCES						
1 (0°)	4.21000	.05275	0	-14,187	-10,021	0
2 (30°)	4.24885	.05275	.14500	-12,265	-10,019	7,081
3 (60°)	4.35500	.05275	.25115	- 7,050	-10,016	12,211
4 (90°)	4.50000	.05275	.29000	0	-10,013	14,022
5 (120°)	4.64500	.05275	.25115	6,975	-10,011	12,080
6 (150°)	4.75115	.05275	.14500	12,039	-10,010	6,950
7 (180°)	4.79000	.05275	0	13,883	-10,009	0
TWO COILS DOWN						
PERIMETER FORCES						
1 (0°)	4.21000	.05275	0	-14,037	- 9,993	0
2 (30°)	4.24885	.05275	.14500	-12,137	- 9,990	7,007
3 (60°)	4.35500	.05275	.25115	- 6,978	- 9,984	12,087
4 (90°)	4.50000	.05275	.29000	0	- 9,977	13,885
5 (120°)	4.64500	.05275	.25115	6,909	- 9,971	11,967
6 (150°)	4.75115	.05275	.14500	11,928	- 9,967	6,886
7 (180°)	4.79000	.05275	0	13,757	- 9,966	0

TOTAL FORCES

	F_X	F_Y	F_Z
	LBS	LBS	LBS
NORMAL OPERATION			
COIL 13 (TOP HALF ONLY)	- 3,722	372,380	329,360
COIL 14 (TOP HALF ONLY)	- 3,721	-372,380	329,360
TOTAL (COILS 13 & 14, TOP & BOTTOM HALVES)	-14,886	0	0
ONE COIL OFF			
COIL 13 (TOP HALF ONLY)	- 1,825	392,400	307,270
COIL 14 (TOP HALF ONLY)	- 2,714	-359,210	312,930
TOTAL (COILS 13 & 14, TOP & BOTTOM HALVES)	- 9,078	66,380	0
TWO COILS OFF			
COIL 13 (TOP HALF ONLY)	- 1,518	394,050	303,600
COIL 14 (TOP HALF ONLY)	- 2,502	-357,910	309,870
TOTAL (COILS 13 & 14, TOP & BOTTOM HALVES)	- 8,040	72,280	0

APPENDIX B-2 SUPPORTING ANALYSES

SUPERCONDUCTOR

GENERAL DYNAMICS Convair Division CODE IDENT NO. 14170	SPECIFICATION NO. 11-38007	REV A
	DATE 6/8/81	PAGE 1 OF 9
	CONTRACT NO. YOE206R	

ELMO BUMPY TORUS PROGRAM

SPECIFICATION FOR SUPERCONDUCTOR

PREPARED BY J. L. Saunders

CHECKED BY

APPROVED BY D. W. Lieurance

SPECIFICATION CHANGE NOTICES—INCORPORATED IN SPEC REVISIONS

SCN NO(S)	INCORP BY	CHECK BY	APPROVED BY	DATE	SPEC REV	REVISION PACKAGE NO.	RELEASE
				7/10/81	A	002	JUL 10 1981

INITIAL PACKAGE NO.	RELEASE	COC TYPE	DISTR CODE
	JUN 8 1981		

☐ PROPOSED ☒ APPROVED	**GENERAL DYNAMICS** *Convair Division* CODE IDENT. NO. 14170 **SPECIFICATION CHANGE NOTICE**	SPECIFICATION NO. 11-38007A SCN NO. 1 PAGE 1 OF 1
ECP NO. N/A	CONTRACT END ITEM NO. N/A	DATE 7/6/81
CONTRACT NO. YOE206R	CONTRACTUAL AUTHORITY N/A	SUPERSEDING SCN DATED --
EFFECTIVITY N/A	TITLE SPECIFICATION FOR SUPERCONDUCTOR	

TEXT CHANGE

Page 6 — Delete: "4.2.3 Surface Finish Inspection

The surface finish requirements of Section 3.5.3 shall be monitored continuously during the final spooling operation using an eddy current monitoring device or equivalent method which is approved by General Dynamics. The purpose of this monitoring device shall be to alert the seller of potential surface defects. In the event that surface defects are identified either visually or by the device, the seller will be responsible for evaluating potential defects and recommending a suitable repair procedure to General Dynamics."

Page 6 — Para. 4.2.2 — Revise to read:

The cleanliness "and surface finish" requirements of Sections 3.5.2 "and 3.5.3"....

PREPARED BY J.L. Saunders 7/10/81	DESIGN	CHECK	RELEASE
GROUP ENGR 7/10/81	STRESS		PACKAGE NO.
MAT. RESEARCH	Q A		DOC. DISTR.

A4187 (1-77)

GENERAL DYNAMICS Convair Division	SPECIFICATION NO. 11-38007	REV A
	DATE 6/8/81	PAGE 2 OF 9
	CONTRACT NO. YOE206R	

1.0 SCOPE

This document establishes the product, quality verification, preparation for shipment, and documentary requirements for procurement of a single grade of superconducting monolith containing niobium-titanium alloy filaments in a copper matrix. This conductor will be used in the thirty-six (36) magnets of GDC Elmo Bumpy Torus Program.

2.0 APPLICABLE DOCUMENTS

The following standards and specifications are part of this document to the extent specified herein. Where there is a conflict between the standards and specifications cited and this specification and the latest revisions thereof, the seller shall notify General Dynamics Convair of the conflict and seek resolution.

2.1 ERDA Standards and Specifications

RDT F 2-4T (December 1974) - Quality Verification Program Requirements

RDT F 3-2T (February 1973) - Calibration Program Requirements

2.2 Miscellaneous

ANSI Y14.5, Dimensioning and Tolerancing.

3.0 PRODUCT REQUIREMENTS

3.1 Conductor Materials

3.1.1 Superconducting Filament Material

The superconductive material shall be a niobium-titanium alloy (46.5 ± 1.5% Wt Nb), meeting the requirements of a specification which has been approved by General Dynamics.

3.1.2 Normal Metal

High conductivity copper with a minimum residual resistivity ratio sufficient to ensure compliance with Section 3.4.2.2 in the finished product.

3.2 Conductor Design

The conductor shall be a rectangular monolith with the following dimensions:

Width	0.1969 ± 0.001 inch (nom: 5.0mm)
Height	0.1142 ± 0.001 inch (nom: 2.9mm)
Corner Radius	0.020 ± 0.004 inch
Cu:Sc Ratio	≥ 2.8:1 (by volume)

The sides shall be flat and parallel to ± 0.0004 in., with adjacent sides at 90.0 ± 0.5 degrees.

3.3 Filament Size, Distribution, and Twist Pitch

The NbTi fraction of the conductor shall be in the form of continuous longitudinal filaments not greater than 66 micrometers in diameter. These filaments shall be uniform in size; at any cross section of the conductor at least 90% of the filaments shall have an area that is within 20% of the average filament area. The filaments shall be confined to an annular region of the conductor. In the filament/copper annulus, the filaments shall be distributed uniformly: the center-to-center distance of at least 90% of the neighboring filament pairs shall be within 20% of the average center-to-center distance. A region of the conductor adjacent to the perimeter and comprising no more than 20% of the conductor area shall be filament-free. In addition, there shall be a filament-free copper region on axis that shall constitute no less than 10% and no more than 15% of the cross sectional area. The conductor shall have the shortest practical twist pitch but in no case shall it be greater than 3.0 inches. Filaments shall be continuous throughout the length of the conductor to the extent that no more than 1% are broken in any six-inch length.

3.4 Conductor Performance

3.4.1 Operating Environment

The conductor will operate in a liquid helium environment at a nominal temperature of 4.2K. The peak "in winding" magnetic field under nominal operating conditions will be 7.4 tesla.

3.4.2 Operating Performance

3.4.2.1 Conductor Critical Current - The guaranteed short sample critical current for 11-38007 conductor at 7.5 tesla and 4.2K shall be greater than 2800 amps. Measurements are to be taken on a sample at 10^{-12} Ω·cm sensitivity, and with the field parallel to the broad face of the conductor.

3.4.2.2 Conductor Composite Resistivity Ratio - The final conductor zero field composite resistivity ratio shall be a minimum of 120.

3.4.2.3 Mechanical Properties - The conductor longitudinal tensile yield strength (.002 offset strain) shall be greater than 30,000 psi when measured at room temperature.

3.4.3 Reliability

The conductor shall be capable of operation under the conditions of Paragraph 3.4.1 for a period of 10 years minimum.

3.4.4 Magnetization Tests

As a design goal, the coupling time constant between filaments, τ_0 , should not exceed one second. The coupling time constant is defined as:

$$\tau_o = \frac{\mu_o \, \ell_o^2}{4 \pi \rho},$$

where:

μ_o = $4\pi \times 10^{-7}$ H/m

ℓ_p = twist pitch length, m

ρ = matrix resistivity at 4.2K and a field of 5.5T, $\Omega \cdot m$

See Section 3.1 for allowable conductor materials. Also refer to Section 3.4.2.2 for required residual resistivity ratio.

The coupling time constant will be measured by ORNL using the methods described by S. S. Shen and R. E. Schwall, Proc. 7th Int. Cryogenic Eng. Conf., IPC Science and Technology Press, Surrey (1979). (This is not a condition for acceptance.)

3.5 Manufacture

3.5.1 Manufacturing/Quality Verification Plan

A detailed manufacturing/quality verification plan shall be prepared by the seller and submitted to General Dynamics Convair for approval. The plan shall identify each processing and inspection step and the procedure to be used. Proprietary details such as heat treat times and temperatures may be omitted.

3.5.2 Cleanliness

Each finished component of the finished product shall be free of visible contamination such as dirt, machine or cutting chips, flux, solder balls, lubricants, residues from fixtures or handling equipment or anything which could change the performance of the components.

3.5.3 Surface Finish

The surface of the conductor shall be free of visible scratches, cracks, cold shuts, blisters, gouges and other injurious imperfections which either exceed the maximum tolerance limit or degrade the performance of either the conductor or the insulation system.

3.5.4 Soldering

The conductor shall be delivered in a condition that will facilitate fabrication of an electrical joint using a commercial lead-tin solder.

3.5.5 Splicing

Splicing shall not be allowed.

3.5.6 Spooling

During spooling operations, the following requirements must be maintained.

a. Rope or/and equivalent material shall be used at the end/start of each layer to assure gentle transitions between layers and damage free conductors.

b. Conductor must lie flat on the shipping spool in an orderly fashion.

c. There shall be no kinks or bends when the conductor is wound on the spool.

d. The conductor must lie on the spool with a pitch of no more than one and one-half conductor widths.

e. Each layer of conductor must be protected by a layer of paper or mylar. The final layer shall be protected with a pliable material, banded, and overwrapped with plastic.

3.5.7 Repair

Components that are not in accordance with design requirements may be repaired in accordance with a written plan which has been submitted and approved by General Dynamics Convair prior to the repair. Reporting of non-conformances shall be accomplished using the GDC Waiver Approval Request Form (WARF) Form #6475, Rev. 1-74.

4.0 QUALITY ASSURANCE

The seller shall plan, establish, and maintain a Quality Verification Program that utilizes those organizational and functional disciplines necessary to furnish objective evidence that the required quality is achieved through the process. The implementation, organization, documentation, reviews, control of quality records, and corrective action requirements of the Quality Assurance Program shall be in accordance with the requirements of the ERDA Standard RDT F 2-4T.

The performance of seller's tests and inspections do not limit the right of General Dynamics Convair to conduct other tests and inspections as General Dynamics deems necessary to assure that the product conforms with all of the requirements of this Specification.

4.1 Materials Verification

Compliance with Section 3.1 shall be established by the results of inspections and tests included with the certifications. Should certifications not be available on any constituent lot of material, a test may be performed for verification of critical characteristics, providing a written test plan is reviewed and approved by GDC.

4.2 In-Process Inspection

4.2.1 Dimensional Inspections

The following in-process dimensional inspections shall be made and documented at representative intervals along the length of each lot of the conductor:

Conductor Dimensions
Conductor Corner Radii

A lot of conductor is defined as a single continuous length subject to the same manufacturing processes such as drawing, heat treat, cabling, etc., which could materially effect the end product mechanical or performance characteristics.

4.2.2 In-Process Surveillance

The cleanliness and surface finish requirements of Sections 3.5.2 and 3.5.3 shall be verified and documented at representative intervals along the length of each lot of conductor.

4.3 Acceptance Tests

Acceptance tests shall be performed on samples from the beginning and end of each lot of completed conductor.

4.3.1 Dimensional Acceptance

The following inspections shall be made and recorded for each sample:

Conductor Height

Conductor Width

Corner Radii

4.3.2 Performance Acceptance

The performance requirements of Paragraph 3.4.2.1, 3.4.2.2, and 3.4.2.3 shall be verified by test on a portion of each sample. (Note: This implies there will be two critical current tests, two composite resistivity tests and two mechanical strength tests for each lot presented for acceptance.)

4.3.3 Filament Size, Distribution, and Twist Pitch

Filament size and distribution compliance shall be established by measurements on a photomicrograph of a representative conductor cross section. Samples for this test are to be obtained during conductor processing at the smallest round size. Dimensions may be scaled to adjust for any remaining area reduction.

Twist pitch compliance shall be established by etching the copper from the center section of a conductor sample but not from the ends. The region from which the copper is removed shall show at least one and a half (1 1/2) twists of the filaments. The ends of the sample shall be held in a plastic holder or other provision made to protect the ends against the etchant and to prevent the sample from untwisting. Samples for this test are to be taken at the final rectangular size.

4.4 Lot Control History Jacket

The following data shall be included in a folder which accompanies each deliverable lot (spool) of conductor.

a. Copies of certifications for all conductor constituent materials.

b. A color photograph of the conductor billet, prior to close, showing the location of constituent materials. The photograph shall be identified to the lot and signed and dated by a representative of the Sellers Quality Assurance organization.

c. Data sheets indicating compliance with the In-Process Inspections of Sections 4.2.1, 4.2.2, and 4.2.3.

d. Data sheets indicating compliance with the Dimensional Acceptance requirements of Section 4.3.1.

e. Data sheets indicating compliance with the Performance Acceptance requirements of Section 4.3.2; including copies of critical current plots, resistivity plots, and stress-strain curves.

f. Data sheets indicating compliance with the General Acceptance requirements of Section 4.3.3.

g. Data sheets indicating conductor length.

h. Non-conformance reports. (WARF).

Each folder shall be identified with the spool lot number. The folder shall be presented to the GDC representative at the time of acceptance. The folder shall be maintained up-to-date and available for review at any time during

the manufacturing/test cycle.

4.5 Measuring and Test equipment shall be controlled by the calibration requirements of RDT F3-2T

4.6 Process Controls

Compliance with the Manufacturing requirements of Section 3.5 shall be established by detailed step-by-step procedures and route cards prepared by the Seller and on file for General Dynamics Convair review. The visibility of processes considered by the Seller to be proprietary shall be restricted to identified General Dynamics Convair personnel by mutual agreement between Seller and General Dynamics Convair.

4.7 Audits

The Seller is subject to audits by General Dynamics Convair to assess the implementation of the Seller's Quality Verification Program at any time during the course of the work.

4.8 Non-conforming Materials

Materials or products which do not meet the requirements of this specification (Ref. paragraph 3.5.7) shall be rejected by the Seller's Quality Control personnel and handled in accordance with the methods prescribed in the Quality Assurance Plan. Examples of this are:

a. Lack of Required Documentation

b. Dimensional Non-conformances

c. Performance Test Failure

4.9 Lot Samples

A 4-meter sample from each end of each conductor lot shall be provided to General Dynamics. Each sample shall be protected by a pliable overwrap and identified with the lot number and end.

5.0 PREPARATION FOR SHIPMENT

5.1 Handling

Handling of all components and the product after final cleaning shall be done in a manner to preclude pickup or entrapment of any dirt, oils, metal chips, or other contamination on their surfaces or in internal parts.

5.2 Marking

Each coil or spool shall be legibly and conspicuously marked or tagged with the

following information:

a. Purchase Order or Contract Number

b. Manufacturer

c. Name of Material

d. Length

e. Lot Number

f. Gross, Net and Tare Weights

g. Q.A. Acceptance Verification

h. General Dynamics Part Number

5.3 Storage

All components and the final product awaiting further processing or shipment shall be handled and stored in a manner which precludes physical damage and contamination.

5.4 Packaging

All material shall be packaged in a manner to maintain cleanliness during handling and shipping and to prevent damage in transit to its destination when properly transported by any common carrier. Each length of conductor shall be wound upon a reel of a diameter to be determined by the seller such that placing or handling the cable shall not degrade the quality, properties, or performance characteristics of the cable.

5.5 Shipping

After receiving approval by General Dynamics Convair to ship the product, shipping shall be performed in accordance with all applicable regulations of the United States Department of Transportation.

APPENDIX B-3 SUPPORTING ANALYSES

STRESS ANALYSIS

EBT-P

4 Sept 81

APPENDIX B-3

STRESS ANALYSIS

HELIUM VESSEL	B-3.1
WINDING	B-3.2
COLD MASS SUPPORTS	B-3.3
VACUUM VESSEL	B-3.4
MISCELLANEOUS	B-3.5
MATERIALS	B-3.6

APPENDIX B-3.1

STRESS ANALYSIS

HELIUM VESSEL

REPORT

PAGE

GENERAL DYNAMICS
Convair Division

EBT-P

HELIUM VESSEL

FINITE ELEMENT MODEL

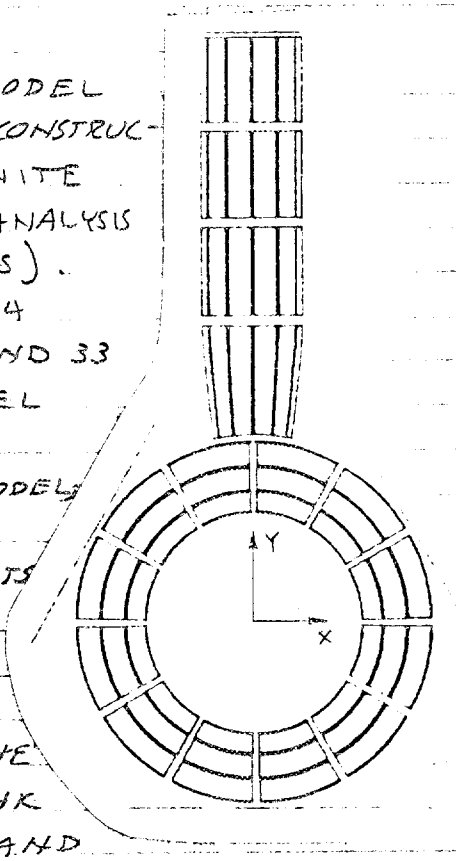

A FINITE ELEMENT MODEL OF THE COLD MASS WAS CONSTRUCTED USING "FEMALE" (FINITE ELEMENT MODELING AND ANALYSIS LANGUAGE FOR ENGINEERS). THE MODEL CONTAINS 144 QUAD 8 PLATE ELEMENTS AND 33 BAR ELEMENTS. THE MODEL CONTAINS 4,575 DOF.

THE OUTER RING IS MODELED AS .75 THK CURVED PLATES IN NODAL INCREMENTS OF 15°. THE INNER RING IS .375 THICK CURVED PLATES ALSO IN 15° NODAL INCREMENTS. THE SIDE PLATES ARE .375 THK AT THE INNER RADIUS AND INCREASE TO .625 THK AT A RADIUS OF 10.92 INCHES. THE STACK IS ALSO MODELED USING CURVED PLATES HAVING 15° NODAL INCREMENTS. THE BOTTOM TWO SEGMENTS ARE .110 THK, THE TOP TWO ARE .035 THK. THE TOP COVER PLATE IS 1.25 THICK REPRESENTING THE COVER FLANGE

PREPARED BY	DATE	CHECKED BY	DATE	REVISED BY	DATE
K. Dawson	9-1-81				

A706-1 (REV. 9-65)

EBT-P

HELIUM VESSEL

INNER BORE

1. THE INNER BORE IS LOADED IN COMPRESSION DURING COIL WINDING.

USING STANSOL RESULTS:

INSULATION MAT'L - NOMEX
WINDING TENSION - 180 LBS.
BOBBIN THICKNESS - .365 IN.

	RADIAL STRESS	HOOP STRESS
I.R. :	0.	-14,865 PSI
O.R. :	-570.75 PSI	-14,295 PSI

FOR EXTERNAL THE RADIAL STRESS AT THE OUTSIDE SURFACE IS EQUAL TO THE APPLIED PRESSURE.

$\therefore P_e = -570.75$ PSI

USING A SHORT TUBE STABILITY ANALYSIS REF "A" TABLE 35, CASE 19

$$q' = .807 \frac{Et^2}{lr} \sqrt[4]{\left(\frac{1}{1-\nu^2}\right)^3 \frac{t^2}{r^2}}$$

Ref "A": Formulas for Stress And Strain, Roark & Young, 5th Ed.

PREPARED BY	DATE	CHECKED BY	DATE	REVISED BY	DATE
R. Dunn	9-2-81				

GENERAL DYNAMICS
Convair Division

EBT-P

HELIUM VESSEL

INNER BORE

$t = .365$
$r = 9.163''$ (MEAN RADIUS)
$\nu = .3$
$E = 28.6 \times 10^6$ PSI
$\ell = 9.544$ IN

$$q' = .807 \frac{(28.6\times10^6)(.365)^2}{(9.544)(9.163)} \sqrt[4]{\left[\frac{1}{1-.3^2}\right]^3 \frac{.365^2}{9.163^2}}$$

$q' = 7{,}532$ PSI

$$MS = \frac{7{,}532}{570.75(4)} - 1 = \underline{\underline{+2.30}} \quad \text{BUCKLING}$$

$$MS = \frac{25{,}000}{14{,}865(1.5)} - 1 = \underline{\underline{+.121}} \quad \text{YIELD}$$

2. THE INNER BORE IS LOADED BY THE CENTERING FORCE ON THE COIL PACK AND THE NORMAL OPERATING PRESSURE

PREPARED BY	DATE	CHECKED BY	DATE	REVISED BY	DATE
K. Dawson	9-2-81				

A706-1 (REV. 9-65)

EBT-P

HELIUM VESSEL

INNER BORE

THIS CONDITION WAS RUN ON THE F/E MODEL. THIS PRODUCED THE FOLLOWING PEAK STRESS.

MAX LONGITUDNIAL STRESS = 7,286 PSI
MAX HOOP STRESS = 1,608 PSI
MAX SHEAR STRESS = 2,840 PSI

VON MISES COMBINED STRESS = 6,630 PSI

$$MS = \frac{25,000}{7,286\ (1.5)} - 1 = +1.29 \text{ YIELD (R.T)}$$

CYLINDER BUCKLING PRESSURE
(REF: 5.2-2, SEC VIII, DIV 2, ARTICLE D-3)

$D_o/t = 18.344/.365 = 50.26$

$L/D_o = 9.544/18.344 = .520$

USING FIG. AGO-28.0 APPENDIX 2

$A = .008$

USING FIG. AHA-28.4 APPENDIX 2

PREPARED BY	DATE	CHECKED BY	DATE	REVISED BY	DATE
R. Dawn	9-2-81				

GENERAL DYNAMICS
Convair Division

EBT-P

HELIUM VESSEL

INNER BORE

$B = 13,600$

$$P_a = \frac{4B}{3(D_o/t)} = \frac{4(13,600)}{3(18.344/.365)}$$

$P_a = 361$ PSI AT R.T.

MARGIN OF SAFETY:

$$MS = \frac{361}{\text{BURST } P = 100} - 1 = +2.61 \text{ (BURST)}$$

SHELL DISCONTINUITY ANALYSIS

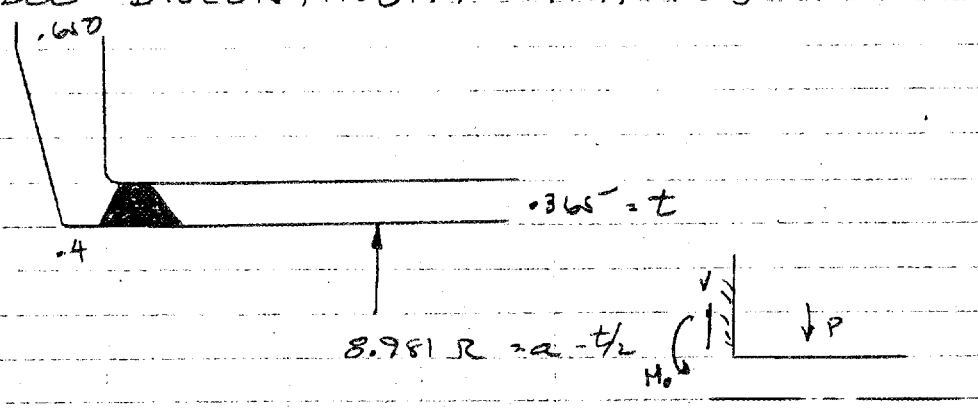

MAT'L - 316 L

$E = 29 \times 10^6$

$\nu = .3$

PREPARED BY	DATE	CHECKED BY	DATE	REVISED BY	DATE
R. Dawson	9-2-91				

A706-1 (REV. 9-65)

GENERAL DYNAMICS
Convair Division

REPORT

PAGE

EBT-P
HELIUM VESSEL

INNER BORE

Assuming that the side plates provide a maximum of 60% fixity moment to the radially loaded bore:

$$M_o = 0.60 \times \frac{p}{2\beta^2}$$

Ref Timoshenko, Theory of plates & shells, pg 475

$$\beta = \left[\frac{3(1-\nu^2)}{a^2 t^2}\right]^{1/4} = \left[\frac{3(1-.3^2)}{\overline{9.164}^2 \times \overline{.365}^2}\right]^{1/4}$$

$$\beta = 0.703$$

p = winding pressure + proof pressure

$$p = 570.75 + 62.5 = 633.25 \text{ psi}$$

$$M_o = \frac{0.60 \times 633.25}{2 \times \overline{.703}^2} = 384.4 \text{ in lbs/in}$$

$$\sigma = \frac{6M}{t^2} = \frac{6 \times 384.4}{\overline{.365}^2} = 17{,}312 \text{ psi}$$

$$MS = \frac{30000}{1.5 \times 17312} - 1 = \boxed{+0.15}$$

PREPARED BY	DATE	CHECKED BY	DATE	REVISED BY	DATE
McCutchen	2-1-82				

A706-1 (REV. 9-65)

GENERAL DYNAMICS
Convair Division

REPORT

PAGE

EBT-P

HELIUM VESSEL

SIDE FLANGES

SIDE FLANGE CORNER STRESS

REF: "A" TABLE 24, CASE 2h

ASSUME UNIFORM LOAD OVER ENTIRE PLATE

LOADS = 50 PSI QUENCH PRESSURE

73,000 LBS FAULT LOAD

EQUIV. FAULT LOAD PRESS = $\frac{73,000}{\pi(R_2^2 - R_1^2)}$

$P_F = \frac{73,000}{\pi(15.025^2 - 9.172^2)}$

Ref "A": Formulas for Stress And Strain, Roark and Young, 5th Ed.

PREPARED BY	DATE	CHECKED BY	DATE	REVISED BY	DATE
K. Dawn	9-2-81				

A706-1 (REV. 9-65)

EBT-P

HELIUM VESSEL

SIDE FLANGES

$P_F = 164$ PSI

PRESS LOAD = 164 + 50 = 214 PSI

$b/a = 9.172/15.025 = .6104$

$\therefore K_{mrb} = -.0153$

$K_{mra} = -.0119$

$\therefore M_b = K_{mrb}\, p\, a^2 = -.0153\,(214)(15.025)^2$

$= 739.2$

$\sigma_b = 6M/t^2 = 6(739.2)/.4^2 = \underline{27,718}$ PSI

$M_a = K_{mra}\, p\, a^2 \quad -.0119\,(214)\,(15.025)^2$

$= 574.9$

$\sigma_a = 6M/t^2 = \underline{8,164}$ PSI

PREPARED BY	DATE	CHECKED BY	DATE	REVISED BY	DATE
[illegible]	9-2-81				

GENERAL DYNAMICS
Convair Division

REPORT

PAGE

EBT-P

HELIUM VESSEL

OUTER RING

MARGIN OF SAFETY

$$MS = \frac{20,000}{22,718(1.5)} - 1 = +.68$$ FAULT COND.

AT 4°K

PREPARED BY	DATE	CHECKED BY	DATE	REVISED BY	DATE
K. Dean	9-2-81				

A706-1 (REV. 9-65)

GENERAL DYNAMICS
Convair Division

REPORT

PAGE

EBT-P

HELIUM VESSEL

STACK

THE HELIUM VESSEL STACK IS A CYLINDER OF VARING WALL THICKNESS. THE BOTTOM SECTION IS .11 THK, THE UPPER SECTION IS .035 THK. MATERIAL IS 316 L.

REF: 5.1-2 SECTION VIII, DIV. 2, ARTICLE D-2 "INTERNAL PRESSURE"

MIN THICKNESS $t = \frac{PR}{S - .5P}$

$S = 16,700(1.15) = 19,200$

$\therefore t = \frac{P(4.3125)}{19,200 - .5P}$

for Proof Pressure of 75 PSI $t = .0169$

$MS = \frac{.035}{.0169} - 1 = +1.07$ PROOF PRESSURE

PREPARED BY	DATE	CHECKED BY	DATE	REVISED BY	DATE
K Zam	9-2-71				

A706-1 (REV. 9-65)

REFERENCES

5.2-1 "FORMULAS FOR STRESS & STRAIN" by ROARK, 5TH ED.

-2 "ASME BOILER & PRESSURE VESSEL CODE

PREPARED BY	DATE	CHECKED BY	DATE	REVISED BY	DATE
R. Dam	9-2-71				

EBTP

HELIUM VESSEL

VAPOR COOLED LEADS

MAXIMUM DESIGN PRESSURE = 30 PSI

MATERIAL PROPERTIES OF 610-CR

F_{TU} = 43.4 KSI

E_T = 3.9×10^6

F_{CU} = 60.1 KSI

E_C = 2.03×10^6

FOR ANALYSIS PURPOSES, ASSUME SEAL DIA IS 2.75" + 2(1.125) = 5.00 DIA

BOLT CIRCLE DIA = 2.75" + 2(1.5") = 5.75" DIA

BLIND FLANGE ANALYSIS:

REF: ASME SEC VIII, DIV 2 ARTICLE D-7

AD-702(b):

$$T = d\sqrt{\frac{CP}{S} + \frac{1.9\,Whg}{Sd^3}}$$

PREPARED BY	DATE	CHECKED BY	DATE	REVISED BY	DATE
R. Dawson	2-20-81				

EBTP

HELIUM VESSEL

VAPOR COOLED LEADS

FROM FIG AD-701.2 (C) $C = .3$

SINCE AN O-RING IS BEING USED, NO BENDING MOMENT IS PRODUCED. THEREFORE LET $h_g = 0$

THEN $T = d\sqrt{\frac{CP}{S}}$

OR $S = \frac{d^2 CP}{T^2} = \frac{(5.0)^2(.3)(30)}{(.625)^2}$

$S = 576$ PSI

$MS = \frac{43,400}{576(3)} - 1 = +$ LARGE

PREPARED BY	DATE	CHECKED BY	DATE	REVISED BY	DATE
R. Dawson	2-20-81				

STACK BELLOWS

50 PSIG WORKING PRESSURE
75 PSIG TEST PRESSURE

10 CONVOLUTIONS
11.0 LONG

8.625" I.D.
9.875" OD

.018" THICK

SPRING RATE:

AXIAL 401 LB/IN

LATERAL 1847 LB/IN

ANGULAR 75 IN LB/DEGREE

APPENDIX B-3.2

STRESS ANALYSIS

WINDING

STANSOL ANALYSIS

PROPERTIES OF TYPE 316 SST -(MATERIAL #1)

1. $E = 29.5 \times 10^{6}$ PSI @ 4K
2. $\alpha = 5.808 \times 10^{-6}$ IN/IN - °F $= 3.0898 \times 10^{-3}$ IN/IN FROM RT TO 4K
3. $\nu = .3$

PROPERTIES OF ANNEALED COPPER

1. $E = 17 \times 10^{6}$ PSI @ 4K
2. $\alpha = 6.205 \times 10^{-6}$ IN/IN - °F $= 3.239 \times 10^{-3}$ IN/IN FROM RT TO 4K
3. $\nu = .3$

PROPERTIES OF NbTi:

1. $E = 7.5 \times 10^{6}$ PSI @ 4K
2. $\alpha = 3.64 \times 10^{-6}$ IN/IN - °F $= 1.9 \times 10^{-3}$ IN/IN FROM RT TO 4K

PROPERTIES OF CONDUCTOR (MATERIAL #5)

1. WIDTH = .1969
2. HEIGHT = .1142
3. CU : SC RATIO = 3.0 (NOM.) OR 75% CU, 25% NT

ELASTIC MODULUS:

$$E = .75\left(17 \times 10^{6}\right) + .25\left(7.5 \times 10^{6}\right) = 14.62 \times 10^{6} \text{ PSI}$$

COEFFICIENT OF THERMAL EXPANSION

$$\alpha = \frac{17 \times 10^{6}\left(3.239 \times 10^{-3}\right).75 + 7.5 \times 10^{6}\left(1.9 \times 10^{-3}\right).25}{17 \times 10^{6}(.75) + 7.5 \times 10^{6}(.25)}$$

$$\alpha = 3.067 \times 10^{-3} \text{ IN/IN FROM RT TO 4K}$$

PROPERTIES OF NOMEX (MATERIAL #4)

1. E (RADIAL) $= 1.0 \times 10^4$
   E (HOOP) $= .25 \times 10^3$
2. $\alpha = 3. \times 10^{-3}$
3. $\nu_{R\theta} = .3$
4. $t = 6.5$ TO 7 MILS

DATA FROM ORNL

PROPERTIES OF G10-CR

SOLID -(MATERIAL #3)

1. $E_\theta = 5.208 \times 10^6$ PSI
   $E_R = 3.2 \times 10^6$ PSI
2. $\nu_{\theta R} = .17$
   $\nu_{R\theta} = .105$
3. $\alpha_R = 7.5 \times 10^{-3}$
   $\alpha_\theta = 2.7 \times 10^{-3}$

(MATERIAL #2)
PERFORATED (46.6% PERFORATED)

$E_\theta = 1 \times 10^2$
$E_R = .534(3.2 \times 10^6) = 1.71 \times 10^6$
$\nu_{\theta R} = .17$
$\nu_{R\theta} = .07$
$\alpha_R = 7.5 \times 10^{-3}$
$\alpha_\theta = 2.7 \times 10^{-3}$

COIL STACK

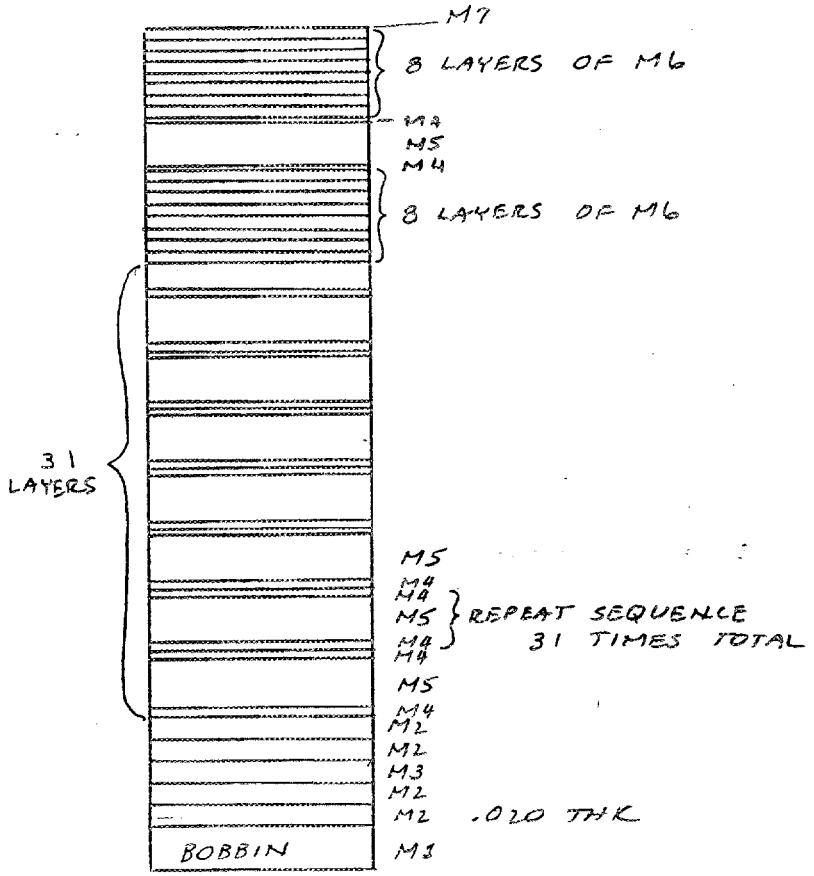

MATERIAL PROPERTIES (INPUT DATA)

MATERIAL 1 STEEL BOBBIN

T1 = .366
WT = .2109
ETH = 29.5E6
VTHR = .3
ATH = 3.0898E-3
ERAD = 29.5E6
VRTH = .3
ARAD = 3.0898E-3

MATERIAL 2 PERFORATED G10-CR

T1 = .02
WT = .2109
ETH = 1.75E6
VTHR = .07
ATH = 2.7E-3
ERAD = 1.75E6
VRTH = .07
ARAD = 7.5E-3

MATERIAL 3 SOLID G10-CR

T1 = .02
WT = .2109
ETH = 5.208E6
VTHR = .105
ATH = 2.7E-3
ERAD = 3.2E6
VRTH = .105
ARAD = 7.5E-3

MATERIAL 4 NOMEX

T1 = .007
WT = .1054
ETH = .25E3
VTHR = .3
ATH = 3.E-3
ERAD = 1.E4
VRTH = .3
ARAD = 3.E-3

MATERIAL 5 CONDUCTOR

TI = .1142
WT = .1969
ETH = 14.62E6
VTHR = .3
ATH = 3.067E-3
ERAD = 14.62E6
VRTH = .3
ARAD = ~~7.5E-3~~ 3.067E-3

MATERIAL 6 PERFORATED 610-CR

TI = .03125
WT = .2109
ETH = .75E6
VTHR = .17
ATH = 2.7E-3
ERAD = 1.7E6
VRTH = .07
ARAD = 7.5E-3

CONDUCTOR STRESS

SUMMATION OF WINDING, COOLDOWN, AND MAGNETIC LOADING PRODUCES THE FOLLOWING hoop STRESS IN THE CONDUCTORS. DATA BASE "EBTPCENSL2DAT." (USING NOMEX CONDUCTOR INSULATION)

X1.=15,105.300
X2.=15,676.300
X3.=16,349.700
X4.=16,573.700
X5.=16,593.800
X6.=16,422.300
X7.=16,094.900
X8.=15,635.300
X9.=15,066.300
X10.=14,487.400
X11.=13,675.100
X12.=12,884.100
X13.=12,047.700
X14.=11,177.400
X15.=10,224.000
X16.=9,377.800
X17.=8,469.000
X18.=7,567.700
X19.=6,684.700
X20.=5,831.500
X21.=5,020.400
X22.=4,265.000
X23.=3,580.470
X24.=2,983.280
X25.=2,492.390
X26.=2,128.630
X27.=1,915.840
X28.=1,880.610
X29.=2,052.410
X30.=2,466.600
X31.=3,159.4[illegible]
X32.=3,096.2[illegible]

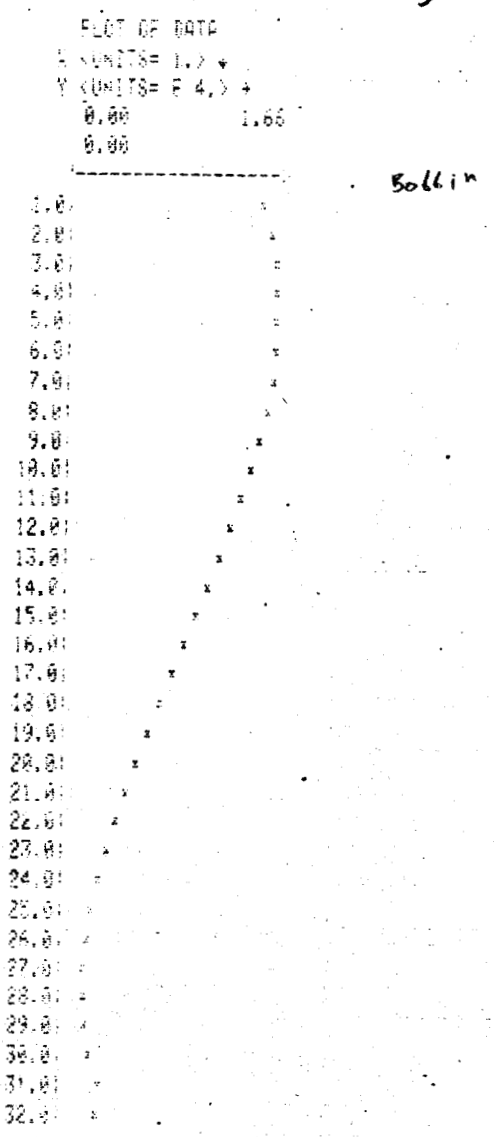

Bollin

GENERAL DYNAMICS
Convair Division

CONDUCTOR STRESS
NOMEX WRAP

7-20, 7-21, 7-27 analyses
summation of winding, cooldown, and magnetic loading produces the following radial stress in the conductors:

NOMEX — RADIAL STRESS IN CONDUCTOR

X1=-6.647
X2=-130.948
X3=-277.941
X4=-319.617
X5=-391.159
X6=-451.225
X7=-501.375
X8=-545.064
X9=-581.740
X10=-613.852
X11=-639.922
X12=-662.860
X13=-682.343
X14=-698.688
X15=-712.108
X16=-722.651
X17=-730.244
X18=-734.713
X19=-735.825
X20=-733.205
X21=-726.424
X22=-714.929
X23=-696.093
X24=-678.140
X25=-645.205
X26=-607.283
X27=-560.201
X28=-502.653
X29=-433.120
X30=-349.911
X31=-251.097
X32=-142.629

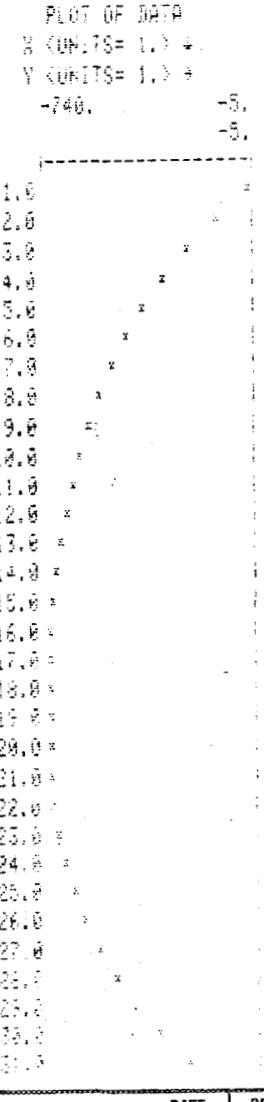

PREPARED BY	DATE	CHECKED BY	DATE	REVISED BY	DATE

A706-1 (REV. 9-65)

CONDUCTOR STRESS

SUMMATION OF WINDING, COOLDOWN AND MAGNETIC LOADING PRODUCES THE FOLLOWING hoop STRESS IN THE CONDUCTORS. DATA BASE "EBTPKAPTONMAGSL2 DAT" (USING KAPTON CONDUCTOR INSULATION)

```
X1=7,150.700
X2=7,743.600
X3=8,141.600
X4=8,471.700
X5=8,746.800
X6=8,976.600
X7=9,169.200
X8=9,330.100
X9=9,465.400
X10=9,579.000
X11=9,674.600
X12=9,755.400
X13=9,824.100
X14=9,883.100
X15=9,934.400
X16=9,979.800
X17=10,021.000
X18=10,059.600
X19=10,096.800
X20=10,133.900
X21=10,172.200
X22=10,212.000
X23=10,254.900
X24=10,301.600
X25=10,352.900
X26=10,409.600
X27=10,472.200
X28=10,541.500
X29=10,618.000
X30=10,702.400
X31=10,795.600
X32=9,652.800
```

```
                PLOT OF DATA
              X (UNITS= 1.) +
              Y (UNITS= E 4.) +
                0.00          1.10
                0.00
              |-----------------
          1.0|          x
          2.0|          x
          3.0|          x
          4.0|          x
          5.0|          x
          6.0|          x
          7.0|          x
          8.0|          x
          9.0|          x
         10.0|          x
         11.0|          x
         12.0|          x
         13.0|          x
         14.0|          x
         15.0|          x
         16.0|          x
         17.0|          x
         18.0|          x
         19.0|          x
         20.0|          x
         21.0|          x
         22.0|          x
         23.0|          x
         24.0|          x
         25.0|          x
         26.0|          x
         27.0|          x
         28.0|          x
         29.0|          x
         30.0|          x
         31.0|          x
         32.0|          x
```

GENERAL DYNAMICS
Convair Division

REPORT

PAGE

CONDUCTOR STRESSES
KAPTON WRAP

7-20, 7-21, 7-27 analyses
Summation of winding, cooldown, and magnetic loading produces the following radial stress in the conductor pack:

KAPTON – RADIAL STRESS IN COND.

X1=-7,119
X2=-44,5[illegible] (–)
X3=-112,84[illegible]
X4=-[illegible]2,366
X5=-7[illegible]4,650
X6=-[illegible]10,640
X7=-1,041,130
X8=-1,[illegible]36,710
X9=-1,237,840
X10=-1,344,990
X11=-1,418,190
X12=-1,478,430
X13=-1,525,710
X14=-1,560,320
X15=-1,582,460
X16=-1,592,620
X17=-1,590,730
X18=-1,577,250
X19=-1,552,020
X20=-1,515,270
X21=-1,467,090
X22=-1,407,490
X23=-1,336,640
X24=-1,254,550
X25=-1,161,350
X26=-1,056,960
X27=-941,470
X28=-814,880
X29=-677,260
X30=-528,507
X31=-366,735
X32=-184,[illegible]

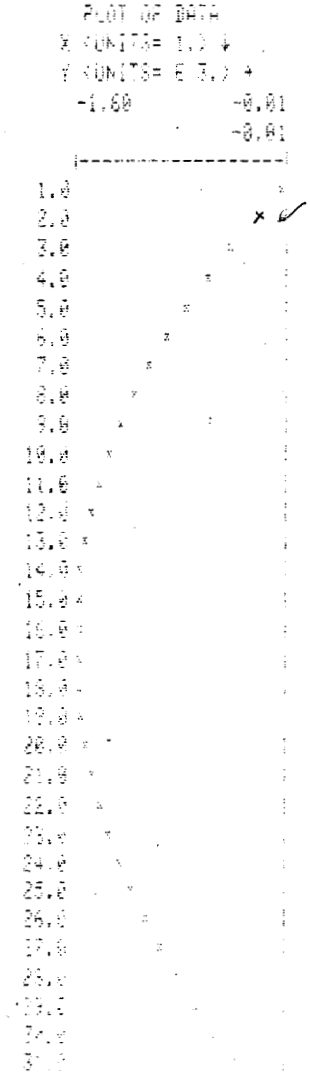

PREPARED BY	DATE	CHECKED BY	DATE	REVISED BY	DATE

A706-1 (REV. 9-65)

STANSOL RESULTS

WINDING LOADS:

BOBBIN STRESS: RADIAL = -571 PSI
HOOP : -14,580 PSI (AVE)
-14,865 PSI (PEAK)

EQUIVALENT EXTERNAL PRESSURE:

$$P_2 = \frac{\sigma_T (R_2^2 - R_1^2)}{-2 R_2^2} = \frac{-14,865 (9.345^2 - 8.98^2)}{2 (9.345)^2}$$

$$P_2 = -569 \text{ PSI}$$

STANSOL RESULTS GIVES P = 571 PSI

CHECK PRESSURE VESSEL STABILITY:

REF: "FORMULAS FOR STRESS & STRAIN" BY ROARK 5TH ED, TABLE 35, CASE 19b

$$q' = .807 \frac{Et^2}{\ell R} \sqrt[4]{\left(\frac{1}{1-\nu^2}\right)^3 \frac{t^2}{r^2}}$$

$$= .807 \frac{(28 \times 10^6)(.365)^2}{8.98 \ (9.163)} \left[\left(\frac{1}{1-.3^2}\right)^3 \frac{.365^2}{9.163^2}\right]^{1/4}$$

$$q' = 7,837 \text{ PSI}$$

$$MS_{Buckling} = \frac{7837}{571 \times 4.0} - 1 = +\text{Large}$$

GENERAL DYNAMICS
Convair Division

REPORT

PAGE

EBT-P

WINDING

AXIAL LOADS - FIELD EFFECTS

The coil has ≈ 38 turns per layer

I have four slices thru conductor pack where there are field values given.

I = 1683 Amps

	Location	Bx	N	NBI	Axial stress (psi)
	1	.14805	4	996	
	5	1.05779	5	8901	
A	9	2.06807	5	17403	
	13	3.33517	5	28065	
	Σ			55366	-2767
	2	.16134	4	1086	
	6	1.16740	5	9824	
B	10	2.36749	5	19922	
	14	4.03605	5	33963	
	Σ			64796	-3239
	3	.15561	4	1048	
	7	1.12667	5	9480	
C	11	2.29051	5	19275	
	15	3.93245	5	33092	
	Σ			62894	-3144
	4	.13277	4	894	
	8	.94962	5	7991	
D	12	1.86457	5	15690	
	16	3.05208	5	25683	
	Σ			50258	-2512

PREPARED BY	DATE	CHECKED BY	DATE	REVISED BY	DATE
M. Cutchen	9-1-81				

A706-1 (REV. 9-65)

EBT-P
WINDING - NOMEX WRAP

CONDUCTOR M.S.

	Conductor #	σ_1 psi	σ_2 psi (x4.0 peaking)	σ_3 psi (x4.0 peaking)	Von Mises Stress (E)	M.S.
INSIDE	5	+16593	-391	-2767	24372	+0.07
	11	+13675	-640	-3239	23247	+0.12
	21	+5020	-726	-3144	15263	+0.70
OUTSIDE	28	+1880	-502	-2512	10536	+1.47

$$\frac{1}{\sqrt{2}}\sqrt{(\sigma_1-\sigma_2)^2+(\sigma_2-\sigma_3)^2+(\sigma_3-\sigma_1)^2} = \text{Von Mises effective stress}$$

$$MS = \frac{\sigma_y}{1.5\,\sigma} - 1$$

σ_y = 30,000 psi @ RT - Spec Minimum

$\sigma_y = 30{,}000 \times \frac{38.5}{29.6} = 39{,}000$ Ref M-216 11-29-77 20°K

PREPARED BY	DATE	CHECKED BY	DATE	REVISED BY	DATE

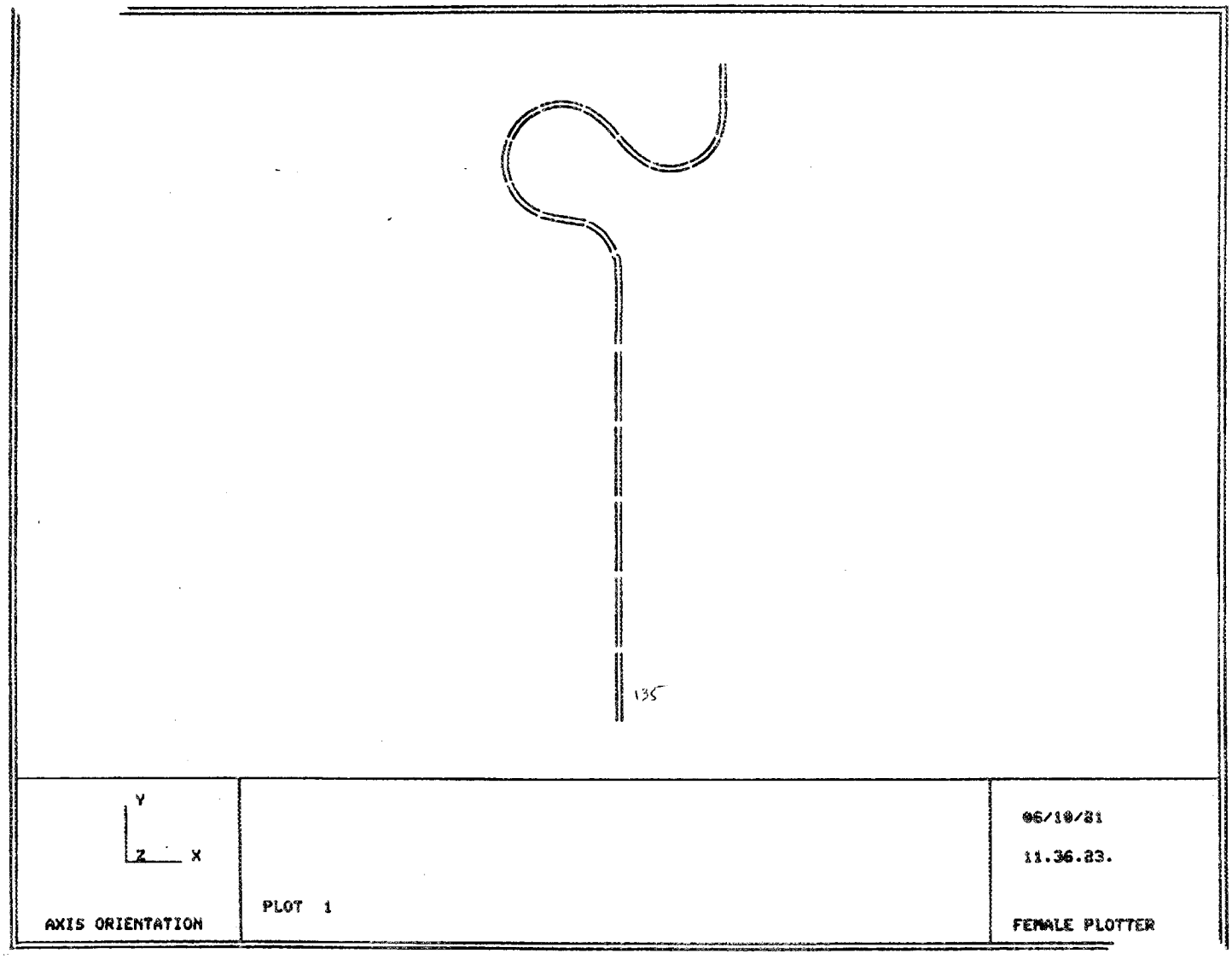
135
Y
Z
X
AXIS ORIENTATION
PLOT 1
06/10/81
11.36.33.
FEMALE PLOTTER

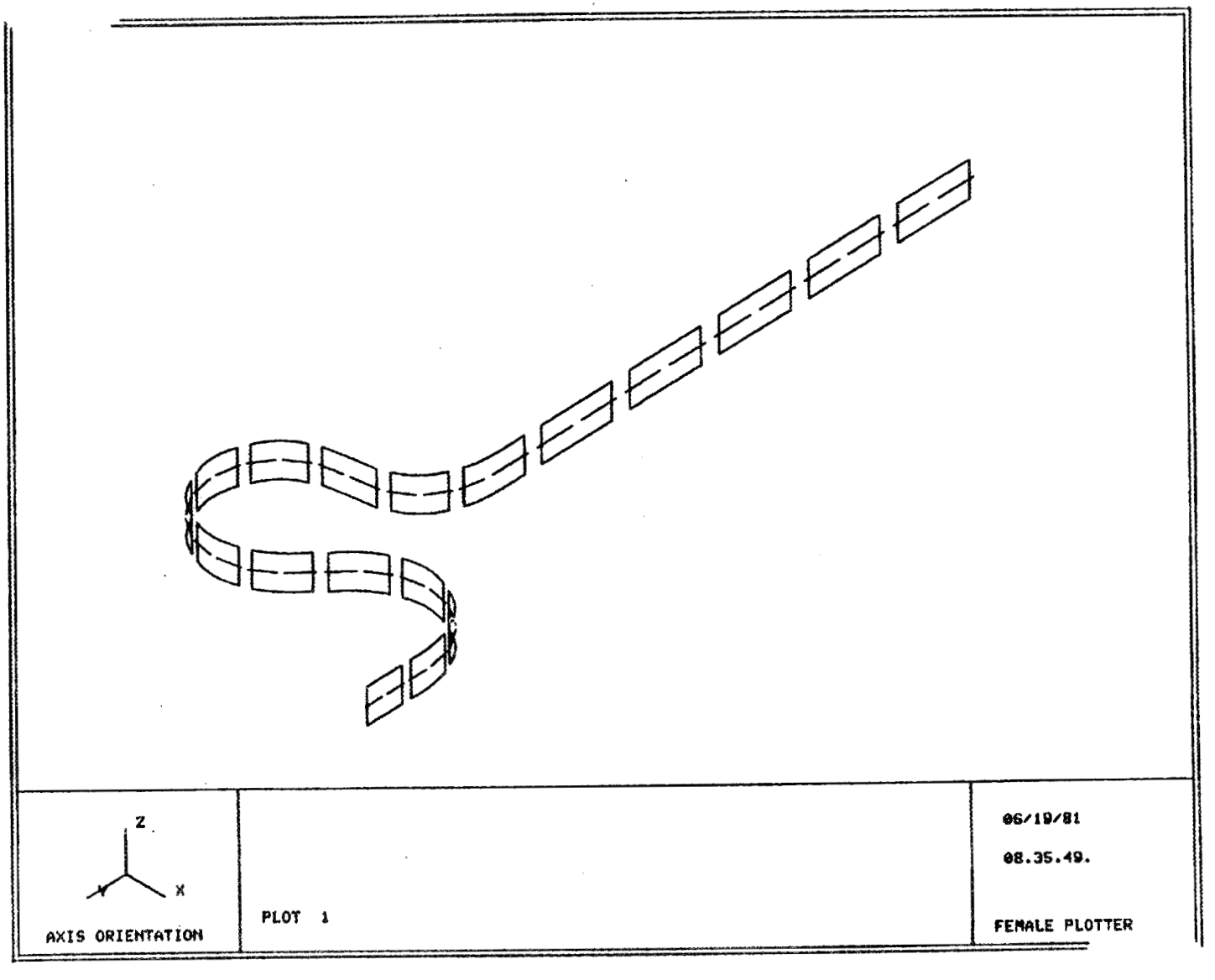
Z
Y
X
AXIS ORIENTATION
PLOT 1
06/19/81
08.35.49.
FEMALE PLOTTER

APPENDIX B-3.3

STRESS ANALYSIS

COLD MASS SUPPORTS

EBT-P
11-38080-6

COLD MASS SUPPORT

The 11-38080-6 cold mass supports provide an almost statically determinate support for the cold mass and react their loads to the vacuum vessel. They are one-piece Ti-6Al-4V machined parts as shown in Figure 1.

Three finite element models of the supports were created as shown in Figure 3. These support models were incorporated into an overall model of the vacuum vessel and Helium vessel as shown in Figure 2.

The combined model was loaded with gravity, centering, fault, pressure, and temperature loads. The NASTRAN results are used in the stress analysis of the supports.

The analysis which follows employs the ASME Boiler And Pressure Vessel Code, Section III, Division 1. This covers nuclear power plant components. This analysis uses subsection NF for Level A & B service limits.

PREPARED BY	DATE	CHECKED BY	DATE	REVISED BY	DATE
H. McCutchen	8-13-81				

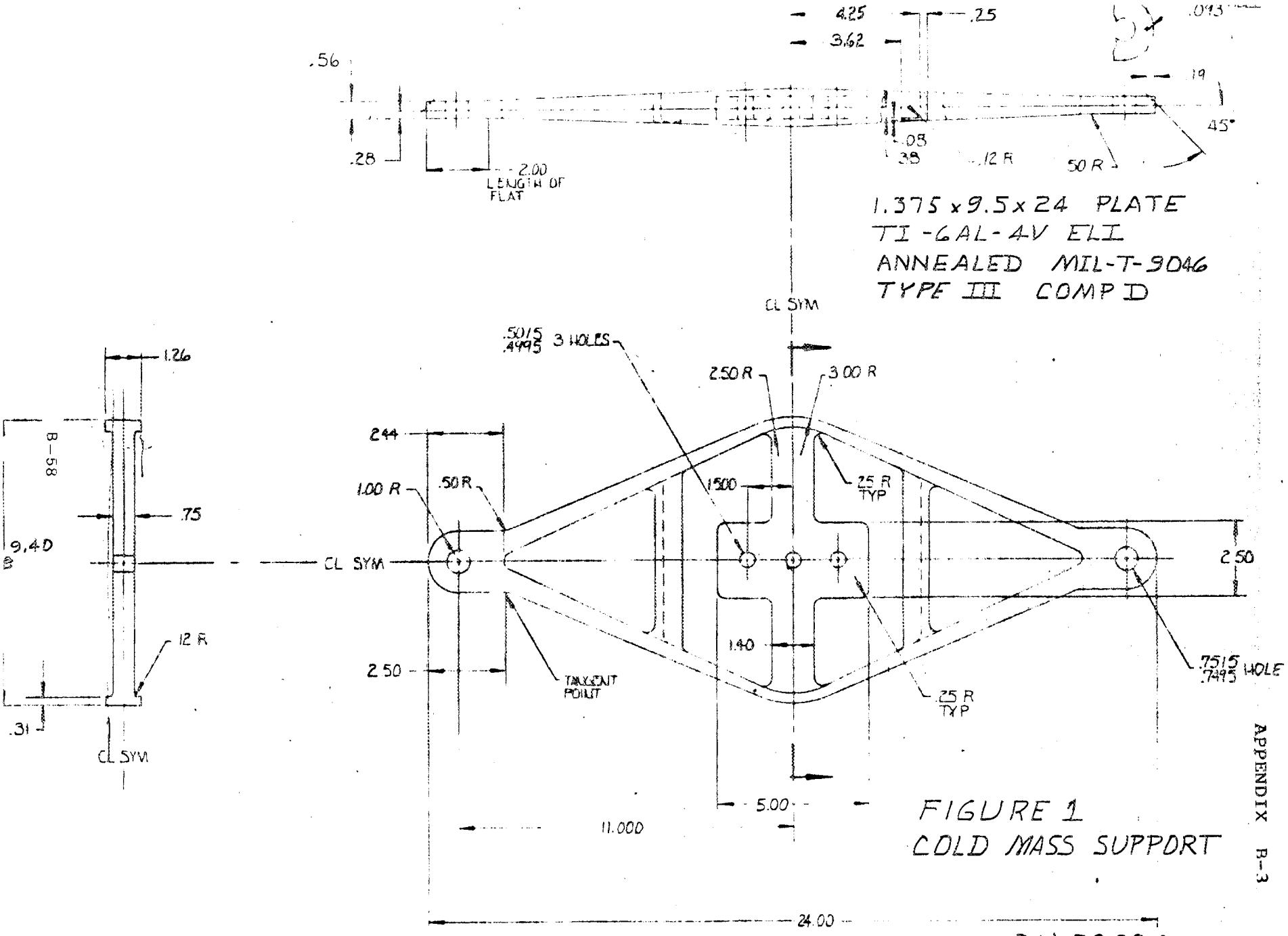

FIGURE 1
COLD MASS SUPPORT

D11-38080

EBT-P
DEWAR - MATH MODEL

COLD MASS SUPPORTS

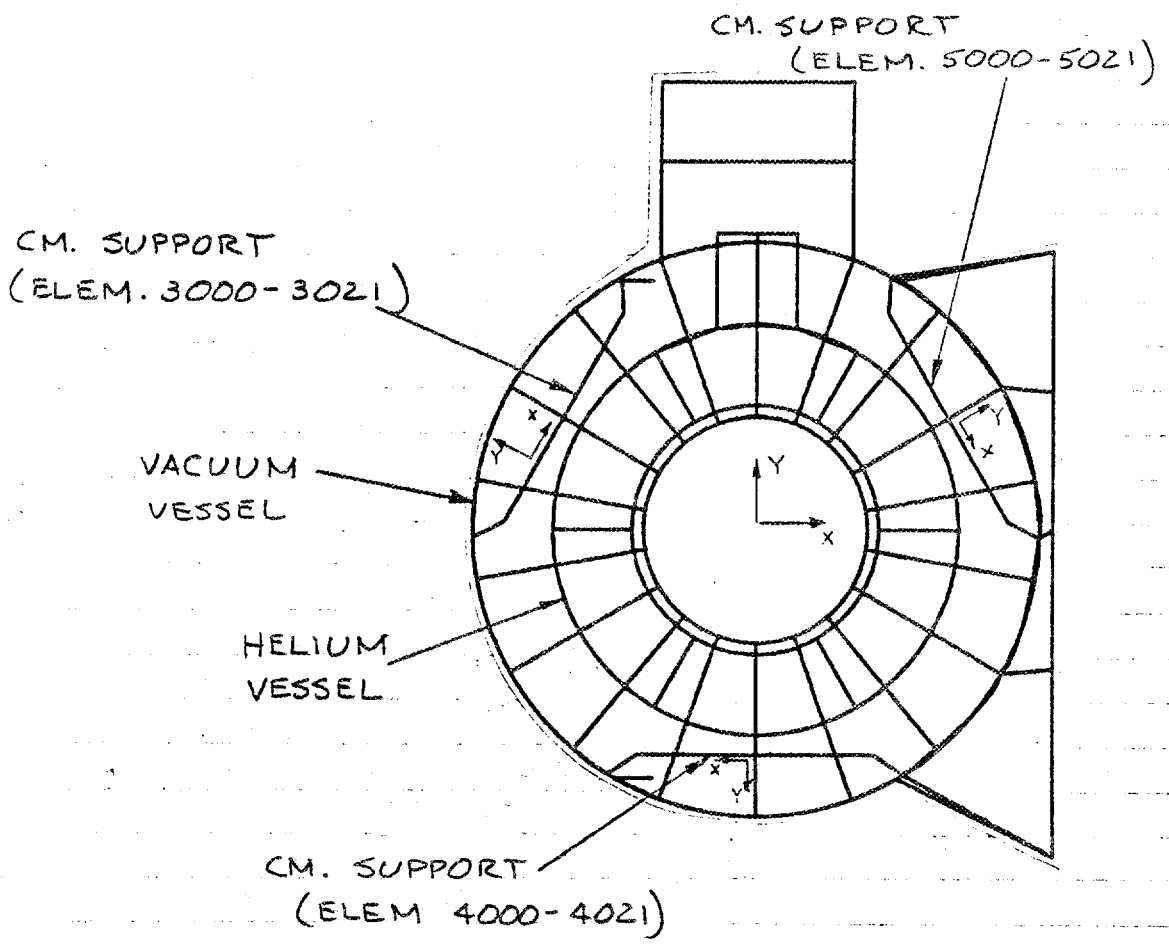

FIG 2

PREPARED BY	DATE	CHECKED BY	DATE	REVISED BY	DATE
K Dawn	5-8-81				

EBT-P
DEWAR - MATH MODEL

COLD MASS SUPPORTS

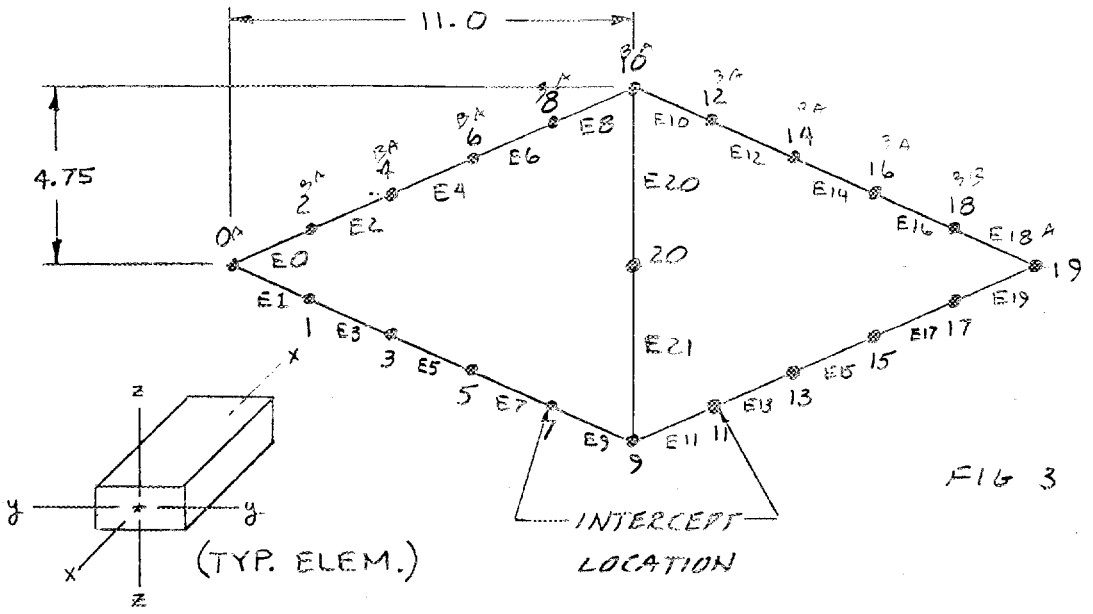

FIG 3

ELEMENT PROPERTIES TABLE 1

ELEM NO.	AREA IN^2	I_z IN^4	I_y IN^4	J IN^4	E PSI	α IN/IN-°F	T °F
E0	.35	.017	.009	.011	16.16E6	4.733E-6	+21
E2	.52	.023	.023	.028	16.36E6	4.87 E-6	-76
E4	.54	.017	.034	.044	16.64E6	4.65 E-6	-173
E6	.52	.011	.045	.096	16.73E6	4.394E-6	-271
E8	.45	.005	.052	.23	17.2 E6	4.117E-6	-330
E20	1.05	0.1717	0.0492	.1309	5.2 E6	5.1 E-6	-396

PREPARED BY	DATE	CHECKED BY	DATE	REVISED BY	DATE
K. Dean	5-8-81				

EBT-P
DEWAR - MATH MODEL

COLD MASS SUPPORTS

NODAL TEMPERATURES

TABLE 2

NODE NO.	TEMP. °F	
0	+ 70.	
2	- 27.5	
4	- 125.	
6	- 222.5	
8	- 320.	4.375 E-6
10	- 339.	4.2773 E-6
20	- 452	3.429 E-6

FORCES ACTING ON COLD MASS

FORCE	MAGNITUDE	DIRECTION
1. GRAVITY	1725 LBS	-Y
2. CENTERING (OP)	17,900 LBS	+X
3. CENTERING (FAULT)	8,000 LBS	+X
4. OUT-OF-PLANE	73,000 LBS	+.087X, +.996Z
5. PRESSURE (OP)	801 LBS	-Y
6. PRESSURE (FAULT)	1602 LBS	-Y

COMBINED FORCES

OPERATING CONDITION : 1, 2, 5
FAULT CONDITION : 1, 3, 4, 6

PREPARED BY	DATE	CHECKED BY	DATE	REVISED BY	DATE
R. Dam	5-8-81				

EBT-P

DEWAR-MATH MODEL

COLD MASS SUPPORTS

NODAL SECTION PROPERTIES TABLE 3

ELEMENT	END	WIDTH	THICK.	AREA	I/c1	I/c2
E0 + E1	A	2.00	.560	1.120	.373	.105
E0 & E1	B	.785	.646	.507	.066	.055
E2 & E3	A	.785	.646	.507	.066	.055
	B	.675	.796	.537	.060	.071
E4 & E5	A	.675	.796	.537	.060	.071
	B	.566	.946	.535	.050	.084
E6 & E7	A	.566	.946	.535	.050	.084
	B	.456	1.096	.500	.038	.091
E8 & E9	A	.456	1.096	.500	.038	.091
	B	.347	1.246	.432	.025	.090
E 20 & 21	A	5.000	.750	3.750	3.125	.469
	B	2.750	.750	2.063	.945	.258

COMBINING AXIAL & BENDING LOADS:

REF ASME SEC III, DIV 1, APPENDIX XVII
PARA. XVII - 2215.2

$$\frac{f_a}{F_a} + \frac{f_{bx}}{F_{bx}} + \frac{f_{by}}{F_{by}} \leq 1$$

PREPARED BY	DATE	CHECKED BY	DATE	REVISED BY	DATE
K. Dawson	5-4-81				

EBT-P

DEWAR

COLD MASS SUPPORTS

THIS CAN BE RE-WRITTEN AS:

$P/A + M_1/I/c_1 + M_2/I/c_2 = \text{DESIGN STRESS}$

MATERIAL ALLOWABLES

TENSILE STRENGTH OF TI-6Al-4V

REF - MIL-HDBK-5 P. 5-67
P. 5-70

F_{TU} (ROOM TEMP) = 130,000

THE EFFECT OF TEMP. IS SHOWN IN FIG 4 AND NODAL TEMP. IS GIVEN IN TABLE 2

TENSILE STRENGTH AT TEMP - TABLE 2

NODE NO.	% INCREASE	F_{TU}
0	0	130,000
2	109	141,700
4	119	154,700
6	132	171,600
8	152	197,600
10	169	219,700

PREPARED BY [illegible] DATE 5-5-81 | CHECKED BY | DATE | REVISED BY | DATE

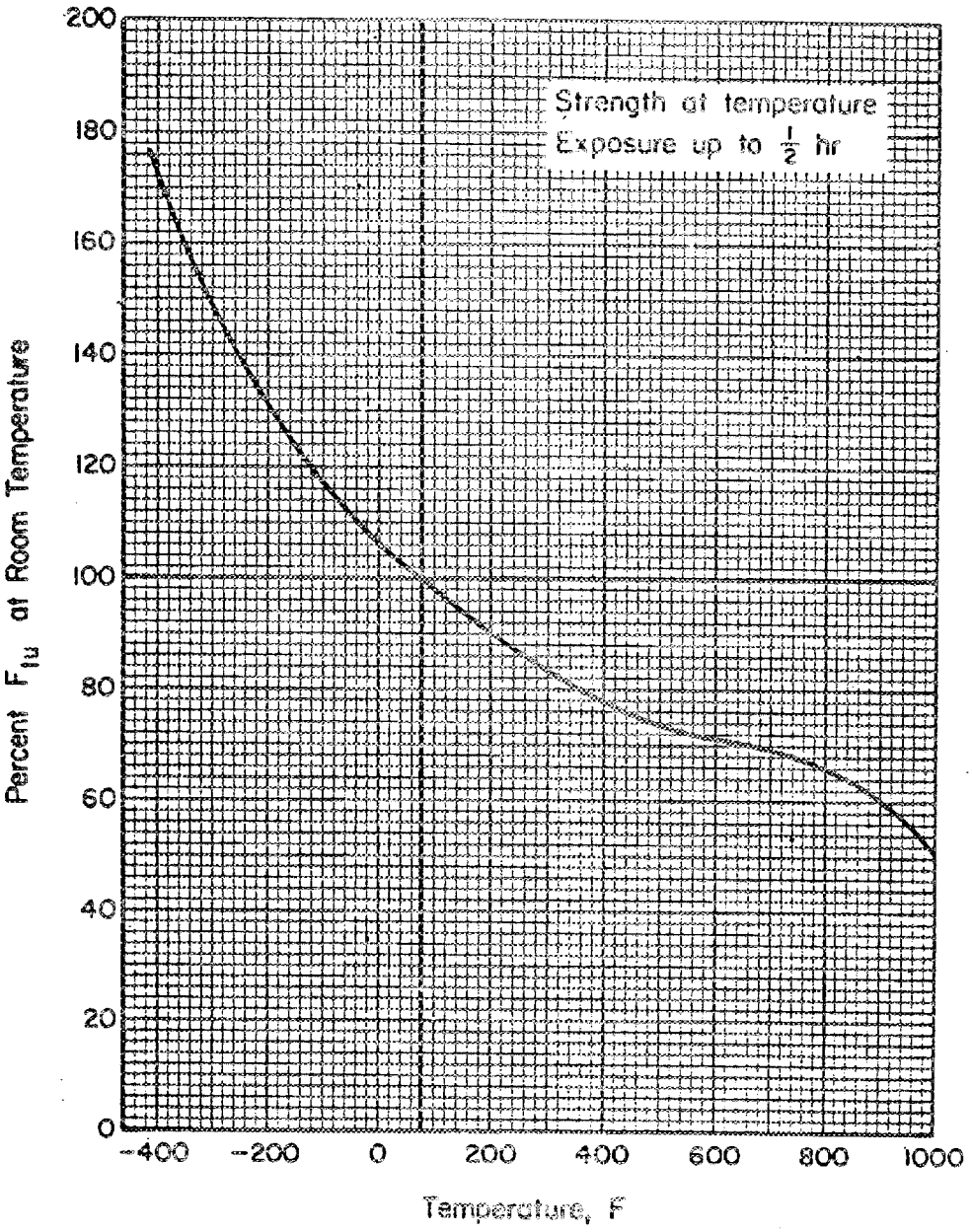

FIGURE 4. *Effect of temperature on the ultimate tensile strength (F_{tu}) of annealed Ti-6Al-4V alloy.*

-EBT-P

DEWAR

COLD MASS SUPPORTS

(Ti-6Al-4V) BEARING STRENGTH = 196,000

610-CR F_{TU} = 125,000 (AT 77°K)
F_{BU} = 33,500 (AT RT)
F_{SU} = 6,260 (AT RT)

FACTORS OF SAFETY

THE BASIC DESIGN CRITERIA OF 1.67 ON YIELD & 2 ON ULT. MAKES ULTIMATE THE LIMITING DESIGN CRITERIA

DESIGN ALLOWABLES - TABLE 3

MATERIAL	LOCATION	PROPERTY	VALUE
Ti-6Al-4V	NODE 0	T/C STRESS	65,000
	NODE 2	T/C STRESS	70,850
	NODE 4	T/C STRESS	77,350
	NODE 6	T/C STRESS	85,800
	NODE 8	T/C STRESS	98,800
	NODE 10	T/C STRESS	109,850
	—	BEARING	98,000
610-CR	—	T/C STRESS	62,500
	—	BEARING	16,750
	—	IL SHEAR	3,130

PREPARED BY K. Dawson DATE 5-5-81 | CHECKED BY DATE | REVISED BY DATE

EBT-P

DEWAR

COLD MASS SUPPORTS

ELEMENT STRESS & MARGINS OF SAFETY - FAULT OPR.

SUPPORT GROUP 3000

TABLE 4

ELEMENT NO.	END A	MS A	END B	MS B
3000	21,931	+1.96	43,846	+.62
3001	21,931	+1.96	21,042	+2.37
3002	43,846	+.62	38,072	+1.03
3003	21,042	+2.37	22,126	+2.50
3004	38,072	+1.03	43,820	+.96
3005	22,126	+2.50	27,832	+2.08
3006	43,820	+.96	51,650	+.91
3007	27,832	+2.08	35,006	+1.82
3008	51,650	+.91	64,764	+.70
3009	35,006	+1.82	46,794	+1.35
3010	64,764	+.70	49,563	+.99
3011	46,794	+1.35	36,793	+1.69
3012	49,563	+.99	41,588	+1.06
3013	36,793	+1.69	29,974	+1.86
3014	41,588	+1.06	35,741	+1.16
3015	29,974	+1.86	24,627	+2.14
3016	35,741	+1.16	40,851	+.73
3017	24,627	+2.14	27,887	+1.54
3018	18,844	+2.45	40,851	+.73
3019	18,844	+2.45	27,887	+1.54
3020	16,297	+2.84	11,420	+4.47
3021	12,869	+3.86	8,446	+6.40

PREPARED BY R. Dawson DATE 5-5-81 | CHECKED BY DATE | REVISED BY DATE

EBTP

DEWAR

COLD MASS SUPPORTS

SUPPORT GROUP 4000

TABLE 4 CONT.

ELEMENT NO.	END A	MS A	END B	MS B	
4000	12,343	+4.27	37,497	+.89	
4001	12,343	+4.27	30,974	+1.29	
4002	37,497	+.89	33,345	+1.32	
4003	30,974	+1.29	28,406	+1.72	
4004	33,345	+1.32	38,448	+1.23	
4005	28,406	+1.72	32,231	+1.66	
4006	38,448	+1.23	45,871	+1.15	
4007	32,231	+1.66	37,717	+1.62	
4008	45,871	+1.15	58,953	+.86	
4009	37,717	+1.62	47,158	+1.33	
4010	58,953	+.86	52,770	+.87	
4011	47,158	+1.33	32,008	+2.09	
4012	52,770	+.87	45,967	+.87	
4013	32,008	+2.09	25,146	+2.41	
4014	45,967	+.87	41,337	+.87	
4015	25,146	+2.41	19,915	+2.88	
4016	41,337	+.87	47,723	+.48	*
4017	19,915	+2.88	22,720	+2.12	
4018	23,034	+1.82	47,723	+.48	*
4019	23,034	+1.82	22,720	+2.12	
4020	32,525	+.92	10,851	+4.76	
4021	28,963	+1.16	8,024	+6.79	

* most critical

PREPARED BY	DATE	CHECKED BY	DATE	REVISED BY	DATE
R. Dawson	5-5-81				

EBT-P

DEWAR

COLD MASS SUPPORTS

SUPPORT GROUP 5000

TABLE 4 CONT.

ELEMENT NO.	END A	MS A	END B	MS B
5000	20,374	+2.19	44,456	+.59
5001	20,374	+2.19	22,449	+2.16
5002	44,456	+.59	38,186	+1.03
5003	22,449	+2.16	20,239	+2.82
5004	38,186	+1.03	42,553	+1.02
5005	20,239	+2.82	24,893	+2.45
5006	42,553	+1.02	48,977	+1.02
5007	24,893	+2.45	31,110	+2.18
5008	48,977	+1.02	60,033	+.83
5009	31,110	+2.18	41,745	+1.63
5010	60,033	+.83	44,520	+1.22
5011	41,745	+1.63	34,786	+1.84
5012	44,520	+1.22	37,602	+1.28
5013	34,786	+1.84	29,510	+1.91
5014	37,602	+1.28	32,847	+1.35
5015	29,510	+1.91	25,789	+2.00
5016	32,847	+1.35	37,329	+.90
5017	25,789	+2.00	28,520	+1.48
5018	13,217	+3.92	37,329	+.90
5019	13,217	+3.92	28,520	+1.48
5020	25,010	+1.50	10,165	+5.15
5021	21,432	+1.92	7,564	+7.26

PREPARED BY	DATE	CHECKED BY	DATE	REVISED BY	DATE
R. Dawson	5-6-81				

EBTP

DEWAR

COLD MASS SUPPORTS

COMBINING AXIAL COMPRESSION & BENDING

REF: ASME SEC III, DIV 1, APPENDIX XVII
PARA. XVII -2215.1

ASSUMPTIONS: 1. AXIAL THERMAL STRESS = 0.
2. SECTION PROP. ARE THOSE AT THE MID-POINT OF EACH SPAN

SECTION PROPERTIES:

AT X = 3.313 (WARM SPAN)

$r_1 = .289(.729) = .211$
$r_2 = .289(.722) = .209$

AT X = 8.813 (COLD SPAN)

$r_1 = .289(.456) = .132$
$r_2 = .289(1.097) = .317$

PREPARED BY	DATE	CHECKED BY	DATE	REVISED BY	DATE
K. Dawson	5-6-81				

A706-1 (REV. 9-65)

EBTP

DEWAR

COLD MASS SUPPORTS

LOADS ACTING ON SECTIONS:

METHOD OF SOLUTION – PERFORM INTERPOLATION OF DATA FROM MATH MODEL USING HEWLETT-PACKARD USERS LIBRARY PROGRAM # 04294D "CUBIC SPLINE CURVE FIT WITH SIMPSON'S RULE INTEGRATION".

EACH SUPPORT HAS 4 WARM & 4 COLD SPANS

TABLE 5

	SUPPORT	W/C	PLANE 1	PLANE 2	AXIAL LOAD	
1	3000	W	-2.899E1	9.000E1	-1.386E4	
2		W	-6.122E1	6.144E1	+1.530E4	
3		W	-4.460E1	-1.499E2	+1.384E4	
4		W	-4.530E1	-1.381E2	-1.531E4	✓
5		C	-7.799E1	-1.043E3	-1.386E4	✓
6		C	-1.620E2	-9.647E2	+1.530E4	
7		C	-1.186E2	-1.020E3	+1.384E4	
8		C	-1.214E2	-9.608E2	-1.531E4	✓
9	4000	W	-6.264E1	6.952E1	+1.276E4	
10		W	-2.340E1	1.855E1	-1.765E4	✓
11		W	-8.017E0	-1.288E2	+1.778E4	
12		W	-7.802E1	-1.157E2	-1.263E4	✓
13		C	-1.636E2	-7.992E2	+1.276E4	
14		C	-6.531E1	-7.356E2	-1.765E4	✓
15		C	-2.133E1	-8.537E2	+1.778E4	

PREPARED BY	DATE	CHECKED BY	DATE	REVISED BY	DATE
K Kaus	5-6-81				

EBTP

DEWAR

COLD MASS SUPPORTS

TABLE 5 CONT.

	SUPPORT	W/C	PLANE 1	PLANE 2	AXIAL LOAD
16	4000	C	-2.075E2	-7.895E2	-1.263E4
17	5000	W	-1.132E1	1.057E2	+1.643E4
18		W	-6.589E1	3.747E1	-1.271E4
19		W	-4.913E1	-1.132E2	+1.298E4
20		W	-2.825E1	-9.721E1	-1.617E4
21		C	-3.223E1	-7.710E2	+1.643E4
22		C	-1.732E2	-7.373E2	-1.271E4
23		C	-1.307E2	-7.591E2	+1.298E4
24		C	-7.515E1	-6.793E2	-1.617E4

DESIGN ALLOWABLES: WARM END $F_a = 74,042$ PSI
$E = 16.5 \times 10^6$

COLD END $F_a = 98,875$ PSI
$E = 18.5 \times 10^6$

EQ 19:

$$\frac{f_a}{F_a} + \frac{C_m f_{bx}}{(1 - f_a/F'_{ex}) F_{bx}} + \frac{C_m f_{by}}{(1 - f_a/F'_{ey}) F_{by}} \leq 1.0$$

$f_a = P/A$

$f_b = Mc/I$

$$F'_e = \frac{12 \pi^2 E}{23 (K l_b / r_b)^2}$$

PREPARED BY	DATE	CHECKED BY	DATE	REVISED BY	DATE
K Dauz	5-6-81				

EBT-P

DEWAR

COLD MASS SUPPORTS

$C_m = .85$

$K = .80$ (PINNED - FIXED)

TAKING THE HIGHEST LOADED CASES FROM TABLE 5 AND ONLY THOSE WITH COMPRESSIVE AXIAL LOADING:

TABLE 6

CASE NO.	W/C	PLANE 1	PLANE 2	AXIAL LOAD
5	C	-7.799 E1	-1.043 E3	-1.386 E4
8	C	-1.214 E2	-9.608 E2	-1.531 E4
14	C	-6.531 E1	-7.356 E2	-1.765 E4
16	C	-2.075 E2	-7.895 E2	-1.263 E4

COLD END CASES

COLD: $F'_{e_x} = \dfrac{12\pi^2(18.5\times10^6)}{23[(.80)(4.375)/(.132)]^2} = 135,500.$

$F'_{e_y} = \dfrac{12\pi^2(18.5\times10^6)}{23[(.80)(11.0)/.317]^2} = 123,617.$

$f_{b_x} = \dfrac{M_1}{.038}$

$f_{b_y} = \dfrac{M_2}{.091}$

$f_a = \dfrac{P}{.50}$

PREPARED BY	DATE	CHECKED BY	DATE	REVISED BY	DATE
K. Dawson	5-6-81				

EBT-P

DEWAR

COLD MASS SUPPORTS

CASE 5

$$f_a = \frac{1.386E4}{98.875} = 27,720$$

$$f_{bx} = \frac{7.799E1}{.038} = 2,052$$

$$f_{by} = \frac{1.043E3}{.091} = 11,462$$

$$\frac{27,720}{98,875} + \frac{.85(2,052)}{(1-27,720/135,500)\,98,875} + \frac{.85(11,462)}{(1-27,720/123,617)\,98,875} \geq 1.0$$

$$.280 + .022 + .127 = .430$$

$$MS = \frac{1.00}{.430} - 1 = \underline{+1.33}$$

CASE 8

$$f_a = \frac{1.531E4}{.5} = 30,620$$

$$f_{bx} = \frac{1.214E2}{.038} = 3,195$$

$$f_{by} = \frac{9.608E2}{.091} = 10,558$$

PREPARED BY	DATE	CHECKED BY	DATE	REVISED BY	DATE
K. Dawson	5-6-81				

A706-1 (REV. 9-65)

EBT-P

DEWAR

COLD MASS SUPPORTS

$$\frac{30,620}{98,875} + \frac{.85(3,195)}{(1-30,620/135,500)98,875} + \frac{.85(10,558)}{(1-30,620/123,617)98,875} \leq 1.0$$

$$.310 + .035 + .121 = .466$$

$$MS = \frac{1}{.466} - 1 = +1.15$$

CASE 14

$$f_a = \frac{1.765E4}{.5} = 35,300 \qquad f_{b_x} = \frac{6.531E1}{.038} = 1,719$$

$$f_{b_y} = \frac{7.386E2}{.091} = 8,084$$

$$\frac{35,300}{98,875} + \frac{.85(1719)}{(1-35,300/135,500)98,875} + \frac{.85(8084)}{(1-35,300/123,617)98,875} \leq 1.0$$

$$.357 + .020 + .097 = .474$$

$$MS = \frac{1}{.474} - 1 = +1.11$$

PREPARED BY	DATE	CHECKED BY	DATE	REVISED BY	DATE
K. Davis	5-6-81				

A706-1 (REV. 9-65)

EBT-P

DEWAR

COLD MASS SUPPORTS

CASE 16 $f_a = \frac{1.263E4}{.5} = 25,260$ $f_{b_x} = \frac{2.075E2}{.038} = 5,460$

$f_{b_y} = \frac{2.895E2}{.091} = 8,676$

$$\frac{25,260}{98,875} + \frac{.85(5,460)}{(1-25,260/135,500)98,875} + \frac{.85(8,676)}{(1-25,260/123,617)98,875} \leq 1$$

$.255 + .058 + .094 = .407$

$MS = \frac{1}{.407} - 1 = \underline{\underline{+1.46}}$

WARM END CASES

$$F'_{ex} = \frac{12\pi^2(16.5\times10^6)}{23[(.8)(4.375)/.211]^2} = 308,790$$

$$F'_{ey} = \frac{12\pi^2(16.5\times10^6)}{23[.8(11.0)/.209]^2} = 47,925$$

CASE 4 $f_a = \frac{1.531E4}{.526} = 29,106$ $f_{b_x} = \frac{4.53E1}{.064} = 708$

$f_{b_y} = \frac{1.381E2}{.063} = 2,192$

PREPARED BY	DATE	CHECKED BY	DATE	REVISED BY	DATE
K. Dawson	1-6-91				

A706-1 (REV. 9-65)

EBT-P

DEWAR

COLD MASS SUPPORTS

$$\frac{29,106}{74,042} + \frac{.85(708)}{(1-29,106/308,790)\,74,042} + \frac{.85(2192)}{(1-29,106/47,925)\,74,042} \leq 1.0$$

$$.393 + .009 + .064 = .466$$

$$MS = \frac{1}{.466} - 1 = \underline{\underline{+1.145}}$$

CASE 10: $f_a = \frac{1.265E4}{.526} = 33,535$ $f_{b_x} = \frac{2.34E1}{.064} = 366$

$$f_{b_y} = \frac{1.853E1}{.063} = 294$$

$$\frac{33,535}{74,042} + \frac{.85(366)}{(1-33,535/308,790)\,74,042} + \frac{.85(294)}{(1-33,535/47,925)\,74,042} \leq 1.0$$

$$.453 + .005 + .011 = .469$$

$$MS = \frac{1}{.469} - 1 = \underline{\underline{+1.13}}$$

CASE 12: $f_a = \frac{1.263E4}{.526} = 24,011$ $f_{b_x} = \frac{7.802E1}{.064} = 1,219$

$$f_{b_y} = \frac{1.157E2}{.063} = 1,836$$

PREPARED BY	DATE	CHECKED BY	DATE	REVISED BY	DATE
K. Dawson	5-6-81				

EBT-P

DEWAR

COLD MASS SUPPORTS

$$\frac{24{,}011}{74{,}042} + \frac{.85(1219)}{(1-24{,}011/308{,}790)\,74{,}042} + \frac{.85(1836)}{(1-24{,}011/47{,}925)\,74{,}042} \leq 1.0$$

$$.324 + .015 + .042 = .382$$

$$MS = \frac{1}{.382} - 1 = \underline{\underline{+1.62}}$$

CHECK INTERLAMINAR SHEAR

THE MAXIMUM SHEARING STRESS ON A RECT. SECTION IS GIVEN AS:

$$S_{v\,max} = \frac{3V}{2A}$$ where V is the vertical shear on the section

SHEAR LOADS GIVEN IN THE F/E MODEL OUTPUT INDICATE MAX SHEAR LOAD LOADING THE COMPOSITE IN THE INTERLAMINAR DIRECTION OCCURS DURING NORMAL OPERATION.

$$V_{MAX} = 396 \text{ LBS.}$$

$$S_{v\,max} = 3(396)/2(2.75)(.75) = 288 \text{ PSI}$$

$$MS = \frac{6260}{288} - 1 = \underline{\text{VERY LARGE}}$$

PREPARED BY	DATE	CHECKED BY	DATE	REVISED BY	DATE
R. Dawson	5-6-81				

EBT-P

DEWAR

COLD MASS SUPPORTS

CHECK END LOADS

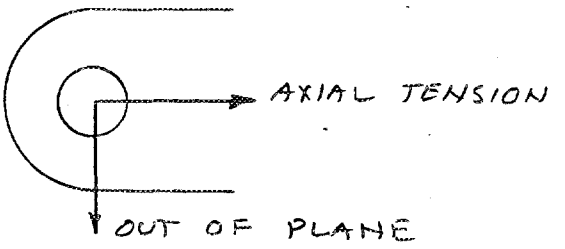

COMPARISON OF END LOADS

TABLE 7

	END	AXIAL	OUT OF PLANE	Σ	θ
1	3000	7,756	12,118	14,388	33°
2	3019	6,093	11,510	13,023	28°
3	4000	3,248	12,030	12,461	15°
4	4019	10,386	13,223	16,814	38°
5	5000	9,265	12,180	15,303	37°
6	5019	3,880	11,605	12,236	18°

DATA FROM F/E MODEL FAULT OPER.

CASE 4 IN TABLE 7 IS WORST CASE

CHECK EDGE DIST.

REF: ASME SEC III, DIV 1, APPENDIX XVII

PARA XVII-2462

PREPARED BY	DATE	CHECKED BY	DATE	REVISED BY	DATE
R. Dawson	5-6-81				

EBT-P

DEWAR

COLD MASS SUPPORTS

EDGE DIST MUST MEET THE FOLLOWING CRITERIA:

EQ 1 $L/d \geq .5 + 1.43\,(f_p/S_u)$

EQ 2 $L/d \geq 1.2$

EQ 3 $f_p/S_u \leq 1.5$

DESIGN $L/d = 1.0/.75 = 1.333$

$S_u = 130{,}000$ PSI

$$f_p = \frac{16{,}814}{.56(.75)} = 40{,}033 \text{ PSI}$$

PER EQ 1 $$.5 + 1.43\left(\frac{40{,}033}{130{,}000}\right) = .94$$

$$MS = \frac{1.333}{.94} - 1 = \underline{+.42}$$

PER EQ 2 $$MS = \frac{1.333}{1.2} - 1 = \underline{+.11}$$

PER EQ 3 $$\frac{f_p}{S_u} = \frac{40{,}033}{130{,}000} = .308$$

$$MS = \frac{1.5}{.308} - 1 = \underline{+3.87}$$

PREPARED BY	DATE	CHECKED BY	DATE	REVISED BY	DATE
R. Dawson	5-6-81				

A706-1 (REV. 9-65)

EBT-P

DEWAR

COLD MASS SUPPORTS

SHEAR ON BOLT REF: ASME SEC III APPENDIX XVII-2461.2

BOLT MATERIAL - INCONEL 718 HT TO 185KSI ULT.

$$\text{SHEAR STRESS} = \frac{16,814}{.375^2\pi} = 38,059 \text{ PSI}$$

$$\text{ALLOWABL SHEAR STRESS} = F_{vb} = \frac{.62\,S_u}{3}$$

$$= \frac{.62(185,000)}{3}$$

$$= 38,233 \text{ PSI}$$

$$MS = \frac{38,233}{38,059} - 1 = +.005$$

COMBINED TENSILE & SHEAR ON BOLT

REF: ASME SEC III, DIV 1 APPENDIX XVII-2461.3

PREPARED BY	DATE	CHECKED BY	DATE	REVISED BY	DATE
K Dawson	5-6-81				

EBT-P

DEWAR

COLD MASS SUPPORTS

$$\frac{f_t^2}{F_{tb}^2} + \frac{f_v^2}{F_{vb}^2} = 1$$

$$f_T = \frac{292\,285}{\pi \cdot .375^2} = 661$$ [TENSILE LOAD AT END 4019]

$$f_V = 38{,}059$$

$$F_{tb} = \frac{185{,}000}{2} = 92{,}500$$

$$F_{vb} = 38{,}233$$

$$\frac{661^2}{92{,}500^2} + \frac{38{,}059^2}{38{,}233^2}$$

$$5.11 \times 10^{-5} + .9909 = .9909$$

$$MS = \frac{1}{.9909} - 1 = \underline{\underline{+.009}}$$

PREPARED BY	DATE	CHECKED BY	DATE	REVISED BY	DATE
K. Dauzn	5-6-81				

A706-1 (REV. 9-65)

EBT-P

DEWAR

COLD MASS SUPPORTS

BEARING STRESS ON BOLT

REF: ASME SEC III, DIV 1, APPENDIX XVII-2461.5

$$F_p = \frac{L S_u}{2d} \leq 1.5 S_u$$

$$F_p = \frac{1(130,000)}{2(.75)} = 86,667$$

$$f_p = \frac{16,814}{.56(.75)} = 40,033$$

$$MS = \frac{86,667}{40,033} - 1 = \underline{+1.16}$$

$$\text{ALSO } MS = \frac{1.5(130,000)}{40,033} - 1 = \underline{+3.87}$$

PREPARED BY	DATE	CHECKED BY	DATE	REVISED BY	DATE
R. Dauzon	5-6-81				

EBT-P

DEWAR

COLD MASS SUPPORTS

CHECK CENTER LOADS

L/D = .75/.25 = 3.0
(BASED ON MIL-HDBK-17
& GOOD DESIGN PRACTICE)

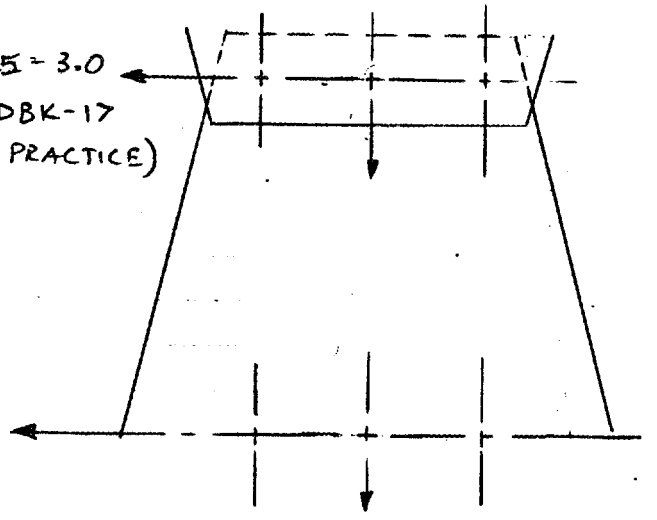

COMPARISON OF LOADS

TABLE 8

	END	AXIAL	LATERAL	Σ
1	3020	-14,562	2,468	14,614
2	3021	8,589		8,677
3	4020	-15,027	9,237	15,721
4	4021	9,127		10,229
5	5020	-14,410	6,363	14,757
6	5021	8,735		9,296

DATA FROM F/E MODEL FAULT OPER.

CASE 3 IN TABLE 8 IS WORST CASE

PREPARED BY	DATE	CHECKED BY	DATE	REVISED BY	DATE
R. Dawn	5-6-81				

EBT-P

DEWAR

COLD MASS SUPPORTS

DIVIDING THIS LOAD EQUALLY ON EACH FASTNER

LOAD = 5,240 LBS PER BOLT.

CHECK EDGE DIST

REF: ASME SEC III, DIV 1, APPENDIX XVII-2462

FOR 610-CR $S_u = 120,000$

$$f_p = \frac{5,240}{.75(.25)} = 27,947 \text{ PSI}$$

PER EQ 1 $.5 + 1.43\left(\frac{27,947}{120,000}\right) = .833$

$$MS = (3/.833) - 1 = +\underline{2.60}$$

PER EQ 2 $MS = \frac{3}{1.2} - 1 = +\underline{1.5}$

PER EQ 3 $\frac{27,947}{120,000} = .233$

$$MS = (1.5/.233) - 1 = +\underline{5.44}$$

PREPARED BY	DATE	CHECKED BY	DATE	REVISED BY	DATE
L. Dawn	5-6-81				

FIND THERMAL STRESS AT CENTER FASTNERS

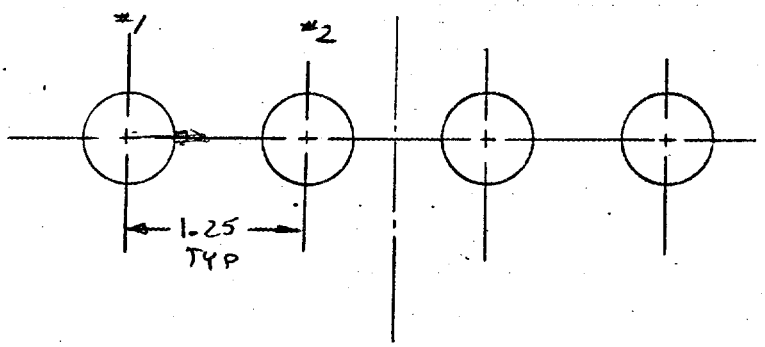

Thermal Expansion of 316 SST : -.00264 IN/IN @ 4°K

Thermal Expansion of Ti-6Al-4V : -.00155 IN/IN @ 4°K

FIND STRAIN RELATIVE TO ℄.

FOR HOLE #1 $\epsilon = 1.875\,(\overbrace{.00264 - .00155}^{.00109})$

$\epsilon = .002044$ IN

FOR HOLE #2 $\epsilon = .625\,(.00264 - .00155)$

$\epsilon = .000681$ IN

UNIT STRAIN = .00264 − .00155 = .00109 IN/IN

FORCE ACTING ON BOLT :

$F = \dfrac{\delta A E}{\ell}$ where $\ell = 1.00$

$A = Dt = .5(.3) = .15$

$E = 17 \times 10^6$

$\delta = .00109$

$F = 2{,}780$ LBS

K. Dam
3-10-81

ADDING THIS TO THE EXISTING SHEAR LOADS
(WORST CASE EL. 90-98)

AXIAL = 4,894
PLANE I = 24,614 + (2,780)4 = 35,734

Σ = 36,068 LBS

$\therefore$ BOLT SHEAR STRESS = $\frac{36,068}{4(.196)}$ = 46,000 PSI

MS = $\frac{47,533}{46,000} - 1$ = +.03 ULT

BEARING STRESS: REF: ASME SEC III XVII-2465

CENTER FASTNERS

$S_b = \frac{36,068}{4(.3).5}$ = 60,113 PSI

MS = $\frac{128,400}{60,113} - 1$ = 1.14

END FASTNER

$S_b = \frac{\overrightarrow{12,864@90^\circ} + 23,815@0^\circ}{.56(.75)}$ = 64,446 PSI BEARING STRESS

LOAD = 27,067 @ 28.4°

MS = $\frac{84,000}{64,446} - 1$ = +.30

EDGE DISTANCE: REF: ASME SEC III XVII-2462

DESIGN EDGE DIST = .900/cos θ = 1.023

$\therefore$ L/d = 1.023/.75 = 1.364

K. Dawn
3-10-81

ACCORDING TO PROCEDURE "a"

$$L/H \geq .5 + 1.43\left(\frac{64,446}{150,000}\right) = 1.114$$

$$MS = \frac{1.364}{1.114} - 1 = +.225$$

$$L/d \geq 1.2$$

$$MS = \frac{1.364}{1.2} - 1 = +.137$$

$$f_p/S_u \leq 1.5$$

$$\frac{64,446}{150,000} = .430$$

$$MS = \frac{1.5}{.43} - 1 = +2.49$$

K. Dam
3-12-81

EBT-P

DEWAR

COLD MASS SUPPORTS

FOR Ti $L/d = .50/.25 = 2.0$

$S_u = 160{,}000(1.69) = 270{,}400$

$f_p = \frac{5{,}240}{.15(.25)2} = 69{,}867$

PER EQ 1 $.5 + 1.43\left(\frac{169{,}867}{270{,}400}\right) = .869$

$MS = (2/.869) - 1 = +1.30$

PER EQ 2 $MS = \frac{2}{1.2} - 1 = +.67$

PER EQ 3 $\frac{169{,}867}{270{,}400} = .251$

$MS = \frac{1.5}{.251} - 1 = +4.98$

SHEAR ON BOLT

REF: ASME SEC III, DIV 1, APPENDIX XVII-2461.2

BOLT - Ti-6Al-4V LOCK BOLT $S_u = 270{,}400$ @ $-340°$

PREPARED BY	DATE	CHECKED BY	DATE	REVISED BY	DATE
K. Dawson	5-6-81				

A706-1 (REV. 9-65)

EBT-P
DEWAR

COLD MASS SUPPORTS

$$\therefore F_{vb} = \frac{.62(270,400)}{3} = 55,883 \text{ PSI}$$

SHEAR STRESS ON BOLT (Double shear)

$$f_{vb} = \frac{5,240}{2\pi(.125)^2} = 53,374 \text{ PSI}$$

$$MS = \frac{55,883}{53,374} - 1 = \underline{\underline{+.05}}$$

BEARING STRESS ON BOLT

REF: ASME SEC III, DIV 1, APPENDIX XVII-2461.5

$$F_b = \frac{.5(219,700)}{2(.25)} \leq 1.5(219,700)$$

$$F_b = 219,700 < 329,550. \text{ PSI}$$

$$f_b = \frac{5,240}{2(.25)(.15)} = 69,867 \text{ PSI}$$

$$MS = \frac{219,700}{69,867} - 1 = \underline{\underline{+2.14}}$$

PREPARED BY	DATE	CHECKED BY	DATE	REVISED BY	DATE
K. Dawson	5-6-81				

EBT-P
DEWAR-MATH MODEL

COLD MASS SUPPORTS

ALTERNATE TITANIUM CENTER BLOCK

(REF: COLD MASS SUPPORT ANALYSIS FOR MODEL DETAILS)

SECTION PROPERTIES:

NODE	AREA	I/C1	I/C2
9 & 10	.688	.315	.029
20	1.250	1.042	.052

ELEMENT LOADS: (FAULT OPERATION)

	END A		END B		
ELEMENT	M1	M2	M1	M2	AXIAL
3020	6.322E3	5.292E2	5.075E1	6.353E2	1.487E4
3021	6.315E3	4.453E2	4.928E1	6.046E2	8.275E3
4020	2.187E4	4.532E2	1.634E2	5.163E2	1.533E4
4021	2.187E4	3.413E2	1.634E2	4.872E2	8.821E3
5020	1.508E4	4.396E2	1.103E2	4.805E2	1.470E4
5021	1.509E4	3.065E2	1.132E2	4.550E2	8.449E3

ELEMENT STRESS

$$\text{STRESS} = \frac{P}{A} + \frac{M1}{I/C1} + \frac{M2}{I/C2}$$

PREPARED BY	DATE	CHECKED BY	DATE	REVISED BY	DATE
K. Dawson	5-9-81				

EBT-P
DEWAR-MATH MODEL

COLD MASS SUPPORTS

ELEMENT	END A (PSI)	END B (PSI)
3020	28,126	43,968
3021	21,232	33,299
4020	41,961	40,840
4021	34,605	30,357
5020	34,677	38,506
5021	27,130	28,532

[ALL STRESS IN LEGS OF SUPPORT ESSENTIALLY THE SAME AS 610-CR DESIGN.]

FACTORS OF SAFETY

(THIS PART TEMP RANGE IS 4K TO 77K, USING PROPERTIES AT 77K)

ASME SEC III, XVII-2214.4 REQUIRES

$$F_b = .6 S_y = .6(214,000) = 128,400 \text{ PSI}$$

MARGIN OF SAFETY

$$MS = \frac{128,400}{41,961} - 1 = +2.06 \text{ YIELD}$$

PREPARED BY	DATE	CHECKED BY	DATE	REVISED BY	DATE
K Dawn	5-4-81				

EBTP
COLD MASS SUPPORTS

DISPLACEMENTS

COLD MASS DISPLACEMENT IS BASED ON THE AVERAGE DISPLACEMENT OF 13 NODES AROUND THE INSIDE PERIMETER OF THE COLD MASS.

LOAD TYPE	X	Y	Z	RX	RY	RZ
GRAVITY	-1.02E-5	-2.25E-3	-2.69E-6	5.10E-7	3.21E-7	1.01E-5
CENTERING	2.05E-2	5.42E-5	-7.96E-5	2.31E-6	-6.01E-6	7.20E-6
OUT OF PLANE	7.01E-3	1.38E-4	9.12E-2	-1.19E-3	1.51E-3	-5.45E-6

SPRING RATE:

VERTICAL : $\frac{1725}{2.25E-3} = 7.67 \times 10^5$ LBS/IN

RADIAL : $\frac{17,900}{2.05E-2} = 8.73 \times 10^5$ LBS/IN

LATERAL : $\frac{73,000}{9.147E-2} = 7.98 \times 10^5$ LBS/IN

PREPARED BY	DATE	CHECKED BY	DATE	REVISED BY	DATE
R. Dawn	5-4-81				

GENERAL DYNAMICS
Convair Division

REPORT

PAGE

EBT-P
11-38080

SUPPORT ASSEMBLY - COLD MASS

FATIGUE - FRACTURE ANALYSIS

The fatigue and fracture analysis of the Ti-6AL-4V ELI cold mass support will be simplified by a series of worst case assumptions.

1. The maximum stress at any section under any load will be used — 40,000 psi

2. The minimum thickness section will be used — 0.310 inches

3. The minimum fillet radius will be used - 0.25 inches

4. All load cycles are assumed to produce maximum stress —

20	Fault
200	Thermal
2000	Charging
2220	
x 10	
22,200	Total cycles required

The outboard lugs are analyzed separately.

PREPARED BY	DATE	CHECKED BY	DATE	REVISED BY	DATE
McCutchen	1-19-82				

EBT-P

11-38080

SUPPORT ASSEMBLY -COLD MASS

Using the 40 ksi flaw growth curve;

62,500
22,200
40,300

The maximum permissable initial flaw size is 0.090 inches.

The drawing requires inspection to MIL-I-6866B, Type I, method A with a maximum acceptable indication of 0.080 inches.

Therefore, the truss-like parts of the support meet all fracture and fatigue requirements.

PREPARED BY	DATE	CHECKED BY	DATE	REVISED BY	DATE

K•E 10 X 10 TO ½ INCH 7 X 10 INCHES KEUFFEL & ESSER CO MADE IN U.S.A.

46 1320

Y.S.
1-5-82

EBT-P SUPPORT ASSEMBLY ANALYSIS

ANALYSIS PARAMETERS

COLLIPRIEST EQUATION:

$C = 4.26 \times 10^{-17}$ } 6AL-4V TI
$n = 8.36$ } (ELI), R.T.; DESSICATED AIR

$K_{IC} = 55$ KSI $\sqrt{IN}$

$K_{TH} = 7$ KSI $\sqrt{IN}$

$F_{TY} = 220$ KSI

1 LIFETIME CONSISTS OF 22,200 LOAD CYCLES (σ_{MAX} = 40 KSI)

$a/2c \simeq 0.5$

0.25 Fillet Radius

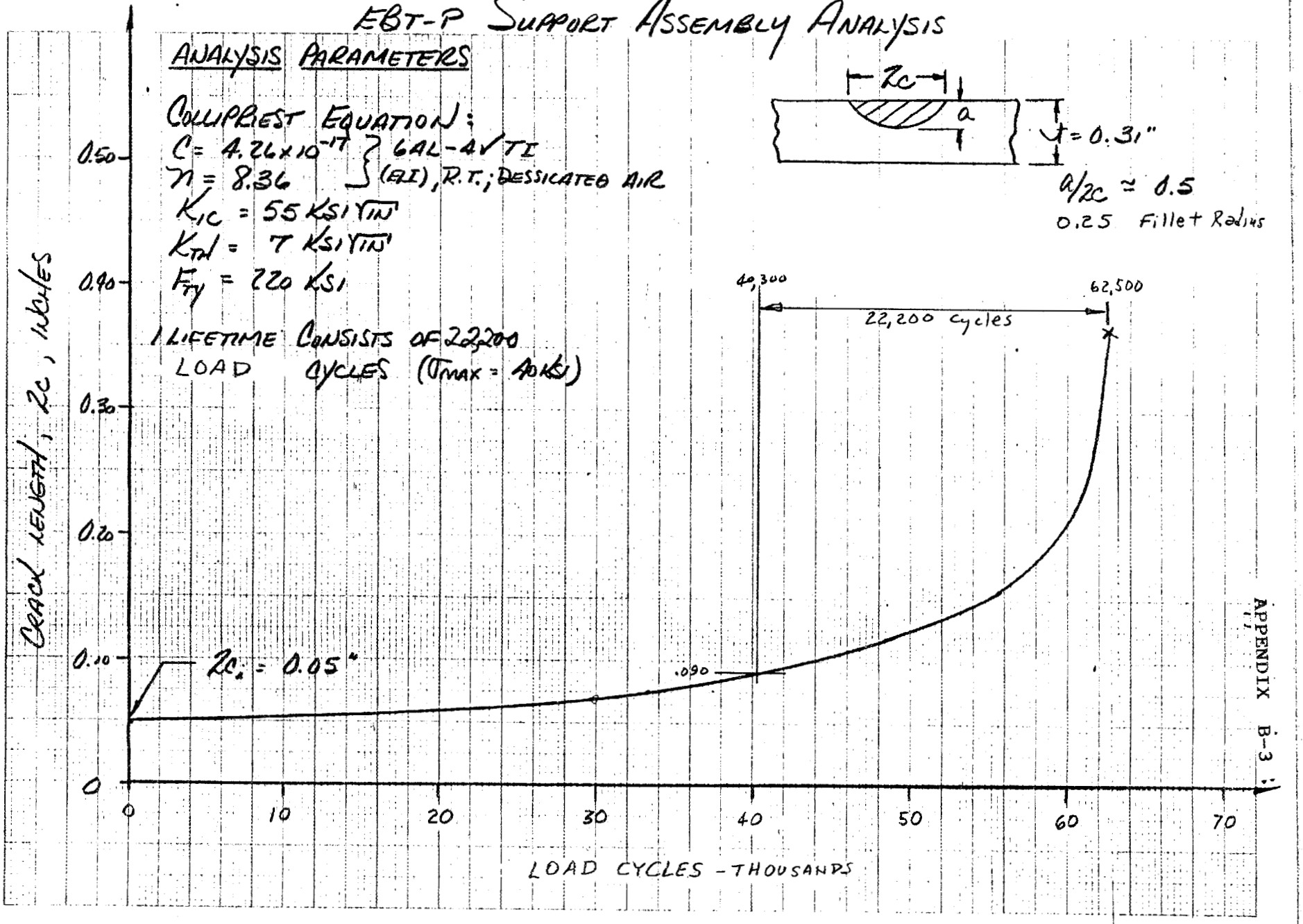

— CRACK GROWTH RATE DATA ~ 6AL-4V TI (ELI)

SOURCE - MCIC-HB-01 FIGURE NTA122

- DESICCATED AIR, R=0, 1" PLATE, ROOM TEMP

$@\Delta K = 20 \text{ ksi}\sqrt{in}$, $\frac{da}{dN} = 3.2 \times 10^{-2}$ in/cycle

$@\Delta K = 30 \text{ ksi}\sqrt{in}$, $da/dN = 9.5 \times 10^{-5}$ in/cycle

$$\frac{da}{dN} = C(\Delta K)^n$$

$$n = \frac{\ln\left(\frac{9.5 \times 10^{-5}}{3.2 \times 10^{-2}}\right)}{\ln\left(30/20\right)} = 8.36$$

$$C = \frac{9.5 \times 10^{-5}}{(30)^{8.36}} = 4.26 \times 10^{-17}$$

$$\frac{da}{dN} = 4.26 \times 10^{-17} (\Delta K)^{8.36}$$

$a_i = 25$ MILS

$\sigma_{max} = 40$ KSI

$W = 310$ MILS

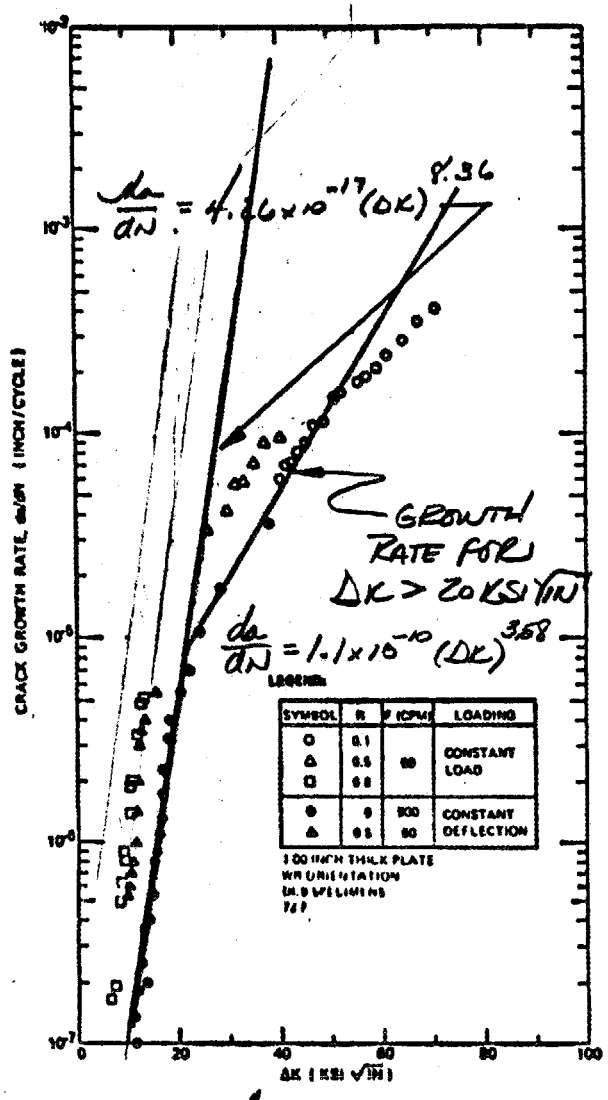

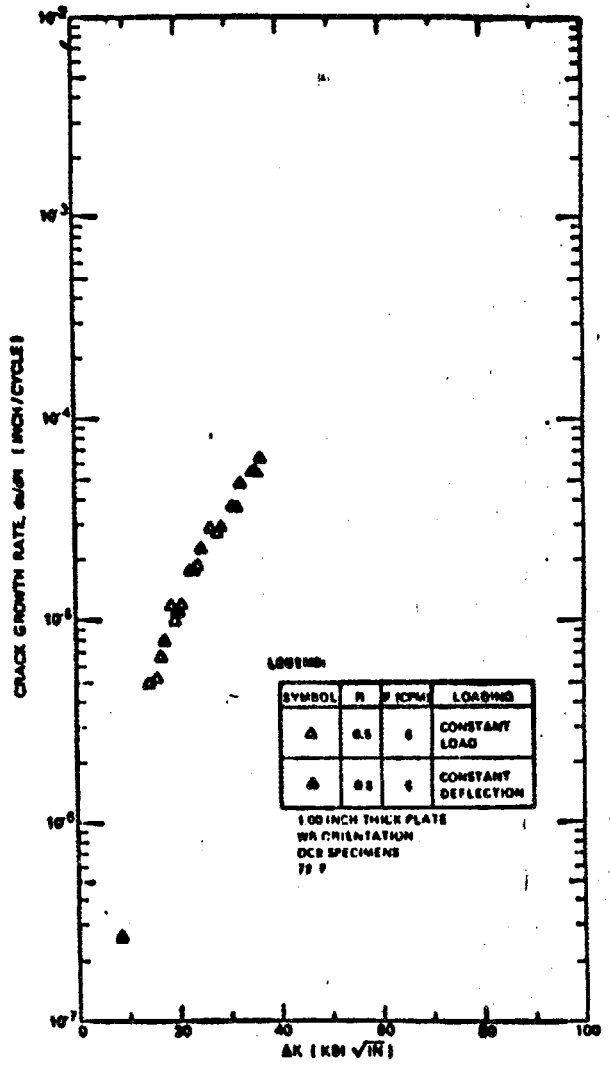

FIGURE ~~NTA122~~. FATIGUE CRACK GROWTH RATES FOR 6Al–4V STANDARD ELI BETA ANNEALED TITANIUM ALLOY IN DESICCATED AIR (88140)

GENERAL DYNAMICS
Convair Division

REPORT

PAGE 12

EBT

D11-38080

SUPPORT - COLD MASS

Ti-6Al-4V ELI
Room Temperature

Lug 4023 Critical

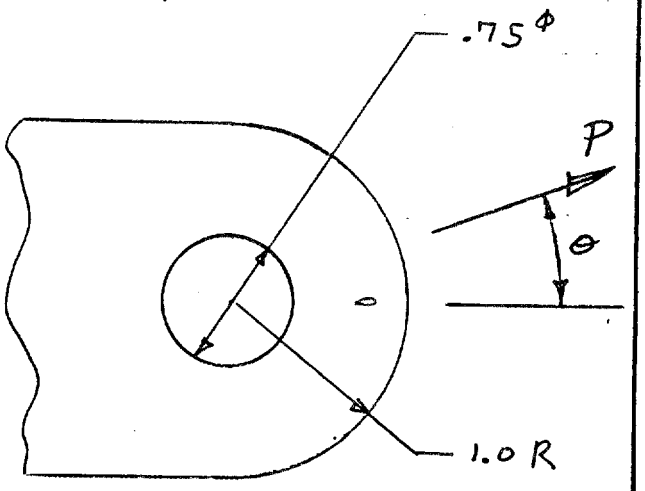

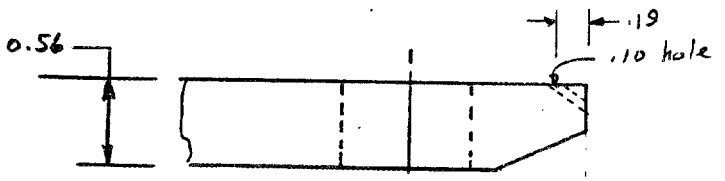

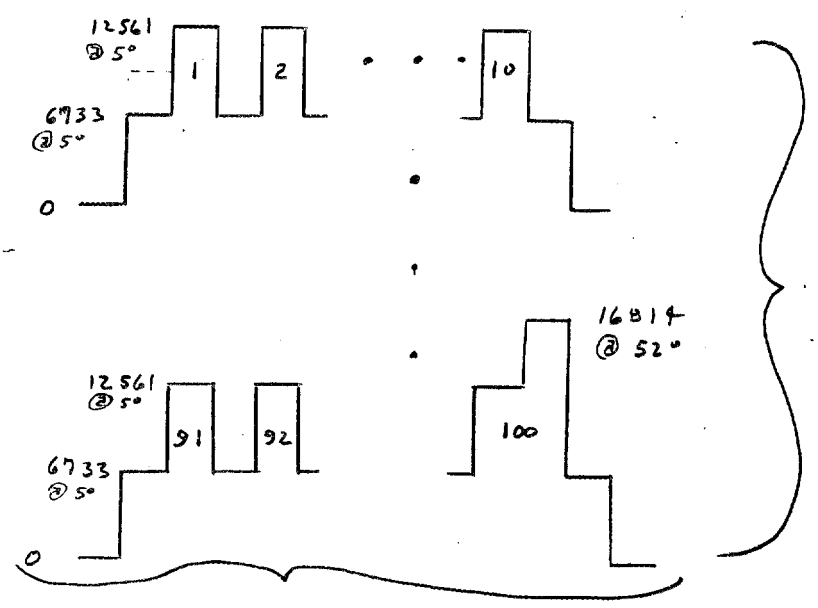

Twice Per Lifetime

1 Fault, 10 Thermal, 100 Normal

PREPARED BY	DATE	CHECKED BY	DATE	REVISED BY	DATE
McCutchen	1-11-82				

GENERAL DYNAMICS
Convair Division

EBT
D11-38080

COLD MASS SUPPORTS

OUTER END LOADS FOR LUG

L.C.	BAR	V1	V2	P (lbs)	θ (°)
4 THERMAL	3022	-303	-6938	6945	2.5
	3023	+304	+6942	6949	2.5
	4022	+586	-6702	6728	5.0
	4023	-587	+6707	6733	5.0
	5022	-277	-6335	6341	2.5
	5023	+276	+6327	6333	2.5
5 NORMAL	3022	-394	-9038	9047	2.5
	3023	+210	+4807	4812	2.5
	4022	89	-1013	1016	5.0
	4023	-1095	+12513	12561	5.0
	5022	-445	-10155	10165	2.5
	5023	136	+3102	3105	2.5
6 FAULT	3022	-12118	-7756	14388	57.4
	3023	-11510	+6093	13023	62.1
	4022	-12031	-3248	12462	74.9
	4023	-13223	+10386	16814	51.9
	5022	-12180	-9265	15303	52.7
	5023	-11605	+3880	12236	71.5
computer - run		KRD	30XS	5-2-81	

PREPARED BY	DATE	CHECKED BY	DATE	REVISED BY	DATE
MCCUTCHEN	1-11-82				

J.S.
1-12-82
①

ERT-P F/M ANALYSIS
SUPPORT ASSEMBLY LUG ANALYSIS

D11-38080

THREE LUGS TO BE ANALYZED -
STRUT ID
- 4023
- 4020
- 5020

FOR ALL ANALYSES 6AL-4V TI (ELI) CRACK GROWTH RATE DATA (DESSICATED AIR) WILL BE USED. THE GROWTH RATE WILL BE ASSUMED TO FOLLOW THE INITIAL, THRESHOLD EFFECTED PORTION OF THE CURVE (CONSERVATIVE). THE FOLLOWING MATERIAL PROPERTIES WILL BE ASSUMED -

CRACK GROWTH RATE: $da/dN = 4.26 \times 10^{-17} (\Delta K)^{8.36}$
$K_{IC} = 55 \text{ KSI}\sqrt{\text{IN}}$
$K_{TH} = 7 \text{ KSI}\sqrt{\text{IN}}$

INITIAL FLAW ASSUMPTIONS -
2 CORNER CRACKS EMANATING FROM THE LUG BORE - $a_i = c_i = 0.080''$

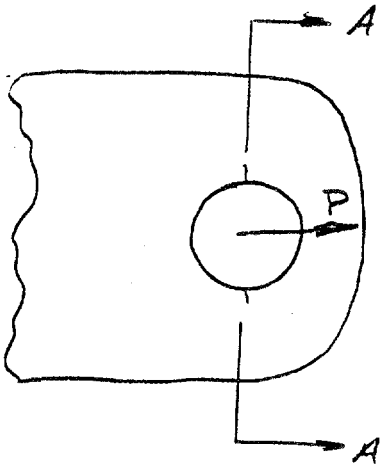

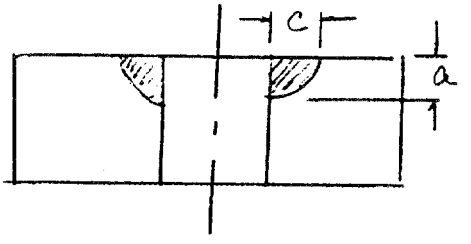

(2)

STRESS INTENSITY FACTOR SOLUTION FOR LUGS REQUIRES STRESS IN TERMS OF σ_g —

$$\sigma_g = P/Wt$$

— STRUT 4023 $W = 2''$, $t = 0.56''$, $D = 1.75''$

LOAD CONDITION	P_{MAX} (LBS)	σ_{MAX} (KSI)
THERMAL	6733	6.0
NORMAL	12561	11.22
FAULT	16814	9.24

STRESS SPECTRUM

σ_{MX}	σ_{MN}	N
6	0	10
11.22	6	100
9.24	3.7	1

1/2 LIFETIME

(3)

— STRUT 4020 $W_{EFF} = 1"$, $t = 0.15"$, $D = .375"$

LOAD CONDITION	P_{MAX} (LBS)	σ_{MX} (KSI)
THERMAL	697	4.7
NORMAL	2053	13.7
FAULT	4443	29.6

STRESS SPECTRUM

σ_{MX}	σ_{MN}	N
4.7	0	10
13.7	4.7	100
29.6	4.7	1

½ LIFETIME

— STRUT 5020 $W_{EFF} = 1"$, $t = 0.15"$, $D = .375"$

LOAD CONDITION	P_{MAX} (LBS)	σ_{MX} (KSI)
THERMAL	666	4.4
NORMAL	2882	19.2
FAULT	3764	25.1

STRESS SPECTRUM

σ_{MX}	σ_{MN}	N
4.4	0	10
19.2	4.4	100
25.1	4.4	1

½ LIFETIME

RESULTS —

CRACK GROWTH AFTER 10 LIFETIMES

STRUT ID	Δ GROWTH (μ-IN)	FINAL CRACK SIZE (IN)
4023	1	0.080001
4020	548	0.080548
5020	50	0.080050

— THUS SUPPORT ASSEMBLY LUGS ARE NOT FRACTURE CRITICAL

APPENDIX B-3.4

STRESS ANALYSIS

VACUUM VESSEL

REPORT

GENERAL DYNAMICS
Convair Division

PAGE

ASME CODE ANALYSIS

VACUUM VESSEL

DETERMINE WALL THICKNESS AND INSPECTION REQUIREMENTS FOR CENTER BORE AND SIDE PLATES.

DESIGN APPROACH:

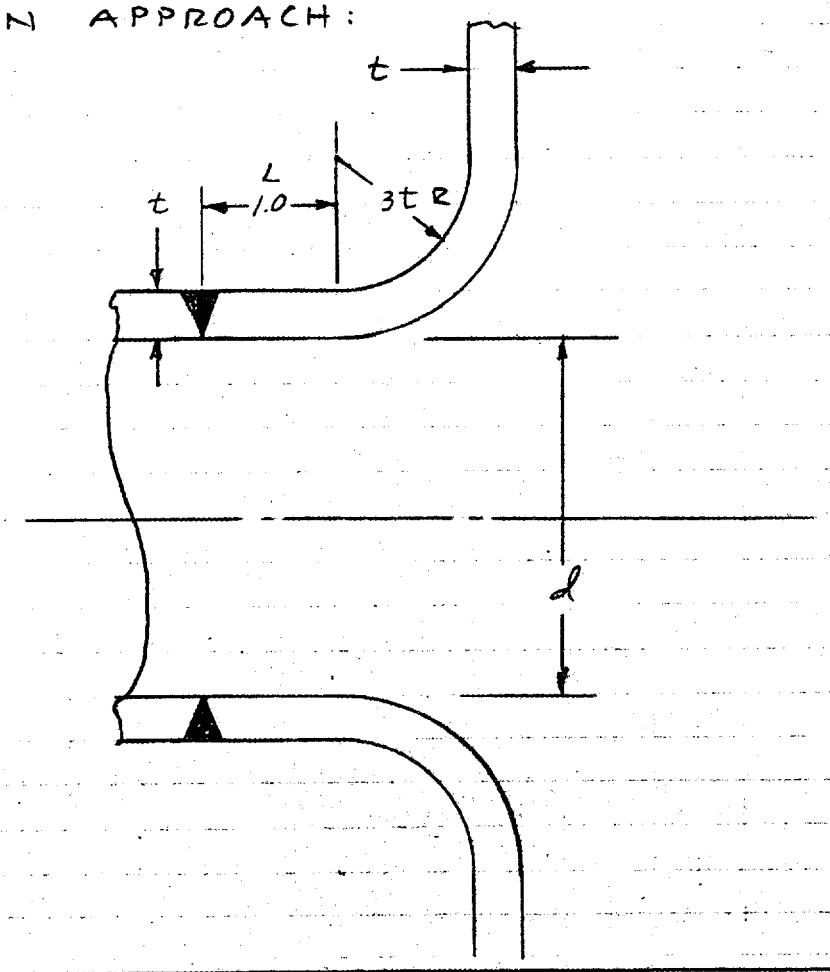

PREPARED BY	DATE	CHECKED BY	DATE	REVISED BY	DATE
R. Dawson	1-30-81				

A706-1 (REV. 9-65)

GENERAL DYNAMICS
Convair Division

ACCORDING TO UG-34

THE MINIMUM REQ'D THICKNES t IS:

$t = d\sqrt{CP/SE}$ WHERE $d = 16.65$
$P = 14.7(1.6)$
$S = 25{,}000$
$t_s = t_h = .25$

$C = .1$ IF $L \geq$ EQ. 6

EQ #6 $l = (1.1 - .8\, t_s^2/t_h^2)\sqrt{d t_h}$

E: (ACCORDING TO TABLE UW-12)

USING SINGLE-WELDED BUTT JOINT WITHOUT BACKING STRIP, DEGREE OF EXAMINATION "C" (NON-RADIOGRAPHIC INSP.)

$\underline{E = .60}$

SOLVING EQ #6 $l = .612$ ∴ SINCE $L = 1.0$ THEN $\underline{C = .1}$

THEN $t = 16.65\sqrt{.1(14.7)(1.6)/25{,}000(.6)}$

$t = .208$

PREPARED BY	DATE	CHECKED BY	DATE	REVISED BY	DATE
R. Dauer	1-30-81				

A706-1 (REV. 9-65)

GENERAL DYNAMICS
Convair Division

MARGIN OF SAFETY

$$MS = \frac{.250}{.208} - 1 = \underline{+.20}$$

THIS ALLOWS FOR NON-RADIOGRAPHIC INSPECTION.

ALIGNMENT TOLLERANCES
TABLE AF-142.1 & PARA AF-142 (p 206)

MAX ALLOWABLE OFFSET = 1/4 t = .063

PREPARED BY	DATE	CHECKED BY	DATE	REVISED BY	DATE
K. Dawson	1-30-81				

A706-1 (REV. 9-65)

GENERAL DYNAMICS
Convair Division

AMSE CODE ANALYSIS

VACUUM VESSEL

THIS ANALYSIS USES AMSE SECTION VIII, DIV. 2 FOR METHODS OF ANALYSIS.

1. BORE TUBE:
CONSIDER AS AN INTERNAL PRESSURE VESSEL.

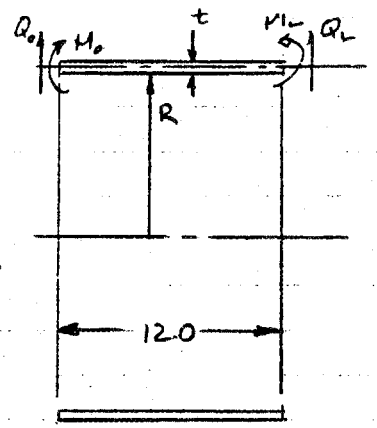

ARTICLE 4-2

R = 8.25

PRIMARY MEMBRANE STRESS

$$S = \frac{pR}{t} + \frac{p}{2}$$

where $p = 14.7(1.6) = 23.52$ PSI
$S = 25{,}000$

SOLVE FOR $t = \frac{pR}{S - p/2} = \frac{23.52(8.25)}{25{,}000 - 23.52/2}$

$t = .008$

PREPARED BY	DATE	CHECKED BY	DATE	REVISED BY	DATE
R. Dawson	1-19-81				

A706-1 (REV. 9-65)

PRIMARY PLUS SECONDARY STRESS:

$$S = \frac{2p\,Y^2}{Y^2-1} \qquad \text{WHERE } Y = R_o/R_i$$

$$S = \frac{2p\,(R_o/R_i)^2}{\left(\frac{R_o}{R_i}\right)^2 - 1} \qquad \text{let } R_o = 8.25 + .010$$

$$S = 19{,}439 \text{ PSI}$$

IF THIS SECTION WERE LOADED AS AN EXTERNAL PRESSURE VESSEL (AD-300.1) $P = 4(14.7) = 58.8$

$D_o/t = 200$ ASSUMING $t = .085$

$L/D_o = 12/16.5 = .727$

FROM FIG AGO-28.0 $A = .00067$

FROM FIG AHA-28.3 (304L) $B = 7{,}800$

$$P_a = \frac{4B}{3(D_o/t)} \cdot 52.0$$

let $t = .090$ THEN $D_o/t = 185.33$

PREPARED BY	DATE	CHECKED BY	DATE	REVISED BY	DATE
R. Tawson	1-19-81				

THEN $A = .00077$

$B = 8300$

$$P_a = \frac{4B}{3(D_o/t)} = 59.713$$

$$MS = \frac{59.713}{58.8} - 1 = \underline{\underline{+.016}}$$ OK $t = .030$

LET $t = .25$, THEN $D_o/t = 66.72$

THEN $A = .0037$

& $B = 11,600$

$$P_a = \frac{4(11,600)}{3(66.72)} = 232 \text{ psi}$$

$$MS = \frac{232}{58.8} - 1 = +2.94$$ BUCKLING

PREPARED BY	DATE	CHECKED BY	DATE	REVISED BY	DATE
R. Dawson	1-19-81				

EBTP

VACUUM VESSEL

OUTLET ASSEMBLY

ANALYSIS OF DRAWING D11-38070

LOADS IMPOSED ON STRUCTURE:

1. ± 14.7 PSI

MATERIAL ALLOWABLES:

1. FASTNERS: MS35308-362 MIN. SPECIFIED TENSILE STRENGTH = 7,020 LBS
   ASME ALLOWABLES PER TABLE ABM-1
   75 KSI MIN TENSILE
   30 KSI MIN YIELD

2. FLANGE: TYPE 304L - ASME ALLOWABLES PER TABLE AHA-1
   70 KSI MIN TENSILE
   25 KSI MIN YIELD

3. ITEM 4 (CROSS): SCH. 10 - MFG. IN ACCORDANCE WITH ASME SPECIFICATIONS. PRESSURE RATING 180 PSI.

PREPARED BY	DATE	CHECKED BY	DATE	REVISED BY	DATE
K. Davis	2-18-81				

EBTP

VACUUM VESSEL

OUTLET ASSY

FASTNER ANALYSIS

REF: ASME SEC VIII, DIV. 2 APPENDIX 3

BOLT LOAD $W_{m1} = .785 G^2 P + (2b)(3.14 G m P)$

where G = DIA. OF GASKET LOAD REACTION
P = DESIGN PRESSURE
b = EFF. GASKET SEAT WIDTH
m = GASKET FACTOR

FROM DWG: $G = 2(1.675) + .239 = 3.589$
$b = .239/8 = .030$ (TABLE 3-320.2)

FROM CODE: $m = 0$ (TABLE 3-320.1)

$\therefore W_{m1} = .785(3.589)^2(14.7)$

$W_{m1} = 148.6$ LBS @ 14.7 PSI & 303.3 LBS @ 30 PSI

ALSO: $W_{m2} = 3.14 b G y$ where y = GASKET UNIT SEATING LOAD = 0 (TABLE 3-320.1)

$= 3.14(.030)(3.589)(0)$

$= 0.$

PREPARED BY	DATE	CHECKED BY	DATE	REVISED BY	DATE
K. Dawson	2-18-81				

EBTP

VACUUM VESSEL

OUTLET ASSY.

REQ'D BOLT AREA:

$A_{m_1} = W_{m1} / S_b$ where S_b = allowable bolt stress

$= \frac{148.6}{30,000} = .005$

AVALIABLE AREA OF BOLTS

BOLT 3/8-24 - BASIC SHANK AREA = .11045 IN^2 (MIL-HDBK-5)

NO. FASTNERS = 6

AREA = 6(.11045) = .663

$MS = \frac{.663}{.005(1.6)} =$ + LARGE (YIELD)

FLANGE ANALYSIS REF: ASME SEC. VIII, DIV 2 APPENDIX 3

FLANGE DESIGN BOLT LOAD $W = W_{m_1} = 148.6$

PREPARED BY	DATE	CHECKED BY	DATE	REVISED BY	DATE
K. Daus	2-18-71				

MOMENTS

$$M_o = \Sigma M = M_D + M_T + M_G$$

$$= H_D h_D + H_T h_T + H_G h_G$$

$$H_D h_D = .785 B^2 P \left(\frac{C-B}{2}\right) = .785(2.63)^2(14.7)\left[\frac{4.7-2.63}{2}\right]$$

$$H_D h_D = 82.611$$

$$H_T h_T = .785 P (G^2 - B^2)\left[\frac{h_D + h_G}{2}\right]$$

$$= .785(14.7)\left[3.589^2 - 2.63^2\right]\left[\frac{(4.7-2.63)/2 + (4.7-3.589)/2}{2}\right]$$

$$H_T h_T = 54.731$$

$$H_G h_G = [W - H]\left[\frac{C-G}{2}\right] = \left[148.6 - .785(3.589)^2(14.7)\right]\left[\frac{4.7-3.589}{2}\right]$$

$$H_G h_G = 0.$$

$$M_o = 82.611 + 54.731 + 0.$$

M_o = 137.3 IN-LBS @ 14.7 PSI M_o = 280.2 IN-LBS @ 30 PSI

PREPARED BY	DATE	CHECKED BY	DATE	REVISED BY	DATE

FLANGE STRESS (REF FIG 3-310.1 SKT 6-1)

$$S_T = \frac{Y M_o}{t^2 B}$$

EVALUATE $A/B = 5.5/2.63 = 2.09$

FROM FIG 3-340.1 $Y = 2.9$

$t = .40$

$$S_T = \frac{2.9(137.3)}{(.4)^2(2.63)} = 946 \text{ PSI @ } 14.7 \text{ PSI}$$

$$= 1{,}931 \text{ PSI @ } 30 \text{ PSI}$$

$$MS = \frac{30{,}000}{946} - 1 = +\underline{30.7} \text{ @ } 14.7 \text{ PSI}$$

$$MS = \frac{30{,}000}{1931} - 1 = +\underline{14.5} \text{ @ } 30 \text{ PSI}$$

PREPARED BY	DATE	CHECKED BY	DATE	REVISED BY	DATE

EBTP

VACUUM VESSEL

OUTLET ASSY

BLIND FLANGE ANALYSIS

REF: ASME SEC VIII, DIV. 2 ARTICLE D-7

AD-702 (b) $T = d\sqrt{\frac{CP}{S} + \frac{1.9\,W h_g}{S d^3}}$

FROM FIG AD-701.2 (c) $C = .3$

$d = 3.589$
$W = 148.6$ @ 14.7 PSI & 303.3 @ 30 PSI
$h_g = .556$
$S = 25{,}000$

$$T = 3.589\sqrt{\frac{.3(14.7)}{25{,}000/1.6} + \frac{1.9(148.6)(.556)}{25{,}000/1.6\,(3.589)^3}}$$

$T = .080$

SOLVING THIS EQ. FOR STRESS

$$S = \frac{.3(\overset{30}{14.7})(3.589)^2 + \frac{1.9(\overset{303.3}{148.6})(.556)}{3.589}}{.25^2} = \frac{1{,}609}{14.7} = \frac{3{,}283}{30}$$

$$MS = \frac{25{,}000}{1{,}609\,(1.6)} - 1 = +8.7 \;\&\; +3.76$$

PREPARED BY	DATE	CHECKED BY	DATE	REVISED BY	DATE
K. Davis	2-19-81				

APPENDIX B-3.5

STRESS ANALYSIS

MISCELLANEOUS

GENERAL DYNAMICS
Convair Division

REPORT

PAGE

EBT
OUT OF PLANE STRUTS

COLUMN CHECK
Ref: ASME SEC III APPENDIX XVII, PAR XVII-2213
D11-38090 gives $\ell = 20.0 + 2 \times 2.8 = 25.6''$

2.00 hex stock 304 L ASTM A276

$F_{ty} = 25$ ksi $P = 22660$ lbs (finite element model)

Ref Roark 5th ed Table 1 Case 9

$a = 2(\tan\alpha)(\rho_2) = 2 \times \tan 30° \times 1.0 = 1.1547$

$\rho_1 = \frac{a}{2 \sin\alpha} = \frac{1.1547}{2 \sin 30°} = 1.1547$

$A = \frac{a^2 n}{4 \tan\alpha} = \frac{1.1547 \times 6}{4 \tan 30} = 3.00 \text{ in}^2$

$r = \left(\frac{6\rho_1^2 - a^2}{24}\right)^{\frac{1}{2}} = \left(\frac{6 \times \overline{1.1547}^2 - \overline{1.1547}^2}{24}\right)^{1/2} = 0.5270$

$I_z = \frac{A\,(12\rho_2^2 + a^2)}{48} = \frac{3 \times (12 \times \overline{1.0}^2 + \overline{1.1547}^2)}{48} = 0.8733$

$k\ell/r = 1.0 \times 25.6 / .5270 = 48.573$

$C_c = \left(\frac{2\pi^2 E}{S_y}\right)^{\frac{1}{2}} = \left(\frac{2\pi^2 \times 28 \times 10^6}{25000}\right)^{\frac{1}{2}} = 148.69$

$F_a = \frac{[1 - (48.573)^2 / 2 \times \overline{148.69}^2]\, 25000}{5/3 + [3 \times 48.573/8/148.69] - [\overline{48.573}^3 / 8 / \overline{148.69}^3]} = 13{,}260$ psi

$f = 22660 / 3.0 = 7553$

$MS = \frac{13260}{7553} - 1 = \underline{\underline{+0.76}}$

Note: this is more critical than $F_{ty}/1.5$

PREPARED BY	DATE	CHECKED BY	DATE	REVISED BY	DATE
McCutchen	9-4-81				

A706-1 (REV. 9-65)

EBT-P
Out of Plane Struts

Rod End Threads

P = 28292 lbs - 1.05 x simple Beam Value

Thread Engagement Length = L

$$L = 4.125 - 2.8 - 2 \times \frac{1}{12} - \frac{1}{8} = 1.033 \text{ inches}$$

The bolt threads are much stronger than the strut threads and the shear plane will not be at the half height point. See next page for solution of fraction of strut thread effective. Round down to 80%.

$$\text{Shear Area} = \pi \times \underset{\text{pitch dia}}{1.1959} \times 1.033 \times 0.8 = 3.105 \text{ in}^2$$

$$f_s = 28292 / 3.105 = 9112 \text{ psi}$$

$$F_{sy} \approx 0.6\, F_{Ty} = 0.6 \times 25000 = 15{,}000 \text{ psi}$$

$$MS = \frac{15000}{1.5 \times 9112} - 1 = \underline{\underline{+0.10}}$$

PREPARED BY	DATE	CHECKED BY	DATE	REVISED BY	DATE
McCutchen	9-4-81				

GENERAL DYNAMICS
Convair Division

REPORT

PAGE

EBT
Out of Plane Struts

Effective Thread Shear Area

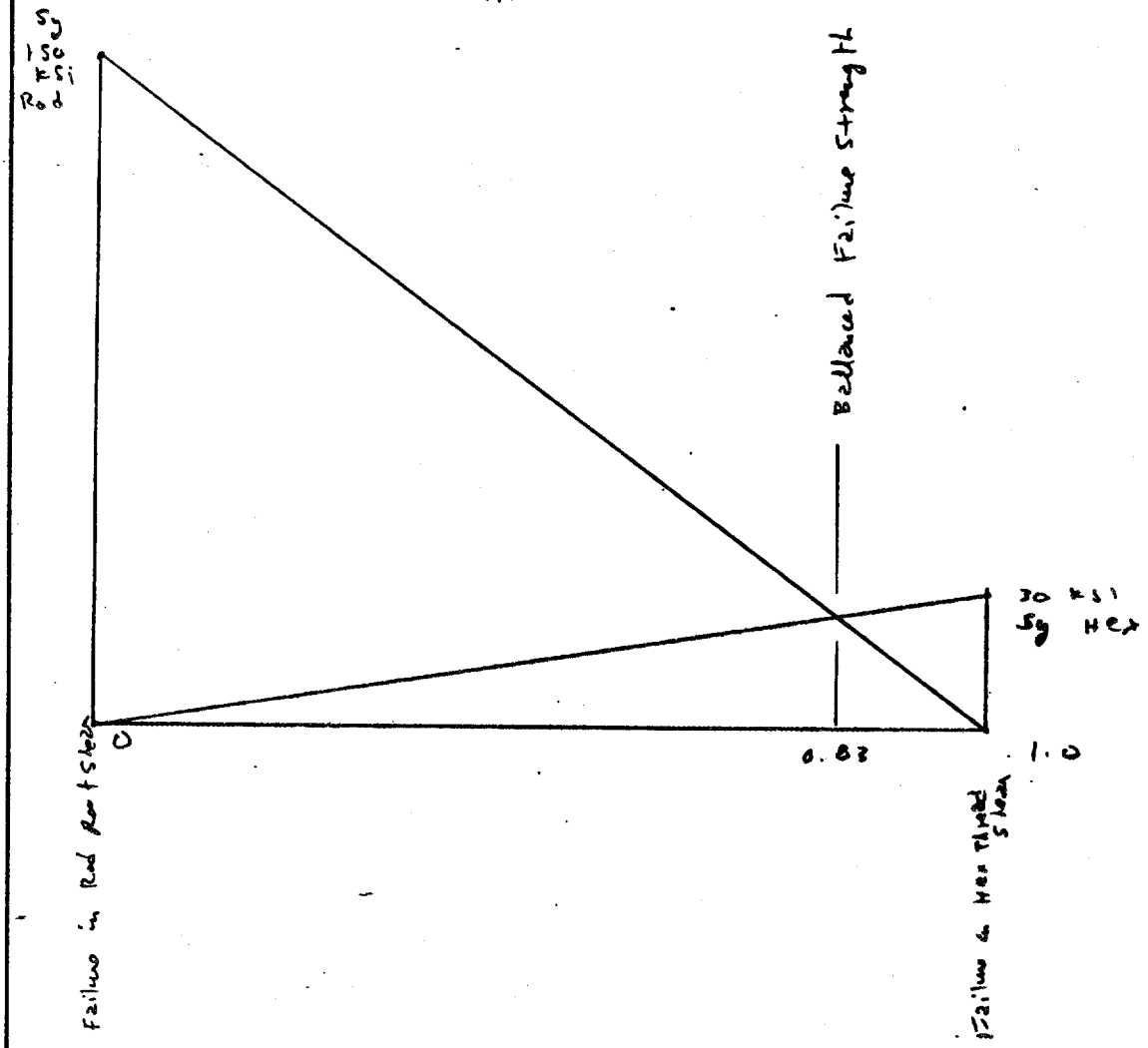

PREPARED BY	DATE	CHECKED BY	DATE	REVISED BY	DATE
McCutchen	9-4-81				

A706-1 (REV. 9-65)

AXIAL STIFFNESS ANALYSIS

INFORMATION PROVIDED BY ORNL INDICATED THAT THE REQUIRED AXIAL STIFFNESS FOR STABILITY OF A TOROIDAL ARRAY IS:

$$k_s > 4\,k_m$$

FOR EBT-P, $k_s > 26{,}700$ lbs/in

FROM NASTRAN MODEL, AXIAL DISPLACEMENT DUE TO AN OUT-OF-PLANE FORCE OF 73,000 POUNDS IS .091482 (MEAN VALUE OF 12 PTS)

THEN:

$$k_s = \frac{73{,}000}{.091482} = 797{,}970 \text{ LBS/IN}$$

$$MS = \frac{797{,}970}{26{,}700} - 1 = \underline{\underline{+28.9}}$$

CHANGING THE OUT-OF-PLANE STRUTS TO SCH 160:

$$k_s = \frac{73{,}000}{.091482 - .002} = 815{,}805 \text{ LBS/IN}$$

$$MS = \frac{815{,}805}{26{,}700} - 1 = \underline{\underline{+29.6}}$$

K. Dawn
3-24-81

AXIAL STIFFNESS REQUIRED

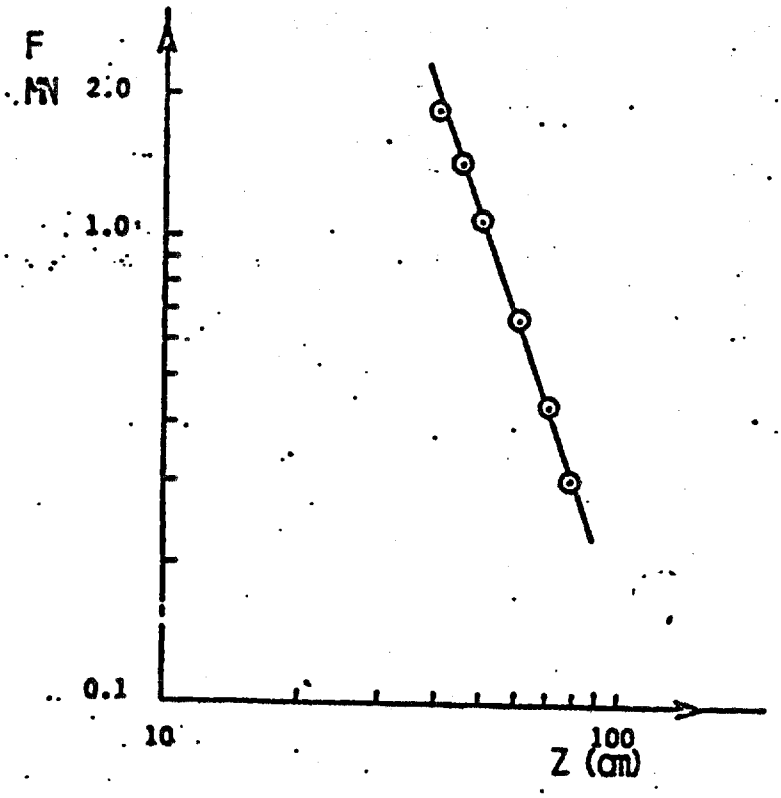

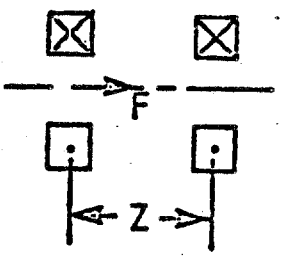

$.70 < Z < .80$ M $\quad F\ (MN) = .1418\ Z^{-3.076}$

$$\left|\frac{dF(.785)}{dZ}\right| = 1.17\ MN/m = k_m$$

FOR STABILITY IN TOROIDAL ARRAY

$$k_s > 4 \cdot k_m$$

$$k_s > 4.68\ MN/m\ (26{,}700\ lb/in.)$$

WHERE:

k_s = *MECHANICAL STIFFNESS IN AXIAL DIRECTION*

APPENDIX B-3.6

STRESS ANALYSIS

MATERIAL PROPERTIES

MATERIAL/PROPERTY	R.T.	4K	USED ON
316L CRES (Annealed)			
Tensile Strength (ksi)	70.	175.	
Tensile Yield (ksi)	25.	60.	
Shear Strength (ksi)	38.	95.	Helium Vessel
Elastic Modulus (msi)	28.	29.2	
Thermal Expansion (in./in.)	0.	-2.95×10^{-3}	
101 OFHC Copper (Annealed)			
Tensile Strength (ksi)	23.	52.	
Tensile Yield (ksi)	8.	10.	Thermal Shields
Shear Strength (ksi)	20.	30.	Tubing
Elastic Modulus (msi)	16.	17.	
Thermal Expansion (in./in.)	0.	-3.25×10^{-3}	
304L CRES (Annealed)			
Tensile Strength (ksi)	70.	170.	
Tensile Yield (ksi)	25.	65.	
Shear Strength (ksi)	40.	100.	Vacuum Vessel
Elastic Modulus (msi)	28.	29.	
Thermal Expansion (in./in.)	0.	-3.0×10^{-3}	
Ti-6Al-4V (Annealed) ELI			
Tensile Strength (ksi)	130.	229.	
Tensile Yield (ksi)	120.	222.	
Shear Strength (ksi)	76.	X	Helium Vessel
Elastic Modulus (msi)	16.	19.	Supports
Thermal Expansion (in./in.)	0.	-1.75×10^{-3}	

Metallic Materials Mechanical Properties

Material/Property	R.T.	77K	4K
G10CR Epoxy/Fiberglass			
Tensile Strength (ksi)			
Warp	60.2	119.	125.
Fill	43.4		
Tensile Strength Modulus (msi)			
Warp	4.1	5.0	5.2
Fill	3.9	4.8	
Compressive Strength (ksi)			
Flatwise	60.1	100.	109.
Compressive Modulus (msi)			
Flatwise	2.03	3.16	
Total Thermal Contraction			
Warp		-0.00235	
Fill		-0.00269	
Normal		-0.00730	
Style 6781 S-2 Glass, G10CR Epoxy			
Tensile Strength (ksi)			
0°	60.0		
Tensile Strength Modulus (ksi)			
0°	5.5		
Total Thermal Contraction			
0°			0.0025

Non-Metallic Material Mechanical Properties

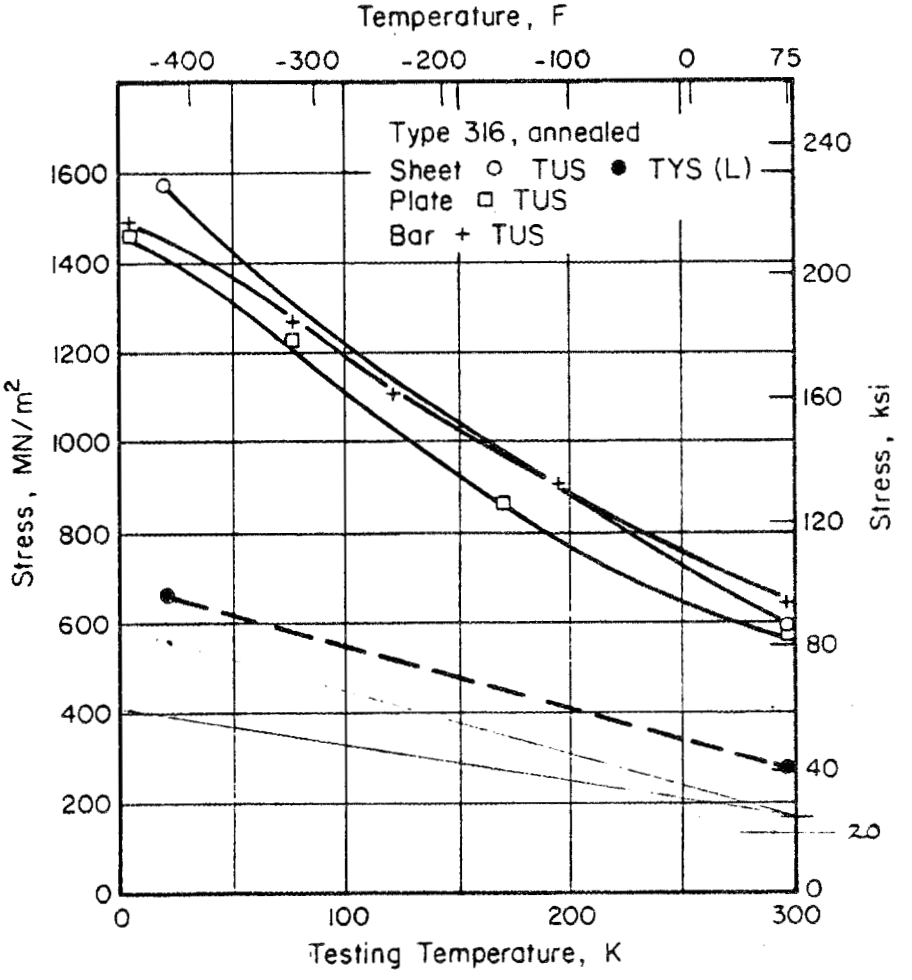

FIGURE 8.1.5-ME1. EFFECT OF TEMPERATURE ON THE STRENGTH OF TYPE 316 STAINLESS STEEL

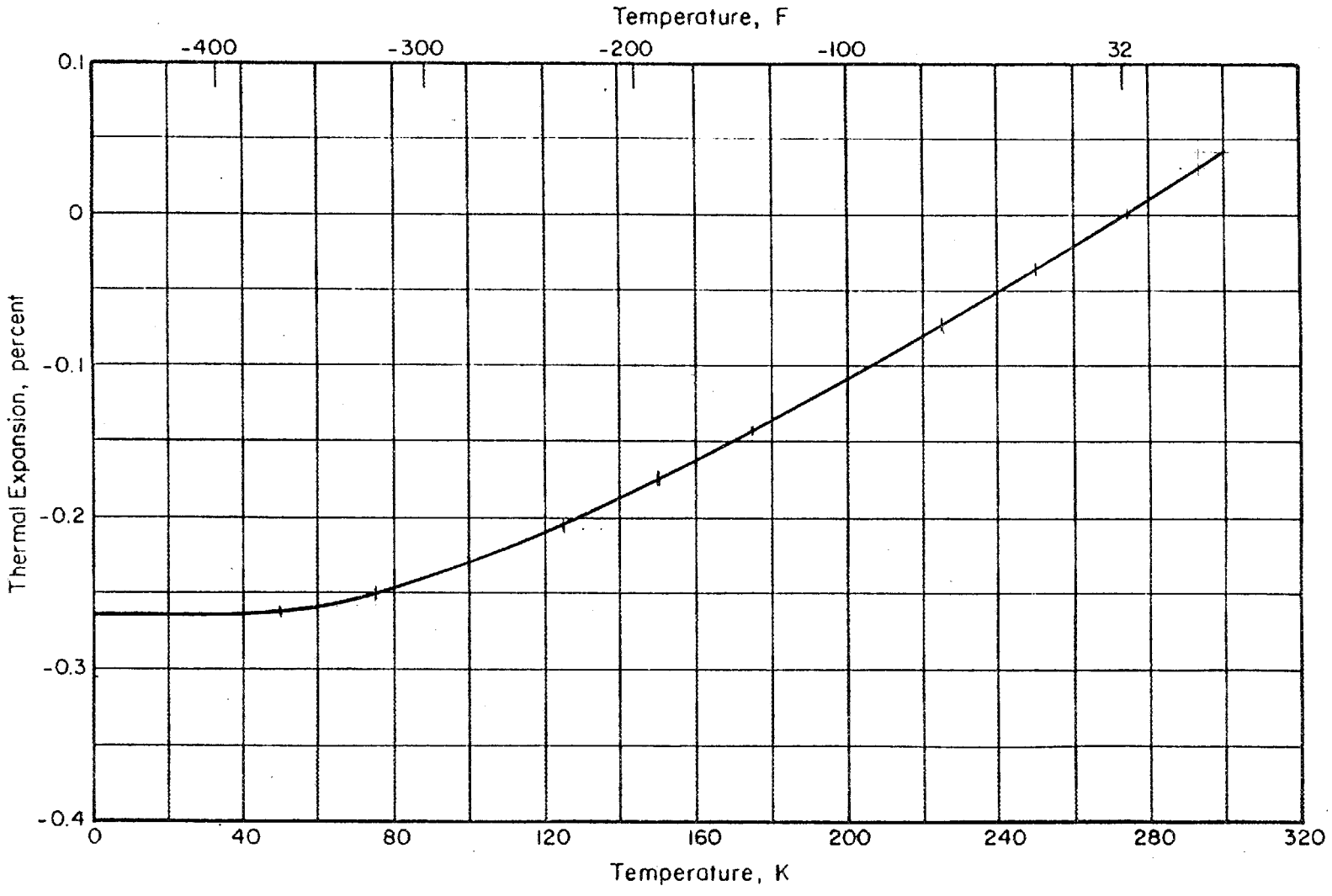

FIGURE 8.1.5-E1. THERMAL EXPANSION VERSUS TEMPERATURE FOR TYPE 316 STAINLESS STEEL

GENERAL DYNAMICS
Convair Division

M-216

29 November 1977

To: Distribution

From: Metals & Ceramics Group, 632-0

Subject: Mechanical Properties of Type 101 OFHC Copper

Reference: Task Control Board Log No. LCP-18 entitled "Material Properties for 1/8 and 1/4 hard OFHC Copper and for G-10 Fiberglass", dated 30 August 1977.

At the request of the Large Coil Program (LCP), reference Task Control Board Log No. LCP-18, a test program was performed to determine the tensile and compression properties of Type 101 OFHC copper. Tests were performed at room and cryogenic (20°K) temperatures on material in various temper conditions, including annealed and 1/8, 1/4 and 1/2 hard.

Test samples were machined from 1/2 inch thick plate obtained from Process Development Laboratory stores. The test samples were properly conditioned by heat treatment (900° F, 30 minutes, air cool) to obtain the annealed condition. This was followed by stretching 20 KSI (about 5%) for the 1/8 hard condition, 28 KSI (about 10%) for the 1/4 hard and 30 KSI (about 15-20%) for the 1/2 hard conditions.

Test specimens were then machined and prepared for testing. Type R_3 (MRG-D-32) tensile specimens and rectangular block compression specimens were used. Strain data was obtained by use of strain gages, extensometers and/or deflectometers. The test data was reduced and the results given in Table 1.

As expected and as is evident from the test data, there is a substantial increase in tensile yield and ultimate strength and compressive yield strength as a result of cold working and/or by decreasing the test temperature. The effects on elastic modulus and ductility (elongation) are less pronounced although there is some increase in modulus at cryogenic temperatures and a decrease in elongation with cold work and low temperatures.

The test data appears to be in good agreement with handbook and literature data and are provided to help support the design and analysis of Convair's LCP magnet.

Prepared by Jack L. Christian
Jack Christian, Group Engineer

cc: D. Hackley
G. Kruse
R. Baldi
J. Burgeson
E. Johnson
R. Bailey
J. Hertz

Table 1 Mechanical Properties of Type 101 Oxygen-Free Copper

CONDITION	TENSILE YIELD STRENGTH (0.2% OFFSET) (KSI) RT	TENSILE YIELD STRENGTH (0.2% OFFSET) (KSI) 20°K	TENSILE STRENGTH (KSI) RT	TENSILE STRENGTH (KSI) 20°K	ELASTIC MODULUS (KSI) RT	ELASTIC MODULUS (KSI) 20°K	TENSILE ELONGATION (% IN 1") RT	TENSILE ELONGATION (% IN 1") 20°K	COMPRESSIVE YIELD (KSI) RT	COMPRESSIVE YIELD (KSI) 20°K
ANNEALED	14.6	21.4	29.2	58.1	17.8	17.2	75	58	14.6	15.0
data probably not valid for annealed	14.0	19.4	27.5	59.1	17.3	21.2	80	68	14.0	15.7
	13.3	18.4	28.6	-	17.1	19.0	79	-	14.0	15.3
	14.0	19.7	28.4	58.6	17.4	19.1	78	63	14.2	15.3
1/8 HARD (5% COLD WORK)	23.0	30.2	31.3	62.9	16.9	18.0	70	63	23.9	25.6
	23.7	27.6	31.0	60.6	17.3	20.0	74	62	22.8	26.5
	24.1	28.6	31.5	61.1	17.7	22.2	76	59	22.6	26.7
	23.6	28.8	31.3	61.5	17.3	20.1	73	61	23.1	26.3
1/4 HARD (10% COLD WORK)	29.6	38.4	33.4	64.8	17.1	21.2	56	53	31.6	37.7
	29.6	39.1	33.5	67.6	17.2	20.0	64	54	31.0	33.5
	29.5	38.1	33.5	65.7	17.4	19.4	61	57	30.8	35.8
	29.6	38.5	33.5	66.0	17.2	20.2	60	55	31.1	35.7
1/2 HARD (20% COLD WORK)	32.5	42.8	34.5	68.9	17.1	19.0	53	51	33.7	38.2
	32.5	42.8	34.5	68.4	17.5	18.3	55	49	32.0	36.5
	32.4	43.2	34.6	69.3	17.0	20.2	55	51	32.5	35.5
	32.5	42.9	34.5	68.9	17.2	19.2	54	50	32.7	36.7

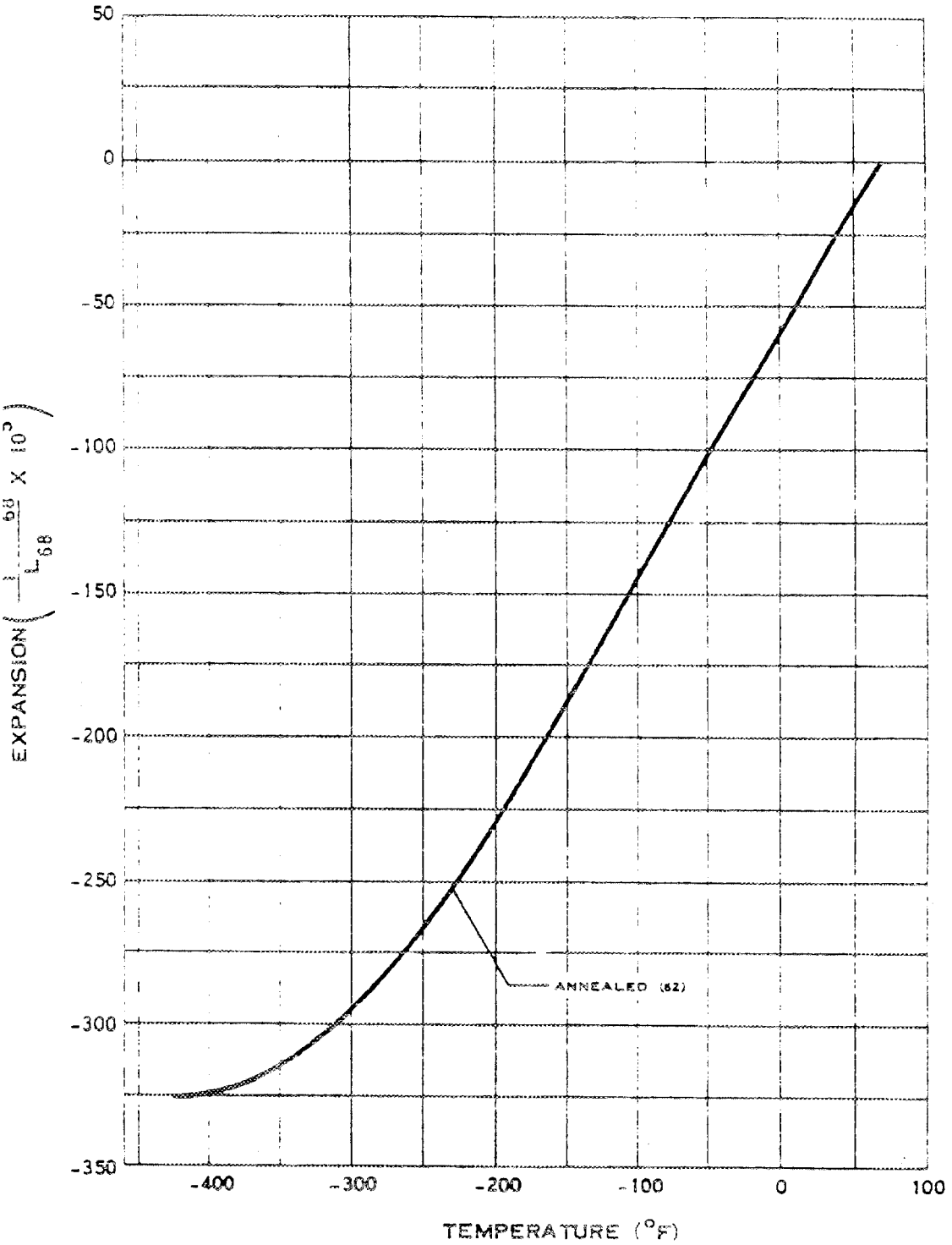

THERMAL EXPANSION OF COPPER

Figure 18

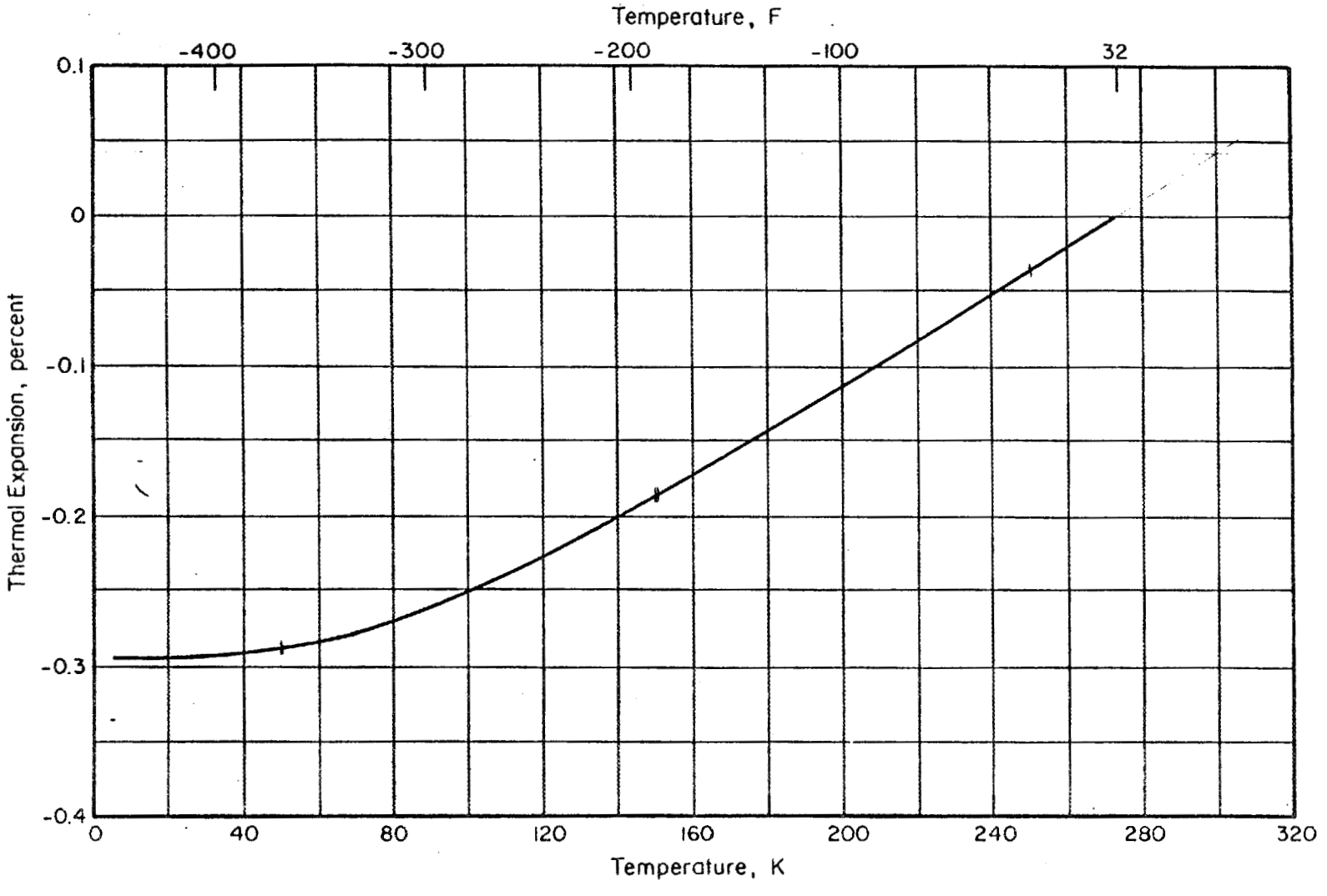

FIGURE 5.1.3-E1. THERMAL EXPANSION VERSUS TEMPERATURE FOR OFHC COPPER

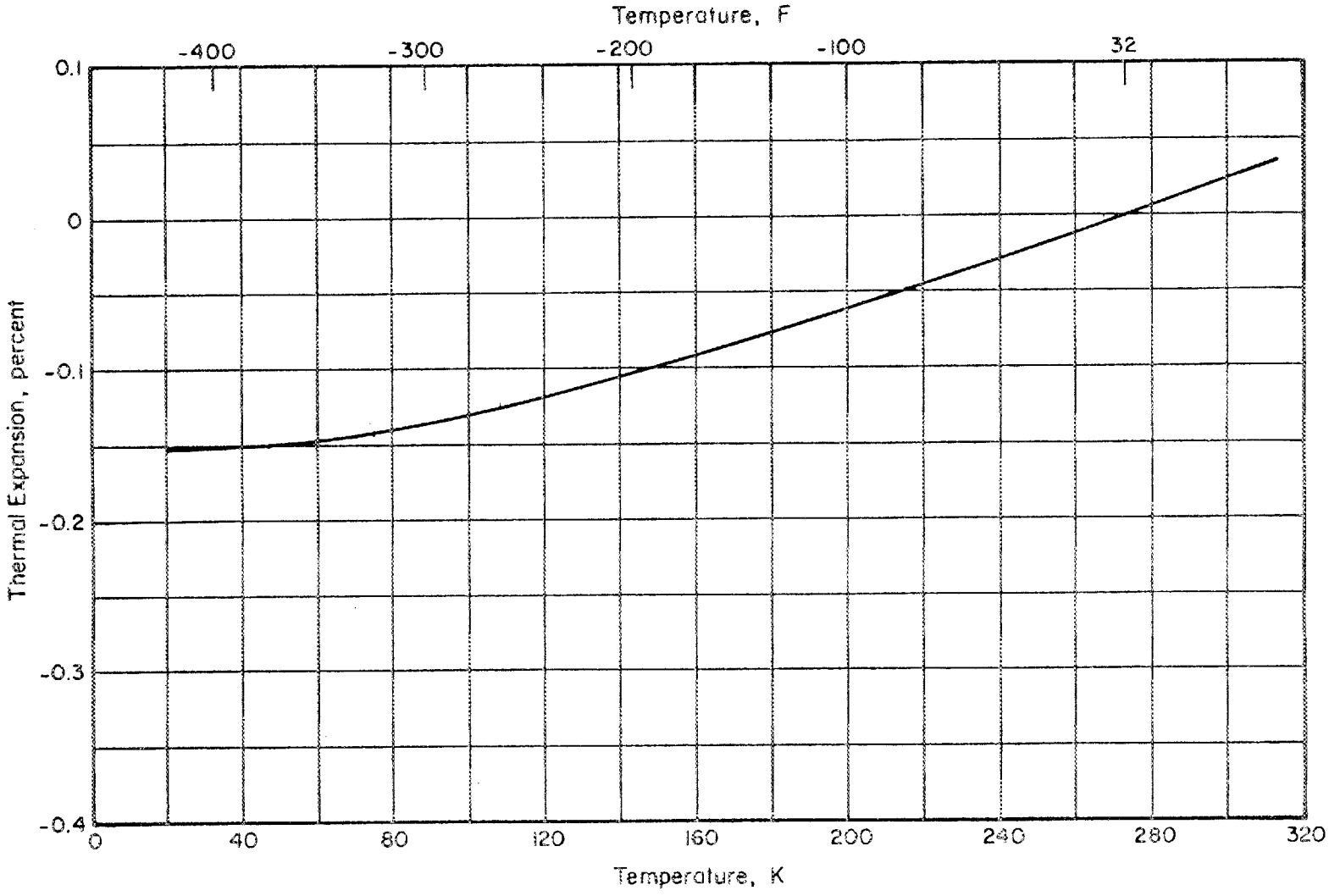

FIGURE 9.3.2-E1. THERMAL EXPANSION VERSUS TEMPERATURE FOR Ti-6 Al-4 V ALLOY

REF: HANDBOOK ON MATERIALS FOR SUPERCONDUCTING MACHINERY

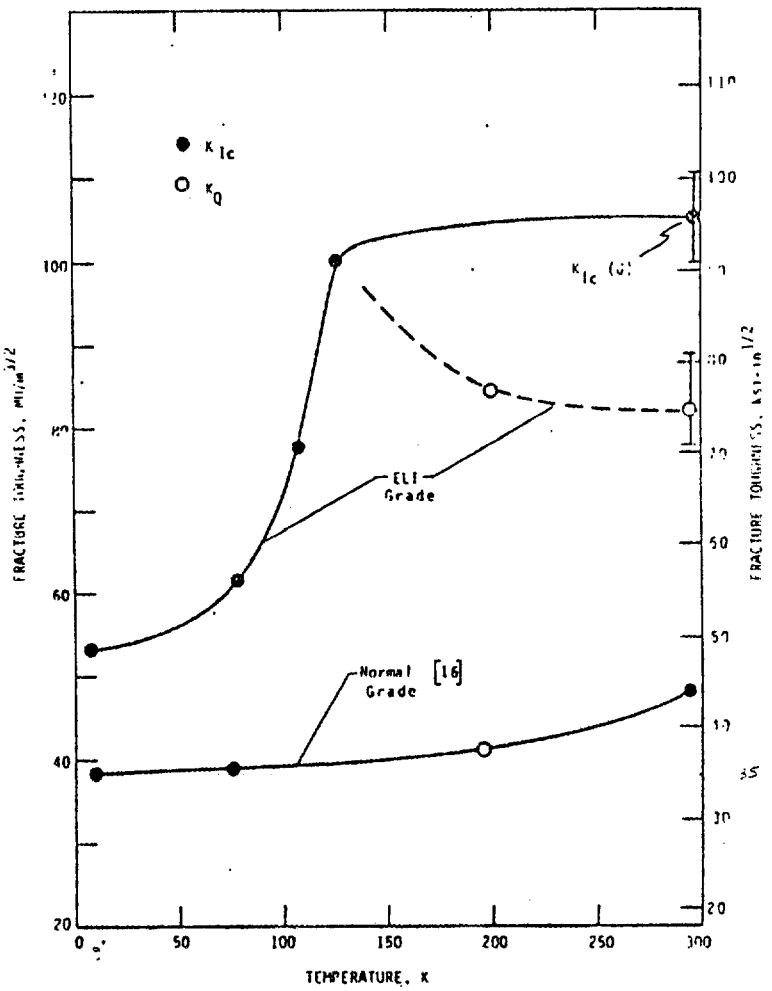

FIG. 11—*Temperature dependence of K_{Ic} for Ti-6Al-4V alloys.*

$K_{IC} = 35$ KSI-IN$^{1/2}$

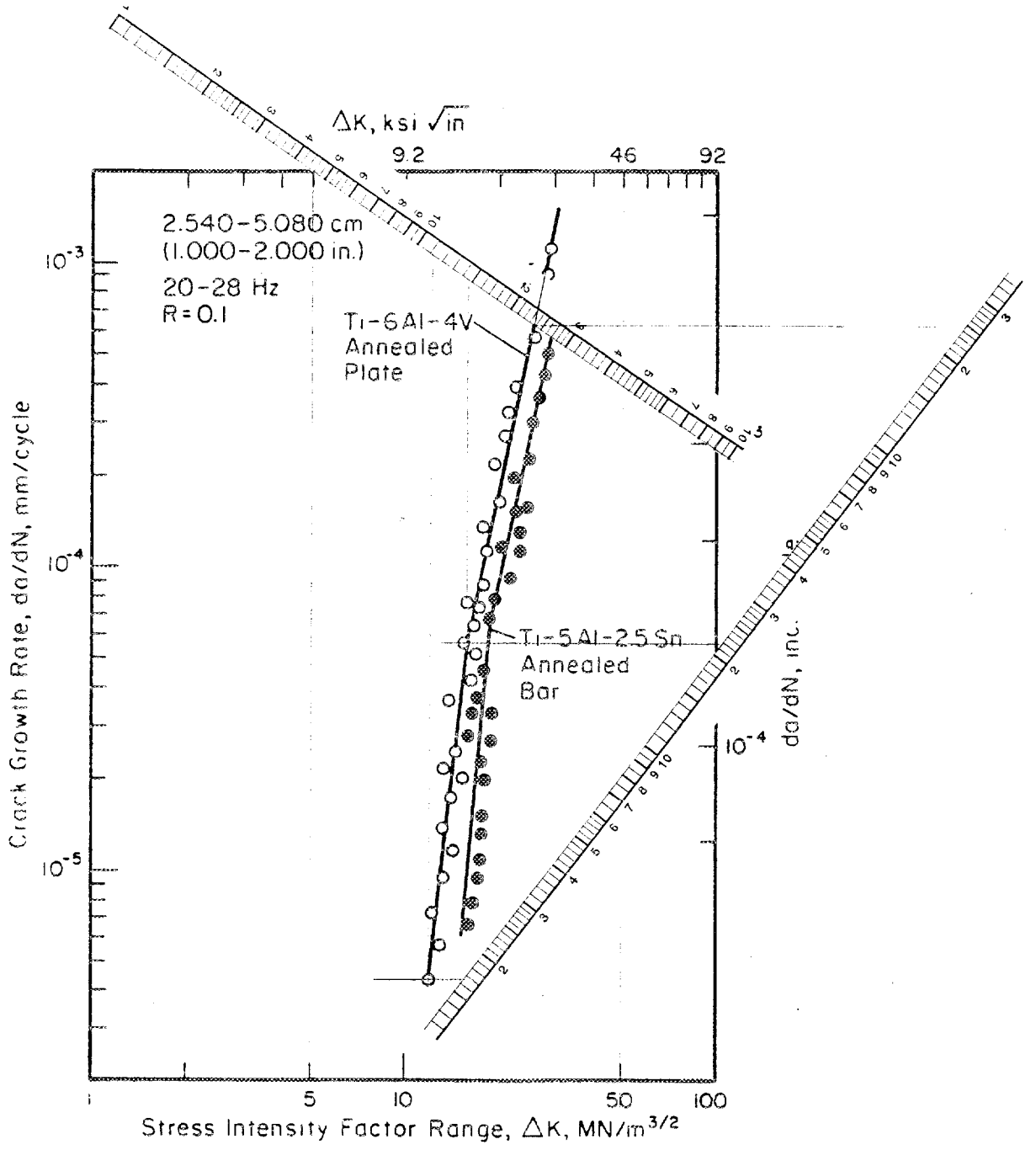

FIGURE 9.2.1-ME6. FATIGUE CRACK GROWTH RATES FOR TITANIUM ALLOYS AT 4 K (-452 F)(94208D)

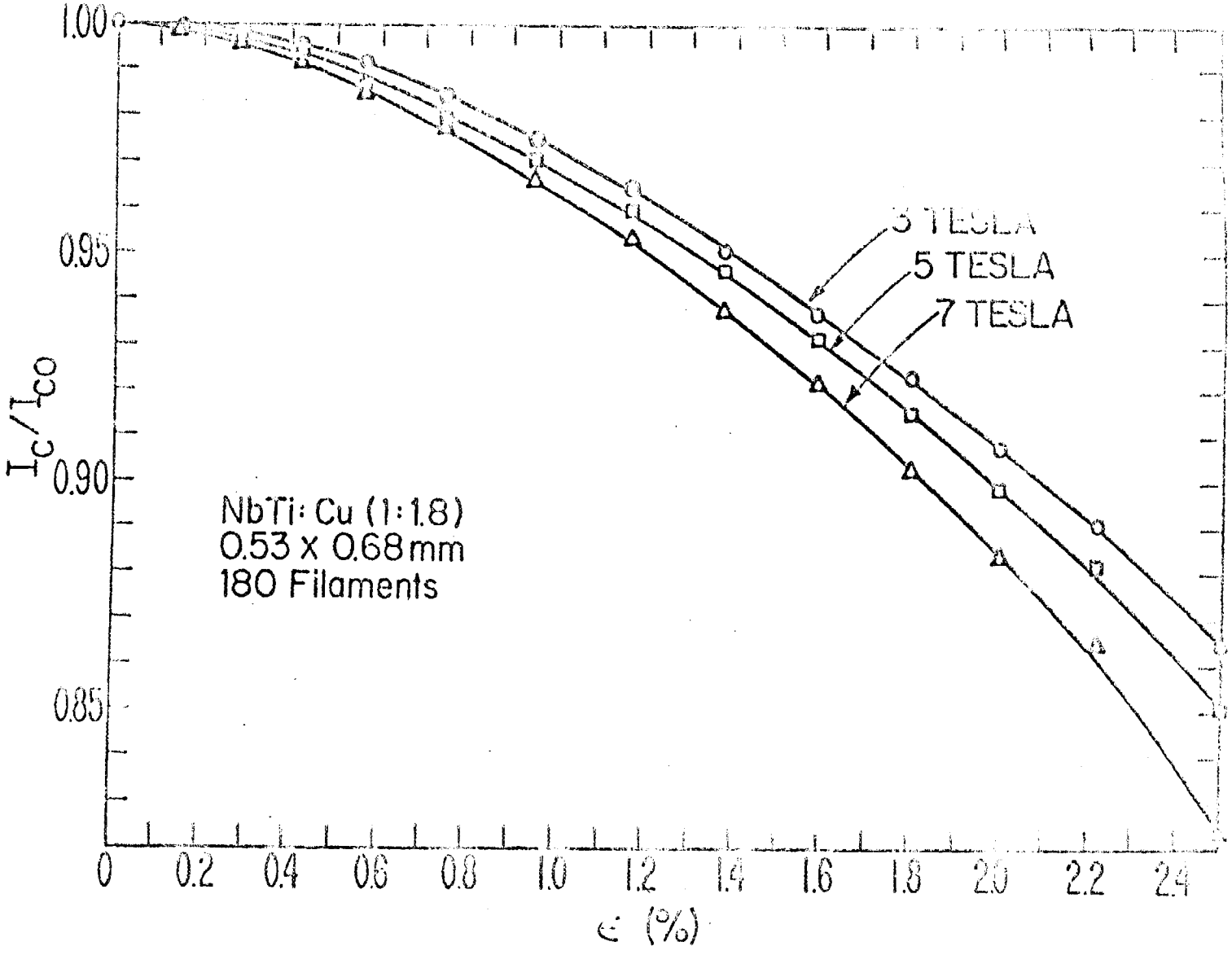
1.00
0.95
0.90
0.85
I_c/I_{co}
0
0.2
0.4
0.6
0.8
1.0
1.2
1.4
1.6
1.8
2.0
2.2
2.4
ε (%)
3 TESLA
5 TESLA
7 TESLA
NbTi: Cu (1:1.8)
0.53 x 0.68 mm
180 Filaments

APPENDIX B-4 SUPPORTING ANALYSES

THERMODYNAMIC ANALYSIS

Appendix A.2-4. Thermal analyses supporting Section 5.3, including stability, credible events, heat transfer within conductor pack, steady state heat loads, quench pressure, and heat transfer coefficients for coldown and warmup.

Computation of the MPZ Energy for EBT-P conductor

Starting from the steady state heat conduction equation:

$$\frac{d}{dx}\left(kA\frac{dT}{dx}\right) = Sq_b - E_q \qquad (1)$$

where k : thermal conductivity
A : cross sectional area of stabilizer
T : conductor temperature
S : effective surface area available for cooling
q_b : heat removal (boiling heat transfer)
E_q : heat generated in the conductor

Eq'n (1) can be rewritten as

$$Q\frac{dQ}{dT} = kASq_b - I^2 L f(T) \qquad (2)$$

where $Q = kA\frac{dT}{dx}$

I : current
L : Lorenz ratio (constant in Wiedeman-Franz law)

and
$$f(T) = 0 \quad ; \quad T < T_{cs}$$
$$= \frac{T - T_{cs}}{T_c - T_{cs}} \quad ; \quad T_{cs} < T < T_c$$
$$= 1 \quad ; \quad T_c < T$$

T_{cs} : current sharing, or saturation, temperature
T_c : critical, or transition, temperature

Finally, normalization of (2) gives

$$Q' \frac{dQ'}{dT} = T\left(\sigma \frac{q_{ca}}{q^{b}_{max}} - f(T)\right) \qquad (3)$$

where $Q' = \dfrac{Q}{I_0\sqrt{L}}$

$\sigma = q^{b}_{max} \Big/ \dfrac{I_0^2 \rho}{A S}$

q^{b}_{max}: maximum or peak nucleate boiling flux

The MPZ energy is ~~that~~ the energy stored in the conductor above the enthalpy of the conductor at bath temperature:

$$\Delta E_{MPZ} = \int_{-\infty}^{\infty} A_t \left[\rho_{cu}\gamma_{cu}\Delta h_{cu}(T) + \rho_{sc}\gamma_{sc}\Delta h_{sc}(T)\right] dx \qquad (4)$$

where A_t = total conductor cross section
ρ = density
γ = ~~[illegible]~~ volumetric fraction of conductor constituent
$\Delta h(T) = h(T) - h(T_{bath})$ = enthalpy of conductor at temperature T, referenced to bath datum
cu subscript refers to copper
sc " " " superconductor

Using $Q = kA\dfrac{dT}{dx}$, Eq'n (4) can be rewritten as a differential eq'n:

$$\frac{d\Delta E}{dT} = \frac{kAA_t}{I_0\sqrt{L}\,Q'}\left[\rho_{cu}\gamma_{cu}\Delta h_{cu} + \rho_{sc}\gamma_{sc}\Delta h_{sc}\right] \qquad (5)$$

The differential equation for the length of the normal zone is

$$\frac{dx}{dT} = \frac{kA}{I_0 \sqrt{L}\, Q'} \qquad (6)$$

Equations 3, 5, and 6 were solved simultaneously using a Runge-Kutta algorithm with σ, the ratio of peak boiling flux to generated flux, as a parameter.

Energy Release From a Radial Slip

Assume conductors lift off bobbin before slipping radially, and that one conductor is held by friction so that it doesn't initially reach its equilibrium position. When/if the conductor slips, the energy released is the product of the frictional force μF_a and the radial slip distance $\Delta\delta_r$, or

$$\Delta U_r = \mu F_a \Delta\delta_r ;$$

where μ = coefficient of friction at slip plane

F_a = accumulated axial force on slipping conductor

$\Delta\delta_r$ = radial strain differential

$$= \frac{r\,\Delta\sigma_H}{E} ;$$

r = conductor radius

E = Young's modulus

$\Delta\sigma_H$ = differential hoop stress before and after slip

$$= \frac{(\Delta F_r - \mu F_a)}{A_c} r ;$$

ΔF_r = differential radial force on slipping conductor due to axial gradient of axial component of magnetic field.

A_c = conductor cross-sectional area

So, $$\Delta\delta_r = \frac{r^2}{A_c E}\left(\Delta F_r - \mu F_a\right) = \frac{\mu F_a r^2}{A_c E}\left(\frac{\Delta F_r}{\mu F_a} - 1\right)$$

and $$\Delta U_r = \frac{(\mu F_a r)^2}{A_c E}\left(\frac{\Delta F_r}{\mu F_a} - 1\right)$$

The axial and radial components of the magnetic field are:

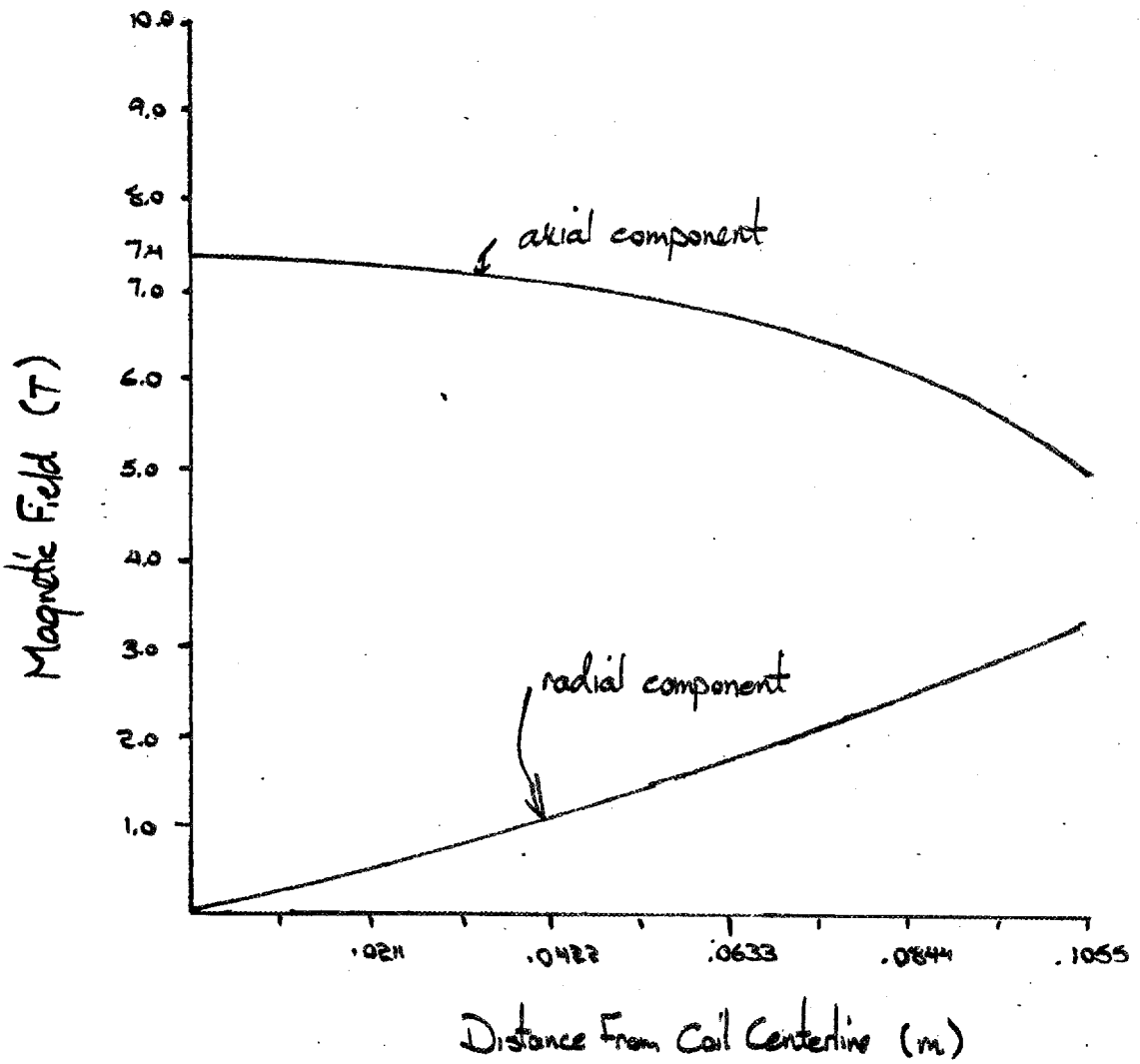

The axial and radial forces acting on the turns in the first layer at 16830 are:

turn# (n)	x (measured from ℄) (m)	F_r (N/m)	ΔF_r (N/m)	F_{a_i} (N/m)	$\sum_{i=1}^{n} F_{a_i}$ (F_a) (N/m)
19	.00268	12290	12.5	124	47530
17	.0134	12240	32.5	621	47040
15	.0241	12160	62.5	1121	45540
13	.0348	11990	90.0	1632	43050
11	.0456	11800	117.0	2160	39520
9	.0563	11520	150.	2708	34930
7	.0670	11200	225.	3270	29230
5	.0777	10620	317.	3867	22390
3	.0884	9930	405.	4474	14360
1	.0991	9000	465.	5097	5097

☆ $\frac{\Delta F_r}{F_a}$ is largest at the first turn, at low field,

$$\left.\frac{\Delta F_r}{F_a}\right|_{max} = .091$$

$$\therefore \quad \mu_{slip} < .091$$

Derivation of energy distribution after slip or collision

Friction is due to the interlocking of surface irregularities as illustrated in the figure. Motion occurs when the local stress at the irregularities

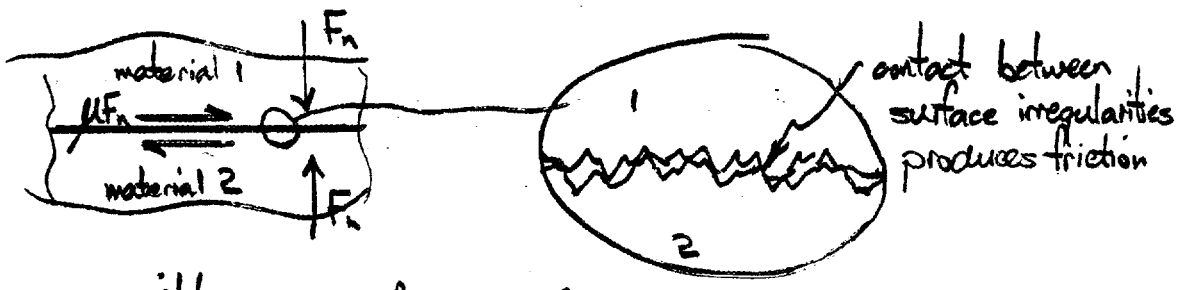

exceeds the ~~shear~~ yield stress of the softer material.

The frictional force is

$$\mu F_n = \sigma_1 A_1 = \sigma_2 A_2$$

where σ : shear stress
A : effective shear stress area

If yield occurs on surface 1, the work done displacing the material is approximately

$$\Delta U_1 = \frac{\sigma_1^2}{2E_1} \Delta V_1$$

where E_1 = modulus of mat'l 1
ΔV_1 = volume of material which yields
ΔU_1 = energy dissipated in mat'l 1

Even though no yielding occurs on surface 2, the strain energy is still dissipated and

$$\Delta U_2 = \frac{\sigma_2^2}{2E_2} \Delta V_2$$

Assuming that $\Delta V_1 \approx \Delta V_2$, the total energy released is

$$\Delta U_{tot} = \Delta U_1 + \Delta U_2$$

and the fraction released in the softer material (mat'l 1) is

$$\frac{\Delta U_1}{\Delta U_{tot}} = \frac{\Delta U_1}{\Delta U_1 + \Delta U_2}$$

$$= \frac{\dfrac{\sigma_1^2 \Delta V}{2E_1}}{\dfrac{\sigma_1^2 \Delta V}{2E_1} + \dfrac{\sigma_2^2 \Delta V}{2E_2}}$$

Since $A_1 \approx A_2$, $\sigma_1 \approx \sigma_2$ and

$$\frac{\Delta U_1}{\Delta U_{tot}} = \frac{1/E_1}{1/E_1 + 1/E_2} = \frac{E_2}{E_1 + E_2}$$

The same arguments and derivation apply to a collision between two bodies with spring constants E_1 and E_2

Estimation of wicking action and possible enhancement of heat transfer due to capillary action in Nomex braid

The static pressure head that is formed by capillary action in a 'tube' formed between braid fibers is approximately:

$$h = \frac{2\gamma\xi}{\rho g r_c} \qquad (1)$$

where h: head
ξ: wettability of Nomex in helium
γ: surface tension of helium
ρ: density
g: acceleration of gravity
r_c: approximate radius of channel formed by void

Assuming the hydraulic diameter is twice the radius,

$$r_c = \frac{d_c}{2} = \frac{2A_c}{P_w} \qquad (2)$$

where A_c = channel cross sectional area
P_w: wetted perimeter of channel

Assume that the fibers are compacted together as shown in the figure. Then

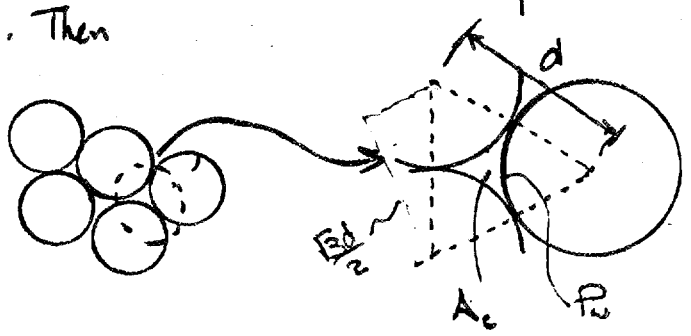

$$P_w \approx \frac{\pi d}{2} \qquad (3)$$

$$A_c \approx d^2\left(\frac{\sqrt{3}}{4} - \frac{\pi}{8}\right) \qquad (4)$$

Thus $$r_c = \frac{2\left[d^2\left(\frac{\sqrt{3}}{4} - \frac{\pi}{8}\right)\right]}{\pi d/2}$$

$$\approx d\left(\frac{\sqrt{3}}{\pi} - \frac{1}{2}\right) \qquad (5)$$

where d = filament diameter

(Note that $\left(\frac{\sqrt{3}}{\pi} - \frac{1}{2}\right) = \frac{\alpha}{1-\alpha}$ where α = void fraction of the braid assuming a close packed braid structure)

Then $$h = \frac{2\gamma\delta}{\rho g d\left(\frac{\sqrt{3}}{\pi} - \frac{1}{2}\right)} \qquad (6)$$

For helium: $\gamma = 0.1$ dyn/cm
$\delta = 1.0$ (because of low intermolecular attractive forces in He)
$\rho = .125$ g/cm^3

and $$h = \frac{.032}{d} \qquad (7)$$

The filament diameter which corresponds to the height of the conductor $h = .5$cm is $d = .064$ cm. The small filaments in the braid were measured using a scanning electron microscope and found to have a

diameter of 2.5×10^{-3} cm, which gives a hydrostatic head of roughly 13 cm

To determine the enhancement of heat transfer due to surface tension, the helium flow rate through the braid is calculated by equating the frictional pressure drop and surface tension head:

$$\frac{2\gamma\delta}{\left(\frac{\sqrt{3}}{\pi}-\frac{1}{2}\right)d} = f\,\frac{l_c}{d_c}\,\frac{\rho V_c^2}{2} \qquad (8)$$

where f = friction factor
l_c = channel length
V = velocity of helium flowing in channel

$$\dot{m}_c = \rho V_c A_c \Rightarrow \rho V_c^2 = \frac{\dot{m}_c^2}{\rho A_c^2} \qquad (9)$$

Using (2), (3), (4), and (5) gives

$$\dot{m}_c = \frac{\pi}{4}\left(\frac{\sqrt{3}}{\pi}-\frac{1}{2}\right)^2 \frac{d^3}{l_c}\,\frac{\rho\gamma\delta}{\mu} \qquad (10)$$

where μ = viscosity of helium and laminar flow has been assumed such that $f = \frac{16}{Re_D} = \frac{4\mu P_w}{\dot{m}_c}$

Using $d = 2.5 \times 10^{-3}$ cm,

$$\dot{m}_c = \frac{2.5 \times 10^{-7}}{l_c} \text{ g/sec}$$

The number of channels within the braid is assumed equal to the number of Nomex filaments n_f, which is determined from the braid area and void fraction:

$$n_f \frac{\pi d^2}{4} = (1-\alpha) A_b \quad ; \quad A_b = \text{braid area}$$

From $\frac{\alpha}{1-\alpha} = \frac{\sqrt{3}}{\pi} - \frac{1}{2} \Rightarrow \alpha = \frac{\frac{\sqrt{3}}{\pi} - \frac{1}{2}}{\frac{\sqrt{3}}{\pi} + \frac{1}{2}} = .049$

$$A_b = (.318\,cm)(.015\,cm) = .00485\,cm^2$$

$$n_f = \frac{(4)(1-.049)(.00485)}{(\pi)(2.58\times10^{-3})^2}$$

$$\approx 1000$$

The braid is capable of a mass flow rate of

$$\dot{m}_b = n_f \dot{m}_c \sim \frac{2.5\times10^{-4}}{l_c}\ g/sec$$

The heat removal rate is $\dot{q} = \dot{m}_b \lambda$, λ = heat of vaporization = 20.4 J/g

$$\dot{q} = \frac{5.1}{l_c}\ mW$$

The area covered by the braid is $w l_c$, w = width of braid = .3175cm

The flux the braid can remove from the conductor is

$$\dot{q}'' = \frac{q}{\pi l_c} = \frac{16}{l_c^2} \text{ mW/cm}^2$$

Taking l_c equal to the width of a conductor (.29 cm)

gives $\dot{q}'' = \frac{16}{(.29)^2} = 190 \text{ mW/cm}^2 = .19 \text{ W/cm}^2$

The point of the analysis is to demonstrate the order of magnitude of flux possible with this heat transfer mechanism. Several of the assumptions made for the sake of the analysis need to be experimentally verified to determine the actual heat transfer due to this mechanism.

Estimate of critical channel heat flux in EBT-P conductor pack

Critical heat fluxes (transition from nucleate to film boiling) in a vertical channel can be estimated according to M.N. Wilson by

$$\dot{q}_c = \sigma \frac{\omega}{\sqrt{z}} \qquad (1)$$

where σ is an empirical constant ≈ 7.0 for vertical channels a few cm high.

According to the theory developed by Sydoriak & Roberts and used by Wilson, the constant σ is a function of $\sqrt{g}$, where g is the component of gravity opposite to the direction of flow.

For a horizontal conductor, the heat transfer channel for a single conductor looks like:

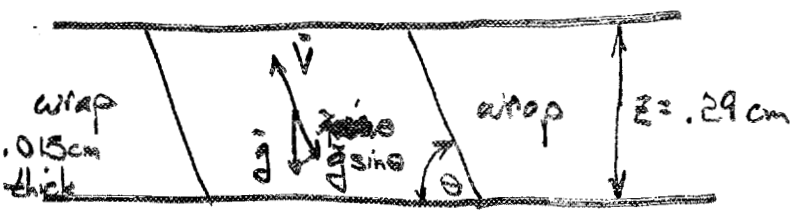

and $\dot{q}_c = \sigma_\theta \frac{\omega}{\sqrt{z}}$, $\sigma_\theta = \sigma_{vertical} \sqrt{\frac{\sin\theta}{\sin \pi/2}}$

The EBT-P conductor is wrapped at roughly a 65° angle, so σ_θ is reduced to

$$\sigma_\theta = 7.0\sqrt{\sin 65^\circ}$$

$$\sim 6.7$$

and $$\dot{q}_c = \frac{(6.7)(.015)}{\sqrt{1.29}}$$

$$\sim .186 \text{ W/cm}^2$$

For a vertical conductor:

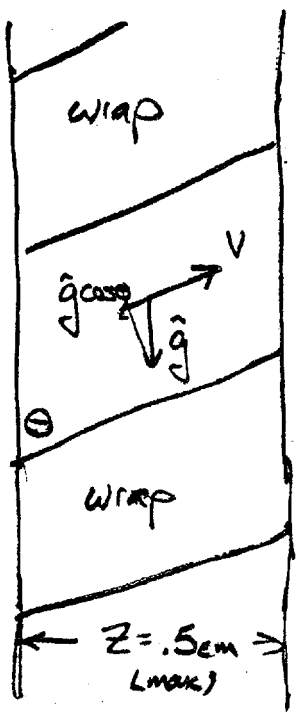

$$\sigma_\theta \sim 7\sqrt{\frac{\cos\theta}{\cos 0}} \sim 4.5$$

$$\dot{q}_c = \frac{(4.5)(.015)}{\sqrt{.5}}$$

$$= .097 \text{ W/cm}^2$$

These estimates assume that the channel "sees" the equivalent of an open pool surrounding the conductor, which is probably not a good assumption. However, the estimates are useful in terms of upper bound, order of magnitude values.

Heat Leak Calculation - Titanium / G-10 Support Concept

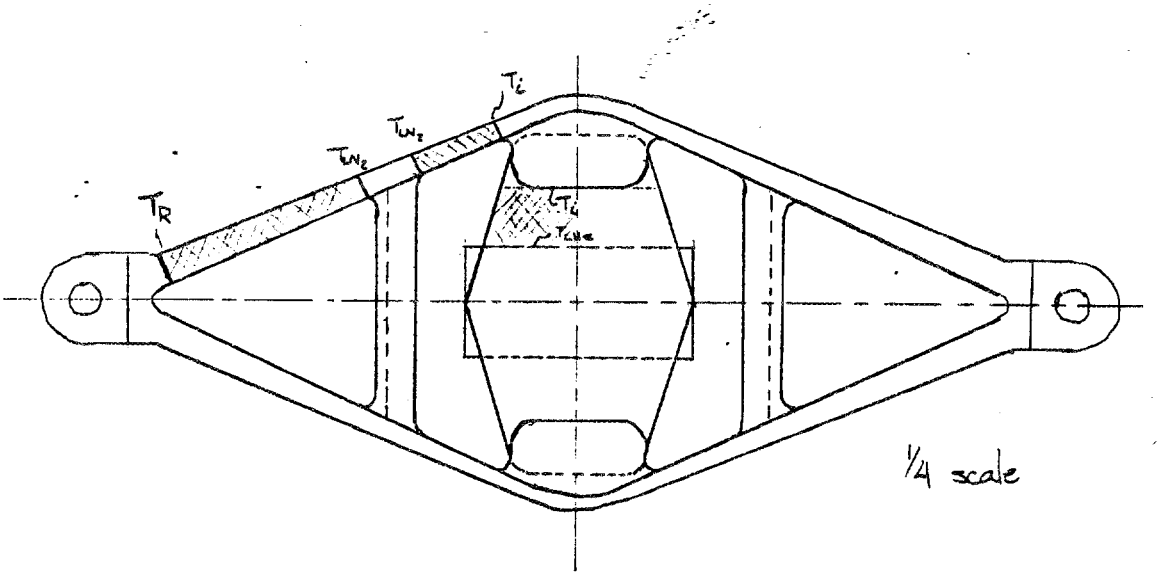

For this preliminary analysis, only the cross-hatched areas shown above are assumed to offer resistance to heat flow between the indicated temperatures for 1/4 of the support.

One-dimensional heat flow is assumed, thus:

$$\dot{Q} = -\frac{\int_{T_1}^{T_2} k\,dT}{\int_{x_2}^{x_1} \frac{dx}{A}}$$

<u>LHe load</u>

In order to determine the LHe load, T_i must be determined.

The s.s. heat conduction in series is

$$\dot{Q}_{LHe} = \frac{\int_{T_i}^{T_{LN_2}} k_{Tit}\, dT}{\int_{x_{LN_2}}^{x_{T_i}} \frac{dx}{A_f}} = \frac{\int_{T_{LHe}}^{T_i} k_{G10}\, dT}{\int_{x_{LHe}}^{x_{T_i}} \frac{dx}{A_s}}$$

where
- T_{LN_2} = temperature at LN_2 heat station = 80 K
- T_i = intermediate temperature at junction of frame and strut
- T_{LHe} = liquid helium temperature = 4.5 K
- x_{T_i} = location of intermediate temperature
- x_{LN_2} = location of heat station
- x_{LHe} = location where the strut meets the lug on the cold mass
- A_f = cross-sectional area of the frame member = .5 in² constant
- A_s = cross-sectional area of strut, variable

Distance from T_{LN_2} to T_i along frame member is ≈ 2 in
Area along frame member constant at .5 in²

$$\text{So} \quad \int_{x_{LN_2}}^{x_{T_i}} \frac{dx}{A_f} = \frac{2\text{ in}}{.5\text{ in}^2} \doteq 4\text{ in}^{-1} = 157\text{ m}^{-1}$$

The cross-sectional area of the G-10 strut at the T_i location is approximately (3.5"X.75") = 2.625 in² total, taking half this area gives 1.313 in²

At the intersection of lug and strut, the cross sectional area is (1.43 X.75") = 3.23 in², half the area is 1.61 in²

The distance between the two locations is ≈ 1.3 inches

Thus $A_s = 1.31 + \frac{(1.61-1.31)}{1.3} x$; x measured from x_{T_i}

$$= 1.31 + .231x \text{ , in}^2$$

$$\int_{x_{T_i}}^{x_{LHe}} \frac{dx}{A_s} = \frac{1}{.231}\int_0^{1.3} \frac{.231\,dx}{1.31+.231x} = \frac{1}{.231}\ln\left[\frac{1.31+(.231)(1.3)}{1.31}\right] = .893\text{ in}^{-1}$$

$$= 35.2\text{ m}^{-1}$$

To determine T_i, must satisfy

$$\frac{1}{157}\int_{T_i}^{T_{LN_2}} k_{Tit}\, dT = \frac{1}{35.2}\int_{T_{LN_2}}^{T_i} k_{G\text{-}10}\, dT$$

T_i (K)	$\int_{T_i}^{80K} k_{Tit}\, dT$ (W/m)	$\int_{4.5K}^{T_i} k_{G\text{-}10}\, dT$ (W/m) *
50	89.0	7.92
60	60.0	10.9
70	30.0	14.3
80	0	17.8

The equality is satisfied for $T_i = 62.5K$, determined by linear interpolation in the above table.

The heat leak to LHe for a quarter strut is, then,

$$\dot{Q}_{\substack{LHe \\ 1/4\ support}} = \frac{1}{35.2}\int_{4.5K}^{62.5K} k_{G\text{-}10}\, dT = \left(\frac{m}{35.2}\right)\left(11.75\,\frac{W}{m}\right) = .333\ W$$

Each support has a heat leak of 1.33 W

Total support heat leak / coil = 4.00 W to LHe

* Conductivity integral of G-10 computed by numerically integrating $k(T)$. Conductivity taken in direction ∥ to weave

LN_2 load

$$\dot{Q}_{LN_2} = \frac{\int_{T_{LN_2}}^{T_R} k_{Tit}\, dT}{\int_{x_R}^{x_{LN_2}} \frac{dx}{A_f}}$$

distance from room temperature location x_R to LN_2 heat station is $\approx$ 4.8 in

A_f is a constant .5 in^2

$$\int_{x_R}^{x_{LN_2}} \frac{dx}{A_f} = \frac{4.8}{.5} = 9.6\ \text{in}^{-1} = 378\ \text{m}^{-1}$$

$$\int_{80K}^{300K} k_{Tit}\, dT = 1225\ \text{W/m}$$

1/4 support heat leak is $\frac{1225}{378} = 3.24$ W

LN_2 heat leak / 1 support = 13.0 W

LN_2 heat leak / coil = 39 W

Scott D Peck

4/29/81

Heat Leak Computation for Ti/Ti strut support concept. APPENDIX B-4

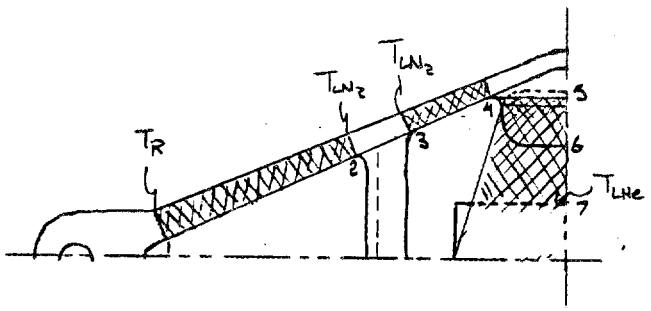

Indicated cross-hatched area offer resistance to heat flow between the indicated temperatures. One dimensional heat flow is assumed.

Conductivity integrals for titanium - 6Al-4V alloy:

$$\int_{80K}^{300K} k\,dT = 1225 \text{ W/m}$$

$$\int_{4.5K}^{80K} k\,dT = 163 \text{ W/m}$$

LHe load:

Area from 3 to 4 assumed constant @ .50 in²
Length " " is approximately 2.0 in

Area from 5 to 6 assumed constant, @ (1.2 in)(1.0 in) = 1.2 in² (for ¼ strut shown)
(includes flanges on frame)

Length from 5 to 6 is approximately 1.0 in

Area of the Ti insert at section 6 is approximately $(1.75\,in)(.25\,in) = .438\,in^2$
(for ¼ strut shown)

Area of Ti insert at section 7 is approximately $(2.15\,in)(.25\,in) = .538\,in^2$
(¼ strut)

Length from 6 to 7 is 1.75 inches

Thus

$$\int_3^7 \frac{dx}{A} = \frac{2.0}{.50} + \frac{1.0}{1.2} + \frac{1.75}{(.538-.438)} \ln\left(\frac{.538}{.438}\right)$$

$$= 8.43\,in^{-1} = 332\,m^{-1}$$

$$\dot{Q}_{LHe} = \frac{163\,W/m}{332\,m^{-1}} = .491\,W/\tfrac{1}{4}\text{ strut}$$

$$= 1.96\,W/\text{strut}$$

$$= 5.89\,W/\text{coil}$$

LN_2 load remains identical to that of the Ti/G-10 strut = 13.0 W/strut
= 39.0 W/coil

Scott D Peck

5/4/81

Heat Leak Calculation - 1 piece titanium support.

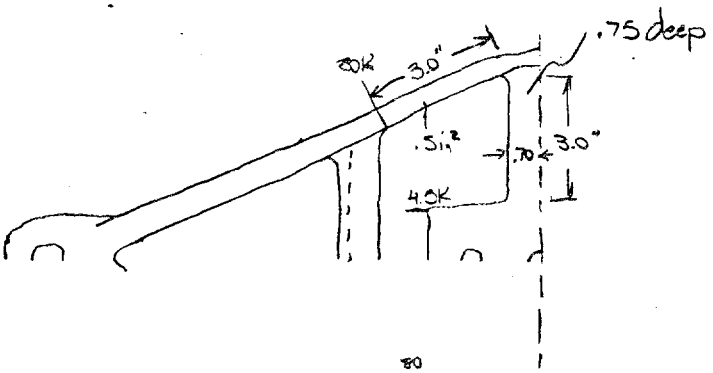

$$\dot{Q}_{1/4\,strut} = \frac{\int_{4.5}^{80} k_{T_i}\, dT}{\int \frac{dl}{A}}$$

$$\int \frac{dl}{A} = \frac{3.0\,in}{.5\,in^2} + \frac{3.0\,in}{(.7)(.75)\,in^2} = \frac{11.7}{in} = \frac{4.61}{cm} = \frac{461}{m}$$

$$\int_{4.5}^{80} k_{T_i}\, dT = 163\,W/m$$

$$\dot{Q}_{1/4\,strut} = .353\,W$$

$$\dot{Q}_{strut} = 1.41\,W$$

$$\dot{Q}_{coil} = 4.24\,W$$

EBT-P Stack Thermal Analysis

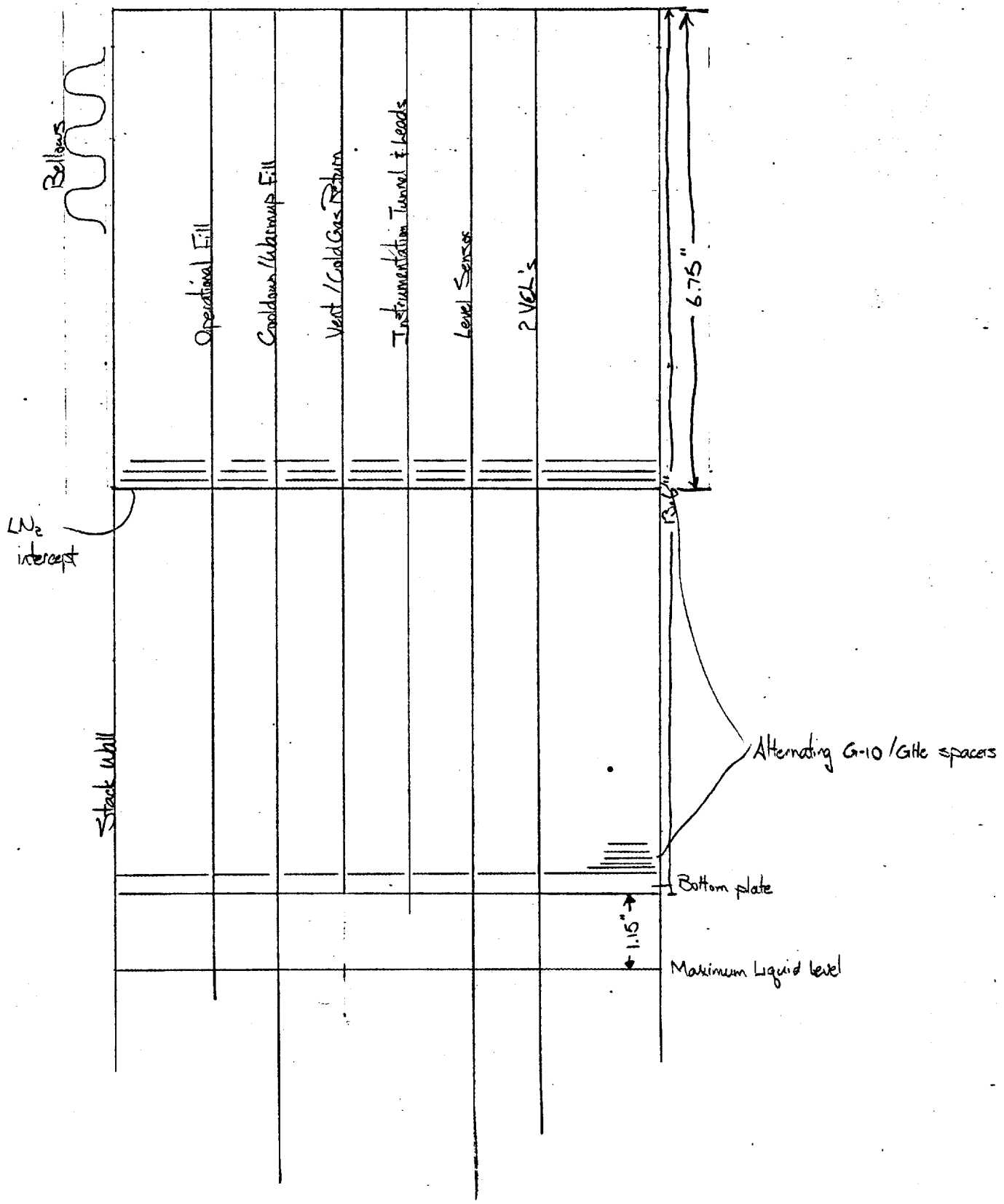

Conduction paths:

- Fill tubes: 2 vacuum jackets + 1 (Cooldown/Warmup) fill
- Vent: vacuum jacket
- Stack: bellows and sleeve
- Wiring tunnel
- Level sensor

GHe/G-10

G-10 buttons/rods

Fill tubes: vacuum jackets are .75" diameter, .035" thick, 304L
fill tubes are .50" diameter, .035" thick, 304L

Vent vacuum jacket: 2.75" OD, .035 thick, 304L

Stack bellows: nominal length 6.75 inches, 10 convolutions, .019 wall thickness

$$\text{bend diameter} = \frac{6.75}{20} = .338''$$

$$\text{straight section} = \frac{OD - ID - d}{2} = \frac{9.875 - 8.625 - .338}{2} = .456''$$

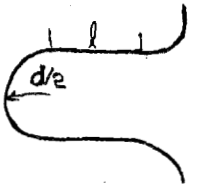

$$\text{length of convolution} = \pi d + 2l$$

$$\text{length of bellows conduction path} = 10(\pi d + 2l)$$

$$= 10[\pi(.338) + (2)(.456)]$$

$$= 19.7''$$

Stack wall (sleeve): 8.39 OD, .030 wall thickness, 304L

Wiring tunnel: 1.25 diameter, .125 wall thickness, G-10CR

Level sensor: assume solid G-10 rod .25" diameter

Instrumentation leads. 30 30AWG copper wires .010" diameter
12 x 7 38AW copper shields .004" diameter

G-10 buttons/rods: assume washer/rod forms solid plug .500" diameter (G-10CR)

G-He/G-10 conduction area: Stack area - VCL - Vent - 1 fill tube - washer

VCL's: 2 tubes 1.1" diameter

Component	Cross-sectional area	L_{300-80}	$L_{80-4.5}$	$L_{300-4.5}$
1 fill tube	.00038 ft^2			1.13 ft
2 fill tube vacuum jackets	.00115 ft^2	.563 ft	.571 ft	
stack bellows	.00383 ft^2	1.64 ft		
stack sleeve	.00549 ft^2		.571 ft	
wiring tunnel	.00341 ft^2			1.13 ft
level sensor	.00034 ft^2			1.13 ft
leads	.0000237 ft^2			1.13 ft
G-10 washers	.00409 ft^2	.563 ft	.571 ft	
GHe/G-10	.322 ft^2	.563 ft	.571 ft	
vent vacuum jacket	.00210 ft^2	.563 ft	.571 ft	

Conductivity integrals:

$\int_{4.5}^{80} k_{304}\,dT = 351$ W/m $\quad \int_{80}^{300} k_{304}\,dT = 2700$ W/m $\quad \int_{4.5}^{300} k_{304}\,dT = 3060$ W

$\int_{4.5}^{80} k_{GHe\,\varnothing\varnothing}\,dT = 5.87$ W/m $\quad \int_{80}^{300} k_{GHe\,\varnothing\varnothing}\,dT = 49.7$ W/m

$\int_{4.5}^{300} k_{Cu}\,dT \simeq 117000$ W/m $\quad \int_{4.5}^{80} k_{G-10}\,dT = 19.5$ W/m $\quad \int_{80}^{300} k_{G-10}\,dT = 134$ W/m $\quad \int_{4.5}^{300} k_{G-10}\,dT = 154$ W

Heat Conduction: $\dot{Q} = \frac{A}{L}\int_{T_c}^{T_h} k\,dT$ if A = constant

	LN_2		LHe	
1 fill tube	--		.314 W	
2 fill vacuum jackets	1.68 W	(1.58)	.216 W	(.327)
stack bellows	1.92 W			
stack sleeve			1.03 W	
wiring tunnel			.142 W	
level sensor			.0141 W	
leads			.748 W	
G-10 washers	.297 W		.0423 W	
GHe/G-10	8.57 W		1.01 W	
vent jacket	3.07 W	(2.88)	.394 W	(.598)

Total LHe: 3.91 W (4.23 W)

Total LN_2: $\dot{Q}_{LN_2} - \dot{Q}_{LHe} =$ 14.0 W (13.4 W) (adjusted for 100K contact at finger springs SAB)

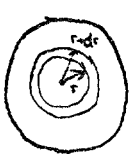

Estimate of temperature rise across LN_2 intercept: assume uniform heat flux over disk, what is temperature distribution:

$$-k(2\pi r t)\frac{dT}{dr} = \dot{q}''\pi r^2$$

$$-\frac{k(2\pi t)}{\dot{q}''}dT = r\,dr$$

$$-\frac{k\,2\pi t}{\dot{q}''}(T_R - T_0) = \frac{r^2}{2} \qquad T_0 - T_R = \Delta T = \frac{\dot{q}''R^2}{4\pi k t}$$

$R \approx \frac{8.4}{2} = 4.2\text{in}$

$$\dot{q}'' = \frac{\dot{q}}{A} = \frac{\dot{q}}{\pi R^2}$$

$$\dot{q}'' R^2 = \frac{\dot{q}}{\pi}$$

$$\Delta T = \frac{\dot{q}}{4\pi^2 k t}$$

$k \approx 280 \frac{\text{BTU}}{\text{hr}\cdot\text{ft}\cdot\text{R}}$ @ 140R

$t = .032" = .00267\,\text{ft}$

$\dot{q} = 14.0\,\text{W} = 47.7\,\text{BTU/hr}$

$$\Delta T = \frac{47.7}{(4\pi^2)(280)(.00267)} = 1.62\text{R} = .90\text{K}$$

Temperature rise across Be-Cu fingers:

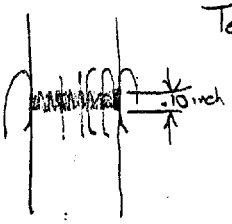

assume .10" band contact around 30% of tube, so area of contact is $\frac{.05\pi D}{144}$ ft^2 (97-310-A)

assume contact coefficient $h = 75 \frac{\text{BTU}}{\text{hr}\cdot\text{ft}^2\cdot\text{R}}$

around fill tubes, $\Delta T = \frac{2.5\,\text{BTU/hr}}{\left(75 \frac{\text{BTU}}{\text{hr}\cdot\text{ft}^2\cdot\text{R}}\right)\left(\frac{.05\pi\ .75}{144}\right)} = 41\text{R}$ unacceptable $= 23\text{K}$

Need to increase contact area by at least 400% around fill tubes.

around vent jacket; $\Delta T = \frac{9.1\,\text{BTU/hr}}{\left(75 \frac{\text{BTU}}{\text{hr}\cdot\text{ft}^2\cdot\text{R}}\right)\left(\frac{.05\pi\ 2.75}{144}\right)} = 40\text{R} = 23\text{K}$

Assume fill tube and vent jackets held to 100K at intercept location.

$\int_{4.5}^{100} k_{304}\,dT = 533\,\text{W/m}$ $\int_{100}^{300} k_{304}\,dT = 2530\,\text{W/m}$

$\dot{Q}_{LHe}$ vent: .598W fill tubes: .327W

$\dot{Q}_{LN_2}$ vent: 2.88W fill tubes: 1.58W

Temperature drop through straps:

strap braids are 1" wide, .045" thick, and ≈ 3.0' long copper.

Each strap must carry ½ of $\dot{q}_{W_2} = \frac{13.4}{7} \approx 2W$

$$\dot{q}_{strap} = \frac{kA}{L} \Delta T$$

k_{Cu} @ 80K = 4.85 W/cm-K

$A = 1 \times .045 \times 2.54^2 = .29\ cm^2$
$L = 3' = 7.6\ cm$

$$\Delta T = \frac{(2W)(7.6cm)}{(.29cm^2)(4.85\ W/cm\cdot K)} = 10.8\ K$$

ΔT through rod at stack wall: stainless steel rod ⅜" diam 7/16" long

$$\Delta T = \frac{(2W)(1.11cm)}{(.713\ cm^2)(.08\ W/cm\cdot K)} = 40K$$

if rod is brass, $k \sim .6\ W/cm\cdot K$

$$\Delta T = \frac{(2)(1.11)}{(.713)(.6)} = 5.2K$$

G-10 plate spacing (thickness): require $Gr < 2000$ based on enclosed horizontal gap

$$Gr_\delta = \frac{\rho^2 g \beta \Delta T \delta^3}{\mu^2}$$

At the bottom plate, $\frac{\dot{q}}{A} = 10.3 \frac{Btu}{hr\text{-}ft^2} = -k \frac{\Delta T_{gap}}{\delta}$

in gaseous He at 4.2K, $k = .00641$ BTU/hr ft °R $\Rightarrow \frac{\Delta T}{\delta} = 1650$ R/ft

$$\Delta T = 1650\,\delta$$

$$Gr = \frac{\rho^2 g \beta (1650)\delta^4}{\mu^2} = \frac{(1.054)^2(32.2)(.370)(1650)\delta^4}{.838\times10^{-6}}$$

$$\delta^4 = \frac{(.838\times10^{-6})(2000)}{(1.054^2)(32.2)(.370)(1650)} = .0167\text{ ft} = .20\text{ inches}$$

A gap spacing of 1/5" will keep natural convection to levels so low only conduction through the gas transfers heat.

Scott D Peck
8/6/81

Radiation loads:

Assume: Outer layer of MLI outside cold wall is at 540R
Inner " " outside " " 144R
Outer " inside " " 144R
Inner layer " inside " " 8R

Use areas of cold wall for heat transfer areas:

A_{or} = area of outer ring
A_{ir} = area of inner ring
A_{sp} = area of 2 side plates
A_{st} = area of stack shield

radius of inner ring = 8.73"
radius of outer ring = 17.57"
width of inner, outer ring = 10.55"
radius of stack = 5.25"
height of stack = 30.38"

$$A_{sp} = 2\left[\pi\left\{\left(\frac{17.57}{12}\right)^2 - \left(\frac{8.73}{12}\right)^2\right\}\right] = 10.14\ ft^2$$

$$A_{or} = 2\pi\left(\frac{17.57}{12}\right)\left(\frac{10.55}{12}\right) = 8.09\ ft^2$$

$$A_{ir} = 2\pi\left(\frac{8.73}{12}\right)\left(\frac{10.55}{12}\right) = 4.02\ ft^2$$

$$A_{st} = 2\pi\left(\frac{5.25}{12}\right)\left(\frac{30.38}{12}\right) = 6.96\ ft^2$$

Flux through MLI blanket is $\dot{q}'' = \frac{k_{MI}}{L}(T_H - T_c)$

for MLI, nominal effective conductivity is

$$k_{eff} = 3.007\times10^{-25}\,\bar{N}^{8.6}\left(\frac{T_H+T_c}{2}\right) + \frac{8.33\times10^{-2}\,\sigma\,(T_H^2+T_c^2)(T_H+T_c)}{\left(\frac{2}{\epsilon}-1\right)\bar{N}}\,\frac{N}{N-1}$$

where $\bar{N}$ = 77 layers/inch (nominal)
N = number of layers
T_H = hot side temperature (R)
T_c = cold side temperature (R)
ϵ = shield emittance (.07)
σ = 1.714×10^{-9} BTU/hr-ft²-R⁴

To account for pins, seams, & penetrations, standard practice is to multiply the above k_{eff} by 4 to get radiation loads. However, must account for perforations also. No good data for perforation degrade, assume 25%, therefore, multiply by 5 instead of 4.

Now, $L = \frac{N}{\bar{N}}$ inches $= \frac{N}{12\bar{N}}$ ft

So $\frac{k_{bi}}{L}(T_h - T_c) = \left(\frac{12\bar{N}}{N}\right)(5 k_{eff})(T_h - T_c)$

$$= 60\,\frac{\bar{N}}{N}\left[3.007\times10^{-25}\,\bar{N}^{9.6}\,\frac{(T_h^2 - T_c^2)}{2} + \frac{8.33\times10^{-2}\,\sigma N}{(\frac{2}{\epsilon}-1)\bar{N}(N-1)}(T_h^4 - T_c^4)\right]$$

$$= 60\left[\frac{3.007\times10^{-25}\,\bar{N}^{9.6}}{2N}(T_h^2 - T_c^2) + \frac{8.33\times10^{-2}\,\sigma\,(T_h^4 - T_c^4)}{(\frac{2}{\epsilon}-1)(N-1)}\right]$$

$$= 60\left[\frac{(3.007\times10^{-25})(77)^{9.6}}{2}\,\frac{(T_h^2 - T_c^2)}{N} + \frac{(8.33\times10^{-2})(1.714\times10^{-9})}{(\frac{2}{.07}-1)}\,\frac{T_h^4 - T_c^4}{N-1}\right]$$

$$= 60\left[1.938\times10^{-7}\,\frac{T_h^2 - T_c^2}{N} + 5.178\times10^{-12}\,\frac{T_h^4 - T_c^4}{N-1}\right]$$

$$= 1.163\times10^{-5}\,\frac{T_h^2 - T_c^2}{N} + 3.108\times10^{-10}\,\frac{T_h^4 - T_c^4}{N-1}$$

for LN_2 loads, $T_h = 540$ R, $T_c = 144$ R: $\dot{q}''_{LN_2} = \frac{3.15}{N} + \frac{26.3}{N-1}$

for LHe loads, $T_h = 144$ R, $T_c = 8$ R: $\dot{q}''_{LHe} = \frac{\overset{(.282)}{.240}}{N} + \frac{\overset{(.184)}{.134}}{N-1}$

Nitrogen radiation loads: $\dot{q}_{LN_2} = 3.15\left[\frac{A_{sp}}{N_{sp}} + \frac{A_{ir}}{N_{ir}} + \frac{A_{or}}{N_{or}} + \frac{A_{st}}{N_{st}}\right]$

$$+ 26.3\left[\frac{A_{sp}}{N_{sp}-1} + \frac{A_{ir}}{N_{ir}-1} + \frac{A_{or}}{N_{or}-1} + \frac{A_{st}}{N_{st}-1}\right]$$

Helium radiation loads: $\dot{q}_{LHe} = .240\left[\frac{A_{sp}}{N'_{sp}} + \frac{A_{ir}}{N'_{ir}} + \frac{A_{or}}{N'_{or}} + \frac{A_{st}}{N'_{st}}\right]$

$$+ .134\left[\frac{A_{sp}}{N'_{sp}-1} + \frac{A_{ir}}{N'_{ir}-1} + \frac{A_{or}}{N'_{or}-1} + \frac{A_{st}}{N'_{st}-1}\right]$$

$$\frac{A_{sp}}{N_{sp}} = \frac{A_{sp}}{N'_{sp}} = \frac{10.14}{20} = .507 \qquad \frac{A_{sp}}{N_{sp}-1} = .534$$

$$\frac{A_{ic}}{N_{ic}} = \frac{A_{ic}}{N'_{ic}} = \frac{4.02}{10} = .402 \qquad \frac{A_{ic}}{N_{ic}-1} = .447$$

$$\frac{A_{oc}}{N_{oc}} = \frac{A_{oc}}{N'_{oc}} = \frac{8.09}{20} = .405 \qquad \frac{A_{oc}}{N_{oc}-1} = .426$$

$$\frac{A_{st}}{N_{st}} = \frac{6.96}{30} = .232 \qquad \frac{A_{st}}{N'_{st}} = \frac{6.96}{10} = .696 \qquad \frac{A_{st}}{N_{st}-1} = .24 \qquad \frac{A_{st}}{N'_{st}-1} = .773$$

$$\dot{q}_{LN_2} = 3.15\left[.507 + .402 + .405 + .232\right] + 26.3\left[.534 + .447 + .426 + .24\right]$$

$$= 48.2 \text{ BTU/hr} = 14 \text{ W}$$

$$\dot{q}_{He} = .240\left[.507 + .402 + .405 + .696\right] + .134\left[.534 + .447 + .426 + .773\right]$$

$$= .775 \text{ BTU/hr} = .227 \text{ W}$$

Heat transfer to helium after loss of vacuum

Assume that the vacuum vessel suddenly disappears, and the entire cold mass is exposed to air. The outer surface of the cryostat walls will instantaneously go to 90K, the temperature of liquid air. The steady state heat load is

$$\frac{\dot{Q}}{A} = -k\frac{dT}{dx}$$

through the steel vessel $\frac{\dot{Q}L_s}{A} = \int_{T_i}^{90K} k_s dT$

and through the ground insulation $\frac{\dot{Q}L_i}{A} = \int_{4.5}^{T_i} k_i dT$

T_i is determined from $\frac{1}{L_s}\int_{T_i}^{90} k_s dT = \frac{1}{L_i}\int_{4.5}^{T_i} k_i dT = \frac{\dot{Q}}{A}$

where T_i = temperature at the interface between steel and ground insulation.

For 304L SS, $k(T) \sim .1T$ W/m-K, T in Kelvin

Conductivity and integrals are shown in the table.

T (K)	k_{304} (W/m·K)	k_{G10} (W/m·K)	$\int k_{304}\,dT$ (W/m)	$\int k_{G10}\,dT$ (W/m)
4.5	.45	.069	0	0
5	.5	.074	.238	.036
6	.6	.084	.788	.115
7	.7	.093	1.44	.203
8	.8	.100	2.19	.300
9	.9	.107	3.04	.404
10	1.0	.114	3.99	.514
12	1.2	.125	6.19	.753
14	1.4	.135	8.79	1.01
16	1.6	.144	11.8	1.29
18	1.8	.152	15.2	1.59
20	2.0	.160	19.0	1.90
25	2.5	.176	30.2	2.74
30	3.0	.190	44.0	3.65
35	3.5	.203	60.2	4.64
40	4.0	.214	79.0	5.68
45	4.5	.224	100.0	6.78
50	5.0	.233	124.0	7.92
60	6.0	.250	179.0	10.3
70	7.0	.264	244.0	12.9
80	8.0	.277	319.0	15.6
90	9.0	.289	404.0	18.4

All around the bobbin winding, $L_i = .00940\,m$ (.037 in)

at bobbin : $L_s = .00965\,m$
side plate : $L_s = .0167\,m$
outer ring : $L_s = .0191\,m$

$$\text{so} \quad \int_{T_i}^{90} k_{304}\,dT = \frac{.00965}{.00094} \int_{4.5}^{T_i} k_{G10}\,dT = 10.3 \int_{4.5}^{T_i} k_{G10}\,dT$$

at inner ring, $T_L = 75K$ at steady state, assume same for bobbin and side plate as well.

$$\text{so } \frac{Q}{A}\Big|_{ss} = \frac{1}{.000940}\int_{4.5}^{75} k_{G10}\,dT = 1.52\ W/cm^2$$

$$k_{eff} = \frac{Q}{A}\Big|_{ss}\frac{L}{\Delta T} = \left(1.52\ \frac{W}{cm^2}\right)\left(.00094 + .00965\right)\left(\frac{1}{85}\right)$$

$$= 1.88\ W/m\text{-}K$$

For transient response, ~~all~~ assume all heat stored in steel, furthermore assume no heat conducted out until steady-state reached to get shortest possible time for steel to warm from 4.5 to 90 K.

Take solution from Heissler chart for slab with both sides subjected to temperature change (center plane insulated). To get α, evaluate c at temperature corresponding to k_{eff}, ie, @ 19 K:

$$c = 4.2\ J/kg\text{-}K$$

$$\rho = 7800\ kg/m^3$$

$$k = 1.88\ W/m\text{-}K$$

$$\alpha = \frac{k}{\rho c} = 5.7\times10^{-5}\ m^2/sec$$

from Heissler chart, steady state reached when

$$\frac{\alpha t}{L^2} \approx 1.5$$

$$t = 1.5 \frac{L^2}{\alpha}$$

$L = .00965\,m$
$\alpha = 5.7 \times 10^{-5}\ m^2/s$

$t = 2.5$ seconds

Area of cryostat $\approx 2 \times 10^4\ cm^2$

Total heat rate $= \left(1.52 \frac{W}{cm^2}\right)\left(2 \times 10^4\ cm^2\right) = 31\ kW$

Max after 1 second (after which heat transfer rate to helium reduced because of gas present) is, assuming linear ramp to steady state, 12.5 kW, which is only 10% of I^2R heating, maximum.

Extreme conservatism of analysis says that heating from loss of vacuum is small and delayed til after helium all gone.

Estimate of heat transfer coefficients for cooldown/warmup models:

Assumptions: all helium flows in annular passage between conductor pack and outer ring

curvature of annulus is insignificant w.r.t. validity of heat transfer correlations for flow in straight ducts (annulus is treated like straight rectangular duct)

effect of temperature variable properties on correlations ignored

Hydraulic diameter of annulus:

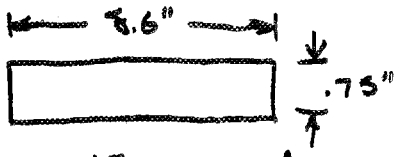

$$D_h = \frac{4A_c}{P_w} = \frac{4\left[\left(\frac{8.6}{12}\right)\left(\frac{.75}{12}\right)\right]}{2\left[8.6+.75\right]/12} = .115\,ft$$

length of passage $= \frac{1}{2}\pi d_a$ $\quad d_a =$ diameter of annulus $\sim$ ~~14"~~ 28" = ~~1.17 ft~~ 2.34 ft

$$L = \left(\tfrac{1}{2}\right)(\pi)(\cancel{1.17}\ 2.34) = \cancel{1.83\,ft}\ 3.68\,ft$$

$L/D =$ ~~15.9~~ 32.0 $\Rightarrow$ developing momentum boundary layer, and since Prandtl number ~ 1, developing thermal boundary layer as well

Reynolds number: $Re_D = \dfrac{\rho V D_h}{\mu}$; $\rho V = \dfrac{\dot m}{A_c}$; $\dfrac{D_h}{A_c} = \dfrac{4}{P_w}$

so $Re_D = \dfrac{4\dot m}{\mu P_w}$ $\qquad P_w = 1.56\,ft$

Temp range (K)	Flow rate / ½ coil (g/sec)	viscosity range ($lb_m/ft\,sec$)	Re_D
300 - 85	3.375	$13.4 - 5.25\times10^{-6}$	1420 - 3640
85 - 50	2.125	$5.25 - 4.27\times10^{-6}$	2290 - 2810
55 - 25	1.688	$4.56 - 2.78\times10^{-6}$	2090 - 3430
30 - 10	1.25	$3.15 - 1.52\times10^{-6}$	2240 - 4650
15 - 4.5	1.00	$2.09 - .863\times10^{-6}$	2720 - 6600

Reynolds number essentially in transition regime between laminar, turbulent flow. Curved passage is flow stabilizer, so assume flow is laminar, developing ~~entry~~ momentum and thermal boundary layers.

from Kays, <u>Convective Heat and Mass Transfer</u>:

since aspect ratio so high, take solution for entry length between parallel planes.

Then

$$Nu_x = \frac{\sum_{n=0}^{3} G_n \exp(-\lambda_n^2 x^+)}{2 \sum_{n=0}^{3} (G_n/\lambda_n^2) \exp(-\lambda_n^2 x^+)}$$

where $x^+ = \dfrac{2\,(x/D_h)}{Re_D Pr}$

and.

n	λ_n^2	G_n
0	15.09	1.717
1	171.3	1.139
2	498.	0.952

in annulus, x varies from 0 to 3.68 ft

$D_h = .115$

$Pr \sim .7$

take average $Re \sim 3000$

so x^+ varies from 0 to .030

There are seven nodal stations around complex model, so look at Nu_x for:

x^+	Nu_x
.0	15.6
.005	9.93
.010	8.52
.015	7.98
.020	7.75
.025	7.64
.030	7.59

$$\overline{Nu} = \frac{1}{L^+}\int_0^L Nu_x \, dx^+ = 8.90$$

Then heat transfer coefficient computed (accounting for temperature differences) from

$$h = \frac{k}{D_h} Nu_x$$

Resistance is calculated by dividing resistance entry in ~~[illegible]~~ resistor data by table entry to get:

$$R = \frac{1}{hA} = \frac{D_h}{k A Nu_x}$$

Let resistor entry $= \dfrac{D_h}{A Nu_x}$

and get variable temperature effect by putting k vs T table entry.

APPENDIX B-5 EBT-P TECHNICAL NOTE # EBT-P-TN-008
21 September 1981

MIRROR COIL X-RAY SHIELD OPTIMIZATION

PREPARED BY G. E. Taylor

APPROVED BY R. J. DANNENMUELLER

APPROVED BY R. E. JUHALA

APPROVED BY for H. F. IMSTER

1.0 SUMMARY: This technical note was prepared to optimize the magnet x-ray shield. The use of tungsten as a magnet shielding material is a very costly design option. The expense would be justified if it were necessary to assure magnet operation or if it saved significantly in magnet refrigeration requirements. However, an all-lead shield design with the same physical envelope will limit x-ray heating of the magnet cold mass to much less than the 10 watts upgrade design criterion. The use of tungsten, as in the baseline concept, decreases x-ray heating by less than a watt at a cost of nearly 3/4 million dollars. On this basis MDAC recommends that an all lead shield be officially adopted as the magnet shielding concept.

The study from which the above conclusions are drawn analyzed several design options including the baseline and the all-lead concepts. An all lead design is preferred due to reduced development, ease of fabrication, reduced costs, and more than sufficient x-ray protection. Second in preference is to mold tungsten into the lead sides adjacent to the inboard limiters. This design reduces total x-ray heating to about the same as the baseline and has the advantages of reducing the tungsten by 75%, easing manufacture and manufacturing tolerances of the tungsten parts, and reducing the peak heating rate by 20% over the baseline. It is still far more complex than the all-lead option. Last in preference of the designs analyzed was the baseline or tungsten throat design. This design requires that the tungsten be manufactured in a complex shape with tight dimensional tolerances. It places the tungsten in an area of minimal x-ray flux and thus makes inefficient use of its shielding ability. Additional development will be required if it is necessary to attach coolant channels to the throat. The design also does little to reduce the peak heating caused by the localized x-ray sources at the inboard limiters.

MDAC does not feel that the increased complexity and cost of a tungsten/lead shield concept can be justified. MDAC recommends that as much shielding be retained as practical while assuring that EBT-P meets optimum physics parameters. The reduced calculated heating provides an additional margin for the stable operation of the magnets and insurance against uncertainties in the physics models used to calculate x-ray intensities.

2.0 SHIELD ANALYSIS MODEL: The calculations were performed by a point kernal shielding code which models the limiters and e-rings as isotropic point source elements distributed in three dimensional space. The shielding was modeled as a series of solid rings. The limiters were not considered to provide shielding although they will provide significant protection, especially against low energy gammas.

2.1 X-Ray Distribution: The x-ray energy distribution is assumed to be that calculated by the MDAC Physics Staff for 2% Al impurity and 2 MeV ring temperature. The total integrated source power is rounded up to 100 watts from 95.7 watts per cavity. All sources are taken as isotropic. This is conservative since any angular concentration of x-rays would tend to be directed radially out of the torus and not toward the cold mass.

2.2 X-Ray Analysis: The x-ray analysis was done by conventional point kernal method. The point kernal is an accurate method of calculating doses and heating provided that reflected gammas are not a dominant contributing factor. The cold mass itself is protected from external reflected sources by a significant thickness of stainless steel which is excellent shielding material against low energy gammas. Any significant reflected flux must come from the magnet dewar and cold mass. Gammas reflected more than 90° have already deposited most of their energy. Therefore, with the conservatisms already built into the calculations, these gammas are not deemed significant.

Figure 1 defines the coordinate system used in the x-ray calculations. The cold mass is divided into volume elements ($r dr d\theta dz$), each of which is considered a target. The limiters are taken as point sources for two reasons. First, the angular and radial distribution of electrons impinging on the limiters is largely unknown. Secondly, treating the limiters as point sources is the worst case with respect to peak heating adding conservatism to the calculation. This has very little effect on total heat deposition since the cold mass intercepts nearly the same solid angle from any sources distributed angularly on the limiters. The electron rings are modeled as circular hoops divided into length elements ($r d\theta$).

The sources considered include both adjacent cavities. Cavities beyond these do not contribute significantly to the doses due to the distance and amount of material between them and the coil. The shielding envelope shown in Figure 2 is modeled as a series of solid rings bounded by r_{min}, r_{max}, z_{min}, and z_{max} as shown in Figures 3-5. For each source/target element combination an effective shield thickness is calculated and attenuation for each of six energy groups is found. The formulation used for each energy group is

$$\dot{D}_E = ((10^5)\ \frac{\mu_a}{\rho}\ P\ B_p(\mu s)/4\pi r^2)\ e^{-\mu s}[f(E)]_{E_1}^{E_2}\ (\text{rad/s})\ .$$

$\frac{\mu_a}{\rho}$ = mass absorption coefficient of target for energy group E

P = x-ray power emitted from source element (in watts)

$B_p(\mu s)$ = empirical secondary flux buildup factor

s = effective shield thickness

r = total distance between source and target

$\dot{D}_E$ = dose rate in rad/s for energy group E

f(E) = normalized energy distribution function

For each target element, contributions to dose are summed over all energy groups and for all source elements to find the total local dose rate. The dose rate is multiplied by the local density to find the heating in the target element. The heating of the target element is summed to find the total heating of the cold mass which includes the conductor, bobbin, and closeout. In one calculation of dose rates the conductor was considered to provide no attenuation. This calculation was provided for conservatism although the resultant heating distribution is unrealistically even across the coil pack. To provide a more realistic, even though, less conservative result the effective attenuation through the conductor to the target was also included.

2.3 X-Ray Code: The x-ray code prints a distribution of dose rates around the magnet at different radii and depths into the magnet. A finer grid of dose rates is calculated at the inboard horizontal midplane of the coil pack since this is where the highest dose rates occur. Peak localized x-ray heating in the conductor was then calculated to be 0.13 milliwatts/cm^3 for the all-lead shield. The heating distribution along outer corner of the conductor is compared for four cases in Figure 6.

3.0 ANALYSIS: Several conclusions can be drawn from the distribution in Figure 6. Ignoring the 5° cant of the electron rings, their contribution to heating is a constant with respect to theta. Therefore, the peaks and valleys are due to the limiter sources. The peak at 0° is due to the close proximity of the limiters and the small angle of the x-rays incident on the shield. This indicates that the most effective location for tungsten in the shield is in the side plates adjacent to the inboard limiters. It is also worth noting that the marked peak at 0° is due to the treatment of limiters as point sources. Since the limiter sources actually have some angular distribution, the peak is lower and the heating distributed over a greater volume than indicated.

Beyond 90° around the magnet, x-rays from the inboard limiters become more incident on the throat of the shield where the thickness is only .75 inch, causing the heating to increase slightly. Therefore, more efficient use could be made of the throat shielding if material were removed from the inboard and moved to the outboard. This can be accomplished by moving the shield bore and toroidal vessel slightly inboard (see Figure 7). The results of this change are shown as Option 4 in Table 1. The same toroidal vessel clear bore and magnet alignment clearance are maintained and additional flux lines for passing particles are cleared by this approach. The disadvantages here are that some of the clearance for throat launch ECRH guides has been eliminated and the toroidal vessel throat is nonconcentric with its flange.

An all-lead design has been developed which reduces the mean throat thickness from .75 to about 0.6 inches (see Figure 8). In this design the S.S. toroidal vessel clears the 16.5 cm flux line inboard and opens additional volume outboard for the throat launch ECRH upgrade. This does not increase the peak heating above the non-concentric option, however, it does increase total heating by about 0.3 watts. The impact of trimming the sides of the shield back to the original 1.25 inches was assessed and found to increase total heating by about 0.15 watts.

4.0 CONCLUSION: A detailed study of local dose and heating rates throughout the magnet cold mass has been completed. Two considerations germane to the shield design are total heat deposition in the cold mass and the maximum local heating rate. A preliminary analysis of photoneutrons indicates insignificant contributions to dose and heating of the cold mass compared to x-rays. A number of shielding options were examined in the study to provide data for design selection. All options studied resulted in significantly less than 10 watts total heating. The baseline shield configuration with the full tungsten throat proved to be an inefficient design. In this design a large volume of tungsten is placed in the throat where the x-ray flux is the least and the tungsten has little effect on peak heating. Placing the tungsten in the side of the shield adjacent to the inboard limiters reduces the overall heating about the same as the baseline but uses only a quarter of the tungsten. This also cuts peak heating to 66% of an all lead design. However, even for the all lead designs, both concentric and non-concentric, the peak heating rates are so small that further reduction appears to be unnecessary. The calculated heat transfer rate is far below that required to cause boiling in the liquid helium. The expense and complication of having tungsten in the shield is, therefore, not justified by the present understanding of source distributions and strengths.

TABLE 1.: 90 GH_z MIRROR COIL X-RAY HEATING SUMMARY

Option	Description	Total Heating (watts)	Coil & Closeout watts	Bobbin watts	Max Coil Heating mwatts/cm^3	Tungsten Required Kg/magnet
1	Tungsten Throat	1.99	0.60	1.39	0.10	162
2	All Lead	2.31	0.85	1.46	0.13	0
3	Tungsten Side Insert	2.08	0.69	1.39	0.08	43
4	All Lead .30" offset bore	2.12	0.78	1.34	0.16	0
5	All Lead, .60" mean throat thickness	2.49	1.00	1.49	0.16	0

FIGURE 1.
COORDINATE SYSTEM FOR X-RAY HEATING CALCULATIONS

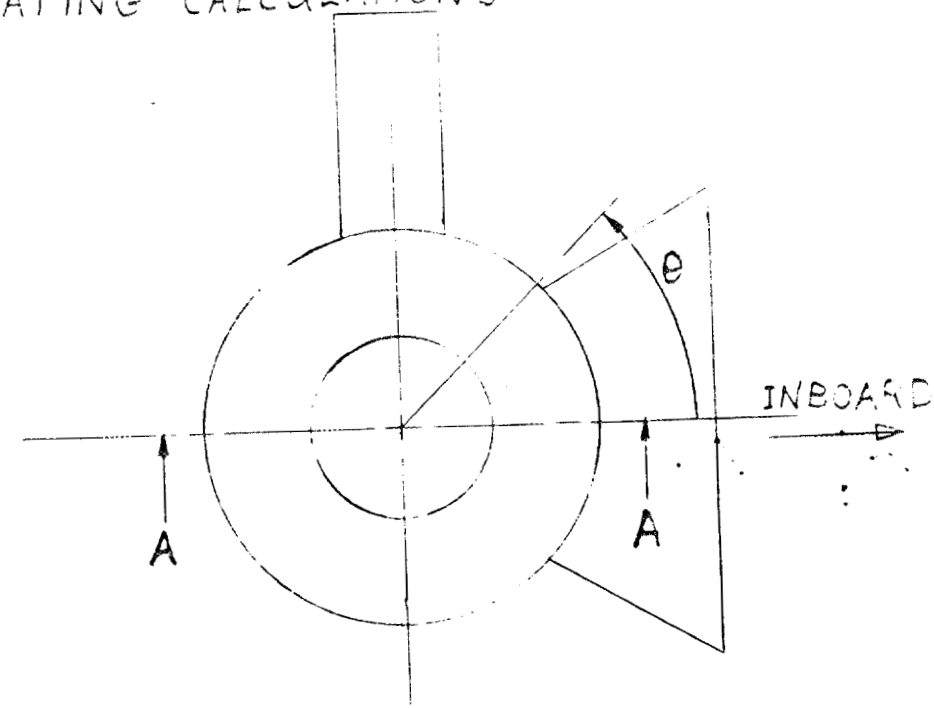

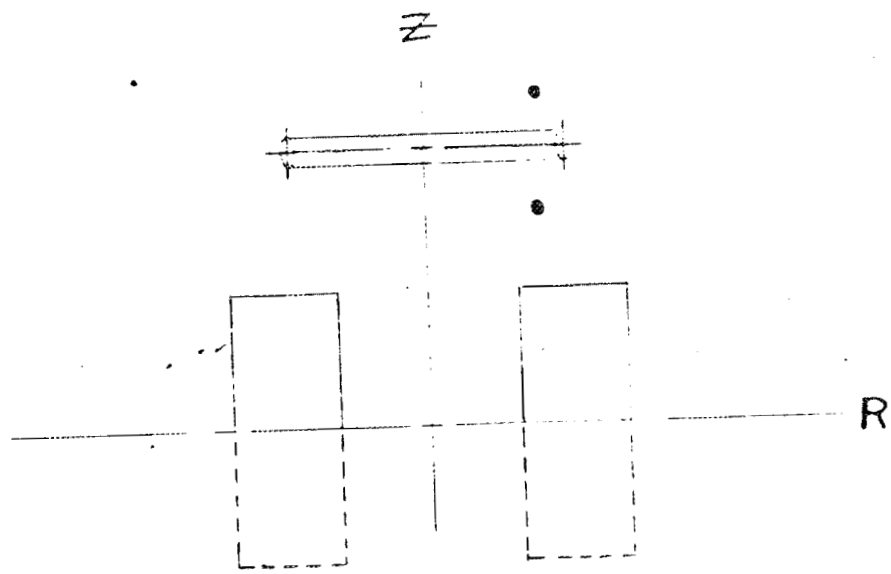

VIEW A-A
(COLD MASS AND X-RAY SOURCES

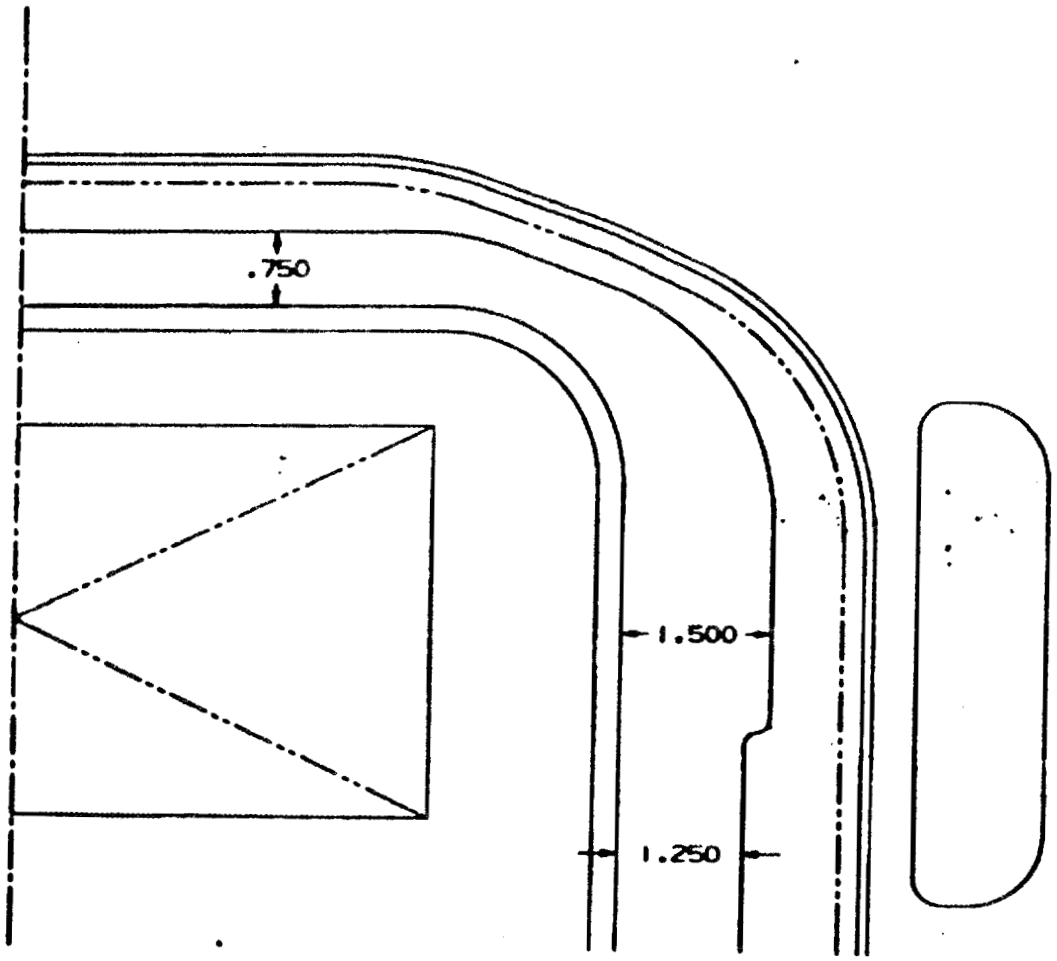

Figure 2.: MIRROR COIL X-RAY SHIELD ENVELOPE

Figure 3: OPTION 1; TUNGSTEN THROAT

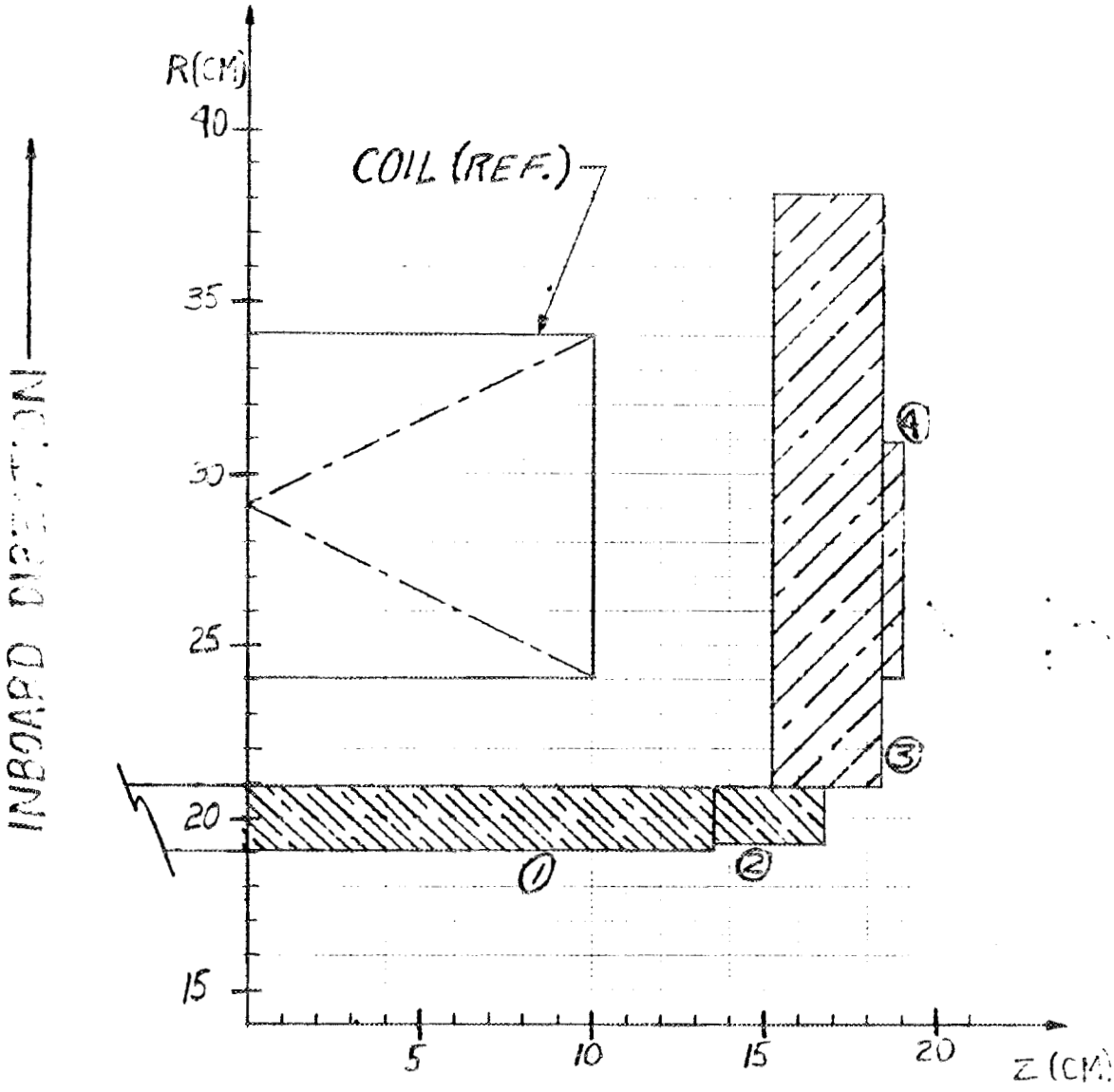

CYL. NO.	MATERIAL	Z_o	Z_i	R_o	R_i
1	TUNGSTEN	-13.59	13.59	19.05	20.95
2	TUNGSTEN	13.59	16.76	19.30	20.95
3	LEAD	15.24	18.42	20.95	38.10
4	LEAD	18.42	19.05	29.10	31.87

Figure 4: OPTION 2; ALL LEAD

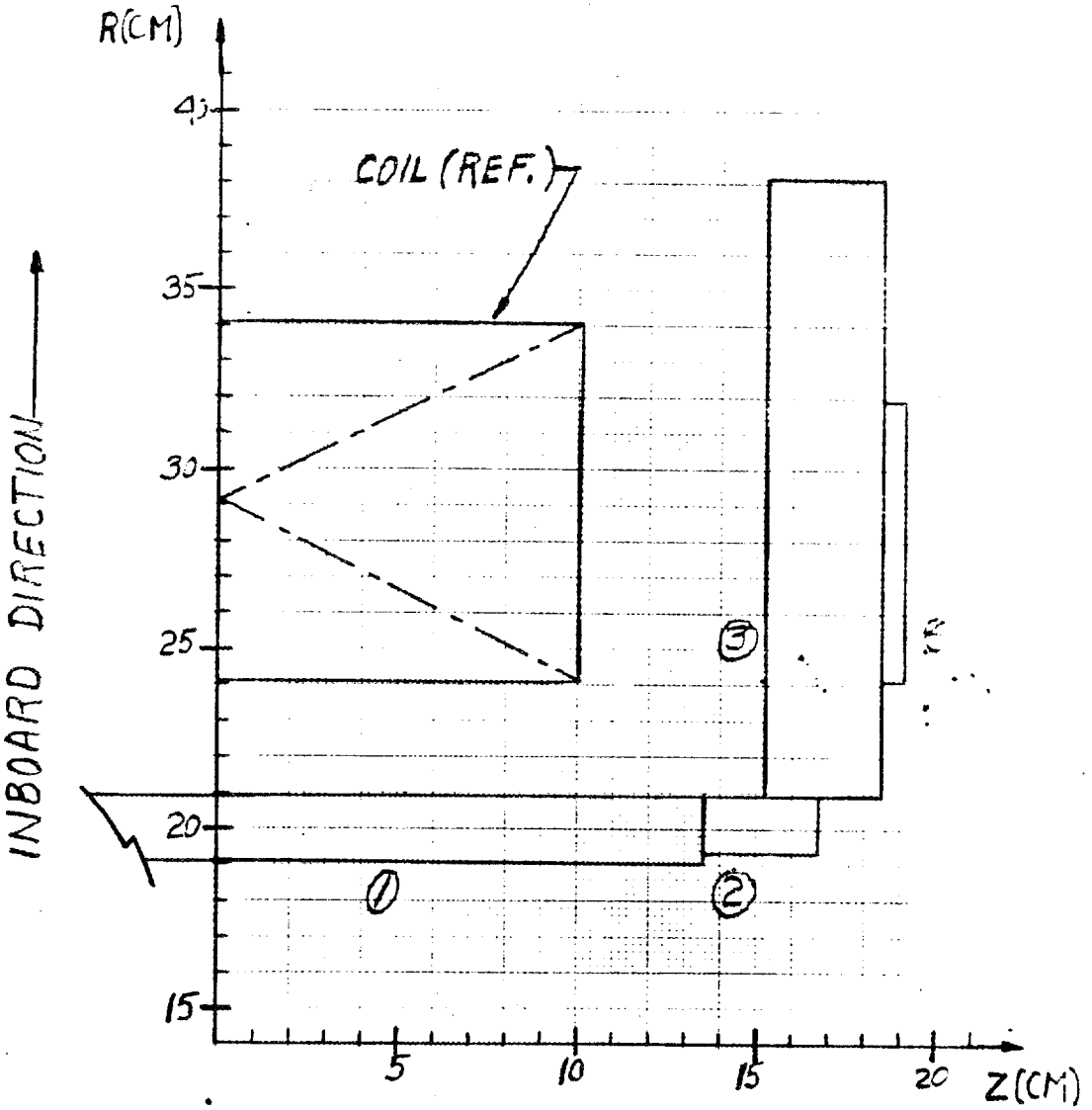

CYL. NO.	MATERIAL	Z_o	Z_i	R_o	R_i
1	LEAD	-13.59	13.59	19.05	20.95
2	LEAD	13.59	16.76	19.30	20.95
3	LEAD	15.24	18.42	20.95	38.10
4	LEAD	18.42	19.05	24.10	31.87

Figure 5: OPTION 3; TUNGSTEN INSERT

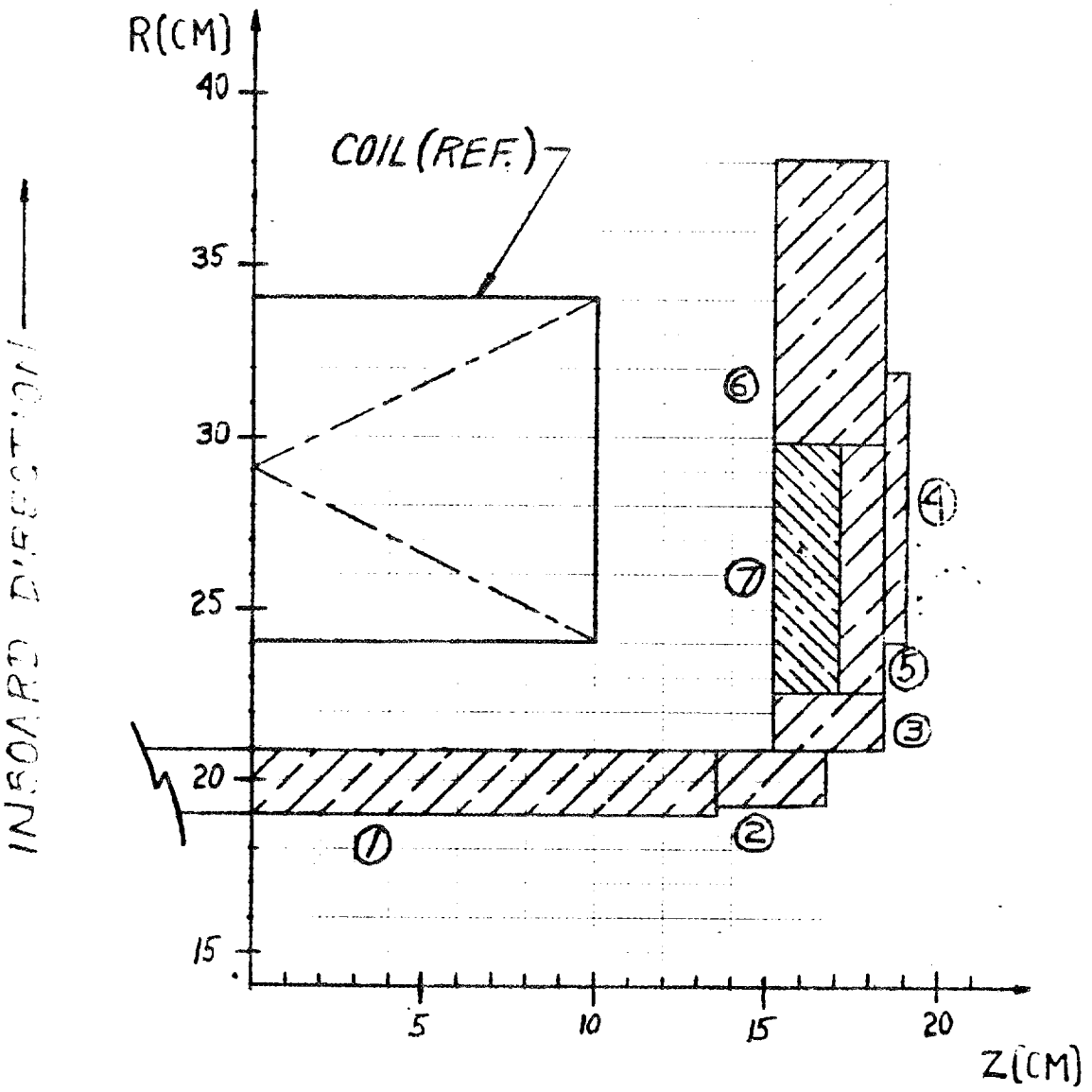

CYL. NO.	MATERIAL	Z_o	Z_i	R_o	R_i
1	LEAD	-13.59	13.59	19.05	20.95
2	LEAD	13.59	16.76	19.30	20.95
3	LEAD	15.24	18.42	20.95	22.61
4	LEAD	18.42	19.05	24.10	31.87
5	LEAD	17.15	18.42	22.61	29.86
6	LEAD	15.24	18.42	29.86	38.10
7	TUNGSTEN	15.24	17.15	22.61	29.86

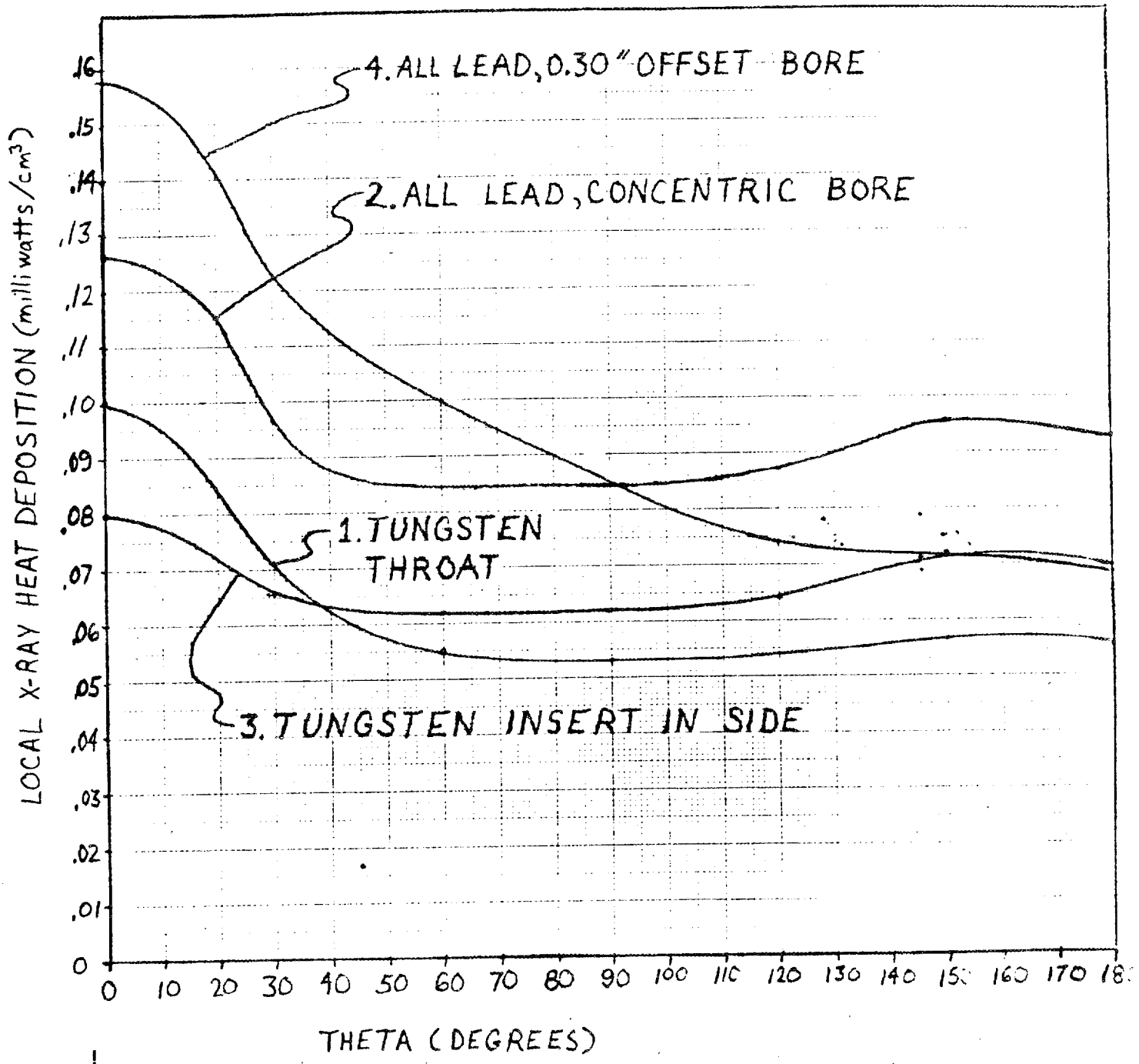

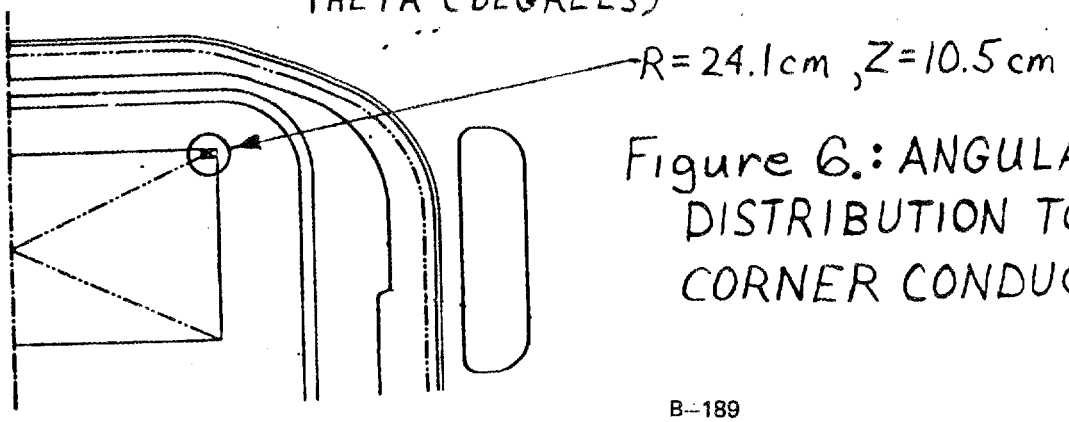

Figure 6.: ANGULAR HEATING DISTRIBUTION TO INSIDE CORNER CONDUCTOR

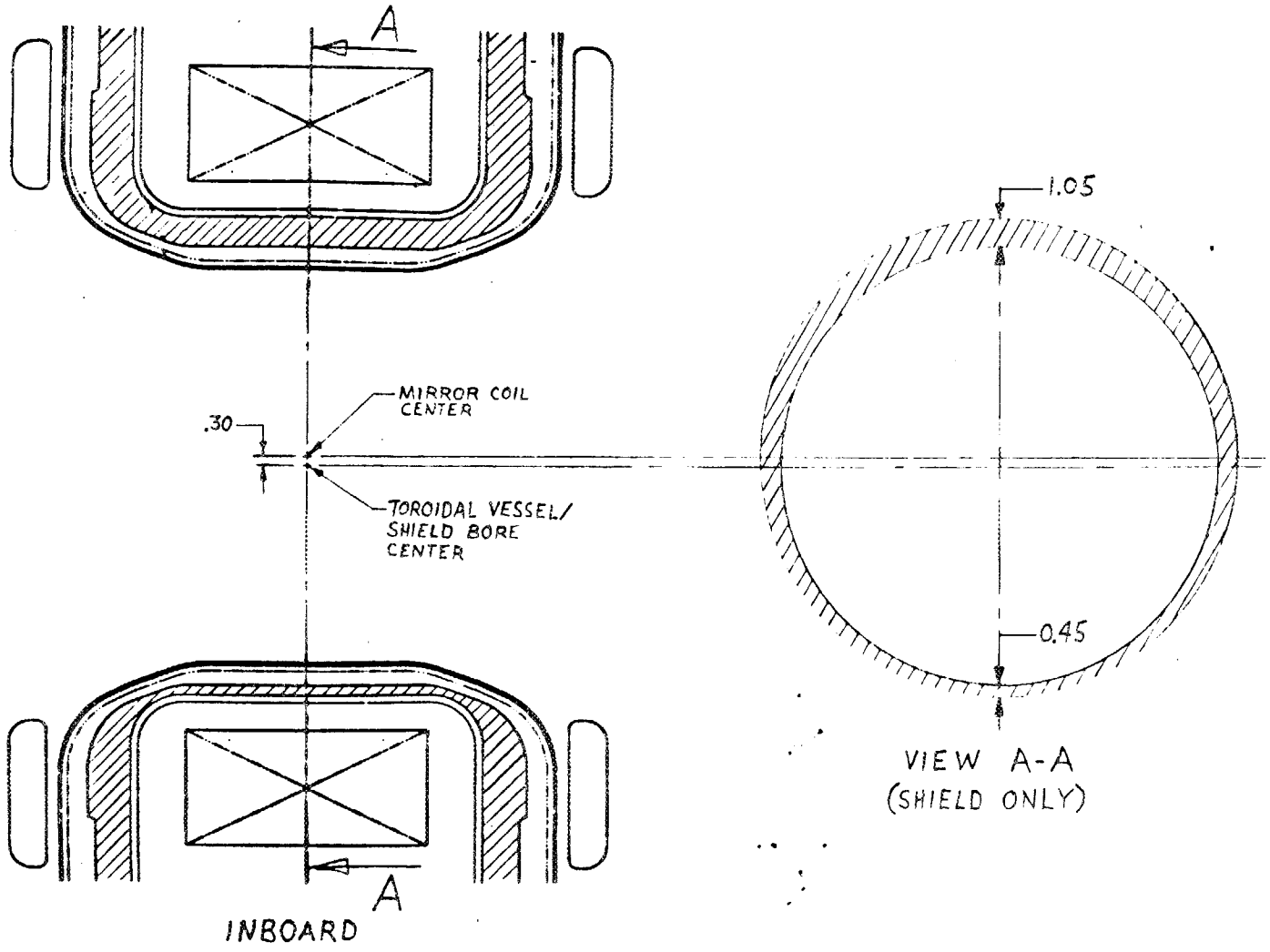

FIGURE 7. : MIRROR COIL X-RAY SHIELD OFFSET BORE ENVELOPE

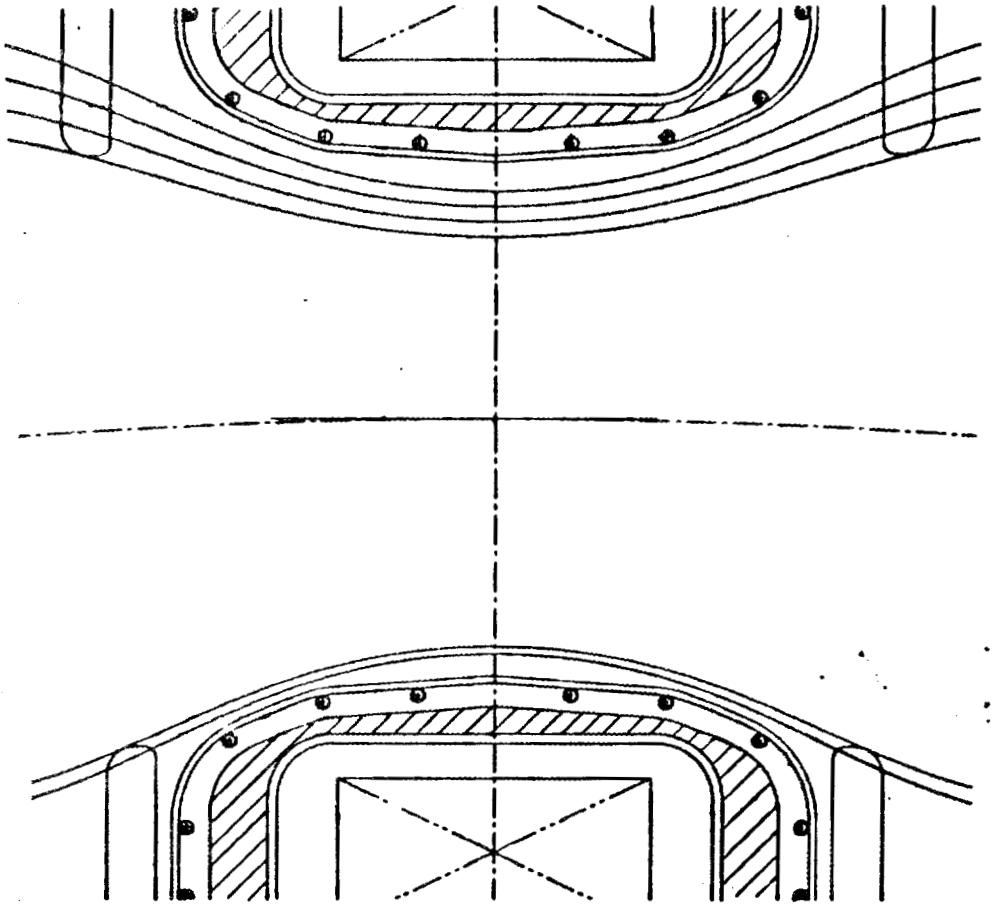

FIGURE 8. CONCENTRIC ALL LEAD SHIELD WITH MEAN THROAT THICKNESS OF 0.6 INCH CONTOURED FOR INCREASED PASSING PARTICLE FRACTION. (SHOWN WITH ALUMINUM VESSEL)

"This plan is preliminary and subject to further revisions and approval during Title II"

EBT-P TECHNICAL NOTE # TN-EBT-P-007

18 September 1981

MAGNETIC SYSTEM ALIGNMENT PLAN

PREPARED BY R. J. Dannenmueller

PREPARED BY J. L. Conlee

APPROVED BY R. E. Juhala

APPROVED BY H. F. Imster

MAGNETIC SYSTEM ALIGNMENT PLAN

This plan describes the proposed approach for the alignment of the mirror coils and supporting structure to limit the cumulative field error as expressed by the quantity of $\Delta B/B$ to 1×10^{-4} when averaged around the torus along the minor axis. The methodology for, and effect of alignment errors on the magnetic field for EBT-P are addressed in Attachments (1), (2), and (3). Systematic errors due to magnet fabrication, power distribution, winding configuration, etc., are addressed in Attachment (4).

The alignment plan described herein can be briefly summarized as follows:

1. Magnetic field measurements will be made on each coil to define axes location with respect to construction balls located on the dewar. (Magnetic axes to within $\pm$ 0.005 inches and $\pm$ 1.5 minutes angularity).
2. Aluminum bucking ring structures reference surfaces on the outer perimeter to be optically aligned to within 0.010 inches and vertical to within 0 degrees, 2 minutes.
3. All magnets are to be installed on the torus before starting alignment. A clearance of 0.30 inch is provided between the magnet base and aluminum ring. This allows for cummulative tolerance buildups and magnet adjustments of 0.17 inches or 0.5 degrees.
4. The magnets are aligned optically to within 0.005 inches.
5. 32 magnets are locked into position using tapered pins.
6. 4 magnets (one in each sector) are temporarily locked into position with jack screws.
7. The magnets are cooled and powered to TBD amperes. Alignment is verified and/or vernier adjustments are made on the 4 magnets with the use of an electron beam to determine field line closure.
8. The final 4 magnets are then permanently pinned in the aligned position.

The tooling bars and scopes required for alignment will be disassembled and removed following alignment verification. In order to provide for misalignments which may occur over the operating life of the machine due to settlements, stress relaxations, etc., it would be highly desireable to incorporate an in place detection scheme for locating suspect coils. It is MDAC's understanding that ORNL is currently exploring the possibility for using a toroidal winding for detecting flux linkages between the toroidal coil and the mirror coils which

are a measure of alignment error. If this technique has the required sensitivity, it would be highly desireable to incorporate it into the EBT-P design and alignment procedure as it could provide coil alignment status during device operation. Additionally, optical realignment of the mirror coils will be hindered after the installation of ARE coils.

Magnet Parameters Measurement

Fabrication tolerances of the magnet limit the magnetic axes angularity with respect to the mechanical axes of the dewar to within ± 9 minutes and coil radial displacement to within ± 0.040. The magnetic axes will be located with respect to construction balls on the dewar during acceptance testing at GDC. Construction ball location shall be as specified in Figure 1. The procedure and equipment required for magnetic field axis determination shall be specified via test data from the ORNL development test program. This plan assumes that the axes location can be identified to within ± 0.005 inches and ± 1.5 minutes angularity. Axes location is transferred to the dewar construction balls in accordance with the following procedures.

1. Move magnet into tooling set-up and adjust to the optical set-up per Figure 2.
   Note: Plane $\boxed{A}$ to be parallel to the vertical sweep plane of Transit #1 within 0.003 inches in 47.5 inches.
   Plane $\boxed{B}$ to be parallel to the vertical sweep plane of Transit #2 within 0.003 inches in 47.5 inches.
2. Obtain data necessary to relate probe contstruction balls (C/B's) to the exterior C/B's.
3. By analytic geometry, determine
   (a) distance from magnetic plane to C/B's.
   (b) distance from the other two orthogonal planes to the C/B's.
4. By analytic geometry, determine the array X, Y, and Z coordinates of the magnet exterior C/B's (assigned to a specific location). Enter array stations on chart, as shown in Figure 3.

Installation of Reference Construction Balls on Concrete Support Ring

The concrete bucking ring will be poured prior to the roof of the torus enclosure. This will allow a cure time of approximately 1 year prior to the

installation of construction balls which establish the torus X, Y, and Z axis datums. The stability of the concrete support ring after 1 year is shown in the cure time/contraction curve of Figure 4. Based on the Figure 4, approximately 91% of the total shrinkage due to drying will occur within the first year. For the concrete bucking ring the shrinkage will be symmetric. The columns will also be getting shorter. At a 40% relative humidity the estimated total change in radius of the concrete support ring is 0.0928 inch. After one year of curing, the concrete will shrink an additional 0.0084 inches. If the ambient relative humidity is 60% the additional change in radius after one year of curing will be 0.0067 inch. These estimates do not include the stainless steel rerods which can reduce the amount of shrinkage by 50%. Other factors that affect the amount of shrinkage are: amount of water per unit volume of concrete, amount of aggregate, size of aggregate, and type of aggregate. At the time alignment is done, updated estimates of the remaining symmetrical shrinkage will be taken into account in future measurements. Because of the symmetry, the residual shrinkage will not alter the accuracy of magnetic field closure. The construction balls will be installed per the following steps:

1. Set-up the optical system around the concrete support ring as shown in Figure 5, and set C/B's 2 and 4 on the lower surface of the concrete ring. The C/B's are to be located on the center of the concrete ring as determined by tape measurements, being cognizant of the location of the aluminum ring attach bolts. C/B's 2 and 4 now represent datum X 0.000. C/B 2 establishes datum Y 100.000.
2. Position C/B's 1 and 3 at datum Y +20.000 ± .003 per Figure 5.
3. Set C/B #5 on the inner vertical surface of the concrete ring. Use a tape to determine the center of ring height. C/B #5 will be Z 0.000 datum.

Aluminum Ring Segment Alignment

The aluminum ring is fabricated and installed in 9 segments. Each segment is aligned to the concrete bucking ring using four C/B's. The C/B's are aligned to within 0.010 inches and vertical to within zero degrees, 2 minutes. Ring segment fabrication tolerance will increase the mirror coil mounting surface tolerance to ± TBD inches and vertical to within TBD minutes.

1. Reposition tooling bar #2 in accordance with Figure 6.
2. Install ring segments 1 and 2 (Note: all ring segments may be installed at this time).
3. Adjust the upper and lower vertical screws as shown in Figure 7, such that the horizontal reference C/B's are at Z station 17.000 ± 0.010.
4. Adjust the radial jack screws and circumferential adjusting turnbuckle to place the reference C/B's at the desired X and Y stations for the specific segment within 0.010. The vertical reference C/B's must be vertical within 0.2 (0.0058" per 10").
5. Recheck for condition of Step 3. If out of tolerance, readjust per Step 3 and 4.
6. Reposition tooling bar #2 per Figure 8.
7. Repeat Step 2 through 5 for segments 3 and 4.
8. Reposition tooling bar #1 and 2 per Figure 9.
9. Repeat Step 2 thru 5 for segment 5 and 6.
10. Reposition tooling bar #2 per Figure 10.
11. Repeat Step 2 thru 5 for segment 7, 8, and 9.

Following alignment, the volume between the aluminum ring and concrete support ring will be filled with grouting to provide a solid interface between the two. If required, the aluminum ring will be supported to prevent movement during the grouting procedure. The grouting will be allowed to cure for TBD days before attachment of the magnets to the ring.

Magnet Alignment on Torus

All 36 magnets, the superstructure, and magnet protection system or simulating mass for the magnet protection system must be installed on the aluminum ring prior to the start of alignment. An initial clearance between the aluminum ring and magnet base is provided for adjustments of up to ± 0.3 inches and/or ± 0.5 degrees. The cryogenic system will be designed to accommodate ± 1.0 inch in any direction. The radial tolerance stack for bucking ring sturcture and magnet assembly is shown in Figure 11. Ten jacking screws are provided, to facilitate magnet alignment; six on the magnet base, and four on the aluminum ring, as shown in Figure 12. The magnets are mounted to the bucking ring using 1 inch bolts with spherical washers for self-alignment. An adjustment insert in the magnet base provides for the radial adjustment. These bolts are shown in Figure 13.

1. Reposition tooling bars #1 and 2 in accordance with Figure 6.
2. For magnet #1 at the 5° position, set outboard C/B at array stations (X, Y and Z) specified in Figure 3 within 0.005.
3. Set upper and lower C/B's on Magnet #1 to array stations (X, Y, and Z) specified in Figure 3 within 0.005 inches.
4. Recheck for Step 2 compliance, if out of tolerance, perform Step 2 and 3.
5. Align magnet 2 through 10 per the above to array stations specified in Figure 3 within 0.005 inches.
6. Reposition tooling bar #2 per Figure 8.
7. Align magnet 11 through 18.
8. Reposition tooling bars 1 and 2 per Figure 9.
9. Align magnet 19 through 28.
10. Reposition tooling bar #2 per Figure 10.
11. Align magnet 29 through 36.

Following alignment of the mirror coils, 32 coils are permanently pinned into position using four tapered pins as shown in Figure 14. The magnet base has been pre-drilled and reamed. The aluminum ring will be match drilled and reamed with the magnet base to accommodate the taper pins. The four remaining coils, one in each quadrant, are temporarily held into position using the jacking screws. These coils are to be utilized for vennier adjustments as required to effect field line closure. The out-of-plane supports are installed and torqued to approximately TBD% of design load. This is to prevent excessive out-of-plane stresses at the magnet base in the event of a quench and circuit breaker failure during subsequent alignment verification testing.

Alignment Verification

The alignment of the mirror coils on the torus will be verified and/or vennier adjustments made for verification with the magnets superconducting at a low field using the electron beam tracing method as utilized on EBT-I. A description of the technique is contained in Attachment (5). Following alignment verification, the final four magnets will be pinned into position in the manner previously described.

Installation Procedure for Out-of-Plane Struts

Alternating struts will be shortened by a small TBD hand applied torque to remove axial freeplay. Then the remaining struts will be shortened to remove their freeplay. The struts will be checked to make sure that there is no binding effecting the adjustment to a no lash condition. The struts will be in slight tension. The struts will be loaded further in tension by a uniform turn of the nut method. The order of adjustment is as described above for freeplay removal and the turn of the nut tightening will be done in two or more increments to the predetermined load level to assure as symmetric and uniform a loading as possible, which it is felt will result in the minimum disturbance of the original alignment. MDAC experience with preload control has shown the scatter of the order of ± 25 percent or more can occur using torque readings alone. For this reason the turn of the nut method, similar to that recommended in building steel construction, has been chosen to assure a repeatable specific shortening of the struts to supply a symmetric preloading with minimal influence on previous magnet alignments. The turn of the nut adjustments will be done with a torque wrench so that any anomalies can be spotted. The torque reading data can then be used as an adjunct to the turn of the nut method to adjust the struts attached to the last four magnets adjusted at quadrant ends or for any replacement magnet to assure uniform adjustment and minimal field error. The strut to dewar fitting bolts will then be tightened to a uniform torque. A locking feature will be utilized to prevent movement of the struts. The alignment of the magnets will then be spot checked. If any adjustments are required then the results of the alignment check will be used to judge what adjustment features will be moved.

MIRROR COIL CONSTRUCTION BALL LOCATIONS

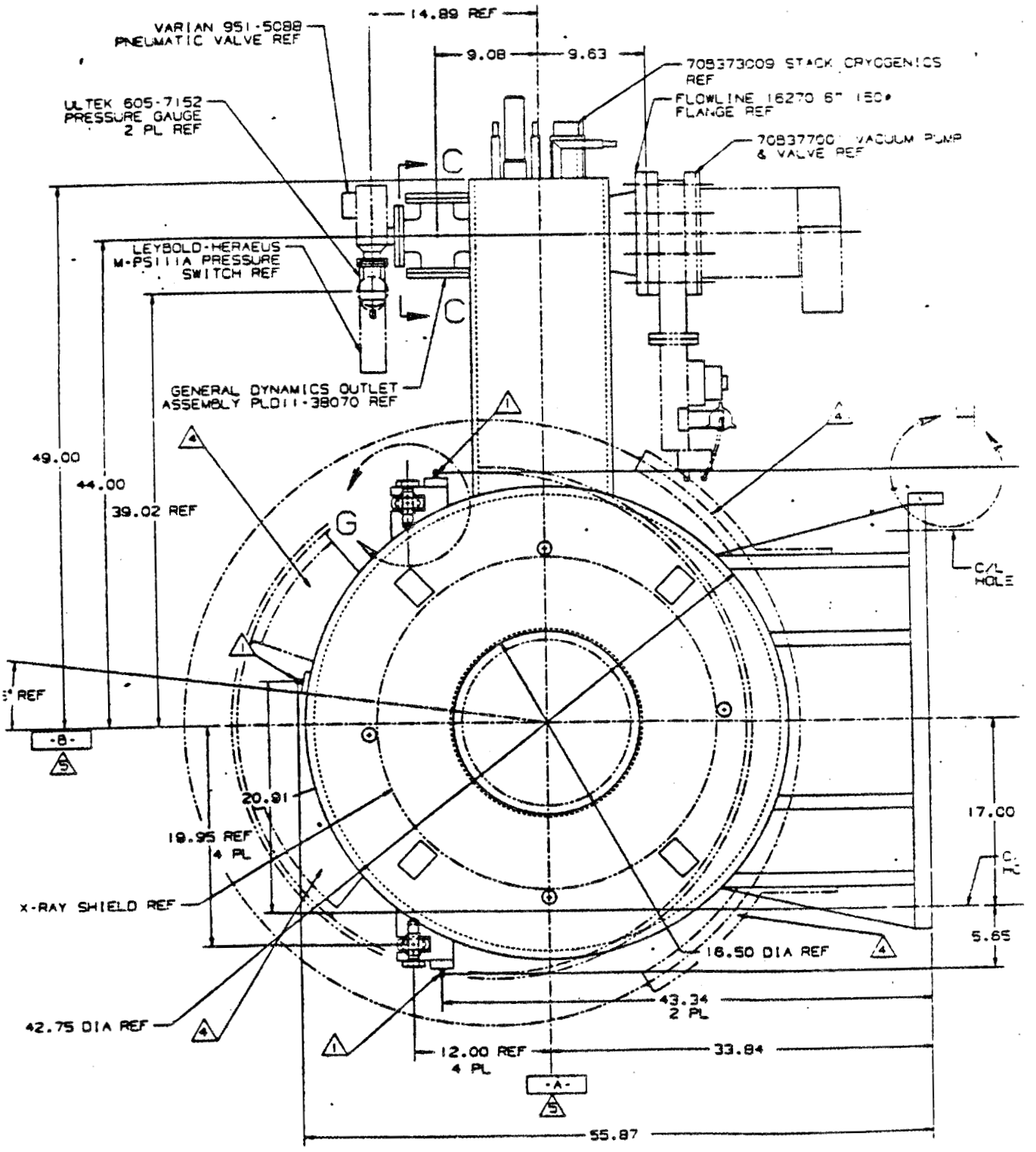

FIGURE 1.

OPTICAL SET-UP FOR MC CONSTRUCTION BALL STATION MEASUREMENTS

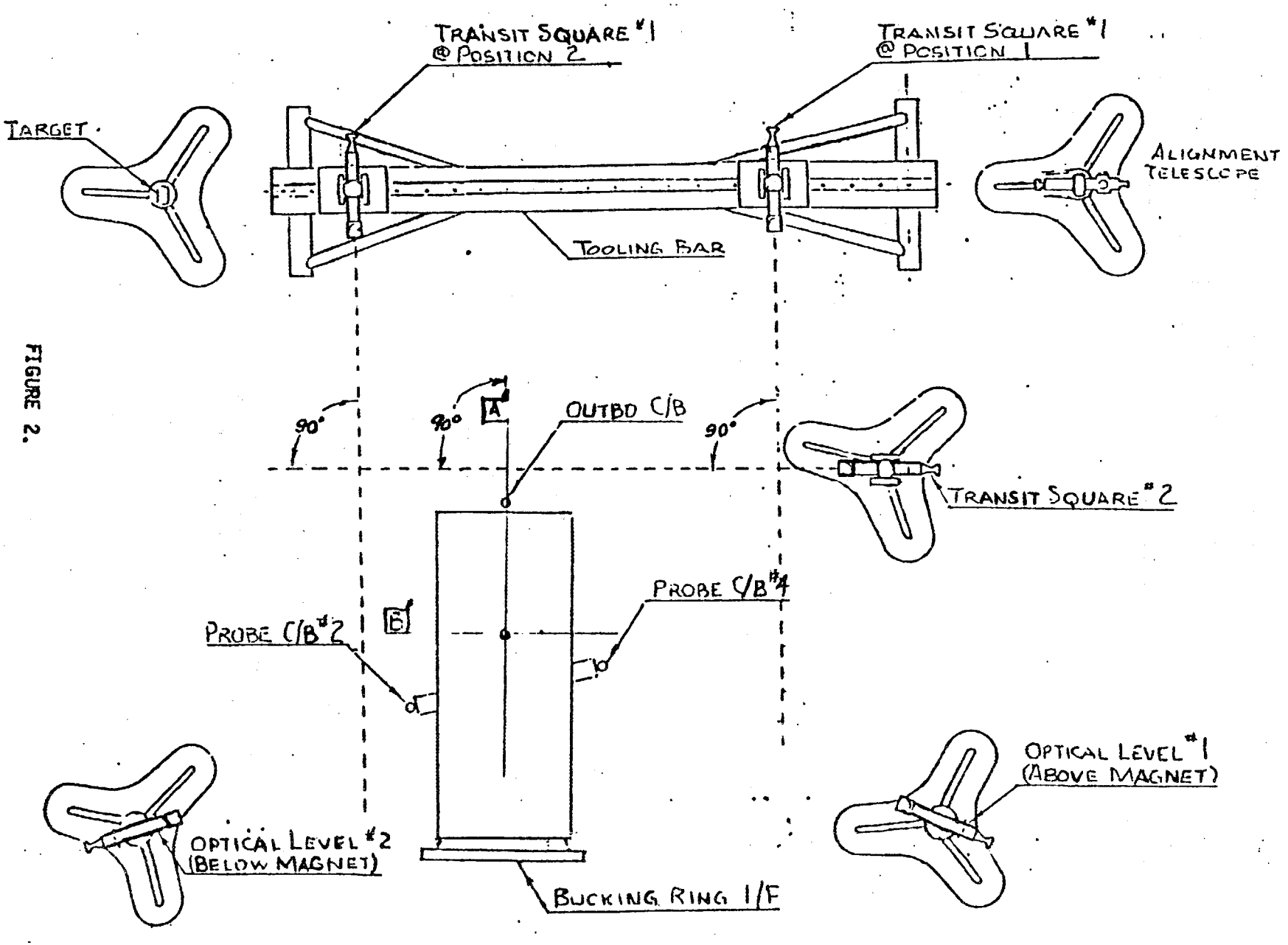

FIGURE 2.

MC C/B STATION ARRAY RECORD

No.	Magnet Position (Degree)	Magnet S/N	Upper C/B Array Station X Y Z	Lower C/B Array Station X Y Z	OUTBP C/B Array Station X Y Z
1	5				
2	15				
3	25				
4	35				
5	45				
6	55				
7	65				
8	75				
9	85				

FIGURE 3.

CONCRETE CURE TIME/CONTRACTION CURVE

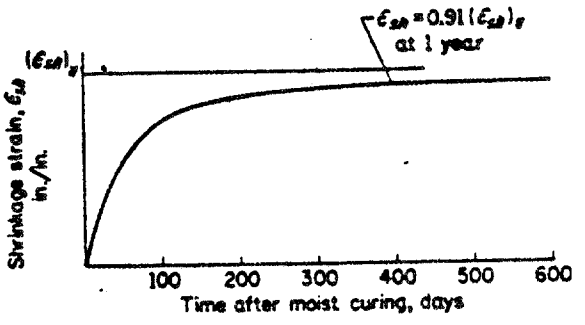

Standard shrinkage strain variation with time after moist curing (for 4 in. or less slump, 40% ambient relative humidity and minimum thickness of member 6 in. or less, after 7 days moist cured).

FIGURE 4.

SET-UP FOR OPTICAL INSTALLATION OF CONCRETE SUPPORT RING C/B'S

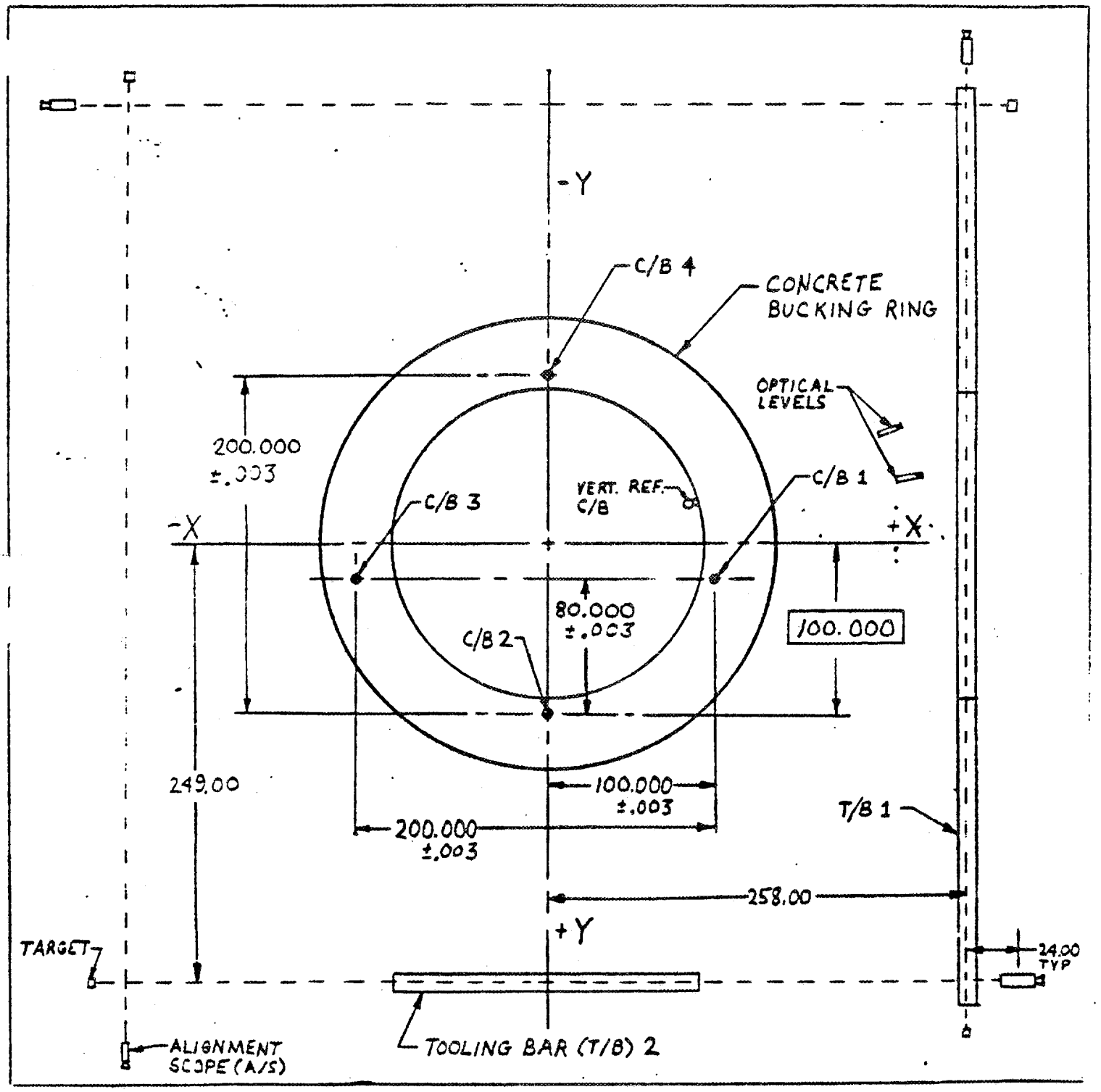

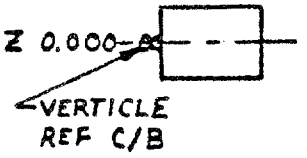

FIGURE 5.

OPTICAL SET-UP FOR INSTALLATION OF ALUMINUM RING SEGMENTS 1 AND 2 AND MAGNETS 2 THROUGH 10

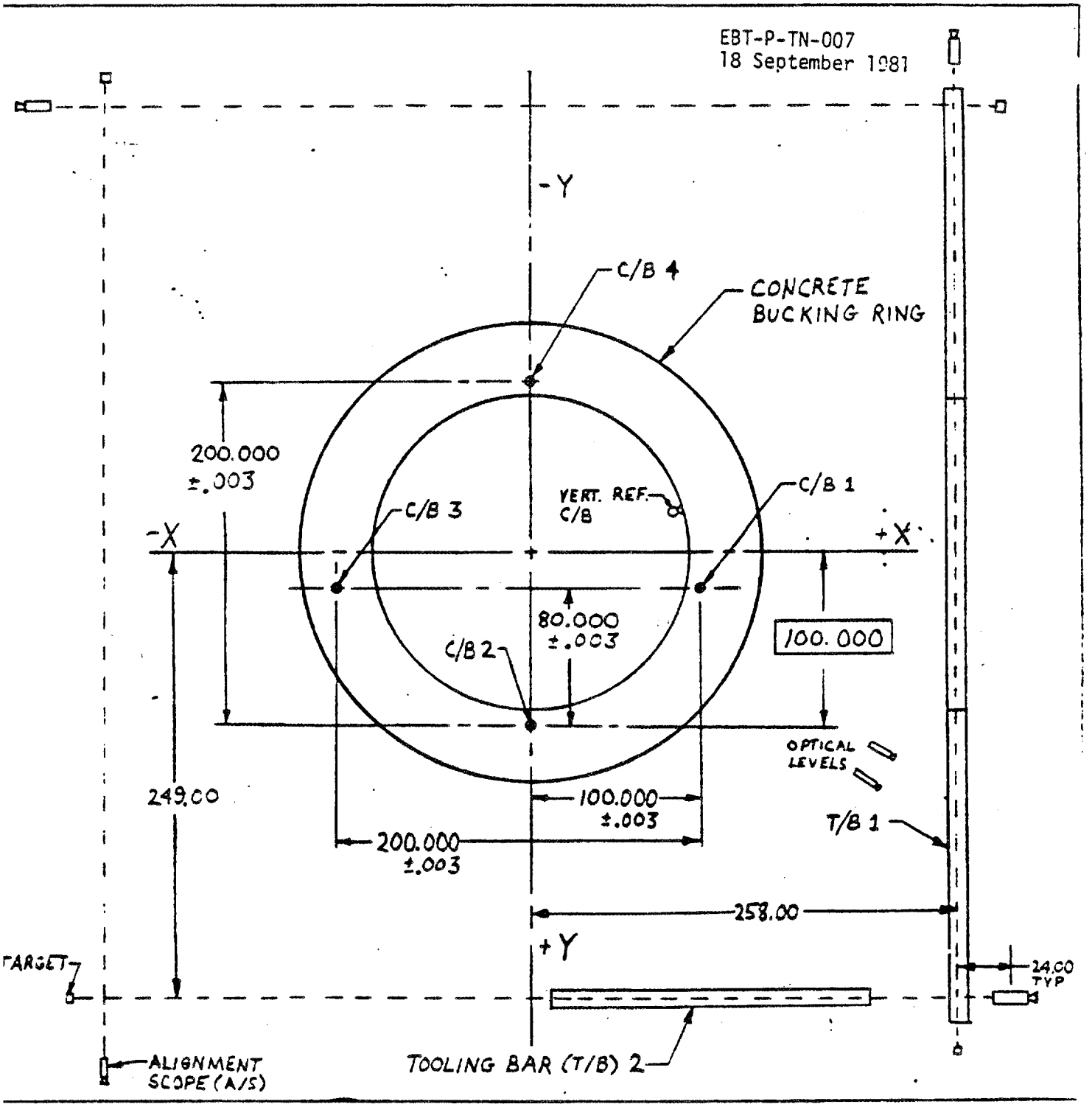

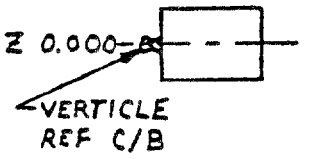

FIGURE 6.

ALUMINUM RING SEGMENT ALIGNMENT

Jack Foot	Displacement						Angular					
No.	Radial		Vertical		Circum.		Roll		Pitch		Yaw	
	IN	OUT	UP	ON	CW	CCW	CW	CCW	UP	DN	CS	CCW
1	In	Out							Out	In	Out	In
2	In	Out							Out	In	In	Out
3	In	Out							In	Out	In	Out
4	In	Out							In	Out	Out	In
5			In	Out			In	Out				
6			In	Out			Out	In				
7			Out	In			Out	In				
8			Out	In			In	Out				

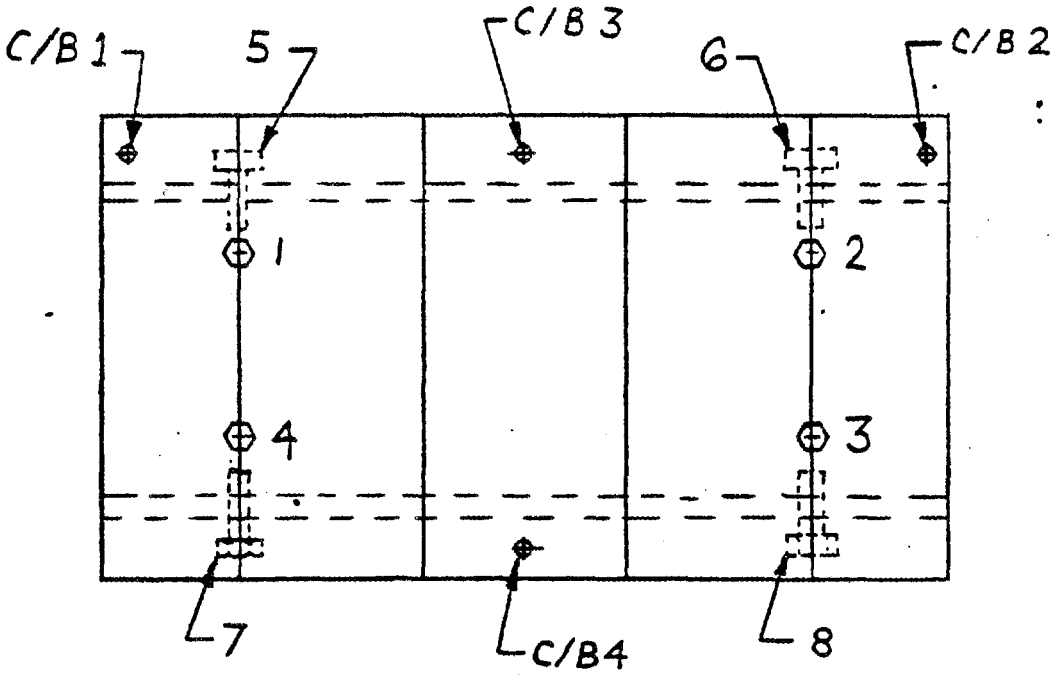

Jack Foot/Turnbuckle Adjustment

FIGURE 7.

OPTICAL SET-UP FOR INSTALLATION OF ALUMINUM RING SEGMENTS 3 AND 4

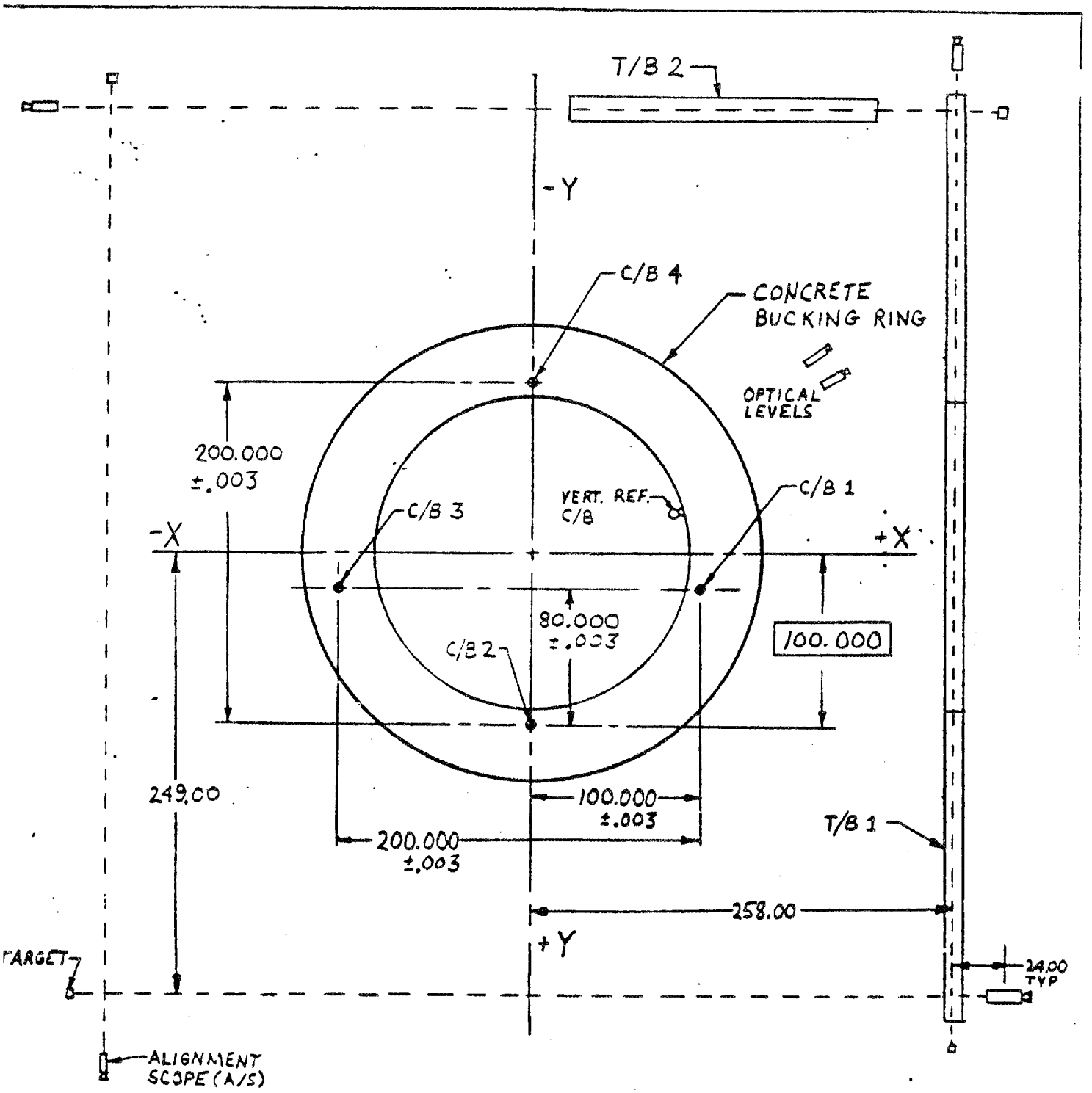

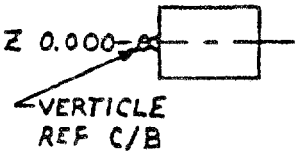

FIGURE 8.

OPTICAL SET-UP FOR INSTALLATION OF ALUMINUM RING SEGMENTS 5 AND 6

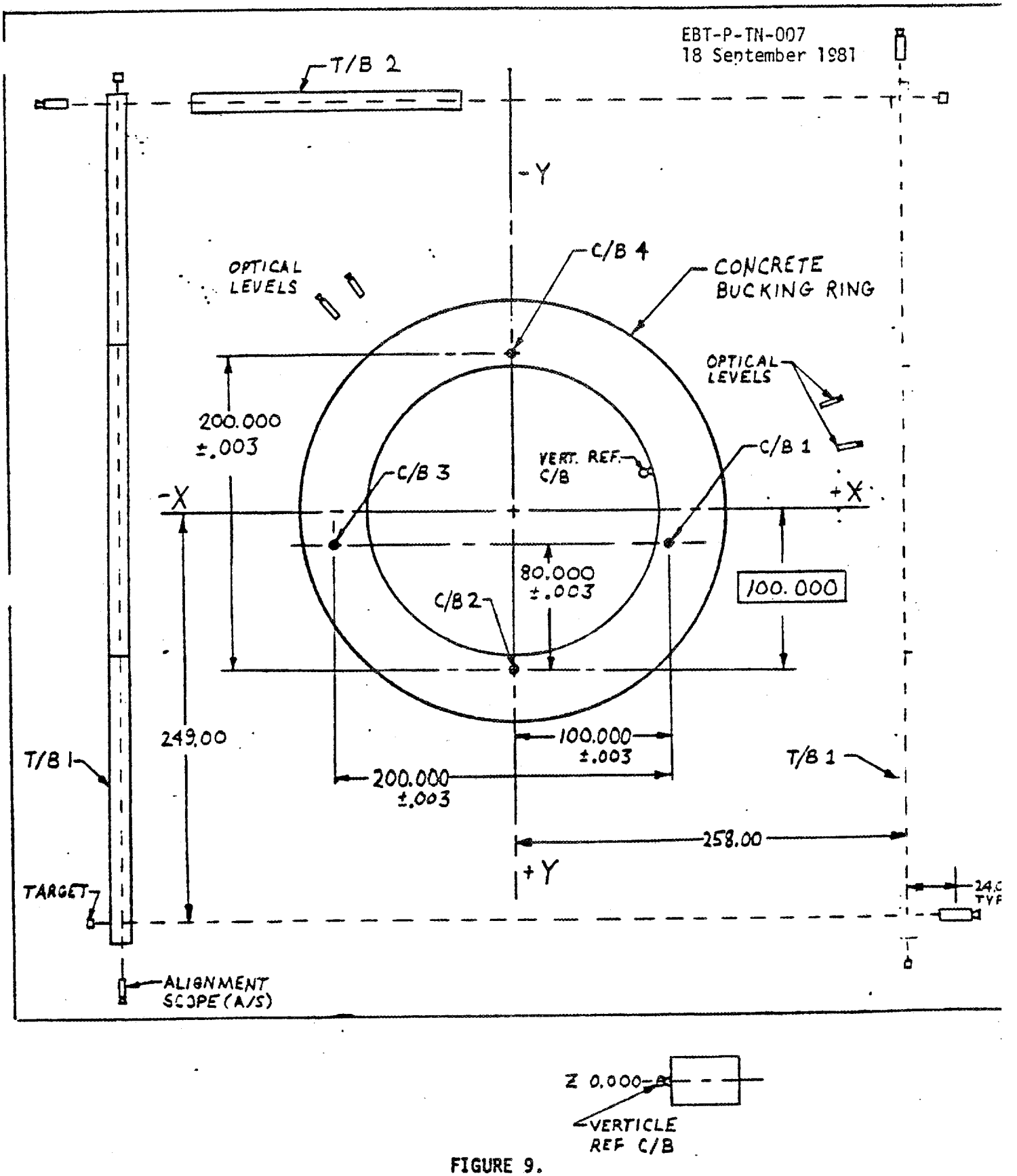

FIGURE 9.

OPTICAL SET-UP FOR INSTALLATION OF ALUMINUM RING SEGMENTS 7, 8, AND 9

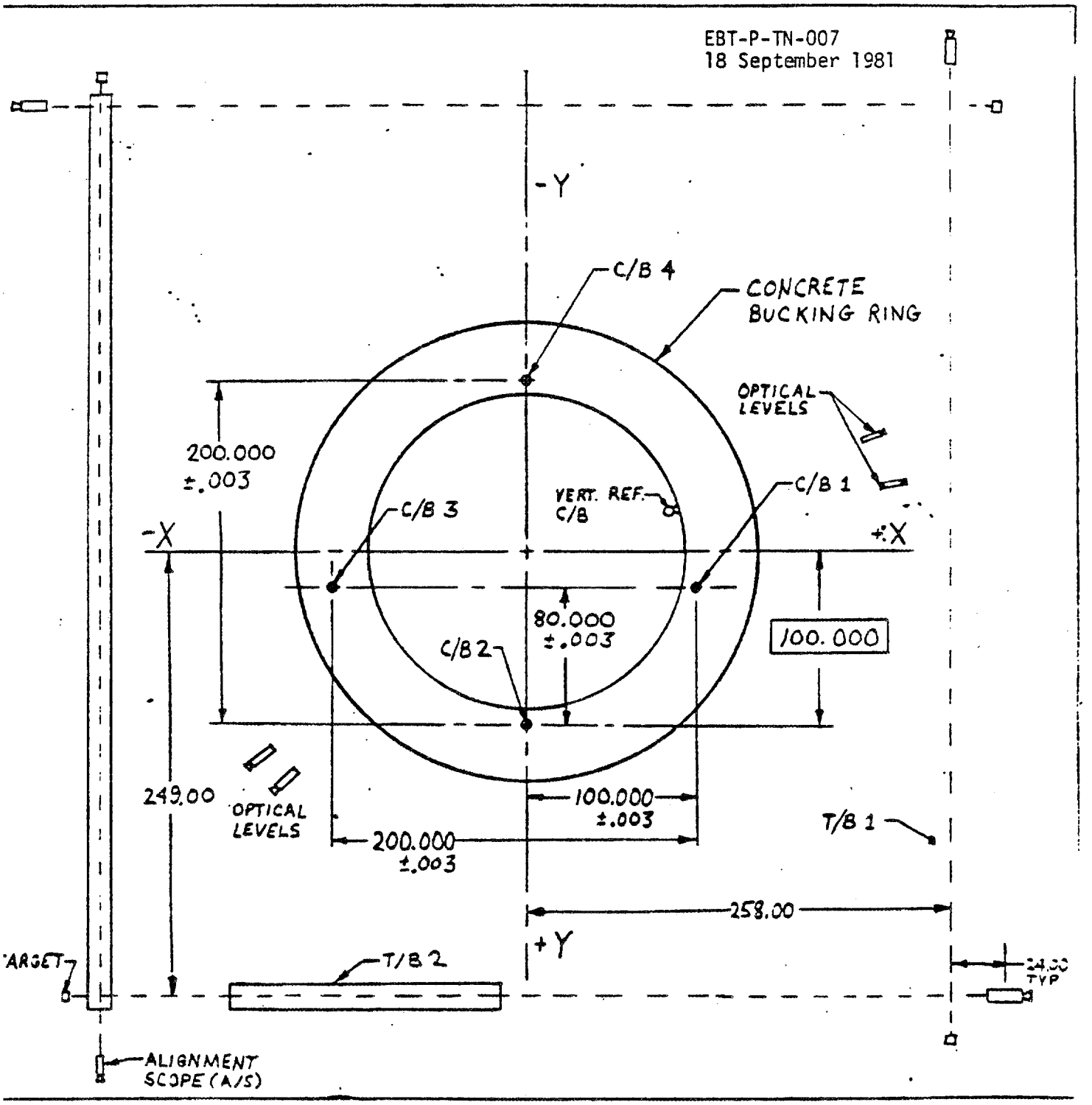

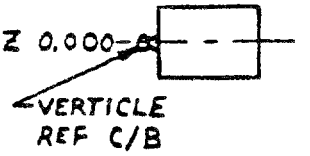

FIGURE 10.

TOLERANCE STACK FOR BUCKING RING STRUCTURE AND MAGNET ASSEMBLY

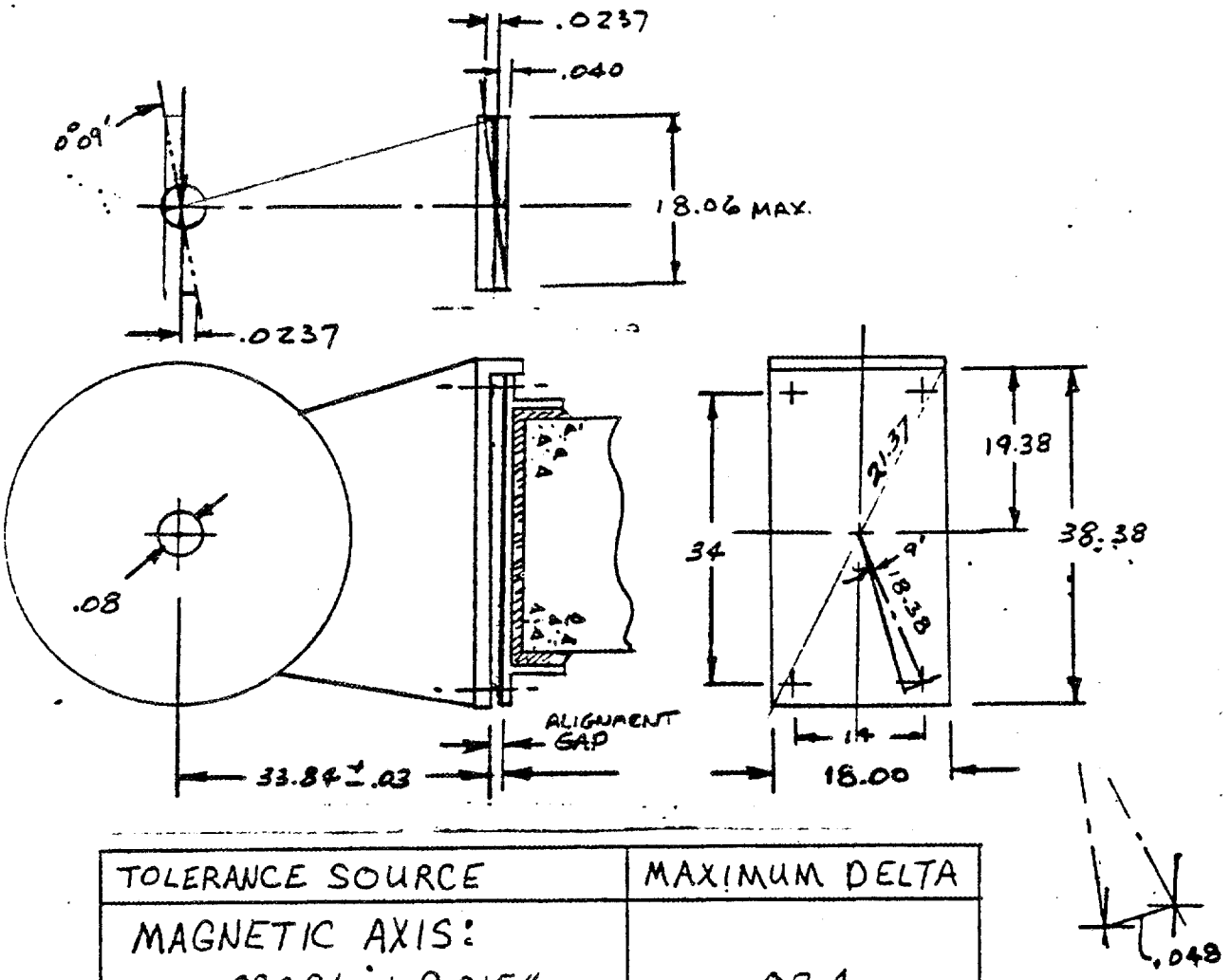

TOLERANCE SOURCE	MAXIMUM DELTA
MAGNETIC AXIS:	
• 0°09' at 9.015"	.024
• 0.040	.040
MAGNET BASE	.030
OUTER RING TOLERANCE:	
• BEAM TOLERANCE	±.040
• LOCATION	±.010
TOTAL	.194

FIGURE 11.

MAGNET ALIGNMENT

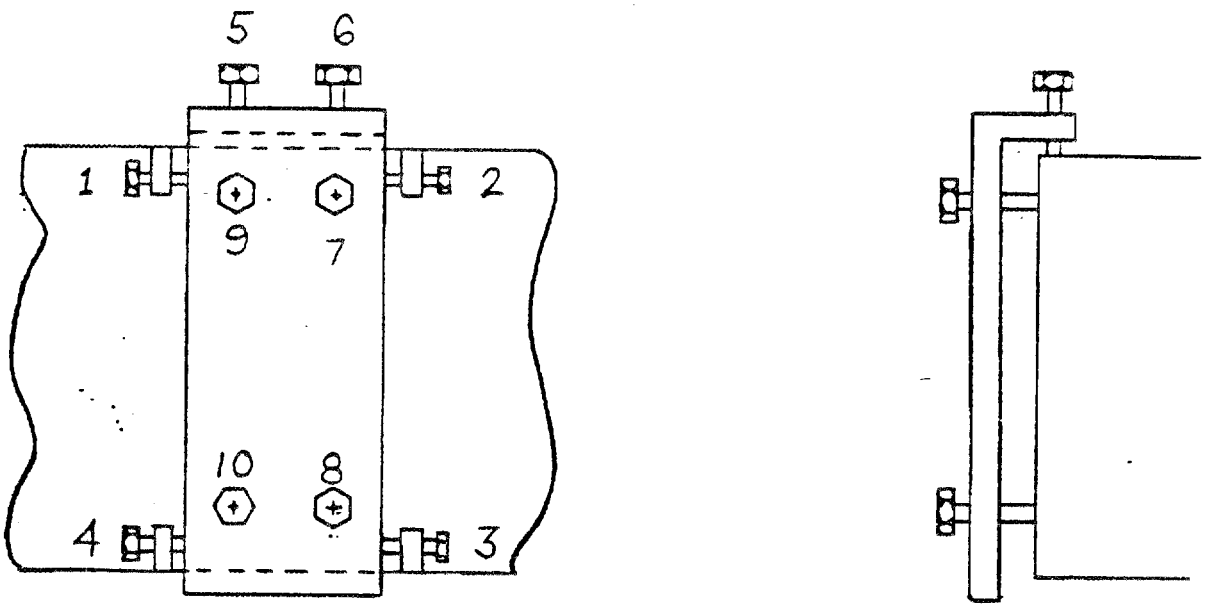

ack Foot	Displacement						Angular					
No.	Radial		Vertical		Circum.		Roll		Pitch		Yaw	
	IN	OUT	UP	ON	CW	CCW	CW	CCW	UP	DN	CS	CCW
1					Out	In	In	Out				
2					In	Out	Out	In				
3					In	Out	In	Out				
4					Out	In	Out	In				
5			In	Out								
6			In	Out								
7	Out	In							Out	In	In	Out
8	Out	In							In	Out	Out	In
9	Out	In							Out	In	Out	In
10	Out	In							In	Out	In	Out

Note: 7, 8, 9 and 10 are magnet attach bolts

FIGURE 12.

MAGNET ATTACH BOLTS

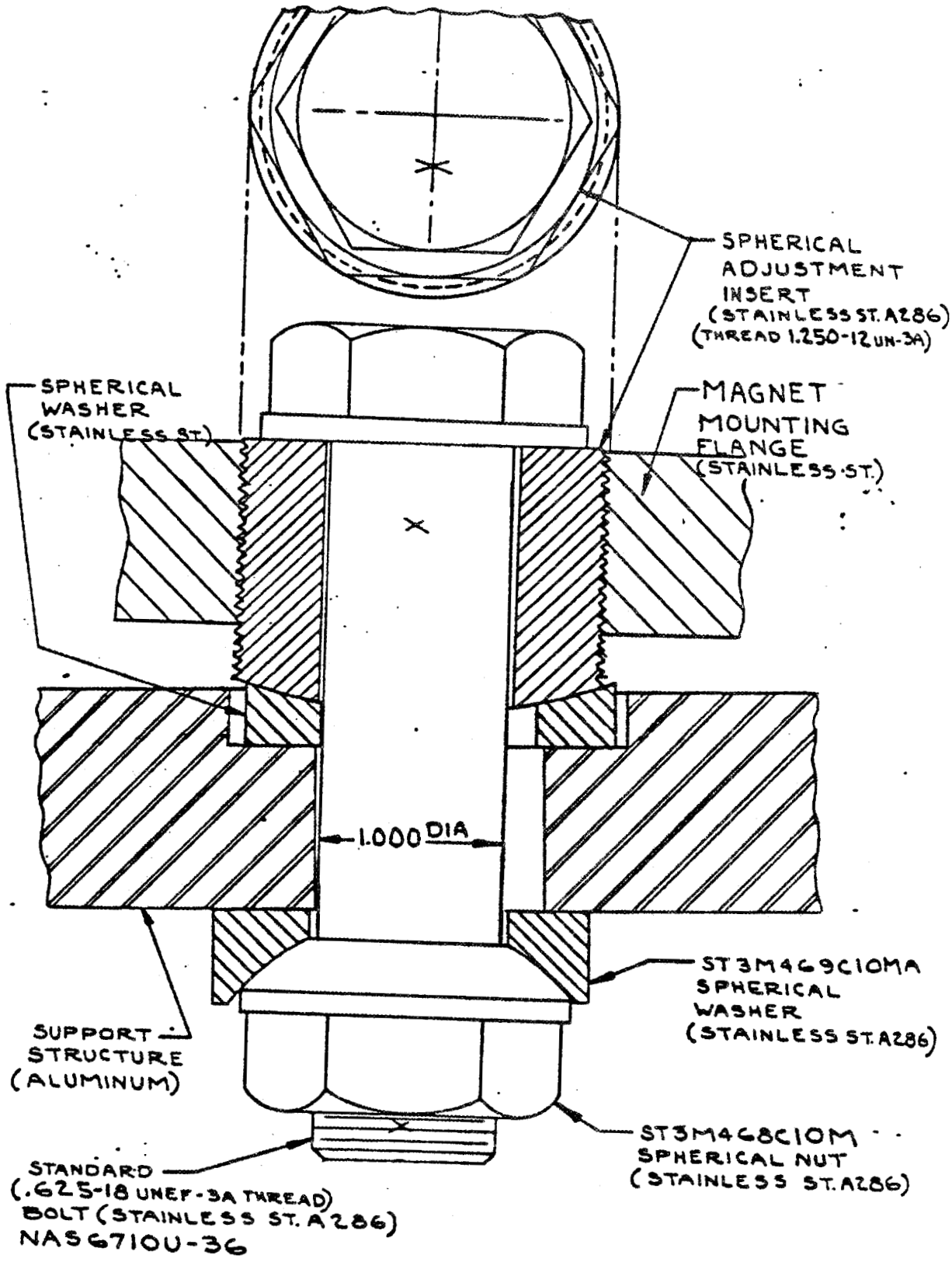

FIGURE 13.

MAGNET TAPER PINS

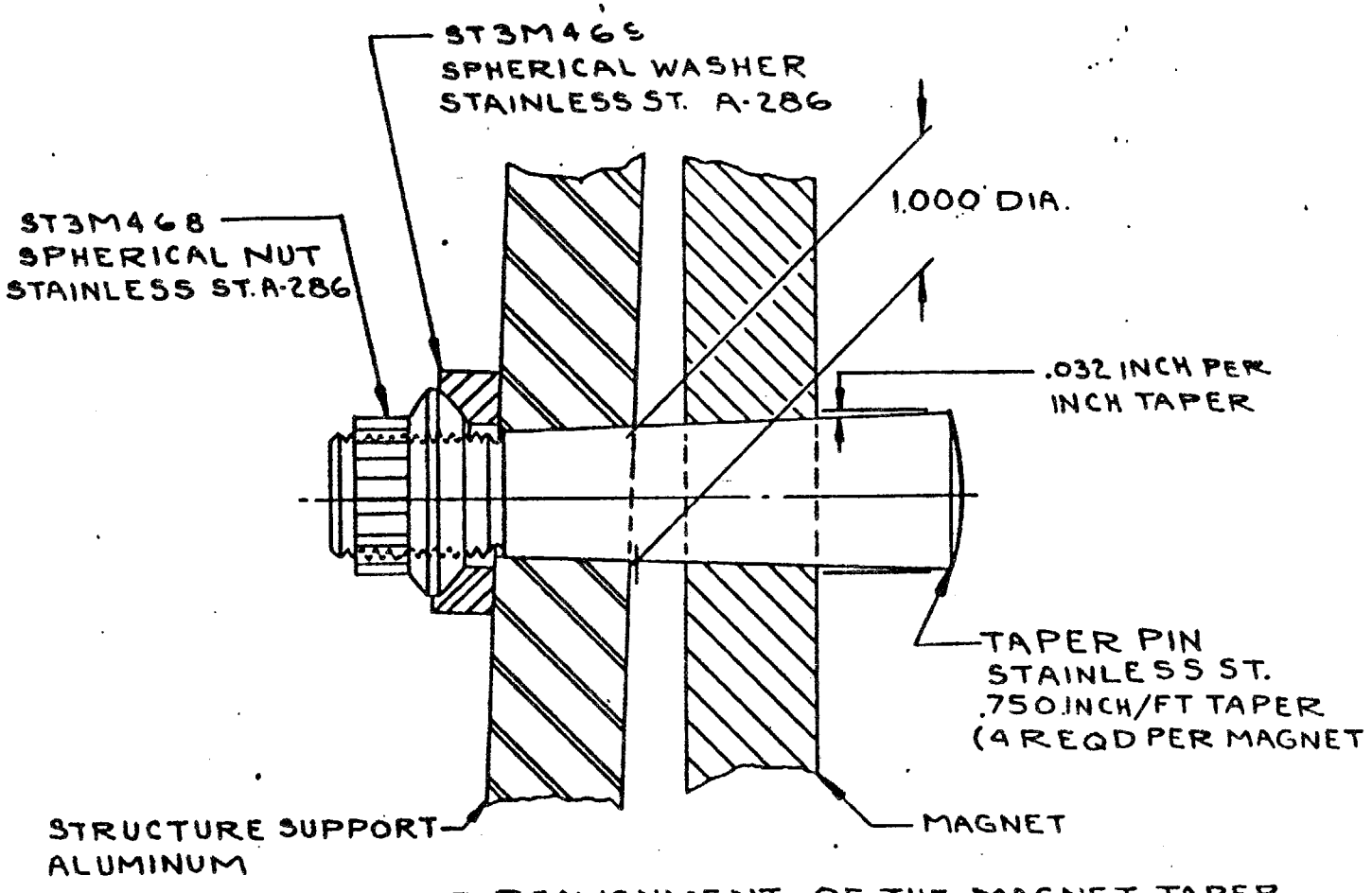

NOTE: FOR A MINOR REALIGNMENT OF THE MAGNET, TAPER REAM ABOVE TWO HOLES FOR A 100% PIN FIT. USE EXISTING PIN. A SPACER WASHER WILL BE REQUIRED BETWEEN SPHERICAL WASHER AND SUPPORT STRUCTURE.

FIGURE 14.

MEMO

EBT-174
29 Feb 80

Subject: MAGNETIC FIELD ERRORS IN EBT-P

To: EBT-Team

From: R. E. Juhala

The specification for field error in the EBT-P RFP calls for a cumulative error in $\delta B/B$ of 1×10^{-4} averaged around the torus along the minor axis. This supercedes an earlier specification of $\delta B/B \sim 6 \times 10^{-4}$ as stated in the reference design report (ORNL/TM-7191).

The systematic field errors are those due to winding helicity, layer to layer transitions, coil leads, electrical bus circuitry, and magnetic materials in the torus structure. In addition, random field errors will be introduced during coil construction, magnet alignment and deviations in magnet current. These errors are to be determined by comparing the field quality to an ideal torus where the coils are simulated by circular current filaments. Using the coordinate system shown in Figure 1 the field errors can be calculated from the following expression:

$$\left\langle \frac{\delta \vec{B}}{B} \right\rangle = \frac{1}{2\pi R_T} \int \frac{\left((B_R - B_R^I)\,\hat{R} + (B_\Theta - B_\Theta^I)\,\hat{\Theta} + (B_Z - B_Z^I)\,\hat{Z} \right) dS}{|\vec{B}|}$$

where the B^I are field components in the ideal torus, and S is an element of arc length along the minor axis ($dS = R_T d\Theta$). The ORNL specification calls for $\left| \left\langle \frac{\delta \vec{B}}{B} \right\rangle \right| \lesssim 10^{-4}$.

The systematic errors need only to be averaged over a machine sector. The random errors can be determined by introducing random displacements in the coil locations and random current increments amongst the magnets and averaging these effects around the torus. The net error will be given by the vector sum of the systematic plus random errors. This net global error can be cancelled to first order by the trim coils which will be designed to compensate field errors up to $\frac{\delta B}{B} \sim 10^{-3}$.

Magnetic materials will also modify the field and therefore must be kept away from the torus. The field exterior to the torus vacuum walls falls rapidly as can be seen in Figure 2. The outermost contour surrounding the minor axis denotes the boundary when $\frac{\delta B}{B} \sim 10^{-4}$. Magnetic materials beyond this boundary (approximately 1.5 meters) should poise no problem to the plasma. For 90 GHz operation the field at 1.5 meters away from the minor axis will be approximately 5 gauss.

Preliminary calculatfons of systematic errors give $\frac{\delta B}{B} \sim 10^{-4}$. These calculations are based on worst case assumptions. For example, the layer to layer transitions are assumed to occur along the vertical axis. In practice these transitions might be spaced uniformily around the coil. Also the error due to helicity, which appears

-2-

EBT-174
29 Feb 80

to be the largest systematic error, can be compensated on the average if necessary by winding right and left hand coils as was suggested previously in the Phase I EBT-P study.

In general field errors are expected to mainly effect the passing particles. These particles sample the field all around the torus many times during a particle lifetime. The experience with EBT-I seems to indicate that a correction for the net radial field error produces a dramatic improvement in plasma confinement (ORNL/TM-6704). The Nagoya Bumpy Torus was designed without correction for the systematic errors in coil construction. A simple calculation shows that a $\frac{\delta B}{B} \sim 10^{-3}$ is expected in this device which is verified by the fact that a global field correction supplied by the torus coils of 10^{-3} is required to operate the plasma in a T-mode. The critical value of $\frac{\delta B}{B}$ for EBT-I is also in this range (the coils are constructed out of similar conductor and roughly the same size) except that systematic winding errors are reduced by having right and left hand windings in the coil (to cancel the helicity error) and by careful attention to coil interconnections and buswork.

From this work at ORNL and Nagoya some understanding of the effect of field errors in confinement has evolved. Applying these criteria to the EBT-P device leads to a critical $\frac{\delta B}{B} \sim 10^{-4}$. Although systematic errors can be most likely held to less than 10^{-4}, the random errors, perhaps mainly due to coil misalignments, are likely to exceed this value. Alignment tolerances of $\pm$ 0.010 in., which are perhaps optimistic, lead to random errors for each coil $\sim$ 4-8 $\times$ 10^{-4}. Thus the net error remaining even when averaged over the torus could exceed the 10^{-4} criteria. This problem remains to be studied in more detail.

R. E. Juhala
EBT - Scientist
Dept. 223, 81/86
Sta. 576-8261

REJ:llm

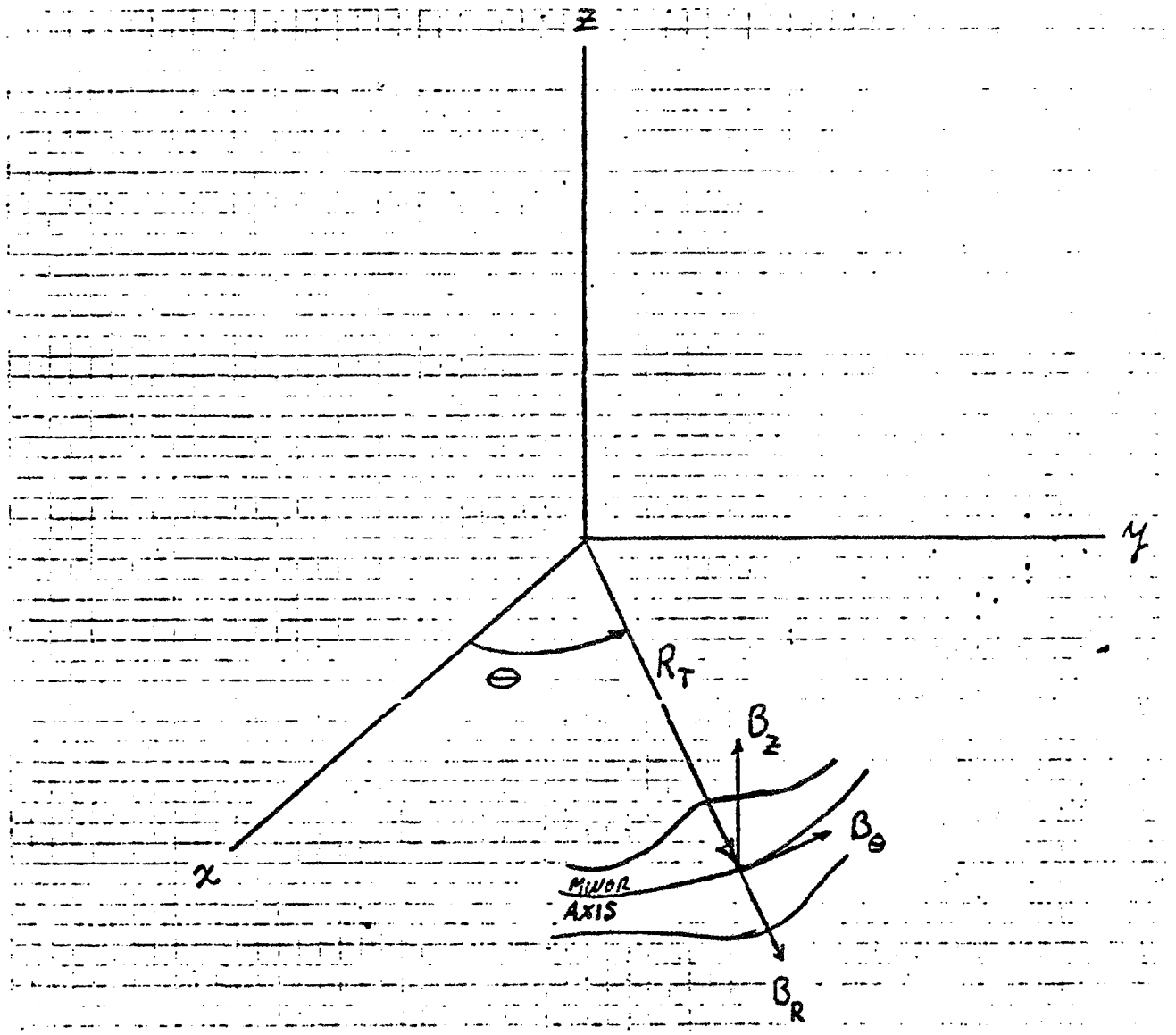

FIGURE 1: TYPICAL COORDINATE SYSTEM FOR MAGNETIC FIELDS IN EBT GEOMETRY

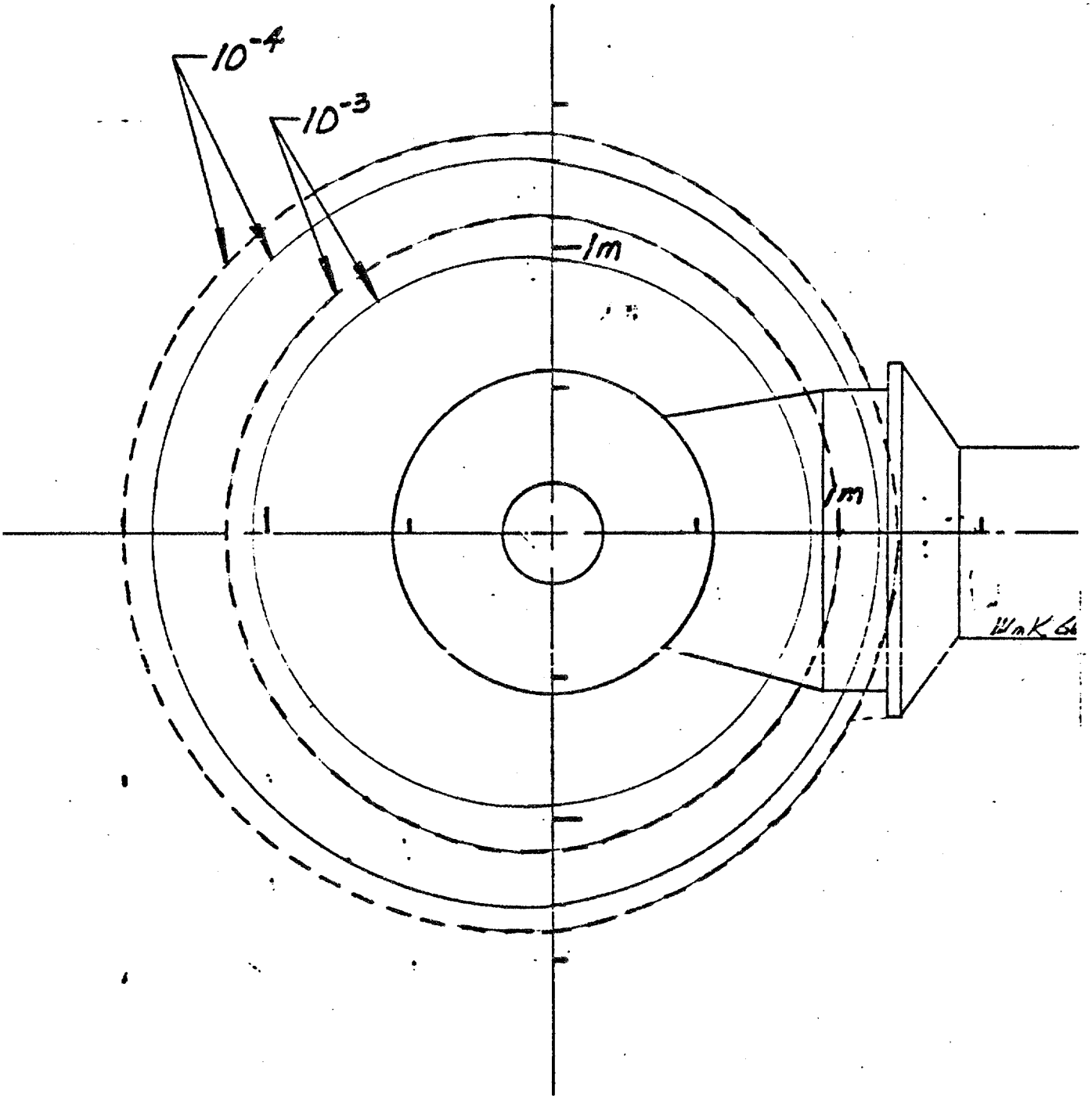

FIGURE 2: Normalized Magnetic Field exterior to the vacuum vessel $B(r)/B_o$ where the solid contours represent fields on a vertical plane through the coil throat (normalized the throat field) and the dashed contours are defined on a vertical plane through the cavity midpoint normalized by the field at midcavity. (Field contours provided by J. Lenz)

MEMO

EBT-182
17 Mar 80

Subject: ALIGNMENT OF THE TOROIDAL FIELD COILS IN EBT-P

To: EBT-Team

From: R. E. Juhala

A discussion of field errors (EBT Memo 174) pointed out the need for precision alignment of the TF coils in EBT-P. This could in principle be accomplished either by geometric alignment of the coil or magnetic alignment. For geometric alignment to be utilized the magnet assemblies must be constructed within very tight tolerances, on the order of $\pm$ 0.005. It would be required that the magnetic coil plane and magnetic axis lie within this tolerance of the respective geometric quantities and that the geometric quantities be indexed with visible markings on the exterior of the magnet assembly to that accuracy. On the other hand, magnetic field measurements can be made on each coil and the required magnetic quantities determined and indexed to this required accuracy on the magnet assembly so that optical alignment can be accomplished in a straight-forward way during installation.

The magnetic plane and magnetic axis are shown in the figure below. The magnetic field is symmetric about this axis, (i.e. $B_\phi = 0$), and also symmetric about the magnetic plane, such that $B_z(r,z) = B_z(r,-z)$. In an ideal coil they coincide with the geometric axis and coil midplane. Also shown in Figure 1 are fiducial surfaces upon which index marks will be placed as determined by field measurements to locate the magnetic axis. The fiducial surfaces should all be spot faced so they lie in a plane. Again field measurements will be used to determine the distance to the magnetic plane from each fiducial surface.

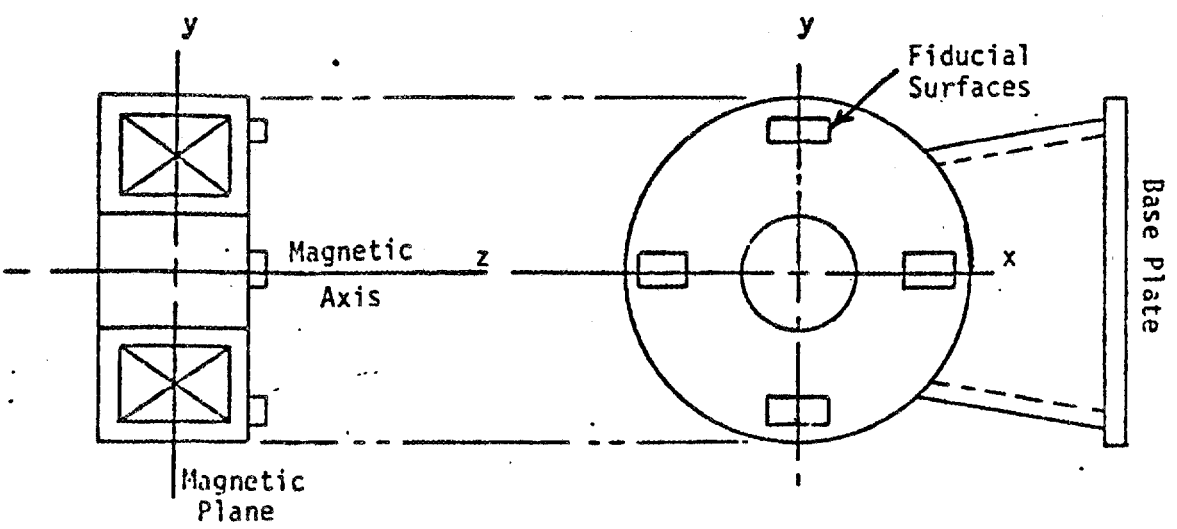

Figure 1: Magnetic Axis and Magnetic Plane for an Ideal Solenoidal Coil

It will be useful to have the geometrical x and y axes indexed on the fiducial surfaces at the time of manufacture. In this case the vertical axis (shown as y in Figure 1) should be made parallel to the baseplate of the magnet. One technique for obtaining the location of the magnetic plane and axis would be to use a matched pair of field sensing probes (either Hall probes or small precision wound flux coils) mounted on a common axis as shown in Figure 2.

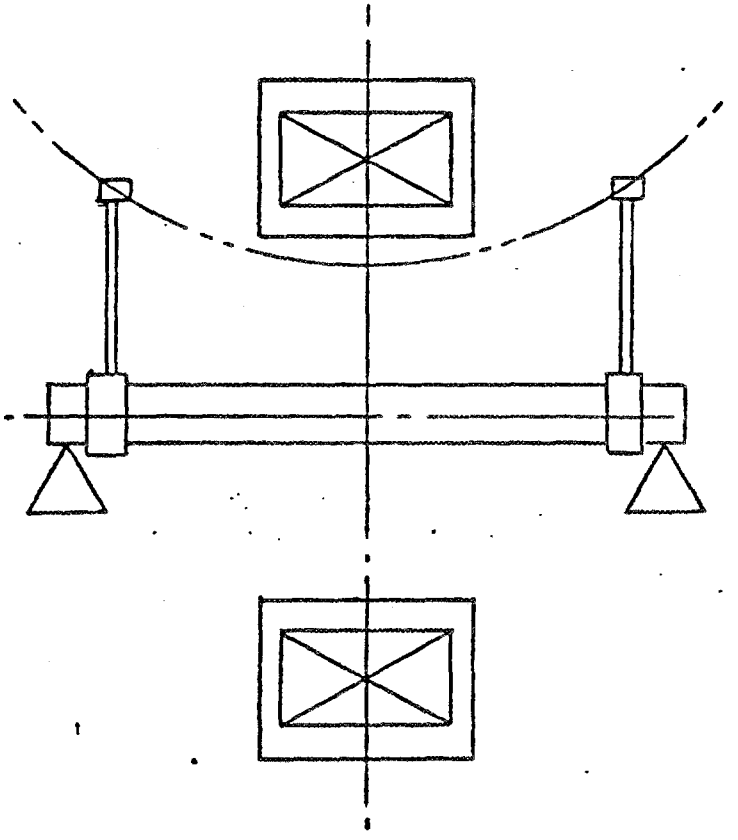

Figure 2: Magnetic Field Measuring Device Located in the Aperture of a Toroidal Field Coil

The probes must be calibrated and balanced to read precisely the same field to a part in 10^{-4} or better. The signal from each would be subtracted from a third probe which remains stationary during the measurement. The probes are rotated together on the common axis and the field differences are recorded simultaneously every 10^{0}, digitized and plotted on an XY recorder. The technique of plotting field differences will allow high resolution from the field probes. The nature of the misalignment will be apparent by inspection of the plotted data with no extensive analysis necessary. The relationship between the two field traces for a tilt of the magnetic plane will be distinctly different from a simple translation of the magnetic axis. By reorientating the field probe axis

-3-

EBT-183
17 Mar 80

the measuring process is repeated until coincidence is achieved between the magnetic and field probe axes. A full 360° rotation of the field probes including the finished data plot should require only a few seconds. Hence, the magnetic alignment process can be accomplished expeditiously during the normal full power testing of each magnet assembly.

Using standard optical alignment techniques the magnet assemblies can be installed and aligned to an accuracy of ∿ ± 0.005". The alignment can be verified by using an electron beam (as in EBT-I). If the field closure requires correction, realignment of the magnet assemblies may be necessary. In this case four magnets, 90° apart around the torus might be arbitrarily selected in order to introduce a global correction to field line closure. Thus, no attempt need be made to realign the entire torus unless gross misalignment is evident. Instead, selected magnets can be reorientated within a small range of tolerances ∿ 0.020 in. to compensate for the alignment error.

R. E. Juhala

R. E. Juhala
Scientist - EBT
Dept. 223, 81/1/86
Sta. 576-8261

REJ:llm

MEMO

EBT-203
9 Jun 80

Subject: EFFECT OF MAGNET ALIGNMENT ERRORS ON THE MAGNETIC FIELD OF EBT-P

To: EBT Team

CC: A. Bay, D. Clifford, R. Lilienkamp

From: J. E. Lenz and R. E. Juhala

Ref:
(a) R. E. Juhala Memo EBT-174, dtd 29 Feb 80
(b) ORNL Report TM-6704
(c) EBT-P Phase II Proposal MDC E2228
(d) R. V. Hogg and A. T. Craig, Introduction to Mathematical Statistics, MacMillian Co., New York, 1970
(e) J. E. Lenz, TM 256.5144, dtd 15 Dec 78
(f) J. C. Sprott, Physics of Fluids, 16, 1157, July 1973.

Encl:
(1) Definition of Magnet Alignment Errors
(2) Probability Distribution Functions Where the Acceptance Measurement is Made After the Manufacturing Process is Completed
(3) Probability Distribution Functions Where the Acceptance Measurement is Used as Part of the Manufacturing Process
(4) Effect of Number of Points and Number of Samples on the Statistics of $\delta B/B$
(5) Translation of Alignment Errors to $\langle \delta B/B \rangle$
(6) Global Field Error Due to Unequal Turns in the TF Magnets
(7) Field Line Tracing With $\delta B/B = 1.66 \cdot 10^{-4}$
(8) Field Line Tracing With $\delta B/B = 1.0 \cdot 10^{-4}$
(9) Correction of Field Line Closure
(10) Effect of $\delta B/B$ on Field Line Closure
(11) Effect of the Alignment Tolerance on the Global Field Error
(12) Histogram of Probability Distribution for $|\langle \delta B/B \rangle|$
(13) Test of Hypothesis That $|\langle \delta B/B \rangle|$ is $n(\bar{x}, s)$

1. This memo describes the effect of alignment errors on EBT-P magnetic fields following the prescription outlined in Ref (a). The experience on EBT-I, Ref (b), indicates that careful attention must be given to field errors during the construction and installation of the EBT-P magnet system. The requirement for EBT-P is that cummulative field error as expressed by the quantity $\delta B/B$ shall be less than 1×10^{-4} when averaged around the torus along the minor axis. Field errors can be either systematic or random. Systematic errors are those due to winding helicity, layer-to-layer transitions, coil leads, electrical bus circuitry, and magnetic materials in the torus structure. Random field errors can also be introduced during coil construction, but will for the most part be introduced by magnet misalignments.

2. The global field error, $\delta B/B$, is defined as:

$$\left\langle \delta\vec{B}/B \right\rangle = \frac{1}{2\pi R_T} \int \frac{\left[(B_R - B_R^I)\hat{R} + (B_\theta - B_\theta^I)\hat{\theta} + (B_Z - B_Z^I)\hat{Z} \right] ds}{|\vec{B}^I|}$$

$$= \frac{1}{n} \sum_{i=1}^{n} \frac{(B_R - B_R^I)_i}{|B^I|_i} \hat{R} + \frac{(B_\theta - B_\theta^I)_i}{|B^I|_i} \hat{\theta} + \frac{(B_Z - B_Z^I)_i}{|B^I|_i} \hat{Z}$$

where: R, θ, z are cylindrical coordinates
B^I are field components in the ideal torus
n is the number of points for comparison around the torus axis .

The systematic errors due to coil design, current leads, and bus-work have been studied and do not exceed the $\delta B/B < 10^{-4}$ criteria. These results are given in the description of the coil design in Ref (c). Errors due to alignment are treated as randomly distributed within assumed tolerances on coil construction, magnetic field mapping (to determine the magnetic axis) and precision of optical alignment techniques which will be used to actually locate the magnets within the torus. In determining $\delta B/B$, a comparison of the magnetic field on axis in a torus where random misalignments have been imposed on the toroidal field coils is made with the field due to an ideal torus with no alignment errors. In order to obtain meaningful statistics on what might be expected during the course of actual construction of the torus, random error assignments were regenerated several times and the quantity $\delta B/B$ calculated for each case. In this way, a mean value of $\delta B/B$ and corresponding standard deviation are determined [cf. Ref (d)].

3. Field errors are introduced by displacements and/or rotations of the coil from its ideal location. Although there are six degrees of freedom, only two of the angular coordinates contribute significantly to the average error in $\delta B/B$. These are rotations about a vertical axis and a major radius which affect the radial and vertical field errors, respectively. Since the global field error is an average taken around the torus, errors due to radial and vertical displacements tend to average out. Displacements along the minor axis (i.e., variations in mirror ratio) do not contribute any significant off-axis component to the global field error. The coordinate system is shown in Encl (1).

4. Aside from the systematic errors which are unique to each particular design, random errors are introduced at each step of the process from individual component fabrication to final alignment of the completed magnet assembly. The distribution function for the errors introduced at each of these steps will depend on the techniques used to insure that the part or process falls within a specified tolerance. Some examples of error distribution which involve different assumptions about the methods used to insure quality are shown in Encls (2) and (3).

The first is a normal distribution where the probability is peaked for a certain occurrence and decreases away from that mean value. This distribution is defined by the mean μ and the standard deviation σ. This type of error distribution will not describe construction or alignment errors because a construction tolerance is established where a part or measurement outside the manufacturing specifications is not accepted. Therefore, the Gaussian curve (I) is truncated at the maximum tolerance (σ), and the probability function appears as II in Encl (2). This probability function is more highly peaked at the mean and is zero outside the tolerance. Depending on the precision of construction, the error distribution may be highly peaked, in which case, the distribution may be more nearly represented by curve III in Encl (3). This triangular distribution could approximate a situation where changing conditions during the course of manufacture brings about a broadening (or narrowing) of the overall tolerance, but it also is in some sense more realistic than a truncated Gaussian, since it does not incorporate the discontinuity at the maximum tolerance. However, since a large number of steps are involved in manufacture of the magnets, a highly-peaked distribution seems unlikely; and although a modified Gaussian, perhaps one with sides falling rapidly but not discontinuously to zero, may be more appropriate a simple step function [Encl (3), curve IV] has been employed. In this case, all errors within the tolerance ranges are equally probable.

5. Random errors due to coil construction are difficult to treat in general, since they are introduced in a large number of different ways. However, the most serious construction errors are manifested by uncertainty in the overall position of the coil pack as a whole and, hence, result in coil misalignments. Of main concern here is the location of the magnetic plane and axis. An alignment which relies on the respective geometric quantities may be subject to errors which are are an order of magnitude larger than those obtainable through the use of magnetic measurements. Thus, the resulting value of $\delta B/B$ that can be obtained will depend only on the accuracy of the field measurements and will be essentially independent of errors in coil construction. The error distribution associated with field measurement and subsequent optical alignment can be reasonably approximated by the flat distribution (Encl (3), curve IV].

6. A computer program has been written for modeling the alignment errors of the TF magnets around a bumpy torus. The torus design and the tolerances for the three errors are input to the program. The magnets are then randomized within these tolerances and $\delta B/B$ is computed using a selectable number of points around the torus. The computer program also allows for statistical sampling by computing statistics on the quantity $\delta B/B$ for N randomized designs. The statistics $\bar{X} = \sum_{i=1}^{N} \frac{X_i}{N}$ (mean) and $S = \left[\sum_{i=1}^{N} \frac{(X_i - \bar{X})^2}{N}\right]^{1/2}$ (standard deviation) are computed for the three components ($X_i = \langle \delta B/B \rangle_R$, $\langle \delta B/B \rangle_\theta$ and $\langle \delta B/B \rangle_z$) and the modulus ($X_i = |\langle \delta B/B \rangle|$) of $\delta B/B$. Encl (4) shows how the statistics for $|\langle \delta B/B \rangle|$ vary with the number of points (n) used to compute $\delta B/B$ around the torus and also with the number of randomized designs sampled (N).

7. Each error was investigated for its effect on $\delta B/B$. Encl (5) lists the results of this investigation. For this initial study, the size of the error was determined for $\pm$.01 " maximum displacement in coil orientation and $\pm$.02" displacement in radial location. This translates to $\pm$.05 degrees ($\pm$ 8 milliradians) for ε and δ with the EBT-P reference design magnets and $\pm$.0005 meters for r. Four cases are shown: three with each error for magnet alignment studied separately and another with all three errors combined. These results indicate the three errors, which are modeled as being independent, affect $\delta B/B$ independently. The alignment error ε results mostly in a R component contribution to $<\delta B/B>$, δ results mostly in a Z component contribution. and r results in both R and θ components. The contribution to $|<\delta B/B>|$ due to r is an order of magnitude smaller than those from ε and δ. Thus, the radial displacement error (r) has a negligible effect on $|<\delta B/B>|$ compared to the two rotation errors, ε and γ, which have an equivalent effect on $|<\delta B/B>|$ for a given tolerance. Also shown in Encl (5) is the effect on $<\delta B/B>$ for random coil rotations along the minor axis (i.e., the angle between each TF coil varies from the ideal sector angle). For a maximum rotation of .01 degrees, which corresponds to .02 inches at the coil, the contribution to $\delta B/B$ is negligible compared to that from δ and ε.

8. Another error analysis, listed in Encl (6), was a study to randomize the turns in each TF coil. Each TF coil will have approximately 1000 turns. Encl (6) lists the global field error due to varying number of coil turns. As is shown, the effect of not having the exact same number of turns in each TF coil has a significant impact on the global field error. This error could be corrected by adjusting the current so that the total ampere turns are the same for each magnet.

9. An important consideration in the programming and analysis of $\delta B/B$ is field line closure. Ref (e) shows the effects of different field line tracing algorithms on the field line symmetry between bumps. However, for this analysis, it is important to have calculated field line closure around the entire ideal torus. Then the effects of $\delta B/B$ in a randomized torus can be studied. A second order Runge Kutta integration algorithm for tracing the field lines was used with 50 points/bump necessary for closure to $\pm$.05 cm in the midplane. This relates to an accuracy of $\Delta\ell/\ell = \frac{.0005}{2\cdot\pi\cdot 4.47} = 1.8E\text{-}5$.

10. Two examples of field line tracing in a randomized torus are shown in Encls (7) and (8). Shown in these two enclosures are the deviations from the ideal torus in the r and z components of a field line in each midplane around the torus. (It will be shown later that for a given randomized torus, each field line within the torus has approximately the same closure error.) Below the deviation graph is a point plot of the randomized ε rotation of each TF magnet and above the graph is a point plot of the *random* δ rotation. As previously shown in Encl (5), a positive (negative) rotation in ε for any TF magnet results in an inward (outward) deviation in the R component of the field line. Likewise, the δ rotation directly affects the deviation in the Z component. These facts then indicate that a manual rotation of a few selected coils about the torus could be used to

cancel the field line closure error in a randomized torus. Encl (9) demonstrates this for the data in Encl (7) by reducing the deviation in the R component. This was done by rotating only the coil at 185° from the field line start in a midplane. The data shows the field line having the exact same tracing about the torus except when it passes through the throat of the adjusted magnet. The deviation in R varies considerably and the Z deviation is unaffected as expected. This example also demonstrates how small misalignment errors in the magnets are magnified into the field line closure and $\delta B/B$. The coil at 185° is rotated .73 degrees which corresponds to .16 inches at the coil pack. This results in a .6-cm or .24-inch deviation in the field lines.

11. An interesting fact is that all the field lines through the aperture of a randomized torus are shifted in the same direction and relatively the same amount. The following table shows the field line closure for several field lines in a randomized EBT-P with $|\langle \delta B/B \rangle| = 1.66E\text{-}4$:

Field Line Start (Midplane)		Closure in Midplane	
r(cm)	z(cm)	Δr(cm)	Δz(cm)
0	0	-.61	.12
-15	0	-.63	.11
15	0	-.67	.12
-15	15	-.63	.17
0	15	-.59	.12
0	-15	-.59	.13

This indicates that these field lines will spiral inward and upward with little dependence on where in the torus they are. Thus, in a randomized torus, the fields lines will spiral away from the minor axis. The direction and amount of shift per spiral is linearly dependent on $\delta B/B$. Encl (10) shows the linear relationship between $\delta B/B$ and the deviation in field line closure ($\Delta \ell$).

12. It is interesting to calculate the confinement time of a passing particle ($v_\parallel/v = 1.0$) constrained to follow a field line (i.e., ignoring curvature and Grad-B drifts). In this case the confinement time is given by the following expression:

$$\tau_p = \frac{a}{V_\parallel \cdot (\delta B/B)}$$

a = minor radius

$V_\parallel$ = velocity of particle along field line

$$= \left[\frac{2 E_{k\parallel}}{m}\right]^{1/2}$$

$\delta B/B$ = global field error

For EBT-P assuming $\delta B/B = 1.10^{-4}$ and 1 keV electrons with $v_\parallel/v = 1.0$, $\tau_p = 0.1$ milliseconds. Since closed drift orbits exist due to precessional motion which has been neglected in the calculations with global field errors present, (Ref f) this is in some sense the shortest time a particle could escape from the plasma.

13. The effects of randomly distributed coil alignment errors on $<\delta B/B>$ are given in Encl (11) for different tolerances. For maximum angular tolerances of $\pm.05°$, which means ±0.010 in. of displacement at the coil pack, the global field error $\delta B/B$ is in the range of $0.48 \pm 0.34 \times 10^{-4}$. For a tolerance range three times wider or $\pm0.15°$ ($\pm.030$ in. at the coil pack), the global field error is correspondingly three times larger or $\delta B/B = 1.4 \pm 1.0 \times 10^{-4}$. In order to achieve coil alignment tolerances of $\pm0.05°$ or better, a determination of the magnetic axis will be required. Standard techniques for accomplishing this can be employed with which the magnetic axis can be determined to less than $\pm.025°$. This limit is actually imposed, not by the field mapping technique, but by optical alignment limitations. It is noted that radial displacement errors, although included in the calculation, made no significant contribution to this averaged quantity $<\delta B/B>$.

14. The position of the cold mass within the vacuum dewar will be difficult to locate to better than ±0.010", since with even very tight tolerances on each component, the cummulative effect of all tolerances during final assembly and especially coil pack motion under large magnetic forces would be expected to limit the accuracy that can be achieved. However, field mapping the magnets to locate the magnetic axis will facilitate alignment accuracy to within $\pm0.025°$.

15. The resulting global error on the assembled torus can be reduced in this separated function design (vacuum cavity separate from the magnet support system) by slight readjustments in the angular orientation of selected coils. Two randomized designs with angular errors of $\pm0.15°$ and $\pm0.30°$ were studied to reduce the global field error. In both cases, the global field error is reduced to much less than 10^{-4} by reorientating only four coils which are 90° apart. For the smaller error ($\pm0.15°$), a coil rotation of 0.10° is required to cancel the error. The larger error requires twice as much rotation in the selected toroidal field coils.

16. As a final analysis of the field error due to misalignment, a level of confidence is considered for the statistics. The statistics $\bar{X}$ (mean) and s (standard deviation) are computed for N samples of randomized bumpy torus designs. The randomized designs are determined from a uniform probability distribution between the tolerances of the three errors in the model. Encl (12) shows a histogram of $|<\delta B/B>|$ for 250 randomized designs. Overlayed above the histogram is a normal distribution which has mean (μ) and standard deviation (σ) equivalent to the mean ($\bar{X}$) and standard deviation (s) of the random sample. It appears that the global field error $|<\delta B/B>|$ follows a normal distribution, as one would expect.

17. There are two confidence levels to be considered. One involves the validity of the random sample statistics $\bar{X}$ and s being used as the mean and standard deviation to describe the probability distribution. Ref (d) derives confidence levels for the mean (μ) and the standard deviation (σ) of a normal distribution determined from the random sample statistics $\bar{X}$ and s. A "goodness of fit" between the random sample and the expected probability distribution can be determined. This was done for the hypothesis that the data in Encl (12) has a normal distribution defined by the statistics of the random sample - mean ($\bar{X}$) and the standard deviation (s). Encl (13) outlines this goodness of fit calculation and shows a 95 percent confidence in the hypothesis that the data is $n(\bar{X}, s)$.

18. Once the probability distribution is known, another confidence level question arises as to how the tolerances affect the probability of success. If $|\langle \delta B/B \rangle|$ is assumed to have a normal distribution described by $\overline{X}$ and s, $n(\overline{X}, s)$, then confidence levels for success can be determined. Some probabilities from a $n(\overline{X}, s)$ distribution are listed:

let X_i = be the ith element of the random sample

then $Pr\ (X_i \leq \overline{X}) = .50$

$Pr\ (X_i \leq \overline{X} + s) = .84$

$Pr\ (X_i \leq \overline{X} + 2s) = .98$

Using a normal distribution table, a confidence level of success for a given tolerance can be determined. The design criteria for 100 percent success is assumed to be $|\langle \delta B/B \rangle| < 1 \cdot 10^{-4}$. Then using Encl (6), the following probabilities for success can be determined.

Tolerance	Probability of Success ($Pr(\lvert\langle \delta B/B \rangle\rvert \leq 1 \cdot 10^{-4})$)
± .2°	.31
± .10°	.50
± .05°	.95
± .025°	.995

19. In summary, it has been determined that a tolerance of ±0.1° in the accuracy of coil alignment leads to global field error $\delta B/B < 1 \times 10^{-4}$ and a probability of 50 percent that realignment will not have to be done. Alignment tolerances equal to one-fourth this value or ±0.025° are possible if field measurements are utilized to locate the magnetic axis and then the probability of a successful first construction is almost 100 percent. Since magnetic field measurements are the most cost effective way to achieve the required alignment accuracy, each magnet should be mapped in sufficient detail to determine the magnetic axis and magnetic plane. Realignment of a few selected toroidal field coils appears to be a reasonable way of reducing the global field error to zero. Initially six magnets uniformily spaced around the torus will be selected for realignment to reduce the global field error to an acceptable level.

J. E. Lenz
Engineer Laboratory
Dept 256, Bldg 102, Sta 25033

R. E. Juhala
Scientist
Dept 223, Bldg 81, Sta 576-8261

DEFINITION OF MAGNET ALIGNMENT ERRORS

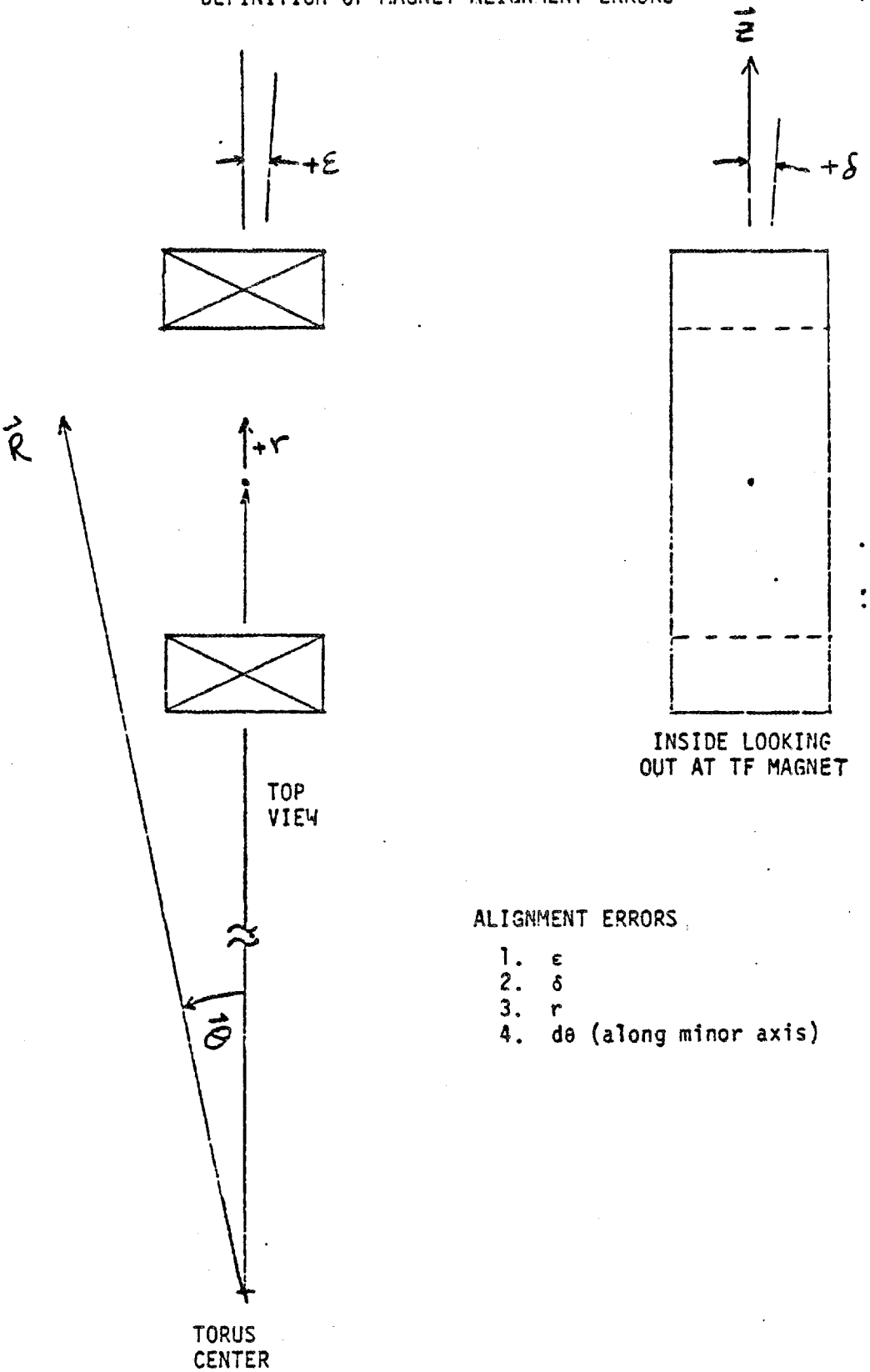

ALIGNMENT ERRORS

1. ε
2. δ
3. r
4. $d\theta$ (along minor axis)

PROBABILITY DISTRIBUTION FUNCTIONS WHERE THE ACCEPTANCE MEASUREMENT IS MADE AFTER THE MANUFACTURING PROCESS IS COMPLETED

NORMAL DISTRIBUTION $n(\mu, \sigma)$

I

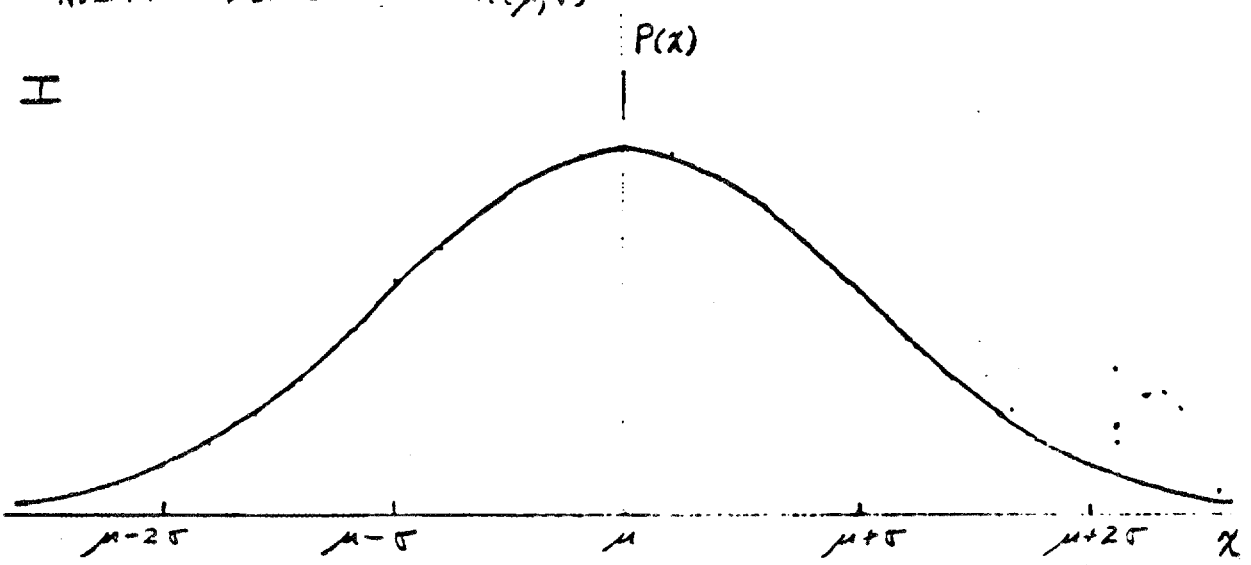

II

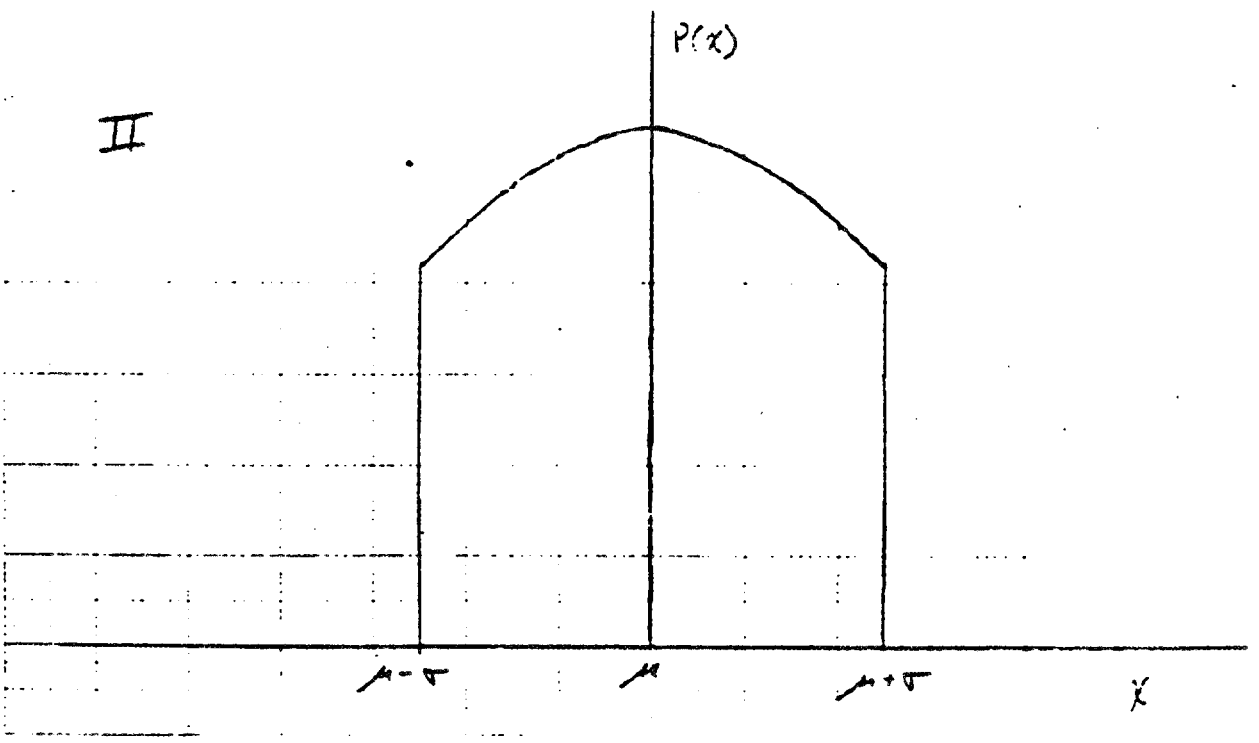

PROBABILITY DISTRIBUTION FUNCTIONS WHERE THE ACCEPTANCE MEASUREMENT IS USED AS PART OF THE MANUFACTURING PROCESS

III

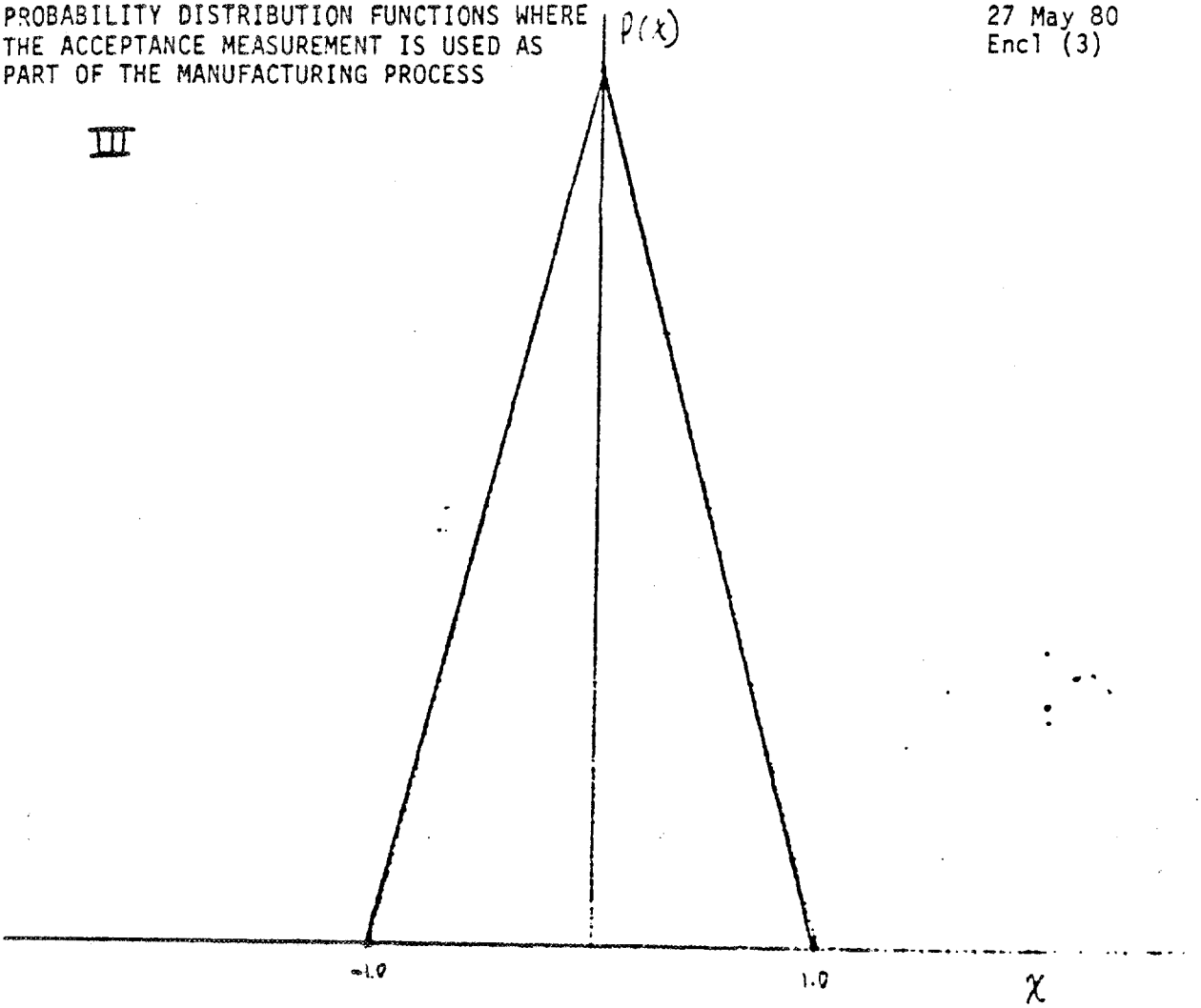

IV

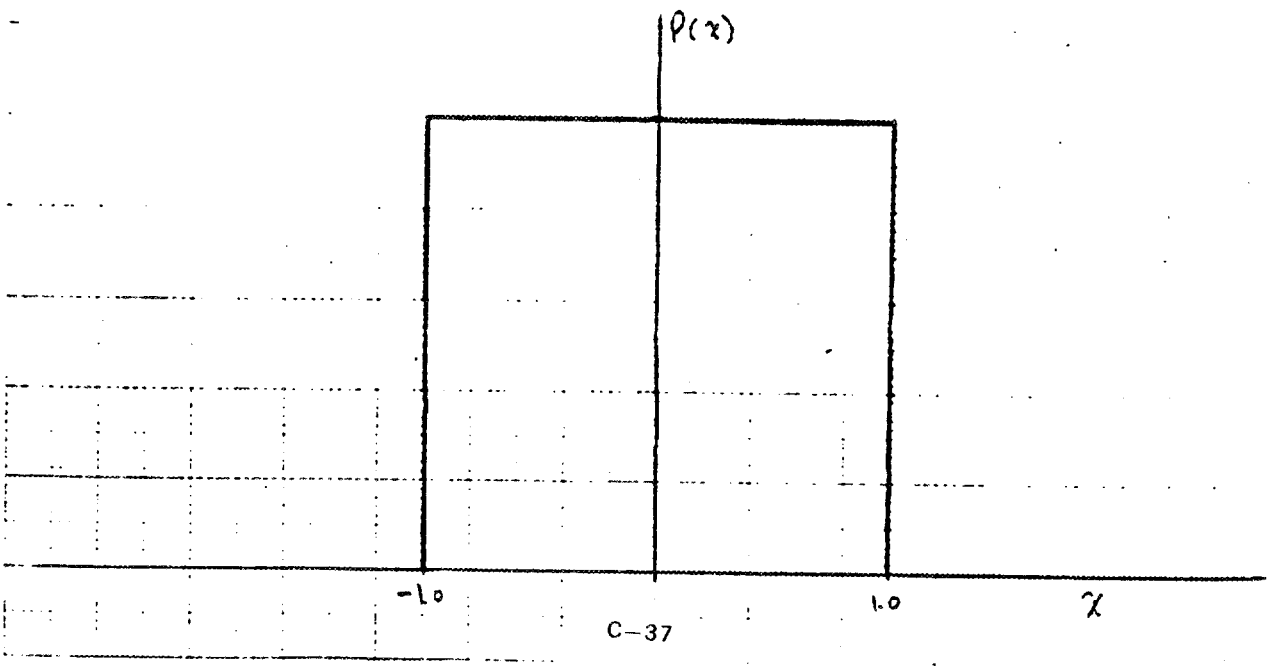

EFFECT OF NUMBER OF POINTS AND NUMBER OF SAMPLES ON THE STATISTICS OF $\delta B/B$

$\varepsilon = \pm .1°$

$\delta = \pm .1°$

$r = \pm .001°$

N = number of randomized designs

n = number of points per bump for comparison

1. n = 10 points/bump

N	$\bar{X}$	S
5	.684507E-4	.27427E-4
10	.732724E-4	.27474E-4
15	.7000E-4	.35713E-4
20	.787613E-4	.52659E-4
25	.776032E-4	.501625E-4
30	.713597E-4	.49487E-4
35	.74857E-4	.485948E-4
40	.76378E-4	.47746E-4
45	.79530E-4	.49069E-4
50	.80571E-4	.518755E-4

2. N = 20 randomized designs

n	$\bar{X}$	S
2	.814651E-4	.590008E-4
5	.809892E-4	.584729E-4
10	.809133E-4	.586201E-4

TRANSLATION OF ALIGNMENT ERRORS TO $\langle \delta B/B \rangle$

n = 10 points/bump
N = 20 randomized designs

	$\langle \delta B/B \rangle_R$		$\langle \delta B/B \rangle_\theta$		$\langle \delta B/B \rangle_Z$		$\lvert \langle \delta B/B \rangle \rvert$	
	$\bar{X}$	S	$\bar{X}$	S	$\bar{X}$	S	$\bar{X}$	S
1. Error in ε only	.285811E-4	.207914E-4	.127719E-4	.906799E-5	0	0	.285812E-4	.208914E-4
2. Error in δ only	.195934E-6	.119226E-6	.157887E-7	.790535E-8	.286385E-4	.208326E-4	.286553E-4	.208107E-4
3. Error in r only	.443124E-5	.123911E-4	.187076E-6	.2202443-6	0	0	.444835E-5	.1238834E-4
4. All three errors modeled	.284513E-4	.20911E-4	.92501E-7	.678644E-7	.287249E-4	.209209E-4	.404382E-4	.295688E-4
5. Error in coil location along minor axis ($d\theta$)	.22123E-5	.1577E-5	.5199E-6	.667E-7	0	0	.2327E-5	.1496E-5

$$\langle \delta B/B \rangle = \langle \delta B/B \rangle_R \cdot \hat{R} + \langle \delta B/B \rangle_\theta \hat{O} + \langle \delta B/B \rangle_Z \hat{Z}$$

Error Tolerance	Displacement of Coil Pack
$\varepsilon = \pm .05°$	.01"
$\delta = \pm .05°$	.01"
$r = \pm .0005m$	.02"
$d\theta = \pm .01°$	.02"

GLOBAL FIELD ERROR DUE TO UNEQUAL TURNS IN THE TF MAGNETS

n = 10 points/bump
N = 20 randomized designs

Error in No. of Turns in TF Coil	$\langle \delta B/B \rangle_R$		$\langle \delta B/B \rangle_\theta$		$\langle \delta B/B \rangle_Z$		$\lvert \langle \delta B/B \rangle \rvert$	
	$\bar{X}$	S	$\bar{X}$	S	$\bar{X}$	S	$\bar{X}$	S
± 1 turn	.50925E-8	.29135E-8	.7404E-4	.5381E-4	0	0	.7404E-4	.5381E-4
± 2 turns	.5543E-8	.3158E-8	.1157E-3	.8987E-4	0	0	.1157E-3	.8987E-4
± 3 turns	.70289E-8	.4101E-8	.17529E-3	.1449E-3	0	0	.17529E-3	.1449E-3

Each TF magnet will require approximately 1000 turns.

FIELD LINE TRACING WITH $\delta B/B = 1.66 \cdot 10^{-4}$

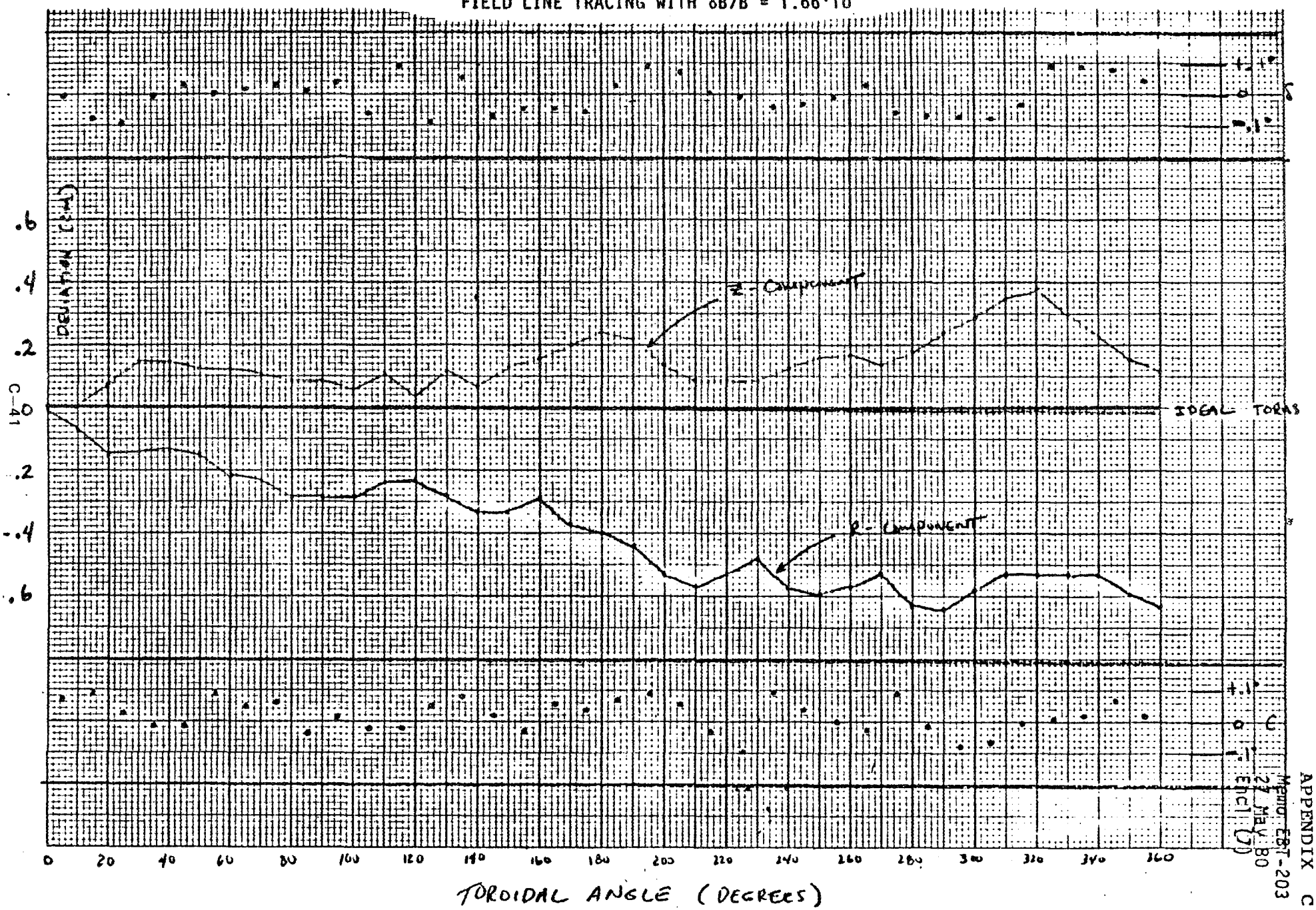

APPENDIX C

Memo EBT-203
27 May 80
Encl (7)

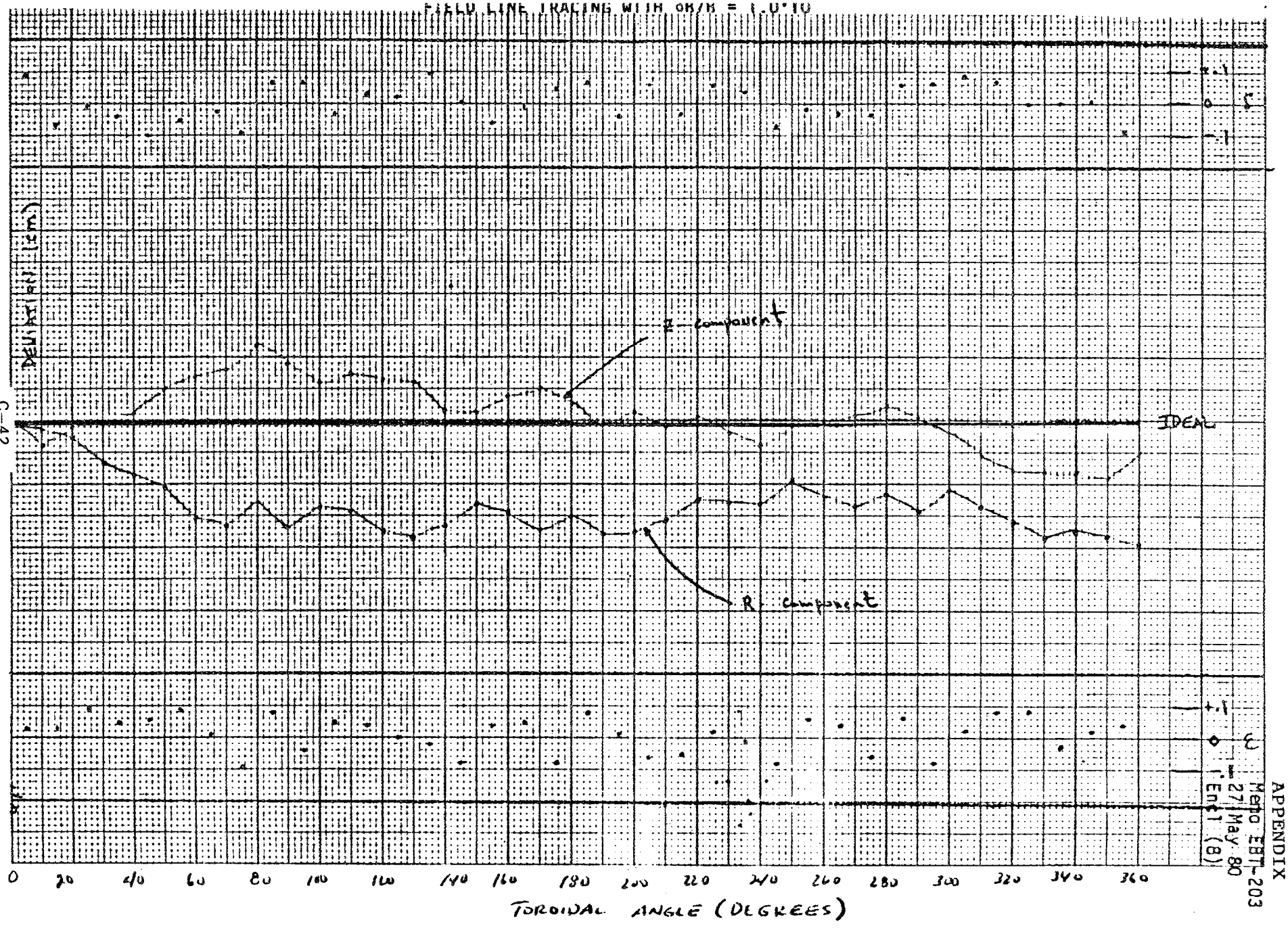
FIELD LINE TRACING WITH DR/R = 1.0*10
Z-component
IDEAL
R-component
0
20
40
60
80
100
120
140
160
180
200
220
240
260
280
300
320
340
360
TOROIDAL ANGLE (DEGREES)

CORRECTION OF FIELD LINE CLOSURE

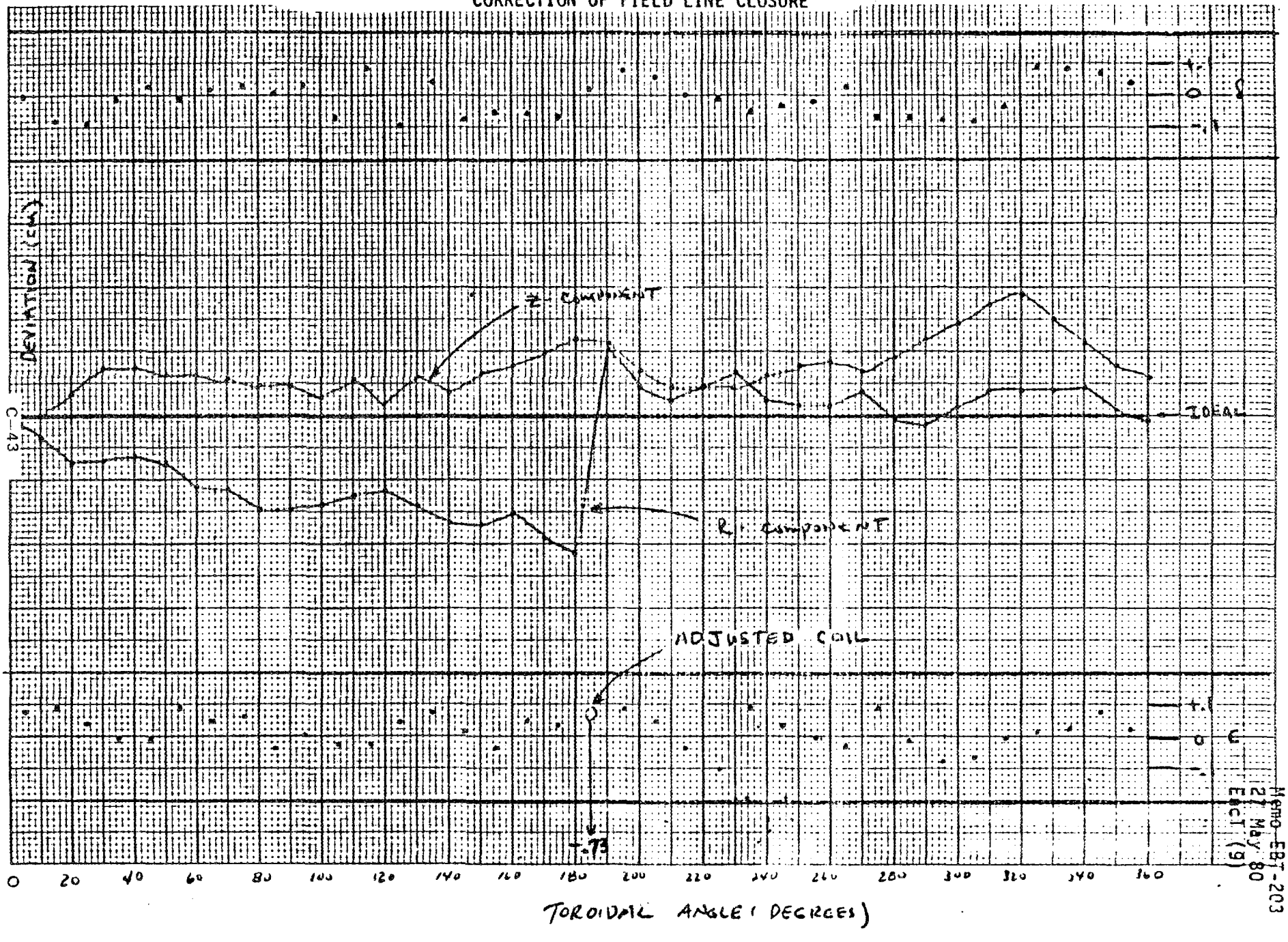

EFFECT OF $\delta B/B$ ON FIELD LINE CLOSURE

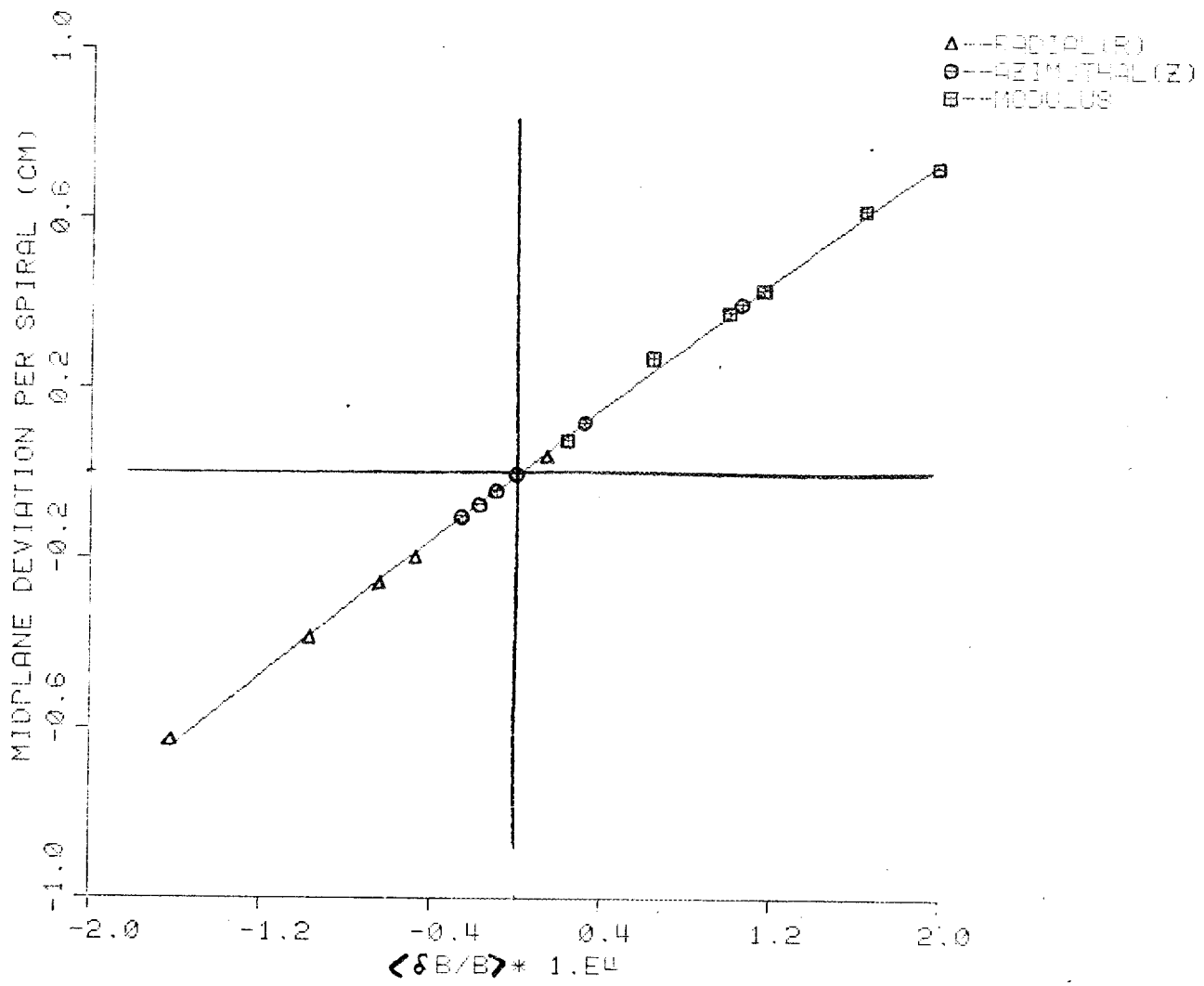

EFFECT OF THE ALIGNMENT TOLERANCE
ON THE GLOBAL FIELD ERROR

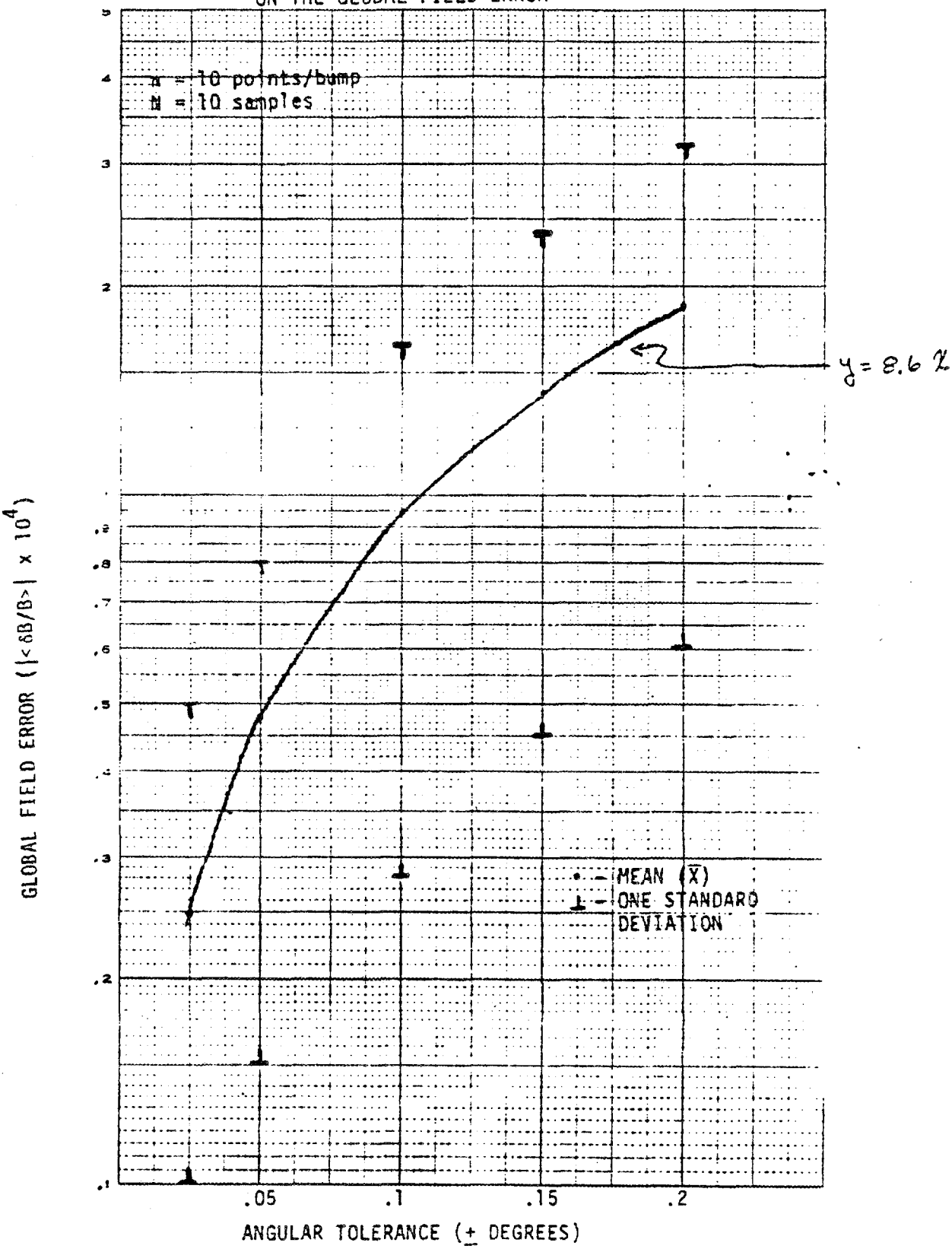

$n = 250$

$$\bar{X} = \sum_{i=1}^{n} \frac{X_i}{n} = .85$$

HISTOGRAM OF PROBABILITY DISTRIBUTION FOR $|\langle \delta B/B \rangle|$

$$s = \left[\sum_{i=1}^{n} \frac{(X_i - \bar{X})^2}{n} \right]^{1/2} = .45$$

Error Tolerance:

$\varepsilon \pm .1°$
$\delta \pm .1°$
$r \pm .001m$

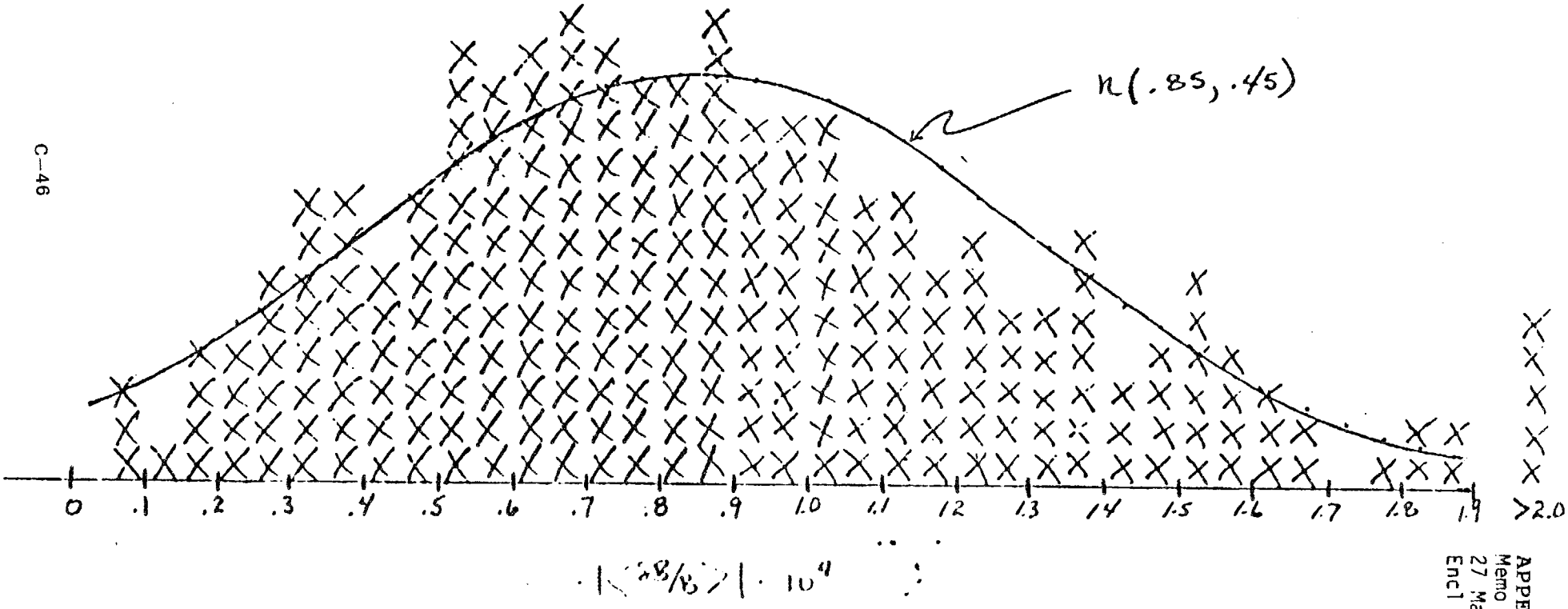

TEST OF HYPOTHESIS THAT $|\langle \delta B/B \rangle|$ is $n(\bar{X}, s)$

A. Hypothesis $X_i = |\langle \delta B/B \rangle|$ is $n(\bar{X}, s)$

where $\bar{X} = \sum_{i=1}^{n} \frac{x_i}{n}$ AND $s = \left[\sum_{i=1}^{n} \frac{(x_i - \bar{x})^2}{n} \right]^{1/2}$

from a random sample of size n.

B. Goodness-of-fit or CHI - squared (χ^2) test

1. The data in Encl (7), as shown, is divided into 40 bins. Let X_i be the occurrence in each bin : X_i $i = 1$ to 40

2. There are 250 random samples (n = 250).

3. For the random sample: $\bar{X} = .85$, $s = .45$

4. For each bin, an expected probability (P_i) can be determined from the normal distribution $n(\bar{X}, s)$.

5. Then the random variable

$$Q = \sum_{i=1}^{150} \frac{(x_i - n P_i)^2}{n P_i}$$

has an approximate CHI squared distribution with 37 degrees of freedom. For the data in Encl (7), Q = 20.7.

6. For $\chi^2(37)$ distribution: $Pr(Q \leq 24) = .95$

C. Since $Q < 24$ there is a 95% confidence in the hypothesis.

Excerpt from Magnetic System Title I report.

The as-built coil configuration was performed using the code COILS2, which was prepared specifically for the EBT-P program. The computer code models the coil using a current-carrying filament which traces out the path followed by the superconductor throughout the winding.

The magnetic model can be described most simply by dividing it into six sections:

a. lead entry down through stack,
b. half of 32nd layer from center to left flange (helix),
c. pancake spiral from 32nd layer to 1st layer,
d. 31 helically-wound layers,
e. half of 32nd layer from right-hand flange to center (helix) and,
f. lead exit up through stack.

The dimensional data can be found from Drawing 11-38006 (Appendix A.1). A more detailed explanation of the model follows.

The computer code models the magnet by sending a single, current-carrying filament down the entry lead path shown in Figure 5.1-5 to the coil pack.

After lead entry, the coil pack itself was modeled by first winding 1/2 of the 32nd layer from the center of the coil to the left-hand flange (as viewed in Drawing 11-38006-1 of Appendix A.1). The filament was wound in a helical manner, consisting of 360-straight line segments per turn, for 19 turns. The conductor then follows a descending spiral path for 34 turns (layers) to the bobbin. Two extra turns (layers) were incorporated in this pancake to compensate for the double-conductor-width insulation between the 31st and 32nd layers (refer to drawing). The model then moves the current element helically in the first layer until it passes the turn of insulation separating the pancaked layers from the rest of the windings. At this point, the main coil pack winding begins. The current element helically progresses from the insulation on the left-hand side to the flange on the right-hand side (as seen in Figure 5.1-8).

Each time a left- or right-hand boundary dimension is met, a layer transition automatically occurs. During a layer transition, the current element travels a path tangent to the point where it contacted the boundary. This tangent takes the element to the next layer, along the boundary, and then begins its helical traverse back to the other side of the coil. The model of the coil pack is then completed by winding the last (32nd) layer from the right-hand flange back to the center of the coil where the lead exits as seen in Figure 5.1-8.

Each helical and/or spiral turn of the conductor was modeled as 360 straight line segments, one segment per degree. The fields, due to each line segment, were calculated and then summed to reach the final field value. A study was performed to determine the deviation caused by using line segments. In this study, the field due to a circular turn of current was compared to those produced by turns of 36,360 and 3600 straight line segments. The field deviations were found to be 0.2%, 2×10^{-3}% and 8×10^{-5}%, respectively. Due to the number of calculations needed when over 1200 turns are segmented into 3600 lines, 360 line segments were determined to be sufficient. Further study of this effect is necessary during Title II.

The field data are presented in Figures 5.1-7 and 5.1-8 for points along the coil axis. Figure 5.1-7 tabulates the non-axial fields at points on either side of the coil. These points are located at the intersections of the axes from two adjacent coils. The data present the effects of individual conductor sections as they influence the field behaviors at these points. The values assigned to these individual sections of conductor may be somewhat misleading. This is due to the fact that the windings of a particular section do not start and stop at the same angular (or circumferencial) positions; therefore, the field error given is partially due to incomplete loops which are completed in another section.

Figure 5.1-8 tabulates the fields at points along the axis from left to right. The average axial field is also shown. In this reference frame, Bx is approximately equal to the axial field and the root mean square of By and Bz is approximately equal to the radial field. With this in mind, the average axial field is 2.49 Tesla and the radial, or error field, is approximately 0.15 gauss. This average should represent a first order attempt at quantifying the toroidal field error due to coil shape. The 0.15 gauss represents a globally-averaged $\Delta B/B$ of approximately 5×10^{-6}.

During the Title II study period, additional field calculations will be necessary. For example, the worst case tolerance buildup effects will be analyzed. The coil model will also be modified so that the layer-layer transitions take place at specified locations. This will include the effects due to next-to-last turn spacers required to equalize the number of turns in each layer.

CONDUCTOR DESCRIPTION

The superconducting cable to be used for the coil windings is described in General Dynamics/Convair Specification No. 11-38007, Rev. A, which is attached as Appendix A.2-2.

Briefly, the superconductive material is a niobium-titanium alloy (45.5 ± 1.5% Wt. Nb) in a high conductivity copper matrix. The conductor as a whole is a rectangular monolith with the follow-

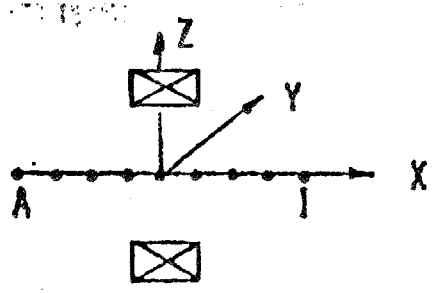

SECTION	LEFT SIDE (PT. A) BY (GAUSS)	LEFT SIDE (PT. A) BZ (GAUSS)	RIGHT SIDE (PT. I) BY (GAUSS)	RIGHT SIDE (PT. I) BZ (GAUSS)
LEAD ENTRY	-1.237	-0.028	+1.349	+0.038
32ND LAYER (LEFT HALF)	-2.623	+1.543	+2.318	-1.102
PANCAKE (LEFT SIDE)	+0.267	+0.513	-0.313	-0.026
LAYERS 1-31	+1.845	-2.809	-1.961	+2.172
32ND LAYER (RIGHT HALF)	+0.518	+0.745	-0.069	-1.078
LEAD EXIT	+1.363	+0.061	-1.224	-0.049
TOTAL:	+0.133	+0.025	+0.100	-0.045

FIGURE 5.1-7. MAGNETIC FIELD AT COIL AXES INTERSECTIONS

GENERAL DYNAMICS
Convair Division

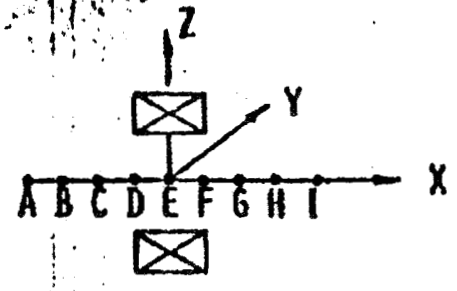

PT	BX (TESLA)	BY (TESLA)	BZ (TESLA)	BR (TESLA)
A	+1.00345	+1.33879E-05	+2.35127E-06	1.3593E-05
B	+1.60879	+1.61234E-05	+4.15350E-07	1.6129E-05
C	+2.61737	+1.88133E-05	+3.07985E-06	1.9064E-05
D	+3.79341	+1.83618E-05	+4.49921E-06	1.8905E-05
E	+4.36235	+1.82903E-05	+8.96304E-06	2.0368E-05
F	+3.79446	+1.59865E-05	-1.13331E-06	1.6027E-05
G	+2.61808	+1.09632E-05	-6.86026E-06	1.2933E-05
H	+1.60906	+9.99710E-06	-5.96136E-06	1.1640E-05
I	+1.00357	+9.97861E-06	-4.35466E-06	1.0887E-05
AXIAL AVERAGE:	+2.49006	+1.4653E-05	+1.1101E-07	1.5505E-05

FIGURE 5.1-8 MAGNETIC FIELD ALONG COIL AXIS

INTRA-LABORATORY CORRESPONDENCE

OAK RIDGE NATIONAL LABORATORY

February 25, 1974

TO: Distribution

FROM: H. Ikegami and R. A. Dandl
H. I. R.A.D.

SUBJECT: ELMO Group Technical Memo No. 14
Magnetic Field Errors on ELMO Bumpy Torus (EBT)

[This report is preliminary. All opinions expressed herein are those of the authors. It is for private circulation only and should not be reproduced or transmitted without the consent of the authors.]

HI:RAD:nb

Attachment

Distribution

C. F. Barnett
C. O. Beasley
L. A. Berry
R. L. Brown
C. E. Bush
J. D. Callen
J. F. Clarke
J. A. Cobble
R. J. Colchin
E. C. Crume
R. A. Dory
J. L. Dunlap
H. O. Eason
P. H. Edmonds
O. C. Eldridge
A. C. England
J. E. Francis
W. F. Gauster
G. E. Guest
E. G. Harris
G. R. Haste
P. Haubenreich
C. L. Hedrick
J. T. Hogan
R. P. Jernigan
T. C. Jernigan
G. G. Kelley
N. H. Lazar
G. F. Leichsenring
H. M. Long
M. S. Lubbell
J. N. Luton
J. F. Lyon
O. D. Matlock
J. R. McNally, Jr.
H. K. Meier
O. B. Morgan
M. Murakami
R. V. Neidigh
D. B. Nelson
C. E. Parker
H. Postma
J. A. Ray
J. W. Reynolds
M. Roberts
J. A. Rome
J. C. Sprott, Univ. Wisc.
D. Steiner
L. D. Stewart
W. L. Stirling
P. L. Walstrom
W. R. Wing
R. E. Wintenberg
W. L. Wright
O. C. Yonts
A. Zucker
Bulletin Board
TD Library (3)

MAGNETIC FIELD ERRORS ON ELMO BUMPY TORUS (EBT)

Hideo Ikegami and R. A. Dandl

The effect of magnetic field errors is known to have deleterious effects on closed-line plasma confinement devices[1] such as bumpy tori and multipoles. In multipole devices, the effect was minimized by applying a toroidal magnetic field. While minimizing field errors, S. Yoshikawa[2] observed that plasma losses to the supported-ring increased as the electron temperature increased and that the losses showed no dependence on ion mass. He ascribed the remaining error field effect in his Spherator experiment to the formation of convective cells. In Tokamak devices, error fields may generate more magnetic islands so as to decrease the effective plasma diameter. In closed-line devices, such as EBT, the error fields cause the toroidal field lines to spiral out so as to connect the plasma to the wall.

It is useful to recall the usual model for plasma escape along field lines spiraling out of the system. In most plasmas, the electron velocity is much larger than the ion velocity so that electrons reach the wall first, thereby generating a space charge along the field line which decelerates electrons and accelerates ions. With the result that both ions and electrons escape to the wall with the same speed, $v_s = \sqrt{T_e/m_i}$ (ion sound velocity), resulting no net current flow. Since electrons are carried to opposite walls, depending on their sign of parallel velocity, there would develop no bulk electric field as might be observed in the case of simple toroidal drift.

Beam Probing

In order to estimate the amount of error field in the ELMO Bumpy Torus, the shift of an electron beam trajectory caused by an artificially imposed error field was studied.

The electron gun and the collector assembly is shown in Fig. 2. The cathode is a tantalum strip of 0.2 mm wound around by 0.05 mm nickel wire and coated by a mixture of BaO and SrO. The segmented collector is composed of five 4 mm x 15 mm electrodes insulated from each other. The electrode #3 is located just behind the beam aperture on the anode plate and is arranged to collect the electron beam coming back along a closed magnetic line.

The electron gun and collector assembly is inserted horizontally into the W4 port. An adjustment which locates collector #3 on the minor toroidal axis also locates collector #1 inside the axis.

The electron beam is a 1.5 mA current pulse at 100 V with 1 μsec width. With the toroidal magnetic field (1820 G) present, the beam current, detected by one of the segmented collectors, is of the order of 150 μA.

The pulse beam technique suppressed the instabilities generated in the beam near electrodes. These instabilities caused scattering and fluctuations of the beam and allowed the observation of very pretty instability growths. The pulsed beam unambiguously indicated a time of flight around the torus of 1.6 μsec, which is the correct time for the 100 V electron beam. The beam collectors were fed into a 100 Ω resistor and displayed on an oscilloscope at 0.1 V/cm and 1 μsec/cm sweep (Fig. 3).

The error field is generated by a pair of air-core coils, one 17.5" outside and the other 23.5" inside from the toroidal axis, assembled in such a way that the coils sandwich the E1 cavity. Magnetic field intensity vs. axial distance, for the half of coils constituting the pair solenoid is shown in Fig. 4. The error field is imposed on the toroidal field in such a way that the field line spirals inwards when the positive current is applied to the error coils. The error field is imposed perpendicularly across the toroidal axis over 30 cm of its circumference. If we assume 10% of the return field crossing back the toroidal axis, the effective error field, ΔB, averaged along the circumference of 30 cm is given by

$$\Delta B \text{ (gauss)} = 4 \text{ I (amp)} \quad ,$$

where I is the current to the error field coils. The toroidal field is kept constant at 1820 G (2000 A) throughout the experiment.

In Fig. 5, the displacement of the beam coming back after one round trip around the torus is plotted against the artificially generated error field. The beam diameter is estimated to be about 2 mm, which is indicated by the shaded regions on the rectangular collectors, as shown in Fig. 5.

It is estimated from Fig. 5 that the horizontal displacement 4.8 mm of the electron beam is produced for every 18 G of the error field, which agrees with the calculated value, if we take the spread of error field ℓ = 46 cm;

$$\Delta r = \frac{\Delta B}{B} \ell$$

$$= \frac{19}{1820} \times 46$$

$$= 0.48 \text{ mm} \quad .$$

Without the artificial error field, the electron beam shows a displacement of 1.5 mm. Provided that this virtual error field is distributed uniformly along the entire toroidal axis, we can estimate the average error value to be

$$\frac{\overline{\Delta B}}{B} = \frac{0.15}{2\pi R}$$

$$= 1.5 \times 10^{-4} \quad .$$

This value, though measured at B = 1820 G, should stay constant for all B. The earth error field, $\overline{\Delta B_o}$, averaged over the toroidal axis, has been measured to be 0.042 G, which gives rise to

$$\frac{\overline{\Delta B_o}}{B} = \frac{0.042}{1820}$$

$$= 2.3 \times 10^{-5} \quad ,$$

which is one order of magnitude smaller than the error field measured so that the error field ($\Delta B = 1.5 \times 10^{-4}$ B) detected by the beam probing is concluded to be due to the asymmetry of toroidal coil assembly. If this error field is homogeneous, it is possible to cancel it by two pairs of deflection coils mounted locally, one vertical and the other horizontal. On the other hand, if the error field is inhomogeneous, that is, its direction is random in space, there is no way to cancel it.

We estimate the loss time for a T_e = 100 eV hydrogen plasma due to an error field. The ion sound velocity for hydrogen is given by

$$v_s = \sqrt{\frac{T_e}{m_i}}$$

$$= 1.7 \times 10^7 \text{ cm/sec} \quad .$$

The loss time may be estimated to be

$$\tau = \frac{a}{v_s(\Delta B/B)}$$

$$= \frac{10}{1.6 \times 10^7 \times 1.5 \times 10^{-4}}$$

$$= 4.2 \times 10^{-3} \text{ sec} \quad ,$$

where a is a minor radius of the ELMO Bumpy Torus, taken to be 10 cm. The Appendix is an elaborate treatment of the plasma decay due to error fields.

APPENDIX I

Calculation of Particle Loss Due to Error Field

Recently, Meade and Fonck[3] discussed the effect of error field on diffusion of plasmas in a closed-line device. His treatment is similar to that of Kadomtsev and Pogutse,[4] in a sense that the first order velocity in Vlasov equation is replaced by

$$V = v_{\parallel} \frac{\Delta B}{B} + V_{\nabla B} \quad ,$$

where $V_{\nabla B}$ is a drift velocity due to the nonuniform field. However, the method of Kadomtsev and Pogutse to describe the diffusion coefficient is valid only when the magnetic surface is closed. In the case of closed-line devices such as shearless multipoles and bumpy tori with the presence of error fields, the method may not be applicable because the error field connects the plasma to the wall by simple flow of particles along the magnetic field lines.

Here we treat the problem with the use of the Fokker-Planck equation, provided the diffusion coefficient D, which may depend on the error field, is known. The electron density $n(x,t;v_{\parallel})$ is assumed to obey the following equation.

$$\frac{dn}{dt} = -\langle w \rangle \frac{dn}{dx} + D \frac{d^2n}{dx^2} + Q \quad , \tag{1}$$

where Q is a source term and w is the radial electron drift velocity due to the error field,

$$w = \frac{\Delta B}{B} v_{\parallel} \quad , \tag{2}$$

which reduces the ion sound velocity when averaged by the electron distribution function, which is deformed into a drift Maxwellian distribution due to the ambipolar electric field to give the ion sound speed,

$$\langle w \rangle = \frac{v_{\parallel}}{|v_{\parallel}|} \frac{\Delta B}{B} \sqrt{\frac{T_e}{m_i}} \quad . \tag{3}$$

For simplicity, the plasma is approximated by an infinitely long belt in y direction with a diameter, 2a, which extends from $-a$ to a in x direction, which is the direction of the error field, ΔB, as shown in Fig. 6. Plasma density is assumed to be uniform in y direction along the toroidal magnetic field and zero for $|x| \geq a$.

If we assume Q = 0, Eq. (1) can be solved by putting

$$n(x,t;w) = n_0 e^{-\alpha t} g(x)$$

to give

$$n(x,t;w) = n_0 \exp\left(-\alpha t + \frac{\langle w \rangle}{2D} x\right) \cos \frac{\sqrt{4\alpha D - \langle w^2 \rangle}}{2D} x \quad . \tag{4}$$

The inverse decay time α is determined from the boundary condition

$$n(\pm a, t; \langle w \rangle) = 0$$

to be

$$\alpha_0 = \left(\frac{\pi}{2a}\right)^2 D + \frac{\langle w \rangle^2}{4D} \tag{5}$$

and we obtain

$$n(x,t;w) = n_o \exp\left(-\alpha_o t + \frac{\langle w\rangle}{2D} x\right) \cos \frac{\pi}{2a} x \quad . \tag{6}$$

In order to eliminate the discontinuity at $x = 0$ in $n(x,t;\langle w\rangle)$, Eq. (6) may be averaged over $v_{\parallel}$ by the Maxwell distribution:

$$n(x,t) = \sqrt{\frac{m}{2\pi T}} \int_{-\infty}^{\infty} n\left(x,t;\frac{\Delta B}{B}\sqrt{\frac{T}{m_i}}\ \frac{v_{\parallel}}{|v_{\parallel}|}\right) \exp\left(-\frac{m}{2T} v_{\parallel}\right) dv_{\parallel}$$

$$= n_o \exp\left\{-\left[\left(\frac{\pi}{2a}\right)^2 D + \frac{T}{4m_i D}\left(\frac{\Delta B}{B}\right)^2\right] t\right\} \cosh\left\{\frac{x}{2D}\left(\frac{\Delta B}{B}\right)\sqrt{\frac{T}{m_i}}\right\} \cos \frac{\pi}{2a} x \quad , \tag{7}$$

where the hyperbolic cosine function reflects the plasma drift towards the wall caused by error field.

The diffusion coefficient for the bumpy torus may be expressed in the following form.[4,5]

$$D \simeq \frac{1}{2}\left(\frac{T}{eBR}\right)^2 \frac{\nu}{\Omega^2 + \nu^2} \quad , \tag{8}$$

where R is the major radius, ω_c is the electron-cyclotron frequency, Ω is the precessional frequency approximately given by

$$\Omega \simeq \frac{T}{(2a)^2\, eB} \tag{9}$$

and ν is the effective collision frequency.

For the collisionless regime, e.g., $T > 100$ eV with $n \sim 10^{12}$ cm^{-3}, we can rewrite Eq. (7) as follows:

$$n(x,t) = n_0 F(x) \exp\left\{ -\left[\frac{\pi^2}{2} \left(\frac{a}{R}\right)^2 \nu + \frac{TR^2}{8m_i a^4} \left(\frac{\Delta B}{B}\right)^2 \frac{1}{\nu} \right] t \right\} , \qquad (10)$$

where $F(x)$ is a form factor. If we take ν_{e-i} to be the Coulomb collision frequency between electrons and ions, the critical value of the error field which dominate the diffusion term is given by

$\nu_{eI} \simeq 25 \frac{n}{T_E^{3/2}}$ @ $T_E = T_I$

$$\left(\frac{\Delta B}{B}\right)_c = 2\pi \left(\frac{a}{R}\right)^2 \frac{a}{\sqrt{\frac{T}{m_i}}} \nu_{e-i} \quad . \qquad (11)$$

For ELMO Bumpy Torus, we choose $a = 10$ cm and $R = 1.5 \times 10^2$ cm. The critical error field is then given by

$M_i = 1836 \times 9.1 \times 10^{-28}$
$= 1.67 \times 10^{-24}$ gms

$$\left(\frac{\Delta B}{B}\right)_c = 1.4 \times 10^{-11} \frac{n(\text{cm}^{-3})}{T^2\,(\text{eV})} \quad , \qquad (12)$$

$\sqrt{m_i} = 1.3 \times 10^{-12}$

which indicates that the error field becomes important for low-density, high-temperature plasmas. For reasonably warm plasmas, $T \sim 100$ eV, the estimated error field $\frac{\Delta B}{B} = 1.5 \times 10^{-4}$ is still below the critical value when the plasma density is larger than 10^{11} cm^{-3}. In the collisional regime, the effect is obviously smaller.

If the electron-neutral collision frequency ν_{e-n} is used instead of ν_{e-i}, the critical error field is given by

$$\left(\frac{\Delta B}{B}\right)_c = 4 \times 10^{-4} \frac{p(10^{-6}\ \text{Torr})}{\sqrt{T(\text{eV})}} \quad .$$

In lightly ionized hydrogen plasmas where the electron-neutral collisions dominate, the error field of ELMO Bumpy Torus becomes effective below a pressure of 4×10^{-6} Torr for $T \cong 100$ eV.

Acknowledgments

The authors wish to express their appreciation to Dr. J. C. Sprott for his special attention on the error field of the ELMO Bumpy Torus. R. L. Livesey is acknowledged for his developing of the electron gun and the detector assembly.

REFERENCES

1. J. C. Sprott, Phys. Fluids 16, 1157 (1973).
2. S. Yoshikawa, Nucl. Fusion 13, 433 (1973).
3. Dale M. Meade and R. J. Fonck, Phys. Fluids 16, 1654 (1973).
4. B. B. Kadomtsev and O. P. Pogutse, Nucl. Fusion 11, 67 (1971).
5. L. Kovrizhnykh, MATT-TRANS-82 (Oct. 1968).

FIGURE CAPTIONS

Fig. 1. Spiraling-in toroidal field lines due to error field imposed.

Fig. 2. Gun and collector assembly.

Fig. 3. Oscilloscope trace of beam current 1 μsec/cm sweep, 0.1 V/cm vertical.

Fig. 4. Magnetic field intensity vs. distance from perturbing field coils with the exciting current held at 5 amperes.

Fig. 5. Shift of the electron beam due to the perturbation field. The abscissa is the current to the perturbing field coils (ref. Fig. 4).

Fig. 6. Slab model of the plasma with toroidal field in y direction and the error field assumed to be in x direction. Plasma is a slab of thickness 2a and infinitely long in y direction.

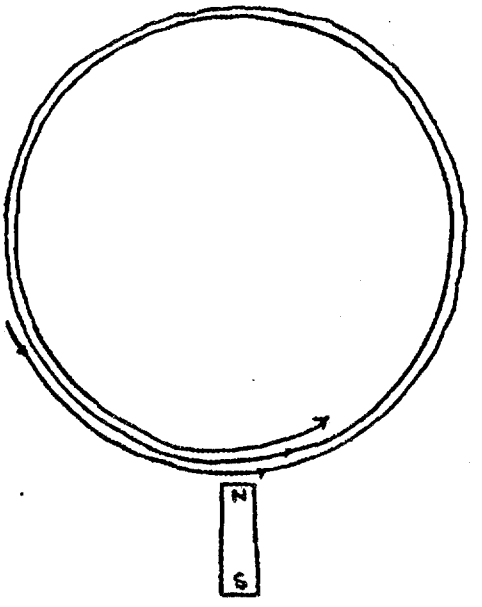

Fig. 1

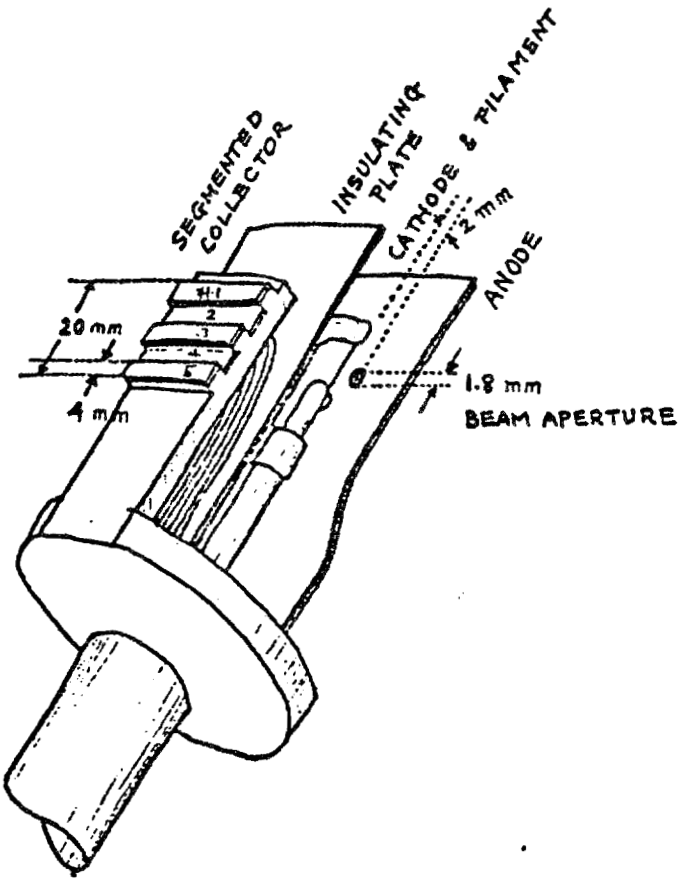
SEGMENTED COLLECTOR
INSULATING PLATE
CATHODE & FILAMENT
2 mm
ANODE
20 mm
4 mm
1.8 mm
BEAM APERTURE

Fig. 2

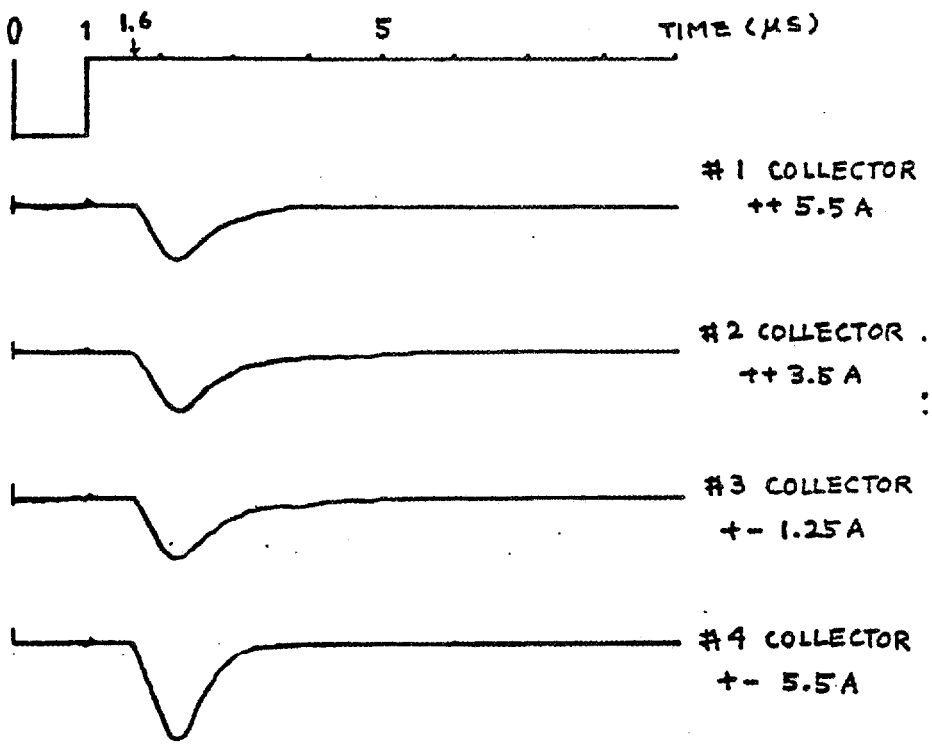
0
1
1.6
5
TIME (μs)
#1 COLLECTOR
++ 5.5 A
#2 COLLECTOR
++ 3.5 A
#3 COLLECTOR
+- 1.25 A
#4 COLLECTOR
+- 5.5 A

Fig. 3

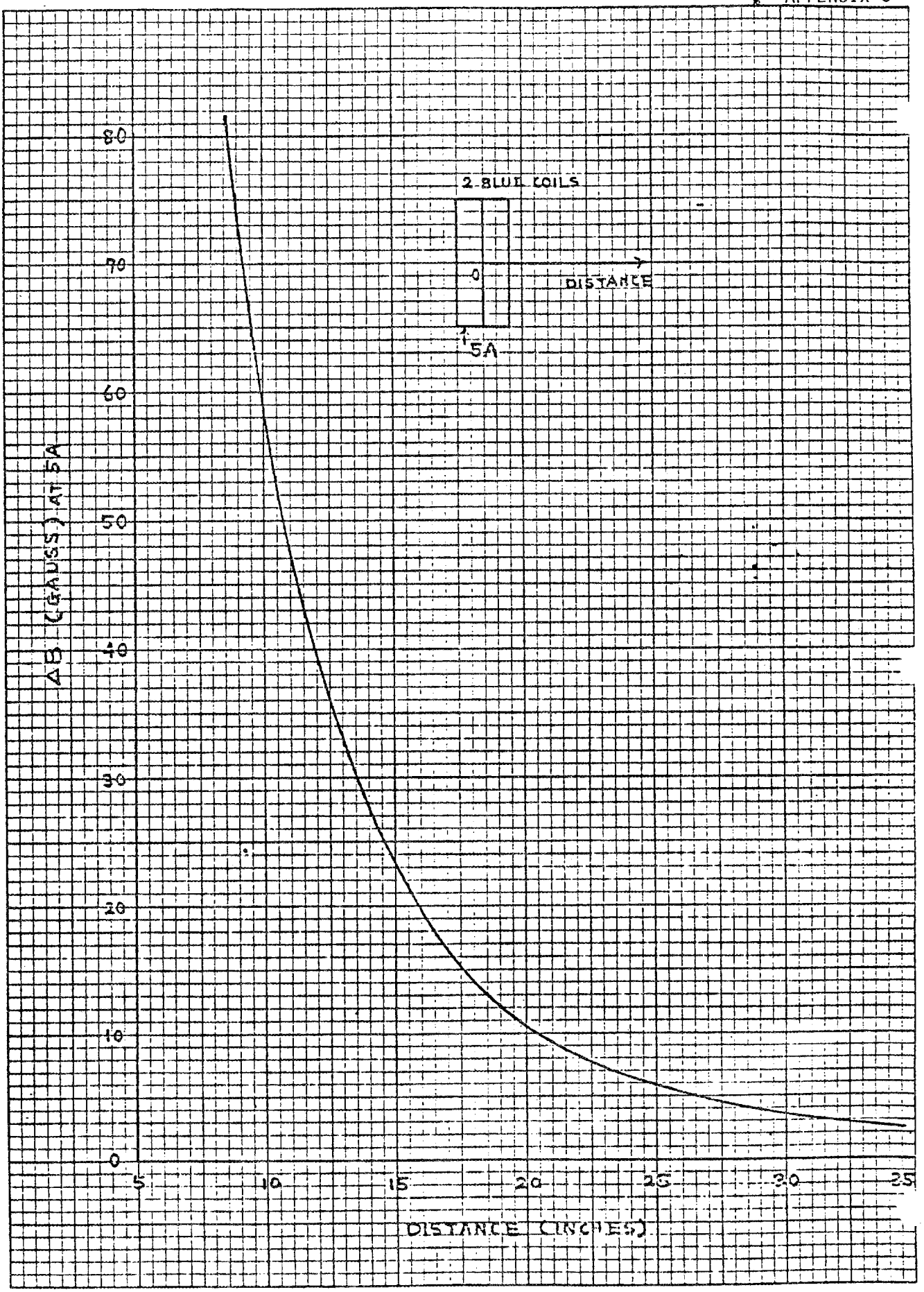
2 BLUE COILS
0
DISTANCE
5A
80
70
60
50
40
30
20
10
0
ΔB (GAUSS) AT 5A
5
10
15
20
25
30
35
DISTANCE (INCHES)

Fig. 4

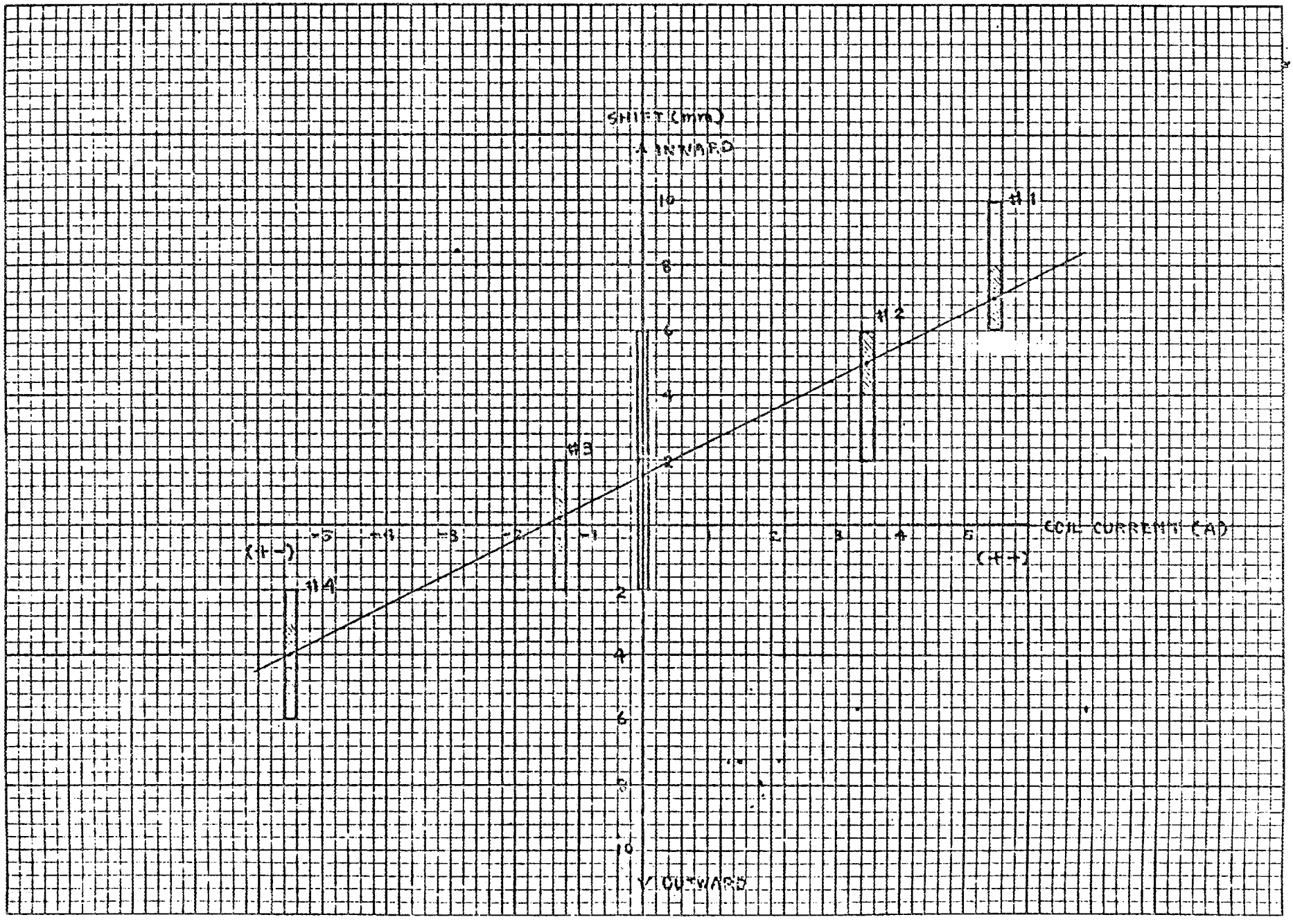
SHIFT (mm)
A INWARD
V OUTWARD
COIL CURRENT (A)
(+-)
(++)
#1
#2
#3
#4
10
8
6
4
2
2
4
6
8
10
-5
-4
-3
-2
-1
1
2
3
4
5

Fig. 5

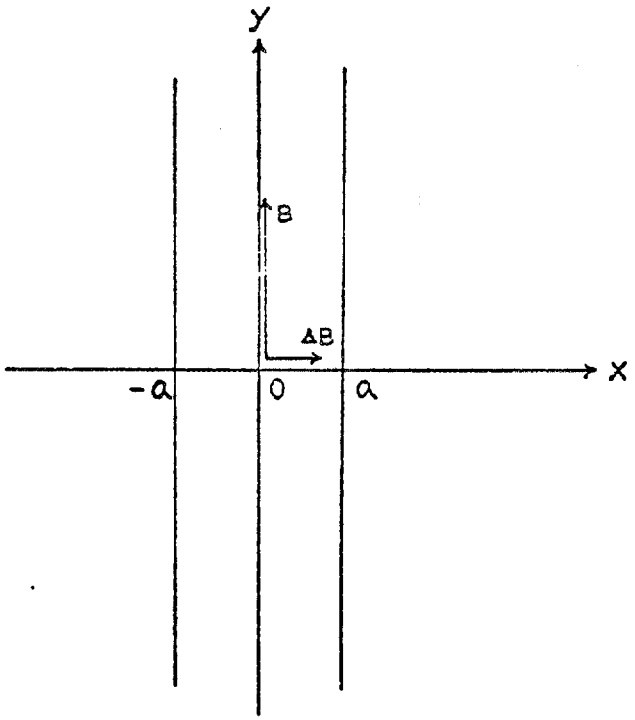

Fig. 6

Océ-Elliott Inc.
"PRECISE" 10X10 TO 1 INCH

REPORT NO. GDC-EBT-81-003

PRELIMINARY MANUFACTURING PLAN

ELMO BUMPY TORUS PROOF-OF-PRINCIPLE (EBT-P)

SEPTEMBER 1981

PREPARED UNDER CONTRACT YOE206R

MC DONNELL DOUGLAS ASTRONAUTICS COMPANY
ST. LOUIS DIVISION

PREPARED BY: R. J. Came
R. J. CAME
OPERATIONS MANAGER

APPROVED BY:
S. L. ACKERMAN
PROGRAM MANAGER

GENERAL DYNAMICS CORPORATION
Convair Division
San Diego, California

SECTION 1

INTRODUCTION

General Dynamics Convair will fabricate, assemble, test, and deliver 36 production EBT-P mirror coil magnets, 3 spare magnets, and the associated instrumentation, power and protection systems.

The work will be performed under contract to McDonnell Douglas Astronautics Company, St. Louis Division, and the magnets will be delivered to Oak Ridge National Laboratory, Oak Ridge, Tennessee.

Period of performance is from September 1982 through September 1984.

This Manufacturing Plan defines all major manufacturing operations required in performance of this task.

SECTION 2

DESCRIPTION OF PRODUCT

The mirror coil magnets covered by this manufacturing plan are an element of the Elmo Bumpy Torus Proof of Principle device, a fusion energy machine to be installed at Oak Ridge, Tennessee.

Each magnet consists of the following major assemblies, which are described in detail under Section 5 of this plan.

- The cold mass, which includes the wound conductor pack and the helium vessel
- The LN_2 cold wall and multilayer insulation, which cover the helium vessel
- The vacuum vessel, which forms the outer container for the entire magnet
- The stack assembly, which contains the high current leads and plumbing components

The completed magnet, Figure 2-1, weighs approximately 3500 pounds and is approximately 43" wide, 80" high, and 12" thick.

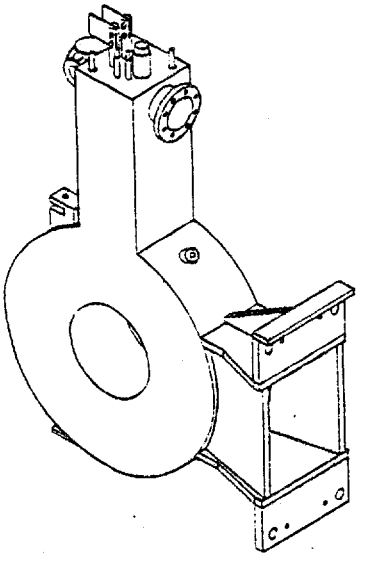

Figure 2-1. Completed Magnet Assembly

SECTION 3

GROUND RULES AND ASSUMPTIONS

Convair Integrated Management Systems (CIMS II) will be implemented on this program.

Engineering designs and specifications created for the EBT-P will be released for Operations and Material Dept. use through the Parts and Data Release System (PADR).

This plan is based on the fabrication, assembly, and test of 36 production mirror coil magnet assemblies, plus three spares.

Convair will perform as prime contractor. The manufacturer of the superconductor is a subcontractor responsible for design and production of the superconductor and for assisting Convair where inputs and analysis are required.

The program will be conducted on a standard 40-hour, 5-day work week with only spot overtime.

The schedule prepared for this program is identified as Master Schedule 81T1-242-3-0008 dated 7/8/81.

Fabrication and assembly will be accomplished in-plant by Dept. 064. Assist will be generated on MBA or similar paper.

Material certification shall be required of vendors. Subcontracting of superconductor services will require off-site inspection.

Tool design reviews will be conducted in accordance with PEDI 0-1-5-5.

The standard operations Planning Control System (PCS) will be utilized for the preparation and release of the fabrication, assembly, test, and preparation for shipment of this coil.

A review of all operations planning will be required prior to release, in accordance with PEDI 0-1-0-9.

The instrumentation, power, and protection systems are the responsibility of the Advanced Energy Systems Laboratory, Dept. 676, and are not included in this plan.

SECTION 4

TOOLING PLAN

The selection of manufacturing methods and the related tools are based upon the lowest combined cost for tools, manufacturing materials, and quality control, including both non-recurring and recurring costs. General Dynamics tooling plan for EBT-P is designed to meet the objective of minimum tooling expenditures while maintaining program quality requirements. The tooling plan is based on one prototype, 36 production articles, and 3 spares which will be fabricated, tested, and delivered.

4.1 TOOLING PHILOSOPHY

Our tooling philosophy highlights the following objectives:

a. Utilize the existing facilities with minimal rearrangement.

b. Strive for maximum utilization of multi-purpose tooling.

c. Use shop aids where possible.

d. Rely on highest level of "craftsman" machinists and welders to minimize tooling complexity and reduce tooling requirements.

4.2 TOOL DESIGN

Tool design concepts are being updated and finalized during this phase of the program. Changes to the tool design are reviewed with and agreed to by the operations manager and representatives of affected departments.

4.3 PLANNING

Operations planning documents for fabrication of details and assemblies are prepared in accordance with planning standard practices. The stamped copy of all planning documents will be retained as part of deliverable data.

4.4 TOOL CONTROL

Orders for the design and fabrication of all tools and manufacturing aids are generated by tool and operations planners using program office approved data. Our tool control system provides for the scheduling of tooling start and due dates in support of end item delivery schedule.

4.5 TOOL FABRICATION

We will accomplish tool manufacturing in a dedicated tool manufacturing facility where modern equipment is used throughout. This includes automated template and master lines layout photo preparation and conventional machine tools. The facility also includes optical equipment for fixture assembly and dimensional calibration.

4.6 TOOL LIST

The tools required to produce a total of 40 magnet assemblies are listed in Table 4-1.

4.7 MAJOR TOOLS

4.7.1 CONDUCTOR TAPING MACHINE. The conductor taping machine Figure 4-1 and 4-2, is a motor-driven mechanism which helically wraps insulating tape around the conductor as the conductor is drawn through the machine. It contains integral photoelectric inspection equipment to monitor uniform spacing of the insulation. As cleaned conductor is drawn through the taping machine, the machine is automatically energized to rotate a hollow spindle around the conductor. The spindle carries a spool of insulating tape. The spindle motion is mechanically coupled to spring loaded rubber rollers which grip the conductor. This coupling maintains a preset pitch of the helical wrapping. As the conductor leaves the spindle, it passes under two fiberoptic, photoelectric inspection heads. These are located an integral number of pitches apart so that each head normally returns the same signal to the electronic monitoring equipment. A difference in these signals causes a warning signal to be sent to the coil winding personnel. The taping machine is driven by a variable speed dc motor which is automatically controlled to vary its speed to match the speed of the conductor.

4.7.2 MAJOR ASSEMBLY FIXTURE. The major assembly fixture (11-38001-1) locates and holds the cold mass in a horizontal position, Figure 4-3, for assembly with the MLI blankets, LN_2 cold wall, and the stack assembly.

This fixture has provisions to compress the upper stack bellows required for final assembly prior to the final closeout weld of the stack assembly and the cold mass.

4.7.3 MAJOR ASSEMBLY STATION. Two assembly stations will be used to maintain the required rate.

Each assembly station, Figure 4-4, will consist of one assembly fixture (11-38001-1 ASFX) and one steel top work table located under an "A" frame (11-38001-1 HATO). The "A" frame has two one-ton electrical hoists and travels on angle iron tracks of sufficient length to cover the entire assembly area.

Table 4-1. Tool List

PART NUMBER	PART NAME	TOOL NAME
11-38001	MAGNET ASSEMBLY	ASSEMBLY FIXTURE (2) HANDLING TOOL (2) SETUP SHEET (3) TURNING WRENCH MANUFACTURING AID
11-38002	COLD MASS ASSEMBLY	WELD FIXTURE SETUP SHEET
11-38003	HELIUM SUPPLY TUBE	CHECK TEMPLATE DRILL JIG BEND FORM
11-38005	OUTER RINGS - COLD MASS	CHECK TEMPLATE MILL FIXTURE BORING FIXTURE WELD FIXTURE
11-38006	WINDING ASSEMBLY	HANDLING TOOL SPECIAL MACHINE
11-38010	SIDE WALL INSULATION	MARK TEMPLATE (8) BLANK DIE (4)
11-38011	CONDUCTOR LEAD HOUSING	PROFILE FIXTURE (2) TRACE PATTERN (2) DRILL JIG (2) DRILL PLATE (2) MILL FIXTURE
11-38013	BOBBIN ASSEMBLY	WELD FIXTURE TURNING FIXTURE (2) CHECK TEMPLATE
11-38016	GROUND INSULATION	MARK TEMPLATE (33)
11-38021	LEAD LUG	PROFILE FIXTURE TRACE PATTERN DRILL JIG

Table 4-1. Tool List (cont'd)

NUMBER	PART NAME	TOOL NAME
11-38030	STACK ASSEMBLY	BEND FORM (3) BLANK DIE (4) DRILL JIG (7) DRILL PLATE (4) DRILL FIXTURE (1) MANUFACTURING AID (3) MARK TEMPLATE (14) MILL FIXTURE (1) TURNING FIXTURE (3) WELD FIXTURE (6)
11-38040	LN_2 COLD WALL ASSEMBLY	BEND FORM (2) BLANK DIE CHECK TEMPLATE (5) DRILL TEMPLATE (4) MARK TEMPLATE (7) PRODUCTION SAMPLE ROUTER FORM WELD FIXTURE (2)
11-38060	VACUUM VESSEL ASSEMBLY	WELD FIXTURE DRILL FIXTURE
11-38062	OUTER RING - VACUUM VESSEL	CHECK TEMPLATE
11-38064	STACK PLATE - VACUUM VESSEL	TURNING FIXTURE
11-38065	STRUT FITTING - VACUUM VESSEL	PROFILE FIXTURE TRACE TEMPLATE
11-38066	SUPPORT ASSEMBLY - VACUUM VESSEL	WELD FIXTURE TURNING FIXTURE (2)
11-38067	SIDE PLATE ASSEMBLY	MILL FIXTURE
11-38068	STACK PLATE ASSEMBLY - VACUUM VESSEL	DRILL PLATE
11-38070	OUTLET ASSEMBLY	PROFILE FIXTURE (3) TRACE TEMPLATE (3) WELD FIXTURE TURNING FIXTURE
11-38080	COLD MASS SUPPORT	HOLDING FIXTURE PRODUCTION TAPE SETUP SHEET TOOLING TAPE
11-38084	COLD MASS SUPPORT INSTALLATION	DRILL FIXTURE SETUP SHEET

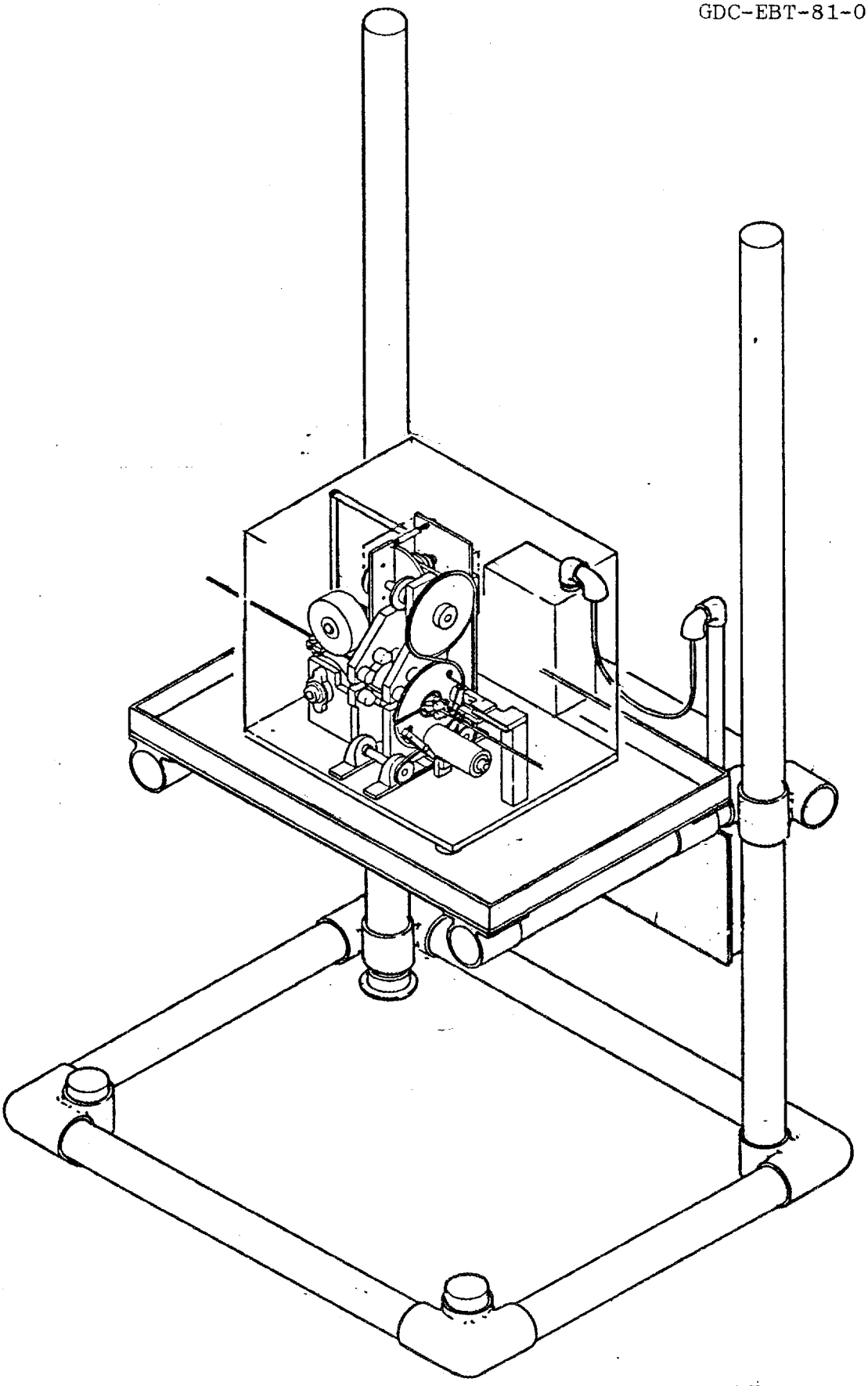

FIGURE 4-1 CONDUCTOR TAPE WINDING MACHINE

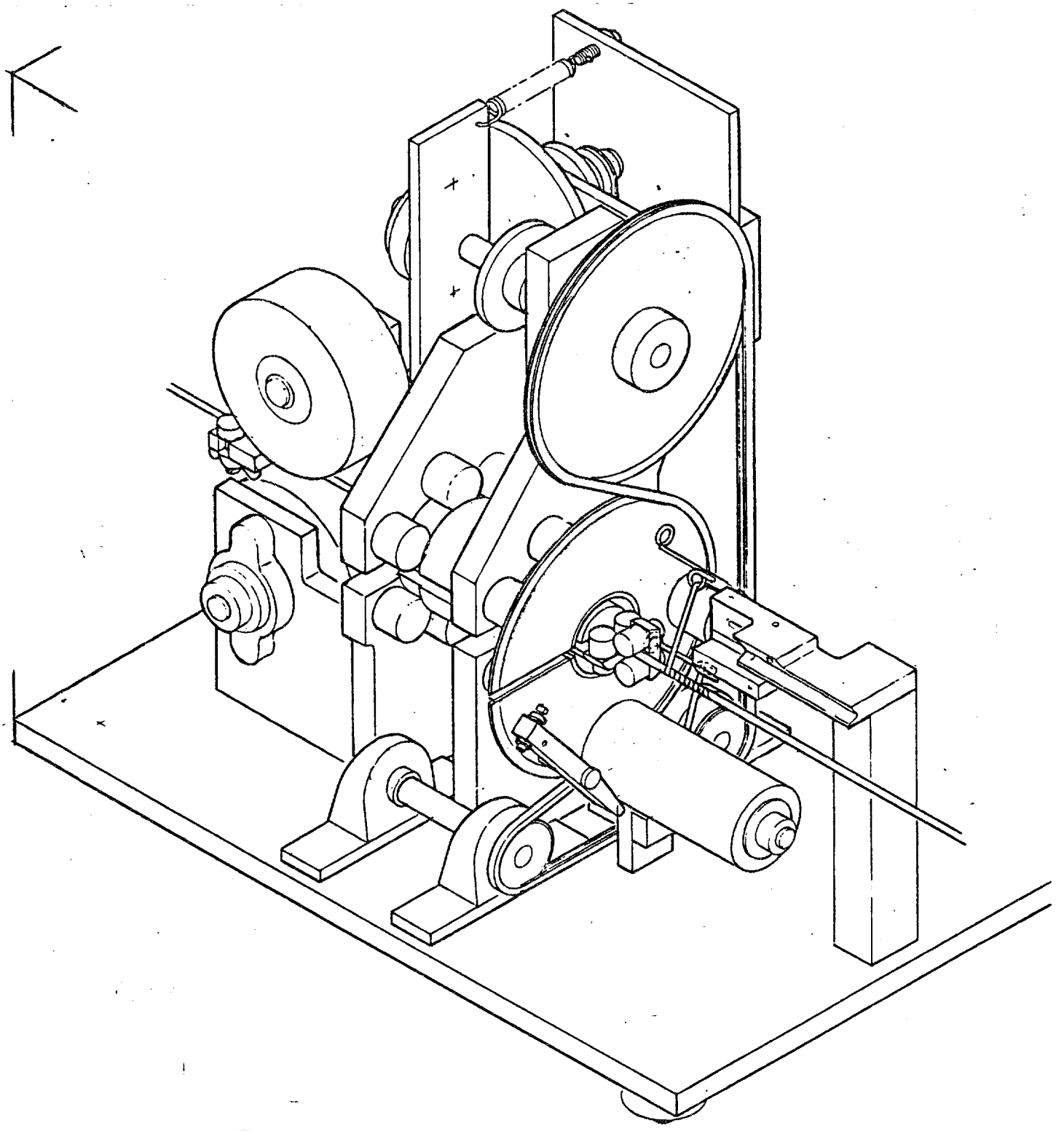

FIGURE 4-2 TAPE WINDING MACHINE HEAD

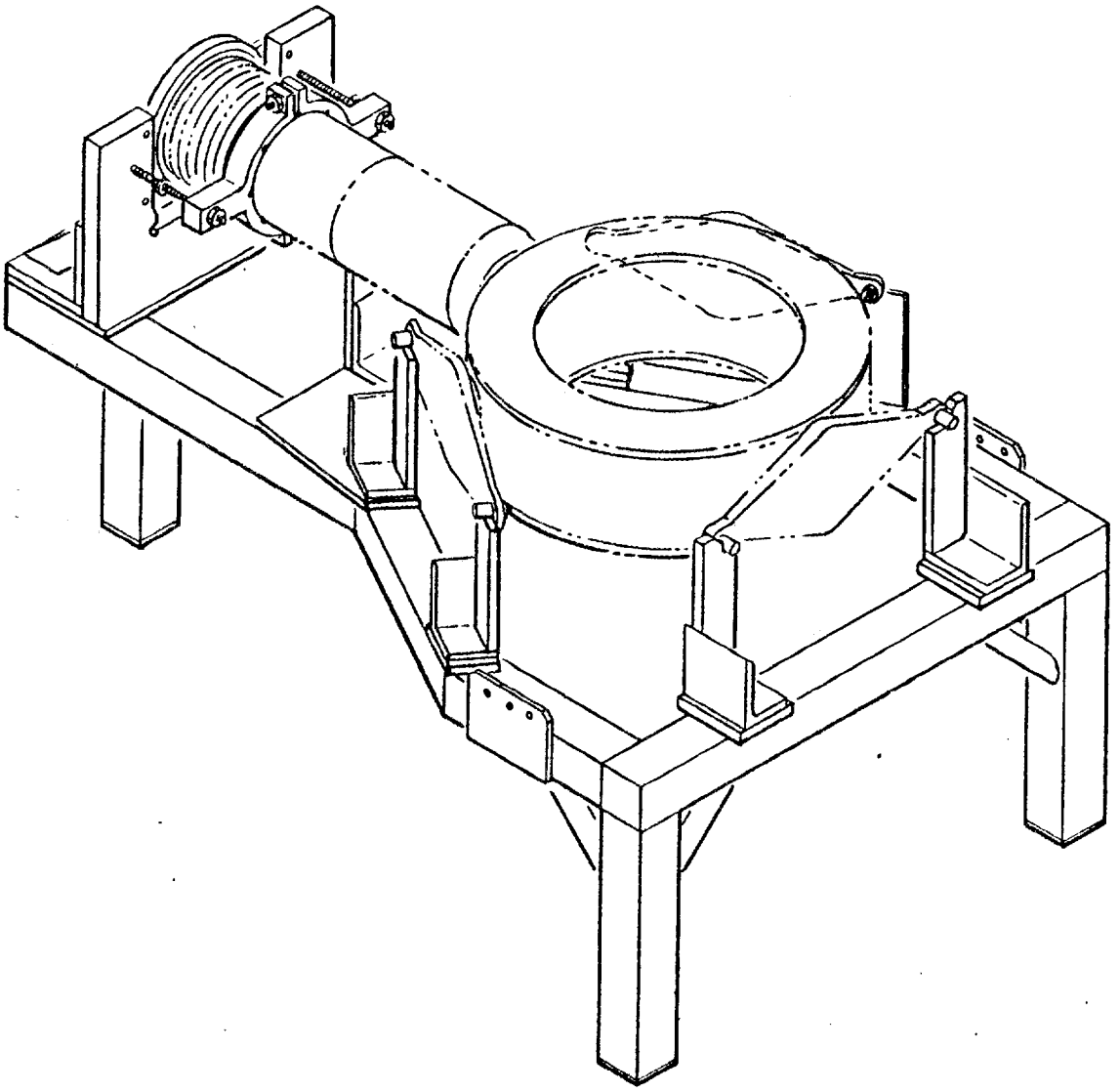

FIGURE 4-3 MAJOR ASSEMBLY FIXTURE

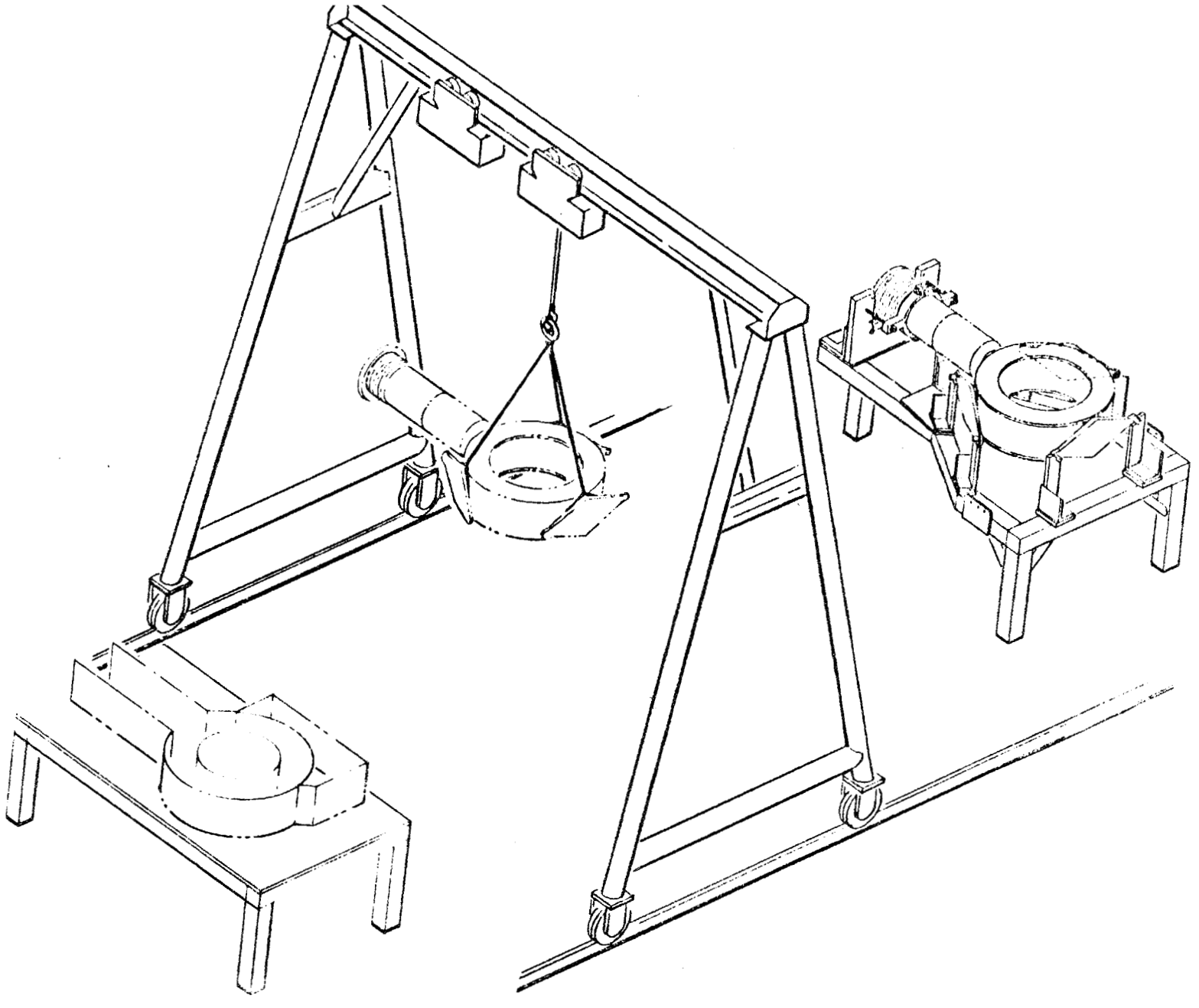

Figure 4-4. Major Assembly Station

SECTION 5

MANUFACTURING ANALYSIS

This section provides a detailed analysis of the fabrication and assembly of each major component of the mirror coil magnet. The Manufacturing Sequence and Flow Plan, Figure 5-1, shows all the major manufacturing operations required to manufacture each magnet.

5.1 COLD MASS ASSEMBLY

The cold mass assembly, as described below, consists of the helium vessel (bobbin and outer ring halves), and the wound conductor with associated insulation, which makes up the conductor pack. The major steps in fabrication, winding, and final assembly are described in the following sections.

5.1.1 BOBBIN. The bobbin assembly shown in Figure 5-2 is made from two 1.0-inch-thick, 30.75-inch-diameter 316L stainless steel plates welded to each end of an 18.00-inch-diameter by 8.5-inch-long tube, roll formed and bevel-welded from .75-inch-thick 316L stainless steel. The side plates are partially machined to create the bobbin weld joint configuration. The

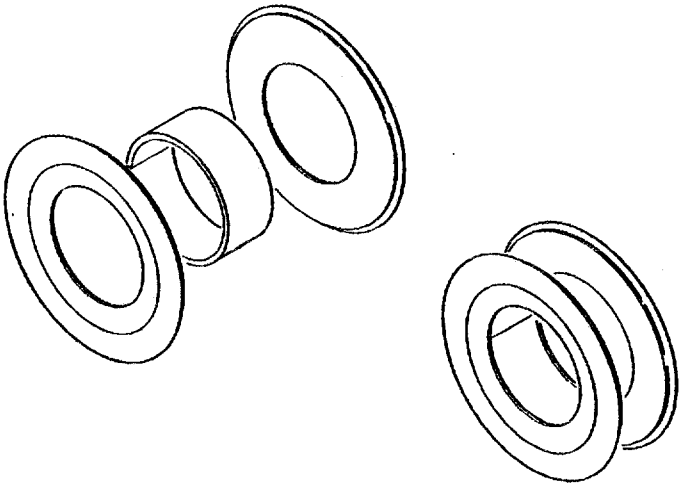

Figure 5-2. Bobbin Assembly

rings and bevel-welded bobbin tube are then placed on the weld positioner, dimensionally aligned and tack-welded in preparation for the final weld operations.

After welding, the bobbin will undergo radiographic and dye penetrant inspection to ensure the welding integrity before stress relief and final machining operations. The precise dimensional control for proper fit of the polyimide and fiberglass insulation, the conductor pack winding and the outer ring installation is guaranteed with our final lathe machining of the bobbin assembly.

5.1.2 INSULATION. The bobbin insulation employs two layers of 5 mil polyimide cut from sheet stock, with two layers of .020 perforated G10CR fiberglass and one solid layer of G10CR fiberglass adhesively bonded to the inside surfaces of the bobbin.

5.1.3 CONDUCTOR PACK. The conductor pack embodies one pancake wind and 32 horizontally (side by side) wound layers.

The winding operations commence with the insulation bobbin mounted to the face of the winding machine, an Aronson weld positioner, shown in Figure 5-3.

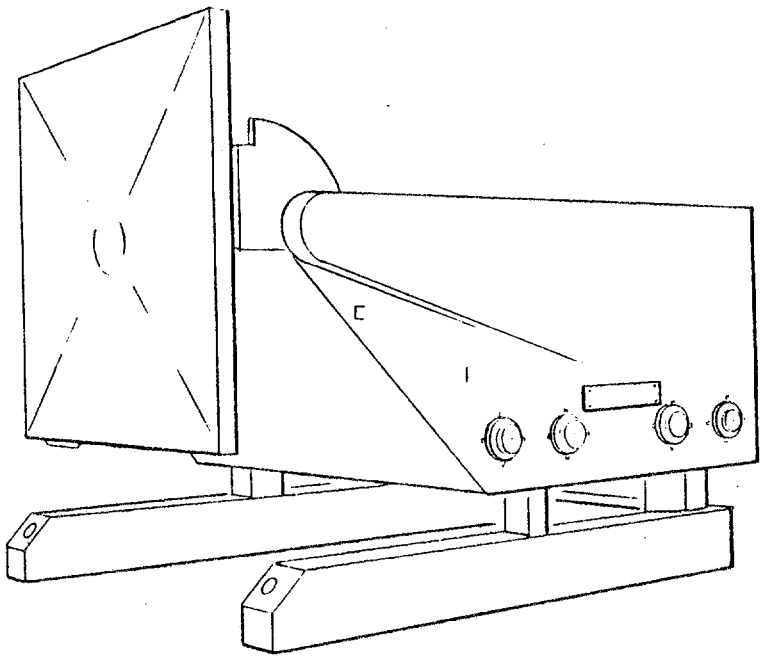

Figure 5-3. Weld Positioner/Winding Machine

An empty spool, for storage of a substantial length of conductor, is placed at the rear of the tensioner in the ultimate position of the supply spool.

The conductor supply spool is mounted beside the bobbin on the winding machine as shown in Figure 5-4.

The conductor is now fed onto the storage spool of sufficient length for the pancake wind plus other requirements for winding.

The conductor is now carefully looped and secured from the supply spool to the bobbin for start of the pancake wind, Figure 5-5.

Feeding from the storage spool through the tensioning, cleaning, counting, and insulation tape winding machine, the pancake layer is wound. Sufficient insulation wound conductor is over wound to make a half layer horizontal wind plus other winding requirements. The pancake wind is now secured and the excess "tail" cut off. Insulation consisting of two perforated and one solid G10CR fiberglass layers is installed beside the pancake wind, insulating it from the horizontal winding. Clamps are installed to secure the pancake wind in position during the horizontal wind process.

At this time, the storage spool is removed from the system and stored for future use. The supply spool is now removed from the winding machine and, without severing the conductor, carefully moved to the position of the storage spool, Figure 5-6.

Reversing the direction of winding, 32 horizontal (side by side) layers are wound on the bobbin alongside the pancake wind, Figure 5-7.

At the 31st layer, eight layers of .030" G10CR fiberglass insulation are installed. The 32nd layer consists of one-half wind from each side to the center for a center conductor tap. Eight more layers of .030" G10CR fiberglass insulation cover the 32nd layer, and two bands (stainless steel hose clamps) are installed. Fiberglass stabilizer blocks are bolted together around the terminals to secure and hold them in place maintaining tension.

Splicing of the conductor will be accomplished as required. This will require a solder station to control heat to assure a sound splice without damage to the conductor. The splicing will be accomplished at the walls of the bobbin at all times to assure a full wind.

5.1.4 <u>OUTER RING 11-38005</u>. Fabrication of the outer ring will start with machining of the weld prep in the flat plate on both edges. The ring is made up of two halves rolled to a 14.43-inch inside radii. Drilling of the stack hole, end trim and weld prep will be performed after fit-up to the bobbin.

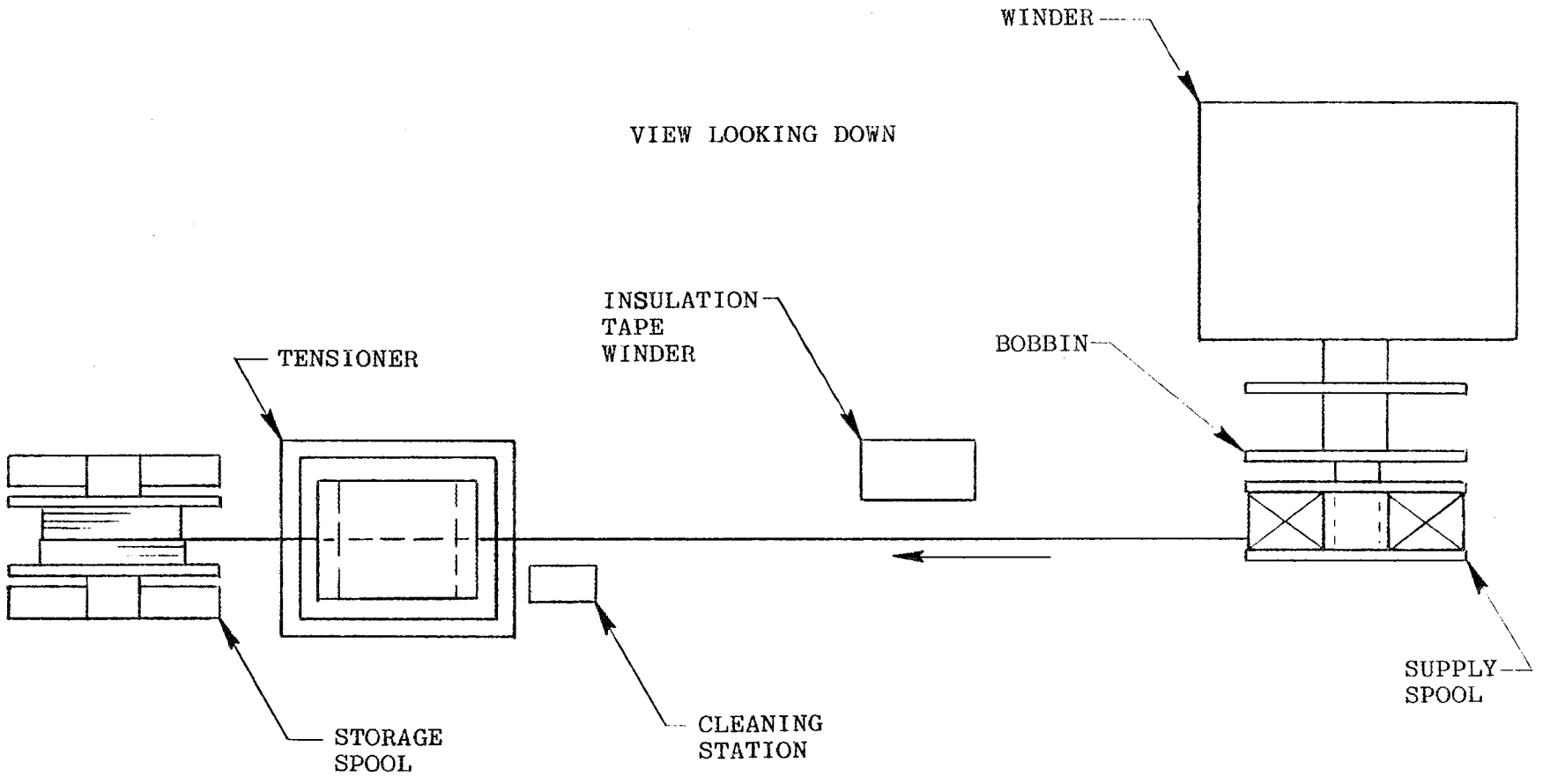

STEP #1

WIND CONDUCTOR ON STORAGE SPOOL FOR PANCAKE COIL. TAPE WINDER AND CLEANING STATION REMOVED FROM LINE

Figure 5-4. Preparation for Winding

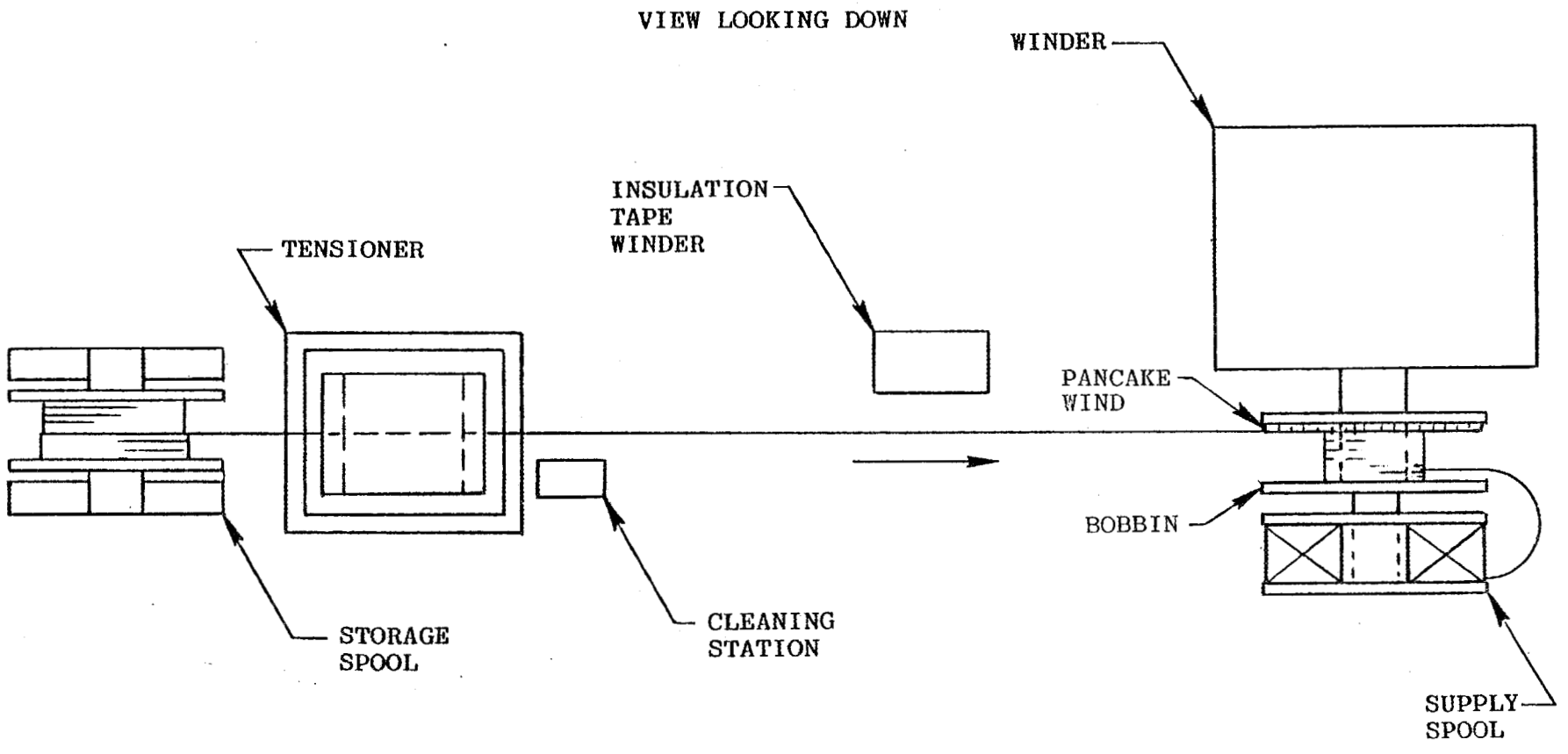

STEP #2

LOOP CONDUCTOR FROM SUPPLY SPOOL ONTO BOBBIN AND SECURE.

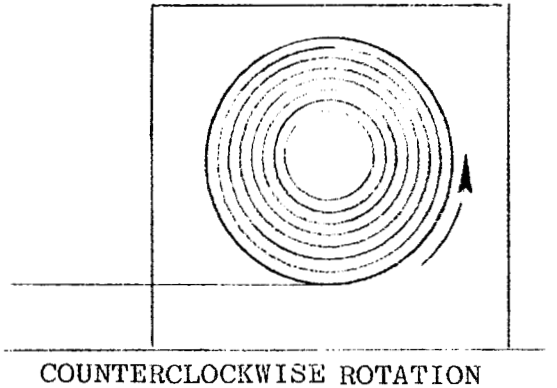

COUNTERCLOCKWISE ROTATION

SIDE VIEW
PANCAKE WIND

Figure 5-5. Pancake Winding

VIEW LOOKING DOWN

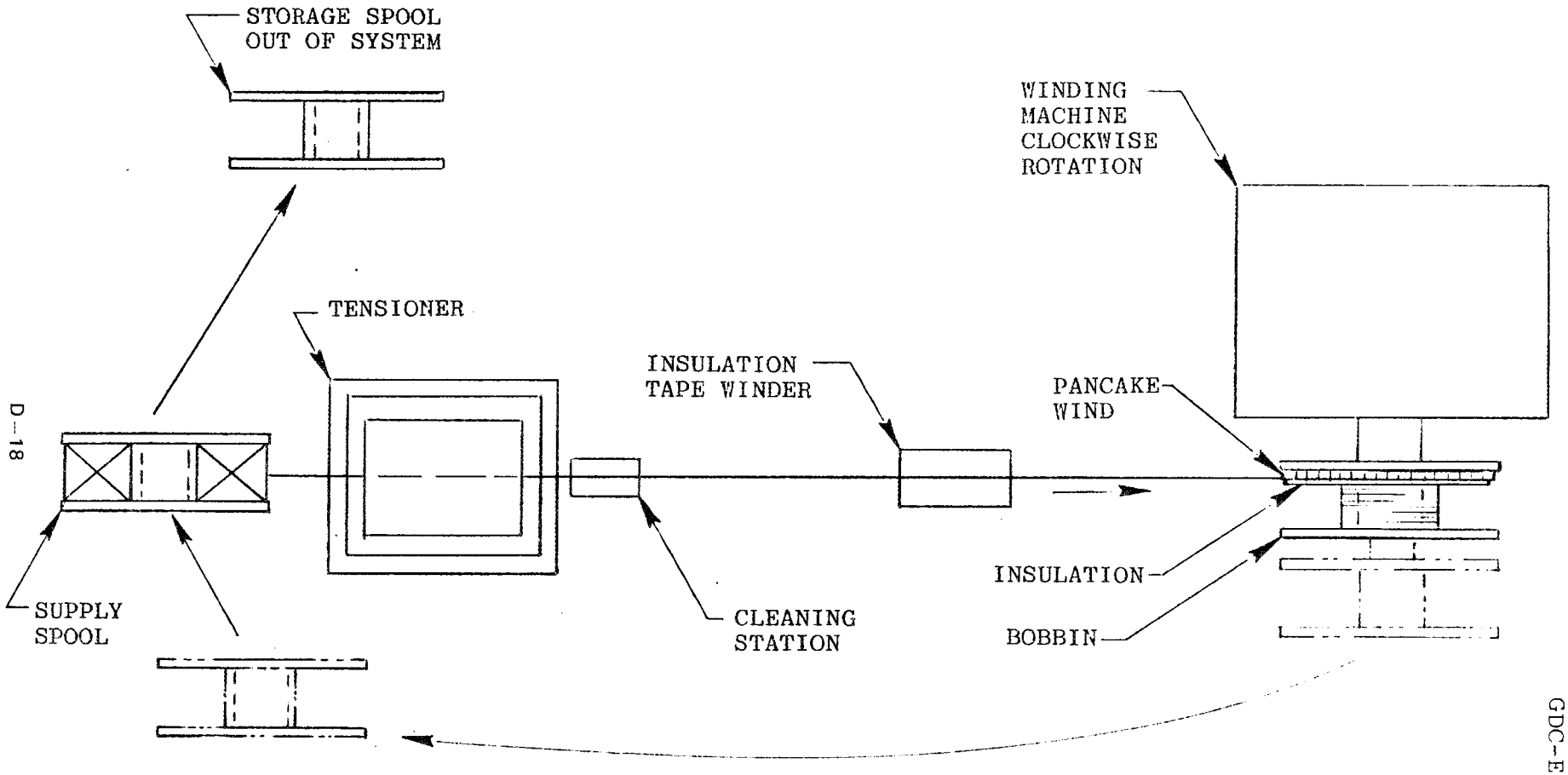

STEP #3

REMOVE STORAGE SPOOL FROM SYSTEM. MOVE CONDUCTOR SUPPLY SPOOL FROM WINDER AND MOUNT IN POSITION OF STORAGE SPOOL INSTALL INSULATION CLAMP PANCAKE COIL TO HOLD IN POSITION. WIND LAYER COIL.

Figure 5-6. Preparation for Layer Winding

SIDE VIEW
LAYER WIND

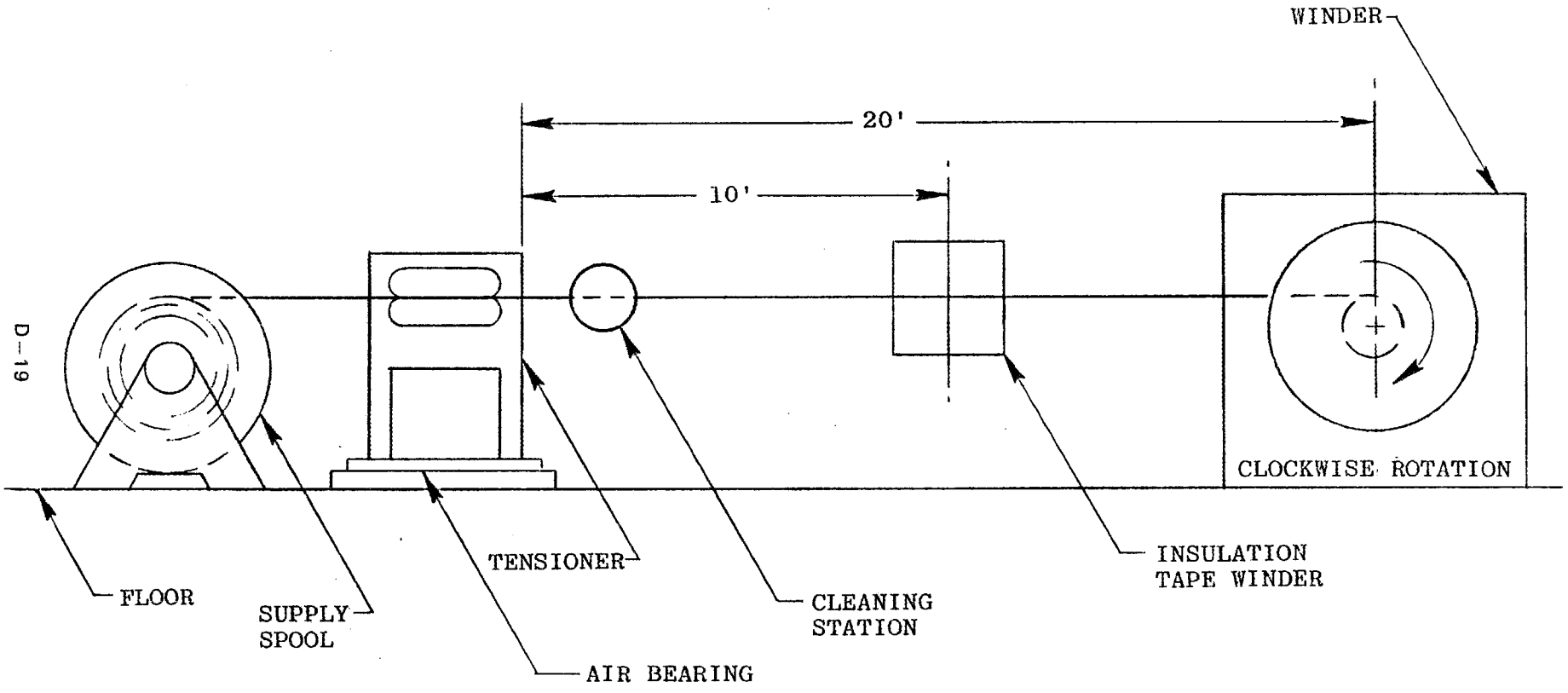

Figure 5-7. Layer Winding

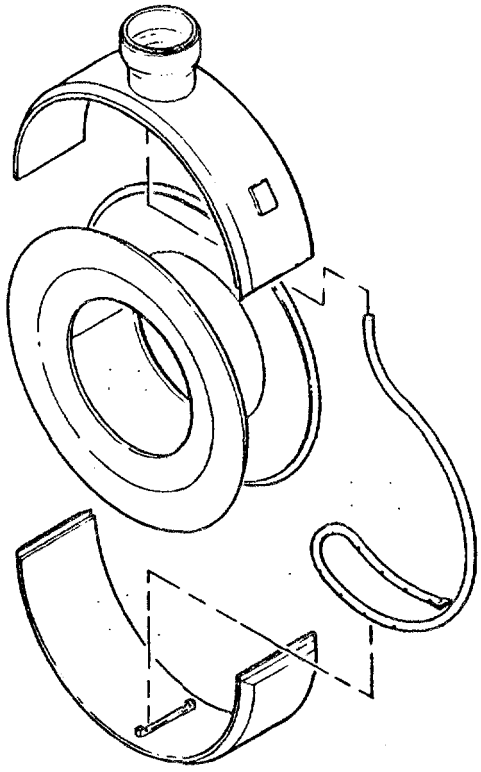

Figure 5-8. Helium Vessel

5.1.5 OUTER RING INSTALLATION. While the bobbin remains in place on the weld positioner/winding machine, the finished outer ring halves are fitted in place and tack-welded. Final closeout welding of the helium vessel, Figure 5-8, is accomplished with semi-automatic equipment. Heat sensors are used to monitor and control heat transfer to the coil winding.

5.2 INSULATION BLANKET 11-38046

There are five different multi-layer insulation blankets used in conjunction with the cold wall. These vary in thickness due to the quantity of alternating layers of aluminized Kapton and Dacron net. They range from .13" for -1 & -5, .26" for -2 & -4 and .39" for -3. The manufacturing of each configuration will be handled by a specialty house. Final fitting will take place when each blanket is installed.

5.3 LN_2 COLD WALL 11-38040

The LN_2 cold wall components in Figure 5-9 consist of three principal subassemblies of the copper envelope and the LN_2 tubes. This assembly is supported from the titanium support struts for the cold mass.

The copper envelope will be fabricated in the GDC facility. The three subassemblies consist of two brazed half sections

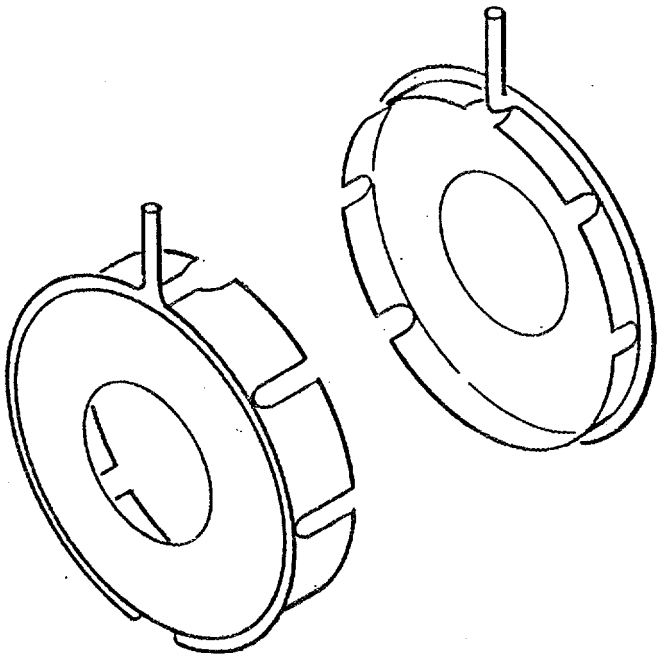

Figure 5-9. LN_2 Cold Wall

split around the circumference which overlap and are riveted together, and the stack tube which is a riveted assembly.

5.3.1 COLD WALL OUTER RINGS. The 0.032-inch-thick copper stock is cut to the finished width of 5.75 and a length of 115.0. The strips are roll-formed to 35.14-inch diameter, inspected with a check template, and trimmed to final configuration and length with a router fixture.

5.3.2 SIDE PLATES. The 0.032-inch-thick copper will be true trace blanked on a punch press to 35.14-inch OD and 17.90-inch ID. These are then brazed to the outer ring sections to form envelope subassemblies.

5.3.3 COLD WALL STACK TUBE. The stack tube is a strip of .032-inch-thick 110 copper rolled to 10.5-inch diameter, trimmed to length, riveted to form a cylinder, and the bottom end trimmed to suit the interface at the shield outer ring. The stack tube is attached to the envelope assembly with riveted angle clips.

5.3.4 ENVELOPE ASSEMBLY. The assembly will be a full size fitup of the envelope and stack pre-assembled with the cold mass with the supports installed but without MLI in place. All rivet holes will be drilled full size at this time,

located from pilot holes in the details, to eliminate contaminates in the MLI blankets.

This pre-assembly will be accomplished with the cold mass mounted in an assembly fixture (11-38001-1). This assembly fixture will also be used to assemble the stack assembly and to assemble the stack with the cold mass, Figure 5-10. After all rivet holes are drilled full size, fitup and trim operations are accomplished.

The parts are disassembled, deburred, and cleaned. They are now ready for final assembly with the cold mass.

LN_2 Line Assembly. Manufacturing the LN_2 line assembly is a straight-forward cutting, fitting, and soldering task. The tooling involved includes a check template for the forming of the tubing and a simple manufacturing aid to simulate the radiation shield envelope with the line joints and terminal points clearly indicated.

5.4 VACUUM VESSEL 11-38060-1

The vacuum vessel is the outer jacket of the magnet assembly. It is a welded assembly consisting of details made from 304L stainless steel, Figure 5-11. The major components include an outer ring, 1" thick X 12" wide X 150" long, rolled to a 40.75" ID. This will be subcontracted to a local specialty house. The two side plates are .25" thick, 42" in diameter with a spun flange in the center having a 16.5" hole for welding the inner ring in place. In the assembly sequence, a .25" X 11.5" X 28" plate will be welded to the side plate to form one wall each of the helium stack. The other two walls are welded to the outer ring. A weld fixture is required.

The bucking cylinder support assembly is a series of rectangular details welded to the outer ring to support the coil. A weld fixture and a turning fixture will be required for this assembly.

The out-of-plane support fittings will be machined in detail with the use of a profile fixture and a trace pattern. They will be welded to outer ring with finish machining of the slot, drilling, and tapping to be performed at the next assembly level.

5.5 STACK SUBASSEMBLIES 11-38030

Subassemblies will be manufactured as outlined on the engineering drawing plus one synthetic subassembly consisting of tube details -19, -20, -33, and one bellows.

Engineering subassemblies are:

11-38030-2 Plate

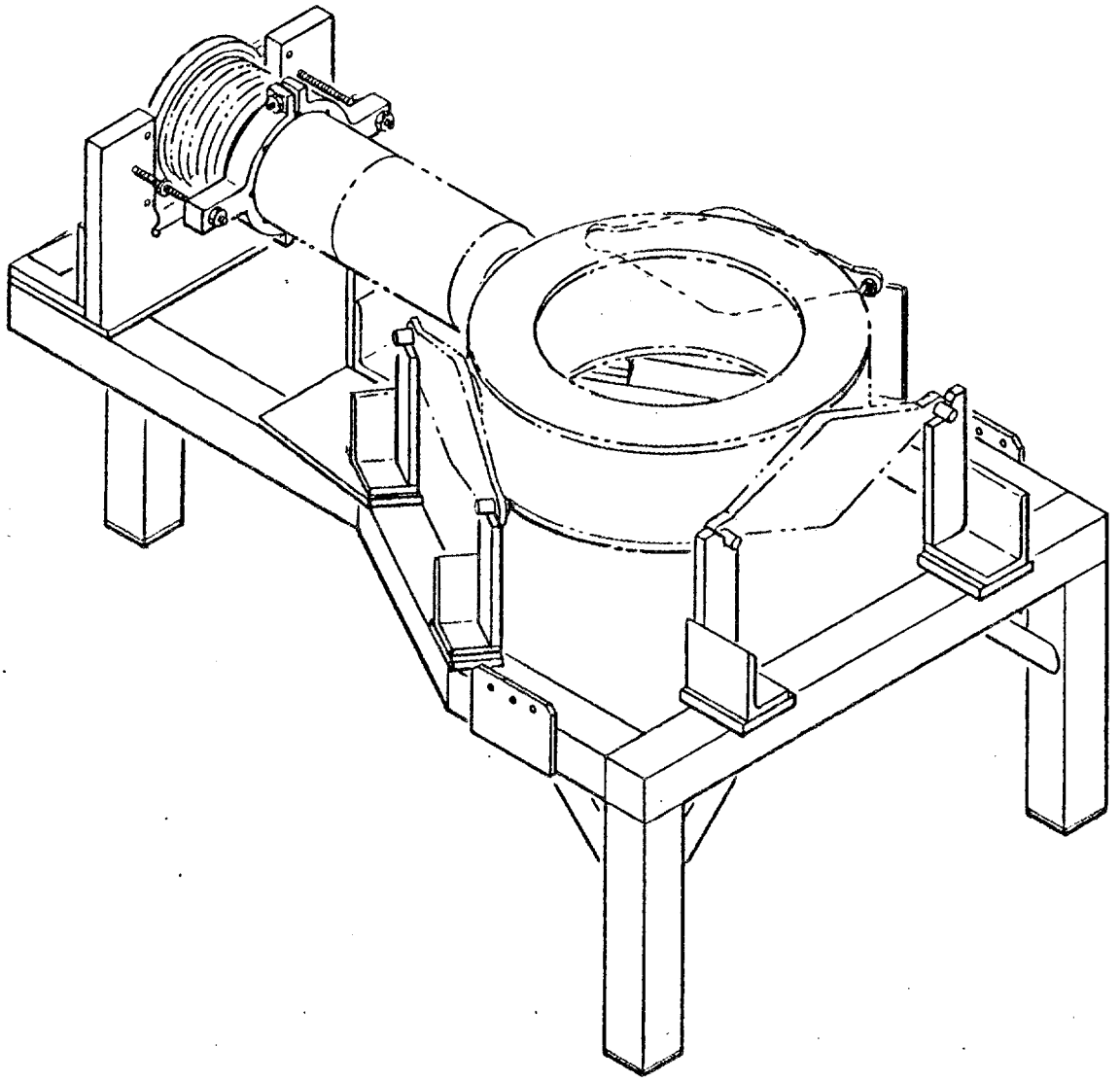

FIGURE 5-10 MAGNET IN ASSEMBLY FIXTURE

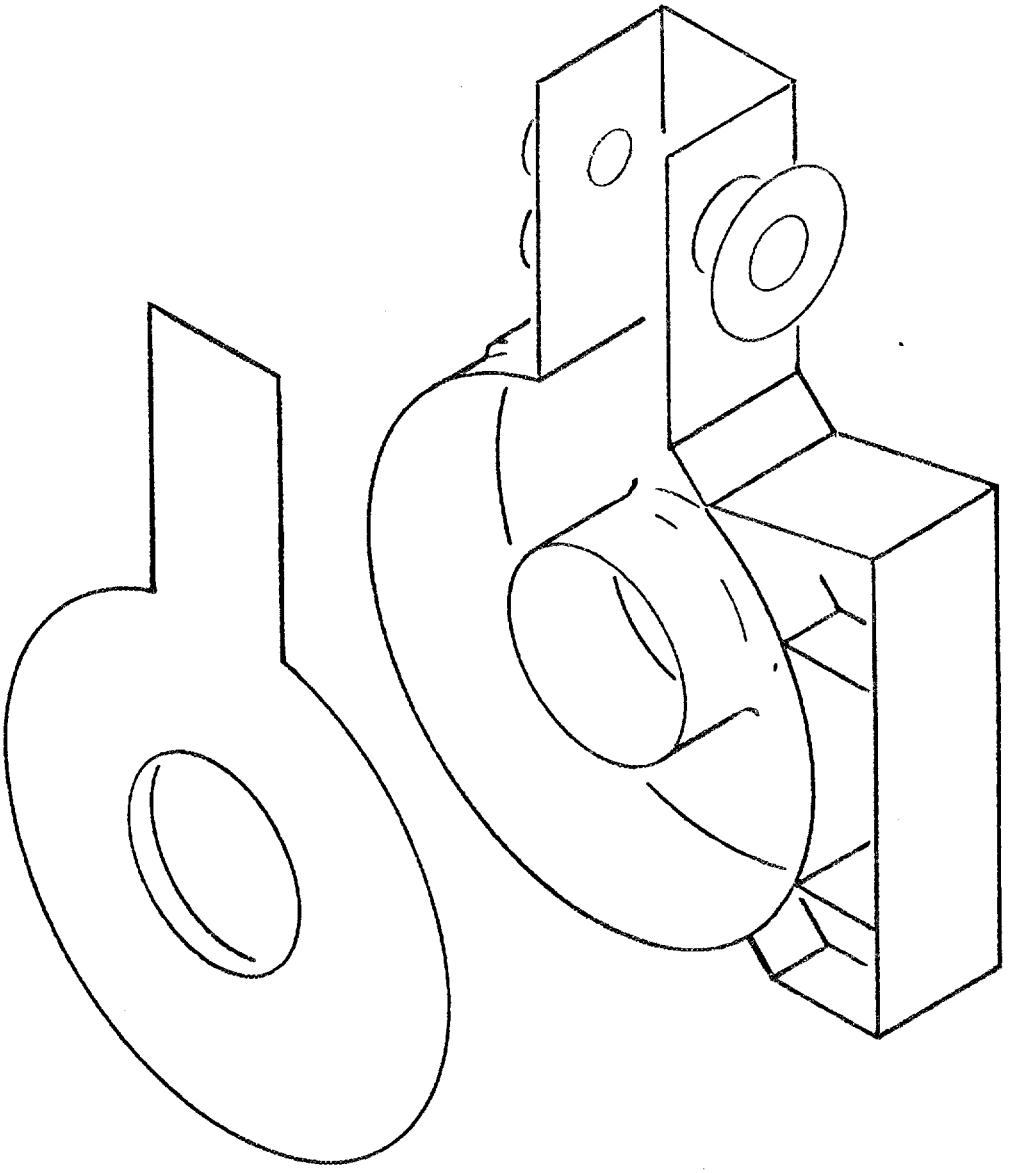

FIGURE 5-11 VACUUM VESSEL SUBASSEMBLIES

11-38030-6	Heat Intercept
-13	Neck
-21	Vent
-26	Tray
-29	Tray
-35 thru -39	Disc
-46	Plate

Final assembly of the stack is accomplished at magnet final assembly.

5.6 COLD MASS SUPPORTS

The three supports are machined from 1.375" X 9.5" X 24" 6AL-4V titanium, Figure 5-12. Numerical control tapes will provide the drilling of the holes, as well as control the machining to ensure consistency and high quality parts. Three parts will be machined simultaneously on a three-spindle, three-axis N/C machine.

The supports will be installed on the cold mass prior to assembly with the LN_2 cold wall.

5.6.1 COLD MASS SUPPORT INST'L 11-38084. This installation consists of the cold mass, three cold mass support fittings, and attaching hardware.

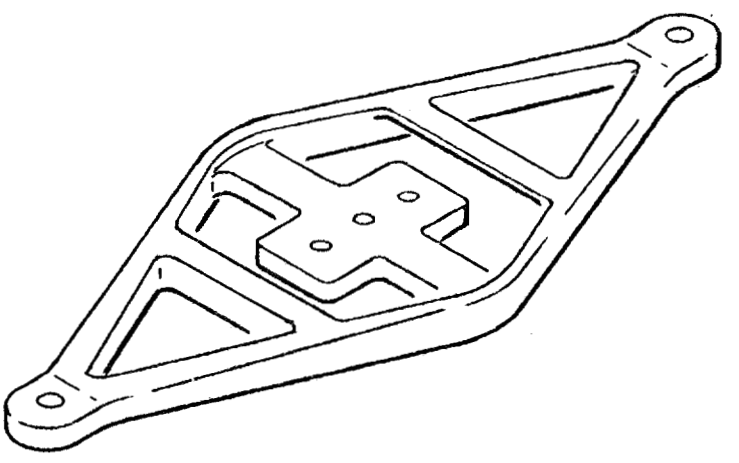

Figure 5-12. Cold Mass Support

The cold mass support fitting pads are machined, drilled, and tapped for the support fittings after welding.

The cold mass with the support struts attached but minus the MLI blanket and cold wall will be located in the vacuum vessel with the aid of a holding fixture. With the vacuum vessel located in a drill fixture attached to our large horizontal boring mill, the operator is now able to locate and drill the holes in the outer ring for the support bosses. These holes provide access for line boring the support strut attachment holes.

At this point, all attach holes in the vacuum vessel support assembly will be drilled. Milling to final size, and drilling and tapping the side support fittings will also be accomplished at this time.

With all machine operations complete, the assembly is removed from the machine and transferred to the welding area. With the cold mass still secured in place, the cold mass support lugs (11-38083) are installed with the shims and welded in place per the engineering drawing.

After welding the support lugs in place, the cold mass is removed and both the cold mass and the vacuum vessel are cleaned of chips, cutting fluids, etc.

At this time, the side outlet assembly (11-38070-1) is welded in place.

5.7 OUTLET ASSEMBLIES 11-38070-1/-2

The outlet assemblies consist of two distinct assemblies. Considerable study has gone into the engineering and fabrication sequence of each assembly. Each purchased cross fitting and machined flange plate will have cleanup cut taken on the plates after being welded into a subassembly. A common drill plate will be used to drill flange holes at the subassembly level. One weld fixture can be used for subassembly welding as well as for the final assembly.

5.8 OUT-OF-PLANE STRUTS 11-38090-1/-2

The out-of-plane struts are large "turnbuckles" manufactured from 2.0 hex 304L stainless steel with rod ends. A close tolerance special bolt manufactured in-house attaches the strut to the vacuum vessel and test stand, Figure 5-13.

Seventy-two struts will be shipped with the magnets as loose pieces.

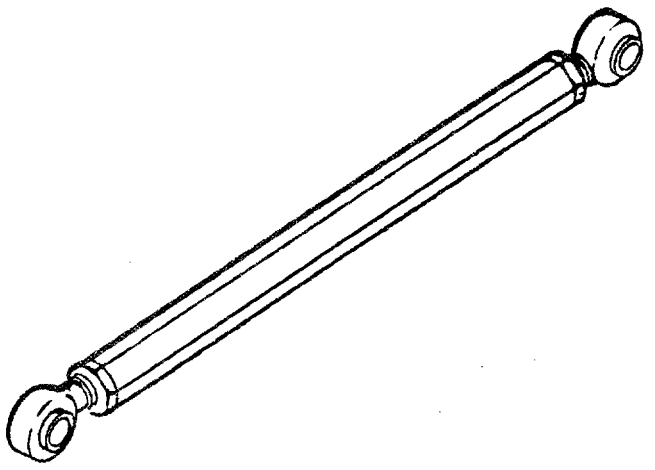

Figure 5-13. Out-of-Plane Strut

5.9 FINAL ASSEMBLY

Two assembly stations consisting of a major assembly fixture within floor-mounted tracks for an "A" frame with two one-ton hoists mounted on trolleys will be provided. A steel top table will also be located within the "A" frame tracks for final installation of the cold mass into the vacuum vessel, Figure 5-14.

5.9.1 COLD MASS SUPPORT INSTALLATION 11-38084. This installation locates in the assembly fixture in a horizontal position with the centerline approximately 36.00 inches above the floor for optimum working height.

5.9.2 STACK ASSEMBLY INSTALLATION 11-38030. This assembly locates on the cold mass assembly in the assembly fixture that has adjustment to facilitate final assembly of the stack and fitup with the cold mass assembly.

Final assembly of the stack is now accomplished by installing the tray assemblies (11-38039), vapor cooled leads (11-38020), LHe tube assembly (11-38031), LHe level sensor (11-38032), stack neck assembly (11-38034), LHe level sensor guide (11-38036).

With all electrical connections and interface tasks completed between the stack assembly (11-38030) and the cold mass assembly (11-38002), the two assemblies are welded together.

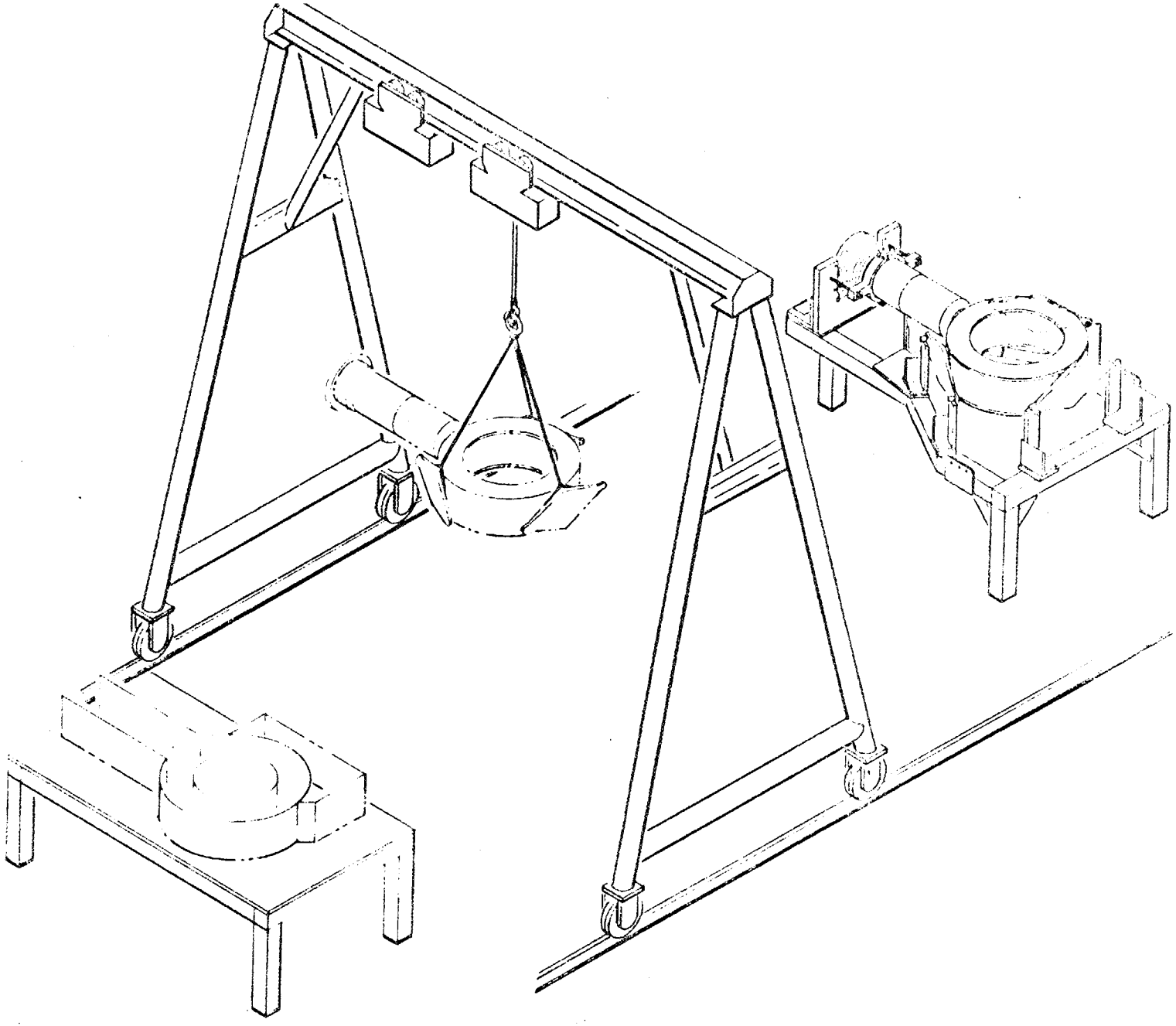

Figure 5-14. Final Assembly Station

5.9.3 LN$_2$ COLD WALL 11-38040 AND MLI BLANKETS 11-38046. The MLI blankets are now installed in conjunction with the assembly and riveting of the LN$_2$ cold wall components.

Upon completing final assembly of the inner MLI blankets and LN$_2$ cold wall, the outer MLI blankets are installed.

Installation of MLI blankets to the outside surfaces of the helium vessel/conductor pack is accomplished with the aid of lofted templates. Cutouts in the template stock identify the specific areas for the bonding of the Velcro material. These templates are matched to the templates used in the fabrication of the MLI blankets. The Velcro strips are bonded in place on the cleaned vessel surface and the MLI blankets merely pressed into position. Helium vessel MLI blankets are installed on the vessel sides and outer ring only.

5.9.4 VACUUM VESSEL ASSEMBLY 11-38001. The completed assembly is now removed from the assembly fixture and located within the vacuum vessel (11-38060). The six cold mass shims (11-38001-4) are assembled between the titanium struts and the cold mass support lugs (11-38083) which were previously welded to the vacuum vessel. The six cold mass support bolts (11-38081) are then installed, torqued, and safety wired.

After final checking, the side plate closeout assembly (11-38001-5) is welded in place.

The last weld between the vacuum vessel (11-38060) and the stack top plate (11-38042) is done with the magnet assembly in the vertical (stack up) position. Final cleanup and installation of top outlet assembly (11-38070-2) completes the assembly.

5.10 ACCEPTANCE TESTING

Production magnets will be subjected to the tests listed below to assure each magnet has been properly manufactured and the requirements of MDAC specifications have been satisfied. The tests listed are final acceptance tests and do not include the manufacturing in-process tests.

1. Winding Insulation Resistance Test*

2. Proof Pressure Test*

3. Final GHe Leak Test*

4. Vacuum Liner GHe Leak Test

5. Magnet Operational Test

6. Magnetic Axes Alignment

7. Heat Leak Test

* Performed prior to installation of shield and vacuum liner.

Additional detail information relative to these tests can be found in Appendix A.5 of this report.

A test facility will be provided to accomplish these tests plus certain in-process tests. The facility is shown in Figure 6-4.

SECTION 6

MANUFACTURING FACILITIES

General dynamics Convair manufacturing facilities include more than 5.9 million square feet under roof. These facilities provide requirements for the complete manufacture of product lines ranging from microcircuits to large steel tools, aircraft, missiles, aerospace ground support equipment, and energy system components.

During our past six years in the energy field, we have developed manufacturing techniques and equipment capabilities relevant to that technology. Our processing and handling functions are facilitized to handle large, heavy steel, copper, titanium, and aluminum products.

6.1 ELMO BUMPY TORUS DEDICATED SPACE

Overall facilities planning for the Elmo Bumpy Torus production program has given prime consideration to the need to minimize program cost while performing in accordance with the program requirements. We have reserved an area of approximately 8,000 square feet in the east end of Building 37 at our Harbor Drive Facility, Figures 6-1 and 6-2, for this program. Figure 6-3 illustrates the planned floor arrangement which provides for the most efficient manufacturing flow from detail parts and material staging thru subassembly, weld, coil winding, closeout weld, x-ray, final assembly, and test.

The close proximity of the Mirror Fusion Test Facility-B program in Buildings 37 and 52 will provide for maximum utilization of support personnel and energy programs equipment.

6.2 EQUIPMENT

We will make maximum use of existing company-owned facilities to minimize cost and avoid schedule delays. All required major capital equipment is company-owned and will be available to manufacture the Elmo Bumpy Torus magnets (Table 6-1). Machine loads and handling equipment projected requirements have been evaluated to assure available capacity for this program.

6.3 LABORATORY AND TEST FACILITIES

In addition to the dedicated EBT-Test Facility (Figure 6-4), which will be located in Building 37, other laboratory and test facilities are available for production and verification test requirements. General Dynamics operates more than 70 R&D, manufacturing development, quality assurance, and test laboratories in San Diego. Our cryogenics, electrical, and materials laboratories have the test facilities and equipment available to support the program.

Table 6-1. Machines and Handling Equipment List

GENERAL DYNAMICS CONVAIR DIVISION MAJOR COMPANY-OWNED EQUIPMENT
AVAILABLE FOR EBT MANUFACTURE AND TEST

TASK	FACILITIES REQUIRED	TYPE	PLANT LOCATION	AVAILABILITY STATUS
ROLLING/BENDING	ROLLS	ROLLS	LF	EXISTING
	BREAKS	BREAKS	LF	EXISTING
DRILLING/TAPPING	HORIZ. OVER-ARM	CINN #2's	LF	EXISTING
	DRILLS	CINN #3's, K&T #3	LF	EXISTING
MILLING	4-AXIS PROFILE MILL	WILSON 4x4 AND 4x6	19	EXISTING
	5-AXIS PROFILE MILL NC	C&L 1x5 NC	LF	EXISTING
	3-AXIS PROFILE MILLS	ARROW PROFILER 1x4	LF	EXISTING
	4-AXIS PROFILE MILLS	ROCKFORD PROFILE MILL	LF	EXISTING
SANDBLASTING	SMALL PARTS BOOTH	SMALL PARTS BOOTHS	KM & LF	EXISTING
	LARGE PARTS AND SUBASSEMBLY BOOTH	LARGE PORTABLE BOOTH TO BE LOCATED IN YARD	19	VENDOR
WELDING	TIG, PORTABLE	MILLER AC/DC 400 AMP	29	EXISTING
	MIG, PORTABLE	MILLER COMBO 600	19	EXISTING
	TUNGSTEN INERT GAS WELDER	COMPUTER CONTROLLED DIMETRICS AUTO. TIG	KM	EXISTING
	MIG, PORTABLE & ACCESSORIES	MILLER COMBO 600	--	*
	WELD POSITIONER	ARONSON	KM	EXISTING
CRANE & RIGGING	0.25 TON TO 5 TON	HOISTS IN MACH. SHOP		EXISTING
		HOUSECRANES IN ASS'Y AREA	ALL	EXISTING
		10-TON MOBILE CRANE		EXISTING
	5 TON TO 9 TON	MULTIPLE HOUSECRANES	ALL	EXISTING
		20-TON MOBILE CRANE		
	9 TON TO 14 TON	20-TON MOBILE CRANE	29	EXISTING
INSPECTION AND TEST	HIGH VOLTAGE MEG OHMMETER	MEG OHMMETER (BIDDLE MOD 210400)	10	EXISTING
	LEAK TEST	HELIUM LEAK DETECTORS	19	EXISTING
	X-RAY	BLDG 3 X-RAY SYSTEM & LAB	LF	EXISTING
	PROCESS & INTERPRETATION EQUIPMENT	PORTABLE X-RAY SYSTEMS	19	EXISTING
WELDING	WELD MACHINES TIB & MIG AUTOMATIC	MILLER	--	*
WINDING	WELD POSITIONER	ARONSON - 20-TON	--	*
WINDING	ELECTRONICALLY CONTROLLED TENSIONER	GENERAL DYNAMICS/DEVOE ENG.	52	EXISTING (TO BE IDENTIFIED)
	ELECTRONICALLY CONTROLLED TENSIONER	GENERAL DYNAMICS/DEVOE ENG.	--	*
GRINDER/SANDER	PEDESTAL GRINDER/SANDER	ROCKWELL 31-352	--	*
SAW	20" BAND SAW	ROCKWELL 28-633	--	*
	POWER HACK SAW	SMALL	--	*
WELD SCREENS	(10) 6'x8' YELLOW SCREENS	MODEL 68CY MUELHISEN	--	*
MISC. HANDLING & STORAGE	(2) STEEL TABLES	36"x48"x84"	--	*
	(1) METAL (4) SHELF STORAGE CABINET	18"x36"x72" SWEDLOW CO.	--	*
	(2) WORK BENCHES	30"x36"x60" WITH MASONITE TOP AND SIDE RACKS	--	*
	ASSORTED PALLET RACKS	LOCAL VENDOR	--	*

* TO BE PURCHASED BY GENERAL DYNAMICS AT TIME OF PRODUCTION AWARD

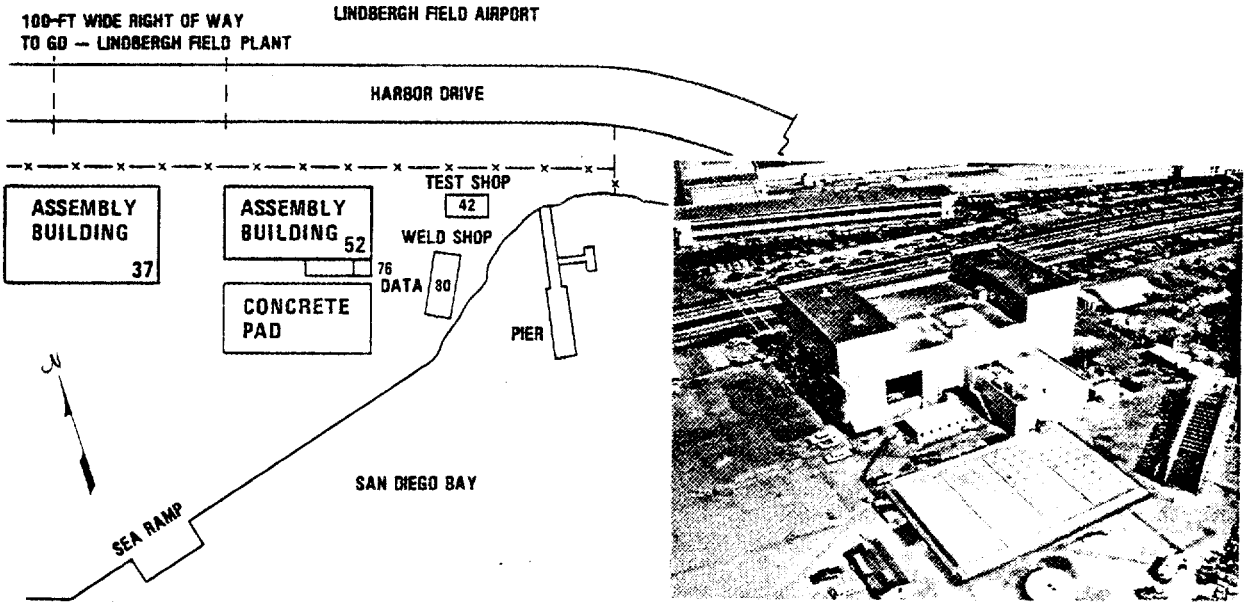

FIGURE 6-1 HARBOR DRIVE FACILITY

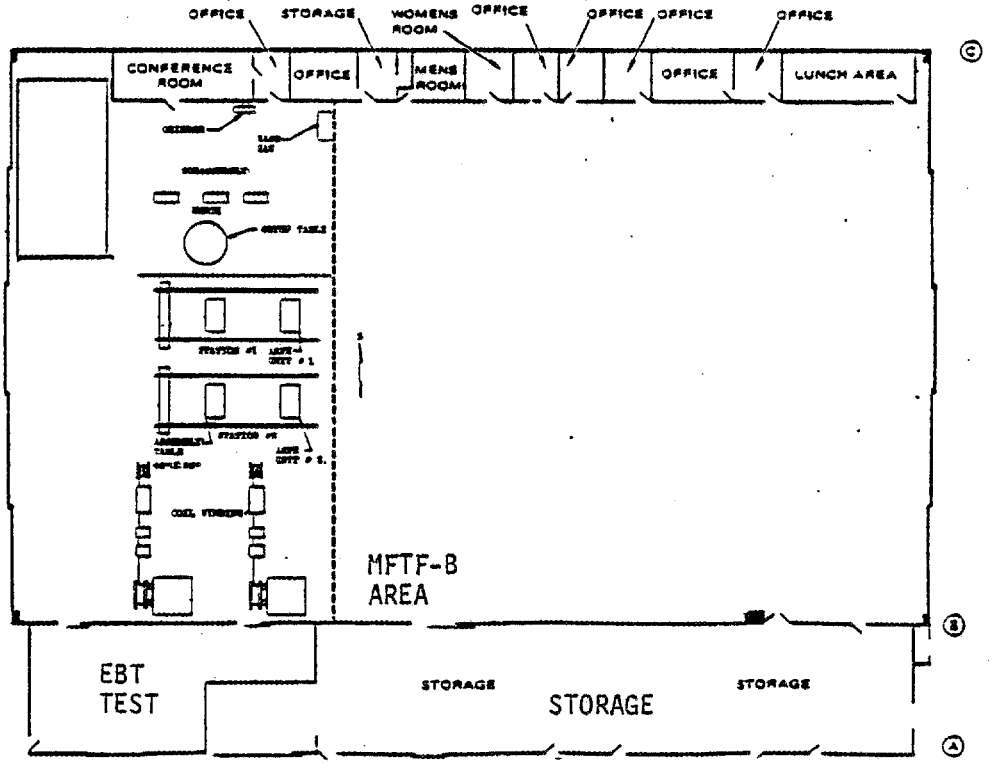

FIGURE 6-2 EBT WILL BE ASSEMBLED IN BUILDING 37

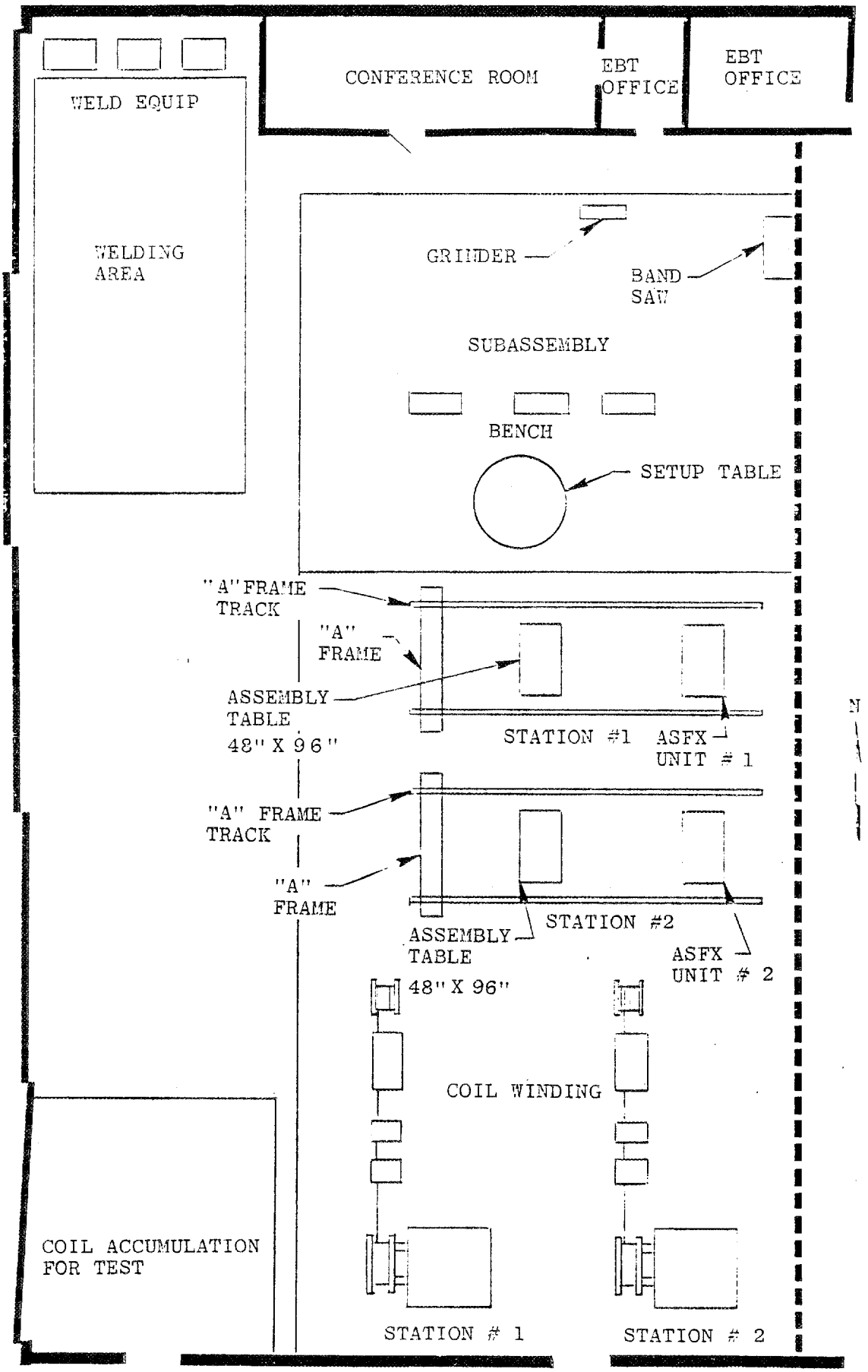

FIGURE 6-3 EBT ASSEMBLY AREA LAYOUT

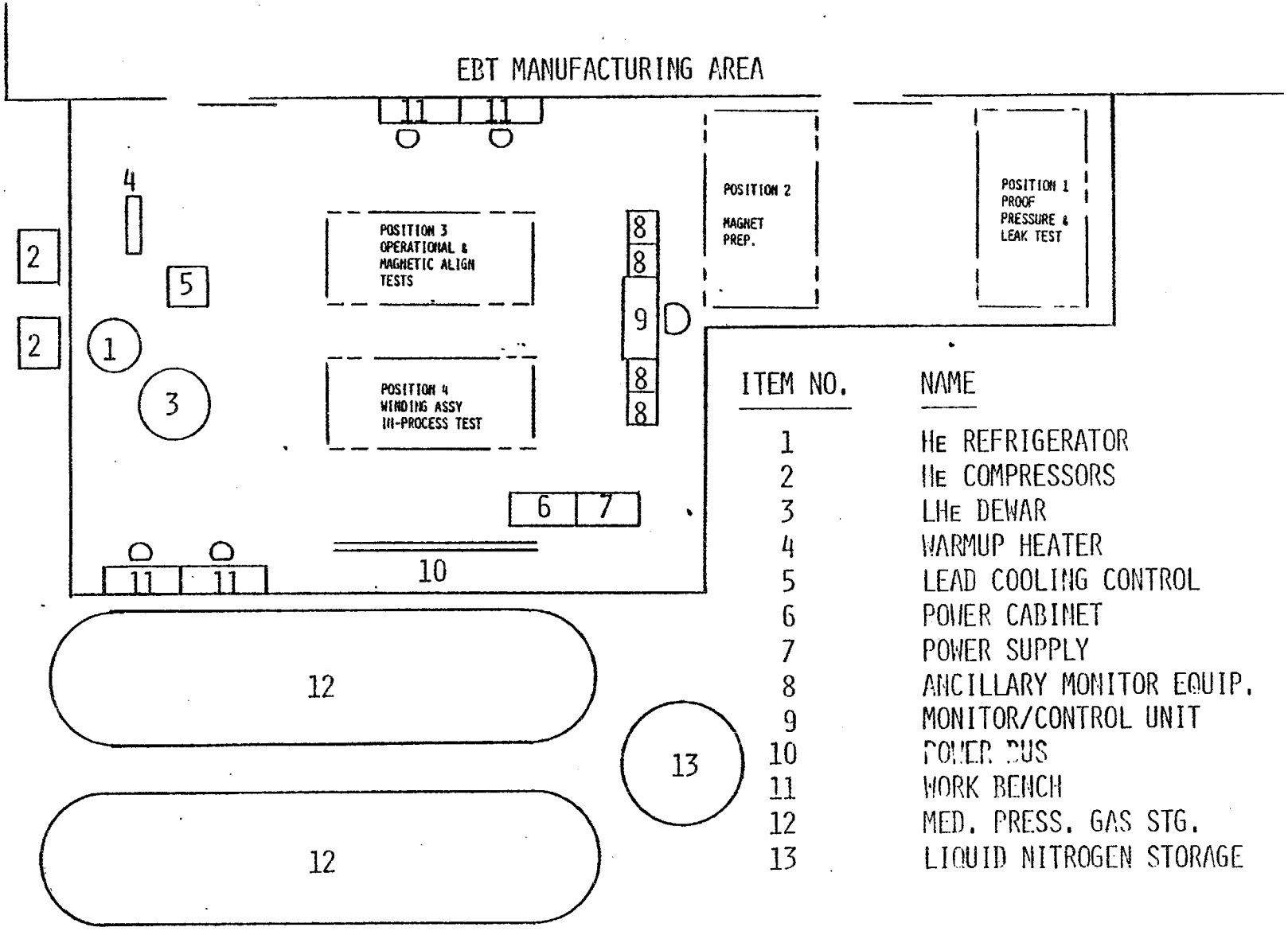

FIGURE 6-4 ELMO BUMPY TORUS PRODUCTION ACCEPTANCE TEST FACILITY

SECTION 7

MAKE OR BUY

The make-or-buy position is based on a comprehensive cost effectiveness analysis. The make-or-buy plan was developed with two key objectives in mind: (1) provide the lowest practical recurring fabrication and assembly cost, regardless of our inherent make capability, and (2) maximize the use of specialized skills and/or facilities available at approved sources.

7.1 MAKE-OR-BUY CRITERIA

Make Determination

- Items that can be produced more economically at the Convair Division.
- Critical items requiring specialized skills or advanced techniques that were developed and demonstrated at Convair and have unique application to the item.
- Items within our capability required to be built at Convair to meet schedule commitments.
- Items requiring a peculiar experience or capability that exists in another of our divisions.
- Items that exceed the capacity of Convair but are within the capacities of other divisions and can be manufactured within schedule more efficiently than by subcontract.

Buy Determination

- Economic factors
- Items requiring a peculiar capability of another manufacturer
- Items that exceed the capacity of General Dynamics but can be procured efficiently and within schedule from a subcontractor.
- Specialty items General Dynamics does not normally produce.

7.2 MAKE-OR-BUY PLAN

Table 7-1 shows the present make-or-buy position for the production units.

TABLE 7-1

MAKE OR BUY PLAN

☐ AIRBORNE

☐ AEROSPACE GROUND EQUIPMENT _____

PAGE 1 OF

DATE _____

CATEGORY	NOMENCLATURE	QUANTITY/VEHICLE	G.F.E.	MAKE	ASSIGNED GENERAL DYNAMICS OPERATING UNIT	BUY: SPEC. CONTROLLED	BUY: SUB CONTRACT	BUY: ITEM/TASK DESCRIPTION (A COST; B DEVELOPMENT MFG/TEST REQ'D CONCURRENT W DESIGN; C REQUIRES SPECIAL TECHNIQUES, PROCESSES & OR FACILITIES; D COMPONENT/SYSTEM RELATIONSHIP REQUIRING SINGLE RESP'TY; E SCHEDULE)
	11-38001-1 Magnet Assy	1		X				
	-2 Side Plate Assy	1		X				
	-3 Sub Assy	1		X				
	11-38002-1 Cold Mass Assy	1		X				
	11-38003-1 Helium Tube	1		X				
	11-38005-1 Cold Mass Outer Ring	1		X				
	-2 Upper Ring - Half	1					X	C
	-3 Lower Ring - Half	1					X	C
	11-38006-1 Winding Assy	1		X				
	11-38007-1 Conductor	A/R				X		C
	11-38009-1 Insulation Slotted	A/R					X	A
	-2 Insulation Slotted	A/R					X	A
	11-38010-1 Sidewall Insulation	6		X				
	-2 " "	2		X				
	-3 " "	2		X				
	-4 " "	1		X				
	-5 " "	2		X				
	-6 " "	118		X				
	-7 " "	86		X				
	11-38010-9 Sidewall Insulation	2		X				
	11-38011-1 Housing-Conductor Lead	1		X				
	-2 " " "	1		X				
	-3 " " "	2		X				
	-4 " " "	1		X				
	11-38011-5 Housing-Conductor Lead	1		X				

A3226 (REV. 5-78)

MAKE OR BUY PLAN

☐ AIRBORNE

☐ AEROSPACE GROUND EQUIPMENT _____

PAGE 2 OF

DATE _____

CATEGORY	NOMENCLATURE	QUANTITY/VEHICLE	G.F.E.	MAKE	ASSIGNED GENERAL DYNAMICS OPERATING UNIT	BUY: SPEC. CONTROLLED	BUY: SUB CONTRACT	ITEM/TASK DESCRIPTION
	11-38012-1 thru 32 Layer Shim Insulation	2 ea				X	C	
	-35 " " "	32				X	C	
	-36 " " "	30				X	C	
	-37 " " "	A/R				X	C	
	11-38012-38 Layer Shim Insul	66				X	C	
	11-38013-1 Bobbin Assy	1		X				
	-3 Bobbin Inner Ring	1				X	C	
	11-38016-1 thru 34 Ground Insul	1 ea		X				
	11-38020-1 Vapor Cooled Leads	1			X		C	
	11-38021-1 Lead Lugs - Cold Mass	1		X				
	11-38030-1 Stack Assy	1		X				
	11-38031-1 Liquid He Tube Assy	1			X		C	
	-3 " " " "	1			X		C	
	11-38032-1 Liquid He Level Sensor	1		X				
	-3 " " " "	1				X	C	
	11-38040-1 LN_2 Cold Wall Assy	1		X				
	11-38046-1 thru -4 MLI Blanket	1 ea				X	A	
	11-38060-1 Vacuum Vessel Assy	1		X				
	11-38062-1 Outer Ring Vacuum Ves	1				X	C	
	11-38063-1 Side Plate-Vacuum Ves	1				X	C	
	-4 " " " "	1				X	C	

A 3226 (REV. 5-78)

A — COST
B — DEVELOPMENT MFG/TEST REQ'D CONCURRENT W DESIGN
C — REQUIRES SPECIAL TECHNIQUES, PROCESSES & OR FACILITIES
D — COMPONENT/SYSTEM RELATIONSHIP REQUIRING SINGLE RESP'TY
E — SCHEDULE

MAKE OR BUY PLAN

☐ AIRBORNE

☐ AEROSPACE GROUND EQUIPMENT _____

PAGE 3 OF

DATE _____

CATEGORY	NOMENCLATURE	QUANTITY/VEHICLE	G.F.E.	MAKE	ASSIGNED GENERAL DYNAMICS OPERATING UNIT	SPEC. CONTROLLED	BUY: SUB CONTRACT	BUY:	ITEM/TASK DESCRIPTION
	11-38064-1 Stack Plate Vacuum Vessel	2		X					
	-2 " " "	1		X					
	-3 " " "	1		X					
	11-38065-1 Strut Ftg Vac Ves	4		X					
	11-38066-1 Support Assy-Vac Ves	1		X					
	11-38067-1,-2 Side Plate Assy, Vacuum Vessel	1	ea	X					
	11-38068-1,-2 Stack Plate Assy, Vacuum Vessel	1	ea	X					
	11-38070-1,-2 Outlet Assy	1	ea	X					
	11-38080-1 Cold Mass Support	3		X					
	11-38081-1 Cold Mass Support Bolt	6					X	A	
	11-38083-1 Cold Mass Support Lug	6		X					
	11-38084-1 Cold Mass Support Inst'l.	1		X					
	11-38090-1 Out-of-Plane Struts	72		X					
	11-38091-1 Out-of-Plane Strut Bolt	144		X					

A 3226 (REV. 5-78)

A COST
B DEVELOPMENT MFG/TEST REQ'D CONCURRENT W DESIGN
C REQUIRES SPECIAL TECHNIQUES, PROCESSES & OR FACILITIES
D COMPONENT/SYSTEM RELATIONSHIP REQUIRING SINGLE RESP'TY
E SCHEDULE

SECTION 8

SUBCONTRACTING

8.1 SUPERCONDUCTOR

Convair will enter into a subcontract agreement with one or more conductor manufacturing companies for the manufacture of the conductor. The subcontractor(s) will be responsible for the development, test, and delivery of the total superconductor requirements for the EBT-P coils. The subcontractor(s), in accordance with the subcontract provisions and approved manufacturing schedules, will deliver the conductor prewound on suitably sized shipping spools.

8.2 STRUCTURAL ELEMENTS

8.2.1 FORMING. The rolling of certain helium and vacuum vessel details will be subcontracted to specially facilitized vendors equipped for the forming of large and thick stainless steel cylindrical shaped parts. Spin forming of the vacuum vessel side plates will also be subcontracted to specialty houses.

8.2.2 MACHINING. Generally speaking, subcontract of machining tasks will be undertaken only to alleviate in-house shop overload conditions.

8.3 INSULATION BLANKETS

The fabrication of the multi-layer insulation blankets will be subcontracted to a specialty firm.

SECTION 9

PROGRAM SCHEDULE

All design, procurement, fabrication, assembly and test activities have been time phased to support program delivery requirements. Provision for reaching rate production of up to five units a month is achieved with the use of two winding and two final assembly stations. The program schedule is shown in Figure 9-1.

REVISIONS:

ORIGINAL ISSUE: 3-18-81
PREDECESSOR: NONE
SUCCESSOR: NONE

ELMO BUMPY TORUS

MASTER SCHEDULE - OVERVIEW

MAGNET SYSTEM DEVELOPMENT

811-242-3-0008
DATE: 9-11-81
PREP BY: M. PARIS X2261
APPVD BY: CONTRACT # 144
REF: PAGE 1 OF 2

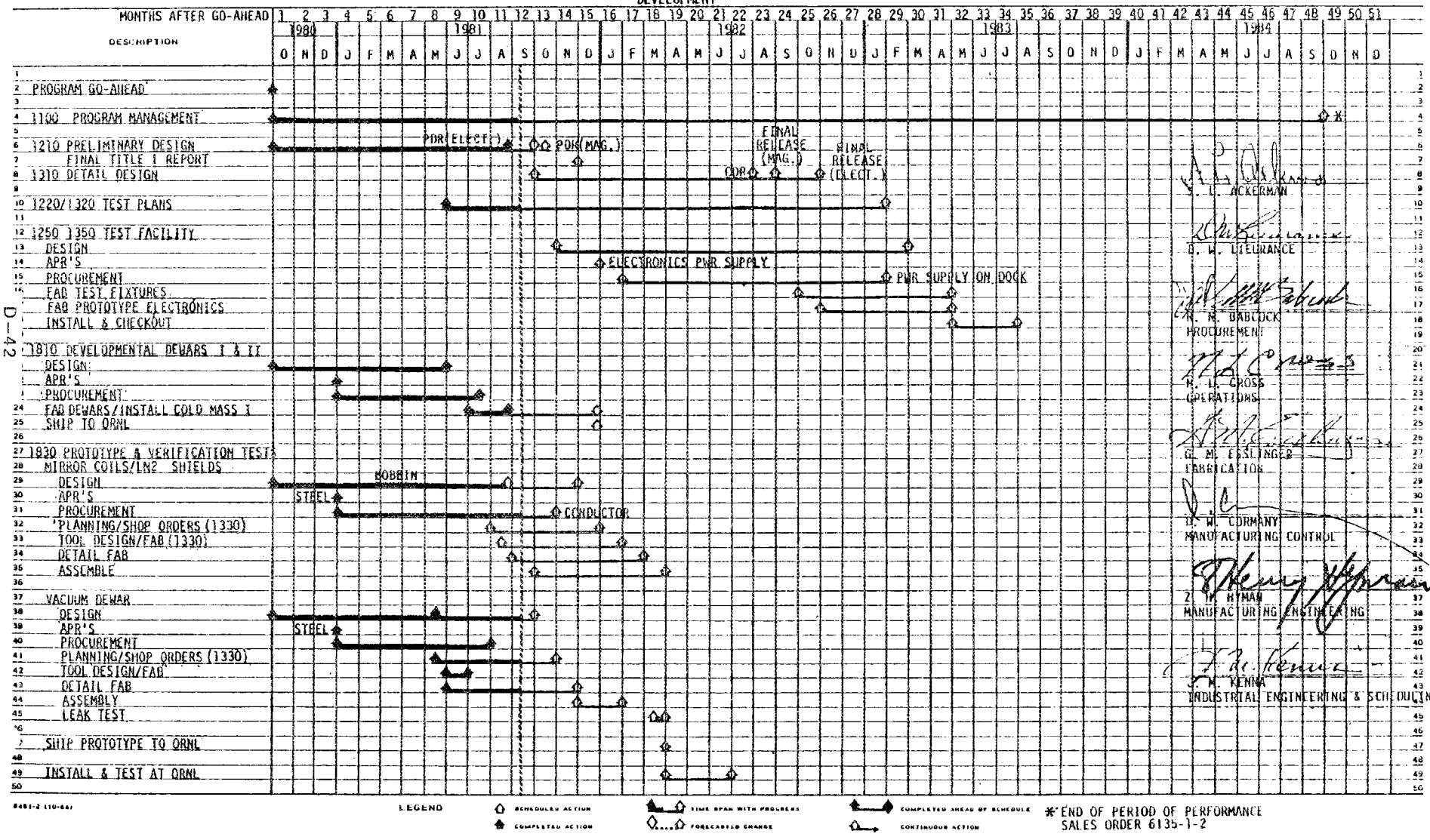

LEGEND
SCHEDULED ACTION
COMPLETED ACTION
TIME SPAN WITH PROGRESS
FORECASTED CHANGE
COMPLETED AHEAD OF SCHEDULE
CONTINUOUS ACTION

* END OF PERIOD OF PERFORMANCE
SALES ORDER 6135-1-2

S. L. ACKERMAN

D. W. LIEURANCE

R. R. BABCOCK
PROCUREMENT

R. L. CROSS
OPERATIONS

G. M. ESSLINGER
FABRICATION

D. W. CORMANY
MANUFACTURING CONTROL

Z. M. HYMAN
MANUFACTURING ENGINEERING

F. M. KENNA
INDUSTRIAL ENGINEERING & SCHEDULING

FIGURE 9-1

REVISIONS:

ORIGINAL ISSUE: 3-18-81

ELMO BUMPY TORUS
MASTER SCHEDULE - OVERVIEW
MAGNET SYSTEM PRODUCTION

01T1-242-3-0008
DATE: 9-11-81
PREP. BY: M. PARIS X2261
APPVD. BY:
REF.: PAGE 2 OF 2

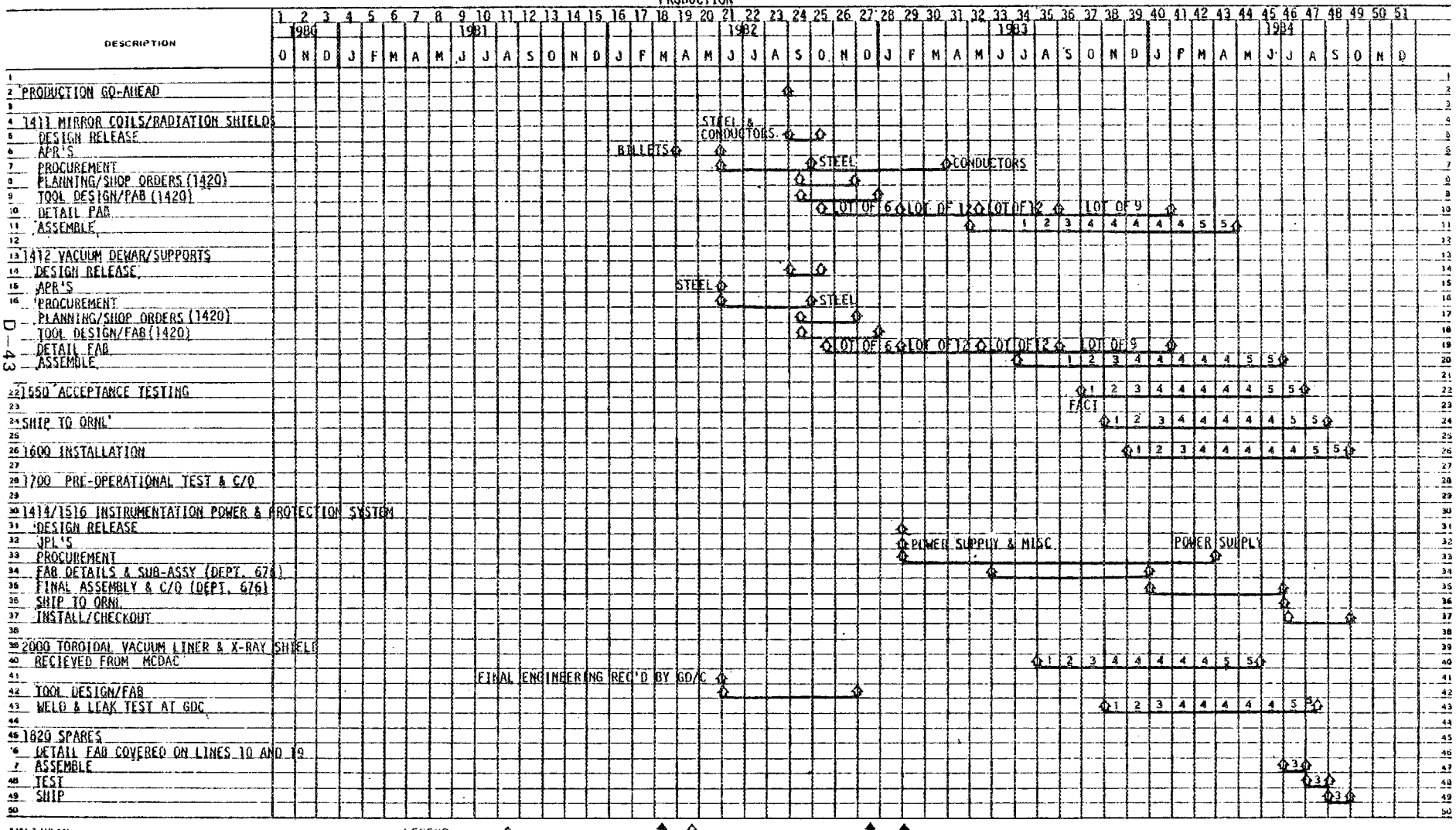

FIGURE 9-1 (CONTINUED)

SECTION 10

QUALITY ASSURANCE

Quality Assurance activities on this program will be conducted in accordance with Report GDC-EBT-81-001, Preliminary Quality Assurance Program Plan, Elmo Bumpy Torus-Proof of Principle.

SECTION 11

PACKAGING AND SHIPPING

Prior to delivery it will be necessary to protect the magnet system against handling and environmental damage. Upon completion of testing at San Diego, all open ends and interfaces will be sealed to preserve the cleanliness of the cooling and vacuum systems. Methods selected for protection against dust and moisture will ensure system integrity and will be subject to MDAC approval.

All closed systems including vacuum, LHe, and LN_2 will be purged and filled with dry nitrogen. Pressure valves will be installed on all entrance lines to the system. All exit line interfaces at the magnet dewar will be shrouded with a fiber-reinforced polyethylene film for protection against dirt and moisture. The shroud will be held in place with pressure sensitive tape and tied with nylon twine. Desiccant will be placed in selected locations where moisture condensation is likely to occur.

11.1 UNIVERSAL TEST FIXTURE/SHIPPING CONTAINER

This fixture, shown in Figure 11-1, consists of a structural steel frame of thick-wall, square tubing, equipped with heavy duty casters for complete mobility and with machined pads for securing the fixture to the ORNL test setup.

Gusseted steel brackets secure the inboard end of the magnet by bolting through the mounting holes in the backing plate and the lower out-of-plane strut fitting. Additional provisions on the fixture provide for securing the magnet shipping container to the truck bed. The wooden container, also a recyclable item, fits over the fixture and bolts directly to the fixture sides to provide a stable, rigid shipping case.

The shipping fixture serves as the in-house manufacturing aid for supporting the magnet assembly for final acceptance testing and preparation for shipping.

11.2 LOADING AND ENVIRONMENTAL PROTECTION

A crane and/or forklift will accomplish the task of loading the magnet assembly at our San Diego facility for truck shipment to ORNL, Oak Ridge, Tennessee. A standard air ride trailer will be used for transporting the magnet assembly. Shock recording devices will monitor shock and vibration encountered in transit.

After loading, the magnet and shipping fixture will be secured to the trailer with a combination of cables, chains and wood blocking.

Representatives of Convair's Engineering, Quality Assurance, and Shipping departments will inspect the load for correct tie-down and blocking requirements. The magnet will then be covered with a waterproof tarpaulin that will be secured to the trailer bed.

Packaging of associated loose equipment will be in accordance with Convair's standard commercial practice.

11.3 TRANSPORTATION AND ROUTING

The magnet system and associated equipment will be transported from San Diego, California, F.O.B., ORNL, Oak Ridge, Tennessee. Estimated transit time is 5-8 days via standard highway routings.

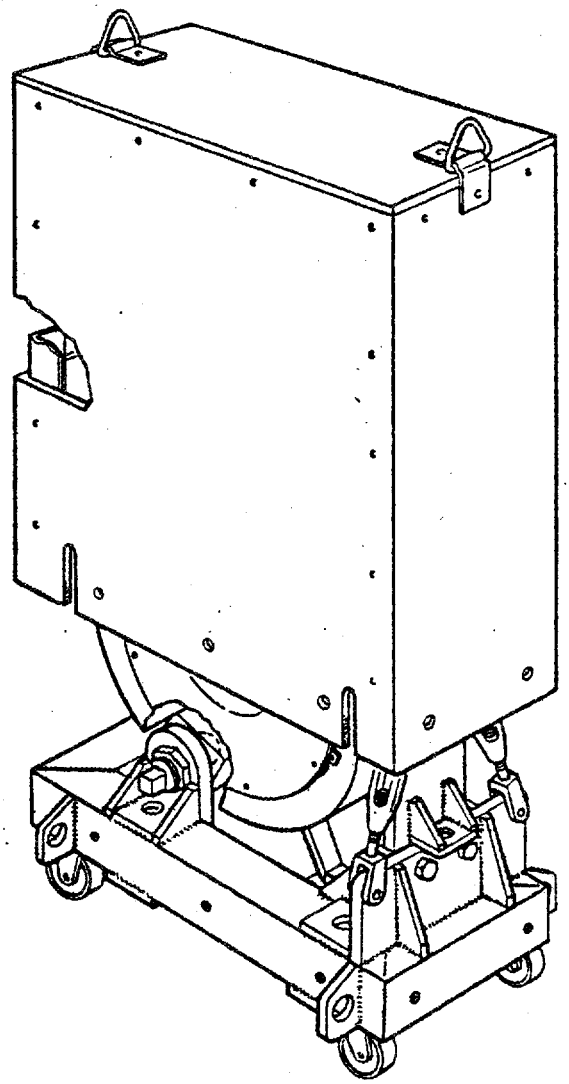

FIGURE 11-1 COMBINATION HANDLING AND SHIPPING FIXTURE

"This plan is preliminary and subject to further revisions and approval during Title II"

APPENDIX E

ACCEPTANCE TEST PLAN

Production magnets will be subjected to the tests listed below to assure each magnet has been properly manufactured. The tests listed are final acceptance tests and do not include the manufacturing in-process tests.

1. Winding Insulation Resistance Test*
2. Proof Pressure Test*
3. Final Magnet GHe Leak Test*
4. Vacuum Liner GHe Leak Test
5. Magnet Operational Test
6. Magnet Axes Alignment
7. Heat Leak Test

* Performed prior to installation of shield and vacuum liner.

Test Plans have been prepared for the Proof Pressure Test, Winding Insulation Resistance Test, and the Magnet Leak Test. These are included in this appendix as Integrated Test Plan (ITP) Sections 4.1.5, 4.1.3, and 4.1.1 respectively. Tests 5, 6, and 7 above are performed at liquid helium temperatures and are described in the following paragraphs.

Prior to the start of cooldown, each magnet will be prepared for test by performing the following operations:

1. The power, protection, control, and instrumentation test equipment systems shall be tested and verified ready for test.
2. The magnet instrumentation shall be tested and verified ready for test.
3. All electrical interfaces between the magnet and test equipment shall be verified.
4. The magnet vacuum vessel shall be evacuated to 10^{-4} TORR.
5. The magnet helium vessel and winding assembly shall be rid of undesirable impurities by evacuating the helium vessel to 100 microns and backfilling with high purity helium gas three times. Any residual impurities will be removed by

the purifiers in the helium refrigerator as gas is circulated during cooldown.

6. The liquid nitrogen system shall be purged with warm dry nitrogen and filled with liquid.

The magnet will be cooled down by supplying gaseous helium at the temperatures, flow rate, and times specified below:

Temperature, °K	Flow, gm/sec	Time, Hours
150	6.75	3
80	6.75	6.5
50	4.25	3.5
25	3.8	3.0
10	2.5	3.0
4.5	2.9	2.9

After cooldown and filling the magnet with liquid helium, thermal stabilization shall be assured prior to performing the tests described in the following paragraphs.

Magnet Operational Test

After the magnet has been cooled down and all instrumentation verified for proper operation, the charging operation will proceed. The charging operation will be performed as follows:

1. Charge magnet to 170 amps at a rate of 25 amps/minute.

2. Verify that all magnet components are functioning properly. This will include, but not be limited to:

   - Pressure transducers
   - Temperature sensors
   - Quench detection system
   - Measurement of voltage across vapor cooled leads to verify superconductivity of magnet coil

3. Initiate an emergency discharge and monitor all instrumentation.

4. If all components are functioning properly, the magnet will be charged to 1700 amps at a rate of 30 amps/minute.

5. This current level will be held for ten minutes while monitoring all components that were checked in Step 2.

6. At the completion of the ten-minute operating period, an emergency discharge will be initiated and all instrumentation will be monitored.

7. If no problems have arisen during or after this emergency discharge, the magnet will be charged to 1700 amps at a rate of 60 amps/minute.

8. This current level will be held for ten minutes while all magnet components are checked for proper operation. This portion of the test will allow a check for any damage that might have been caused by the emergency discharge.

This will finish the fully operational portion of the test, and if the magnet is shown to operate properly, the Magnet Axes Alignment and heat leak tests will follow immediately. At the completion of the Magnet Axes Alignment test and the heat leak test, a normal discharge will be initiated in the magnet.

Magnet Axes Alignment

Magnetic field mapping tests shall be conducted to identify the location of the conductor midplane axes. The technique and instrumentation for this test is currently under development by ORNL; however, the data expected from this test is listed below:

Perpendicular Distance from Plane C to Upper Construction Ball Center

Perpendicular Distance from Plane C to Lower Construction Ball Center

Perpendicular Distance from Plane B to Outboard Construction Ball Center

Perpendicular Distance from Plane B to Magnetic Center

Perpendicular Distance from Plane C to Magnetic Center

Perpendicular Distance from Plane A to Magnetic Center

$\cos \theta_x$

$\cos \theta_y$

$\cos \theta_z$

The definitions of planes, axes, and angles are as follows:

1. Plane A is a plane through the centers of the three reference construction balls (see magnet envelope interface drawing 70B376001 for construction balls' location).

2. Plane B is a plane through the centers of the upper and lower construction ball and is perpendicular to Plane A.

3. Plane C is a plane through the center of the outboard construction ball and is perpendicular to Planes A and B.

4. X Axis is the intersection of Plane A and Plane C.

5. Y Axis is the intersection of Plane B and Plane C.

6. Z Axis is the intersection of Plane B and Plane A.

7. Magnetic plane — plane perpendicular to the magnetic axis about which the magnetic field is symmetrical.

8. Magnetic center — intercept of the magnetic axis and the magnetic plane.

9. θ_x — Angle between the magnetic axis and the X axis.

10. θ_y — Angle between the magnetic axis and the Y axis.

11. θ_z — Angle between the magnetic axis and the Z axis.

Heat Leak Test

This test will consist of measuring the time required to vaporize a volume of liquid helium. The volume will be determined by using the liquid helium level sensor located in the magnet stack. The sensor provides a continuous level readout over a distance of 14 inches. Since other items of equipment are located in the volume occupied by the level sensor, it will be necessary to calibrate the volume as a function of liquid level. After the vaporized volume and time required are known, the heat leak into the magnet is easily calculated. This test will be performed with the magnet fully charged and no liquid helium supply to the magnet.

INTEGRATED TEST PLAN

ELMO BUMPY TORUS MAGNET SYSTEM

CASD-EBT-81-011

SECTION 4.1.1

LEAK DETECTION TEST PLAN

FOR THE

EBT DEVELOPMENT COIL/VACUUM VESSEL

27 JULY 1981

APPROVALS:

Prepared by: J. Peterson 7/24/81

Approved by Chief Engr.: D. W. Lawrence 8/27/81

Approved by Requestor: S. D. Zullo 8/27/81

Approved by Program Mgr.: [illegible]

LEAK DETECTION TEST PLAN FOR THE ELMO BUMPY TORUS MAGNET

INTRODUCTION

This plan is to provide guidelines for leak testing of the EBT magnet components and subassemblies at various stages in the manufacturing and assembly process.

The objectives of this plan are to attempt to minimize risk and rework, while still minimizing leak test costs. Each stage of leak test proposed is the last stage of manufacture and assembly in which a leakage test can be made, still allowing easy leakage test access and repair without any disassembly.

LEAK TEST METHODS

Leak tests will be conducted in accordance with ASTM Designation: E498-73, Standard Methods of Testing for Leaks using the mass spectrometer leak detector or residual gas analyzer in the tracer probe mode, method A. A Veeco MS17AB mass spectrometer leak detector or equivalent (nominal sensitivity: 1.6×10^{-10} scc He/sec or 6×10^{-11} scc air/sec) will be used. An auxiliary pumping station will be used with the leak detector, for testing large volumes. The leak detector will be used alone for smaller items. The sensitivity will be set to a standard calibrated leak, which is traceable to the NBS, before and after each test or once a day, whichever is less.

The requirement to enclose the test item in helium atmosphere (a bag purged with helium) will not be performed when the test is on a small, localized area, i.e., checking the weld of a flow pipe to the radiation shield.

LEAKAGE MEASUREMENT ACCEPTANCE CRITERIA

1. During testing, any leak pinpointed will be repaired.

2. Small piece parts: 1×10^{-8} to 1×10^{-10} scc He/sec leaks - GDC will search for a leak a maximum of 8 working hours. After 8 hours, MDAC will be notified and a QAR initiated. For leaks greater than 1×10^{-8}, a QAR will be initiated and a disposition will be given by the MRB.

3. Assemblies: Leaks less than 1×10^{-8} scc He/sec are acceptable.

4. Assemblies: 1×10^{-6} to 1×10^{-8} scc He/sec leaks - GDC will search for a leak a maximum of 8 working hours. After 8 hours, MDAC will be notified and a QAR initiated. For leaks greater than 1×10^{-6}, a QAR will be initiated and a disposition will be given by the MRB.

The above leakage criteria are guidelines for test personnel only. Large leaks can be accepted by a Material Review Board (MRB) if deemed appropriate.

LEAKAGE TEST SEQUENCE

The tests to be performed are listed below. Each step below is indicated on the first article schedule by an encircled number corresponding to the test number given.

1. Bellows Leak Test (8ELE-50-10) - Blank off ends of bellows. Evacuate interior of bellows and perform leak test. This leak test will be done by the vendor prior to shipment.

2. LN_2 Tubes (D11-38040) - Thermal shock and leak test all LN_2 tubes after they have been brazed to the LN_2 cold wall. The thermal shock test will consist of flowing LN_2 into the LN_2 tubes. When the LN_2 flows out of the other end of the LN_2 tubes, the test will be considered complete. For the leak test, only a bag test need be done if there is no visible evidence of damage. If the bag test reveals excessive leakage, spray tests will be done to locate damage for repair.

3. He Lines (D11-38031) - After the helium supply lines have been connected to the helium stack, perform leak test. Evacuate vacuum jacket. Bag line and purge bag with He.

4. Instrumentation Outlet Assemblies - After the instrumentation connectors have been installed on the outlet assemblies, but prior to installing the instrumentation outlet assemblies onto the helium stack, perform leak test on the assemblies.

5. Cold Mass (X2E-1470-0015) - Prior to installation of the MLI blankets, perform leak test on the completed cold mass. Blank off stack openings, evacuate and spray along welds. Repair as required.

6. Neck Welds on Stack - After the stack has been welded to the cold mass, the welds will be leak tested. Blank off the helium vent and helium cooldown tube. Remove the LHe operation tube and evacuate the stack and helium vessel. Spray all welds and repair as required.

7. Completed Magnet Leak Test - Blank off ports in stack assembly. Evacuate vacuum vessel and spray the external welds. Flood the helium vessel with helium.

REVISIONS:

ORIGINAL ISSUE: 2-4-81
PREDECESSOR: 81T1-242-3-0008
SUCCESSOR: NONE

ELMO BUMPY TORUS

WBS ELEMENT SCHEDULE (1810)

DEVELOPMENTAL DEWARS I & II

81T3-242-3-0022
DATE: 9-16-81
PREP BY: M. PARIS, X2261
APPVD BY: CONTRACT #144
REF

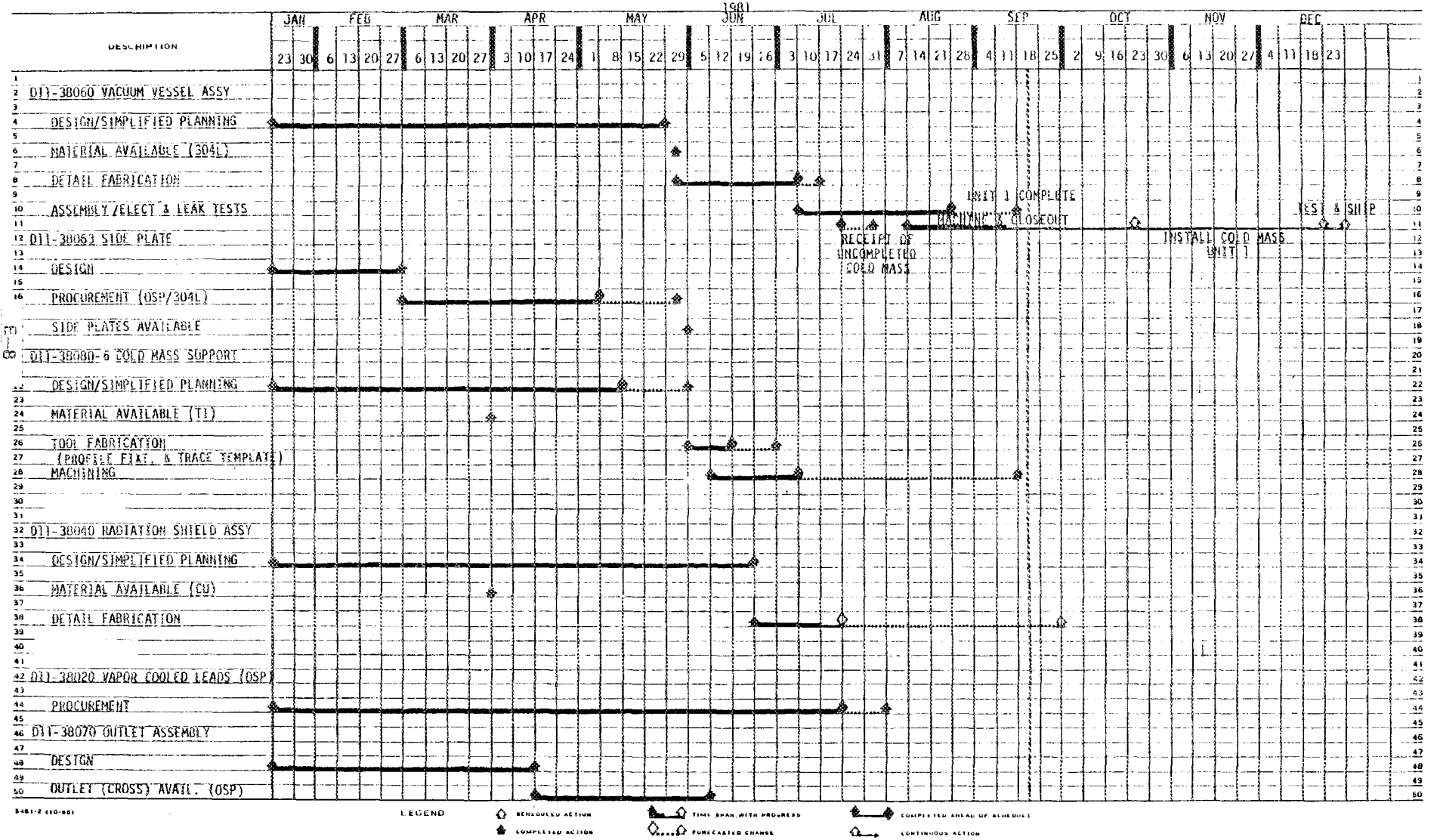

3481-2 (10-80)

LEGEND
RESCHEDULED ACTION
COMPLETED ACTION
TIME SPAN WITH PROGRESS
FORECASTED CHANGE
COMPLETED AHEAD OF SCHEDULE
CONTINUOUS ACTION

APPENDIX E

BIT3-242-3-0022

REVISIONS:

ORIGINAL ISSUE: 2-4-81
PREDECESSOR: BITT-242-3-0008
SUCCESSOR: NONE

ELMO BUMPY TORUS
WBS ELEMENT SCHEDULE (1810)
DEVELOPMENTAL DEWARS I & II

PAGE 2 OF 2

DATE: 9-16-81
PREP. BY: M. PARIS, X2261
APPVD. BY: CONTRACT #144
REF.:

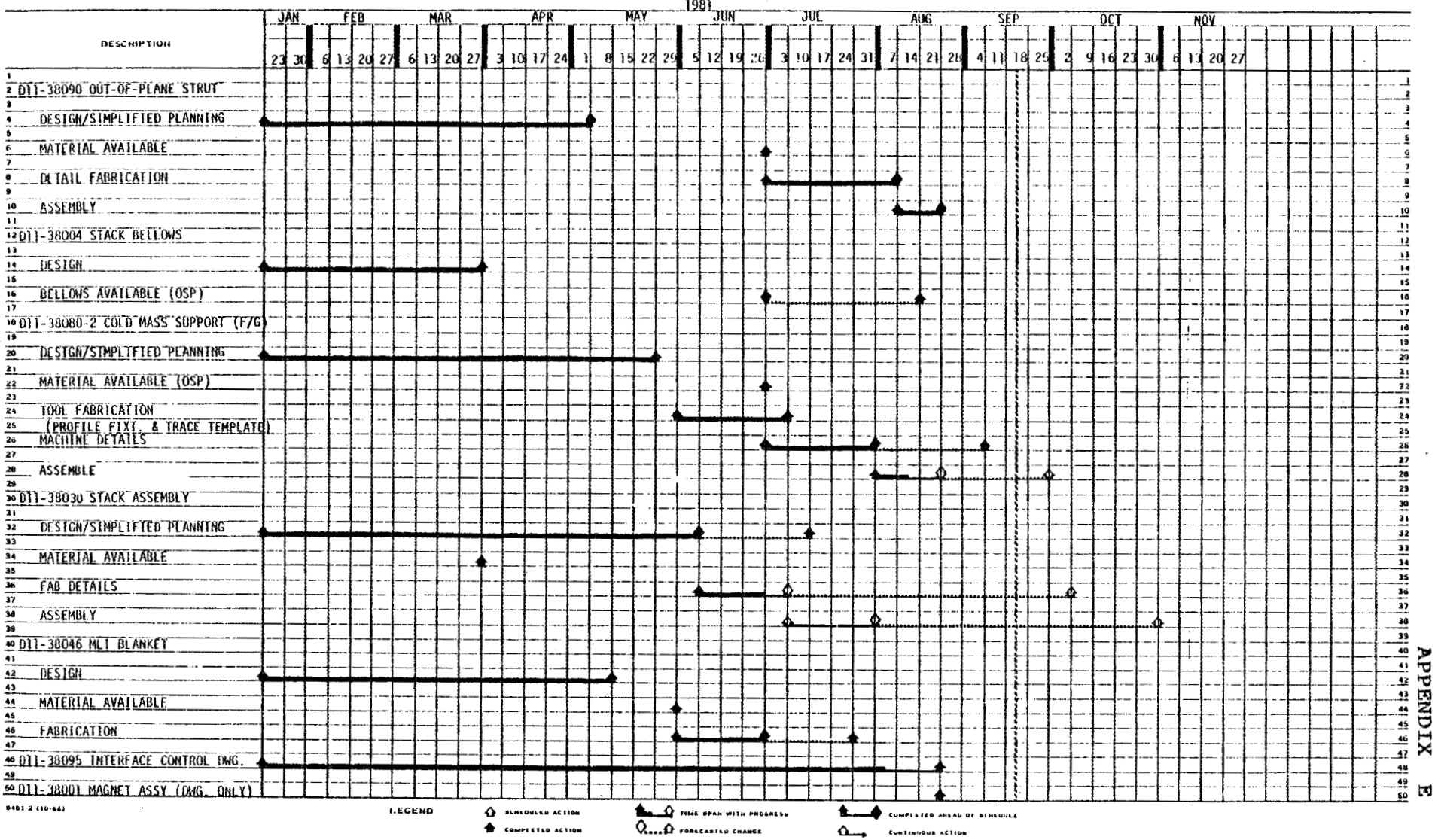

LEGEND

- SCHEDULED ACTION
- COMPLETED ACTION
- TIME SPAN WITH PROGRESS
- FORECASTED CHANGE
- COMPLETED AHEAD OF SCHEDULE
- CONTINUOUS ACTION

INTEGRATED TEST PLAN

ELMO BUMPY TORUS MAGNET SYSTEM

CASD-EBT-81-011

SECTION 4.1.3

WINDING INSULATION RESISTANCE TEST

22 JULY 1981

APPROVALS:

Prepared by: Jay Petersen

Approved by Chief Engr.: D. W. Lawrence

Approved by Requestor: D. W. Lawrence

Approved by Program Mgr.: _____

EBT-P INTEGRATED TEST PLAN
CASD-PMS-81-011

SECTION 4.1.3

WINDING INSULATION RESISTANCE TEST

I. SUMMARY

The magnet insulation strength shall be verified as significant points in the winding process as specified in the attached data sheet. Verification shall be conducted by the application of an insulation resistance test.

II. PURPOSE

The purpose of these tests is to demonstrate that the magnet winding shall withstand a high voltage test without breakdown, arcing or puncturing.

III. REQUIREMENTS

The insulation resistance tests require that the magnet shall be subjected to 2800 VDC for a period of one minute. The tests shall be performed at the points specified in the attached data sheet. The insulation resistance between any one conductor and ground shall be measured and shall not be less than twenty-five (25) megohms. Test procedure shall conform to MIL-STD-202 Method 302.

IV. CONFIGURATION

Owing to the very low dielectric strength of helium gas at room temperature, tests in this environment are to be avoided. Therefore, tests shall be conducted in air at ambient atmospheric conditions. The insulation resistance tests shall require the complete electrical isolation of the windings from ground potential. The magnet shall be inspected before the initiation of the first resistance test, to assure that no part of the winding is at or near a ground.

V. INSTRUMENTATION

The instrumentation for the insulation resistance tests shall consist of standard, commercially available Megohmmeters. The Associated Research 5220 D.C. Hypot is satisfactory for these tests.

VI. PROCEDURES

Measurements shall be performed at potential of 2800 plus or minus 50 volts dc, using an insulation resistance instrument with a minimum accuracy of 10 percent. Apply the voltage for a length of time determined as follows:

a) In all cases, wait for short term needle swings (line transients) to die out.

b) If the meter needle steadies at an unchanging value, the reading may be taken at any time after 1 second.

c) If the meter needle continues to move, take the reading at 120 $\pm$ 5 seconds.

d) If only a qualitative assessment is being made (readings will not be recorded), the circuit may be judged satisfactory if, at any time during the first 60 seconds, an increasing meter reading passes through the specified insulation resistance value.

Data shall be recorded on the attached data sheet at specific points in the winding process as specified therein.

SAFETY: Owing to the high voltages employed in these tests, all safety precautions shall be followed.

a) Warn all personnel that insulation tests are about to begin.

b) Check to make sure all personnel are at least ten (10) feet away from all parts of the winding machine.

c) Conduct insulation resistance tests with extreme care.

d) Give an all clear signal at the conclusion of the tests.

VII. DOCUMENTATION

Documentation regarding the Associated Research 5220 D.C. Hypot is given here. In addition, the MIL-STD-202 section regarding insulation resistance testing is attached. A data sheet specifying the points at which insulation tests are to be conducted is included.

EBT-P DATA SHEET FOR
INSULATION RESISTANCE TESTS

	REQUIRED RESISTANCE	ACTUAL RESISTANCE	DATE	TIME	INSP
Completion of coil winding (prior to open dewar test)	25 mΩ	----	--	--	--
Completion of open dewar test	25 mΩ	----	--	--	--
After lead connection (prior reducer neck closeout weld)	25 mΩ	----	--	--	--
Final acceptance	25 mΩ	----	--	--	--

INTEGRATED TEST PLAN

ELMO BUMPY TORUS MAGNET SYSTEM

GDC-EBT-81-011

SECTION 4.1.5

PROOF PRESSURE TEST PLAN

25 AUGUST 1981

APPROVALS:

Prepared by: J. Peterson

Approved by Chief Engr.: 9/1/81

Approved by Requestor: S. D. Zullo

Approved by Program Mgr.:

EBT-P INTEGRATED TEST PLAN
GDC-EBT-81-011
SECTION 4.1.5

I. SUMMARY

This plan is to provide guidelines for proof pressure testing of the magnet to 62.5 psig so the structural integrity of the magnet can be verified.

II. PURPOSE

The purpose of this test is to verify the structural integrity of the EBT magnet helium vessel.

III. TEST REQUIREMENTS

The magnet will be pressurized to 62,5 psig using gaseous helium and this pressure held for five minutes. The magnet will then be inspected to verify that no evidence of permanent set, external leakage, or failure of any kind resulting from the test exists.

The test pressure of TBD psi is in accordance with Paragraph UG-100, Section VIII, Division 1 of the ASME Code, 1977 Edition, with the Winter of 1978 Addenda, i.e., 1.25 times the design pressure.

IV. CONFIGURATION

The completed EBT magnet (D11-38001) shall be the test specimen.

V. INSTRUMENTATION

A pressure gage accurate to 0.5 psi will be used.

VI. PROCEDURE

A. Blank off helium vent and helium operation ports.

B. Attach pressure line to helium cooldown port (with helium cooldown tube removed).

C. Pressurize the helium vessel to 62.5 psig with gaseous helium at a rate less than 5 psi/sec.

D. Hold pressure for five minutes and then verify that no decay in pressure has occurred.

E. Vent the gas in the helium vessel.

F. Visually inspect the magnet for any sign of permanent set, leakage, or other failure.

VII. DOCUMENTATION

This test will be documented in the Quality Assurance Document with a stamp to verify that the test has been performed.

VIII. PROOF PRESSURE OPERATION SAFETY REQUIREMENTS

The following precautions will be taken to ensure safety during the test:

- Only personnel associated with the test will be allowed in the testing area.
- The magnet will be in an enclosed area, isolated from all personnel. This enclosure will consist of sandbags stacked to stop any magnet fragments that might be generated by a test failure.
- A safety relief valve will be used on the pressure line to prevent any structural damage from over-pressurizing.

"PRELIMINARY"

ELMO BUMPY TORUS
PRODUCTION ACCEPTANCE TEST FACILITY
REQUIREMENTS DOCUMENT

"PRELIMINARY"

ELMO BUMPY TORUS
PRODUCTION ACCEPTANCE TEST FACILITY
REQUIREMENTS DOCUMENT

1.0 INTRODUCTION

This document defines the requirements for the test facility required to accomplish the production acceptance testing of the 39 EBT magnet assemblies. The facility shall have the capability of performing a fully-operational test of the magnet using liquid helium. The primary purpose for the facility is final acceptance testing; however, it may be desirable to accomplish some of the in-process testing in this facility. These requirements will be developed concurrently with the detail production facilities planning and manufacturing planning. It is currently planned to locate the test facility adjacent to the EBT production facility in building 37 at the Harbor Drive Test Site.

2.0 REQUIREMENTS

2.1 GENERAL

a. The facility shall be completed, validated and ready for production acceptance testing by 1 October 1983 per schedule 81T-242-3-0008.

b. The facility shall have the capability of testing 39 magnet assemblies over an 11-month period at the following rate:

month:	1	2	3	4	5	6	7	8	9	10	11
magnet:	1	2	3	4	4	4	4	4	5	5	3

c. The cost of the facility shall be minimized; however, trade studies relating to labor costs vs. equipment costs are encouraged to reduce overall program costs.

d. The facility shall be capable of operating continuously on a 24-hour a day, 7-day a week basis. Periodic preventitive maintenance shall not exceed a duration of four hours.

e. Magnet cleanup, vacuum pumping, cooldown and warmup shall assume a 24-hour a day operation, if required. The actual testing of the magnet shall be accomplished on a one-shift-a-day basis unless studies verify two shifts are desirable.

f. As a guideline, all equipment sizing, timelines, etc. shall include a 20% minimum margin to accommodate unforeseen problems.

g. The facility shall be designed, constructed, inspected and tested in accordance with the most recent requirements of the following codes and standards:

1. The ASME Code for Unfired Pressure Vessels

2. American Standard Code for Pressure Piping

3. National Electrical Code

4. Occupational Safety and Health Act

h. The facility shall be maintained in a state of readiness for 10 years after the completion of the EBT-P contract.

i. To the maximum extent possible, standard "off-the-shelf" equipment shall be used.

j. Spare parts for both the EBT contract and the 10 year maintenance period shall be provided.

k. Drawings and instructions for the installation, operation, and maintenance shall be provided for all equipment.

2.2 TESTING

a. The facility shall provide the capability to accomplish the final acceptance tests on each production magnet assembly in accordance with procedure (TBD).

b. Prior to testing a production magnet, the facility shall be validated by performing compatibility test procedure (TBD). The prototype magnet shall be used for this validation.

c. The facility shall be capable of accomplishing in-process tests defined in procedures (TBD).

d. Testing shall be accomplished in accordance with schedule (TBD).

2.3 CRYOGENIC SYSTEM

a. The system shall have the capability of cooling down the magnet assembly from room temperature to 4.5^{o}K in 24 hours using gaseous helium. The flowrate, temperature and time requirements for the gas supply to the magnet are:

Temperature, ^{o}K	Flow, gm/sec	Time/hours
150	6.75	3
80	6.75	6.5
50	4.25	3.5
25	3.8	3.0
10	2.5	3.0
4.5	2.0	2.0

The refrigeration required to cool the magnet as a function of gas exiting temperature from the magnet is:

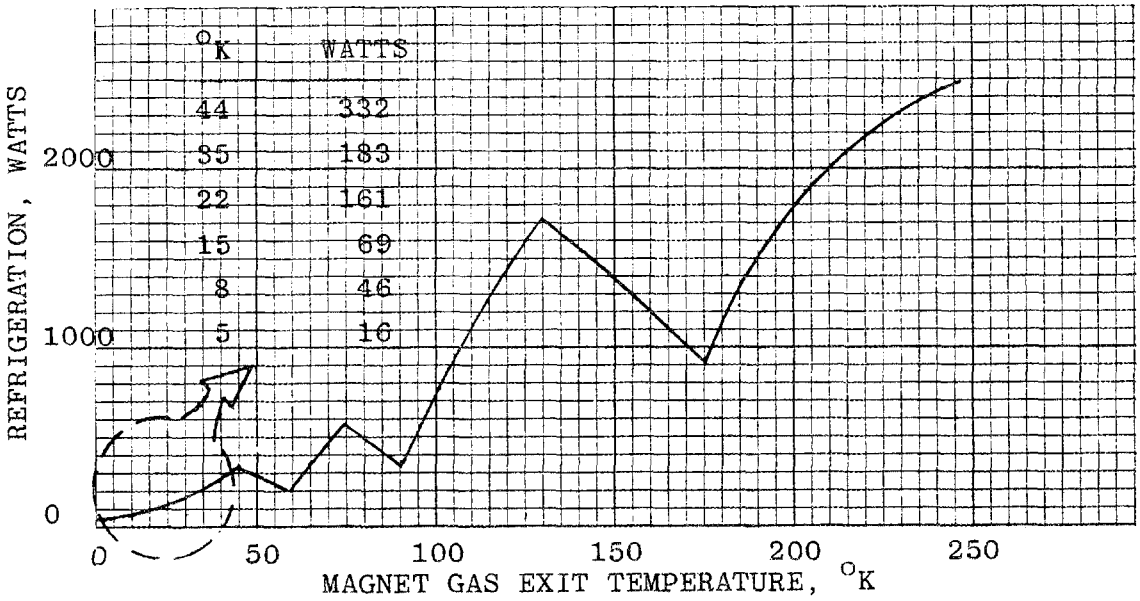

b. During steady-state operation, the system shall be capable of supplying 19.3 watts of refrigeration at 4.6°K plus 5.0 liters per hour of liquid helium.

c. The system shall be capable of maintaining the magnet cold mass at 4.2°K under steady-state conditions.

d. The system shall supply liquid nitrogen to the magnet assembly at a flowrate of (TBD) and pressure of

e. Fluid system interfaces with the magnet shall be as shown on drawing 11-38001.

2.4 VACUUM SYSTEM

a. The system shall be capable of producing a vacuum of 10^{-4} Torr in four hours within the vacuum vessel of the magnet assembly.

b. The system shall be capable of maintaining a vacuum of 10^{-5} Torr with a gaseous helium leak rate of (TBD) into the vacuum vessel.

c. The system shall be designed with adequate safeguards to eliminate vacuum vessel oil contamination due to a system malfunction.

d. Vacuum vessel volume, materials of construction and connection interfaces shall be defined by drawing (TBD).

2.5 POWER, PROTECTION AND INSTRUMENTATION

a. The system shall be designed to interface either a completed magnet assembly or the cold mass being tested in the open dewar.

b. The power supply shall be capable of providing a maximum of 2000 adc at a voltage of $\pm$ 10 vdc.

c. The power supply shall be controlled at the control console by the facility process controller.

d. The protection system shall include monitoring devices to detect all potential magnet anomalies; a circuit breaker driver and circuit breaker to isolate the magnet in case of a fault and a dump resistor to absorb magnet energy during a fault (emergency discharge).

e. Instrumentation equipment shall be used both to monitor magnet operation and to verify the proper function of all magnet instrumentation.

f. Facility electronics shall be as similar as possible to the EBT-P electronics. Prototype EBT-P electronics will be used in the facility after a complete verification.

g. The facility shall include a magnet simulator to verify proper function of all electronics.

2.6 FACILITY

a. With the exception of gaseous helium and liquid nitrogen storage tanks, all equipment shall be located inside a building.

b. The portion of the test facility normally occupied by personnel shall be heated to 65°F minimum, light level shall be 100-foot candles minimum and the routine equipment noise level shall not exceed 50 decibels. Air conditioning shall not be provided for any portion of the facility; however, ventilation shall be provided at a rate of TBD room changes per hour for the complete facility at all times while personnel are present.

c. Normal and routine venting of gases shall be ducted to a safe place outside the building.

d. The facility shall be designed to limit personnel exposure to magnetic fields per MDAC Specification 76301 Paragraph 3.9.8.

e. Electrical power, equipment cooling water, and space requirements are derived requirements and shall be determined early in the design phase.

f. The facility shall contain no ferromagnetic materials within TBD feet of the magnetic axes test stand.

g. The facility shall contain workbenches, desks and files suitable for the following personnel:

1. Two (2) engineers

2. Four (4) mechanics/technicians

3. One (1) quality control.

APPENDIX F

LONG LEAD PROCUREMENT

Long lead procurement will be required in three principal areas: the superconductor, certain stainless steel, and several electronic/electrical components. As the master schedule indicates, GDC recommends that the niobium titanium billets contract be awarded in April 1982 for the production mirror coils. In August, the conductor manufacturer should be allowed to proceed with the procurement of copper and other critical die materials. Fabrication of the conductor could begin immediately after prototype verification tests have been completed.

Depending on the "open" capacity of the vendor(s) selected to produce the conductor, it may be desirable to further accelerate this procurement. This schedule could be advanced if open-dewar tests are completed and are highly successful. Stainless steel for the first lot mirror coil production should be ordered by 1 September 1982. At times, these materials are in short supply, and due to the cyclic nature of the steel industry, it may be necessary to place steel orders much earlier and for multi-lot quantities. The power supply for the production magnets is a long-lead-time item. This procurement should be released as soon as the procurement specification has been completed and approved, in any event no later than January 1982. Electrical connectors, especially those that are hermetically sealed, should be placed on order approximately 30 weeks before required. Again, due to the cyclic nature of such material, it may be necessary to make earlier commitments for these components as well.

APPENDIX G PRELIMINARY HAZARD ANALYSIS REPORT

REPORT NO. GDC-EBT-81-002

PRELIMINARY HAZARD ANALYSIS REPORT

ELMO BUMPY TORUS
PROOF-OF-PRINCIPLE
(EBT-P)

21 AUGUST 1981

PREPARED UNDER CONTRACT YOE206R

MC DONNELL DOUGLAS ASTRONAUTICS COMPANY
ST. LOUIS DIVISION

PREPARED BY:

M. R. BROWN
SYSTEM SAFETY ENG.

APPROVED BY:

D. R. NASH
QUALITY ADMINISTRATOR

APPROVED BY:

S. L. ACKERMAN
PROGRAM MANAGER

APPROVED BY: _____

MC DONNELL DOUGLAS ASTRONAUTICS COMPANY
ST. LOUIS DIVISION

GENERAL DYNAMICS CORPORATION
CONVAIR DIVISION
SAN DIEGO, CALIFORNIA

TABLE OF CONTENTS

		PAGE
I.	INTRODUCTION	1
II.	FORM AND METHODS	1
III.	MAJOR HAZARDS	3
	Magnetic	3
	Electrical	4
	Radiation	4
	Cryogenic	5
	Vacuum Pumping	5
	Mechanical and Structural	5
APPENDIX A		6

PRELIMINARY HAZARD ANALYSIS REPORT

I. INTRODUCTION

The following Preliminary Hazard Analysis (PHA) is presented as part of the Preliminary Design Review for the Mirror Coils, Vacuum Dewar, and associated Electronics subsystems for the Elmo Bumpy Torus Proof-of-Principle (EBT-P). This PHA is the first of several safety studies to be performed by General Dynamics Convair Division and submitted to McDonnell Douglas Astronautics Company (MDAC), St. Louis.

The PHA is performed in order to obtain an initial safety evaluation of the EBT-P magnet subsystem with its interfacing subsystems. The information from the PHA will be incorporated into the final design of the experimental magnet subsystem. The PHA provides the basis for design requirements and subsequent system safety analysis by identifying safety critical areas and the hazards involved, and by delineating the planned preventative action.

The format used in the following PHA is the same as that used by General Dynamics Convair Division in previous superconducting magnet safety studies and has been approved by MDAC Safety.

II. FORM AND METHODS

Safety hazards will be highlighted using the PHA Matrices found in Appendix I. The Matrices include all hazards found in the PHA listed according to type of hazard. The types of hazards correspond to EBT-P subsystems that interface with the magnet/dewar subsystem. The division of subsystems is the same as that defined by Union Carbide Corporation in their Request for Proposal. The organization is similar to that of a flow chart, i.e., hazards are considered from the event causing a hazardous condition through the accident and its effects. The last three column headings were developed as follows:

The hazard classification is the severity of the accident that could occur if no corrective actions were taken. The classifications are:

1. Minor Injury
2. Serious Injury
3. Disabling Injury - Single Fatality
4. Multiple Fatalities

The accident probability is the chance of occurrence of the accident if no corrective actions were taken. The classifications are:

L - Low; unlikely to occur during the life of the EBT-P
M - Medium; may occur during the life of the EBT-P
H - High; likely to occur during the life of the EBT-P

The planned preventative actions are those actions thought to be sufficient to reduce the particular accident risk to a level deemed acceptable after review. These planned actions are judgements made early in the design process. The actual corrections and the appropriate residual risks will be determined when more specific design information is available and will be included in subsequent hazard analyses.

The order of precedence for satisfying system safety requirements and receiving identified hazards shall be as specified:

a. Design for minimum hazard: From the first, design to eliminate hazards. If an identified hazard cannot be eliminated, control hazards through design selection.

b. Safety devices. Hazards that cannot be eliminated or controlled through design selection shall be controlled to an acceptable level through the use of fixed, automatic, or other protective safety design features or devices. Provisions shall be made for periodic functional checks of safety devices.

c. Warning devices. Hazards that cannot be eliminated or controlled through design selection shall be controlled to an acceptable level through the use of fixed, automatic, or other protective safety design features or devices. Provisions shall be made for periodic functional checks of safety devices.

d. Procedures and training. Where it is impossible to eliminate or adequate control a hazard through design selection or use of safety and warning devices, procedures and training shall be used to control the hazard. Procedures may include the use of personal protective equipment. Precautionary notations shall be standardized as specified by the managing activity. Safety critical tasks and activities may require certification of personnel proficiency.

(Taken from MIL-STD 882A, Section 5.4.2)

There are several subsystems that affect magnet safety directly. These subsystem hazard types specific to the magnet are:

- Magnetic
- Electrical
- Radiation, Radioactivity
- Cryogenic
- Vacuum Pumping
- Mechanical and Structural

III. MAJOR HAZARDS

The following describes each of the hazard types previously mentioned. Particular safety critical areas and those areas under further study are described.

MAGNETIC

It appears that exposure to fringing fields of about 4 Tesla is possible. Fields of this size have three basic effects:

- Disturbance of instrumentation
- Attraction of ferromagnetic objects
- Effects of exposure to personnel

If the fringing fields are changing, a further hazard is eddy current. Eddy currents could circulate in artificial limbs or ograns of personnel causing malfunction of the limb or organ.

Although the Department of Energy has provided standards on constant magnetic field exposure (see Table 1), further study is required on the biological effects of both constant and changing magnetic fields on personnel, the specific strength of the magnetic field in the vicinity of all instrumentation and ferromagnetic objects, and the absolute maximum eddy currents possible in artificial limbs or organs.

Table 1 Constant Magnetic Fields

	For an 8 hr. work-day	for exposures of 1 hr. or/less	for exposures of 10 min. or less
Whole Body or Head Exposure	0.01 Tesla	0.1 Tesla	0.5 Tesla
Exposure of Extremeties	0.1 Tesla	1 Tesla	2 Tesla

(Taken from the Procurement Specification for EBT-P, Section 3.9.8)

ELECTRICAL

Included in the Electrical subsystem are the Power and Distribution, Protection, and Instrumentation and Control subsystems. Hazards in these areas have been considered.

The major electrical hazards occur during transient situations (charge or dump) and especially during a quench or fast dump. This is because it is only during a transient situation that significant voltage can appear on terminals, taps, and wires.

The basic hazards include arcing from coil-to-coil or coil-to-ground, heat from power dissipated in wires, fire, and electrical shock from high voltage taps. Because the planned preventative action we recommend is isolation, either through limited access or insulated terminals, we will perform further studies of the exact positions and routes of electrical lines. Once these are known, we can better evaluate the specific electrical hazards to personnel.

A failed instrument could lead to dangerous situations, particularly during a quench. Any of the hazardous situations mentioned can be further aggravated if they remain undetected by instrumentation. Should a quench occur, instruments must be able to reliably communicate temperature, pressure, voltage, current and atmospheric information to control personnel so that they may react quickly and safetly.

Further study is required of the exact positions of instrumentation so that we may better understand the effects of magnetic fields, low temperatures and high voltages on them.

RADIATION

The microwave (90 GHz) and RF radiation produced by the Electron Cyclotron Resonant Heating (ECRH) and the Ion Cyclotron Resonant Heating (ICRH) subsystems present a possible hazard to personnel. In addition, neutron flux and other ionizing radiation from the plasma can have hazardous ramifications should shielding fail. Radioactivity can also decay organic insulation and adhesives producing hydrogen. Hydrogen, when introduced into an excited helium atmosphere significantly reduces the electrical breakdown strength of helium (Penning Effect). This can result in arcing. Also considered under the radiation heading are X-ray and Gamma-ray radiation.

We require further study as to the amount of radiation byproducts produced, and their containment.

CRYOGENIC

Liquid helium and nitrogen will be used in large quantities as a cooling medium in the magnet subsystem. Hazardous conditions occur due to extreme cold, potential high pressure, and inert gases. The extreme cold can result in cold burns from personnel contact with cold cyropanels, lines, leaks and spills. The high pressure resulting from a sudden liquid-to-gas phase change can result in overstress to the magnet structure and explosion of the dewar. The inert gases could result in asphyxiation should gaseous helium or nitrogen displace oxygen in a personnel occupied area.

We require further study of the exact positions and routes of all cyrogenic lines so we can determine the potential hazards of leaky or ruptured lines.

VACUUM PUMPING

The hazards involved in the vacuum jacket around the magnet subsystem have been studied. Vacuum related hazards include stress initiated by the vacuum condition and any leaks in the vacuum that might cause poor insulation. These hazards could result in an implosive rupture of the vessel or undesired helium boil-off.

The vacuum system is presently under study to determine further hazardous conditions.

MECHANICAL AND STRUCTURAL

Mechanical and structural hazards have been studied and noted. The primary hazard is overstress due to vacuum, thermal fluctuation, magnetic fields and earthquake which could lead to structure failure. Although the structure has been designed to tolerate these stresses, the potential hazards should not be overlooked. Also included in this section are general industrial hazards. These include falls from elevations, slip and trip situations, noise, and movement of large machinery. Prevention of accidents due to these hazards will primarily be accomplished by compliance with general industrial safety measures.

Further study will include use of structural analyses to determine the severity of mechanical and structural hazards.

APPENDIX A

PRELIMINARY HAZARD ANALYSIS MATRICES

GENERAL DYNAMICS

EBT-P----PRELIMINARY HAZARD ANALYSIS (PHA) MATRICES

PAGE: 1

SUBSYSTEM: MAGNET

TYPE OF HAZARD: MAGNETIC

PREPARED BY: MICHAEL BROWN

DATE: AUG. 19,1981

KEY: HAZARD CLASS
1 = MINOR INJURY
2 = SERIOUS INJURY
3 = DISABLING INJURY - FATALITY
4 = MULTIPLE FATALITIES

ACCIDENT PROBABILITY
L = LOW, UNLIKELY
M = MEDIUM, POSSIBLE
H = HIGH, LIKELY

ITEM	HAZARDOUS ELEMENT	OPERATIONAL MODE	EVENT CAUSING HAZARDOUS CONDITION	HAZARDOUS CONDITION	ACCIDENT INITIATION	POTENTIAL ACCIDENT	EFFECTS	HAZ. CLASS	ACC. PROB.	PLANNED PREVENTATIVE ACTION
1	MAGNETIC FIELDS	OPERATION	FERROMAGNETIC OBJECTS IN VICINITY OF LARGE MAGNETIC FIELDS	FERROMAGNETIC OBJECTS MOVING AT HIGH SPEEDS	PERSONNEL USING FERROMAGNETIC OBJECTS IN MAGNETIC FIELD	PERSONNEL HIT BY MOVING OBJECT	PERSONNEL INJURIES	3	H	PROHIBIT ALL FERROMAGNETIC OBJECTS FROM MAGNET AREA DURING OPERATION
2	MAGNETIC FIELDS	OPERATION	OPERATION OF MAGNET	UNSHIELDED INSTRUMENTATION IN VICINITY OF MAGNET	INSTRUMENTS GIVE FALSE INFORMATION ABOUT TEMP., PRESSURE, ETC.	PERSONNEL CONTACT WITH HAZARDOUS SITUATION WITHOUT WARNING	PERSONNEL INJURIES	3	H	SHIELD OR REMOVE ALL INSTRUMENTATION FROM HIGH MAGNETIC FIELDS
3	MAGNETIC FIELDS	OPERATION	OPERATION OF MAGNET BY PERSONNEL	PERSONNEL IN VICINITY OF LARGE MAGNETIC FIELDS (>50G)	PERSONNEL PRESENT	PERSONNEL OVER-EXPOSED TO LARGE MAGNETIC FIELDS	PERSONNEL INJURIES	2	H	LIMIT ACCESS DURING OPERATION
4	FALLING STRUCTURE	OPERATION (TRANSIENT)	OPERATION OF MAGNET	MECHANICAL STRESS (B AND DB/DT)	OVERSTRESS	STRUCTURE FAILURE	FATALITY OR SEVERE INJURY	4	L	DESIGN AND CONSTRUCT STRUCTURE TO WITHSTAND 1.5 TIMES MAXIMUM POSSIBLE FIELD STRENGTH
5	MAGNETIC FIELDS	TRANSIENT	CHANGES IN MAGNETIC FIELD	INDUCED EDDY CURRENTS IN STRUCTURE	PERSONNEL CONTACT WITH METALLIC SURFACE	PERSONNEL SHOCKED BY EDDY CURRENT	PERSONNEL INJURY	2	L	GROUND STRUCTURE
6	MAGNETIC FIELDS	TRANSIENT	CHANGES IN MAGNETIC FIELD	INDUCED EDDY CURRENTS IN ARTIFICIAL LIMBS/ ORGANS OF PERSONNEL	PERSONNEL WITH ARTIFICIAL LIMBS/ ORGANS PRESENT	ELECTRIC SHOCK OR FAILURE OF LIMB/ ORGAN	PERSONNEL INJURY	3	H	WARN PERSONNEL WITH ARTIFICIAL LIMBS/ ORGANS OF HAZARD
7	MAGNETIC FIELDS	OPERATION	OPERATION OF MAGNET	STRESS ON CONDUCTOR PACK	HIGH RESISTANCE IN CONDUCTOR	SEE ELECTRICS ITEM 7				

SUBSYSTEM: MAGNET TYPE OF HAZARD: ELECTRICAL PREPARED BY: MICHAEL BROWN DATE: AUG. 19, 1981

KEY: HAZARD CLASS
1 = MINOR INJURY
2 = SERIOUS INJURY
3 = DISABLING INJURY - FATALITY
4 = MULTIPLE FATALITIES

ACCIDENT PROBABILITY
L = LOW, UNLIKELY
M = MEDIUM, POSSIBLE
H = HIGH, LIKELY

ITEM	HAZARDOUS ELEMENT	OPERATIONAL MODE	EVENT CAUSING HAZARDOUS CONDITION	HAZARDOUS CONDITION	ACCIDENT INITIATION	POTENTIAL ACCIDENT	EFFECTS	HAZ. CLASS	ACC. PROB.	PLANNED PREVENTATIVE ACTION
1	FALLING STRUCTURE	TRANSIENT	COIL IS SHORTED	FORCE IMBALANCE BETWEEN COILS	ADJACENT COILS WITH DIFFERENT CURRENTS	STRUCTURE FAILURE	FATALITY OR SEVERE INJURY	4	L	DESIGN TO WITHSTAND 1.5 TIMES MAXIMUM POSSIBLE YIELD STRENGTH, PREVENT SHORTING
2	ELECTRICAL FIRE	TRANSIENT	COIL IS SHORTED BY ARCING	BURNING FIBERGLAS OR PLASTIC	SPARK FROM ARCING COIL	DESTRUCTION OF COILS AND STRUCTURE BY FIRE	PERSONNEL INJURIES BY FIRE, DEBRIS, TOXIC GAS	3	L	FIRE PROOF INSULATION WITHOUT JEOPARDIZING CRYOGENIC CONDITIONS, INSTALL SPRINKLERS
3	TOXIC OR NOXIOUS VAPORS	TRANSIENT	COIL IS SHORTED BY ARCING	TOXIC OR NOXIOUS BREAKDOWN PRODUCTS FROM FIBERGLAS OR PLASTIC	ELECTRICAL ENERGY DECOMPOSES ORGANIC MATERIAL	PERSONNEL EXPOSED TO TOXIC ATMOSPHERE	PERSONNEL INJURIES BY INHALATION OF VAPORS	3	M	VENTILATE ENCLOSURES, LIMIT ACCESS DURING OPERATION
	FALLING STRUCTURE	TRANSIENT	COIL IS SHORTED BY ARCING	ARC MELTS HOLE IN VESSEL	HEAT FROM ARC	IMPLOSION OF VESSEL	PERSONNEL INJURIES BY EXPLOSION	4	L	DESIGN TO PREVENT PUNCTURE AND ARCING, ACCEPT RISK
5	ELECTRICAL POWER	TRANSIENT (QUENCH)	EXPOSED WIRE OR TERMINAL	HIGH VOLTAGE	PERSONNEL CONTACT WITH ELECTRICAL COMPONENTS	ELECTRICAL SHOCK	PERSONNEL INJURIES BY HIGH VOLTAGE	3	H	COVER ALL EXPOSED WIRES AND TERMINALS, LIMIT ACCESS
6	ELECTRICAL POWER	TRANSIENT (QUENCH)	COIL GOES NORMAL	HIGH VOLTAGE	PERSONNEL CONTACT WITH ELECTRICAL COMPONENTS	ELECTRICAL SHOCK	PERSONNEL INJURIES BY HIGH VOLTAGE	3	H	COVER ALL EXPOSED WIRES AND TERMINALS, LIMIT ACCESS
7	ELECTRICAL POWER	TRANSIENT (QUENCH)	BROKEN OR HIGH RESISTANCE	HIGH VOLTAGE	PERSONNEL CONTACT WITH ELECTRICAL COMPONENTS	ELECTRICAL SHOCK	PERSONNEL INJURIES BY HIGH VOLTAGE	3	H	COVER ALL EXPOSED WIRES AND TERMINALS, LIMIT ACCESS
8	HEAT	TRANSIENT	I2R POWER DISSIPATED IN LEADS	HOT LEADS	PERSONNEL CONTACT HOT LEADS	SEVERE BURNS	PERSONNEL INJURIES BY BURNING	3	H	ISSUE PROTECTIVE CLOTHING TO MAINTENANCE PERSONNEL
9	HEAT	TRANSIENT	I2R POWER DISSIPATED IN LEADS	HOT LEADS	COMBUSTION OF FLAMMABLE MATERIAL	FIRE	SEE ELECTRICS (ITEM 2)			
10	HEAT	TRANSIENT	I2R POWER DISSIPATED IN LEADS	HOT LEADS	HELIUM BOIL	SEE CRYOGENICS (ITEM 1)	SEE CRYOGENIC (ITEM 1)			
11	ELECTRICAL POWER	TRANSIENT	CONDUCTIVE CONTAMINENTS IN INSULATION	HIGH VOLTAGE	PERSONNEL CONTACT WITH ELECTRICAL COMPONENTS	ELECTRICAL SHOCK	PERSONNEL INJURIES BY HIGH VOLTAGE	3	L	PROVIDE ADEQUATE INSPECTION OF INSULATION
12	ELECTRICAL POWER	TRANSIENT	CONDUCTIVE CONTAMINENTS IN INSULATION	SHORTING	PERSONNEL CONTACT WITH ELECTRICAL COMPONENTS	ELECTRICAL SHOCK	PERSONNEL INJURIES BY HIGH VOLTAGE	3	L	PROVIDE ADEQUATE INSPECTION OF INSULATION

SUBSYSTEM: MAGNET TYPE OF HAZARD: ELECTRICAL (CONT') PREPARED BY: MICHAEL BROWN DATE: AUG. 19, 1981

KEY: HAZARD CLASS
1 = MINOR INJURY
2 = SERIOUS INJURY
3 = DISABLING INJURY - FATALITY
4 = MULTIPLE FATALITIES

ACCIDENT PROBABILITY
L = LOW, UNLIKELY
M = MEDIUM, POSSIBLE
H = HIGH, LIKELY

ITEM	HAZARDOUS ELEMENT	OPERATIONAL MODE	EVENT CAUSING HAZARDOUS CONDITION	HAZARDOUS CONDITION	ACCIDENT INITIATION	POTENTIAL ACCIDENT	EFFECTS	HAZ. CLASS	ACC. PROB.	PLANNED PREVENTATIVE ACTION
13	ELECTRICAL POWER	TRANSIENT	CONDUCTIVE CONTAMINENTS IN INSULATION	SHORTING	ADJACENT COILS WITH DIFFERENT CURRENTS	STRUCTURE FAILURE	FATALITY OR SEVERE INJURY	4	L	PROVIDE ADEQUATE INSPECTION OF INSULATION
14	PCB (POLYCHLORINATED BUTYLS)	ALL	PCB'S USED IN ELECTRICAL EQUIPMENT	PCB'S IN ENVIRONMENT	PCB CONTAINMENT LOST	PERSONNEL INGEST PCB'S	PERSONNEL INJURIES BY INGESTED PCB'S	3	L	SUBSTITUTE SAFER MATERIALS
15	OZONE	ALL (QUENCH)	HIGH VOLTAGE COMPONENTS PRODUCE OZONE	EXCESSIVE OZONE CONCENTRATION IN AIR	PERSONNEL EXPOSED TO OZONE	PERSONNEL EXPOSED TO TOXIC ATMOSPHERE	PERSONNEL INJURIES BY INHALATION OF VAPORS	2	M	DESIGN TO LIMIT GENERATION, VENTILATE IF NECESSARY
16	OZONE	ALL (QUENCH)	HIGH VOLTAGE COMPONENTS PRODUCE OZONE	EXPLOSIVE CONCENTRATION OF OZONE IN AIR	IGNITION SOURCE	EXPLOSION	PERSONNEL INJURIES BY EXPLOSION	2	M	DESIGN TO LIMIT GENERATION, VENTILATE IF NECESSARY
17	FAILED INSTRUMENT	ALL	NON-UNIFORM QUENCH	UNEQUAL CURRENTS AND UNBALANCED FORCES	PERSONNEL RECEIVE INCORRECT TEMPERATURE OR VOLTAGE INFORMATION	OVERSTRESS AND STRUCTURE FAILURE	SEE MECHANICS SECTION (# 6,9, 12,13)			
18	FAILED INSTRUMENT	WARM-UP	UNDETECTED TEMPERATURE CHANGE	CRYOPANELS REMAIN AT CRYOGENIC TEMPERATURES	PERSONNEL RECEIVE INCORRECT TEMPERATURE OR PRESSURE INFORMATION	CONTACT WITH CRYOGENS	SEVERE COLD BURN	2	L	USE REDUNDANT INSTRUMENTATION
19	FAILED INSTRUMENT	ALL	INERT ATMOSPHERE UNDETECTED	INERT ATMOSPHERE	PERSONNEL RECEIVE INCORRECT ATMOSPHERIC INFORMATION	SEE CRYOGENICS SECTION (ITEM 5)	SEE CRYOGENIC (ITEM 5)			
20	FAILED INSTRUMENT	ALL	HIGH PRESSURE UNDETECTED	MECHANICAL STRESS	OVERSTRESS	STRUCTURE FAILURE, RUPTURE OF CHAMBER	FATALITY OR SEVERE INJURY	4	L	DESIGN TO WITHSTAND 10 TIMES EXPECTED LIFE CYCLE FATIGUE, PROVIDE BURST DISKS
21	FAILED INSTRUMENT	ALL	LARGE STRESS/STRAIN UNDETECTED	MECHANICAL STRESS	OVERSTRESS	STRUCTURE FAILURE	FATALITY OR SEVERE INJURY	4	L	DESIGN TO WITHSTAND 1.5 TIMES MAXIMUM POSSIBLE YIELD STRENGTH
22	FAILED INSTRUMENT	WARM-UP	HIGH DISCHARGE VOLTAGE UNDETECTED	ARCING	PERSONNEL RECEIVE INCORRECT TEMPERATURE OR VOLTAGE INFORMATION	SEE ELECTRICS SECTION (ITEMS 2, 3 AND 4)	SEE ELECTRICS (# 2,3,4)			
23	FAILED INSTRUMENT	WARM-UP	LOW DISCHARGE VOLTAGE UNDETECTED, HIGH I2R	THERMAL STRESS	OVERSTRESS	STRUCTURE FAILURE	SEVERE INJURIES	3	M	DESIGN TO WITHSTAND 1.5 TIMES MAXIMUM POSSIBLE YIELD STRENGTH
24	FAILED INSTRUMENT	WARM-UP	LOW DISCHARGE VOLTAGE UNDETECTED, HIGH I2R	HELIUM BOIL AND RESULTING HIGH PRESSURE	OVERSTRESS	STRUCTURE FAILURE	SEVERE INJURIES	3	M	DESIGN TO WITHSTAND 1.5 TIMES MAXIMUM POSSIBLE YIELD STRENGTH

SUBSYSTEM: MAGNET TYPE OF HAZARD: ELECTRICAL (CONT') PREPARED BY: MICHAEL BROWN DATE: AUG. 19, 1981

KEY: HAZARD CLASS
1 = MINOR INJURY
2 = SERIOUS INJURY
3 = DISABLING INJURY - FATALITY
4 = MULTIPLE FATALITIES

ACCIDENT PROBABILITY
L = LOW, UNLIKELY
M = MEDIUM, POSSIBLE
H = HIGH, LIKELY

ITEM	HAZARDOUS ELEMENT	OPERATIONAL MODE	EVENT CAUSING HAZARDOUS CONDITION	HAZARDOUS CONDITION	ACCIDENT INITIATION	POTENTIAL ACCIDENT	EFFECTS	HAZ. CLASS	ACC. PROB.	PLANNED PREVENTATIVE ACTION
25	FAILED INSTRUMENT	WARM-UP	LOW DISCHARGE VOLTAGE UNDETECTED	MELTED WIRE OR INSULATION	SHORTING OR ARCING	SEE ELECTRICS SECTION (ITEM 1)	SEE ELECTRICS (ITEM 1)			

SUBSYSTEM: MAGNET TYPE OF HAZARD: RADIATION PREPARED BY: MICHAEL BROWN DATE: AUG. 19, 1981

KEY: HAZARD CLASS
1 = MINOR INJURY
2 = SERIOUS INJURY
3 = DISABLING INJURY - FATALITY
4 = MULTIPLE FATALITIES

ACCIDENT PROBABILITY
L = LOW, UNLIKELY
M = MEDIUM, POSSIBLE
H = HIGH, LIKELY

ITEM	HAZARDOUS ELEMENT	OPERATIONAL MODE	EVENT CAUSING HAZARDOUS CONDITION	HAZARDOUS CONDITION	ACCIDENT INITIATION	POTENTIAL ACCIDENT	EFFECTS	HAZ. CLASS	ACC. PROB.	PLANNED PREVENTATIVE ACTION
1	NEUTRON RADIATION	OPERATION	OPERATION OF REACTOR	NEUTRON FLUX	PERSONNEL PRESENT	PERSONNEL OVER-EXPOSED TO NEUTRON FLUX	PERSONNEL INJURIES BY FLUX	2	L	USE MATERIALS TO MINIMIZE ACTIVATION, LIMIT ACCESS
2	RADIATION	ALL	NEUTRON FLUX	PRESENCE OF RADIOACTIVE MATERIALS, 3H, 14C, 42AR, ETC.	PERSONNEL PRESENT	PERSONNEL OVER-EXPOSED TO RADIATION	PERSONNEL INJURIES BY RADIATION	2	L	USE MATERIALS TO MINIMIZE ACTIVATION, LIMIT ACCESS
3	RADIATION	OPERATION	NEUTRON FLUX, X-RAY	RADIATION PRESENT	RADIATION DEGRADES STRUCTURE	OVERSTRESS	FATALITY OR SEVERE INJURIES	4	L	USE MATERIALS TO MINIMIZE ACTIVATION
4	RADIATION	OPERATION	RADIOLYSTIC DECOMPOSITION OF ORGANIC INSULATION, GLUE, ETC.	HYDROGEN PRESENT	PRESENCE OF HYDROGEN LOWERS DIELECTRIC CONSTANT OF HELIUM (PENNING EFFECT)	ARCING	SEE ELECTRICS SECTION (ITEMS 2, 3 AND 4)			
5	RADIATION	OPERATION	RADIOLYSTIC DECOMPOSITION OF ORGANIC INSULATION	DECOMPOSED INSULATION	UNPROTECTED CONDUCTORS IN CLOSE PROXIMITY	ARCING AND/OR SHORTED COILS	SEE ELECTRICS SECTION (ITEMS 2, 3 AND 4)			
6	RADIATION	OPERATION	RADIATION DAMAGE TO STABILIZER OR SUPERCONDUCTOR	HIGH RESISTANCE IN CONDUCTORS	COIL GOES NORMAL	SEE ELECTRICS SECTION (ITEM 7)	SEE ELECTRICS (ITEM 7)			
7	X-RAY RADIATION	OPERATION	NORMAL FLOW OF PLASMA	X-RAYS, GAMMA RAYS	PERSONNEL PRESENT	PERSONNEL OVER-EXPOSED TO X-RAYS AND GAMMA RAYS	PERSONNEL INJURIES BY RADIATION	2	L	SHIELD VESSEL DURING OPERATION, LIMIT ACCESS
8	X-RAY RADIATION	TRANSIENT (QUENCH)	HIGH VOLTAGE	X-RAYS	PERSONNEL PRESENT	PERSONNEL OVER-EXPOSED TO X-RAYS	PERSONNEL INJURIES BY X-RAYS	2	L	SHIELD VESSEL DURING OPERATION, LIMIT ACCESS
9	MICROWAVE RADIATION	OPERATION OF ECRH	MICROWAVE SHIELDING FAILS	PRESENCE OF MICROWAVES	PERSONNEL PRESENT	PERSONNEL OVER-EXPOSED TO MICROWAVE RADIATION	PERSONNEL INJURIES BY RADIATION	2	L	SHIELD ECRH DURING OPERATION, LIMIT ACCESS
10	MICROWAVE RADIATION	OPERATION OF ECRH	MICROWAVE SHIELDING FAILS	PRESENCE OF MICROWAVES	MICROWAVES DEGRADE ORGANIC INSULATION	ARCING AND/OR SHORTED COILS	SEE ELECTRICS SECTION (# 2,3,4)	2	L	SHIELD ECRH DURING OPERATION, LIMIT ACCESS

SUBSYSTEM: MAGNET TYPE OF HAZARD: CRYOGENIC PREPARED BY: MICHAEL BROWN DATE: AUG. 19, 1981

KEY: HAZARD CLASS
1 = MINOR INJURY
2 = SERIOUS INJURY
3 = DISABLING INJURY - FATALITY
4 = MULTIPLE FATALITIES

ACCIDENT PROBABILITY
L = LOW, UNLIKELY
M = MEDIUM, POSSIBLE
H = HIGH, LIKELY

ITEM	HAZARDOUS ELEMENT	OPERATIONAL MODE	EVENT CAUSING HAZARDOUS CONDITION	HAZARDOUS CONDITION	ACCIDENT INITIATION	POTENTIAL ACCIDENT	EFFECTS	HAZ. CLASS	ACC. PROB.	PLANNED PREVENTATIVE ACTION
1	FALLING STRUCTURE	ALL (QUENCH)	UNANTICIPATED LIQUID-TO-GAS PHASE CHANGE	HIGH PRESSURE	OVERSTRESS	STRUCTURE FAILURE, RUPTURE OF CHAMBER	FATALITY OR SEVERE INJURY	4	L	DESIGN ADEQUATE RELIEF VALVES AND VENTING SYSTEM
2	CRYOGENS	ALL	FROZEN CONTAMINANTS IN LINES	HIGH PRESSURE	OVERSTRESS	STRUCTURE FAILURE, RUPTURE OF CHAMBER	FATALITY OR SEVERE INJURY	4	L	PROVIDE RELIEF VALVES/ VENTS AND ADEQUATE HELIUM PURIFICATION
3	FALLING STRUCTURE	ALL	CRYO LINE CRIMPED	HIGH PRESSURE	OVERSTRESS	STRUCTURE FAILURE, RUPTURE OF CHAMBER	FATALITY OR SEVERE INJURY	4	L	PROVIDE RELIEF VALVES, DESIGN TO PREVENT CRIMP
4	CRYOGENS	COOLDOWN, WARMUP	THERMAL STRESS	SEVERE TEMPERATURE CHANGE	OVERSTRESS	STRUCTURE FAILURE, RUPTURE OF CHAMBER	FATALITY OR SEVERE INJURY	4	L	DESIGN TO WITHSTAND STRESSES
5	CRYOGENS	ALL	CONDENSED AND FROZEN O2,O3,H2,D2 ON CRYO-PANELS	EXPLOSIVE SUBSTANCES	IGNITION SOURCE	EXPLOSION	FATALITY OR SEVERE INJURY	4	L	PROVIDE ADEQUATE CRYOGEN PURIFICATION
6	CRYOGENS	ALL	LEAK IN LINE	UNCONTAINED CRYOGENS PRESENT	UNDETECTED SPILL OR LEAK	PERSONNEL CONTACT WITH CRYOGENS	SEVERE COLD BURN	2	M	DESIGN TO PREVENT LEAKS, LIMIT ACCESS
7	CRYOGENS	MAINTENANCE	EXPOSED CRYOPANELS	EXTREME COLD AT CRYO-PANELS	PERSONNEL CONTACT WITH CRYOPANELS	PERSONNEL CONTACT WITH CRYOPANELS	SEVERE COLD BURN	2	L	ISOLATE PANELS, LIMIT ACCESS
8	CRYOGENS	ALL	CRYO VENTING	COLD AND INERT ATMOSPHERES PRESENT	PERSONNEL BREATHE VAPORS	PERSONNEL ASPHYXIATION AND/ DAMAGE TO LUNGS	FATALITY OR SEVERE INJURY	4	M	EVALUATE MAGNITUDE OF PROBLEM, BACK-FILL WITH AIR, USE EXTERNAL VENTS

SUBSYSTEM: MAGNET TYPE OF HAZARD: VACUUM PUMPING PREPARED BY: MICHAEL BROWN DATE: AUG. 19, 1981

KEY: HAZARD CLASS
1 = MINOR INJURY
2 = SERIOUS INJURY
3 = DISABLING INJURY - FATALITY
4 = MULTIPLE FATALITIES

ACCIDENT PROBABILITY
L = LOW, UNLIKELY
M = MEDIUM, POSSIBLE
H = HIGH, LIKELY

ITEM	HAZARDOUS ELEMENT	OPERATIONAL MODE	EVENT CAUSING HAZARDOUS CONDITION	HAZARDOUS CONDITION	ACCIDENT INITIATION	POTENTIAL ACCIDENT	EFFECTS	HAZ. CLASS	ACC. PROB.	PLANNED PREVENTATIVE ACTION
1	FALLING STRUCTURE	UNDER VACUUM	EVACUATING VESSEL	STRUCTURAL STRESS	OVERSTRESS	RUPTURE OF CHAMBER	INJURIES	3	M	DESIGN TO WITHSTAND 10 TIMES EXPECTED LIFE CYCLE FATIGUE
2	FALLING STRUCTURE	UNDER VACUUM	PUNCTURE OF VESSEL WALL BY ELECTRICAL ARC, PROJECTILE, ETC.	PERSONNEL NEAR IMPLODING VESSEL	RUPTURE OF CHAMBER	IMPLOSION FROM PRESSURE DIFFERENTIAL	FATALITY OR SEVERE INJURY	4	L	DESIGN TO PREVENT PUNCTURE
3	VACUUM	UNDER VACUUM	LEAK IN VACUUM	POOR INSULATION	RAPID HEAT TRANSFER	HELIUM BOIL AND RESULTING HIGH PRESSURE	SEE CRYOGENIC SECTION (ITEM 1)			
4	OIL	OPERATION	PUMPS PRODUCE AIR/OIL MIXTURE	AIR/OIL MIXTURE	IGNITION SOURCE	FIRE, EXPLOSION, AND SUBSEQUENT DESTRUCTION	PERSONNEL INJURIES BY BURNS, DEBRIS	3	L	PROVIDE EXHAUST AND VENTILATION TO PUMPS, PROVIDE FILTERS
5	NOISE	OPERATION	PUMPS MAKES NOISE	EXCESSIVE NOISE IN WORK ENVIRONMENT	PERSONNEL PRESENT IN HIGH NOISE AREA	HEARING IMPAIRED	HEARING IMPAIRED	2	H	LOCATED PUMPS AWAY FROM PERSONNEL, PROVIDE ADEQUATE SOUND ATTENUATION

SUBSYSTEM: MAGNET TYPE OF HAZARD: MECHANICAL AND STRUCTURAL PREPARED BY: MICHAEL BROWN DATE: AUG. 19, 1981

KEY: HAZARD CLASS
1 = MINOR INJURY
2 = SERIOUS INJURY
3 = DISABLING INJURY - FATALITY
4 = MULTIPLE FATALITIES

ACCIDENT PROBABILITY
L = LOW, UNLIKELY
M = MEDIUM, POSSIBLE
H = HIGH, LIKELY

ITEM	HAZARDOUS ELEMENT	OPERATIONAL MODE	EVENT CAUSING HAZARDOUS CONDITION	HAZARDOUS CONDITION	ACCIDENT INITIATION	POTENTIAL ACCIDENT	EFFECTS	HAZ. CLASS	ACC. PROB.	PLANNED PREVENTATIVE ACTION
1	MECHANICAL EQUIPMENT	OPERATION	STRUCTURE FAILURE	FALLING STRUCTURE	PERSONNEL PRESENT	PERSONNEL CRUSHED	FATALITY OR SEVERE INJURY	4	L	DESIGN TO WITHSTAND 1.5 TIMES MAXIMUM POSSIBLE YIELD STRENGTH
2	MECHANICAL EQUIPMENT	OPERATION	MAGNETIC FIELD	LARGE MAGNETIC FORCES FATIGUE STRUCTURE	OVERSTRESS	STRUCTURE FAILURE	FATALITY OR SEVERE INJURY	4	L	DESIGN TO WITHSTAND 1.5 TIMES MAXIMUM POSSIBLE YIELD STRENGTH
3	MECHANICAL EQUIPMENT	OPERATION	THERMAL STRESS	LARGE THERMAL GRADIENT FATIGUES STRUCTURE	OVERSTRESS	STRUCTURE FAILURE	FATALITY OR SEVERE INJURY	4	L	DESIGN TO WITHSTAND 1.5 TIMES MAXIMUM POSSIBLE YIELD STRENGTH
4	MECHANICAL EQUIPMENT	OPERATION	PULLING A VACUUM IN VESSEL	VACUUM WEAKENS AND FATIGUES STRUCTURE	OVERSTRESS	STRUCTURE FAILURE	FATALITY OR SEVERE INJURY	4	L	DESIGN TO WITHSTAND 10 TIMES EXPECTED LIFE CYCLE FATIGUE
5	FIRE	ALL	SPARK, HEAT, EXPLOSION	COMPONENTS EXPOSED TO HEAT	COMPONENT IGNITES	MATERIAL BURNS, STRUCTURE FAILURE	PERSONNEL INJURY BY FALLING DEBRIS, TOXIC GAS	4	L	USE NON-FLAMMABLE MATERIALS WHERE POSSIBLE (MLI HAZARD RECOGNIZED, ACCEPT RISK), LIMIT SPREAD, INCORPORATE DETECTION DEVICES, DESIGN TO WITHSTAND STRESS
6	MECHANICAL EQUIPMENT	OPERATION	NEUTRON FLUX AND NUCLEAR DEGRADATION OF STRUCTURE	RADIATION WEAKENS AND FATIGUES STRUCTURE	OVERSTRESS	STRUCTURE FAILURE	FATALITY OR SEVERE INJURY	4	L	DESIGN TO WITHSTAND 1.5 TIMES MAXIMUM POSSIBLE YIELD STRENGTH, PROVIDE SHIELDING
7	MECHANICAL EQUIPMENT	OPERATION	INADEQUATE DESIGN, IMPROPER INSTALATION	DESIGN OF STRUCTURE INADEQUATE TO WITHSTAND STRESSES	OVERSTRESS	STRUCTURE FAILURE	FATALITY OR SEVERE INJURY	4	L	DESIGN TO WITHSTAND 1.5 TIMES MAXIMUM POSSIBLE YIELD STRENGTH
8	MECHANICAL EQUIPMENT	OPERATION	STRUCTURE FAILURE	BROKEN COILS MOVING AT HIGH SPEEDS, ACCELERATED BY LARGE FIELDS	PERSONNEL PRESENT IN PATH OF MOVING OBJECT	PERSONNEL HIT BY MOVING OBJECT	FATALITY OR SEVERE INJURY	4	L	DESIGN TO WITHSTAND 1.5 TIMES MAXIMUM POSSIBLE YIELD STRENGTH
9	MECHANICAL EQUIPMENT	OPERATION	MOTION OF COILS	FORCES INDUCED BY DB/DT	OVERSTRESS	STRUCTURE FAILURE, OR SEVERE INJURY	FATALITY OR SEVERE INJURY	4	L	DESIGN COILS TO PREVENT MOTION
10	EARTHQUAKE	ALL	EARTHQUAKE	ADDITIONAL STRESS ON COMPONENTS	OVERSTRESS	STRUCTURE FAILURE, RUPTURE OF CHAMBER	FATALITY OR SEVERE INJURY	4	L	DESIGN TO SATISFY AREA EARTHQUAKE STANDARDS, ACCEPT RISK
11	EARTHQUAKE	MAINTENANCE	EARTHQUAKE CAUSES COILS TO MOVE	CLEARANCE DECREASES	PERSONNEL BETWEEN MAGNET AND VESSEL WALL	PERSONNEL CRUSHED	FATALITY OR SEVERE INJURY	4	L	DESIGN TO SATISFY AREA EARTHQUAKE STANDARDS, ACCEPT RISK
12	MECHANICAL EQUIPMENT	TRANSIENT (QUENCH)	COIL IS SHORTED	MAGNETIC FORCE IMBALANCE (COIL GOES NORMAL)	OVERSTRESS	STRUCTURE FAILURE	FATALITY OR SEVERE INJURY	4	L	DESIGN TO WITHSTAND 1.5 TIMES MAXIMUM POSSIBLE YIELD STRENGTH
13	MECHANICAL EQUIPMENT	TRANSIENT (QUENCH)	BROKEN OR HIGH RESISTANCE CONNECTION	MAGNETIC FORCE IMBALANCE (COIL GOES NORMAL)	OVERSTRESS	STRUCTURE FAILURE	FATALITY OR SEVERE INJURY	4	L	DESIGN TO WITHSTAND 1.5 TIMES MAXIMUM POSSIBLE YIELD STRENGTH

SUBSYSTEM: MAGNET TYPE OF HAZARD: MECHANICAL AND STRUCTURAL (CONT') PREPARED BY: MICHAEL BROWN DATE: AUG. 19, 1981

KEY: HAZARD CLASS
1 = MINOR INJURY
2 = SERIOUS INJURY
3 = DISABLING INJURY - FATALITY
4 = MULTIPLE FATALITIES

ACCIDENT PROBABILITY
L = LOW, UNLIKELY
M = MEDIUM, POSSIBLE
H = HIGH, LIKELY

ITEM	HAZARDOUS ELEMENT	OPERATIONAL MODE	EVENT CAUSING HAZARDOUS CONDITION	HAZARDOUS CONDITION	ACCIDENT INITIATION	POTENTIAL ACCIDENT	EFFECTS	HAZ. CLASS	ACC. PROB.	PLANNED PREVENTATIVE ACTION
14	LARGE MECHANICAL STRESS	ALL	STRESS RAISES RESISTANCE OF CONDUCTORS	HIGH RESISTANCE CONDUCTORS	OVERSTRESS	STRUCTURE FAILURE	FATALITY OR SEVERE INJURY	4	L	DESIGN TO WITHSTAND 1.5 TIMES MAXIMUM POSSIBLE YIELD STRENGTH
15	LARGE MECHANICAL STRESS	ALL	STRESS WEAKENS OR CRACKS INSULATION	WEAKENED OR CRACKED INSULATION	SHORTING OR ARCING	SEE ELECTRICS SECTION (ITEMS 1, 2,3,4)	SEE ELECTRICS (# 1,2,3, 4)			
16	LARGE MECHANICAL STRESS	ALL	STRESS CONSTRICTS OR BREAKS CRYO LINES	BLOCKED OR BROKEN CRYO LINES	LEAK IN LINE, HIGH PRESSURE	SEE CRYOGENIC SECTION (ITEMS 3 AND 7)	SEE CRYOGENIC (# 3, 7)			
17	PERSONNEL WORKING AT ELEVATIONS	MAINTENANCE	MAINTENANCE	PERSONNEL AT ELEVATIONS	TRIP, SLIP	PERSONNEL OR OBJECTS FALL	POSSIBLE FATALITY	3	M	DESIGN HANDRAILS, TOEBOARDS, SCAFFOLDING ONTO STRUCTURE. REQUIRE HARDHATS
18	FIRE	ALL	SPARK, HEAT, EXPLOSION	COMPONENTS EXPOSED TO HEAT	COMPONENT IGNITES	MATERIAL BURNS	PERSONNEL INJURY BY BURNS OR TOXIC GAS	3	M	USE NON-FLAMMABLE MATERIALS WHERE POSSIBLE (MLI HAZARD RECOGNIZED, ACCEPT RISK), LIMIT SPREAD, INCORPORATE DETECTION DEVICES
	MOVING MACHINERY	FABRICATION, OPERATION	FABRICATION AND OPERATION OF SYSTEM	RAPIDLY MOVING MACHINE PARTS	PERSONNEL PRESENT NEAR MOVING PARTS	PERSONNEL CAUGHT BY MOVING PARTS	PERSONNEL INJURIES BY MOVING PARTS	3	M	LIMIT ACCESS DURING OPERATION
20	MASS OF MAGNET	FABRICATION, TRANSPORTATION	MOVING THE MAGNET	HUGE MOVING MASS	PERSONNEL PRESENT UNDER OR AROUND MAGNET	PERSONNEL CRUSHED	PERSONNEL INJURIES BY WEIGHT OF MAGNET	3	L	MONITOR FABRICATION AND TRANSPORT OF MAGNET
21	TOXIC OR NOXIOUS FUMES	OPERATION	HEAT ON POLYURETHANE BLADDER PRODUCES FUMES	TOXIC AND NOXIOUS FUMES	PERSONNEL PRESENT	PERSONNEL EXPOSED TO TOXIC ATMOSPHERE	INJURY BY INHALATION OF FUMES	2	L	PROVIDE ADEQUATE VENTING OR CONTAINMENT (NOTE: THIS IS NOT A CONCERN FOR EBT-P)
22	NOISE	OPERATION	PUMPS MAKES NOISE	EXCESSIVE NOISE IN WORK ENVIRONMENT	PERSONNEL PRESENT IN HIGH NOISE AREA	HEARING IMPAIRED	HEARING IMPAIRED	2	H	LOCATED PUMPS AWAY FROM PERSONNEL AREAS, PROVIDE ADEQUATE SOUND ATTENUATION

APPENDIX H

MAGNET DEVELOPMENT PROGRAM

APPENDIX

By acceptance of this article, the publisher or recipient acknowledges the U.S. Government's right to retain a nonexclusive, royalty-free license in and to any copyright covering the article.

DESIGN AND CONSTRUCTION OF THE EBT-P DEVELOPMENT COILS*

J. K. Ballou, T. J. McManamy, R. L. Brown, W. H. Gray, and M. S. Lubell
Oak Ridge National Laboratory
P. O. Box Y, Oak Ridge, Tennessee 37830

Summary

The ELMO Bumpy Torus Proof-of-Principle (EBT-P) plasma physics device is a large mirror fusion machine scheduled to begin operation in 1985. It will have 36 superconducting mirror magnets arranged in a bumpy torus on a 4.5-m radius. Presented here are several of the design parameters and the supporting design/analysis that have not been published until now due to contractural arrangements between ORNL and the EBT-P subcontractors.

Introduction

Historical Perspective

The EBT-P magnet development program[1,2] began in May 1979 to support the construction schedule by taking advantage of the time between the start of the EBT-P program and the selection of the industrial subcontractors to perform some of the magnet development work. Briefly stated, the basic plan was for the Oak Ridge National Laboratory (ORNL) to design, build, and test two full-sized development magnets (D1 and D2) and transfer the technical information obtained during the development work to the industrial manufacturer in charge of magnet construction. The magnet manufacturer would then wind a prototype magnet, with basically the same design parameters, which would be tested in a three-magnet array simulating the magnetic conditions of EBT-P.

The EBT-P magnet design parameters were agreed upon during Phase I of the EBT-P project by ORNL Fusion Energy Division (FED) staff members, Department of Energy - Office of Fusion Energy (DOE-OFE) staff members, and the four competing industrial teams during a series of meetings in the Fall of 1979. Naturally, the chosen parameters were the result of a series of compromises among several factors; the most significant were: (1) EBT physics constraints, (2) EBT-P performance goals, (3) acceptable risk levels, and (4) projections of available funding.

Present Status

To date ORNL has fabricated and successfully tested magnets D1 and D2. (For the details of the tests see Ref. 3 which is a companion paper to this one and also located in the proceedings of this conference.) Oak Ridge National Laboratory is presently transferring the technical information gleaned from the magnet development work to General Dynamics Convair Division (the industrial manufacturer in charge of magnet construction for EBT-P). The remainder of this report presents some of the more interesting aspects of and novel ideas for the ORNL EBT-P development magnets.

*Research sponsored by the Office of Fusion Energy, U.S. Department of Energy, under contract W-7405-eng-26 with the Union Carbide Corporation.

EBT-P Design Parameters

The 36 mirror magnets are solenoids wound in a U-shaped winding cavity. The winding pack has a length of 21.1 cm with inner and outer radii of 24 and 34 cm, respectively. A schematic of the winding design, to be discussed, is shown in Fig. 1. The peak magnetic field at the windings with the magnets assembled as a bumpy torus will be 7.4 T. This magnetic field is achieved with an average current density over the winding pack of 10,000 A/cm^2.

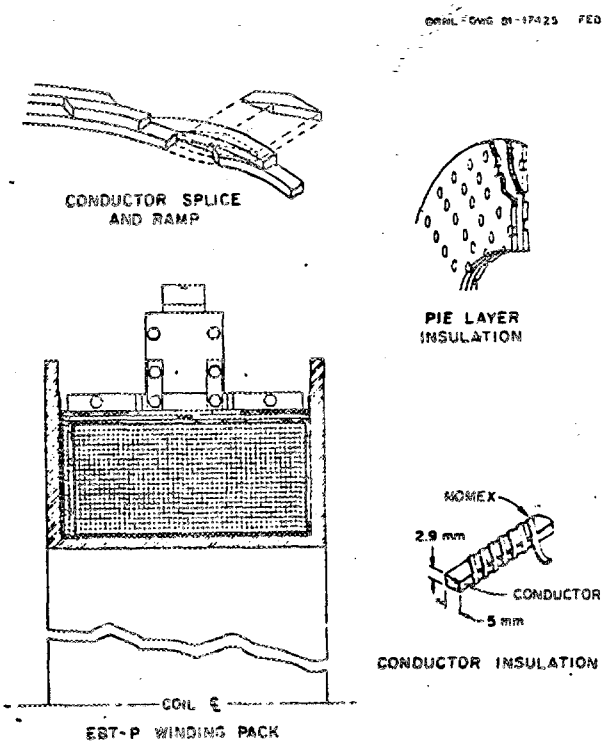

Fig. 1 Schematic of the EBT-P development coil design.

The conductor is a 2.9 x 5.0 mm compacted monolith[4] of copper and NbTi. The measured critical currents are 3600 A at 7.5 T for the high field conductor and 4300 A at 6 T and 3020 A at 7.5 T for the low field conductor.[3] Magnet D1 is wound with both conductor grades; D2 is wound with only the low field conductor, due to other concerns. The high field conductor was delivered with a 71% copper fraction, and the low field conductor was delivered with a 76% copper fraction. The expected operating current for the magnets is about 1700 A for 7.4 T at the windings when operated in the full EBT-P torus. When tested separately, these magnets require about 6% more current for 7.4 T to make up for the effect of the other magnets in the torus. The total stored energy in the magnet is about 1.5 MJ.

Of course, these magnets cannot be cryostable at these fields and average current densities, but as stable a design as possible was chosen. Dresner[2] indicates that a conductor with a copper fraction of about 75% and an operating current to critical current ratio of about 50-60% for a pool-boiling cooled magnet is the optimum for this configuration. Pool boiling was chosen because of high expected x-ray heat load on the magnet's windings. Nomex* lacing tape (applied in a spiral wrap with 50% converage) was chosen as an insulation because of our previous experience with this material and because it is easy to use.

EBT-P Development Magnet Construction

The bobbin and closure ring for the first and second development magnets (D1 and D2) were fabricated from 304L stainless steel. A U-shaped bobbin was chosen to minimize the required spatial envelope and to provide an accurately machined winding cavity. The ground wall insulation consisted of a single 0.94-mm thickness of solid G-10 next to the bobbin and a 1.2-mm-thick perforated G-10 sheet next to the windings. This sheet was perforated to allow for improved helium circulation. The corners were insulated with Mylar* tape.

A layer winding scheme was not used because of the magnetic field error that would have been created by the distance that separated the leads, and a pancake winding was avoided because of the number of splices that would have been required. A hybrid scheme was developed for the winding. With this scheme, a single pie or one-half pancake was wound on one side, and the remainder of the coil was layer wound, thus permitting both leads to come out close together near the middle of the last layer. Besides minimizing the magnet field error due to current leads, this scheme also had the advantages of (1) not requiring any splices if the conductor was long enough and (2) not requiring any connection to or penetration of the steel bobbin. The conductor was wound with 800 N of tension, and strain gauges on the bobbin bore were used to monitor the prestress added by each layer.[5] A justification for the stated superconductor pretension is presented in the next section. A special device spiral-wrapped Nomex insulation onto the rectangular superconductor during winding and was geared to give 50% coverage. The sequence of steps used to produce the hybrid winding is shown in Fig. 2 and is given below:

(1) Mount both bobbin (B) and superconductor (SC) which is on spool #1 onto winding machine (WM). Attach leader (1) and route through tensioner (T). Start leader on spare spool #2 (S2).
(2) Pull a pancake (PC) and one-half layer length of superconductor through tensioner and wind on spare spool #2.
(3) Form crossover of the superconductor and firmly attach to bobbin. Apply tension to superconductor and wind pancake and extra conductor.
(4) Remove superconducting spool #1 with the remaining superconductor from winding machine without cutting the superconductor.
(5) Temporarily, wind entire length of superconductor on bobbin. Attach leader to superconductor and route through tensioner to spare spool #2. Remove spool #1.
(6) Wind all of the remaining superconductor on spool #2.

*Reference to a company or product name does not imply approval or recommendation of the product by Union Carbide Corp. or the U.S. Department of Energy to the exclusion of others that may be suitable.

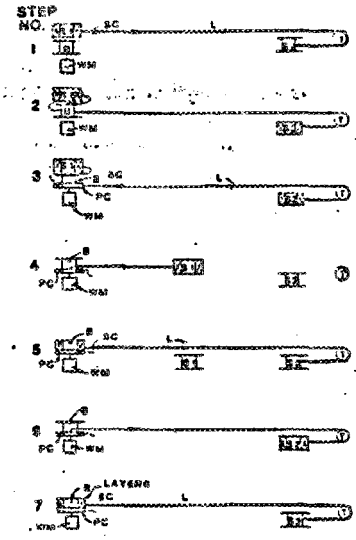

Fig. 2 Winding sequence to produce the EBT-P development coils.

(7) Apply tension and wind superconducting layers on bobbin. The last layer would be an even numbered layer. Wind layer to the middle and band.
(8) Unwind the excess conductor from the pancake and then rewind on the last layer to bring the leads together on the center.

The spiral wrap and tension machine required one end of the lead to be threaded through them. A number of the above steps, such as (5) and (6), could be eliminated with an advanced design that allowed conductor to be inserted from the side with the ends on different spools.

As shown in Fig. 1, insulation is required between the pancake and layer-wound section and between the last and next-to-last layers. The insulation design provided a safety factor greater than 2 (including the effects of voltage enhancement at the corners) while allowing for free helium circulation.[6]

Polycarbonate double wedge shaped pieces were used to form joggles and to provide a ramp-up from one layer to the next. Experience has shown the joggles to be easier to wind than a pure helical winding for this size coil.

Splices were required on the first and second coil because the conductor length on a single spool was insufficient for a complete coil. Also, the first coil used two grades of conductor requiring a splice at the end of the high field region. Three potential solders were evaluated experimentally: (a) 50 Sn, 50 Pb; (b) 97.5 Pb, 2.5 Ag; (c) 97.5 Pb, 1.5 Ag, 1 Sn. Pull tests on soldered conductor samples were accomplished at room temperature, 80 K, and 4.2 K. Both high lead solders (b and c) were significantly stronger at 4.2 K than the 50-50 solder (a). Solder (b) was slightly stronger than (c) and was selected for the high field grade splice. Our results were consistent with the findings given in Ref. 7. A typical splice and ramp is shown in Fig. 1.

Since this magnet is wound in a U-shaped bobbin, special care was required to ensure a tight winding pack in the axial direction. Special, angled face micarta blocks were fabricated for use while winding. The windings were axially compressed by hammering on

these blocks. During winding, the spread of the side flanges was measured to determine the effectiveness of this technique.

Copper lead blocks and G-10 pieces were fabricated to allow the layer side and pancake side leads to pull against each other without connection to the bobbin (see Fig. 3).

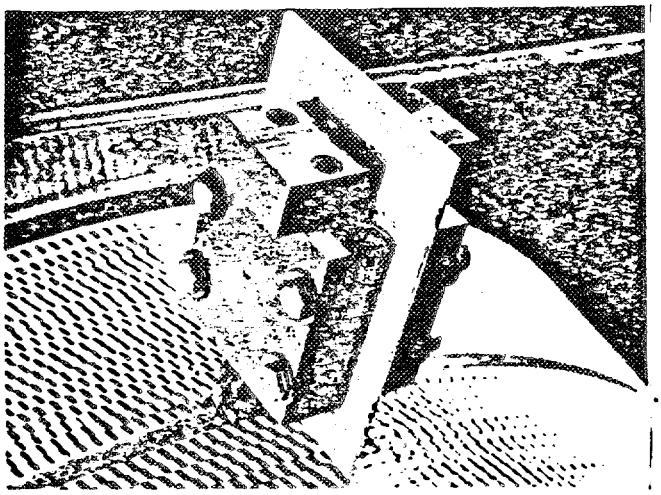

Fig. 3 Photograph showing the lead blocks, the last layer of the coil, and the insulation between the two coil parts.

The last layer and G-10 sidewall insulation is 19 mm below the radius at which the closure ring will be welded to the side walls of the bobbin. With this separation, the peak insulation and conductor temperatures can be kept below approximately 120°C during the welding operation, which General Dynamics Convair Division will perform.

EBT-P Winding Pack Stress Analysis

In this section an application of solenoid stress analysis with gaps is shown as it predicts the radial and tangential stress distributions in the winding pack of the EBT-P development magnets. Due to several external design constraints, chiefly high magnetic field (7.4 T) and conductor current density (11,725 A/cm^2) requirements and small dimensional limitations for bobbin thickness (0.96 cm), a satisfactory design could not be achieved that maintained a compressive interface pressure between the inner turns of the superconducting windings and the outer bobbin surface. Applying more winding preload to overcome this deficiency would have exceeded the room-temperature design-allowable compressive yield stress of the bobbin. (The design-allowable yield stress was chosen to be two-thirds of the material yield stress.) A simple linear calculation was not sufficient to predict the state of stress in the superconductor when the magnet is fully energized (see Fig. 4) since a tensile radial stress exists at the bobbin-insulation-superconductor interface of this well-ventilated magnet design. A nonlinear theory described in Ref. 8 was used to predict the stress state in the superconductor when the magnet is fully energized (as shown in Fig. 5).

Notice that the tangential force which was fictitiously permitted to accumulate in the bobbin with the linear calculation is redistributed mainly over the

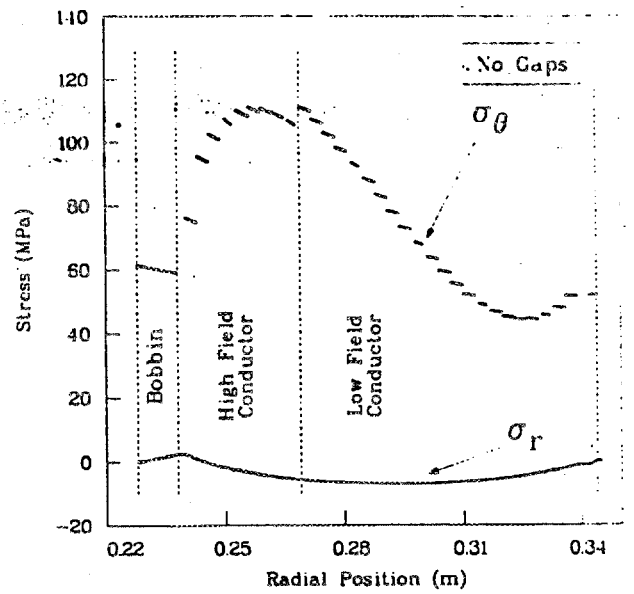

Fig. 4 The radial and tangential stress distribution at design field for the EBT-P prototype magnet, assuming no gaps can develop within the windings. The superconductor is graded in this magnet. There are 9 layers in the high field region and 23 layers in the low field region.

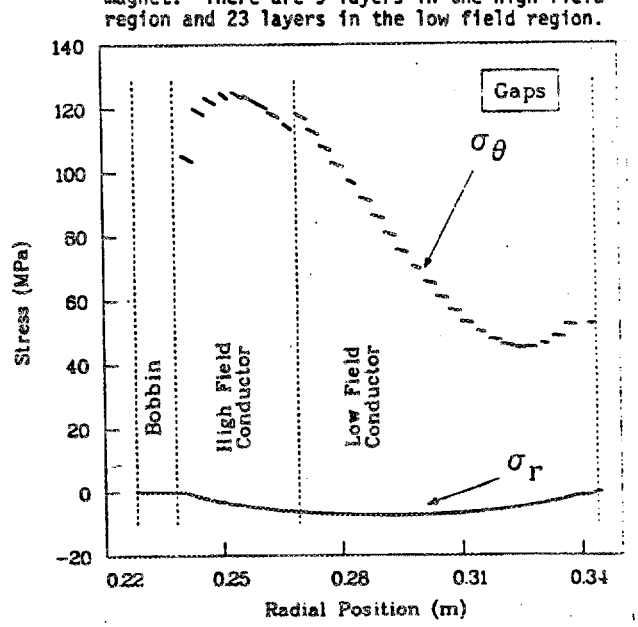

Fig. 5 The stress distribution at design field for the EBT-P prototype magnet, assuming gaps can develop within the windings.

first few turns of the superconductor with the nonlinear calculation. The calculated current for lift off of the winding from the bobbin is approximately 10% higher than that experimentally measured for a virgin energization after cooldown. Subsequent energizations without warmup produce decreasing changes in strain at lift off, thus indicating more complex mechanical behavior within the magnet's winding pack. An analytical method to predict this behavior is being developed.

EBT-P Magnet Case Stress Analysis

The EBT-P magnet case is 19 mm thick on each piece except for the inner bobbin, which has a 9.5-mm thickness. An axisymmetric finite-element model using PAFEC[9] was developed using approximately 500 four-node quadrilaterial elements to model the behavior of the EBT-P magnet case. The material properties of the model were uniformly chosen to be that of stainless steel (200 GPa). No attempt was made to take into account the conductor stiffness; only the coil case itself was modeled - a conservative and generally accepted engineering practice in magnet design/analysis.

This model simulates the cold mass support system by artifically restraining the center-outside-top node of the outer ring against movement in the axial direction. No restraint was supplied in the radial direction.

Three load cases were defined. The first two were defined as a 1.6-MPa side pressure load (due to a hypothetical fault condition) and a 6.8-MPa inner bobbin pressure load (attained from STANSOL calculations early in the conceptual design phase). The third loading case was chosen to be a 1.4-MPa uniform internal pressure acting upon the four inner surfaces of the coil case - thus simulating a quench multiplied by a factor of 4 (since there is some error involved in accurately calculating this number).

Linear superposition of the three loading cases combines all the loads that we have assumed to occur during a worst case fault condition. The combined loading case is dominated by loading case two and is shown in Fig. 6. The deflections have been greatly exaggerated so that they could be visually interpreted on this plot. Also, the contours represent areas of progressively larger von Mises stress. This model predicts that design allowable stress (two/thirds of the yield stress) will not be exceeded even with the conservatively magnified loads.

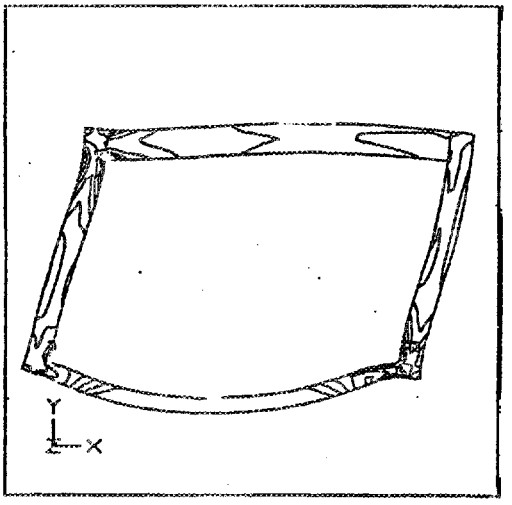

Fig. 6 The predicted von Mises stress contour distribution for the combined loading case design condition. On this plot the deflections have been greatly exaggerated so that they could be visually interpreted.

Summary

Both development coils have been tested in a large general purpose laboratory Dewar. Each coil met or exceeded design specifications. The tests and results will be presented in another paper in this conference.

References

1. J. K. Ballou, T. J. McManamy, W. H. Power, and H. T. Yeh, Proc. 8th Symp. Engineering Problems of Fusion Research, Vol. 2, p. 755 (1979).

2. EBT-P Proposed Reference Design Report, Oak Ridge National Laboratory ORNL/TM-7191 (January 1980).

3. J. R. Miller et al., these proceedings.

4. S. O. Hong, E. Adam, E. Gregory, D. Koop, and W. Maroncik, IEEE Trans. Magn. MAG-17, 916 (1981).

5. W. H. Gray, T. J. McManamy, J. K. Ballou, and R. L. Brown, "A Comparison Between Experimental and Analytical Winding Prestrain for a Circular Solenoid," these proceedings.

6. S. W. Schwenterly, Oak Ridge National Laboratory, private communication.

7. P. M. Rackov and C. D. Henning, "Superconductor Joining Methods for Large CTR Magnets," 6th Symp. on Engineering Problems of Fusion Research (1975).

8. W. H. Gray, "Stress Analysis of Solenoids that Develop Gaps," Proc. COMPUMAG - Chicago (to be published).

9. J. E. Akin, B. R. Dewey, and R. D. Henshell, "PAFEC - Programs for Automatic Finite Element Calculations," Structural Mechanics Software Series, University of Virginia Press, Vol. 3 (1979).

By acceptance of this article, the publisher or recipient acknowledges the U.S. Government's right to retain a nonexclusive, royalty-free license in and to any copyright covering the article.

TESTS OF THE FIRST DEVELOPMENT COILS FOR EBT-P*

J. R. Miller, J. W. Lue, and S. S. Shen
Oak Ridge National Laboratory
Oak Ridge, Tennessee 37830

Summary

Two superconducting coils have been built and tested as part of a development program aimed at proving the technology for production of a 36-coil toroidal set for the Elmo Bumpy Torus Proof-of-Princple (EBT-P) machine. Both coils have demonstrated the capability of being charged reliably and rapidly to maximum fields in excess of 7.4 T. The capability for essentially continuous operation with simulated x-ray heat loads in excess of 10 W has also been demonstrated in both coils.

Introduction

The EBT-P machine will use 36 superconducting solenoids in a toroidal array for plasma containment. The plasma will be heated with a high power microwave source presently under development. Initially, this source will be operated at 60 GHz, which requires the magnet coils to be operated at a level corresponding to a maximum field in the windings of 5 T. It is planned to extend the operation of the microwave source to 90 GHz as a second phase of machine operation. The coils will then be required to operate with 7.4-T maximum field in the windings.

The coils in an EBT machine see essentially steady magnetic fields in contrast to the environment of tokamak coils. However, they generally can be expected to have significant steady heat loads deposited directly into the windings by x-radiation. The total heat load is expected to be as high as 10 W in EBT-P. The requirement for operation with steady heat load directly in the windings gives an advantage to a ventilated coil design over a potted design. Two nearly identical coils of ventilated design have been built to demonstrate both practical coil fabrication techniques and applicable NbTi conductor technology.

Coil and Conductor Specifications

The two development coils (referred to here as D1 and D2) were wound with rectangular, copper-stabilized, NbTi superconductor of the compacted bundle type developed by Airco Superconductors.[1] Two grades of conductor (high field and low field) were used in D1, and a single grade was used in D2. Important features of these conductors are listed in Table 1.

A ventilated winding was achieved by applying a "barber pole" wrap of Nomex† braid with approximately 50% coverage to the conductors as they were being wound into the coils. Each coil was for the most part layer wound but had a single "pancake" portion at one end as a convenience for bringing out the "start" end of the conductor with minimal disturbance to the solenoidal field. Details of coil construction are given elsewhere.[2] The similarity of the coils is evident from the brief list of parameters in Table 2.

Test Objectives and Procedures

There were two major objectives for the tests of the development coils: (1) to demonstrate reliable operation at the "60-GHz" and "90-GHz" levels (5-T and 7.4-T maximum field at the windings, respectively) and (2) to examine performance under a simulated x-ray heat load. Additionally, it was desired to determine whether training was required to reach the performance goals, to provide assurance that degradation was not experienced during normal operation, to verify that the coils could be charged at a convenient rate, and to document quench and dump characteristics in order to aid in the design of production coil and dewar assemblies.

The initial tests were performed in a large "bucket" dewar with the coil axis horizontal. These tests have been referred to as "open dewar" tests in contrast to planned future tests that will utilize the integral dewar assemblies like those for production coils that conform closely to the windings. In the range of 500 to 600 liters of liquid helium surrounded the coil during an open dewar test.

The coils themselves were sparsely instrumented for the tests. Only a pair of voltage taps at the coil terminals was directly connected to the windings. The relatively high operating current density and the desire not to occlude helium passages influenced the decision not to allow instrument leads inside the winding pack. However, the coil bobbin, the test dewar, helium recovery lines, and magnet current delivery leads were well instrumented.

Strain gages on the bore of the bobbin provided some information about the stress state in the windings. CLTS's† on the bobbin, cryostat parts, and coil terminals and busses provided cooldown information and helped verify proper operation. A pressure transducer in the dewar was used to provide transient data during quenches. Carbon resistance thermometers at two levels in the bath verified equilibrium helium conditions in the dewar before testing. Hall probes mounted on the midplane of each coil, at the center and at 223-mm radius, checked performance against calculation. Continuous monitoring of helium consumption was accomplished by level detectors in the bath and by manifolding all helium recovery lines through a single external mass-flow meter.

The basic test procedure was intended to consist simply of ramping the coil to a current corresponding 7.4-T maximum field to verify achievement of that performance goal and then using a fast-response, 300-V, 2000-A bipolar power supply to superimpose a 0.5-Hz ac ripple current at various dc levels sufficient to

*Research sponsored by the Office of Fusion Energy, U.S. Department of Energy, under contract W-7405-eng-26 with the Union Carbide Corporation.

†A DuPont trade name for an aramid fiber insulating material. Reference to a company or product name does not imply approval or recommendation of the product by Union Carbide Corporation or the U.S. Department of Energy to the exclusion of others that may be suitable.

†A Micro-Measurements designation for a strain-gage type temperature sensor. Reference to a company or product name does not imply approval or recommendation of the product by Union Carbide Corporation or the U.S. Department of Energy to the exclusion of others that may be suitable.

Table 1. Conductor description

	D1		D2
	High Field	Low Field	
Conductor type	(compacted bundle, Nb-46.5 wt.%Ti/Cu composite)		
Number of filaments	37 x 529	9 x 517	9 x 517
Conductor cross section (mm^2)	5.0 x 2.9	5.0 x 2.9	5.0 x 2.9
Cu:SC ratio	2.5:1	3.2:1	3.1:1
R_{300}/R_{10}	110	194	—
I_c^* at 7.5 T (A)	3720	2835	3020
I_c^* at 6.0 T (A)	—	4330	4290
Length used (m)	625	1642	2297

*At 10^{-12} Ωcm effective resistivity.

Table 2. Brief coil description

	D1	D2
Winding type	"Layer-cake"	"Layer-cake"
Winding OD (m)	0.694	0.696
Winding ID (m)	0.480	0.480
Winding height (m)	0.211	0.212
Number of turns	1225	1240

produce total heat loads at least as great as 10 W. The heat load from ac losses produced by the ripple was judged to be an adequate simulation of an x-ray heat load, both in distribution and effect. Actual heat load was measured using an on-line computer to calculate losses from compensated voltage and current signals. Figure 1 shows typical digitally stored and processed data. Losses are extracted from the data both by integrating and averaging the ripple current-voltage product and by converting to a magnetization vs field curve which can be integrated to give the loss per cycle. It is not necessary to do the computer integrations for each test level since (as Fig. 2 clearly demonstrates) losses for particular coil operating conditions scale directly as the square of the ripple current amplitude. Because of various equipment problems, several variations and repetitions of the basic procedure were actually carried out.

Results

In terms of the objectives of the test program, the results are simple and satisfying. The coils were shown to be capable of being charged rapidly and reliably to over 7.4-T maximum field without any problems directly related to the coil. Table 3 lists several of the coil operating characteristics. Coil D1 was charged to this level at 32 $A \cdot s^{-1}$ and D2 at 25 $A \cdot s^{-1}$ without quenching, although D2 did quench at this rate as the charge was continued to 7.7 T. Both coils eventually were shown to be capable of essentially continuous operation with a steady direct heat load in excess of 10 W at fields up to 7.4 T. In some instances heat was applied for over 20 min, but usually 1 min was considered a sufficient test steady heat load performance goal the first time it was tested and D2 did not. However, we do not believe that this indicates a difference in the coils. Rather, we believe it is a manifestation of the differences in the actual test procedure.

Figures 3, 4, and 5 give the chronology of all cases for both coils where coil current was ramped to a significant level. The vertical axis in each

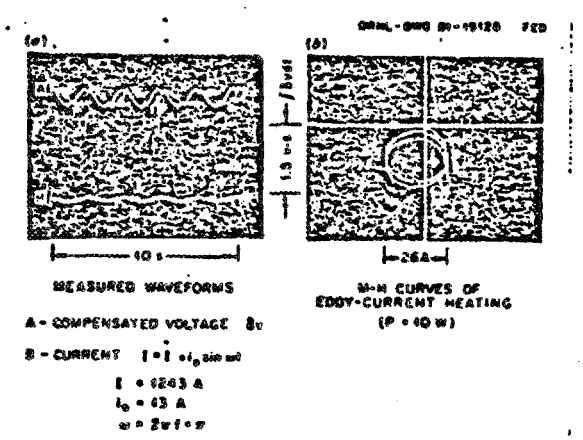

Fig. 1. Display of digitally stored data from a typical steady heating test.

Table 3. Coil operating characteristics

	D1	D2
B_0/I (T/A)	2.506×10^{-3}* $2.51 \pm 0.01 \times 10^{-3}$†	2.528×10^{-3}* $2.53 \pm 0.01 \times 10^{-3}$†
B_{max}/I (T/A)	4.072×10^{-3}* 4.05 ± 0.02†	4.075×10^{-3}* $4.06 \pm 0.02 \times 10^{-3}$†
Inductance (H)	0.86 ± 0.01†	0.88 ± 0.01†
Stored Energy (MJ) (at I = 1850 A)	1.47†	1.51†
B_{max} (T) (at I = 1850 A)	7.53*	7.56*
I/I_c (at I = 1850 A)	0.50†	0.51†
$J_{overall}$ (A/mm²) (at I = 1850 A)	100.4*	100.2*

*Calculated from details of winding configuration.

†Direct or indirect measurement.

indicates coil current, while the horizontal axis merely indicates sequence of events. No time scale is implied. A solid slanting line indicates that the particular coil was ramped steadily up or down in a controlled fashion to some level. When a number appears alongside a slanted line it indicates ramp rate. A solid horizontal line means that coil current was held at the indicated level while an ac ripple was superimposed to produce heating. The number above a

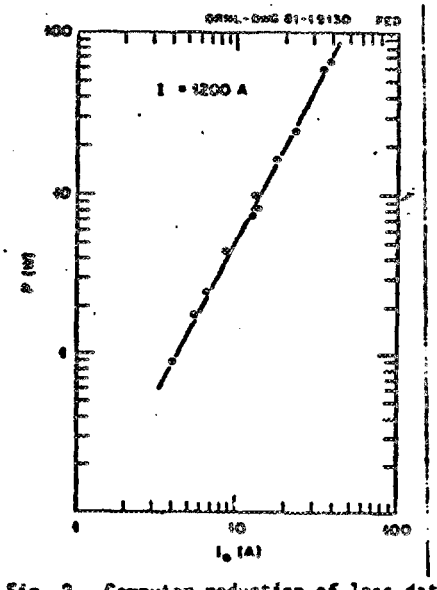

Fig. 2. Computer reduction of loss data showing heating power P varying as the square of the ripple current amplitude i_0.

horizontal line gives maximum heat load during that event. A broken vertical line means that the coil was either quenched and was dumped or just dumped. However, it was observed from boil-off records that every dump resulted in a quench so that for most considerations the two events are the same. A number alongside a vertical line counts the quench or dump number. A separation between events on the sequence axis indicates that these tests were not done on the same day. Events on each chronology chart were done during the same cooldown. Temperature was usually maintained at 4.2 K, but never exceeded 77 K.

Note that the first time the performance of D1 against steady heating was tested, it had already been ramped to high currents and quenched or dumped several times. The first test of D2 against steady heating was done after one charge in excess of 1800 A and no hard quenches. Modest performance was observed in D2 after three moderate quenches.

Since quenches sometimes occurred after tens of seconds at a particular ripple amplitude, it seemed more reasonable that an effect involving helium replenishment or bubble clearing was responsible. Quenches caused by conductor motion would have been sudden and would presumably have occurred the first time a given current level was attained. Strain gages on the bobbin indicated that windings lifted off the bobbin, thus relieving prestress, as the coil was charged. After a charge to 1800 A and discharge, prestress was not returned to the bobbin. Figure 6 is a typical strain gage record. This might be explained in terms of "bedding in" of the winding pack that prevented complete return of the windings to the bobbin. After the first charge and discharge, the amount of prestress relieved did not change significantly; i.e., during subsequent ramps the bobbin strain followed a trace essentially like the upper leg of Fig. 6. However, it seems that good performance against steady heating was achieved only after several

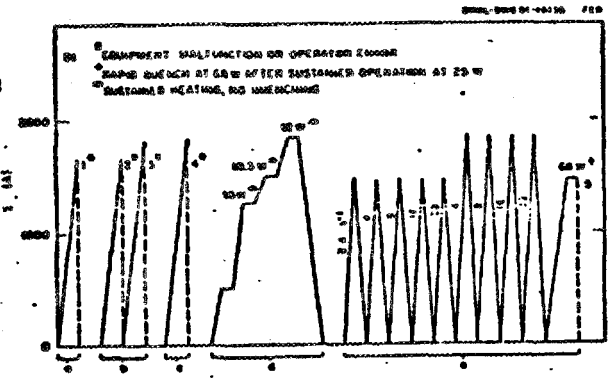

Fig. 3. Chronology of the test of the first development coil, D1.

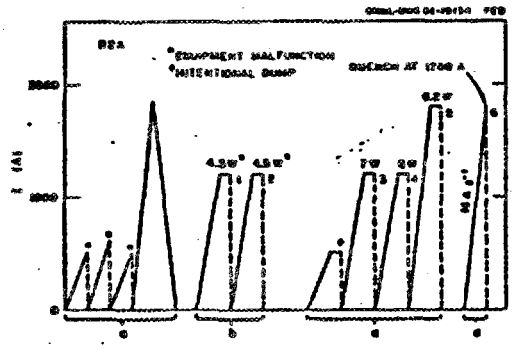

Fig. 4. Chronology of the first test of the second development coil, D2.

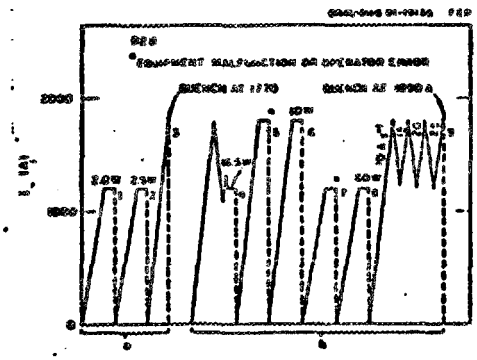

Fig. 5. Chronology of the second test of the second development coil, D2. The coil was warmed to room temperature and the dewar evacuated before cooldown for this test.

hard quenches preceded a test. Figure 5 shows that during the second cooldown and test of D2, 60 W at the 5-T level was required to produce a quench after seven quenches had preceded. On the first test at 5 T in this series with no preceding quenches (or ramps to 1800 A), only 2 W was required.

Conclusions

Two nearly identical development coils for EBT-P have been built and tested. It has been demonstrated that they can be charged rapidly and reliably to

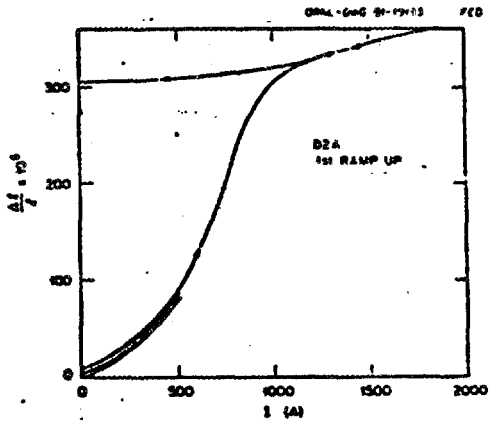

Fig. 6. A typical record of a strain gage attached to the inside of the coil bobbin at the midplane during the initial charge. Subsequent charges essentially repeated the upper leg of the trace.

maximum fields greater than 7.5 T with no apparent training. No degradation of this capability was observed after many cycles to the same level. Both coils were shown to be capable of withstanding steady heat loads greater than 10 W total. However, cooldown, charging, and quench history may have a pronounced effect on this aspect of performance.

Acknowledgments

The authors would like to thank R. C. Dixon, C. W. Proctor, D. L. James, and H. R. DeArmond for their assistance in construction, instrumentation, and installation of the test coils and J. P. Rudd and W. J. Kenney for assistance in running the tests. We also thank J. K. Ballou and T. J. McManamy for helpful discussions in interpreting results.

References

1. S. O. Hong, E. Adam, E. Gregory, D. Koop, and W. Marancik, IEEE Trans. Magn. MAG-17, 916 (1981).

2. J. K. Ballou, et al., paper 3A-08, these proceedings.

By acceptance of this article, the publisher or recipient acknowledges the U.S. Government's right to retain a nonexclusive, royalty-free license in and to any copyright covering the article.

NEW DEVELOPMENTS IN PROGRAM STANSOL VERSION 3*

W. H. Grey
Fusion Energy Division
Oak Ridge National Laboratory
Oak Ridge, TN 37830

STANSOL is a computer program that applies a solution for the mechanical displacement, stress, and strain in rotationally-transversely isotropic, homogeneous, axisymmetric solenoids. Careful application of the solution permits the complex mechanical behavior of multilayered, nonhomogeneous solenoids to be examined. Loads applied to the solenoid model by program STANSOL may consist of differential temperature, winding preload, internal and/or external surface pressure, and electromagnetic Lorentz body forces and may vary arbitrarily from layer to layer. STANSOL version 3, the latest update to the original version of the computer program, also permits structural analysis of solenoid magnets in which frictionless interlayer gaps may open or close. This paper presents the new theory coded into version 3 of the STANSOL program, as well as the new input data format and graphical output display of the resulting analysis.

Introduction

Program STANSOL[1,2] (Structural Analysis of Solenoids) was the first computer program that integrated the mechanical behavior of axisymmetric solenoid magnets due to winding prestress, internal and/or external surface pressure, thermal contraction and/or expansion, and electromechanical Lorentz body force. Based upon the theory derived in Ref. 3 for an axisymmetric, plane-stress solenoid magnet with rotationally-transversely isotropic material properties, program STANSOL has been used to perform stress analyses upon several successful superconducting and normal magnets designed and built at the Oak Ridge National Laboratory (ORNL). Two recent solenoid magnets that were partially designed with the information from a STANSOL analysis were CWTX[4] and EBT-P.[5] Copies of program STANSOL have been distributed free-of-charge to nearly every Department of Energy (DOE) laboratory, to seven private industrial corporations, and to eleven universities.

Presented here are the most significant additions that have been programmed into STANSOL to change it from version 2 to version 3. Four major changes have occurred between version 2 and 3: (1) all input data is accepted in free-format; (2) a summary of the extremum of the stress and strain is printed out; (3) a computer graphics capability has been added so that plots of the mechanical displacement, stress, and strain are drawn; and (4) the solution algorithm can develop frictionless gaps that may open or close during magnet cooldown (warmup) and energization.[6] The following sections discuss each of these four modifications individually.

Free-Format Input Data

Originally, program STANSOL was coded to accept input data on card images based upon input fields that were eight characters wide. (This scheme was a holdover from input to COSMIC/NASTRAN.) STANSOL version 3 now accepts input card images in free-format, an option available with most higher level FORTRAN run-time operating systems. Briefly described in the Appendix are the ten types of input card images program STANSOL version 3 understands. Card images that contain more than one data variable per image must separate the variables by a comma and/or a space. With the exception of card type 4 there is no restriction placed upon where the variable data must be located upon a card image, as long as the data is present in the order the variables are listed for a specific card type in the Appendix. Standard FORTRAN variable declarations are used throughout; i.e., variable names that begin with the letter I through N, inclusive, are automatically defined as integers. All other variables are defined as real or double precision.

Output Extremum Summary

Originally, program STANSOL presented the results of a solenoid stress analysis as a voluminous numerical tabulation of the mechanical displacement, stress, and strain for each layer of the solenoid under consideration. With version 3 of program STANSOL, this output data is still available as it is printed out on a data channel for future examination; however, two more concise methods are available to inspect the results of an analysis. The best method is graphical examination — the subject of the next section of this paper. The quickest method is to examine the output extremum table that is typed out on the user's terminal.

The output extremum summary individually lists maximum and minimum stress and strain for each material type in the solenoid. Rapid evaluations of the overall stress analysis are possible from the quick examination of the extremum summary. Parametric studies benefit enormously from this output data.

Output Data Representation Using Computer Graphics

To replace having to digest the printout of program STANSOL, a computer graphics capability has been developed for examining the results of an analysis. A subroutine was added to program STANSOL to plot the mechanical displacement, stress, and strain directly on the screen on a user's Tektronix terminal (or any compatible equipment) using standard Tektronix software. Figures 1 and 2 are representative example plots produced by version 3 of program STANSOL.

The general problem and case description are plotted as page titles for future output identification as well as the date and time of program execution. The units used to represent the data are drawn as annotation to the x- and y-axis labels. The title of the plot is indicative of the type of load that has been applied to produce the variable's distribution. Distinguishing symbols are used to differentiate between material types. To simplify the plotting subroutine, a straight line is drawn between the dependent variable values at the inner and outer radial locations for a given layer material, instead of drawing a smooth curve. This technique is generally sufficient since the distance within one layer is usually a small interval.

Another method of producing plots is available with the new version of program STANSOL. A special data file is created by the plotting subroutine that contains coordinates of the end points of the lines that represent the requested variable's distribution. This special data file is written in a format suitable for the MAPPER[7] program. By using a LOCATE MAPPER

*Research sponsored by the Office of Fusion Energy, U.S. Department of Energy, under contract W-7405-eng-26 with the Union Carbide Corporation.

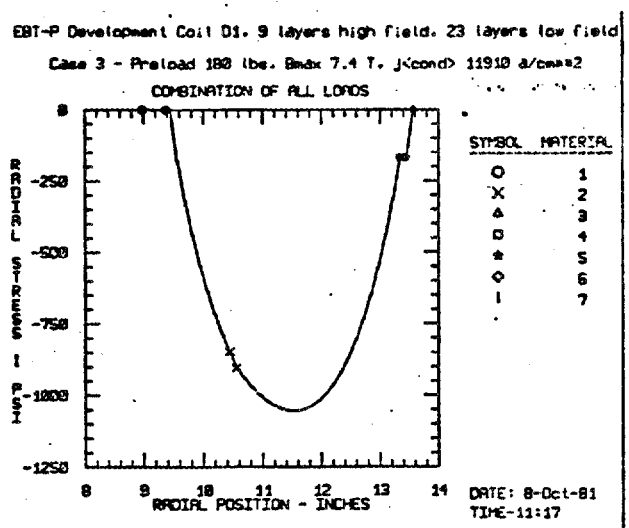

Fig. 1. A plot generated by version 3 of program STANSOL showing the predicted radial distribution throughout the EBT-P development coil D1.

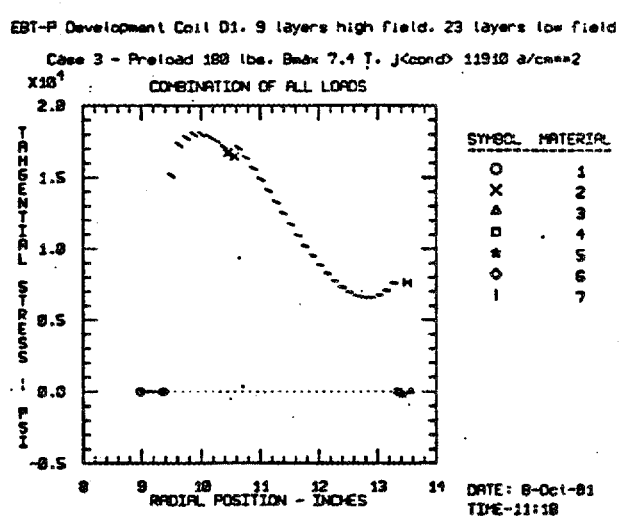

Fig. 2. A plot generated by version 3 of program STANSOL showing the predicted tangential distribution throughout the EBT-P development coil D1.

command and a few other easy to learn instructions, plots like Fig. 3 can be generated.

Frictionless Gap Solution Capability

By using the linear solution derived in Ref. 3 and incremental loading, a piecewise-continuous, nonlinear solution may be assembled for magnets in which frictionless gaps are permitted to open and close. By choosing load increments that correspond to incipient frictionless gap formation or termination, complex, geometrically nonlinear structural behavior can be mathematically modeled. Within each loading increment a linear solution is calculated for each continuous section of the solenoid. (In the limit there could be as many sections as there are layers since, in principle, there could be a gap between each layer.)

Each gap formation modifies the solution boundary conditions by introducing another interface where the radial stress (and, therefore, the interface pressure) must be zero. Each gap termination removes the corresponding gap-introduced radial stress boundary condition. The solution increment for each section is added to the current solution, and the magnet is redivided (or recombined) into sections based upon the new gap definition. The next load increment is calculated, and the process is repeated until all the loads have been fully applied. Thus, because of this updating of the model's geometry, the solution becomes nonlinear even though within any solution increment a linear small displacement theory is used. This theory was programmed into version 3 of the STANSOL computer program using the mathematical steps presented in Ref. 6.

Conclusions

The latest updates to program STANSOL version 3 have been presented in this paper. Briefly summarized, these updates (1) permit more flexibility in input data formatting, (2) enhance the output capabilities of the program by using computer graphics and extremum

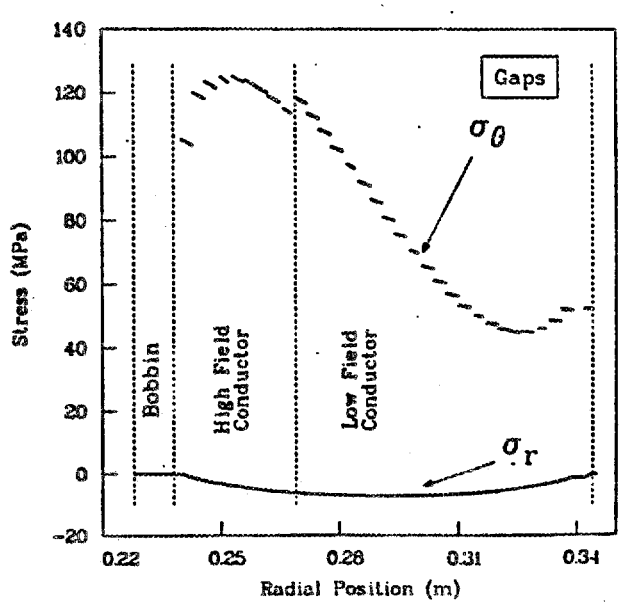

Fig. 3. A plot generated by MAPPER using data output from version 3 of program STANSOL showing the predicted radial and tangential stress distribution throughout the EBT-P development coil D1.

summaries, and (3) add an additional solution capability to calculate the mechanical behavior of solenoids if frictionless gaps develop.

References

1. N. E. Johnson, W. H. Gray, and R. A. Weed, in Proc. 6th Symp. on Engineering Problems of Fusion Research, Vol. 1, p. 243 (1975).
2. N. E. Johnson, Adv. Cryog. Eng. 22, 490 (1977).
3. W. H. Gray and J. K. Ballou, "Electromechanical Stress Analysis of Transversely Isotropic Solenoids," J. Appl. Phys. 48(7), 3100 (1977).
4. J. K. Ballou, R. L. Brown, W. A. Fietz, J. W. Forseman, W. H. Gray, W. J. Kenney, R. B. Wysor, W. D. Markiewicz, and R. G. Van Alstyne, "Design and Testing of a Dual 8-T 380-mm/12-T 220-mm Split Superconducting Solenoid for ORNL," IEEE Trans. Magn. MAG-17 (5), 2238 (1981).
5. J. K. Ballou, T. J. McManamy, R. L. Brown, W. H. Gray, and M. S. Lubell, "Design and Construction of an EBT-P Development Coil," these proceedings.
6. W. H. Gray, "Stress Analysis of Solenoids That can Develop Gaps," Proc. COMPUMAG-Chicago (to be published).
7. B. A. Clark, K. N. Fisher, D. A. Dahl, "MAPPER User's Manual," Computer Science Division, Oak Ridge National Laboratory, Oak Ridge, Tennessee (1979).

Appendix: Free-Format Input Data Summary for Version 3 of Program STANSOL

Card Type 1

DESC Eighty columns of alphanumeric characters are read and stored as a general problem description. This data is used as a major heading for all subsequent output during this execution of program STANSOL. The first input card image is used for this purpose.

Card Type 2

DESCA Eighty columns of alphanumeric characters are read and stored as the case description. This data is used as a minor heading for all subsequent output during this execution of program STANSOL. The second input card image is used for this purpose.

Card Type 3

COMMENT Any comments which the user desires to include as distinguishing remarks for future interpretation of his input and/or output data. There is no limit to the number of comment cards.

Card Type 4

CT The type 4 input data card is a comment terminator. The dollar sign ($) character typed in column 1 serves as a delimiter for comments and thus terminates comment input data cards.

Card Type 5

r_{in} The variable r_{in} is the inner radius of the assembled magnet in inches.

w_1 The variable w_1 is the assembled length in the axial direction of the magnet in inches.

p_{in} The variable p_{in} represents a surface pressure to be applied to the inner surface of the assembled magnet. The units of p_{in} are psi.

p_{out} The variable p_{out} represents a surface pressure to be applied to the outer surface of the assembled magnet. The units of p_{out} are psi.

DMULT This variable is no longer supported.

MODE This variable is no longer supported.

IPLTCN The variable IPLTCN controls the generation of computer graphic output. If IPLTCN is equal to zero, then computer graphics output is not generated. If IPLTCN is not equal to zero, then it is used to indicate which variable distribution is to be drawn.

Card Type 6

Since program STANSOL is a general purpose program that permits multilayered, nonhomogeneous solenoids to be mathematically modeled, a convenient method was derived to allow the multilayered design of a solenoid to be input to the program with a minimum of effort. As most solenoids have a repetitive design to their winding pack, the method chosen was based upon the concept of layer sets. A layer set is defined as a set of layers of materials that repeat themselves somewhere within the magnet. For example, consider a magnet with 50 radial turns of superconductor that is insulated turn-to-turn with a spiral wrap of insulation and further insulated layer-to-layer with a sheet of insulating material. Use material number 1 to represent the superconductor, number 2 to represent the turn-to-turn insulation, and number 3 to represent the sheet insulation, then the layer geometry may be described by the material number sequence 2,1,2,3 repeated 50 times. Program STANSOL simplifies the required amount of input data by reading a repeat count for the number of layer sets followed by the layer set material number definition. Obviously, if a nonrepetitive material, such as a bobbin, is to be input, then a repeat count of 1 followed by a single material number can be specified.

MNLSET The variable MNLSET is the number of material layer sets defined on this card. It is the repeat count for the following material number layer definition. Layer set one begins with the first layer and proceeds radially outward through the magnet.

$MN_1,\ldots,MN_8$ The variables MN_1 through MN_8 represent the material numbers for this layer set. Currently, there can be a maximum of 8 material numbers per layer set definition.

A blank card terminates card type 6 input data.

Card Type 7

Like the material layer sets defined and used on card type 6, the concept of a load layer set is used to simplify input data for the load definition. Usually, these data are an echo of the material layer set definition; however, there are special cases where the added flexibility of having a different load number from that of a material number for a given layer is required.

LNLSET The variable LNLSET is similar to MNLSET except it refers to the repeat count for the load layer sets defines on this card.

$LN_1,\ldots,LN_8$ The variables LN_1 through LN_8 represent the load numbers for this layer set. Currently, there can be a maximum of 8 load numbers per load layer set definition.

A blank card terminates card type 7 input data.

Card Type 8

Type 8 input data card images define the material properties for a particular material number. The material number is the pointer used on card type 6 to identify the magnet geometry by associating a layer material number with a group of material properties.

MN The variable MN is the material number to be associated with the following set for material properties. MN has a one-to-one correspondence with a material number input on card type 6.

TT The variable TT is the layer thickness in inches for material number MN.

WT The variable WT is the axial length of the magnet used to determine the winding preload for material number MN.

E_θ The variable E_θ is the Young's modulus in the tangential (or hoop) direction for material number MN. The units of E_θ are psi.

$\nu_{\theta r}$ The variable $\nu_{\theta r}$ is the major Poisson's ratio $(-\varepsilon_r/\varepsilon_\theta)$ for material number MN.

a_θ The variable a_θ is the thermal coefficient of contraction (expansion) in the tangential direction for material number MN. The units of a_θ are in/in/K. The material is assumed to be isotropic if the remainder of the data card is blank.

E_r The variable E_r is the Young's modulus in the radial direction for material number MN. The units of E_r are psi.

$\nu_{r\theta}$ The variable $\nu_{r\theta}$ is the minor Poisson's ratio $(-\varepsilon_\theta/\varepsilon_r)$ for material number MN. The reciprocal relationship will be used to define this variable if it is not defined on this data card.

a_r The variable a_r is the thermal coefficient of contraction (expansion) in the radial direction for material number MN. The units of a_r are in/in/K.

There must be one type 8 input data card for every layer material number defined on the type 6 input data cards. A blank card terminated type 8 input data.

Card Type 9

These input card images define the load types and magnitudes for a particular load number. The load number is the pointer used on card type 7 to identify the layers that are loaded.

LN The variable LN is the load number used on card type 7.

DENST The variable DENST is the current density in the units of A/cm^2 for load number LN.

PLDT The variable PLDT is the winding preload in units of lb_f/in of axial length for load number LN.

WPT The variable WPT is the axial length of the magnet used to determine the winding preload for load number LN. The units of WPT are inches.

TEMPT The variable TEMPT is the differential temperature to be applied to the layer for load number LN. The units of TEMPT are ^{0}C or K.

There must be one type 9 input data card for every layer load number defined on the type 7 input data cards. A blank card terminated type 9 input data.

Card Type 10

These input card images define the magnetic field distribution for the magnet. The magnetic field distribution is input as a table of points of radii versus magnetic field. The radii, magnetic field point pair must be input in order of sequentially increasing radii. The radii do not have to correspond to any physical location in the magnet as a table lookup is automatically performed for the user when the value of the magnetic field is needed at a particular radial coordinate. The units for the radii, magnetic field point data are inches and Tesla, respectively. A blank radii, magnetic field point pair terminates type 10 input data. There can be a maximum of four radii, magnetic field points per card type 10.

R_1, B_1 The variables R_1, B_1 represent the magnetic field B at the radial coordinate R.

•

•

R_4, B_4 The variables R_4, B_4 represent the magnetic field B at the radial coordinate R.

By acceptance of this article, the publisher or recipient acknowledges the U.S. Government's right to retain a nonexclusive, royalty-free license in and to any copyright covering the article.

ON MECHANICAL STRESSES IN SOLENOIDS CONSTRUCTED OF TRANSVERSELY ISOTROPIC MATERIALS*

W. H. Gray and W. D. Cain
Fusion Energy Division
Oak Ridge National Laboratory
Oak Ridge, TN 37830

Equations relating the mechanical stress, strain, and displacement of elastic, axisymmetric solenoid magnets to the solenoid's geometry, current density, magnetic field, and material properties have been derived by several authors. For the special case of rotational transverse isotropy, these equations are singular for certain values of the ratio of the orthotropic elastic moduli. This paper discusses the mathematical conditions for which a singularity of this type exists and presents a general solution to these equations at their singular points.

Introduction

In previous papers[1,2] solutions have been given for mechanical stresses and displacements in axisymmetric, plane-stress, rotationally transversely isotropic solenoids that can be multilayered and nonhomogeneous. These solutions consider loads due to winding prestress buildup, internal and external pressure, thermally induced contraction or expansion, and electromagnetically induced Lorentz body forces. This theory forms the basis for the STANSOL[3,4] computer program.

While performing a stress analysis with STANSOL some time ago, an anomalous behavior was observed when the ratio of orthotropic moduli for a particular material was four. At first, it was assumed that there was a bug in the coding of the STANSOL program. Upon further examination, it was determined that what was occuring was, in fact, a singular point exhibited by the equations as presented in Ref. 1. Presented here is a reformulation of the equations presented in Ref. 1 with special consideration to singular points that can occur in the general solution. The new equations are developed with the terminology expressed in Ref. 5, instead of Ref. 1, due to the succinctness of the nomenclature used in Ref. 5. (Also, by citing over 30 references, Ref. 5 contributes an excellent historical review of the development and gradually increasing sophistication of the analytical and numerical solutions for mechanical stresses and displacement in axisymmetric solenoids.)

A General Solution for the Mechanical Behavior of Rotationally Transversely Isotropic Solenoids Including Singular Points

The following equations apply to an axisymmetric, plane-stress, rotationally transversely isotropic solenoid that can be multilayered and nonhomogeneous. Assume that a solenoid can be modeled as a series of concentric, homogeneous circular rings. Then for the ith layer, the equilibrium equation in polar coordinates, assuming the presence of an electromagnetically induced Lorentz body force, is expressed as

$$\frac{\partial \sigma_{r,i}}{\partial r} + \frac{\sigma_{r,i} - \sigma_{\theta,i}}{r} = -J_i B_{z,i}(r) \qquad (1)$$

The kinematic relationships for the ith layer equate the strains to the displacement and for the purpose of this analysis, like those in Refs. 1, 2, and 5, are based upon the assumption of infinitesimally small displacements. They are expressed as

$$\epsilon_{r,i} = \frac{\partial u_i}{\partial r} \qquad (2a)$$

$$\epsilon_{\theta,i} = \frac{u_i}{r} \qquad (2b)$$

The material constitutive equations for the ith layer relate the stresses to the strains and are expressed as

$$\sigma_{r,i} = \frac{E_{r,i}}{(1 - \nu_{\theta r,i}\nu_{r\theta,i})}(\epsilon_{r,i} + \nu_{\theta r,i}\epsilon_{\theta,i}) \qquad (3a)$$

$$\sigma_{\theta,i} = \frac{E_{\theta,i}}{(1 - \nu_{\theta r,i}\nu_{r\theta,i})}(\nu_{r\theta,i}\epsilon_{r,i} + \epsilon_{\theta,i}) \qquad (3b)$$

assuming rotational transverse isotropy, and the following reciprocality relationship is valid:

$$\frac{\nu_{\theta r,i}}{E_{\theta,i}} = \frac{\nu_{r\theta,i}}{E_{r,i}} \qquad (4)$$

Further, it is assumed that the magnetic field can be expressed as a polynomial in r.

$$B_{z,i}(r) = \sum_{k=0}^{n_b} b_{k,i} r^k \qquad (5)$$

By substituting (2) through (5) into (1), the following second-order, nonlinear, nonhomogeneous equation governing the displacement of the ith layer is obtained:

$$\frac{\partial^2 u_i}{\partial r^2} + \frac{\partial u_i}{r\partial r} - \alpha_i^2 \frac{u_i}{r^2} = -J_i K_i \sum_{k=0}^{n_b} b_{k,i} r^k \qquad (6)$$

where

$$K_i = \frac{(\alpha_i - \nu_{\theta r,i}^2)}{E_{\theta,i}}$$

*Research sponsored by the Office of Fusion Energy, U.S. Department of Energy, under contract W-7405-eng-26 with the Union Carbide Corporation.

and

$$\alpha_i = \left(\frac{E_{\theta,i}}{E_{r,i}}\right)^{1/2}$$

The solution of (6), which is in the form of Cauchy's equation,[6] can be obtained by transforming the independent variable to $t = \ln(r)$ thus transforming (6) into a second-order, linear, nonhomogeneous equation in terms of t as

$$\frac{\partial^2 u_i}{\partial t^2} - \alpha_i^2 u_i = -J_i K_i \sum_{k=0}^{n_b} b_{k,i} e^{(k+2)t} \tag{7}$$

The roots of the characteristic equation of (7) are $\pm\alpha_i$; therefore the complementary solution of (7) is

$$(u_i)^c = C_{1,i} e^{\alpha_i t} + C_{2,i} e^{-\alpha_i t} \tag{8}$$

By inspection the particular solution of (7) can be written as

$$(u_i)^p = J_i K_i \sum_{k=0}^{n_b} b_{k,i} \frac{e^{(k+2)t}}{[\alpha_i^2 - (k+2)^2]} \tag{9}$$

When the positive root of the characteristic equation of (7) is equal to the power of r in the particular solution, i.e., $k + 2 = \alpha_i$, then the particular solution expressed in (9a) is singular because of a repeated root [notice the denominator in (9a)]. Modification of the particular solution due to this single repeated root in the characteristic equation is accomplished by multiplying (9a) by t, thus yielding a solution for displacement at this singular point.

$$(u_i)^p = -\frac{J_i K_i b_{k,i} t e^{(k+2)t}}{2(k+2)} \tag{9b}$$

Combining (8) and (9) and expressing the result in terms of the original independent variable r yields the general solution to (6)

$$u_i = C_{1,i} r^{\alpha_i} + C_{2,i} r^{-\alpha_i} + (u)^p_{k,i} \tag{10a}$$

$$(u)^p_{k,i} = J_i K_i \sum_{k=0}^{n_b} b_{k,i} \frac{r^{k+2}}{[\alpha_i^2 - (k+2)^2]} \Big|_{k+2 \neq \alpha_i} \tag{10b}$$

$$(u)^p_{k,i} = -\frac{J_i K_i b_{k,i} r^{k+2} \ln(r)}{2(k+2)} \Big|_{k+2 = \alpha_i} \tag{10c}$$

where $C_{1,i}$ and $C_{2,i}$ represent undetermined coefficients that are dependent upon the boundary conditions of the continuum model. The undetermined coefficients are solved for by applying boundary conditions upon the radial stress distribution; therefore, equations for mechanical strain and stress must be formulated in terms of the undetermined coefficients. Substituting (10) into (2) determines the radial and tangential strains in terms of the undetermined coefficients. The radial strain is expressed as

$$\epsilon_{r,i} = \alpha_i C_{1,i} r^{\alpha_i - 1} - \alpha_i C_{2,i} r^{-(\alpha_i + 1)} + (\epsilon_r)_{k,i} \tag{11a}$$

$$(\epsilon_r)_{k,i} = J_i K_i \sum_{k=0}^{n_b} b_{k,i} \frac{(k+2) r^{k+1}}{[\alpha_i^2 - (k+2)^2]} \Big|_{k+2 \neq \alpha_i} \tag{11b}$$

$$(\epsilon_r)_{k,i} = -\frac{J_i K_i b_{k,i} [1 + (k+2)\ln(r)] r^{k+1}}{2(k+2)} \Big|_{k+2 = \alpha_i} \tag{11c}$$

The tangential strain is expressed as

$$\epsilon_{\theta,i} = C_{1,i} r^{\alpha_i - 1} + C_{2,i} r^{-(\alpha_i + 1)} + (\epsilon_\theta)_{k,i} \tag{11d}$$

$$(\epsilon_\theta)_{k,i} = J_i K_i \sum_{k=0}^{n_b} b_{k,i} \frac{r^{k+1}}{[\alpha_i^2 - (k+2)^2]} \Big|_{k+2 \neq \alpha_i} \tag{11e}$$

$$(\epsilon_\theta)_{k,i} = -\frac{J_i K_i b_{k,i} r^{k+1} \ln(r)}{2(k+2)} \Big|_{k+2 = \alpha_i} \tag{11f}$$

Substituting (11) into (3) determines the radial and tangential stresses in terms of the undetermined coefficients. The radial stress is expressed as

$$\sigma_{r,i} = \frac{1}{K_i}[(\alpha_i + \nu_{\theta r,i}) C_{1,i} r^{\alpha_i - 1} - (\alpha_i - \nu_{\theta r,i}) C_{2,i} r^{-(\alpha_i + 1)} + (\sigma_r)_{k,i}] \tag{12a}$$

$$(\sigma_r)_{k,i} = J_i K_i \sum_{k=0}^{n_b} b_{k,i} \frac{(k+2+\nu_{\theta r,i}) r^{k+1}}{[\alpha_i^2 - (k+2)^2]} \Big|_{k+2 \neq \alpha_i} \tag{12b}$$

$$(\sigma_r)_{k,i} = -J_i K_i b_{k,i} \frac{[1+(k+2+\nu_{\theta r,i})\ln(r)]r^{k+1}}{2(k+2)} \Big|_{k+2=\alpha_i} \quad (12c)$$

The tangential stress is expressed as

$$\sigma_{\theta,i} = \frac{1}{K_i}[(\alpha_i+\nu_{\theta r,i})\alpha_i C_{1,i} r^{\alpha_i-2} + (\alpha_i-\nu_{\theta r,i})\alpha_i C_{2,i} r^{-(\alpha_i+1)} + (\sigma_\theta)_{k,i}] \quad (12d)$$

where $(\sigma_\theta)_{k,i}$ for $k + 2 \neq \alpha_i$ is expressed as

$$(\sigma_\theta)_{k,i} = J_i K_i \sum_{k=0}^{n_b} b_{k,i} \frac{[\alpha_i^2 + \nu_{\theta r,i}(k+2)]r^{k+1}}{[\alpha_i^2 - (k+2)^2]} \quad (12e)$$

where $(\sigma_\theta)_{k,i}$ for $k + 2 = \alpha_i$ is expressed as

$$(\sigma_\theta)_{k,i} = -J_i K_i b_{k,i} \frac{\{\nu_{\theta r,i}+[\nu_{\theta r,i}(k+2)+\alpha_i^2]\ln(r)\}r^{k+1}}{2(k+2)} \quad (12f)$$

By setting the radial stress to zero at the inner and outer radii of the ith layer, two simultaneous equations can be generated that uniquely determine $C_{1,i}$ and $C_{2,i}$. When these equations are solved the undetermined coefficients can be expressed as

$$C_{1,i} = \frac{[(\sigma_r)_{k,i}]_{in} r_{in}^{1+\alpha_i} - [(\sigma_r)_{k,i}]_{out} r_{out}^{1+\alpha_i}}{(\alpha_i+\nu_{\theta r,i})(r_{out}^{2\alpha_i} - r_{in}^{2\alpha_i})} \quad (13a)$$

$$C_{2,i} = \frac{[(\sigma_r)_{k,i}]_{out} r_{out}^{1-\alpha_i} - [(\sigma_r)_{k,i}]_{in} r_{in}^{1-\alpha_i}}{(\alpha_i-\nu_{\theta r,i})(r_{out}^{-2\alpha_i} - r_{in}^{-2\alpha_i})} \quad (13b)$$

and

$$(\sigma_r)_{k,i} = J_i K_i \sum_{k=0}^{n_b} b_{k,i} \frac{(k+2+\nu_{\theta r,i})r^{k+1}}{[\alpha_i^2 - (k+2)^2]} \Big|_{k+2\neq\alpha_i} \quad (13c)$$

$$(\sigma_r)_{k,i} = -J_i K_i b_{k,i} \frac{[1+(k+2+\nu_{\theta r,i})\ln(r)]r^{k+1}}{2(k+2)} \Big|_{k+2=\alpha_i} \quad (13d)$$

Conclusions

The general solution for mechanical displacement, stress, and strain in axisymmetric solenoids was shown to be singular when the relationship $k + 2 = \alpha_i$ is satisfied. A modification to the general solution was derived that permits evaluation of the mechanical behavior of axisymmetric solenoids when a singular point is encountered.

Nomenclature

Variable	description
B	magnetic field
E	Young's modulus
J	conductor current density
r	radial position
t	ln(r)
u	displacement
α	moduli ratio
ε	strain
σ	stress
ν	Poisson's ratio

Subscript	description
,i or i	refers to the ith layer
in	refers to the inner surface of a layer
out	refers to the outer surface of a layer
r	refers to the radial direction
z	refers to the axis of revolution direction
θ	refers to the tangential direction

Superscript	description
c	complementary solution
p	particular solution

References

1. W. H. Gray and J. K. Sallou, "Electromechanical Stress Analysis of Transversely Isotropic Solenoids," J. Appl. Phys. 48(7), 3100 (1977).
2. W. E. Johnson, W. H. Gray, and R. A. Weed, in Proc. 6th Symp. on Engineering Problems of Fusion Research, Vol. 1, p. 243 (1975).
3. W. E. Johnson, Adv. Cryog. Eng. 22, 490 (1977).
4. W. H. Gray, "New Developments in Program STANSOL Version 3," in Proc. 9th Symp. on Engineering Problems of Fusion Research, to be published.
5. E. S. Bobrov and J. E. C. Williams, "Stresses in Superconducting Solenoids," in Proc. Winter Annual ASME Appl. Mech. Div., Francis C. Moon, Ed., AMD-41, 13 (1980).
6. Erwin Kreyszig, Advanced Engineering Mathematics, John Wiley and Sons, Inc., New York, 1967, p. 166.

acceptance of this article, the publisher or recipient acknowledges a U.S. Government's right to retain a nonexclusive, royalty-free license in and to any copyright covering the article.

A COMPARISON BETWEEN EXPERIMENTAL AND ANALYTICAL WINDING PRESTRAIN FOR A CIRCULAR SOLENOID*

W. H. Gray, T. J. McManamy, J. K. Ballou, and R. L. Brown
Fusion Energy Division
Oak Ridge National Laboratory
Oak Ridge, TN 37830

A series of practice winding experiments were done during the winding of the development magnets for ELMO Bumpy Torus Proof-of-Principle (EBT-P — a large, experimental fusion device using 36 superconducting mirror magnets). The experimental method involved layer winding conductor on the bobbin and monitoring the hoop strain accumulation on the inside of the bobbin's bore tube and thus inferring the effectiveness of winding tension as a means of controlling operational stress levels within the magnets. The experiments were done with bare conductor and with several types of spiral wrapped insulation on the conductor. Experiments were also performed varying the type of ground-plane insulation between the bobbin and the inner turn of the conductor, as well as experiments that varied the location of the layer wound section on the bobbin. Good agreement between experimental data and a computational stress model was obtained. The effect of time-dependent viscoelastic material behavior was observed.

Introduction

Using winding tension to compress the inner turns of a magnet's conductor is a generally accepted practice to decrease the operational stress level of a circular solenoid. Tension applied to the conductor while it is being wound is transferred to the solenoid as a radial surface pressure on the previous outer conductor layer. The solenoid equilibrates this induced radial surface pressure by producing compressive radial and hoop (tangential) stress distributions throughout the solenoid. Layer by layer the compressive stress distribution accumulates so that it is theoretically possible to develop stresses large enough to yield or buckle the solenoid's bobbin or its inner turns. Since the electromagnetic Lorentz force induces tensile hoop stresses when equilibrated by the solenoid, the magnet designer, in principle, can adjust the operational hoop stress level to satisfy magnet design criteria by carefully controlling the winding tension. In fact, it is theoretically possible to produce a solenoid that has essentially zero hoop stress at its operating condition by varying the amount of winding tension from layer to layer. Practically, however, designs of this type are difficult to achieve.

Although using winding tension to decrease the operational hoop stress in solenoid magnets has been a common practice for many years, to the authors' knowledge little experimental data is available to verify this practice as, in general, there is little mechanical data available on the construction and operation of solenoids. Operational success of solenoids implies satisfaction of design criteria and by inference adequate magnet prestress.

One recent paper[1] does show good agreement between theory and experiment for the displacement of the bobbin of a solenoid magnet. This magnet was a small-bore, high magnetic field NMR device wound with circular superconducting wire and impregnated with epoxy. The winding tension was optimized to produce the desired stress distribution when coupled with the other design criteria; it produced a successful magnet.

Previous Work at ORNL

Three recent magnets designed and constructed at the Oak Ridge National Laboratory (ORNL) have used ventilated winding packs made with monolithic or cabled, composite superconductors. These magnets have used a 50% barber pole wrap of Nomex† lacing tape on a rectangular conductor to provide turn-to-turn and layer-to-layer insulation. This insulation design also provides the space for helium percolation through the winding pack, but has a disadvantage in that it produces poor radial and axial structural stiffness.

The first of these ventilated ORNL magnets was a small-bore 8-T solenoid designed with back-of-the-envelope stress calculations. It is used routinely as a laboratory magnet and operates successfully at design field. It was wound to test out the ventilated winding pack design, but because of its modest stress level no sophisticated stress analysis was done. The second ventilated ORNL magnet built was CWTX.[2] CWTX is a large (38-cm bore), high magnetic field (8 T), split superconducting solenoid. Including the more fundamental aspects of solenoid mechanical design, two criteria were imposed during the design/analysis of CWTX that were to be solved by the judicious choice of winding tension. They are listed below.

(1) In order to prevent lift-off of the superconductor from the bobbin, the winding tension was calculated to produce at least 100-psi compressive radial stress at the bobbin-insulator-superconductor interface during magnet operation at 8 T. This imposed criteria implies that no sudden conductor motion is possible in the high field region of the magnet and is a generally accepted magnet community idea; although the absolute value of the compressive interface stress is a value that varies from individual to individual.

(2) A lower than normal design stress was chosen for the superconductor because of the following mechanical effect. CWTX's superconductor is a composite of Cu/NbTi cable wrapped around a rectangular copper core and then soldered together. When mechanically tested, this superconductor exhibited a bilinear stress vs strain material behavior before its mechanical yield point. This is believed to be caused by local inelastic behavior of the solder. In order to prevent the added heat input from the inelastic material behavior of the solder in the magnet, a lower than normal design stress was chosen for the superconducting composite.

A winding tension was calculated to satisfy the design criteria including the two mentioned above. The bobbin was instrumented with strain gauges, and the bobbin strain was monitored after every layer to determine the accuracy of the prestrain calculation. Much to our surprise, the bobbin of CWTX had a negligible hoop winding prestrain. It was concluded that the viscoelastic material behavior of the impregnated Nomex lacing tape insulation caused a stress relaxation within the windings, thereby preventing compressive stress accumulation during winding. CWTX,

*Research sponsored by the Office of Fusion Energy, U.S. Department of Energy, under contract W-7405-eng-26 with the Union Carbide Corporation.

†Reference to a company or product name does not imply approval or recomendation of the product by Union Carbide Corp. or the U.S. Department of Energy to the exclusion of others that may be suitable.

however, is a success in spite of the violation of the two winding tension related design parameters, probably because of the superior winding pack ventilation. Dissatisfied with the lack of agreement between winding theory and experiments for CWTX, the following experiments were done to get a better understanding about how winding tension influences magnet stress for the third ventilated ORNL magnet design – the development magnets for EBT-P (ELMO Bumpy Torus Proof-of-Principle).

Practice Winding Tests on the EBT-P Development Coils

The design and construction of the EBT-P development magnets is the subject of a companion paper[3] presented at this conference. Presented here is the influence of the winding tension upon the mechanical behavior of the EBT-P development magnet's bobbin. In Ref. 3 these data are used to predict the operational stress level in the EBT-P magnets.

A series of experiments were done during the practice winding to verify the computational stress models for the EBT-P development magnets. These computational models used STANSOL[4] to predict the accumulation of compressive strain at the inner radius of the bobbin due to the applied winding tension. The experimental method involved layer winding rectangular copper conductor on the bobbin and intermittently monitoring the hoop strain accumulation on the inside of the bobbin's bore tube. In order to save time, the layer wound section was only 50 mm wide (approximately 10 conductor widths) and seven layers thick (see Fig. 1). Both EBT-P development magnet bobbins are 215 mm wide and are designed to hold 32 layers of superconductor spiral wrapped with insulation. Practice winding experiments were done with bare conductor and with several types of spiral wrapped insulation on the conductor. Experiments were also performed varying the type of ground-plane insulation between the bobbin and the inner turn of the conductor, as well as experiments that varied the location of the layer wound section on the bobbin.

By progressively introducing different materials into the practice winding, changes in the bobbin response were distinguishable, and, if necessary, the computational stress model was empirically updated to match the new behavior. This method was used to empirically determine the compressive Young's modulus of the spiral wrapped insulation used in the EBT-P development magnets. The following sections briefly present the progressive steps taken during the practice winding and their corresponding comparisons between experimental data and analytical predictions. A complete report presenting all the experimental data and detailing all the analytical calculations is available in Ref. 5.

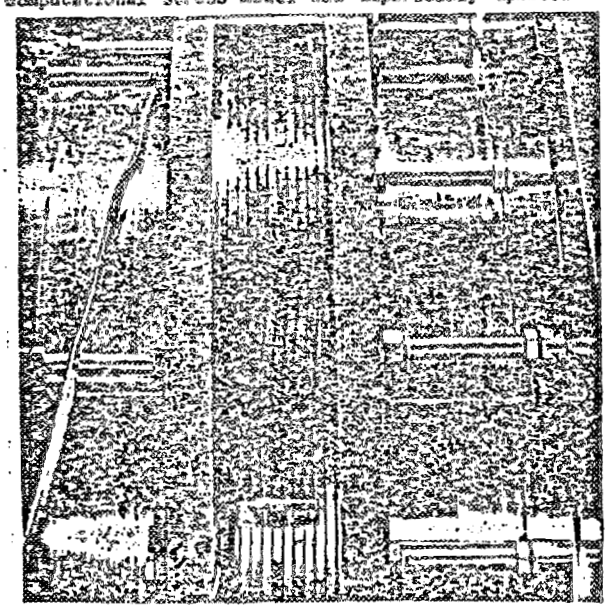

Fig. 1. A photograph of the experimental winding section. This section was 50 mm wide and 7 layers high.

Winding Bare Conductor on a Bare Bobbin

By choosing to practice wind bare conductor onto a bare bobbin, the number of variable parameters was minimized. The accumulation of compressive hoop strain in the bobbin is a function of material dimensions, elastic material properties, and winding tension. The material dimensions were accurately measured. The Young's modulus and Poisson's ratio for stainless steel and copper at room temperature are well known, and the winding tension was accurately set at 610 N (although some adjustment to this value was necessary due to winding table friction and conductor-spool inertia).

Also, a correction was applied to the Young's modulus of the bobbin in the STANSOL computational stress model because of the increase in bobbin stiffness due to partially winding a layer on a long cylinder. This correction was calculated by applying a ring of pressure to an infinite cylinder (see Refs. 5 and 6) and is not an adjustable parameter. Figure 2 presents a comparison between bobbin hoop strain gauge data and the analytical prediction. Good agreement was obtained.

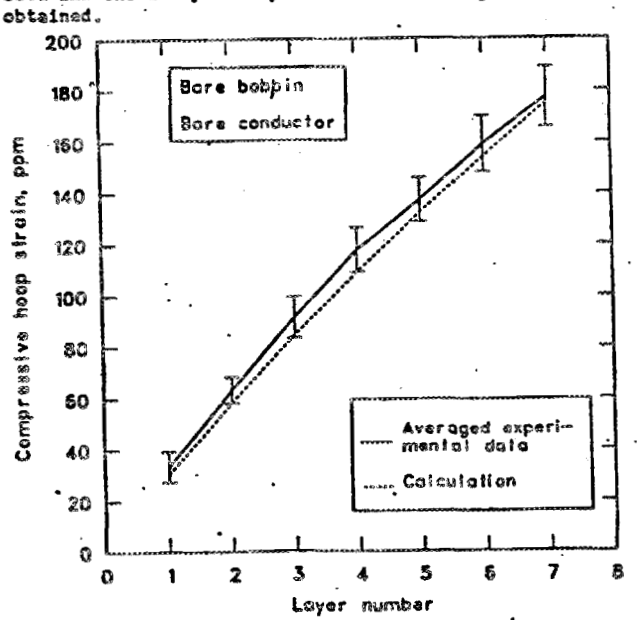

Fig. 2. A comparison between bobbin hoop strain and analytical prediction vs layer number for practice winding bare conductor onto a bare bobbin. The solid line is drawn through the mean strain gauge data averaged from several strain gauges each read after a layer was wound. These gauges were uniformly circumferentially positioned on the inner bobbin bore tube at the axial midplane of the magnet. In principle, each gauge should have read the same value. The error bars represent the standard deviation in the experimental data. The dashed line represents the analytical prediction from the STANSOL computational stress model. (All figures in this paper use the same distinguishing lines and symbols to differentiate between experimental data and analytical calculation.)

Winding Bare Conductor on an Insulated Bobbin

The next step in the practice winding introduced several layers of 50% perforated G-10 and a solid G-10 layer between the bobbin and the first conductor layer. The G-10 material was the same type used for the ground-plane insulation in the EBT-P development magnets. The practice winding was repeated, and the computation model was updated to reflect the addition of the new materials. Room temperature material property data for G-10 was used with the 50% perforated layers having their material properties modified by the simple rule-of-mixtures. Figure 3 shows the results of the practice winding for this geometry. Again good agreement was obtained.

Winding Insulated Conductor on an Insulated Bobbin

By performing the two previous experiments, we confirmed that using a STANSOL computational stress model adequately predicts winding prestrain accumulation in a magnet. Another practice winding experiment was performed to examine the effect of introducing impregnated Nomex lacing tape into the winding using it as a 50% spiral wrap of insulation on the conductor. Again the viscoelastic phenomenon, observed with the winding of CWTX, occurred.

The practice winding was repeated with a 50% wrap of nonimpregnated Nomex lacing tape. Again the viscoelastic phenomenon was observed; however this time the effect was considerably less. The stress relaxation of the winding prestrain on the practice winding with nonimpregnated Nomex took days to lose a few microstrain, instead of hours to lose tens of microstrain with impregnated Nomex. Figure 4 shows the results of the practice winding that included the 50% spiral wrap of nonimpregnated Nomex lacing tape. These experimental data are essentially instantaneous strain values since the experiment took less than one hour to perform. Therefore, the STANSOL model was modified to include the effect of the elastic behavior of the nonimpregnated Nomex lacing tape (a viscoelastic model is being developed).

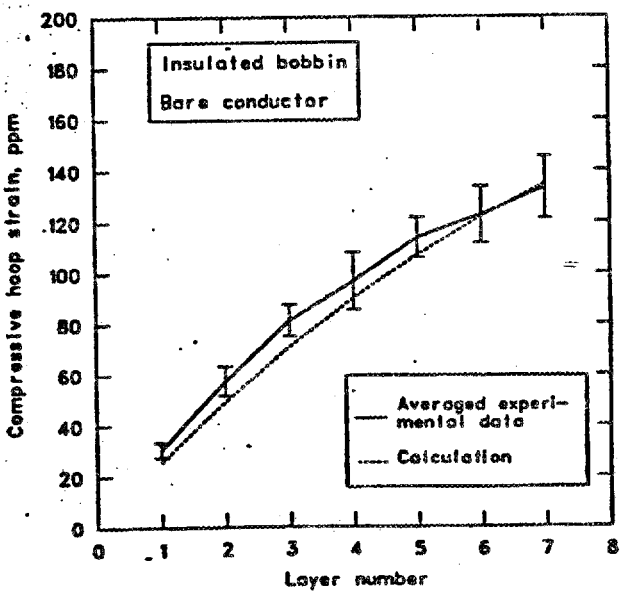

Fig. 3. A comparison between bobbin hoop strain and analytical prediction vs layer number for practice winding bare conductor onto an insulated bobbin. The winding tension used in this experiment was the same as that of the experiment shown in Fig. 2. (See the caption of Fig. 2 for an explanation of the symbolic nomenclature.)

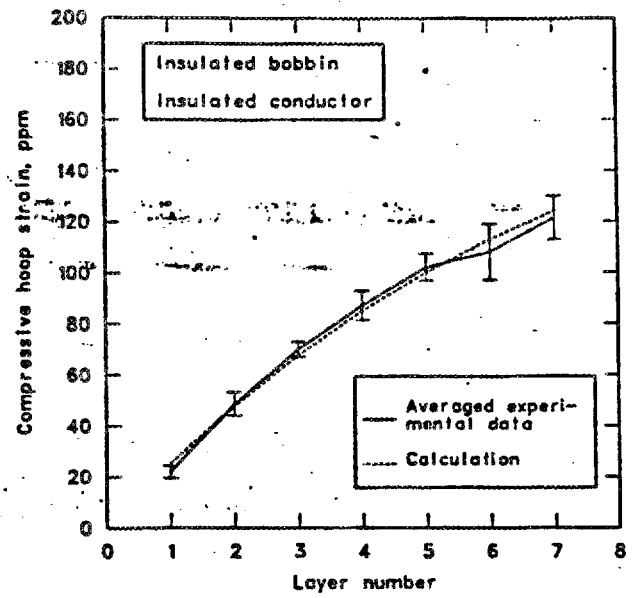

Fig. 4. A comparison between bobbin hoop strain and analytical prediction vs layer number for practice winding insulated conductor onto an insulated bobbin. The material properties of the Nomex conductor insulation were adjusted to match the experimental data, as they were the only parameters in the calculation that could be reasonably adjusted to make the experimental data and the computational stress model agree. The winding tension used in this experiment was the same as that of the experiment shown in Fig. 2. (See the caption of Fig. 2 for an explanation of the symbolic nomenclature.)

To achieve the good agreement between theory and experiment for this practice winding, the Young's modulus of the nonimpregnated Nomex was adjusted to fit the experimental data. This empirical determination of the nonimpregnated Nomex lacing tape's material properties is justifiable because of the lacing tape's nonhomogeneous nature — a bundle of uncoupled strands of nylon. It is difficult to use composite theory to calculate a modulus for this type of material.

Reference 5 details several other practice winding experiments performed prior to winding the EBT-P development magnets. These experiments included winding layers close to the bobbin side walls and using a 50% spiral wrap of Kapton H-film† as a conductor insulation. (It was hoped that the Kapton H-film would not exhibit viscoelastic behavior. Unfortunately, it did.) The magnitude of the stress relaxation was slightly less than that of the nonimpregnated Nomex lacing tape. Kapton H-film did give a slightly tighter winding pack when compared to an equivalent winding pack using nonimpregnated Nomex lacing tape. Because of previous experience and ease of fabrication, nonimpregnated Nomex lacing tape was chosen for the development magnets.

Winding Data for EBT-P development Magnet D1

Using the data and experience gleaned from the practice winding, the EBT-P development magnet D1 was wound. Prior to the winding the computational stress model was updated to reflect the superconductor material properties and dimensions which were slightly different from those of the plain copper conductor used in the practice winding. A winding tension of 670 N was selected to ensure that the compressive yield

stress of the bobbin would not be exceeded during winding. The first layer was wound and it was then decided to depend upon stress relaxation occurring so the winding tension was increased to 800 N for the remainder of the layers. (The 800 N represents the upper limit of the tensioning device.) Figure 5 shows the comparison between the bobbin hoop strain experimental data and the prediction based on the computational model. The difference is attributed primarily to the viscoelastic behavior of the nonimpregnated Nomex insulation. The viscoelastic phenomenon is clearly visible around layer nine's experimental data. At layer nine a several week delay in the winding occurred due to the design, verification, and fabrication of a splice between the high and low field graded superconductor. Other bumps in the experimental data can be directly attributed to holidays and weekends occurring over the course of the winding.

Since the computational stress model does not take into account stress relaxation, another method was desired to verify the elastic portion of the stress computation. By examining the incremental bobbin hoop stress vs layer number, a more reasonable comparison of experimental data with prediction can be made. Figure 6 presents the incremental bobbin hoop stress vs layer number. These data reduce the appearance of viscoelasticity on the data. Good agreement is obtained between the experimental data plotted in this manner and the elastic computation. (Ref. 5 presents similar data for the second EBT-P development magnet.)

Conclusions

Instrumenting practice winding experiments is a reasonable method of verifying computational stress models. Experimental data obtained from monitoring the accumulation of bobbin hoop strain during winding can be used to determine material properties that are not amenable to calculation with classical composite material calculation methods. When winding ventilated magnets, viscoelastic material behavior of the conductor insulation can stress-relieve the accumulated bobbin hoop strain. This stress relaxation and other inelastic behavior during operation[7] reduce the amount of compressive hoop stress in the conductor. Because of this, it is prudent and conservative not to depend on winding tension to decrease the conductor operational stress level within a magnet, if one of the winding pack materials exhibits viscoelastic material behavior.

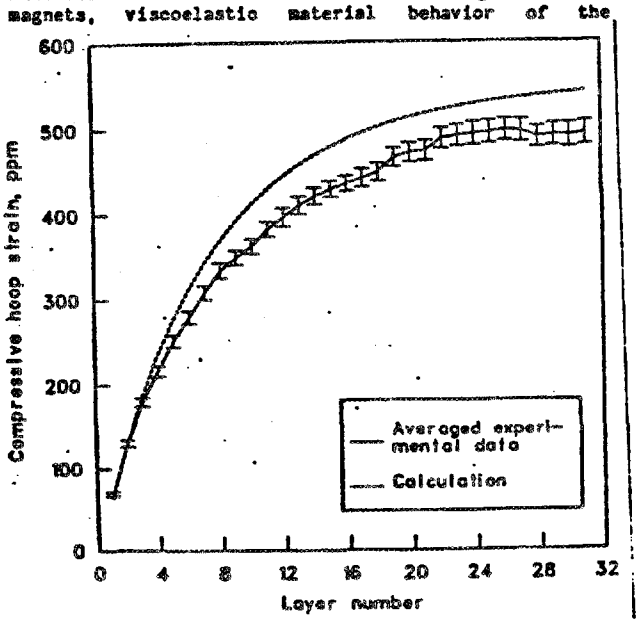

Fig. 5. A comparison between bobbin hoop strain and analytical prediction vs larger number for the first EBT-P development magnet. The difference between experiment and theory is attributed to primarily viscoelastic material behavior in the nonimpregnated Nomex insulation. (See the caption of Fig. 2 for an explanation of the symbolic nomenclature.)

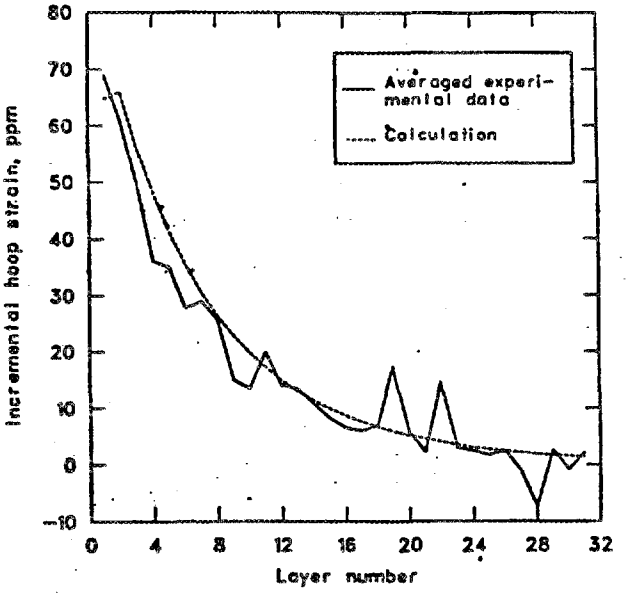

Fig. 6. A comparison between incremented bobbin hoop strain and analytical prediction vs layer number for the first EBT-P development magnet. By plotting the data in this manner, the appearance of viscoelastic material behavior is reduced. Good agreement is shown between the elastic calculation and the experimental data. (See the caption of Fig. 2 for an explanation of the symbolic nomenclature.)

References

1. E. S. Bobrov and J. E. C. Williams, "Stresses in Superconducting Solenoids," in Proc. Winter Annual ASME Appl. Mech. Div., Francis C. Moon, Ed., AMD-41, 13 (1980).
2. J. K. Ballou, R. L. Brown, W. A. Fietz, J. W. Forseman, W. H. Gray, W. J. Kenney, R. B. Wysor, W. D. Markiewicz, and R. G. Van Alstyne, "Design and Testing of a Dual 8-T 380-mm/12-T 220-mm Split Superconducting Solenoid for ORNL," IEEE Trans. Magn. MAG-17 (5), 2238 (1981).
3. J. K. Ballou, T. J. McManamy, R. L. Brown, W. H. Gray, and M. S. Lubell, "Design and Construction of an EBT-P Development Coil," these proceedings.
4. W. H. Gray, "New Developments in Program STANSOL Version 3," in Proc. 9th Symp. on Engineering Problems of Fusion Research, these proceedings.
5. W. H. Gray, T. J. McManamy, J. K. Ballou, and R. L. Brown, "The ORNL EBT-P Development Magnet Winding Experiments," Oak Ridge National Laboratory, to be published.
6. S. Timoshenko and S. Woinowsky-Krieger, Theory of Plates and Shells, McGraw-Hill Book Company, New York, 1967, p. 471.
7. J. R. Miller, J. W. Lue, and S. S. Shen, "Tests of the First Development Coils for EBT-P", these proceedings.

STRESS ANALYSIS OF SOLENOIDS THAT DEVELOP GAPS

W. H. Gray

Abstract - Several large superconducting magnets recently built or under construction at the Oak Ridge National Laboratory use ventilated winding-pack designs. Due to external constraints, it is not always possible to develop enough prestress to ensure compressive layer-to-layer interface pressures. Unless there is some mechanism to support tensile interface pressures (such as epoxy bonding, which is not possible in ventilated magnet designs), the magnet will develop gaps at these interfaces. Presented herein is a theory for determination of the nonlinear mechanical behavior of axisymmetric solenoids that can develop frictionless gaps which may open and close during magnet cooldown and energization. Also discussed are the implementation of this theory within a computer program and an example application of this theory to several magnets.

INTRODUCTION

Several large superconducting magnets recently built or under construction at the Oak Ridge National Laboratory (ORNL) use ventilated winding-pack designs. To achieve a porous structure with good ventilation capability and numerous liquid helium paths throughout, a 50% spiral wrap of turn-to-turn insulation is used with no epoxy potting or other layer-to-layer support. These magnets depend upon winding-pack prestress and cooldown thermal strain to maintain compressive layer-to-layer interface pressures during magnet operation. Due to external design considerations and constraints (for example, exceeding the design-allowable bobbin compressive stress or buckling of the inner winding layers), it is not always possible to develop enough prestress to ensure compressive layer-to-layer surface pressures. Unless there is some mechanism to support tensile interface pressures (such as epoxy bonding), the magnet will develop gaps at these interfaces.

In previous papers [1,2], solutions have been given for mechanical stresses and displacements in axisymmetric, plane-stress, rotationally-transversely isotropic solenoids that can be multilayered and nonhomogeneous. These solutions consider loads due to winding prestress buildup, internal and external pressure, thermally induced contraction or expansion, and electromagnetically induced Lorentz body forces; however, they assume that the solenoid is mechanically continuous and that no gaps can develop. In order to apply these solutions rigorously, care must be taken to ensure that enough winding prestress is used. This paper removes this restriction by presenting a technique for the calculation of mechanical stresses and displacements in solenoids that are not mechanically continuous and that can develop frictionless gaps which may open or close during magnet cooldown (warmup) and/or energization. Presented herein are the modification of the above theory and the incorporation of this new technique into the STANSOL [3] computer program.

A REVIEW OF SOLENOID STRESS ANALYSIS WITHOUT GAPS

As the basis for the frictionless gap solution presented in subsequent sections of this paper is a gapless (continuum) solution, the formulation and solution of equations for mechanical stresses and displacement in continuum solenoids are briefly reviewed in this section. The following equations apply to an axisymmetric, plane-stress, rotationally-transversely isotropic solenoid that can be multilayered and nonhomogeneous. The formulation of these equations is presented in detail in Refs. [1] and [2]; however, they are developed here with the terminology expressed in Ref. [4], because of the succinctness of the nomenclature used in Ref. [4]. (Also, by citing over 30 references, Ref. [4] contributes an excellent historical review of the development and gradually increasing sophistication of the analytical and numerical solutions for mechanical stresses and displacement in axisymmetric solenoids.)

The Continuum Solenoid Stress Model

Assume that a multilayered, nonhomogeneous solenoid can be modeled as a series of concentric homogeneous circular rings. Then for the ith layer, the plane-stress equilibrium equation in polar coordinates, assuming both magnet axisymmetry and the presence of an electromagnetically induced Lorentz body force, is expressed as

$$\frac{\partial \sigma_{r,i}}{\partial r} + \frac{\sigma_{r,i} - \sigma_{\theta,i}}{r} = -J_i B_{z,i}(r) \tag{1}$$

The kinematic relationships for the ith layer equate the strains to the displacement and for the purpose of this analysis, like those in Refs. [1], [2], and [4], are based upon the assumption of infinitesimally small displacements. They are expressed as

$$\varepsilon_{r,i} = \frac{\partial u_i}{\partial r} \tag{2a}$$

$$\varepsilon_{\theta,i} = \frac{u_i}{r} \tag{2b}$$

The material constitutive equations for the ith layer relate the stresses to the strains and are expressed as

$$\sigma_{r,i} = \frac{E_{r,i}}{(1 - \nu_{\theta r,i}\nu_{r\theta,i})} (\varepsilon_{r,i} + \nu_{\theta r,i}\varepsilon_{\theta,i}) \tag{3a}$$

$$\sigma_{\theta,i} = \frac{E_{\theta,i}}{(1 - \nu_{\theta r,i}\nu_{r\theta,i})} (\nu_{r\theta,i}\varepsilon_{r,i} + \varepsilon_{\theta,i}) \tag{3b}$$

assuming rotational transverse isotropy, and the following reciprocality relationship is valid:

$$\frac{\nu_{\theta r,i}}{E_{\theta,i}} = \frac{\nu_{r\theta,i}}{E_{r,i}} \tag{4}$$

Further, it is assumed that the magnetic field can be expressed as a polynomial in r,

$$B_{z,i}(r) = \sum_{k=0}^{n_b} b_{k,i} r^k \tag{5}$$

By substituting (2) through (5) into (1), the following eqaution governing the displacement of the ith layer is obtained:

$$\frac{\partial^2 u_i}{\partial r^2} + \frac{\partial u_i}{r\partial r} - \alpha_i^2 \frac{u_i}{r^2} = - \frac{(\alpha_i - \nu_{\theta r,i}^2)}{E_{\theta,i}} J_i \sum_{k=0}^{n_b} b_{k,i} r^k \tag{6}$$

Solution of (6), which is in the form of Cauchy's equation [5], yields the following expression for the displacement within the ith layer:

$$u_i = C_{1,i} r^{\alpha_i} + C_{2,i} r^{-\alpha_i} + J_i K_i \sum_{k=0}^{n_b} b_{k,i} \frac{r^{k+2}}{[\alpha_i^2 - (k+2)^2]} \tag{7}$$

where

$$K_i = \frac{(\alpha_i - \nu_{\theta r,i}^2)}{E_{\theta,i}}$$

where $C_{1,i}$ and $C_{2,i}$ represent undetermined coef- ficients that are dependent upon the boundary conditions of the continuum model and α_i is defined as

$$\alpha_i = \left(\frac{E_{\theta,i}}{E_{r,i}} \right)^{1/2}$$

<u>The Multicontact Elastic Ring Problem</u>

The solution of (7) for layers $i = 1, 2, \ldots, l$ requires the formulation of a multicontact elastic ring problem. This section briefly reviews the method used by STANSOL [3] to solve this type of problem. First, the coefficients $C_{1,i}$ and $C_{2,i}$ are solved for by assuming that the ith layer is self-supporting; i.e.,

$$(\sigma_{r,i})_{in} = (\sigma_{r,i})_{out} = 0 \tag{8}$$

thus uniquely determining the displacement of the ith layer. However, the resulting displacements for layers $i = 1, 2, \ldots, l$ using (8) as the sole boundary condition are incompatible; i.e., there is no guarantee that

$$(u_i)_{out} = (u_{i+1})_{in} \tag{9}$$

which must be true if there is to be a continuum solution. To enforce (9) for layers $i = 1, 2, \ldots, l - 1$, a set of interface pressures is introduced to restore compatibility. By solving for these unknown interface pressures, a general solution for the ith layer can be obtained that uses the interface pressures as the boundary conditions for the determination of the coef- ficients $C_{1,i}$ and $C_{2,i}$ in (7), instead of the boundary condition expressed in (8).

A similar technique can be used for the thermally induced stresses within a magnet simply by changing the right-hand side of (1) and (7) and introducing thermal strains into the kinematic and material constitutive equations. Winding preload stress distributions can be calculated by setting the right-hand side of (1) and (7) to zero and simulating the actual winding process by building up the magnet geometry layer by layer. For each newly applied layer $i = 1, 2, \ldots, lp$, a set of interface pressures is calculated, based upon the current magnet build and specification of the outer-most interface pressure, to be

$$p_{lp-1} = \frac{P_{lp}}{w_{lp}(r_{lp})_{in}} \tag{10}$$

thus forcing the outermost interface pressure to depend upon the winding tension.

Linear superposition of the solutions for winding prestress layer by layer, thermally induced stress via cooldown (or warmup), and electromagnetically induced stress for a continuum of layers permits the modeling of complex mechanical behavior in solenoids. Reference [6] contains the details of how the interface pressures are calculated for a particular load type and how to correctly superimpose all of the solutions.

Isotropy, Transverse Isotropy, and Orthotropy

Reference [4] presents a derivation for mechanical stresses and displacement in axisymmetric, plane-stress, rotationally orthotropic solenoids that can be multilayered and nonhomogeneous. The difference between rotational orthotropy [4], rotational transverse isotropy [1,2], and isotropy [7] as they relate to solenoid mechanics is discussed below. For isotropic materials there is no distinction between material direction; i.e., $E_r = E_\theta = E$ and $\nu_{r\theta} = \nu_{\theta r} = \nu$.

For rotationally-transversely isotropic materials, there are two distinct material directions and the reciprocality relationship expressed in (4) is valid. For rotationally orthotropic materials, there are two distinct material directions and the reciprocality relationship expressed in (4) is not valid, thus creating an unsymmetric material constitutive matrix. Practically, however, there is little difference between the two solutions presented in Refs. [1,2] and Ref. [4]., since (4) is used to simplify the solution presented in Ref. [4]. The difference amounts to replacing the material property coefficient $(\alpha - \nu_{\theta r}^2)/E_\theta$ for transverse isotropy with $(1 - \nu_{r\theta}\nu_{\theta r})/E_r$

for orthotropy which, of course, may be degenerated into $(1 - \nu^2)/E$ for simple isotropy.

SOLENOID STRESS ANALYSIS WITH GAPS

By using the above linear solution and incremental loading, a piecewise-continuous, nonlinear solution may be assembled for magnets in which frictionless gaps are permitted to open and close. In Ref. [4] a brief discussion is presented for modifying a linear solenoid stress analysis to permit a gap to open but not to close it. In fact, Ref. [4] shows a magnet analysis where a single gap opens and presents an excellent comparison between magnet behavior and theory. The gap theory presented here is more complete, as multiple gaps are permitted to open and close.

By choosing load increments that correspond to incipient frictionless gap formation or termination, complex, geometrically nonlinear structural behavior can be mathematically modeled. Within each loading increment a linear solution is calculated for each continuous section of the solenoid. (In the limit there could be as many sections as there are layers, since, in principle, there could be a gap between each layer.) Each gap formation modifies the solution boundary conditions by introducing another interface where the radial stress (and, therefore, the interface pressure) must be zero. Each gap termination removes the corresponding gap-introduced radial stress boundary condition. The solution increment for each section is added to the current solution, and the magnet is redivided (or recombined) into sections based upon the new gap definition. The next load increment is calculated, and the process is repeated until all the loads have been fully applied. Thus, because of this updating of the model's geometry, the solution becomes nonlinear even though within any solution increment, linear small displacement theory is used.

This theory was programmed into a modified version of the STANSOL computer program using the mathematical steps listed below. Also

presented below are the physical and mathematical conditions for frictionless gap formation and termination.

(1) First, if any preload is specified, a solution based upon winding prestress is calculated. During the prestress analysis, it is assumed that no gaps can occur. The solution for the preload mechanical stresses and deflections for layers i = 1, 2, ..., l is saved as the initial mechanical stress state.

$$(u_i)^o = (u_i)^{preload} \tag{11a}$$

$$(\sigma_{r,i})^o = (\sigma_{r,i})^{preload} \tag{11b}$$

$$(\sigma_{\theta,i})^o = (\sigma_{\theta,i})^{preload} \tag{11c}$$

If no preload is specified, $(u_i)^o$ is set to zero. Also, the gap definition table is initially set to zero to indicate that there are no gaps.

(2) The subsequent steps apply to either the thermal mechanical behavior or the electromagnetic mechanical behavior by simply changing to the appropriate forcing function [the right-hand side of (1)]. The thermal mechanical behavior is considered first.

(3) The incremental load factor, f, is set to 1.0 and a solution based upon the current gap definition is calculated. If there are gaps, then each continuous section of the solenoid is treated as an independent continuum. If there are no gaps, the entire solenoid is treated as a continuum and the following gap close test is skipped. (Of course, each sectioned continuum can contain many layers, each of which can be of a different material.)

(4) A check is made to determine if any opened gap will close during application of this load increment by evaluating of the expression

$$(\delta_i)^{new}_{out} = (u_{i+1})^{o}_{in} + (u_{i+1})^{f}_{in} - (u_i)^{o}_{out} - (u_i)^{f}_{out} \tag{12}$$

If the value of the new deflection difference is greater than or equal to zero for layer interfaces with gaps, then no gap will close and step (5) is skipped.

(5) If the value of the new deflection difference is less than zero, then a gap would close using this large a load increment. A new load increment factor is calculated according to the expression

$$f_{cg} = \min \left[\frac{(u_{i+1})^{o}_{in} - (u_i)^{o}_{out}}{(u_i)^{f}_{out} - (u_{i+1})^{f}_{in}} \right], \; i = \text{gapped layers} \tag{13}$$

which is the load increment factor that brings the solenoid to incipient gap termination.

(6) A check is made to determine if a new gap will open within the load increment. For every gapless interface, the value of the radial stress is calculated as

$$(\sigma_{r,i})^{new}_{out} = (\sigma_{r,i})^{o}_{out} + (\sigma_{r,i})^{f}_{out} \tag{14}$$

If the value of the new radial stress is less than or equal to zero (or some programmable tolerance) for layers without gaps, then no new gaps develop and step (7) is skipped.

(7) If the value of the new radial stress is greater than zero for any gapless layer, then a gap would open using this large a load increment. A new load increment factor is calculated according to the expression

$$f_{og} = \min \left[\frac{(\sigma_{r,i})^{o}_{out}}{(\sigma_{r,i})^{f}_{out}} \right], \; i = \text{gapless layers} \tag{15}$$

which is the load increment factor that brings the solenoid to incipient gap formation.

(8) Using the minimum of f_{og}, f_{cg}, and f, a new load increment factor is obtained and the solution is updated to the point of incipient gap formation or termination according to the expression

$$(u_i)^{o} = (u_i)^{o} + (u_i)^{\min(f_{og}, f_{cg}, f)} \tag{16}$$

The gap definition table is updated to connect (or subdivide) the solenoid geometry and a new load increment factor is calculated as

$$f = 1.0 - \min(f_{og}, f_{cg}, f) \tag{17}$$

(9) Steps (4) through (8) are repeated until no new gap develops and no previously existing gap closes within a loading increment.

(10) Steps (3) through (9) are repeated for the electromechanical body force loading.

APPLICATIONS

Three sample applications of solenoid stress analysis with gaps are presented in this section. The first one involves a magnet recently built at ORNL and used as a prototype for a future fusion experiment. The last two are interesting, though academic, examples that demonstrate the capabilities of the modified computer program to calculate stress in magnets with multiple gaps.

EBT-P Stress Analysis

In this section an application of solenoid stress analysis with gaps is shown as it predicts the radial and tangential stress distributions in the winding pack of a prototype superconducting (Cu/NbTi) magnet for the ELMO Bumpy Torus Proof-of-Principle experiment (EBT-P)[8]. Due to several external design constraints, chiefly high magnetic field (7.4-T) and conductor current density (11,910-A/cm^2) requirements and low dimensional limitations for bobbin thickness (0.96 cm), a satisfactory design could not be achieved that maintained a compressive interface pressure between the inner turns of the superconducting windings and the outer bobbin surface. Applying more winding preload to overcome this deficiency would have exceeded the room temperature design-allowable compressive yield stress of the bobbin. (The design-allowable yield stress was chosen to be two-thirds of the material yield stress.) A simple linear calculation was not sufficient to predict the state of stress in the superconductor when the magnet is fully energized, see Fig. 1, since a tensile radial stress exists at the bobbin-superconductor interface of this well-ventilated magnet design. The theory described in this paper was used to predict the stress state in the superconductor when the magnet is fully energized, as shown in Fig. 2.

Notice that the tangential force which was fictitously permitted to accumulate in the bobbin with the linear calculation is redistributed mainly over the first few turns of the superconductor with the nonlinear calculation. This magnet has been successfully energized and the current at which lift-off of the conductor from the bobbin occurred compares favorably with the nonlinear calculation after stress relaxation is taken into account. More details about this magnet and its geometry, material properties, and test results can be obtained from Refs. [8] and [9].

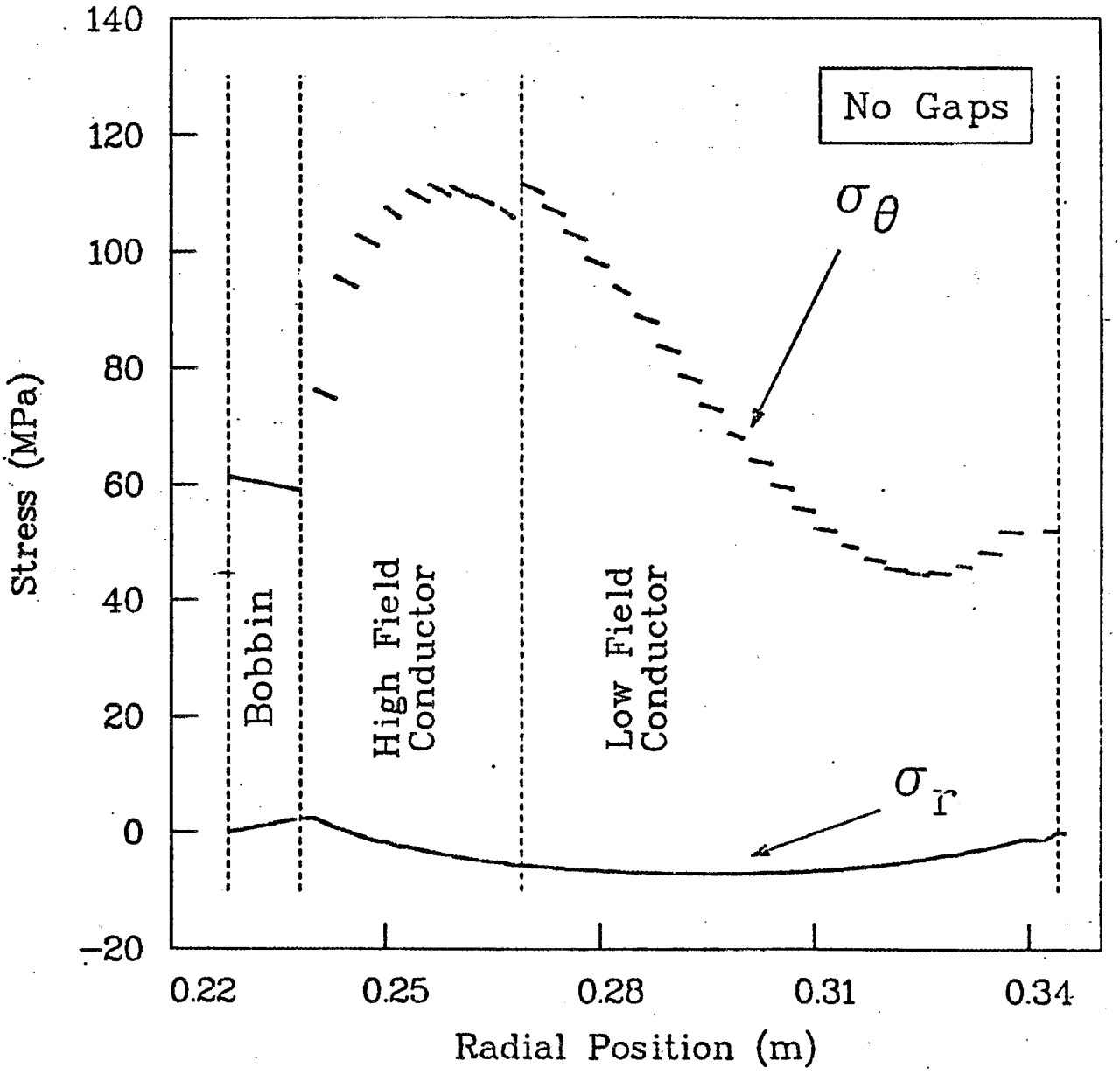

Fig. 1. The radial and tangential stress distribution at design field for the EBT-P prototype magnet, assuming no gaps can develop within the windings. The superconductor is graded in this magnet. There are 9 layers in the high field region and 23 layers in the low field region.

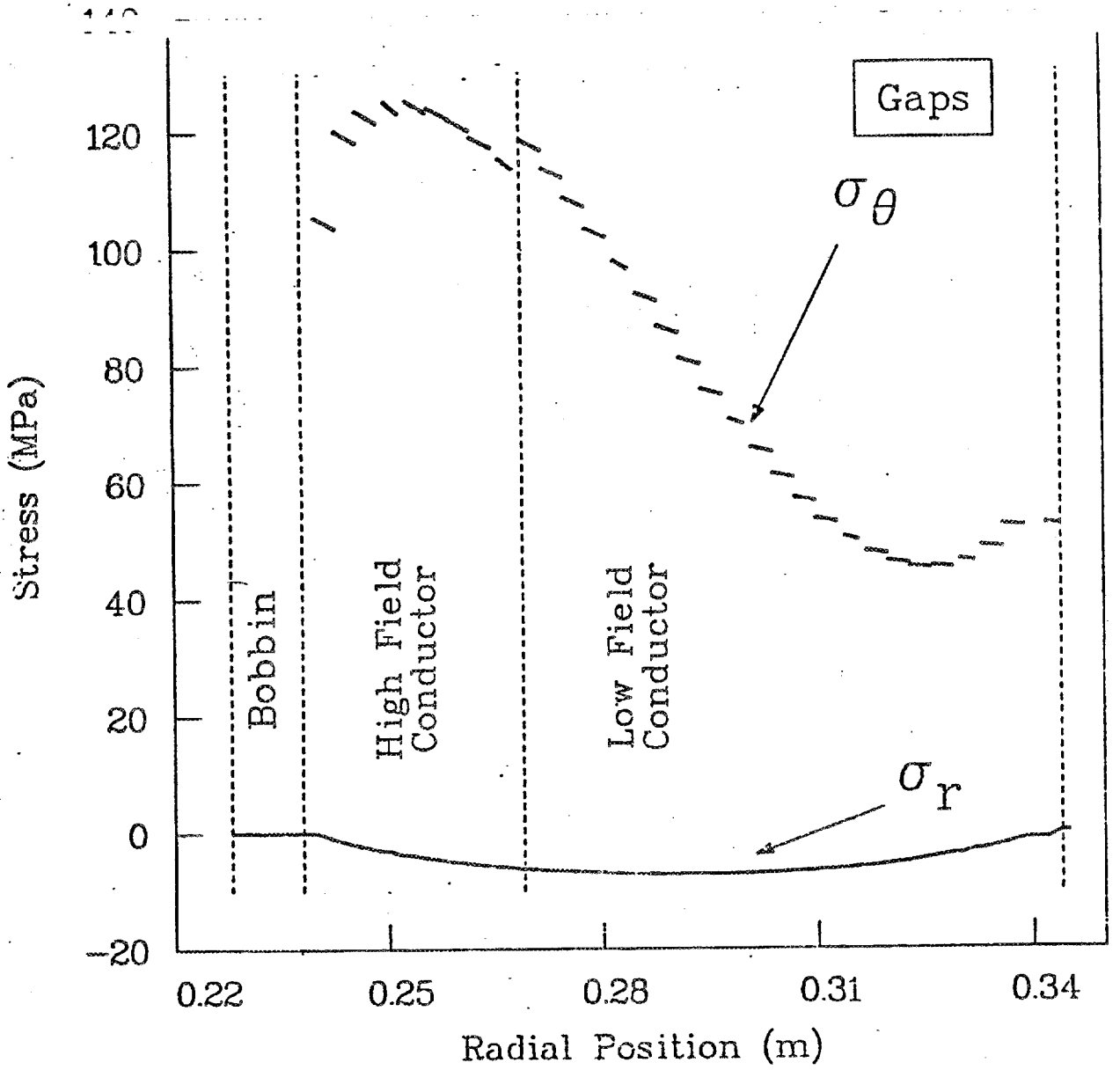

Fig. 2. The radial and tangential stress distribution at design field for the EBT-P prototype magnet, assuming gaps can develop within the windings.

Multiple Gap Sample Problem

Consider a magnet with no bobbin, a layer width of 1.0 cm, negligible layer-to-layer insulation, and inner and outer radii of 15.0 cm and 80.0 cm, respectively. The layer width was arbitrarily chosen so that there are 65 layers in this magnet. By neglecting prestress and thermally induced stress this calculation magnifies the effect of gapping and therefore is an interesting, through academic, example problem. For this problem the current density is assumed to be 1000.0 A/cm^2 and the magnetic fields at the inner and outer radii are 7.34 T and -0.49 T, respectively. Magnets with this large a radial build have large regions of tensile radial stresses, as shown in Ref. [1], when electromagnetically induced loads are considered as the only loading condition. Figure 3 shows the radial and tangential stress distributions for this magnet when no gaps are assumed to occur. Assuming that the layer-to-layer interfaces of this example magnet cannot support the tensile radial stress distribution shown in Fig. 3 and permitting gaps between layers where tensile radial stresses occur, the new radial and tangential stress distributions are calculated to be those shown in Fig. 4. Figure 4 shows that the first 23 layers are calculated to separate from one another while the remaining 42 layers act together as a single continuum.

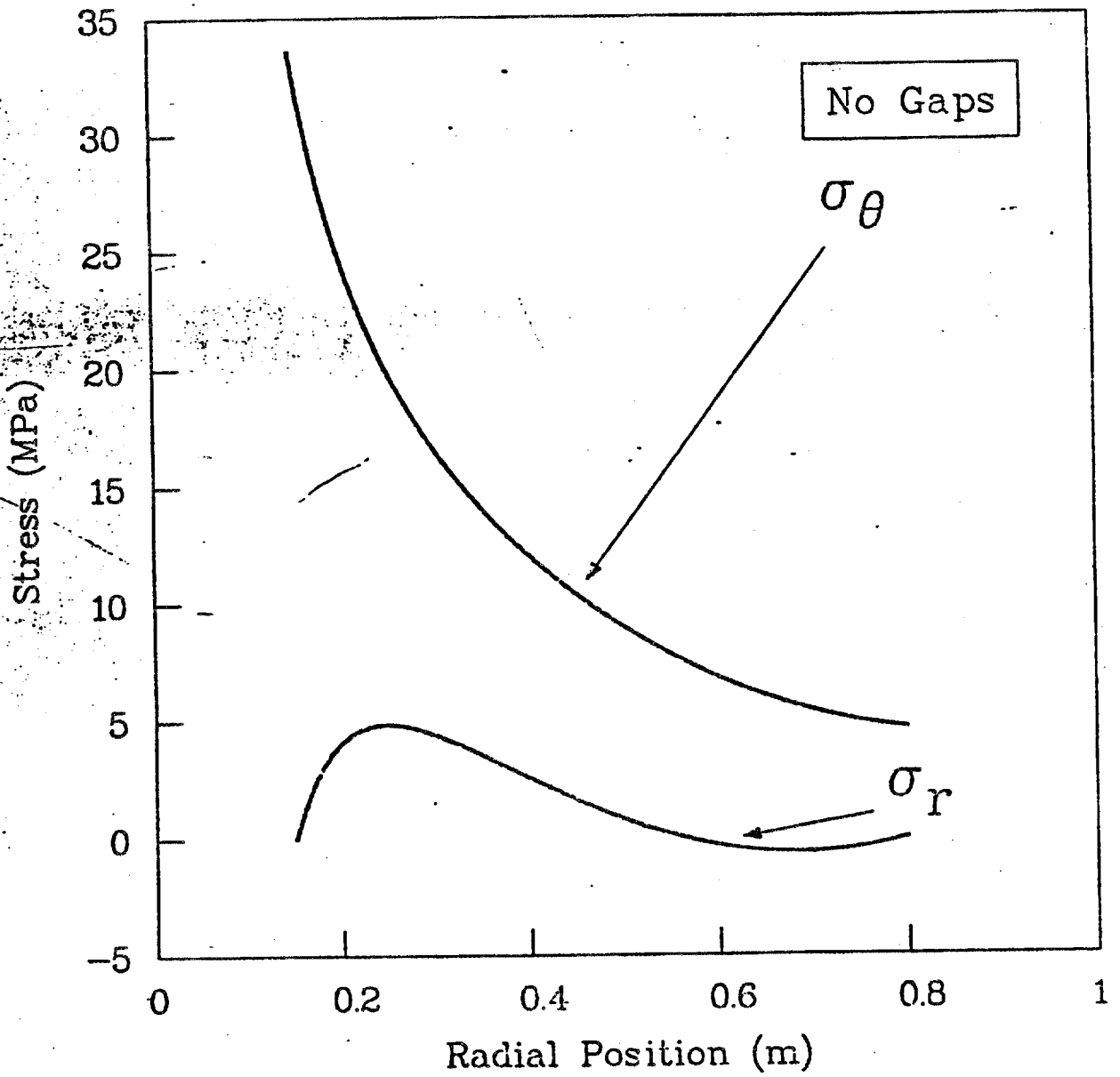

Fig. 3. The radial and tangential stress distributions for the 65-layer sample problem when no gaps are permitted to occur. Notice the tensile radial stress that is developed between several of the inner layers.

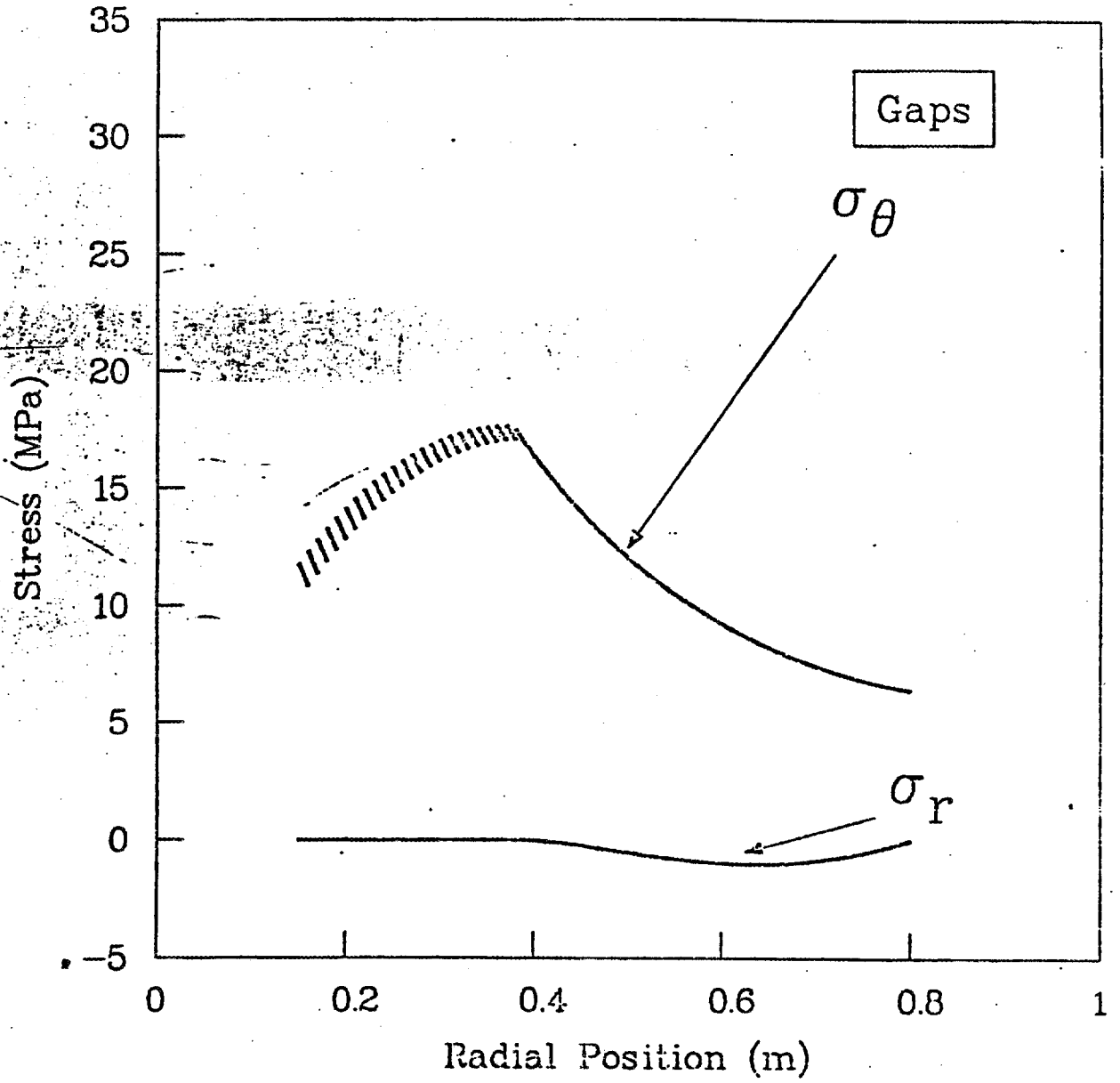

Fig. 4. The radial and tangential stress distributions for the 65 layer sample problem when gaps are permitted to develop by the computer software. The modified computer program calculates that the first 23 layers of this solenoid are self-supporting.

Gap Open and Then Close Sample Problem

By introducing into the second sample problem a 2.54-cm stainless steel inner bobbin, a stainless steel outer restraining ring of the same thickness, and a 0.05-cm Mylar wrap of turn-to-turn insulation, a more meaningful sample problem that demonstrates gap opening and then closing can be generated. The material properties of copper are used for the 65 layers of conductor. Assuming that the conductor is wound with a small amount of preload, that the magnet is operated at liquid nitrogen temperature, and that no gaps can develop, the radial and tangential stress distributions can be calculated to be those shown in Fig. 5. This example was chosen because in the absence of a shrink fit of the stainless steel outer ring, a gap develops between it and the outer conductor layer during cooldown. Furthermore, during energization of the magnet, the coil expands enough, due to the electromagnetic load, for the previously opened gap to close. Figure 6 shows the radial and tangential stress distributions for this magnet when gaps are allowed to open and close during magnet cooldown and energization.

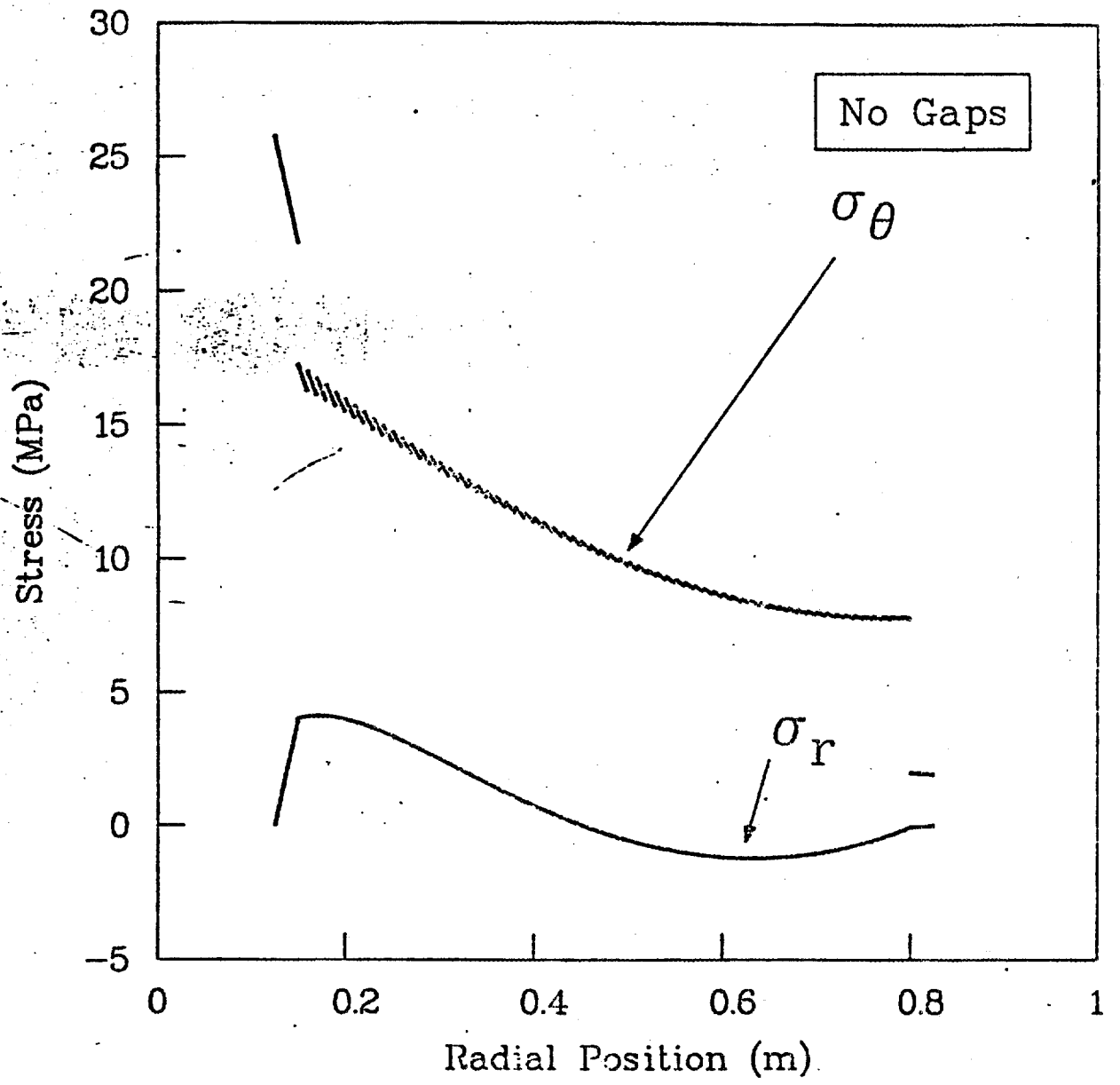

Fig. 5. The radial and tangential stress distributions for the third sample problem when no gaps are permitted to occur.

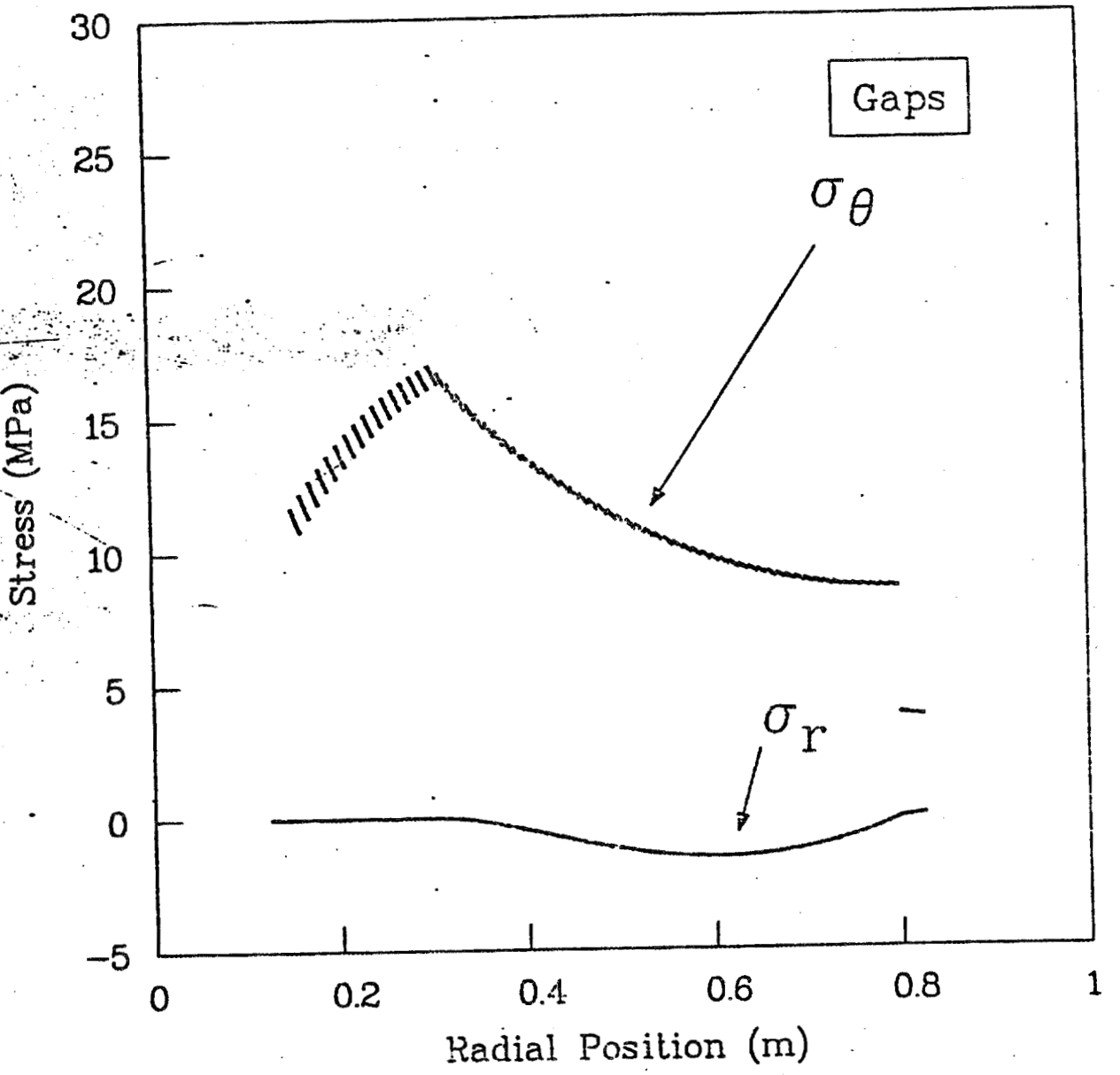

Fig. 6. The radial and tangential stress distributions for the third sample problem when gaps are permitted to develop by the computer software.

CONCLUSIONS

A theory has been presented for the determination of the nonlinear mechanical behavior of axisymmetric solenoids that can develop frictionless gaps which may open or close during magnet operation. This theory takes into account material properties that can be rotationally-transversely isotropic and magnets that can be multilayered and nonhomogeneous. Also discussed were the implementation of this theory within a computer program and example applications of this theory to several magnets.

NOMENCLATURE

Variable	description
B	magnetic field
E	Young's modulus
f	incremental load factor
J	conductor current density
p	pressure
P	preload force
r	radial position
u	displacement
w	width of turn (z direction)
α	moduli ratio
δ	displacement difference
ε	strain
σ	stress
ν	Poisson's ratio

Subscript	description
cg	refers to closing of a gap
,i or i	refers to the ith layer

in	refers to the inner surface of a layer
lp	refers to layer at which preload is applied
og	refers to opening of a gap
out	refers to the outer surface of a layer
r	refers to the radial direction
z	refers to the axis of revolution direction
θ	refers to the tangential direction

Superscript description

f	an incremental value calculated using f
new	a new value
o	an initial value
preload	a value calculated for preload only

REFERENCES

1. W. H. Gray and J. K. Ballou, "Electromechanical Stress Analysis of Transversely Isotropic Solenoids," J. Appl. Phys. 48(7), 3100 (1977).
2. N. E. Johnson, W. H. Gray, and R. A. Weed, in Proc. 6th Symp. on Engineering Problems of Fusion Research, Vol. 1, p. 243 (1975).
3. N. E. Johnson, Adv. Cryo. Eng., 22, 490 (1977).
4. E. S. Bobrov and J. E. C. Williams, "Stresses in Superconducting Solenoids," in Proc. Winter Annual ASME Appl. Mech. Div., Francis C. Moon, Ed., AMD-41, 13 (1980).
5. Erwin Kreyszig, Advanced Engineering Mathematics, John Wiley and Sons, Inc., New York, 1967, p. 166.
6. N. E. Johnson, "The Structural Analysis of Nonhomogeneous Solenoids Using the STANSOL Computer Program," MRI-C2754-TR-3, Mechanics Research Inc., Oak Ridge, Tennessee (1975).
7. L. M. Lontai and P. G. Marston, "A 100 Kilogauss Quasi-Continuous Cryogenic Solenoid – Part 1," in Proc. Int. Symp. on Magnet Technology, Vol. 1, p. 723 (1965).

8. J. K. Ballou, W. H. Gray, T. J. McManamy, and R. L. Brown, "Design and Tests of the Prototyye Coils for EBT-P," to be presented at the 9th Symp. on Engineering Problems of Fusion Research (proceedings to be published).

9. W. H. Gray, T. J. McManamy, J. K. Ballou and R. L. Brown, "A Comparison Between Experimental and Analytical Winding Pre-Strain for a Circular Solenoid," to be presented at the 9th Symp. on Engineering Problems of Fusion Research (proceedings to be published).

OAK RIDGE NATIONAL LABORATORY
OPERATED BY
UNION CARBIDE CORPORATION
NUCLEAR DIVISION

POST OFFICE BOX Y
OAK RIDGE, TENNESSEE 37830

August 11, 1982

To: Attached Distribution Lists

EBT-P PROJECT TITLE I DESIGN REPORT

Publication of the final Title I Design Report for the Elmo Bumpy Torus Proof-of-Principle (EBT-P) Project has been completed by McDonnell Douglas Corporation with approval of the ORNL EBT-P Project Office. The full report includes the following nine volumes:

Volume I - Device Summary

Volume II - Toroidal Vessel

Volume III - Magnet System

Volume IV - Microwave System

Volume V - Vacuum Pumping System

Volume VI - Instrumentation and Control

Volume VII - Cryogenic System

Volume VIII - Device Utilities

Volume IX - Support Structure

Attached for those on Distribution List A are Volumes I thru IX; for those on Distribution List B, Volume I is attached. Volume I - Device Summary contains general project information and a summary of the other technical volumes.

Please advise the EBT-P Project Office should you need additional copies or have any questions in regard to the Title I Report.

James D. Stout

for A. L. Boch
EBT-P Project Manager

ALB:JDS:gce

Attachment

Distribution List A

EBT-P Project Title I Design Report

Volumes I thru IX

1. R. G. Alsmiller
2. J. K. Ballou
3. L. A. Berry
4. J. A. Blair
5. A. L. Boch
6. C. Bridgman
7. A. Y. Broverman
8. R. A. Brown
9. D. B. Campbell
10. Central Research Library
11. R. G. Clark
12. K. D. Cook
13. H. O. Eason
14. R. S. Edwards
15. D. A. Everitt
16. FED Library
17. FED Reports Office
18. W. M. Fletcher
19. C. L. Garren
20. J. C. Glowienka
21. R. J. Hadley
22. W. R. Hamilton
23. G. R. Haste
24. R. A. Jump, DOE/ORO
25. K. L. Kilby
26. H. D. Kimrey
27. Lab Records (2)
28. C. M. Loring
29. H. C. McCurdy
30. T. J. McManamy
31. L. K. Price, DOE/ORO
32. J. P. Schubert
33. J. D. Stout
34. D. W. Swain
35. R. D. Wall
36. J. E. Warwick
37. T. L. White

Distribution List B

EBT-P Project Title I Design Report

Volume I

1. R. G. Affel
2. S. W. Ahrends, DOE/ORO
3. T. D. Anderson
4. S. I. Auerbach
5. J. A. Auxier
6. F. W. Baity
7. D. B. Batchelor
8. P. Brewington, DOE/ORO
9. E. H. Bryant
10. R. D. Burris
11. D. D. Cannon
12. J. A. Cobble
13. H. I. Cobert
14. R. J. Colchin
15. W. A. Davis
16. J. K. Denton
17. R. H. Dilworth
18. R. A. Dory
19. B. C. Duggins
20. K. T. Dziedzic, DOE/ORO
21. G. G. Fee
22. D. E. Ferguson
23. P. C. Fourney
24. W. O. Harms
25. H. H. Haselton
26. P. N. Haubenreich
27. C. L. Hedrick
28. D. L. Hillis
29. S. Hiroe
30. G. W. Horde
31. G. R. Jasny
32. V. C. Kruzic
33. J. A. Lenhard, DOE/ORO
34. M. S. Lubell
35. F. C. Maienschein
36. J. R. McGuffey
37. O. B. Morgan
38. H. H. Osborne
39. F. S. Patton
40. H. Postma
41. D. A. Rasmussen
42. M. W. Rosenthal
43. T. L. Ryan
44. M. J. Saltmarsh
45. T. E. Shannon
46. J. Sheffield
47. K. W. Sommerfeld
48. P. H. Stelson
49. P. B. Thompson
50. H. E. Trammell
51. D. B. Trauger
52. T. C. Trotter
53. N. Uckan
54. T. Uckan
55. J. R. Weir
56. J. C. White
57. A. Zucker